NASA Technical Memorandum 4594

Lunar Ultraviolet Telescope Experiment (LUTE) Phase A Final Report

Robert O. McBrayer
LUTE Task Team Manager
George C. Marshall Space Flight Center, MSFC, Alabama 35812

National Aeronautics and Space Administration
George C. Marshall Space Flight Center, MSFC, Alabama 35812

April 1994

ACKNOWLEDGMENTS

SPECIAL

Special acknowledgment is given to Mr. Max Nein for applying his special insight into the design of telescopes, to Mr. John Frazier for ensuring that all aspects of LUTE engineering were properly addressed, and to both of them for maintaining focus in the phase A activities. Special acknowledgment is also given to Ms. Barbara Walker for her dedication in the compilation, typing, and editing of this report.

SCIENCE

Dr. John McGraw, University of New Mexico, LUTE Principal Investigator—Developed the concept of a lunar transit telescope and served as a principal proponent of the LUTE as a pathfinder derivative of this concept.

Dr. Jason Porter, Marshall Space Flight Center, LUTE Study Scientist—Served as a science representative to the LUTE Task Team and prepared the science and educational objectives for this report.

Dr. Jack Burns, New Mexico State University, LUTE Environmental Package Principal Investigator—Defined a group of instruments to supplement the lunar environmental data that will inherently be collected from the LUTE.

Dr. Stewart Johnson and Dr. Koon Meng Chua, University of New Mexico, Lunar Environment—Provided council and support in the definition of lunar environmental parameters that should be considered in the LUTE design.

March 18–20, 1993, LUTE Science Workshop Participants—Provided a comprehensive description of the scientific objectives for the development of LUTE.

TECHNICAL

Kauffman, Tim Johnson, Brian	Systems Requirements
Gerry, Mark Tyler, Tony Frank, Thomas	Layouts
Jones, Bill	Optical System and Focal Plane Instrument
Luz, Paul Oliver, Karen	Structural Analysis
Rice, Terrie	Materials

Williams, Don Huie, Harold Willowby, Doug	Electrical Power
Walker, Sherry Alexander, Reggie	Thermal Analysis and Control
Blevins, Harold Lowery, D.O.	Communications and Data Handling
Carrington, Connie	Pointing and Alignment
Chandler, Holly	Mass Properties
Hilliard, Jim	Software
Robinson, Keith	Operations Planning
McCarter, Jim Johnson, Les Hilchey, John	Landing Site Analysis and Lunar Environment
Dickerson, Tom Mulqueen, Jack Schmitt, Terri	Lander
Trentham, Ed Galuska, Mike Higgins, Art	Safety and Mission Assurance
Wright, Belinda	Schedules
Prince, Andy	Financial Planning
Korsch Optics, Inc. Korsch, Dietrich	Design of the Aplanatized Third Order Corrected LUTE Optic
Hughes/Danbury Stier, Mark Ruthven, Greg	Optical System Studies
Itek Solomon, Len	Optical System Studies
System Studies & Simulations Smith, Jan	Project Planning/Risk Assessment

TABLE OF CONTENTS

	Page
1.0 INTRODUCTION	1
1.1 Purpose	1
1.2 Scope	1
1.3 Background	1
1.4 Project Management	4
2.0 SCIENCE AND EDUCATIONAL OBJECTIVES	5
2.1 UV Survey Characteristics, Expected Astronomical Capabilities and Progress	5
2.2 Role in Education	8
3.0 PERFORMANCE REQUIREMENTS	9
3.1 Requirements Summary	9
3.2 Level I Requirements	9
3.3 Level II Telescope Requirements Summary	9
4.0 LUTE REFERENCE DESIGN CONCEPT	11
4.1 System Description	11
4.1.1 Objectives and Requirements for the LUTE Reference Design	11
4.1.2 Primary Interfaces	12
4.1.2.1 Launch Vehicle	12
4.1.2.2 Generic Lander	13
4.1.3 Major LUTE Systems/Elements	14
4.1.3.1 Optics	14
4.1.3.2 Optical Bench Assembly	15
4.1.3.3 Baffles	15
4.1.3.4 Metering Structure	15
4.1.3.5 Baseplate	16
4.1.3.6 Power System	16
4.1.3.7 Communications and Data Handling (C&DH)	16
4.1.3.8 Mechanisms	18
4.1.3.9 Telescope Protection System	18
4.1.3.10 Reference Design Configuration Summary	20
4.2 Subsystems Design	20
4.2.1 Optical Configuration	20
4.2.2 Focal Plane Instrument	21
4.2.3 Baseline Structural Design	21
4.2.3.1 Requirements	22
4.2.3.2 Structural Mass Estimate	23
4.2.3.3 Primary Mirror	23
4.2.3.4 Mirror Support Structures	24

TABLE OF CONTENTS (Continued)

	Page
4.2.3.5 Metering Structure	25
4.2.3.6 Optical Baffles	26
4.2.3.7 Light Shade	26
4.2.3.8 Electronics Box Support Structure	27
4.2.3.9 Aperture Cover	28
4.2.3.10 Baseplate	28
4.2.3.11 Integrated Structural Model	28
4.2.3.12 Conclusion	29
4.2.4 Electrical Power System (EPS)	29
4.2.5 Thermal Control System (TCS)	31
4.2.5.1 Requirements	31
4.2.5.2 Environment	32
4.2.5.3 Summary of TCS Reference Design	33
4.2.5.4 Summary of Thermal Analysis Results	33
4.2.6 C&DH System	35
4.2.7 Pointing and Alignment	37
4.2.8 Mass and Inertia Summary	41
4.2.8.1 Mass Statement	41
4.2.8.2 Mass Properties	42
4.2.8.3 Stability	42
4.2.9 LUTE Software	43
4.3 Mission Operations	45
4.4 LUTE Lunar Environment Instruments	45
5.0 SUBSYSTEM TRADES	47
5.1 Optics	47
5.1.1 Telescope Design	49
5.1.2 Figure Error Correction Using a Deformable Mirror	49
5.1.3 Effect of Bulk Temperature Changes on the Performance of the Optical Telescope System	50
5.1.4 LUTE Sunshade/Light Baffle	55
5.1.4.1 Methodology	55
5.1.4.2 Results	56
5.1.4.3 Future Analyses	58
5.1.5 Error Budget	58
5.1.6 900 cm Effective Focal Length (EFL) Optical System	60
5.1.7 Resolution Versus EFL and Pixel Size	61
5.2 LUTE Focal Plane Array (FPA)	62
5.3 Structural Trades and Analysis	65
5.3.1 FE Models	66
5.3.2 Requirements and Loads	67
5.3.3 Structural Material Selection	69
5.3.4 Mitigation of Mirror Deformations in Lunar-Based Telescopes	70
5.3.4.1 Temperature Effects on Structures	71

TABLE OF CONTENTS (Continued)

		Page
	5.3.4.2 Mirror Support Trades	73
	5.3.4.3 Primary Mirror	75
	5.3.4.4 Primary Mirror Trade Summary	84
	5.3.4.5 Analysis Summary for SiC Primary Mirror	85
5.3.5	Metering Structure	86
	5.3.5.1 Design Trade Space	86
	5.3.5.2 Back Focal Distance Thermal Disturbances	87
	5.3.5.3 Stress Analysis Results	88
5.3.6	Light Shade	88
	5.3.6.1 Light Shade Construction Trade	88
	5.3.6.2 Buckling Analysis of Baseline Light Shade	89
	5.3.6.3 Stress Analysis of Baseline Light Shade	89
	5.3.6.4 Light Shade Mass	90
5.3.7	Electronics Box Support Structure	90
5.3.8	Aperture Cover	90
5.3.9	Baseplate	92
5.3.10	Component Trade Summary	93
5.3.11	Integrated LUTE Structural Model	93
	5.3.11.1 Interface Hardpoints From Lute to the Lander Mount	94
	5.3.11.2 Interface Loads	94
	5.3.11.3 Stress Analysis	94
	5.3.11.4 Normal Modes Analysis	95
5.3.12	Structural Mass Estimate	96
5.3.13	Analysis Conclusion	96
5.4	Electrical Power System (EPS)	97
5.4.1	LUTE Power System Trade and Selection Criteria	97
5.4.2	EPS Candidate Comparison	98
5.4.3	LUTE Power Requirements	99
5.4.4	Use of Solar Array	99
	5.4.4.1 Solar Array Requirements	101
	5.4.4.2 Solar Array Performance	102
5.4.5	Use of an RTG	103
	5.4.5.1 RTG Requirements	103
	5.4.5.2 RTG Performance	103
5.5	Thermal Control System	104
5.5.1	Procedure	104
5.5.2	Trade Description	105
5.5.3	Telescope Thermal Control	105
	5.5.3.1 Requirements	105
	5.5.3.2 Initial Thermal Analysis	107
	5.5.3.3 Model Description	107
	5.5.3.4 Material Properties	110
	5.5.3.5 Initial Results	112
	5.5.3.6 Mirror Construction and Support Structure Effects	127

TABLE OF CONTENTS (Continued)

		Page
5.5.3.7	Mirror Material Trades	130
5.5.3.8	Site Latitude Trade	131
5.5.3.9	Use of Heaters on Primary Mirror	135
5.5.3.10	Metering Structure Axial Gradient	136
5.5.3.11	Declination Effect on Mirror Temperature	138
5.5.4	Detector Thermal Control	139
5.5.4.1	Requirements	140
5.5.4.2	Concepts	140
5.5.4.3	Detector TCS Recommendations	145
5.5.5	Subsystem Thermal Control	145
5.5.5.1	Requirements	145
5.5.5.2	Electronics Analysis	146
5.5.5.3	Power System Analyses	148
5.5.5.4	Mechanism Analysis	150
5.5.5.5	Thermal Control Conclusion	150
5.6	Communications and Data Handling	151
5.7	Pointing and Alignment	153
5.7.1	Guidelines and Assumptions	153
5.7.2	Acquisition Sensor Trades	153
5.7.3	Telescope Mount Trades	154
5.7.4	Kinematic and Static Equilibrium Equations	156
5.7.5	Hexapod Mount Trades	157
5.7.6	Tilt-Plate and Azimuth-Elevation-Roll Mount Trades	164
5.7.7	Component Selection and Weight and Power Estimates	170
5.7.8	Conclusions, Issues, and Concerns	173
5.8	Landing Site Selection Analysis	173
5.8.1	Introduction	173
5.8.2	Requirements	173
5.8.3	Sky Coverage	174
5.8.4	Sunlight Avoidance	176
5.8.4.1	Site Lighting Geometry	176
5.8.4.2	Solar Light Shade	176
5.8.4.3	Light Shade Size	177
5.8.4.4	Unavoidable Sunlight Intrusion Near Sunrise and Sunset	178
5.8.5	Earthshine Avoidance	178
5.8.5.1	Earth Motion in the Lunar Sky	178
5.8.5.2	Light Shade Requirements for Earthshine Avoidance	181
5.8.5.3	Sunlight and Earthshine Constraints on LUTE Operations	182
5.8.5.4	LUTE Operation Time Variation With Viewing Declination	183
5.8.6	Continuous Opportunity for Earth Communications	183
5.8.7	Communications Antenna Pointing	184
5.8.8	Galactic Pole Viewing	184
5.8.9	Avoiding Lyman-α Emissions in the Geocorona	186
5.8.10	Lunar Surface Thermal Radiation	186

TABLE OF CONTENTS (Continued)

Page

5.8.11 The Lunar Terrain 187
5.8.12 Micrometeoroid Avoidance 188
5.8.13 The Focal Plane Array 188
5.8.14 Summary of LUTE Site Selection 188
5.8.15 Cosmic Rays 189
5.8.16 Lunar Dust 189
5.8.17 Lunar Thermal Environment 190
5.8.18 LUTE Lunar Environment Instruments 190
5.9 Software 191
5.9.1 Software Management Plan Document Outline 191
5.9.2 LUTE Software Development Life Cycle 192
5.9.3 LUTE Software Content Outline 193
5.9.3.1 LUTE Flight Software 193
5.9.3.2 Science Data Software 193
5.9.3.3 EGSE Software 193
5.9.3.4 Development and Verification Software 193
5.9.3.5 Simulation Software 193
5.9.3.6 Opertions Software 193
5.9.3.7 Sensor Data Base Software 193
5.10 Lander 194
5.10.1 Common Subsystem Study 194
5.10.2 LUTE Level II Requirements Imposed on Lander 194
5.10.3 Parametric Sizing Study for Lander 194

6.0 SAFETY AND MISSION ASSURANCE 197

6.1 Safety 197
6.2 Reliability 198
6.3 Quality Assurance 198

7.0 SCHEDULE AND COST 199

7.1 Future Planning 199
7.2 Funding Requirements 199
7.2.1 Predevelopment Funding Requirements 199
7.2.2 Development Funding Requirements 199
7.2.3 Ground Rules and Assumptions 202
7.2.4 Minimum Configuration 203
7.2.5 NWODB 203

8.0 FUTURE WORK 204

8.1 Near-Term Effort 204
8.1.1 LUTE Optical Systems Analysis 204

TABLE OF CONTENTS (Continued)

		Page
8.1.2	Large-Area Detector Array	204
8.1.3	Enviromental Measurement Package	205
8.2	Long-Range Plans	205
9.0	CONCLUSION	206
REFERENCES		209
APPENDIX A	LUTE PRELIMINARY PROJECT PLAN	213
APPENDIX B	LEVEL I SYSTEMS REQUIREMENTS DOCUMENT (LUTE)	233
APPENDIX C	LEVEL II SYSTEMS REQUIREMENTS DOCUMENT (TELESCOPE)	245
APPENDIX D	LEVEL II SYSTEMS REQUIREMENTS DOCUMENT (LANDER)	287
APPENDIX E	LUTE/ARTEMIS	317
APPENDIX F	LUTE HARDWARE TREE	323
APPENDIX G	APERTURE COVER CONCEPTS	331
APPENDIX H	MECHANISMS	343
APPENDIX I	LUTE MISSION OPERATIONS PLAN	365
APPENDIX J	LUTE MIRROR MATERIALS REPORT	371
APPENDIX K	MIRROR MATERIAL PROPERTIES	395
APPENDIX L	LUTE TELESCOPE STRUCTURAL DESIGN STUDY REPORT (STUDY REPORTS BY OPTICAL COMPANIES)	401
APPENDIX M	MATERIAL PROPERTIES FOR THERMAL ANALYSES	461
APPENDIX N	LUTE SYSTEM SAFETY PLAN	659
APPENDIX O	LUTE PRELIMINARY HAZARD ANALYSIS REPORT	667
APPENDIX P	LUTE RELIABILITY PLAN	707
APPENDIX Q	LUTE INTEGRATED PROGRAM PLAN FINAL REPORT	727

LIST OF ILLUSTRATIONS

Figure	Title	Page
1.	Recent MSFC lunar-based optical astronomy facilities studies	2
2.	LUTE in operational configuration, integrated with the lander, deployed on the lunar surface	3
3.	Celestial map	6
4.	LUTE reference configuration	12
5.	Atlas II 3.3 m payload envelope	13
6.	Lander/payload interface hardpoints	13
7.	LUTE hardware tree	14
8.	Optical bench assembly	14
9.	Optical bench envelope dimensions	15
10.	Launch configuration	16
11.	C&DH equipment locations	17
12.	Deployment mechanisms	19
13.	LUTE configuration	20
14.	Optical layout	21
15.	Primary mirror internal construction	24
16.	Baseline primary mirror support	24
17.	Metering structure finite element model	25
18.	Light shade	26
19.	T-stringer geometry	27
20.	Electronics box support structure	27
21.	Galileo RTG for LUTE	30
22.	RTG EPS chracteristics	31

LIST OF ILLUSTRATIONS (Continued)

Figure	Title	Page
23.	Heat sources and sinks for LUTE in the operating environment	32
24.	Primary mirror temperature (reference configuration)	34
25.	The LUTE with RTG	34
26.	Effect of RTG heat load on primary mirror	35
27.	LUTE C&DH simplified block diagram	36
28.	Pointing system components	38
29.	Artemis lander with estimated strut hardpoint coordinates	39
30.	Deck-tilt due to one crushed leg	39
31.	LUTE mass properties	42
32.	Lander stability	43
33.	LUTE software functional configuration	44
34.	Primary and secondary baffles	47
35.	Geometric distortion in the focal plane	48
36.	Primary figure error (positive deformation)	51
37.	Primary figure error (negative deformation)	51
38.	Secondary figure error (positive deformation)	52
39.	Secondary figure error (negative deformation)	52
40.	Tertiary figure error (positive deformation)	53
41.	Tertiary figure error (negative deformation)	53
42.	Baffle designs for LUTE	56
43.	Power scattered to detector	57
44.	LUTE wavefront error budget	59

LIST OF ILLUSTRATIONS (Continued)

Figure	Title	Page
45.	Resolution (arcsec) versus EFL and pixel size	61
46.	LUTE focal plane CCD array	62
47.	Schematic representation of CCD/TDI technique	63
48.	Fiber optic field flattener and UV converter	64
49.	Structural load paths for LUTE reference design	69
50.	Temperature effects on a beam	71
51.	Thermal deformation versus baseplate CTE	72
52.	Mirror support concepts	73
53.	Thermal deformation versus support stiffness	74
54.	Analysis process for mirror deformations	75
55.	Transient thermal distortion coefficient	78
56.	Transient thermal distortion coefficient (plotted with beryllium and SiC data)	78
57.	Steady-state thermal distortion coefficient	79
58.	Beryllium primary mirror thermal load at 40° lunar latitude	80
59.	Beryllium primary mirror thermal deformations at 40° lunar latitude	80
60.	Ceraform™ SiC primary mirror thermal deformations at 40° latitude	82
61.	Mirror tilt angle	83
62.	Lunar gravity deformations	83
63.	Metering structure design concepts	86
64.	Secondary mirror enclosure options	87
65.	Metering structure thermal deformations	88

LIST OF ILLUSTRATIONS (Continued)

Figure	Title	Page
66.	Aperture cover mass estimate	91
67.	Aluminum cover mass versus thickness	91
68.	Interface hardpoints from LUTE to the lander mount	92
69.	First natural frequency mode shape	96
70.	EPS solar array description	99
71.	LUTE solar array Sun angle	100
72.	LUTE photovoltaic power system	100
73.	LUTE solar array performance	101
74.	Solar array temperatures	102
75.	LUTE power requirements by phase	102
76.	EPS RTG description	103
77.	RTG power output versus background temperature	104
78.	Baseline model geometry	108
79.	Lunar surface simulation	108
80.	Mirror construction	109
81.	Reduced LUTE TMG™ model	110
82.	Detailed LUTE TMG™ model	111
83.	Primary mirror temperature for baseline	112
84.	Baseline primary mirror temperature distribution (top view)	112
85.	Baseline light shade temperature distribution	113
86.	Sources of temperature differential in primary mirror	113
87.	Isothermal enclosure options (side view)	115

LIST OF ILLUSTRATIONS (Continued)

Figure	Title	Page
88.	Mirror temperature distribution for isothermal rings (noon)	116
89.	Mirror temperture distribution for isothermal bucket (noon)	116
90.	Mirror temperature distribution for isothermal baseplate (noon)	116
91.	Mirror temperature distribution for isothermal baseplate and ring (noon)	117
92.	Mirror temperature distribution for isothermal light shade (noon)	117
93.	Primary mirror temperature differential for enclosure options	118
94.	Light shade shape and orientation options	119
95.	Mirror temperature distributions for 65° north with tilt option	121
96.	Light shade temperature distributions for 65° north with tilt option	121
97.	External ground shade encloses LUTE east, west, and north sides	122
98.	Primary mirror temperature differential for light shade options	123
99.	Heat flux contribution of lunar surface	124
100.	Angled baffle concept	125
101.	Baffles can be arranged to achieve symmetric view to space	126
102.	Horizontal ring baffle concept	126
103.	Flared light shade concept	127
104.	Effect of flare angle on north/south temperature differential (local noon)	128
105.	One-piece mirror with ring support	128
106.	Separate primary and tertiary with ring support	128
107.	Titanium flexures supporting primary mirror on baseplate	129
108.	Primary mirror gradient for different methods of support	129
109.	Primary mirror temperature distribution at noon (beryllium)	130

LIST OF ILLUSTRATIONS (Continued)

Figure	Title	Page
110.	Primary mirror temperature distribution at noon (SiC)	130
111.	Primary mirror temperature distribution at noon (fused silica)	131
112.	Temperature differential for beryllium and SiC primary	132
113.	Temperature differential for beryllium and fused silica primary	132
114.	Telescope orientation at latitudes studied	133
115.	Summary of mirror and light shade maximum temperatures	134
116.	Temperature differential across primary mirror	135
117.	Mirror average and maximum temperature differential	135
118.	Light shade temperature at lower and upper edge of metering structure	137
119.	Estimate of metering structure axial thermal gradient	138
120.	Light shade configurations for 30° and 40° point declinations	138
121.	Location of CCD detector and radiator	139
122.	Passive radiator concepts for detector heat rejection	141
123.	Results of passive detector radiator trade study	142
124.	Illustration of TEU	143
125.	New detector location to alleviate thermal control problems	144
126.	Electronics box analysis positions	146
127.	Thermal control methods for electronics box	147
128.	RTG dimensions and optical properties	148
129.	RTG outer shell temperature	149
130.	Solar array configuration analyzed	149
131.	Solar array temperature predictions	150

LIST OF ILLUSTRATIONS (Continued)

Figure	Title	Page
132.	Tilt-plate mount	155
133.	Tilt range for tilt plate configuration	155
134.	Rollring trades	156
135.	Kinematic constraint loop closure equations	157
136.	Hexapod mount trades	158
137.	Option 1—tilt angle	159
138.	Option 1—actuator lengths at maximum tilt angle for 0.813 m actuators	159
139.	Option 1—actuator workspace for 0.813 m actuators	160
140.	Option 3—three-strut configuration	161
141.	Option 3—sensitivity to upper half angle at 0.56 m rollring radius	161
142.	Option 3—sensitivity to rollring radius for 10° upper half angle	162
143.	Option 3—actuator forces and lengths at maximum tilt	162
144.	Option 3—roll angle capability over entire tilt region	162
145.	Option 3—actuator workspace and region available for subsystem packaging	163
146.	Option 4—maximum tilt angle for various actuator lengths	163
147.	Mount options for 42° tilt requirement	164
148.	Hexapod mount tilt capability	165
149.	Azimuth-elevation-roll and tilt-plate concepts	165
150.	Azimuth-elevation-roll mount	166
151.	Two-actuator tilt-plate dual-rollring mount	167
152.	Top view and tilt region without lower rollring for two-actuator tilt-plate dual-rollring mount	167
153.	Single-actuator tilt-plate roll mount	168

LIST OF ILLUSTRATIONS (Continued)

Figure	Title	Page
154.	Two-actuator tilt-plate roll mount concept	169
155.	Top view and tilt region for two-actuator tilt-plate roll mount	169
156.	Elevation axis actuators	170
157.	Upper and lower racering bearings	171
158.	Motor-driven pinion gear drive assembly for upper and lower racerings	171
159.	Secondary mirror actuator	172
160.	Sky area surveyed by LUTE depends on viewing declination and telescope FOV	175
161.	Geometry of the Earth/Moon system	175
162.	Sky coverage of a transit telescope for small FOV's	176
163.	Path of the Sun relative to the LUTE light shade	177
164.	Light shade angle depends on viewing declination	177
165.	Recommended LUTE light shade angle	178
166.	Lunar sunrise relative to the LUTE light shade	179
167.	Optical libration in latitude	179
168.	Optical libration in longitude	180
169.	Earth motion as viewed from a lunar site	180
170.	Earth confinement region relative to the LUTE light shade	181
171.	Light shade angles	181
172.	LUTE operation times during a 2 year mission with no sunlight or earthshine interference	182
173.	Solar-powered LUTE operation time for two different viewing declinations	183
174.	Earth visibility from the Moon	184

LIST OF ILLUSTRATIONS (Continued)

Figure	Title	Page
175.	Antenna pointing direction for Earth communications	185
176.	Site location required for galactic pole viewing	185
177.	Avoidance of hydrogen Lyman-α in the geocorona	186
178.	Avoidance of surface thermal radiation	187
179.	Software life cycle	192
180.	LUTE level II requirements imposed on lander	194
181.	Ground rules and assumptions	195
182.	LUTE/lander/launch vehicle relationships	195
183.	LUTE/lander/launch vehicle mass/cost summary	196
184.	Performance and cost	196
185.	LUTE (in-house project)	200
186.	LUTE cost estimate	201
187.	LUTE cost matrix	201
188.	Potential LUTE savings as a result of NWODB	203
189.	LUTE programmatics	207
190.	LUTE documentation	208

LIST OF TABLES

Table	Title	Page
1.	Advantages of astronomy from the Moon	2
2.	Functional analysis for structures	22
3.	Structural mass estimate for baseline design	23
4	LUTE linear static stress analysis with Atlas IIAS launch load	28
5.	LUTE structural natural frequency	29
6.	Systems requirements affecting the thermal control system	31
7.	Thermal control mass summary	33
8.	LUTE C&DH subsystem equipment list	37
9.	Mechanism and alignment requirements	40
10.	LUTE mass statement	41
11.	Summary of structural trade studies	66
12.	Finite elements in structural model	67
13.	Minimum glass design factors	68
14.	Room temperature mechanical properties of candidate structural materials	69
15.	Structural material selection for baseline design	70
16.	HDOS ranking of mirror construction geometries (from "best" to "worst")	76
17.	Room temperature properties of candidate mirror materials	76
18.	Comparison factors for mirror material trades	77
19.	Thermal-structural performance of primary mirror materials at 40° latitude ("best" material to "worst" material)	81
20.	Flat (0° tilt) LUTE primary mirror at 40° lunar latitude	84
21.	Primary mirror quasi-static launch stress	84
22.	Structural analysis summary for SiC primary mirror	85

LIST OF TABLES (Continued)

Table	Title	Page
23.	Light shade trade summary	89
24.	Buckling margin of safety summary for stiffened light shade	89
25.	Light shade mass summary	90
26.	Baseplate launch stresses versus material selection	92
27.	Impact of mirror material selection on structural mass	93
28.	Summary of structural trade results	94
29.	Quasi-static reactions forces (N) for 40° latitude mount	95
30.	LUTE linear static stress analysis with Atlas IIAS launch loads	95
31.	LUTE structural natural frequency	96
32.	Structural mass estimate for baseline design	97
33.	EPS requirements/selection criteria	98
34.	EPS candidate comparisons	98
35.	Power requirements (W) for each mission phase	99
36.	Analysis tools	105
37.	Summary of trade studies performed	106
38.	Model initial temperatures	109
39.	LUTE thermal analysis materials	111
40.	Summary of isothermal enclosure trade results	118
41.	Summary of light shade trade results	122
42.	Absorbed heat loads, at noon, for various optical properties	124
43.	Comparison of baffle options to baseline at local noon	127
44.	Summary of mirror material trade results	131

LIST OF TABLES (Continued)

Table	Title	Page
45.	Summary of latitude trade results	133
46.	Results of pointing declination thermal trade	139
47.	Detector radiator temperature summary	142
48.	Subsystem thermal control requirements	145
49.	LUTE frequency options	152
50.	Ground rules used for LUTE site selection	174

LIST OF ACRONYMS AND ABBREVIATIONS

AGN	active galactic nuclei
AXAF	Advanced X-Ray Astrophysics Facility
BOL	beginning of life
BRDF	bidirectional reflectance distribution function
C&DH	communications and data handling
CCD	charge coupled device
CG	center of gravity
CTE	coefficient of thermal expansion
	charge transfer efficiency
CTI	CCD transit instrument
	charge transfer inefficiency
DOE	Department of Energy
DOF	degrees of freedom
DSN	Deep Space Network
EFL	effective focal length
EGSE	electrical ground support equipment
EOL	end of life
EPS	electrical power system
ESMC	Eastern Space and Missile Center
FAUST	far ultraviolet space telescope
FE	finite element
FEM	finite element model
FOV	field of view
FPA	focal plane array
FUV	far ultraviolet
FY	fiscal year

GE	General Electric
GPHS	general purpose heat source
GSE	ground support equipment
GSFC	Goddard Space Flight Center
HDOS	Hughes Danbury Optical Systems
HST	Hubble Space Telescope
IPS	instrument pointing system
IR	infrared
ISM	interstellar medium
JSC	Johnson Space Center
JPL	Jet Propulsion Laboratory
KSC	Kennedy Space Center
LCTE	lunar cluster telescope experiment
LEO	low-Earth orbit
LLT	large lunar telescope
LTT	lunar transit telescope
LUTE	Lunar Ultraviolet Telescope Experiment
LVDT	Linear Variable Differential Transducer
MGSE	mechanical ground support equipment
MLI	multilayer insulation
MSFC	Marshall Space Flight Center
MSI&T	mission system integration and test
MY	man-year
NASA	National Aeronautics and Space Administration
NASCOM	NASA cost model
NRL	Naval Research Laboratory
NWODB	new ways of doing business

OSR	optical solar reflector
PMS	program mission support
PRD	projects requirements document
QSO	quasars
RF	radio frequency
RHU	radioisotope heating unit
RTG	radioisotope thermoelectric generator
RY$	real year dollars
SICM	scientific instrument cost model
SINDA	systems improved numerical differencing analyzer
SNR	supernova remnants
SRD	systems requirements document
SSTDC	steady-state thermal distortion coefficient
STASS	skin-stringer tank analysis spreadsheet system
SWG	science working group
TBD	to be determined
TCS	thermal control system
TDI	time delay and integration
TEU	thermoelectric units
TLI	translunar injection
TMG™	thermal model generator
TRASYS	thermal radiation analyzer system
3-D	three-dimensional
TTDC	transient thermal distortion coefficient
UIT	ultraviolet imaging telescope
ULE	ultralow expansion
UV	ultraviolet

SYMBOLS AND UNITS

α	solar absorptivity—thermal expansion coefficient
b/s	bits per second
δ	conic constant
ε	emissivity
Å	Angstrom
ρ	density—radial coordinate
C_p	specific heat
cm	centimeters
dB	decibel
ΔT	temperature difference
f_p	focal length of primary mirror
f_s	focal length of secondary mirror
f_t	focal length of tertiary mirror
GaSb	gallium antimonide
Hz	Hertz
k	thermal conductivity—stiffness
K	Kelvin
kbs	kilobits per second
kg	kilogram
km	kilometer
kPa	kilopascal
kW	kilowatts
MPa	megapascal
m_s	secondary mirror magnification
m_t	tertiary mirror magnification

m	meters
Mbs	megabits per second
micron	10^{-6} meters
mm	millimeters
mrad	milliradian
nm	nanometer
Nm	Newton meter
ppm	parts per million
rms	root mean square
rss	root of the sum of squares
SiC	silicon carbide
W	Watt

TECHNICAL MEMORANDUM

LUNAR ULTRAVIOLET TELESCOPE EXPERIMENT (LUTE) PHASE A FINAL REPORT

1.0 INTRODUCTION

1.1 Purpose

The purpose of the Lunar Ultraviolet Telescope Experiment (LUTE) phase A study was to determine the feasibility of placing an unmanned, 1 m aperture, transit telescope on the Moon and operating it from Earth for a minimum period of 2 years.

1.2 Scope

The scope of the LUTE phase A study included identifying the scientific and engineering requirements, developing a feasible reference design configuration that satisfies the scientific and engineering requirements, developing an operational approach to recovering and processing LUTE data, and documenting the trade studies that were accomplished during the phase A activity. The educational aspects of LUTE were assumed to be included in the scientific and engineering requirements and will be addressed in phase B. The LUTE project incorporates new ways, recently identified by NASA, of planning and implementing projects.

1.3 Background

Over the past 25 years, a scientific revolution has occurred in astrophysics as a result of two advancing fronts. First, instruments and telescopes have been developed to make more sensitive measurements throughout the entire electromagnetic spectrum. Second, access to space has permitted observations without the influence of our atmosphere. The lunar surface is another advantageous location for astrophysical observations, and many studies show that the Moon is a logical place to utilize these advances in sensing technology and to establish space observatories. The unique advantages of the Moon would enable instruments to achieve high resolution, operate over longer useful lifetimes, and make observations in specialized areas of concern in ways not feasible with current telescopes operating in Earth orbit.

Lunar-based telescopes will capitalize on a number of advantages the Moon offers as an observing platform (table 1). The lunar environment will enable important observations in the ultraviolet (UV), which are constrained on Earth and in low-Earth orbit (LEO). Observation times for lunar-based telescopes will not be handicapped by frequent interruptions due to occultations by the Earth, Sun, and Moon. The dark lunar sky and the Moon's slow rotation will facilitate observation of very faint objects. This remote location also minimizes the geocoronal effect on observations. Lunar seismic activity is far less than Earth's, simplifying the choice of a stable site for a telescope. In addition, the low-gravity environment will enable the use of lightweight structures and optics, as well as the positive preloading of telescope joints and bearings.

Studies of lunar observatories (fig. 1) at Marshall Space Flight Center (MSFC) sponsored by NASA Headquarters Astrophysics Division have shown that the design of telescopes that will reliably operate on the Moon differ in many aspects from the traditional ground-based and orbiting telescopes.

Table 1. Advantages of astronomy from the Moon.

Vacuum environment	No atmospheric absorption or attenuation
Dark, cold sky/surface	Facilitates observation of faint objects; minimizes light pollution and radio interference; aids IR observations
Magnetic field very low	Magnetic field 10^{-4} to 10^{-2} times less than Earth's
Full sky view	28 days rotation; Earth subtends <3° from Moon; site selection to place Earth 10° above horizon
Instrument support	Natural lunar structures
Long baselines feasible	Enhances construction of interferometers
Stable platform	Lunar seismic activity far less than Earth's (~2.5 Richter)
Low gravity	Facilitates light weighted structures and optics; positive preloading of joints; bearings feasible; no tethers required

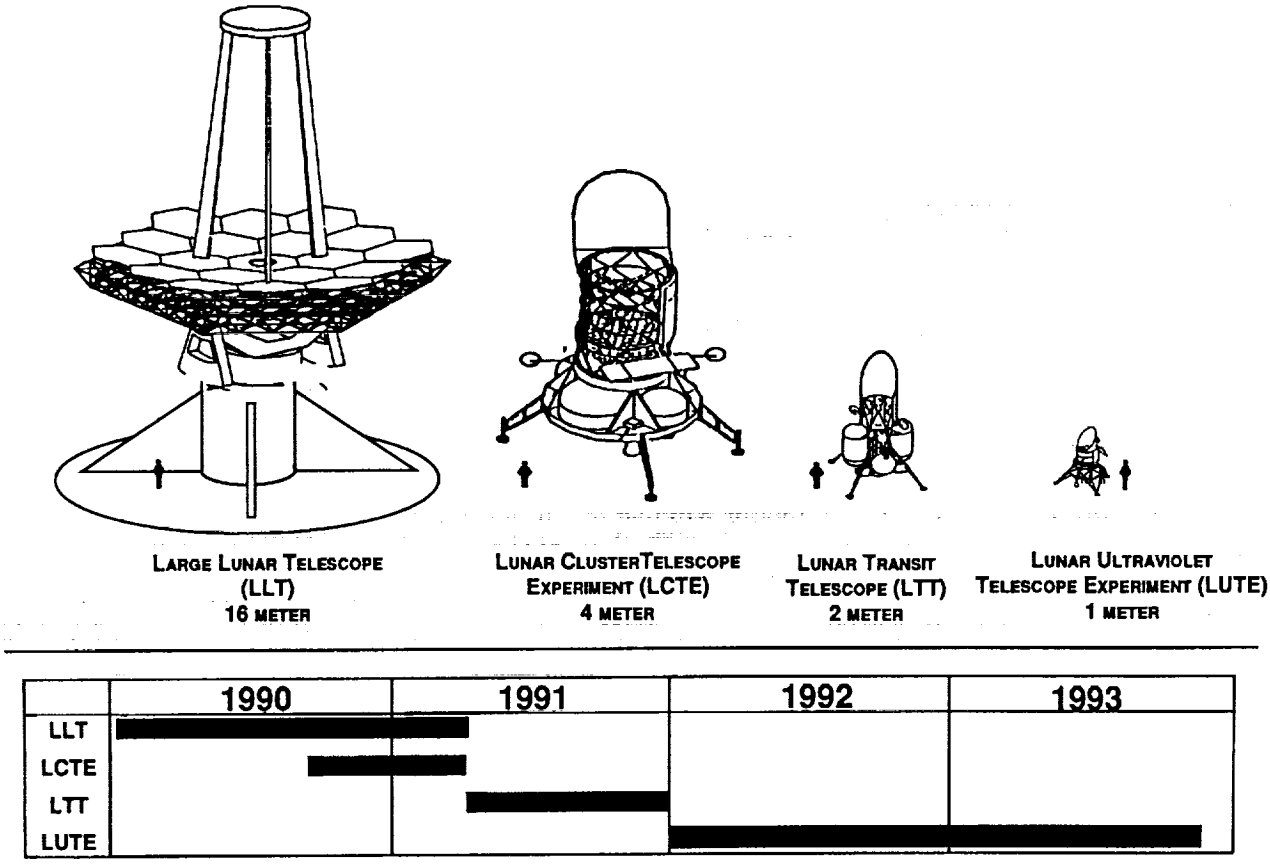

Figure 1. Recent MSFC lunar-based optical astronomy facilities studies.

The primary reason is the temperature extremes associated with the long lunar day and night cycle. Therefore, the development of a small, scientifically productive telescope would also serve as a technology pathfinder for future lunar observatories. The LUTE would provide this learning experience prior to deploying a major astronomical facility on the Moon like the 2 m lunar transit telescope (LTT), the 4 m lunar cluster telescope experiment (LCTE), or the 16 m large lunar telescope (LLT).

The LUTE project will also be utilized as a pathfinder for implementing new approaches to the management of new NASA projects. On July 28, 1992, an in-house MSFC LUTE Task Team was formed to focus and complete the remaining phase A activity and to perform the project planning for design, fabrication, testing, launch, and 2 year operation of a telescope on the lunar surface. The LUTE project will provide for an extended phase B activity, with a 5 year span from the start of phase B to launch. The LUTE mission characteristics include: scientific merit, educational opportunities, low cost, and high benefit-to-cost ratio. The LUTE project will provide opportunities to use and develop new ways of doing business (NWODB) in the design, development, and procurement phases while serving as a technological pathfinder for future lunar science hardware design. The NWODB's are described in several NASA briefings.[1-3]

The LUTE is a 1 m class, fixed pointing declination, UV imaging telescope that can be placed on the Moon by an unmanned lander as an early scientific payload (fig. 2). It could produce a multiple bandpass (1,000 to 3,500 Å) UV survey of more than 300 square degrees of the sky, with a resolution of less than 0.5 arcsecond, and repeat observations at intervals to allow studies of stellar variability. The concept of this high-resolution survey of the UV sky is proposed by the "Decade Report of the Astronomy and Astrophysics Survey Committee."[4] In addition, the LUTE concept is specifically endorsed by the UV Missions Operations Working Group as the highest priority early lunar astronomical instrument and by the Lunar Astrophysics Management Operations Working Group as an excellent candidate precursor lunar science payload. Both working groups are sponsored by NASA's Office of Space Science and Applications.

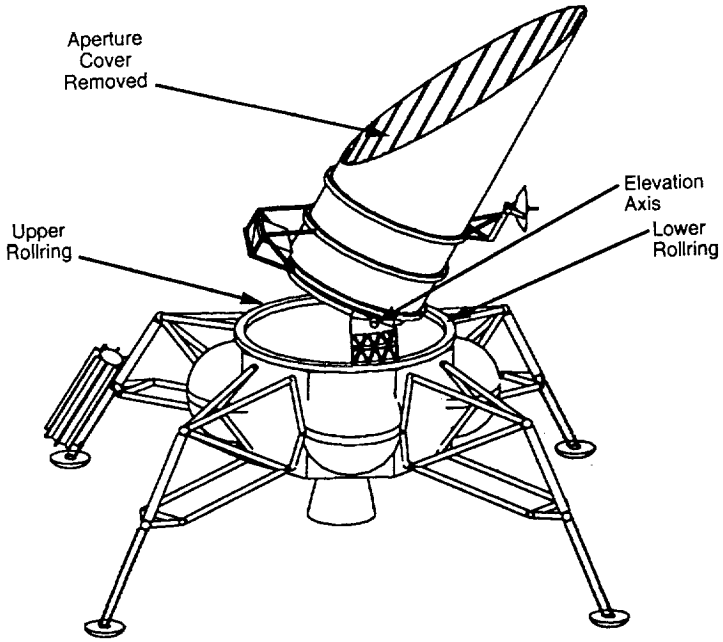

Figure 2. LUTE in operational configuration, integrated with the lander, deployed on the lunar surface.

1.4 Project Management

The LUTE Task Team was established to manage the development of the LUTE project. The task team was given ground rules to use LUTE as a pathfinder project for new "small, fast, low-cost" projects. These ground rules were (1) keep the telescope simple, (2) keep the cost low, and (3) keep the development time short. Implementing this approach required NWODB within NASA. NWODB applicable to LUTE include the following: extended phase B effort (including more early year funding), early appointment of a project manager, concurrent engineering, reduced organizational complexity, advanced design and configuration control methods, completion of preliminary design review before the start of phase C/D, utilization of performance specifications, three project review gates before phase C/D, the early use of breadboards to reduce phase C/D engineering changes, and utilization of a program commitment agreement.

The LUTE Task Team was established approximately half-way through the phase A activity. The task team core was comprised of four full-time members: a manager, deputy manager, chief engineer, and secretary. Approximately 15 full-time equivalent people (engineers, scientists, and program analysts) from Program Development, Science and Engineering Directorate, and the Safety and Mission Assurance Office were utilized in a matrix organization to complete the phase A activity. The organizational interfaces worked smoothly, and resources were efficiently utilized for the LUTE phase A final activity with this approach. The phase B activity will require some additions to the core group of full-time team members and additional matrix support.

The LUTE phase A final effort under the task team was expanded to concurrently involve people from other elements of the MSFC organization with hands-on hardware development experience. This expertise was utilized to augment the special talent in Program Development for performing feasibility studies. This resulted in development of LUTE phase A final products that are usually not available until the phase B activity: draft LUTE level I and level II systems requirements document, lander systems requirements document, preliminary project plan (appendix A), preliminary reliability plan, preliminary safety plan, preliminary hazard analysis, and a preliminary project logic flow diagram have been prepared as part of the phase A effort. These documents are some specific, tangible examples of involving a wide range of engineering disciplines in the project early enough to ensure that considerations are given to all aspects of the project during its formative stages.

A three-dimensional (3-D) electronic engineering drawing system was utilized during the LUTE phase A final study to improve the analytical process. The drawings prepared by the assembly and layout analyst were utilized by the thermal analyst, the structures analyst, and the pointing and control analyst to evaluate the LUTE configuration. This eliminated the need for separate layouts for each discipline's analysis. Since the assembly and layout analyst made all changes in the layout computerized drawings, there was assurance that all analysts were working on the same configuration. This configuration was electronically transferred to the Visual Information Division at MSFC and utilized in the development of an animation of the LUTE mission scenario. Some of this same material was utilized in the development of a "penny folder" on the LUTE project that was printed at MSFC using an advanced reproduction process. The MSFC internal graphics and printing capability made an animation and "penny folder" possible with severely limited LUTE funding.

This report outlines the mission science and educational criteria that were used for the phase A activity, the reference design concept that resulted from phase A, the subsystem trades that were accomplished to develop the reference design concept, safety and mission assurance considerations, the project schedule and cost estimates that were developed from the phase A effort, a summary of future work, and conclusions that can be drawn from the phase A activity.

2.0 SCIENCE AND EDUCATIONAL OBJECTIVES

2.1 UV Survey Characteristics, Expected Astronomical Capabilities and Progress

The scientific value of the LUTE will be primarily in its role as the first high-resolution astronomical survey in the UV and far ultraviolet (FUV) regions of the electromagnetic spectrum. Although there have been observations in this wavelength range, these have been mostly limited to spectra of selected objects, with the targets chosen because of their interesting appearance in some other spectral regime. There have been a few previous imaging surveys. Those with the Far Ultraviolet Space Telescope (FAUST) and very wide field camera onboard Spacelab 1 had several hundred times less sensitivity and spatial resolution than will be provided by LUTE. The ultraviolet imaging telescope (UIT) on Astro-1 had comparable sensitivity to that projected for the LUTE, but the LUTE will have approximately 3 times the spatial resolution and 10 times the spatial coverage (per year). In contrast to these earlier surveys which sampled only nearby or extremely UV-bright objects, or objects in a fairly restricted volume of space, the LUTE will furnish a statistical sample of the UV sources in the universe as a whole. The value of such a sampling in this previously neglected region of the spectrum will be immense, comparable to a celestial census. The worth of the LUTE as a survey instrument will also be considerably enhanced by other complementary missions (e.g., Hubble Space Telescope (HST) and Advanced X-ray Astrophysics Facility (AXAF)). The relative sensitivities of the instruments are entirely appropriate for this use. Interesting objects can be identified from the LUTE sample, then examined in more detail with longer observations by the other instruments.

The wavelength range planned for the LUTE, approximately 1,000 to 3,500 Å, is of great interest to astronomers because of the physical insight it gives into dynamic processes in the universe. Emission at these wavelengths is characteristic of plasmas that are hotter than the surface temperatures of most stars. Although many objects show a bit of UV emission, for something to be really bright in this regime it must usually be dynamic, heated by some sort of energetic process. Examples are flares in the outer atmospheres of relatively cool stars like our own Sun, or accretion disks of matter spiraling into black holes. UV observations allow us to see directly into the heart of many astrophysical phenomena.

The LUTE is planned to be a 1 m f/3 imaging telescope. Operating as a transit telescope, the LUTE will have fixed pointing, allowing the Moon's rotation to move it along a ribbon of sky. Its field of view (FOV) will sweep out a circular swath on the celestial sphere, 1.4° (1° unvignetted) wide, once each month. The choice of power source will determine what fraction of this swath can be observed each month. The use of solar arrays would restrict operation to approximately lunar daytime, i.e., at most, about half of the circle could be observed in any given month. (There are other possible operational constraints which may reduce the observable fractions somewhat more, such as avoiding periods near lunar sunrise and sunset during the lunar summer when direct sunlight might enter the telescope aperture. See section 5.8 for a discussion of these constraints.) The use of a radioisotope thermoelectric generator (RTG) would permit around-the-clock observations (subject to the other possible constraints). The total annual coverage will exceed 300 square degrees, but the number of repeats of any given portion of the swath will be larger with an RTG. Increasing the number of repeats is desirable for all of the science objectives since combining the observations can dramatically increase the signal to noise. Science objectives concerning time varying objects are particularly sensitive to the number of repeats. Figure 3 shows a map of the celestial sphere.[5] The thin curved line represents the plane of the galaxy, and the three labeled points correspond to the north and south galactic poles and the galactic center. The thicker curved lines show two of the many possible survey strips for the LUTE. The upper one of these is the preferred survey. Here, the lunar site and instrument pointing (selenographic declination +30°) have been selected to include the north galactic pole in the observed area. It is desirable to have the swath approach the galactic pole as closely as possible because the dense clouds of dust and gas within our own galaxy

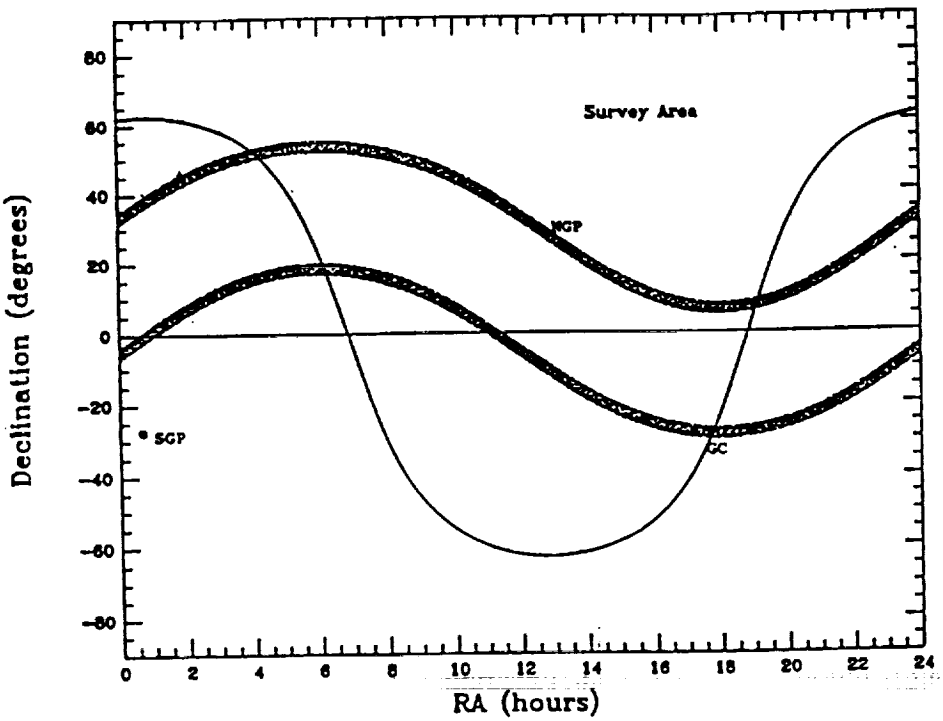

Figure 3. Celestial map.

obscure more distant objects; looking out the pole where our galaxy is thinnest will permit observation of distant targets. This obscuration is not a simple function of galactic latitude; if operational or hardware constraints (section 5.8) preclude pointing directly at the pole, it should still be possible to choose the LUTE orientation so as to include suitable lines of sight out of the galaxy within the swath. The approximate spectral range of the LUTE will be 1,000 to 3,500 Å. This is to be covered in three filter bandpasses, each about 800 Å wide. Resolution of 0.33 arcsecond per pixel is planned. The point source sensitivity at a signal-to-noise ratio of 10 for a B0 star at 1,500 Å is currently estimated to be $V \geq 25$ (after correction for reddening). The planned combination of sensitivity and spatial coverage ensure that the LUTE will sample a statistically significant volume of the universe. Together with the expected spatial and temporal resolution, this will enable the LUTE to contribute substantially to many current scientific investigations. These include (but are not limited to) the following topics:

(1) Extragalactic Astronomy:

Imaging and morphology of distant galaxies: More than 10^6 galaxies will be imaged within the annual strip.

Galaxy evolution: Regions of recent star formation can be identified from the presence of hot young UV-bright stars. Star formation rate as a function of galactic redshift and morphological type can be determined.

Search for gravitational lenses and lensed objects: UV-bright objects such as quasars (QSO's) can be detected at large distances and so are excellent candidates for lensing. The LUTE survey will determine the frequency of occurrence of gravitational lenses. Combining this with the separation of the lensed images gives an estimate of the mass density of the universe.

Search for cosmic strings: Special case of gravitational lenses—cosmic strings have been postulated as "seeds" for the observed structure of the universe. One could search for clusters of identical pairs of galaxies lensed by a continuous string to demonstrate the existence of strings or limit their space density.

Distribution of extragalactic background light: How much of the UV background is diffuse or discrete? Is it all composed of galaxies? Also map windows through "nearby" haze for intensive observation by other missions.

Active galactic nuclei (AGN's) and QSO's: The UV survey will find an entirely new sample of these objects. The statistics of this population are of great interest. Monthly variability may be common, resulting from occultation of the central broad-line region by dark orbiting narrow-line material. The time scales of the variability can be used to determine the size of the regions involved.

(2) Galactic Astronomy

Measure motions of stars/kinematics of the galaxy: Repeated observation of the field will allow derivation of proper motions at the subpixel level. A parallax program for stars at distances of hundreds of parsecs can be initiated.

Discover and monitor interacting binaries: Detailed studies of cataclysmic variables, x-ray binaries, V471 Tauri systems, and binary Wolf-Rayet systems will be possible.

Study of the interstellar medium (ISM): Supernova remnants (SNR's) interact with the ISM as they spread outward, heating and locally enriching it to enhance emission in the UV. Also reflection of other radiation sources by interstellar dust ("reflection nebulae") can be studied.

Discover and monitor variability of chromospherically active stars: Much flare energy goes into UV lines, so the output variations of these stars will appear at high contrast. Monitoring of starspot cycles analogous to the solar magnetic cycle may greatly enhance our understanding of the Sun's own dynamo. This is one area in particular where increasing the number of repeated observations (via an RTG) could greatly enhance the science return.

Production mechanisms for white dwarfs: Stars just cooling to the white dwarf stage are strong UV emitters.

(3) Solar System Astronomy

Distribution of zodiacal dust: This is constantly removed and replenished. Observations of proper motion and parallax can define the circulation patterns.

Very early/late coma on comets and transient coma on asteroids: Water vapor and its dissociation products can be easily detected.

The LUTE science working group (SWG) met during the course of this phase A study (March 18–20, 1993). One topic considered by the SWG was whether the telescope, which had served as the basis for the early phase A, represented the best choice of design parameters or if the scientific return might be enhanced by an alternate design. The early phase A strawman was the same telescope reported here, a 1 m f/3 telescope with detector pixels covering 0.33 arcsecond each. The specific alternative considered, within the constraint of the 1 m size, was a change to a telescope that would be slower (f/9), but

have greater spatial resolution (0.11 arcsecond per pixel). This change would have some advantages. There would be a significant improvement in the ability of the LUTE to accurately measure the positions of objects (astrometry). Other objectives that could benefit from the increased spatial resolution would be the studies of UV-bright stars within other galaxies and the studies of AGN's and QSO's, because of the increased ability to discern the radial distributions of UV sources within these distant targets. However, the group consensus was that more would be lost than gained by such a change. One negative effect of the change would be a reduction in the area covered by the survey by a factor of three. This would adversely affect the statistical value of the sample of all types of objects, but would be especially bad for some of the rarer types, such as SNR's or stars just cooling to the white dwarf stage. So few of these might be found in the smaller survey strip that no general conclusions about the group could be made at all. Furthermore, the studies of diffuse targets, the ISM, SNR's, and the UV background would be severely curtailed by the reduced speed of the instrument. This is because there is a fixed noise per pixel. Spreading the image of a faint extended object over more pixels (to achieve higher spatial resolution) has the unfortunate disadvantage of adding more noise to the image. The conclusion of the SWG was that the strawman parameters were optimal for the 1 m UV telescope.

2.2 Role in Education

In addition to its scientific goals, the LUTE has excellent potential as an educational tool. At the graduate and undergraduate level, research involving the LUTE data base will differ from most astronomical research. Traditionally, astronomers formulate a question, make observations with a (pointing) telescope, then reduce and analyze the data. The LUTE survey data will be archived immediately, with no individual data rights. Data bases of positions and varying intensities of cataloged objects will be formed, allowing research to be done at the level of data access rather than telescope access. A scientist/student can simply formulate a problem and begin accessing data. Problems of many types can be attacked, including statistical analyses of various classes of objects and selection of specific targets, either for intensive analysis of LUTE data itself (e.g., for time variation) or as candidates for follow-on observations at other telescopes. This data base query system is designed to promote "lateral thinking"—the interactive nature of commanding and graphically representing large data sets allows one to investigate interesting phenomena as they appear in the data. This mode of operation opens up discovery space to any user. Knowing that one could make an entirely unanticipated discovery enhances the excitement of working in this way and encourages constant critical thinking. In particular, while the professional astronomer with training in astrophysics, experimentation, and critical thinking has an advantage in discovery, the student being trained in these and other aspects of physical sciences has a real possibility of making exactly the same discovery. At elementary and secondary education levels, the LUTE data will have a different sort of appeal. The complete public access to the data will make it possible for the data to be received by schools in near real time. The excitement of seeing "live" astronomical observations from the Moon should inspire many young scientists and engineers, and be the basis for spinoff lessons in many different fields of physics, engineering, and astronomy.

3.0 PERFORMANCE REQUIREMENTS

A preliminary project requirements document (PRD) has been developed by systems engineering for the LUTE project. Ordinarily, project management would not initiate the development of a PRD so soon, but according to NWODB, it is both prudent and cost-effective to begin generating such a document, even as early as phase A. With that in mind, a comprehensive list of science and design requirements was compiled for the LUTE project. This preliminary PRD serves not only as a holding tank and tracking device for derived system requirements, but also as a head start on an effort that would likely be much more time- and cost-intensive if it were delayed until later in the program. These requirements are written in a format that will lend itself to the development of an official document in the future. Accordingly, these requirements have been organized using the prescribed format of the generic systems requirements specification document, and even though the PRD is far from complete, it is fully capable of evolving into a baseline document as the LUTE project enters new phases. These requirements, though preliminary, helped to accelerate LUTE development by providing a clear requirements status to the LUTE technical discipline leads early in the project. Requirements regarding science, materials, mechanisms, optics, thermal control, structures, dynamics, power, command and data management, software, weight and center of gravity (CG), mission analysis, and mission environments have been included in the document and provide a reference point not only to the present development team but also to any new team members. The PRD has been through several informal reviews to date and will continue to be reviewed and updated as necessary.

3.1 Requirements Summary

The systems integration team joined the LUTE phase A Task Team in October 1992, and began by generating a preliminary set of level II LUTE systems requirements. These requirements were transformed into a level II systems requirements document (SRD) according to NASA and MSFC generic systems requirements documentation standards. This initial document included science, design, mission, operations, and performance requirements which were derived from the overall LUTE scientific goals. Consistent with the LUTE level I SRD, the level II SRD serves as the basis for lower level requirements and also drives the development of support plans, interface documentation, specifications, and drawings to be compiled in later phases of the program.

3.2 Level I Requirements

The level I SRD was prepared by the Task Team, but has not been baselined by NASA Headquarters. A copy of this document is included in appendix B.

3.3 Level II Telescope Requirements Summary

The level I mission requirements of the LUTE (section 3.1) drive the telescope requirements at level II and specify what kind of data are needed from a lunar-based UV telescope. The level II requirements are derived from them and specify the parameters that will keep the LUTE within the bounds set at the highest level. For example, the requirements in section 3.1 indicate what kind of data are desired from the LUTE, and the level II requirements define the lunar site selection criteria and landing orientation that will be conducive to obtaining that data. The system has been divided into two major elements: the telescope and the lander that delivers it to the lunar surface. Together, these two major elements are called the integrated payload and, for the sake of simplicity, they are treated separately at level II. This method will allow the development of the two separate elements to proceed independent of each other

even though they perform as a connected unit for nearly all functional, mechanical, and operational purposes. The level II requirements, which drive the telescope design, are addressed in this section. The level II telescope and lander systems requirements are included in appendices C and D.

4.0 LUTE REFERENCE DESIGN CONCEPT

The following sections describe the reference design concept to date. The design is derived from requirements described in the previous sections, and supported by trade study results in the individual subsystems areas. The trade studies, as described in detail in section 5.0, provided conclusions that were incorporated into the following reference design. The configuration was generated using an integrated design and engineering analysis software tool. The software consists of both solid modeling generation and structural/thermal analysis tools. The software integrates these tools into one package with a common interface and a shared application data base. Geometric concepts and designs developed in the solid modeling package were utilized by the structures and thermal analysis groups to aid in building their finite element models. This integrated approach maintained a consistent configuration across engineering disciplines and was used extensively during the phase A analytical process.

4.1 System Description

The configuration design effort was directed toward a LUTE concept that would be compatible with requirements imposed by the launch vehicle, lander, and overall performance of a lunar based telescope. A reference concept was established after analysis and trade studies were conducted, examining both physical and performance characteristics of each subsystem. A landing site of 66.5° north latitude and 24.2° west longitude was selected to meet a number of site selection constraints and after numerical thermal analyses had been done for 65° latitude. Some of the results described in section 5 refer to 40° north latitude because initial studies were based on this latitude. An overall description of the LUTE reference design concept will be given in this section.

4.1.1 Objectives and Requirements for the LUTE Reference Design

In developing the reference LUTE design to meet the scientific objectives outlined in section 3, goals were established to minimize the need for active thermal control and minimize weight. The LUTE optical design was developed by D. Korsch. This compact design lent itself to the limited volume of the Atlas II 3.3 m diameter payload fairing, which also houses the lander. Additional design requirements were derived from the launch vehicle, accommodation of the optical design, optimum science return, the lunar environment, the continuous operation of the telescope, structural efficiency, and thermal designs. During the initial phase of the design activity, the LUTE payload was baselined to use the Artemis common lunar lander. The Artemis concept, a generic lander to be launched on a Delta II vehicle, was proposed by Johnson Space Center (JSC) as a cost-effective approach to delivering various payloads to the lunar surface. After extensive study, it was determined that the Delta/Artemis vehicle was both performance- and volume-limited for the LUTE payload (see appendix E.) Therefore, a generic lander was sized for use on an Atlas II launch vehicle. The lander provides a structural interface (identical to Artemis) and a power interface for the RTG.

The harsh lunar environment created thermal control problems. It was desired to maximize the operation time of the telescope throughout the day/night cycle. The radiators needed to have an unobstructed view to deep space and also be located in close proximity to the heat source. Doing so would maximize heat transfer and minimize weight. The detector, located in the plane of the secondary mirror, required a cold environment. Lunar surface radiation impinging on the upper interior surface of the light shade tended to heat the detector and the mirrors, causing nonuniform temperature gradients. One solution involved the use of solar baffles, another changing the site latitude, and the third was a combination of the two. The omnidirectional and high-gain antenna, on the other hand, needed to be mounted near the periphery of the telescope to preclude any view obscuration or obstruction. The lander could not guarantee a specific landed attitude or orientation; therefore, the LUTE was required to provide roll and

tilt capability to align the electronics box, high-gain antenna, and focal plane detector. This would be accomplished automatically by a signal to the low-gain antenna to start the telescope activation. The reference configuration, as shown in figure 4, was strongly influenced by these considerations.

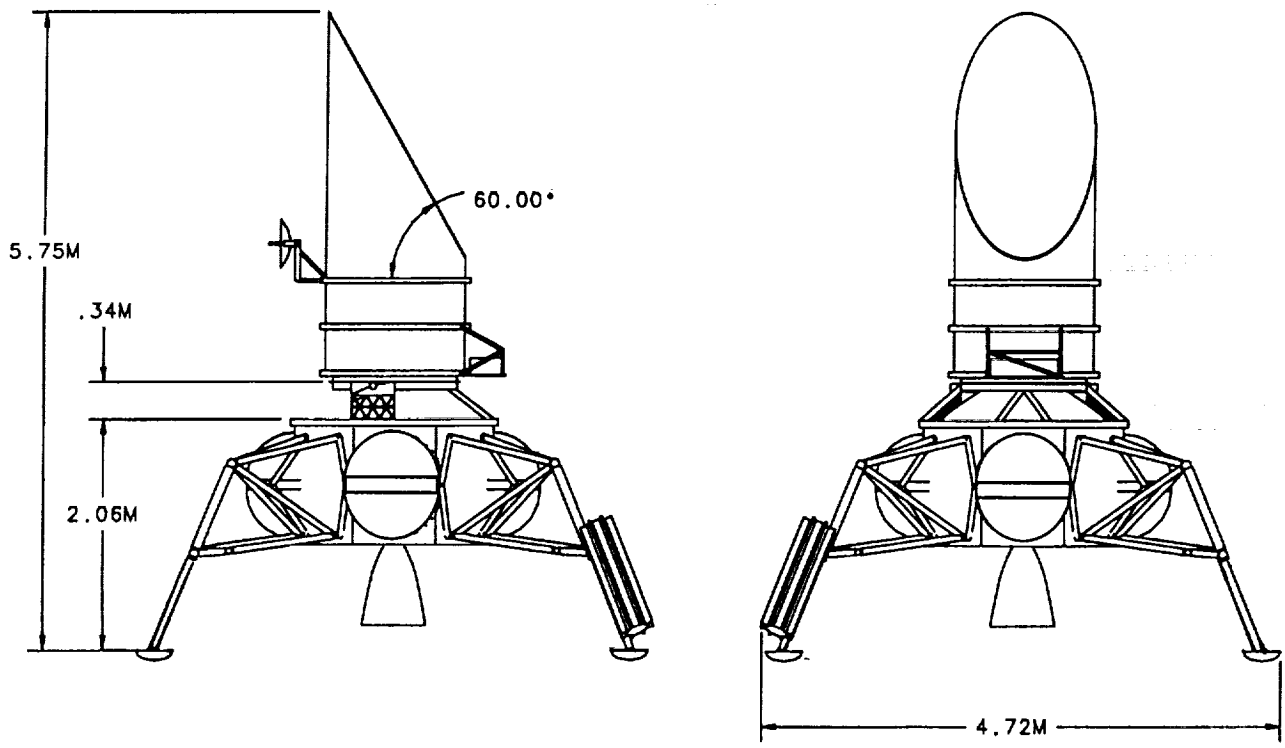

Figure 4. LUTE reference configuration.

4.1.2 Primary Interfaces

The following two sections will cover the LUTE primary interfaces: the launch vehicle and the lander.

4.1.2.1 Launch Vehicle

The LUTE/lander payload is designed to be launched on an Atlas II vehicle utilizing a Centaur third stage. The 3.3 m external diameter payload fairing, with a 2.9 m diameter dynamic envelope, determines the maximum outer dimensions of the LUTE/lander payload. The Atlas II User's Mission Planning Guide is the reference used in determining the dynamic envelope, as shown in figure 5. It is assumed that space vehicle primary structure first lateral modes are above 10 Hz and first axial modes are above 15 Hz. These envelopes include allowances for payload fairing static and dynamic deflections, manufacturing tolerance, out-of-round conditions, and misalignments. Additional information on the capabilities of the Atlas II will also be found in the guide.

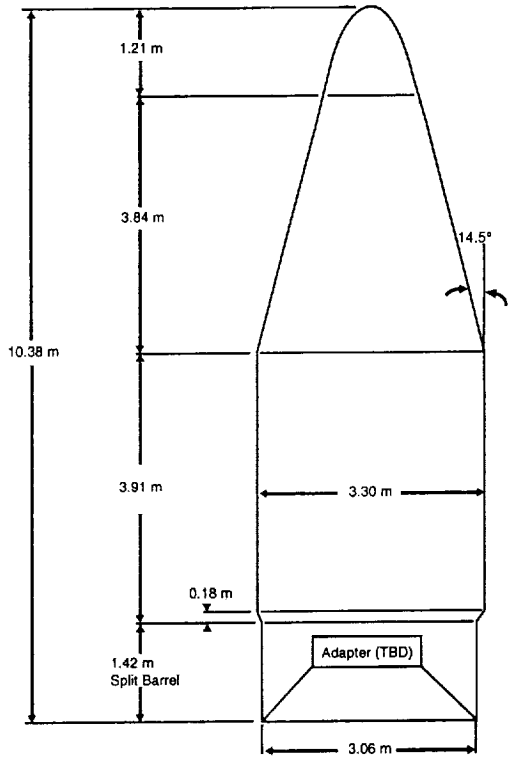

Figure 5. Atlas-II 3.3 m payload envelope.

4.1.2.2 Generic Lander

A study was performed to determine the physical size of a lander required to accommodate the LUTE. A four-tank lander configuration, with a single 4,000 N Marquardt gimbaled engine, was assumed. Using a total propellant load of 1,650 kg of nitrogen tetroxide/monomethylhydrazine, each tank would have volumetric requirements of 0.39 m^3. The spherical domed tanks were located 90° apart on a 1.82 m diameter circle. The body of the lander is an octagonal structure with the four legs located between the tanks. An RTG is attached to one of the lander legs. The overall stowed diameter of the lander stage is 2.70 m, with an overall length of 1.78 m. The lander provides 12 hardpoints, to be used only for payload attachment. Six hardpoints are located on a 1.82 m diameter circle and the remaining six are located on a 0.76 m diameter circle, as shown in figure 6.

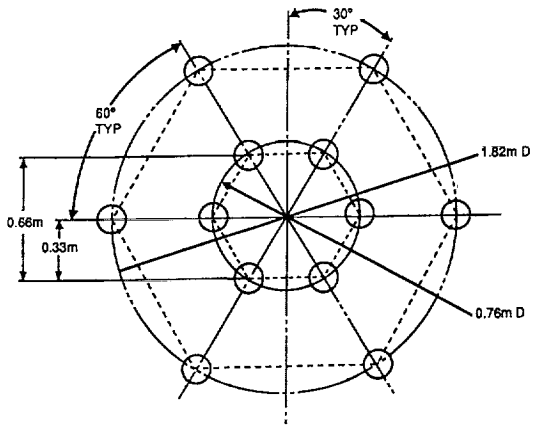

Figure 6. Lander/payload interface hardpoints.

4.1.3 Major LUTE Systems/Elements

The hardware tree, shown in figure 7, contains a first- and second-order subassembly breakdown of the LUTE payload. Some of the elements are common to more than one system. Further subassembly breakdown is provided in appendix F. The following sections define functional requirements and design concepts for the major LUTE assemblies. Additional analysis and trade studies will be conducted to determine the best ways of implementing design requirements.

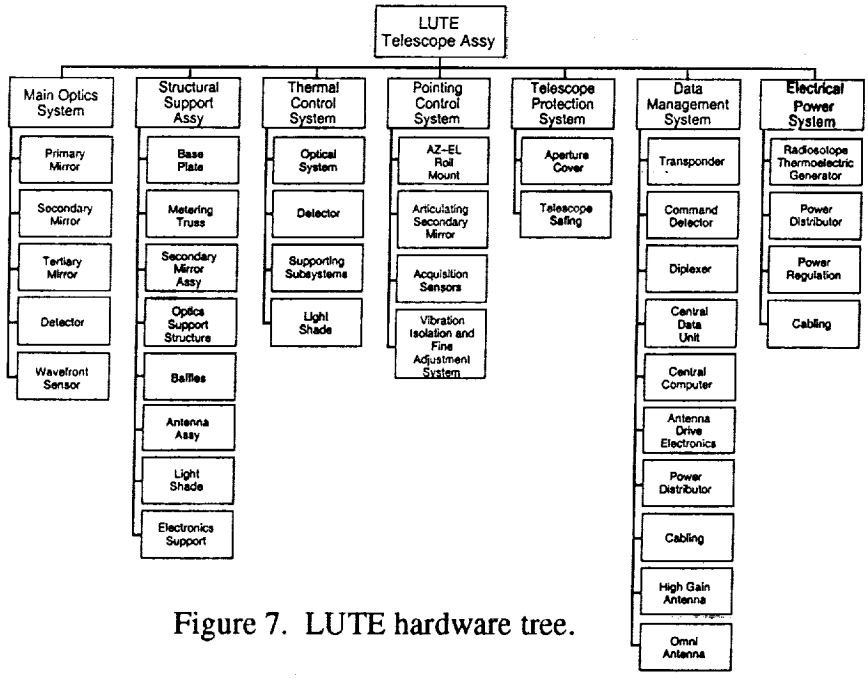

Figure 7. LUTE hardware tree.

4.1.3.1 Optics

The selected three-mirror system is shown in figure 8. The primary mirror diameter is 1 m with a 0.5 m central hole. The secondary mirror is 0.38 m in diameter with a 0.15 m central hole. The tertiary mirror is 0.28 m in diameter and located in the same plane as the primary mirror. The focal plane detector is located in the same plane as the secondary mirror. The separation distance between the primary/tertiary and secondary mirror is 0.65 m.

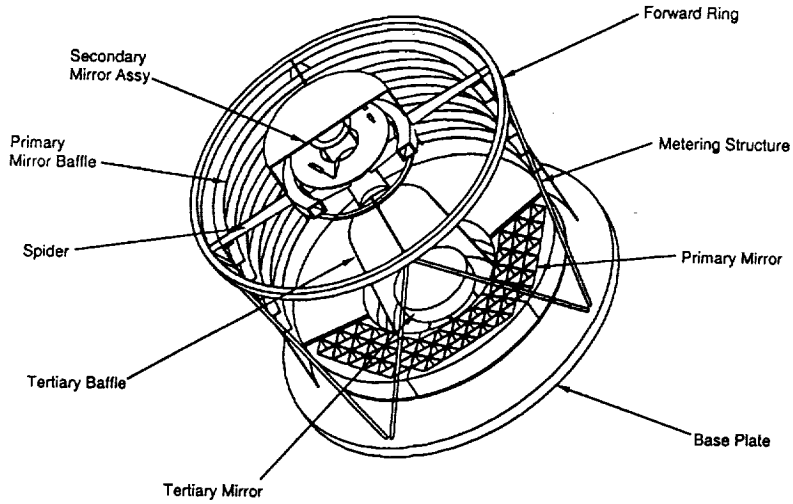

Figure 8. Optical bench assembly.

4.1.3.2 Optical Bench Assembly

The primary function of the optical bench assembly is to hold the relative alignment of the optics and detector within an allowable tolerance. This is accomplished by using thermally stable materials, isolating the structure from the changing environment, and providing an articulating secondary mirror. The spacing and attitude of the secondary mirror relative to the primary can be adjusted to compensate for thermally induced motions. The design goal of minimizing thermal growth was incorporated to limit the frequency and degree of adjustments. The major structural elements of the optical bench assembly are mirrors, focal plane detector, light baffles, metering structure, and base plate support.

4.1.3.3 Baffles

The function of the baffles is to attenuate any stray light entering the optical bench assembly. Baffle geometry is also specified by the optical design. The envelope dimensions of the optical bench and relative locations of the baffles are shown in figure 9.

Main Baffle—The main baffle is a cylindrical shell with open ends having internal rings and external longerons. The shell has an outside diameter of 1.08 m and overall length of 0.82 m. The aft end of the shell is attached to the baseplate.

Internal Baffles—Truncated conical baffles enclose the secondary mirror, tertiary mirror, and the focal plane detector. The secondary mirror baffle is attached to the hub ring supporting the secondary mirror assembly. The tertiary mirror baffle is attached to the baseplate. The detector baffle is integrated into the support structure for the detector.

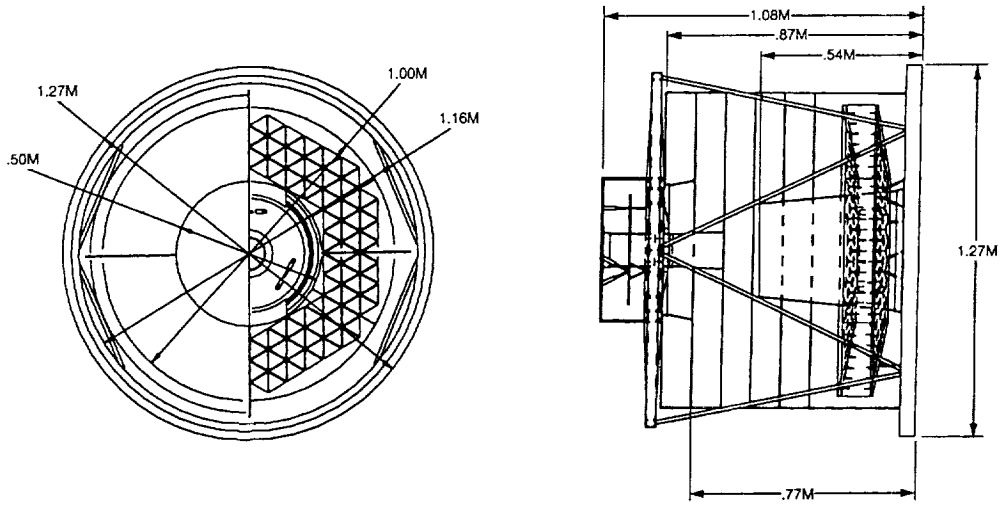

Figure 9. Optical bench envelope dimensions.

4.1.3.4 Metering Structure

The key function of the metering truss is to provide a stable support for the optics and focal plane assembly. A single bay truss, with eight struts, spans between the base plate and the forward metering ring. The truss assembly interfaces with the secondary mirror support spider. The truss length is 0.83 m, with a diameter of 1.19 m. An alternate metering structure considered is a cylindrical shell structure that also supports the secondary mirror via the spider assembly. The construction would be a closed shell consisting of longitudinal stringers and formed rings.

Spider—The reference design has the secondary mirror and focal plane assembly nested inside a circular ring frame. Beams extend radially from this ring to the metering structure where all four are rigidly connected. The four beams are arranged in a cruciform structure.

4.1.3.5 Baseplate

The baseplate is the central structural element of the LUTE payload. It serves as the integrating structure for the optical bench assembly, pointing system, and light shade. The metering truss, attached to the forward side of the plate, supports the secondary mirror assembly. The primary and tertiary mirrors are supported by the baseplate through flexure mounts. The aft end of the light shade and tertiary mirror baffle are cantilevered from the plate. A motor and bearing assembly mounted on the aft side of the baseplate provides ±180° rotation of the LUTE about the optical axis for initial orientation after landing.

4.1.3.6 Power System

The power system generates, regulates, and distributes the electrical energy output from the RTG to the lander during its operational phase and then, after landing, to the LUTE. The power is distributed to the electromechanical devices and avionics subsystems which perform the various spacecraft functions.

When activated, the RTG produces power continuously, therefore, cooling provisions will be required in the Atlas II fairing. Figure 10 shows the LUTE/lander stowed in the Atlas II fairing. The RTG is located on one of the lander legs to maximize its distance from the optical assembly during LUTE operation. The RTG requires a thermal isolator which is included in the phase A design concept.

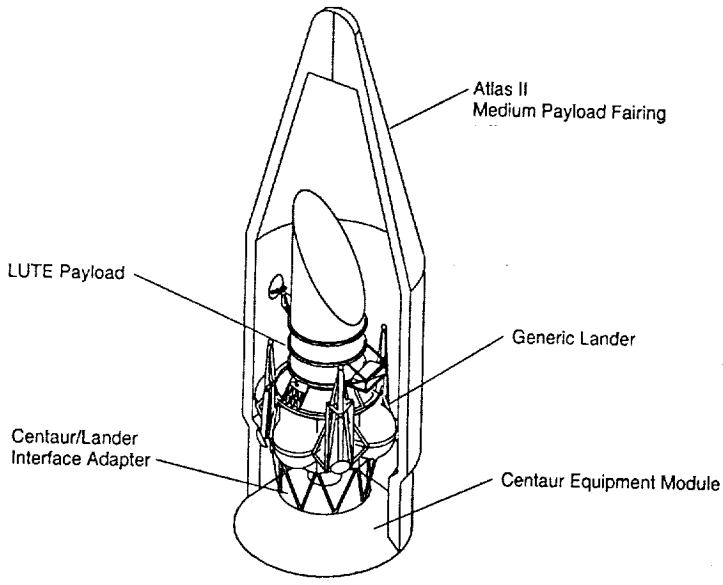

Figure 10. Launch configuration.

4.1.3.7 Communications and Data Handling (C&DH)

The reference design C&DH system includes all the equipment required to manage the flow of data to and from the LUTE and lander. This includes the receipt, processing, and execution of commands; the storage and transmission of information from LUTE systems; and the routing of scientific

data and subsequent transmission to the ground. The LUTE configuration was required to accommodate the placement of a high-gain antenna, four omnidirectional antennae, and a standard complement of C&DH components as defined in section 4.2.6.

High-Gain Antenna Assembly—The high-gain antenna dish is 0.46 m in diameter. The antenna utilizes a double axis gimbal system to acquire and track Earth. Due to limitations in the lander design, a specific attitude and orientation of the LUTE could not be assured. Therefore, the LUTE will provide some means of initial alignment. This is accomplished by mounting the antenna assembly on a mast. The mast is structurally attached to the light shade external ring frames.

Omnidirectional Antennae—Omni-antennae will be used for initial acquisition of LUTE. It is anticipated that four omnidirectional antennae will be needed to ensure adequate pattern coverage. This is necessary due to the uncertainty of landing orientation and the potential obscuration of the Earth from the light shade. The exact location of the omni-antenna is subject to further analysis; however, it is expected that they will be equally spaced around the lander periphery.

Integrated Electronics Box—A major assumption in the study was the use of an integrated electronics box. It was decided that a single box containing the power, C&DH, and sensor electronics would be easier to accommodate than numerous individual components. Also, many of the existing off-the-shelf electronic components would have to be requalified or redesigned to sustain the harsh lunar environment. The box, with dimensions of 0.3 by 0.6 by 0.15 m, is located on the north side of the telescope. The electronics box is attached to a strut supported shelf, as shown in figure 11.

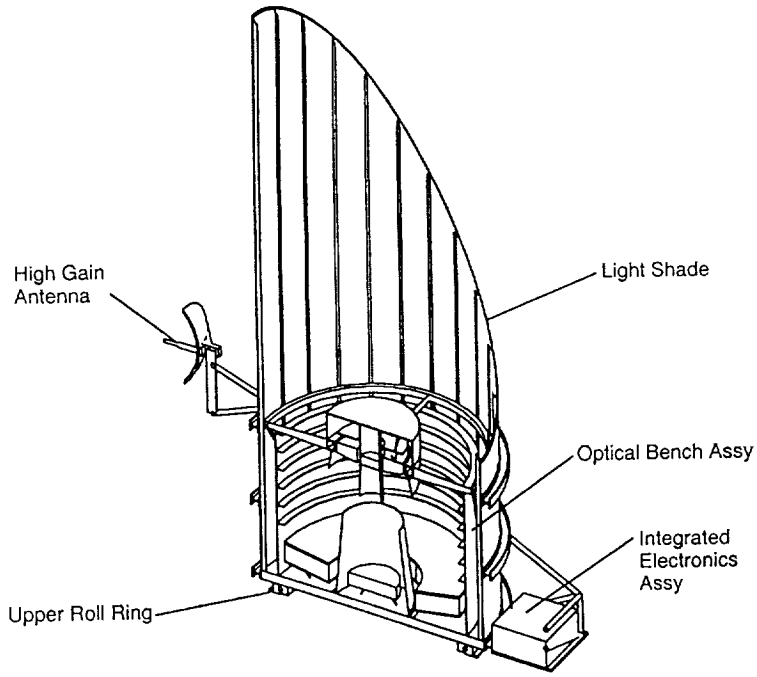

Figure 11. C&DH equipment locations.

The need to be located on the anti-Sun side of the telescope during lunar operation was dictated by thermal control requirements of unobstructed view to space. The upper surface of the box served as the radiator. Thermally activated louvers were included in the design of the radiator. Louvers are an active element that have been used in different forms on numerous spacecraft. They can provide variable

heat rejection from fully closed to fully open without any power consumption. A bimetallic spring actuated rectangular blade (venetian blind) type was selected for the phase A concept.

It was assumed that the volume of the integrated electronics box would be equal to the summation of the volumes of the individual components. This assumption will be refined in phase B.

4.1.3.8 Mechanisms

LUTE cannot be launched in its operational configuration because of shroud envelope limitations. To function, the LUTE must be placed in an operational configuration which includes articulation to align the telescope to the proper declination. It may also be necessary to make fine pointing adjustments to keep the payload functioning properly over its expected 2 year life. The mechanisms required include those found on the telescope pointing system, aperture cover, high-gain antenna, and electronics box thermal louvers. The telescope pointing system mechanism is discussed in detail in the guidance, navigation, and control section along with its operational function. The high-gain antenna and electronics box thermal louver discussions are found in the C&DH section of the document. It is understood that each time a mechanism is required to deploy or orient a device, a failure mode is created. Therefore, a primary goal in the phase A was to minimize the number of mechanisms. This approach should be retained in subsequent phases of the project.

4.1.3.9 Telescope Protection System

Aperture Cover—An aperture cover is required for protection of the optical system from contamination entering the telescope tube. This could occur any time during shipping, launch, in transit to the Moon, or after landing on the lunar surface. For this study, it was assumed that the hinge and latch mechanisms are required to operate only once and are single fault tolerant. Various design options were assessed (see appendix G). The detailed design of the deployment mechanisms would depend on how the cover is to be opened. Also important is the interface between the cover and the telescope tube. The presence of an O-ring seal could change or eliminate several of the methods for opening the cover. Redundancy requirements and the need for multioperation mechanisms can also be major design drivers. A hinged aperture cover provides not only a pivot point for the door, but also a good location to apply the torque required for opening the door. Motor-driven hinges which feature high redundancy/reliability would be suited for applications requiring repeated operation. They require thermal control and more complex electronics than "one shot" schemes. The simplest concept for opening the aperture cover would be a hinge with the required torque applied by a torsional spring, as shown in figure 12. This type of configuration has flown in the past as a solar array deployment mechanism. The design is currently being developed for AXAF-S. With proper design and materials selection, a similar design could be adopted for the LUTE application.

If a passive spring hinge system is used, some method of controlling rate and/or stopping may be required. This will help minimize disturbance of any dust that settles on the cover during landing and prevent damage to the barrel section or other telescope parts. Candidate mechanism that limit rate include torsional springs which oppose the motion, viscous dampers, friction brake, magnetic brake, or eddy current damper. These are essentially passive devices that require no control other than initial setup. Eddy current dampers have been used for many spacecraft and are to be used for AXAF-S. The mechanism may need to be thermally conditioned to stay within its qualification range. A latching system will also be required for the aperture cover. These latches will serve as launch locks and allow opening of the door on command. If repeatability is required, a motor-driven latch system is preferred. Appendix H shows a high redundancy motor-driven latch used on the HST. This type of system would also require complex electronic and thermal control. For a "one shot" system, pyrotechnics provide an

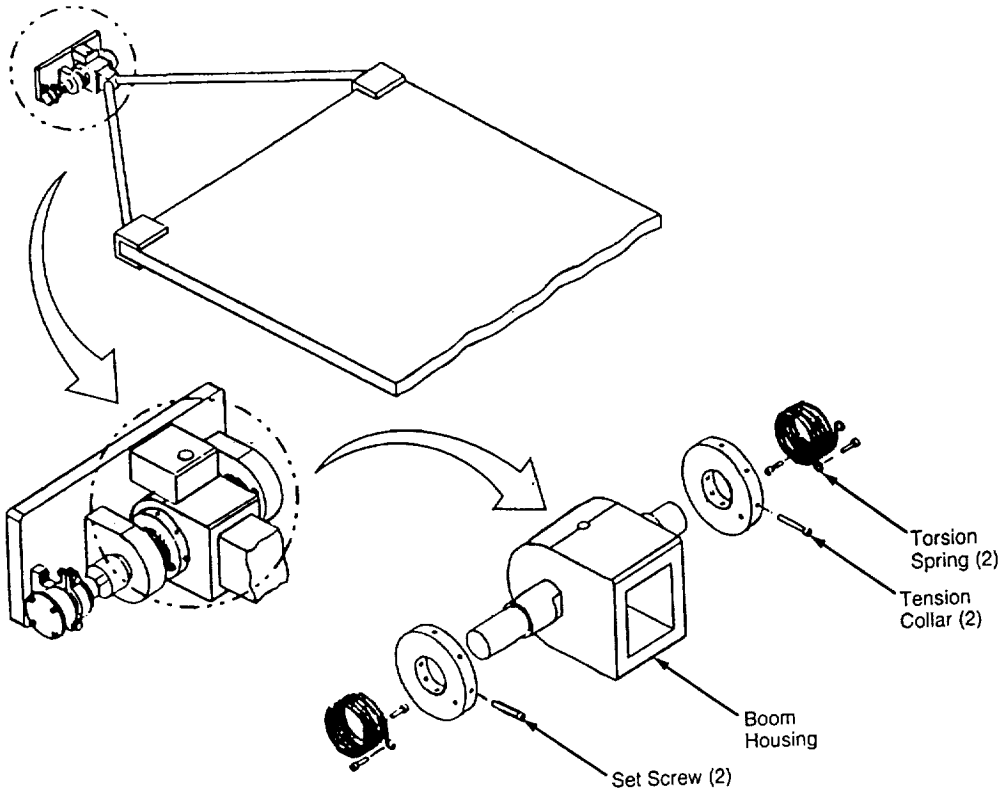

Figure 12. Deployment mechanisms.

attractive system. Small pyrotechnic devices, such as guillotines, pin pullers, and nut separators, produce very little shock and contain the gases from firing. Proper isolation can help attenuate the shock they produce. Pyrotechnic latch systems have been used on many spacecraft and are to be used for AXAF-S and most likely on AXAF-I. They are also relatively inexpensive, have built-in redundancy, and are well proven. Paraffin devices were also investigated for latch design. Some of the same methods used for pyrotechnic latch design (nut separator and pin puller) could also be used with a paraffin actuator. A resettable nut separator qualified for space applications, and resettable paraffin operated latches are available. These latch designs offer a very simple system with much lower shock loads than pyrotechnics. The main disadvantage of paraffin actuators is that temperature is the triggering device. Paraffin devices would have to be thermally isolated or the high lunar temperatures would prematurely activate them. For this reason, paraffin technology is not recommended for LUTE. Another possible method of a latching/release system for the door would be thermal knives. The thermal knife system is more expensive than pyrotechnics, but would produce less shock to the spacecraft. Additional information on eddy current dampers, pyrotechnic devices, paraffin actuators, and thermal knives is given in appendix H. In summary, the following configuration is recommended for the LUTE aperture cover:

Drive	– torsional spring located at hinge line
Rate Control	– eddy current damper
Latches	– pyrotechnic nut separator.

Configuration of the LUTE aperture cover, required redundancy, repeatability requirements, method of opening the door, acceptable levels of shock, available power, and thermal control will be considered in phase B.

Light Shade—The light shade is designed to keep direct sunlight from entering the telescope tube and impinging on the optical bench assembly. The light shade is an open-ended circular shell with a diameter of 1.27 m and an overall length of 3.35 m. The forward end is sliced at a 60° angle with

respect to the horizontal. However, the angle of the slice is dependent on the viewing declination selected. The shape is maintained with ring frames and longerons. The ring frames are external in the region surrounding the optical bench assembly and internal elsewhere. The internal ring frames also serve as baffles. The 24 longerons are located internal to the light shade and are equally spaced around the circumference.

4.1.3.10 Reference Design Configuration Summary

The configuration effort concentrated on striking a balance between the diverse requirements and evolving a concept that would be feasible and ultimately could be developed. The primary considerations for the optimized design included limiting the weight of the LUTE, ensuring compatibility with the lander, fitting within the Atlas-II launch vehicle fairing, satisfying the thermal control requirements, and maintaining a high reliability while minimizing the complexity of the overall design. This optimized design, shown in figure 13, would change as the design requirements change. Studies performed by JSC indicate that the Delta-II launch vehicle, originally assumed for the lift-off to translunar injection, did not have adequate performance to carry the launch weight of the Artemis/LUTE combination. Once the Artemis took its share of the 2.9 m diameter Delta fairing, the volume left for the LUTE was marginally adequate. Therefore, it was decided to utilize the Atlas-II launch vehicle. The additional performance allowed the use of an RTG, giving virtually continuous operational capability. In addition, a dedicated lander allowed the sharing of some common subsystems, eliminating duplication inherent in the approach pursued previously. There also exists the possibility of a more efficient structural arrangement. These changes, intuitively, would reduce the total mass that the launch vehicle would have to carry to orbit.

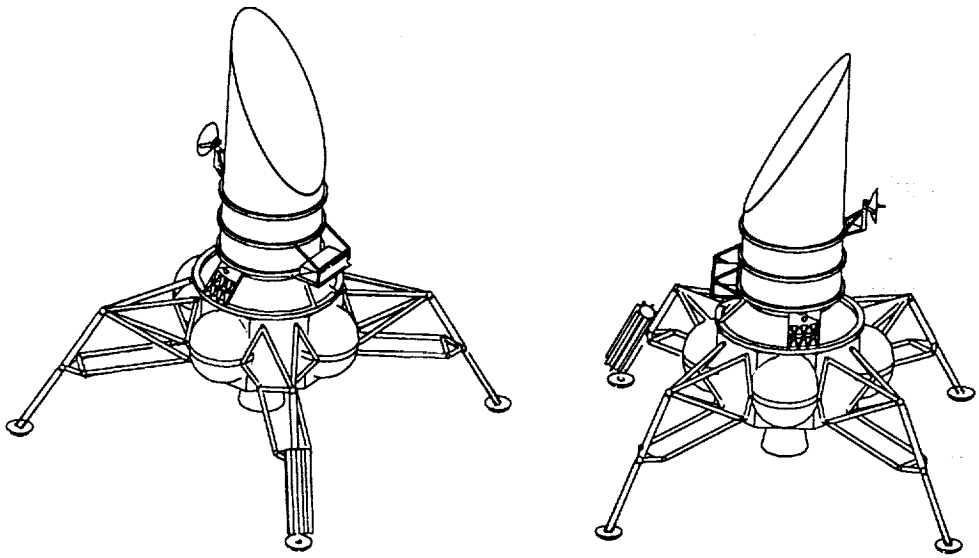

Figure 13. LUTE configuration.

4.2 Subsystems Design

4.2.1 Optical Configuration

The optical design of the LUTE was primarily driven by the requirement for a wide field-of-view, which requires a three- or four-mirror telescope. A three-mirror system (fig. 14) was selected because an additional reflection resulting from a fourth mirror would further reduce the throughput of the telescope. Also, the location of the focal plane in front of the telescope, a result of the three-mirror

configuration, is advantageous. While in most practical systems the focal plane is located behind the primary, the location of the focal plane in front of the telescope has the added advantage of facilitating the required radiative cooling of the detector array. The current optical design is a compact 1 m aperture, three-mirror telescope with a field-of-view of 1.4° and a system focal length of 300 cm. The image diameter is 7.4 cm. The back focal distance, i.e., length of the optical train between the tertiary and secondary mirrors, is 65 cm. A more detailed discussion of the optical design and the trade studies involved in the design of the optics is given in section 5.1.

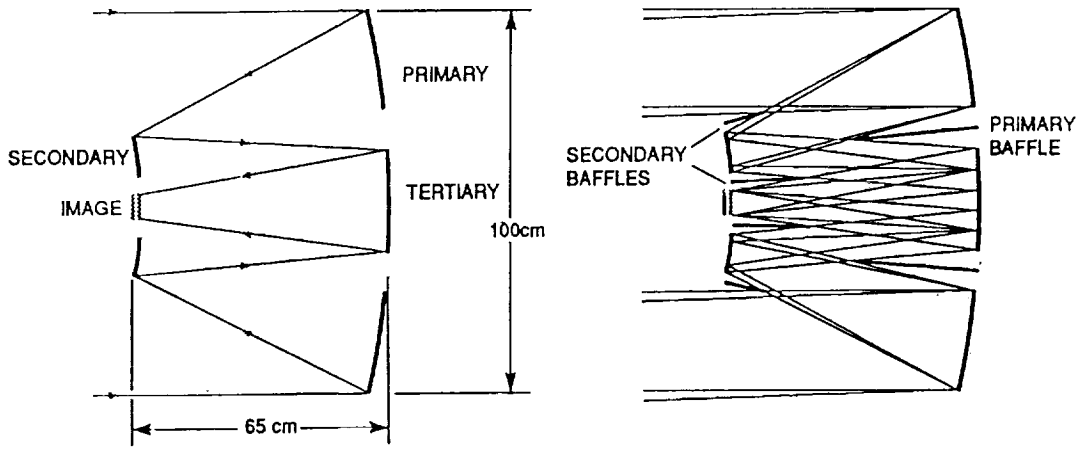

Figure 14. Optical layout.

4.2.2 Focal Plane Instrument

The focal plane instrument for the LUTE consists of an array of charge-coupled device (CCD) detectors operated in a time delay and integration (TDI) mode, wherein the charge image is clocked from column-to-column across the CCD's at just the proper rate to remain synchronized with the optical image (see section 5, fig. 47). This approach improves the faint-object sensitivity of the instrument and at the same time eliminates the need for mechanically driving the telescope assembly to compensate for the apparent motion of the stars and other celestial objects across the lunar sky. The focal plane instrument, as currently envisioned, covers the UV portion of the spectrum from approximately 1,000 to 3,500 Å in three bands of approximately 800 Å each. There are two image sensors for each bandpass. These sensors are physically separated on the focal plane. This layout of sensors allows measurement of short-term variability of stellar objects. In addition to the UV detectors, visible band (optical) detectors are situated at the edges of the usable image area. These detectors are useful for assessing the overall performance of the optical system and assist in the alignment of the telescope. A more detailed description of the focal plane instrument and component elements is provided in section 5.2.

4.2.3 Baseline Structural Design

The following sections describe the individual structural components in the baseline LUTE design. The structural trades and analyses supporting their design will be discussed in section 5.3 of this report.

Methodology—The structural components were analyzed with a combination of hand calculations,[6] spreadsheet analyses, and finite element (FE) analyses with the I-DEAS™ finite element modeling (FEM) and model solution software codes. After each component was analyzed and a baseline

design chosen, an integrated I-DEAS™ model of the structural components was assembled, primarily to calculate natural frequencies for the combined structure. This section discusses the LUTE structural requirements, mass estimate, primary mirror, mirror support structure, metering structure, optical baffles, light shade, aperture cover, electronics box support structure, and baseplate. Stress and natural frequency results for the integrated LUTE FE model are presented.

Results—Individual detailed component analyses and trade studies were completed and are documented in section 5.3. Thermal deformations for the SiC optics were calculated and found to be acceptable by optical analyses. In addition, the LUTE components were analyzed as an integrated whole structural system. Natural frequencies for the combined structure meet Atlas IIAS requirements, and computed launch stresses are safe from material failure. The mass estimate for the structural system is 122 kg. These analyses show that the structural system for LUTE is adequate and safe.

4.2.3.1 Requirements

To identify the requirements affecting the structural system, a functional analysis for the LUTE structures was performed. Derived requirements are summarized in table 2.

Table 2. Functional analysis for structures.[7–11]

Functions	Requirements
• Minimize mass	Structural mass requirement not given
• Survive launch loads and vibrations	Launch vehicle = assumed Atlas IIAS • Frequency: 1st lateral mode > 10 Hz, 1st axial mode > 15 Hz. • Max LF ≈ 6.0 g's axial at BECO, 2.0 g's lateral at BECO/BPJ. • System random LF's ≈ 2.1 g's axial, 2.0 g's lat. • Component-level random load criteria = TBD.
• Survive lander loads and vibrations	Lander = assumed Artemis • Interface at 2 hex. frames with 6 hardpoints each. • Landing loads < launch vehicle loads. • Frequency constraints = TBD. • Random vibration loads criteria = TBD.
• Operate in lunar environment	• Surface ΔT = 93 to 395 K. • Optics ΔT = 65 to 265 K. • Minimum operating life requirement = 2 years. • Contamination requirements = TBD.
• Minimize disturbances to optics: – Maintain dimensional stability – Reduce thermal paths – Minimize light blockage	Mirror surface figure (requirements w/o actuators) • Vertical peak-to-valley deformation ≤ TBD microns. • Curvature deformation ≤ TBD μ radians. (Deformations supplied to Optics for acceptance)
• Assure adequate strength and safety	• General safety factor = 1.4. • Safety factor for glass analysis = 3.0.

The structural design of the LUTE was primarily driven by two objectives. The first was to minimize degradation of the LUTE optical performance due to thermal deformations. The second objective was to minimize structural mass.

4.2.3.2 Structural Mass Estimate

A summary of the structural mass estimate for the baseline LUTE preliminary design appears in table 3.

Table 3. Structural mass estimate for baseline design.

Component	Material	Mass (kg)
Mirror Support Structure		
Flexures		
– Primary	Graphite/Epoxy	1
– Secondary	Graphite/Epoxy	1
– Tertiary	Graphite/Epoxy	1
Launch Locks	TBD	TBD
Metering Structure	Graphite/Epoxy	
– Truss rods		11
– Spider		9
– Secondary mirror housing		1
Optical Baffles	Al 2219	
– Primary baffle		12
– Secondary baffle		0.5
– Tertiary baffle		1
– Science instrument		0.2
Light shade	Al 2219	
– Skin		11
– Support frames		12
– Skin stringers		14
Miscellaneous		
– Power system attachment	TBD	TBD
– Electronic box support	Al 2219	8
– Aperture cover	Aluminum	15
Telescope Baseplate	Graphite/Epoxy	24
Total		122

4.2.3.3 Primary Mirror

The LUTE primary mirror has an outside diameter of 100 cm and an inside diameter of 50 cm. The internal mirror construction, as pictured in figure 15, consists of two faceplates, 3 mm thick, separated by a 6 cm thick core of triangular cells. Each cell of the sandwich core is an equilateral triangle with sides that are 5 cm in length and 1 mm thick. The mirror also has a 2 mm thick hatband around the outer circumference. It is anticipated that the secondary and tertiary mirrors will have similar construction schemes, albeit with different geometric dimensions.

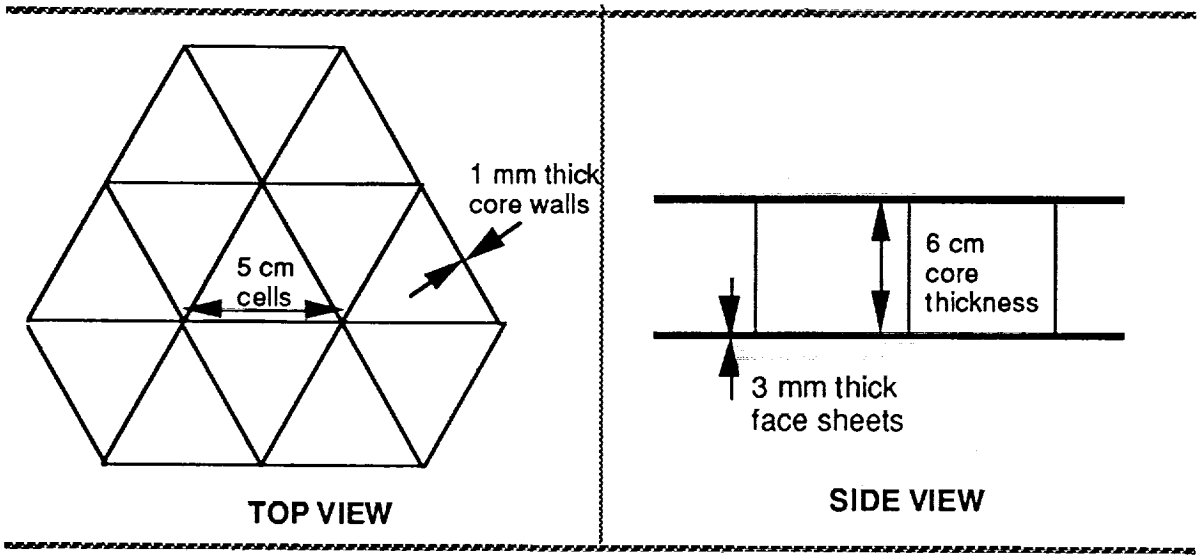

Figure 15. Primary mirror internal construction.

Mirror Material—Thermal deformations for three primary mirror candidates were analyzed with I-DEAS™ 6.1 and are described in detail in section 5.3.4.3, with the mirror material trade study. From that trade, SiC was selected as the baseline mirror material. Optical studies and trades also favored SiC as the mirror material choice.

4.2.3.4 Mirror Support Structures

Structural supports for the primary and tertiary mirrors connect these mirrors to the baseplate. These supports must minimize stress and deformations in the mirrors during operation, by allowing the mirrors to expand and contract in the thermal environment. A statically determinant support with three bottom-mounted flexures, pictured in figure 16 and discussed in section 5.3.4.2, has been chosen as the reference design for the primary, secondary, and tertiary mirrors.

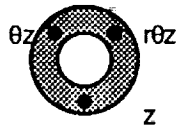

at 41.67-cm radially in Finite Element model

	θ = 30°	θ = 150°	θ = 270°
Restrained d.o.f.	rθz	θz	z

Figure 16. Baseline primary mirror support.

The three bottom-mounted support flexures were radially located at the neutral surfaces of the three mirrors. The primary mirror's neutral surface is at a radial location of 39.5 cm. Figure 16 shows supports at 41.67 cm in the FE mesh because this was the closest nodal location to 39.5 cm. The tertiary mirror's neutral surface is at 9.9 cm radially, and the secondary mirror's neutral surface is at 14.4 cm radially.

4.2.3.5 Metering Structure

The metering structure supports the secondary mirror and the science instrument. Its primary structural function is to maintain the focal distance from the primary and tertiary mirrors to the secondary mirror and science instrument. The structure must have extremely small deflections and low thermal expansion for dimensional stability during the lunar thermal cycle. Another objective is to minimize heat transfer to the secondary mirror and science instrument by selecting materials with low thermal conductivity and by reducing the number of heat conduction paths. Light blockage must also be minimized so that the FOV of the primary and tertiary mirrors is not obscured. A picture of the metering structure finite element model is shown in figure 17. The configuration is based on the design of the HST's metering truss.

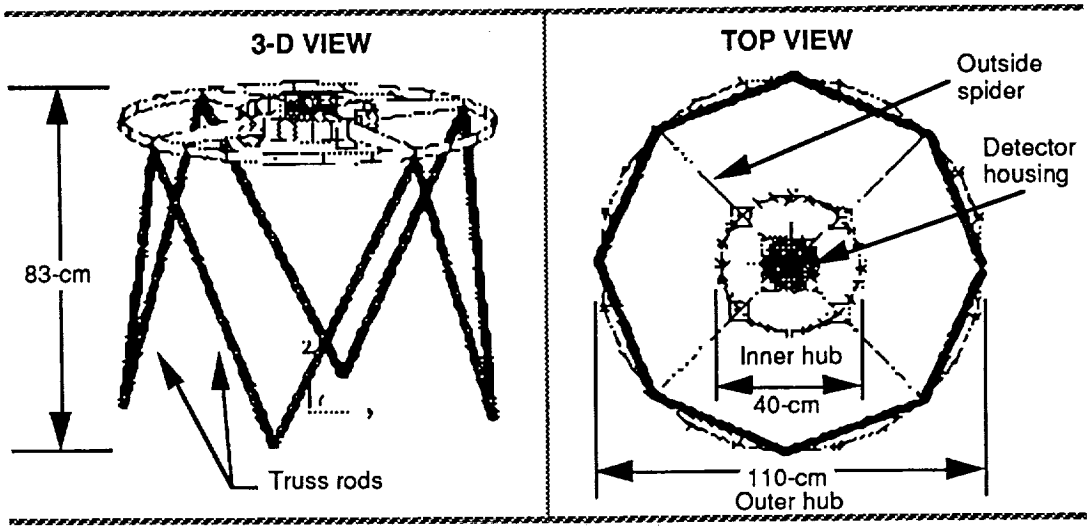

Figure 17. Metering structure finite element model.

Geometry—The diameter of the truss and outer hub were assumed to be 110 cm (the primary mirror is 100 cm in diameter and the baseplate is 120 cm in diameter). The metering truss is 83 cm tall, with 65 cm separation distance between the optics. The outer hub is 3 cm tall. The inner hub diameter is 40 cm and the detector housing is 14 cm in diameter. They are both 6 cm tall. The structural model was one design iteration behind the configuration; the latest configuration has both the detector housing and inner hub at 40 cm in diameter.

The metering truss tubes are 5 cm in diameter, with a 5 mm wall thickness. The outer hub thickness is 2.5 cm, and the inner hub thickness is 6 mm. The outside spider thickness is 1.5 cm, and the inside spider thickness is 1 cm. The sides of the detector housing are 1.5 cm thick, and the detector cover is assumed to be 6 mm thick.

Materials—Graphite/epoxy is the reference material for the metering structure.

4.2.3.6 Optical Baffles

The optical baffles block stray light from impinging on the LUTE mirrors. None of the baffles in the baseline design are load-carrying. The baffles were assumed to be aluminum with a minimum gauge thickness of 1 mm for the mass estimate. Hand calculations for the secondary and tertiary baffles predict that the 1 mm gauge thickness will be sufficient to prevent buckling during launch.

4.2.3.7 Light Shade

The light shade blocks direct sunlight, earthlight, and lunar surface reflections from the optics. In the current LUTE design, the light shade is mounted onto the baseplate. It does not support the optical assembly but does support multilayer insulation (MLI), the high-gain antenna, aperture cover, and electronics box. As a goal, the light shade should minimize vibrational transmission into the baseplate and optical assembly during operations. The baseline light shade model is shown in figure 18.

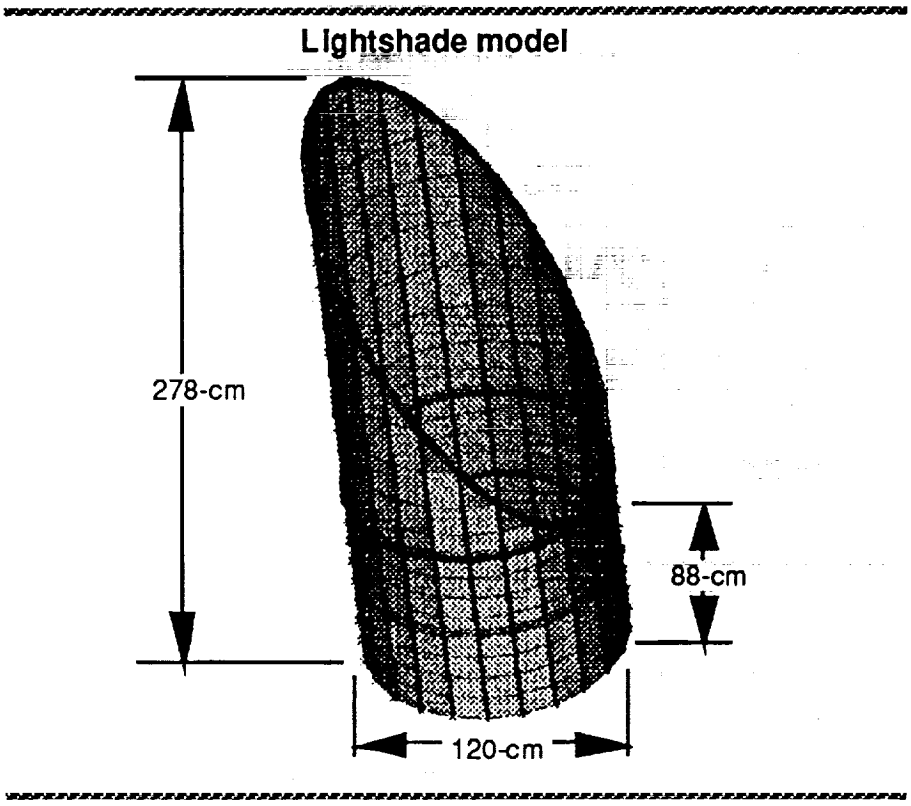

Figure 18. Light shade.

Geometry—The structural model of the LUTE light shade is 120 cm in diameter and 278 cm tall, with 88 cm being the cylindrical section's height. The skin thickness is 0.508 mm with 24 T-section skin stringers attached to the inside circumference of the light shade at 15° intervals. The skin thickness and number of stringers were determined from a trade study summarized in section 5.3.6. The spacing between stringers is 15.7 cm. The geometry of the skin stringers is shown in figure 19.

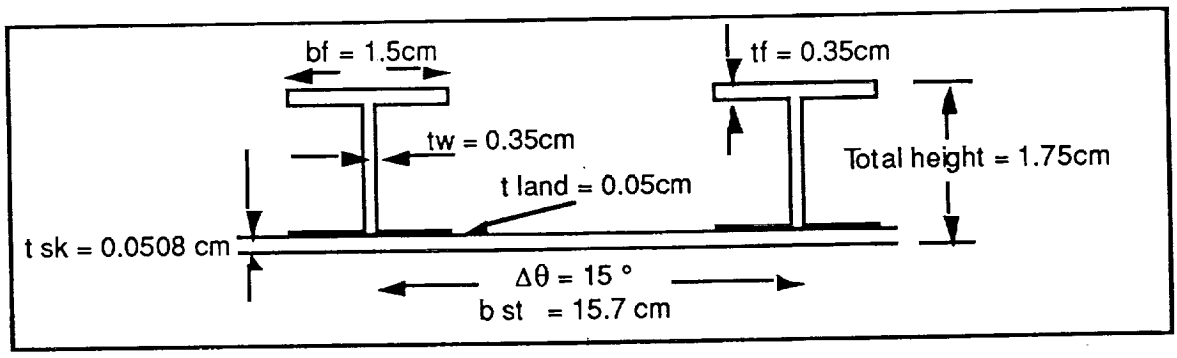

Figure 19. T-stringer geometry.

The skin stringers act to increase the stiffness of the structural design. Likewise, one intermediate Z-frame is located halfway up the cylindrical section of the light shade to provide reinforcement for the skin stringers to prevent column buckling. The Z-frame has 1.27 cm wide flanges, a height of 2.54 cm, and a web thickness of 0.254 cm.

In addition, two major frames, to be assembled with the light shade, have been identified as necessary to increase stiffness and to provide structural attachments for the high-gain antenna, aperture cover, electronics box, and potentially the power system. Both frames were assumed to be simple box beams.

4.2.3.8 Electronics Box Support Structure

The electronics box support structure, shown in figure 20, is attached to the north side of the light shade (the shortest side). The structure provides a stable support for the electronics box while maintaining an open view to space for thermal radiative heat transfer. The support structure is an aluminum truss consisting of a 1 cm thick electronics box shelf and 11 circular rods which are 1.25 cm in diameter.

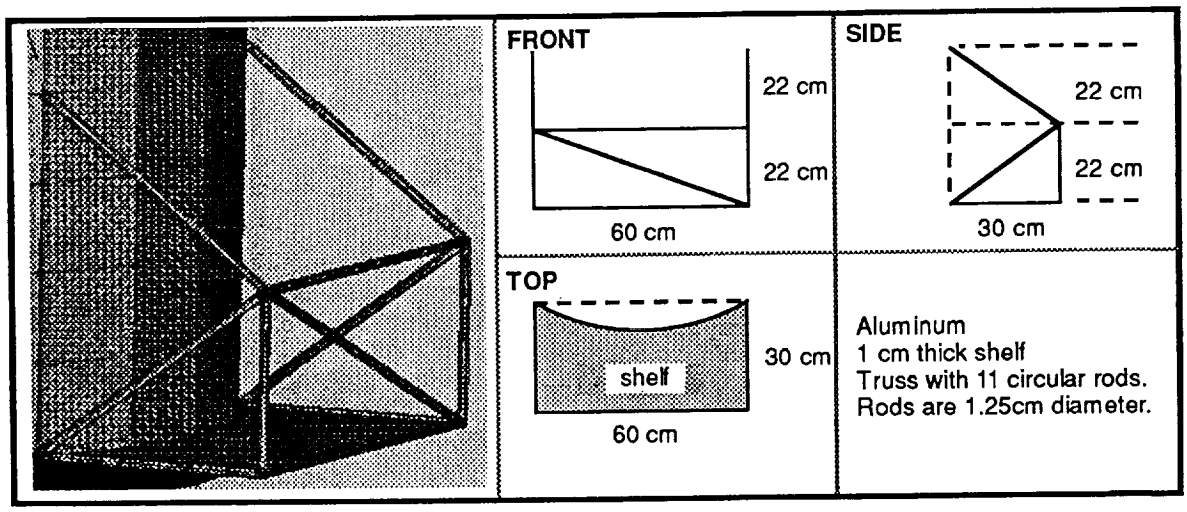

Figure 20. Electronics box support structure.

4.2.3.9 Aperture Cover

The function of the aperture cover is contamination control. Although a reference design has not been selected, a mass estimate of 15 kg for an aluminum cover was derived by scaling the masses of the HST and AXAF sunshade doors. This mass estimate is described in section 5.3.8.

4.2.3.10 Baseplate

The structural function of the LUTE baseplate is to provide support for the entire optical assembly and light shade. It will also interface with the telescope mount.

Geometry—The baseplate is 120 cm in diameter in the structural model. It is modeled as a honeycomb structure with two faceplates. Internal dimensions for the baseplate construction have been assumed to be identical to the primary mirror construction (fig. 15), pending detailed stress analysis.

Materials—Since the reference optics are SiC, the baseplate has been modeled as graphite/epoxy, in an effort to maintain athermalization between the optics and baseplate thermal growth.

4.2.3.11 Integrated Structural Model

After baseline designs for each component were selected, the components were incorporated into an integrated FEM of the LUTE structural system. This model was used to calculate launch stresses and normal mode dynamics.

Stress analysis—A linear statics stress analysis conducted with I-DEAS™/model solution determined that the reference designs and mass estimates for the LUTE structural components are reasonable. Quasistatic loads of 6 g's axial and 2 g's lateral, representing maximum launch vehicle loads on an Atlas IIAS, were applied to the model. Table 4 summarizes the results of the FE stress analysis.

Table 4. LUTE linear static stress analysis with Atlas IIAS launch loads.

Structure	Max. Launch Stress (kPa)	Location	Allowable Strength (MPa)	Stress M.S.	Results
Integrated FE model	40,000	Metering structure.	–	–	–
Baseplate	–9,640	Above hexapod mount.	356.07	>20	Safe
Primary mirror	426	Outside and inside, near mounts.	>1	–	Safe
Metering structure					
Spider	40,000	Attachments to secondary housing.	356.07	7.9	Safe
Truss	–680	Near baseplate attachment.	356.07	High	Safe
Light shade					
Skin	–18,390	At elec. box upper attach.	236.36	11.9	Safe
T-stringers	–14,700	Near elec. box lower attach.	236.36	15.1	Safe
Electronics box support	12,170	Upper light shade attach. rods.	236.36	>20	Safe
			SF = 1.4		

Stresses developed in the LUTE structural components are safe from material failure, with high margins of safety. Positive margins will be maintained for the structural system even if combined quasi-static and random vibration load factors were to increase up to 53 g's axially and 16 g's laterally. For some components, especially the mirrors and metering structure, stiffness and deflection requirements will probably drive the structural design more so than the stress requirements. Buckling requirements must also be considered.

Normal modes analysis—A normal modes analysis run with I-DEAS™/model solution determined that the reference structural design does not violate Atlas IIAS payload frequency constraints. A summary of the natural frequencies analyzed for the LUTE structure appears in table 5.

Table 5. LUTE structural natural frequency.

Mode	Natural Frequency (Hz)	Description	Violates Atlas II Constraints
1.	20.8	Lateral (E to W) vibration of light shade conic section.	No
2.	22.9	Axial vibration of light shade conic section.	No
3.	23.7	Lateral (N to S) vibration of light shade.	No
4.	36.7	(Pictorial output not obtained.)	No
5.	38.5	(Pictorial output not obtained.)	No
6.	38.9	(Pictorial output not obtained.)	No

Atlas IIAS frequency constraints, listed in section 4.2.3.1, are that the first lateral mode must be above 10 Hz and that the first axial mode must be above 15 Hz.

4.2.3.12 Conclusion

Individual detailed component analyses and trade studies were completed and are documented in section 5.3. Thermal deformations for the SiC optics were found to be acceptable by optical analyses. The LUTE components were analyzed as an integrated whole structural system. Natural frequencies for the combined structure meet Atlas IIAS requirements, and computed launch stresses are safe from material failure. Launch loads were the driving load condition. The mass estimate for the structural system is 122 kg (with two TBD's identified). These analyses show that the structural system for LUTE is adequate and safe. It is assumed the RTG is mounted on the lander structure and, therefore, does not affect the telescope structure.

4.2.4 Electrical Power System (EPS)

The LUTE power system is based upon the use of existing design features and configuration of the Galileo spacecraft RTG, as shown in figure 21. During the trade studies, a 150 W RTG, based upon use of one-half of an existing design, was evaluated as a candidate power source. However, during the course of the phase A final study, it became apparent that utilizing an existing 300 W RTG design could supply the power needed during lunar descent and would offer to LUTE the capability of future power growth. Location and characteristics of the existing RTG design are shown in figure 22.

RTG Design Features

An RTG is comprised of two major elements a thermoelectric power generator and a modular radioisotope heat source. Heat generated by the decaying radioisotope is converted directly into electrical energy by use of thermocouple technology. Current space RTGs commonly use Plutonium-238 fuel pellets and silicon germanium thermocouples. Other features include:

- Radioisotope fuel pellets encapsulated in iridium shells and graphite reentry modules
- Thermoelectric power assembly comprised of 572 multiply-redundant silicon germanium "unicouples" each producing more than 1/2 watt
- Qualified for launch environments and cooling requirements

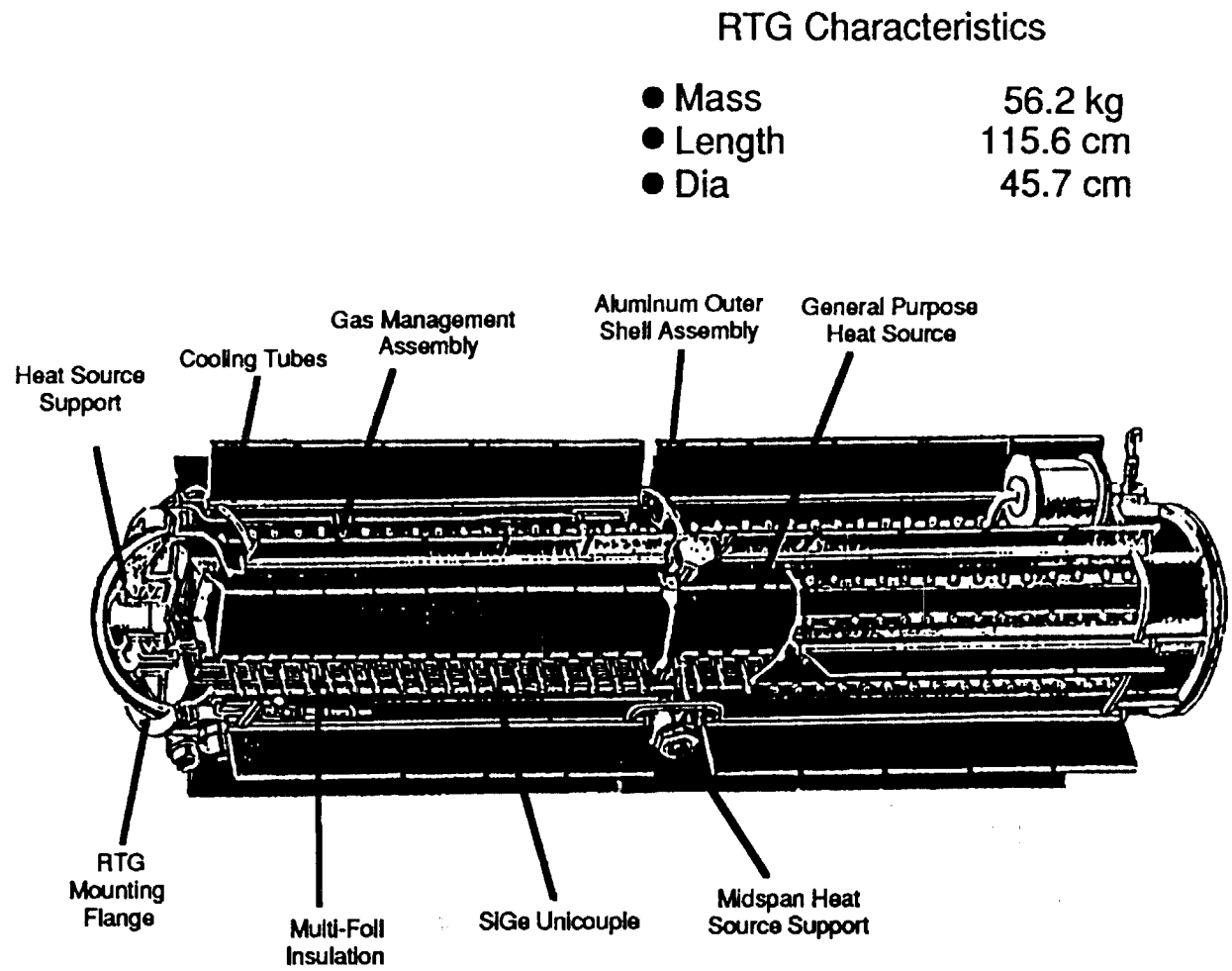

Figure 21. Galileo RTG for LUTE.

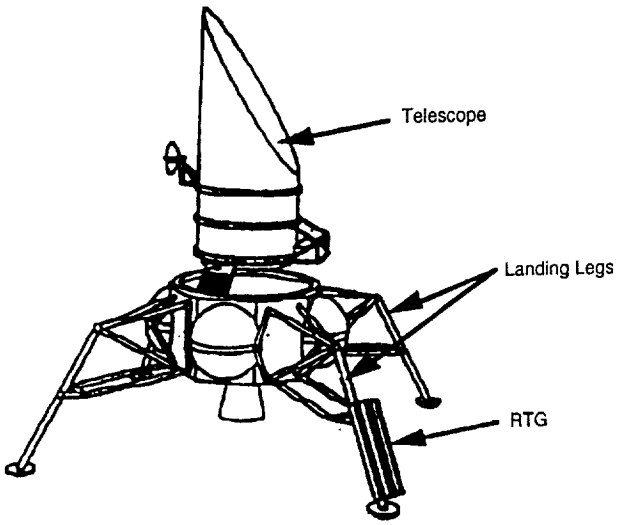

RTG EPS Characteristics

Power Capability (BOL)	300 watt
EPS Mass	
RTG	56.2 kg
Regulator	12 kg
Distribution	10 kg

Figure 22. RTG EPS characteristics.

4.2.5 Thermal Control System (TCS)

The objective of the LUTE thermal control system is to maintain the primary mirror, optical system, detector, and subsystem equipment within the required temperature range with minimum expenditure of mass and power. In addition, thermal gradients in the primary mirror and optical system must be minimized. Power availability is very limited. An RTG will be available to provide small amounts of heater power during the night periods. Mass for the thermal control system is also very limited since the LUTE is designed to be launched on a Delta or an Atlas vehicle.

4.2.5.1 Requirements

Specific requirements influencing the thermal control system are listed in table 6. The launch vehicle selected defines the ascent and transit environment for the LUTE. Material selection and degraded insulation and coating property assumptions must allow for the 2 year minimum useful life requirement. The allowable temperature range and the maximum temperature differential for the optics, which depend on the optics configuration, material, construction, and performance requirements, will be defined after preliminary trade studies have been completed. The focal plane detector is an array of

Table 6. Systems requirements affecting the thermal control system.

Launch vehicle	Atlas class vehicle
Lander	Undefined
Useful life	2 years
Optics temperature range	TBD, based on optical req./design
Optics maximum temperature differential	Less than TBD
Detector temperature range	77 to 210 K
Detector heat rejection	TBD, estimate 2 to 10 W
Detector temperature stability	TBD
Electronics temperature range	223 to 398 K
Electronics heat rejection	≈90 W in subsystem box(s)

CCD's which has a temperature stability requirement as well as maximum and minimum operating temperature requirement. The total heat load to be removed from the detector array is modeled at 10 W. The LUTE electronics, which will be located in one or more boxes, have maximum and minimum temperature requirements, as shown in table 6. Total heat dissipation for these items is estimated at 90 W. Other components, such as motors and mechanisms, may dissipate small amounts of heat or require some thermal conditioning. These are currently undefined and will be treated in later studies.

4.2.5.2 Environment

The LUTE must function properly in its operating environment on the lunar surface, as well as withstand its handling and transit environments without degradation. Transit phase environments for the Atlas II vehicle were used to analyze the present design configuration.

Prelaunch—During prelaunch activity, the temperature within the payload fairing will be held between 277 and 303 K, with a relative humidity at or below 50 percent.

Ascent—The payload fairing protects the spacecraft from aerodynamic heating to a nominal altitude of 113,000 m, during which the peak heat flux radiated by the inner fairing is less than 400 W/m^2 at the warmest location. After fairing jettison, the maximum free-molecular heat flux is 1,135 W/m^2. Solar heating, Earth albedo and thermal heating, and radiation to the lander and upper stage are also present during this phase. The heat flux from these sources is configuration dependent.

Transit—The thermal environment for the LUTE during transit from Earth orbit to the lunar surface is dependent on payload configuration, orientation, and trajectory. Further definition of these parameters will support a more complete analysis. However, the design impact of this environment is not expected to be as severe as the lunar environment.

Operating—The LUTE operating environment on the lunar surface is a more severe thermal environment than that encountered by orbital space telescopes because the lunar surface acts as a heat source during the lunar day and also complicates heat rejection by limiting the view to deep space. Surface temperatures may vary from 85 to 390 K during the 14 day hot and cold soak periods, whereas the typical 30 minute dark period for an Earth-orbiting telescope results in much smaller temperature swings. In addition, Earth-orbiting telescopes have more flexibility than lunar telescopes to maintain a particular orientation with respect to the Sun. Telescope thermal interaction with the lunar surface is illustrated in figure 23.

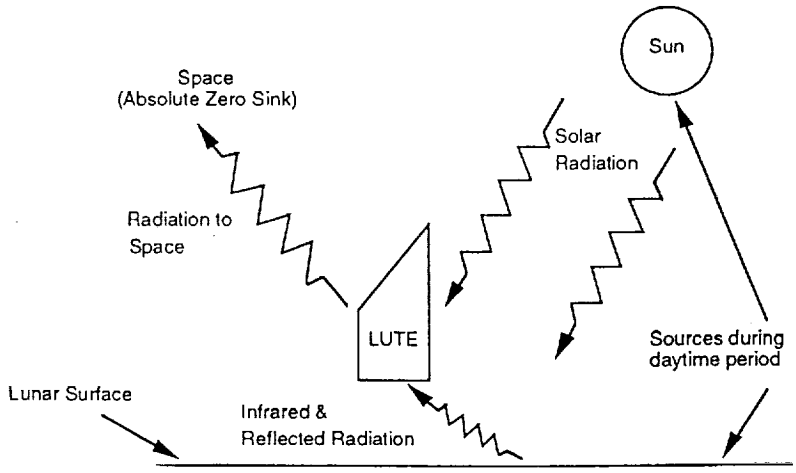

Figure 23. Heat sources and sinks for LUTE in the operating environment.

4.2.5.3 Summary of TCS Reference Design

The LUTE reference design consists of the cylindrical light shade truncated at a 60° angle with external MLI, heat pipes on the baseplate, and lower light shade to approximate the isothermal baseplate and ring concept, separate primary and tertiary mirrors with three points, flexure supports, a northerly location for the electronics box, and a louver/radiator system with heaters and MLI for electronics thermal control. Thermal control of the detector is by a heater and radiator system. Insulation thicknesses for the light shade and baseplate are described in section 5.5.3 of this document. The power requirements for the LUTE thermal control system are 10 W during parts of the lunar day and night.

Table 7 summarizes the LUTE thermal control system mass. This estimate is based on the dimensions of the components, as currently defined, and does not include any contingency factor. TCS mass was estimated for a 1.25 m diameter light shade with a maximum height of 2.87 m and a shade angle of 60°. The detector radiator mass is based on a 0.5 m diameter circular radiator. The subsystem radiator and insulation masses are based on an electronics box with external dimensions of 0.6 by 0.33 by 0.15 m tall.

Table 7. Thermal control mass summary.

Component	Component (kg)	System (kg)
Optical System		11.7
Heat pipe assembly	11.2	
Thermal isolation	0.5	
Detector TCS		3.5
Radiator	2	
Thermal shield	1	
Heaters	0.25	
Heat transfer device	0.25	
Subsystem TCS		6.7
Radiator	3	
Insulation	2.2	
Coatings	0.5	
Heater devices	1	
Light Shade		4.9
Insulation	3.2	
Coatings	1.7	
Total		26.8

4.2.5.4 Summary of Thermal Analysis Results

The thermal model of the reference configuration consists of the LUTE with SiC primary and tertiary mirrors, a light shade truncated at a 60° angle, simulated heat pipes on the baseplate and lower light shade, and an RTG. Three-point supports are used for the mirrors in this model. The telescope is located at 65° north latitude and is tilted to view at a 40° north declination. The RTG, simulated in this model, generates 350 W of electrical power. The primary mirror temperature is plotted for one diurnal

cycle in figure 24. The maximum mirror temperature is 173.5 K and the minimum temperature is 84.3 K, for a total bulk temperature swing of 89.2 K. The maximum predicted temperature gradient in the primary mirror is 0.17 K, which occurs shortly after dawn. If the rapid temperature change, which occurs in the 30 to 40 h just after dawn, is omitted (i.e., the telescope is not operated at that time), the maximum predicted gradient over all other times is 0.06 K.

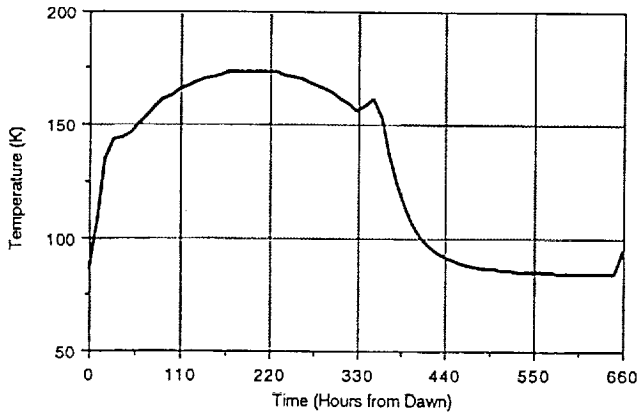

Figure 24. Primary mirror temperature (reference configuration).

The focal plane array, composed of CCD's, is cooled by a radiator located forward of the secondary mirror. For the reference configuration and site, the array temperature can be maintained at or below 190 K, even if the heat dissipation requirement is as high as 10 W. To control the rate of temperature change of the focal plane array, 10 W has been included in the budget for heaters. The electronics box is mounted on the north side of the LUTE light shade after post lunar landing alignment and is equipped with thermally actuated louvers on the top to prevent both overheating during the lunar day and excessive cooling during the lunar night. As long as the equipment is operating, added heat will probably not be required to maintain allowable temperatures during the lunar night, but 10 W heaters are included to maintain minimum temperature within the box in case the telescope systems should be shut down during the night. Figure 25 shows that the RTG will be located on one of the legs of the LUTE lander. The telescope with the RTG on the lander was modeled to determine the effect of the RTG heat load on the primary mirror. Because the telescope's pointing direction relative to the RTG location is unknown, mirror temperatures were calculated for an RTG located on the north and south sides of the telescope.

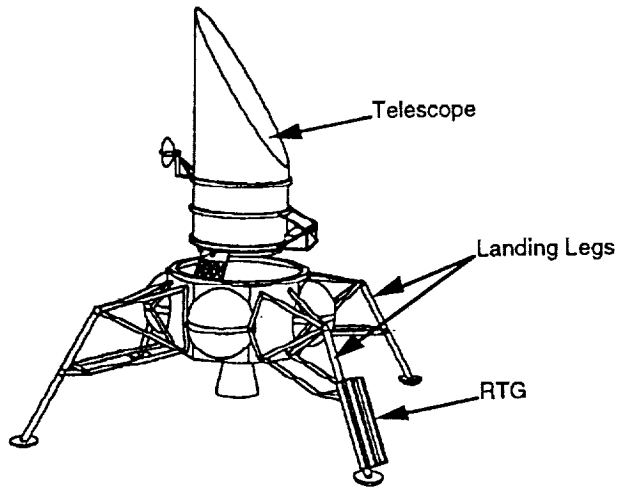

Figure 25. The LUTE with RTG.

Figure 26 is a comparison of the primary temperature results of an analysis without an RTG versus those of analyses with an RTG. These results indicate that the RTG heat load reduced the bulk temperature swing of the primary mirror by about 27 K, while only increasing the peak temperature at lunar noon by about 5 K. Note that the results also show that the mirror temperature is not affected by the location of the RTG.

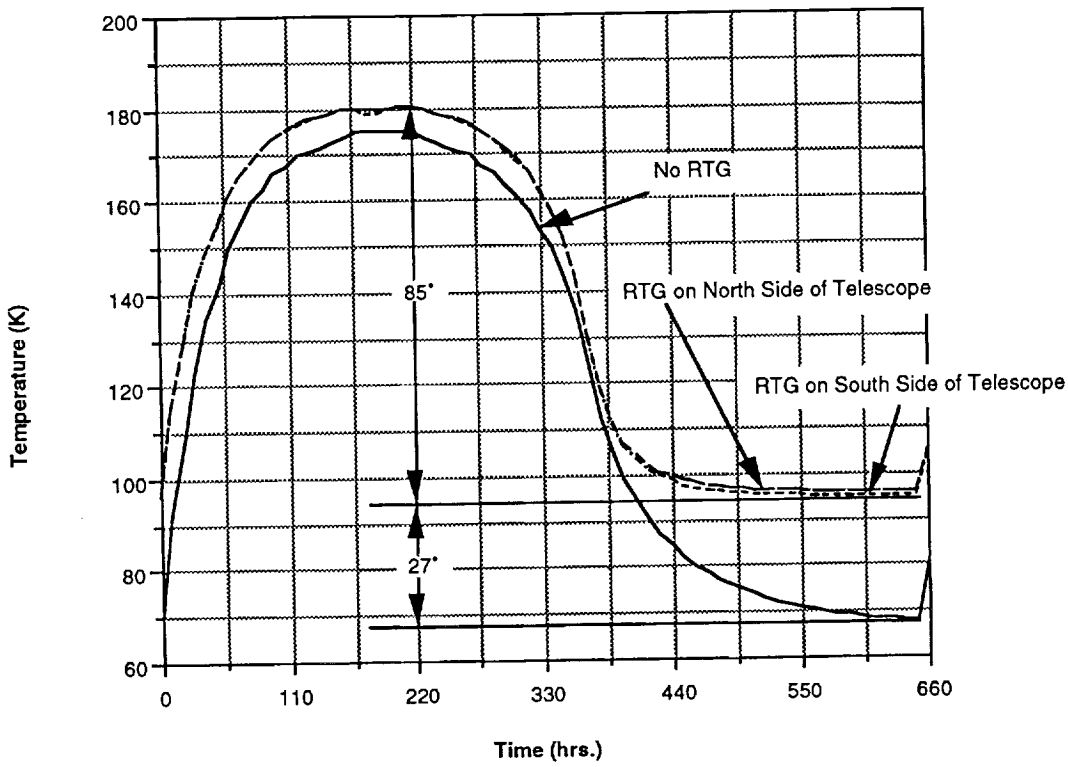

Figure 26. Effect of RTG heat load on primary mirror.

4.2.6 C&DH System

The C&DH subsystem for the LUTE will be required to collect, process, and transmit the science and engineering data from the telescope to Earth. The C&DH subsystem will also provide communications with the LUTE for receiving and processing all commands from the ground station. Based on the current focal plane instrument, the raw science data rate has been estimated to be about 2.6 megabits per second (Mbs).

Because of power and antenna size restrictions, some method of reducing the transmission bandwidth is necessary. Transmission of all the raw data is desirable; however, data compression is necessary to reduce the transmitted data rate to approximately 200 kilobits per second (kbs). It will be possible to preserve the highest information content of the data while using low-loss data compression. The C&DH subsystem for this study has, therefore, been based on this 200 kbs transmitted rate. If the data rate should increase from the baseline 200 kbs, some adjustments in the C&DH subsystem will be necessary. A data rate increase will necessitate an increase in the output radio frequency (RF) power or an increase in the antenna size or both. For example, a data rate increase to 400 kbs, now under consideration, would require the RF power output to be doubled. Except for a minimal increase in transmitter weight and volume, the impacts of increasing data rates to 400 kbs are not considered to be significant.

With an RTG, the LUTE will be able to operate continuously while it is on the lunar surface, which requires that the Earth be in view at all times to provide constant communication. This creates a requirement on the LUTE site selection. The Earth subtends an angle of 1.8° at the lunar distance, allowing coverage of the whole Earth without moving the telescope antenna. However, the Earth appears to move in a 16° by 18° box over a period of 18.6 years, requiring periodic adjustment of the antenna as the Earth changes position. Thus, the antenna for the LUTE is specified as a steerable parabolic reflector with two degrees-of-freedom (DOF). Omnidirectional antennas will be provided for initial contact and setup of the telescope. Another ground rule for this study was that the telescope and the lunar lander would have independent, noninterfacing communication systems. When the lander is defined, an option to share the omnidirectional antennas will be explored.

The NASA Deep Space Network (DSN) has been selected as the primary facility for receiving the data from the LUTE. The DSN, operated by the Jet Propulsion Laboratory (JPL), is NASA's largest and most sensitive telecommunications and radio navigation network. The DSN has locations at Goldstone, CA; Madrid, Spain; and Canberra, Australia. Each complex consists of stations with large parabolic dish antennas; these antennas have diameters of 26, 34, and 70 m. Each complex also has a data processing center which is constantly manned and capable of receiving and processing signals from several spacecraft simultaneously.

Due to weight and power limitations, the system has been designed with a minimum number of components. Figure 27 shows a simplified block diagram of the LUTE C&DH subsystem. A typical weight and power breakdown for such a system is given in table 8. Some weight and power savings may be achieved by selectively choosing specific components at later phases of the study. Component weight, power, and size will be influenced by the phase B design activity.

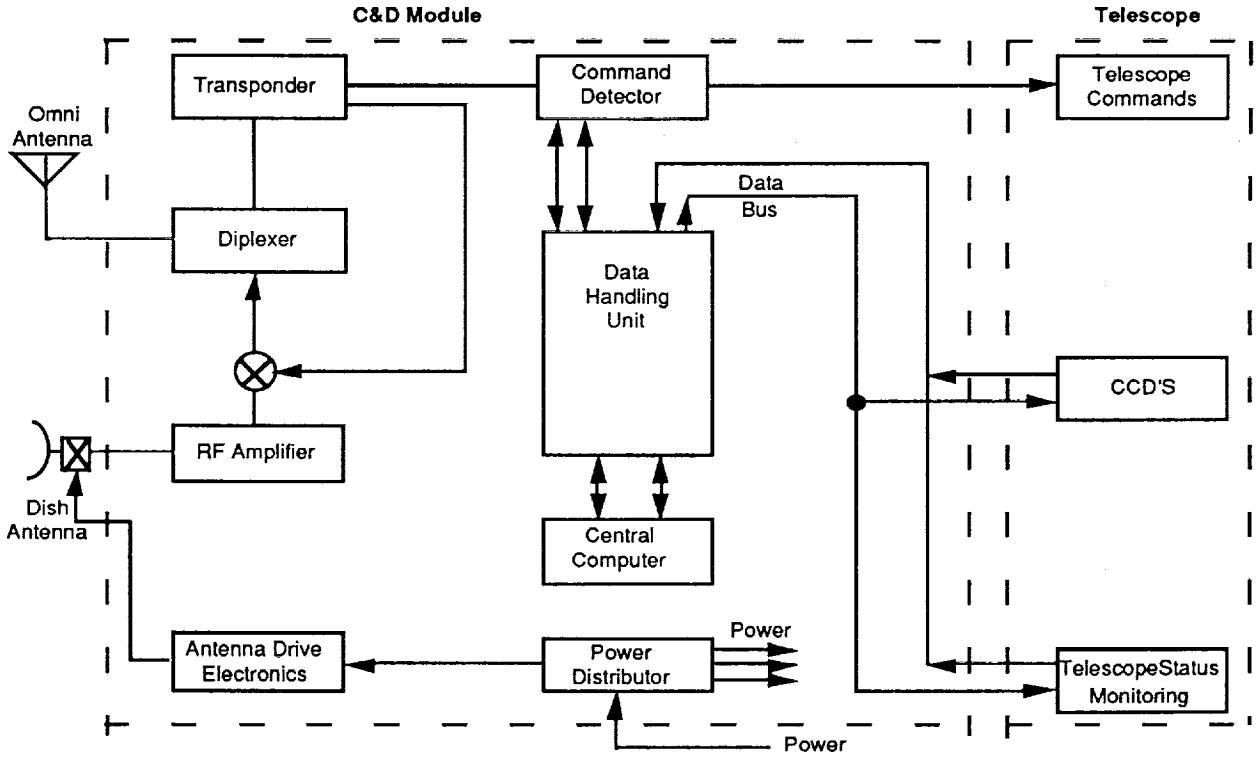

Figure 27. LUTE C&DH simplified block diagram.

Table 8. LUTE C&DH subsystem equipment list.

	Quantity	Weight (kg)	Average Power (W)	Unit Size (cm)
Module Components				
Transponder	1	6.8	18	36×11×25.2
Command Detector	1	1.4	10	3×10×15
Diplexer	1	1.0	–	5×15×3
Central Data Unit	1	14.5	15	18×15×12
Central Computer	1	14.5	15	22.7×17.8×20.3
Ant. Drive Elect.	1	2.3	10	3×4×1
Power Dist.	1	1.4	7	5×10×15
Structure and Cabling	1	6.4	–	–
Subtotal		28.3	75	
External Components				
Omni Antennas	2	1.0	–	3×3×30
High-Gain Antenna	1	2.3	–	TBD
Antenna Mount	1	1.8	–	–
Antenna Drive	1	3.2	8	10D×30
Subtotal		8.3	8	
Total		36.6	83	

4.2.7 Pointing and Alignment

The lunar site selection, the surface characteristics, and the capability of the lander, combined with the focal plane alignment requirements, drive the telescope mount and mechanisms design. A summary of alignment requirements and lander attitude capability is presented in this section.

As the Moon rotates, stars will track curved paths from east to west across the telescope focal plane. The curvature of these paths is a function of the telescope line-of-sight declination from the Moon's equator (see sec. 5.2(2)). To ensure that a star path does not stray more than one-tenth of a pixel in the north-south direction, the focal plane array orientation must be held to 14.6 arcseconds in the east-west direction, for a device integration time of 883 seconds. The tilt alignment requirement for the focal plane is specified by the sensitivity of star-path curvatures to declination misalignment; for a telescope line-of-sight declination of 40°, the tilt accuracy is 5 arcminutes in the north-south direction. These arcminute tilt and arcsecond roll alignment requirements on the focal plane array drive the pointing requirements for the telescope. Although there are no east-west alignment requirements on the optics due to its symmetry, the arcminute tilt requirement applies to the entire line-of-sight assembly.

Since alignment is critical for telescope function and the lander does not ensure any roll orientation after landing, the LUTE telescope mount must be designed to accommodate any roll or tilt errors. The lander will provide a stable base after landing, so that the lander and LUTE will not tip over. The LUTE telescope mount will have to provide alignment capability to accommodate ±180° roll and a tilt range for lunar slope, leg crushing, and surface rocks.

The telescope mount has three DOF (azimuth, elevation, and roll), and is composed of upper and lower rollrings and two elevation actuators mounted on a support structure. Pointing system components are identified in figure 28. The launch lock is a rotating support bolted to the upper rollring and is

deployed after landing by either a pyrotechnic nut splitter or a pyrotechnic pin puller. A vibration isolation and fine adjustment system will provide the periodic alignments necessary for disturbance compensation. A Sun sensor mounted on the antenna bracket provides initial acquisition attitude information for rolling and tilting the assembly before the aperture cover is removed. Alignment CCD's on the edges of the focal plane provide fine alignment sensing for both roll and tilt. A five DOF steerable secondary mirror will provide focus and tilt adjustments for the three-mirror optics. A wavefront sensor for optical assembly alignment is optional.

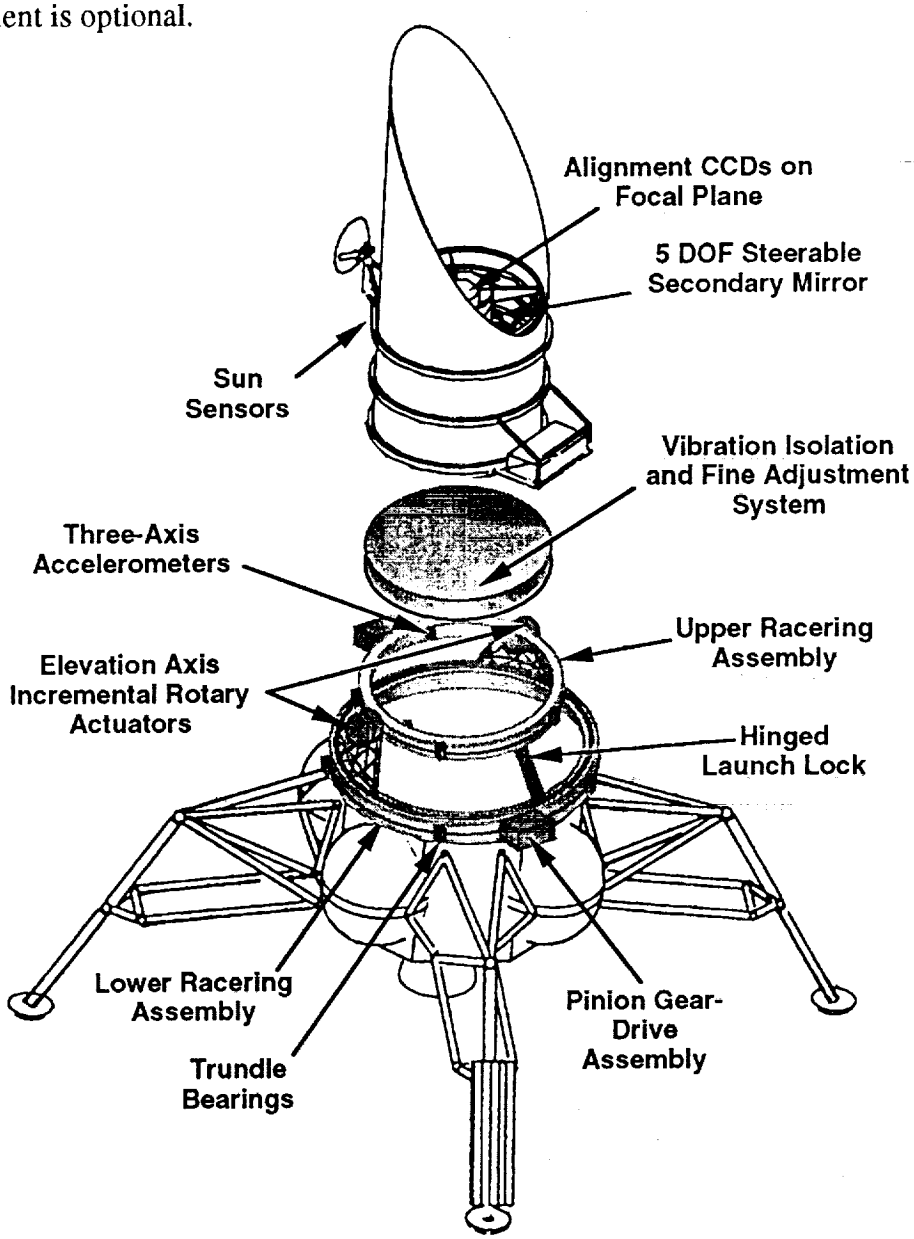

Figure 28. Pointing system components.

It was assumed that the lander would accommodate up to 12° of lunar slope on mature mare, with a 3σ landing error of 3 kg, and would sustain a maximum vertical velocity of 1.74 m/s and 1.53 m/s maximum horizontal velocity.[12] Parametric curves are available to estimate the leg stroke for landing energy attenuation as a function of vertical velocity.[13] It has been assumed as a worst case that the legs will permanently deform and shorten by the leg stroke. To determine the shortening of struts in the legs, coordinates of strut hardpoints are needed. The dimensions of the lander were estimated from the

engineering drawings. The coordinates shown in figure 29 were scaled from the 1.818 m diameter for the hexagonal interface hardpoints.[13] The maximum deck-tilt angle occurs when one leg sustains all the crushing. To estimate the deck-tilt as a function of attenuation stroke, the difference between pre- and postlanding positions of the feet was determined, as well as the corresponding tilt angle for a flat deck. Two cases were studied: one in which all crushing is sustained by the middle leg strut, and the other case in which one side leg strut is crushed. These two cases are extremes, since leg crushing would most likely involve permanent deformation of all three struts. Both of these cases are plotted in figure 30. A crushed side strut produces the larger tilt angle, and for a maximum stroke length of 0.18 m, the worst case deck-tilt is 1.9°.

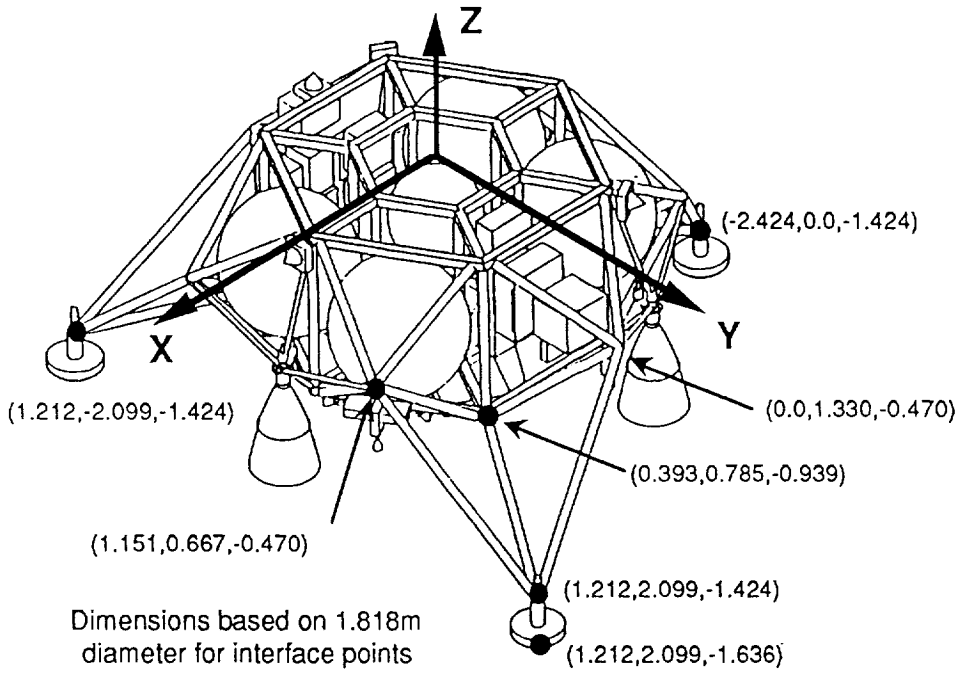

Figure 29. Artemis lander with estimated strut hardpoint coordinates.

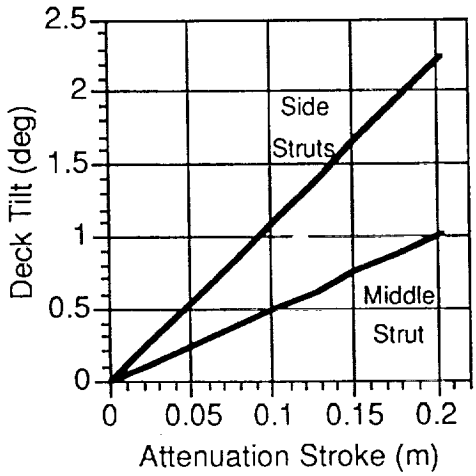

Figure 30. Deck-tilt due to one crushed leg.

To provide a worst-case estimate of deck-tilt, the effect of one surface rock under an uphill foot was included. Lunar surface rocks are discussed in a summary of Apollo and Surveyor data by Shoemaker and Morris.[14] Surveyor sites 5 and 6 represent mature mare, and provide a worst-case estimate of 10 cm for large rock diameters. Shoemaker notes that this 10 cm is a maximum dimension, usually parallel to the surface, and that rocks are generally one-half to one-third buried in the surface. Hence, a maximum height of 5 cm is assumed for our analysis, and a worst-case estimate with one rock under an uphill foot produces a deck-tilt angle of 0.79°.

Landing error also contributes to the amount of tilt required by the telescope mount to bring the line-of-sight to zenith. Using a landing error requirement of 3 km (3σ) and a lunar mean radius of 1,738 km, a worst-case (north or south) tilt error of 0.1° was obtained. Addition of the identified errors gives a worst-case estimate of 14.8° for the elevation range necessary for the telescope mount to point to zenith. For a 66.5° latitude landing site and a pointing declination of 40°, the mount must provide a 26.5° tilt capability from zenith. Therefore, adding all tilt requirements, a 41.3° capability is necessary.

Table 9 contains a summary of LUTE mechanism and alignment requirements, and identifies components in the baseline configuration that nominally satisfy those requirements. The light shade, high-gain antenna, electronics box, and optical assembly, including the detector, are all one unit that rotates and tilts together. The assembly must be tilted so that the optical axis points south to a 40° northern declination. The antenna base is aligned during preflight component integration so that it will

Table 9. Mechanism and alignment requirements.

Component	Pointing Direction	Mechanism Requirements		Baseline Configuration
		Range	Accuracy	
Light Shade				
• Roll	South	±180°	±1°	Upper Rollring
• Declination (from lunar equator)	40°	42°	±1°	Lower Rollring, Elev. Actuators
High-Gain Antenna				
• Declination	40°	42°	±1°	Lower Rollring, Elev. Actuators
• Elevation (above local horizontal)	31.2°	14.8°+{31.2°}	±1°	Elev. Actuators+{config.}
• Azimuth	153.9°	±180°	±1°	Upper Rollring
• Tracking	Earth (2°)	±11° "half-cone"	TBD	High-Gain Drive
Optical Assembly				
• Roll	None	None	None	Upper Rollring
• Declination	40°	42°	±5 arcminutes	Lower Rollring, Elev. Actuators
Focal Plane Array				
• Roll	E–W	±180°	±14.6 arcseconds	Upper Rollring
• Declination	40°	42°	±5 arcminutes (over 883 seconds integration)	Lower Rollring, Elev. Actuators
Steerable Secondary Mirror	Primary Mirror	Unknown	Unknown	Secondary Mirror Actuators
Electronics Box				
• Roll	North	Unknown	Unknown	Upper Rollring
• Declination	NA	NA	NA	Lower Rollring, Elev. Actuators

{ } Implies that range requirement is met by a specific fixed configuration

point at the correct declination above the lunar surface when the light shade is tilted to the 40° declination. An antenna drive unit will provide two DOF for tracking the 2° image of Earth as it moves within a cone of approximately 11° half-angle. Range and accuracy requirements for the steerable secondary mirror will be identified when a complete analysis of optical assembly deformations is available. Requirements for the vibration isolation and fine adjustment system will also be identified when disturbance characteristics have been determined. This fine alignment system will periodically adjust telescope pointing to compensate for thermal warping of the mount structure and lander disturbances.

4.2.8 Mass and Inertia Summary

4.2.8.1 Mass Statement

The LUTE system mass statement (table 10) contains the masses for the optical system, structural components, and supporting subsystems. The total system dry mass of approximately 400 kg includes a 30 percent engineering contingency. If the RTG is included in the LUTE weight, the total LUTE weight would be increased to 472 kg.

Table 10. LUTE mass statement.

	(kg) (w/o RTG)	(kg) (w RTG)
Optical System		
Primary Mirror (1 m diameter)	19.6	
Secondary Mirror (38 cm diameter)	3.5	
Tertiary Mirror (28 cm diameter)	2.3	
Optical Baffles	13.7	
Detector	5.0	
Structural Support Assembly		
Metering Structure	21.0	
Mirror Support Structure	3.0	
Telescope Baseplate	24.0	
Electronics Box Support Structure	8.0	
Telescope Protection System		
Light Shade	37.0	
Aperture Cover	15.0	
Launch Locks	4.0	
Supporting Subsystems		
Pointing System	66.0	
Electrical Power System (RTG)	22.0	(56)
C&DH	36.6	
Thermal Control System	26.8	
Subtotal	307.5	(363)
Contingency (30 percent)	92.2	(109)
Total	399.7	(472)

4.2.8.2 Mass Properties

The mass properties of the LUTE system (fig. 31) were developed for the analysis of the launch CG, the vehicle dynamics at lunar landing, and the telescope pointing. These properties are referenced from the right-handed coordinate system shown. The system origin is located at the center of the lander interface plane for the LUTE mass properties.

The CG location is important both at launch and during lunar landing. At launch, launch vehicle performance is generally related to the CG distance above the separation plane. During landing, a low CG produces greater landing stability. The lander for LUTE will accommodate the LUTE mass properties.

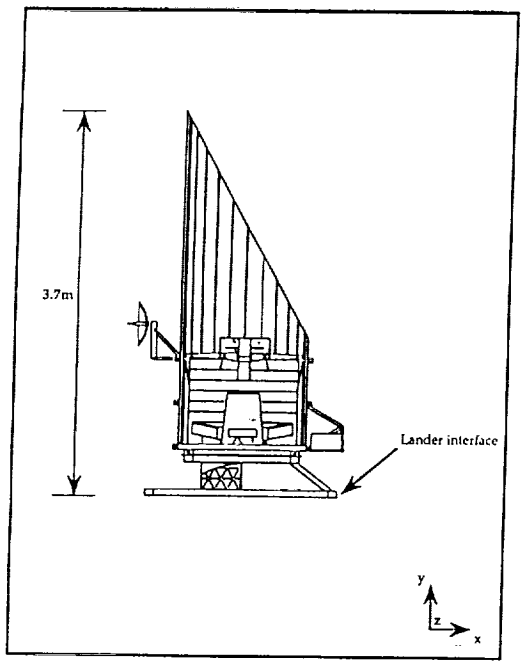

Telescope Mass * = 400 kg
Telescope Center of Mass (from Lander interface)
x-c.g.= 0.17 m
y-c.g.= 0.63 m
z-c.g.= 0.00 m
Telescope Moments of Inertia
Ixx = 322 kg m^2
Iyy = 240 kg m^2
Izz = 419 kg m^2

* LUTE mass excluding RTG

Figure 31. LUTE mass properties.

4.2.8.3 Stability

The lander will place the telescope/lander assembly in an upright position on the lunar surface if the center of mass remains within the lander footprint throughout touchdown. During landing, the landing gears will crush and deform the footprint of the lander, tilting the lander deck and producing an offset of the lander/telescope center of mass from the footprint center. The composite telescope/lander center of mass must remain within this footprint to ensure stability (fig. 32).

Assuming the lander has been balanced so that its center of mass is close to its centerline, the 14.7° tilt will shift the lander center of mass within the footprint a distance of 0.195 m from the center out toward the edge. The telescope-mount elevation axis is offset from the telescope centerline by 0.199 m, producing a worst-case footprint offset of 0.517 m. The telescope assembly is rotated to the 40° pointing declination, which when added to the 0.1° for landing site errors, provides an additional 26.6° as a worst case, and shifts the telescope center of mass a maximum of 0.824 m in the footprint. The composite telescope/lander center of mass is shifted 0.29 m from the center of the footprint in this worst case. This offset is significantly less than the 1.209 m minimum distance for stability, and so the

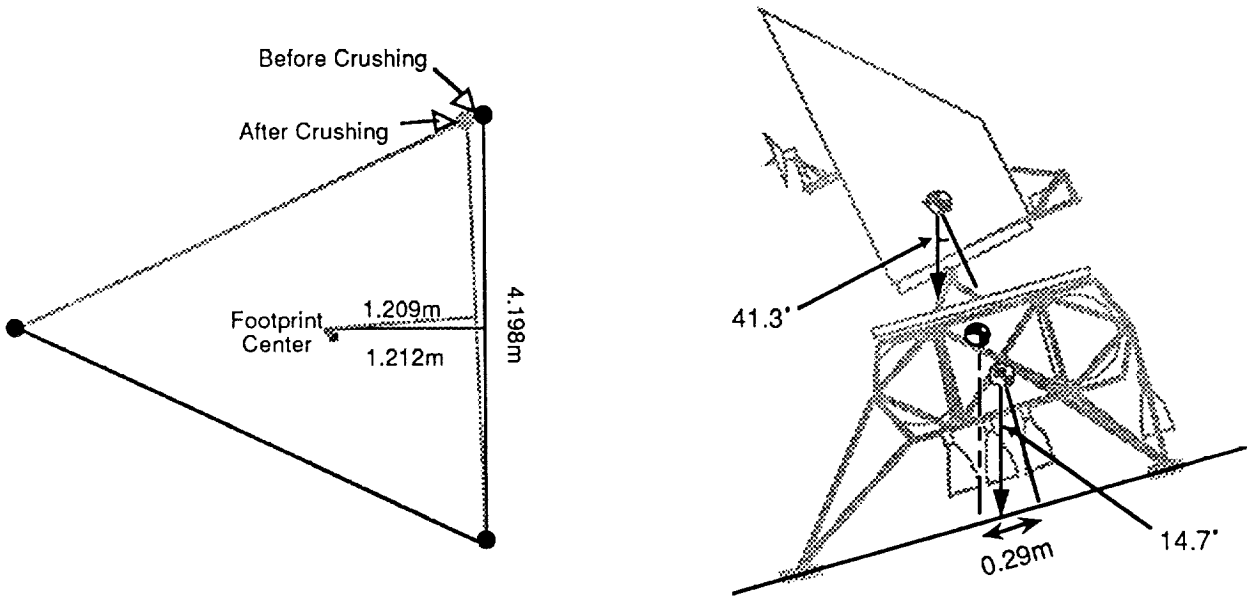

(a) Lander footprint, before and after crushing.

(b) Center-of-mass offset after landing and pointing to 40° declination.

Figure 32. Lander stability.

lander/telescope is in no danger of tipping over if the lunar slope is less than 12° and the landing conditions do not exceed the lander design requirements. Dynamic stability is a function of the landing gears ability to absorb energy and to reduce the transfer of landing energy into oscillations or bouncing. Landing dynamics will be analyzed in phase B.

4.2.9 LUTE Software

The LUTE software reference design will require seven major systems: flight software, science software, electrical ground support equipment (EGSE) software, development and verification software, simulation software, operations software, and sensor data base software.

The flight software will be designed and implemented primarily for command and data management. Flight software will also be responsible for the health and welfare of all the flight subsystems such as environmental control, optics calibration, electrical power management, dynamics and pointing control, vehicle interfaces, and system safing. This software will have the capability for onboard loading and dumping of the flight computer memory from the ground control center.

The science software will consist of requests to command science data requirements and receive telemetry for data processing and display. Science software will also be designed to retrieve ephemeris and basic science data. This software will reside in the LUTE operations center facility.

The EGSE software will be designed, developed, implemented, and utilized for test and checkout of the flight C&DH hardware and verification and validation of the LUTE software. EGSE software will consist of acquisition, processing, and display capability of the LUTE commands and telemetry. Spacecraft integration launch and lander vehicle interface software will also reside within the EGSE system.

The development and verification system for the LUTE software will be used to automate, as much as practicable, the design and documentation of software test procedures to maximize benefits

from emerging technology. This system will also be utilized to support flight and EGSE software development and unit test. Software documentation will also be a function of this system.

Software simulation can be implemented as a means for LUTE subsystems modeling and vehicle interfacing. The C&DH function of the LUTE can also be simulated by software. The software simulator will serve as a very important function for flight software verification and for training personnel for the operational concepts of LUTE.

The major functions of the operations software will be timeline management, telemetry acquisition, LUTE commanding, processing, and display of telemetry. Operations will be responsible for data archive and playback of the timeline data.

Sensor data base and generation will be contained in a separate facility. This system will also be responsible for engineering measurement identification and data base configuration control.

LUTE design requires that the downlink data be transmitted as low as 200 kbs in a compressed data stream. This will require that all of the ground support systems have a data processor with the capability of sorting the data and processing the portion required to support other individual functions. The LUTE, lander, and launch vehicles will utilize the same uplink and downlink data streams. This does not present any foreseeable problems for the defined LUTE software. For more details of the LUTE software, see section 5.0.

A functional diagram of the relationship of these major systems is provided in figure 33. The vertical dashed line on this figure identifies a functional interface between the onboard software and the ground/flight operations software.

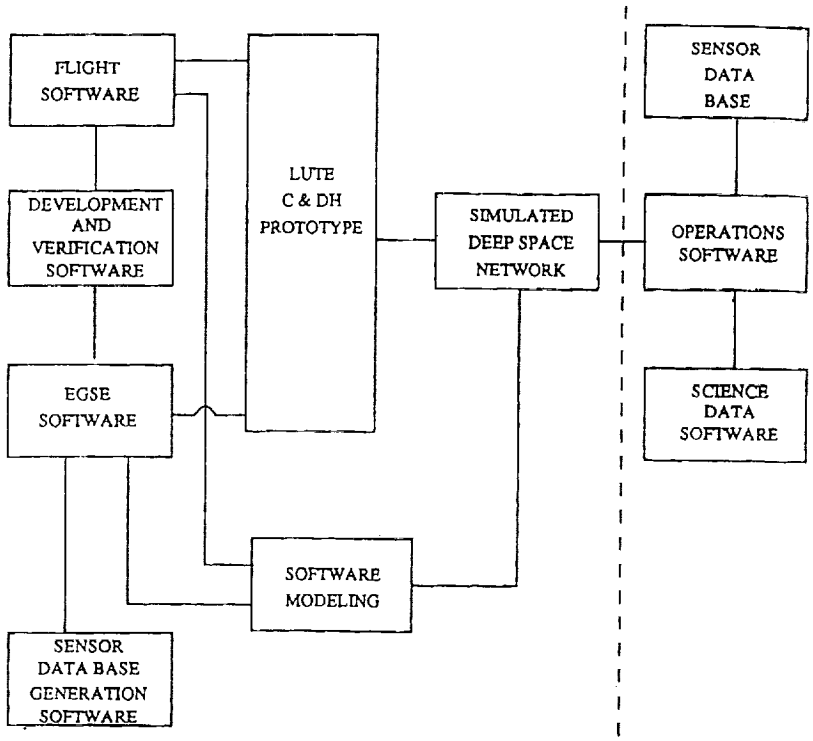

Figure 33. LUTE software functional configuration.

4.3 Mission Operations

NASA will provide for the necessary facilities required to operate the instrument from the ground for the operational period of the LUTE. The LUTE and the operations facilities will be developed for use by the scientific, engineering, and educational communities. The capabilities of the operations center will include services which will allow ground controllers to monitor engineering and scientific information from the instrument and distribute scientific data. Ground controllers will also have the capability to command the instrument. It is desired that all LUTE information be made readily available to the public. The operations center will have a substantial capability to provide scientific and engineering information to individuals and institutions. NASA will select a location for the operations of LUTE based on several factors. It is desired to draw upon existing resources of the NASA infrastructure along with scientific and educational institutions in developing the operational facilities for LUTE. It is intended that these facilities be designed and developed to be operated and maintained by the scientific and educational community. An institution with a vested interest in the instrument performance and science return will serve as the operations center for LUTE. A plan will be developed to dictate mission operations in order to ensure that the mission goals will be accomplished. NASA will be responsible for the development of this plan consistent with NASA policy and with guidance from the scientific community. A draft of this plan is included as appendix I.

4.4 LUTE Lunar Environment Instruments

A large data base on lunar environmental conditions has been assembled through remote measurements and by instruments carried on unmanned lunar landers and the Apollo missions; however, there are many areas in which the data are either insufficient or lacking. The design of future lunar telescopes, rovers, and lunar bases would therefore benefit substantially from further data on the lunar environment. In addition, analysis of the science and engineering data returned from the LUTE telescope could be aided by a detailed knowledge of the environmental conditions to which the telescope and its subsystems are subjected. Design of the LUTE mission should therefore consider incorporating a lunar environmental monitoring package which would ride along on the LUTE lander platform, would be deployed on the lunar surface, and would operate in conjunction with the LUTE power and telemetry system.

Researchers at the New Mexico State University have suggested such an environmental monitoring system. A group of four instruments to monitor the lunar environment has been outlined and is currently under study at New Mexico State University.

The instruments are as follows:

(1) Micrometeorite Detector—Detect and determine the velocity vector and mass of micrometeorites up to 100 mm in diameter.

(2) Dust Detector/Deflector—Incorporate a charged dust deflector into the design of the LUTE telescope and characterize the local, time-varying dust conditions. Determine particle sizes of dust and local natural electric field variations.

(3) Lunar Atmosphere Detector—Determine the composition and time variation of ionized atmosphere components using a ion mass spectrometer.

(4) Cosmic Ray Detector—Determine the rate and energy distribution of cosmic rays using a stacked-detector instrument.

These instruments would be mounted on a common pallet with the LUTE telescope and would share power and communications with it. The micrometeorite and cosmic-ray detectors should be mounted high enough to see a full 2 π steradians view of the sky without blockage by the telescope. The instruments are expected to operate over the full 2 year lifetime of the LUTE telescope. Preliminary estimates of instrument parameters are approximately 30 kg, with a volume of 0.05 m^3 and a power requirement of about 20 W.

5.0 SUBSYSTEM TRADES

The subsystem trades, identified by discipline in the following paragraphs, provide the background of activity that led to the LUTE phase A final design concept described in section 4.0. These trade studies are recorded as an indication of the options that have been investigated and evidence of the thoroughness with which the feasibility of LUTE has been explored. These data are shared with the intent of providing a stepping stone in analyzing hardware that will eventually be placed on the lunar surface.

5.1 Optics

The optical design of the 1 m aperture LUTE was derived from the design of a 2 m aperture LTT. The optical configuration of the LTT, as well as the LUTE, was primarily driven by the requirement for a wide FOV. Two-mirror telescopes of the Cassegrain as well as of the Gregorian configuration can only be corrected for spherical aberrations, specifically astigmatism and field curvature, limiting the high resolution field to no more than a few arcminutes. Furthermore, the use of a refractive corrector, which might solve the FOV problem, would result in a major reduction in throughput and severe limitation of the spectral range; the only available option is a multimirror system. Satisfactory performance can be obtained with both three- and four-mirror designs.

There are two important differences between three- and four-mirror systems. The first, and most obvious, is the number of mirrors and, therefore, also the number of reflections. The second is the location of the focal plane. While in most practical systems the focal plane of a four-mirror telescope is located behind the primary, the focal plane of a three-mirror system is located behind the secondary.

Because of higher throughput and greater simplicity, the three-mirror configuration was selected as the candidate concept for the LUTE, as mentioned in paragraph 4.2.1. The location of the focal plane in front of the telescope has the added advantage of facilitating the required cooling of the detector arrays. The basic configuration of the LUTE optical system and its dimensions are shown in figure 34. Additional design parameters are given in paragraph 5.1.1. The secondary and tertiary baffles, which are for an unvignetted circular field of 1.4°, are indicated in figure 34, which also shows a full-field ray trace. An exaggerated illustration of the geometric distortion in the focal plane is given in figure 35. Preliminary performance optimization and analysis indicates that the residual aberrations at the edge of the FOV can be reduced to less than 1 mrad.

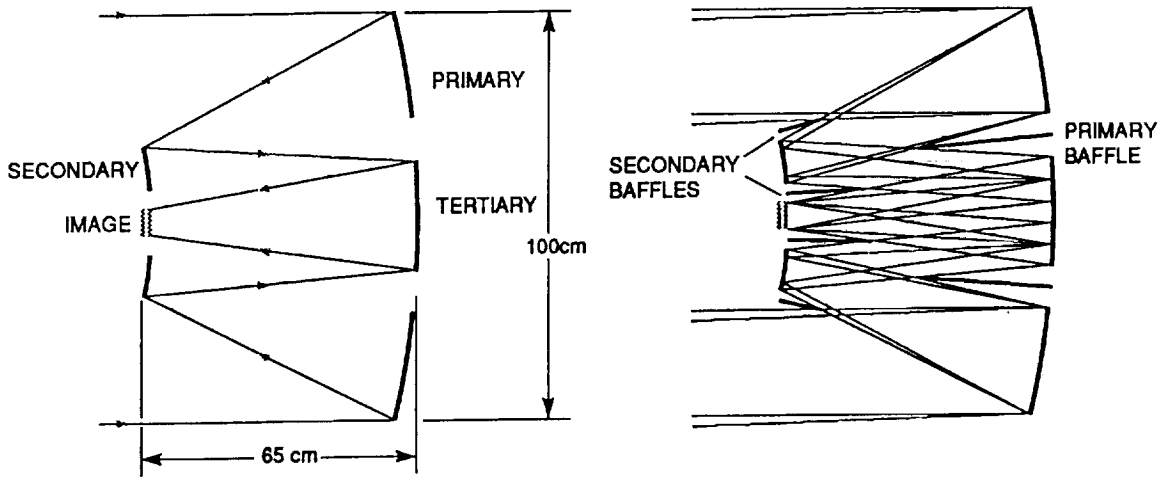

Figure 34. Primary and secondary baffles.

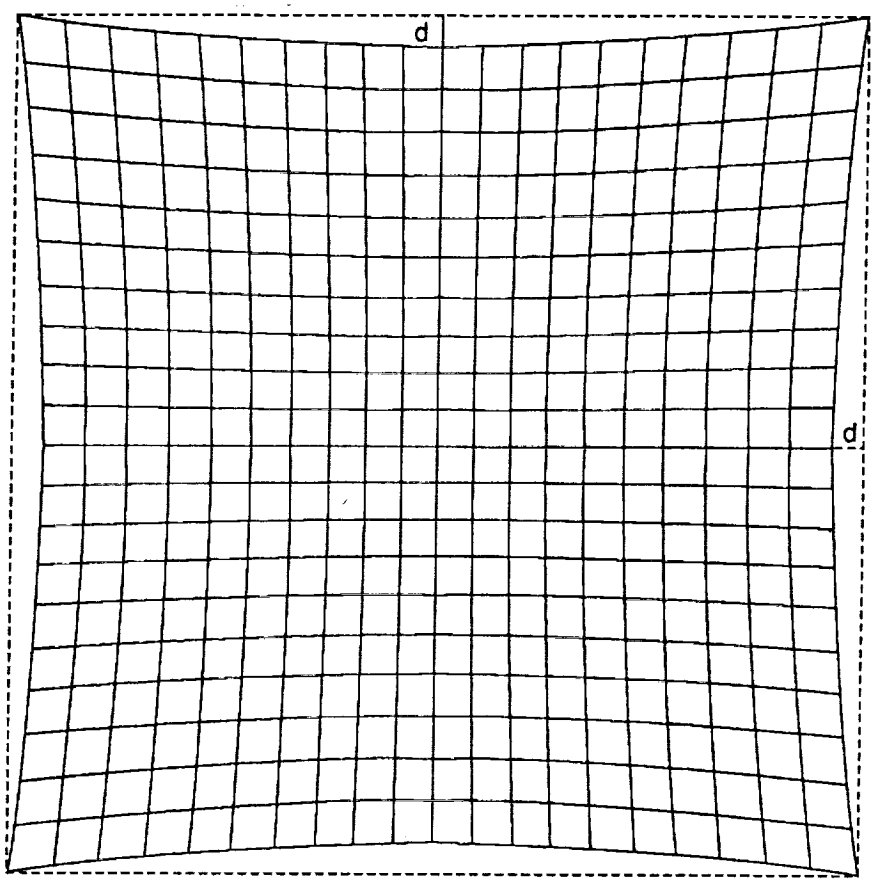

Figure 35. Geometric distortion in the focal plane.

Of all the problems to be expected when moving into a new and unknown territory, attaining and maintaining the desired optical performance in the harsh lunar environment is one of the major concerns. Apart from the dust that could contaminate the mirror surfaces, if not properly protected, the extreme temperature fluctuations between lunar day and night place the optical performance of the telescope in serious danger. To analyze this problem, two different aspects of temperature variation are considered. First, there is a temporal change of the average uniform or base temperature; and second, there is a spatial difference, or temperature gradient, which is particularly detrimental when any of the three mirrors that make up the telescope are affected.

Since a change in the base temperature only changes the size of the components (i.e., the vertex radii of the mirrors, but not their shapes), excellent performance restoration can be achieved, even for temperature changes of 100 K or more, by simply readjusting the mirror separation. A special case exists, if the entire optical system, mirrors as well as structural components, is fabricated from the same material. A uniform scale change without affecting the optical performance is the result, as long as all the mirrors attain the same temperature.

A more complicated problem is that of temperature gradients. Even though the telescope will be thermally isolated, some residual gradients may be present, and the resulting wavefront error, induced by the surface deformations, must be corrected. Performance restoration can no longer be achieved by a simple realignment. This problem requires the use of adaptive optics; at least one of the mirrors must be deformable in a controlled fashion to compensate the figure errors of the other mirrors. Since the telescope system is by design aplanatic (corrected for spherical aberration and coma), it would take at least

two deformable mirrors to maintain aplanatism. As will be shown later, use of adaptive optics was avoided by minimizing mirror thermal gradients. The goal is to find out which of the three telescope mirrors would make the most effective corrector by first introducing the optical design of the LUTE.

5.1.1 Telescope Design

A diagram of the LUTE is shown in figure 4. Because of phase A weight and space limitations, compactness was an important design consideration. Primary and secondary baffles were configured to prevent outside radiation from reaching any point of the 1.4° image field either directly or after only a single reflection. The root-mean-square (rms) spot diameter is 1 mrad at the edge of the field and smaller everywhere else. A summary of the important LUTE design parameters is given in the following:

Primary Diameter	100 cm
Primary Hole	50 cm
Secondary Diameter	38 cm
Secondary Hole	15 cm
Tertiary Diameter	28 cm
Image Diameter	7.4 cm
PrimaryVertex Curvature	–0.00500000/cm
Secondary Vertex Curvature	–0.01135531/cm
Tertiary Vertex Curvature	–0.00295858/cm
Image Curvature	+0.0062/cm
Secondary Distance	–65 cm
Tertiary Distance	+65 cm
Image Distance	–65 cm
System Focal Length	+300 cm.

The surface equation for the three mirrors is:

$$z = h^2c/[1+(1-(1+\delta)\,h^2c^2)^{-0.5}]+Ac6h^6+Ac8h^8\ .$$

The conic constant, δ, and the aconic coefficients, $Ac6$ and $Ac8$, for the three surfaces are summarized in the following:

	δ	$Ac6$	$Ac8$
primary	–1.2241	+2.067E-14	+1.5E-18
secondary	–3.7020	+1.400E-11	0
tertiary	–66.750	+2.500E-11	0

5.1.2 Figure Error Correction Using a Deformable Mirror

To determine which of the three telescope mirrors is best suited for the correction (as a deformable mirror), the following computer experiments were carried out: a surface deformation was introduced to one of the mirrors until a noticeable performance degradation was observed, then each of the other two mirrors were reconfigured alternately until system stigmatism was restored. The measurement for the state of correction is the geometric rms spot size on and off axis.

For the purpose of this preliminary study, only axially symmetric surface deformations were considered. In practice, asymmetric deformations are not only likely to occur, but can also be corrected as long as magnitude and spatial frequency are compatible with the range and the density of the actuators that drive the deformable mirror.

The surface deformations were introduced by changing the conic constant of the respective mirror. To distinguish between a positive and a negative deformation, the sign of $\Delta\delta$ must be observed. A positive $\Delta\delta$ causes an increased edge bending, while a negative $\Delta\delta$ causes a decrease or flattening of the surface. Since positive and negative deformations affect the system aberrations differently, both cases were considered separately.

A special program is used to determine the shape of the deformable mirror. This program is based on the method described by D. Korsch in "Reflective Optics."[15] With two mirror surfaces given, this program automatically finds the shape of the third deformable mirror, the corrector, to render the system rigorously stigmatic.

The results of these computer experiments are represented in figures 36 through 41. Each graph shows the state of correction of the system with one of the three mirrors deformed before and after correction, using alternately each of the other two mirrors as correctors. Each graph also shows the ideal or design performance for comparison.

The amounts of deformation introduced were $\Delta\delta = \pm 0.0021$ for the primary, $\Delta\delta = \pm 0.011$ for the secondary, and $\Delta\delta = \pm 1.0$ for the tertiary. The edge bending caused by these deformations was ± 2 μm for the primary and the secondary, and ± 10 μm for the tertiary.

Most noticeable in every graph is the comparatively weak influence of tertiary deformations on the system aberrations. It takes significantly stronger deformations of the tertiary than of the primary or secondary to cause a comparable image degradation. On the other hand, the tertiary is the most ineffective corrector and is therefore least suited as a corrective mirror. The effectiveness of the primary and secondary mirrors are about equal, and the practical considerations will determine the final selection.

5.1.3 Effect of Bulk Temperature Changes on the Performance of the Optical Telescope System

During operation of the LUTE on the lunar surface, the primary, secondary, and tertiary mirrors will cool to temperatures far below those experienced during mirror fabrication. Temperatures will range from approximately 80 K (–193 °C) at lunar sunrise to 260 K (–13 °C) at lunar noon. No known mirror material has a zero coefficient of thermal expansion (CTE) over such a large range of temperature. Even materials such as Corning's low expansion ULE titanium silicate, which has a near-zero CTE near room temperatures, exhibit a positive CTE at much lower temperatures.

The combination of nonzero CTE and the wide temperature range that the LUTE will experience will lead to changes in the shapes of the mirrors, which will affect the imaging characteristics of the telescope. The purpose of this note is to document the effect of thermally induced changes in mirror shape.

It should be noted at this point that variations in temperature will cause dimensional changes in virtually all of the structural elements of the LUTE, not just the mirrors. For instance, the metering structure will change length as the temperature decreases. This will affect the performance of the LUTE. Dimensional changes in the supports for the mirrors can be manifested both as a displacement of the

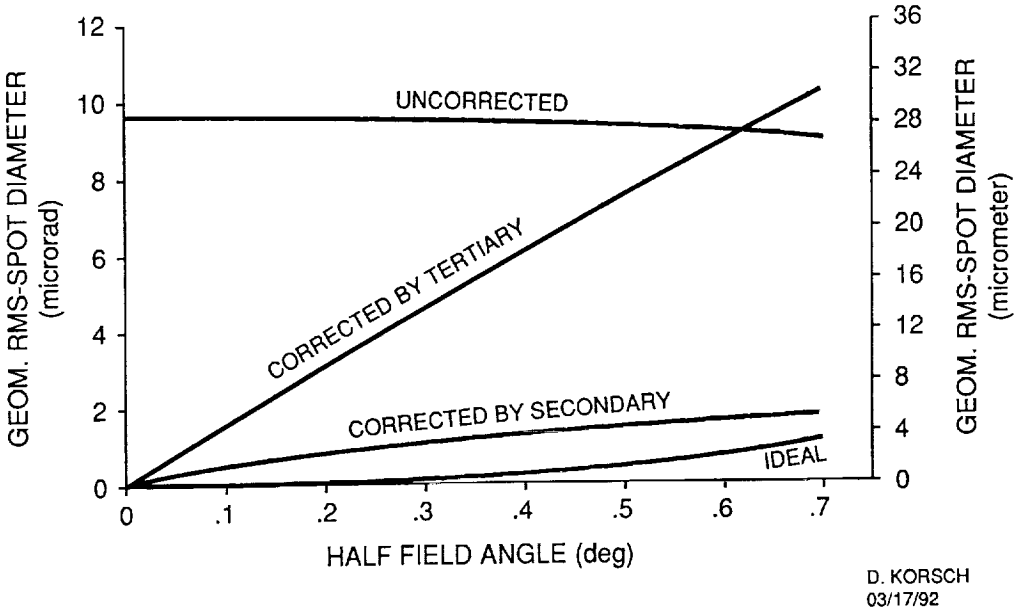

Figure 36. Primary figure error (positive deformation).

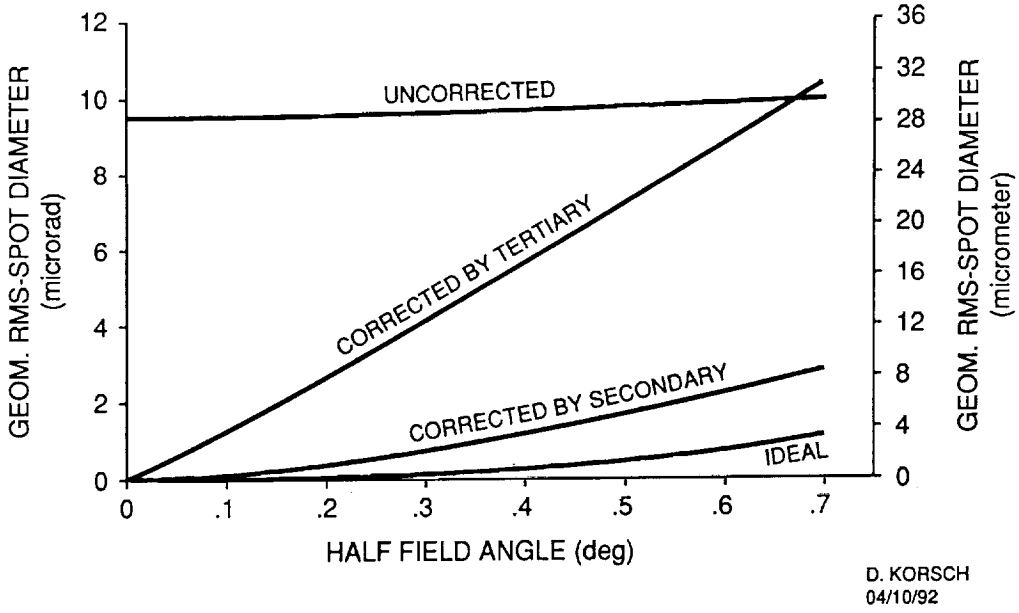

Figure 37. Primary figure error (negative deformation).

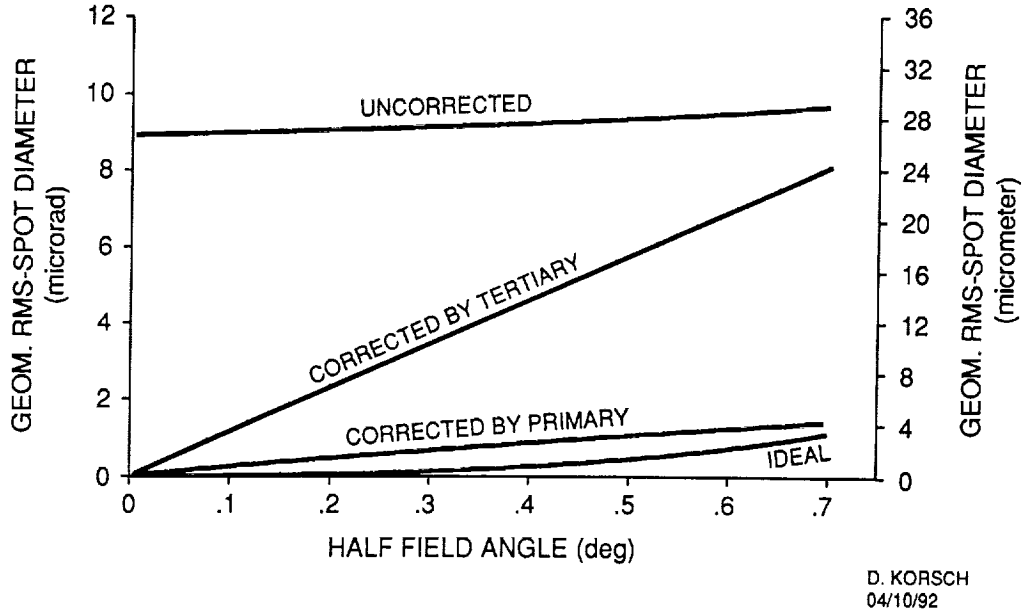

Figure 38. Secondary figure error (positive deformation).

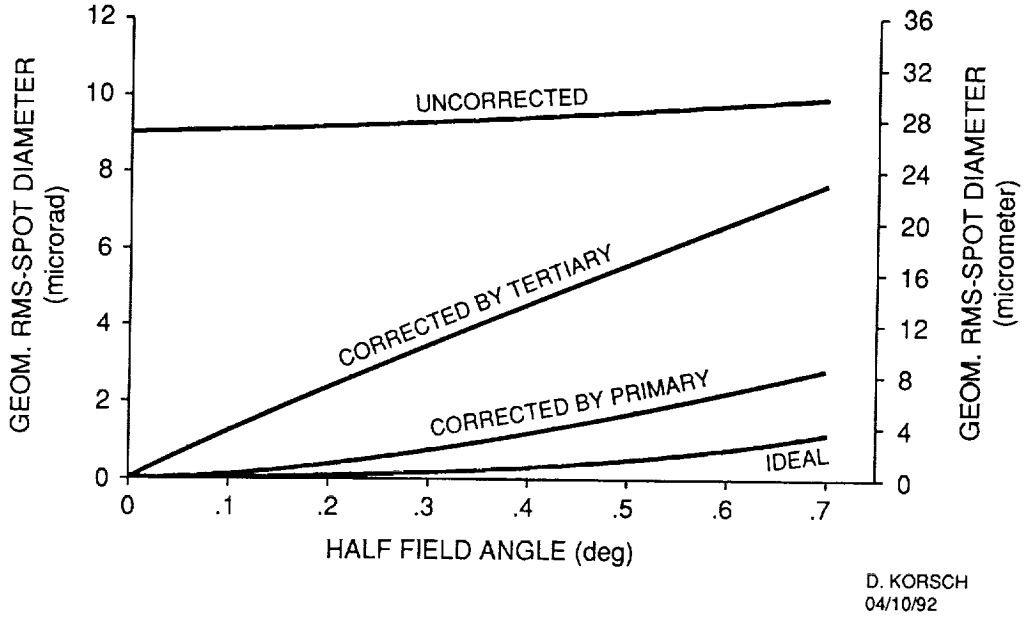

Figure 39. Secondary figure error (negative deformation).

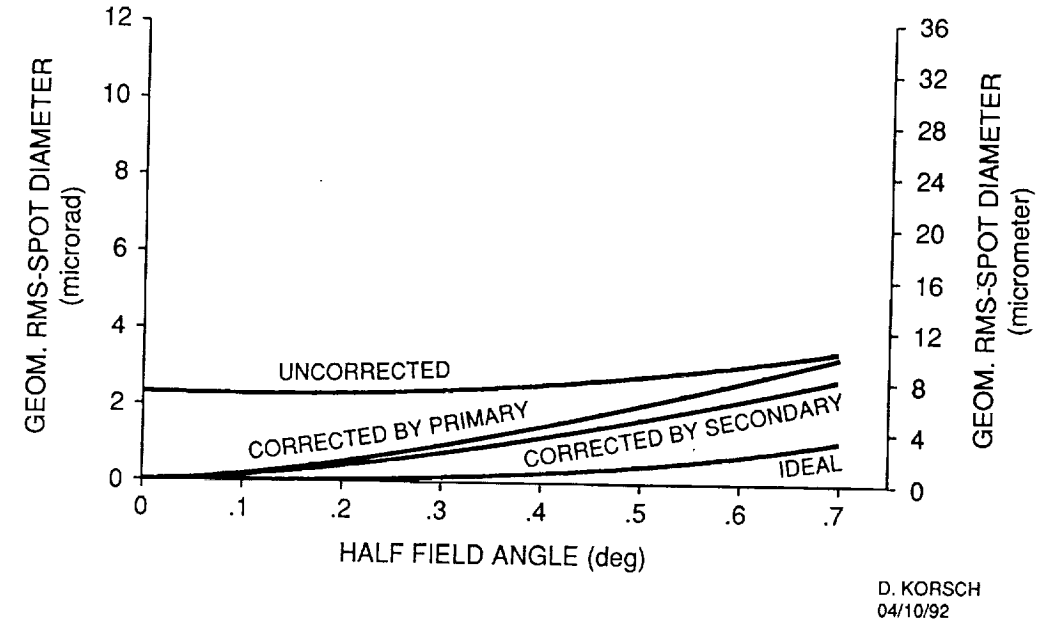

Figure 40. Tertiary figure error (positive deformation).

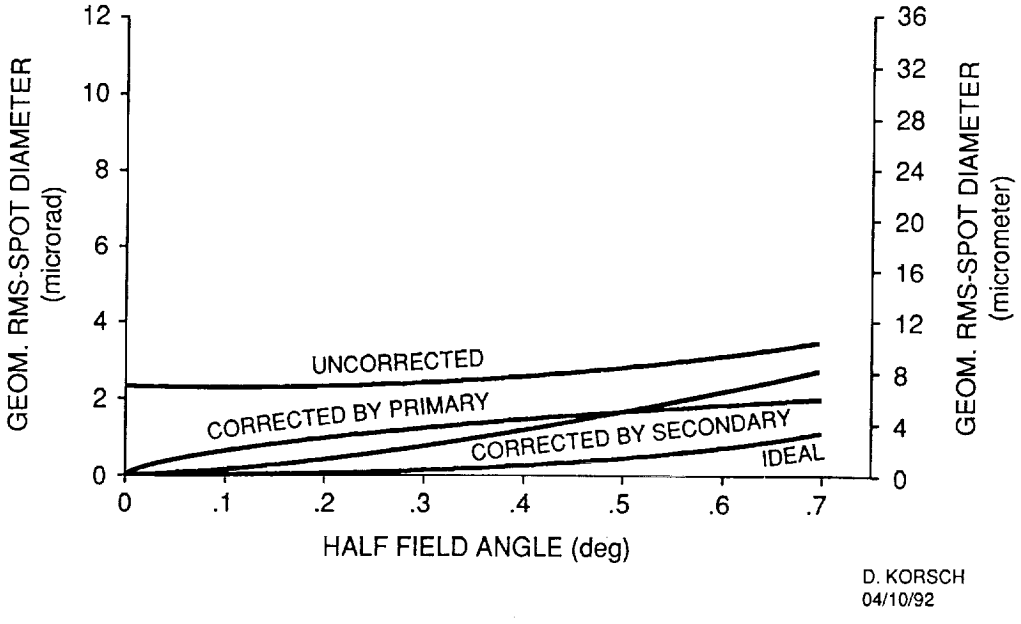

Figure 41. Tertiary figure error (negative deformation).

mirror away from the nominal position, and as a mechanical distortion of the mirror, if the forces are not isolated by the use of an appropriate mount-ing scheme that supports the mirror in a stress-free condition.

The thermal distortion of the LUTE mirrors can be divided into two cases: so-called "bulk" temperature effects and effects caused by temperature gradients across or through the mirrors. Bulk temperature effects will be considered first, since they are simpler to understand.

Bulk effects arise from temperature changes of the entire mirror substrate, hence the term "bulk." A two-step process is used to assess the effect of bulk changes on the optical performance. First the effect on mirror shape is determined, then this result is used to assess the impact on overall image quality. Also, this procedure does not admit to any inhomogeneity in the CTE.

Effect on Mirror Shape—In general, any conic section (the curve resulting from the intersection of a plane and a cone) can be described mathematically by the following equation:

$$z(r) = \frac{\rho r^2}{1+\sqrt{1-(1+k)\rho^2 r^2}} , \tag{5-1}$$

where

ρ = vertex curvature = $1/R$

r = radial coordinate = $\sqrt{x^2+y^2}$

k = conic coefficient

$z(r)$ = sag (vertical displacement).

The coordinates used here are those of a right-handed system with the optical axis oriented along the z-axis of the coordinate system.

The conic coefficient k determines the type of surface (sphere, parabola, ellipse, or hyperbola). The range of values for each of these types of surfaces is listed as follows:

Conic Coefficient	Type of Surface
0	Sphere
$-1 < k < 0$	Ellipsoid
-1	Paraboloid
<-1	Hyperboloid

It is possible for k to be positive. In this case, an oblate ellipsoid is obtained, however this surface is not a conic section. For the LUTE, all the surfaces have conic coefficients <-1, thus all the surfaces are hyperboloids.

When the temperature of a piece of material changes, in general its dimensions will change as well. Let α denote the ratio of lengths at the two temperatures. Define two new variables r' and z', related to r and z by $r' = \alpha r$ and $z' = \alpha z$. Substituting these expressions into the equation of the surface and doing a few lines of algebraic rearrangement, the following result is obtained:

$$z'(r) = \frac{\rho' r'^2}{1+\sqrt{1-(1+k)\rho'^2 r'^2}} \quad , \tag{5-2}$$

where $\rho' = \rho/\alpha$.

The effect of contraction (or expansion) of the mirror substrate material is to change the vertex curvature without any effect on the conic coefficient, so that a parabola remains a parabola, a sphere remains a sphere, and a hyperbola remains a hyperbola with the same conic coefficient.

To apply this result to the LUTE optical system, it is first necessary to determine the change in curvature of each of the mirrors. This will be a function of the total expansion of the mirror substrate material. The results are summarized in the following:

Element	Design Vertex Radius (cm)	Beryllium	ULE
α		0.99875	1.000020
Primary	+200.00	+199.75	+200.004
Secondary	–88.064	–87.9539	–88.0658
Tertiary	+338.00	+337.5775	+338.0067

5.1.4 LUTE Sunshade/Light Baffle

5.1.4.1 Methodology

The primary tool used for stray light analyses of the LUTE was the APART™ computer code from Breault Research Organization. This code is the industry standard for straylight analysis. However, the code requires a more detailed description of the system being analyzed (optics, baffles, vanes, etc.) than had been defined during the phase A effort. Therefore, in order to complete the analyses, some assumptions were made, such as the size and shape of the truncated conical baffles, the absorptive coatings used on the baffles, and the surface finish of the mirrors.

5.1.4.1.1 Baffle Design

The truncated baffles were designed to reduce the maximum amount of straylight without blocking any of the desired signal radiation. The main baffle is a right circular cylinder with 4 cm deep baffle rings spaced 10 cm apart. It is located around the outside of the primary mirror. The truncated conical baffles are the secondary, tertiary, and detector baffles. These enclose the secondary mirror, tertiary mirror, and detector, respectively. The dimensions of these baffles (cm) are summarized in the following:

Baffle	Inner Base Radius	Outer Base Radius	Tip Radius	Height
Main	50.00	50.00	50.00	65.00
Secondary	19.25	20.00	24.21	10.75
Tertiary	18.66	18.66	16.28	34.32
Detector	6.00	7.50	6.48	18.38

The orientation of the baffles and mirror surfaces are shown in figure 42.

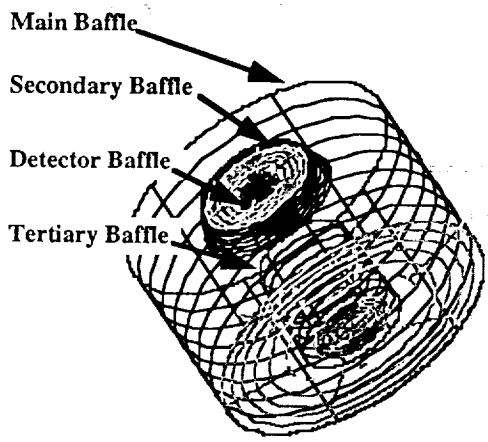

Figure 42. Baffle designs for LUTE.

5.1.4.1.2 Baffle Coating

Two coatings from the APART™ library, IITRI, and Ebinol C, were evaluated as candidates for coating the baffles. IITRI is an experimental conductive black coating developed by the Illinois Institute of Technology Research Institute. It consists of a silica-graphite pigment in an elastomeric silicone binder. Ebinol C is produced by a process that makes black cupric oxide coatings on copper and on copper alloys containing 65 percent or more copper. Ebinol C is chemically and thermally stable, while IITRI has been reported to have problems with debonding. The Ebinol C performed better than IITRI in absorbing stray radiation.

5.1.4.1.3 Mirror Finish

One of the most important elements in any stray light evaluation is the surface finish of the mirrors, typically expressed in terms of the bidirectional reflectance distribution function (BRDF). A BRDF was assumed such that the magnitude was 0.001 at an angle of 0.57°, with a roll-off exponent of –2. The BRDF at other angle is given by

$$\mathrm{BRDF} = 0.001*((\beta-\beta_0)/0.01)^{-2},$$

where β and β_0 are the direction cosines of the position vector of the observation point and the position vector of the specular reflection vector. Alternatively, β and β_0 can be defined as the sines of the angles of observation and reflection with respect to the surface normal. The values assumed for the BRDF are values typical for mirrors with "normal" levels of contaminants.

5.1.4.2 Results

To reduce the amount of stray light in a system, the primary sources of light scattering must first be determined. The most effective and practical way to do this is to determine the critical objects and illuminated objects. Critical objects are those objects which the detector can "see," either directly or through a mirror. For the LUTE design, the critical objects are the mirrors, the detector conical baffle, the inside of the secondary and tertiary conical baffles, the main baffle, and the struts supporting the secondary mirror assembly. Illuminated objects are those components which are directly illuminated by

an outside source of radiation. In the LUTE, the illuminated objects are the light shade, the struts supporting the secondary mirror assembly, the main baffle, the mirrors, and the outside of the secondary and tertiary conical baffles.

Stray radiation enters the detector by scattering from the illuminated objects to the critical objects, and then scattering from the critical objects to the focal plane. Each time the light scatters from an object, it loses some amount of energy. Scatter paths, which include more than two (nonmirror) surfaces, usually lose too much energy to be considered further. If a critical object is also an illuminated object, then stray radiation can reach the detector in a single scatter. These direct scatter paths usually contribute the most stray light in the system. For the LUTE design, the critical objects that can be directly illuminated by outside sources are the main baffle, the support struts, and the primary mirrors.

The APART™ code determines the power scattered to the detector for various off-axis angles. The power is relative to a plane wave irradiance of 1.0 W/cm^2 at the primary mirror. On-axis the total power entering the system would be 5,890.5 W. This is useful for comparing the scattered light power to the power from the object being observed. For instance, a point source at an angle 2° off-axis, just slightly outside the field view of the LUTE instrument, would scatter 0.000597 W of radiant energy to the detector. This is $1.01*10^{-7}$ times the amount of energy this same source would transfer if it were on-axis. The total power scattered to the detector as a function of angle is shown in figure 43. The individual contributions of five components of the system are also shown. Each of these components is the dominant scattering source at some off-axis angle.

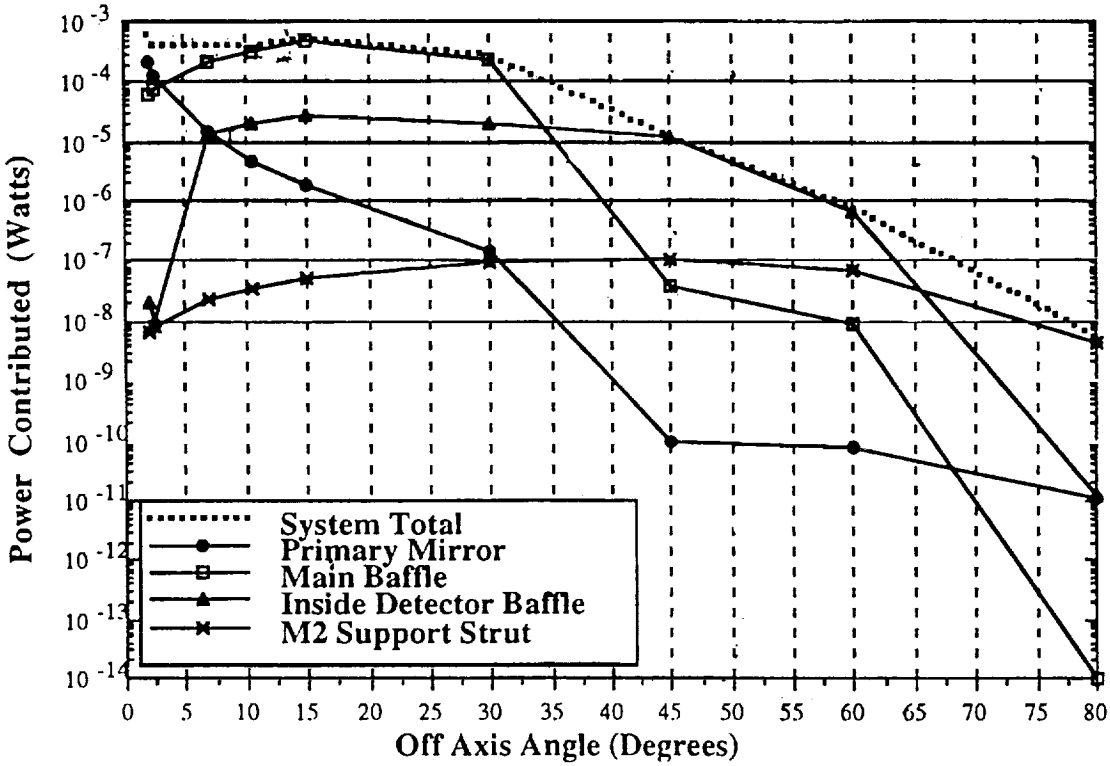

Figure 43. Power scattered to detector.

5.1.4.3 Future Analyses

The baffle designs and coatings used in this analysis should not be considered as the best possible design, but are instead a "first-cut" of how the baffles could be designed. As the design for the instrument evolves and matures, further analyses would be needed to determine the optimum baffle design, vane structure, coating material, and optical layout. It is possible that a few internal vanes on the detector and tertiary conical baffles might further reduce stray light levels. Scatter from the main baffles is primarily due to edge scatter from the vanes, so a restructuring of these vanes might be effective in reducing the scattered light. In addition, alternate coatings should be identified and coating properties measured in the UV. If the optical configuration changes, then baffle design would need to be adjusted for that configuration.

Because the mirrors are critical elements for stray light reduction, it is important that they remain as clean as possible since contamination will degrade the BRDF of the mirrors. This effect is more pronounced in the UV since any particulates that collect on the surfaces of the mirrors will be large compared to the wavelength of the light. An estimate of the particulate contamination of the mirrors should be made and that value used in the stray light analysis of the mirrors.

5.1.5 Error Budget

Figure 44 presents the preliminary wavefront error budget. For each of the mirrors, an accuracy of 1/50th wave (0.02) at the helium-neon laser wavelength of 6,328 Å was assumed (all wavefront errors are rms at 6,328 Å, unless otherwise noted). For reference, the HST primary mirror was polished to an accuracy of 0.017 (≈1/60th wave), as was the Itek demonstration mirror that is currently being used in the CDD transit instrument (CTI). Alignment errors were assumed to contribute about 1/50th wave per surface to the error budget, and a residual wavefront design error was assigned a value of 1/50th wave. This is somewhat less than the error shown by the code V runs, but it is possible the design can be improved somewhat. An error of 1/100th wave was assigned to uncertainty and noise in measuring the individual optics and the overall assembly.

Provision is made to include the effect of light scattered by dust or other contaminates which may collect on the surface of the optics. The effect of dust on the optical performance will be to increase the amount of scattered light, which will reduce the contrast ratio of the stellar images. This is equivalent to moving light energy from the central portion of the focused spot and redistributing it to the outer portions of the image spot in a manner very similar to wavefront errors introduced by imperfect optics and/or imperfect alignment. At this time, there is no accurate estimate of the level of scatter that can be expected due to dust collecting on the mirror surfaces.

The environmental errors are listed as TBD. Although several cases for thermally distorted optics have been analyzed, these analyses have only considered the primary mirror, and have not included any effects due to the secondary and tertiary mirrors or to distortion of the optical metering truss.

Independent analysis by Hughes Danbury Optical System (HDOS) and Litton Itek Optical Systems show that the thermal excursions must be controlled in order to avoid active optics (appendix L).

The various error terms are combined together in a root-sum-squares (rss) manner. This is appropriate if the sources of error are not correlated, which is likely to be the case for polishing and alignment. For thermally induced errors, correlation between terms would be likely, so the errors should be added together.

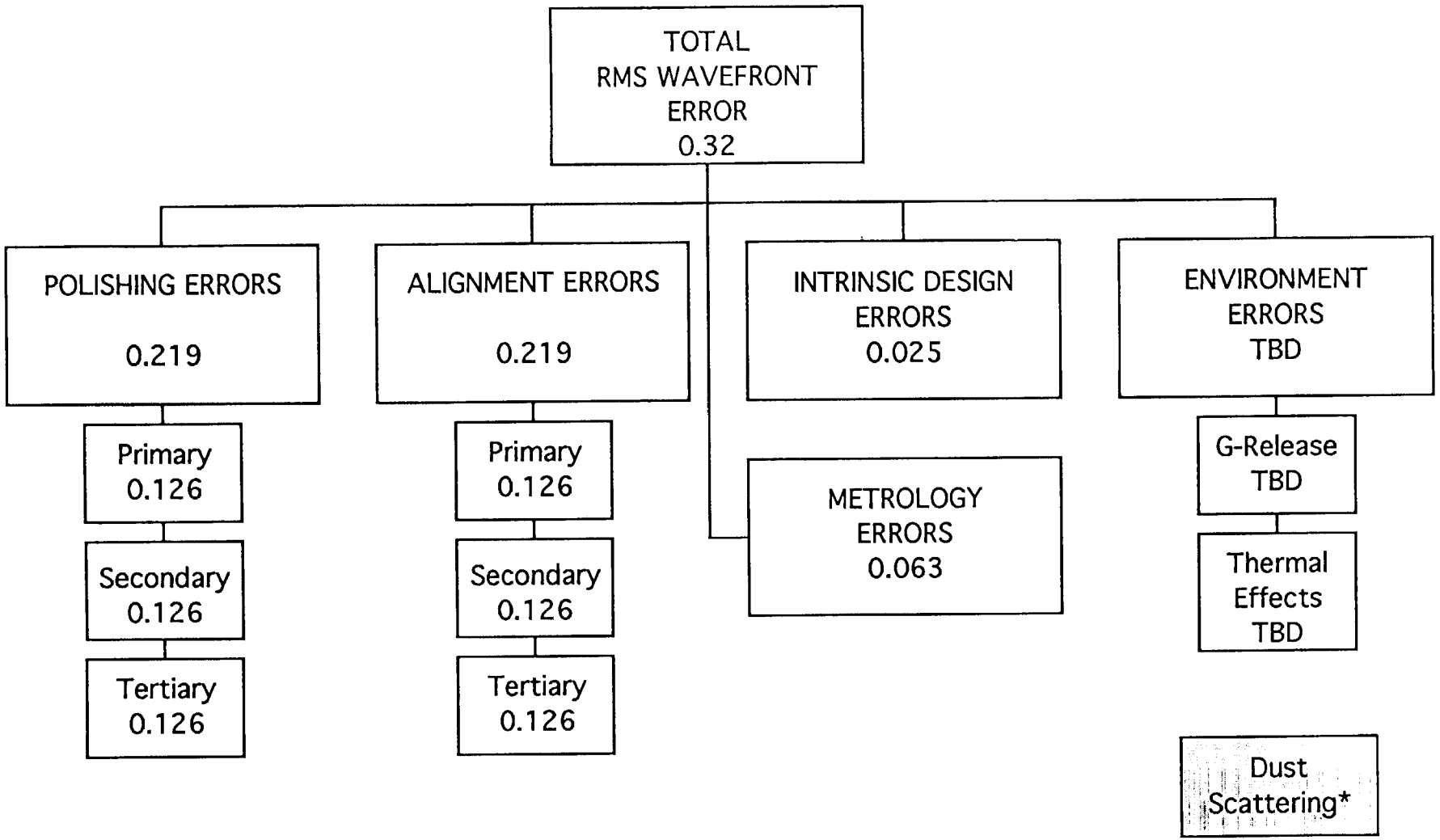

Figure 44. LUTE wavefront error budget.

Considering only the quantities for which there are numerical estimates, the total rss wavefront error is about 0.05 (about 1/20th wave) at 6,328 Å, which would be considered diffraction-limited (anything better than about 1/14th wave is considered diffraction-limited). But this number must be multiplied by 6.328 to determine the wavefront error at 1,000 Å, which gives a value of 0.317 wave, which is not diffraction-limited. When the effect of distorted optics is included, the total wavefront error will become larger.

5.1.6 900 cm Effective Focal Length (EFL) Optical System

The LUTE focal plane detectors are envisioned to be CCD photodetector arrays, clocked at the lunar sidereal rate. Current microelectronic technology can produce CCD's whose individual photodetectors are approximately 7 μ square. An extension of this technology may produce CCD's with 5 μ square pixels. Even using these smaller pixels, the basic resolution of the LUTE will be set by the pitch of the CCD's, not by the resolving power of the optics themselves. This is equivalent to stating that the available detector arrays do not make use of the resolution of the telescope optics. It can be shown that in order to fully utilize the resolving power of the telescope, there should be four pixels spanning the Airy diameter. For the LUTE, this would require a pixel pitch of less than 1.0 μ. Since CCD's with pixels this small are unlikely to be available in the foreseeable future, the only other avenue available to increase the angular resolution of the LUTE is to increase the system focal length. This approach has the disadvantage that the angular coverage is reduced in proportion to the increase in focal length if the overall dimensions of the focal plane array are held constant. The tradeoff between angular coverage and resolution and the quality of the science that can be obtained is discussed elsewhere.

It can be shown that the EFL of the optical system is equal to the product of the primary mirror focal length, the secondary mirror image magnification, and the tertiary mirror magnification. The existing D. Korsch optical design has a primary mirror focal length of 100 cm, a secondary mirror magnification of –4.875, and a tertiary mirror magnification of –0.6154, yielding an effective focal length of 300 cm.

The approach taken to increase the EFL was to hold the primary mirror focal length constant at 100 cm. This approach was used because the overall length of the telescope was constrained to be as short as possible, so that the experiment would fix within the launch vehicle payload shroud and so that the CG of the experiment would be as low as possible, to minimize the possibility of the experiment tipping over on uneven terrain.

As before, the EFL of the optical system is the product of the primary focal length, the secondary magnification, and the tertiary magnification. Since the primary focal length has been maintained at 100 cm, the product of the secondary and tertiary must be ±9 so that the product of primary focal, secondary magnification, and tertiary magnification is 900 cm. The relationship between magnification, mirror spacing, mirror curvature, and the back focal distance is given by the following expression:

$$m = m_s \cdot m_t = \frac{(i_s \cdot i_t)}{(o_s \cdot (dsd - i_s))} \quad , \tag{5-3}$$

where

i_s = secondary image distance

i_t = tertiary image distance

o_s = secondary object distance

dsd = primary-to-secondary distance.

The relationship between o_s, dsd, and the focal length of the primary mirror, f_p, is given by:

$$o_s = dsd - fp\,. \tag{5-4}$$

Although the original design had a back focal distance of 65 cm to match the primary-secondary and secondary-tertiary distances, there could be some advantages for detector cooling to making the back focal distance larger, thus placing the image surface higher to avoid thermal radiation from the sunshade.

The solution of this equation for a 900 cm EFL gives secondary and tertiary curvatures of –0.00818 and –0.02189 cm^{-1}, respectively. Compared to the 300 cm EFL design, the secondary is somewhat flatter, but the tertiary is much more steeply curved. Also, both elements are now convex, whereas before, the secondary was convex, but the tertiary was concave.

Of much greater concern is the strong curvature of the image surface. This is due to the strong convex shapes of the secondary and tertiary mirrors, which are not offset by the relatively weaker positive curvature of the primary mirror. Generally, as the discussion in section 5.2 will indicate, focal surface curvature can be accommodated by "mosaicking" the focal plane with sensors chips, at the expense of a more complicated design and fabrication procedure. The curvature of the focal surface in this case (radius ≈19 cm) is such that the CCD's would be prohibitively small, so that it does not appear that a 900 cm EFL instrument with 65 cm vertex spacing is feasible.

5.1.7 Resolution Versus EFL and Pixel Size

The formal resolution of the LUTE instrument is a function of two factors: the EFL of the telescope optics and the pixel pitch of the CCD's. Figure 45 shows this relationship in tabular form. The baseline pixel pitch is 5 μm, and the baseline focal length is 300 cm, yielding a resolution of 0.68 arcsecond. However, it is not certain that 5 μm pixel CCD's will be available for the LUTE. In that

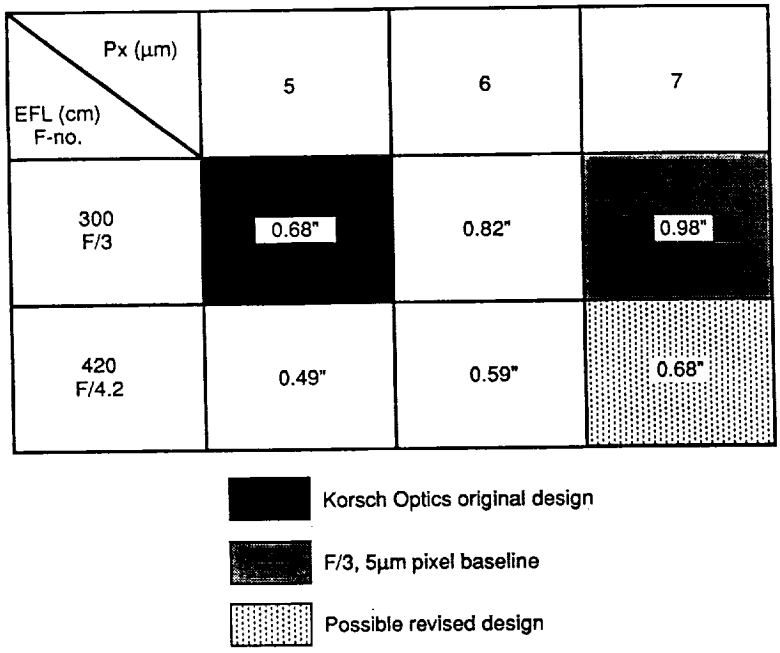

Figure 45. Resolution (arcsecond) versus EFL and pixel size.

case, CCD's with larger pixels may have to be used. If the baseline optics are retained, then the formal resolution of the instrument will become 0.98 arcsecond. One approach to maintaining the resolution of the instrument would require increasing the focal length by a factor of 7/5, to 420 cm. However, the diameter of the primary mirror would need to remain at 100 cm due to the physical space constraints imposed by the launch shroud. Thus, the f-number of the telescope would increase from f/3.0 to f/4.2.

The preceding discussion indicates that regardless of whether 5 or 7 μm pixel CCD's are used in the LUTE instrument, the resolution will be determined by the size of the detector pixels, not by the resolving power of the optics.

5.2 LUTE Focal Plane Array (FPA)

The sensor array for the LUTE uses an array of frame transfer CCD optical detectors which convert the optical image formed by the optical system into electronic charges. These electronic charges are subsequently converted to digital form and transmitted to Earth for storage and analysis. For a more detailed description of CCD operation, consult one of the standard texts on CCD's, such as reference 16. Figure 46 gives an overall view of the FPA architecture.

The technique used to acquire the star field image is termed drift scanning, since the telescope is pointed in a fixed direction and the star images appear to drift across the focal plane in an east to west direction due to the rotation of the Moon. This approach is shown schematically in figure 47. If the CCD's are aligned so that the rows of pixels run east and west, and the CCD is clocked at the apparent sidereal rate, the electronic charge image of the star field will remain exactly fixed under the optical image. This prevents blurring or smearing of the image, and allows a longer image integration time, thereby improving the overall sensitivity of the detection process. The process of synchronizing the motion of the optical and electronic images is referred to as TDI.

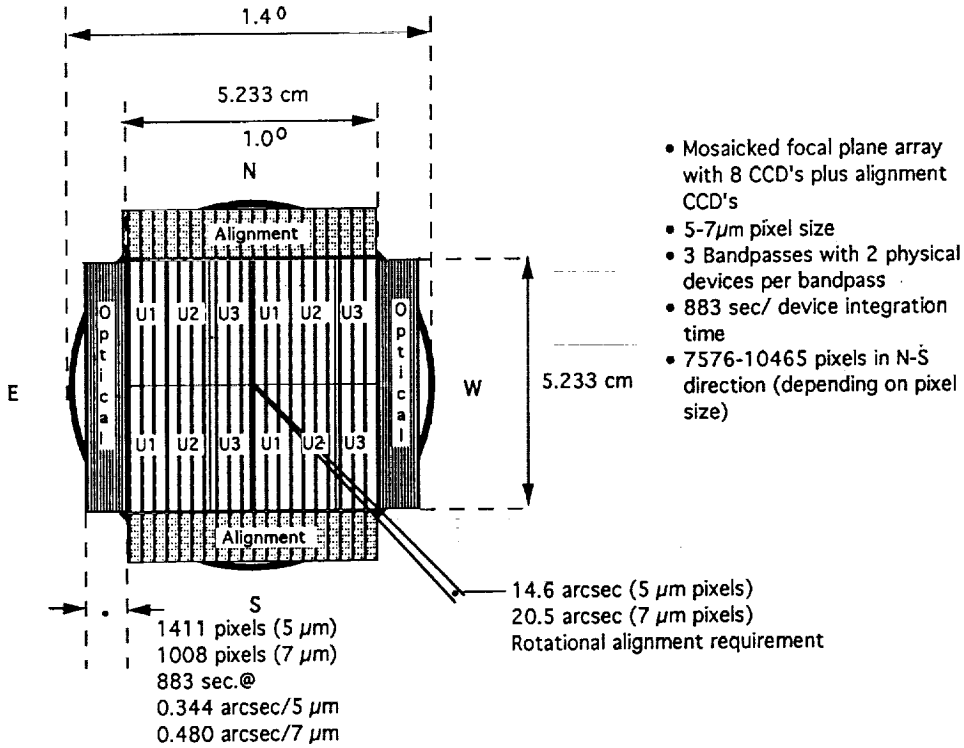

Figure 46. LUTE focal plane CCD array.

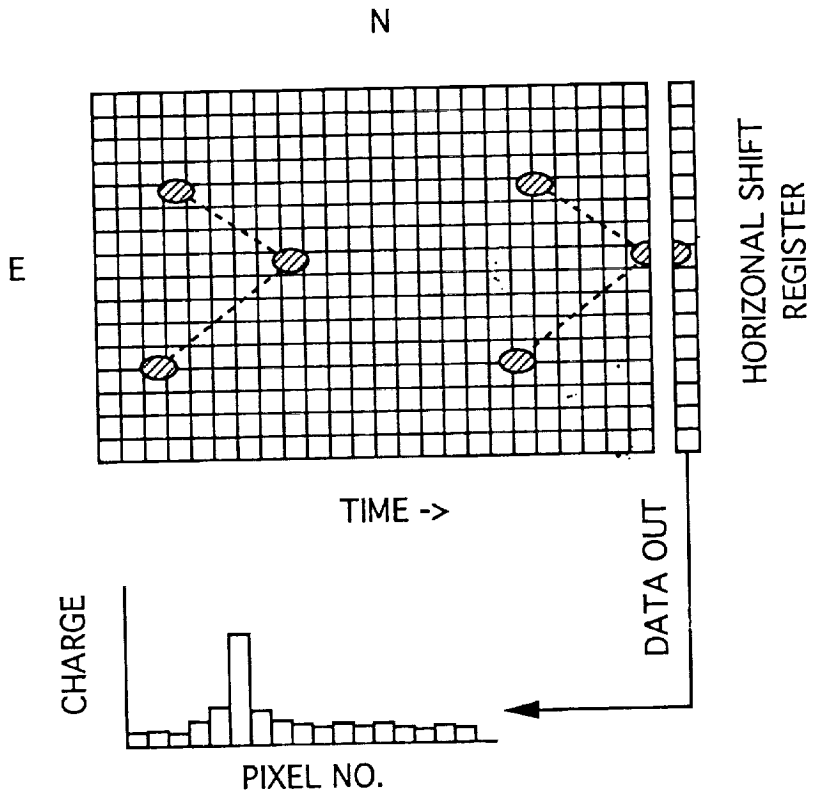

Figure 47. Schematic representation of CCD/TDI technique.

As the charge image reaches the western edge of the CCD, the accumulated electronic charges are transferred into an analog shift register, and then sequentially shifted into the output amplifier. The amplifier output is digitized (16 bit resolution) and the resulting data are transferred to the C&DH system for transmission to Earth. For additional details on this observational technique.[17,18]

Although the preceding description has discussed using CCD's as the sensing element, alternate approaches exist. One alternate approach to conventional CCD's would be photon counting detector arrays, although much development work remains before these devices will be mature enough for use. Yet another approach is the use of active-pixel devices now under development in the U.S. and Japan.[19] This technology, which is still in the early stages of development, might allow area-of-interest image processing which would greatly reduce the bandwidth required to return the data to Earth.

There are a number of items that must be considered in the detailed design of the FPA. These items are:

(1) Curvature of the focal "plane"

(2) Curved star trails

(3) Pixel size (focal length, resolution, etc.).

(1) Curvature of the focal plane—The baseline LUTE optics were designed to have negligible curvature of the image surface so that flat CCD's can be used without an undue amount of image blurring due to defocus. If the CCD's used in the FPA are no more than 14 by 14 mm, then a focal surface radius of curvature ≥100 cm results in only a small increase (≈1 μm) in the image spot of light from a point source. If larger sensor chips are used, then the minimum permissible image surface radius of curvature is correspondingly larger. For example, a sensor 20.5 by 20.5 mm (corresponding to an array of 4,096 by 4,096 pixels at a 5 μm/pixel pitch) would require that the focal surface radius of curvature be greater than 215 cm, which is flatter than the existing baseline design. Sensor chips of this size therefore could not be used unless: (a) the optical design was altered to produce an image surface with less curvature, or (b) the image quality requirements were relaxed somewhat.

Even though the departure of the image surface is negligible over the dimensions of an individual sensor chip, over the diameter of the entire focal plane the deviation is appreciable (≈417 μm at the edges of the FPA). This amount of curvature can be accommodated by building up the FPA as a "mosaic" of CCD's which conforms to the approximate shape of the focal surface. Alignment of the individual CCD's on the focal plane has been addressed by other researchers and is a manageable task.[20] Deforming the CCD's in two dimensions, such as is done with the film for a Schmidt camera, is a technique whose feasibility is unproved.

As an alternative to the focal plane mosaic approach, a fiber optic field flattener might be interposed between the image surface proper and the CCD's. This approach has been used to convert and detect x rays and is shown in figure 48. The drawback to this approach is limited resolution. Since the fibers typically must be in the 4 to 6 μm diameter range, the spatial resolution in the focal plane cannot be any better than this. Other unknowns are possible resolution degradation introduced by the conversion phosphor, and questions regarding the durability of the phosphor in ground handling, during launch, and in the lunar environment. These questions and others must be satisfactorily answered before this approach could be selected.

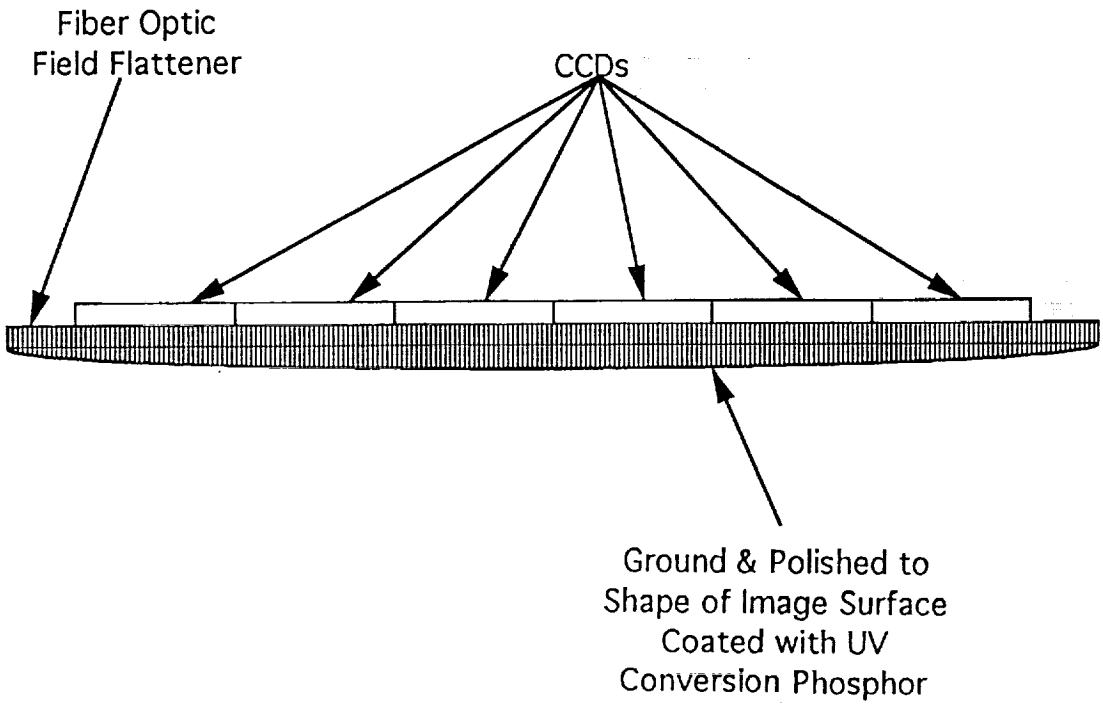

Figure 48. Fiber optic field flattener and UV converter.

(2) Curved Star Trails—As the Moon rotates on its axis, the FOV of the LUTE instrument sweeps across the lunar sky. As a star moves into the FOV, its image on the telescope focal plane moves along a slightly curved path. The exact amount of curvature of this path depends on the pointing declination of the telescope's optical axis and the declination of the star. The star image track on the focal plane is a portion of an ellipse for viewing declinations greater than 45°, a parabola for a viewing declination equal to 45°, and a hyperbola for declinations less than 45°. These curved star tracks can be precisely described by mathematical expressions modified only by distortions in the telescope optical system.[21 22] The practical consequence of this is that "standard" CCD's, with a rectilinear arrangement of pixels, will not align properly with the curved star image tracks, resulting in an image mistrack, or "smear," from one horizontal row of pixels to the adjacent row. This would degrade the resolution of the instrument and, to some extent, defeat any sensitivity gain from the TDI scheme. This difficulty will be exacerbated as the resolution of the telescope increases (either smaller pixels or longer focal length or a combination of both).

One possible solution to this difficulty is to fabricate custom CCD's with the rows of pixels laid out on curved tracks. In principal the curvature of the tracks can be adjusted so that the star images remain exactly centered on the row of pixels. The principal drawback to this approach is the higher costs associated with custom CCD's, since each chip will need to be designed for a specific location on the focal plane. Another drawback is the extreme pointing accuracy and alignment requirement for the telescope with a detector that has been designed for star track curvatures corresponding to a specific declination. Pointing accuracy ranges are typically a few arcseconds.

(3) Pixel Size—In addition to the consideration discussed in the preceding paragraphs regarding the apparent necessity of having curved rows of CCD pixels, there are tradeoffs on the size of the CCD pixels themselves. As discussed previously, the size of the pixels influences the angular resolution of the LUTE telescope. The pixel size also influences the dynamic range of the instrument, since pixel size and full well capacity (number of photoelectrons that can be stored and transferred along the row of pixels) are related. At the same time, readout noise is relatively independent of the pixel size or well capacity and sets the lower limit on detectability. At the present time, commercially available CCD's have minimum pixel sizes around 7 μm, with full well capacities on the order of 60,000 e^-. Fabrication of CCD's with smaller pixels is possible, and could be pursued in parallel with efforts to develop CCD's with curved tracks. The challenge will be to maintain good device yield and reasonable full well capacity as the size of the pixels is reduced.

5.3 Structural Trades and Analysis

The LUTE structural reference design, described in section 4.2.3, evolved through analyses and trade studies described below. A combination of hand calculations, simple and detailed I-DEAS™/FEM models, and consultation with vendor representatives were used to develop and evaluate options for the LUTE structural systems. Table 11 summarizes the trade studies that were performed.

Structural analyses in this section compare temperature effects on structures, mirror support trades, primary mirror material trades, metering structure design options, light shade construction trades, and aperture cover design options. The effects of mirror material selection on other structural telescope components are also given.

Table 11. Summary of structural trade studies.

Structural Components	Trades	Options	Analysis
Mirrors	Temperature effects.	Bulk temperature, axial gradient, diametral gradient.	Hand
	Athermalization.	Baseplate-optics ΔCTE from 0 to 11.3 ppm/K.	I-DEAS™/FEM
	Substrate trades.	One-piece versus separate mirrors.	Vendor (HDOS)
	Construction trades.	Closed back, open back, meniscus, single arch.	Vendor (HDOS)
	Material trades.	Thermal deformations: Be, SiC, fused silica.	I-DEAS™/FEM
	Tilt from 0° to 90°.	Deformation due to lunar gravity.	I-DEAS™/FEM
Mirror support structure	Support concepts.	Outer, inner, bottom three-point mounts.	I-DEAS™/FEM
	Support stiffness.	Flexure stiffness k = 0.01 N/m to ∞.	I-DEAS™/FEM
Metering structure	Design concepts.	Seven options identified for trade space.	
	Material trades.	Thermal deformations: Be and Gr/Ep cylinders.	Hand
Light shade	Construction trades.	Varied skin thickness and number of stringers.	Spreadsheets
Aperture cover	Mass versus thickness.	Assumed aluminum, compared to historical data.	Hand
	Alternate designs.	Two fabric/mylar concepts identified for trade space.	
Baseplate	Athermalization.	Baseplate-optics ΔCTE.	I-DEAS™/FEM
	Material trades.	Stress: beryllium, graphite/epoxy, titanium.	I-DEAS™/FEM
	Interface reactions.	Loads with 40° site mount. 65° site mount TBD.	I-DEAS™/FEM

Definitions—The structural terms "allowable strengths" and "stress margins of safety" will often appear in the text. For clarity, these terms have been defined below, as they are used in the structural documentation.

$$\text{allowable strength} = \sigma_{\text{allowable}} = \text{material yield strength/safety factor} \qquad (5\text{-}5)$$

$$\text{stress margin of safety} = \text{M.S.} = (\sigma_{\text{allowable}}/\text{calculated stress}) - 1 \ . \qquad (5\text{-}6)$$

For stress margin of safety, positive values indicate a safe design while negative values indicate structural failure.

5.3.1 FE Models

The reference structural design and geometry is described in section 4.2.3, Baseline Structural Design. This section shall briefly describe some of the FE models that were generated from this geometry.

Primary Mirror—The reference primary mirror FE model has 192 nodes. Mesh increments are 6 cm vertically, 15° circumferentially, and 8.33 cm radially. There are 240 elements in the model. Faceplates are thin-shell linear quadrilateral elements, and the mirror's sandwich core is modeled with solid linear bricks. To approximate the sandwich construction, the solid elements were assigned a

density equal to 5.3 percent of the material's normal value to simulate the sandwich cell mass and a Young's modulus equal to 3.5 percent of the material's normal value to simulate the honeycomb's stiffness.[23]

Metering Structure—The metering structure model has 149 nodes. There are 125 elements in the model: 8 rods for the metering truss tubes, 104 thin-shell linear elements, and 13 lumped masses for inertial loading. The lumped masses represent the secondary mirror, science instrument, etc.

Electronics Box Support Structure—The structure was modeled as an aluminum truss with 8 nodes, 11 circular rods, and a 1 cm thick electronics box shelf.

Baseplate—There are 650 nodes in the FE model. In addition, there are 1,054 elements in the model: 648 thin-shell linear elements for the faceplates and 324 solid elements for the honeycomb core. For preliminary design, the solid elements were assigned a density equal to 10 percent of the material's normal value to simulate the sandwich cell mass and a Young's modulus equal to 3.5 percent of the material's normal value to simulate the honeycomb's stiffness.

Integrated Structural Model—Table 12 lists the number of nodes and elements in the model.

Table 12. Finite elements in structural model.

Component	Nodes	Elements						
		Lumped Masses	Springs	Rods	Beams	Thin Shells	Solids	Total
Integraded FE model	1,339	79	6	19	408	1,269	396	2,177
Baseplate	650					648	324	972
Primary mirror	192		6			168	72	246
Secondary mirror	–	4						4
Tertiary mirror	–	3						3
Primary baffle	–	36						36
Secondary baffle	–	4						4
Detector	–	1						1
Radiator	–	4						4
Metering structure	149			8		104		112
Light shade	360				408	348		756
Aperture cover	–	24						24
High-gain antenna	–	1						1
Electronics box support	8			11		1		12
Electronics box	–	2						2

5.3.2 Requirements and Loads

The requirements used in the structural trade studies are listed in the reference design chapter in section 4.2.3.1. The LUTE is currently designed to launch on an Atlas IIAS, which imposes challenging mass and geometrical constraints. The baseline TCS, consequently, is designed to be passive. The baseline optical system is inactive with the exception of a focusing actuator on the secondary mirror cell. Operating in the lunar environment under these conditions imposes some substantial requirements on the

optical structures. Thermal data show that the lunar surface temperature can vary from 93 K at sunrise to as hot as 395 K at local noon during the 14 day lunar day/night cycle.[10]

Design Factors for Glass Structures—Some glass structures design information and safety factors appear in MSFC-HDBK-505. LUTE mirrors are to be qualified through analysis and testing of the flight hardware, a protoflight test. A summary of the minimum design factors for glass appears in table 13.

Table 13. Minimum glass design factors.

Glass Condition	Analysis Factor of Safety	Qualification Test Factor	Protoflight Test Factor
Nonpressurized (Analysis and Test)	3.0	N/A	1.2
Bonds for Structural Glass	2.0	1.4	1.2

Also specified in MSFC-HDBK-505, "the material strength allowables for adhesives shall meet the requirements of MSFC-STD-506" and "the material properties of glass shall meet the requirements of MSFC-STD-506."

Launch Vehicle Loads—Preliminary loads for the three LUTE/lander launch vehicle candidates of Atlas IIAS, Titan III/TOS, and Titan IV/Centaur can be found in their mission planner's guides. These loads include design load factors, acoustic environments, and shock response spectrum for the three launch vehicles. The Atlas IIAS has been chosen as the baseline launch vehicle for LUTE.

Random loads have not been identified for the LUTE/lander interface, and are to be accounted for in future analyses.

Random vibration levels are given for the payload to launch vehicle interface in General Dynamics's "Mission Planner's Guide for the Atlas Launch Vehicle Family," dated July 1990. Using the methods detailed in JA-418, "Payload Flight Equipment Requirements for Safety Critical Structures," NASA/MSFC, August 1984, and the natural frequencies listed for the baseline LUTE structure in section 4.2.3.12, random vibration load factors were derived to be 2.1 g's axially and 2.0 g's laterally for the overall system. A component-level random loads analysis must be performed in phase B.

Structural Load Paths—The structural load path diagram associated with the baseline LUTE design is drawn in figure 49.

The baseplate is one of the most important structural components of the LUTE, since all other LUTE structural components are affected by its performance. Likewise, the light shade and metering structure provide structural attachments for several components. The complexity of maintaining the spacing between the primary and tertiary mirrors with the secondary mirror is also evident, from the number of structural components through which loads must pass.

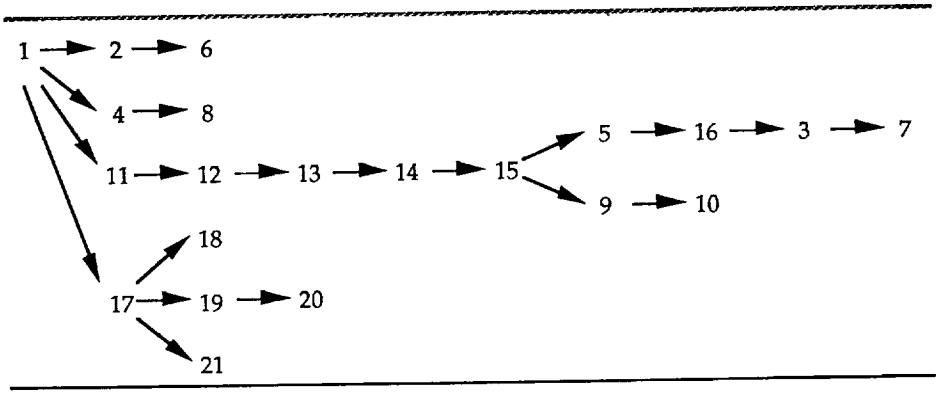

1 **Baseplate**
— **Mirror Supports**
— • Structure
2 - Primary flexures
3 - Secondary flexures
4 - Tertiary flexures
— • Control mech. (rigid body)
5 - Secondary actuators
— **Optics**
6 • Primary mirror
7 • Secondary mirror
8 • Tertiary mirror
— **Science Instrument**
9 • Detector support
10 • Detector

— **Metering Structure**
11 • Truss (or Cylindrical Shell)
12 • Outer hub
13 • Spider
14 • Inner hub
15 • Secondary mirror enclosure
16 **Thermal Isolation Plate**
17 **Lightshade**
18 **Aperture Cover**
— **Electronics**
19 • Electronics box support structure
20 • Electronics box
21 **High Gain Antenna**

(Baffles assumed to be non-load bearing)

Figure 49. Structural load paths for LUTE reference design.

5.3.3 Structural Material Selection

A detailed discussion of the candidate materials in the LUTE preliminary design appears in appendix J of this report. Although not included in this report but of great value in the LUTE phase A study, a data book was compiled from the literature search done in preparing the "LUTE Mirror Materi als Report" contained in appendix J. When selecting materials for LUTE structural components, low mass was an important requirement. Materials with high strength-to-mass ratios and high stiffness-to-mass ratios are desirable, unless other requirements, such as thermal deformation constraints or material-based athermalization designs, dictate otherwise. Table 14 lists the materials which were considered for LUTE structural components.

Table 14. Room temperature mechanical properties of candidate structural materials.

Material	Type	Density (kg/m^3)	YTS (MPa)	E (GPa)	Specific Strength [YTS/rho] (KJ/kg)	Specific Stiffness [E/rho] (MJ/kg)	CTE (ppm/K)	Poisson's Ratio mu (–)
Aluminum	2219-T81	2,823	330.9	74.5	117	26	22.14	0.33
Al-Li	2195	2,700	690.0	78.6	256	29	–	–
Al/SiC	Metal matrix composite							
Beryllium	I-250 (structural grade)	1,850	= 544.7	303.0	294	164	11.3	0.08
Graphite/Epoxy	GY70/934, ±12°	1,689	498.5	268.2	295	159	–0.54	–
Invar	36	8,080	= 248.2	= 144.0	31	18	0.00177	–
Titanium	Ti-5Al-2.5Sn	4,484	758.4	106.9	169	24	10.26	0.33
					high is good	high is good		

Room temperature material properties for the optical components of the LUTE are given in the primary mirror trade section, section 5.3.4.3. Temperature-varying properties for beryllium and SiC appear in appendix K.

Table 15 shows which candidate materials were selected for each structural component for the baseline design of LUTE, based on specific component requirements. The structural trade results responsible for many of these selections will be discussed with the component analyses.

Table 15. Structural material selection for baseline design.

Component	Material Candidates (ALL-CAPS were selected)	Section Rationale	Analysis Method
Optics	SILICON CARBIDE Beryllium Fused Silica	Minimize thermal deformations during lunar operations. Good UV performance	I-DEAS™/FEM and Model Solution.
Mirror Support Structure	GRAPHITE/EPOXY Titanium Berylliium Invar	Compatibility with mirror material. Minimize stress and deflections in the mirrors.	Hand analysis.
Metering Structure	GRAPHITE/EPOXY Beryllium	Low CTE to maintain focal length between optics.	Engineering judgment. I-DEAS™ FE models.
Optical Baffles	ALUMINUM Aluminum-Lithium Beryllium Graphite/Epoxy	Nonload bearing structures, wanted a cheap material, easy to manufacture.	Hand analysis.
Light Shade	ALUMINUM Aluminum-Lithium Graphite/Epoxy	Well-understood manufacturing process. Cheap. Technical simplicity.	PD22 spreadsheet analytical tool. I-DEAS™ FEM.
Aperture Cover	To be determined		Historical data for mass.
Electronics Box Support	ALUMINUM	Cheap, easy to manufacture.	Hand and FE analysis.
Power System Attachment	To be determined		
Telescope Baseplate	GRAPHITE/EPOXY Titanium Beryllium	Thermal distortion compatibility with optics. Optics-baseplate material athermalization desired.	I-DEAS™ FEM.

5.3.4 Mitigation of Mirror Deformations in Lunar-Based Telescopes

Structural design and analysis of the optical systems for lunar-based telescopes is a challenging task. A concern during this study was the degradation of the LUTE optical figure due to thermal deformations. In addressing this task, a multidisciplinary analysis process was developed, temperature effects were characterized, and primary mirror thermal deformations were calculated for use in the optical analyses. Trade studies evaluated the qualitative performance of various design schemes. Results indicate that statically determinant mirror supports with bottom-mounted flexures render less optical disturbance under thermal loading than mirror supports at the inner or outer periphery. Another trade

C-2

indicated that a telescope's baseplate should be athermalized with respect to the mirrors by matching thermal distortion coefficients. A comparison of three materials for the primary mirror indicated that SiC would be the best material for LUTE's operational environment.

5.3.4.1 Temperature Effects on Structures

Thermal data show that the lunar surface temperature can vary from 93 K at sunrise to as hot as 395 K at local noon.[10] During this 14 day lunar day/night cycle, thermal analysis predicts that the temperature of LUTE's primary mirror will vary from 65 to 265 K at 40° latitude, 0° longitude, which was considered early in the phase A final study. Operating in the lunar environment under these thermal conditions is very challenging, and a primary concern is the degradation of LUTE's optical performance due to thermal deformations.

A general understanding of the temperature effects on structures will provide some valuable insights to guide the design of lunar-based telescopes. To illustrate, the characteristic deformations of a beam under three basic thermal loads are sketched in figure 50.

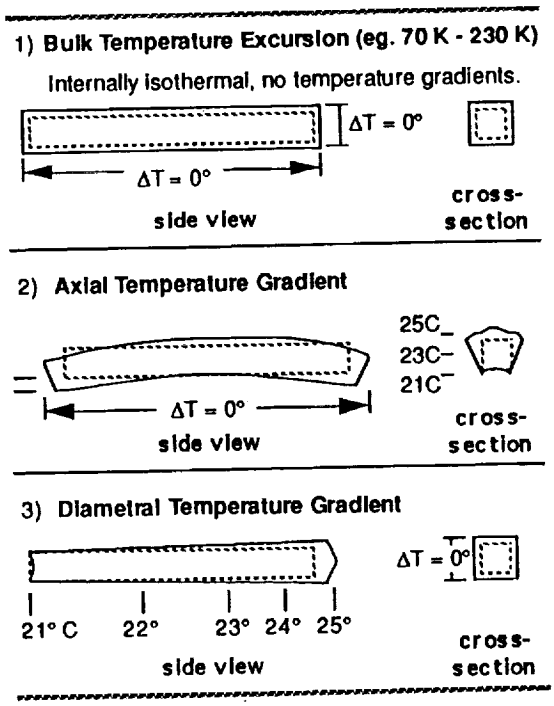

Figure 50. Temperature effects on a beam.

Hand analysis shows that a pure axial (through the thickness) temperature gradient is more significant than a pure diametral (across the span) temperature gradient in causing vertical deformation. For instance, in a beam with no constraints, having a span of l and a thickness of t, a diametral gradient of $[(l/t)^2/2]$ is needed to equal the vertical tip deflection caused by a 1 K axial gradient. If the beam had a span of 50 cm and a thickness of 6.6 cm, a 28.7 K diametral gradient would cause the same vertical tip deflection as a 1 K axial gradient.

Athermalization—Athermalization schemes may be material-based, geometry-based, or a combination of the two. This analysis will assume material-based techniques. Krim discusses the concept of athermalization in detail.[24] If care is not taken to athermalize lunar-based telescopes, bulk temperature excursions will drive the deformations. To illustrate, FE analyses with I-DEAS™ were conducted to evaluate the interaction between mirror thermal deformation and baseplate athermalization. A beryllium LUTE primary mirror was mounted to a baseplate via three flexures on the mirror's outside edge. The CTE of the baseplate was allowed to vary between 0 and 11.3 ppm/K (11.3 ppm/K equals the CTE of beryllium). The variation in baseplate CTE represented different candidates for the baseplate material selection. The thermal deformations of the primary mirror's figure, in response to an assumed temperature loading of 96 K bulk temperature excursion, 0.1 K axial gradient, and 0.6 K diametral gradient, are plotted in figure 51.

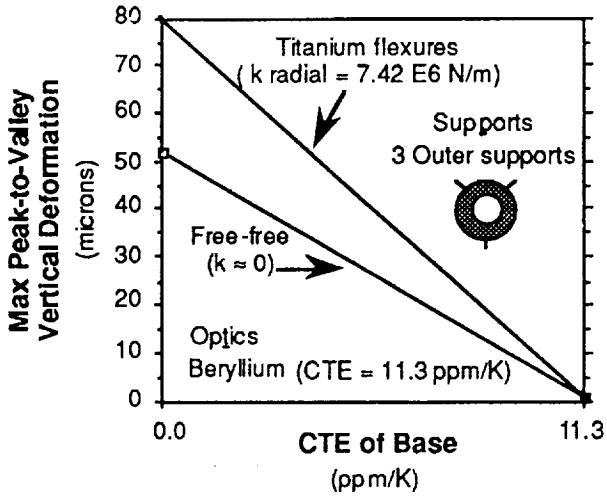

Figure 51. Thermal deformation versus baseplate CTE.

When the difference between CTE's of the baseplate and optics becomes wider, the mismatch in their thermal growth during the 96 K bulk temperature excursion results in larger deformations.

Utilizing an athermalization scheme is recommended for the baseplate-optics system and for any other sensitive component such as the metering structure. For the LUTE, current athermalization plans are to match the CTE's of the baseplate and optics as closely as possible. Matching other thermal-distortion indicators, such as the steady-state and transient-thermal distortion coefficients, may also be necessary. The mirror support trade and mirror material trade, discussed later, assumed an athermalized baseplate-optics system.

A concern, however, is whether athermalization can accommodate large bulk temperature swings (e.g., the 200 K range predicted for the LUTE optics). Material-based athermalization schemes work best when the operating temperature is held within a narrow band, since the athermalized design can be tailored for those specific temperatures. If the temperature variation is outside this band, though, athermalization may break down. For example, when a design has been athermalized using material-based techniques, there exists a ratio C between the CTE's of two materials that allows the structure to be athermalized at a given temperature T_0:

$$C = \mathrm{CTE}_1\ (T=T_0)/\mathrm{CTE}_2\ (T=T_0)\ . \qquad (5\text{-}7)$$

If the temperature T should change by an appreciable amount, the design will only remain athermalized if the ratio between the thermal expansion slopes of these two materials equals the same ratio constant C:

$$C = \frac{\int (\partial \mathrm{CTE}_1/\partial T)dT}{\int (\partial \mathrm{CTE}_2/\partial T)dT} \approx \frac{(\partial \mathrm{CTE}_1/\partial T)\Delta T}{(\partial \mathrm{CTE}_2/\partial T)\Delta T} = \frac{(\partial \mathrm{CTE}_1/\partial T)}{(\partial \mathrm{CTE}_2/\partial T)} \quad . \tag{5-8}$$

A more detailed discussion on athermalization is beyond the scope of this report.

5.3.4.2 Mirror Support Trades

Before a mirror material trade was conducted, a design for the mirror support structure was baselined. Structural supports for the primary and tertiary mirrors hold these optics above the baseplate and must allow the mirrors to expand and contract in the thermal environment. Otherwise, stress and additional warpage will be introduced into the mirrors. The mirror support trade was conducted to assess the impact of different mirror support concepts on a primary mirror's thermal deformations. The affect of mirror support stiffness on thermal deformations was also evaluated. Launch and lunar gravity loads were not considered in this trade.

Method—For the mirror support trade, a beryllium primary mirror was modeled. An assumed temperature loading of 96 K bulk temperature excursion, 0.1 K axial gradient, and 0.6 K diametral gradient was applied to the model to assess the thermal deformation figure change when the mirror was supported along its outside edge, inside edge, and bottom with three flexures. The bottom supports, utilizing a statically determinant support concept, were mounted close to the neutral surface of the mirror. The three designs are illustrated in figure 52.

The supports were modeled with spring elements. Several runs were made with each design to assess the thermal deformations as the spring constants were varied. These deformations are plotted in figure 53.

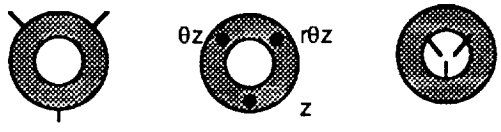

Support Locations	RESTRAINED D.O.F. Outer supports	Bottom supports	Inner supports
30°	rθz	rθz	rθz
150°	rθz	θz	rθz
270°	rθz	z	rθz

Figure 52. Mirror support concepts.

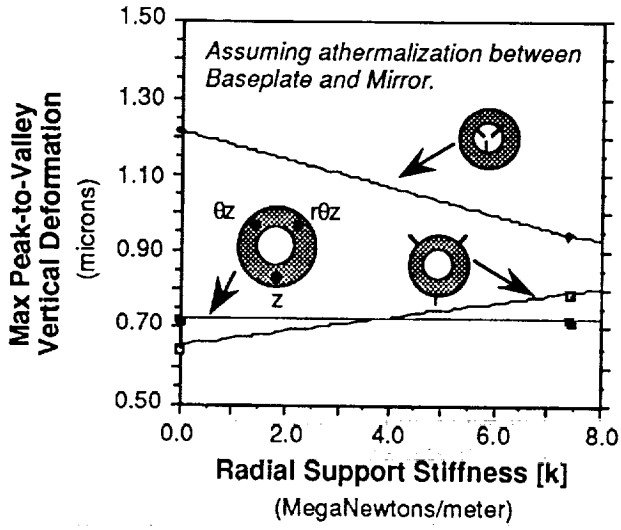

Figure 53. Thermal deformation versus support stiffness.

Results—Figure 53 indicates that the resulting deformations of the mirror using the outer supports and bottom supports are less than when using inner supports. The current data are not conclusive in showing whether bottom supports are better than outer supports. The assumed thermal loads were not large enough to create a discernible difference between these options. Kinematic bottom supports, however, are statically determinant, i.e., having the advantage of not being influenced by the stiffness of the flexures.

The statically determinant support concept with three bottom-mounted flexures was chosen as the baseline design for the LUTE primary and tertiary mirrors during preliminary design. The mirror support flexures have been radially located at the mirrors' neutral balance point. The location of the neutral balance point was estimated by calculating the radial distance r, where the mirror's outer radial mass equaled the mirror's inner radial mass:

$$\pi\,(R_{outer}^2 - r^2)\,t\rho = \pi\,(r^2 - R_{inner}^2)\,t\rho\ . \tag{5-9}$$

This equation was then simplified to derive an expression for the radial balance point r:

$$r = \sqrt{(R_{outer}^2 + R_{inner}^2)/2}\ . \tag{5-10}$$

Using this equation, hand calculations approximated the primary mirror's neutral balance point at a radial location of 39.5 cm and the tertiary mirror's neutral balance point at 9.9 cm radially. The secondary mirror's balance point is at approximately 14.4 cm radially.

Launch Locks—Stress analysis is required and has not been performed to determine if the mirror support flexures can withstand launch and lunar landing loads without damage. If the flexures cannot support the mirror safely, launch locks will be required to support the LUTE optics during launch and landing.

5.3.4.3 Primary Mirror

Extreme temperature swings in the mirrors of lunar-based telescopes with passive TCS's will necessitate that the optical structures be designed carefully in an effort to reduce thermal deformations of the mirrors and to maintain satisfactory optical performance. It is desirable to maintain the dimensional stability of the optical structures, to reduce thermal conductivity paths to the mirrors, and to minimize light blockage. The analysis of thermal deformations on the LUTE optics has been a very detailed undertaking. In addressing this task, an interactive, multidisciplinary analysis process, as sketched in figure 54, was developed.

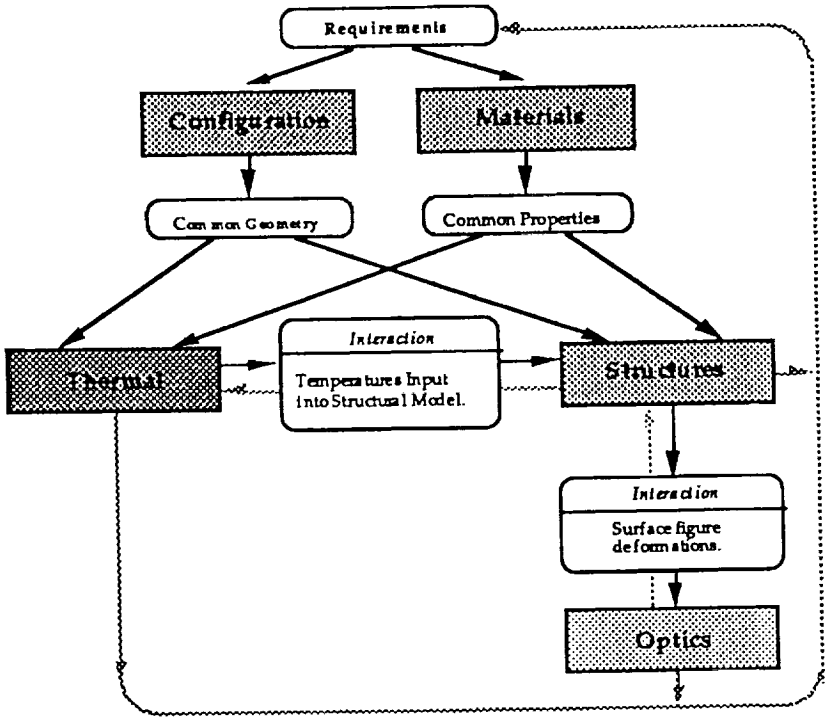

Figure 54. Analysis process for mirror deformations.

This process was used to calculate primary mirror thermal deformations. Numerical data generated by the process were transmitted electronically between disciplines. The configuration, thermal, and structures disciplines used the I-DEAS™ software package for FE design and analyses of the LUTE.

Structural analyses compared the qualitative performance of various design schemes. To conduct the design trades for the LUTE optics, analyses were based on the I-DEAS™ FE model of the primary mirror. The primary mirror geometry and construction are described in section 4.2.3.3. The FE model is described in section 5.3.1. Models were not built for the secondary and tertiary mirrors. It is anticipated that the primary mirror results will be pertinent to the design of lunar-based telescopes in general, even if their thermal control systems are not entirely passive. Trades resulted in the selection of a baseplate athermalized with respect to the mirrors by matching thermal distortion coefficients, statically determinant mirror supports with three bottom-mounted flexures, and SiC as the baseline mirror material.

Integrated Primary-Tertiary Versus Separate Primary-Tertiary Mirror—The baseline primary-tertiary mirror assembly has the mirrors ground on separate blanks. Another option reviewed was to grind the primary and tertiary mirrors on a single blank. This option was not chosen, however, because consultation with industry indicated that it would be difficult to grind a primary and tertiary on one blank, because of alignment of the two foci. Normally, the mirrors are ground separately and then aligned. Similarly, during operation, the mirrors may experience a misalignment which could be corrected by rigidly moving one or the other.

Another advantage to having the LUTE primary and tertiary mirrors ground on separate blanks is reduced weight. If these mirrors were ground on a single blank, the weight would be 17 percent higher than the combined weight of the separate primary and tertiary.

Mirror Construction Trades—The baseline mirror geometry with closed-back construction was primarily chosen due to heritage from previous studies. A study on mirror construction trades was undertaken by HDOS during the LUTE preliminary design. HDOS investigated a number of different geometries, including single-arch, closed-back, open-back, and meniscus constructions. Results of their study are summarized in table 16. A copy of HDOS's report appears in appendix L.

Table 16. HDOS ranking of mirror construction geometries (from "best" to "worst").

Based on Wave Front Error (WFE)	**Based on Deflection**
1. Single arch (supported at inner radius)	1. Closed back
2. Closed back (supported at 2/3R)	2. Open back
3. Open back (supported at 2/3R)	3. Single arch
4. Meniscus (supported at 2/3R)	4. Meniscus
calculated from 1g sag and fundamental frequency	

Mirror Material Property Comparison—Selection of the mirror material is one of the first steps in the design of a telescope's optical structures. After a mirror material is selected, the material for the mirror support structure can be chosen. The baseplate material selection will be impacted by the choice of a mirror material. The metering structure material selection may also be influenced. Room temperature properties for the LUTE optical system material candidates are listed in table 17. Beryllium and SiC temperature-varying mechanical properties are listed in appendix K.

Table 17. Room temperature properties of candidate mirror materials[24–30]

Material	Type	Density rho (kg/m^3)	YTS (MPa)	Elastic modulus E (GPa)	CTE (ppm/K)	Conductivity k (W/(m-K))	Specific heat Cp (J/(kg-K)	Poisson's ratio mu [—]
Beryllium	O-50	1827 - 1855	172 - 207	303	11.3 - 11.5	182 - 220	1825 - 1926	0.04
Silicon dioxide	(quartz)	2650	—	—	—	6.2 - 10.4	745	—
Silicon dioxide	(fused silica)	2187 - 2220	—	72	0.54 - 0.56	≈ 1.4	745	0.244
Silicon		≈ 2330	—	—	2.5	≈ 148	712	—
Silicon Carbide		2920 - 4595	—	311	2.6 - 3.24	112-156,490	675 - 1255	—
SiC/Al	MMC	2910	—	117	12.4	123	1004	—
ULE	Ti Silicate, 7971	2187 - 2205	UTS 50	68	0 ± 0.054	1.3	766	0.17
Zerodur	M	2519 - 2570	—	89	0 ± 0.09	1.6	812	0.25

An effort was undertaken to identify all comparison factors, or figures of merit, pertinent to a telescope's mirror material selection and to assemble them in a systematic summary chart. There are many factors to be considered when selecting a suitable mirror material. Table 18 lists some of these comparison factors.

Table 18. Comparison factors for mirror material trades.

PARAMETER	DEFINITION	UNITS	CRITERIA
• Specific stiffness	E / rho	MJ / kg	high is good
• Specific strength	YTS / rho	kJ / kg	high is good
• Microyield strength	stress which causes 1% creep in TBD hours	MPa	high is good
• Fracture toughness	K1c		
• Anisotropy (homogeniety of properties)	ratio of directional props.	dimensionless	near 1 is good
• Hysteresis due to thermal cycling	change in optical figure	TBD	low is good
• Steady state thermal distortion coefficient	CTE / k	cm / Megawatt	near 0 is good
• Transient thermal distortion coefficient	(CTE-rho-Cp)/k	10E-6(sec/cm^2-K)	near 0 is good
• Surface figure — Peak-to-valley deformation — Curvature tilt	departure of actual from undeformed.	μm (microns) micro-radians	low is good near 0 is good
• Surface microroughness	departure of surface from plane.	Angstroms (Å) rms	low is good
• Optical scatter (scatter ∝ roughness^2)	TBD	Angstroms (Å) rms	low is good
• Bidirectional reflectance distribution function (BRDF)	angle off specular, amount of light	TBD TBD	low is good
• UV reflectance (normal incidence)	R = [(n λ - 1)^2 + λk^2] / [(nλ + 1)^2 + λk^2]	percent (%)	high is good
• Cost	Price / diameter	$ / cm	low is good

Mirror material trades and mirror support trades were complicated by the requirement that the optics withstand a bulk temperature excursion of approximately 65 to 265 K. Ground- and space-based telescopes typically do not have to contend with the harsh thermal environment affecting lunar-based telescopes. Consequently, the structural results presented herein will focus primarily on the ability of a material to resist deformation due to thermal loads. Steady-state thermal distortion coefficients, transient thermal distortion coefficients, and FE analyses of the primary mirror's surface figure in response to thermal loads will be discussed.

The transient thermal distortion coefficient (TTDC) is a figure of merit that indicates a material's tendency to deform under transient thermal loads. It is calculated from a material's density, coefficient of thermal expansion, specific heat, and thermal conductivity:

$$\mathrm{TTDC} = \mathrm{CTE} \times \rho \times C_p / k \ . \tag{5-11}$$

A TTDC near zero is considered good because it indicates that the material tends not to deform under transient thermal gradients at a given temperature. A plot of TTDC versus temperature is shown in figure 55.

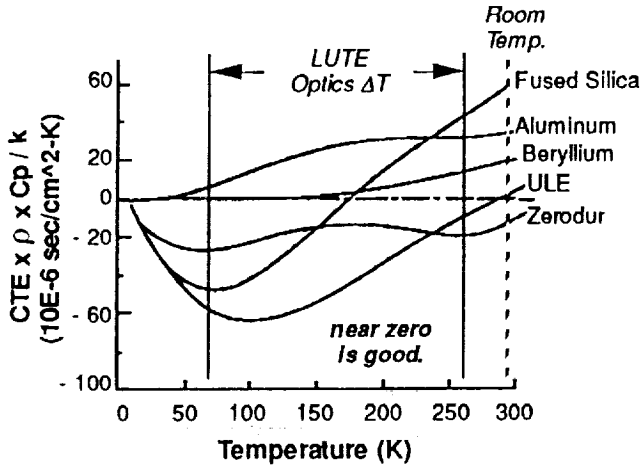

Figure 55. Transient thermal distortion coefficient.

Figure 55 was reproduced with permission from data presented by Paquin in 1986.[31] According to the plot, beryllium and Zerodur resist transient thermal distortion better than other materials in the LUTE primary mirror temperature range of 65 to 265 K.

However, the information displayed in figure 55 does not include some materials like SiC.[32 33] Beryllium and SiC temperature varying material properties were obtained from literature and discussions with vendors.[34] Beryllium and SiC temperature-varying mechanical properties are listed in appendix K. The transient thermal distortion coefficients of these materials were then calculated and plotted in figure 56. The curves indicate that SiC tends to resist transient thermal deformations better than beryllium.

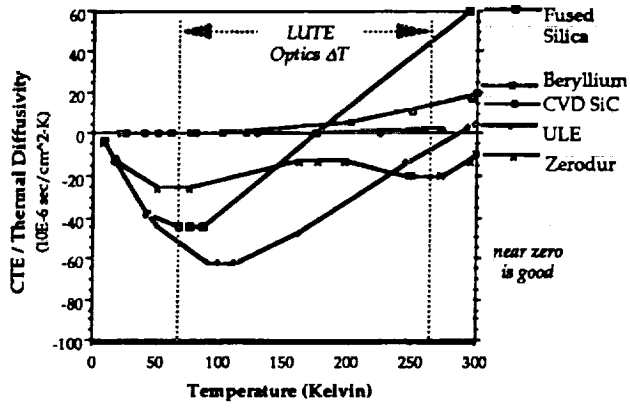

Figure 56. Transient thermal distortion coefficient
(plotted with beryllium and SiC data).

The steady-state thermal distortion coefficient (SSTDC) is another figure of merit for a material's resistance to thermal deformation. It is calculated from a material's thermal conductivity and CTE:

$$SSTDC = CTE/k \ . \tag{5-12}$$

Values of SSTDC near zero are considered good because they indicate that the material tends not to deform under steady-state thermal gradients at a given temperature. After temperature-varying material properties were obtained, the SSTDC was calculated and plotted for beryllium, CVD™ SiC, and Ceraform™ SiC in figure 57.[35] This figure indicates that SiC tends to resist steady-state thermal deformations better than beryllium.

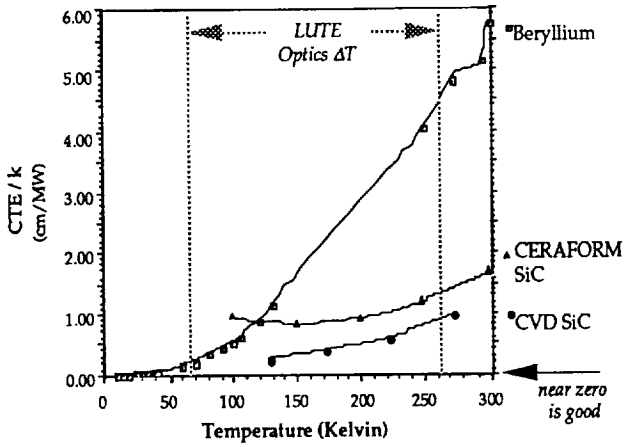

Figure 57. Steady-state thermal distortion coefficient.

The TTDC and SSTDC figures of merit provide some direction for the structural analysis of the primary mirror. Results from FE structural analyses were used to compare the surface figure thermal deformations of a beryllium, SiC, and fused silica primary mirror.

Mirror Material Trade: Figure Deformations Under Thermal Loads—Thermal deformation analyses were utilized in the preliminary design of the LUTE to characterize temperature effects, to study the interaction of the baseplate and optics material selection on thermally induced deformations, to compare various design concepts for the mirror support structure, and to conduct mirror material trades. Both hand and FE analyses were conducted.

After the athermalized baseplate-optics design and the statically determinant support concept with bottom-mounted flexures were baselined, a mirror material trade was conducted. The trade used FE analyses to calculate thermally induced figure deformations of the primary mirror during lunar operation. The thermal load case applied to the FE models represented an isothermal light shade and baseplate at a 40° latitude, 0° longitude landing site. Beryllium, SiC, and fused silica were compared during the study. Detailed analyses for SiC will be discussed later, but only the summarized results for fused silica will be presented. Beryllium and SiC temperature-varying mechanical properties are listed in appendix K.

Beryllium thermal deformations—Beryllium was the first material analyzed because of its good thermal properties and low density. SiC and fused silica were then analyzed.

Figure 58 depicts one of the thermal load cases, at a given time step, for the beryllium primary mirror.

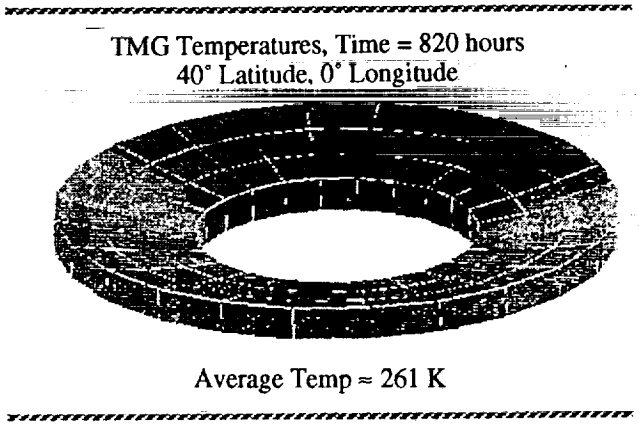

Figure 58. Beryllium primary mirror thermal load at 40° lunar latitude.

Figure 59 illustrates the maximum thermal deformations calculated with I-DEAS™/model solution for the beryllium LUTE primary mirror.

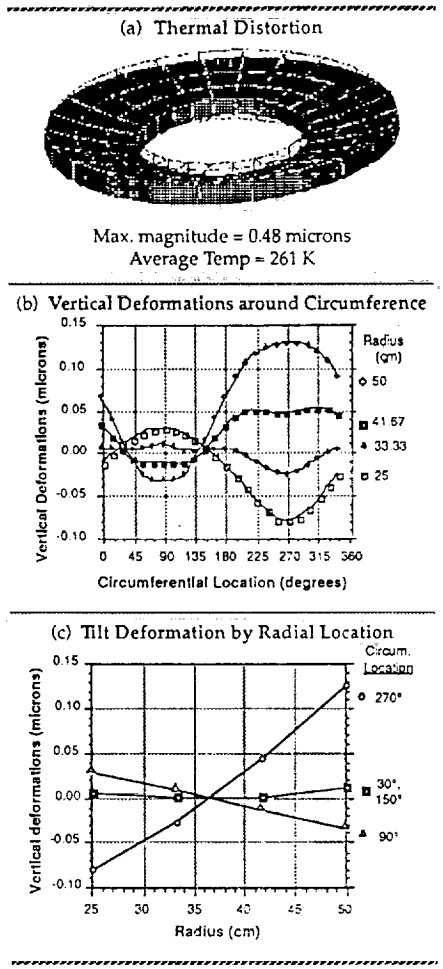

Figure 59. Beryllium primary mirror thermal deformations at 40° lunar latitude.

Figure 59 represents the results from only one thermal load case, the temperature case causing maximum thermal deformation. In all, beryllium primary mirror temperatures and deformations were calculated for three critical time steps during the lunar day/night thermal cycle. The output temperatures and deformations are summarized in table 19(b).

The time steps in table 19(b) were chosen because the largest temperature gradients in the mirror existed at these times. The bulk temperature range was 65 to 262 K. The maximum vertical peak-to-valley thermal deformation was about 0.16 μm, with a maximum curvature tilt of about 56 μ deg. The maximum thermal stress in the mirror was 102.6 kPa, resulting in a high margin of safety.

Table 19. Thermal-structural performance of primary mirror materials at 40° latitude ("best" material to "worst" material).

(a) SiC (Ceraform™) Mass = 16.9 kg + 15 percent = 19.4 kg $\sigma_{allowable}$ = TBD (>1 MPa)

Time (h)	Descriptor	Average Temperature (K)	Temperature Gradient (K)	Maximum Peak-to-Valley Vertical Deformation (μ)	Maximum Curvature Tilt (μ deg)	Thermal Stress (kPa)
820	Noon	261.3	0.20	0.048	10.66	27.8
1000	Afternoon	157.1	0.09			
				Low is good	Near zero is good	

*Used room temperature properties, except CTE as f(T). Assumed Poisson's ratio = 0.25.

(b) BERYLLIUM O-50 Mass = 10.7 kg + 15 percent = 12.3 kg $\sigma_{allowable}$ = 122.86 MPa (1.4 SF)

Time (h)	Descriptor	Average Temperature (K)	Temperature Gradient (K)	Maximum Peak-to-Valley Vertical Deformation (μ)	Maximum Curvature Tilt (μ deg)	Thermal Stress (kPa)
650	Morning	123.2	0.11	0.035	13.42	102.6
820	Noon	261.2	0.18	0.160	55.75	
1000	Afternoon	159.5	0.09	0.054	-15.70	
				Low is good	Near zero is good	

*Used temperature-varying properties.

(c) FUSED SILICA Mass = 12.7 kg + 15 percent = 14.6 kg $\sigma_{allowable}$ = TBD (>1 MPa)

Time (h)	Descriptor	Average Temperature (K)	Temperature Gradient (K)	Maximum Peak-to-Valley Vertical Deformation (μ)	Maximum Curvature Tilt (μ deg)	Thermal Stress (kPa)
690	Morning	177.7	7.07	0.459	794.66	53.7
820	Noon	260.1	3.34	0.210	197.53	41.8
1000	Afternoon	159.0	7.80	0.460	-873.50	82.6
1030	Afternoon	104.8	2.73			
				Low is good	Near zero is good	

*Used room temperature material properties.

SiC Thermal Deformations—Figure 60 illustrates the maximum thermal deformations calculated with I-DEAS™ for the SiC LUTE primary mirror. As with the beryllium mirror, a statically determinant mount with three bottom-mounted flexures was used, and the thermal load case applied to the FE model represented an isothermal light shade and baseplate at a 40° latitude landing site.

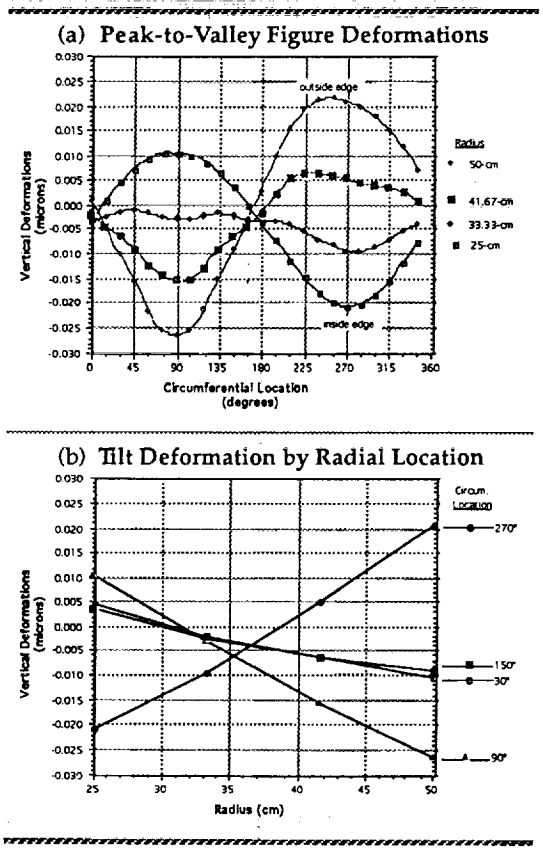

Figure 60. Ceraform™ SiC primary mirror thermal deformations at 40° latitude.

Figure 60 represents the results from the temperature case causing maximum thermal deformation. The output temperatures and deformations are summarized in table 19(a). The time steps in table 19(a) were chosen because the largest temperature gradients in the mirror existed at these times. The bulk temperature range was 65 to 262 K. The maximum vertical peak-to-valley thermal deformation was about 0.05 μm, with a maximum curvature tilt of about 11 μ deg. The maximum thermal stress in the mirror was 27.8 kPa, resulting in a high margin of safety.

Thermal Deformation Trade Results—Structural analyses were conducted with I-DEAS™/model solution for SiC, beryllium, and fused silica primary mirrors. Thermal deformation results are summarized in table 19. The thermal stresses developed in all three materials were low, below 1 MPa, and acceptable.

Table 19 shows that SiC resisted thermal deformation better than the other two mirror materials, since its maximum peak-to-valley and tilt deformations were the lowest. The results from this material trade, based on FE analysis of the thermal deformations, concurred with the TTDC and SSTDC material property comparisons in figures 55 through 57. Optical studies also favored SiC as the mirror material.

As a result, SiC has been chosen as the baseline mirror material for the LUTE phase A final reference configuration.

Note that the SiC structural analysis was based on room temperature properties, except CTE as a function of temperature. SiC temperature-varying mechanical properties are listed in appendix K. Typical temperature-varying properties for SiC from 65 to 265 K will be better than the room temperature properties. Therefore, the tabulated thermal deformation for SiC represents a "worst-case" scenario, and it is expected that the qualitative results in table 19 will still hold if temperature-varying properties are used for SiC in a more detailed analysis.

Figure Deformations Under 1/6 Gravity as a *f* (Nonzenith Pointing)—In addition to thermal deformations, the primary mirror's surface figure will be affected by the lunar gravity of 1/6 g. An FE analysis with I-DEAS™ was completed to assess primary mirror figure deformations for SiC and beryllium.

LUTE will be tilted on the Moon, to assure correct pointing declination. Mirror tilt angles, as illustrated in figure 61, were varied from 0° (horizontal) to 90° (vertical) for the lunar gravity deformation analysis.

Figure 61. Mirror tilt angle.

The peak-to-valley and curvature deformations of a beryllium and SiC primary mirror are plotted in figure 62.

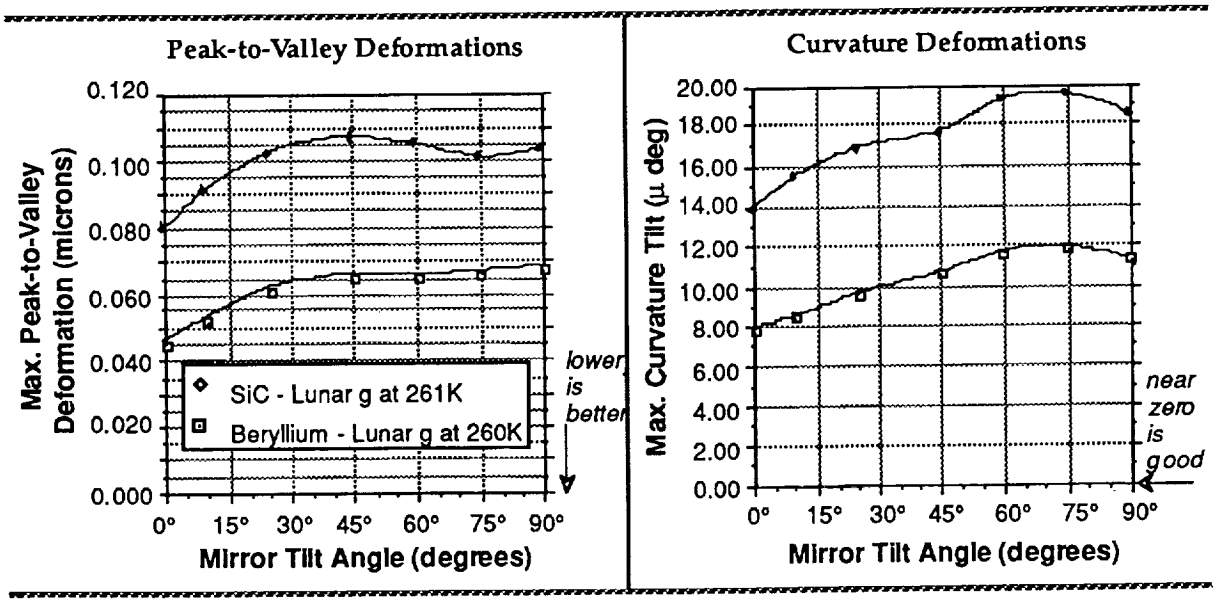

Figure 62. Lunar gravity deformations.

In figure 62, the beryllium mirror deformed less than SiC due to lunar gravity, as was expected since its specific stiffness is higher.

Combined Thermal and Lunar Gravity Loading—When only thermal deformations are considered, SiC is better than beryllium at maintaining low deformations. When only lunar gravity deformations are considered, though, beryllium is better than SiC. As an indication of mirror performance under combined loading, the maximum 40° latitude thermal deformations for each material were added to the lunar gravity deformations of the primary mirrors with a 0° tilt angle.

Table 20 shows that the SiC primary mirror performed better than the beryllium mirror, when maximum thermal deformations were added to lunar gravity deformations, for mirrors with 0° tilt.

Table 20. Flat (0° tilt) LUTE primary mirror at 40° lunar latitude.

Condition	Beryllium		Silicon Carbide	
	Peak-to-Valley Deformation (μ)	Curvature Deformation (μ deg)	Peak-to-Valley Deformation (μ)	Curvature Deformation (μ deg)
Thermal	0.16	56	0.05	11
Lunar g	0.05	8	0.08	14
Sum ≈	0.21	64	0.13	25

Low values are better

Launch Stresses—Structural stresses were calculated for beryllium, SiC, and fused silica primary mirrors during launch on an Atlas IIAS launch vehicle. Maximum quasi-static loads of 6 g's axial and 2 g's lateral were applied to the FE models.

Table 21 indicates that all three candidate mirror materials will survive launch on an Atlas IIAS, assuming quasi-static loads and the mirror construction of section 4.2.3.3. Random vibration loads will be significant and must be considered in future analyses.

Table 21. Primary mirror quasi-static launch stress.

Material	Maximum Launch Stress	Analysis Safety Factor	Allowable Strength	Result
Beryllium	246.7 kPa	1.4	122.86 MPa	Safe
Fused Silica	299.0 kPa	3.0	TBD (>5 MPa)	Safe
SiC	397.0 kPa	3.0	TBD (>5 MPa)	Safe

5.3.4.4 Primary Mirror Trade Summary

Degradation of the optical performance due to thermal deformations, during the lunar day/night cycle, was an important concern of the LUTE preliminary design study. This task necessitated close interaction between the materials, configuration, thermal, structures, and optics disciplines.

Three modes of thermal loading—bulk temperature excursion, axial temperature gradient, and diametral temperature gradient—on the optics were identified. Axial gradients are more significant than diametral gradients in causing thermal deformations. However, structural analyses indicated that the primary mirror bulk temperature excursion during the lunar day/night cycle will drive the vertical peak-to-valley deformation in the optics unless the primary mirror and baseplate are athermalized with respect to each other. Athermalization, in this case, may be accomplished by matching thermal distortion similarity parameters for the optics and baseplate, such as the coefficients of thermal expansion or transient thermal distortion coefficients. A concern, however, is whether athermalization can accommodate the large bulk temperature swings predicted for LUTE.

Trade studies for the primary mirror were discussed, including a mirror support trade and a mirror material trade. Using separate primary and tertiary mirrors, the mirror support trade evaluated various inner, outer, and bottom support concepts. Analysis, based on an assumed beryllium primary mirror thermal loading, indicated that inner supports were worse than the other concepts, since thermal deformations were larger. Outer supports and bottom supports resulted in similar deformations. However, kinematic bottom supports had the advantage of being statically determinant. As a result, a statically determinant support with three bottom-mounted flexures was baselined. Using this support configuration, an FE mirror material trade evaluated the thermal and lunar gravity deformations of a beryllium, SiC, and fused silica primary mirror. At a 0° longitude, 40° latitude landing site, the maximum peak-to-valley and curvature tilt primary mirror deformations were smaller with SiC than with beryllium or fused silica. SiC has therefore been baselined as the mirror material for the LUTE preliminary design.

5.3.4.5 Analysis Summary for SiC Primary Mirror

I-DEAS™/FEM was used to analyze launch stresses, operating thermal deformations, and lunar gravity deformations of the SiC primary mirror. The analysis results are summarized in table 22, given a statically determinant mount with three bottom-mounted flexures.

Table 22. Structural analysis summary for SiC primary mirror.

		SURFACE FIGURE		STRESS	
CONDITION	LOAD	Peak-to-Valley deformation (microns)	Curvature deformation (μ deg)	Max. Stress	Result
Launch	Quasi-static 6g's axial + 2g's lateral	—	—	397.0 kPa	Safe
Operate 40° Lat.	Thermal: 261K with 0.20K gradient.	0.048	10.6	27.8 kPa	Safe
Operate 40° Lat.	Lunar gravity: 1/6 g with 0° Tilt.	0.079	13.8	< Launch	Safe
Operate 65° Lat.	Thermal load less than 40° Lat.	TBD (< 40° Lat)	TBD(<40° lat)	< 40° Lat.	Safe
Operate 65° Lat.	Lunar gravity: 1/6g with 25° Tilt.	0.101	16.8	< Launch	Safe
					SF = 3.0

When the 40° latitude thermal deformation results were used in the optical analysis, optical performance was found to be acceptable, i.e., the optical spot diagram and encircled energy performance were satisfactory.

Note that the baseline LUTE landing site is 66.5° latitude by 24.2° longitude, not 40° latitude by 0° longitude. Thermal analysis has shown that thermal loads will be smaller at 65° latitude. Thermal deformations will also be smaller at 65° latitude. Consequently, the optical performance at 65° latitude will still be satisfactory.

5.3.5 Metering Structure

The primary structural function of the metering structure is to maintain the separation distance from the primary and tertiary mirrors to the secondary mirror and the science instrument. The structure must be very stiff and have low thermal expansion for dimensional stability during the lunar thermal cycle. Another objective is to minimize heat transfer to the secondary mirror and science instrument by selecting materials with low thermal conductivity and by reducing the number of heat conduction paths. Also, light blockage must be minimized, so that the FOV's of the primary and tertiary mirrors are not obscured.

5.3.5.1 Design Trade Space

Figure 63 shows the design trade space for the LUTE metering structure.

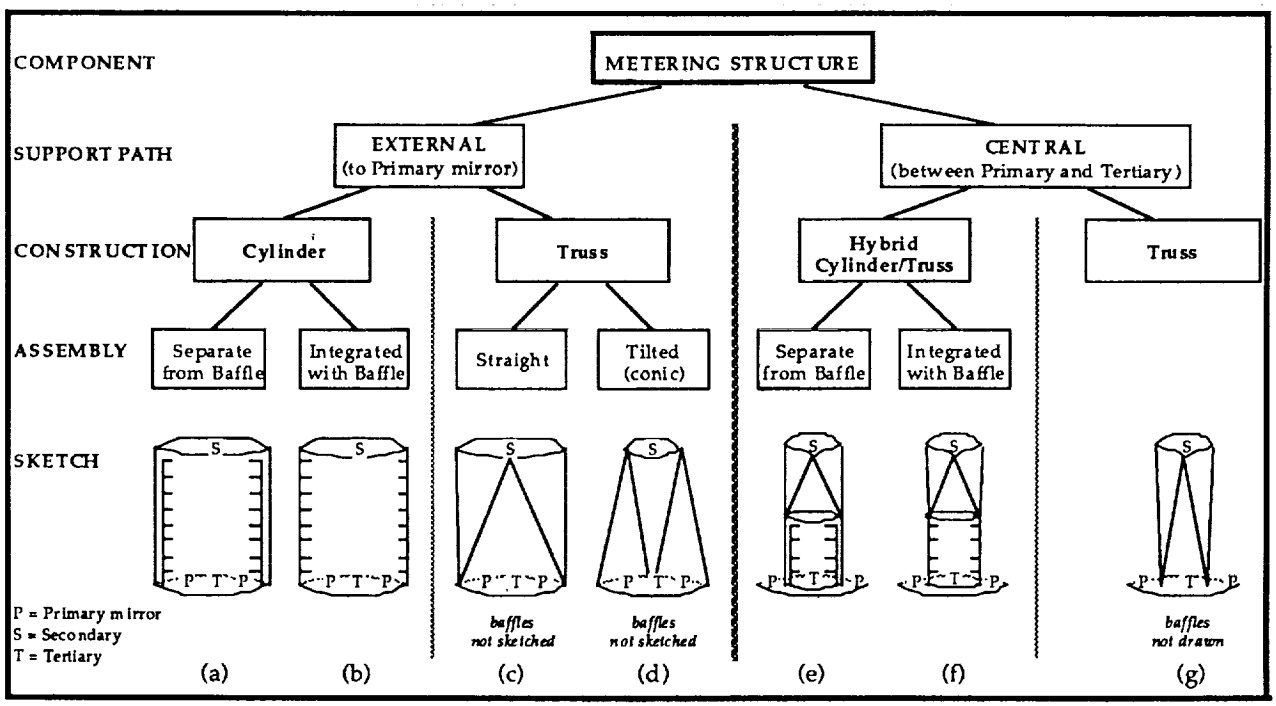

Figure 63. Metering structure design concepts.

Figure 63 only shows the primary to secondary mirror portion of the metering structure. Figure 64 illustrates three possible designs for the portion of the metering structure that lies in the plane of the secondary mirror.

Structural trades have not yet been completed to compare the seven different metering structure design concepts. Due to heritage from previous telescope studies, the baseline design for the LUTE metering structure was chosen to be option "c" in figure 63, a derivative of the HST straight metering truss, external to the optics, with the structure in the plane of the secondary mirror being similar to option "b" in figure 64.

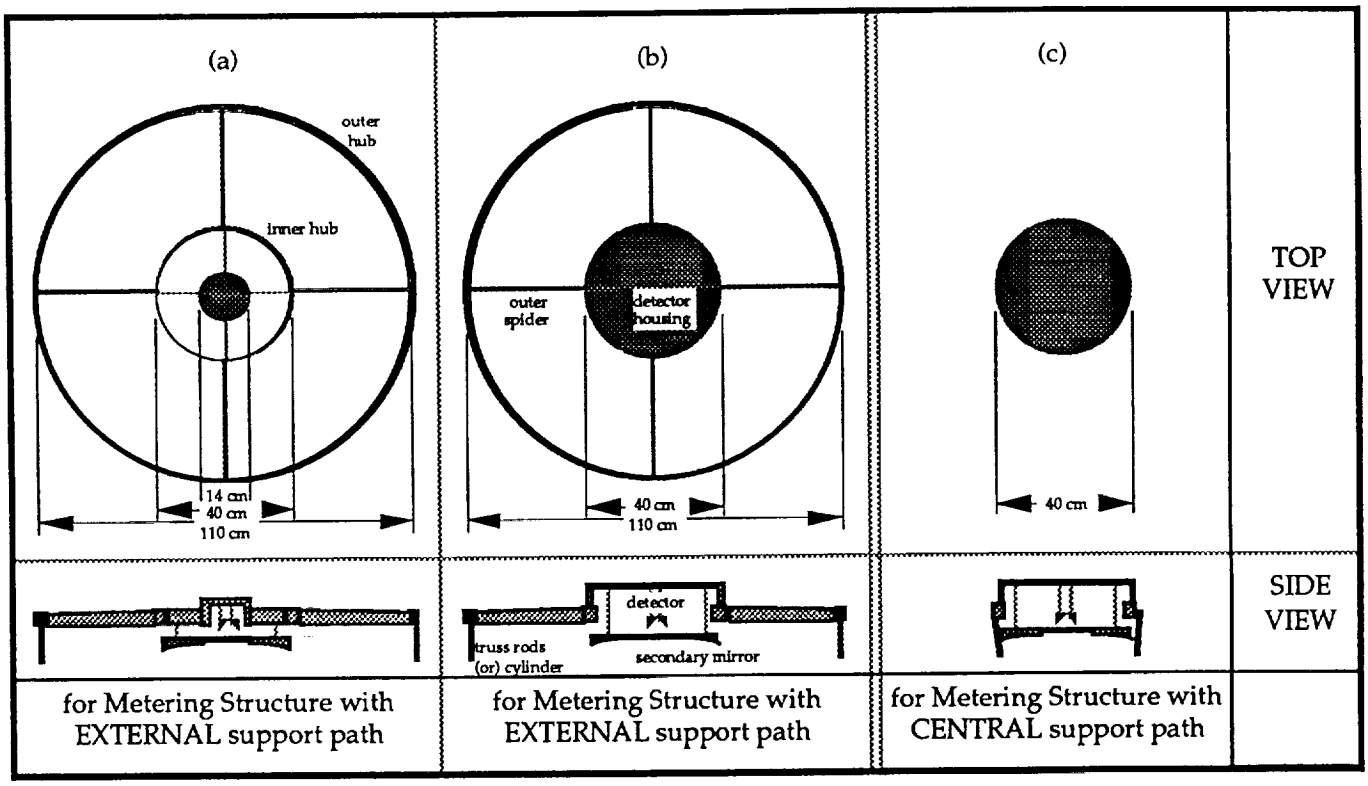

Figure 64. Secondary mirror enclosure options.

5.3.5.2 Back Focal Distance Thermal Disturbances

A dimensional stability requirement for the separation distance between the secondary mirror and the other two mirrors has not yet been defined. It is possible that the LUTE metering structure may not be able to maintain thermal deformations within the focus requirement for the entire lunar day. Consequently, the effect of focal length thermal disturbances on the back focal length of the LUTE optical system requires additional analysis in phase B.

A hand analysis of these deformations was conducted to develop an initial bounding estimate for the preliminary design. For ease of analysis, the metering structure configuration was assumed to be an 83 cm tall cylinder external to the optics (similar to metering structure design option "a" in figure 63). Room-temperature isotropic material properties for beryllium and graphite/epoxy were used. The thermal loading affecting the focal length was assumed to be a pure bulk temperature excursion; no internal temperature gradients were applied. Based on these assumptions, the change in focal length was calculated and plotted in figure 65 as the bulk temperature excursion varied from 0 to 200 K.

The LUTE optics are currently predicted to experience a bulk temperature excursion of 200 K from 65 to 265 K. If it is assumed that the metering structure is designed to a 165 K reference and that its temperature range will be 165±100 K, then figure 65 shows that a beryllium cylinder will have a maximum back focal distance change of about 940 μ while a graphite/epoxy cylinder will have a maximum back focal length distance change of about 45 μ. These numbers represent an initial bounding estimate, which is within available actuator capabilities.

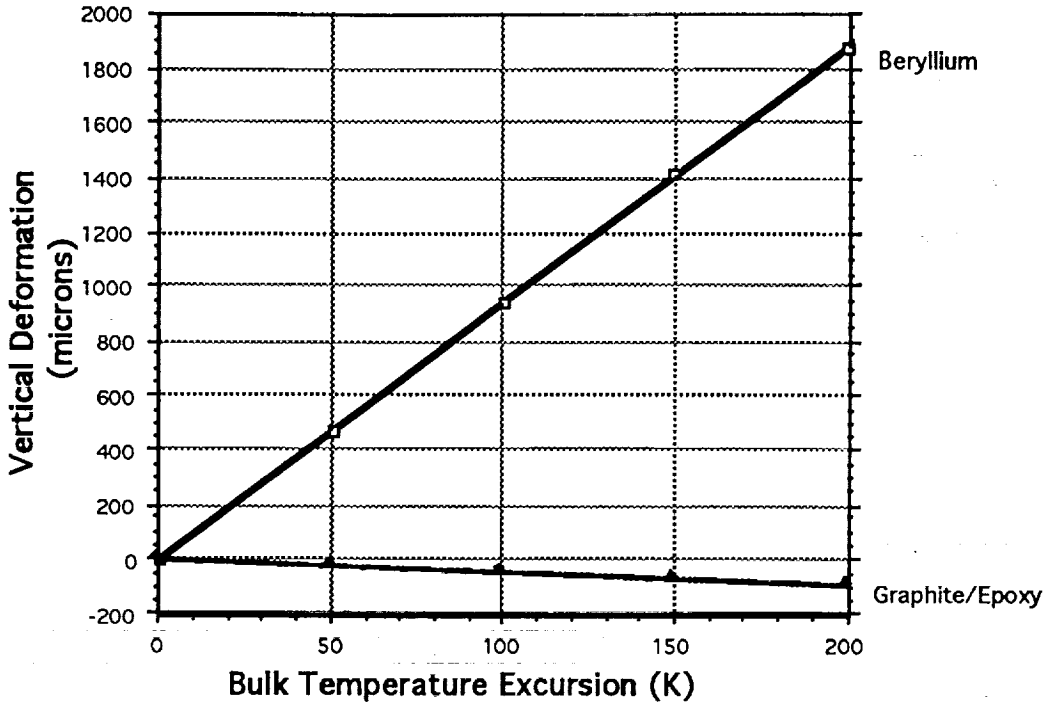

Figure 65. Metering structure thermal deformations.

5.3.5.3 Stress Analysis Results

I-DEAS™ was used to analyze the launch stresses in the metering structure. Quasi-static launch loads of 6 g's axial and 2 g's lateral resulted in a maximum stress of 40 MPa, located in the structural attachments to the secondary mirror housing. The metering structure is safe with a margin of safety equal to 7.9, which indicates that the structure can withstand combined quasi-static and random vibration loads of 53 g's axial and 18 g's lateral before material failure.

5.3.6 Light Shade

The light shade FE model, geometry, and construction are described in section 4.2.3.7 of this report. The light shade is constructed of aluminum. It has major support frames around the aperture opening and at the top of its cylindrical section. There is also an intermediate Z-frame located at the middle of the cylindrical section to provide additional support against buckling.

5.3.6.1 Light Shade Construction Trade

A light shade construction trade was conducted to determine the required skin thickness and number of T-section skin stringers needed to prevent buckling of the light shade cylinder during launch. The trade was run with skin-stringer tank analysis spreadsheet system (STASS) 1.0, an extensive system of analysis spreadsheets developed for the analysis of skin-stringer-stiffened cylindrical shells under compression. This tool calculates buckling margins of safety for six failure conditions, including general instability (Shanley and Becker criteria), stringer crippling, local elastic buckling, wide column buckling, and sheet buckling.

A 1.4 safety factor and Atlas IIAS quasi-static launch loads of 6 g's axial and 2 g's lateral were used to calculate loads for the trade, resulting in a compressive axial force of 12,855 Newtons (N) (2,890 lb) and bending moment of 2,960 N-m (26,200 in-lb). Analysis with STASS 1.0 showed that sheet buckling was the dominant failure condition. The margins of safety (MS) and mass (kg) estimates for the construction trade are summarized in table 23.

Table 23. Light shade trade summary.

Skin Thickness	No. of T-Section Skin Stringers		
	12	18	24
0.0508 cm (0.02 in)	M.S. = –0.70 m = 30 kg	M.S. = –0.31 m = 34 kg	***M.S. = 0.27**** ***m = 37 kg***
0.0762 cm (0.03 in)	M.S = –0.18 m = 36 kg	M.S. = 0.78 m = 39 kg	M.S. = 2.17 m = 43 kg
0.1016 cm (0.04 in)	M.S. = 0.68 m = 42 kg	M.S. = 2.57 m = 45 kg	M.S. = 5.23 m = 49 kg

*Selected option.

Positive values for buckling margin of safety indicate a safe design while negative values indicate structural failure. From table 23, six of the nine design options had positive skin buckling margins of safety. The lowest mass option, 24 T-section skin stringers and 0.0508 cm skin thickness, was chosen as the baseline light shade structural design.

5.3.6.2 Buckling Analysis of Baseline Light Shade

The baseline light shade has 24 T-section skin stringers, 0.0508 cm skin thickness, an intermediate "Z"-frame, and two major support frames attached to the skin of the light shade. Spreadsheet analysis with STASS 1.0 has determined that the stiffened light shade is safe during launch on an Atlas IIAS. The minimum margin of safety was positive 0.27, as shown in table 24. Component-level random vibration and shock loads have not yet been quantified.

Table 24. Buckling margin of safety summary for stiffened light shade.

Failure Condition	Buckling Margin of Safety (Launch Loads)	Result
General Instability		
– Shanley	>30	Safe
– Becker	>30	Safe
Stringer Crippling	26	Safe
Column Allowable	17	Safe
Skin Buckling	0.27	Safe

5.3.6.3 Stress Analysis of Baseline Light Shade

I-DEAS™ was used to analyze launch stresses in the baseline light shade. Quasi-static launch loads of 6 g's axial and 2 g's lateral resulted in a maximum stress of minus 18,390 kPa, where the upper

attachments of the electronics box support structure connect to the light shade skin. The light shade skin is safe from material failure with a margin of safety equal to 11.9. The light shade can withstand combined quasi-static and random vibration loads up to 77 g's axial and 26 g's lateral before material failure.

5.3.6.4 Light Shade Mass

The mass estimate for the baseline light shade structure is given in table 25.

Table 25. Light shade mass summary.

Parts	Comment	Cylindrical Section	Conic Section	Light Shade
Skin	0.0508 mm Al 2219-T81	4.7 kg	5.0 kg	9.7 kg
Stringer land	Attachment for 24 stringers	0.5 kg	0.5 kg	1.0 kg
T-stringers	24 T-section stringers	5.8 kg	6.2 kg	12.0 kg
Z-frame	Cylindrical section only	1.1 kg	–	1.1 kg
			Subtotal =	23.8 kg
+Major frame: Aperture opening				6.4 kg
+Major frame: Top of cylinder				2.4 kg
			Total =	32.6 kg
+ 15 percent for attachments and fittings				4.9 kg
			Grand Total =	37.5 kg

5.3.7 Electronics Box Support Structure

An analysis of the LUTE electronics box support structure was performed with the structure modeled as an aluminum truss with 8 nodes, 11 circular rods, and a 1 cm thick electronics box shelf. The reference geometry is detailed in section 4.2.3.8. Using Atlas IIAS launch loads of 6 g's axial and 2 g's lateral, element forces were calculated with I-DEAS™/FEM analysis. Hand analysis, using the tangent modulus theory, indicated that rods sized to be 1.25 cm in diameter would resist the compressive element forces calculated by I-DEAS™ without buckling. The first rod to fail is predicted to have a critical buckling load of 1,790 N with a critical buckling stress of 14.6 MPa. The electronics box support structure weighs 8 kg.

I-DEAS™/FEM was also used to analyze the launch stresses in the electronics box support structure. Quasi-static launch loads of 6 g's axial and 2 g's lateral resulted in a maximum stress of 12.2 MPa. This indicates that the electronics box support structure is safe since the maximum launch stress of 12.2 MPa is below the critical buckling stress of 14.6 MPa. It is estimated that the structure can survive combined quasi-static and random vibration loads up to 7.2 g's axial and 2.4 g's lateral before buckling.

5.3.8 Aperture Cover

Based on historical data of HST and AXAF-I, a mass of 15 kg was estimated for a LUTE aperture cover. The mass estimate assumes the aperture cover to be aluminum, like HST and AXAF. The mass estimate is shown in figure 66.

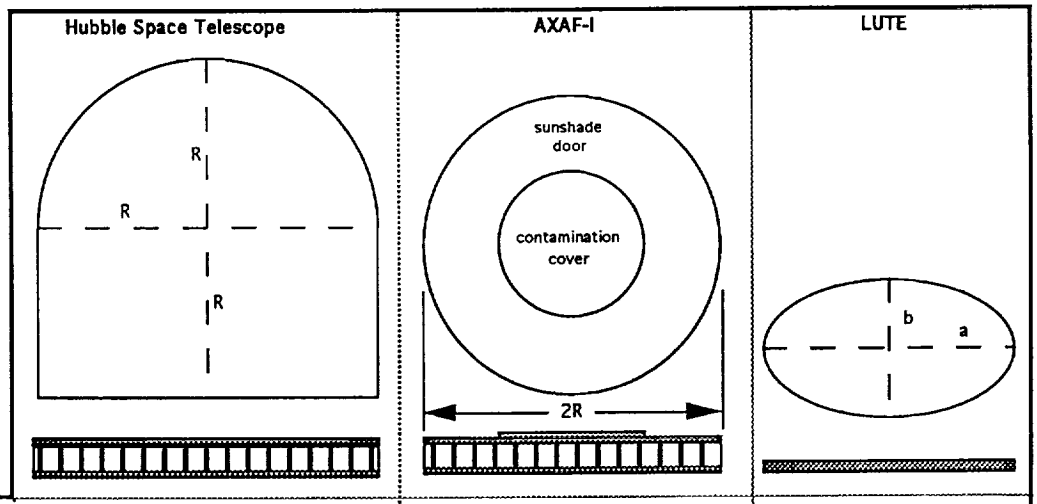

	Hubble Space Telescope	AXAF-I	LUTE
Deployment mech.	Opens/Closes, reusable.	5.8 kg mech., opens once only.	TBD (will open once only)
Construction	Al facesheets, t = 0.03 cm. Al honeycomb core, t = 3.7 cm.	Gr/Ep facesheets Al honeycomb core	TBD
Size	2R = 304.8 cm	2R = 266.7 cm	2a = 224 cm, 2b = 120 cm.
Surface area	SA = 8.29 m^2	SA = 5.59 m^2	SA = 2.12 m^2
Structure			
Structural mass	44.3 kg	39.5 kg	TBD
Structure/SA ratio	5.34 kg/m^2	7.07 kg/m^2	TBD
Scaled to LUTE SA =	11.3 kg	15.0 kg	—

Figure 66. Aperture cover mass estimate.

Figure 67 shows how the mass would vary with thickness for a flat aluminum elliptical aperture cover.

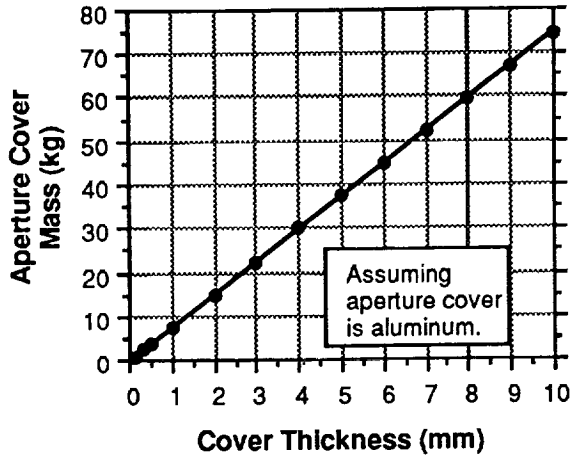

Figure 67. Aluminum cover mass versus thickness.

Two lightweight options for a fabric or mylar aperture cover have been identified in appendix G. A design for the aperture cover has not been performed.

5.3.9 Baseplate

At 40° latitude, hexapod mounts were circumferentially located at 20°, 40°, 140°, 160°, 260°, and 280° along the outside edge of the baseplate, as shown in figure 68(a). The reference landing site for LUTE has been moved to 66.5° latitude. Landing at this latitude required a new mount to accommodate the pointing requirement of the 40° declination. Restraints for this new mount have not yet been incorporated into the structural baseplate model, although the two mounts are fairly similar. It is expected that analysis results will remain valid in either case.

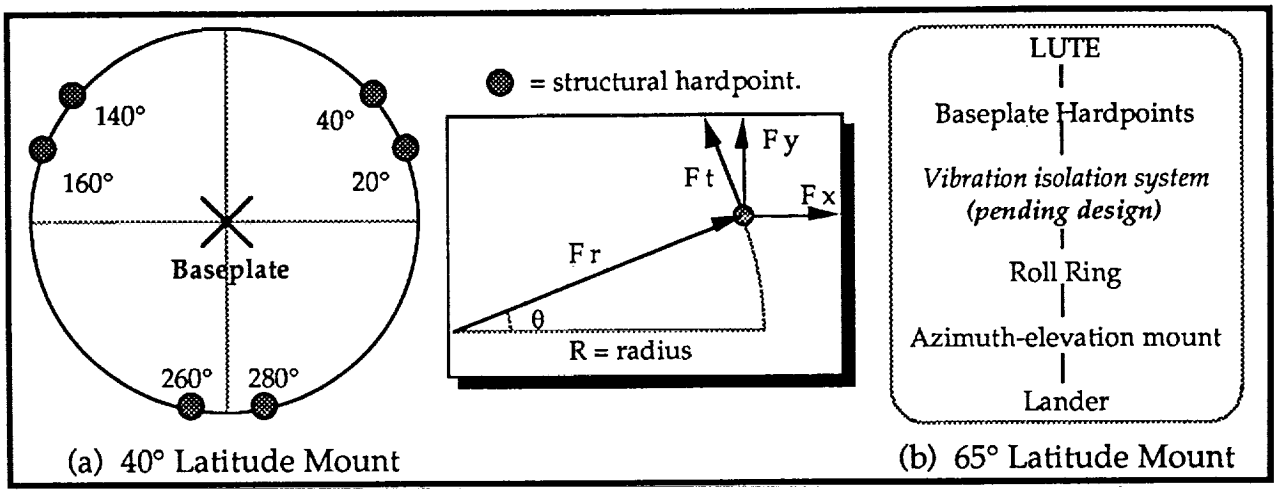

Figure 68. Interface hardpoints from LUTE to the lander mount.

Launch Stress Versus Baseplate Material—Using the reference baseplate geometry described in section 4.2.3.11, FE analyses evaluated the stresses that would develop in different baseplate materials during launch on an Atlas IIAS. Results from these analyses are summarized in table 26.

Table 26. Baseplate launch stresses versus material selection.

Baseplate Material	Mass	Max. Launch Stress	Allowable Strength	Stress margin of safety	Result
Beryllium	26 kg	6.3 MPa	389.1 MPa	60.8	Safe
Titanium	63 kg	4.3 MPa	541.7 MPa	125.0	Safe
Graphite/Epoxy	24 kg	6.8 MPa	356.1 MPa	95.5	Safe
			SF = 1.4		

The baseplate launch stress analyses show that all baseplate materials will be safe during launch on an Atlas IIAS, with high margins of safety. It is anticipated that the baseplate structures will still be safe with the new 66.5° latitude mount.

Baseplate Material Selection—The choice of a baseplate material is largely dependent on the material selection of the mirrors that will be supported by it. As discussed in section 5.3.4.1, athermalization between the optics and baseplate, by matching coefficients of thermal expansion, is very

desirable because this will reduce optical deformations induced by bulk temperature excursions. When beryllium optics were being considered, a beryllium or titanium baseplate appeared feasible. However, now that the reference optics are SiC, a graphite/epoxy baseplate would be a better material choice.

5.3.10 Component Trade Summary

Most of the structural analysis trades focused on thermal deformation analysis, mirror support trades, and mirror material trades for the LUTE optical system. The selection of an optical mirror material must be one of the first considerations when designing a lunar-based telescope, since the mirror material selection influences the selection of materials for the rest of the telescope, as illustrated in table 27, due to athermalization schemes and back focal distance requirements.

Table 27. Impact of mirror material selection on structural mass.

Impacted Structural Components	Mirror Material Selection			
	Beryllium		Silicon Carbide	
	Material	Mass (kg)	Material	Mass (kg)
Mirror (P&T)	Beryllium 0-50	12+1	SiC	19+2
Mirror Support Flexures (P&T)	Ti-5Al-2.5Sn	3+2	Graphite/Epoxy (or) Invar	1+1 5+4
Baseplate	Beryllium (or) Ti-5Al-2.5Sn	26 63	Graphite/Epoxy (or) SiC/Al MMC	24 41
Metering Structure – Truss rods – Spider – Secondary mirror housing	 Graphite/Epoxy Be I-250 Ti-5Al-2.5Sn	 11 10 2	 Graphite/Epoxy Graphite/Epoxy Graphite/Eoxy	 11 9 1
Secondary Mirror	Beryllium 0-50	2	SiC	4
Total =		69 or 106	72, 79, 89, or 96 kg	

Results from the other component structural trades are summarized in table 28. These results have been incorporated into the reference structural design described in section 4.2.3, Baseline Structural Design.

5.3.11 Integrated LUTE Structural Model

As designs for components were selected, they were incorporated into an integrated FE model of the LUTE structural system. The FE's used in the structural model are listed in section 5.3.1, figure 68. The integrated structural model was used to calculate interface loads, stresses, and frequencies for the baseline configuration.

Table 28. Summary of structural trade results.

Structural Components	Trades	Results
Mirrors	Temperature effects. Athermalization. Substrate trades. Construction trades. Material trades. Tile from 0° to 90°.	Axial gradient more significant than diametral gradient. Match thermal distortion parameters of baseplate and optics. Separate substrates for primary and tertiary mirrors. Closed back design, heritage from past studies, is reasonable. SiC baselined. Lunar g deformations tend to increase with mirror tilt angle.
Mirror support structure	Support concepts.	Kinematic supports with three bottom-mounted flexures.
Metering structure	Design concepts. Material trades.	External metering truss due to heritage from past studies. Graphite/epoxy chosen over beryllium.
Light shade	Construction trades.	24 T-section skin stringers and 0.0508 cm skin thickness.
Aperture cover	Design concepts.	Three designs identified but not analyzed.
Baseplate	Athermalization. Material trades. Interface reactions.	Match thermal distortion parameters of baseplate and optics. Graphite/epoxy due to athermalization with SiC. Loads calculated for 40° site mount, pending for 65° site mount.

5.3.11.1 Interface Hardpoints From LUTE to the Lander Mount

The LUTE was initially planned to land at 40° latitude and 0° longitude. The interface points for the 40° latitude mount are shown in figure 68(a). Hardpoint locations were determined by the controls system; hexapod actuators were to be attached to the LUTE baseplate at these hardpoints for the 40° latitude mount.

The interface hardpoints from LUTE to the lander mount, at 65° latitude, have not been defined, because the vibration isolation system between the baseplate and roll ring is pending design in phase B.

5.3.11.2 Interface Loads

Interface reactions for the 40° latitude mount were calculated in both cylindrical and cartesian coordinates. Coordinates are shown in table 29. The interface reactions represent limit loads with a factor of 1.0 and were calculated using Atlas IIAS quasi-static launch loads of 6 g's axial and 2 g's lateral.

The analytical work on the 66.5° latitude mount will be performed in phase B.

5.3.11.3 Stress Analysis

A linear statics stress analysis with I-DEAS™/model solution determined that the reference designs and mass estimates for the LUTE structural components were reasonable. Quasi-static loads of 6 g's axial and 2 g's lateral, representing maximum launch vehicle loads on an Atlas IIAS, were applied to the model. Table 30 summarizes the results of the FE stress analysis.

Table 29. Quasi-static reactions forces (N) for 40° latitude mount.

Point	Cylindrical		Cartesian		Vertical	Magnitude
	Radial Fr	Tangential Ft	Fx	Fy	Fz	
20°	-5265	-1974	-4272	-3656	6562	8642
40°	-3248	474	-2792	-1725	2747	4280
140°	-1063	-13	822	-674	1101	1530
160°	28	-401	111	386	-694	801
260°	-1290	237	457	1229	-85	1314
280°	-4212	1677	920	4439	4635	6484

Table 30. LUTE linear static stress analysis with Atlas IIAS launch loads.

Structure	Maximum Launch Stress (kPa)	Location	Allowable Strength (MPa)	Stress M.S.	Result
Integrated FE model	40,000	Metering structure.	–	–	–
Baseplate	–9,640	Above hexapod mount.	356.07	>20	Safe
Primary mirror	426	Outside and inside, near mounts.	? (>1)	–	Safe
Metering structure					
Spider	40,000	Attachments to secondary housing.	356.07	7.9	Safe
Truss	–680	Near baseplate attachment.	356.07	high	Safe
Light shade					
Skin	–18,390	At electric box upper attach.	236.36	11.9	Safe
T-Stringers	–14,700	Near electric box lower attach.	236.36	15.1	Safe
Electronics box support	12,170	Upper light shade attach. rods.	236.36	>20	Safe
			SF = 1.4		

Stresses developed in the LUTE structural components are acceptable, with high margins of safety. Positive margins will be maintained for the structural system even if the combined quasi-static and random vibration load factors increase up to 53 g's axially and 16 g's laterally. For some components, especially the mirrors and metering structure, stiffness and deflection requirements will probably influence the structural design more than the stress requirements.

5.3.11.4 Normal Modes Analysis

A normal modes analysis with I-DEAS™/model solution determined if the reference structural design violated Atlas IIAS payload frequency constraints. Figure 69 shows the first mode shape of the integrated structural model at 20.8 Hz.

A summary of all the frequencies from the FE normal modes analysis appears in table 31. Note that the first three normal modes involved vibration of the conic section of the light shade. Conic sections are inherently less stable and stiff than cylindrical sections. Equipment must be attached to the cylindrical section of the light shade instead of the conic section. If equipment must be attached to the conic section, it should be attached as low as possible.

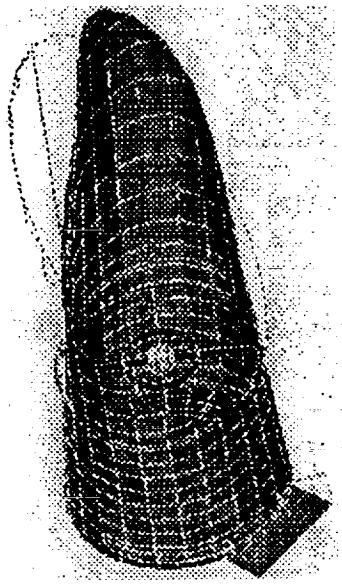

Figure 69. First natural frequency mode shape.

Table 31. LUTE structural natural frequency.

Mode	Natural Frequency (Hz)	Description	Violates Atlas II Constraints?
1.	20.8	Lateral (E to W) vibration of light shade conic section.	No
2.	22.9	Axial vibration of light shade conic section.	No
3.	23.7	Lateral (N to S) vibration of light shade.	No
4.	36.7	(Pictorial output not obtained.)	No
5.	38.5	(Pictorial output not obtained.)	No
6.	38.9	(Pictorial output not obtained.)	No

Analysis predicts that the LUTE will not violate the Atlas IIAS payload frequency constraints. Atlas IIAS frequency constraints, listed in section 4.2.3.1, are that the first lateral mode must be above 10 Hz and that the first axial mode must be above 15 Hz.

5.3.12 Structural Mass Estimate

A summary of the structural mass estimate for the baseline LUTE preliminary design appears in table 32.

5.3.13 Analysis Conclusion

Individual detailed component analyses and trade studies were completed and documented. Thermal deformations for the SiC optics were calculated and found to be acceptable. The LUTE components were analyzed as an integrated structural system. Natural frequencies for the combined structure meet Atlas IIAS requirements, and computed launch stresses are below material failure criteria. Launch loads were the driving load condition. The mass estimate for the structural system is 122 kg. These analyses show that the structural system for LUTE is adequate and safe.

Table 32. Structural mass estimate for baseline design.

Component	Material	Mass (kg)	Scaled	Hand	FE
Mirror Support Structure					
Flexures					
– Primary	Graphite/Epoxy	1		X	
– Secondary	Graphite/Epoxy	1		X	
– Tertiary	Graphite/Epoxy	1		X	
Launch Locks	TBD	TBD			
Metering Structure	Graphite/Epoxy				X
– Truss rods		11			
– Spider		9			
– Secondary mirror housing		1			
Optical Baffles	Al 2219				
– Primary baffle		12		X	
– Secondary baffle		0.5		X	
– Tertiary baffle		1		X	
– Science instrument		0.2		X	
Light Shade	Al 2219				
– Skin		11		X	X
– Support frames		12		X	X
– Skin stringers		14		X	X
Miscellaneous					
– Power system attachment	TBD	TBD			
– Electronic box upport	Al 2219	8		X	X
– Aperture cover	Aluminum	15	X	X	
Telescope Baseplate	Graphite/Epoxy	24		X	X
Total =		122			

5.4 Electrical Power System (EPS)

5.4.1 LUTE Power System Trade and Selection Criteria

The lunar surface environmental conditions, coupled with the lunar cycle of approximately 28 Earth days (14 Earth days of sunlight followed by 14 Earth days of darkness), placed a significant driver on the selection of a LUTE power system. The early goal of keeping the total LUTE mass to 200 kg placed further constraints on the EPS design. Using the above criteria, the logical candidate power source was a solar array without an energy storage system or an RTG. Study guidelines of minimizing program cost and a 1998 launch date would also influence the selection. To a lesser degree, the power systems selection would be influenced by the expected LUTE system power growth and the relatively short mission life. It was recognized that the solar array selection would restrict LUTE operations to the lunar day. Additionally, the absence of electric power during the lunar night limits the design approach of the thermal control system to meet the thermal requirements of the various subassemblies. For these reasons the option of using an RTG was kept as a candidate for the power system. EPS requirements are summarized in table 33.

Table 33. EPS requirements/selection criteria.

- Primary power system (i.e., no energy storage)
- 2 year minimum life
- Operate in lunar environment (dust, temperature, radiation, etc.)
- Accommodate growth in power requirement as study matures (initial requirement 85 We ave.)
- Program cost
- Program management

Primary Candidates

- Solar Array—Sunlit period operation only
- RTG continuous operation*

*Selected for current design.

5.4.2 EPS Candidate Comparison

Some of the major engineering and program management considerations that need to be considered in the final selection of the LUTE power system are listed in table 34. It should be emphasized that these comparisons are not intended to be totally inclusive. As the study matures, increases in mass, overall complexity, interaction with other subsystems, and cost will play a significant role in the final selection of the LUTE power system.

Table 34. EPS candidate comparisons.

	S/A	RTG
Launch/Prelaunch	Stowed	Requires cooling on pad
Transit	Stowed	Could supply power to lander
Initial Deployment	Primary battery required	Self sufficient
Life	Degrade with thermal cycling radiation and dust (25 percent allocated)	More complex, voltage regulation required.
Lunar Environment	S/A fabrication to accommodate temperature extremes	Minimal effects
System Impacts	Required solar orientation	Thermal and radiation environment impacts
Growth	Governed by packaging volume, deployment complexity, and mass budget	Current technology up to 300 W/unit
Cost	Minimal cost system	5–6 times S/A cost
Program Management	Well understood MSFC experience	Complex: Heavy DOE involvement; no MSFC experience

5.4.3 LUTE Power Requirements

LUTE power requirements for each mission phase are shown in table 35. The normal LUTE operating power is 79 W. However, during the mission phase of optical train alignment power requirements approach 95 W. The intermittent mission phase accounts for the possible occurrence of minor realignment of the optical train due to mechanical thermal disturbance. For this phase of the mission, 92 W is expected to be the maximum power requirement.

Table 35. Power requirements (W) for each mission phase.

Subsystem	Acquisition*	Operation	Intermittent*
Sun Sensor	2.8		
Roll Ring Assembly	10.0		
Mount Actuators	42.0	2.0	42
Secondary Mirror Actuators		2.4	30
Detector Electronics		10.0	
C&DH	50.0	65.0	50
Antenna Drive	18.0		18
Maximum/Phase	94.8	79.4	92

*All items not on simultaneously.

5.4.4 Use of Solar Array

The use of solar array power system, based on an average lunar day power requirement of 80 W, is described in figure 70. The solar array area is based on 130 W/m^2 performance with allowances made for temperature degradation and lunar dust effects. A total degradation of 25 percent was allowed as a result of radiation damage and dust accumulation.

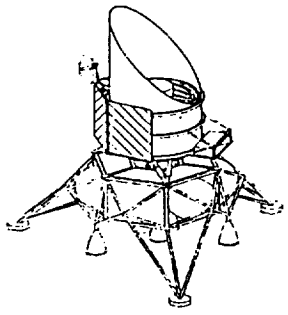

Stowed S/A

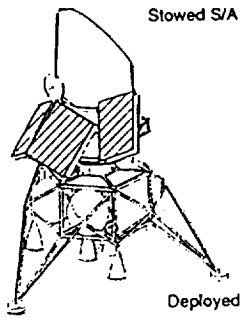

Deployed S/A

Power Req.	85 Watts	
Power System Description		
• Solar Array (fixed)	2.8 m^2	10 kg
• Primary Battery (for deployment)		5 kg
• Power Distr. Reg.		9
		24 kg*

*Mounting hardware & development mechanisms not included

Figure 70. EPS solar array description.

The solar arrays are mounted above the rollring and are oriented with the centerline along the north-south direction by the telescope pointing system. The arrays are nontracking and, therefore, must be oversized to accommodate the Sun incidence angle loss. The arrays must be deployed from their stowed positions to align the normal of the arrays to the plane of the solar vector. The angle of deployment is equal to 90° minus the latitude of the LUTE landing site (fig. 71). This angle is preset before launch. The array has a tent cross-section (fig. 72). The tent configuration is modeled such that the power at sunrise and sunset is equal to that at high noon. The final configuration (see fig. 70) consists of four panels, panels 1 and 4 are fixed while panels 2 and 3 require deployment. Panels 1 and 4 are illuminated only during low Sun angles and are not sensitive to latitude. Designing the array as a four-panel configuration helps accommodate packaging within the allowable constraints.

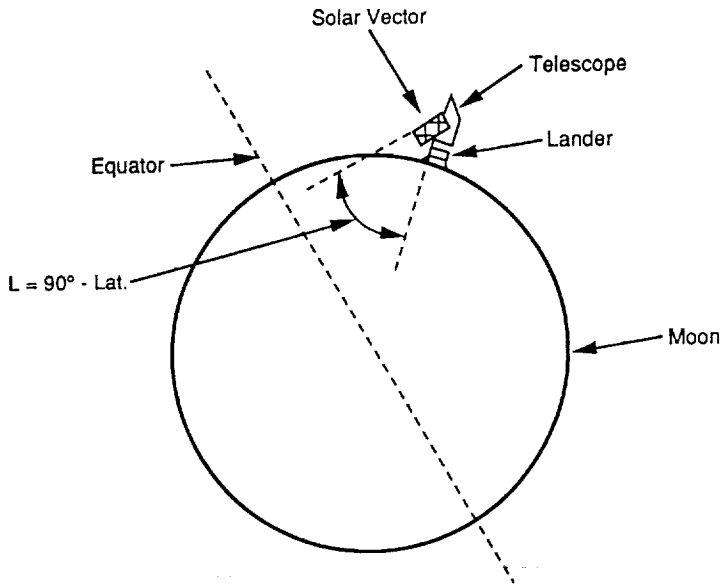

Figure 71. LUTE solar array Sun angle.

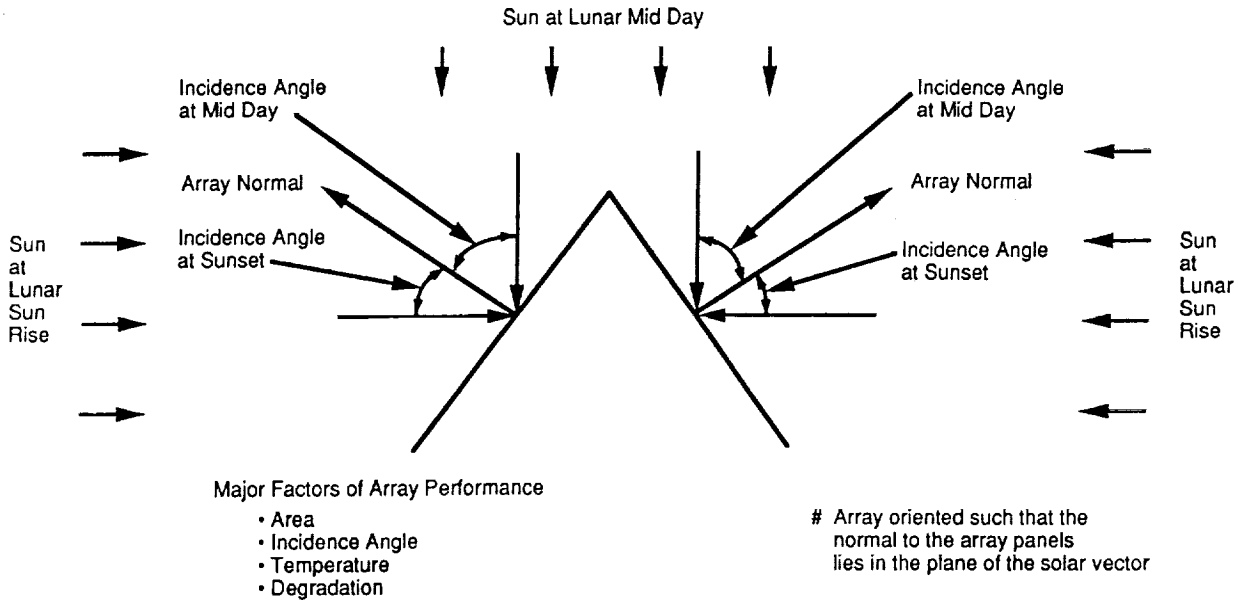

Figure 72. LUTE photovoltaic power system.

5.4.4.1 Solar Array Requirements

The power source, when utilizing a solar array, must be designed for the nominal operation power condition; however, as noted from the power requirement of table 35, there are expected power levels during the acquisition phase as power levels approach 95 W. During this phase, a supplemental primary lithium battery could be used to supply power to the Sun sensor and rollring assembly. The battery is sized, however, to have the required energy to completely perform the entire mission phase of acquisition. The normal operational power required by LUTE is approximately 79 W. The array must be designed and sized to supply this amount of power under the worst case condition at the end of life (EOL). From figure 73, it would be represented by the combined array output when operating at approximately 58 percent of the array's capability. Due to the temperature rise of the array as the lunar day progresses and the incident angle of the Sun vector to the plane of the arrays, the output power will vary for the eastward and westward pointed array, as shown. By utilizing the inherent characteristic of this solar array configuration and the effects of solar cell temperature, the average power output is sufficient during parts of the lunar day to supply the intermittent power requirement if these power consuming functions are timed to occur at high Sun incidence and low temperature conditions, as shown in figure 73. The power level requirement for the intermittent phase is expected to be 92 W. These power levels can be accommodated early in the mission, but at the EOL, the power required exceeds the worst-case design capability. However, this can still be accommodated by proper time of day selection to perform the alignment. Figure 73 shows that the array can provide the required power except at the minimal output periods at approximately the 10 and 2 o'clock Sun positions. Timing actuator operations should alleviate this problem.

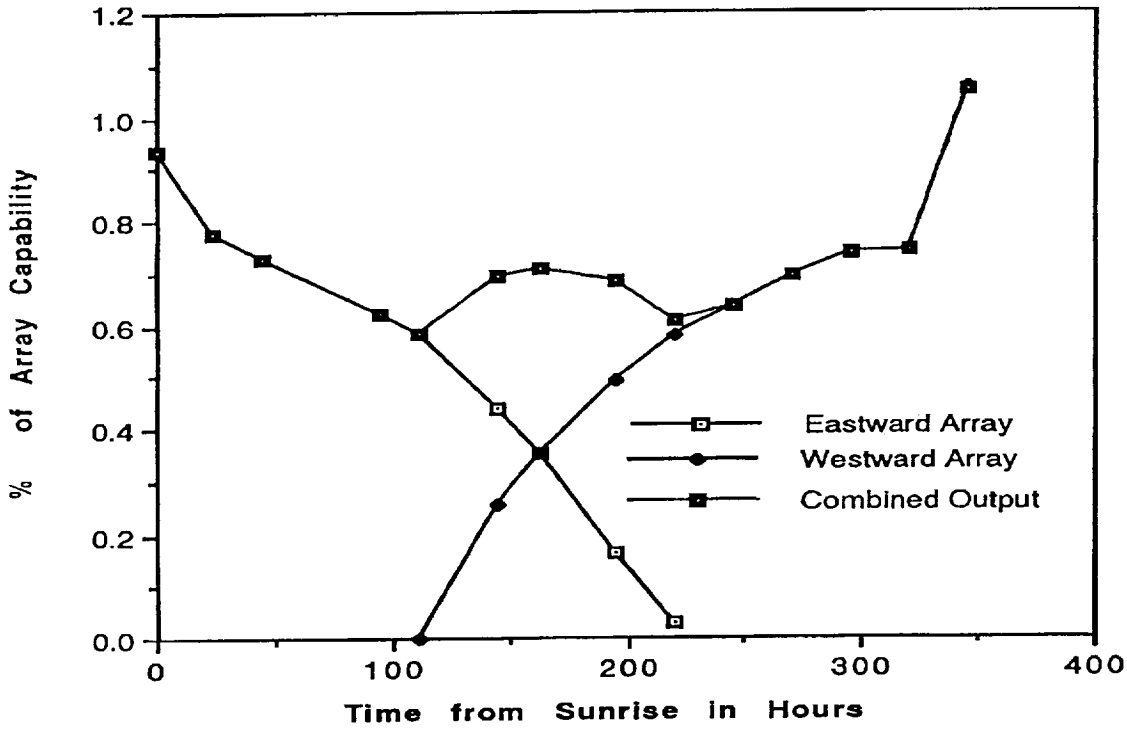

Figure 73. LUTE solar array performance.

5.4.4.2 Solar Array Performance

Solar array cell performance is significantly affected by cell temperature; therefore, it was necessary to determine the expected solar array temperature for a lunar day/night cycle. Figure 74 shows a plot of these temperatures. The high temperature is approximately 370 K and the low temperature is approximately 78 K. It should also be noted that the eastward pointing array and the westward array experience the same temperature delta, but at different times of the lunar day. This fact has been utilized to improve LUTE system performance as addressed in figures 74 and 75.

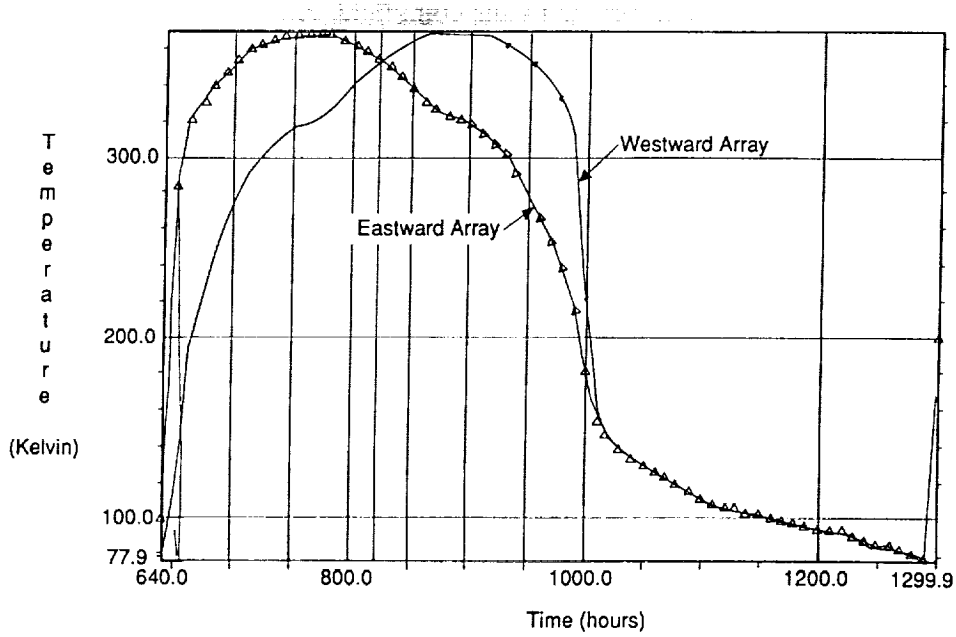

Figure 74. Solar array temperatures.

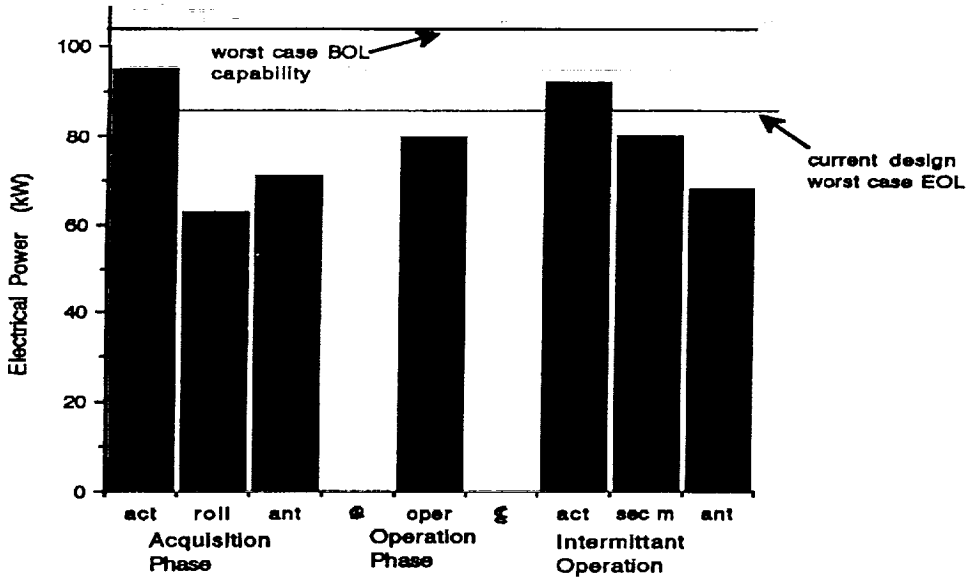

Figure 75. LUTE power requirements by phase.

5.4.5 Use of an RTG

The use of an RTG for the LUTE EPS is described in figure 76.

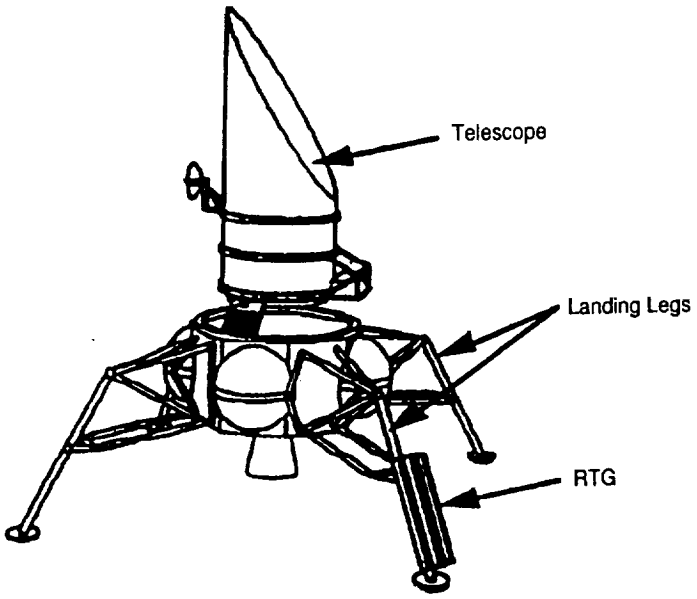

Power Capability	300 watt
EPS Mass	
RTG	56.2 kg
Regulator	12 kg
Distribution	10 kg

Figure 76. EPS RTG description.

Consultation with the Department of Energy (DOE) and General Electric (GE) Aerospace on the configuration, mass, and cost of an RTG has shown the configuration that represents the least cost and earliest availability approach consists of one-half (150 W) of the current general purpose heat source (GPHS) RTG. The power level, delivered by this configuration, is compatible with the current LUTE requirement with approximately 100 percent growth. However, the full 300 W RTG has been selected for LUTE, as discussed in the following.

5.4.5.1 RTG Requirements

The requirements of the LUTE RTG would be to maximize the use of the current RTG. This configuration would minimize design, qualification test, and to some degree, meet the required compliance of the National Nuclear Safety Policy. These conditions can be best met by using the GPHS RTG, used on the Galileo and Cassini spacecrafts. If the 150 W power level were desirable, the physical configurations and designs of this RTG could be used by reducing the thermoelectric converters and plutonium general purpose heat sources of the GPHS RTG by 50 percent and retaining the end cap and mounting flange. The gas management assembly would have to be redesigned.

5.4.5.2 RTG Performance

The design of the Galileo-type RTG is based upon a considerably longer lifetime requirement than that proposed for LUTE. This RTG offers a distinct advantage. Additionally, the ability for lunar day and night operation, with possibly only a minor drop in power output, will offer considerably more flexibility for LUTE performance and system operations. The RTG, as designed, for Galileo has a restriction upon the ambient temperature maximum limit of 563 K. In addition to the physical dimension

changes to the GPHS and thermoelectric generator, there is some reduction in output power of the RTG as the cold junction of the thermoelectric generator increases the effect of background temperature on the available power, as shown in figure 77.

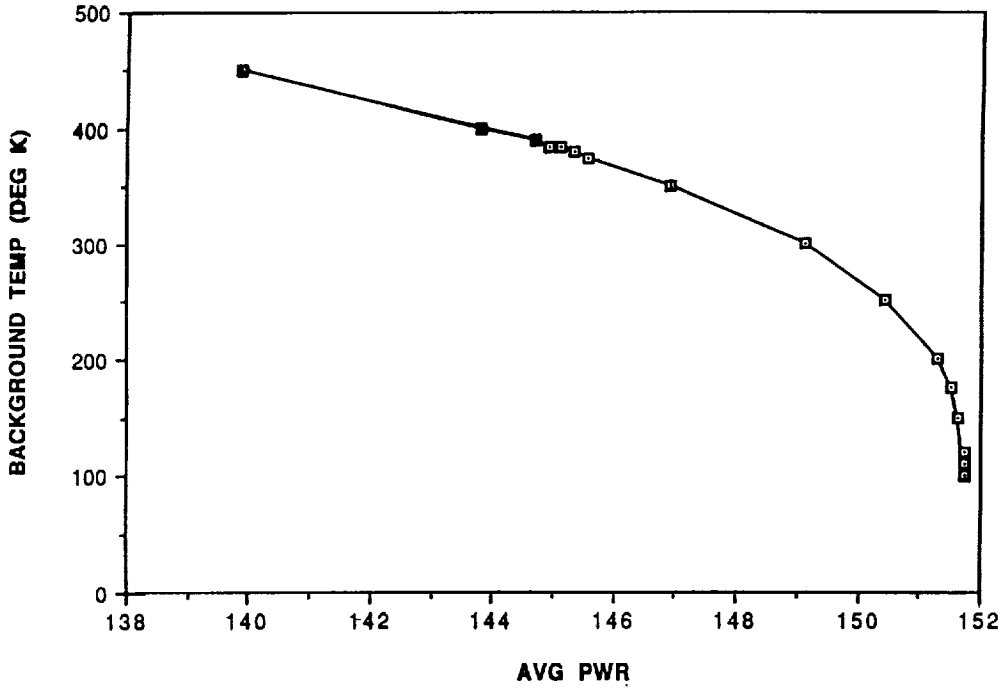

Figure 77. RTG power output versus background temperature.

5.5 Thermal Control System

The procedures and requirements used to define the LUTE TCS are described below. In addition, the trade studies and analyses conducted are discussed and general conclusions are presented. Telescope, detector, and subsystems thermal control are treated separately. A baseline telescope system is described for use as a reference point in the trade studies. Please note that this baseline is not the LUTE reference configuration.

5.5.1 Procedure

A combination of hand calculations, simple and detailed math models, and consultation with vendor representatives has been used to develop and evaluate options for the LUTE TCS. The analysis tools used are listed in table 36.

As indicated, spreadsheet calculations were used for quick estimates and preliminary assessments. Thermal Radiation Analyzer System (TRASYS) and Systems Improved Numerical Differencing Analyzer (SINDA) models were used in conjunction for heat transfer analyses, primarily of the detector radiator and the subsystem radiator. Models constructed using I-DEAS™ were used in the thermal model generator (TMG™) program for more detailed analyses of the primary mirror, light shade, and subsystems. The TRASYS and TMG™ programs calculate radiation conductors and orbital heating at

Table 36. Analysis tools.[36–40]

Code	Platform	Function
Excel	Macintosh	Spreadhseet, quick estimates of temperature, heat rejection capability, etc.
TRASYS	VAX	Radiative heating calculations
SINDA '85	VAX	Heat transfer calculations with input from TRASYS model
I-DEAS™	SG 4D/35 W/S	Model generation and postprocessing of results
TMG™	SG 4D/35 W/S	Radiative heating and heat transfer analyses

specified times during an orbit, based on the model geometry and orientation. SINDA and TMG™ are used to conduct either transient or steady-state heat transfer analyses, considering thermal capacitance, radiation, convection, and conduction. Boundary conditions are specified by the user. Output from a transient analysis is in the form of time-varying element temperatures, supplemented by heat flux through specific conductors, if desired.

5.5.2 Trade Description

Trade studies were conducted in several areas, indicated in table 37, to understand the implications of different TCS and configuration options, to provide a basis for evaluating them, and to support selection of a preferred option.

The TCS trade criteria included performance of the optical system (related to mirror temperature differential and bulk temperature swing) and the performance of other elements of the TCS, such as the detector radiator and the subsystem thermal control.

5.5.3 Telescope Thermal Control

The thermal analysis of the telescope has focused on the LUTE primary mirror and light shade. Some temperature predictions are also available for the tertiary mirror, but will not be discussed in this report. No temperature predictions have been made for the secondary mirror or the metering structure. Thermal requirements for the telescope, as well as analyses and results for the baseline configuration and trade studies, are discussed in the following sections.

5.5.3.1 Requirements

The telescope thermal requirements will be derived from the optical requirements listed in table 6. Deformations induced by temperature gradients within the mirror and its supporting structure have an adverse effect on optical performance. In addition, due to bulk temperature swings experienced by the mirror and its supporting structure, changes in the shape, spacing, and orientation of the optical elements require correction. For these reasons, both temperature differential within the mirror and bulk temperature changes during the operating period must be minimized as much as practical. As used here, temperature differential refers to the maximum temperature difference between any two points on the mirror at a particular time. Bulk temperature change refers to the difference between the maximum and

Table 37. Summary of trade studies performed.

Trade	Options
Isothermal Enclosure	Isothermal Rings Isothermal Basket Isothermal Light Shade Isothermal Baseplate and Ring Isothermal Baseplate
Light Shade	Cylindrical With Insulation Cylindrical Without Insulation Thermal Control Baffles 65°N Latitude With 25° Tilt Low Emissivity Light Shade Interior External Ground Shade
Site Latitude	40° 48.5° 57° 65°
Mirror Construction and Support Structure	One-Piece Primary/Tertiary With Ring Two-Piece Primary/Tertiary With Ring Two-Piece Primary/Tertiary With Three-Point Flexures
Lunar Surface Optical Properties	Low α, Low ε High α, Low ε Low α, High ε Low α, High ε, Low ε Light Shade
Light Shade Baffles	Angled Rings
Light Shade Flare Angle	5° 10° 15°
Mirror Material	Beryllium SiC Fused Silica
Effect of RTG Location	North Side on Lander Leg South Side on Lander Leg
Detector Cooling	Passive Radiator TEU plus Radiator Alternatives
Electronics Box Radiator Position	North Side East/West Side South Side
Electronics Box Night Heat Source	Heater Electronics Operating Phase Change Material
Electronics Box Radiator Cover	Louvers Insulated Door

minimum temperature of the mirror during a lunar day/night cycle. As will be seen, light shade temperature has a significant effect on mirror temperature differential, mirror bulk temperature swing, and detector performance. Therefore, mirror temperature differential, bulk temperature swing, and light shade maximum temperature will be used to evaluate telescope thermal control options.

The allowable temperature gradient and total bulk temperature change has not yet been quantified and can only be determined by much more detailed thermal, structural, and optical analyses. It is expected that the allowable gradient will eventually be specified as a set of temperature differentials in the axial, diametral, and circumferential directions. The bulk temperature change allowable may be specified as a maximum and minimum allowable temperature during operation, with or without a maximum rate of change specified. These requirements will be influenced by the choice of mirror material and construction and by the support structure design.

Mass and power constraints strongly suggest a passive thermal control system, although low power heaters may be an option, with the availability of an RTG.

5.5.3.2 Initial Thermal Analysis

I-DEAS™ TMG™ thermal models were used to predict mirror temperatures and to determine what factors influence the primary mirror temperature distribution. A reduced model with approximate geometry and a greatly reduced number of elements was used to determine factors influencing light shade internal temperatures and evaluate concepts in a quick fashion, while a more detailed model with accurate mirror geometry was used for actual mirror temperature predictions.

The geometry for the baseline configuration is shown in figure 78. The model is assumed to be located on a flat site at 40° north latitude with the sunshade rotated so that its highest point is to the south. Note that for the reference configuration, LUTE is located at a 65° north latitude, but still views at a 40° declination.

5.5.3.3 Model description

The two basic computer models used for this effort will be referred to as the reduced model and the detailed model. Both consist of the same basic elements: light shade, external insulation, mirror, lander body, lunar surface, and subsoil. In both cases the mirrors and light shade are beryllium, the external insulation is MLI, the lander body is aluminum, and the lunar surface properties are based on information obtained during the Surveyor and Apollo programs.[41]

Figure 79 shows how the lunar surface was simulated in the model and the arrangement of elements simulating the surface. The curvature of the Moon was simulated and a large enough portion of the lunar surface was modeled to adequately represent radiation interchange between the LUTE and the surface. Surface material thickness and subsoil temperature were varied to obtain a day/night temperature profile that simulates measured lunar surface temperatures.

The 40° north latitude location was simulated by tilting the entire model 40° from the solar vector and placing the model in a planet oriented orbit about the Earth at a radius of 390,290 km. The solar declination was specified as –23.5° and the orbit inclination was specified as 25° to simulate correct lighting conditions for midsummer on the Moon, which is the hot case lighting condition. The solar flux is 1,353 W/m^2, the Earth infrared flux is 236 W/m^2, and the Earth albedo factor is 0.35.

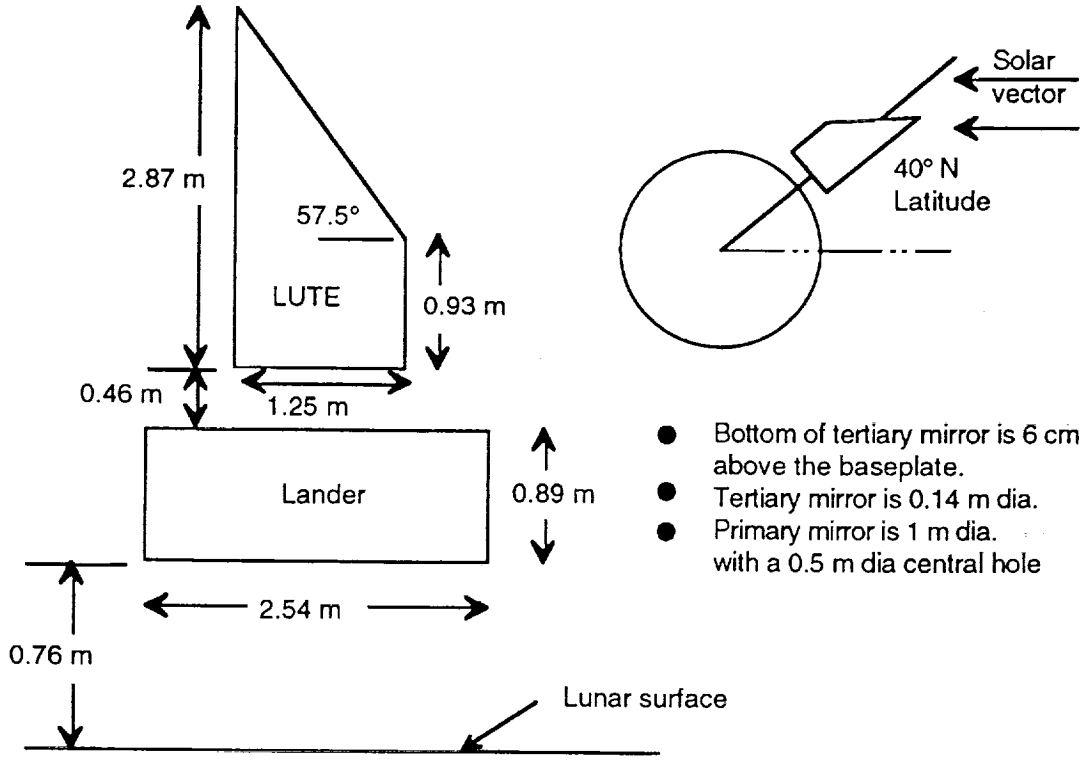

Figure 78. Baseline model geometry.

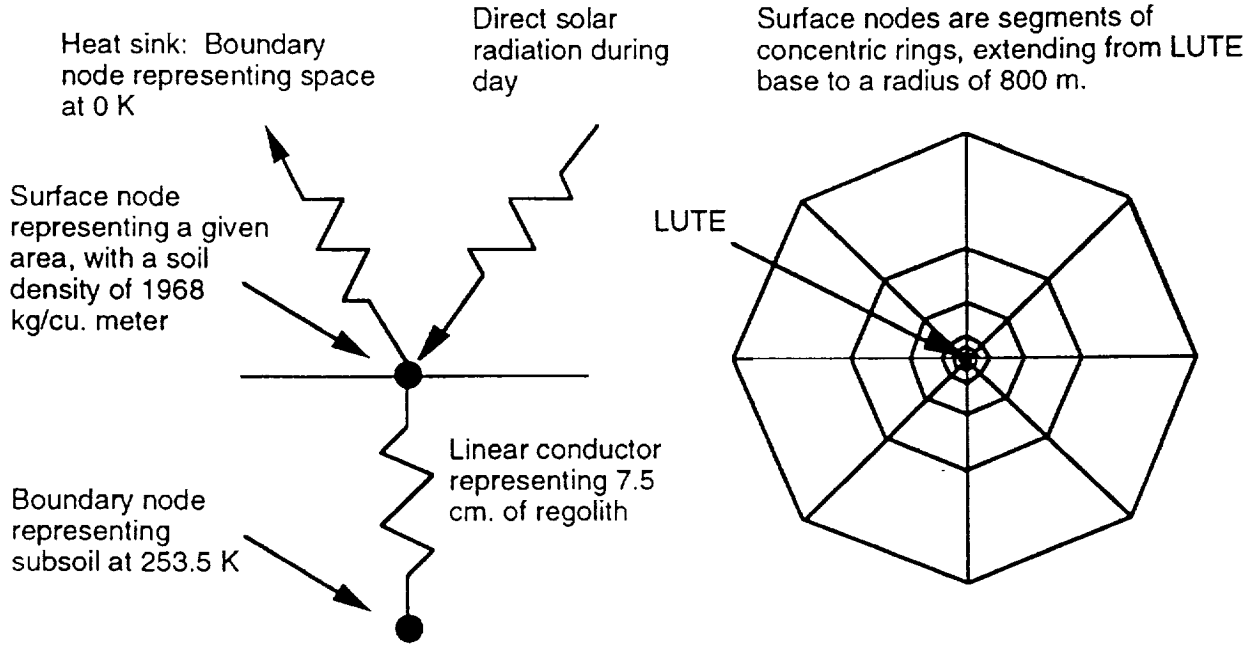

Figure 79. Lunar surface simulation.

Preliminary analyses indicated that if the thermal analyses are begun with the initial temperatures, as shown in table 38, the effect of the initial temperature is eliminated by the second diurnal cycle. All results presented are for the second diurnal cycle of a simulation. All simulations begin at sunrise and output is typically recorded at 10 hour intervals.

Table 38. Model initial temperatures.

Component	Initial Temperature (K)
Mirrors	100
Light shade	110
Baseplate	110
MLI	110
Lander	110
Lunar surface	100
Subsoil	253.5
Space	0

Assumed internal construction of the primary and tertiary mirrors is shown in figure 80. The sandwich core of the mirrors was simulated as a linear conductance based on the area of the core material in contact with the face sheets. This construction was used for all mirror materials evaluated.

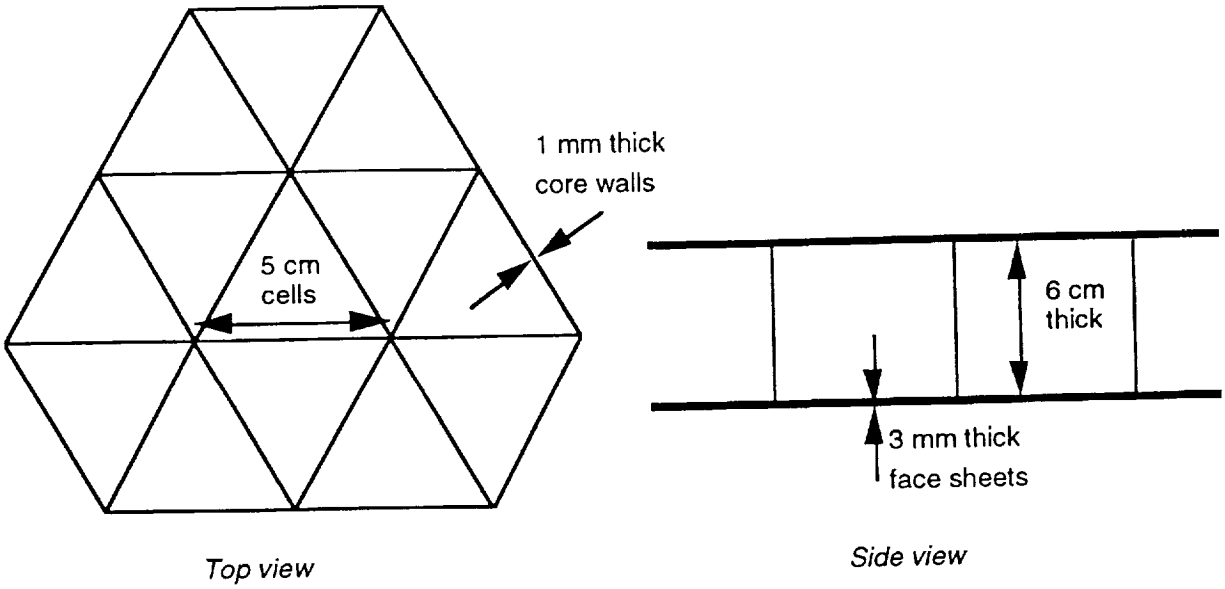

Figure 80. Mirror construction.

The reduced model, shown in figure 81, has a square light shade and mirror to reduce the number of elements in the model, which reduces the time between concept generation and availability of analysis results.

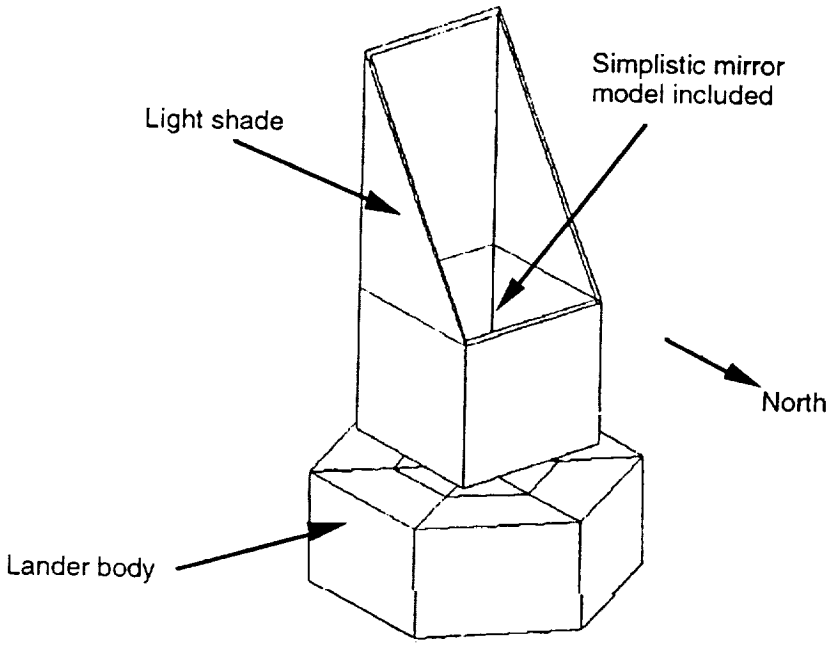

Figure 81. Reduced LUTE TMG™ model.

The total number of elements included is 210, with 20 of those representing the telescope and the rest representing the lander and the lunar surface. The primary mirror is composed of four elements, two on the top surface and two on the bottom surface. These are oriented to represent the north and south halves of the mirror.

The detailed thermal model, shown in figure 82, has 112 elements representing the primary mirror and 64 representing the tertiary mirror for the thermal analyses. The primary and tertiary mirrors are located on the same blank of material and are connected by a ring of elements. The primary mirror is assumed to be supported by a continuous ring at the outer diameter. The model consists of 575 elements with run times of 13 to 36 hours, depending on the degree of element merging and presence of additional elements required for a particular trade study.

Internal baffles, metering structure, and secondary mirror are not included in this thermal model. These components will have some effect on mirror temperatures and should be evaluated in future activities.

There is some concern about the precision of the analytical results from these models. Model inputs such as material properties, optical properties, and geometry are typically known to one or two significant figures. Results have been presented to two significant figures in most cases. However, errors of 5 to 10 K are not uncommon for a thermal model. Additional information on the environment and physical construction will improve the accuracy in phase B.

5.5.3.4 Material Properties

Table 39 indicates the major parts of the LUTE and identifies the material, thickness, and optical properties used for each. The baseline model was generated before the concept was well defined and does not necessarily represent the reference configuration. For instance, the light shade is not beryllium in the reference configuration and the lander body is not necessarily aluminum. In addition, beryllium

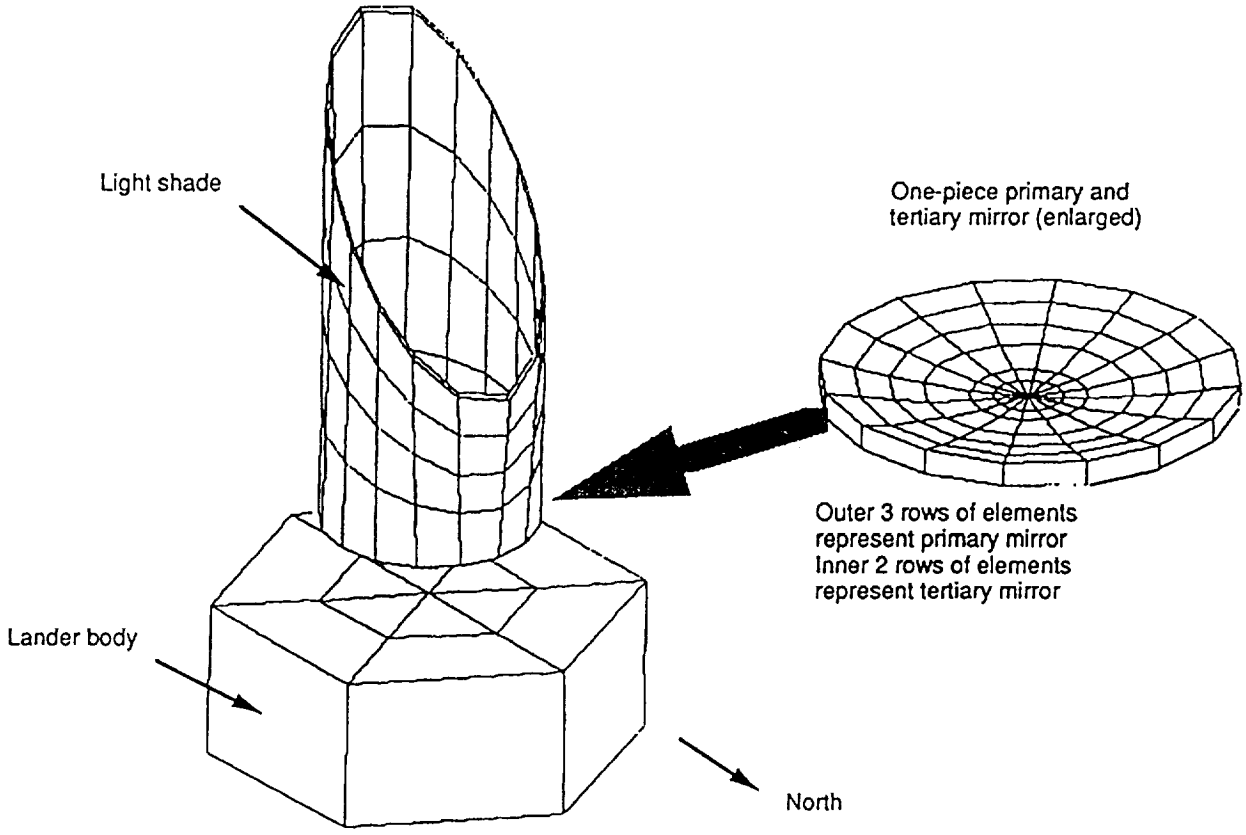

Figure 82. Detailed LUTE TMG™ model.

may not be the material selected for the optical elements. These assumptions were made in the early part of the study and the materials have not been changed to preserve the consistency of the trade studies done with the models. In general, the trends observed should be valid, even though the actual temperatures will be affected if significant material changes are made.

Insulation thicknesses were chosen based on previous work done for the LTT.[42]

Table 39. LUTE thermal analysis materials.

Component	Material	Thickness	Emissivity (e)	Absorptivity (a)
Mirror (front)	Beryllium	see fig. 82	0.03	0.09
Mirror (back)	Beryllium	see fig. 82	0.5	0.05
Light shade	Beryllium	0.11 cm	0.8	0.8
Baseplate	Beryllium	1.0 cm	0.8	0.8
Light shade ins.	MLI	0.625 cm	0.78	0.2
Baseplate ins.	MLI	1.27 cm	0.2	0.2
Lander	Aluminum	1.0 cm	0.78	0.28

5.5.3.5 Initial Results

These results are for the detailed thermal model, pointing to zenith at the 40° north location, with nominal optical properties and insulations and no heat pipes or other devices to reduce temperature gradients. Primary mirror temperature versus time is shown in figure 83. The total mirror temperature swing is 161 K and occurs, roughly, between dawn and local noon. The maximum primary mirror temperature differential is 0.35 K and the average temperature differential is 0.25 K.

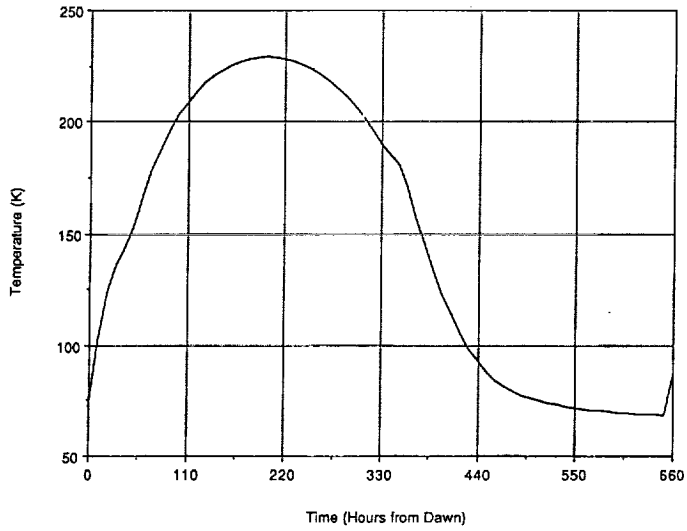

Figure 83. Primary mirror temperature for baseline.

A representation of the mirror temperature distribution for local morning, noon, and late afternoon is shown in figure 84. This illustrates the hot spot on the primary mirror, which is located on the north side at midday, but generally moves from the east to north to west during the day. Figure 85 shows the light shade temperature at local morning, noon, and late afternoon, which influences the mirror hot spot. The upper internal surface of the light shade is significantly warmer than the lower portion at

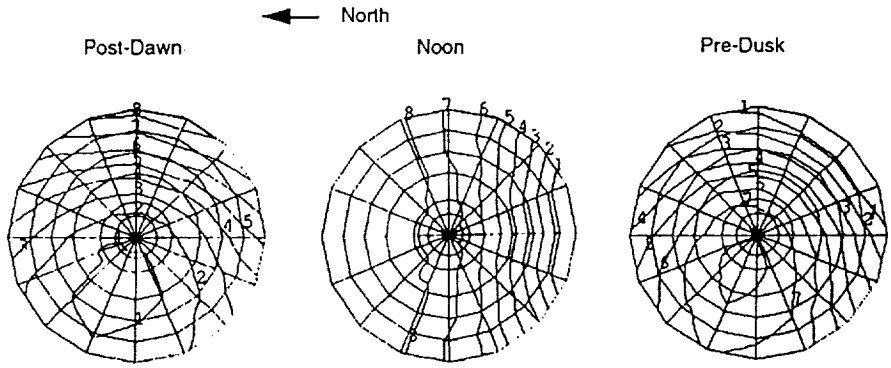

Contour	Temp. (K)
1	123.91
2	123.94
3	123.98
4	124.01
5	124.04
6	124.07
7	124.11
8	124.14

Contour	Temp. (K)
1	228.17
2	228.20
3	228.22
4	228.24
5	228.27
6	228.29
7	228.31
8	228.34

Contour	Temp. (K)
1	184.96
2	184.98
3	185.01
4	185.04
5	185.06
6	185.09
7	185.12
8	185.14

Figure 84. Baseline primary mirror temperature distribution (top view).

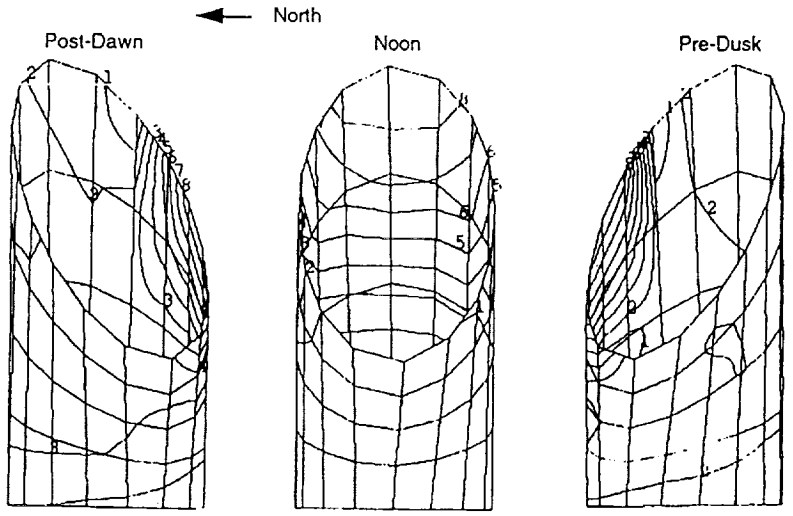

Contour	Temp. (K)	Contour	Temp. (K)	Contour	Temp. (K)
1	119.42	1	233.42	1	175.17
2	131.76	2	242.35	2	182.81
3	144.11	3	251.27	3	190.46
4	156.45	4	260.20	4	198.10
5	168.80	5	269.13	5	205.75
6	181.14	6	278.06	6	213.39
7	193.49	7	286.98	7	221.04
8	205.83	8	295.91	8	228.68

Figure 85. Baseline light shade temperature distribution.

midday because of radiation interchange between the upper light shade (high emissivity) and the lunar surface (high emissivity and ≈368 K) illustrated in figure 86. Another contributing factor to the mirror hot spot is early morning and late afternoon "peek over" of solar radiation, in which sunlight impinges directly on the upper east or west edge of the light shade interior as shown in figure 85. This phenomenon occurs near local midsummer and is due to the slight tilt of the Moon's axis of rotation with respect to the ecliptic pole. A third contributor to the temperature differential across the primary mirror is the asymmetric view to space of the primary mirror illustrated in figure 86. The light shade is truncated at a 57.5° angle to prevent sunlight from impinging directly on the north side of the light shade and heating the shade. The 57.5° shade angle also precludes earthlight from entering the telescope. However, this causes the south side of the mirror to have a more favorable view to space than the north side of the mirror. Finally, the mirror temperature is influenced by the baseplate and light shade, which radiate and conduct heat to it, but are not heated uniformly by the environment.

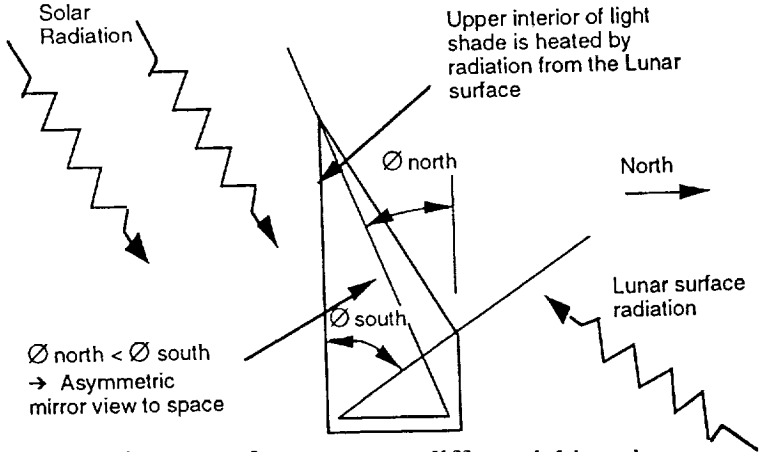

Figure 86. Sources of temperature differential in primary mirror.

5.5.3.5.1 Isothermal Enclosure Trades

The objective of this trade was to examine the influence of the primary mirror's surroundings on temperature differential and bulk temperature swing and to identify options to reduce those parameters. The five isothermal enclosures examined are isothermal rings, isothermal bucket, isothermal light shade, isothermal baseplate and ring, and isothermal baseplate, which are shown along with the baseline in figure 87. Thermal analysis and results for the baseline configuration (fig. 87(a)) have been discussed previously. The enclosure options examined and corresponding analysis results are discussed in the following paragraphs.

Isothermal Rings—The four rows of light shade elements in the TMG™ model were modified by using four merge sets so that the model simulates four highly conductive rings around the light shade as shown in figure 87(b). Each of the four rings is isothermal. In addition to the light shade rings, the baseplate inner surface was forced to be isothermal. Primary mirror temperature distribution at noon is shown in figure 88. The mirror maximum temperature differential is 0.3 K, the average temperature differential is 0.16 K, and the bulk temperature swing is 174.6 K. This represents a slight improvement in mirror temperature differential, but an increase in bulk temperature swing from the baseline. In addition, it may be impractical to achieve this effect.

Isothermal Bucket—In this concept, illustrated in figure 87(c), elements of the inner light shade below the secondary mirror position were merged so that they are forced to an average temperature. This simulates a highly conductive bucket, including the baseplate, which encloses the optical system. Primary mirror temperature distribution at noon is shown in figure 89. The maximum primary mirror temperature differential was 0.06 K, which is a significant reduction from the baseline case. The mirror bulk temperature swing is essentially the same as for the baseline case. An additional advantage of this option is that the metering structure temperature differential would also be reduced from the baseline. However, an isothermal bucket such as this one may be difficult to achieve without significant mass penalties.

Isothermal Light Shade—All elements forming the inner light shade surface, including the baseplate, were merged and forced to an average temperature so that all light shade surfaces visible to the mirror would be at the same temperature at a given time. This is illustrated in figure 87(d). Primary mirror temperature distribution at noon is shown in figure 90. The maximum primary mirror temperature differential of 0.09 K is a significant reduction from the baseline case, though the reduction is not quite as large as for the isothermal bucket option. An interesting result of this analysis is that the remaining gradient across the mirror (about 0.09 K) can be attributed entirely to the asymmetric view to space of elements on the primary mirror. The maximum mirror temperature, and thus the bulk temperature swing, for this option is higher than for the isothermal bucket option or the baseline. This warmer mirror results in a larger temperature differential across the mirror than for the isothermal bucket option because the asymmetric mirror view factor to space is more influential for higher mirror temperatures.

Isothermal Baseplate and Ring—In an effort to determine the minimum isothermal area, which would be effective in reducing the temperature differential across the primary mirror, the lower ring of elements on the light shade interior and the baseplate elements were merged as illustrated in figure 87(e). Primary mirror temperature distribution at noon is shown in figure 91. The maximum mirror temperature differential of 0.06 K and the bulk temperature swing of 160.6 K are essentially the same as for the isothermal bucket case. In addition, the area requiring modification via heat pipes or other very conductive material is much less, so this concept should have a mass advantage.

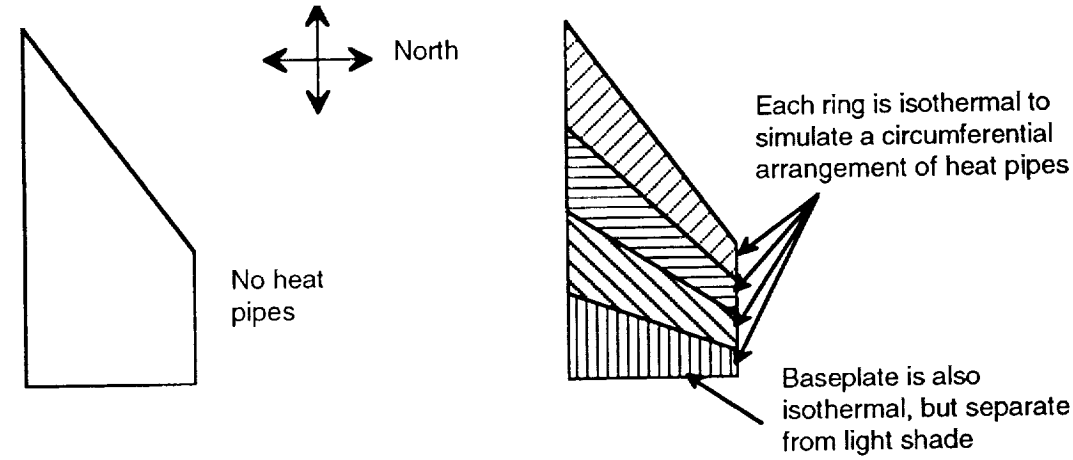

(a) Baseline

(b) Isothermal rings

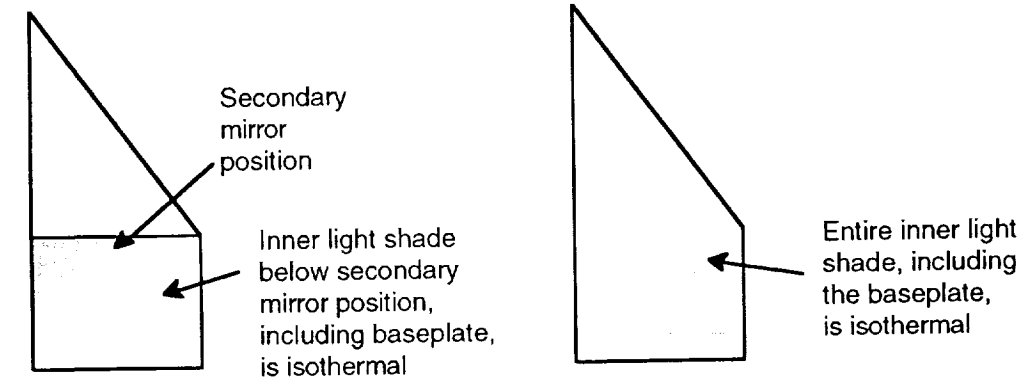

(c) Isothermal bucket

(d) Isothermal light shade

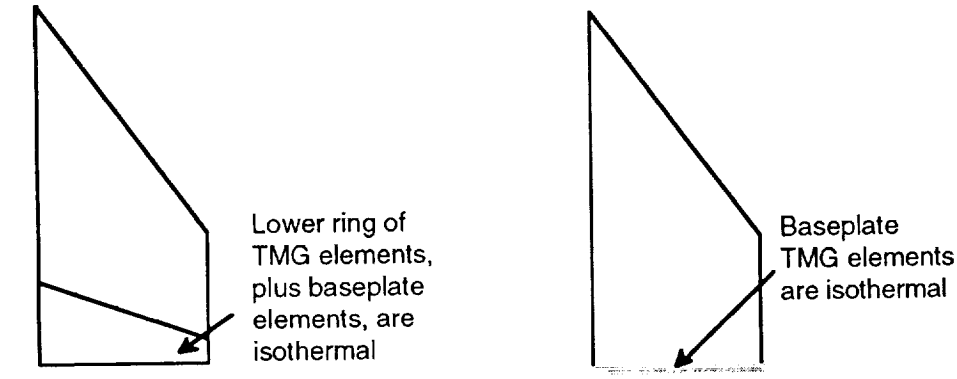

(e) Isothermal baseplate & ring

(f) Isothermal baseplate

Figure 87. Isothermal enclosure options (side view).

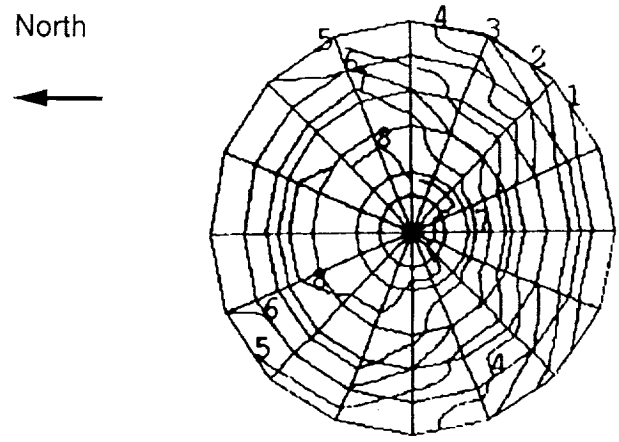

Contour	Temp. (K)
1	242.78
2	242.78
3	242.79
4	242.80
5	242.80
6	242.81
7	242.82
8	242.82

Figure 88. Mirror temperature distribution for isothermal rings (noon).

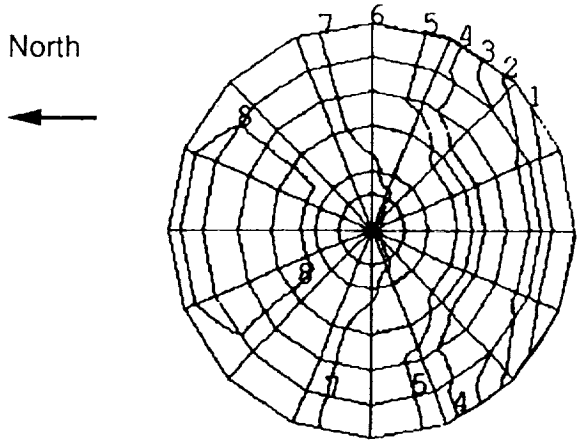

Contour	Temp. (K)
1	227.90
2	227.90
3	227.91
4	227.92
5	227.92
6	227.93
7	227.94
8	227.94

Figure 89. Mirror temperature distribution for isothermal bucket (noon).

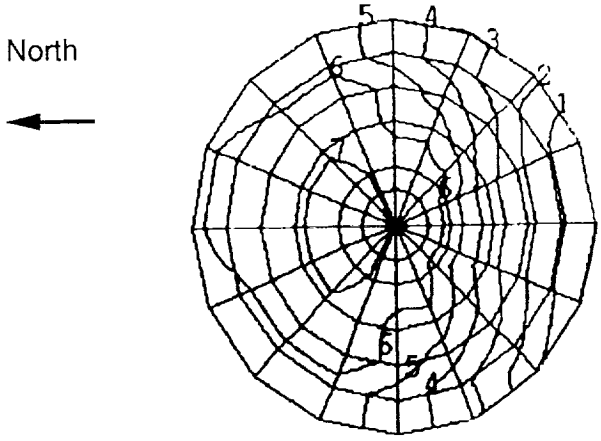

Contour	Temp. (K)
1	261.41
2	261.42
3	261.43
4	261.44
5	261.44
6	261.45
7	261.46
8	261.47

Figure 90. Mirror temperature distribution for isothermal light shade (noon).

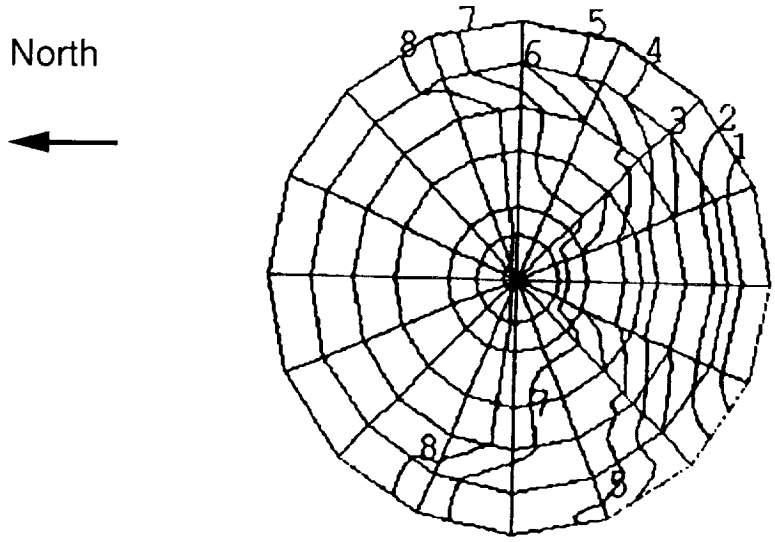

Contour	Temp. (K)
1	227.89
2	227.89
3	227.90
4	227.91
5	227.91
6	227.92
7	227.93
8	227.93

Figure 91. Mirror temperature distribution for isothermal baseplate and ring (noon).

Isothermal Baseplate—This option considered the effect of having an isothermal baseplate, as illustrated in figure 87(f). No portion of the light shade wall was forced to be isothermal. The maximum primary mirror temperature differential was 0.22 K, which is somewhat lower than for the baseline, but not as low as for the isothermal bucket or isothermal baseplate and ring options. The bulk temperature swing for this option is essentially the same as for the baseline. Primary mirror temperature distribution at noon is shown in figure 92. Although this option is the simplest of the five to fabricate, it does not reduce the mirror temperature differential as much as when the ring is also included (above).

Summary of Enclosure Trades—Table 40 summarizes the results of this trade study. The isothermal bucket and isothermal baseplate and ring options have the lowest primary mirror temperature differential and bulk temperature swing.

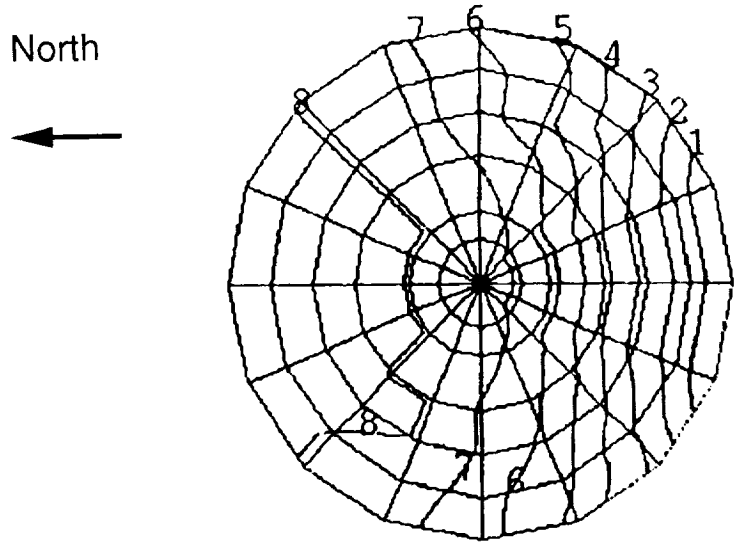

Contour	Temp. (K)
1	228.81
2	228.83
3	228.85
4	228.87
5	228.88
6	228.90
7	228.92
8	228.94

Figure 92. Mirror temperature distribution for isothermal baseplate (noon).

Table 40. Summary of isothermal enclosure trade results.

Option	Maximum ΔT (K)	Mirror Maximum (K)	Night/Day Swing (K)	Shade Maximum (K)	Average ΔT (K)
Baseline	0.35	229.3	161.0	304.8	0.25
Iso. Rings	0.3	243.6	174.6	273.2	0.16
Iso. Bucket	0.06	228.3	161.6	304.8	0.05
Iso. Shade	0.09	261.6	194.4	262.1	0.06
Iso. BP and Ring	0.06	228.0	160.6	304.8	0.05
Iso. BP	0.22	229.2	160.8	304.8	0.16

Primary mirror temperature differential during the day is shown for each option in figure 93. Sunset occurs at about 330 hours on this graph. Peaks after sunrise and sunset are caused by the rapid temperature change in the environment. The isothermal baseplate and ring seems to be the best isothermal enclosure option for LUTE.

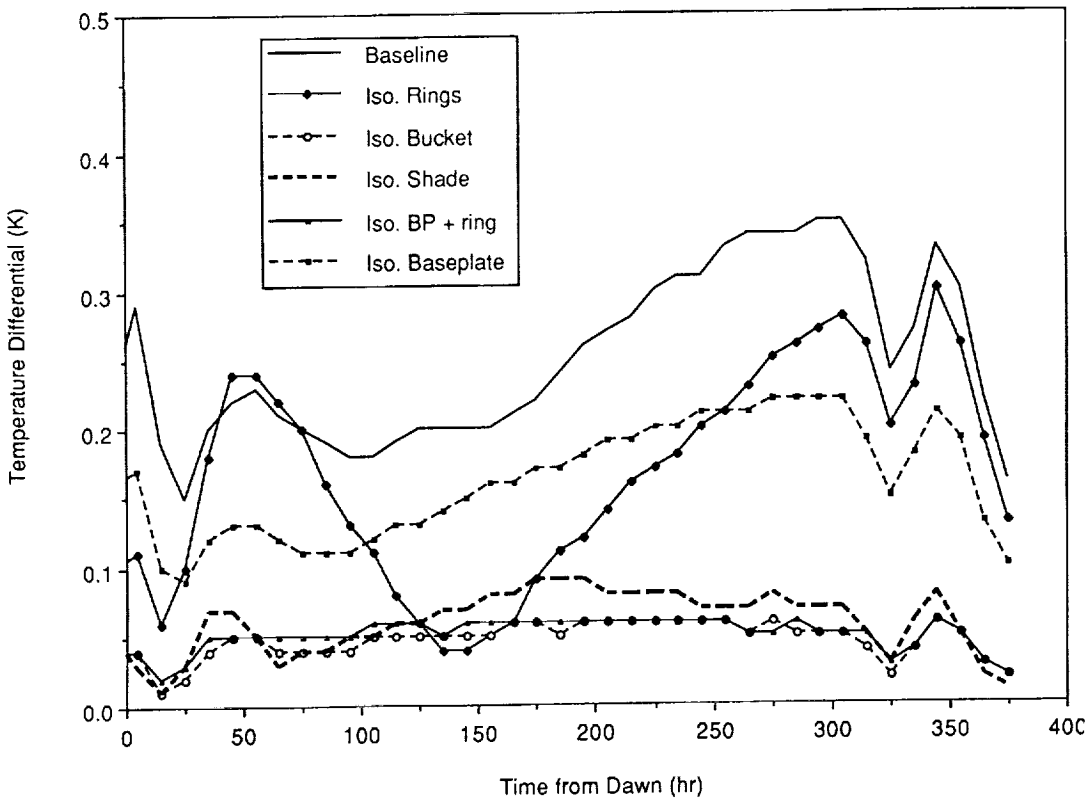

Figure 93. Primary mirror temperature differential for enclosure options.

Results for the isothermal shade indicate that a significant mirror temperature differential (0.09 K) is caused by the asymmetric light shade geometry. The difference in results for the isothermal bucket and isothermal shade options (0.06 K versus 0.09 K) indicates that this differential is strongly dependent on mirror maximum temperature and increases with mirror maximum temperature. Thus, lowering the mirror maximum temperature will also help to reduce the mirror temperature differential.

5.5.3.5.2 Light Shade Trades

As indicated earlier in table 37, several options for light shade shape, orientation, and construction were considered as part of the light shade trade. Two alternate light shade shapes and one alternate orientation are illustrated in figure 94. In addition, a concept in which the upper portion of the light shade was coated with a low emissivity material and an option with an external, three-sided ground shade were considered. These options are discussed in the following paragraphs.

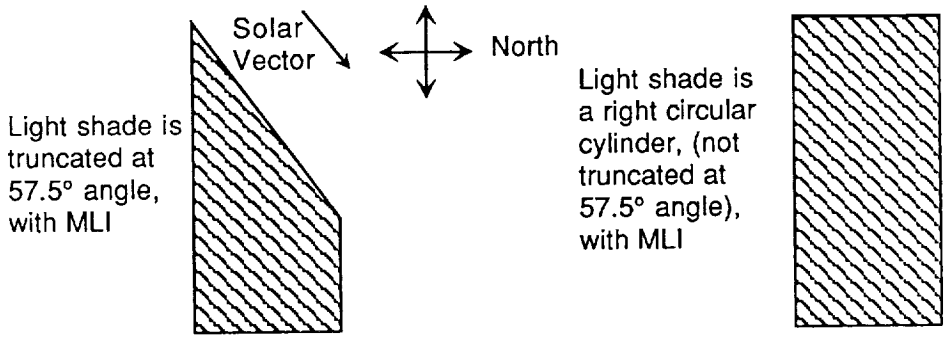

(a) Baseline

(b) Cylindrical with MLI

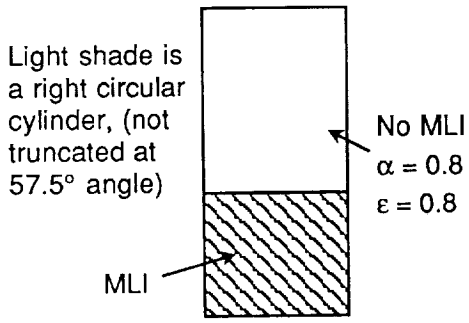

(c) Cylindrical without MLI

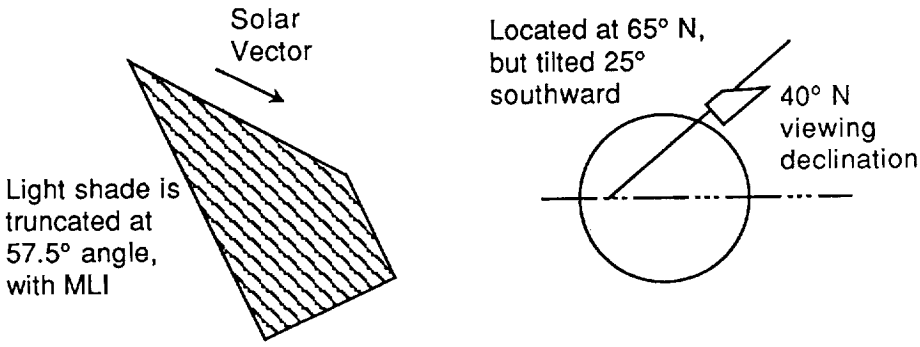

(d) 65° N with 25° tilt to south

Figure 94. Light shade shape and orientation options.

Cylindrical Shade with Insulation—A cylindrical light shade was proposed to provide a symmetric view to space for the north and south sides of the primary mirror. This concept is illustrated in figure 94(b). The interior of the light shade has $\alpha = 0.8$ and $\varepsilon = 0.8$ and the entire exterior is insulated with MLI. The maximum mirror temperature of 371.7 K is much hotter than for the baseline case (229.3 K) due to the hotter light shade temperature (410.4 K versus 304.8 K) caused by direct solar absorption on the north side of the light shade interior. This direct solar heating of the light shade interior causes the mirror hot spot to move from east to south to west during the day. For the baseline configuration, the hot spot moved from east to north to west during the day. Mirror maximum temperature differential also increased from the baseline, although the average temperature differential decreased to 0.16 K. This concept is not recommended because of the elevated temperatures in the vicinity of the detector radiator, which must reject heat at approximately 200 K inside the upper light shade. In this concept, not only was the radiator FOV reduced, but the temperature of the radiator surroundings increased to about 400 K at midday.

Cylindrical Shade Without Insulation—In an attempt to reduce the light shade temperature while maintaining a symmetric light shade, the MLI was removed from the upper light shade and the optical properties of the shade exterior were changed to $\alpha = 0.8$ and $\varepsilon = 0.8$, as shown in figure 94(c). This provides for more even heating of the shade from solar radiation and interchange with the lunar surface. The mirror temperature differential is reduced during the middle part of the day, but is increased at low Sun angles, primarily because at that time only one side of the shade receives direct solar radiation and the surface temperature at that time of day is lower than the light shade temperature. The maximum and average mirror temperature differentials are 0.86 and 0.05 K, respectively. The maximum mirror temperature remained high, at 348.7 K, contributing to a bulk temperature swing of 278.7 K, over 100 K greater than for the baseline. The maximum light shade temperature of 363.8 K is also higher than the baseline and, like the previous option, will adversely affect detector heat rejection capability. This option is not recommended.

65° North Latitude With 25° Tilt—Moving the telescope to a more northerly latitude, then tilting it southward to view at 40° declination reduces the upper light shade radiative interchange with the lunar surface. The case examined was a latitude of 65° north with a resulting 25° southerly tilt as illustrated in figure 94(d). Results showing primary mirror and light shade temperature distributions are presented in figures 95 and 96, respectively. The mirror average temperature differential of 0.13 K is a significant reduction from the baseline concept. The maximum mirror temperature differential and maximum mirror temperature were also reduced from the baseline. The bulk temperature swing of 105.1 K is significantly lower than the 161 K for the baseline. The maximum upper light shade temperature was reduced from 304.8 K in the reference to 198.6 K, providing a much better environment for the detector radiator which must reject heat at 200 K.

Low Emissivity Light Shade Interior—Since heating of the upper light shade is primarily from radiative interchange with the lunar surface, a low emissivity coating was suggested for this surface rather than the high emissivity coating previously examined. The coating analyzed was $\alpha = 0.7$, $\varepsilon = 0.07$. The effect was actually to increase the temperature of this surface from 304.8 K in the baseline to 336 K, since some reflected solar radiation from the surface was still absorbed, but could not be rejected by radiation to space as effectively as when the emissivity was 0.8. The result was radiation of a lesser amount of heat from the surface, but with a lower emissivity and, therefore, at a slightly higher temperature. Mirror temperature gradient and bulk temperature swing were essentially the same as for the baseline.

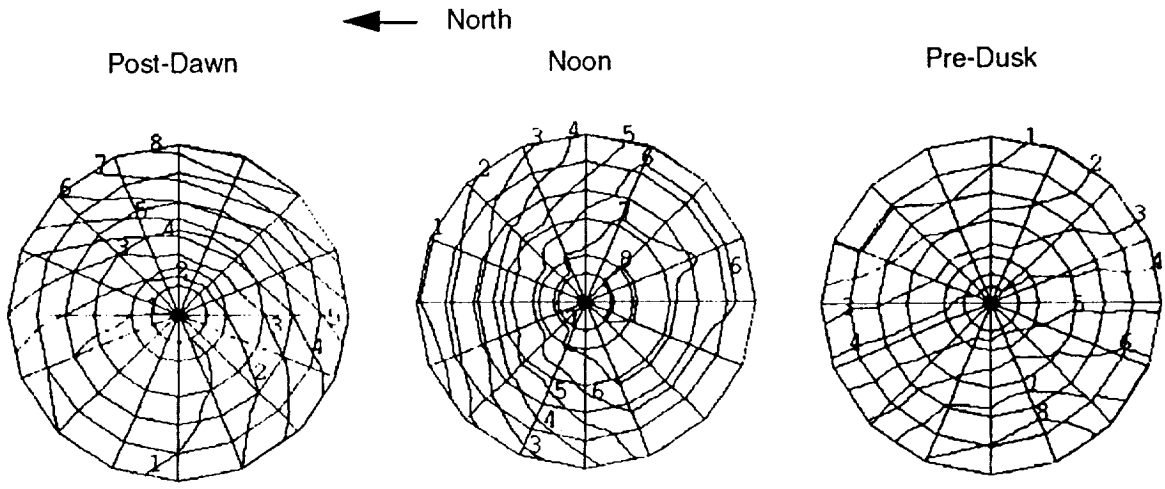

Contour	Temp. (K)	Contour	Temp. (K)	Contour	Temp. (K)
1	121.69	1	169.35	1	157.03
2	121.72	2	169.36	2	157.05
3	121.75	3	169.37	3	157.07
4	121.78	4	169.38	4	157.09
5	121.81	5	169.40	5	157.12
6	121.84	6	169.41	6	157.14
7	121.87	7	169.42	7	157.16
8	121.90	8	169.43	8	157.18

Figure 95. Mirror temperature distributions for 65° north with tilt option.

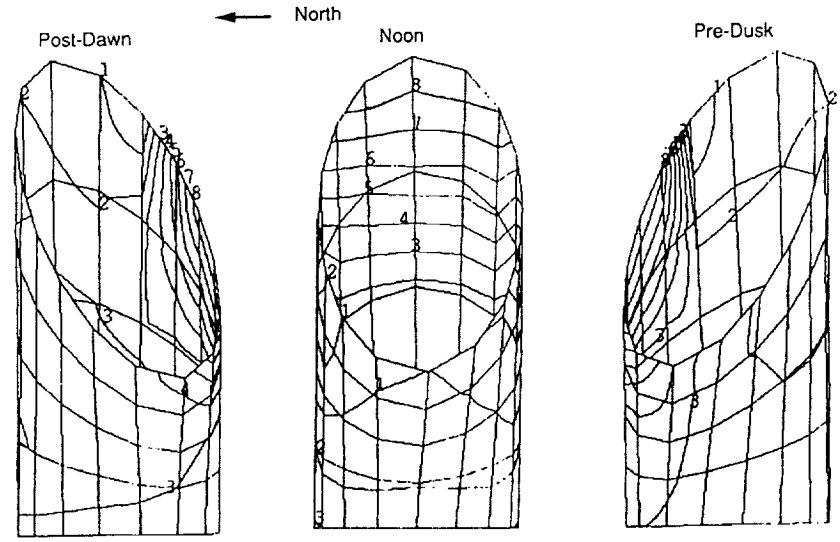

Contour	Temp. (K)	Contour	Temp. (K)	Contour	Temp. (K)
1	107.03	1	161.41	1	134.05
2	120.45	2	166.06	2	145.09
3	133.88	3	170.70	3	156.13
4	147.30	4	175.35	4	167.17
5	160.72	5	180.00	5	178.21
6	174.14	6	184.65	6	189.25
7	187.57	7	189.29	7	200.29
8	200.99	8	193.94	8	211.33

Figure 96. Light shade temperature distributions for 65° north with tilt option.

External Ground Shade—An external ground shade was suggested to reduce heating of the upper light shade from the lunar surface. This was examined in the form of a three-sided shade as illustrated in figure 97. The shade was MLI with an internal absorptivity of 0.2 and emissivity of 0.78 and an external (away from telescope) absorptivity of 0.15 and emissivity of 0.15. Results indicate increased temperature differential, temperature swing, and light shade temperature as compared to the baseline, because the ground shade temperature is similar to the lunar surface temperature, but is much closer to the telescope. This concept is not viable unless a tall southerly shade can also be provided to eliminate direct solar absorption by the enclosure or the interior of the shade can be made specular.

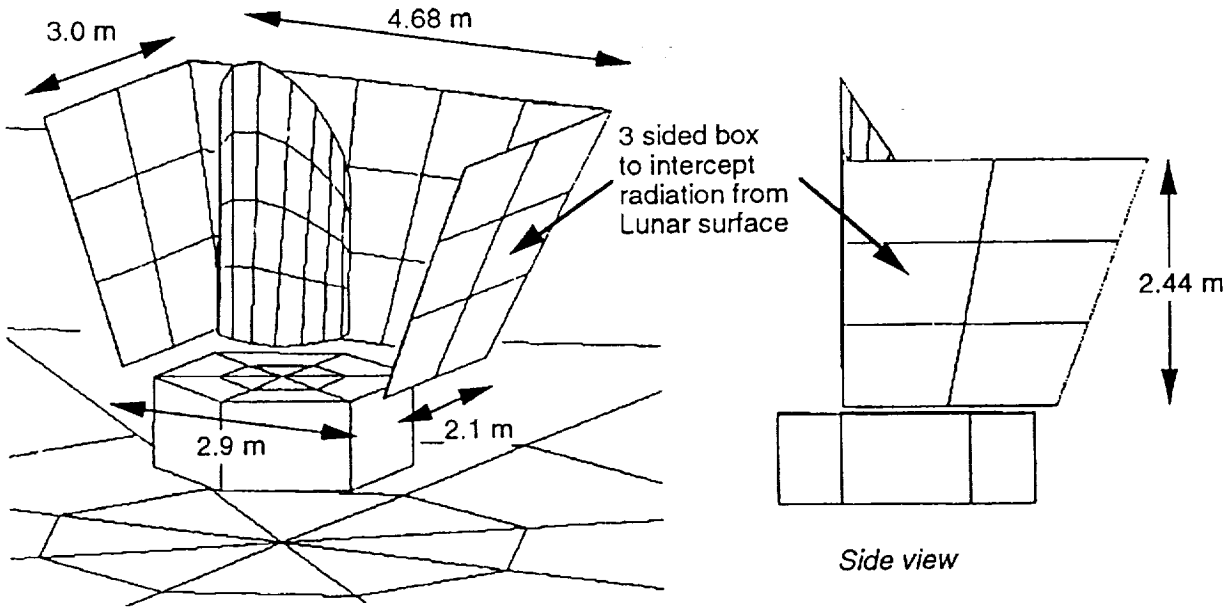

Figure 97. External ground shade encloses LUTE east, west, and north sides.

Summary of Light Shade Trades—Table 41 summarizes the results for all light shade options examined. The only clear improvement over the baseline is the 65° north location with the LUTE tilted 25° to the south. This reduces mirror temperature differential, bulk temperature swing, and light shade maximum temperature. The cylindrical light shades reduce the average mirror temperature differential, but increase bulk temperature swing and light shade temperature dramatically. These side effects are probably unacceptable for LUTE.

Table 41. Summary of light shade trade results.

Option	Maximum ΔT (K)	Mirror Maximum (K)	Night/Day Swing (K)	Shade Maximum (K)	Average ΔT (K)
Baseline	0.35	229.3	161.0	304.8	0.25
Cylindrical	0.61	371.7	301.1	410.4	0.16
Cylindrical, no MLI	0.86	348.7	278.7	363.8	0.05
65° N, tilted	0.27	170.1	105.1	198.6	0.13
Low emissivity	0.35	229.1	160.8	336	0.24
Ground shade	0.54	280.0	213.4	331.8	0.32

Figure 98 shows the primary mirror temperature differential versus time for all light shade options and the baseline. The 65° north option gives the lowest overall temperature differential. Note that the differential for this option is also quite constant for most of the viewing period.

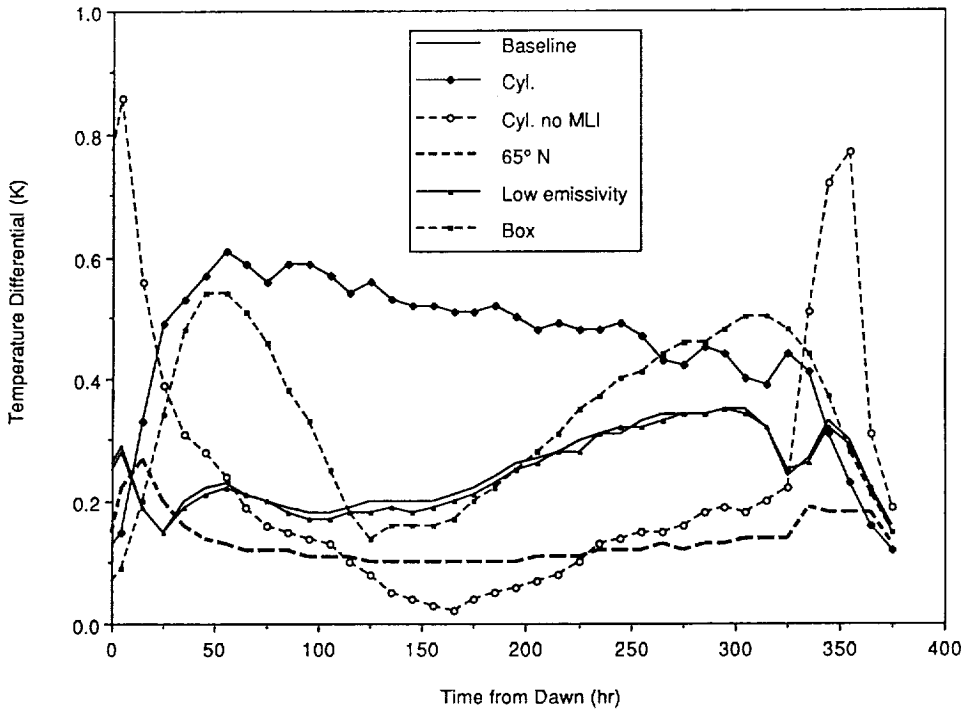

Figure 98. Primary mirror temperature differential for light shade options.

5.5.3.5.3 Alteration of Lunar Surface Properties

The lunar surface has a high solar absorptivity and a high emissivity. Consequently, it absorbs most of the solar radiation incident upon it and reradiates this energy very effectively as heat. The inner light shade, with its high emissivity, absorbs this radiated heat, and the resulting high light shade temperature causes thermal gradients in the primary mirror. Past studies have suggested that the optical properties of the lunar surface near a lander might be modified by spraying a powder on the surface or deploying a fabric cover. Analysis indicates that a majority of the heat absorbed by the upper light shade is from the surface within a 20 m radius of the landing site, as illustrated in figure 99. Using the reduced thermal model, the effect of altering the optical properties of the lunar surface within a 20 m radius of the LUTE was examined. Properties were only modified on the north side of the LUTE, since the light shade interior has no view to the south. Both the light shade and lunar surface elements are diffuse in this model.

Table 42 summarizes the results of this study. Reducing lunar surface absorptivity (α) resulted in increased reflected solar radiation absorbed by the light shade. As long as the surface α/ε ratio is about 1 (first and second cases), the lunar surface temperature is essentially unchanged. If the surface absorptivity remains high, but the emissivity is reduced (third case), the surface temperature increases. This results in decreased light shade heating by reflected solar radiation but increased heating by thermal radiation from the surface. If the surface absorptivity is reduced, but the emissivity remains high (fourth case), the surface temperature is reduced considerably. This decreases light shade heating by thermal radiation from the surface but substantially increases heating by reflected solar radiation.

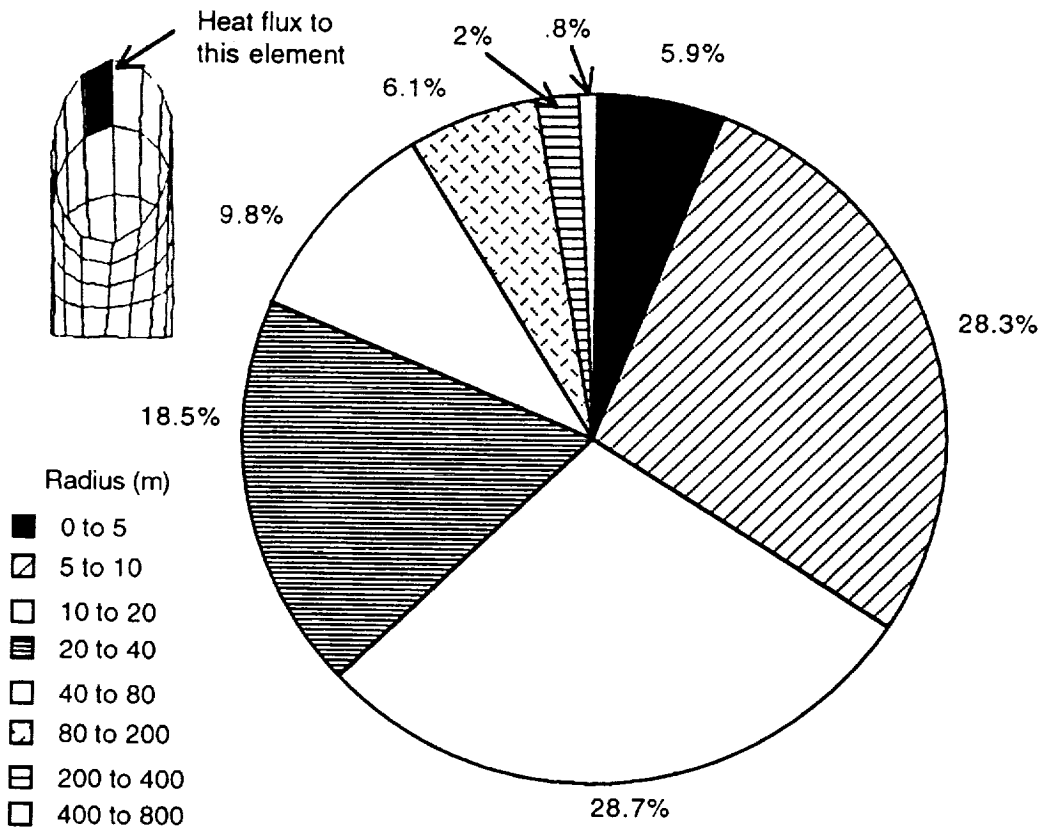

Figure 99. Heat flux contribution of lunar surface.

Table 42. Absorbed heat loads, at noon, for various optical properties.

Case	Shade α/ε	Shade Temperature (K)	Surface α/ε	Modified Surface Temperature (K)	Absorbed Solar (W)	Absorbed IR (W)
1	0.08/0.08	275.4	0.93/0.95	367.4	27.4	248.2
2	0.80/0.80	275.0	0.20/0.20	366.5	197	131.6
3	0.80/0.80	274.9	0.80/0.20	521.3	57.5	270.2
4	0.80/0.80	275.3	0.20/0.80	261.0	197	90.1
5	0.20/0.80	252.9	0.20/0.80	261.0	60.2	119.6

It was apparent from these results that changing the lunar surface properties, and thus lunar surface temperature, was not sufficient to change the light shade temperature significantly. However, a combination of reduced absorptivity on the light shade, plus the lunar surface property combination, which resulted in the lowest surface temperature (fifth case), reduced the light shade temperature from 275 to 253 K. Thus, a low absorptivity coating on the upper light shade to reduce solar absorption with a high emissivity to radiate to space effectively, coupled with a reduced lunar surface temperature, is one means of reducing the light shade temperature. This approach may complicate stray light baffling. Other options that might have a similar effect are a specular, high emissivity coating on the upper light shade or a specular coating on the lunar surface. No investigation of the practicality of these options has been made.

5.5.3.5.4 Light Shade Baffles

Baffles on the light shade were identified as an option to influence the light shade and mirror temperatures. Both angled baffles and horizontal ring shaped baffles were considered. These analyses were performed using the reduced model and the TMG™ analysis program.

Angled Baffles—Because of the desire for a symmetrical light shade shape, reduced radiative exchange between the lunar surface, and a moderate temperature in the vicinity of the detector radiator, the concept illustrated in figure 100 was developed. The upper ring baffles on the open side of the light shade are parallel to the nominal solar vector (50° from the horizontal) and treated with a low ε coating on the undersides and a high ε coating on the top for minimum surface heat absorption and maximum heat rejection to space. This arrangement gives the mirror a symmetric view to space, and the baffles block over 50 percent of the radiation from the lunar surface to the upper light shade as shown in figure 101. Primary mirror temperature differential is reduced from the baseline, although maximum mirror temperature (i.e., mirror temperature swing) and upper light shade maximum temperature are increased. These temperature increases occur because of reduced view to space. Although these baffles complicate the placement of other subsystems, such as electronics and solar panels, this option should be studied further because it addresses two key issues in primary mirror thermal control (mirror temperature swing and upper light shade temperature) and may lend itself to incorporation into the aperture cover.

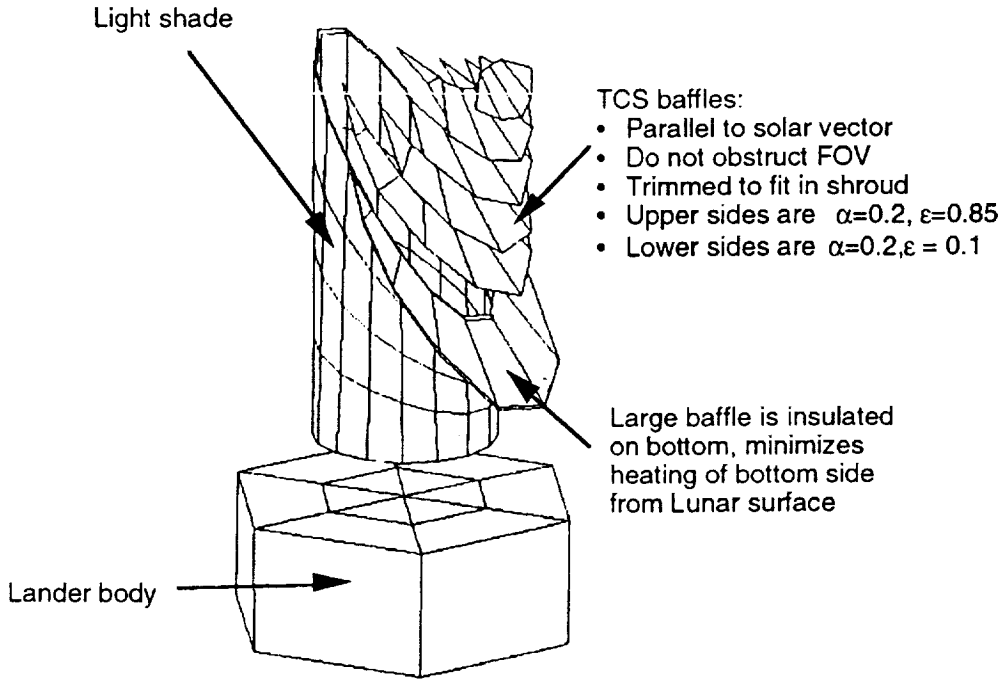

Figure 100. Angled baffle concept.

Ring Baffles—Large flat ring-shaped baffles above a short cylindrical light shade were suggested as a means to block solar radiation while providing a symmetric view to space for the mirror. This option, illustrated in figure 102, could also be deployed by a simple mechanism and would result in a shorter stowed configuration. During early morning and late afternoon, when the Sun is low in the

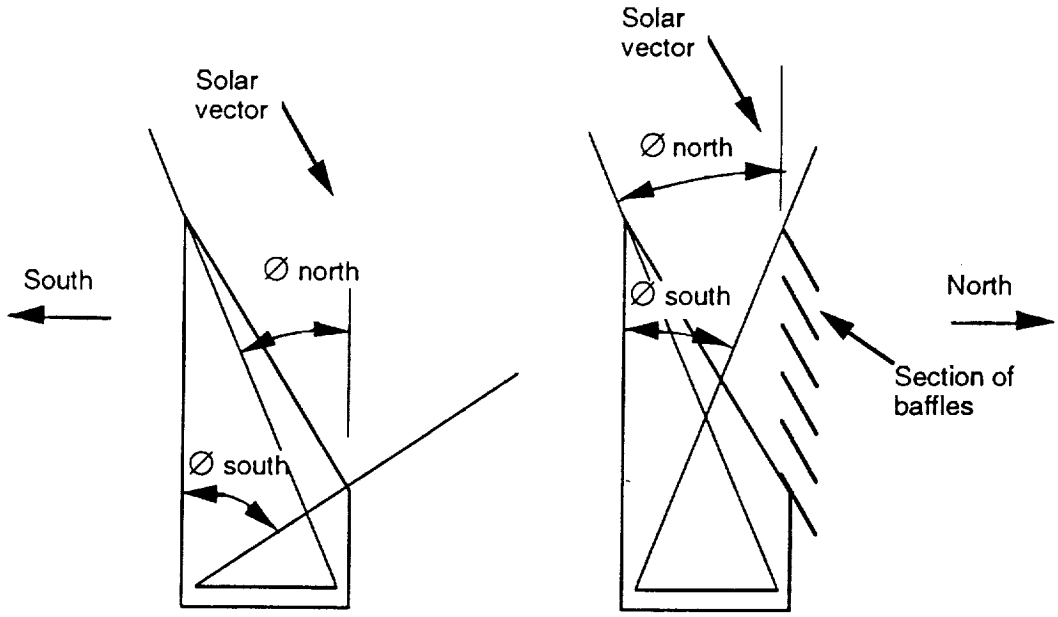

Figure 101. Baffles can be arranged to achieve symmetric view to space.

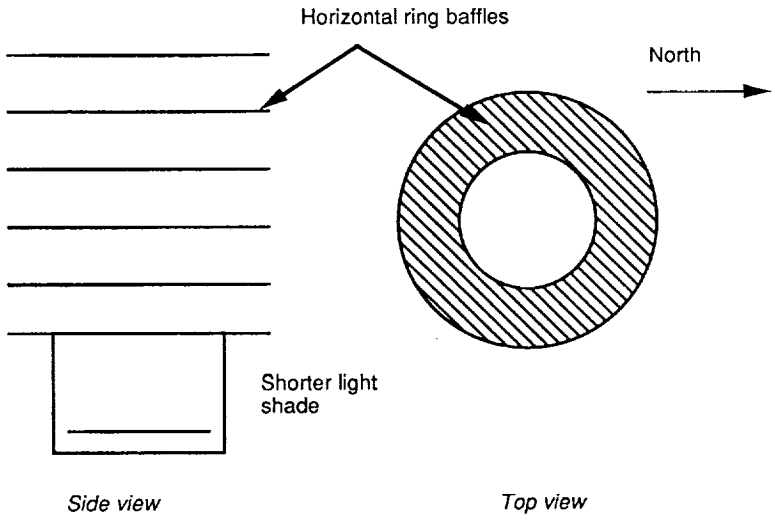

Figure 102. Horizontal ring baffle concept.

sky, most solar radiation passes between the baffles. Near local noon, when the Sun is near maximum elevation, the baffles completely shade the telescope interior. However, during midmorning and mid-afternoon, some solar radiation passes between the baffles and is absorbed by surface inside the telescope. This results in elevated temperatures inside the telescope. Local high gradients would be expected between shaded areas and those in direct Sun, although the model is not sufficiently detailed to detect this phenomenon. Any influence this might have on optical performance will be addressed in phase B.

Summary of Baffle Trades—Results for the two baffle options are summarized in table 43. The angled baffles indicate some improvement, but the ring baffles cannot be recommended, primarily because of the high bulk temperature swing which will result from the 336 K maximum mirror temperature.

Table 43. Comparison of baffle options to baseline at local noon.

Option	Mirror North Side Temperature (K)	Mirror South Side Temperature (K)	Mirror Temperature Differential (K)	Light Shade Temperature (K)
Baseline	238.29	238.22	0.07	275.4
Angled	268.81	268.84	0.03	278.87
Ring	336.14	336.06	0.08	N/A

5.5.3.5.5 Flared Light Shade

One method suggested to reduce the temperature of the upper light shade is to flare it, as shown in figure 103. This simultaneously reduces its view to the lunar surface and the primary mirror, and increases its view to deep space. Using the reduced TMG™ model, 0°, 5°, 10°, and 15° flare angles were analyzed.

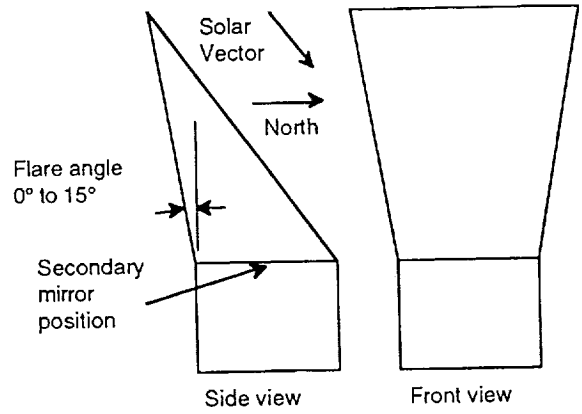

Figure 103. Flared light shade concept.

Analysis results are summarized in figure 104. Flare angles of 10° or less provide little improvement in the temperature differential. Unfortunately, flare angles of 15° or greater become extremely large and difficult to deploy successfully. For these reasons, the flared sunshade was not considered in further studies. Although any flare is positive, flare angles large enough to significantly reduce thermal control complexities pose packaging and deployment concerns.

5.5.3.6 Mirror Construction and Support Structure Effects

The mirror support structure can significantly influence the temperature distribution in the mirror. For all the studies discussed above, a ring support on the outer edge of the primary mirror was used and the primary and tertiary mirrors were ground on a continuous beryllium blank (no center hole). Structural analysis indicated that a three-point support using titanium flexures was preferable for the large temperature excursions experienced by the mirror. Titanium was chosen because its coefficient of thermal expansion closely matches that of beryllium, and it has good strength and stiffness properties. Other flexure materials, such as Invar™, might be more appropriate for mirror materials other than beryllium. Separate primary and tertiary mirrors are also preferable to a one-piece design for manufacturing considerations. To assess the impact of these mirror construction and support differences, the three cases below were analyzed. The isothermal light shade model described above was used for all three cases.

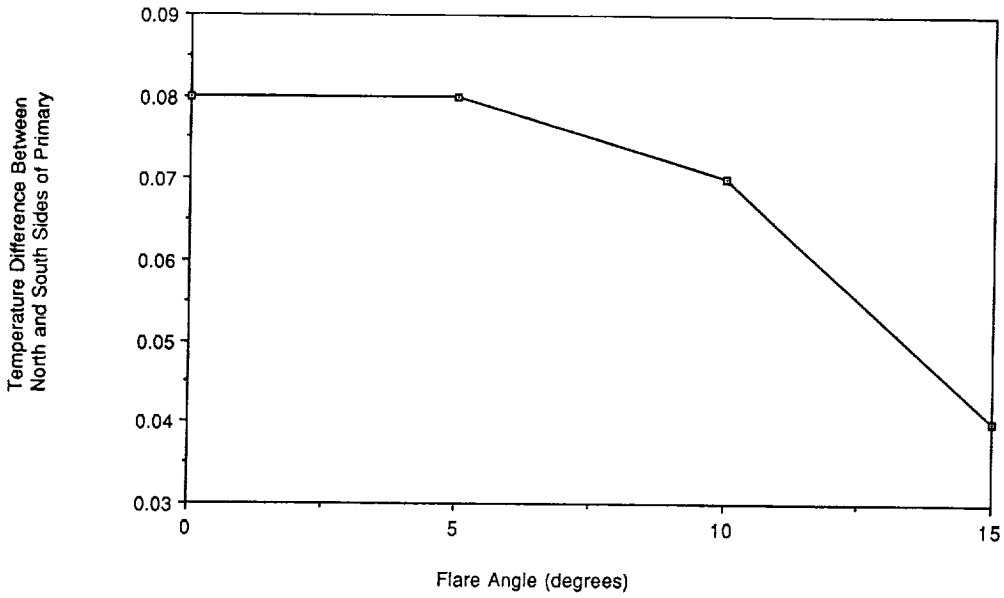

Figure 104. Effect of flare angle on north/south temperature differential (local noon).

One-Piece Primary/Tertiary with Ring Support—For this case, the primary and tertiary mirrors are ground on a continuous blank of beryllium and supported by a continuous ring around the outer edge as shown in figure 105. The ring is assumed to be 1 cm tall, with a total area (for conduction calculations) of 3.9 cm^2. The maximum temperature differential for the primary mirror elements is 0.08 K.

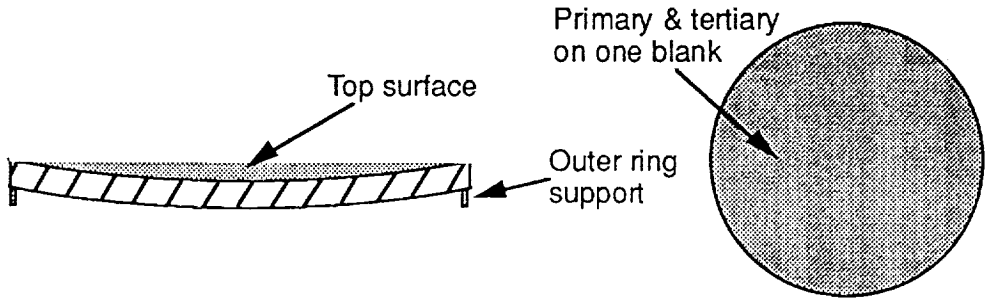

Figure 105. One-piece mirror with ring support.

Separate Primary/Tertiary With Ring Support—For this case, the primary mirror has a center hole, as shown in figure 106, and is supported by a continuous ring around the outer edge as described previously. The maximum temperature differential for the primary mirror elements is 0.18 K. This center hole in the primary mirror increases the gradient across the diameter of the mirror.

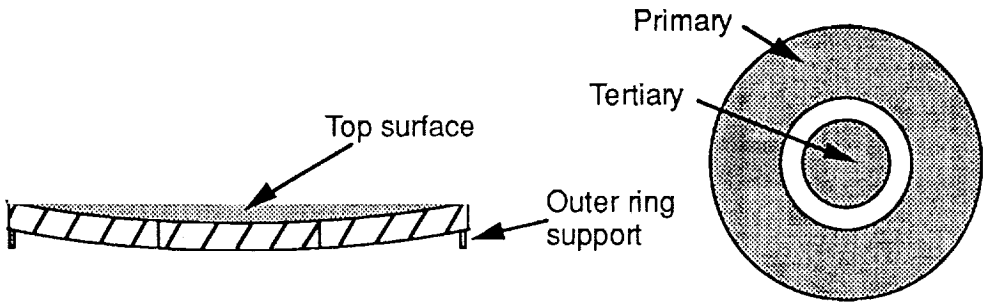

Figure 106. Separate primary and tertiary with ring support.

Separate Primary/Tertiary With Three-Point Flexure Support—For this case, the primary mirror is supported by three titanium flexures, located midway between the inner and outer radii and spaced at 120° intervals. Each flexure consists of two titanium rods, 3.2 mm in diameter and 6 cm long, as shown in figure 107. No insulating buttons at the ends of the rods were included, although it may be possible to incorporate such insulators in the design of the flexures. The maximum temperature differential for the primary mirror elements is 0.18 K, which is the same as for the previous case.

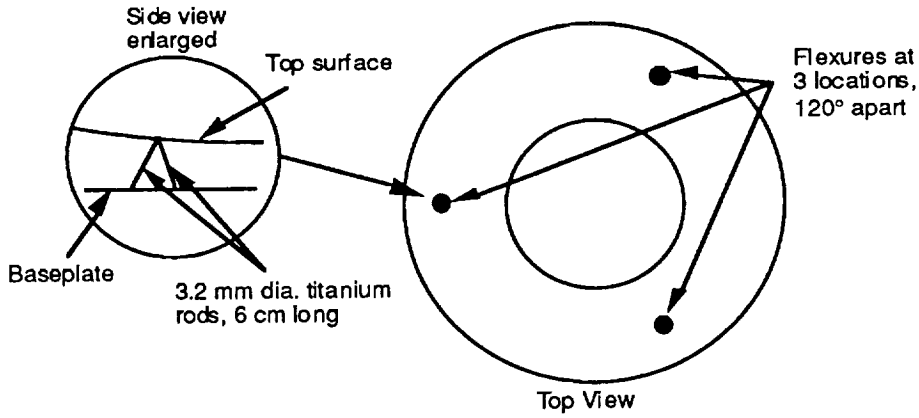

Figure 107. Titanium flexures supporting primary mirror on baseplate.

Summary of Mirror Construction and Support Structure Effects—Results of this trade are shown in figure 108. Both of the mirrors with center holes (two-piece) have larger temperature differentials than the one-piece mirror. However, for most of the operating period, there is little difference between the flexure and ring supports for the mirrors with a center hole. The flexure support creates slightly higher mirror temperature differentials during the early morning and late afternoon periods when the mirror is undergoing relatively rapid temperature changes. This is primarily caused by rapid local heating or cooling of the mirror in the vicinity of the flexure. Mirror construction and support had no effect on bulk temperature swing or light shade temperature.

Figure 108. Primary mirror gradient for different methods of support.

5.5.3.7 Mirror Material Trades

The baseline for all trade studies conducted previously was a beryllium primary and tertiary mirror. Beryllium was initially chosen because of its high thermal conductivity and relatively low CTE. In this trade, other primary and tertiary mirror materials were examined. The support structure used was a three-point support with titanium flexures at each point (described previously). The construction of the mirrors was not changed, except the primary and tertiary were separate mirrors, not ground on a single blank as stated previously. This was for consistency with structures and optical system models. Results from the thermal analyses described were transferred to the structural analyst for deformation analysis. The materials considered were beryllium, Ceraform™ SiC, and fused silica. In the final analysis, mirror material selection will be based on optical performance over the temperature range, plus other factors such as surface quality, manufacturability, etc. All three material options were run with an isothermal light shade as described above.

Beryllium—The maximum temperature differential for the beryllium primary mirror is 0.18 K. Figure 109 illustrates the temperature distribution on the primary mirror at local noon.

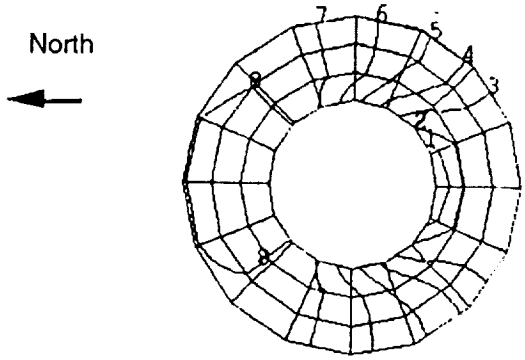

Contour	Temp. (K)
1	261.23
2	261.25
3	261.27
4	261.29
5	261.30
6	261.32
7	261.34
8	261.36

Figure 109. Primary mirror temperature distribution at noon (beryllium).

Silicon Carbide—The maximum temperature differential for the Ceraform™ SiC primary mirror is 0.22 K. Figure 110 illustrates the temperature distribution on the primary mirror at local noon. The SiC results differ little from those for beryllium. This is not surprising since the thermal conductivity and specific heat of the two materials are similar. Values for specific heat of SiC below room temperature were not available, so a projected value was used. This analysis should be reevaluated if temperature-dependent data become available.

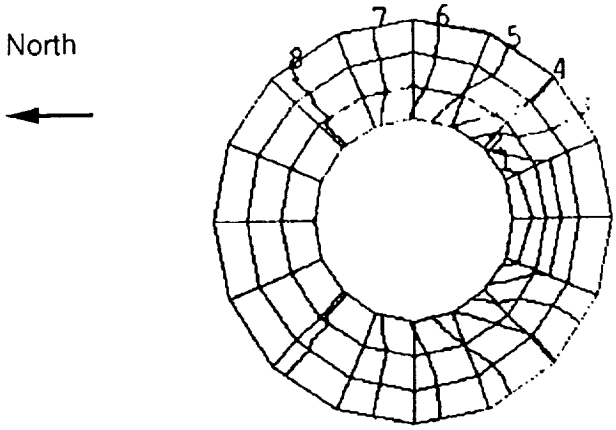

Contour	Temp. (K)
1	261.16
2	261.18
3	261.21
4	261.23
5	261.25
6	261.27
7	261.30
8	261.32

Figure 110. Primary mirror temperature distribution at noon (SiC).

Fused Silica—The maximum temperature differential for the fused silica mirror is 13.08 K. Figure 111 illustrates the temperature distribution on the primary mirror at local noon. This is much larger than the differential for beryllium or SiC, primarily because of the lower thermal conductivity of fused silica. However, fused silica also has a much smaller coefficient of thermal expansion than the other two materials. A deflection analysis must be performed to determine which material will have the smallest distortion due to thermal loading.

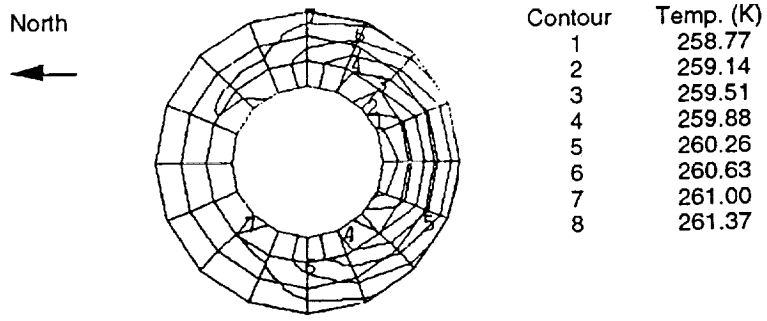

Figure 111. Primary mirror temperature distribution at noon (fused silica).

Summary of Mirror Material Trades—Table 44 summarizes the results of the mirror material trade study. The only parameter affected by the mirror material is the mirror temperature differential.

Table 44. Summary of mirror material trade results.

Option	Maximum ΔT (K)	Mirror Maximum (K)	Night/Day Swing (K)	Average ΔT (K)
Beryllium	0.18	261.4	194.2	0.12
SiC	0.22	261.7	194.4	0.14
Fused Silica	13.08	261.4	194.5	4.19

The temperature differential across the primary mirror is shown in figure 112 for beryllium and SiC and in figure 113 for beryllium and fused silica. Beryllium, SiC, and fused silica primary mirror temperature profiles for the LUTE operational period were transferred to LUTE structural analysis personnel for evaluation of temperature-induced deformations. Names and descriptions of output files for these and other telescope thermal analyses discussed are listed in appendix M.

5.5.3.8 Site Latitude Trade

Changing the latitude of the LUTE landing site from 40° north to 66.5° north, while still viewing at a 40° declination, reduced the detector radiator temperature to an acceptable value and reduced the mirror bulk temperature swing. To assess the sensitivity of light shade interior temperature, mirror bulk temperature swing, and mirror temperature differential to telescope latitude, landing sites of 40° north, 48.5° north, 57° north, and 65° north have been modeled with the TMG™ program. Figure 114 illustrates the orientation of the telescope relative to the lunar surface, the lander, and the solar vector at each landing latitude.

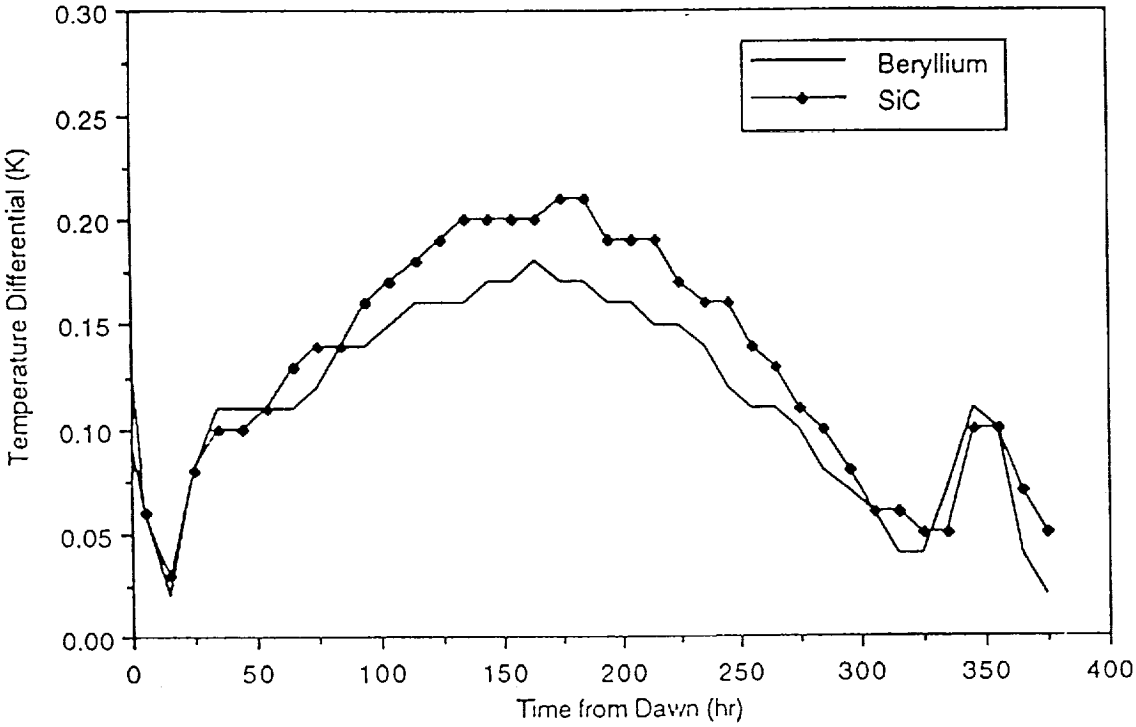

Figure 112. Temperature differential for beryllium and SiC primary.

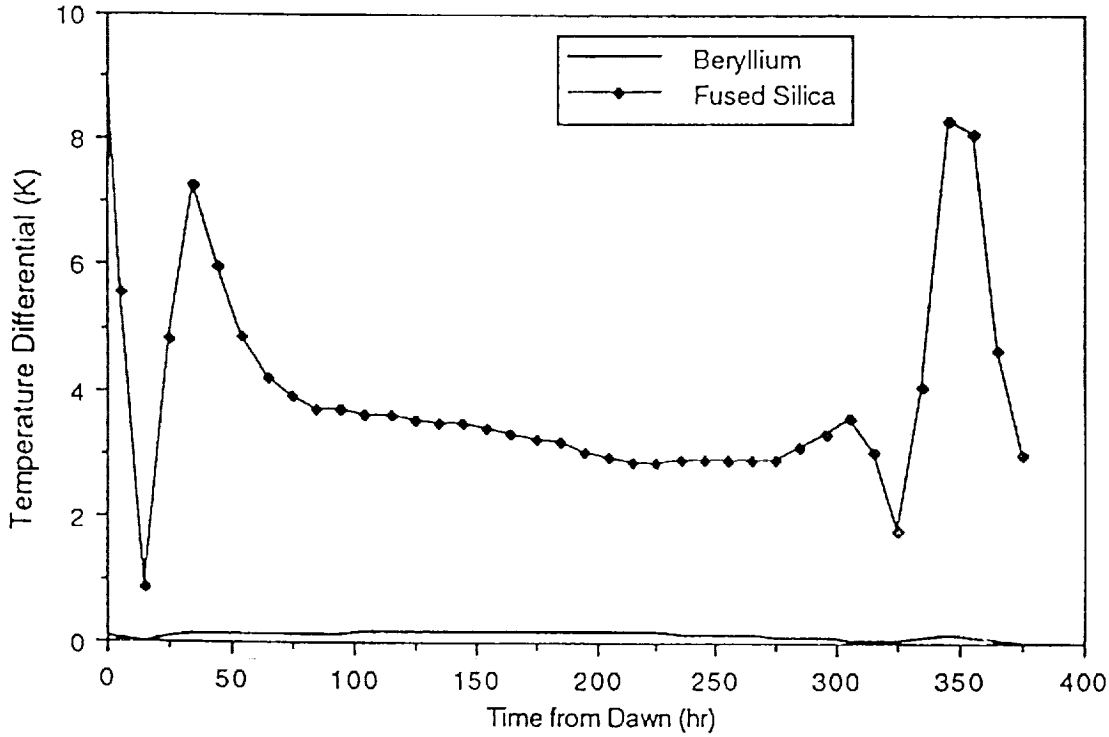

Figure 113. Temperature differential for beryllium and fused silica primary.

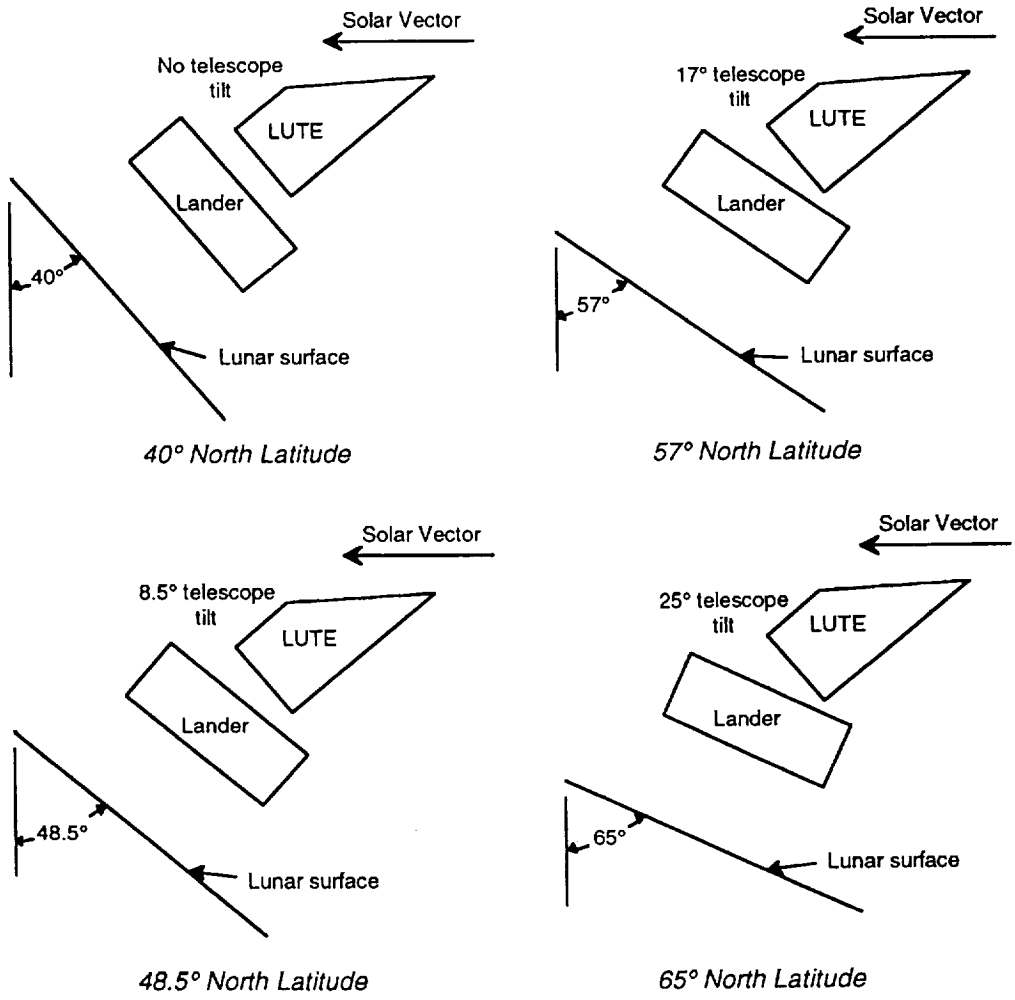

Figure 114. Telescope orientation at latitudes studied.

In all cases, the LUTE is pointing at a 40° declination, the primary and tertiary mirrors are beryllium and are ground on a single blank, and the primary mirror is supported by a ring at its outer radius. Table 45 summarizes the results of the latitude trade study. Generally, mirror temperature differential (ΔT), maximum temperature, temperature swing, and light shade temperature decrease with increasing latitude. The detector radiator temperature will be somewhat lower than the light shade interior temperature.

Table 45. Summary of latitude trade results.

Latitude	Maximum ΔT[9] (K)	Average ΔT (K)	Mirror Maximum (K)	Night/Day Swing (K)	Light Shade Interior Temperature (K)
40.0	0.35	0.25	229.3	161.0	304.8
48.5	0.27	0.19	211.5	143.0	284.6
57.0	0.21	0.15	194.1	125.9	258.9
65.0	0.20	0.13	170.1	105.1	198.6

Maximum light shade temperature, mirror temperature, and mirror day/night temperature swing are shown in figure 115 for the latitudes studied. Note that the light shade temperature decrease is larger between 57° and 66.5° than between 48.5° and 57°. This indicates that even lower light shade interior temperatures could be obtained for locations north of 66.5°.

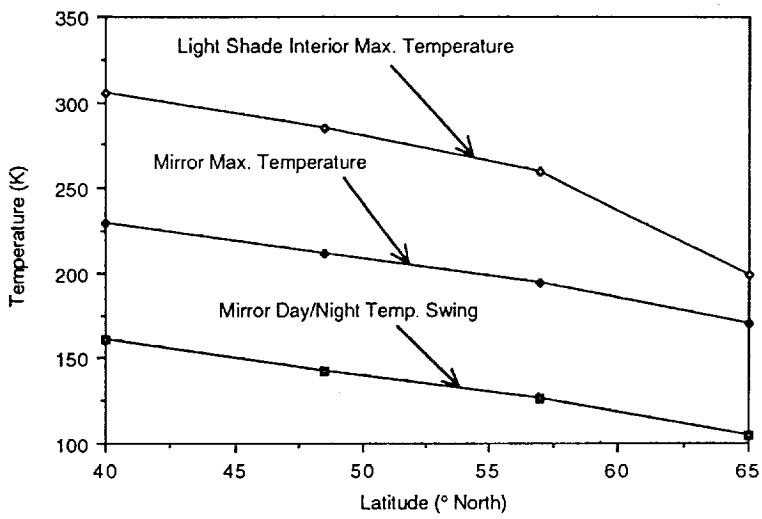

Figure 115. Summary of mirror and light shade maximum temperatures.

The primary driver for the reduction of mirror temperature, temperature swing, and temperature differential is the reduction of the light shade interior temperature. This reduction is caused by the southward tilt of the telescope (shown in fig. 114) that is required to view at a 40° declination from landing sites higher than 40° north. The tilt reduces the inner light shade view to the lunar surface and increases its view to space—its ultimate heat sink. The reduced view to the lunar surface lowers the heat load to the light shade, and the increased view to space allows rejection of the heat load at a lower temperature. The temperature differential across the primary mirror is shown in figure 116 for the four latitudes studied. The average mirror differential is lower for higher latitude locations because the cooler light shade interior causes less heating of the north side of the mirror. Maximum and average mirror temperature differential are shown for each latitude in figure 117.

The trend is toward lower differentials at higher latitudes, but the curves begin to flatten between 57° and 65°. This indicates that the differential cannot be reduced indefinitely by moving to higher latitudes. The portion of the differential, which is due to the asymmetric view factor of the mirror to space and the nonuniform temperature of the baseplate, will not be affected by the change in latitude. In summary, significant thermal control benefits can be obtained by moving the LUTE landing site to a latitude higher than 40° north, as long as the telescope can be tilted to continue viewing at a 40° declination angle. The reduction in primary mirror maximum temperature differential is clearly nonlinear and locations north of 65° will probably result in little additional reduction. However, the analysis results indicate that maximum light shade temperature (hence detector radiator operating temperature), mirror temperature, and mirror temperature swing will continue to decrease for locations north of 65°.

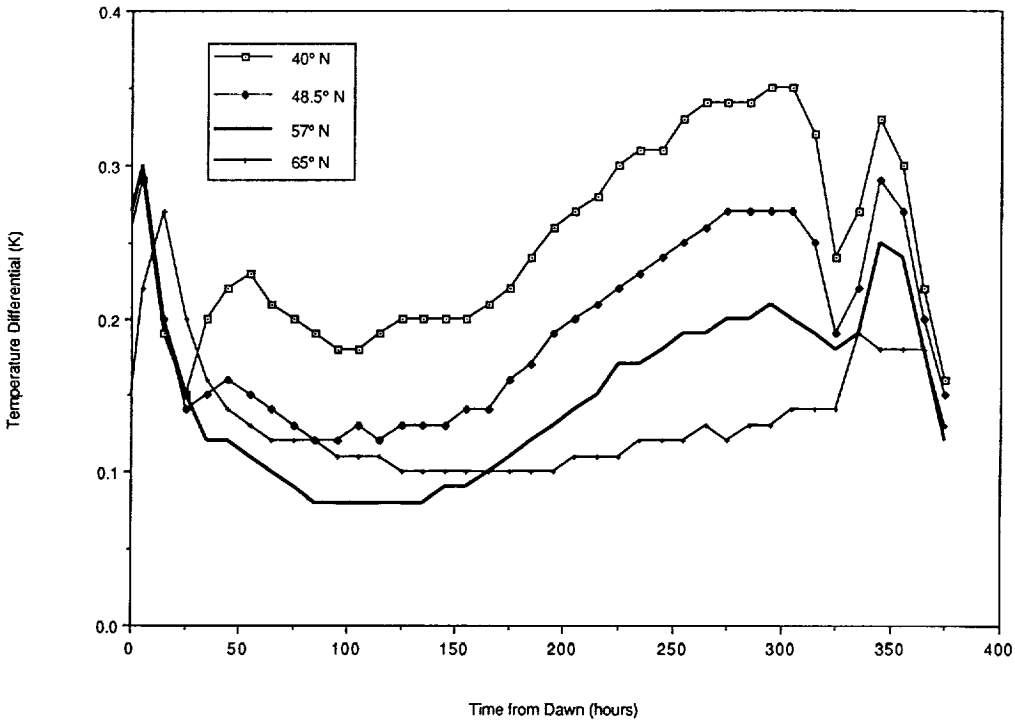

Figure 116. Temperature differential across primary mirror.

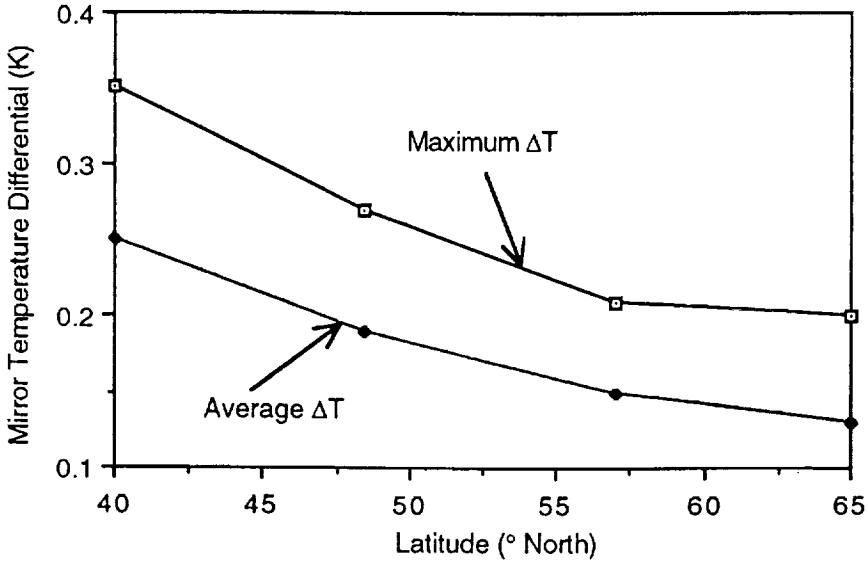

Figure 117. Mirror average and maximum temperature differential.

5.5.3.9 Use of Heaters on Primary Mirror

The LUTE primary mirror experiences a large diurnal temperature swing with only passive thermal control. With the possibility of an RTG power source and resulting power availability during the lunar night, it becomes reasonable to examine active thermal control in the form of heaters for the primary mirror. The purpose of the heaters is to increase the minimum temperature of the mirror and, thus, decrease the total temperature swing of the primary mirror. For the first case analyzed, the LUTE is located at 40° north latitude, pointing at a 40° declination, has beryllium primary and tertiary mirrors ground on a single blank, and has a ring supporting the primary mirror at its outer radius. The data pre-

No heat pipes, heaters, or other active thermal control techniques were used for the light shade or mirror. With passive thermal control, the minimum mirror temperature is 71.8 K and the maximum mirror temperature is 239 K, for a total temperature swing of 167.2 K. If the minimum temperature is to be raised to 220 K, a maximum of 34.2 W of heater power is required. The power required varies from zero to the maximum value, and heat must be applied for a total of 480 hours of the 654 hour diurnal cycle.

The second case analyzed places the LUTE at 65° north latitude, pointing at a 40° declination, and retains the beryllium primary and tertiary mirrors and the outer support ring. The data presented are taken from TMG™ thermal analysis results using the model mentioned previously. No heat pipes, heaters, or other active thermal control techniques were used for the light shade or mirror. With passive thermal control, the minimum mirror temperature is 67.8 K and the maximum mirror temperature is 175 K, for a total temperature swing of 107.2 K. If the minimum temperature is to be raised to 160 K, a maximum of 10.2 W of heater power is required. The power required varies from zero to the maximum value, and heat must be applied for a total of 440 hours of the 654 hour diurnal cycle.

For the cases previously described, heat was applied directly to the back of the primary/tertiary mirror. If this is not feasible, then a heater plate must be added between the baseplate and the mirror. It is not feasible to apply heat directly to the baseplate because it is not thermally isolated from other large LUTE components. Use of a heater plate is less efficient than applying heat directly to the mirror back and might require as much as 25 percent more power to maintain the same mirror temperature. In addition, because the design of the mirror support is not well defined, a 15 percent contingency factor should be applied to the calculated heater power estimates previously described. The benefits of reduced mirror temperature swing should be weighed against the costs of a heater system. The benefits include simplified analyses, optimized temperature range selection, traceability of image quality degradation, etc. These costs include, additional mass (approximately 1.5 kg), additional system complexity, and greater potential for significant temperature gradients within the mirror, particularly if a heater unit should fail.

5.5.3.10 Metering Structure Axial Gradient

Knowledge of the temperature gradients, which will exist in the LUTE metering structure, is needed for the design of the metering structure and secondary mirror support system. The existing LUTE thermal models do not include a simulation of the metering structure or secondary mirror. A detailed thermal model of the metering structure cannot be constructed at this time because several metering structure concepts are being considered, and design details are not available for any of the concepts. For preliminary purposes, the axial gradient of the light shade in the vicinity of the metering structure may be used as an estimate of the gradient which will exist in the metering structure. The metering structure is in close proximity to the light shade, so use of the light shade temperature predictions should provide a reasonable approximation of the metering structure temperature. However, circumferential and diametral metering structure gradients cannot be estimated based on the light shade temperature predictions because of the "spider" structure supporting the secondary mirror. This structure will provide conduction paths across the metering structure which do not exist for the light shade.

For the case documented, the LUTE is located at 40° north latitude, pointing at a 40° declination, has beryllium primary and tertiary mirrors ground on a single blank, and has a ring supporting the primary mirror at its outer radius. For higher latitude locations, pointing at the same declination, the light shade axial gradient would be somewhat lower than for the case documented. Since this is a preliminary estimate, it is appropriate to use the higher gradient. The data presented in the following are taken from TMG™ thermal analysis results using the model previously mentioned. No heat pipes, heaters, or other

active thermal control techniques were used for the light shade or mirror. Figure 118 shows the temperature variation of the light shade at the upper and lower edge of metering structure for one lunar cycle. For the purpose of this report, the "upper edge" means the light shade at approximately the level of the secondary mirror, rather than the actual end of the light shade. The thermal analysis documented is for "midsummer" lighting conditions. Point A in the figure indicates an elevated light shade temperature caused by direct sunlight inside the light shade shortly after dawn. A similar phenomenon, caused by direct sunlight inside the light shade before sunset, is indicated by point B on the graph. The lower edge of the light shade is essentially unaffected by the direct sunlight "peek-over" into the upper light shade. After sunset (about 350 hours) the lower edge is warmer than the upper edge because it loses heat to space less rapidly. The upper edge cools more rapidly because of its higher view factor to the deep space heat sink.

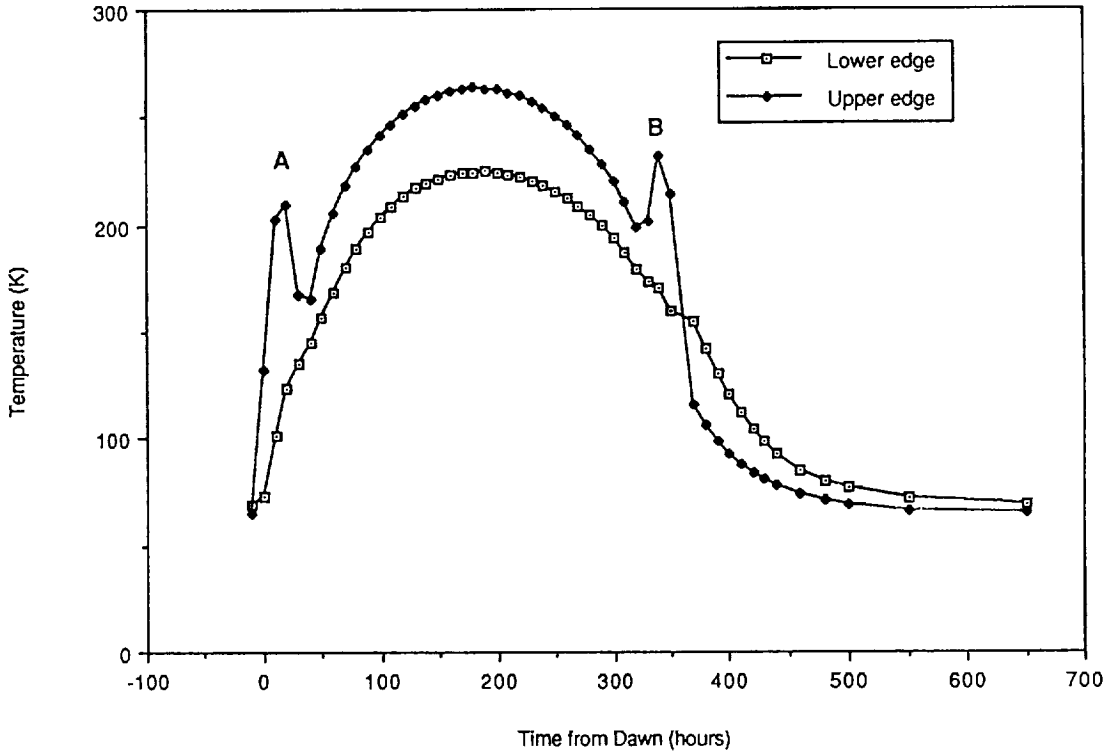

Figure 118. Light shade temperature at lower and upper edge of metering structure.

Figure 119 shows the axial temperature difference between the upper and lower edges of the metering structure, as indicated by the light shade temperature. The gradient is positive when the upper edge is warmer than the lower edge. The maximum gradient is about 100 K and occurs shortly after local sunrise. If the seasonal effects of sunlight peeking over the light shade are neglected, the maximum axial gradient is about 40 K.

When the metering structure and secondary mirror support structure design has been better defined, a more detailed thermal analysis of the metering structure may be appropriate. That analysis might be expected to yield a time-varying temperature profile of the entire metering structure, which could be used in a structural analysis to predict thermal deformations of the metering structure.

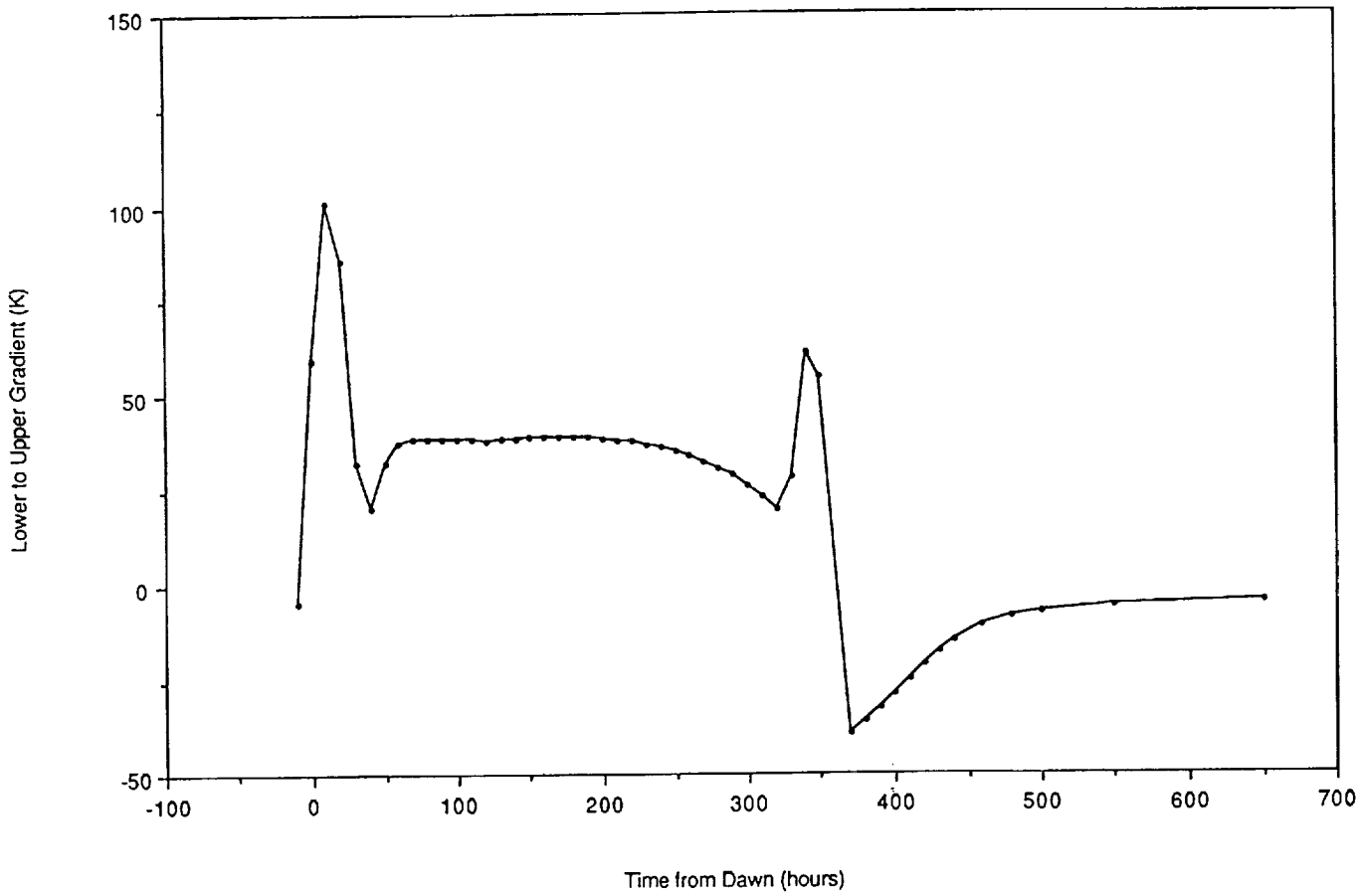

Figure 119. Estimate of metering structure axial thermal gradient.

5.5.3.11 Declination Effect on Mirror Temperature

Previous thermal analyses were conducted for a pointing declination of 40° north, however, a declination of 30° north is of considerable scientific interest. In order to accommodate this lower declination, the light shade angle must be increased to approximately 70°, which increases the length of the light shade by over 1 m. The thermal effects of the two declinations have been compared for a telescope with beryllium optics at a 65° north latitude location. Sketches of the two configurations are shown in figure 120.

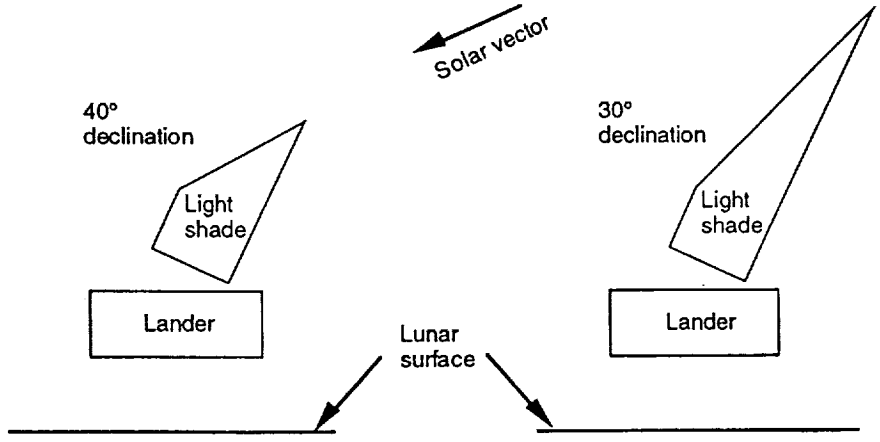

Figure 120. Light shade configurations for 30° and 40° point declinations.

Table 46 summarizes the analysis results for the two declinations. The lower declination causes an 8.4 K increase in the mirror maximum temperature. This increase is primarily driven by the larger light shade required for a 30° pointing declination. No increase in temperature gradient over the primary mirror was noted due to change in pointing declination. The increase in mirror maximum temperature and day/night temperature swing resulting from the lower declination is undesirable. However, the magnitude of the change is relatively small and can probably be tolerated, if required. The increase in light shade size required to accommodate the 30° declination is probably a more serious design problem than the resulting thermal effects.

5.5.4 Detector Thermal Control

The detector is an array of several CCD's and is located in the central hole of the secondary mirror. Figure 121 shows the location of the detector.

Table 46. Results of pointing declination thermal trade.

Pointing Declination	Mirror Temperature			Light Shade Maximuum Temperature (K)
	Maximum	Minimum	Day/Night Swing	
30°	183.5 K	67.4 K	116.1 K	183.1 K
40°	175.1 K	67.8 K	107.3 K	178.3 K

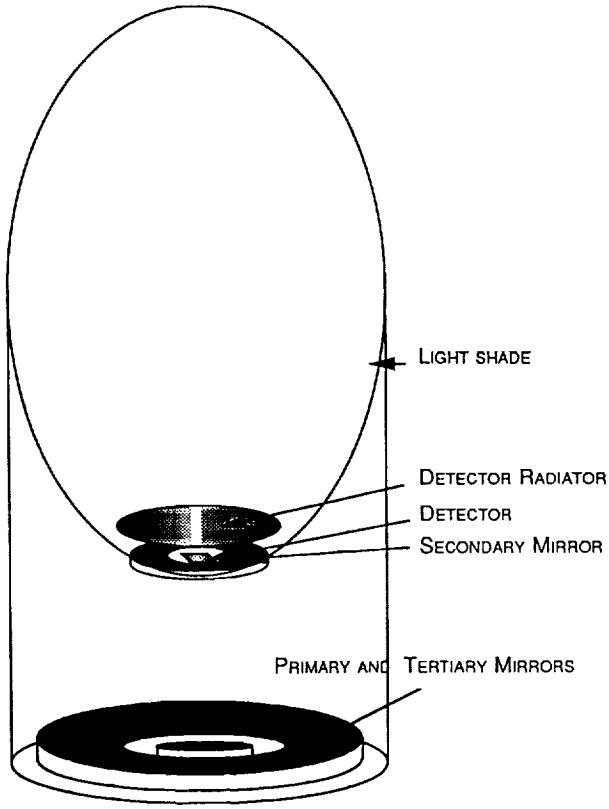

Figure 121. Location of CCD detector and radiator.

5.5.4.1 Requirements

Thermal requirements for CCD's vary with the application, size, and wavelength of interest. For the LUTE application, the maximum allowable CCD temperature for UV and visible applications is about 210 K. Over short periods of time, the detector temperature must be stable to tenths of a degree, so rapid temperature changes must be eliminated. The heat to be removed from the detector comes from conduction through the wires leading into the array, heat produced by reading the information from the CCD's, and radiation from the environment. The total heat to be removed from the focal plane array is estimated at not more than 5 to 10 W. Because the LUTE is mass and power limited, passive thermal control of the detector is preferred. This does not preclude the use of heaters, but suggests minimum usage of such devices.

5.5.4.2 Concepts

Concepts for thermal control of the CCD include a passive radiator, a thermoelectric unit (TEU) with a radiator, a cryo-cooler, and cryogenic fluid. Each concept is discussed in detail below.

Passive Radiator—The first step in the design of the thermal control system for the detector was determining how much heat could be radiated from a radiator attached to the detector. The radiator area was assumed to be the same as the secondary mirror area. A 10 K temperature rise was assumed between the radiator and the detector, giving a target maximum radiator temperature of 200 K. Initial analyses involved some hand calculations using assumed view factors based on a TMG™ model of a similar geometry. These analyses, assuming a radiator temperature of 200 K, showed that the radiator would be absorbing heat during operating times rather than rejecting heat. A TRASYS model of light shade, lunar surface and the radiator were built to more accurately represent the radiation environment of the radiator. The output of the TRASYS model was used as input for a SINDA model to determine the amount rejected or absorbed by the radiator and the temperature at which it radiates. Steady-state analyses were run for a hot environment and also for a cold environment. The hot environment represented the midday when the lunar surface may reach temperatures of 385 K, and the interior light shade may have an average temperature of 270 K. The cold environment represented the time during the lunar night just before dawn where the lunar surface temperature falls to about 85 K, and the interior light shade temperature is about 80 K. Two different analyses were run for both the hot and cold cases: one to calculate how much heat can be rejected or absorbed at a radiator temperature of 200 K and the other to determine the radiator's temperature with a constant heat load of 10 W. For this trade study, the telescope was located at a 40° north latitude, unless noted. The radiator, telescope, and lunar surface were also modeled using TMG™. The model was run to calculate the transient radiator temperature, assuming a 10 W heat load, during the lunar cycle.

Trade Studies—Figure 122 shows the four concepts for thermal control of the detector which were analyzed. Concept 1 is a horizontal radiator behind the secondary mirror. The radiator diameter is limited to 0.5 m to avoid obscuration of the primary mirror and the radiator has optical properties of $\alpha = 0.8$ and $\varepsilon = 0.8$. In this location, the radiator has a view to space which is limited by the light shade. Because the radiator has a view to the light shade interior, the radiator heat rejection capability is dependent on the light shade temperature.

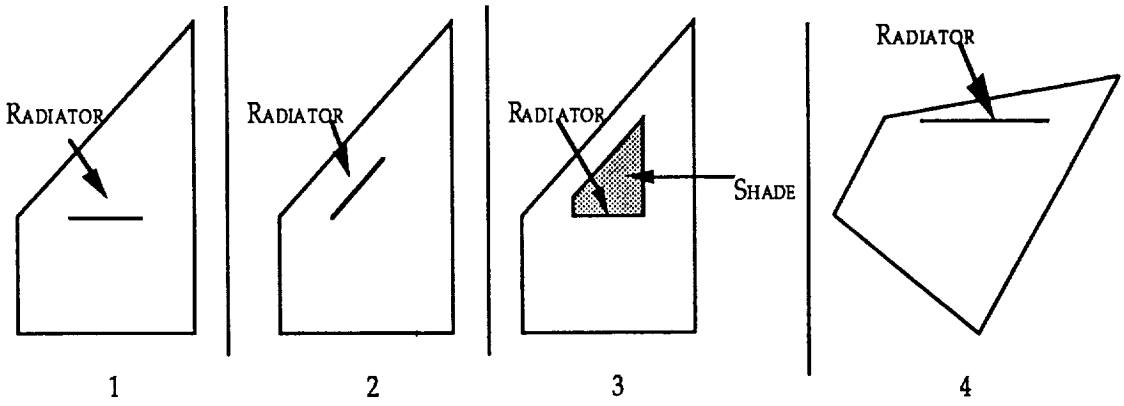

Figure 122. Passive radiator concepts for detector heat rejection.

Concept 2 is a radiator slanted 50° so it will be parallel to the solar vector. The radiator's projected area would be the surface area of the secondary mirror. This concept has two benefits: the surface area of the radiator increases so that there is potential to radiate more heat, and the radiator has a better view to space and a limited view of the light shade. The major drawback of this concept is that it has a view of the lunar surface, which severely limits the heat rejection capability of the radiator during the operating period.

In concept 3, the radiator is placed in its own shade to block radiation from both the light shade and the lunar surface. The shade around the radiator again limits the radiator's view to space, thus limiting its heat rejection capability.

Concept 4 involves moving the telescope to a higher latitude (65° north, as discussed previously). At this latitude, the light shade interior surface has a reduced view to the lunar surface, thereby reducing the interior shade temperature. Also, the radiator can be oriented parallel to the lunar surface to avoid lunar surface radiation and moved forward in the telescope to reduce the radiator's view of the light shade. This concept allows a nearly 100 percent view to space, and increases the heat rejection capability of the radiator.

Results—Each of the concepts mentioned above was analyzed using TRASYS and SINDA. The results shown in figure 123 and table 47 indicate that the environment for concept 1 would heat the radiator to a temperature of 228 K, or 28 K above the target radiator temperature, even with no heat load from the detector. The same is true for concept 2, where the lunar surface radiation raises the temperature, with no detector heat load, to 227 K. The calculated temperature for concept 3 with no heat load is 240 K . However, for concept 4, the radiator temperature is 117 K with no heat load and 190 K with a heat load of 10 W. This is 10 K below the maximum target radiator temperature of 200 K. Based on these results, moving to a 65° latitude will allow the use of passive cooling to maintain the detector within acceptable temperature limits during operation.

TEU Plus Radiator—Because no heat could be passively rejected in the baseline configuration, other methods of thermal control were pursued. One of these is cooling using TEU's, which are small devices that transfer heat when current is passed through them. The amount of cooling is proportional to the current passed through the device, and the heat flow direction is determined by the direction of the current. A TEU has hot and cold sides as shown in figure 124. The cold side would be attached to the

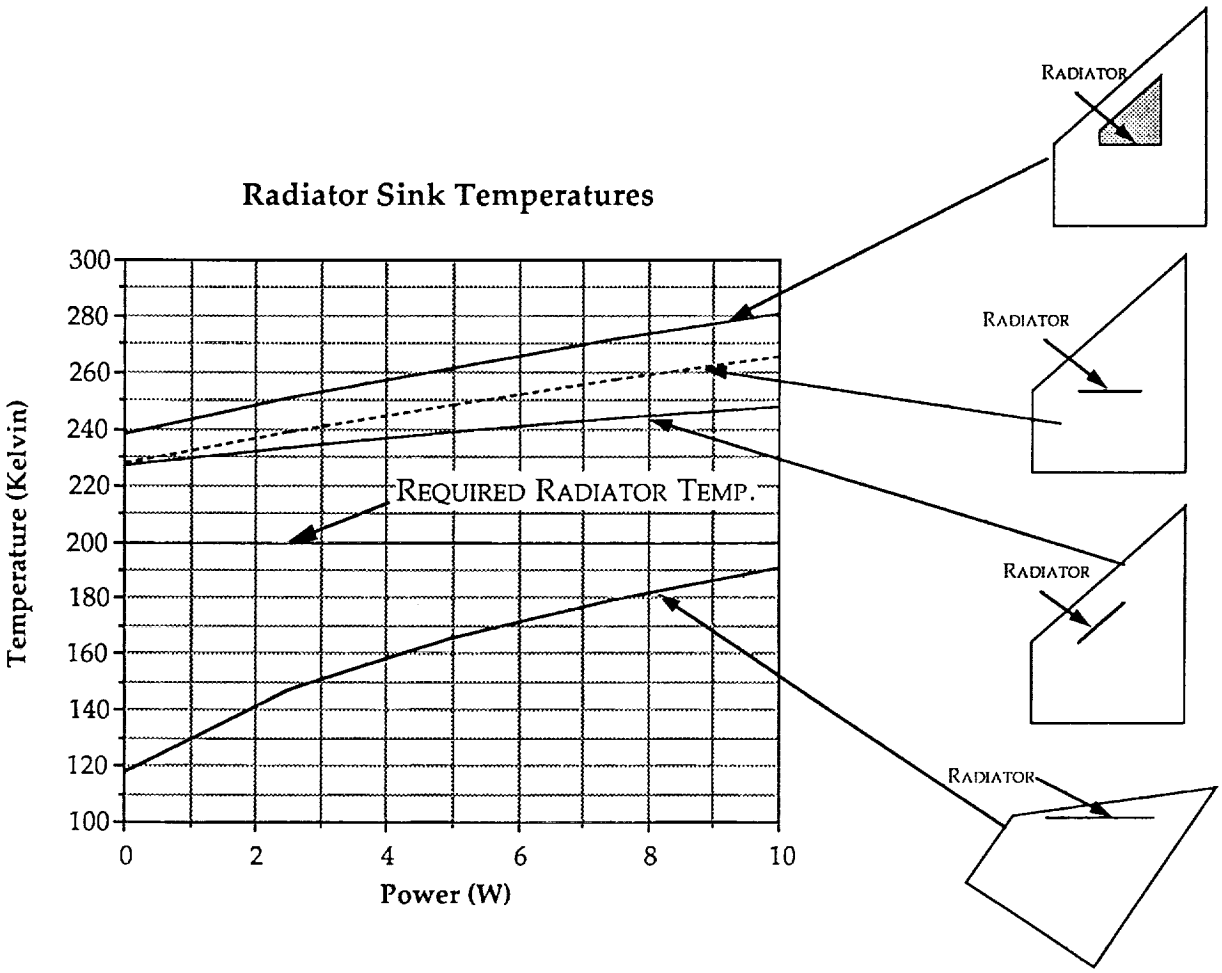

Figure 123. Results of passive detector radiator trade study.

Table 47. Detector radiator temperature summary.

Concept	Temperture With No Heat Load	Temperature With 10 W Heat Load
1	228	265
2	227	247
3	240	280
4	117	190

LUTE detector, and the hot would be attached to a heat pipe or directly to a radiator to reject heat to space. These devices can require large amounts of power depending on the temperature difference (ΔT) between the hot and cold sides and how much heat must be transferred. The efficiency of these devices is generally low and decreases as the ΔT increases. As a result, more power is required to remove the unwanted heat from the instrument for larger temperature differentials.

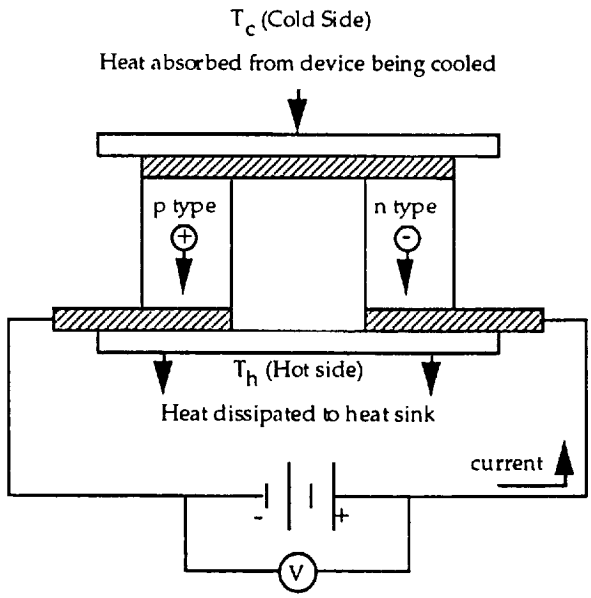

Figure 124. Illustration of a TEU.

The major problem with using a TEU in this application is the large ΔT between the cold side and the radiator. The radiator needs to operate above 300 K to reject the required heat load in its warm environment, while the detector needs to be cooled to 210 K. Another problem is the amount of heat that needs to be rejected. The TEU would require 400 W of power to remove 10 W from the detector if an appropriate TEU were available. Based on conversations with vendors, the cost of fabricating a TEU that would perform as required would be prohibitive. The TEU is not a viable option for the baseline configuration and requirements. These devices require considerable power and can only pump small amounts of heat. A change in the thermal control method or a change in the detector constraints is needed.

Alternate TCS Options—Since the detector heat rejection options discussed above seem to be unacceptable for the LUTE reference location (40° north latitude), several other options have been identified. These are cryo-coolers, cryogenic fluids, alternate detector locations, an alternate telescope location, and altering detector requirements by changing the detector design.

Cryo-cooler: One alternative option for a detector thermal control is a cryo-cooler. Cryo-coolers are mechanical devices that can operate at temperatures as low as 4 K. Drawbacks to using these devices are the large power requirement and the vibration they induce in the system. Because there is some vibration associated with this device, attaching it to the detector would probably reduce the image quality. Cryo-coolers with no moving parts are being developed to reduce vibration and extend life, but these currently have very low efficiencies and high power requirements.

Cryogenic fluid: A cryogenic fluid such as nitrogen or helium could be used to provide a heat sink for the detector. Telescopes such as AXAF-S will use this method to maintain instruments at the proper temperatures. However, for AXAF-S, nearly the entire spacecraft is a dewar which contains the superfluid helium coolant. The dewar itself, which would have to be designed to minimize boiloff in the harsh lunar surface environment for 2 years, would probably be a large portion of the LUTE mass budget. The cryogenic fluid required or 2 years operation would further increase the system mass.

Alternate detector location: Enlarging the radiator would allow rejecting more heat or rejecting the same amount of heat at a lower temperature. However, because the detector is located inside the telescope light shade and cannot obstruct the FOV, the thermal radiator is limited in size. Also, with the current radiator location, radiation from the light shade drives the heat rejection capabilities of the detector radiator. One solution to these problems is to move the detector. Moving it to the side of the light shade, as shown in figure 125, would allow use of a radiator that could "see" mostly space and would also allow an increased radiator surface area if needed. One disadvantage to this idea is that moving the detector would mean moving the focal plane and changing the optical design. Also, the radiator would probably have to be deployable because of space limitations in the launch vehicle shroud. Additional structure might be needed to support the radiator after deployment.

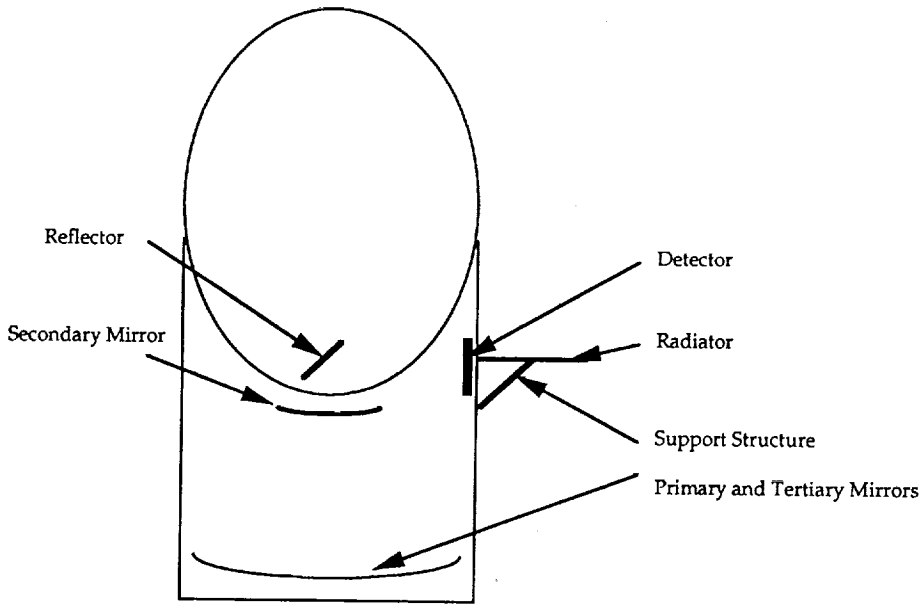

Figure 125. New detector location to alleviate thermal control problems.

Alternate telescope location: The major driver of the detector radiator thermal environment is the light shade. Analyses have shown that the upper light shade reached average temperatures over 270 K. The radiation of this heat to the detector radiator dramatically limits its capability. Changing the thermal environment of the light shade is necessary to radiate 10 W of heat at 200 K from inside the light shade. One way of changing this environment is to locate the telescope at a higher latitude and tilt it so that its view of the lunar surface is reduced. Reducing the view to the hot lunar surface allows the light shade temperature to drop down to about 200 K, which reduces the amount of radiation from the light shade to the radiator. Coupling the cooler light shade with a radiator-oriented parallel to the lunar surface provides an almost ideal radiation environment.

Alteration of detector thermal requirements: The thermal requirements for the detector are preliminary. If an adequate TCS to maintain the detector within its specified operating limits cannot be designed, then the feasibility of the LUTE is questionable. It may be necessary to alter the requirements so that a more functional TCS can be designed for the detector. If the allowable detector temperature were increased, the radiator could operate at a higher temperature decreasing the ΔT between hot and cold sides on a TEU and decreasing the amount of power needed to remove the heat from the detector. However, raising the operating temperature of the detector would decrease the quality of the images obtained since temperatures above 210 K will increase noise. Therefore, it appears unlikely that the

detector maximum temperature will be increased. A reduction in the amount of heat dissipated to a level of 0.5 W or less may make the use of a TEU more feasible because it would decrease the amount of power needed to remove the heat from the detector at the specified temperature difference. The heat load assumed for the analyses is based on limited information about the detector. More detail about the detector and its connections would allow better characterization of the thermal environment and may reduce the heat load assumed.

5.5.4.3 Detector TCS Recommendations

Locating the telescope at a higher latitude is the most attractive solution. The temperature and heat rejection requirements can be easily met with this option. Not only is the thermal environment affecting the detector radiator less severely, but the radiator's view to space is increased so that the heat can be more effectively radiated. This option also requires the least weight and power from the TCS perspective, because it is totally passive. The other passive radiator concepts examined do not meet the detector maximum temperature requirements. Of the active cooling concepts examined, the TEU and cryo-cooler have large power requirements and the cryogenic fluid system has a large mass requirement. None of these options is feasible with the current system power and mass limitations. Changing the detector location has been suggested as a means to provide a larger detector radiator in a better location, but this would be undesirable because it results in an optical configuration with a fourth reflector. It is also unlikely that a detector can be developed to operate at 260 K and produce an image of acceptable quality in time for the LUTE mission. The other passive radiator concepts examined do not meet the detector maximum temperature requirement.

5.5.5 Subsystem Thermal Control

LUTE subsystem equipment requiring thermal control includes the electronics, solar arrays, and various mechanisms, motors, and other equipment. The major subsystem components have been illustrated previously. Passive thermal control options were strongly favored for thermal control of this equipment.

5.5.5.1 Requirements

For an operating range of 208 to 398 K, heat rejection requirements for subsystem components are shown in table 48.

Table 48. Subsystem thermal control requirements.

Module Components	Average Power (W)	Temperature (K)
Transponder	18	208 to 398
Command Detector	10	208 to 398
Diplexer	–	208 to 398
Central Data Unit	15	208 to 398
Central Computer	15	208 to 398
Antenna Drive Electronics	10	208 to 398
Power Distribution	7	208 to 398
ACS Electronics	–	208 to 398

5.5.5.2 Electronics Analysis

The LUTE electronics consists mainly of the command and data handling and power conditioning equipment. Thermal control of the electronics presented some challenging problems. The equipment needs to be maintained within a temperature range of 208 K (nonoperating) to 398 K (operating). As stated earlier, the electronics dissipate about 90 W of heat. During the LUTE operating period, the lunar surface temperatures may rise to 385 K while being exposed to solar radiation for about 14-Earth days. This hot environment creates problems when trying to reject the heat generated by the electronics during operation. On the other hand, there is a concern for the survival of the electronics during the lunar night when lunar surface temperatures drop to as low as 85 K during the 14-Earth day/night time period, if the electronics are not operating and producing power internally during this time.

Because of limited power, passive thermal control is necessary. To simplify the TCS and make temperature control of components more manageable all electronics were located in one box. This also minimizes the radiator surface area needed and TCS mass.

Placement of the box is important to providing proper viewing for the radiator. Reduction of direct solar heating on the radiator and avoidance of lunar surface radiation is necessary while providing view to space to radiate the heat produced in the box.

The radiator surface area needed to reject heat generated by electronics was calculated using an Excel spreadsheet. TRASYS and SINDA models were built to more accurately characterize the thermal environment and calculate radiator temperatures. The radiator was modeled in four different positions around the light shade as is shown in figure 126. The hot lunar environment was assumed as the boundary condition for the analyses. The box was assumed to be well insulated and to have no conduction through any structural attachments. Steady-state radiator temperatures were calculated assuming a 90 W heat load on the radiator.

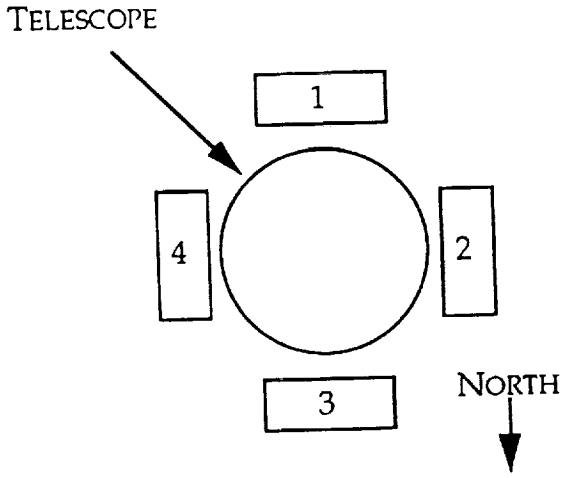

Figure 126. Electronics box analysis positions.

For the night case, it was assumed the radiator has a perfect view to space. The objective of this analysis was to determine the emissivity necessary to limit the heat loss from the box and also determine how much heat would be needed to maintain the box at survival temperature. Because the box will be in the cold environment for an extended period, it will be necessary to provide some heat. This heat could

come from an RTG, a phase change material, or an radioisotope heating unit (RHU), or from leaving the components operating at night. Using an RTG as a power source, the LUTE could operate continuously providing power necessary for the electronics' survival. A phase change material could be used to store heat from the daytime operation and maintain the temperature of the electronics above the minimum during the night, but calculations from a previous study showed that the amount of mass needed would be prohibitive. RHU's show the most promise to provide heat during the night. These devices are small and provide heat continually, almost indefinitely, at no increase in power system mass.

The thermal analysis showed that the radiator could be located in any position, provided that it is an optical solar reflector (OSR). An OSR is a radiator that has a thin coating on the surface to minimize the amount of absorbed solar energy while allowing the surface to radiate. At night, though, the emissivity of the radiator would have to be modified to about 0.45 to reduce the box heat loss by radiation to an acceptable level. To accomplish this with an OSR, a cover with a low emissivity would have to be moved into position over the radiator at night. This would require a mechanism to open and close the cover as shown in figure 127. A more practical method of accomplishing this surface modification is using louvers. Louvers have a range of effective emissivity of 0.2 to 0.7. No power is required to close louvers and they have been used for space applications for many years. A drawback to using louvers is that to maximize their radiation capability, solar radiation must be avoided because they have a high solar absorbtivity. A cover could be used to protect the louvers from solar heating, but the effective emissivity would be reduced, significantly decreasing their radiation capability during daytime operation.

The radiator surface area was determined to be 0.2 m^2 radiating at 343 K. If the radiating surface were modified to have an emissivity of 0.45, 10 W of heat would have to be added to maintain the electronics above its lower temperature limit.

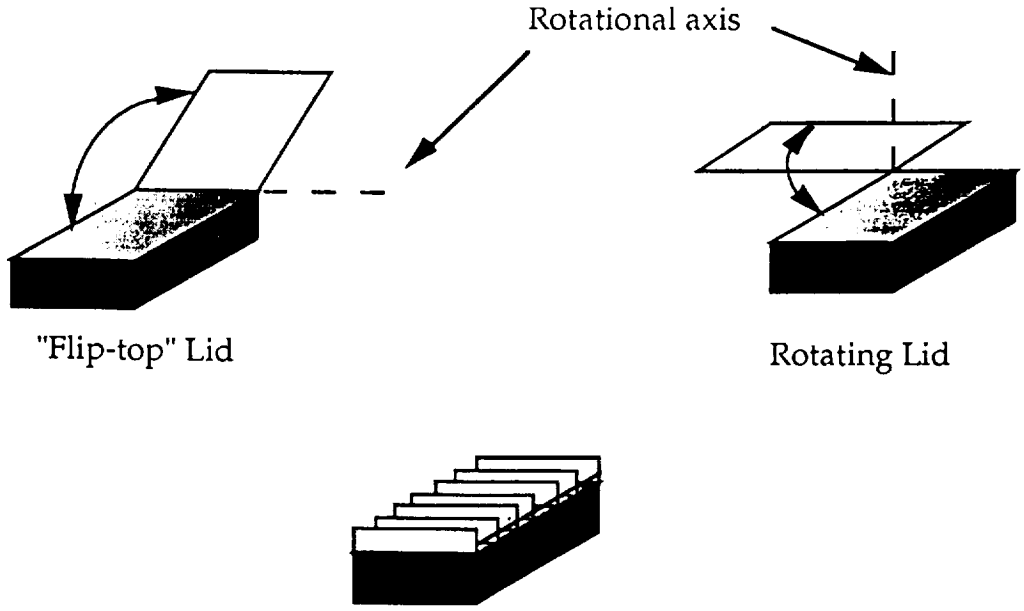

Figure 127. Thermal control methods for electronics box.

5.5.5.3 Power System Analyses

RTG Analysis—The purpose of this analysis was to calculate the operating temperature of a 300 W RTG on the lunar surface during the lunar day/night cycle and to determine whether the temperature of the RTG will exceed its allowable operating temperature. The upper temperature limit of the RTG was determined to be 533 K.[43] If the RTG temperature had been above 533 K, other methods of thermal control would have been required or the RTG could not have been used. Because the LUTE is power and mass limited, the thermal control of the RTG is limited to passive methods. But, as has been discussed in an earlier document, the model run is simply the RTG located 2 m above the lunar surface. The RTG is 1.17 m long and 0.23 m in diameter with eight fins extended radially 0.091 m and located around the circumference of the RTG, as shown in figure 128. A 4,100 W heat load was applied to the body of the RTG, which was assumed to be located 2 m above the lunar surface. Other heat sources are solar energy and radiated energy from the lunar surface. The thermal model was run for one lunar day/night cycle. Output from the analysis was taken every 10 hours during the 660 hour cycle.

The analysis results show that there is a hot spot in the area of the RTG nearest the lunar surface. The higher temperature was expected because this area of the RTG is exposed directly to the lunar surface and receives the most thermal radiation from the surface. However, figure 129 shows that the temperature at this spot only reaches about 505 K, which is about 28 K below the maximum allowable temperature.

The analysis results show that the RTG can effectively radiate the heat it generates in the lunar environment. If the maximum calculated temperature had exceeded the allowable limit of 533 K, the optical properties of the RTG surface could be modified to enable more effective radiation of the heat load. But, if modifying the optical properties did not achieve the required result, an alternative method of thermal control would have to have been employed, which might have required additional mass and volume.

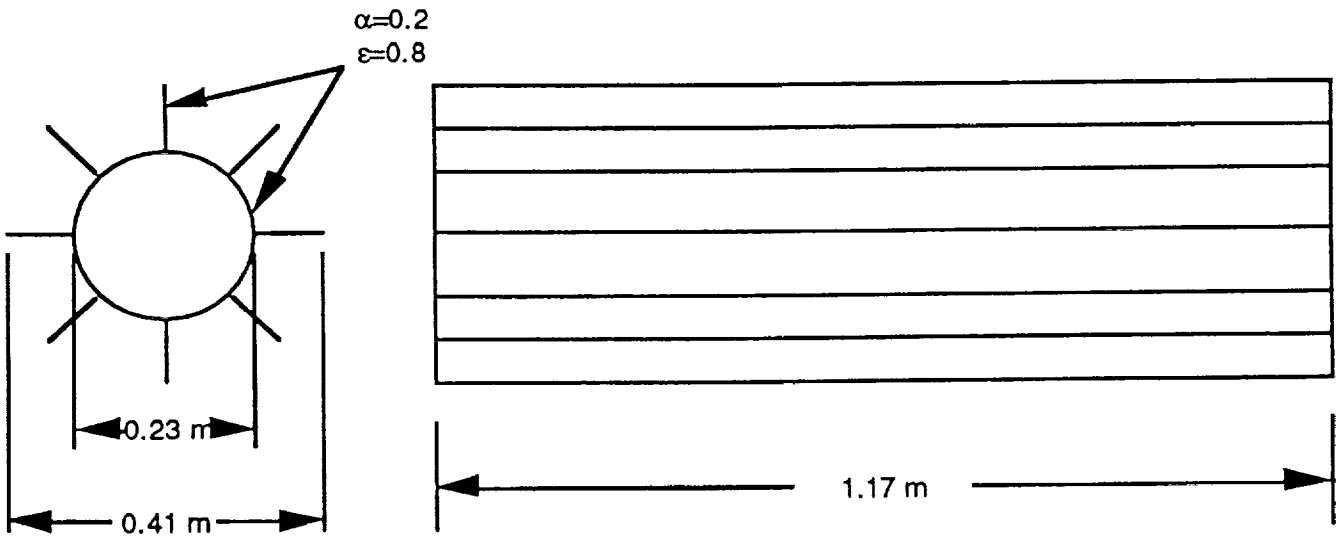

Figure 128. RTG dimensions and optical properties.

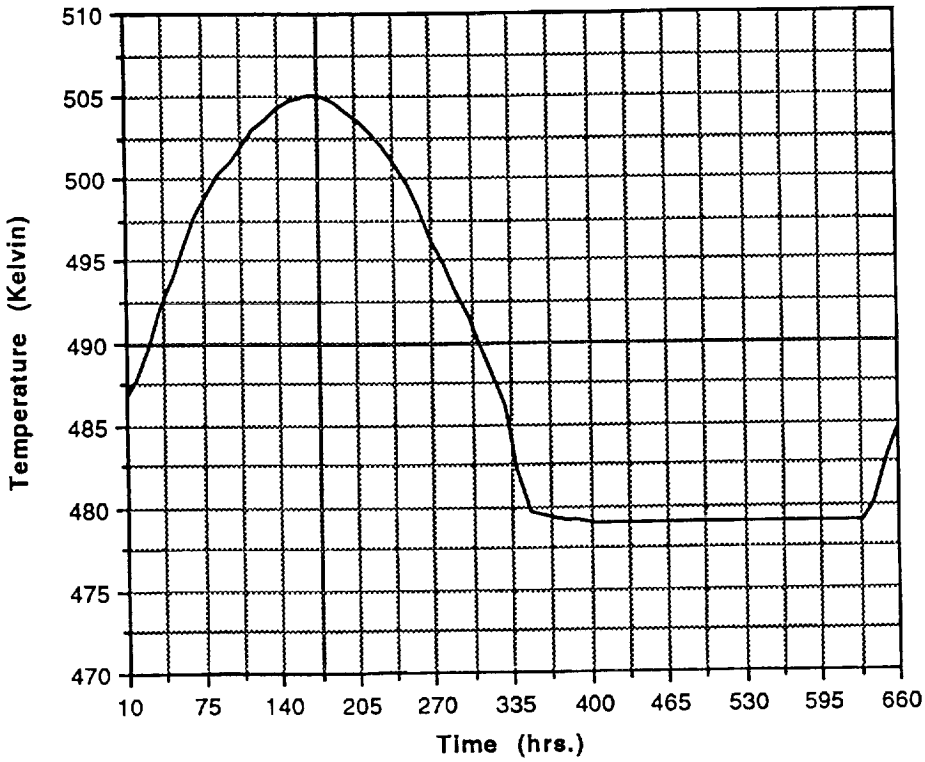

Figure 129. RTG outer shell temperature.

Solar Array Analysis—The temperature of the solar array affects the efficiency of the solar cells. For this reason, a preliminary thermal analysis using an I-DEAS™ TMG™ model was done for the original solar array configuration (the arrays were later enlarged), which is shown in figure 130.

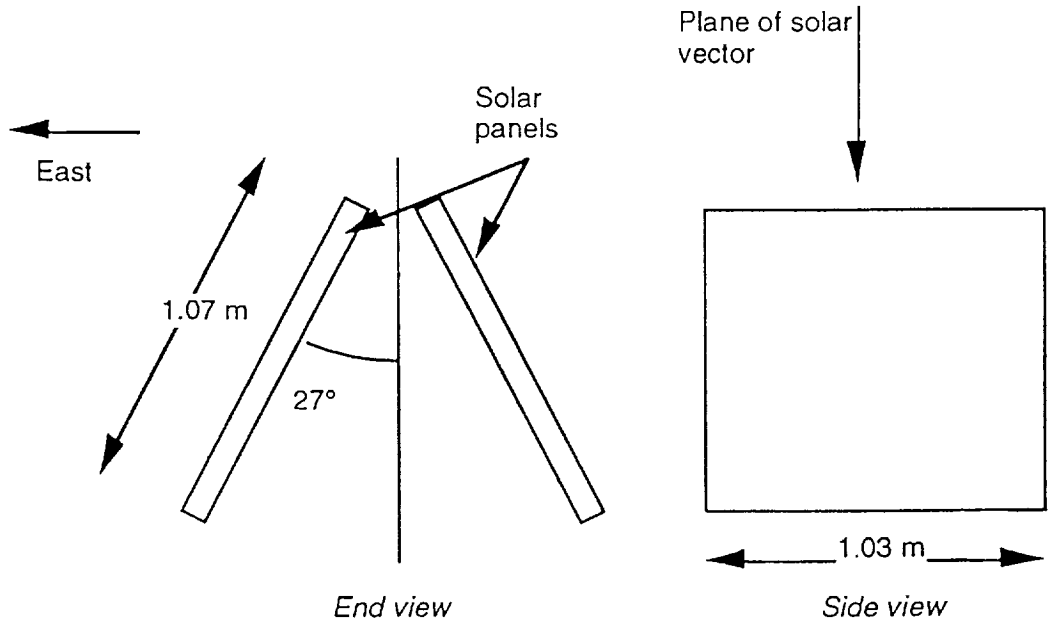

Figure 130. Solar array configuration analyzed.

The solar array front surface was modeled as having $\alpha = 0.667$, $\varepsilon = 0.8$, and the back surface was modeled as having $\alpha = 0.8$, $\varepsilon = 0.7$. In addition, it was assumed that there was good conduction between the solar array front and back surfaces. The predicted temperatures for the two panels are shown for one diurnal cycle in figure 131. The maximum solar array temperature of approximately 370 K results in some degradation of the cell efficiency.

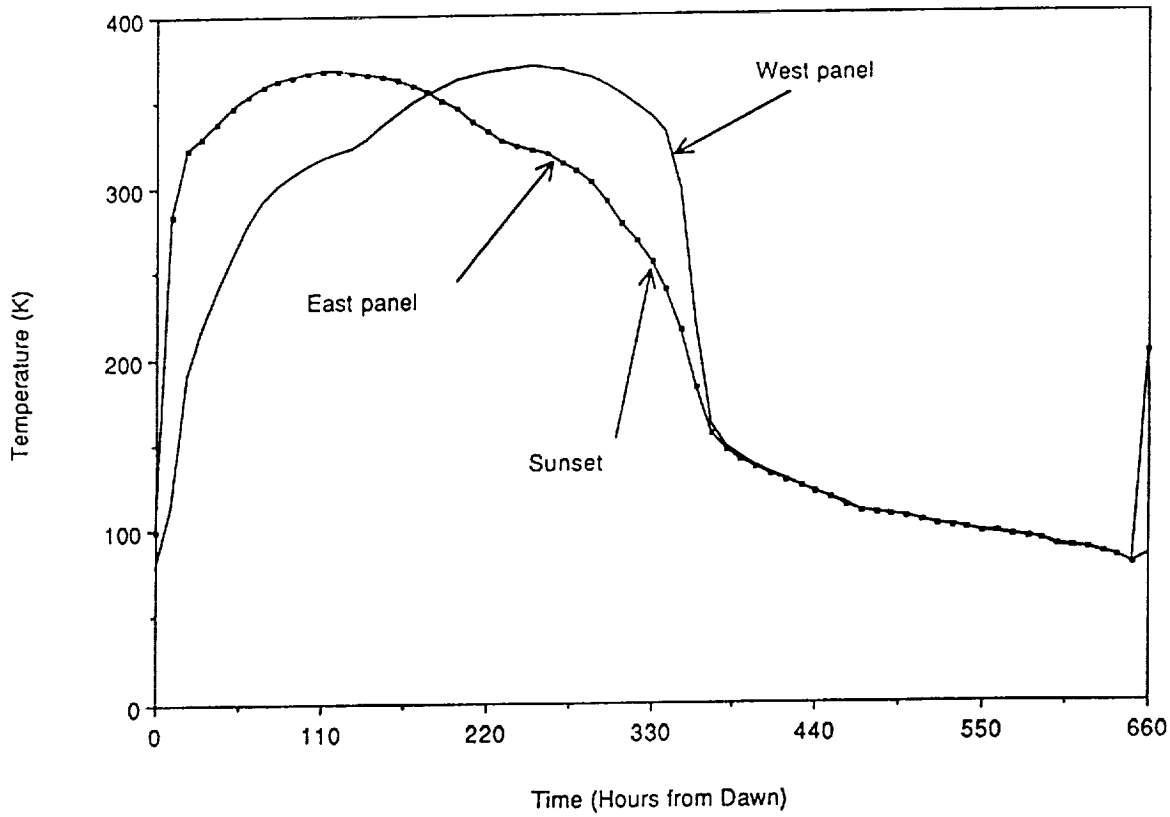

Figure 131. Solar array temperature predictions.

5.5.5.4 Mechanism Analysis

Several mechanisms are included on LUTE. These have not been analyzed, but motors are available which can withstand the expected temperature excursions (approximately 70 to 380 K). In addition, thermal control coatings and paints can be used to reduce the expected temperature excursion on selected components, if needed. While none have been identified to date, a few components may require heaters to assure proper operation.

5.5.5.5 Thermal Control Conclusion

Thermal analyses and trade studies performed for the LUTE show that the lunar surface significantly influences the thermal control systems of the telescope and supporting subsystem equipment. Radiation from the lunar surface during the day heats the light shade interior, which then heats the optical system and the detector radiator. The asymmetric light shade opening, coupled with the radiation from the upper light shade, produces a temperature differential across the primary mirror during the lunar day. Heat pipes or other highly conductive devices placed in and around the LUTE baseplate can be used to reduce the temperature differential in the primary mirror.

Mirror construction also affects the temperature differential in the mirror. Under the same conditions, a mirror with a center hole will have a larger differential than one without a hole. Of the mirror materials examined, beryllium has the smallest temperature differential, followed closely by SiC, but the low thermal diffusivity of fused silica results in a very large temperature differential. The mirror support system (three-point flexures or a ring) has little influence on temperature differential. Mirror construction and material do not influence mirror maximum temperature and diurnal temperature swing. Applying heat to the primary mirror to raise the minimum temperature can reduce the diurnal temperature swing, but if very precise temperature control is required, heat should be applied to the mirror at all times.

Locating the telescope at a latitude near 65° north and tilting it southward to view at a 40° declination provides several benefits to the thermal control system. Mirror maximum temperature differential, maximum temperature, and diurnal temperature swing are all reduced by locating the LUTE at 65° north latitude rather than 40° north latitude. In addition, the focal plane array can then be passively cooled by a radiator situated forward of the secondary mirror. Passive cooling of the detector is not feasible at lower latitude sites.

Thermal analyses have not revealed any serious problems in the area of subsystem thermal control. Electronics box heat can be rejected at all locations studied, but the recommended location is on the north side of the telescope. This location allows the use of louvers to regulate heat rejection and avoid excessive heat rejection during the lunar night. The RTG can radiate 4,100 W of waste heat in the proposed location and orientation. Its maximum case temperature will be approximately 505 K, which is well within allowable limits. Future thermal analysis efforts for LUTE should identify thermal control systems for the metering structure and the secondary and tertiary mirrors. Also, the effect of the stray light baffles on optical system temperatures should be quantified. Eventually, a parametric assessment must be done considering the effects of variations in local environment, such as lunar surface properties, terrain, and landing slope, to determine the worst case thermal performance of the LUTE. In a similar vein, some estimation of the uncertainty of thermal model results should be undertaken, either by comparison with test results, or by analysis of the solution algorithms and computer hardware precision.

5.6 Communications and Data Handling

The DSN has the capability to operate at S-Band, X-Band, and Ka-Band frequencies. The 26 m DSN subnet, using S-band communications, is generally used for Earth orbit and near-space applications. Advantages of this option are the large numbers of space qualified equipment choices and the magnitude of experience with this equipment. Disadvantages include higher power requirements, larger antenna size, and the difficulty in obtaining frequency allocations due to the large number of spacecraft using S-band. Table 49 compares the three bands along with a sample calculation of link margin using the LUTE baseline requirements. This chart shows that with the 200 kb data rate, using a 0.3 m diameter antenna at the telescope and 10 W of RF power on the DSN 26 m S-Band antenna, the link margin is a positive 7.2 dB. This is a sufficient margin for good communications and a reasonable power allocation for the current power system. Using X-Band would give a +18.7 dB margin and would permit a power reduction or a data rate increase and still have an acceptable link margin. As requirements become more fully defined, the various transmission band options will be reexamined.

Table 49. LUTE frequency options.

	S-Band	X-Band	Ka-Band
Frequency/Wavelength	2.25 GHz 13.3 cm	8.4 GHz 3.57 cm	39.0 GHz 0.77 cm
Antenna Gain Comparison (Theor.)	Ref.	+11.5 dB	+23.1 dB
Weather/Atmospheric Link Degradation	Least Sensitivity	Little Sensitivity	–0.5 dB @ 30 el. –7.0 dB @ 10 el.
Power Amplifier Efficiency	TWTA 30–50%	TWTA 30–40%	TWTA 30–35%
Technology	Mature/Proven	Mature/Proven	Technology Ongoing
Link Margin (200 kHz, 1 ft, 10 W, 26 m DSN)	7.2 dB	18.7 dB	30.3 dB
DSN Availability	Yes	Yes	Yes
Design Impacts	Largest Antenna and Power Requirement Frequency Allocations	Smaller Antenna Lower Power Lower Beam Width	Smallest Antenna Lowest Power Req. Low Beam Width May Require Frequent Pointing. Attn. at Low Elev. Angles.

If the data rate should increase from the baseline 200 kbs, some adjustments will be necessary in the C&DH subsystem. A data rate increase will necessitate an increase in the output RF power or an increase in the antenna size or both. For example, a data rate increase to 400 kbs would require the RF power output to be doubled (to keep the same RF link margin). This would also double the required dc input power to the transmitter. Conversely, doubling the data rate at the same power will result in a 3 dB reduction in the current link margin, or to +4.2 dB in the current design. Antenna size effects are proportional to the area change (or the square of the diameter). Doubling the antenna diameter increases the area by four times with a 6 dB increase in the link margin. However, another factor comes into play with increased antenna size and that is beam width, which decreases with antenna size. Doubling the size of the current antenna from 0.3 m to 0.6 m would reduce the beam width from 30.4° to 15.2°. This would require the LUTE antenna to be repositioned more frequently to track the Earth.

Other potential impacts are in hardware weight and volume, software capabilities, and data handling and storage capacity at the ground station. Except for a minimal increase in transmitter weight and volume, these impacts are not considered to be significant. All of these factors will need to be examined if the data rate increases, to see what combination gives the most efficient system with the least impact.

5.7 Pointing and Alignment

5.7.1 Guidelines and Assumptions

The objective of the pointing system is to meet the telescope alignment requirements and accommodate attitude errors present after landing. Design goals are to provide a lightweight, low-power, and low-cost system utilizing hardware and designs that have previously flown. No sensor information from the lander will be available for use by the telescope subsystems. The telescope operates in a transit mode, in which no tracking of celestial targets or reorientation is necessary after initial attitude acquisition. Hence, control systems were not required for this telescope, particularly in light of the risk, complexity, and cost of these systems. Compensation for disturbances was not required of the pointing system, since small variations in the observed region of sky could be identified by processing data from the alignment CCD's. It is not clear at this time whether the response to alignment disturbances will be small enough to continuously satisfy the arcsecond east-west requirements. Small periodic alignment adjustments may be necessary during operation. Assuming all disturbances are thermally induced, the mirror deformations are being accommodated by the thermal control system, and deformable or actively controlled mirrors will not be used. A five DOF steerable secondary mirror has been identified as necessary for focus and tilt adjustments.

The emphasis of phase A tasks has been on estimation of alignment requirements, identification of suitable pointing system components, and component and configuration trades. The mount must provide a 42°-tilt capability in all directions so that the 40°-declination requirement can be met from a 66.5° latitude with a maximum 15° lander tilt. To avoid changes to the telescope configuration, the mount was required to attach to the telescope at the baseplate. The mount must interface with the lander bolt hole pattern, not change the configuration of the lander, or intrude on the region below the interface points. Redundancy of certain components may be desirable, but is not a major criterion. Alignment requirements are discussed in section 4.2.7; the pointing requirements are 14.6 arcseconds in roll about the line-of-sight, and 5 arcminutes of north-south tilt, over a device integration time of 883 seconds. The function of the pointing system is to acquire the proper telescope attitude after lunar landing, and then maintain that attitude over the 2 year lifetime of the telescope. A nominal list of tasks for attitude acquisition include initial estimation of both axis and angle of tilt, rotation of the evaluation axis to the proper azimuth, elevation of the telescope to the proper declination, and roll of the light shade/antenna/electronics assembly to their proper orientation. After the aperture cover is removed and any other deployables are positioned, alignment sensing and mount adjustments are initiated.

5.7.2 Acquisition Sensor Trades

Attitude acquisition begins immediately after landing, so that estimates of tilt and roll angles can be used to align the light shade/antenna/electronics assembly to their proper orientation. Tilt direction must be sensed for proper orientation of the elevation axis, since the combination of lander deck tilt and 40° pointing declination cannot be determined before landing. Tilt direction and angle could be sensed by a tiltmeter; laboratory tiltmeters are available that sense tilt within 1 arcsecond. Unfortunately, no readily available space-qualified tiltmeters could be identified, although the pendulum sensor on the Saturn guidance platform was suggested as a possible alternative. Lander tilt estimates of approximately 1 arcminute could be provided by the dc component from the lander accelerometers, and the lander star tracker may provide additional attitude information if it is not pointed at the Sun or the Earth, but study guidelines preclude any use of lander information by the telescope. Hence, an accelerometer set on the mount is recommended. Pointing declination and roll angle sensing can be provided by a Sun sensor mounted to the light shade or antenna. Unfortunately, Sun sensors will not operate or even survive over

a full lunar thermal cycle. Preliminary estimates of the antenna bracket temperatures indicate a swing from 80 to 370 K over the full lunar day. Sensor head operational temperatures must be maintained within 263 to 333 K, and nonoperational temperatures range from 233 to 343 K. Since no thermal control will be provided for the Sun sensor head, it will be functional for only about 24 hours after landing, and so initial attitude acquisition must be accomplished during this time. A NASA-qualified two-axis fine digital Sun sensor, providing a 64° by 64° FOV, has been baselined, and a supplemental coarse Sun sensor is recommended.

5.7.3 Telescope Mount Trades

Various telescope mount designs were considered for use on LUTE. Lightweight, low-power, short designs that have already been space-qualified or flown are characteristics to be used in design selection. Alignment requirements indicate that as a minimum the three rotational DOF are necessary (azimuth, elevation, and roll can be used to characterize these DOF). Translational DOF have not been identified as necessary during the phase A final study, since the telescope design has not progressed to the point where translational balancing should be considered. An evaluation of lander postlanding attitude capabilities shows that the telescope mount must provide a ±180° roll capability, but only 42° of tilt capability is necessary for the selected lunar site and pointing declination.

Traditional telescope mounts,[44] such as horseshoe, frame, or English mounts, require broad bases that are unsuitable for the small interface surface provided by a lunar lander. German mounts are suitable only for designs without height constraints, and yoke or fork mounts are generally massive. All of these mounts are designed to support and rotate the telescope about its center of mass, which was not suitable for the LUTE configurations. Lightweight balloon-borne telescope mounts were examined,[45–47] but these mounts are designed to be hung below a gondola, and counter-rotational controls with counterweights are one of the main design considerations for these mounts. Single-column mounts, such as the shuttle-based IPS, were also considered, but in many cases they are too tall or weigh too much for our application. The telescope was zenith-pointing during the first part of the study, requiring only a maximum tilt of 15° to accommodate the lander crushing, surface slope, and site errors. Hence, the first half of the study examined mounts with small tilt capabilities, a tilt-plate mount, and the hexapod mount design baselined in earlier telescope studies like the 2 m LTT.[48]

The tilt-plate design, shown in figure 132, consists of two actuators and a ball socket mounted on a rollring. For the 21.8° strut angle shown, the nominal actuator length is 0.875 m, with a stroke length of 0.292 m. The ball socket is elevated to a height of 0.3251 m above the rollring, so that the optical assembly is vertical during launch and landing. The rollring provides ±180° about the line-of-sight for east-west alignment of the focal plane. Unfortunately, this design does not provide moment control about the horizontal centerline that runs between the two actuators and through the outer ball joint. For equal actuator lengths, the telescope will rotate about this axis until the baseplate rests on an actuator. The tilt capability for this configuration about other azimuthal axes is shown in figure 133. The right half of the tilt range is defined by a 5° limit on the angle between the strut and the lander mounting surface, preventing horizontal strut configurations that produce infinite loads. The left half of the tilt range is defined by the maximum and minimum strut lengths due to stroke. For axes with tilt capability greater than 90°, a value of 90° has been assigned. Tilt angles at the 0° and 180° axes are not defined, since all angles will satisfy the kinematic equations for these axes. This configuration problem is resolved if the upper hardpoints of the actuators are not colocated, but the tilt capability will change. The maximum tilt angle that can be guaranteed about any axis is 22.1°. Actuator resolution is probably adequate for tilt accuracy specifications, but focal plane roll alignment requires arcsecond accuracy for the rollring. Since the tilt-plate concept requires more design definition, and the hexapod mount has been defined in previous studies, the hexapod concept was selected early in phase A when small tilt capability was required.

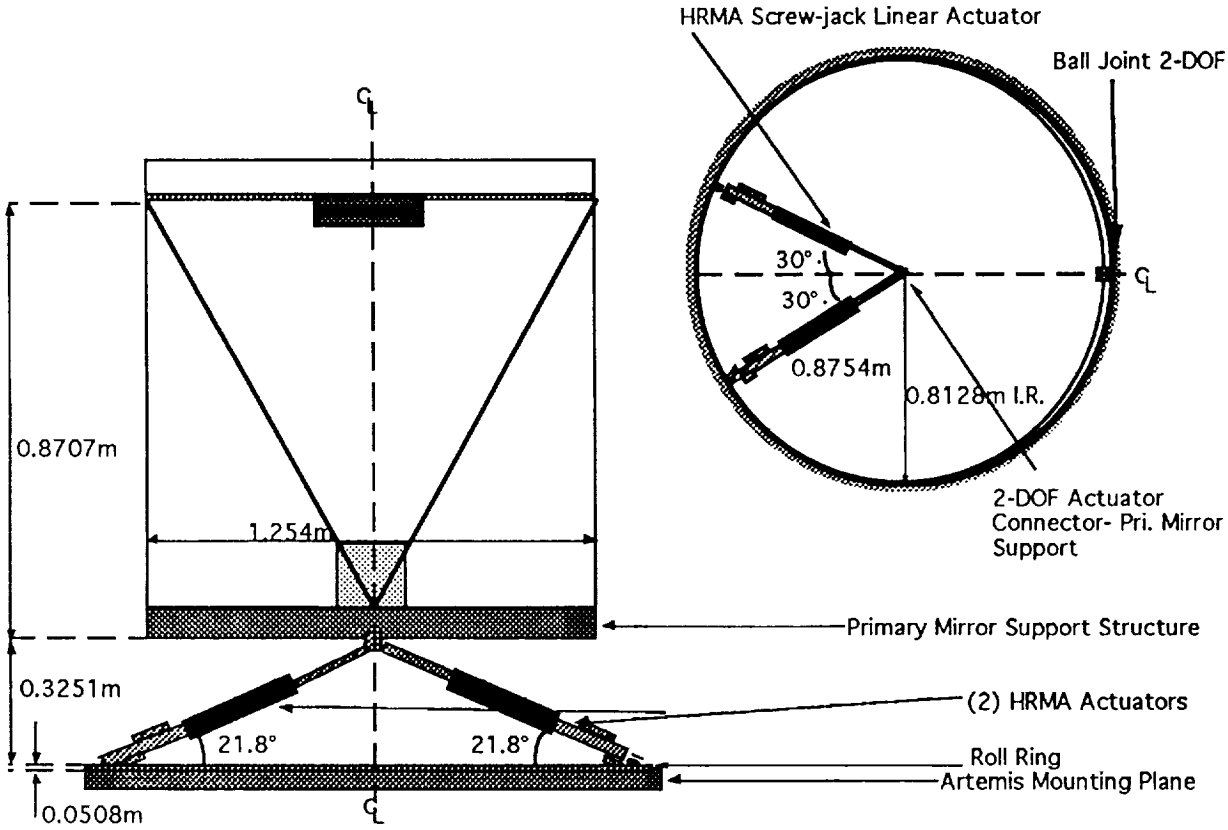

Figure 132. Tilt-plate mount.

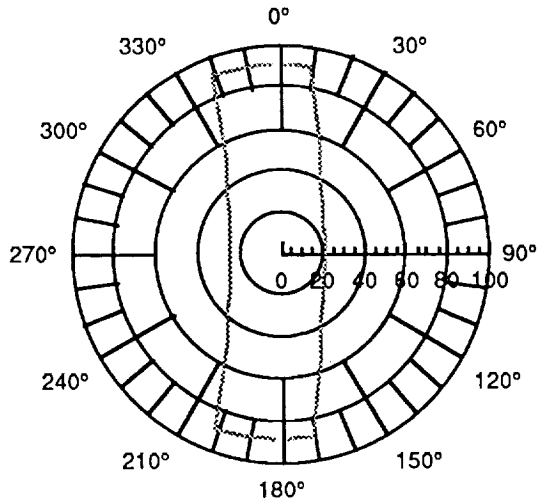

Figure 133. Tilt range for tilt-plate configuration.

Hexapod mounts have been used for many years for precision alignment and support of secondary mirrors, for both ground- and space-based telescopes. Although they provide six DOF, applications with symmetric optics do not generally require roll alignment, and so hexapod mounts are treated as five DOF redundant systems. Hexapods also provide small ranges of motion, which were appropriate for early LUTE tilt requirements, but not for roll. Hence, a rollring assembly was added to the hexapod mount to provide roll range and gross alignment capability, and the hexapods were used for fine roll alignment.

Since pointing requirements for the light shade, high-gain antenna, and the electronics box were on the order of degrees in the first half of the study, a trade was done early to determine if a separate fine-alignment rollring could be used for the focal plane and another rollring for the rest of the assembly. Since the optics do not need to roll, the bigger rollring would just rotate the light shade/antenna assembly, and the electronics box, as shown in figure 134(a). This option requires a complex design to accommodate load-paths between the outer rotating assembly and the telescope mount, adds another mechanism near the detector, and may increase the overall diameter of the telescope. Since the focal plane rollring and motor should not obscure incoming light and also not contribute to the heat rejection of the detector, this option was not considered.

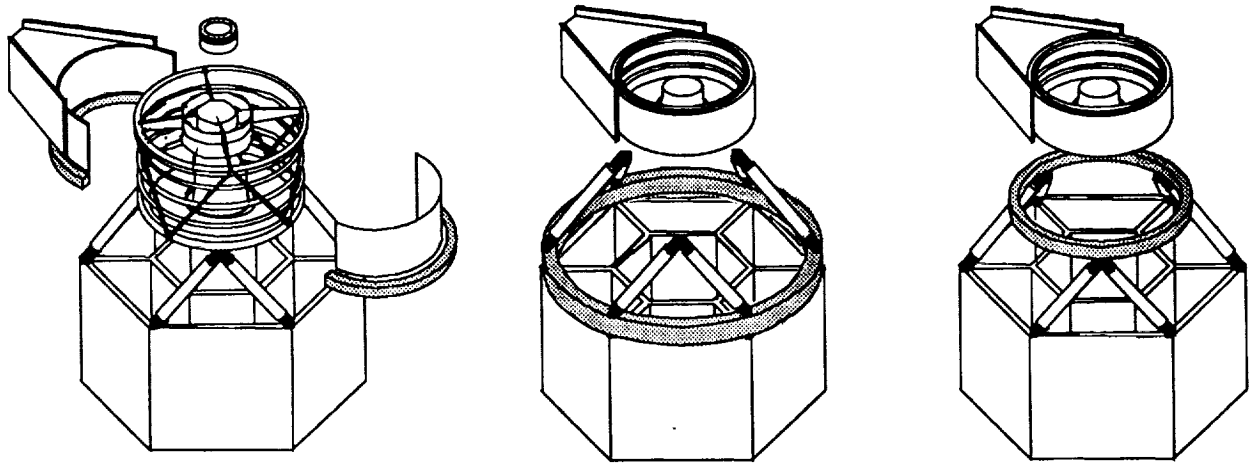

(a) Separate focal plane rollring. (b) Rollring at lander interface. (c) Rollring at telescope interface.

Figure 134. Rollring trades.

For the single rollring configuration, two locations were considered. A rollring at the lander interface, shown in figure 134(b), has the potential for accuracy due to the large diameter, but would also be heavier than locating the rollring at the top interface, as shown in figure 134(c). This last option also has the potential of weight reduction by integrating the rollring with the telescope baseplate structure. Since the hexapod actuators are nominally capable of providing fine roll adjustments, the option in figure 134(c) was chosen for the baseline rollring configuration during the first half of phase A.

5.7.4 Kinematic and Static Equilibrium Equations

To analyze the capability of various mount configurations, kinematic and static equilibrium equations were derived and programmed in MATLAB™.[49] The center of the lander interface surface will be treated as the origin of an inertial coordinate frame $\boldsymbol{I}, \boldsymbol{J}, \boldsymbol{K}$, where the $\boldsymbol{K}$-axis is normal to the interface surface. A body-fixed coordinate system $\boldsymbol{i}, \boldsymbol{j}, \boldsymbol{k}$ aligns the $\boldsymbol{k}$-axis along the line-of-sight, and has an origin at the center of mass. The telescope mass has six DOF, represented by the Cartesian inertial

translational coordinates $\{x, y, z\}$, and the azimuth, elevation, and roll angles $\{\gamma_i, i = 1,...,3\}$. Each actuator has three DOF, represented by the spherical coordinates $\{r_i, \theta_i, \phi_i, i = 1,...,6\}$, to provide orientation with respect to the inertial reference frame. The system is constrained, however, by the ball joints at each end of the actuator, so that motion of the telescope mass and the actuators is not independent. The constraint equations are derived by writing vector loop closure equations for each actuator, as shown in figure 135. The vector $\boldsymbol{R}$ from the origin to the actuator base hardpoint is added to the vector $\boldsymbol{r}$ along the actuator, and this in turn is added to the vectors $\boldsymbol{s}$ and $\boldsymbol{l}$ in body-coordinates, where $\boldsymbol{s}$ runs from the upper hard-point in to the center of the telescope base, and $\boldsymbol{l}$ runs up to the center of mass. The inertial-coordinate vector from the center of mass to the origin $-(x\boldsymbol{I}+y\boldsymbol{J}+z\boldsymbol{K})$ is added to this sum, and the total around the loop is set to zero. Each actuator's vector loop equation provides three scalar constraint equations. The system is represented by the 24 coordinates $\{x, y, z\}$, $\{\gamma_i, i = 1,...,3\}$, and $\{r_i, \theta_i, \phi_i, i = 1,...,6\}$, but with the 18 constraint equations the motion still has six DOF.

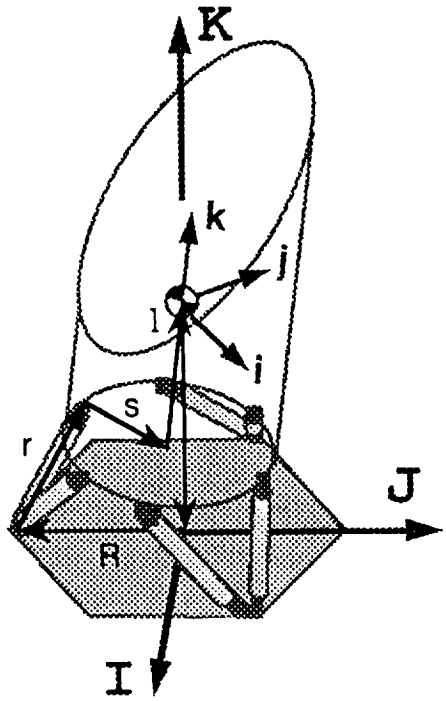

Figure 135. Kinematic constraint loop closure equations.

Traditional solutions[50 51] to the loop closure equations would utilize iterative methods like Newton-Raphson to solve for the attitude and translational variables in terms of the six actuator lengths, which are the commanded variables. In the solution technique used for this analysis, the constraint equations for the actuator variables are solved after specifying values for the six attitude and translational coordinates. Then the actuator lengths are checked to meet the stroke length constraints. Checks are made for singular configurations or geometries in which the actuators intrude below the lander interface. This technique solves the inverse problem, which provides sufficient but not necessary configurations. For use in a control algorithm, however, one would need to ensure that the solutions are necessary and unique as well as sufficient.

5.7.5 Hexapod Mount Trades

The design goal was to determine a hexapod configuration that is short, lightweight, utilizes the lander interface hardpoints, and meets the alignment requirements. Maximum tilt capability is the

primary consideration, with roll capability as a function of tilt to be defined after a configuration is selected. Although no translational requirements have been defined, excessive motion of the telescope center of mass may cause the lander to shift in the lunar soil, and so the mount has been designed to constrain telescope CG translation. Strut forces should not be excessive. The lander interface surface was identified early in the study as a possible location for mounting the subsystems, and so the actuator workspace needed to provide an adequate region below the rollring for this packaging. The mounting of antennas and the electronics box on the sunshade requires us to locate the rollring at the telescope base rather than higher on the barrel of the telescope, and, although additional capability can be found by placing this ring at a higher location, that configuration parameter could not be adjusted in these studies. Nominal actuator length is defined at midstroke, and stroke length throughout this analysis is sized as one-third of the nominal strut length. Calculation of forces was based on an early estimate of 133 kg for the telescope moving mass, and the mount capability was determined for a center of mass at 0.58 m above the rollring, along the line-of-sight. The lander hardpoint locations were provided by JSC;[12] the outer hardpoints are located 0.909 m from the centerline, and the inner hardpoints are 0.381 m from the centerline.

Four hexapod configuration options were analyzed, as shown in figure 136. Option 1 utilizes the outer lander hardpoints, with upper actuator hardpoints located at 120° apart. Option 2 relaxes colocation of the upper actuator hardpoints in option 1. Option 3 is the vertical inverse of option 1, and provides flexibility by varying the angle between upper hardpoints. Option 4 utilizes the lander inner hardpoints with the option 1 configuration.

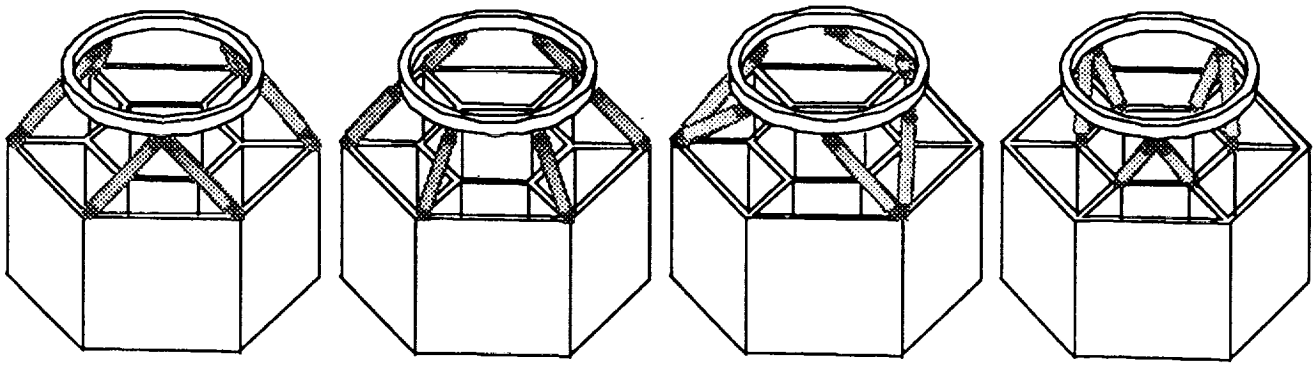

Figure 136. Hexapod mount trades.

Analysis for option 1 included tilt angle capability for various actuator lengths, strut forces, actuator workspace, and sensitivity to configuration changes. The maximum tilt angle for a particular horizontal axis varies as that axis changes from 0° to 360° around the base. Most hexapod configurations will produce three- or six-sided tilt regions, as shown in figure 137(a). The maximum tilt angle that can be guaranteed in any direction is the radius of an inscribed circle for this region. Figure 137(b) plots the maximum tilt angle as a function of nominal actuator length. A 0.813 m actuator will provide 15.3° of tilt, as shown in figure 137(a), with a stroke length of 0.271 m. The actuator lengths corresponding to the maximum tilt angle are plotted in figure 138. The actuator workspace and corresponding region available for subsystem packaging are plotted in figure 139. Note that each pair of upper hardpoints traces out a planar ellipse as the actuators tilt the telescope. The upper surface of the subsystem packaging region is defined by the motion of the telescope base. Variations in upper and lower hardpoint radii showed that option 1 is sensitive to lander hardpoint locations.

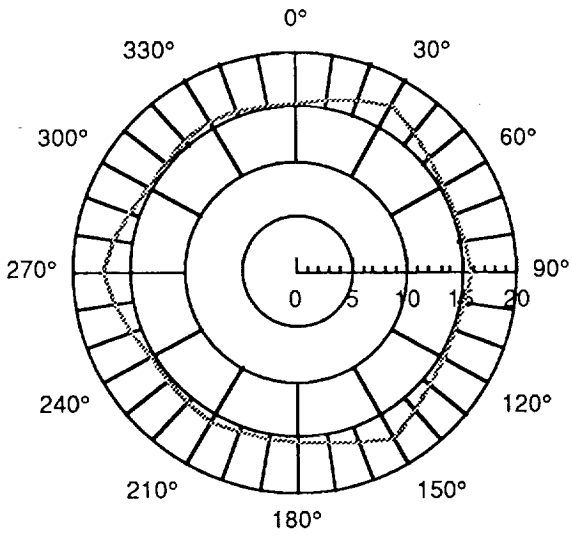

(a) Tilt range of motion for 0.813 m actuator

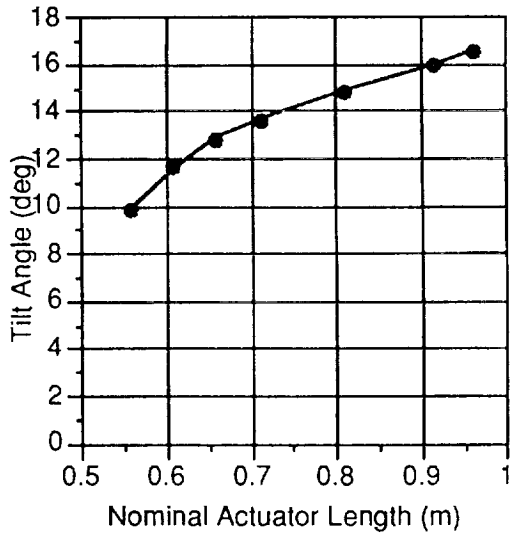

(b) Maximum tilt angle

Figure 137. Option 1—tilt angle.

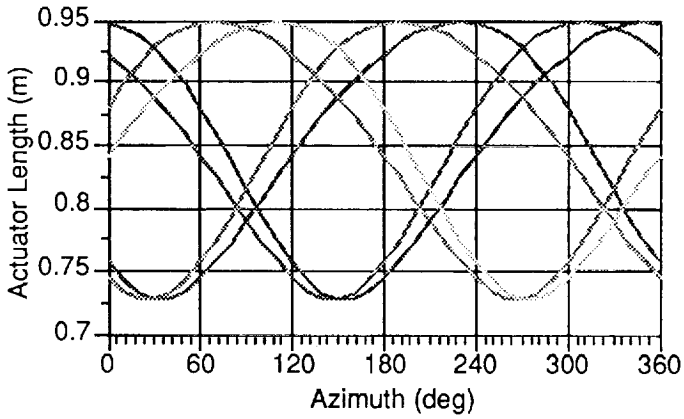

Figure 138. Option 1—actuator lengths at maximum tilt angle for 0.813 m actuators.

Several upper hardpoint locations were considered in evaluation of option 2. Locating the upper hardpoints directly over the lower hardpoints (at 60° separations) provided the largest tilt angles for a given actuator length, but the equilibrium solution for the strut forces in this configuration showed that it is statically indeterminate. This configuration also had the potential for kinematic instability, in which the struts would allow the telescope to collapse down to the lander interface surface. Hence, this configuration was not pursued.

Option 3 provides the flexibility to optimize placement of the actuator upper hardpoints to maximize tilt. Variations in the angle between upper hardpoints indicated that smaller angles between pairs, in which the actuators are more vertical, produced more tilt angle for a given actuator length. In fact, a maximum tilt angle is produced when the angle is reduced to zero and the pair collapses to a single actuator. This configuration is also statically determinate, since the redundant struts from option 2 have been removed. Unfortunately, the three-strut configuration is kinematically unstable, as shown in the free-body diagram of figure 140. The struts are two-force members, either in tension or compression, so that actuator forces must be applied to the upper plate along the strut longitudinal directions. These

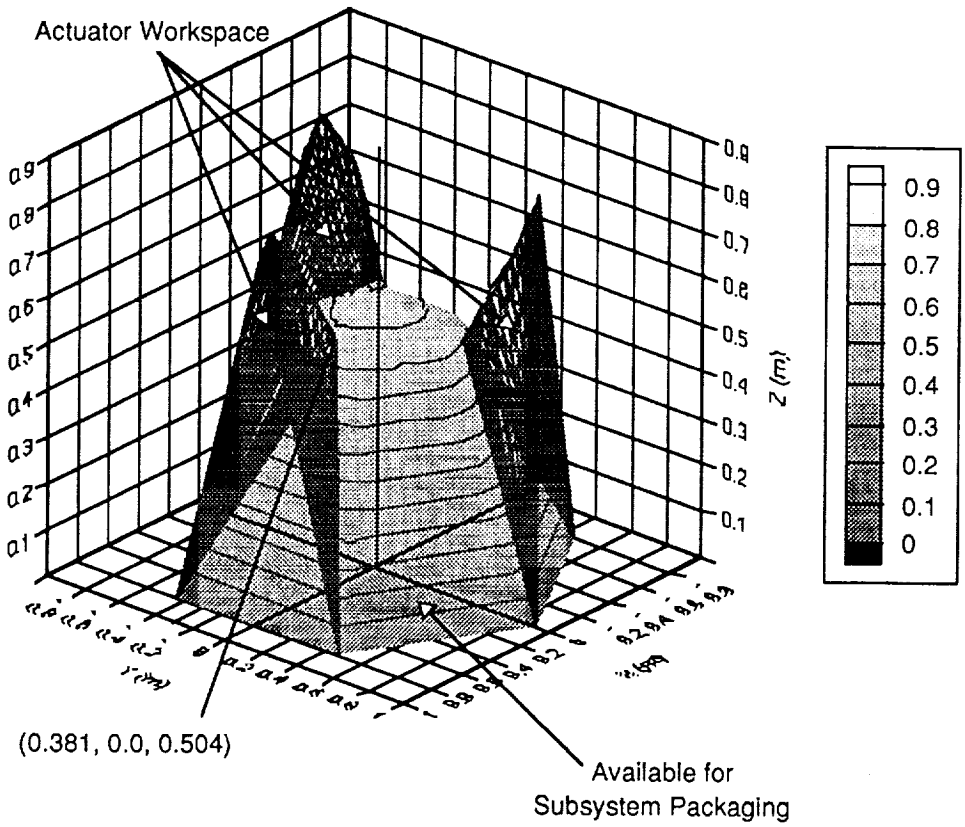

Figure 139. Option 1—actuator workspace for 0.813 m actuators.

forces each produce a moment $r \times F$ perpendicular to the plane defined by the strut and the radial vector from the center to the upper hardpoint. These three moments sum to zero in the horizontal plane, but produce a nonzero sum in the vertical direction, causing the plate to rotate and fall to the interface plane. Hence, the three-strut configuration is eliminated, and a six-strut configuration that can provide forces in directions that counteract these nonzero moments must be used.

To determine the upper geometry for six actuator configurations in option 3, the sensitivity to angular separation between actuator pairs and rollring radius was analyzed. A strut length of 0.508 m was chosen for this analysis. Angular separation was parametrized using the upper half-angle between an actuator pair; for a 0.56 m rollring radius, the maximum tilt angle and strut force are plotted in figure 141. Small angular separation produces larger tilt angles, as shown before, but also requires larger strut forces, and so an upper half-angle of 10° that just meets the 15°-tilt requirement from the first half of phase A was selected. For a 10° upper half-angle configuration, the sensitivity to rollring radius is plotted in figure 142. The tilt angle is maximized for a rollring radius of approximately 0.56 m, providing the required 15° of tilt. Note that this rollring radius is close to the 0.55 m radius determined in option 1.

Using a 0.508 m nominal strut length, a rollring radius of 0.56 m, and a 20° total upper separation angle between actuator pairs, option 3 provides a 15.32° tilt capability. Strut forces range between 458 N in compression and 334 N in tension, as shown in figure 143(a); actuator length at the maximum tilt angle is plotted in figure 143 (b). Roll angle capability decreases to zero as the tilt angle increases, as shown by the surface in figure 144. A 16.7° maximum roll capability is available for 0° tilt, and the average over this tilt region is 5.9°. This roll capability will be used for fine roll adjustments to achieve the arcsecond alignment requirements for the focal plane.

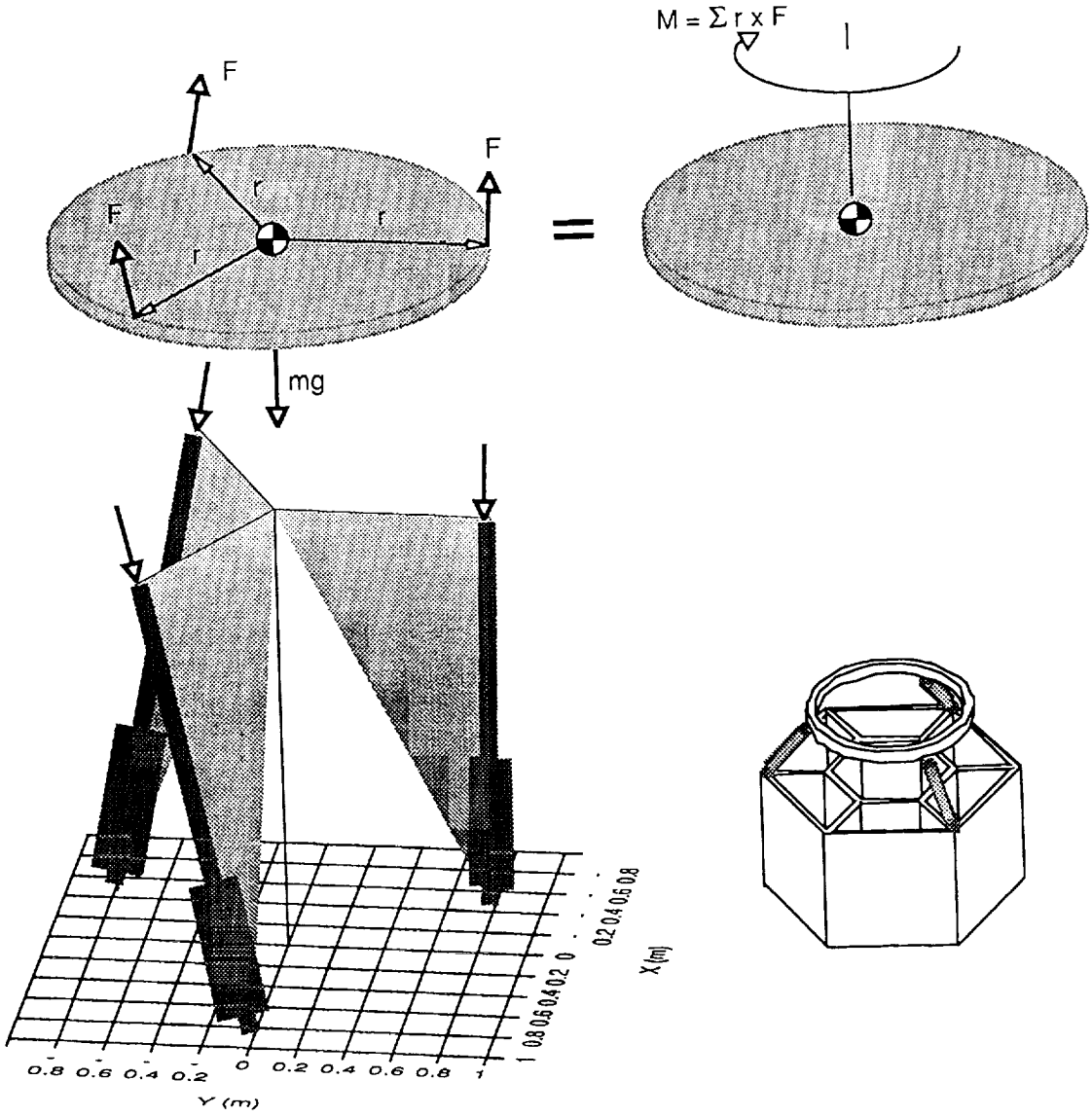

Figure 140. Option 3—three-strut configuration.

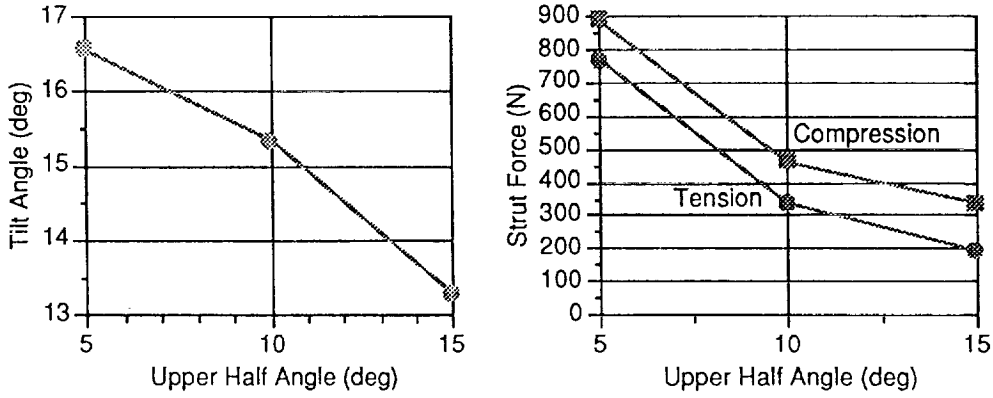

Figure 141. Option 3—sensitivity to upper half angle at 0.56 m rollring radius.

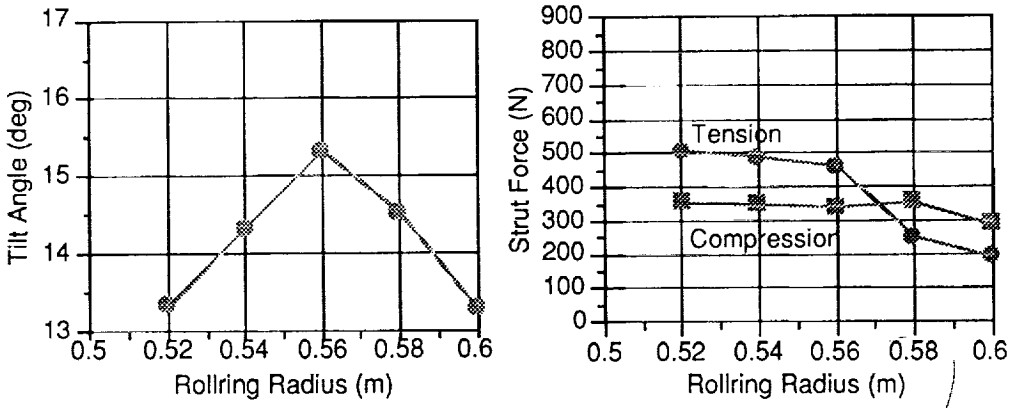

Figure 142. Option 3—sensitivity to rollring radius for 10° upper half angle.

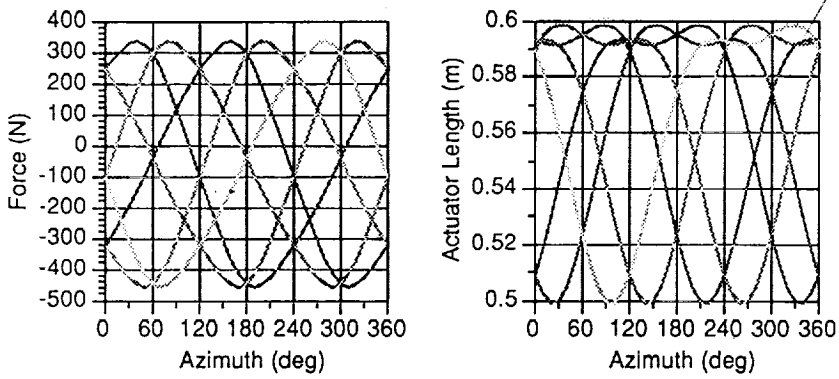

(a) Strut forces (b) Strut lengths

Figure 143. Option 3—actuator forces and lengths at maximum tilt.

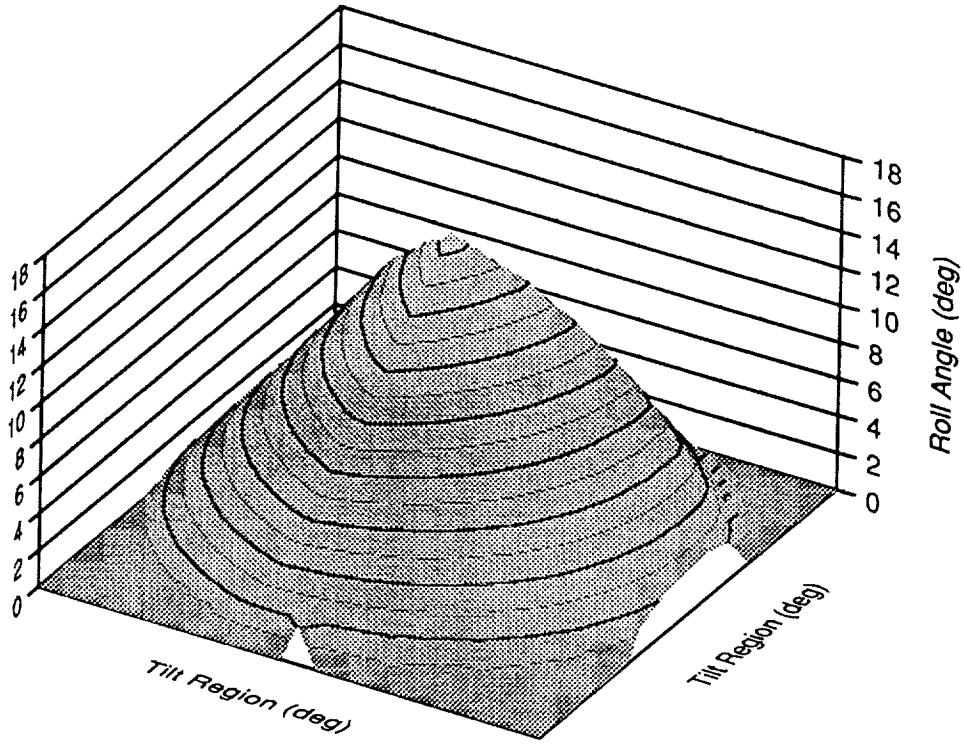

Figure 144. Option 3—roll angle capability over entire tilt region.

The hexapod workspace for option 3 is shown in figure 145, and coordinates of lowest actuator points are indicated to determine packaging space on the lander interface surface.

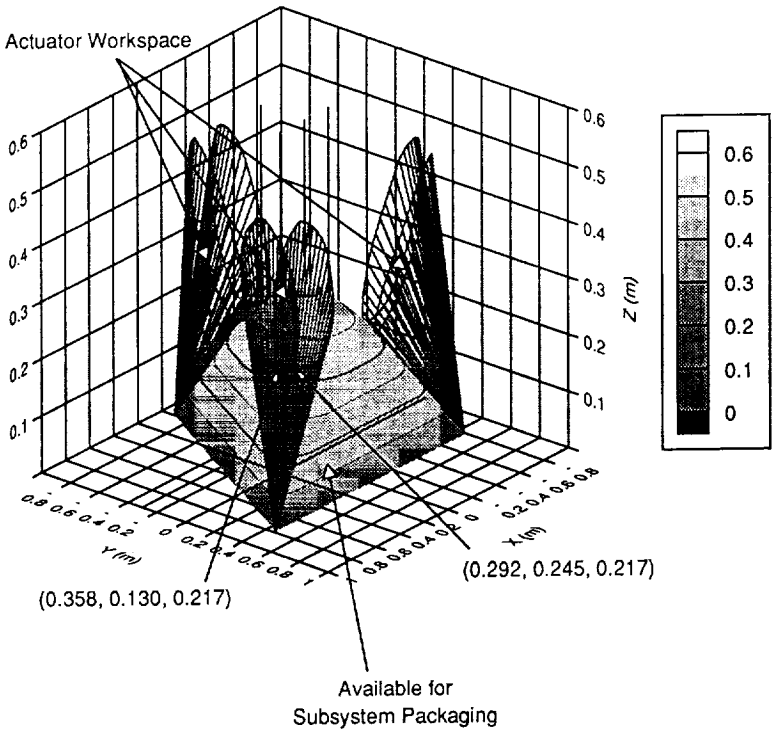

Figure 145. Option 3—actuator workspace and region available for subsystem packaging.

Option 4 utilized the lander inner hardpoints, at a radius of 0.381 m. For a rollring radius of 0.56 m, the maximum tilt angle as function of actuator length is plotted in figure 146. This option requires a 1.118 m actuator to meet the 15° tilt requirement, so it will not be pursued.

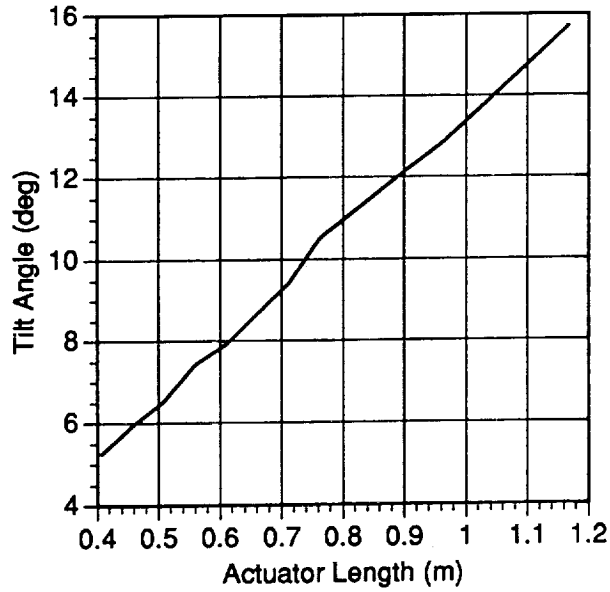

Figure 146. Option 4—maximum tilt angle for various actuator lengths.

In summary, four hexapod configurations shown in figure 136 were analyzed. The first option provides no choice for upper and lower hardpoint locations, and required a 0.813 m actuator to meet the 15° tilt requirement needed during the first half of the study. The maximum actuator force was 120 N for this configuration. Option 2 required a 0.559 m actuator for the 15° tilt capability, but the best configuration was statically indeterminate. Option 3 was found to provide 15° tilt with a 0.508 m actuator, required 460 N maximum actuator force, and the triangular region on the lander interface surface below the actuator workspace had a height of 0.22 m. Option 4 provided no choice for upper or lower hardpoints, and required a 1.118 m actuator to meet the tilt requirement. Hence, option 3 with a 20° angular separation between actuator pairs is the preferred configuration for hexapod mounts.

During the second half of the study, the site selection and pointing declination were changed to improve the thermal environment for the optics. The tilt range requirement changed from 15° to 42°, and hexapod mounts were no longer a suitable candidate. Hence, tilt-plate mounts and azimuth-elevation mounts were reconsidered.

5.7.6 Tilt-Plate and Azimuth-Elevation-Roll Mount Trades

The tilt requirements applicable during the second half of the study required a revisit to the mount trades. Figure 147 shows some of the mount options considered. The actuator lengths in hexapod configurations tend to grow as the tilt requirement is increased, increasing the telescope/lander stack size. The overall height could be decreased by attaching the lower actuator hardpoints on the lower struts of the lander, which would require some redesign of the lander to ensure room for actuator motion, or attaching the upper actuator hardpoints above the telescope base. Both of these options violate guidelines, and so the mount is constrained to lie between the lander upper surface and the telescope base. Figure 148(a) shows a parametric study of tilt capability as a function of actuator length for the hexapod configuration selected earlier. The tilt space for a 3.048 m actuator meets the 42° tilt requirement, as shown in figure 148(b), but this length is unsuitable for this application. Hence, hexapod mounts were eliminated from consideration. Lander accommodation of large tilt errors, either by adjusting the legs or the lander structure, was also eliminated, since those options would produce large shifts in the composite telescope/lander center of mass that could affect stability and would require modifications to the lander.

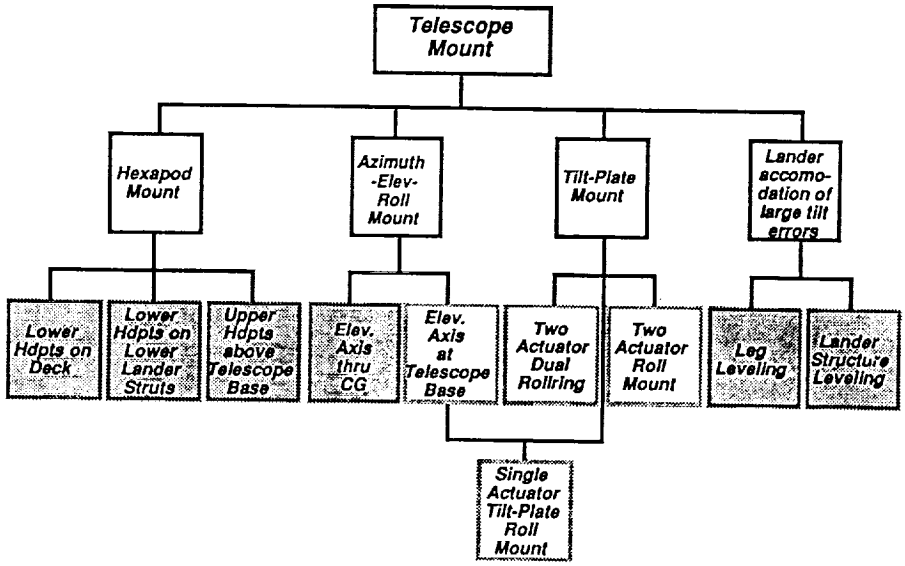

Figure 147. Mount options for 42° tilt requirement.

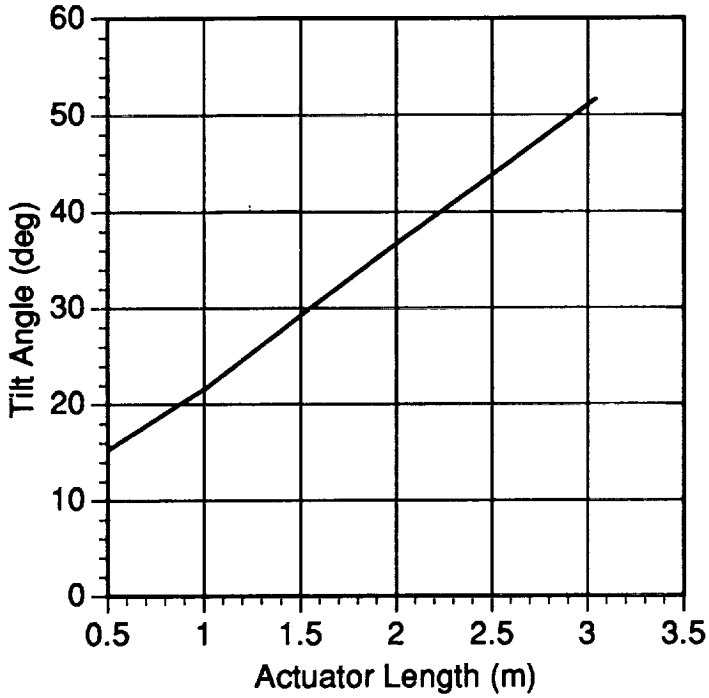

(a) Tilt capability versus actuator length.

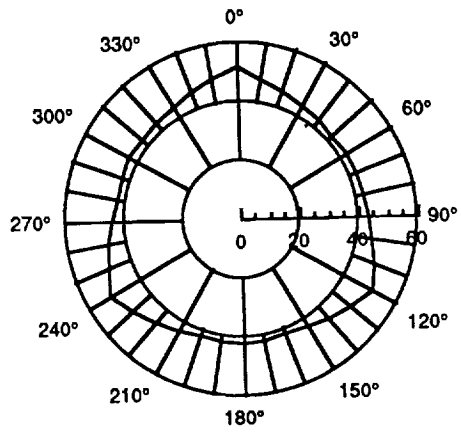

(b) Tilt space for 3.048 m actuator.

Figure 148. Hexapod mount tilt capability.

Viable options included azimuth-elevation-roll mounts and variations on the tilt-plate mount considered earlier. Aligning the elevation axis through the telescope center of mass reduces loads on the bearings, but would require that the mount extend up past the telescope base and violate the mount guidelines. Hence, the elevation axis of the azimuth-elevation-roll mount will be located at the telescope base. Tilt-plate mounts include two-actuator dual-rollrings and single-actuator dual-rollrings. The single-actuator tilt-plate rollring mount is a blend of tilt-plate and azimuth-elevation-rollring mounts. These four concepts are shown in figure 149.

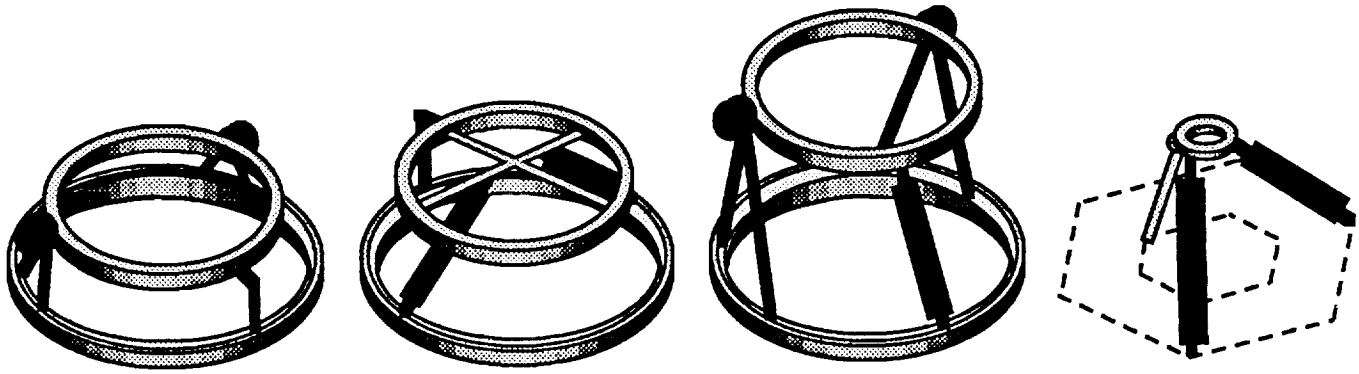

Azimuth-Elevation-Roll Mount

Two-Actuator Tilt-Plate Dual-Rollring

Single-Actuator Tilt-Plate Roll Mount

Two-Actuator Tilt-Plate Roll Mount

Figure 149. Azimuth-elevation-roll and tilt-plate concepts.

The azimuth-elevation-roll mount is composed of upper and lower rollrings and elevation actuators mounted on a support structure, as shown in figure 150. The lower rollring rotates until the elevation axis is aligned perpendicular to the deck tilt vector, in the plane of the lander deck. The elevation axis is offset from the telescope centerline by 0.199 m, which aligns the telescope center of mass vertically over the elevation axis when the telescope is tilted 26.5°. This minimizes the moment about the elevation axis. Compensation for lander tilt error will shift the telescope center of mass within a 15° cone around this position, producing a maximum static torque load of 53 Nm on the elevation axes (based on a 305 kg moving mass estimate). A 100 Nm torque is required to initially tilt the telescope by 26.5° from its launch-lock position to align the center of mass over the elevation axis, and will be used to size the elevation motors. The upper rollring rotates the telescope and detector to its proper east-west orientation, which puts the high side of the light shade and the antenna on the southern side of the telescope. The 0.4 m vertical clearance between the two rollrings provides a 90° tilt capability.

The two-actuator tilt-plate dual-rollring concept shown in figure 151 utilizes the same two rollrings considered in the previous concept. The elevation axis has been replaced by two linear actuators and a ball-joint attached to the upper rollring. The location of the upper and lower hardpoints for the actuators and ball-joint were varied to maximize tilt capability and minimize mount height. Both radial and azimuthal variations of the upper and lower hardpoints were analyzed for various actuator lengths. The optimum location for the actuator hardpoints is diametrically opposite each other, with the upper hardpoints located 0.24 m apart. A 0.82 m actuator length provides a 42° tilt capability on the ball-joint side, as shown in figure 152, but only a 24° capability on the "free" side. Hence, the lower rollring is necessary to align the maximum tilt capability with the required azimuth. The vertical separation between the two rollrings is 0.46 m when the actuators are backed down to their minimum lengths. The upper rollring still aligns the telescope assembly to its proper east-west orientation.

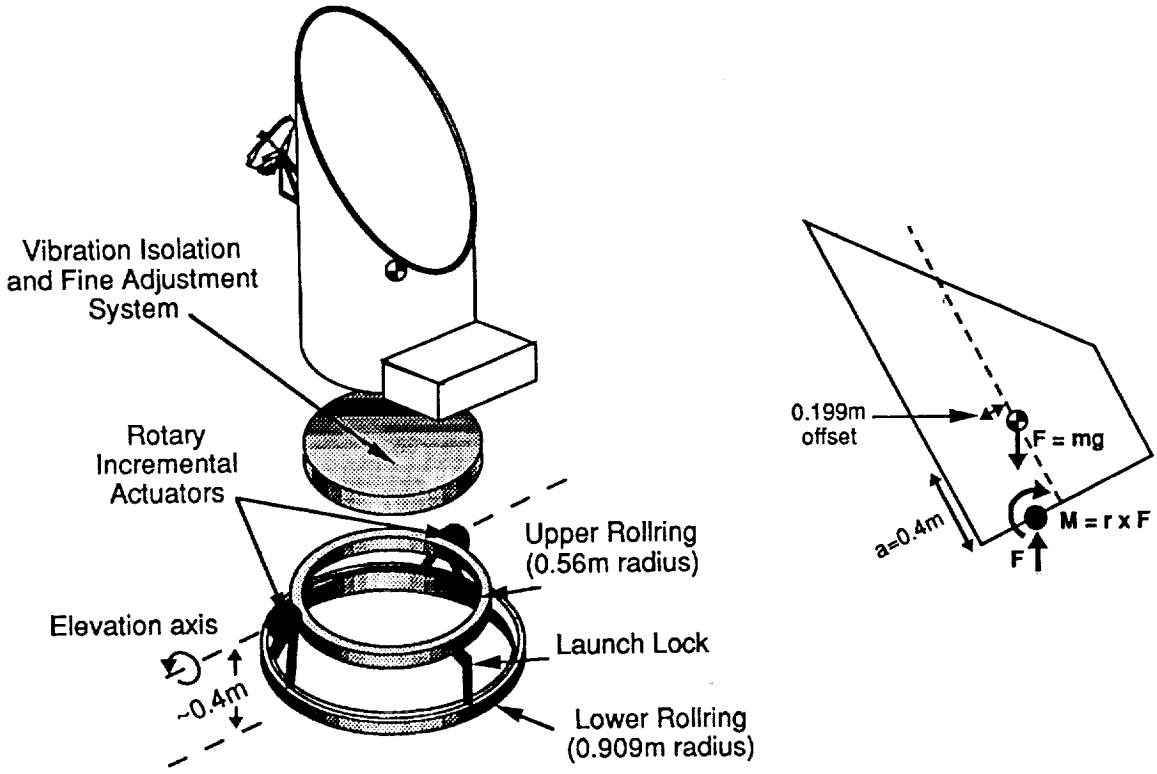

Figure 150. Azimuth-elevation-roll mount.

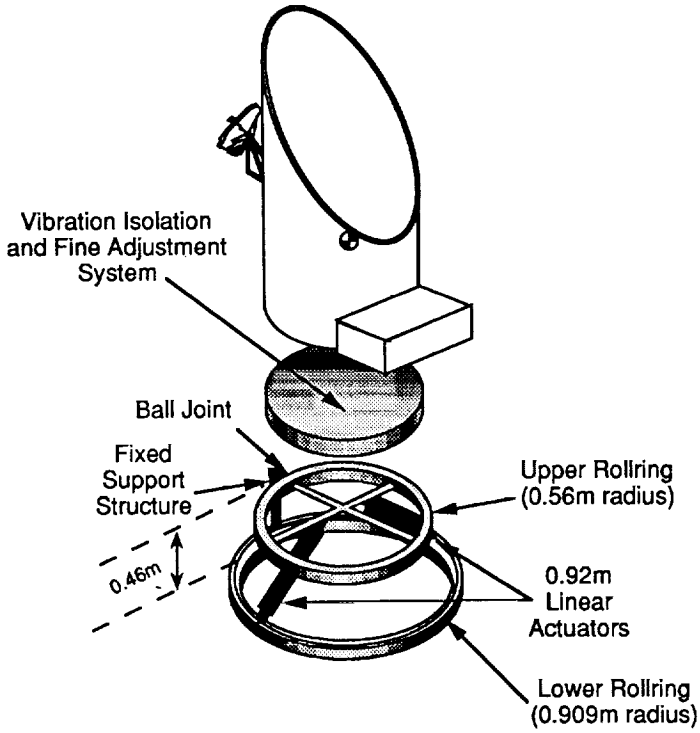

Figure 151. Two-actuator tilt-plate dual-rollring mount.

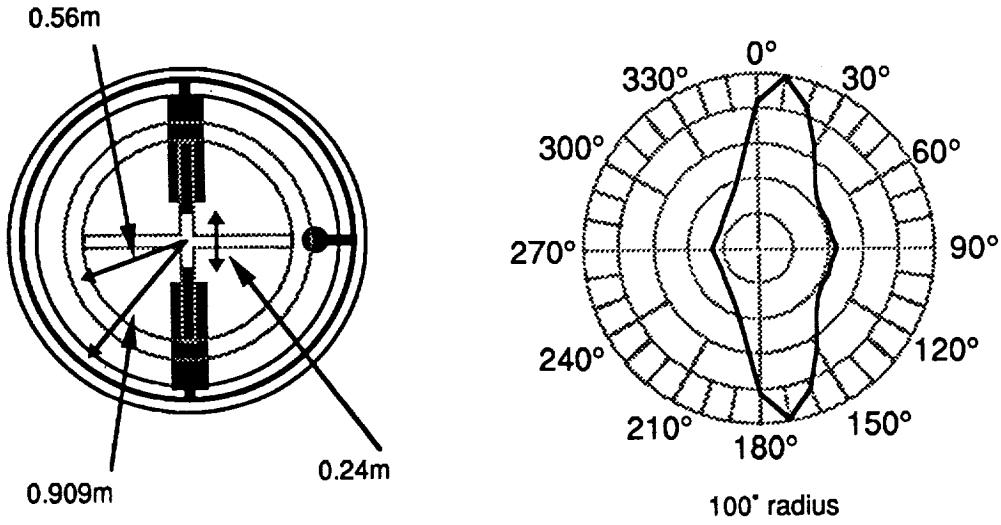

Figure 152. Top view and tilt region without lower rollring for two-actuator tilt-plate dual-rollring mount.

Since the previous configuration still requires two rollrings to provide ±180° tilt capability, a single-actuator tilt-plate roll concept will perform the same function with one less actuator. This mount concept is shown in figure 153. The lower rollring aligns the elevation axis for tilt by the single linear actuator. The elevation axis is a simple single DOF rotational joint, with no motors or sensors, and is offset from the telescope centerline by 0.199 m to minimize the bearing loads. A 1.63 m linear actuator with 0.54 m stroke provides a uniform 42° of tilt capability, but requires a 1.36 m vertical separation between the upper and lower rollrings. Telescope east-west alignment is still provided by the upper roll-ring, which can be designed to an appropriate diameter.

C-3.

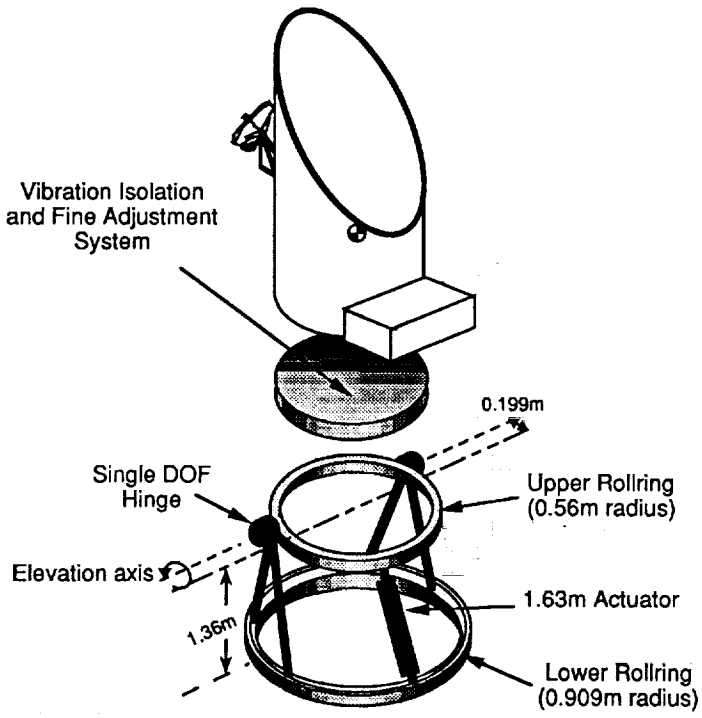

Figure 153. Single-actuator tilt-plate roll mount.

In an attempt to eliminate the lower rollring, the two-actuator dual-rollring mount was revisited. A parametric study was made of actuator lengths, upper hardpoint locations, and ball-joint location, with goals of minimizing mount height and maximizing tilt capability. As shown in figure 154, the optimum mount configuration requires 1.0 m actuators, with lower hardpoints located at the outer lander interface points and upper hardpoints located at a 0.187 m distance apart, diametrically opposite each other on the upper rollring. The ball-joint location was varied in the study, but the most even tilt coverage was found for the ball-joint at the same radius as the actuator upper hardpoints. The tilt region for this configuration is shown in figure 155; a 90° tilt capability is provided on the ball-joint side, and a minimum of 42° in tilt is provided on the actuator side. The minimum actuator length, with the ball screws backed into the actuators, is the limiting factor for this tilt capability. As in the previous mount concept, the upper rollring has not been sized. The figure shows a small rollring directly over the upper hardpoints of the actuators and the ball joint, but a larger rollring such as that shown in the previous mount concept is also possible with additional support structure.

A top-level assessment was made of the four mount concepts shown in figure 149. The two-actuator tilt-plate dual-rollring concept, although short at 0.46 m, utilizes two actuators as well as the lower rollring to meet the 42° tilt requirement, and needs a two DOF elevation point. Its DOF's are also not independent of each other, so that tilt commands must coordinate the motion of both actuators. The single-actuator tilt-plate roll concept does exhibit independent DOF, and a single DOF elevation axis, but is very tall, requires a long actuator, and still needs the lower rollring. The two-actuator tilt-plate roll mount concept does not require the lower rollring, but exhibits interdependent DOF and needs the two DOF elevation point. The azimuth-elevation-roll mount is the shortest concept considered, has independent DOF, and is amenable to drive-motor redundancy on the elevation axis. It requires the lower rollring. The azimuth-elevation-roll mount concept was chosen for the phase A reference design.

Since the LUTE holds the same fixed pointing attitude over its lifetime, the mount must provide enough range to initially acquire the proper right ascension and declination, and enough precision to

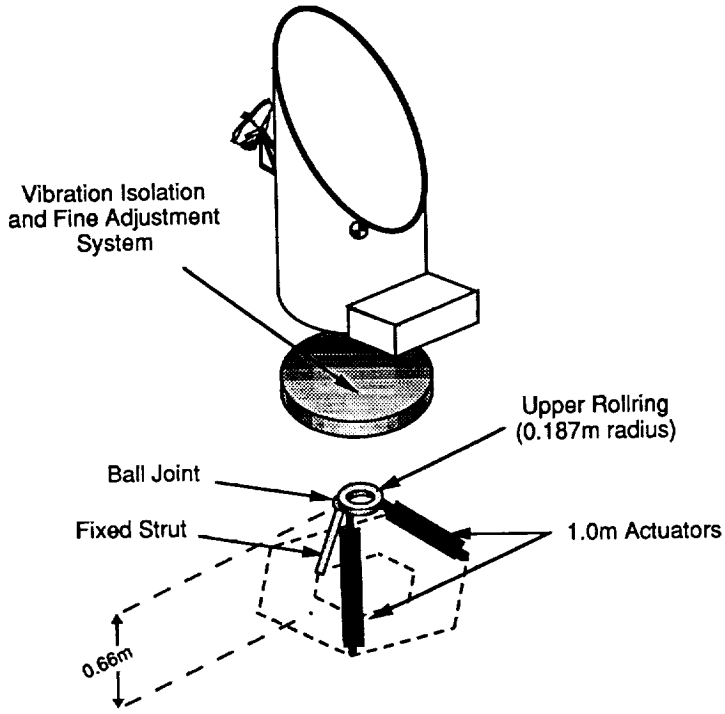

Figure 154. Two-actuator tilt-plate roll mount concept.

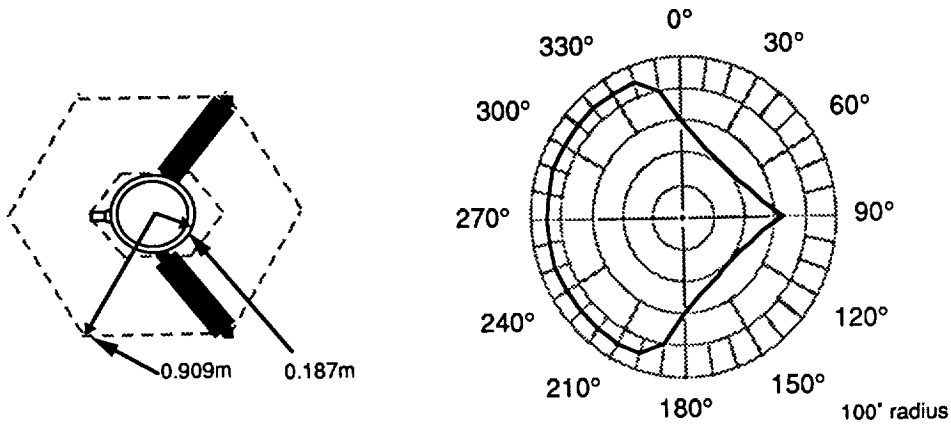

Figure 155. Top view and tilt region for two-actuator tilt-plate roll mount.

hold that attitude. The mount concepts considered here are two-tiered systems, in which the lower system provides the DOF for the proper orientation, and the upper system interfaces between the lower mount and the telescope baseplate. This upper system will provide vibration isolation and fine adjustment capability to accommodate any disturbances to the telescope attitude. A major source of disturbances will be the warping and structural distortions of the lander and lower mount due to lunar thermal cycling. These disturbances will occur at very low frequencies, and will most likely require an active isolation and adjustment system. Other sources of disturbances may be thermal expansion and contraction of tanks, joints, and structural components in the lander, which may occur at high frequencies and at unpredictable times during the telescope operation. Since a specific lander has not been chosen for this telescope, no assessment has been made of frequency and amplitude characteristics for the disturbances, which would be necessary to design the upper isolation system. A preliminary weight and power estimate for the isolation system has been provided, however, based on a recent study of passive and active damping using magnetostrictive actuators.[52]

Since the telescope power source is located on the lander, power may be transmitted across the mount by either sliprings or power rollrings, or by a cable bundle that rotates with the mount structure. The latter choice is baselined for the LUTE. Although the cable bundle will provide a nonuniform load on the mount during operation, this design simplifies the rollring components of the mount bearings and actuators, allowing selection of racerings supported by bearings. The racering and bearing system for the Space Station *Alpha* joints[53] has been used as a design template for the upper and lower rollrings in the mount.

5.7.7 Component Selection and Weight and Power Estimates

To provide weight and power estimates, a nominal set of hardware was selected for some components of the pointing system. The elevation axis motors are rotary incremental actuators, as shown in figure 156. The selected motor is a permanent magnet stepper with an output of 0.004° per step, and a harmonic drive ratio of 200:1. Optical disk and absolute encoders are located in a small chamber in the motor housing. The output torque capability for a typical load is 136 Nm, with a maximum torque of 272 Nm. Typical unpowered holding-torque capability is 90 Nm, and 200 Nm for powered capability. Total mass for each elevation actuator is 7.7 kg, with an average power estimate of 16 W each during usage.

The upper and lower rollring assemblies utilize pinion-gear-driven racerings supported by redundant tapered roller bearings, as shown in figures 157 and 158. These racering assemblies have been scaled from the 3.2 m diameter Space Station *Freedom* solar array rotary joint. Six sets of trundle bearings have nominally been allocated to each LUTE racering; a design analysis will be necessary to determine the minimum number of bearings and to optimize their location for our application. The upper and lower drive motors include resolvers and utilize 10 W apiece during operation. The upper racering assembly mass estimate is 7 kg, and the lower assembly is 15 kg. An additional 10 kg is allocated for the structure to support the elevation axis and upper rollring, and 2 kg for the launch lock and its support structure. Although the mount structure has not been designed in this preliminary assessment, it should exhibit dimensional stability over the range of lunar temperature variations.

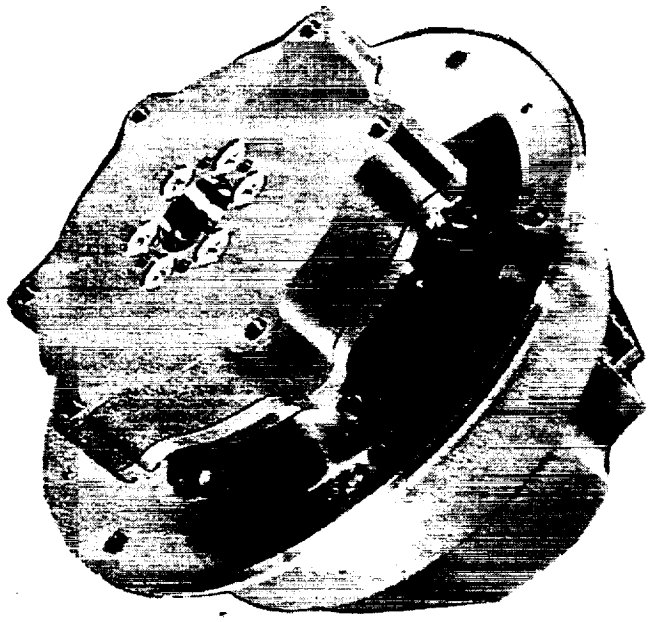

Figure 156. Elevation axis actuators.

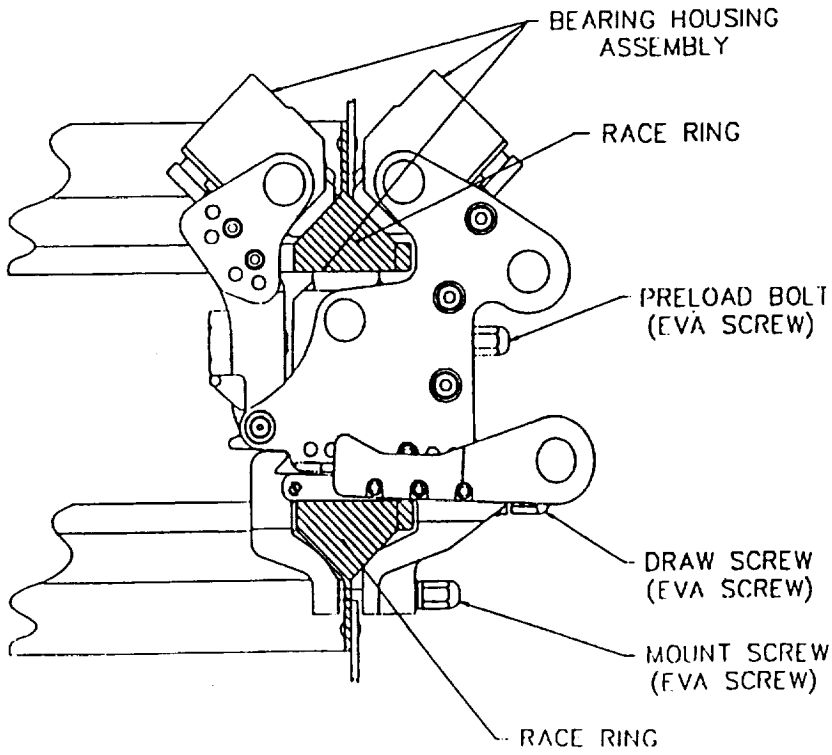

Figure 157. Upper and lower racering bearings.

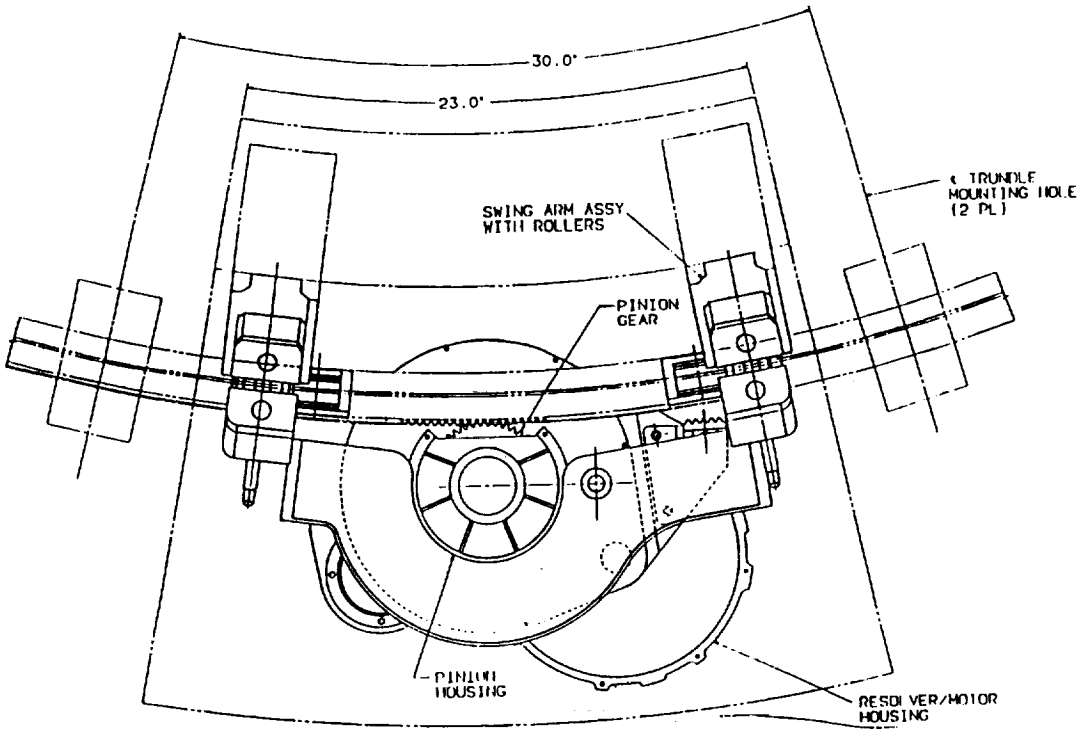

Figure 158. Motor-driven pinion gear drive assembly for upper and lower racerings.

The Sun sensor, which is used only during initial acquisition after landing, has a mass of 1.3 kg including its remotely-located electronics, and requires 2.8 W. The three-axis accelerometer that provides tilt-sensing after landing and possibly some vibrational disturbance sensing has a mass of 0.34 kg and requires 3 W.

The vibration isolation and fine adjustment system has a mass allocation of 10 kg. If six magnetostrictive actuators/transducers are utilized, a nominal power estimate of 60 W would be needed during their short periods of use.

The secondary mirror actuators tilt, focus, and despace the secondary mirror. An optical assessment of the necessary rigid body displacements of the secondary mirror has not been completed, but a nominal set of actuators was chosen for weight and power estimates. The secondary actuators have both coarse and fine strokes. Each coarse stroke stepper motor provides 750 μm stroke with 0.2 μm resolution, and requires 0.35 W continuously and 16 W peak power. Its remotely located drive electronics requires 2 W. The fine stroke phase-change actuator has a 2 μm stroke, with less than 0.006 μm resolution, and requires less than 0.05 W; its drive electronics at a remote location also requires 2 W of power. Linear Variable Differential Transducers (LVDT's) provide displacement sensing for feedback control of the coarse actuators, and require 2.4 W of continuous power. The total mass of each actuator is 0.23 kg, and includes the stepper motor, harmonic driver, LVDT, two circular flexure springs, a guide tube, mounting hardware, a mirror-mount button, and the fine stroke phase-change actuator. A breadboard actuator is shown in figure 159.

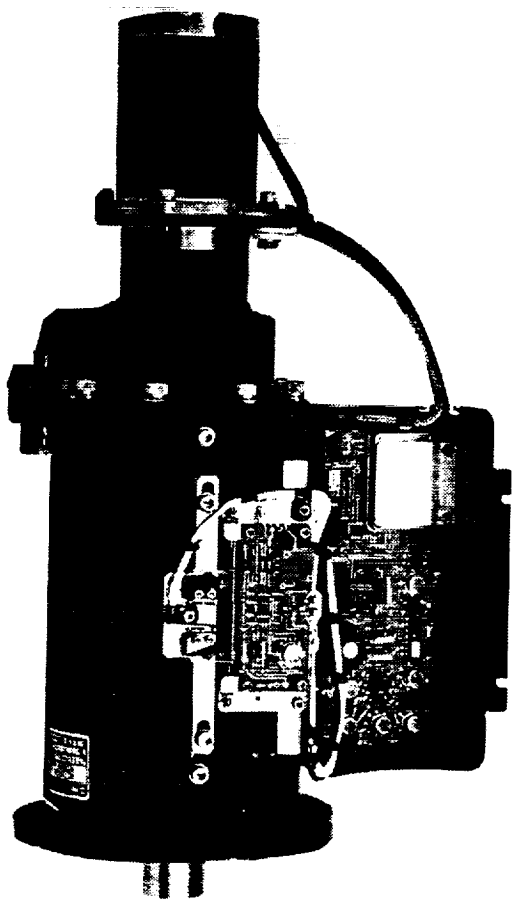

Figure 159. Secondary mirror actuator.

With a 3 kg nominal estimate for cables, the total mass estimate is 66 kg. Initial acquisition requires 6 W for sensors, and 42 W for the lower racering and elevation actuators. The upper racering assembly requires 10 W, and will probably be used after the lower actuators have been moved. The vibration isolation and fine adjustment system may require 60 W, but it will most likely be activated for very short periods of time during telescope operation. The secondary mirror actuators require 30 W during periods of their operation.

5.7.8 Conclusions, Issues, and Concerns

A telescope pointing system has been defined to meet telescope declination requirements and to accommodate attitude errors of the lander. Acquisition sensors and a telescope mount have been identified by design trades, and weight and power estimates have been completed for components.

There are, however, some remaining issues and concerns with the pointing and alignment system that have to be addressed in phase B. The Sun sensor head used for initial attitude acquisition will only be operational during the first 24 hours after landing on the lunar surface, due to the significant temperature increase and the absence of thermal protection. Hence, alignment must be completed during this first 24 hours, and operational timeline analysis has not indicated if this is adequate. The telescope mount actuators were selected for a 305 kg moving mass located 0.4 m above the telescope base, and may be inadequate for a heavier mass estimate. Racering and bearing size and location have not been determined for the loads encountered during telescope operation. Material selection for the mount structure and bearing surfaces should be made with consideration of the lunar thermal variations and 2 year lifetime. Requirements for both the vibration isolation and fine adjustment system and the secondary mirror actuator system have not been identified, so actuator selection may not be adequate, and the frequency of use with the corresponding power profile is unknown. The need for tertiary mirror tilt actuators has not been identified. Control algorithms necessary for operation were not developed during the phase A final study.

5.8 Landing Site Selection Analysis

5.8.1 Introduction

The selection of the landing site for LUTE is driven by scientific goals and design considerations that influence its performance. Of particular concern are the site influences on thermal performance communications and attitude and alignment requirements.

5.8.2 Requirements

A complete list of specific science requirements for lunar astronomy is currently in the formative stages in the astrophysics community. Until these detailed requirements are agreed upon and made available, the ground rules listed in table 50 are used to serve as a guide for selecting a lunar site for LUTE. Included in table 50 are the locations on the Moon where each ground rule can most easily be satisfied.

Table 50. Ground rules used for LUTE site selection.

Requirement	Favored Location
1. Maximize sky coverage	Equator
2. Avoid sunlight in telescope aperture	Mid and higher latitudes
3. Avoid earthshine in telescope aperture	Prime meridian, mid to high latitudes
4. Provide continuous communication with Earth	Near side
5. Provide galactic pole viewing	30° latitude
6. Minimize telescope alignment requirements	Smooth, flat mare regions
7. Minimize lunar surface thermal radiation	High latitudes, polar region
8. Avoid geocorona Lyman-α background	Eastern or western limb
9. Locate in area of lower micrometeoroid flux and velocities	Eastern limb

5.8.3 Sky Coverage

The LUTE is a "transit" telescope. After landing on the Moon, it will be aligned to view a selected lunar declination. Other than this initial alignment (and perhaps occasional alignment adjustments), no capability to point the optical axis to other areas of the sky is required. The rotation of the Moon on its axis causes the optical FOV to sweep a swath across the lunar sky. This is illustrated in figure 160. In 27 days, 7 hours, 43 minutes, 11.5 seconds, the Moon rotates 360° with respect to the stars (or about 13.18°/day). As indicated in figure 160, the sky coverage becomes less for higher viewing declinations. The maximum sky coverage is achieved for a pointing direction that is perpendicular to the Moon's spin axis: for example, a zenith-pointing telescope located at the Equator or a telescope at 45° latitude tilted 45° southward from zenith. Although a viewing declination of 0° maximizes sky coverage, later discussion will reveal the difficulty in adequately shielding the telescope from sunlight and earthshine while oriented in this direction.

In addition to the Moon's rotation about its polar axis, the polar axis itself has a motion which affects the amount of sky that can be observed. Figure 161 shows the geometry of the Earth-Moon system relative to the ecliptic plane.

As indicated in figure 161, the Moon's spin axis is tilted from the ecliptic pole by a constant angle of approximately 1.5°. Furthermore, the spin axis "cones" about the ecliptic pole making a complete circuit every 18.6 years. This motion occurs because of (1) the precession of the Moon's orbit plane about the ecliptic pole, and (2) the fact that the nodes of the lunar equator on the ecliptic remain aligned with the nodes of the lunar orbit plane on the ecliptic. This motion of the Moon's spin axis causes the monthly visibility swath (fig. 161) to shift slightly from month-to-month. Eventually, after the Moon's orbit plane (and its spin axis) has completed its 18.6 year precessional cycle, the telescope will have seen as much of the celestial sphere as is possible for the LUTE FOV. Figure 162 shows how sky coverage changes with viewing declination for various LUTE FOV's assuming continuous LUTE operation. The use of solar power as a sole power source would preclude LUTE operation when the Sun is below the horizon. LUTE operations would, therefore, be limited to approximately 2 weeks each month

(about 194° of Moon rotation with respect to the stars). Hence, slightly more than half of the visibility swath shown in figure 160 will be seen in a month. The following month, the observable swath strip will be shifted eastward by about 30°. This eastward shift, in the view swath, is caused by the motion of the Earth-Moon system in its orbit about the Sun. About 5 1/2 months after the initial 2 week operational period, a complete band around the celestial sphere will have been viewed by the LUTE. The use of an RTG as now baselined, however, would allow viewing operations to continue into the lunar night.

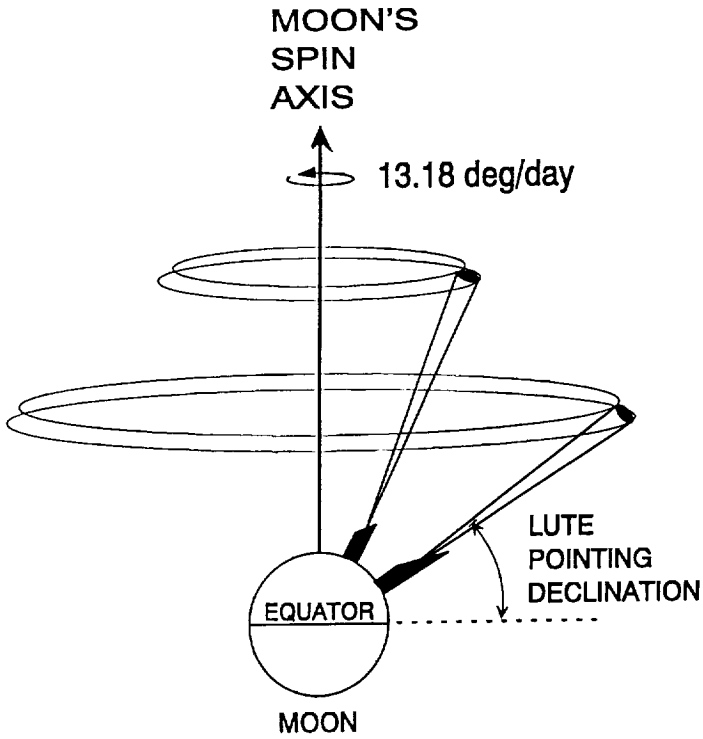

Figure 160. Sky area surveyed by LUTE depends on viewing declination and telescope FOV.

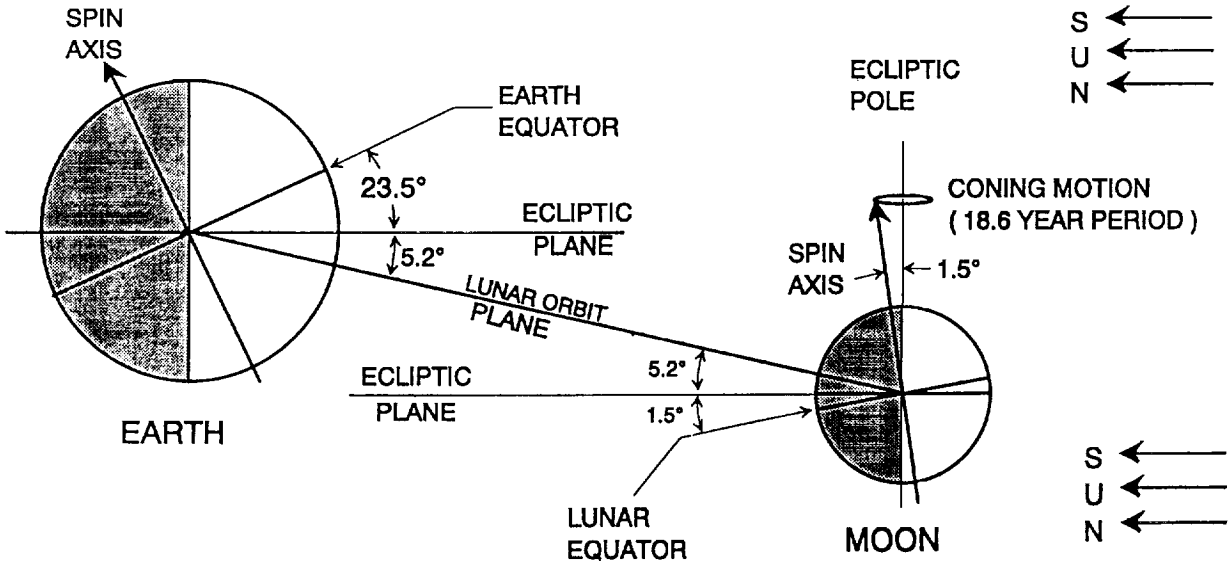

Figure 161. Geometry of the Earth/Moon system.

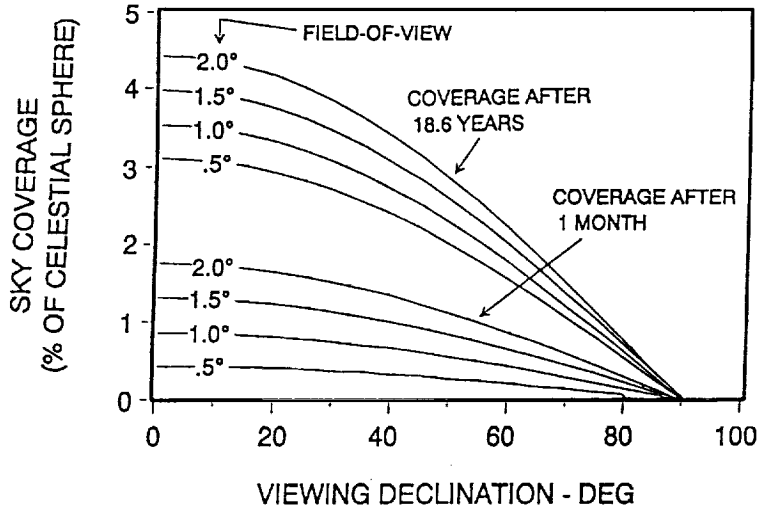

Figure 162. Sky coverage of a transit telescope for small FOV's.

5.8.4 Sunlight Avoidance

The focal plane sensor to be employed in the LUTE consists of an array of CCD's that must operate at temperatures less than about 210 K. To minimize sources of thermal energy that could damage the sensor and stray light that could mask the incoming UV data, it is necessary to provide an appropriate shade to prevent sunlight from entering the LUTE aperture.

5.8.4.1 Site Lighting Geometry

As illustrated in figure 161, the Moon's spin axis is tilted 1.5° from the pole of the ecliptic plane, causing the Moon to experience "seasons" as the Earth-Moon system orbits the Sun. For a LUTE site in the Northern Hemisphere, lunar summer solstice is the "worst-case" scenario for Sun-shading because light from the upper limb of the Sun reaches its highest lunar declination. As the Moon rotates the LUTE site into view of the Sun, the Sun will rise in the east, reach a maximum elevation angle at local noon with the Sun directly south of the telescope, and then set in the west.

5.8.4.2 Solar Light Shade

Based on the Moon's rotational motion and the geometrical constraints discussed previously, the solar light shade must be an enclosure around the telescope mirror structure with its upper portion cut at an angle. Such a shade is illustrated in figure 163 as a truncated cylinder. The tall side of this shade must be on the south side (for northern sites) of the telescope, and the angle between the plane of the shade opening, and the local horizontal plane must be large enough so that the solar vector spends most of its time on the south side of the plane. The required light shade angle is determined by the telescope's viewing declination (equal to site latitude for a zenith-pointing telescope) as illustrated in figure 164. Assuming lunar summer solstice as a worst case, the Sun will have a declination of about 1.5°. Adding 0.25° to account for the angle subtended by the Sun's radius yields the highest declination that the limb of the Sun will have—1.75°. For this case, a shade angle of $90°-\delta_{view}+\text{Max}\ \delta_{Sun}+\alpha_{Sun}$ would allow sunlight to enter the shade interior throughout the lunar day except at the instant of local noon; hence, additional shade angle is necessary to provide a longer period of sunlight protection. As will be discussed in a later section, the light shade angle must be approximately 10° larger than the above value in order to provide

complete Earth-shine protection. Satisfying the Earth-shine avoidance requirement will result in an adequate shade for sunlight protection since the Earth reaches higher lunar declinations than does the Sun.

5.8.4.3 Light Shade Size

As the lunar day progresses, the Sun will rise in the lunar sky (as seen from the LUTE site), reaching its highest elevation angle at local noon. At the Equator, this elevation angle is greater than 88.5°, or almost directly over the LUTE viewing axis (for a zenith-pointing LUTE). It would be impossible to keep sunlight out of the telescope aperture in this situation. Likewise, even at a latitude of 30°, the light shade angle required for effective shading would be about 70°. This would result in a light shade that is about 2¾ m taller than the telescope metering structure (from the bottom of the diagonal slice to the tip of the shade) assuming a 1 m telescope diameter. This shade, along with the LUTE lander, cannot be accommodated by the volume constraints of a Delta II launch vehicle. An Atlas IIAS launch vehicle, however, seems to have adequate space for such a configuration. Figure 165 shows the recommended light shade angles to be used at different pointing declinations. These light shade angles would ensure complete sunlight protection for most of the lunar daylight period.

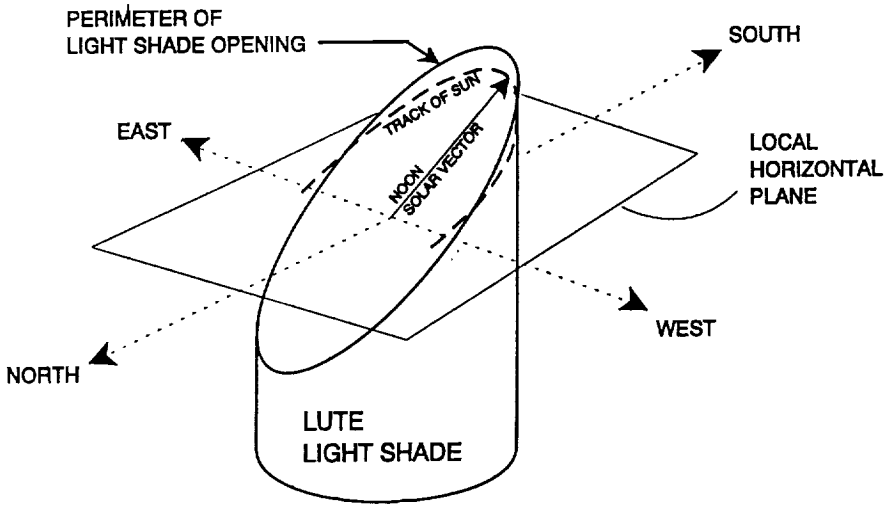

Figure 163. Path of the Sun relative to the LUTE light shade.

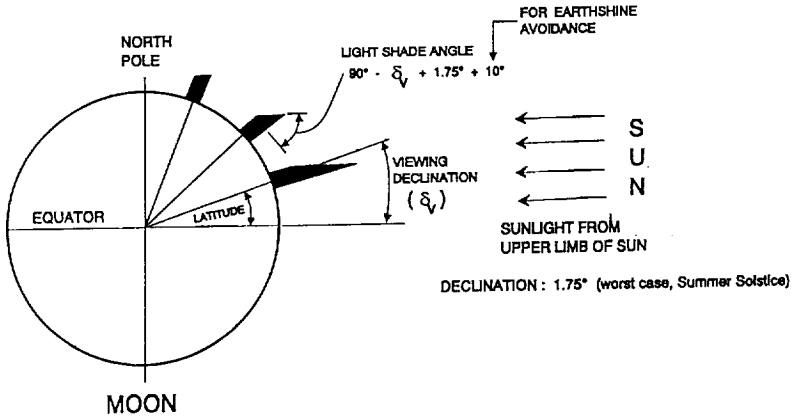

Figure 164. Light shade angle depends on viewing declination.

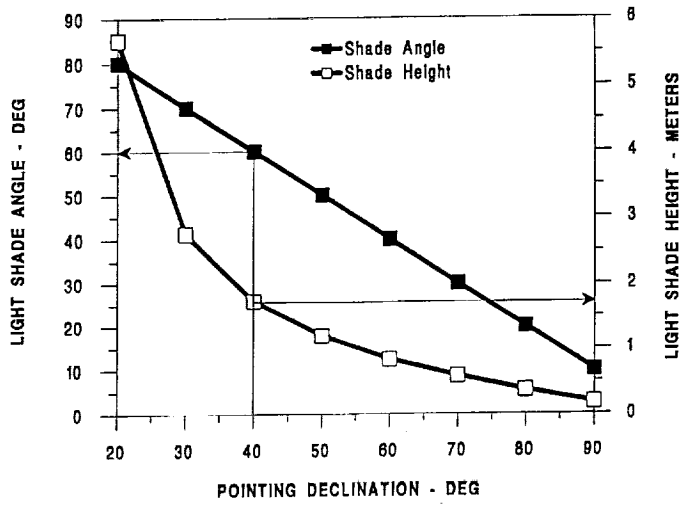

Figure 165. Recommended LUTE light shade angle.

5.8.4.4 Unavoidable Sunlight Intrusion Near Sunrise and Sunset

In lunar spring and summer, the Sun actually rises slightly north of due east and sets slightly north of due west. For some period to time after sunrise, sunlight will illuminate a portion of the light shade interior. The same will occur just before sunset. In figure 163, if a view is taken along the east-west axis in the plane of the shade opening, the view illustrated in figure 166 is seen. This figure shows that immediately after sunrise (and also before sunset), there is a period of time that sunlight will illuminate the shade interior until the solar disk is fully on the south side of the plane of the shade opening. This situation occurs only in lunar spring and summer when the selenocentric declination of the Sun is positive. This effect cannot be avoided for a passive and immovable light shade unless effective light baffling inside the shade can be provided. The duration of this Sun interference period (worst case) is about 26.8 hours for a viewing declination of 30° and a light shade angle of 70°. This Sun interference period can be significantly longer for lower shade angles. For example, a 60° shade angle would impose an operation wait time after sunrise of approximately 205 hours ($8\frac{1}{2}$ days). The time after sunrise that the LUTE must wait for complete sunshading is a function of shade angle, viewing declination, and site latitude. The path of the Sun in the lunar sky, relative to local horizontal, changes with site latitude. If the LUTE site were on the Equator, the path of the Sun in figure 166 would be nearly vertical with respect to the horizon.

5.8.5 Earthshine Avoidance

The Earth is another source of radiation that can interfere with LUTE observations. Fortunately, the shade designed for Sun-shading (as described previously) can also serve as a shade for reflected light from the Earth. Recall that for Sun-shading, the tall side of the truncated cylinder shade must be oriented toward the south so that shading is effective when the Sun is at its maximum elevation angle (which occurs at local noon when the Sun is due south of the LUTE). To assess the effectiveness of this shade for earthshine, it is necessary to determine the motion of the Earth in the lunar sky.

5.8.5.1 Earth Motion in the Lunar Sky

The same side of the Moon generally faces the Earth at all times because the Moon's rotation rate is precisely equal to its orbital period around the Earth. There is, however, an apparent "wobble" in the Moon's orientation as viewed from Earth. The effect of this apparent motion is to cause the Earth-Moon line to deviate from the mean center of the Moon's disk. This drift of the Earth-Moon line on the

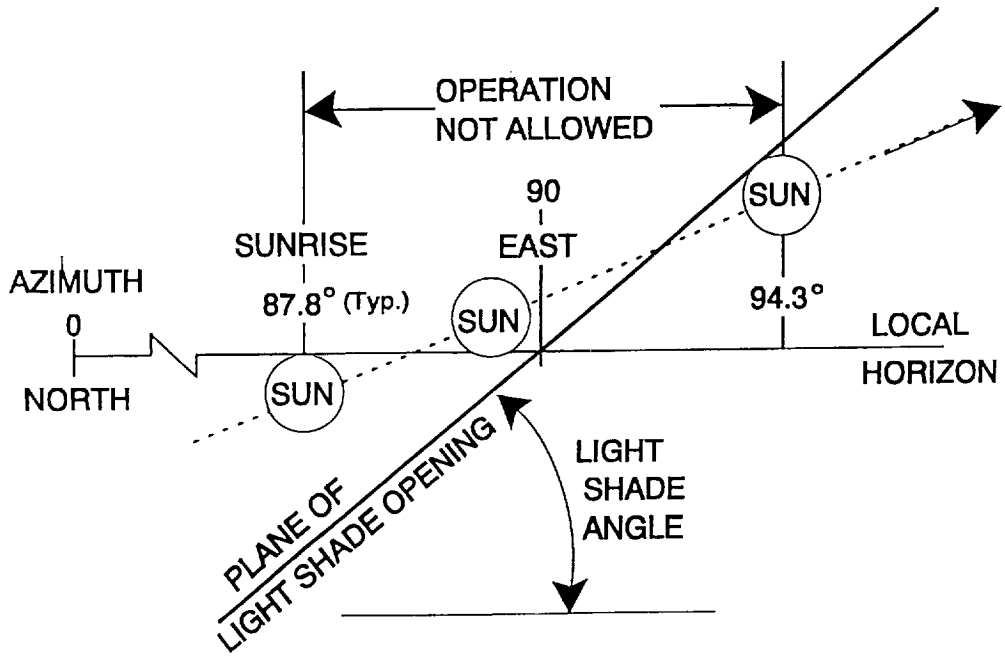

Figure 166. Lunar sunrise relative to the LUTE light shade.

lunar surface is never more than ±8° in longitude, nor ±7° in latitude (selenographic coordinates). This variable orientation of the Moon relative to the Earth is caused by the optical librations. From a position on the Moon looking at the Earth, these librations will cause the Earth to move in the lunar sky. The optical libration in latitude is described in figure 167. This phenomenon occurs because the Moon's spin axis is not perpendicular to its orbit plane. At one position in the Moon's orbit, the lunar north pole is tilted toward the Earth, placing the Earth over the +6.7° latitude line. Approximately 2 weeks later, the Moon has moved 180° in its orbit where the lunar north pole is tilted away from the Earth. At this position, the Earth is over the –6.7° latitude as shown in figure 167.

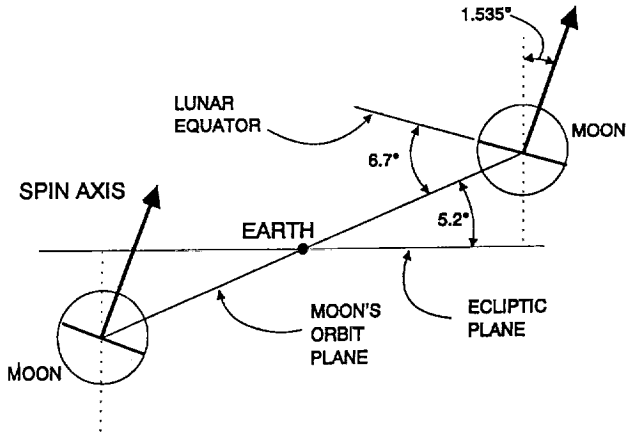

Figure 167. Optical libration in latitude.

The optical libration in longitude occurs because the Moon is moving around the Earth at a variable angular rate, but the Moon is spinning on its axis at a constant rate. This is illustrated in figure 168, which shows a view of the Earth-Moon system from above the ecliptic plane. In 1 month, the central meridian of the Moon moves west, then east of the Earth-Moon line due to the mismatch between the Moon's constant spin rate and its variable orbital rate.

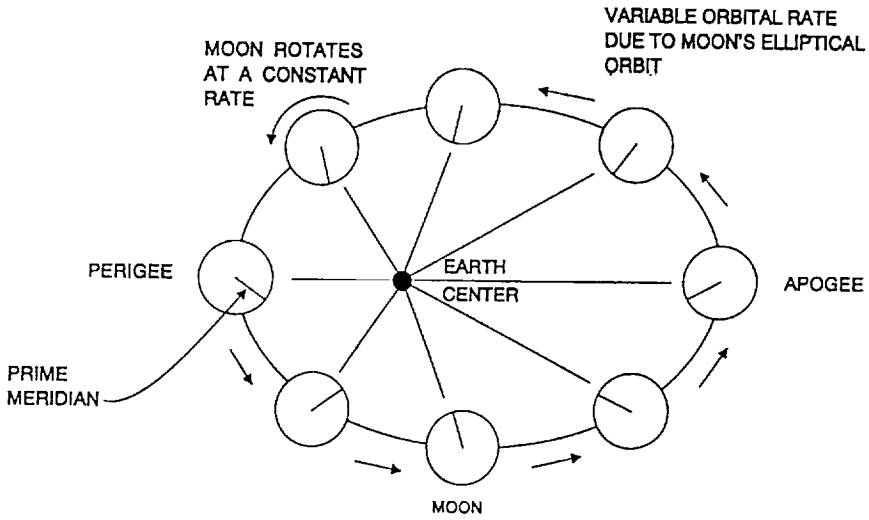

Figure 168. Optical libration in longitude.

Figure 169 shows an azimuth-elevation track of the path of the Earth as viewed from a lunar site at 40° north latitude and 4.4° west longitude. The circles represent the Earth at intervals of 1 day. Trajectories are shown for two sample months: January 1997 and January 2000.

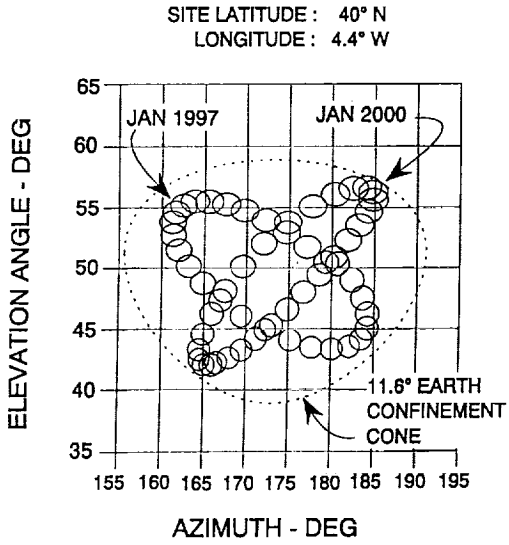

Figure 169. Earth motion as viewed from a lunar site.

The Earth's movement in the lunar sky, as observed from a lunar site, is always confined to a relatively small region. This region can be approximated by an 11.6° cone (half angle) emanating from the site. (The actual shape of the region in which the Earth can move is closer to a rectangle than a cone. The 11.6° cone approximation encompasses the corners of the actual rectangular region.) For any site on the Moon where the Earth is visible, this cone is fixed, and its pointing direction depends on the lunar site. For the sample site used in figure 169, the Earth confinement cone is centered at about a 174° bearing and a 50° elevation angle (slightly east of due south). For locations near the Moon's limb, the Earth will disappear beneath the horizon, causing interruptions in communications with Earth.

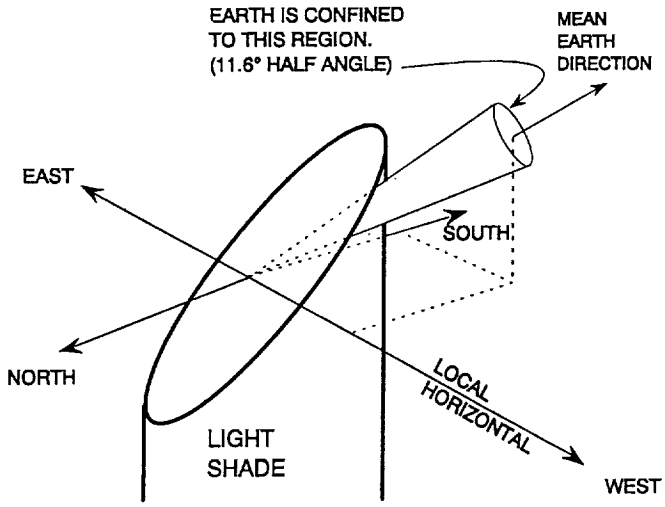

Figure 170. Earth confinement region relative to the LUTE light shade.

5.8.5.2 Light Shade Requirements for Earthshine Avoidance

Ensuring that reflected Earth light never enters the telescope aperture requires that the entire Earth confinement cone (referred to in the previous section) is on the south side of the plane of the LUTE light shade opening. Figure 170 illustrates this geometry. For a given LUTE location, the portion of the sky (the cone) that contains the Earth has a fixed direction from the site. Orienting the plane of the shade opening until it is just tangent to the cone will define the minimum shade angle that will ensure no Earth light intrusion into the telescope. This criterion was used to determine the light shade angles for any northern site on the Moon's near side. These data are shown in figure 171.

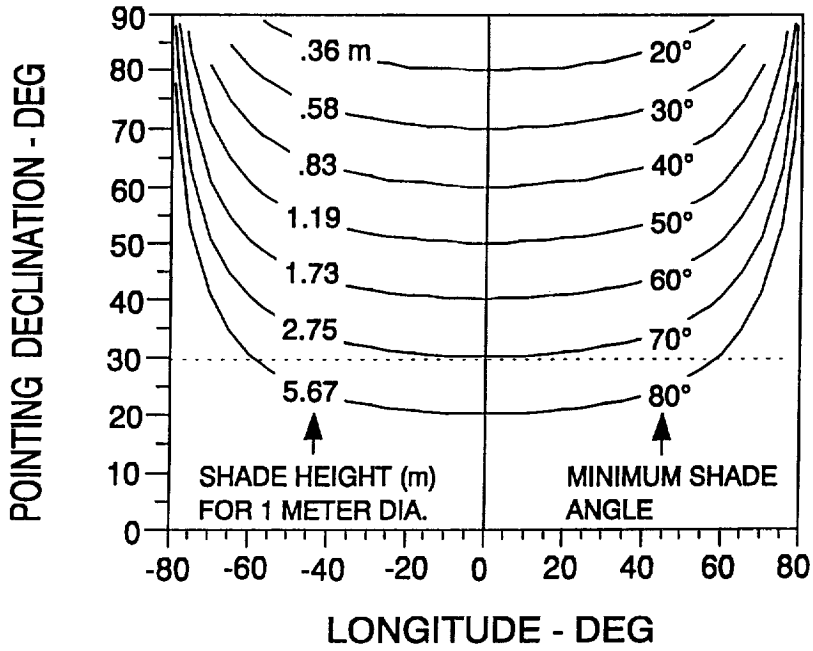

Figure 171. Light shade angles.

The illumination from the geocorona was not considered in computing these shade angles—only the reflected light from the physical disk of the Earth (full Earth assumed). In figure 171, the shade angle is the angle between the plane of the light shade opening and the plane perpendicular to the telescope's optical axis. The shade height is the distance from the tip of the light shade to the bottom of the "slice" (measured along the optical axis). The data show that for a given viewing declination site longitudes approaching the eastern or western limb of the Moon require taller light shades. The reason for this is that the shade must have its tallest side oriented toward the south for optimum Sun-shading. (It is assumed that the LUTE has no out-of-plane misalignment with the local meridian plane). With this orientation and the LUTE near the eastern or western limb, the Earth (i.e., the Earth confinement region) is no longer directly south of the light shade, but rather southeast (or southwest). The Earth can rise above the plane of the light shade opening if the shade angle is not increased from its prime meridian value.

5.8.5.3 Sunlight and Earthshine Constraints on LUTE Operations

A computer simulation, which models the motion and orientation of the Moon with respect to the Sun and Earth, was used to compute the times that LUTE can operate. This simulation included the effects of optical librations in latitude and longitude and in lunar orbit plane precession. The criteria for LUTE operation from a light avoidance point of view are: (1) light rays from the Sun or Earth must not enter the light shade opening, and (2) the Sun must be above the local horizon for a solar-powered LUTE. Figure 172 shows the total operation time achieved during a 2 year mission starting on January 1, 1998. Results are shown for a range of light shade angles for both a solar-powered LUTE and an RTG-powered LUTE located at 66.5° north latitude and 24.2° west longitude. The viewing declination is 30°. The LUTE, in this case, must be tilted from the zenith direction toward the south by an angle equal to site latitude minus viewing declination to enable the telescope to point at 30° declination. The results shown in figure 166 indicate that, for this sample case, a light shade angle of 70° is needed to completely avoid all earthshine in the telescope aperture. A light shade angle less than about 53° provides no earthshine protection at all. Since the RTG powered version can operate during lunar night, approximately twice as much "on" time is achieved compared to the solar powered version. For large shade angles (>70°), the RTG version is completely shaded against sunlight and earthshine intrusion at all times except for the period between sunrise and the instant the solar vector is on the south side of the shade opening plane. (Refer again to figure 166. This effect only occurs during lunar summer.)

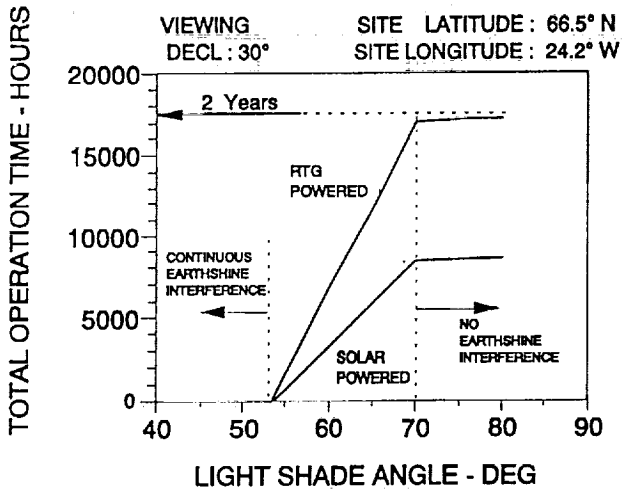

Figure 172. LUTE operation times during a 2 year mission with no sunlight or earthshine interference.

5.8.5.4 LUTE Operation Time Variation With Viewing Declination

Figure 173 shows the percent time in operation during a 2 year mission for viewing declinations of 30° and 40°. In both case, the LUTE site location is 66.5° north latitude and 24.2° west longitude. This figure shows that about 10° more light shade angle is necessary to achieve the same operation time at 30° as was available at 40° viewing declination. Using a 60° light shade angle and viewing at 40° declination allows a solar-powered LUTE to accumulate nearly three times more operation time than viewing at 30° declination with the same light shade. A 70° shade would be more appropriate for the 30° viewing declination. In general, the best light shade angle is approximately 100° minus the viewing declination. This will ensure sunlight protection during most of the lunar day while also ensuring no intrusion of reflected earthlight.

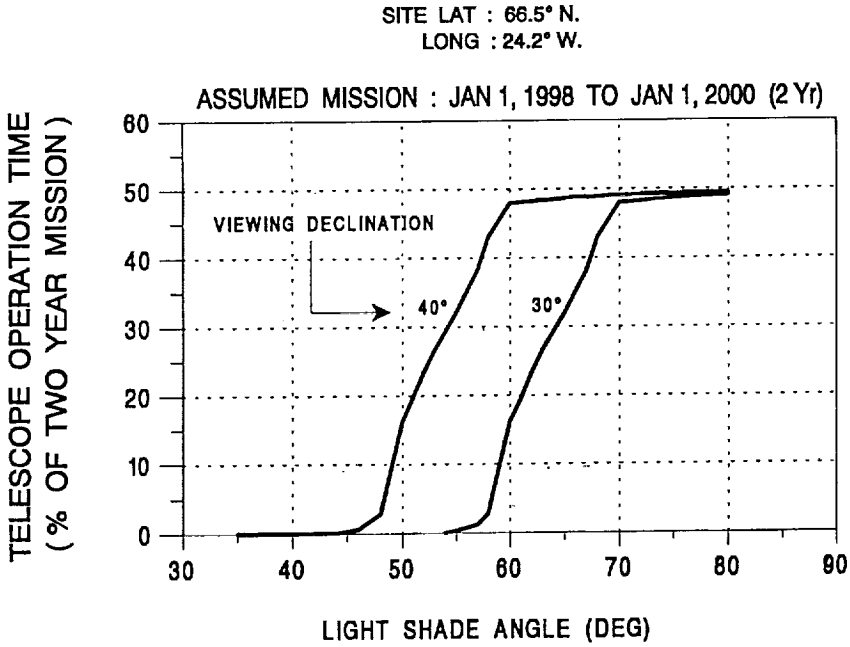

Figure 173. Solar-powered LUTE operation time for two different viewing declinations.

5.8.6 Continuous Opportunity for Earth Communications

In section 5.8.5.1, "Earth Motion in the Lunar Sky," a description is given of the optical librations in latitude and longitude. These phenomena explain why the Earth-Moon line drifts across the surface of the Moon with excursions in latitude of almost ±7° and excursions in longitude of almost ±8°. A consequence of these effects is that the Earth's elevation angle, as viewed from a lunar site, varies between a minimum value and a maximum value over the course of a month; that is, the Earth rises and sets. For a continuous opportunity of line-of-site communications between the LUTE and Earth, it is necessary that the Earth never set below the lunar horizon. This condition is satisfied if the LUTE is within about 80° (measured along a great circle) of the mean central point of the Moon (0° latitude, 0° longitude). Figure 174 shows the limits placed on site selection for line-of-site Earth visibility.

Placing LUTE at any site within the closed contour ensures that the entire Moon-side hemisphere of the Earth is always visible. If the telescope is placed at a high latitude, the available longitudes are limited. For example, at 70° latitude, LUTE must be within ±60° longitude to achieve full-time Earth line-of-site. The LUTE site indicated in figure 174 is a potential site which is in a relatively smooth area in a generally mountainous part of the Moon. (A later section will explain the desirability of a high

latitude.) Placing the telescope on the far side of the Moon would certainly have its benefits, such as the elimination of the earthshine shading problem. A far-side site, however, would necessitate either relay satellites in lunar orbit (a "halo" orbit about a stable Earth-Moon libration point may be one possibility) or lunar surface relay antennas remote from the LUTE site. A site selected on the near side of the Moon represents the most cost-effective solution for continuous Earth communications.

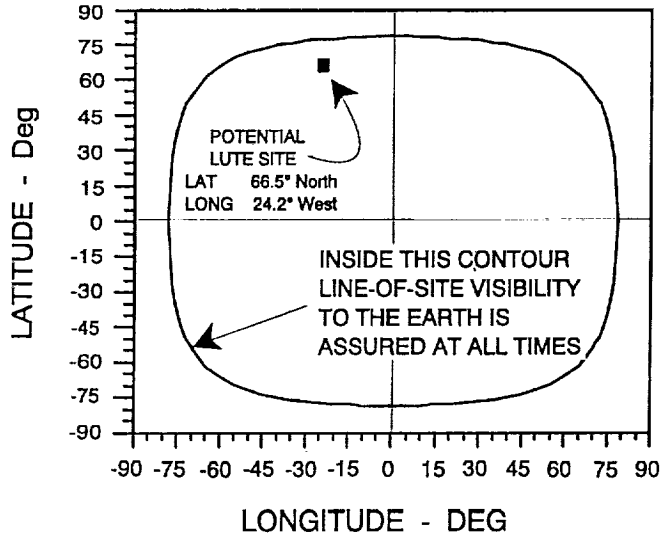

Figure 174. Earth visibility from the Moon.

5.8.7 Communications Antenna Pointing

Figure 175 describes how the high-gain communications antenna must be oriented to point toward the Earth. The mean direction of the Earth from any LUTE site is parallel to the lunar equatorial plane, as indicated in the figure. The elevation angle and azimuth direction are easily computed by transforming a 0° latitude/0° longitude vector (in the selenographic coordinate system) to the LUTE site reference frame. The dot product between this vector and the local zenith will yield the elevation angle. The dot product between the horizontal projection of this vector and the north horizontal vector yields the mean antenna pointing azimuth. The Earth's position deviates from this azimuth/elevation point by no more than approximately 10.6° in any direction. The antenna system must have sufficient pointing capability to follow the Earth as it moves through this region if the beam width of the transmitted signal is not sufficient to cover the entire 11.6° region (10.6° plus 1° Earth radius).

5.8.8 Galactic Pole Viewing

The LUTE is designed to view and record very faint UV emissions from very distant objects. Viewing in the galactic plane will provide some valid science data, but attempting to view distant objects through the bright UV background of our own galaxy, could completely mask the desired UV detections. Therefore, it is desirable to provide viewing opportunities as close as possible to the galactic north pole. Some galactic plane viewing is unavoidable, however, because the rotation of the Moon will swing the LUTE optical axis through the plane two times each month. For LUTE viewing declinations greater than 60°, the Moon's rotation will cause the optical axis to approach the galactic plane to within approximately 60° minus the declination, but the viewing axis will remain on the north side of the galactic plane. The galactic pole is located at a celestial latitude of about 29.8°. This is illustrated in

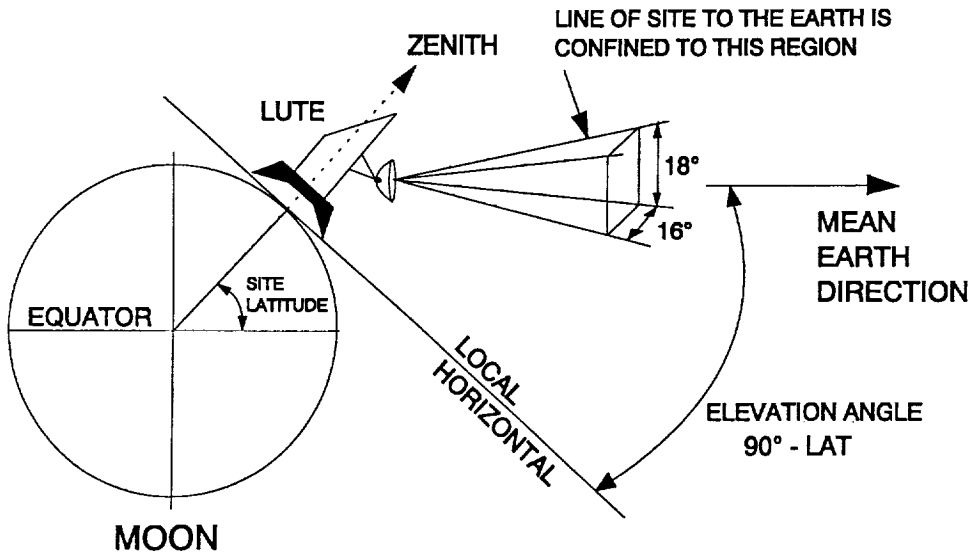

Figure 175. Antenna pointing direction for Earth communications.

figure 176. Also shown in this figure is the Moon with its full range of orientations with respect to the ecliptic plane. The Moon's equatorial plane is tilted at a constant angle from the ecliptic plane of approximately 1.5°. Furthermore, the Moon's spin axis cones about the ecliptic pole making a complete circuit in 18.6 years. If the LUTE is oriented to point at a lunar declination of 29.8°, it will point within 1.5° (the exact value depends on the lunar season) of the galactic pole once each month. This will remain true regardless of the position of the lunar pole in its coning cycle. Figure 176 depicts a zenith-pointing LUTE located at the optimum latitude for galactic pole viewing (29.8°). For a solar-powered LUTE, which can operate only during the lunar day, the galactic pole will be on the sunlit side of the Moon only during about half of the year. This is due to the orbital motion of the Earth-Moon system around the Sun. When the galactic pole is viewable during lunar day and the LUTE is oriented to view the 29.8° declination, the LUTE viewing axis is within 10° of the galactic pole for only a 42 hour period every lunar month. Therefore, the total yearly viewing time within 10° of the galactic pole is only about 105 days.

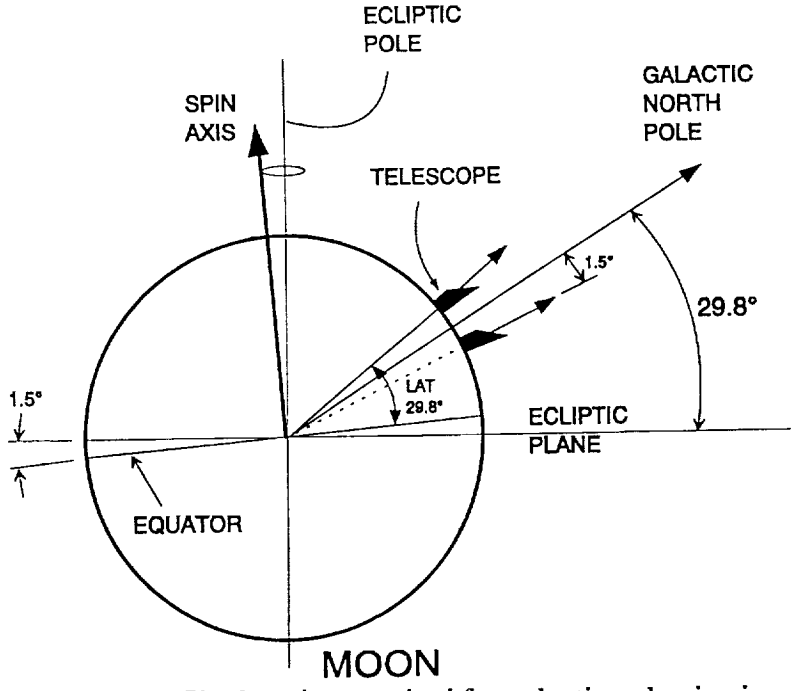

Figure 176. Site location required for galactic pole viewing.

5.8.9 Avoiding Lyman-α Emissions in the Geocorona

Detection and measurement of the hydrogen Lyman-α emissions from the stellar targets is one of the objectives of the LUTE telescope. These emissions can be masked by the Lyman-α emissions that are present in the Earth's geocorona. It would be desirable to avoid this interference as much as possible by viewing in a direction that would minimize the Lyman-α illumination seen by the LUTE. Figure 177 depicts a view of the Earth-Moon system with the geocorona from above the ecliptic plane. Data from the NRL's far-UV camera/spectrograph, which was operated on the lunar surface during the Apollo 16 mission, showed that the hydrogen Lyman-α geocorona has a "tail" in the anti-Sun direction. The Moon will travel through this tail each month, and the LUTE will unavoidably encounter some increased Lyman-α background. However, the proper choice of site longitude and/or viewing declination would point the viewing axis perpendicular to the direction of the Earth. Referring to figure 174 again, a zenith-pointing LUTE could be located at any latitude and longitude along with closed contour and still satisfy the continuous communication requirement while achieving the best Lyman-α reduction geometry. Locating on the far side of the Moon could be a solution to this problem but, as previously discussed, this would complicate the continuous Earth communications requirement. Besides, it is not clear whether a far-side location with LUTE pointing antiearthward would encounter lower Lyman-α interference than viewing perpendicular to the Earth direction.

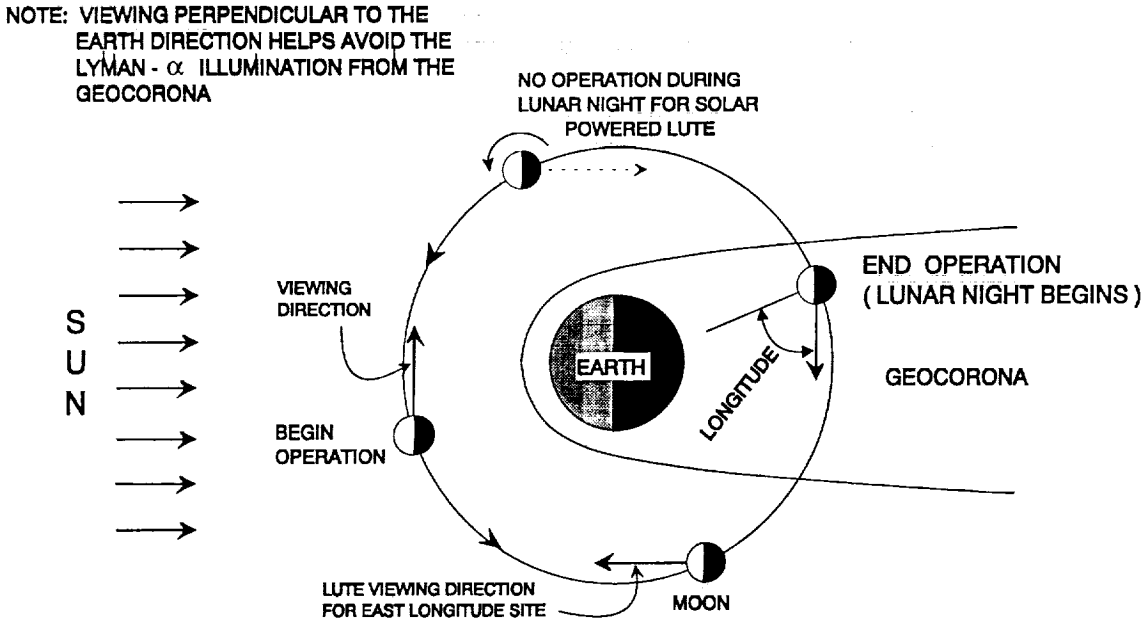

Figure 177. Avoidance of hydrogen Lyman-α in the geocorona.

5.8.10 Lunar Surface Thermal Radiation

The upper interior portion of the LUTE light shade receives thermal radiation emitted from the lunar surface on the north side of the telescope. Preliminary studies have shown that the resulting heat input to the mirror and detector is difficult to reject. At locations near the equatorial regions, the thermal load is especially high because of the high Sun-incidence angles encountered during the lunar day. One possible solution for reducing this thermal load on the light shade is to locate the telescope at a more northerly latitude and tilt the telescope southward to point at the desired lunar declination (e.g., 29.8° to provide galactic pole viewing). This geometry is illustrated in figure 178.

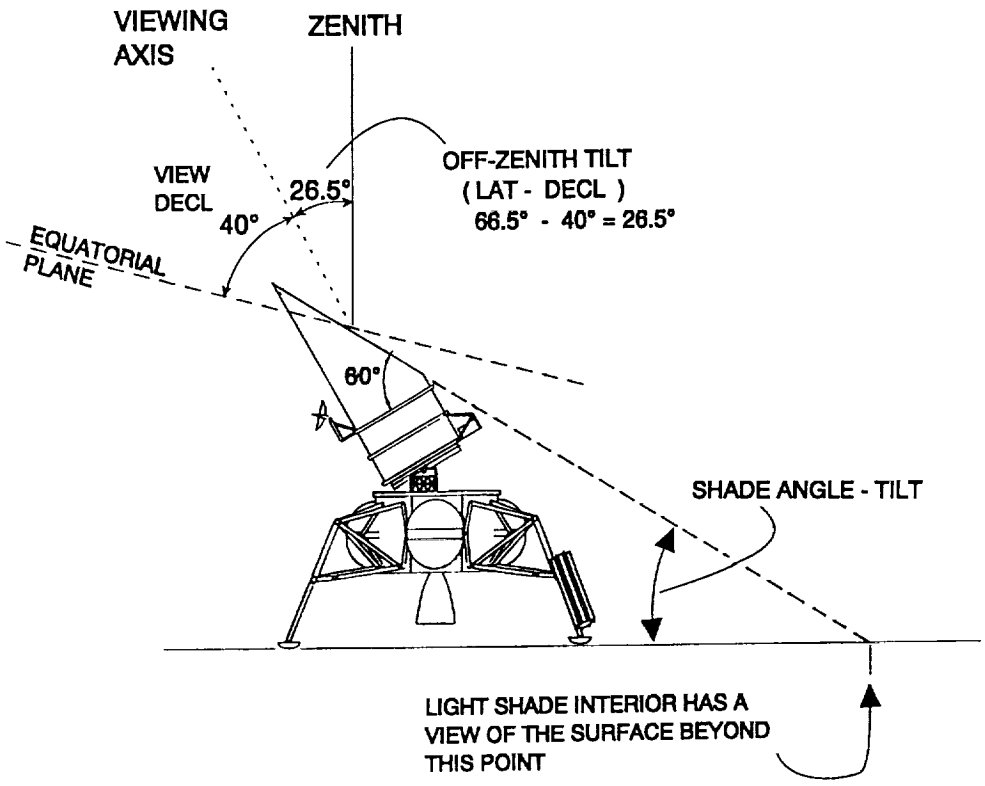

Figure 178. Avoidance of surface thermal radiation.

The example shown in this figure is for a LUTE site at 66.5° north latitude with the telescope tilted southward by 36.5°. This points the viewing axis at 30° declination. Tilting the telescope southward causes the view that the upper light shade interior has of the lunar surface to be at a greater horizontal distance from the telescope. This reduces the intensity of the radiation seen by the shade interior and thus the heat load. Thermal analyses have verified that for a viewing declination of 30°, a light shade angle of 70°, and the telescope site at 66.5° latitude, the resulting 36.5° southward tilt substantially reduces the thermal load on the primary mirror and telescope detector to acceptable limits. To implement this scenario, however, adds the complexities of a mechanism to perform the tilting operation after landing the telescope.

5.8.11 The Lunar Terrain

A tilting telescope can be used to reduce the lunar surface radiative thermal loads as described in the previous section. A dominant factor in determining the tilt requirements to be used in designing the tilt mechanism is the slope of the lunar surface at the landing site. To help ensure that steep terrain slopes are avoided, a landing site in one of the smooth maria is recommended. However, there are no maria at the high latitudes that are needed for a southward tilting LUTE. Lunar orbit photographs were examined in an attempt to locate areas that are relatively free of large craters or other prominences. A somewhat smooth area was found at 66.5° north latitude and 24.2° west longitude. From this site, the LUTE can be tilted 36.5° southward to view the 30° declination region. The resolution of the lunar orbiter photographs is not fine enough to ascertain the specific texture of the lunar surface. The highest resolution photographs that are available resolve objects (boulders and craters) only to about 2 m. These photographs reveal that essentially every square meter of the lunar surface is pock-marked with craters. It will be difficult to acquire knowledge of the terrain roughness at the LUTE touchdown point without higher resolution surveys of the proposed telescope site.

5.8.12 Micrometeroid Avoidance

Locating the LUTE near the eastern limb of the Moon may result in a lower flux of micrometeroid hits. This location is sometimes referred to as the "trailing" limb because it is on the side of the Moon opposite the Moon's Earth-orbital velocity vector. However, the Earth-Moon system is moving through interplanetary space at a velocity of about 30 km per second. This means that, with respect to a Sun-fixed frame of reference, the Moon's velocity varies from 29 km per second near the "new" Moon position to 31 km per second near the "full" Moon position. Relative to interplanetary space (a Sun-fixed frame), the eastern limb is "trailing" only in the "full" Moon position; it is "leading" in the "new" Moon position. There may be a slight benefit achieved by placing LUTE at an eastern longitude near the Moon's limb. This site is on the trailing side of the Moon when the Moon's velocity is greatest—31 km per second. Therefore, it will avoid collisions with micrometeroids whose velocities (component in the direction of the Moon's velocity) are less than 31 km per second. Compare this site to one on the western limb of the Moon where the site is on the trailing side of the Moon when the Moon's velocity is at a minimum (29 km per second). This situation provides protection against micrometerites whose velocities are less than 29 km second.

5.8.13 The Focal Plane Array

Based on current technology, the sensor at the telescope's focal plane will probably be a design that is currently in use in Earth-based telescopes. These devices consist of a plate covered by a mosaic of frame transfer CCD's. In the LUTE, the sensor will be aligned so that the columns of pixels in the CCD's are in an east-west direction. As the optical images of stars travel across the sensor, they traverse down the columns of pixels on the CCD's. The CCD detectors are clocked at the apparent sidereal rate of the Moon's rotation as the electrical images are integrated along each column of pixels, At the end of each column of pixels on a CCD, the integrated result is read out and recorded. As the Moon rotates on its axis, an image of a star will traverse across the focal plane sensor in a slightly curved path. The curvature of the path is a function of both the selenocentric declination of the star and the pointing declination of the telescope's optical axis. After establishing the desired pointing declination of the telescope, the focal plane array must be constructed such that the columns of pixels on each CCD are tangent to the curved star image tracks. If the LUTE is slightly misaligned, the image track curvature will be different from what the focal array was designed for, and the image will smear across the pixel columns at a small angle. Assuming a maximum allowed smear of 0.1 pixel-per-pixel column and a 3,000 pixel length for a CCD, it has been computed that the angle between the star image track and the pixel columns cannot exceed 6.87 arcseconds. This translates into about a 5 arcminutes declination pointing accuracy at 40° declination. Furthermore, the east-west alignment of the focal plane sensor must be within 6.87 arcsecond accuracy. These stringent alignment requirements would vanish by designing a sensor that does not depend on a custom fabrication to closely match an expected star track curvature.

5.8.14 Summary of LUTE Site Selection

The preceding analyses indicate that it is difficult to find a telescope site on the Moon which mutually satisfied all of the ground rules listed in table 50. For example, for a simple zenith-pointing LUTE:

(l) Maximizing sky coverage from an equatorial site encounters the highest lunar surface temperatures, misses galactic pole viewing by 29.8°, and is impossible to shade against sunlight or earthshine.

(2) Providing galactic pole viewing by locating at 29.8° latitude (on the central meridian) requires a tall light shade that may be difficult to accommodate within the weight and volume limits of the launch vehicle.

(3) Locating farther north than 29.8° to permit a practical light shade and a cooler lunar surface compromises galactic pole viewing and further reduces sky coverage.

(4) Total earthshine protection requires increased light shade height (angles) for sites east or west of the prime meridian.

(5) Locating on the limb of the Moon (or far side) to view 90° to the Earth's direction for Lyman-α interference reduction provides less than 100 percent Earth communication opportunity.

(6) Relaxing the light shade height requirements for full sunshine and earthshine shading will reduce the total telescope operation time.

For a zenith-pointing LUTE, it was finally decided to relax the galactic pole viewing ground rule and locate the LUTE at 40° north latitude. The light shade needed to provide sufficient light protection (neglecting possible baffling benefits) is about 60°. Since moving east or west of the prime meridian would require a taller light shade, and since the smooth Mare Imbrium is in this region, a longitude near the central meridian was selected. The exact placement in longitude was selected to be 4.4° west after inspection of lunar orbiter photographs revealed that this site fell between major local craters and mountains. For a LUTE designed to tilt southward to lessen the effects of lunar surface thermal radiation, a site at 66.5° north latitude and 24.2° west longitude was selected. The amount of tilt (from zenith) required to point the LUTE at 40° declination (assuming a horizontal landing site) is 26.5°. Viewing at 30° declination to achieve galactic pole viewing would require a tilt of 36.5°. As more specific science requirements become known, the site selection process will be revisited to determine if other locations on the Moon would better satisfy them.

5.8.15 Cosmic Rays

Lunar-based astronomical instruments will be exposed to a solar and galactic cosmic-ray environment, more severe than that present on the Earth or in LEO. The Moon is located outside the Earth's protective atmospheric envelope, which acts as a thick shield for highly-energetic cosmic-ray particles from space. The Moon lacks the benefit of the Earth's protective geomagnetic and atmospheric envelopes, which serve to deflect energetic cosmic rays. Cosmic rays can produce noise in the detector CCD's and could impact the lifetime of these CCD's.

5.8.16 Lunar Dust

Dust contamination on the telescope optics from any source is another concern in placing the LUTE on the lunar surface. The Apollo missions have shown that any activity can easily disturb lunar dust and launch even the smallest grains in ballistic paths that stretch far across the lunar surface. The lofted dust may be transferred onto the telescope, obscuring the sensitive optics, scattering light resulting in distorted observations, degrading the performance of thermal control coatings, and potentially interfering with mechanical devices forming a part of the telescope.

5.8.17 Lunar Thermal Environment

The lunar thermal environment is characterized by large temperature swings and long soak times at the temperature extremes. This environment presents a challenge for any equipment which must operate on the lunar surface, but is especially challenging for telescopes which must maintain precise spatial relationships between optical components. The lunar surface temperature varies from approximately 90 K at sunrise to as hot as 390 K at local noon. The surface temperature rises rapidly after sunrise, remaining above 300 K for a period of about 240 hours. The surface temperature also falls rapidly at sunset and is near 100 K for about 290 hours. Without adequate thermal control, these large temperature changes and long soak periods can cause misalignment of optical components, damage to electronic components, and failure of mechanical devices.

5.8.18 LUTE Lunar Environment Instruments

A large data base on lunar environmental conditions has been assembled through remote measurements and by instruments carried on unmanned lunar landers and the Apollo missions; however, there are many areas in which the data are either insufficient or lacking. The design of future lunar telescopes, rovers, and lunar bases would, therefore, benefit substantially from further data on the lunar environment. In addition, analysis of the science and engineering data returned from the LUTE telescope could be aided by a detailed knowledge of the environmental conditions to which the telescope and its subsystems are subjected. Design of the LUTE mission should, therefore, consider incorporating a lunar environmental monitoring package which would ride along on the LUTE lander platform, be deployed on the lunar surface, and operate in conjunction with the LUTE power and telemetry system. Researchers at New Mexico State University have suggested such an environmental monitoring system. A group of four instruments to monitor the lunar environment has been outlined and is currently under study at New Mexico State University. The instruments are:

(1) Micrometeorite Detector—Detect and determine the velocity vector and mass of micrometeorites up to 100 mm in diameter.

(2) Dust Detector/Deflector—Incorporate a charged dust deflector into the design of the LUTE telescope and characterize the local, time-varying dust conditions. Determine particle sizes of dust and local natural electric field variations.

(3) Lunar Atmosphere Detector—Determine the composition and time variation of ionized atmosphere components using an ion mass spectrometer.

(4) Cosmic Ray Detector—Determine the rate and energy distribution of cosmic rays using a stacked-detector instrument.

These instruments would be mounted on a common pallet with the LUTE telescope and share power and communications with it. The micrometeorite and cosmic-ray detectors should be mounted high enough to see a full 2π steradians view of the sky without blockage by the telescope. The instruments are expected to operate over the full 2 year lifetime of the LUTE telescope. Preliminary estimates of instrument parameters are approximately 30 kg, with a volume of 0.05 m^3 and a power requirement of about 20 W.

5.9 Software

A management plan outline, development schedule, and content outline for LUTE software have been included in this section. In addition, a brief description is provided for the seven different types of software required for the LUTE project. This effort is consistent with the NWODB in a phase A activity and provides a strong basis for the development of a more detailed software program at the start of phase B.

All the required software for LUTE and its related interfaces will be designed, developed, and tested according to the latest version of MSFC "Software Management and Development Requirements Manual," MMI 8075.1.

5.9.1 Software Management Plan Document Outline

INTRODUCTION
- Purpose
- Scope
- Description

RELATED DOCUMENTS

PURPOSE AND DESCRIPTION OF LUTE SOFTWARE
- Flight Systems
- Science Data
- Electrical Ground Support Equipment
- Lunar Lander
- Launch Vehicle

CONFIGURATION MANAGEMENT
- Level III Change Control Board
- Level IV Change Control Board
- Software Review Board

ORGANIZATIONAL RESPONSIBILITIES
- Program Manager
- Program Engineer
- Program Science Adviser
- Astrionics Laboratory
- Software Quality Assurance Office
- Systems Analysis and Integration Laboratory
- Mission Operations Laboratory

UNITS OF MANAGEMENT
- Work Breakdown Structure
- Software Configuration End Item
- Related Software Documentation

SOFTWARE MAINTENANCE
- Software Development Folders
- All Systems Software
- User Training

SOFTWARE REVIEW MANAGEMENT
- Project Requirements Review
- Software Requirements Review
- Preliminary Design Review
- Critical Design Review
- Test Readiness Review
- Configuration Inspection
- Acceptance Review

LUTE SOFTWARE DOCUMENTATION

5.9.2 LUTE Software Development Life Cycle

LUTE development at MSFC will utilize NWODB and the development life cycle, projected in figure 179, reflects this approach.

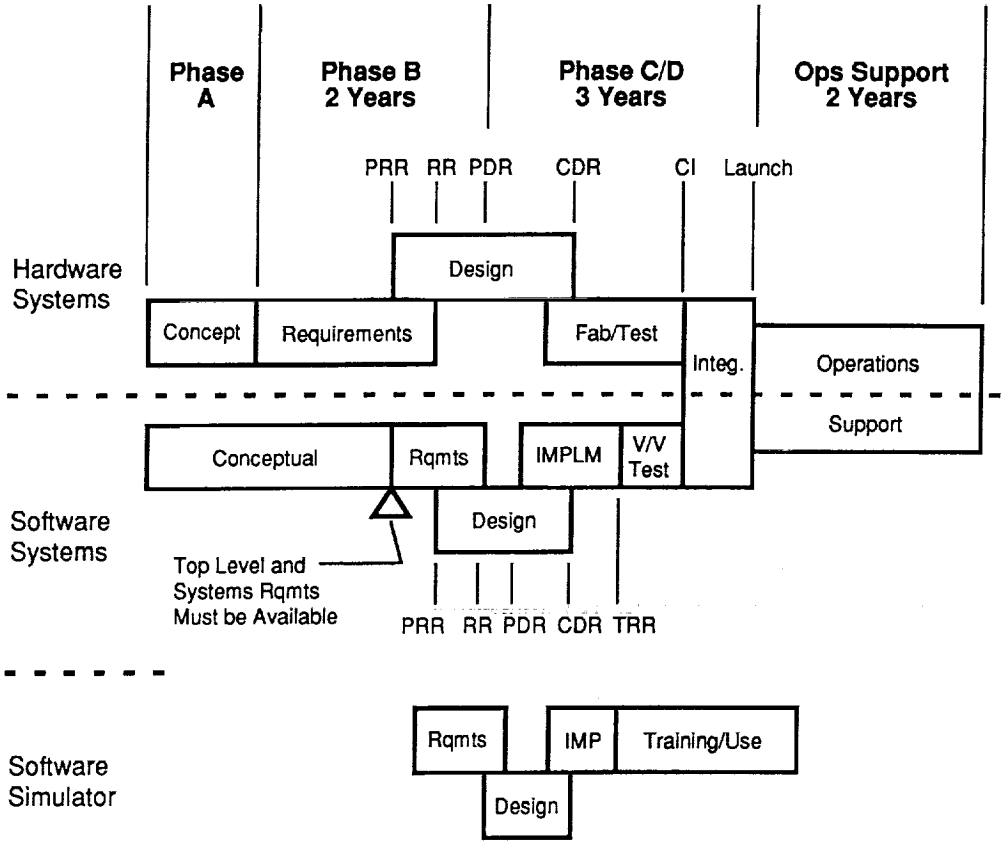

Figure 179. Software life cycle.

5.9.3 LUTE Software Content Outline

Software for the LUTE is divided into seven systems: flight software, science software, EGSE software, software development and verification, simulation, operations, and sensor data base.

5.9.3.1 LUTE Flight Software

The LUTE flight software consists of the following components: executive controller, command and data management, dynamics and pointing control, optics calibration and processing, electrical power management, thermal control, launch vehicle interface, and lander vehicle interface.

5.9.3.2 Science Data Software

It is projected that the science software will be a separate system and will consist of the following: ephemeris data, data acquisition and processing, command requests and telemetry, data display, and science data base.

5.9.3.3 EGSE Software

Phase A final results indicate this software will include the following systems: executive software, data acquisition and processing, data display, spacecraft integration, command and telemetry, launch vehicle interface, and lander vehicle interface.

5.9.3.4 Development and Verification Software

This software is projected to include the following components: support of flight software development, software configuration management, software archives, documentation development, test procedure development, test procedure interpreter, and test procedure execution.

5.9.3.5 Simulation Software

The software defined for simulation will contain the following: system modeling, commands and telemetry, launch and lander interfaces, and training.

5.9.3.6 Operations Software

Operations software will contain the following systems: data acquisition and processing, timeline management, command and data management, data display, and data archive and playback.

5.9.3.7 Sensor Data Base Software

The sensor data base software will be designed as a separate system and contain the following: data acquisition, data processing and display, measurement identification, data base generation, and data base configuration and control.

5.10 Lander

5.10.1 Common Subsystem Study

After the total mass of LUTE increased to the point of exceeding the performance capability of Artemis, a mass reduction study was initiated. Since both Artemis and LUTE have individual power and C&DH subsystems, an investigation was made to determine if significant mass reductions could be realized by using common subsystems. The results of the study showed that a potential mass reduction of 30 kg (5 kg from power and 25 kg from C&DH) may be available. Future LUTE and lander studies will take advantage of the mass savings (although small) resulting from combining subsystems.

5.10.2 LUTE Level II Requirements Imposed on Lander

The constraints under which LUTE must operate directly affects the design of the lander. Figure 180 lists the level II requirements imposed on the lander by LUTE.

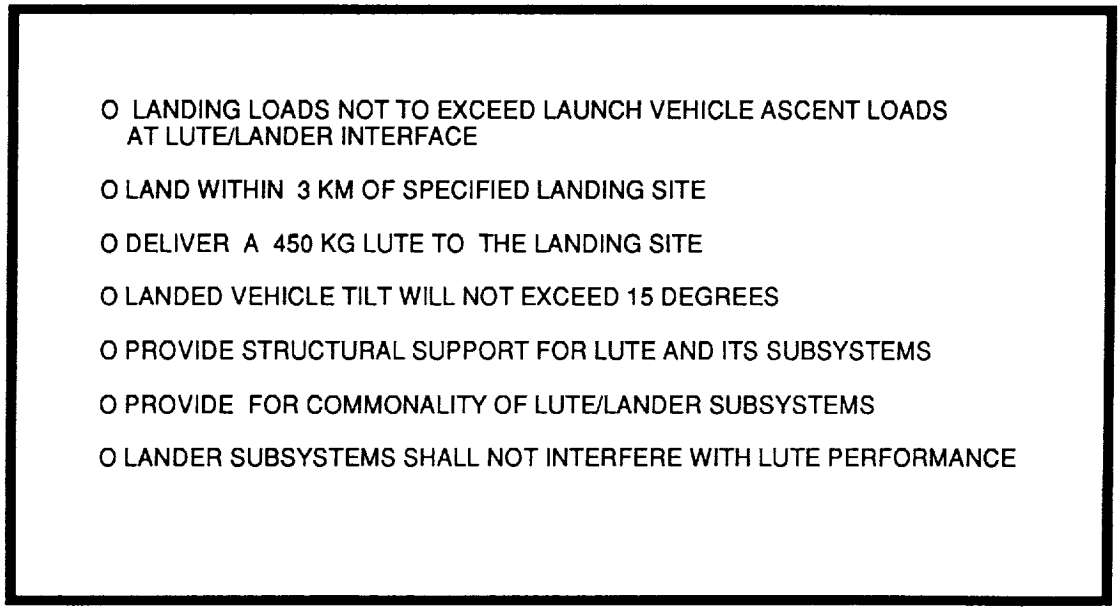

Figure 180. LUTE level II requirements imposed on lander.

5.10.3 Parametric Sizing Study for Lander

Early in the LUTE preliminary design process, the Artemis lander was baselined as the delivery vehicle for placing LUTE on the lunar surface. As LUTE became better defined, its mass increased beyond the performance capability of Artemis. At this point, a parametric study was begun to scale up the Artemis lander to accommodate LUTE masses which were varied from 338 kg to 1,200 kg. Launch vehicles were also selected which would be required to inject the variable LUTE/lander masses into a 5 day transfer to the Moon. Total costs of the LUTE, lander, and launch vehicle were also developed. A mass contingency of 32 percent was included in the burnout mass of the upscaled Artemis. The ground rules and assumptions used in this assessment are shown in figure 181.

- Potential launch vehicles—Delta, Atlas, Titan series, proton
- Use LUTE masses of 338 kg (1 m aperture), 700 kg (1.5 m), and 1,200 kg (2 m)
- Use Artemis as basic lander design
- Use historical lunar logistics system (LLS) storable propellant landers as additional data point
- Compute stage mass fractions from Artemis and LLS data
- All systems/subsystems scaled by mass fraction
- A 10 percent mass contingency is added in addition to the Artemis 20 percent contingency giving a total contingency of 32 percent
- Launch vehicle performs all burns through TLI to $C_3 = -1.9$ km^2/s^2
- 120 hour, 5 day transfer time
- No hardware jettisoned from TLI through landing
- Use Artemis Delta V budget of 2,781 m/second from TLI through landing
- Storage propellant with $I_{sp} = 310$ seconds

Figure 181. Ground rules and assumptions.

Figure 182 shows the mass relationship between LUTE, lander, and launch vehicle capability. For a 1 m aperture LUTE, the lander mass including residuals is approximately 671 kg (including the RTG) and requires a propellant mass of approximately 1,510 kg. The total mass at translunar injection (TLI) amounts to approximately 2,561 kg and requires the Atlas II AS launch vehicle. A payload growth margin of approximately 239 kg is available for this configuration.

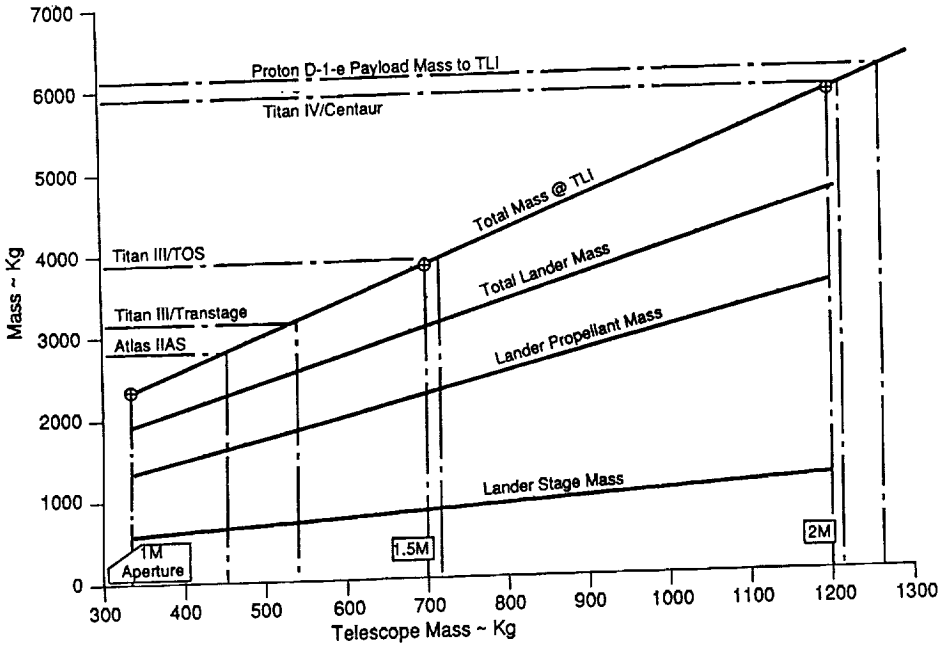

Figure 182. LUTE/lander/launch vehicle relationships.

A gross estimate of the LUTE, lander, launch vehicle, and cost relationships is shown in figure 183. The total cost for placing a 338 kg,1 m LUTE on the lunar surface is $521 million. A more detailed cost estimate for the LUTE reference design concept is provided in section 8.0.

	Aperture Size					
	1 M		1.5 M		2 M	
	Mass (kg)	Cost (M$)	Mass (kg)	Cost (M$)	Mass (kg)	Cost (M$)
• LUTE	338	126	700	155	1200	185
• Lander	2181	266	3150	332	4700	402
• Total LUTE/Lander at TLI	2519	392	3850	487	5900	587
• Launch Vehicle Req'd	Atlas IIAS	129	Titan III/ TOS	236	Titan IV/ Centaur	352
• Total		521		723		939

Figure 183. LUTE/lander/launch vehicle mass/cost summary.

Figure 184 shows the mass and cost relationships for varying LUTE masses. The total mass including the LUTE and lander at TLI and the total costing including the LUTE, lander, and launch vehicle are displayed as a function of LUTE mass. The step functions of the "total cost" plot result from the total mass of the LUTE and lander increasing to the point that a larger launch vehicle is required.

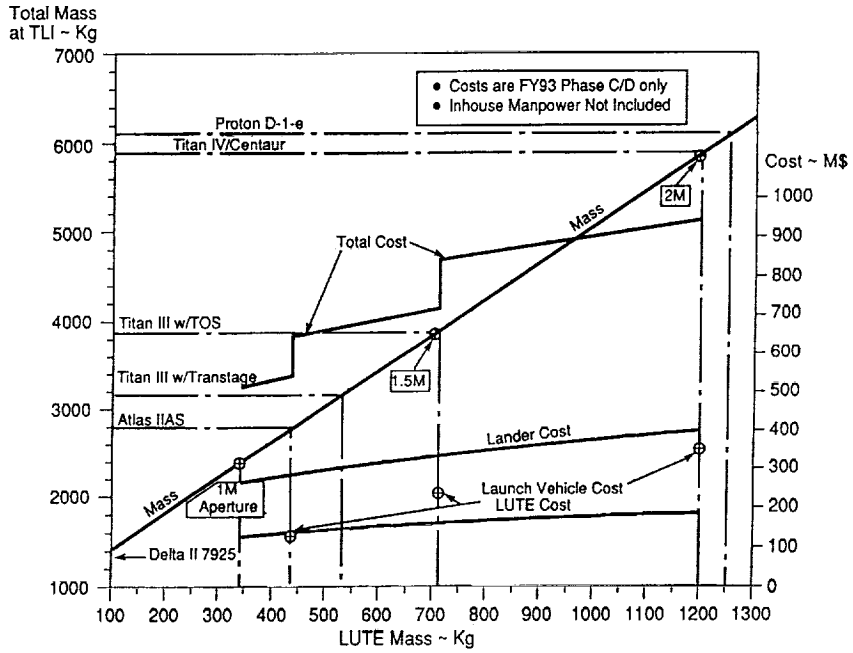

Figure 184. Performance and cost.

6.0 SAFETY AND MISSION ASSURANCE

6.1 Safety

A preliminary system safety plan was prepared during the phase A final study which established the system safety objectives. The system safety responsibilities and hazard analysis methods are discussed in this plan, which is enclosed in appendix N. A preliminary hazard analysis was prepared which identified potential safety hazards and potential techniques for eliminating or controlling these hazards.

The preliminary hazard analysis, which is enclosed in appendix O, addresses the LUTE as an independent experiment from the lunar lander or the launch vehicle. The LUTE will be launched into space by an expendable launch vehicle, and no manned contact is planned following the launch. Therefore, the only system safety concern will be ground processing and on the range during launch. If the LUTE is launched from the Eastern Space and Missile Center (ESMC) and processed at Kennedy Space Center (KSC), it will be required to comply with safety requirements specified by ESMC 127-1, "Eastern Space and Missile Center Range Safety Requirements," and KHB 1710.2, "KSC Safety Practices Handbook."

At this point of design maturity, LUTE has potential range safety hazards associated with power, thermal control, structures and materials, pressurization, command and data management, and pointing and alignment systems. During phase A, two options for the electrical power system were studied. One option for a power source was a solar array system and the other was an RTG-powered system. The RTG option was selected for the phase A design concept. However, the hazard analysis for the solar array system was included in the preliminary hazard analysis. An RTG is classified as a major ionizing radiation source. A user of a major ionizing radiation source is required to follow the space nuclear safety review process and obtain approval for use by the Executive Office of the President through the Office of Science and Technology Policy. This review and approval process is also required if the LUTE uses a Russian-built RTG, lander, and/or is launched by a Russian launch vehicle. During the ground processing of a spacecraft with an RTG at ESMC or KSC, radiation protection controls that are identified by ESMC-160-1, "Radiation Control Program," and KHB 1860.1, "Radiological Controls for Major Sources and Nuclear Assemblies," will be implemented. Also, redundant methods of cooling the RTG during ground processing will be required. During all mission phases, the potential of failures of the launch vehicle, transfer stage, lunar lander or the LUTE, which may result in a hazardous radiological release, must be assessed for acceptable risk.

In the thermal control system, RHU's, heat pipes, and electrical heaters were evaluated for their hazard potential. If the RHU's are used, radiation protection controls will be implemented during ground processing. If heat pipes are used, controls will be provided to prevent rupture, which produces shrapnel, and the subsequent release of potential flammable substances. As with all heater systems, personnel touch temperature hazards will be considered in the design.

The mechanical ground support equipment (GSE) and the flight structure will be designed in accordance with MSFC structural design practices to ensure that personnel injury and damage to flight hardware and ground processing facilities are avoided. All GSE and flight pressurized systems will be designed to MSFC standards.

The materials used on LUTE will be selected using MSFC materials' standards. All solvents and plastic films used during ground processing will be approved by the ESMC and KSC launch site safety offices. These are generic-type hazards associated with all structures and materials.

The LUTE C&DH has the capability to cause a potential range safety hazard during ground testing and processing. This potential hazard is a personnel exposure to high levels of nonionizing radiation from the LUTE radio frequency system transmitter, which may be caused by inadvertent commands or inadequate personnel shielding. The proper number of inhibits for transmitter operation and precautions for personnel protection will be provided to control this hazard. The pointing and alignment system will have the capability to roll and tilt the LUTE.

If the pointing and alignment system were to inadvertently roll or tilt the LUTE after it is encapsulated in the missile fairing, a potential exists to damage the launch pad facility and the launch vehicle. Also, during ground processing and transportation, an inadvertent roll or tilt may injure ground personnel or damage site facilities. The roll and tilt mechanisms will be structurally designed to the required MSFC standards and the required mechanism power supply inhibits will be provided which will control this hazard.

Overall, given the present LUTE design concept, all the safety design concerns for the LUTE have been previously addressed in the design of spacecraft that have previously flown.

6.2 Reliability

The MSFC Reliability Office will be actively involved in the design and buildup of the LUTE. A reliability program plan was prepared during phase A (see appendix P). The plan will serve as the implementing directive for management of reliability program activities for LUTE. The activities described in the plan are structured to reflect the unique nature of the LUTE program. The reliability plan will be updated, as appropriate, for the different phases of the program. How stringent the reliability requirements are will depend on the payload classification. It is recommended that LUTE be a class B payload per NMI 8010.1A.

6.3 Quality Assurance

The MSFC Quality Assurance Office will become more involved with the LUTE project as it moves into phase B. This involvement will continue through the buildup and test/checkout of the payload. A formal quality assurance program, including closed-loop problem reporting and analysis, will be developed and implemented. A formal qualification and acceptance test program will also be required. A quality program plan will be prepared during phase B and will be updated as required.

7.0 SCHEDULE AND COST

7.1 Future Planning

A phase A management assessment of LUTE at the end of 1993 will yield the go-ahead (or no-go) for a full in-house phase B. The project will then follow timescale of approximately 2 years for a phase B (definition phase) and approximately 3 years for phases C (design and development phase) and D (fabrication, integration, and test). The schedule depicted in figure 185 shows a generic timescale from the start of phase B through the end of the project. The uncertainty of the start of phase B and the funding availability dictate a generic timescale. The lander milestones will be added when a definitive agreement is reached for the lunar lander.

7.2 Funding Requirements

The current estimated funding requirements for LUTE are defined by programmatic considerations such as the in-house development approach and the inclusion of NWODB, as well as technical parameters such as weight and power. The following two sections, Predevelopment Funding and Development Funding, illustrate the current LUTE baseline cost and civil service manpower estimates. Section 7.2.3, Ground Rules and Assumptions, details the philosophies underlying the baseline cost estimate. The alternative minimum configuration cost estimate is discussed in section 7.2.4. The application of NWODB is explained in section 7.2.5.

7.2.1 Predevelopment Funding Requirements

The predevelopment funding for LUTE is of vital importance. One of the main goals of NWODB is to define and understand the problems and requirements early. Therefore, the funding and manpower demands for prephase C/D are necessary to ensure that the NWODB cost savings can be realized. The LUTE predevelopment funding and civil service manpower estimates are given in figure 186. This exhibit gives the full funding and manpower profile for LUTE, from the predevelopment phase through 2 years of operations and data analysis. The predevelopment funding and manpower estimates are shown under FY94. The cost is 19.2 RY$M and manpower is 44.3 man-years.

Predevelopment estimates are the sum of two requirements: adequate prephase C/D resources and early development/long lead procurement. The prephase C/D resources have been estimated as 10 percent of the development phase cost and manpower (FY95 through FY98). To ensure adequate resources for the predevelopment phase, and to allow for early development and the procurement of long lead items, 5 percent of the phase C/D estimated cost and manpower was shifted into FY94. The sum of these two percentages yield the FY94 numbers shown in figure 186.

7.2.2 Development Funding Requirements

The funding and civil service manpower needs for the development of the LUTE are shown in figure 187. The development funding and manpower is inclusive of the years FY95 to FY98. The cost and manpower shown for FY99 and FY00 are for 2 years of operations and data analysis. The total cost for the development phase is 134.6 RY$M. Total civil service manpower for designing, developing, and building the LUTE is 280.6 MY, with an additional 35.0 MY required to fulfill project office requirements. Cost for operations and data analysis is estimated to be 14.5 RY$M plus 6.0 project office man-years. A detailed cost and manpower matrix for LUTE is shown in figure 187. This matrix provides detailed cost and manpower estimates by various subsystems and system level cost elements for the baseline and minimum configurations.

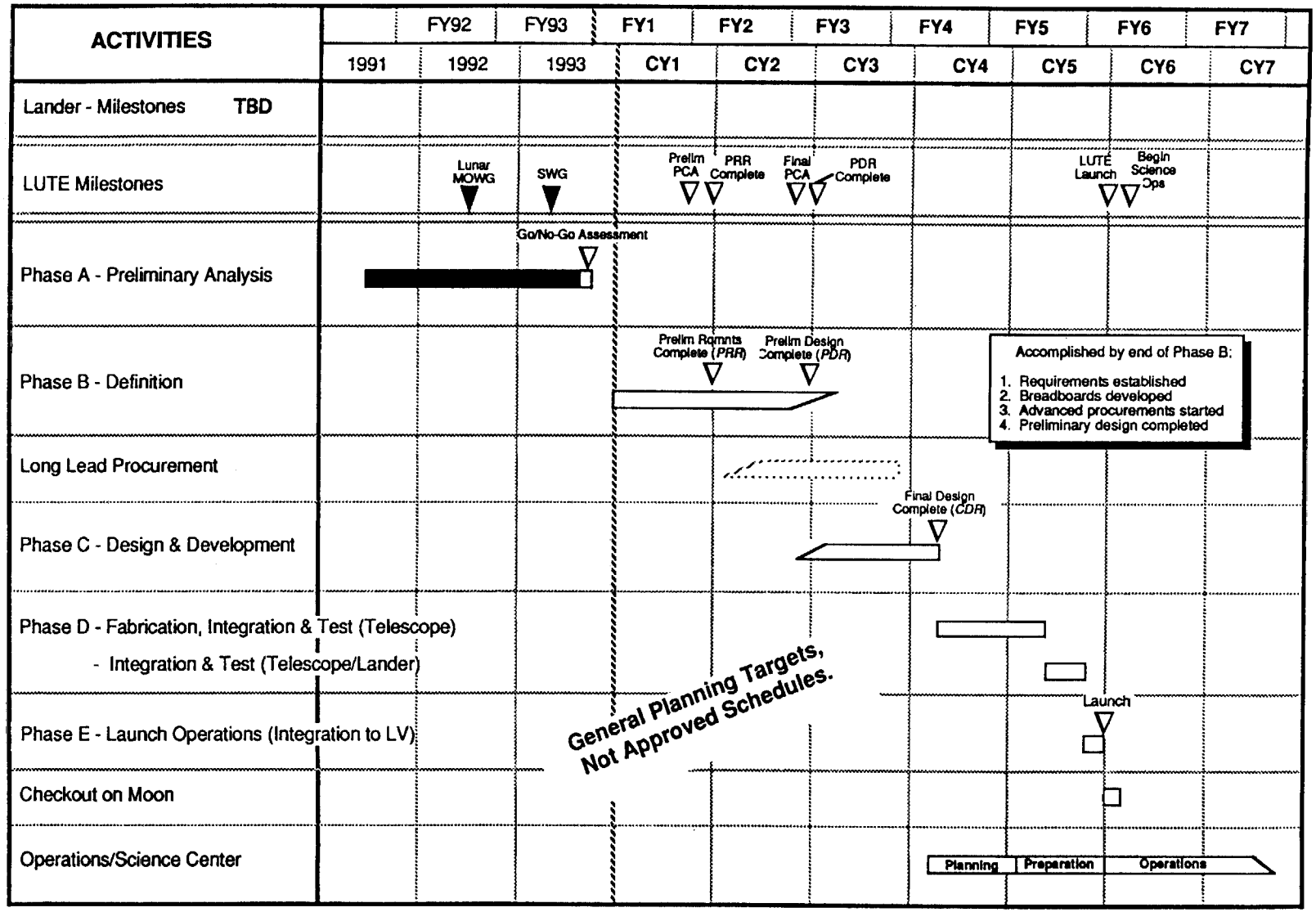

Figure 185. LUTE (in-house project).

LUTE COST ESTIMATE
ONE METER

NEW WAYS OF DOING BUSINESS
IN-HOUSE

FY	COST (RY$M)	C. S. MANPOWER DESIGN & DEVELOPMENT	C. S. MANPOWER PROJECT OFFICE
93			
94	19.2	44.3	
95	23.9	52.7	4.4
96	54.8	115.6	10.2
97	45.0	91.1	10.2
98*	10.9	21.2	10.2
99	7.1		4.0
00	7.4		2.0
TOTAL	168.3	324.9	41.0

* Launch Year

Note: The total cost for a Prime Contractor Business as Usual Approach is 263.9 RY$M.

Figure 186. LUTE cost estimate.

	BASELINE		MINIMUM CONFIGURATION		
ELEMENT	MPR/PMS MY/RY$M	COST RY$M	MPR/PMS MY/RY$M	COST RY$M	MINIMIZING ASSUMPTIONS
PHASE B	44.3 / 1.0	18.2	39.7 / 0.9	9.5	Reduced Development in CCD & Optics Technology
DETECTOR		12.2		7.1	Used Available CCD Technology
OPTICAL SYSTEM (OPTICS & STRUCTURE)		30.8		23.3	Adapted Optical System to Match Available CCD's
POWER REGULATION & DISTRIBUTION	10.6 / 0.3	1.3	10.3 / 0.2	1.3	
COMMUNICATIONS & DATA MANAGEMENT	63.7 / 1.5	7.6	62.0 / 1.5	7.5	
STRUCTURE	23.2 / 0.6	2.8	22.5 / 0.5	2.7	
MECHANISMS	15.4 / 0.4	1.8	15.0 / 0.4	1.8	
POINTING/VIBRATION ISOLATION/FINE ADJUST	31.8 / 0.8	3.8	31.0 / 0.7	3.8	
THERMAL CONTROL SYSTEM	34.7 / 0.8	4.1	33.8 / 0.8	4.1	
ATTITUDE DETERMINATION & CONTROL					
PROPULSION SYSTEM					
GROUND SYSTEM DEVELOPMENT	32.8 / 0.8	3.9	19.7 / 0.5	2.4	Reduced Systems Cost
TELESCOPE/LANDER INTEGRATION	14.5 / 0.4	1.7	9.4 / 0.2	1.1	Integration Simplified Without RTG
PAYLOAD/LAUNCH VEHICLE INTEGRATION					
ASSEMBLY & TEST	63.7 / 1.5	7.6	56.3 / 1.3	6.8	Removal of RTG Assembly & Test Responsibility
GROUND SUPPORT EQUIPMENT	11.6 / 0.3	1.4	10.3 / 0.2	1.3	
PROJECT MANAGEMENT	13.5 / 0.3	1.6	12.2 / 0.3	1.5	
RTG		45.9			Part of Lander
MISSION OPERATIONS (2 YEARS)	6.0 / 0.2	14.6			Not Included
TOTAL MANPOWER (MY/$)	365.8 / 8.8		322.2 / 7.7		
TOTAL HARDWARE		159.3		74.2	
TOTAL COST		168.1		81.9	

NOTES:
- HARDWARE COST INCLUDES PROGRAM SUPPORT, CONTINGENCY, AND FEE
- CIVIL SERVICE MANPOWER INCLUDES PROJECT OFFICE (INDIRECT) AND DESIGN AND DEVELOPMENT (DIRECT)
- UNCOSTED ITEMS ARE CONSIDERED TO BE LANDER UNIQUE
- MINIMUM CONFIGURATION ASSUMES DESCOPED TELESCOPE AND DETECTOR WITH MISSION OPERATIONS FUNDED SEPERATELY; ASSUMES RUSSIAN COOPERATION FOR THE LAUNCH VEHICLE, LANDER, AND RTG

Figure 187. LUTE cost matrix.

7.2.3 Ground Rules and Assumptions

The LUTE cost and manpower estimate includes all life cycle elements with only the cost of the lander and the launch vehicle excluded. The major cost elements of the LUTE estimate are the telescope, supporting subsystems, assembly and test, telescope/lander integration, and ground systems development. The telescope consists of the optics, CCD detector, metering structure, light baffles, and the primary mirror support structure. The supporting subsystems are the support and pointing structure, the RTG based power subsystem, the communications and control subsystem, and the thermal control subsystem. These subsystems are necessary to maintain and operate the telescope following lunar landing; therefore, they have been included as part of the cost estimate. Assembly and test accounts for the integration of the telescope with the supporting subsystems and testing of the full package ensure reliability. Tests include thermal vacuum, vibration, and mirror accuracy. The telescope/lander integration is to support the integration of the complete LUTE package with the lander. It is assumed that the interface between the telescope and lander is a simple structural and power interface. Ground system development consists of the software, computers, networks, and facility modifications necessary to operate LUTE, receive the data, analyze the data, and distribute the data to the scientists, universities, and schools. The ground system is currently the least well-defined portion of the LUTE; therefore, the ground system development cost estimate has the lowest confidence level.

All of the LUTE's major cost elements are estimated using parametric approaches. The cost models used are the MSFC instrument cost model, the MSFC NASA cost model (NASCOM), the GSFC mission system integration and test (MSI&T) cost model, and the GSFC ground systems cost model. Weight is used as the cost driver for all of the models, with the exception of the ground systems cost model. A 10 percent contingency is included for all weights (for costing purposes only).

Cost for two of the elements, the detector and RTG, is taken directly from outside sources. The detector costs were estimated by the Space Science Laboratory. Development of the detector is considered the highest risk activity for LUTE; and therefore, carries a very conservative cost estimate. The DOE provided the RTG cost estimate. The RTG is a follow-on unit to the type used on Galileo and Cassini. Both the RTG and detector are considered full out-of-house developments and do not incorporate NWODB cost savings. The optical system is also assumed to be an out-of-house purchase, but NWODB credits are taken against the cost.

In addition to the above subsystems, the estimated cost also includes program support, contingency, program mission support (PMS), and fee. Program support, contingency, and fee are estimated as percentages. The program support percentage is 5 percent, fee is 10 percent on the detector and optics, 5 percent on all other elements, and the contingency is estimated at 15 percent. The low contingency percentage is consistent with NWODB. PMS is estimated at 21 FY93$k per civil service man-year.

In-house civil service manpower was estimated using a civil service manpower model developed from data compiled for the Engineering Cost Group. The model estimated total in-house manpower for the in-house design and development. The estimated manpower was then allocated at 10 percent to the project office and 90 percent to the hardware design, development, fabrication, and test. The reduction in out-of-house cost was estimated using data from the Cosmic Background Explorer.

Operations and data analysis cost and manpower is estimated using a percentage factor developed from a JSC study. The JSC study indicated that operations and data analysis would cost about 3 percent of the total phase C/D cost (and in this case, in-house manpower) per year.

7.2.4 Minimum Configuration

An alternative cost estimate is shown in figure 187 (LUTE cost matrix). This estimate, titled "minimum configuration," incorporates several changes to reduce the cost. These changes reduce manpower by 43.6 MY and save 86.2 RY$M. The minimum configuration LUTE requires 322.2 MY and 81.9 RY$M. One of the important changes is to use available CCD detector technology rather than developing new technologies in the areas of pixel size and detector shape. Using available detector technology not only reduces detector cost but also enables a lower cost optical system. Phase B funding requirements can be reduced since advanced development is not required for the detector and the optical system. The second important change is the deletion of the RTG and mission operations cost. The RTG is assigned to the lander, and lander items are not costed in this study. Mission operations costs are assumed to be funded separately, and thus are not included. Finally, ground system development cost is reduced due to the overall flight hardware cost reductions.

7.2.5 NWODB

The LUTE cost and manpower estimate reflects a new approach to the way that NASA does business. Called NWODB, this methodology estimates the impact to program cost for changes in the procurement process, phase B funding, funding stability, management approaches, design methods, and production processes.

Implicit in the NWODB cost savings are several changes in the relationship between NASA, Congress, and the contractors. The NASA/Congressional relationship must change to allow for adequate phase B funding and phase C/D funding stability. Adequate phase B funding will enable problems to be identified and resolved early, with resulting savings in cost and manpower. Funding stability during phase C/D will eliminate cost growth due to schedule slips and funding shortfalls. The NASA/contractor relationship is assumed to change from a hands-on detailed oversight role to a performance specification driven hands-off approach. The goal is to allow the contractor to find the best design solution for a set of performance specifications. It is believed that such a change in the NASA/contractor relationship will result in savings in both contractor dollars and NASA civil service manpower. This will require careful definition of the performance specification and discipline by NASA/contractor management and technical personnel.

The estimated effects of these NWODB changes of the LUTE cost are shown in figure 188. The total possible NWODB cost savings is 25 percent. As can be seen in figure 188, the estimated LUTE savings is less. The reason for lower estimated savings is that the limited timeframe for implementing LUTE reduces the possibility for incorporating these changes into NASA's culture.

	Cost/Manpower Savings		
Proposed Culture Change	Cost	Design & Development	Project Office
More Extensive Phase B	5.8%	5.8%	
Multi-year Funding Stability	5.5%	5.5%	5.5%
Enhanced Quality/Management Methods	8.2%	8.2%	8.2%
Advanced Design Methods	2.0%	2.0%	
Advanced Production Methods			
Improved Procurement Processes	2.0%		2.0%
Total	21.5%	19.9%	15.0%

Figure 188. Potential LUTE savings as a result of NWODB.

8.0 FUTURE WORK

8.1 Near-Term Effort

The next technical effort for LUTE, either as an initial part of phase B or a precursor to phase B, is described in detail in the following paragraphs.

8.1.1 LUTE Optical Systems Analysis

Design studies of the LUTE optical system have been performed during the phase A final study. The resulting optical configuration, material selection, metering structure design, mirror support schemes, etc., have been conceptually developed and evaluated to the depth which is normally commensurate with a phase A level. Since the LUTE telescope is a very sophisticated optical system and is constrained principally by cost and also by launch weight, further development of the design is necessary to derive the best optical approach within these constraints. These studies must consider manufacturing, assembly, and testing aspects within the current ability of optical houses and NASA.

Therefore, overall optical system analyses and evaluations should be performed by optical companies with space telescope expertise, as an initial task in phase B or a precursor task to systems preliminary design. These studies should address changes to the design that would optimize performance, manufacturability, testing, cost and schedule, etc., made possible by relaxation of the mass constraints and the availability of additional power for thermal control. The applicability of 7 μm pixels in the CCD detector should be part of these analyses with regard to the effects on focal length, optical prescription, overall telescope design, and the primary/tertiary mirror structural design.

Results from these studies, with the assessments of LUTE overall assembly and testing concepts, can then be utilized to derive contractor and Government cost estimates, and the technical results can be utilized early in the phase B activity.

8.1.2 Large-Area Detector Array

Analyses of the large-area detector during the phase A studies pointed toward a detector pixel size of 5 μm. The resolution of the current LUTE f/3 three-mirror D. Korsch design is considerably better than the limits imposed by the 5 μm pixels; however, 5 μm pixels are currently beyond the commercial manufacturing state-of-the-art. Thus, it would be necessary to develop this manufacturing capability in industry and research laboratories. While such efforts should be continued, and since CCD detectors of such pixel size are of interest to many researchers, another approach should be investigated for LUTE, in which the pixel size of the detector elements is increased to commercially available dimensions. This approach will save time and money, but its impact on the identified scientific objectives for LUTE must be assessed.

Another area of concern with the CCD focal plane array derives from the requirement that the observed stars describe curved tracks on the image plane which are in direct relation to the declination at which the telescope is pointed. Thus, the rows of pixels in the array must be curved according to preselected pointing declination. This is not only difficult to accomplish, it also requires accurate alignment to that declination after the telescope has been deployed on the Moon. A more flexible and possibly simpler solution might be obtained through the development of an array which responds to software corrections of the star tracks in the time-delay-integration charge transfer. It is, therefore, proposed to assess if such a declination-independent array could be designed and the algorithms developed. We propose to proceed with a two-pronged approach, where modest funding continues the 5 μm pixel development and

larger funding is dedicated to the development of a LUTE focal plane array using larger pixels. Evaluation of developing curved pixel tracks versus applying software methods of star track registration is recommended.

The capability of industry to produce large area CCD detectors, either fabricated directly on a spherical substrate or sufficiently thinned that they could be "stretched" to conform to a spherical surface, to allow matching the detector to the image field curvature must be investigated further. If a photon counting rather than a drift scan detection mode is contemplated, software solutions to the distortion problems must be investigated.

Using the optical analyses described previously, a breadboard CCD array of commercially obtainable wavers should be developed to the requirements of typical dimensions and curvature of the LUTE focal plane.

8.1.3 Environmental Measurement Package

One of the key supporting systems for LUTE and for future lunar instrument development is a lunar environmental measurement package, which has been proposed and is currently under study at New Mexico State University. Because this assembly of instruments enhances the LUTE mission and works with information from the LUTE optical system, the analyses and design of this measurement system should be expanded. Study results on weight, power requirements, communication and data relay, etc., will directly affect the LUTE subsystems and total weight and volume estimates.

8.2 Long-Range Plans

A preliminary outline of LUTE programmatics, with 5 years from the start of phase B to launch of the LUTE and a 2 year operational phase, are described in figure 189. In addition, the required documentation to support these programmatics is outlined on figure 190. The development stage for each document is indicated as (P) for preliminary, (U) for update, or (B) for baseline. Several preliminary documents, mentioned above, such as safety plan, reliability plan, and hazard analysis plan, are available at the end of phase A, ahead of the documentation plan outlined.

Another effort to accomplish some early long-range planning and to identify risks in the project was also accomplished through a small, disadvantaged business contract. The fidelity of the data available to include in planning activities of this nature is reflected directly in the results. However, the activity forced early consideration of real hardware processes, was instructive to all the team members participating in the activity, and provided a lower level of detail on tasks and sequencing of tasks than the top level planning described above. The report on this long-range planning and risk-assessment activity is included in appendix Q.

9.0 CONCLUSION

The LUTE has been studied at MSFC for more than 1 year. Extensive evaluations of the scientific merits were made by the astronomical community during a series of reviews and a LUTE science workshop. Based on the scientific, technical, and programmatic assessments, it can be concluded that the LUTE mission is scientifically justifiable, technically feasible without major new technology development, and possible within schedule and cost envelopes which support the science and pathfinder mission objectives. Significant by-products of this scientific mission are new engineering insight into long-term lunar design criteria and requirements and the use of science data as an educational tool at all levels of the educational system.

The unique LUTE UV survey will provide valuable tools for astrophysical research. It will be a primary data source for the study of point and diffuse UV sources of all classes and will identify prime targets for high resolution study with orbital instruments.

Production of the LUTE telescope is well within the capability of existing manufacturing facilities and current technology, as shown by detailed analyses of the LUTE optical system and the telescope supporting subsystems. The detector is the only area where a current technological challenge exists and an alternative approach should be considered. The LUTE telescope was initially laid out with a very fast f/3 optical system, which is desirable from a scientific aspect. This system ideally requires a focal plane CCD detector array with a pixel size smaller than 5 μm, which is not currently available. While 5 μm pixel CCD's will eventually be developed, the LUTE design should be based on a technically mature CCD pixel size. Introducing currently available 7 μm pixels for the LUTE CCD would change the system to a f/4.2 (still a very fast system) and increase the back focal length, i.e., the telescope length by only 26 cm, which can easily be accommodated in the design. Reviews by the scientific community should confirm that this approach will not have a significant impact on the science objectives as defined by the LUTE Science Working Group in March 1993. Assessment of the LUTE development schedule has shown that a 5 year development program is reasonable within the boundaries of detailed design, manufacturing, and testing. NWODB, now being implemented by industry and Government, will reduce the amount of documentation required via concurrent engineering practices, and thus shorten schedules and reduce cost. These concepts have been included in the schedule and costing analyses for LUTE.

During the studies of LUTE, various options for delivery to and landing of the telescope on the Moon have been analyzed. Because a definitive lunar landing vehicle is not currently available, a generic lunar lander was devised as a representative lander and lunar platform for LUTE. In this context, the LUTE design is conservative because a guideline that LUTE be a self-sufficient system has been strictly maintained during the study.

The only interfaces with the generic lander are structural connections and an electrical cable interface with the RTG mounted on one of the lander legs. Pointing and alignment, power distribution, thermal control, and communication are telescope functions in the current design. When a specific lander vehicle becomes available or is defined, some of the telescope supporting subsystems, such as electronic equipment and computers, communication and data handling, and others, may become integral with the equivalent lander systems, which will reduce system weight and cost.

Independent documented assessment of the telescope optics by experienced optical houses and selected subsystem evaluation by aerospace industries further confirm the overall technical feasibility of the LUTE.

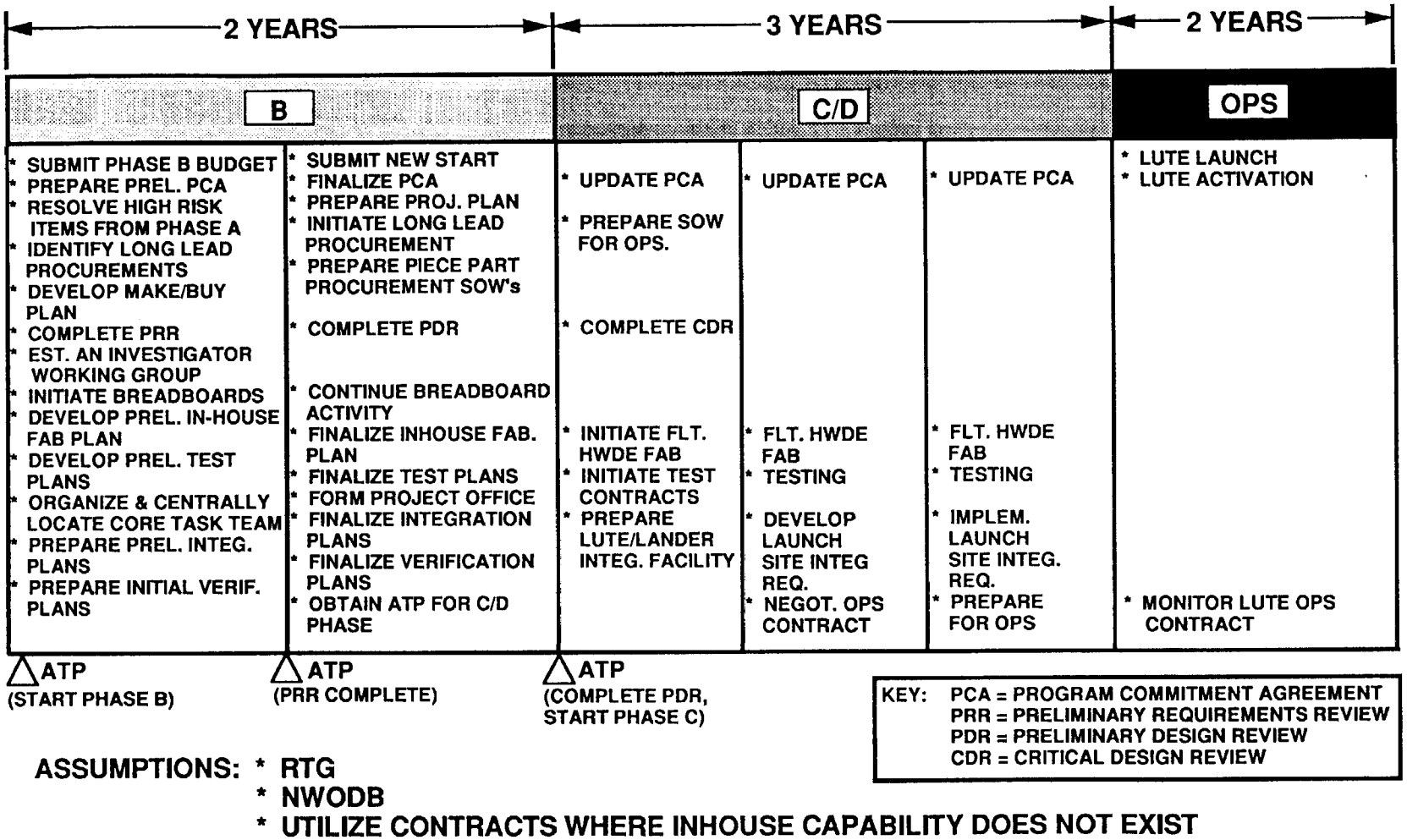

Figure 189. LUTE programmatics.

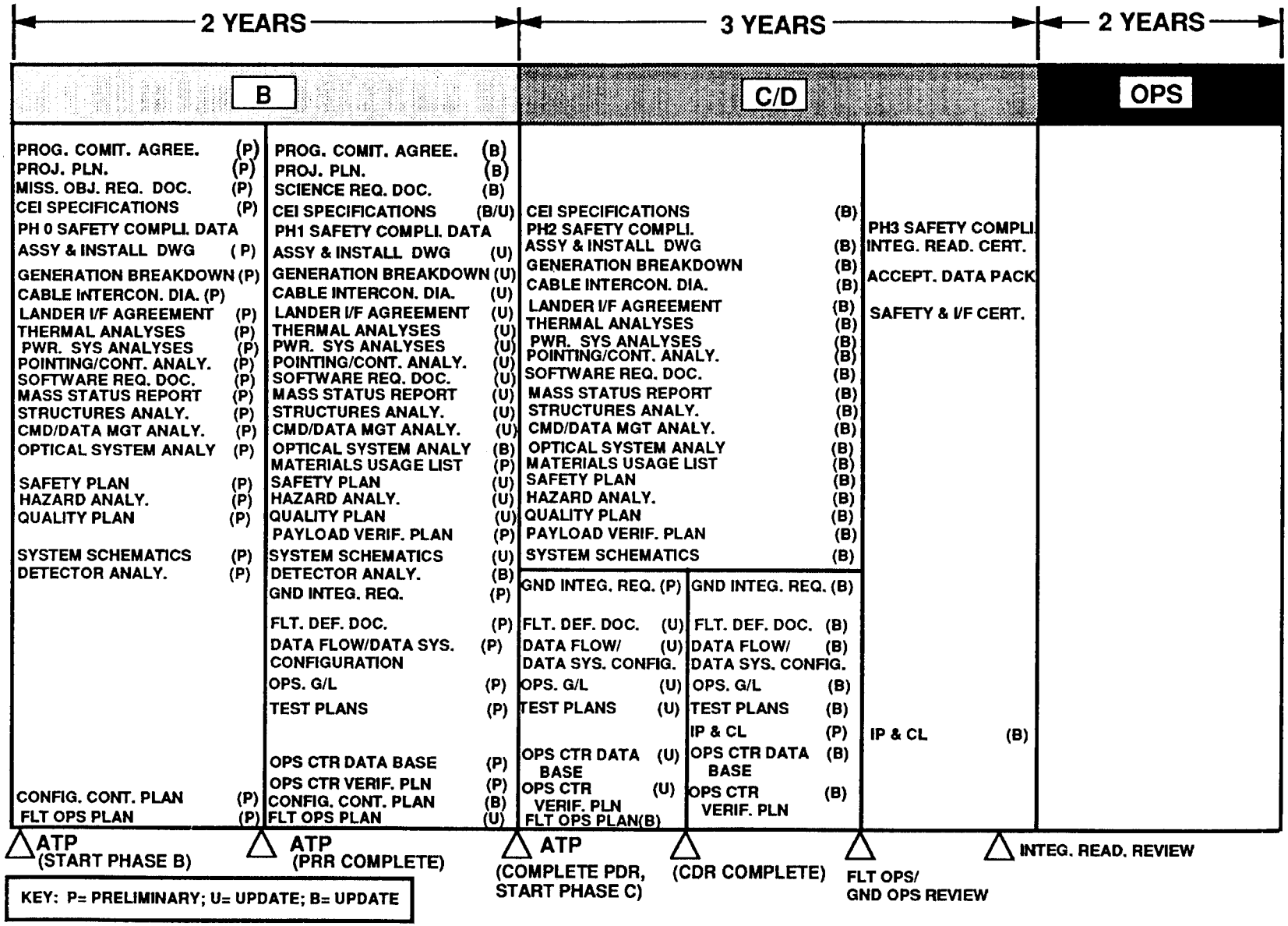

Figure 190. LUTE documentation.

REFERENCES

1. Hamaker, J.: "New Ways of Doing Business Cost Quantification Analysis." MSFC/Program Development, August 1992.

2. Lee, J.: "Institutional Team on Program/Project Planning—Findings and Recommendations." MSFC, December 1992.

3. Dr. Robins: "Policy Revision Proposals for Management of Major Development Programs and Projects—Program Excellence Team Report to NASA Senior Management." NASA Headquarters, December 21, 1992.

4. "The Decade of Discovery in Astronomy and Astrophysics by the National Research Council." National Academy Press, Washington, DC, 1991.

5. McGraw, J.T.: "An Early Lunar-Based Telescope: The Lunar Transit Telescope (LTT)." Astrophysics From the Moon, American Inst. of Physics, AIP Conf. Proc. No. 207, M.J. Mumma and H.J. Smith, editors, 1990, p. 433.

6. Young: "Roark's Formulas for Stress and Strain." Sixth edition, 1989.

7. General Dynamics Commercial Launch Services, Inc., *Mission Planner's Guide for the Atlas Launch Vehicle Family,* revision 2, July 1990.

8. Derived system random vibration LF based on methods in JA-418, "Payload Flight Equipment Requirements for Safety Critical Structures." NASA/MSFC, August 1984.

9. "Artemis Conceptual Flight Profile." Systems Engineering Division, NASA/JSC, August 1992.

10. Cremers, C.J., Birkebak, R.C., and White, J.E.: "Thermal Characteristics of the Lunar Surface Layer." International Journal of Heat and Mass Transfer, vol. 15, 1972.

11. "Structural Strength Program Requirements." MSFC-HDBK-505 (Rev. A), 1981.

12. JSC Artemis Design Team, *Artemis System Requirements Review*, October 1992.

13. JSC Artemis Design Team, *Common Lunar Lander Detailed Design Study*, June 1992.

14. "Rock Distributions on the Lunar Surface," *Lunar Engineering Models, General and Site Specific Data*. NASA Exploration Programs Office, May 1992, pp. 88–93.

15. Korsch, D.,: "Reflective Optics." Section 12.5, Academic Press, 1991.

16. Beynon, J., and Lamb, D.: "Charge-Coupled Devices and Their Application." MacGraw-Hill, London, 1980.

17. McGraw, J., Stockman, H., Angel, J., Epps, H., and Williams, J.: "Charge-Coupled Device (CCD)/Transit Instrument (CTI) Deep Photometric and Polarimetric Survey—A Progress Report." SPIE, vol. 331, Instrumentation in Astronomy IV, 1982.

18. Mackay, C.: "Drift Scan Observations With a Charge-Coupled Device (CCD)." SPIE, vol. 331, Instrumentation in Astronomy IV, 1982.

19. Fossum, E.: "Active-Pixel Sensors Challenge CCD's." Laser Focus World, June 1993, pp. 83–87.

20. Burke, B., Mountain, R., Daniels, P., and Harrison, D.: "420 × 420 Charge-Coupled-Device Imager and Four-Chip Hybrid Focal Plane." Opt. Eng., vol. 26(9), 1987, pp. 890–896.

21. Green, R.M.: "Spherical Astronomy." Cambridge University Press, Cambridge, 1985.

22. McCarter, J., and Korsch, D.: "Lunar Transit Telescope Feasibility Study." MSFC Program Development, LTT-004, January 1992.

23. Anon., "Mechanical Properties of Hexcel Honeycomb Materials." TSB 120, Hexcel Corporation, 1992.

24. Krim, M.: "Athermalization of Optical Structures: Selected Room Temperature Properties and Some Commentary." Working papers, Hughes Danbury Optical Systems, November 20, 1991.

25. Anon., "Beryllium Optical Properties." Brush Wellman, Inc., Beryllium/Mining Division, (419) 862-2745, date unknown.

26. Anon., "Glass Ceramics Zerodur M." Schott Glass Technologies Inc., Duryea, PA 18642, (717) 457-7485, date unknown.

27. Anon., "ULE Titanium Silicate, Code 7971." Corning Glass Works, Corning, NY 14831, (607) 974-4418, date unknown.

28. Dibble, M.A., Staff Editor: "Material Selection." Machine Design: 1992 Basics of Design Engineering Reference Volume, vol. 64, No. 12, June 1992.

29. Incropera and DeWitt: "Fundamentals of Heat and Mass Transfer." Third edition, 1990.

30. Parsonage, T.: "Selecting Mirror Materials for High-Performance Optical Systems." Dimensional Stability, SPIE, vol. 1335, 1990, pp 119–126.

31. Paquin, R.: "Hot Isostatic Pressed Beryllium for Large Optics." Optical Engineering, vol. 25, No. 9, September 1986, p. 1004.

32. Killpatrick, D.H.: "Report on the Properties of Beryllium." Oak Ridge National Laboratory, May 1990.

33. Swenson: "HIP Beryllium: Thermal Expansivity From 4 to 300 K and Heat Capacity From 1 to 108 K." Journal of Applied Physics, vol. 70(6), September 1991.

34. Anon., "CVD Silicon Carbide™." CVD Materials, Technical Bulletin No. 107, Morton Advanced Materials, date unknown.

35. Anon., "UTOS Ceraform™ Silicon Carbide (Siliconized SiC)." United Technologies Optical Systems, date unknown.

36. Microsoft® Excel User's Guide for the Apple® Macintosh™, Version 1.03, copyright Microsoft Corporation, 1985 and 1986.

37. JSC-22964, Thermal Radiation Analyzer System (TRASYS) User's Manual, NASA, Johnson Space Center, April 1988.

38. MCR-86-594, Systems Improved Numerical Differencing Analyzer and Fluid Integrator (SINDA '85/FLUINT) User's Manual, Martin Marietta Corporation, Denver Aerospace.

39. I-DEAS™ Finite Element Modeling™ User's Guide, copyright, Structural Dynamics Research Corporation, Milford, OH, 1990.

40. I-DEAS™ Thermal Model Generator (TMG™), Version 6, Maya Heat Transfer Technologies Ltd., Montreal, PQ, Canada.

41. Jones, W.P., Watkins, J.R., and Calvert, T.A.: "Temperatures and Thermophysical Properties of the Lunar Outermost Layer." *The Moon 13*, D. Reidel Publishing Company, Dordrecht, Holland.

42. Walker, S.T., and Waters, R.: "Lunar Transit Telescope, Thermal Analysis and Control." LLT-004.

43. Campbell, R.W.: "Joint Ulysses and Galileo Orbiter RTG Requirements Specifications." August 23, 1989.

44. Marx, S., and Pfau, W.: *Observatories of the World.* Van Nostrand Reinhold Co., 1982.

45. Polites, M.: *Literature Search into Precise Pointing Systems for Balloon-Borne*

46. Fazio, G.: *Balloon-Borne Three-Meter Telescope for Far-Infrared and Submillimeter Astronomy.* Semiannual Status Report No. 4, Smithsonian Astrophysical Observatory, October 1985.

47. Perkin-Elmer Space Science Division, *NASA-MSFC Stabilized Balloon Platform Study Final Report.* February 1988.

48. MSFC Program Development, *Lunar Transit Telescope (LTT), 2-m Aperture UV/VIS/IR Telescope, A Feasibility Study*, January 1992.

49. The Math Works, Inc., *MATLAB*, South Natick, MA.

50. Mabie, H. and Reinholtz, C.: *Mechanisms and Dynamics of Machinery.* John Wiley & Sons, 1987.

51. Haug, E.J.: *Computer-Aided Kinematics and Dynamics of Mechanical Systems.* Allen and Bacon, 1989.

52. Fenn, R.C., and Gerver, M.J.: "Passive and Active Damping Enhancement Using Magnetostrictive Transduction." SatCon Technology Corp., NASA SBIR phase I Final Report, Contract No. NAS8-39828, Marshall Space Flight Center, August 1993.

53. Lockheed, McDonnell Douglas, GE, Honeywell, and IBM, "Space Station *Freedom* Work Package 02 Solar Alpha Rotary Joint Detailed Design Review," March 1993.

APPENDIX A

LUTE PRELIMINARY PROJECT PLAN

LUNAR ULTRAVIOLET TELESCOPE EXPERIMENT (LUTE)

PRELIMINARY PROJECT PLAN

NOVEMBER 12, 1993

PROJECT PLAN

LUNAR ULTRAVIOLET TELESCOPE EXPERIMENT (LUTE)

NOVEMBER 1993

APPROVAL:

T. J. Lee
Director
Marshall Space Flight Center

Wes Huntress
Associate Administrator
Office of Space Science

TABLE OF CONTENTS

1.0 INTRODUCTION
- 1.1 Purpose
- 1.2 Scope

2.0 PROGRAM SUMMARY

3.0 MISSION OBJECTIVES
- 3.1 Science
- 3.2 Lunar Science/Exploration Technology

4.0 BACKGROUND AND RELATED STUDIES

5.0 SUMMARY OF TECHNICAL PLAN
- 5.1 LUTE Description
- 5.2 LUTE Operations
  - 5.2.1 Integration/Test, Launch, and Flight Activities
  - 5.2.2 Communications
- 5.3 Technological Products

6.0 MANAGEMENT APPROACH
- 6.1 Introduction
- 6.2 Organization
  - 6.2.1 Office of Space Science
  - 6.2.2 Russian Space Program
  - 6.2.3 LUTE Task Team
    - 6.2.3.1 Task Team Manager
    - 6.2.3.2 Deputy Task Team Manager
    - 6.2.3.3 Chief Engineer
    - 6.2.3.4 Project Scientist
    - 6.2.3.5 Principal Investigators (PIs) and Universities
    - 6.2.3.6 Program Development
    - 6.2.3.7 MSFC Science Engineering (S&E) Directorate
    - 6.2.3.8 Project Control
  - 6.2.4 Procurement
  - 6.2.5 Safety & Mission Assurance (S&MA)
  - 6.2.6 Contracted Effort
- 6.3 Requirements Definition & Documentation
- 6.4 Schedule
- 6.5 Resources - Cost and Manpower Estimates
- 6.6 Risk Assessments

7.0 PROCUREMENT APPROACH

1.0 INTRODUCTION

1.1 Purpose

This document describes the planned activities, interfaces, and objectives for the MSFC developed Lunar Ultraviolet Telescope Experiment (LUTE). The New Ways of Doing Business (NWODB) philosophies will be used to achieve streamlined documentation which will evolve as the project progresses. This document will be used to satisfy documentation required between the Administrator and Program Associate Administrator (PAA) and the PAA and the Field Installation Directors (FIDs).

1.2 Scope

The scope of the LUTE project, as described by this plan, includes the in-house definition, design, development, production, integration/test, and operation of the LUTE with contracted effort only in specific areas of need.

This document will outline the management plan, technical interfaces, procurement strategy, schedule and resource estimate, and technical/ programmatic risks for the LUTE project. The NWODB for the LUTE project will be discussed as it applies to these areas.

2.0 PROGRAM SUMMARY

In 1989 a National commitment was made by the President of the United States to achieve the goals of human and robotic exploration of the Moon and Mars, as soon as possible, within the constraints of the national resources. The LUTE project will respond to these goals by developing a one meter ultraviolet telescope which will take advantage of the unique aspects of the moon to perform astrophysics astronomy. The LUTE will serve as a technological pathfinder for the design of future lunar surface instruments, as well as, as a scientifically viable, small, quick, inexpensive initial step in our return to the moon.

The LUTE project falls under the responsibility of the Office of Space Science. Through the authority of the Astrophysics Division of the Office of Space Science, the MSFC has been designated as the lead project management and development center for the LUTE. Close relationships will exist between NASA Headquarters, the LUTE Task Team, the Principal Investigator (PI) groups, and the Russian space program.

A cooperative effort to integrate the LUTE project with the Russian space program is envisioned for the lander, launch vehicle, and Radioisotope Thermoelectric Generator (RTG).

3.0 MISSION OBJECTIVES

3.1 Science

The LUTE will take advantage of the unique aspects of the moon (i.e., fixed rotation rates, vacuum environment, etc.) to perform astrophysics astronomy.

The LUTE will be able to produce an ultraviolet imaging survey of the universe over a larger fraction of the sky than has ever been produced. The astronomy performed by the LUTE will complement the earth orbiting telescope program. Furthermore, the data retrieved by the LUTE will support research on hundreds of astronomical point-sources, ranging from analysis of UV colors in main sequence stars to studies of active galactic nuclei and quasars.

The LUTE science will also be used in the educational and public outreach programs. The transmission of LUTE images will have direct application to science and astronomy at all levels of the educational system.

3.2 Lunar Science/Exploration Technology

The LUTE plans to serve as a pathfinder for the design of future lunar surface instruments. The LUTE will provide information about the lunar environmental effects on operational systems hardware by serving as a long duration exposure facility (2 year minimum). The operation of the LUTE will also provide important lunar engineering data in the area of material degradation due to the lunar thermal fluctuations, dust contamination, radiation, and vacuum effects. The information obtained by LUTE will be significantly beneficial to the future exploration missions to the Moon.

4.0 BACKGROUND AND RELATED STUDIES

The MSFC has gained experience in the definition, design, and development of telescopes through the Hubble Space Telescope. Furthermore, there are several conceptual telescope studies which have been developed prior to the LUTE. These precursor studies are depicted by Figure 4.0. This figure depicts how the desire for a lunar telescope started with the study of a large 16 meter telescope, the Large Lunar Telescope (LLT); was reduced in size and studied as a 4 meter cluster telescope, the Lunar Cluster Telescope Experiment (LCTE); and then was further reduced to the 2 meter Lunar Transit Telescope (LTT) before being studied as a 1 meter telescope.

The LTT went through an extensive feasibility study. This study, completed in early 1992, produced two significant documents: the LTT Feasibility Study (Doc #LLT-004, January 1992) and the LTT Project Description (March 1992). The LUTE is derived from the LTT study and therefore a brief overview of the LTT, taken from these two documents, is beneficial in understanding the origin of the LUTE.

The LTT study involved a fixed-declination, 2 m-class, optical telescope with an observing capability in the ultraviolet, visible, and infrared regions of the spectrum. This unmanned, transit telescope was to be placed on the lunar surface in the early stages of returning to the Moon.

The LTT used an all-reflective optical system composed of a very low weight two meter primary mirror plus the active optics of two correcting mirrors. The elements of the telescope, including the optics, the metering structure, the baffles, the light shield, and the sunshade were to be mounted on a central core structure which would also support the propulsion subsystem, the landing mechanisms and other subsystems serving the LTT.

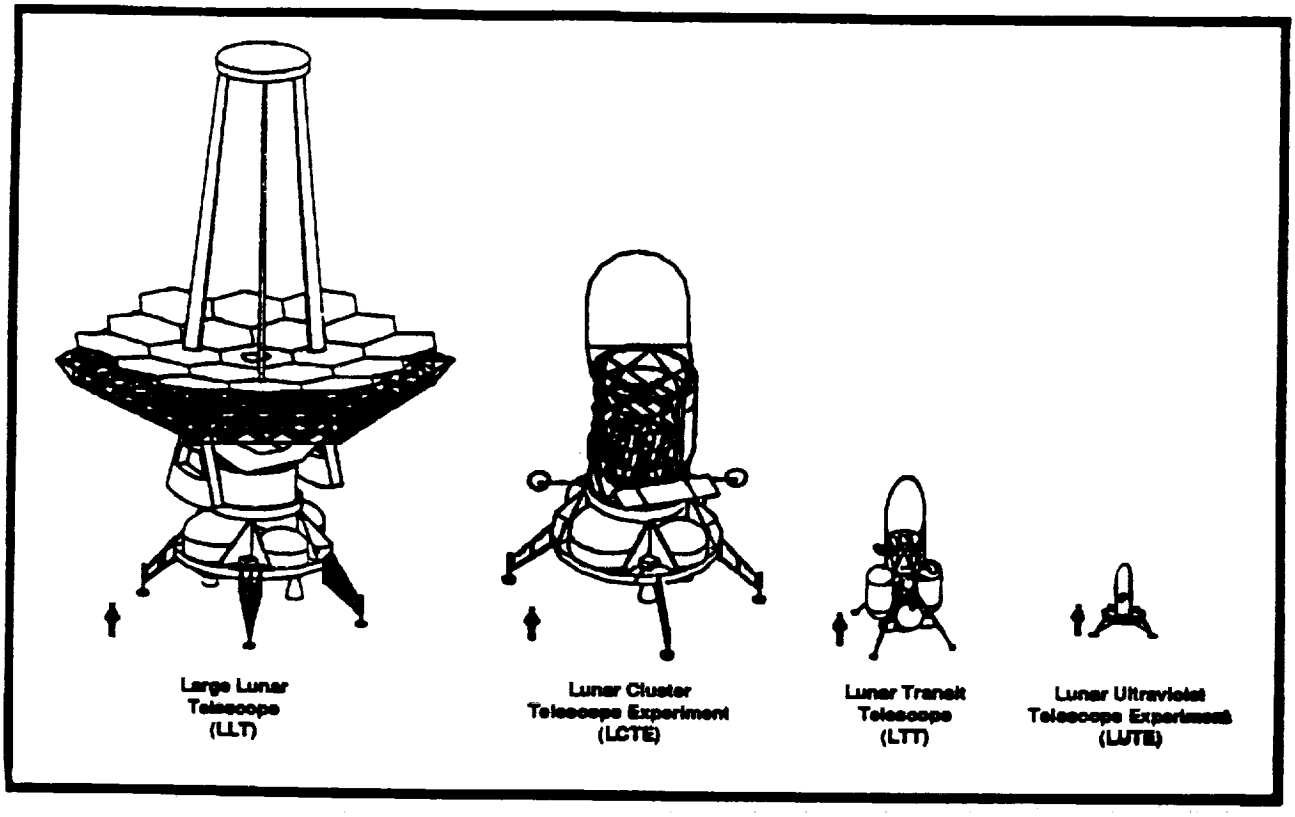

FIGURE 4.0 - LUTE Precursor Studies

The propulsion, power, communication, guidance, navigation, and reaction control and landing mechanism subsystems, were designed to place the LTT on the lunar surface accurately at a designated site with the required orientation. Once the LTT was settled on the Moon, the core structure, landing structures, and mechanisms were to serve as the pedestal and fixed mount for the telescope throughout science operations.

The landing subsystem concept developed during MSFC studies was to support the LTT mission in its initial configuration, and grow to meet the needs of future lunar observatories. The LTT integrated landing system/payload was planned for launch to the Moon aboard a Titan IV - Centaur launch vehicle.

The study showed that LTT could become a "flagship" project, leading the way to increased system procurement and management effectiveness. New, creative and imaginative management techniques were planned for application to the development of the LTT system to effect the maximum savings in time and cost.

The LUTE, being a smaller, less expensive telescope is a perfect place to start in the developmental evolution of these larger telescopes. The early operation of the LUTE will provide vital information which will facilitate larger lunar telescope design.

5.0 SUMMARY OF TECHNICAL PLAN

5.1 LUTE Description

The LUTE is a stationary, 1-meter ultraviolet optical telescope designed for a two year life on the Moon. (See Figure 5.1.) The LUTE will be the first major instrument to profit from the unique advantages of the Moon (i.e., a superstable astronomical platform with negligible atmosphere).

The LUTE will achieve a wide field of view with a compact three mirror optical system using lightweight mirror materials. The focal plane instrument is a two-dimensional mosaic of charge coupled devices (CCD's), arranged to give a 1.4-degree-wide field of view. The LUTE will not track specific targets, but will be pointed continuously at a chosen declination. As the Moon rotates about its axis during its 28-day period, the LUTE will observe continuously along a 1.4-degree-wide path across the celestial sphere.

The LUTE will produce a UV imaging survey of a swath of the universe to a limiting visual magnitude of 27 with high angular resolution and broad wavelength coverage. Each year the LUTE will survey greater than 300 square degrees of the celestial sphere with a resolution of 0.5 arcsec or better. Most of this swath will be examined at least 24 times to enable astrometric and variability assessments of interesting targets. The bandwidth accessible with the LUTE extends from 1000 to 3500 Å in three bandpasses currently assumed to be 800 Å wide. This ensures acquisition of a statistically complete sample of both point and extended sources which are bright in the UV.

The LUTE data will support research on hundreds of astronomical point-sources ranging from asteroid coma and cometary H and OH, through analysis of UV colors in main sequence stars, investigations of cataclysmic variables and accreting binaries, out to studies of active galactic nuclei and quasars.

The LUTE will also serve as a lunar long duration exposure facility. Its data stream will include information about the lunar environmental effects on operational lunar systems.

5.2 LUTE Operations

5.2.1 Integration/Test, Launch, and Flight Activities

Integration and end to end test of the LUTE will be performed at the MSFC. Integration of the LUTE to the Russian lander will be performed by MSFC personnel and the Russian lander organization. Testing of the integrated telescope/lander system will be performed at TBD.

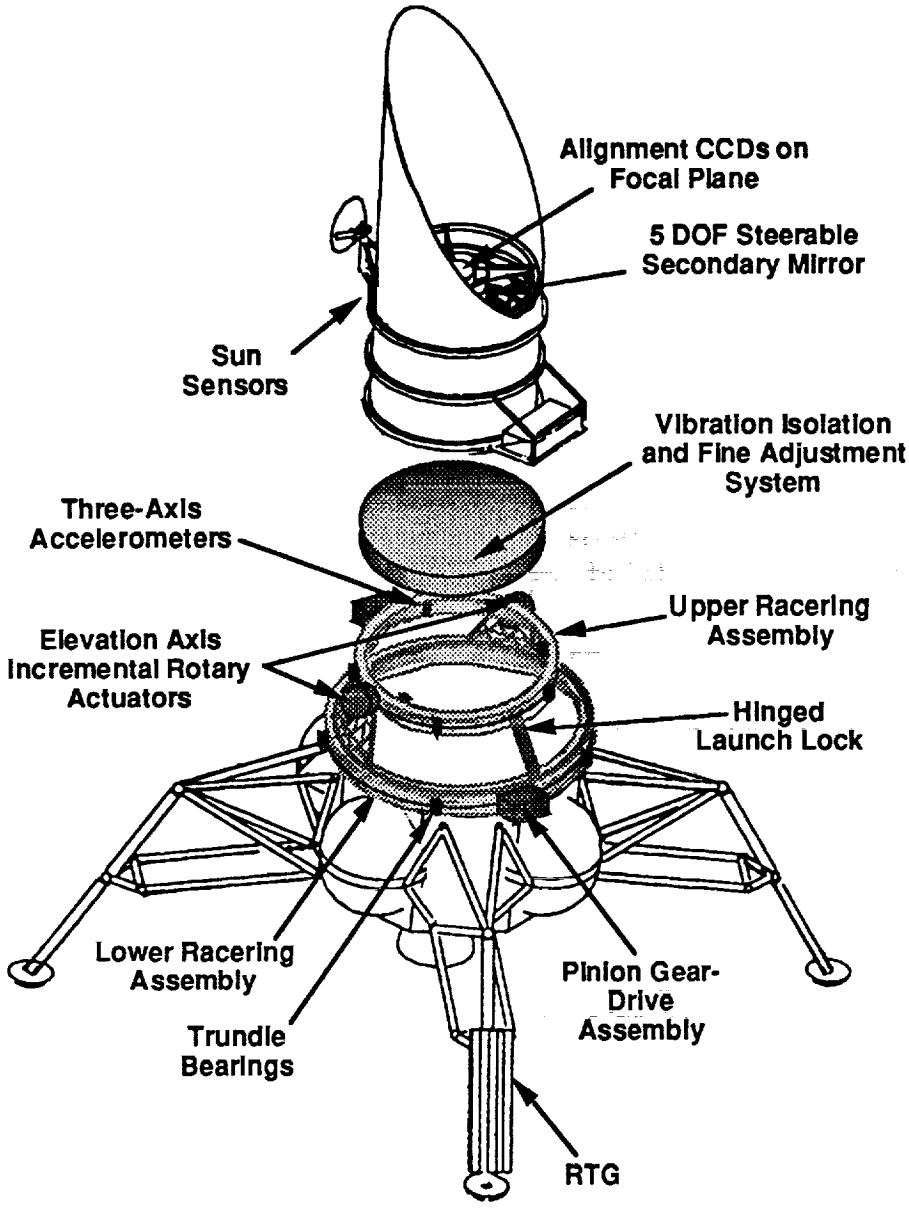

FIGURE 5.1 - Lunar Ultraviolet Telescope Experiment (LUTE) on a Generic Lander (Exploded View)

Integration of the telescope/lander system to an expendable launch vehicle will be done in conjunction with the Russian space program. All testing and control of the launch vehicle will be managed by TBD. Launch of the LUTE will occur at the TBD launch site.

Upon launch of the LUTE, control will be given to the MSFC. The flight will be monitored and controlled from the LUTE Operations Control Center (LOCC).

5.2.2 Communications

The LUTE will generate a continuous, minimum 200 kilobit telemetry stream to Earth utilizing the NASA Deep Space Network. Data will be routed to the LUTE Operations Control Center (LOCC) located at the TBD institution. The LOCC will process and distribute the downlink information from the LUTE to the Scientific Data Center (SDC), the Engineering Support Center (ESC), and the Educational and Media Service Center (EMSC). The LOCC will also provide the capability to control the instrument by ground initiated commands.

The SDC will distribute and archive the science information from the telemetry downlink for the scientific community. The ESC will provide information to engineering support personnel to monitor health and status of the LUTE. The EMSC will coordinate the dissemination of LUTE operations information to scientific, educational, and media services.

The LOCC will utilize many existing institutional electronic data transfer networks to communicate with the SDC, ESC, and the EMSC. These centers may be located within the LOCC or electronically connected.

5.3 Technological Products

Several technological products and contributions to future lunar telescopes will result from the LUTE project. Three significant areas where there will be technological contributions are in the thermal, structural, and pointing & alignment systems of the LUTE.

Innovative application of existing thermal control technology will result from the operation of the LUTE. Significant knowledge of material degradation and the lunar thermal environment will be applicable to any future lunar operations: habitats, unmanned science/robotic exploration missions, rover, etc.

In the structures area, the LUTE will (1) gain insight into the design of optical structures for large bulk temperature cycles and internal temperature gradients, (2) gain significant information into the design of telescopes for a surface gravity of one-sixth earth gravity, and (3) help to characterize the degradation of structural materials exposed to the lunar environment.

Long term attitude and alignment sensing will require the development of sun sensors, LED systems, star trackers, and other sensors that will operate accurately in the lunar thermal and dust environment. This development will not only be necessary for future lunar telescopes, but for any structure requiring precision alignment and knowledge.

6.0 MANAGEMENT APPROACH

6.1 Introduction

The management of the LUTE project will involve the use of new philosophies to minimize cost and schedule. These NWODB include: streamlined documentation and review process, concurrent engineering, organization of

task team in Phase A, integration of Program Development and S&E personnel in Phase A, more extensive Phase B, and others.

6.2 Organization

The proposed LUTE Organization is shown in Figure 6.2. The organizational structure, which specifically addresses the Phase A study, reflects the integration of Program Development and S&E personnel. This new way of doing business deals with the importance of having all parties involved in the project in its earliest stages to facilitate a smooth transition into later stages of the project.

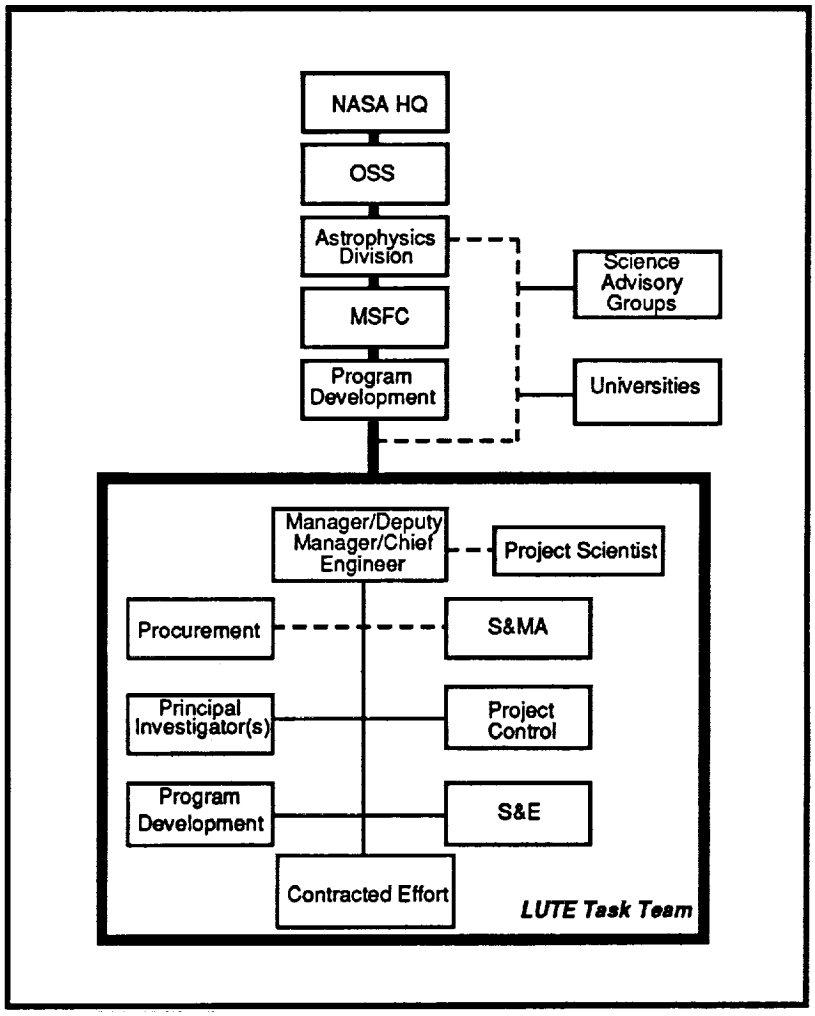

FIGURE 6.2 - LUTE Project Organization

In the following paragraphs, the responsibilities for the organizations shown in Figure 6.2 will be described. These responsibilities will evolve into more detailed tasks as the project progresses.

6.2.1 Office of Space Science

The Astrophysics Division of the Office of Space Science has overall responsibility for the LUTE. The Astrophysics Division has designated the MSFC as the lead project management and development center for the LUTE.

6.2.2 Russian Space Program

TBD

6.2.3 LUTE Task Team

6.2.3.1 Task Team Manager

The LUTE Task Team Manager is responsible for the overall management of the LUTE's definition, design, development, integration, test, and operation within the constraints of cost, schedule, and performance. Furthermore, the Task Team Manager is responsible for the

- development of the LUTE goals and objectives;
- management of contracts and agreements with industry, universities, other NASA centers; and International Space Agencies
- maintenance of management milestones and reviews; and
- integration of all mission elements.

6.2.3.2 Deputy Task Team Manager

The Deputy Task Team Manager assists and supports the Task Team Manager in the overall management of the LUTE as described in 6.2.3.1 and serves as Task Team Manager in his absence.

6.2.3.3 Chief Engineer

The Chief Engineer is responsible for the engineering and technical aspects of the LUTE project. The Chief Engineer is responsible for

- the identification of engineering required to accomplish the project,
- ensuring staffing to address project engineering and technical aspects, and
- the identification of technical issues which require resolution.

6.2.3.4 Project Scientist

The LUTE Project Scientist is responsible for the science definition and integration. The Project Scientist is responsible for the

- development of the LUTE science rationale, goals, and objectives;
- participation in the planning of mission science operations to ensure the attainment of mission goals; and
- consultation with the LUTE Task Team Manager on all science matters.

6.2.3.5 Principal Investigators (PIs) and Universities

The Principal Investigators will be responsible for

- supporting the development of the LUTE science rationale, goals, and objectives;
- participation in the planning of mission science operations;
- definition and design of the focal plane instrument; and
- consultation with the LUTE Task Team Manager and Project Scientist on all science matters.

6.2.3.6 Program Development

The Program Development Directorate has the overall authority for the LUTE Task Team. Personnel from the Program Development support in the subsystem definition and design of the LUTE. Subsystem support is provided in the following areas: thermal analysis, electrical power, communications & data management, configurations/mechanisms, pointing & alignment, and structures.

6.2.3.7 MSFC Science & Engineering (S&E) Directorate

The S&E Directorate is supporting the Task Team by providing personnel in the definition and design phases. These personnel are responsible for

- overall design integration of the optical system;
- focal plane instrument software design and integration; and
- support to the LUTE design in the following areas: systems analysis, operations, structures, electrical power, communications & data management, pointing & alignment, thermal control, mechanical design, stress & dynamics, materials, fabrication planning, software planning, and integrated test planning.

6.2.3.8 Project Control

The Project Control function of the LUTE Task Team is made up of personnel from the Program Development Directorate. The functions of these personnel are as follows:

- cost estimation for the design, development, production, and operation of the LUTE;
- overall project planning: development, maintenance, and monitoring of schedules; development and management of logic networks; and
- overall resource management: establish and control cost and manpower requirements and the implementation of procurement strategies.

6.2.4 Procurement

The procurement organization will provide the necessary support to develop and facilitate the acquisition of the optical telescope assembly and detector for the LUTE.

6.2.5 Safety & Mission Assurance (S&MA)

S&MA will provide the safety, reliability, and quality functions during all phases of the LUTE project.

The systems safety function of the LUTE Task Team will be provided by the Systems Safety Engineering Office. Their responsibilities will include the following:

- During the Feasibility and Concept Phase (Phase A), a preliminary hazard assessment based upon the Phase A LUTE configuration will be performed.
- During the definition phase, the LUTE System Safety Plan will be developed and specific safety criteria will be established.
- During the design phase, a detailed LUTE hazard analysis and safety assessment will be performed. An integrated LUTE and lander hazard analysis will also be performed.

The reliability function will be provided by the Systems Safety and Reliability Office. Their responsibilities will include the following:

- A reliability program plan will be prepared and coordinated with the LUTE Task Team during the Feasibility and Concept Phase (Phase A). The reliability plan will address the appropriate set of tasks and requirements to assure a project reliability commensurate with the designed "class of payload" and acceptable project risks. The plan will address in-house required tasks as well as identification of the reliability effort to be performed under any contracted agreements.
- Basic reliability tasks will be performed starting with the Definition Phase (Phase B) and proceeding through the Design/Development Phase (Phase C/D). These tasks include: Failure Mode and Effects (FMEA) and Critical Items List (CIL) preparation, support to the design review process, problem reporting and assessment, and acceptability of the EEE parts program.

6.2.6 Contracted Effort

To date, the known contracted effort will include the procurement of the 1-meter optical assembly and the detector. These are long lead procurement items which must be procured as early in the process as possible. Specialized testing of the LUTE will also be a contracted effort, however, the specific testing required will be defined early in Phase B.

6.3 Requirements Definition & Documentation

During Phase A, the LUTE requirements will be developed, maintained, and integrated by the LUTE Task Team and approved by the LUTE Task Team Manager. The required documentation is depicted in Figure 6.3.

6.4 Schedule

The LUTE schedule is shown in Figure 6.4. The schedule was developed as a five year in-house development using NWODB which includes a streamlined requirements and design review process. The LUTE project will meet all required programmatic documentation and reviews according to NMI 7120.4. Generic years are used after 1993 pending Phase B go ahead decision and out year funding commitment.

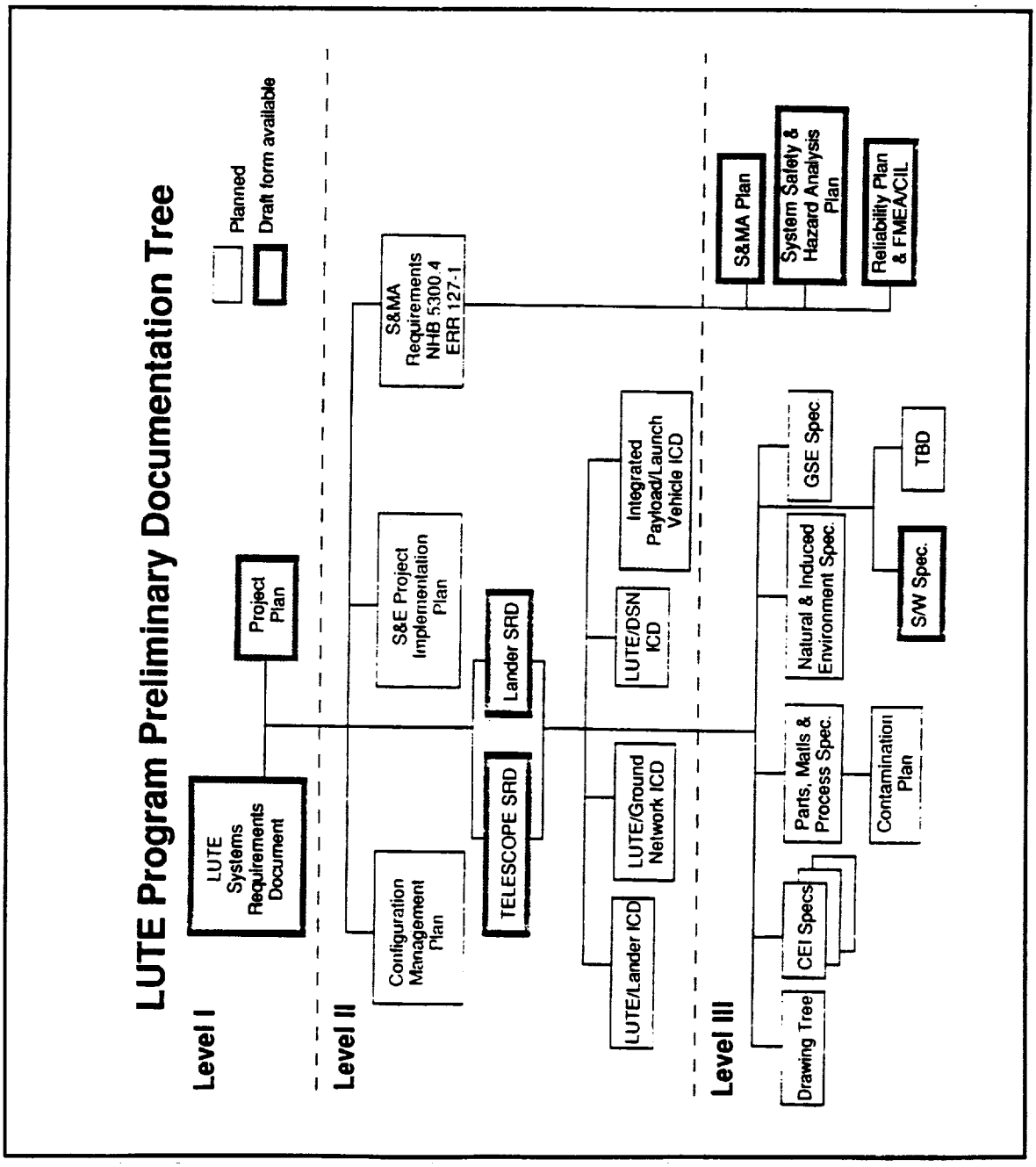

Figure 6.3 Documentation Matrix

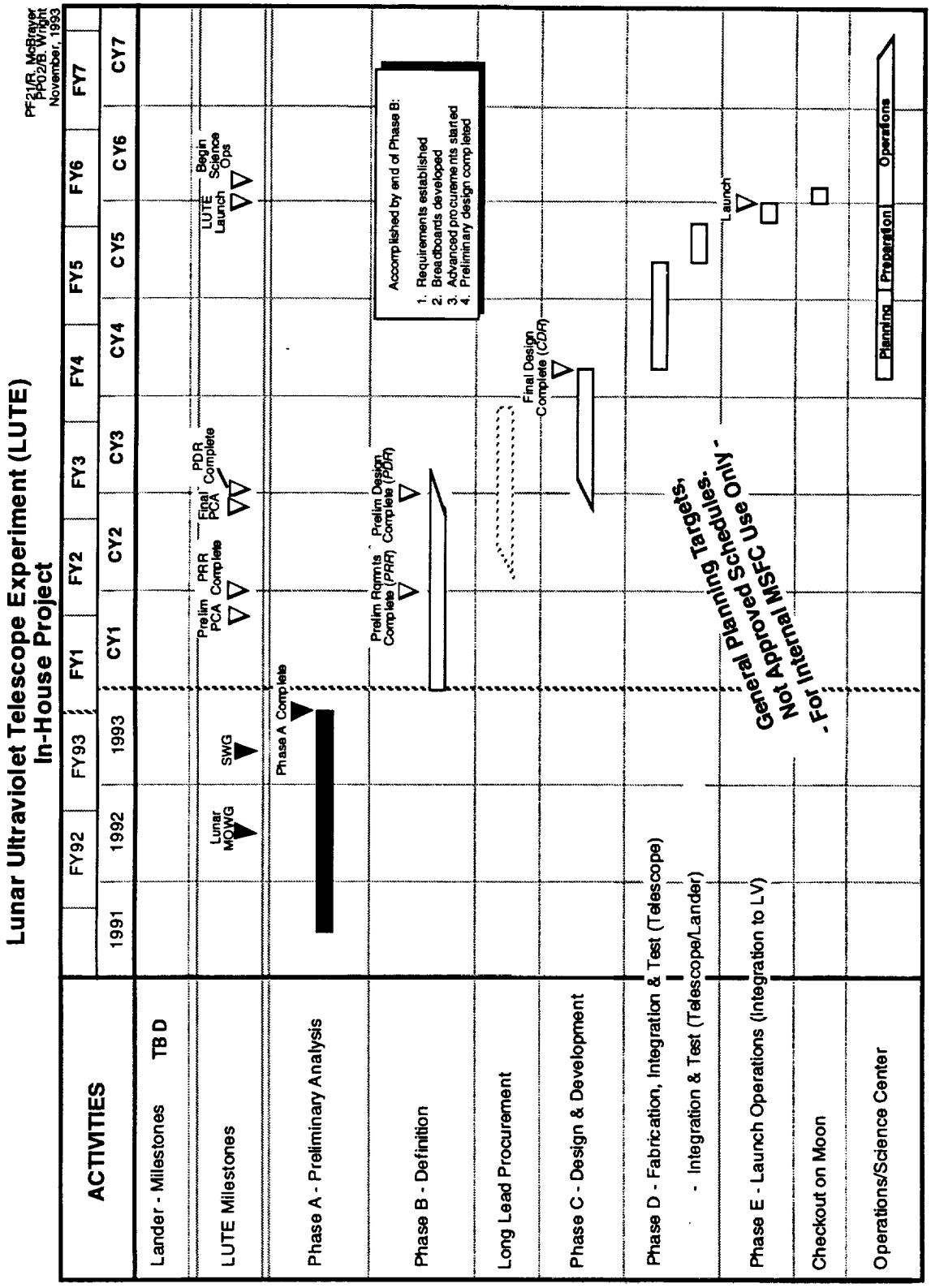

FIGURE 6.4 LUTE Schedule

6.5 Resources - Cost and Manpower Estimates

The LUTE cost estimate is based on standard parametric assumptions and techniques. The estimate is for the design, development, and build of a single flight telescope with corresponding supporting subsystems. Costs are also estimated for an in-house Phase B, ground systems development, and post-flight operations. Descriptions of the telescope and supporting subsystems provided by the LUTE Task Team form the inputs to the estimate.

Several key assumptions are made concerning the planned development of LUTE in order to facilitate the cost estimate. Among these assumptions are the following: in-house design, development, and build; standard integration, fee, and contingency percentages; use of a 60% cost/50% time beta curve to spread the cost; and use of the latest NASA Headquarters Inflation Index for all cost escalation. The most important assumption is the New Ways of Doing Business (NWODB) factors to reduce the cost. These factors assume that changes will be made in the way that NASA does business, thus reducing cost. The NWODB include a more extensive Phase B, multi-year funding stability, enhanced quality/management methods, advanced design methods, and procurement/contract management reform.

The cost models used for the LUTE estimate are the MSFC Instrument Cost Model to estimate the telescope cost and the NASA Cost Model (NASCOM) to estimate the supporting subsystems cost. The detector costs are provided by the Space Science Lab (SSL) and the RTG costs are provided by the Department of Energy (DOE). Ground systems development cost is estimated using the GSFC Ground Systems Cost Model. Operations and data analysis cost is based on the JSC Spacecraft Operations Cost Model. In-house manpower is determined using analogies to previous in-house NASA projects and MSFC developed estimating relationships. All estimates assume a protoflight approach.

The current cost estimate includes all expected costs from Phase B through launch, plus two years of operations. Only two items are not costed: the launch vehicle and the lander. Though these items represent a cost to NASA, it is not expected that the cost will be attributed to the LUTE project.

The baseline cost and manpower estimate is $168.3 million and 366 civil service man-years (see Figures 6.5A and 6.5B). These numbers are based on a one year Phase B, a four-year development schedule with Phase C/D start in FY93, launch in CY98, and two years of data analysis. NWODB credits are fully taken. Without the NWODB reductions, cost and manpower increase to $208.4 million and 481 man-years. (For comparison purposes, a total out-of-house approach with no NWODB reductions would cost $263.9M and require 185 man-years for the project office.)

6.6 Risk Assessments

Many technical and programmatic risk areas exist that could increase the cost of the LUTE mission. Technical areas of high risk are development of the detector array, thermal control of the detector, control of deformations in the optical system, and weight. The detector array is high risk because it involves the development of new technologies; the risk is always great for cost overruns when developing new technologies. The thermal control system is

complicated by the extreme temperature environment of the moon and the sensitivity of the optics (and other subsystems) to temperature gradients and changes.

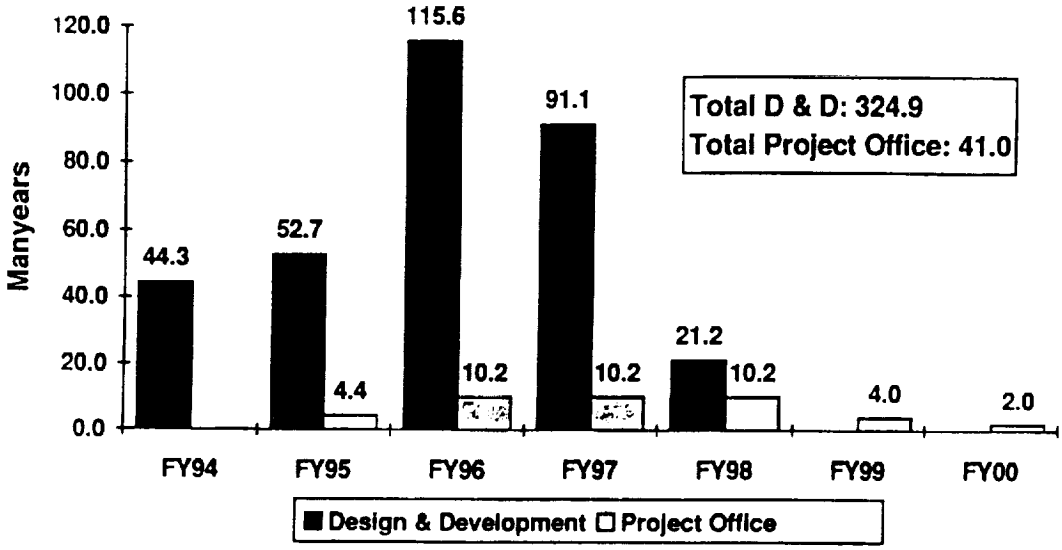

FIGURE 6.5A LUTE Civil Service Manpower Spread

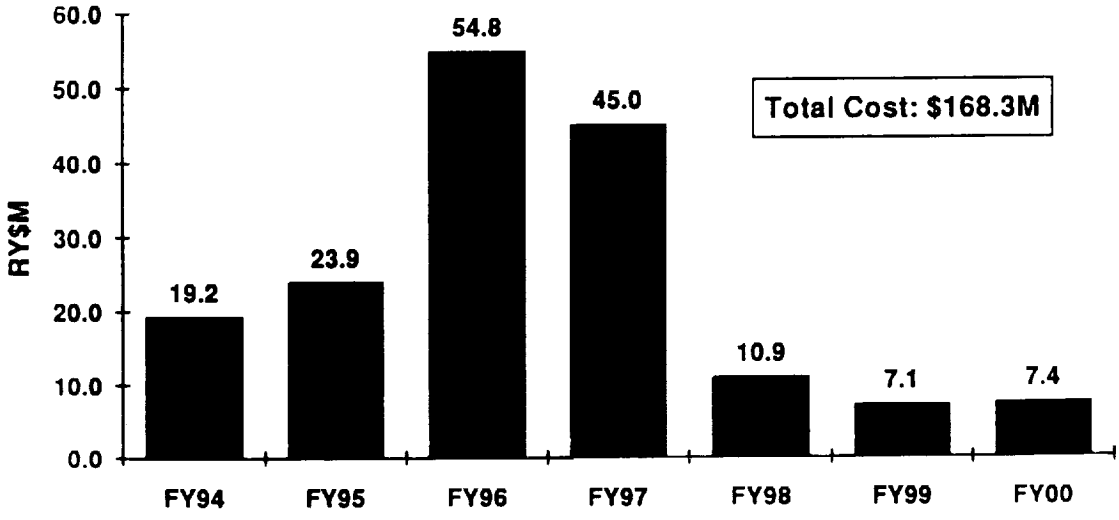

FIGURE 6.5B - LUTE Cost Spread

The largest programmatic risk is the use of the New Ways of Doing Business (NWODB) factors. Many of the cost reductions realized using these factors are beyond the control of the task team. If any of the NWODB assumptions are not met, cost increases will occur. Other programmatic assumptions that carry significant risk are unanticipated events during the in-house development effort which may require the use of outside engineering support. This engineering support may require additional expenditures. These uncosted items are not high risk, but are necessary and may require additional funds (a few can possibly be done totally in-house). These costs will either be charged directly to the project office or born by some other part of NASA.

7.0 PROCUREMENT APPROACH

The procurement approach for the LUTE involves some contracted activity in parallel with the MSFC in-house activity throughout the conceptual, definition, design, and development phases of the LUTE.

During the conceptual phase several studies, awarded as grants, were performed by universities. Also, several procurement contracts were initiated and completed with the optical industry and Small Disadvantaged Businesses. It is anticipated that the LUTE project will use these types of procurements to obtain other relevant studies in future phases of the project.

The only major procurement to be utilized by the LUTE project is the acquisition of the optical telescope assembly and the detector. It is anticipated that these items will be a long lead procurement, acquired through a full and open competition. The NWODB approach to managing this contract by using performance specifications (i.e., NASA as a technical advisor rather than monitor) will decrease cost and schedule.

APPENDIX B

LEVEL I SYSTEMS REQUIREMENTS DOCUMENT (LUTE)

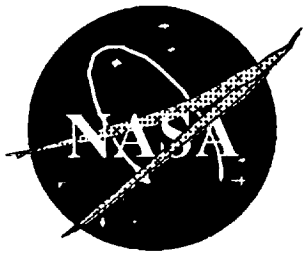

NASA-RQMT-XXXX
AUGUST 31, 1993

National Aeronautics and
Space Administration

National Aeronautics and Space Administration
Washington, D.C. 20546

D-R-A-F-T

LUNAR ULTRAVIOLET TELESCOPE EXPERIMENT

LEVEL I SYSTEMS REQUIREMENTS DOCUMENT

Prepared by:
Science and Engineering Directorate
Systems Analysis and Integration Laboratory
Systems Integration Division
Systems Integration Branch

Table of Contents

ACRONYMS AND ABBREVIATIONS 1
LEVEL I SYSTEMS REQUIREMENTS FOR THE LUTE PROJECT 2
1.0 SCOPE AND CONTROL 2
2.0 MISSION REQUIREMENTS 2
2.1 LUTE Mission 2
2.2 In-flight Transportation 2
2.3 Lunar Operational Life 2
2.4 Environmental Effects 3
2.5 Calibration 3
2.6 Verification 3
2.7 Ground Integration 3
3.0 FLIGHT SYSTEMS REQUIREMENTS 3
3.1 Telescope 3
3.1.1 Mission Requirements 3
3.1.2 Observatory Requirements 3
3.1.3 Telescope Subsystems Requirements 4
3.2. Lander 4
3.2.1 Mission Requirements 4
3.2.2 Operational Capability 5
3.2.3 Lunar Lander Subsystem Requirements 5
3.3 Integrated Payload Subsystem Requirements 6
3.3.1 Thermal Control Subsystem 6
3.3.2 Data Management Subsystem 6
3.3.3 Power Supply and Distribution Subsystem 6
3.3.4 Flight Software 6
4.0 SAFETY 7
5.0 RELIABILITY 7
6.0 MISSION GROUND SUPPORT REQUIREMENTS 7
6.1 LUTE Operations Support Center (LOSC) 7
6.2 LUTE Science Center (LSC) 7
6.3 Autonomy 7

ACRONYMS AND ABBREVIATIONS

CCAFS	Cape Canaveral Air Force Station
GN&C	Guidance, Navigation and Control
IP	Integrated Payload
km	kilometer
LOI	Lunar Orbit Insertion
LOSC	LUTE Operations Support Center
LSC	LUTE Science Center
LUTE	Lunar Ultraviolet Telescope Experiment
NASA	National Aeronautics & Space Administration
NASCOM	NASA Communications Network
NMI	NASA Management Instruction
OSSA	Office of Space Science and Applications
TBD	To Be Determined
TCS	Thermal Control System
TLI	Trans-Lunar Injection
UTC	Universal Time Coordinated
UV	Ultraviolet

LUTE PROJECT LEVEL I SYSTEMS REQUIREMENTS

1.0 SCOPE AND CONTROL

This program requirements document establishes the Level I requirements for the Lunar Ultraviolet Telescope Experiment (LUTE) program. Currently the LUTE program includes the development of both the LUTE and the Lunar Lander, which together form the Integrated Payload (IP). The IP is designated as a Class B payload per NMI 8010.1A in terms of the total approach to development, reliability, and quality assurance. The requirements specified in this document are established on the basis of science requirements which exist at the time of Phase A development of the program, and include functional, physical and procedural requirements for the LUTE mission. The LUTE system shall be designed to meet these requirements unless specific waivers have been approved by the Associate Administrator of the Office of Space Science and Applications (OSSA), NASA Headquarters. This is a Level I document that is controlled, and maintained at Level I by NASA Headquarters, OSSA.

2.0 MISSION REQUIREMENTS

2.1 LUTE Mission

The LUTE mission is to transport an ultraviolet(UV) astronomical observatory to the lunar surface and to collect useful astronomical data during the operational life of the experiment for both scientific and educational purposes. The two year mission of the LUTE will be to ensure acquisition of a statistically complete sample of both point and extended sources which are bright in the UV. By utilizing the moon and its natural rotation as a moving observation platform, the UV telescope will gather scientific data and relay it to earth for analysis.

2.2 In-flight Transportation

2.2.1 The LUTE shall be delivered to a nominal low earth orbit by TBD {Atlas IIAS/Proton} Launch vehicle.

2.2.2 The TBD {Centaur} upper stage shall initiate the first phase of Trans-Lunar Injection (TLI) and the main propulsion system of the Lunar lander shall complete TLI.

2.2.3 The Lander shall provide a controlled, powered descent to the predetermined landing site.

2.3 Lunar Operational Life.

2.3.1 The LUTE shall be have a 2 year fully operational life, with operations continuing after the 2 years as capabilities allow.

2.3.2 The LUTE shall be considered fully operational if all subsystems are functioning to their design requirements.

2.3.3 The LUTE shall be considered operational as long as useful science data can be obtained.

2.3.4 The IP systems shall have a fail-safe fail-op capability to assure safety and operability of all LUTE systems and subsystems after launch.

2.4 Environmental Effects.

All reasonable precautions shall be taken during development, transportation, launch, and operations to protect against environmental conditions which could jeopardize the scientific performance of the LUTE.

2.5 Calibration

The LUTE shall be calibrated on the ground and on the lunar surface to provide quantitative values to all parameters which will be required for future data analyses. The calibrations shall be performed with the goal of determining the operational performance with accuracies of 1 percent or better, whenever scientifically important and technically feasible.

2.6 Verification

A verification program for a Class B payload shall be conducted to insure that the LUTE meets all program requirements. The verification program shall include the transmission of data through the NASA Communication Network (NASCOM), Lunar Operations Support Center (LOSC), LUTE Science Center (LSC), to demonstrate the compatibility of ground support systems. The verification program shall insure the interface compatibility between the LUTE/Lander and launch vehicle.

2.7 Ground Integration

2.7.1 The LUTE and Lander shall undergo final acceptance prior to delivery to the launch site {CCAFS/TBD}. Final integration and verification of launch readiness shall occur at the launch site.

2.7.2 Ground integration activities shall be compatible with existing launch site facililities.

3.0 FLIGHT SYSTEMS REQUIREMENTS

3.1 Telescope

3.1.1 Mission Requirements

3.1.1.1 The Telescope shall provide for viewing within approximately 10° of the Galactic pole.

3.1.1.2 The Telescope placement and viewing direction shall minimize the optical depth of the geocorona through which observations must be made.

3.1.2 Observatory Requirements

3.1.2.1 The observatory shall be a wide field, three mirror, aplanatic ultraviolet Telescope with a nominal 1.0 meter aperture.

3.1.2.2 The observatory shall be a capable of imaging a 1.4-degree-wide field of view.

3.1.3 Telescope Subsystems Requirements

3.1.3.1 Optical Subsystem

3.1.3.1.1. The optical subsystem shall have a nominal back focal length of TBD {65} cm, and a nominal outer diameter of 1.0 m.

3.1.3.1.2. The optical subsystem shall have a focal ratio of TBD {3} (F/3).

3.1.3.1.3. The optical subsystem shall produce UV imaging in a bandwidth that extends from approximately 1000Å to 3500Å in three band passes 800Å in width (exact limits TBD).

3.1.3.2 Structural Support Subsystem

The LUTE structural support subsystem shall provide the structure to mount all associated subsystems and the three-mirror observatory.

3.1.3.3 Pointing Control Subsystem

After landing, the Pointing Control Subsystem shall be capable of making a one-time adjustment to the LUTE subsystems to position them in the orientation needed to fulfill requirement 3.1.1.3.

3.1.3.4 LUTE Contamination Control

The LUTE contamination control shall prevent catastrophic loss of subsystems.

3.2. Lander

3.2.1 Mission Requirements

3.2.1.1 The lunar lander shall be capable of delivering the LUTE Telescope to within TBD km of a specified landing site.

3.2.1.2 The Lander shall deliver LUTE to the lunar surface without disrupting the operability of the LUTE systems.

3.2.1.3 The Lander shall provide the final stage of trans-lunar injection (TLI), lunar orbit insertion (LOI), and descent to the lunar surface.

3.2.1.4 The Lander systems and subsystems shall not interfere with LUTE performance.

3.2.1.5 The Lander shall determine and transmit landing site orientation and coordinates after stabilization on the lunar surface.

3.2.2 Operational Capability

3.2.2.1 As a platform, the lander shall have a 2-year fully operational life, with operations continuing after the 2 years as capabilities allow.

3.2.2.2 The Lander systems not common with LUTE shall operate on the lunar surface only to the point of ensuring the safety and operability of the LUTE systems.

3.2.3 Lunar Lander Subsystem Requirements

3.2.3.1 Propulsion Subsystem

3.2.3.1.1 The Lander shall provide the thrust required to execute TLI, LOI, and a controlled landing.

3.2.3.1.2 The propulsion subsystem shall generate control torques to achieve and maintain vehicle attitudes during TLI, LOI, and landing.

3.2.3.2 Structural Support Assembly

3.2.3.2.1 The Lander shall provide a structural interface with fixed mounting points to support all LUTE systems.

3.2.3.2.2 The Lander shall be capable of supporting static and dynamic loads incurred on the IP during all preflight, flight, landing, and operation phases.

3.2.3.2.3 The Lander shall provide a post-landing stable platform.

3.2.3.3 Guidance, Navigation and Control (GN&C) Subsystem

The GN&C subsystem shall maintain attitude and directional control during all phases of the flight from TLI to lunar landing.

3.2.3.4 Tracking Subsystem

The Lander shall incorporate a tracking subsystem to support descent and landing.

3.3 Integrated Payload Subsystem Requirements

3.3.1 Thermal Control Subsystem

3.3.1.1 The TCS must accommodate a variety of flight attitudes during all phases of the mission.

3.3.1.2 The TCS shall provide the capability to keep all IP subsystems operational within the temperature limits of the lunar environment.

3.3.1.3 The TCS shall minimize power consumption and subsystem weight.

3.3.2 Data Management Subsystem

3.3.2.1. Transmission Links

3.3.2.1.1. All normal data transmissions to and from the IP shall be via the Deep Space Network and NASCOM.

3.3.2.1.2. The Data Management Subsystem shall be capable of simultaneous and separate transmission of science and engineering data.

3.3.2.2 Data Acquisition

3.3.2.2.1 Data shall be recorded and transmitted with high accuracy and reliability such that no more than 5% of the acquired data shall be lost in transmitting data from the spacecraft to the LSC.

3.3.2.2.2 All flight and ancillary data (i.e., translunar flight coordinates, lunar landing location, universal time, etc.) shall be available to the LSC within 72 hours after receipt at the LOSC.

3.3.3 Power Supply and Distribution Subsystem

The Power Supply and Distribution Subsystem shall provide sufficient power to all of the IP systems.

3.3.4 Flight Software

3.3.4.1 The IP Flight Software shall provide the data processing modules necessary to control and monitor all aspects of the IP operations.

3.3.4.2 The Flight Software shall provide the capability to restore memory data in the onboard computer and also provide the capability to dump the onboard computer memory to ground support.

4.0 SAFETY

The design of the LUTE integrated payload shall assure that safety of the Launch Vehicle, launch vehicle operations personnel and ground support personnel are not compromised at any time under normal or any credible mode of operation.

5.0 RELIABILITY

Except for structural assemblies, including pressure vessels, no credible single point failure will jeopardize the mission. No two credible failures shall cause loss of life or damage to surrounding facilities (transporters, launch pads, launch vehicle, etc.).

6.0 MISSION GROUND SUPPORT REQUIREMENTS

6.1 LUTE Operations Support Center (LOSC)

The LOSC shall provide the ability to monitor, evaluate, operate, and control the performance of all LUTE flight systems for the duration of the LUTE mission and shall provide a communications link from the IP to the LSC.

6.2 LUTE Science Center (LSC)

The LSC shall provide science planning, data reduction and analysis, archiving and dissemination of data, and a focal point for interaction with the scientific community.

6.3 Autonomy

The LUTE shall be designed with an appropriate balance between autonomous operation and supporting ground communication and interaction, in a manner to maximize life and minimize life cycle costs.

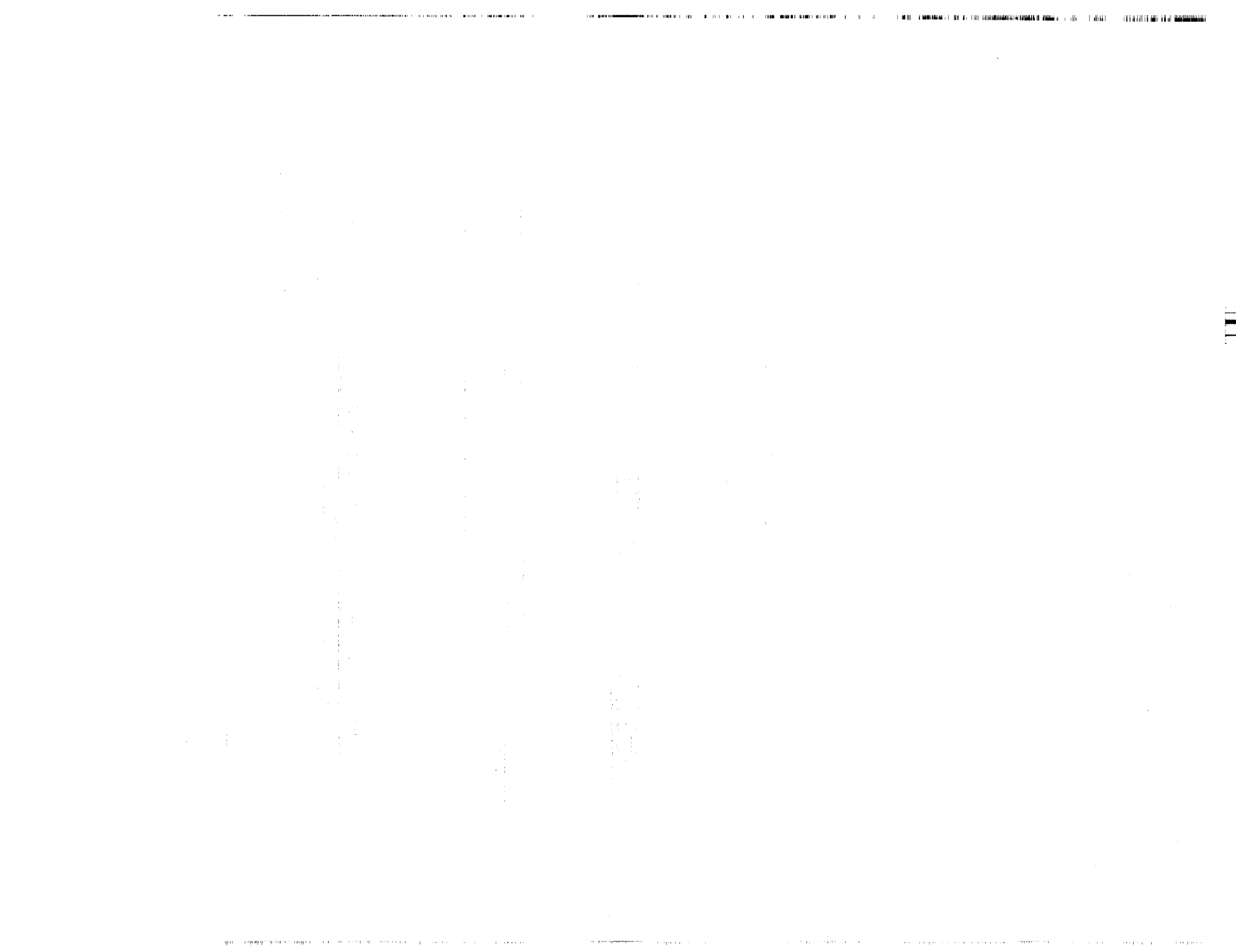

APPENDIX C

LEVEL II SYSTEMS REQUIREMENTS DOCUMENT (TELESCOPE)

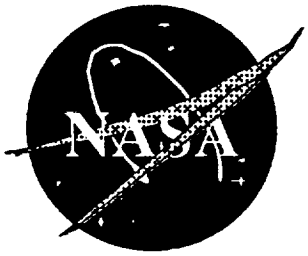

MSFC-RQMT-XXXX
September 3, 1993

National Aeronautics and
Space Administration

George C. Marshall Space Flight Center
Marshall Space Flight Center, Alabama 35812

D-R-A-F-T

LUNAR ULTRAVIOLET TELESCOPE EXPERIMENT

TELESCOPE

LEVEL II SYSTEMS REQUIREMENTS DOCUMENT

Prepared by:
Science and Engineering Directorate
Systems Analysis and Integration Laboratory
Systems Integration Division
Systems Integration Branch

Lunar Ultraviolet Telescope Experiment (LUTE)
Level II Systems Requirements Document

PREPARED BY:

EL44 DATE

APPROVED BY:

PF21 DATE
LUTE Project Manager

APPROVED BY:

EL44 DATE
Chief,
Systems Integration Branch

EJ23 DATE
LUTE Chief Engineer

EL41 DATE
Chief,
Systems Integration Division

STRESS (ED01) DATE

EL01 DATE
Director, Systems Analysis
and Integration Laboratory

MATERIALS (EH01) DATE

Release Date: ___/___/___	Marshall Space Flight Center **SPECIFICATION/DOCUMENT CHANGE INSTRUCTION** **Spec./Doc. No.** _____	Page of _____ Copy No.:

Change No./Date	SCN/DCN No./Date	CCBD No./Date	Replacement Page Instructions

MSFC-Form 4140 (Revised September 1990)

NOTE: After revising the document, file this sheet in document preceeding Table of Contents

TABLE OF CONTENTS

LIST OF FIGURES vi
ACRONYMS AND ABBREVIATIONS vii
1.0 INTRODUCTION 1
1.1 Purpose 1
1.2 Scope 1
1.3 Document Format 1
1.4 Project Description 1
1.5 Control 2
1.6 Reference Configuration 3
2.0 APPLICABLE DOCUMENTS 4
3.0 REQUIREMENTS 7
3.1 Mission Requirements 7
3.1.1 In-Flight Transportation 7
3.1.2 Mission Parameters 7
3.1.3 Landing Orientation 7
3.1.4 Lunar Operational Life 8
3.2 Operational Requirements 8
3.2.1 IP Configuration 8
3.2.2 Launch Configuration 8
3.2.3 Ground Operations 8
3.2.4 Flight Operations 8
3.2.5 Post-landing 9
3.3 Optical Systems 10
3.3.1 Field of View 10
3.3.2 Wavelengths 10
3.3.3 Sensitivity 10
3.3.4 Stray light 10
3.4 Electrical Power System 11
3.4.1 Power Usage 11
3.4.2 Continuous Operation 11
3.4.3 EPS Interfaces 11
3.4.4 Wire Protection 11
3.4.5 Electrical Grounding 11
3.5 Reserved 11
3.6 Ground Support Equipment (GSE) 11
3.6.1. Mechanical Ground Support Equipment (MGSE) 11
3.6.2 Electrical Ground Support Equipment 11
3.6.3 Ground Support Software 11
3.6.4 Servicing 11
3.7 Propulsion 11
3.8 Thermal Control System TCS 12
3.8.2 Optical Temperature/Gradient Requirements 12
3.8.3 Detector Temperature Requirements 12
3.8.4 Electronics Temperature Requirements 12
3.8.5 Mechanisms 12
3.10 Communications and Tracking System (C&TS) 13
3.10.1 Functional Requirement 13
3.10.2 DSN Compatibility 13
3.10.3 Uplink and Downlink Transmission 13
3.10.4 High Gain Antenna (HGA) 13

3.10.5 Data Transmission 13
3.11 Data Management System 13
3.11.1 Functional Requirements 13
3.11.2 Timing and Clock Frequencies 13
3.11.3 Science and Engineering Data 14
3.11.4 Data Transmission Rates 14
3.11.5 Command Capability 14
3.11.6 Data Processing 14
3.11.7 Computer(s) Reloading 15
3.11.8 Error Detection and Correction 15
3.12 Software 15
3.12.1 Software Management 15
3.12.2 Preflight Test Software 15
3.12.3 Flight Software Design Parameters 15
3.13 Mechanism and Pointing Control Systems 15
3.13.1 High Gain Antenna 15
3.13.2 Focal Plane Array 15
3.13.3 Optical Assembly 16
3.13.4 Light shade 16
3.13.5 Spider assembly 16
3.13.6 Steerable Secondary Mirror 16
3.14 Physical Standards 16
3.14.1 Coordinate System 16
3.14.2 Envelopes/Dimensions 16
3.14.3 Mass Requirements 16
3.14.4 NASA Standard Components 16
3.14.5 Measurement Unit System 16
3.14.6 Factors of Safety 17
3.14.7 Fatigue 17
3.15 Reliability Requirements 17
3.15.1 Single Point Failure 17
3.16 Maintainability Requirements 17
3.16.1 Fracture Control Program 17
3.17 Quality Assurance Requirements 17
3.18 Safety and Mission Assurance Requirements 17
3.18.1 S&MA Plan 17
3.18.2 Launch Vehicle Mission Assurance 17
3.18.3 Ordnance Devices 18
3.18.4 Range Safety 18
3.19 Environment Requirements 18
3.19.1 Natural Environment 18
3.19.2 Induced Environments 19
3.19.3 Contamination 20
3.19.4 Magnetic 20
3.20 Transportability/Transportation Requirements 20
3.20.1 Shipping Container Design 20
3.20.2 Transportation Environment 20
3.20.3 Prime Mode of Transportation 20
3.21 Storage Requirements 20
3.21.1 Storage Cleanliness 20
3.21.2 Shelf Life 20
3.21.3 On-pad Stay Time 20
3.22 Design and Construction Requirements 20
3.22.1 Main Optics System 20

3.22.2 Structural Support Assembly 21
3.22.3 Thermal Control System 23
3.22.4 Pointing Control System 24
3.22.5 Telescope Protection System 25
3.22.6 Data Management System 26
3.22.7 Power Distribution System 27
3.22.8 Weight Allocation 27
3.22.9 Materials Construction 28
3.22.10 Ground Support Equipment Design 29
3.23 Interface Requirements 29
3.23.1 Telescope to Science Instrument 29
3.23.2 LUTE to Lander 29
3.23.3 Telescope to Mirror Assembly 29
3.23.4 LUTE to Ground Systems 30
4.0 VERIFICATION 30
4.1 General 30
4.2 Verification Types 30
4.3 Verification Requirements Matrix 30
4.4 Verification Facilities and Equipment 30
4.5 Spacecraft Hardware Requirements 30
4.5.1 Payload Classifications 30
4.5.2 Previously Flown Hardware 30
4.5.3 Controlled Prototype Hardware 30
4.5.4 Off-the-shelf Parts 31
5.1 Preparation, Packaging and Shipment 31
6.0 NOTES 31
7.0 APPENDIX -- A Verification Matrix 31

LIST OF FIGURES

FIGURE	TITLE	PAGE
1-1	LUTE Documentation Tree	2
1-2	LUTE Coordinate System	3
1-3	LUTE Subsystems Configuration	3

ACRONYMS AND ABBREVIATIONS

Å	Angstrom
arcmin	arc minute
arcsec	arc second
B0	Star Class indication
BER	Bit Error Rate
CCD	Charge Coupled Devices
CVD	Chemical Vapor Deposition
DMS	Data Management System
DOF	Degrees of Freedom
DSN	Deep Space Network
EGSE	Electrical Ground Support Equipment
EPS	Electrical Power System
GSE	Ground Support Equipment
HGA	High Gain Antenna
Hz	hertz
ICD	Interface Control Document
ID	Inner Diameter
kg	kilogram
KSC	Kennedy Space Center
λ	Lambda (Wavelength measured in Å)
LOSC	LUTE Operations Support Center
LOST	LUTE Operations Support Team
LUTE	Lunar Ultraviolet Telescope Experiment
Ly-a	Lyman alpha
m	meter
MAPTIS	Materials and Processes Technical Information Systems
MgF_2	Magnesium Fluoride
MGSE	Mechanical Ground Support Equipment
micron	10^{-6} meters
MSFC	Marshall Space Flight Center
m_V	Visual Magnitude
NHB	NASA Handbook
NMI	NASA Management Instruction
OD	Outer Diameter
RF	Radio Frequency
rms	root mean square
rpm	revolutions per minute
RQMT	Requirement
RTG	Radio-isotope Thermal Generator
S&MA	Safety and Mission Assurance
SEI	Space Exploration Initiative
SI	International System of Units
SRD	Systems Requirements Document
TBD	To Be Determined
TCS	Thermal Control System
TLI	Trans-Lunar Injection
UTC	Universal Time Coordinated
{ }	Indicates possible value for TBD

LEVEL II SYSTEMS REQUIREMENTS FOR THE LUTE PROJECT

1.0 INTRODUCTION

1.1 Purpose

The purpose of this document is to define the Level II design and development requirements for the LUTE project. The performance requirements outlined in this document represent the minimum performance levels of the Telescope to be used in carrying out the requirements of the LUTE program throughout its mission life.

1.2 Scope

This document establishes the systems requirements for all elements of the LUTE and shall comply with the LUTE Level I Program Requirement Document.

1.3 Document Format

The Level II Systems Requirements Document (SRD) is organized in a standard format of five sections as described below.

Section Number	Title	Content
1.0	Introduction	Defines the purpose and scope of the document and includes a description of the LUTE project.
2.0	Applicable Documents	Lists the applicable documents cited in Section 3.0.
3.0	Requirements	Defines the functional and performance requirements imposed upon the LUTE design.
4.0	Verification	Defines the verification of Section 3.0 requirements.
5.0	Preparation for delivery	Instructions for preparation packaging and shipment.
6.0	Notes	
7.0	Appendix	

1.4 Project Description

The purpose of the LUTE program is to take advantage of the unique aspects of the lunar environment for astronomy observations in the ultraviolet wavelengths, collect environmental data to support the design of future lunar equipment, and to provide a source of educational material for wide distribution to primary and secondary educational systems both for the United States and the international community. The LUTE Lander shall both transport the LUTE telescope to the lunar surface and provide a stable platform for the Telescope

1.5 Control

This document shall be controlled at Level II by the MSFC Advanced Projects Office, Lunar Ultraviolet Telescope Experiment Task Team, PF21. For further reference regarding documentation flow, refer to Figure 1-1, below.

Figure 1-1 LUTE Systems Requirements Documentation Tree

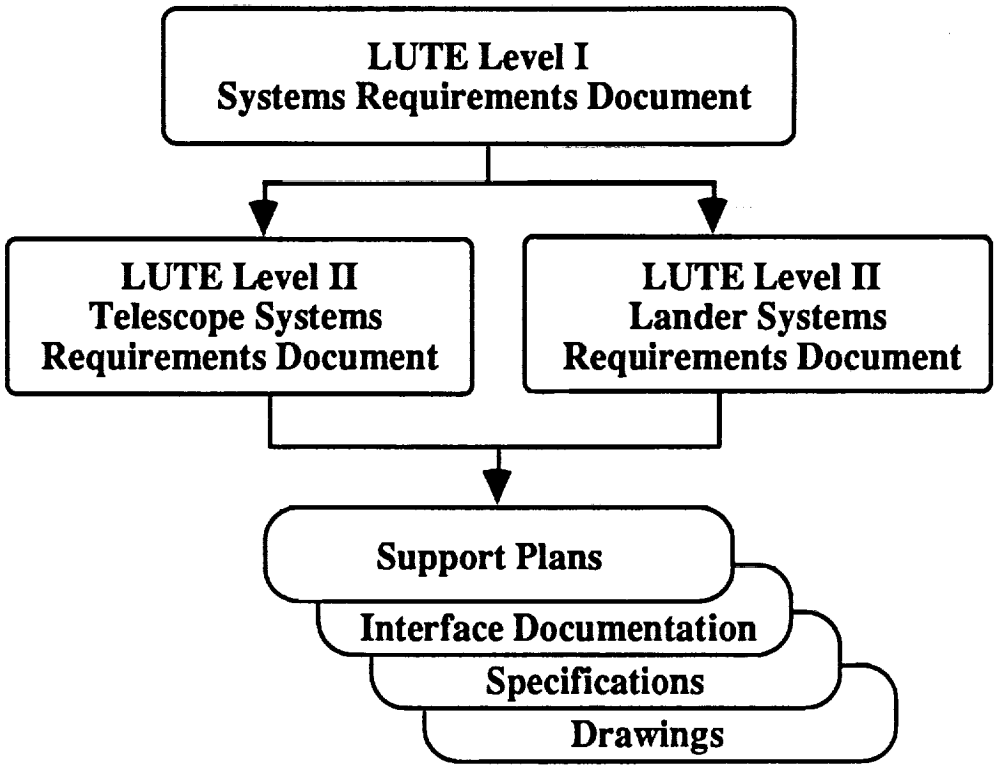

1.6 Reference Configuration

Figure 1-2 represents the coordinate system for the latest LUTE reference configuration.

Figure 1-2: LUTE Configuration Reference Coordinates

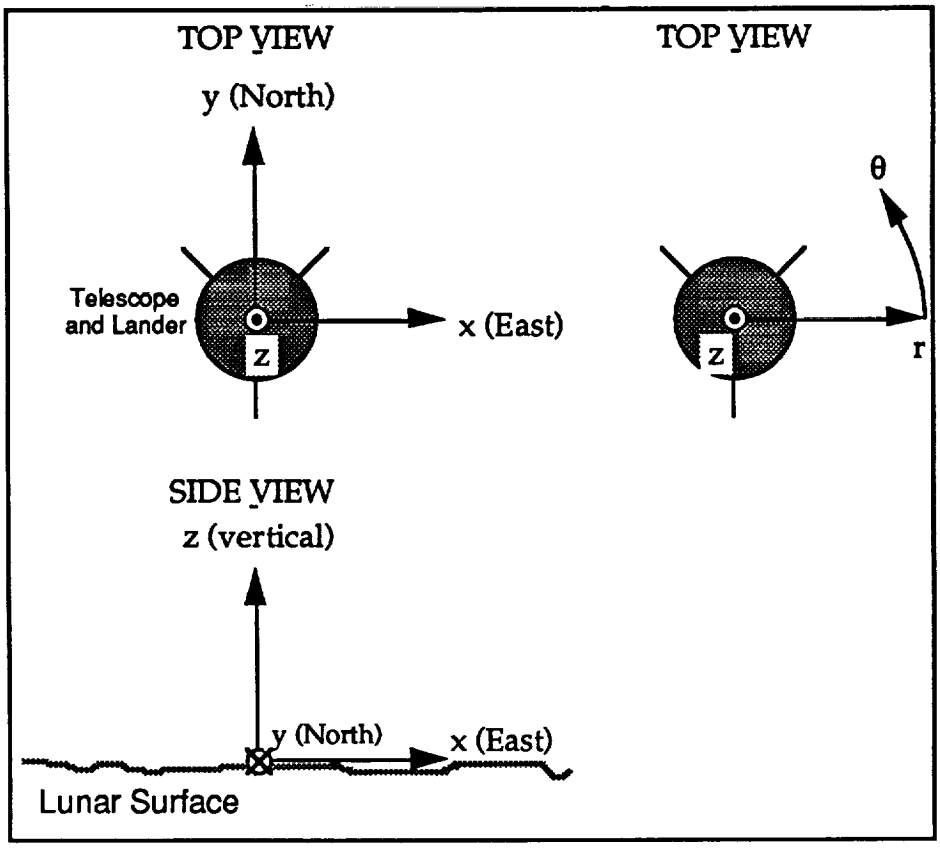

Figure 1-3 represents the latest reference configuration for the LUTE subsystems.

Figure 1-3 Telescope Reference Configuration

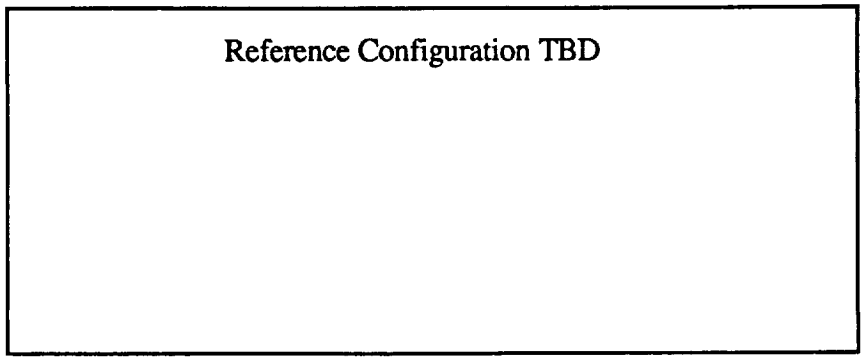

1.7 Definition of Terms

Deck Tilt - The angle at which the deck of the Lander is tilted away from the local horizontal plane. This angle must be stated in conjunction with the θ angle.

Viewing Declination - For a certain θ angle, the viewing declination angle is equal to the latitude minus Deck tilt angle minus the tilt of the optical assembly.

Integrated Payload(IP) - This term is used to refer to the integrated LUTE telescope and the Lunar Lander as one package.

Lander - Refers to the LUTE Lunar Lander.

2.0 APPLICABLE DOCUMENTS

The following documents form a part of these requirements to the extent specified herein. In the even of conflict between documents referenced below and other project documentation, the requirements specified herein shall govern.

DOCUMENT NO.	TITLE	PARA. NO.
K-STSM-14.1	Launch Site Accomodations Handbook for Payloads	3.2.3.1
MSFC-PLAN-904	OCC/LOSC Functional Requirements on the HOSC	3.2.4.2.3
MSFC-SCPE-1548	GSE Requirements for MSFC STS Experiments	3.6
DSN-TBD	LUTE/Lander Compatibility with DSN	3.10.2
DOC-TBD	IP Software Management Plan	3.12.1
NASA TM-X-73343	TBD	3.14.1
MSFC-HDBK-1453	Fracture Control Handbook	3.16.1
MSFC-PLAN-TBD	Safety and Mission Assurance Plan for the Lunar Telescope	3.18
NHB 5300.4(1D-2)	Safety, Reliability, Maintainability and Quality Provisions for the Space Shuttle program	3.18.1.1

NHB 5300.4(1C)	Inspections Systems Provisions for Aeronautical and Space System Materials, Parts, Components and Services	3.18.1.1
NASA-TM-TBD	Natural Environment Design Specifications for the Lunar Telescope	3.19.1.1
NASA-T BD-DOC	Meteoroid, Orbital and Lunar Debris Design Specifications for the Lunar Telescope	3.19.1.2
NHB 5300.4(1C)	Inspection Systems Provisions for Aeronautical and Space System Materials, Parts, Components, and Services	3.22.7.5
NHB 5300.4(3I)	Requirements for Printed Wiring Boards	3.22.7.5
NHB 5300.4(3K)	Design Requirements for Rigid Printing Wiring Boards and Assemblies	3.22.7.5
MSFC-STD-506C	Materials and Process Control	3.22.9.1
MSFC-HDBK-527F	Materials Selection List for Space Hardware Systems	3.22.9.1
JSC-SP-R-0022A	General Specification, Vacuum Stability Requirements of Polymeric Materials for Spacecraft Applications	3.22.9.2
MSFC-SPEC-1443	Outgassing Test for Non-metallic Materials Associated with Sensitive Optical Surfaces	3.22.9.2
MSFC-SPEC-1238	Thermal Vacuum Bakeout Specification for Contamination-sensitive Hardware	3.22.9.2

MSFC-SPEC-250A	Protective Finishes for Space Vehicles, Structures, and Associated Flight Equipment; General Specification	3.22.9.4 3.22.9.5 3.22.9.6
NHB-8060.1C	Flammability, Odor, and Offgassing Requirements and Test Procedures for Materials in Environments that Support Combustion	3.22.9.7
MSFC-SPEC-522B	Design Criteria for Controlling Stress Corrosion Cracking	3.22.9.9
NMI-8010.1	Classification of NASA Payloads	4.5.1
MMI-8030.2	Policy on MSFC Payloads	4.5.1
MMI-8080.5	Policy for Certification/Qualification of Flight Hardware and Program Critical Ground Support Equipment	4.5.1
MSFC-HDBK-527F	Materials Selection List for Space Hardware Systems	4.5.4
MSFC-STD-506C	Materials and Process Control, Standard	4.5.4

3.0 REQUIREMENTS

3.1 Mission Requirements

The LUTE shall be designed to serve as an international lunar ultraviolet astronomical observatory. Its design shall incorporate those features required to adequately serve the academic and scientific world by using the moon as a platform for exploring the universe. The LUTE shall adhere to the following mission requirements:

3.1.1 In-Flight Transportation

LUTE shall be delivered to orbit by a TBD launch vehicle, delivered to translunar flight and injected into lunar orbit by TBD upper stage vehicle, and delivered to the lunar surface by a TBD Lander

3.1.2 Mission Parameters

3.1.2.1 Operational Environment

The LUTE shall be designed to operate in a nominal lunar environment and survive the induced environments incurred on a payload during launch, flight and touchdown of the IP as described in Section 3.19.

3.1.2.2 Lunar Site Selection Criteria

3.1.2.2.1 The landing site shall allow for minimizing sunlight that enters the telescope aperture.

3.1.2.2.2 The landing site shall allow for minimizing earthshine that enters the telescope aperture.

3.1.2.2.3 The landing site shall be on the near side of moon to provide continuous earth communications.

3.1.2.2.4 The landing site shall be selected to minimize the lunar thermal environment on the LUTE and its supporting subsystems.

3.1.3 Landing Orientation

3.1.3.1 The LUTE systems shall accommodate a maximum deck tilt of 14.8°.

3.1.3.2 The LUTE shall utilize its own mechanisms to provide proper rotational orientation {about the Z axis} such that the.

3.1.3.3 The final selenographic declination of the LUTE after landing shall be +TBD° {+65°} with an accuracy of ±1°.

3.1.3.4 The final landing orientation of the LUTE shall provide for viewing within 10° of the north Galactic pole.

3.1.3.5 The final landing orientation shall ensure acquisition of a statistically complete sample of both point and extended sources which are bright in the UV.

3.1.4 Lunar Operational Life

The LUTE shall be designed to be fully operational for at least two years of operation after landing on the lunar surface.

3.2 Operational Requirements

3.2.1 IP Configuration

The LUTE telescope shall interface with the Lander in accordance with the interface requirements defined in Paragraph TBD.

3.2.2 Launch Configuration

The LUTE shall interface with TBD launch vehicle in accordance with the interface requirements defined in Paragraph TBD.

3.2.3 Ground Operations

3.2.3.1 Installation and Removal

The LUTE, in conjunction with the launch site, shall provide for checkout, servicing, maintenance, Lander and launch vehicle integration, and verification of launch readiness. Operations shall be compatible with K-STSM-14.1 (ATLAS/CCAFS) or TBD (Proton/Balkanour), as appropriate.

3.2.4 Flight Operations

3.2.4.1 LUTE Operations Support Team (LOST)

All flight operations from TLI through post-landing safing shall be under the control of the LOST.

3.2.4.2 LUTE Operations Support Center

3.2.4.2.1 The LOSC will be located in the Huntsville Operations Support Center (HOSC) at the Marshall Space Flight Center (MSFC).

3.2.4.2.2 The LOSC shall provide support for development, verification, and operations irrespective of other operations activities within the HOSC.

3.2.4.2.3 LOSC/LUTE requirements on the HOSC shall be documented in MSFC-PLAN-904.

3.2.4.3 Autonomy

The LUTE shall operate autonomously until LOI at which time the LOST will provide checkout and verification of the LUTE systems before allowing the LUTE to operate autonomously again. When LUTE systems return to autonomous operation, they shall remain so until landing.

3.2.4.4 Commanding

3.2.4.4.1 A multi-rate command capability shall be implemented to optimize commanding in real time and memory load modes and to maximize link margin for contingency operation.

3.2.4.4.2 The LUTE shall have the capability to accept real-time commands from the LOSC and execute them without interfering with the execution of stored commands.

3.2.4.4.3 The LOSC shall have the capability to uplink real-time commands to the LUTE.

3.2.4.4.4 The LOSC shall not transmit a command to the LUTE without controlled constraint checks.

3.2.4.5 Telemetry

The LUTE shall have the capability to downlink all the data necessary for facility control and monitoring.

3.2.4.6 Post-Landing Safing

3.2.4.6.1 The LUTE shall be capable of its required post-landing safing and shutdown without ground intervention.

3.2.4.6.2 The LUTE shall provide a positive signal to the LOSC verifying post-landing safing.

3.2.5 Post-landing

3.2.5.1 Safing Modes

3.2.5.1.1 Landing Safe Mode

LUTE shall be designed to enter a safe mode of autonomous acquiescence automatically upon landing, and to remain there until the LOSC determines that dust cover removal and aperture door removal operations are appropriate.

3.2.5.1.2 Operational Safe Mode

In case of post-activation contingencies, or loss of signal, LUTE shall be capable of autonomous

powered self-stabilization until further contact is made from the LOSC.

3.3 Optical Systems

3.3.1 Field of View

3.3.1.1 The telescope shall be a capable of imaging a 1.4-degree-wide field of view, with a 1.4-degree-wide unvignetted field of view for science.

3.3.1.2 The Telescope shall have a resolution of TBD {0.1} arcsec or better using the Rayleigh criterion for contrast.

3.3.1.3 The Telescope shall have a full-width half-intensity diameter of TBD {0.1} arcsec.

3.3.1.4 70% of the total energy of a stellar image shall be contained within a radius of TBD {0.10} arcsec of the primary mirror.

3.3.2 Wavelengths

3.3.2.1 The LUTE system shall produce UV imaging in a bandwidth that extends from 1000Å to 3500Å in three band passes 800Å in width (exact limits TBD).

3.3.2.2 LUTE shall have an on-axis static wavefront error of no more than TBDλ {0.075λ (λ=6328Å)} rms under lunar operation conditions.

3.3.3 Sensitivity

The LUTE point source sensitivity for a Class B0 star at 1500Å shall be greater than or equal to 25 m_V (after correction for reddening) with a signal to noise ratio of TBD {10}, and a resolution of at least TBD {0.33} arcsec per pixel.

3.3.4 Stray light

3.3.4.1. The LUTE design shall attenuate stray light such that the straylight irradiance at the focal plane is less than the irradiance of the image of a region of sky having the radiance of a TBD {23} m_V star per arcsec.

3.3.4.2. The LUTE shall have a light shade configuration which is capable of avoiding stray light from sunshine, lunar surface reflection and the bright earth limb, and fits within the TBD launch vehicle payload shroud.

3.4 Electrical Power System

3.4.1 Power Usage

The LUTE power system shall provide TBD watts {100W} maximum power to the IP subsystems.

3.4.2 Continuous Operation

The LUTE power system shall be furnished continuously for the life of the LUTE mission.

3.4.3 EPS Interfaces

The EPS shall interface with TBD IP subsystems.

3.4.4 Wire Protection

TBD

3.4.5 Electrical Grounding

The EPS shall have access to a single-point ground.

3.5 Reserved

3.6 Ground Support Equipment (GSE)

GSE shall be in accordance with MSFC-SPEC-1548.

3.6.1. Mechanical Ground Support Equipment (MGSE)

3.6.1.1 The LUTE MGSE shall include all equipment required to support subsystem and system verification, assembly, integration, and transportation, and launch support.

3.6.2 Electrical Ground Support Equipment

3.6.2.1 System EGSE, hardware and software, shall be provided to enable system level pre-launch checkout of the LUTE and the IP.

3.6.3 Ground Support Software

TBD

3.6.4 Servicing

TBD

3.7 Propulsion

N/A

3.8 Thermal Control System TCS

3.8.2 Optical Temperature/Gradient Requirements

3.8.2.1 The TCS shall maintain the following operating temperature range and gradient for the optical system:

Minimum Temperature: 65° K
Maximum Temperature: 250° K
Maximum Gradient: TBD (°K/cm)

3.8.2.2 The TCS shall be capable of rejecting TBD Watts and adding TBD Watts to stabilize the temperature of the optical system.

3.8.2.3 The TCS shall prevent thermal distortions in the LUTE structural support systems from interfering with the LUTE optics.

3.8.3 Detector Temperature Requirements

3.8.3.1 The TCS shall maintain the following operating temperature range and gradient for the detector system:

Minimum Temperature: 77° K
Maximum Temperature: 210° K
Maximum Gradient: TBD (°K/cm)

3.8.3.2 The TCS shall be capable of rejecting TBD Watts from the detector during the Lunar day.

3.8.3.3 Heating for detectors shall not be required at night.

3.8.4 Electronics Temperature Requirements

3.8.4.1 The TCS shall maintain the following operating temperature range and gradient for the electrical system:

Minimum Temperature: 220° K
Maximum Temperature: 358° K
Maximum Gradient: TBD (°K/cm)

3.8.4.2 The TCS shall be capable of rejecting TBD Watts from the electronics box during the Lunar day.

3.8.5 Mechanisms

LUTE mechanisms shall be designed to minimize the need for active thermal conditioning, and thermal conditioning shall be provided to the LUTE mechanisms where necessary.

3.9 Thermal Protection System

TBD

3.10 Communications and Tracking System (C&TS)

3.10.1 Functional Requirement

The C&TS shall provide the capability to transmit engineering and scientific data, receive and demodulate commands, and provide tracking.

3.10.2 DSN Compatibility

The C&TS shall be compatible with the DSN per DSN TBD {810-5}.

3.10.3 Uplink and Downlink Transmission

3.10.3.1 All uplink and downlink data transmission to and from LUTE shall be via the Deep Space Network (DSN).

3.10.3.2 The LUTE shall be capable of continuous uplink and downlink transmission.

3.10.4 High Gain Antenna (HGA)

3.10.4.1 HGA shall have an unobstructed view of earth.

3.10.4.2 The HGA shall have pointing capability for tracking the earth so as to provide maximum signal to the ground receiving station.

3.10.4.3 The HGA shall be capable of providing coverage via DSN to accommodate command, monitoring, and engineering data.

3.10.5 Data Transmission

3.10.5.1 RF Link Margins

TBD

3.10.5.3 Bit Error Rates (BER)

Data transmitted (sensor to user) shall have no more than one error in TBD bits.

3.11 Data Management System

3.11.1 Functional Requirements

The DMS shall perform command processing for the Lander subsystems, provide the required storage for data and commands, provide the central timing, and provide computation support for all Lander subsystems.
3.11.2 Timing and Clock Frequencies

3.11.2.1 The LUTE shall provide time in Universal Time Coordinated (UTC) format and required clock frequencies at

constant frequency with a resolution of one microsecond and a stability of TBD Hz in 24 hours.

3.11.2.2 The time in UTC format shall be relatable to UTC within TBD milliseconds.

3.11.3 Science and Engineering Data

The LUTE shall be capable of simultaneous and separate transmission of science and engineering data.

3.11.4 Data Transmission Rates

3.11.4.1 The LUTE shall be capable of transmitting uncompressed data at a rate of 200 kbits/s utilizing data reduction and data stitching at the landing site.

3.11.4.2 The LUTE data transmission system shall provide an RF signal of TBD watts so as to provide sufficient link margins for the transmitted data signal.

3.11.4.3 The data system shall operate continuously.

3.11.4.4 Bit Error Rates (BER)

Data transmitted (sensor to user) shall have no more than one error in TBD bits.

3.11.5 Command Capability

3.11.5.1 Command Optimization

Commanding shall be optimized the link margin maximized for contingency operation in the real time and memory load modes by implementing a multi-rate command capability.

3.11.5.2 Command Storage

The LUTE shall have the capability for onboard command storage of TBD thousand words.

3.11.5.3 Command Error

The onboard data management system shall allow for no more than one erroneous command in TBD commands to go undetected.

3.11.5.4 Command Confirmation

The LUTE shall have the capability to verify command reception and engineering data transmission during all phases of its mission.

3.11.6 Data Processing

The DMS shall contain a digital computer(s) for data processing.

3.11.7 Computer(s) Reloading

The DMS digital computers shall have the capability to reload or patch the computer(s) software upon ground command.

3.11.8 Error Detection and Correction

TBD

3.12 Software

3.12.1 Software Management

The management and development of the Lander flight software and supporting computer software shall be included in the LUTE Lunar Lander Software Management Plan, using MM 8075.1 as a guideline.

3.12.2 Preflight Test Software

TBD

3.12.3 Flight Software Design Parameters

TBD

3.13 Mechanism and Pointing Control Systems

3.13.1 High Gain Antenna

3.13.1.1 A gimbal capability of ±11° half cone angle shall be provided for the HGA with a tracking accuracy of TBD° in order to keep the LUTE in constant contact with the LOSC.

3.13.1.2 The mean pointing direction of the antenna shall be due South and 50° above Lunar horizontal with a ±180° azimuth range and a pointing accuracy of ±1°.

3.13.1.3 The HGA elevation range shall be approximately ±14.8° to accommodate an unfavorable deck tilt angle of the lander, with a pointing accuracy of ±1°.

3.13.2 Focal Plane Array

3.13.2.1 The focal plane array shall have the capability to roll in an east-west direction with an azimuth range capability of ±180° and a pointing accuracy of ±14.6 arcsec.

3.13.2.2 The focal plane array shall have the capability to point toward the zenith with a range of ±14.8° and a pointing accuracy of ±5 arcmin.

3.13.3 Optical Assembly

3.13.3.1 The optical assembly shall point to 40° above the south Lunar horizon with a pointing accuracy of ±5 arcsec and the ability to compensate for a deck tilt up to 14.8°.

3.13.4 Light shade

3.13.4.1 The light shade positioning mechanism shall have the capability to position the high side of the light shade due south with a ±180° range of movement and a positioning accuracy of ±1°.

3.13.4.2 The light shade positioning mechanism shall have the capability to point the light shade in the zenith direction by accommodating a maximum deck tilt of 14.8°, with an accuracy of ±1°.

3.13.5 Spider assembly

TBD

3.13.6 Steerable Secondary Mirror

TBD

3.14 Physical Standards

3.14.1 Coordinate System

The LUTE coordinate system shall be in accordance with NASA TM-X-73343, as shown in Figure 1-2, page 3 of this document.

3.14.2 Envelopes/Dimensions

The IP shall reside within the TBD usable static envelope provided by the TBD launch vehicle payload shroud.

3.14.3 Mass Requirements

The total mass of LUTE including interface hardware shall not exceed TBD {305}kg.

3.14.4 NASA Standard Components

The LUTE shall incorporate, NASA standard and other proven or qualified parts or components.

3.14.5 Measurement Unit System

International System (SI) units shall be used. Expression in both SI and US Customary Units is acceptable where the use of SI units alone would obviously impair communication or reduce the usefulness of a report to the primary recipients. When both systems of units are used, the units used for the principal measurements and

calculations will be stated first, followed by the other system in parentheses.

3.14.6 Factors of Safety

TBD

3.14.7 Fatigue

TBD

3.15 Reliability Requirements

3.15.1 Single Point Failure

Single point failures that would cause permanent loss of command capability, engineering telemetry or scientific data shall be individually dispositioned.

3.16 Maintainability Requirements

3.16.1 Fracture Control Program

Fracture control program will follow MSFC-HDBK-1453 where appropriate (TBD).

3.17 Quality Assurance Requirements

TBD

3.18 Safety and Mission Assurance Requirements

3.18.1 S&MA Plan

A S&MA Plan, MSFC-PLAN-TBD, shall be prepared, maintained, and implemented for the LUTE program. The plan shall describe the organization and method of implementation of the S&MA program for the Lander design, development, production, test, and flight with respect to safety, reliability, and quality assurance requirements.

3.18.2 Launch Vehicle Mission Assurance

3.18.2.1 The safety and mission assurance for the LUTE will meet the requirements of NHB 5300.4(1D-2) and NHB 5300.4(1C) as appropriate, per the LUTE payload classifications on specific materials, parts, components and services (TBD).

3.18.2.2 No hazard associated with the LUTE or its deployment procedures shall prevent the safe execution of the launch vehicle mission.

3.18.3 Ordnance Devices

Ordnance devices shall not be used on the LUTE.

3.18.4 Range Safety

The LUTE shall not preclude the launch vehicle from properly executing a launch vehicle mission abort sequence should one be considered necessary.

3.19 Environment Requirements

3.19.1 Natural Environment

3.19.1.1 General Requirement

The LUTE design shall comply with the natural environment specified in NASA TM-TBD.

3.19.1.2 Meteoroid, Orbital, and Lunar Debris Impact

The LUTE shall provide protection against loss of functional capability when subjected to the debris flux models as defined in TBD-DOC.

3.19.1.3 Radiation/Nuclear Radiation

TBD

3.19.1.4 Thermal

3.19.1.4.1 The LUTE shall be capable of withstanding the following temperature extremes:

Earth Orbit
Minimum: TBD° K
Maximum: TBD° K

Translunar Flight
Minimum: TBD
Maximum: 70° K

Lunar Surface Temperature
Minimum: 93° K
Maximum: 395° K

3.19.1.4.2 The LUTE shall demonstrate survivability in simulated environments representing each phase of its mission life before integration with the Lander system. (i.e., Thermal-Vacuum test, vibrations test, etc.)

3.19.2 Induced Environments

3.19.2.1 Provisions shall be made to preclude over pressurization damage to any part of the LUTE during the in-flight segment.

3.19.2.2 The LUTE shall be capable of being rotated at TBD revolutions per minute (rpm) for TBD days during translunar flight in order to avoid overheating of the LUTE systems and elements.

3.19.2.3 Launch Vehicle Induced loads

3.19.2.3.1 Acoustics

The LUTE shall be designed to assure structural integrity and functionality upon exposure to the maximum acoustic levels within the launch vehicle payload shrouds.

3.19.2.3.2 Random Vibration

The LUTE shall be designed to withstand the random vibration environments during lift-off and transonic flight.

3.19.2.3.3 Shock

The LUTE shall be designed for the shock levels generated by the facility and launch vehicle separation devices. The shock levels at the separation interface shall be attenuated throughout the structure to component/sub-assembly locations.

3.19.2.3.4 Low Frequency and Steady State Accelerations

The LUTE shall be designed to withstand the low frequency and stead-state acceleration environments that occur during the launch, ascent, and on-orbit flight elements.

3.19.2.3.5

LUTE system shall accommodate the following quasi-static loads induced by the launch vehicle: TBD {6.5 g's axially and 3.5 g's laterally}. Frequency constraints are TBD.

3.19.2.4 Lander Induced Loads

3.19.2.4.1 The LUTE system and interface hardware shall accommodate the following loads induced by the lander: TBD. Frequency constraints are TBD.

3.19.2.4.2 The LUTE system shall accommodate a maximum powered descent thrust equal to TBD {3914N at -15° pitch and a touchdown thrust of 979N at 90° pitch}.

3.19.3 Contamination

3.19.3.1 The LUTE shall be maintained in a class TBD environment during and following assembly.

3.19.3.2 All LUTE elements involved shall be maintained in a 10K clean environment when optics are exposed.

3.19.4 Magnetic

TBD

3.20 Transportability/Transportation Requirements

3.20.1 Shipping Container Design

The LUTE shall be shipped in a container specifically designed to protect the LUTE during surface and air transportation.

3.20.2 Transportation Environment

The LUTE transportation container shall maintain an environment that meets cleanliness specifications for ground processing as outlined in section 3.17 of this document.

3.20.3 Prime Mode of Transportation

The prime mode of transportation of the LUTE between ground sites shall be by TBD mode of transportation.

3.21 Storage Requirements

3.21.1 Storage Cleanliness

3.21.1.1 The LUTE shall be stored in a class 100K environment during idle periods after assembly and lander vehicle integration.

3.21.2 Shelf Life

3.21.2.1 The LUTE shall be capable of nominal operations after TBD years of idle storage.

3.21.3 On-pad Stay Time

TBD

3.22 Design and Construction Requirements

3.22.1 Main Optics System

3.22.1.1 The LUTE shall be a wide field, three mirror, aplanatic ultraviolet telescope with a nominal 1.0 meter aperture.

3.22.1.2 Mirror deformation shall be less than TBD {0.1} microns without actuators.

3.22.1.3 The primary, secondary and tertiary mirrors shall be aluminized with a TBD {silicon} polishable overcoat.

3.22.1.4 The primary, secondary and tertiary mirror blanks shall be constructed of TBD material {Chemical Vapor Deposition (CVD) Silicon Carbide}.

3.22.1.5 The back focal length shall be TBD {300} cm.

3.22.1.6 Optical axis shall be aligned within TBD arcmin of the pre-planned pointing delineation.

3.22.1.6.1 Primary Mirror

TBD

3.22.1.6.2 Secondary Mirror

3.22.1.6.2.1 The secondary mirror shall be articulated by hexapod actuators for piston, tilt and lateral displacement.

3.22.1.6.2.2 The secondary mirror shall have an outer diameter (OD) of 38 cm, and an inner diameter (ID) of 15 cm.

3.22.1.6.3 Tertiary Mirror

The tertiary mirror shall have a 28 cm OD (ID = 0 cm.)

3.22.1.6.4 Detector

3.22.1.6.4.1 Detectors shall have fine East-West alignment with TBD arcsec resolution.

3.22.1.6.4.2 The detector shall be a CCD array.

3.22.1.6.4.3 The detector array shall be constructed of 5-7.5mm pixels (typical).

3.22.1.6.5 Wavefront Sensor

TBD

3.22.2 Structural Support Assembly

The LUTE structure subsystem shall provide the structure to mount all associated components and the optical assembly.

3.22.2.1 Base Plate

3.22.2.1.1 The base plate shall provide support for the entire optical assembly and light shade.

3.22.2.1.2 The base plate shall interface with the roll ring and hexapod mounts.

3.22.2.1.3 The base plate rate of thermal expansion shall be compatible with that of the optical systems.

3.22.2.2 Metering Structure

The metering structure supports the secondary mirror and science instrument.

3.22.2.2.1 The metering structure shall maintain the back focal length (the distance between the optics) to within ±TBD microns.

3.22.2.2.2 The metering structure shall minimize conductive heat transfer to the optics and minimize light blockage.

3.22.2.2.1 Spider

TBD

3.22.2.2.2 Inner Hub Ring

TBD

3.22.2.2.3 Outer Ring

TBD

3.22.2.3 Secondary Mirror Assembly

3.22.2.3.1 Housing

TBD

3.22.2.3.2 Reaction Plate

TBD

3.22.2.3.3 Launch Locks

TBD

3.22.2.4 Optics Support Structure

3.22.2.4.1 Flexures

TBD

3.22.2.4.2 Launch Locks

TBD

3.22.2.5 Baffles

TBD

3.22.2.6 Antenna Assembly

TBD

3.22.2.7 Light Shade

3.22.2.7.1 The light shade shall be capable of supporting multi-layer insulation, an aperture cover and the electronics box.

3.22.2.7.2 Light shade angle and length shall be determined according to landing site as shown in Figure TBD.

3.22.2.7.3 Orientation of the light shade (highside) shall be due South.

3.22.2.8 Electronics Support

TBD

3.22.3 Thermal Control System

3.22.3.1 Optical System

3.22.3.1.1 Heat Pipes

TBD

3.22.3.1.2 Thermal Isolators (for mirrors)

TBD

3.22.3.2 Detector

3.22.3.2.1 Radiator

TBD

3.22.3.2.2 Heat Transfer Device

TBD

3.22.3.2.3 Thermal Shield

LUTE thermal protection shall be passive to the maximum extent possible.

3.22.3.3 Supporting Subsystems

3.22.3.3.1 Radiator

TBD

3.22.3.3.2 Louvres/Door

TBD

3.22.3.3.3 Insulation

TBD

3.22.3.3.4 Coatings

TBD

3.22.3.3.5 Heaters

3.22.3.4 Light Shade

3.22.3.4.1 Insulation

TBD

3.22.3.4.2 Coating

TBD

3.22.4 Pointing Control System

3.22.4.1 Hexapod Mount

3.22.4.1.1 Rotary Incremental Actuators

TBD

3.22.4.1.2 Encoders, Potentiometers, Ball Screws and Nuts

TBD

3.22.4.1.3 Guide Tubes

TBD

3.22.4.1.4 Harmonic Drives

TBD

3.22.4.1.5 End Joints

TBD

3.22.4.2 Light Shade & Antenna Roll Assembly

3.22.4.2.1 Rolling

TBD

3.22.4.2.2 Motor

TBD

3.22.4.2.3 Cables

TBD

3.22.4.3 Articulating Secondary Mirror

3.22.4.3.1 Course & Fine Stroke Actuators

TBD

3.22.4.3.2 Drive Electronics

TBD

3.22.4.4 Acquisition Sensors

3.22.4.4.1 Sensors

TBD

3.22.4.4.2 Electronics

TBD

3.22.4.5 Deformable Primary Mirror (optional)

TBD

3.22.5 Telescope Protection System

3.22.5.1 Aperture Cover

3.22.5.1.1 Deployment Mechanism

TBD

3.22.5.1.2 Launch Locks

TBD

3.22.5.1.3 Seals

TBD

3.22.5.2 Telescope Safing

The LUTE structure subsystem shall provide an aperture door system to satisfy contamination protection requirements.

3.22.6 Data Management System

3.22.6.1 Transponder

TBD

3.22.6.2 Command Detector

TBD

3.22.6.3 Diplexer

TBD

3.22.6.4 Central Data Unit

TBD

3.22.6.5 Central Computer

3.22.6.51 The LUTE shall provide the capability to restore memory data in the onboard computer.

3.22.6.52 The LUTE shall provide the capability to dump the onboard computer memory to ground support.

3.22.6.6 Antenna Drive Electronics

TBD

3.22.6.7 Power Distributor

TBD

3.22.6.8 Cabling

TBD

3.22.6.9 High Gain Antenna

TBD

3.22.6.10 Omni Antenna

TBD

3.22.7 Power Distribution System

3.22.7.1 Radio-isotope Thermoelectric Generator

LUTE electrical power requirements shall be met by Radio-isotope Thermal Generator (RTG) battery.

3.22.7.2 Battery (optional)

The LUTE electrical power system shall be accompanied by a small primary battery for start up.

3.22.7.3 Power Distributor

TBD

3.22.7.4 Power Regulator

Electrical/electronic processes shall be controlled per the requirements of NHB 5300.4(3A-2, 3G, 3H, and 3J).

3.22.7.5 Cabling

Electrical/electronic design and parts shall meet the requirements of NHB 5300.4(1F, 3I, and 3K).

3.22.7.51 All deployable appendages shall have redundant systems which will insure proper deployment upon lunar landing.

3.22.7.6 LUTE to TBD Lunar Lander Interface

3.22.7.61 LUTE shall utilize mechanical interface consisting of TBD discrete hardpoints as defined in TBD lunar lander Document XXXX. The TBD lunar lander/LUTE interface will be located at launch vehicle station TBD.

3.22.8 Weight Allocation

	Program (kg)Est.
Optical System	
Primary Mirror	12
Secondary Mirror	4
Tertiary Mirror	2
Detector	5
Structural Support Assembly	
Metering Structure	23
Mirror Support Structure	4

281

Telescope Baseplate	44
Light Shade	42
Light Baffles	14
Miscellaneous Hardware	6
Telescope Protection System	
Aperture Cover	10
Electronic Box Support	8
Launch Locks	4
Supporting Subsystems	
Power System Attachment	TBD
Antenna Bracket	TBD
Pointing System	36
Electrical Power System	24
Command & Data Handling	37
Thermal Control System	26
Contingency (10%)	30
Total	330

3.22.9 Materials Construction

3.22.9.1 Materials and Processes

Materials and processes used in the construction of the LUTE shall meet the requirements of MSFC-STD-506C. The materials selection list, MSFC-HDBK-527F, or the MAPTIS Database shall be used during design.

3.22.9.2 Outgassing of Materials

All materials used in the construction of the LUTE shall meet the thermal vacuum stability requirements of JSC-SP-R-0022A and MSFC-SPEC-1443. Cables, connectors, and other equipment shall be baked out per MSFC-SPEC-1238.

3.22.9.3 Castings

Castings shall not be used in the LUTE design without specific MSFC approval.

3.22.9.4 Corrosion of Metal Parts

Metal parts shall be protected from corrosion in accordance with MSFC-SPEC-250, provided that such protection is compatible with the operating and space environmental requirements.

3.22.9.5 Dissimilar Metals

The use of dissimilar metals (as defined in MSFC-SPEC-250) in direct contact is discouraged. When dissimilar metals are required to be joined, their facing surfaces shall be adequately insulated,

preferably by an approved sealing compound, to assure protection from electrolytic corrosion.

3.22.9.6 Finish

The LUTE finish shall be in accordance with MSFC-SPEC-250A except for special thermal and baffle finishes.

3.22.9.7 Flammability

All nonmetallic materials used in construction of the LUTE shall meet the flammability requirements of NHB-8060.1.

3.22.9.8 Corrosion Resistant Metals

Metals in contact with fluid media shall be corrosion resistant and shall be compatible with the media to which they are exposed. Use of metals and their weldments subject to embrittlement at low temperatures shall be avoided in all cryogenic applications.

3.22.9.9 Stress Corrosion

MSFC-SPEC-522B shall be used as a requirement for stress corrosion susceptibility of various materials.

3.22.10 Ground Support Equipment Design

3.22.10.1 Electrical Ground Support

TBD

3.22.10.2 Mechanical Ground Support

TBD

3.23 Interface Requirements

3.23.1 Telescope to Science Instrument

The Telescope to Science Instrument interface shall be in accordance with the Telescope to Science Instrument Interface Control Document (ICD).

3.23.2 LUTE to Lander

The LUTE to Lander interface shall be in accordance with the LUTE to Lander ICD.

3.23.3 Telescope to Mirror Assembly

The Telescope to Mirror Assembly interface shall be in accordance with the Telescope to Mirror Assembly ICD.

3.23.4 LUTE to Ground Systems

The LUTE to Ground Systems interface shall be in accordance with the LUTE to Ground Systems ICD.

4.0 VERIFICATION

4.1 General

TBD

4.2 Verification Types

TBD

4.3 Verification Requirements Matrix

TBD

4.4 Verification Facilities and Equipment

TBD

4.5 Spacecraft Hardware Requirements

4.5.1 Payload Classifications

LUTE shall use liberalized payload classifications based upon use of proven flight design, parts, and materials with applicable testing, as required in the following documents:

NMI 8010.1
MMI 8030.2
MMI 8080.5

4.5.2 Previously Flown Hardware

LUTE shall reuse previously flown hardware which has been refurbished and tested as required.

4.5.3 Controlled Prototype Hardware

LUTE shall make use of controlled prototype hardware as flight hardware by manufacturing to baselined engineering requirements with quality verifications which have not subjected the hardware to structural or life-limiting environments exceeding program flight requirements.

4.5.4 Off-the-shelf Parts

LUTE shall make use of "off-the-shelf" parts, materials and components qualified for flight use, per the information contained in the following documents:

MSFC-HDBK-527F
MSFC-STD-506C

5.0 PREPARATION FOR DELIVERY

5.1 Preparation, Packaging and Shipment

6.0 NOTES

TBD

7.0 APPENDIX -- A Verification Matrix

TBD

APPENDIX D

LEVEL II SYSTEMS REQUIREMENTS DOCUMENT (LANDER)

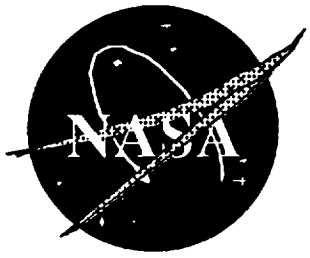

MSFC-RQMT-XXXX
September 3, 1993

National Aeronautics and
Space Administration

George C. Marshall Space Flight Center
Marshall Space Flight Center, Alabama 35812

D-R-A-F-T

LUNAR ULTRAVIOLET TELESCOPE EXPERIMENT

LANDER

LEVEL II SYSTEMS REQUIREMENTS DOCUMENT

Prepared by:
Science and Engineering Directorate
Systems Analysis and Integration Laboratory
Systems Integration Division
Systems Integration Branch

Lunar Ultraviolet Telescope Experiment (LUTE) Lunar Lander Level II Systems Requirements Document

PREPARED BY:

EL44 DATE

APPROVED BY:

EL44 DATE
Chief,
Systems Integration Branch

EL41 DATE
Chief,
Systems Integration Division

EL01 DATE
Director, Systems Analysis
and Integration Laboratory

APPROVED BY:

PF21 DATE
LUTE Project Manager

EJ23 DATE
Lander Chief Engineer

STRESS (ED01) DATE

MATERIALS (EH01) DATE

Release Date: ___/___/___	Marshall Space Flight Center **SPECIFICATION/DOCUMENT CHANGE INSTRUCTION** Spec./Doc. No. _____	Page of _____ Copy No.:

Change No./Date	SCN/DCN No./Date	CCBD No./Date	Replacement Page Instructions

MSFC-Form 4140 (Revised September 1990)

NOTE: After revising the document, file this sheet in document preceeding Table of Contents

TABLE OF CONTENTS

LIST OF FIGURES v
ACRONYMS AND ABBREVIATIONS vi
1.0 INTRODUCTION 1
1.1 Purpose 1
1.2 Scope 1
1.3 Document Format 1
1.4 Project Description 1
1.5 Control 2
1.6 Reference Configuration 3
1.7 Definition of Terms 4
2.0 APPLICABLE DOCUMENTS 4
3.0 REQUIREMENTS 6
3.1 Mission Requirements 6
3.1.1 Trans-Lunar Injection (TLI) 6
3.1.2 Lunar Orbit Insertion (LOI) 6
3.1.3 Lunar Descent 6
3.1.4 Lunar Landing 7
3.1.5 Post Landing Safing, Shutdown and Mission Operations 7
3.1.6 Operational Environment 7
3.1.7 Lunar Operational Life 7
3.2. Operational Requirements 8
3.2.1 IP Configuration 8
3.2.2 Launch Configuration 8
3.2.3 Ground Operations 8
3.2.4 Flight Operations 8
3.3 Electrical and Power System (EPS) 9
3.3.1 Power Requirements 9
3.3.3 Wire Protection 9
3.3.4 Electrical Grounding 9
3.4 Airborne Support Equipment 9
3.5.1 Mechanical Ground Support Equipment (MGSE) 10
3.5.2 Electrical Ground Support Equipment (EGSE) 10
3.5.3 Ground Support Software 10
3.5.4 Servicing 10
3.6 Propulsion Performance 10
3.6.1 Main Propulsion System (MPS) 10
3.6.2 Reaction Control System (RCS) 11
3.7 Thermal Control System 11
3.8 Thermal Protection System 11
3.9 Communications and Tracking System (C&TS) 11
3.9.1 Functional Requirement 11
3.9.2 DSN Compatibility 11
3.9.3 Uplink and Downlink Transmission 11
3.9.5 Data Transmission 12
3.10 Data Management System (DMS) 12
3.10.1 Functional Requirements 12
3.10.2 Timing and Clock Frequencies 12
3.10.3 Command 12
3.10.4 Lander Engineering Telemetry 13
3.10.5 Format Capability 13

3.10.6 Data Processing 13
3.10.7 Computer(s) Reloading 13
3.10.8 Error Detection and Correction 13
3.11 Software 13
3.11.1 Software Management 13
3.11.2 Preflight Test Software 13
3.11.3 Flight Software Design Parameters 13
3.12 Guidance, Navigation and Control (GN&C) System 14
3.12.1 Functional Requirements 14
3.12.2 Performance Requirements 14
3.13 Mechanical System Requirements 14
3.14 Physical Standards 14
3.14.1 Coordinate System 14
3.14.2 Envelopes/Dimensions 14
3.14.3 Mass Requirements 14
3.14.4 NASA Standard Components 14
3.14.5 Loads and Frequency Requirements 14
3.14.7 Factors of Safety 15
3.14.8 Fatigue 15
3.15 Reliability Requirements 15
3.15.1 Single Point Failure 15
3.16 Maintainability Requirements 15
3.16.1 Fracture Control Program 15
3.17 Quality Assurance Requirements 15
3.18 Safety and Mission Assurance (S&MA) Requirements 15
3.18.1 S&MA Plan 15
3.18.2 Launch Vehicle Mission Assurance 15
3.18.3 Ordnance Devices 16
3.18.4 Range Safety 16
3.19 Environment Requirements 16
3.19.1 Natural Environment 16
3.19.2 Induced Environment 17
3.19.3 Contamination 17
3.19.4 Magnetic 17
3.20 Transportability/Transportation Requirements 18
3.20.1 Shipping Container Design 18
3.20.2 Transportation Environment 18
3.20.3 Prime Mode of Transportation 18
3.21 Storage Requirements 18
3.21.1 Storage Cleanliness 18
3.21.2 Shelf Life 18
3.21.3 On-pad Stay Time 18
3.22 Design and Construction Requirements 18
3.23 Interface Requirements 18
3.23.1 Launch System Interface 18
3.23.2 Lander to LUTE 18
3.23.3 Lander to Deep Space Network 18
4.0 VERIFICATION 19
5.0 PREPARATION FOR DELIVERY 20
6.0 NOTES 20
7.0 APPENDIX -- A Verification Matrix 20

LIST OF FIGURES

FIGURE	TITLE	PAGE
1-1	LUTE Documentation Tree	2
1-2	LUTE Configuration Reference Coordinates	3
1-3	Integrated Payload Reference Configuration	4

ACRONYMS AND ABBREVIATIONS

BER	Bit Error Rate
C&TS	Communications and Tracking System
DMS	Data Management System
DOC	Document
DSN	Deep Space Network
EGSE	Electrical Ground Support Equipment
EPS	Electrical and Power System
GN&C	Guidance, Navigation and Control
GSE	Ground Support Equipment
HOSC	Huntsville Operations Support Center
IP	Integrated Payload
JSC	Johnson Space Center
kg	kilogram
KSC	Kennedy Space Center
LOI	Lunar Orbit Insertion
LOSC	LUTE Operations Support Center
LOT	Lander Operations Team
LUTE	Lunar Ultraviolet Telescope Experiment
m	meter
MGSE	Mechanical Ground Support Equipment
MLI	Multi-Layer Insulation
MMI	Marshall Management Instruction
MPS	Main Propulsion System
MSFC	Marshall Space Flight Center
NASA	National Aeronautics and Space Administration
NFPA	National Fire Protection Association
NHB	NASA Handbook
NMI	NASA Management Instruction
RCS	Reaction Control System
RF	Radio Frequency
rpm	revolutions per minute
RQMT	Requirement
S&MA	Safety and Mission Assurance
SEI	Space Exploration Initiative
SI	International System of Units
SPEC	Specification
SRD	Systems Requirement Document
TBD	To Be Determined
TCS	Thermal Control System
TLI	Trans-Lunar Injection
UTC	Universal Time Coordinated
{ }	Indicates possible value for TBD

LEVEL II SYSTEMS REQUIREMENTS FOR THE LUTE LUNAR LANDER PROJECT

1.0 INTRODUCTION

1.1 Purpose

The purpose of this document is to define the Level II design and development requirements for the LUTE Lunar Lander project. The performance requirements outlined in this document represent the minimum performance levels of the Lander to be used in carrying out the requirements of the LUTE program throughout its mission life.

1.2 Scope

This document establishes the project requirements for all elements of the LUTE Lunar Lander and shall comply with the LUTE Level I Program Requirement Document.

1.3 Document Format

The Level II Systems Requirements Document (SRD) is organized in a standard format of five sections as described below.

Section Number	Title	Content
1.0	Introduction	Defines the purpose and scope of the document and includes a description of the Lunar Lander project.
2.0	Applicable Documents	Lists the applicable documents cited in Section 3.0.
3.0	Requirements	Defines the functional and performance requirements imposed upon the Lunar Lander design.
4.0	Verification	Defines the verification of Section 3.0 requirements.
5.0	Preparation for delivery	Instructions for preparation packaging and shipment.
6.0	Notes	
7.0	Appendix	

1.4 Project Description

The purpose of the LUTE program is to take advantage of the unique aspects of the lunar environment for astronomy observations in the ultraviolet wavelengths, collect environmental data to support the design of future lunar equipment, and to provide a source of educational material for wide distribution to primary and secondary educational systems both for the United States and the international

community. The LUTE Lander shall both transport the LUTE telescope to the lunar surface and provide accommodations for the operation of the Telescope

1.5 Control

This document shall be controlled at Level II by the MSFC Advanced Projects Office, Lunar Ultraviolet Telescope Experiment Task Team, PF21. For further reference regarding documentation flow, refer to Figure 1-1 below.

Figure 1-1 LUTE Systems Requirements Documentation Tree

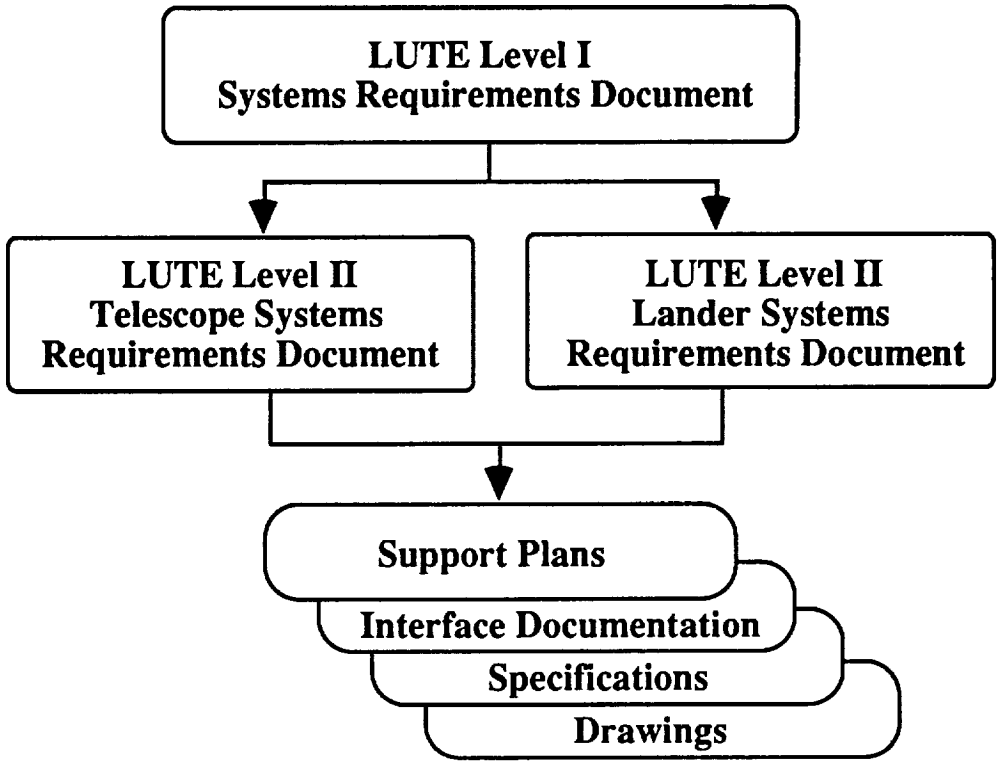

1.6 Reference Configuration

Figure 1-2 represents the latest design reference configuration for the LUTE and Lander coordinate system.

Figure 1-2: LUTE Configuration Reference Coordinates

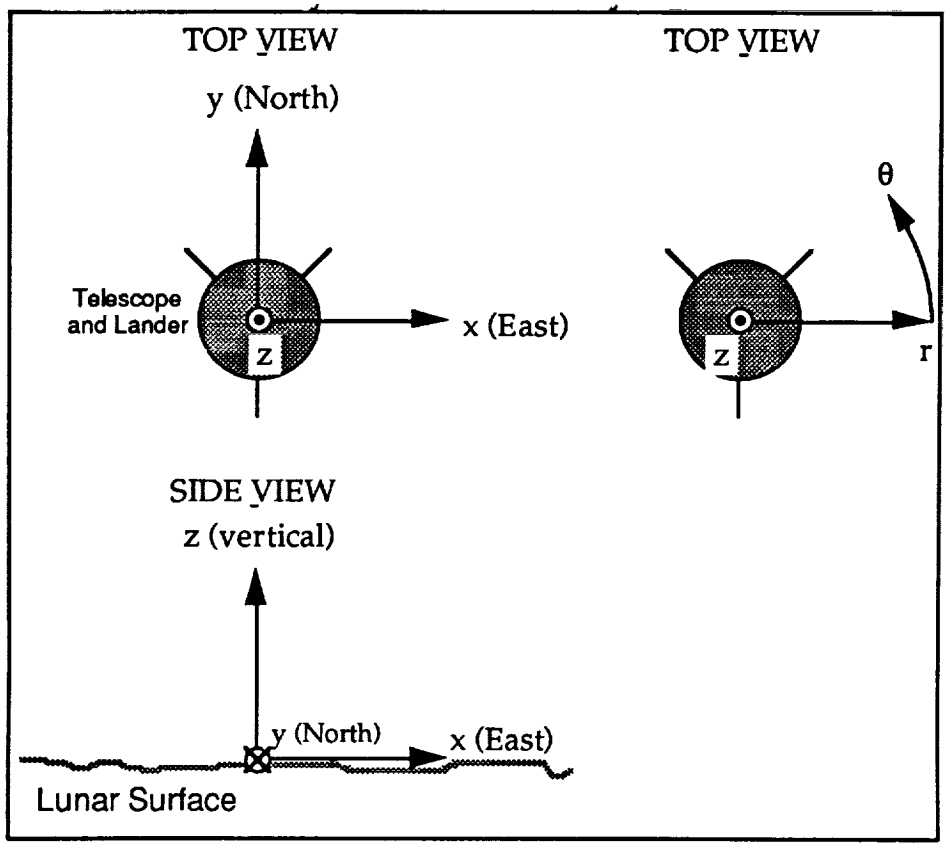

Figure 1-3 represents the latest reference configuration for the LUTE Lunar Lander subsystem configuration

Figure 1-3 Integrated Payload Reference Configuration

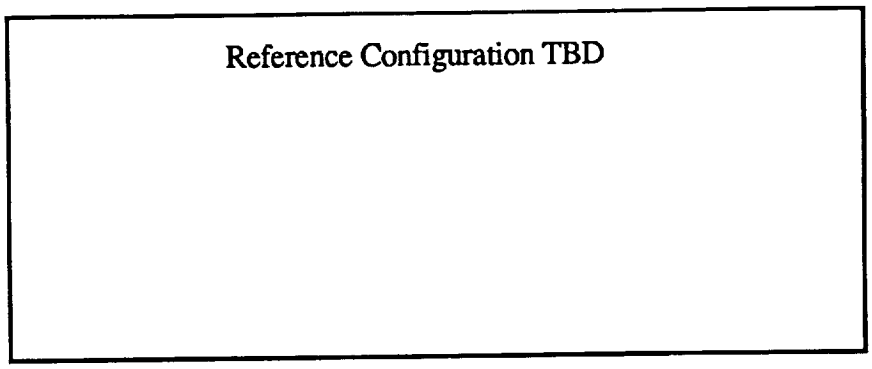

1.7 Definition of Terms

Deck Tilt - The angle at which the deck of the Lander is tilted away from the local horizontal plane. This angle must be stated in conjunction with the θ angle.

Viewing Declination - For a certain θ angle, the viewing declination angle is equal to the latitude minus Deck tilt angle minus the tilt of the optical assembly.

Integrated Payload(IP) - This term is used to refer to the integrated LUTE telescope and the Lunar Lander as one package.

Lander - Refers to the LUTE Lunar Lander.

2.0 APPLICABLE DOCUMENTS

The following documents form a part of these requirements to the extent specified herein. In the even of conflict between documents referenced below and other project documentation, the requirements specified herein shall govern.

DOCUMENT NO.	TITLE	PARA. NO.
K-STSM-14.1	Launch Site Accomodations Handbook for Payloads	3.2.3.1
MSFC-PLAN-904	OCC/LOSC Functional Requirements on the HOSC	3.2.4.2.3
MSFC-SPEC-1548	GSE Requirements for MSFC STS Experiments	3.5
DSN-TBD	LUTE/Lander Compatibility with DSN	3.9.2

DOC-TBD	IP Software Management Plan	3.11.1
NASA TM-X-73343	TBD	3.14.1
MSFC-HDBK-1453	Fracture Control Handbook	3.16.1
MSFC-PLAN-TBD	Safety and Mission Assurance Plan for the Lunar Telescope	3.18.1
NHB 5300.4(1D-2)	Safety, Reliability, Maintainability and Quality Provisions for the Space Shuttle program	3.18.2.1
NHB 5300.4(1C)	Inspections Systems Provisions for Aeronautical and Space System Materials, Parts, Components and Services	3.18.2.1
NASA-TM-TBD	Natural Environment Design Specifications for the Lunar Telescope	3.19.1.1
NASA-T BD-DOC	Meteoroid, Orbital and Lunar Debris Design Specifications for the Lunar Telescope	3.19.1.2
NMI-8010.1	Classification of NASA Payloads	4.5.1
MMI-8030.2	Policy on MSFC Payloads	4.5.1
MMI-8080.5	Policy for Certification/Qualification of Flight Hardware and Program Critical Ground Support Equipment	4.5.1
MSFC-HDBK-527F	Materials Selection List for Space Hardware Systems	4.5.4
MSFC-STD-506C	Materials and Process Control, Standard	4.5.4

OTHERS: To Be Determined (TBD)

3.0 REQUIREMENTS

3.1 Mission Requirements

The Lander mission requirements are to deliver to the lunar surface from Trans Lunar Injection the LUTE telescope without disrupting the operability of the LUTE telescope systems. The Lander must also provide throughout the required operation time a stable platform for the LUTE telescope and certain other spacecraft accommodations as required below.

3.1.1 Trans-Lunar Injection (TLI)

3.1.1.1 Control

The Lander shall not provide the delta-V burn required for TLI however it shall automatically make midcourse corrections to set up for proper Lunar Orbit Insertion.

3.1.1.2 Attitude

The Lander shall maintain a rotational rate at TBD revolutions per minute (rpm) for TBD hours during TLI. This requirement shall be accordance with the Telescope thermal requirements.

3.1.2 Lunar Orbit Insertion (LOI)

3.1.2.1 Lunar Circular Orbit Requirements

3.1.2.1.1 The Lander shall insert itself into a circular orbit (eccentricity less than TBD) at an altitude above the lunar surface of TBD (100 km).

3.1.2.1.2 The circular orbit chosen shall provide for a nominal descent to the lunar site selected by the LUTE TBD.

3.1.2.2 Control

The Lander shall automatically make midcourse corrections and insert the payload into the required lunar circular orbit at which time it will wait for a command from the LOT to proceed with descent.

3.1.2.3 Lunar Circular Orbit Verification of Subsystems

TBD

3.1.3 Lunar Descent

3.1.3.1 Control

Upon receiving the go ahead command from the LOT the Lander shall perform a descent to the specified lunar site.

3.1.3.2 Attitude

TBD

3.1.4 Lunar Landing

The Lander shall provide a controlled landing according to the requirements listed below

3.1.4.1 The Lander shall limit descent and landing loads to TBD.

3.1.4.2 The Lander shall touchdown on the lunar surface within 3 km of the specified landing site.

3.1.4.3 The Lander shall accommodate for the final selenographic declination of +TBD° {+65°} with an accuracy of ±1° for LUTE after landing.

3.1.4.4 The final touchdown shall not result in a deck tilt of more than TBD degrees.

3.1.4.5 The Lander shall be capable of landing under daylight.

3.1.4.6 Upon landing the Lander shall provide its location and orientation to the LOSC.

3.1.5 Post Landing Safing, Shutdown and Mission Operations

3.1.5.1 System Safing and Shutdown Requirements

TBD days after landing, the Lander, from that point on, shall not adversely affect the operation of the LUTE.

3.1.5.2 Post Landing Mission Requirements

3.1.5.2.1 LUTE Accommodations Requirements

TBD

3.1.6 Operational Environment

The Lander shall be designed to operate in a nominal lunar environment and the induced environments during launch, flight and touchdown of the Lander as described in Section 3.19.

3.1.7 Lunar Operational Life

Upon landing on the lunar surface, Lander systems required for LUTE operation shall have a 2-year fully operational life, with operations continuing after the 2 years as capabilities allow.

3.2. Operational Requirements

3.2.1 IP Configuration

The Lander shall interface with the LUTE telescope in accordance with the interface requirements defined in Paragraph TBD.

3.2.2 Launch Configuration

The Lander shall interface with TBD launch vehicle in accordance with the interface requirements defined in Paragraphs 3.14.2 and 3.23.1.

3.2.3 Ground Operations

3.2.3.1 Installation and Removal

The Lander, in conjunction with the launch site, shall provide for checkout, servicing, maintenance, LUTE and launch vehicle integration, and verification of launch readiness. Operations shall be compatible with K-STSM-14.1 (ATLAS/CCAFS) or TBD (Proton/Balkanour), as appropriate.

3.2.4 Flight Operations

3.2.4.1 Lander Operations Team (LOT)

All flight operations from TLI through post-landing safing shall be under the control of the LOT.

3.2.4.2 LUTE Operations Support Center

3.2.4.2.1 The Lander Operations Team (LOT) shall conduct flight operations from the LUTE Operations Support Center (LOSC), located in the Huntsville Operations Support Center (HOSC) at the Marshall Space Flight Center (MSFC).

3.2.4.2.2 The LOSC shall function within the guidelines established for the HOSC. The LOSC shall provide support for development, verification, and operations irrespective of other operations activities within the HOSC.

3.2.4.2.3 LOSC/LUTE requirements on the HOSC shall be documented in MSFC-PLAN-904.

3.2.4.3 Autonomy

The Lander shall nominally operate autonomously until LOI at which time the LOT will provide checkout and verification of the Lander systems before giving control back to the Lander systems. Upon Lander receiving control in lunar orbit, it will again operate autonomously until landing.

3.2.4.4 Commanding

3.2.4.4.1 All commanding of the Lander shall be performed from the LOSC.

3.2.4.4.2 A multi-rate command capability shall be implemented to optimize commanding in real time and memory load modes and to maximize link margin for contingence operation.

3.2.4.4.3 The Lander shall have the capability to accept real-time commands from the LOSC and execute them without interfering with the execution of stored commands.

3.2.4.5 Telemetry

The Lander shall have the capability to downlink all the data necessary for facility control and monitoring.

3.2.4.6 Post-Landing Safing

3.2.4.6.1 The Lander shall be capable of performing the post-landing safing and shutdown without the need of ground intervention.

3.2.4.6.2 The Lander shall provide a positive signal to the LOSC verifying post-landing safing.

3.3 Electrical and Power System (EPS)

3.3.1 Power Requirements

The Lander shall provide power for the LUTE operations. The LUTE will operate on the lunar day and night cycle for 2 years.

3.3.2 EPS Interfaces

The EPS interfaces with TBD LUTE subsystems.

3.3.3 Wire Protection

TBD

3.3.4 Electrical Grounding

The Lander shall provide LUTE with single-point ground.

3.4 Airborne Support Equipment

TBD

3.5 Ground Support Equipment (GSE)

Lander GSE shall be in accordance with MSFC-SPEC-1548.

3.5.1 Mechanical Ground Support Equipment (MGSE)

3.5.1.1. The Lander MGSE shall include all equipment required to support subsystem and system verification, assembly, integration, and transportation, and launch support.

3.5.2 Electrical Ground Support Equipment (EGSE)

3.5.2.1. System EGSE, hardware and software, shall be provided to enable system level pre-launch checkout of the Lander and the IP.

3.5.3 Ground Support Software

TBD

3.5.4 Servicing

TBD

3.6 Propulsion Performance

3.6.1 Main Propulsion System (MPS)

3.6.1.1. Functional Requirement

The MPS shall provide the required thrust for LOI, lunar descent, and landing.

3.6.1.2. Propellant Requirements

The MPS shall provide the propellant necessary to perform the velocity change maneuvers required by the mission.

3.6.1.3. Propellant Quality

TBD

3.6.2 Reaction Control System (RCS)

3.6.2.1. Functional Requirement

The RCS shall generate the required control torques to achieve and maintain vehicle attitudes during TLI, LOI, and landing.

3.6.2.2. Propellant Requirements

The RCS shall provide the propellant necessary to perform the maneuvers in paragraph 3.6.2.1.

3.6.2.3. Propellant Quality

TBD

3.7 Thermal Control System

The TCS shall maintain all Lander system and component temperatures within the specified limits during all mission phases. The thermal design shall be based on worst case mission parameters of attitude, altitude, beta angle, and heat rates. The design shall also be based on worst case estimates of interface conductance, multilayer insulation (MLI) performance, power configuration, and mission timeline. Passive thermal control shall be used.

3.8 Thermal Protection System

TBD

3.9 Communications and Tracking System (C&TS)

3.9.1 Functional Requirement

The Lander C&TS shall provide the capability to transmit engineering and scientific data, receive and demodulate commands, and provide tracking.

3.9.2 DSN Compatibility

The C&TS shall be compatible with the DSN per DSN TBD {810-5}.

3.9.3 Uplink and Downlink Transmission

3.9.3.1 All uplink and downlink data transmission to and from IP shall be via the Deep Space Network (DSN).

3.9.3.2 The Lander shall be capable of continuous uplink and downlink transmission from LOI to post landing shutdown.

3.9.4 High Gain Antenna

The HGA shall be capable of providing coverage via DSN to accommodate command, monitoring, and engineering data.

3.9.5 Data Transmission

3.9.5.1 Transmission Rates

TBD

3.9.5.2 RF Link Margins

TBD

3.9.5.3 Bit Error Rates (BER)

Data transmitted (sensor to user) shall have no more than one error in TBD bits.

3.10 Data Management System (DMS)

3.10.1 Functional Requirements

The DMS shall perform command processing for the Lander subsystems, provide the required storage for data and commands, provide the central timing, and provide computation support for all Lander subsystems.

3.10.2 Timing and Clock Frequencies

3.10.2.1 The IP shall provide time in Universal Time Coordinated (UTC) format and required clock frequencies at constant frequency with a resolution of one microsecond and a stability of TBD Hz in 24 hours.

3.10.2.2 The time in UTC format shall be relatable to UTC within TBD milliseconds.

3.10.3 Command

3.10.3.1 Command Capability

A multi-rate command capability shall be implemented to optimize commanding in the real time and memory load modes and to maximize link margin for contingency operation.

3.10.3.2 Command Storage

The Lander shall have the capability for onboard command storage of TBD thousand words.

3.10.3.3 Command Error

The onboard data management system shall allow for no more than one erroneous command in TBD commands to go undetected.

3.10.3.4 Command Confirmation

The Lander shall have the capability to verify command reception and engineering data transmission during all phases of its mission.

3.10.4 Lander Engineering Telemetry

Data shall be contained in an engineering data stream to determine the health and status of all on-board systems.

3.10.5 Format Capability

The DMS shall provide re-programmable and fixed format capability and the capability to select formats.

3.10.6 Data Processing

3.10.6.1 The DMS shall contain a digital computer(s) for data processing.

3.10.6.2 The data system will be capable of processing uplink and downlink transmissions from LOI to post landing shutdown.

3.10.7 Computer(s) Reloading

The DMS digital computer(s) shall have the capability to reload or patch the onboard software upon ground command.

3.10.8 Error Detection and Correction

TBD

3.11 Software

3.11.1 Software Management

The management and development of the Lander flight software and supporting computer software shall be included in the IP Software Management Plan, using MM 8075.1 as a guideline.

3.11.2 Preflight Test Software

TBD

3.11.3 Flight Software Design Parameters, TBD

3.12 Guidance, Navigation and Control (GN&C) System

3.12.1 Functional Requirements

3.12.1.1 The GN&C contains the necessary hardware and software to autonomously execute the IP vehicle attitude and control during all Lander powered flight phases.

3.12.1.2 The Lander shall incorporate a tracking system to support descent and landing at the specified lunar landing site.

3.12.2 Performance Requirements

TBD

3.13 Mechanical System Requirements

TBD

3.14 Physical Standards

3.14.1 Coordinate System

The Lander coordinate system shall be in accordance with NASA TM-X-73343, as shown in Figure 1-2, page 3 of this document.

3.14.2 Envelopes/Dimensions

The IP shall reside within the TBD usable static envelope provided by the TBD launch vehicle payload shroud.

3.14.3 Mass Requirements

The total mass of Lander including interface hardware shall not exceed TBD kg.

3.14.4 NASA Standard Components

The Lander shall incorporate NASA standard and other proven or qualified parts or components.

3.14.5 Loads and Frequency Requirements

The Lander shall withstand the structural and thermal loads produced by natural and induced environments as required in Section 3.19.

3.14.6 Measurement Unit System

International System of Units (SI) shall be used. Expression in both SI and US Customary Units is acceptable where the use of SI units alone would obviously impair communication or reduce the usefulness of a report to the primary recipients. When both systems of units are used, the units used for the principal measurements and calculations will be stated first, followed by the other system in parentheses.

3.14.7 Factors of Safety

TBD

3.14.8 Fatigue

TBD

3.15 Reliability Requirements

3.15.1 Single Point Failure

No single point failure within the LUTE/Lander subsystems shall cause a loss of the IP or permanent loss of command capability, engineering telemetry, or scientific data.

3.16 Maintainability Requirements

3.16.1 Fracture Control Program

Fracture control program will follow MSFC-HDBK-1453 where appropriate (TBD).

3.17 Quality Assurance Requirements

TBD

3.18 Safety and Mission Assurance (S&MA) Requirements

3.18.1 S&MA Plan

A S&MA Plan, MSFC-PLAN-TBD, shall be prepared, maintained, and implemented for the LUTE program. The plan shall describe the organization and method of implementation of the S&MA program for the Lander design, development, production, test, and flight with respect to safety, reliability, and quality assurance requirements.

3.18.2 Launch Vehicle Mission Assurance

3.18.2.1 The safety and mission assurance for the IP will meet the requirements of NHB 5300.4(1D-2) and NHB 5300.4(1C) as appropriate, per the IP payload classifications on specific materials, parts, components and services (TBD).

3.18.2.2 No hazard associated with the Lander or its deployment procedures shall prevent the safe execution of the launch vehicle mission.

3.18.3 Ordnance Devices

Ordnance devices utilized in the Lander/Launch vehicle interface shall not degrade the performance of the IP.

3.18.4 Range Safety

The Lander shall not preclude the launch vehicle from properly executing a launch vehicle mission abort sequence should one be considered necessary.

3.19 Environment Requirements

3.19.1 Natural Environment

3.19.1.1 General Requirement

The Lander design shall comply with the natural environment specified in NASA TM-TBD.

3.19.1.2 Meteoroid, Orbital, and Lunar Debris Impact

The Lander shall provided protection against loss of functional capability when subjected to the debris flux models as defined in TBD-DOC.

3.19.1.3 Radiation/Nuclear Radiation

TBD

3.19.1.4 Thermal

3.19.1.4.1 Flight Environment

The Lander shall be capable of withstanding the following temperature extremes:

Earth Orbit
Minimum: TBD° K
Maximum: TBD° K

Trans-Lunar Flight
Minimum: TBD
Maximum: 70° K

Lunar Surface Temperature
Minimum: 93° K
Maximum: 395° K

3.19.1.4.2 Ground Environment

GSE shall be provided to accommodate thermal control requirements for the Lander when subjected to the ground environments defined in TBD-DOC which are experienced during pre-flight assembly, test, and transport.

3.19.2 Induced Environment

3.19.2.1 General Requirement

The Lander shall be capable of meeting its performance requirements after exposure to any environment or combination of environments specified in DOC-TBD.

3.19.2.2 Acoustics

The Lander shall be designed to assure structural integrity and functionality upon exposure to the maximum acoustic levels within the launch vehicle payload shrouds.

3.19.2.3 Random Vibration

The Lander shall be designed to withstand the random vibration environments during lift-off and transonic flight.

3.19.2.4 Shock

The Lander shall be designed for the shock levels generated by the facility and launch vehicle separation devices. The shock levels at the separation interface shall be attenuated throughout the structure to component/sub-assembly locations.

3.19.2.5 Low Frequency and Steady State Accelerations

The Lander shall be designed to withstand the low frequency and stead-state acceleration environments that occur during the launch, ascent, and on-orbit flight elements.

3.19.2.6 Overpressurization and Control

Provisions shall be made to preclude over pressurization damage to any part of the Lander during launch.

3.19.3 Contamination

The Lander shall be maintained in a class TBD environment during and following assembly.

3.19.4 Magnetic

A magnetic cleanliness program with magnetic materials and wiring control shall be implemented.

3.20 Transportability/Transportation Requirements

3.20.1 Shipping Container Design

3.20.1.1 The Lander shall be shipped in a container specifically designed to protect the IP during surface and air transportation.

3.20.2 Transportation Environment

3.20.2.1 The Lander transportation container shall maintain an environment that meets cleanliness and thermal specifications for ground processing as outlined in section 3.19 of this document.

3.20.3 Prime Mode of Transportation

3.20.3.1 The prime mode of transportation of the Lander between ground sites shall be by TBD mode of transportation.

3.21 Storage Requirements

3.21.1 Storage Cleanliness

3.21.1.1 The Lander shall be stored in a class 100K environment during idle periods after assembly and Lander vehicle integration.

3.21.2 Shelf Life

3.21.2.1 The Lander shall be capable of nominal operations after TBD years of idle storage.

3.21.3 On-pad Stay Time

TBD

3.22 Design and Construction Requirements

TBD

3.23 Interface Requirements

3.23.1 Launch System Interface

The Lander shall interface with the TBD launch vehicle and its related facilities as defined in TBD-DOC.

3.23.2 Lander to LUTE

The Lander shall interface with the LUTE as defined in ICD-TBD.

3.23.3 Lander to Deep Space Network

The Lander shall interface with the DSN as defined in ICD-TBD. (-3-600041)

4.0 VERIFICATION

4.1 General

TBD

4.2 Verification Types

TBD

4.3 Verification Requirements Matrix

TBD

4.4 Verification Facilities and Equipment

TBD

4.5 Spacecraft Hardware Requirements

4.5.1 Payload Classifications

The Lander shall use liberalized payload classifications based upon use of proven flight design, parts, and materials with applicable testing, as required in the following documents:

NMI 8010.1
MMI 8030.2
MMI 8080.5

4.5.2 Previously Flown Hardware

The Lander shall reuse previously flown hardware which has been refurbished and tested as required.

4.5.3 Controlled Prototype Hardware

The Lander shall make use of controlled prototype hardware as flight hardware by manufacturing to baselined engineering requirements with quality verifications which have not subjected the hardware to structural or life-limiting environments exceeding program flight requirements.

4.5.4 Off-the-shelf Parts

The Lander shall make use of "off-the-shelf" parts, materials and components qualified for flight use, per the information contained in the following documents:

MSFC-HDBK-527F
MSFC-STD-506C

5.0 PREPARATION FOR DELIVERY

5.1 Preparation, Packaging and Shipment

TBD

6.0 NOTES

TBD

7.0 APPENDIX -- A Verification Matrix

TBD

APPENDIX E

LUTE/ARTEMIS

APPENDIX E

LUTE/ARTEMIS

List of Figures:

Figure 1 LUTE/Artemis Layout

2 Launch Configuration

3 Operational Configuration

Lunar Ultraviolet Telescope Experiment

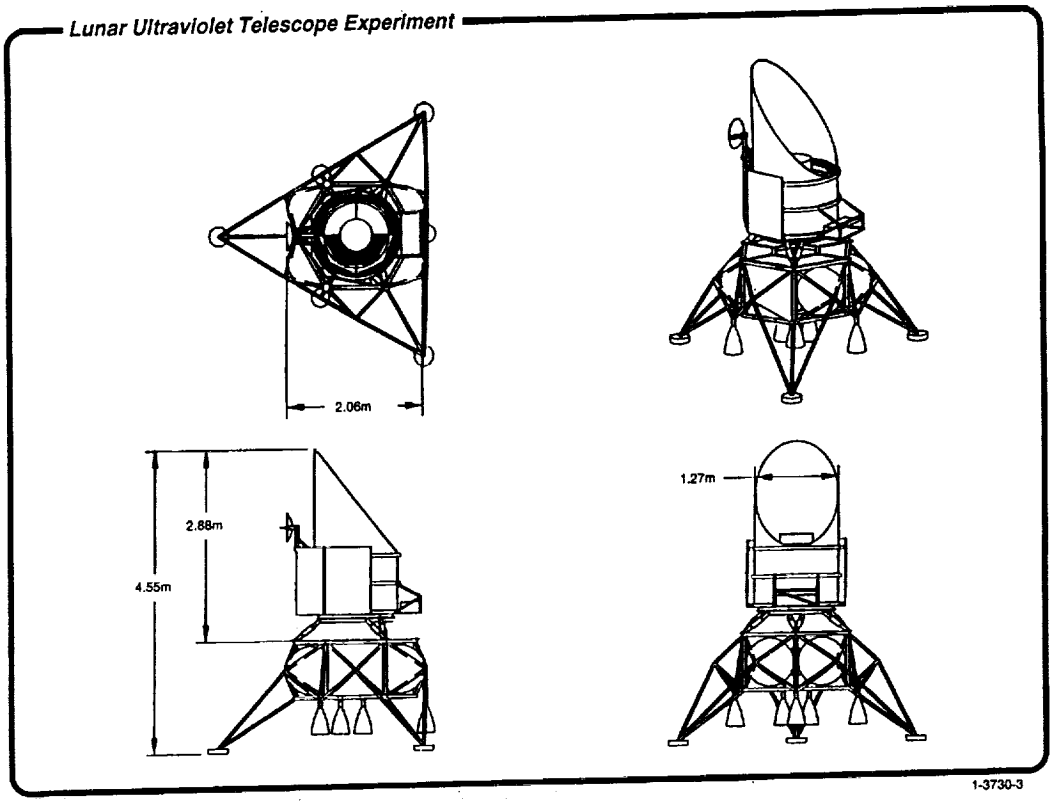

1-3730-3

Lunar Ultraviolet Telescope Experiment

Launch Configuration

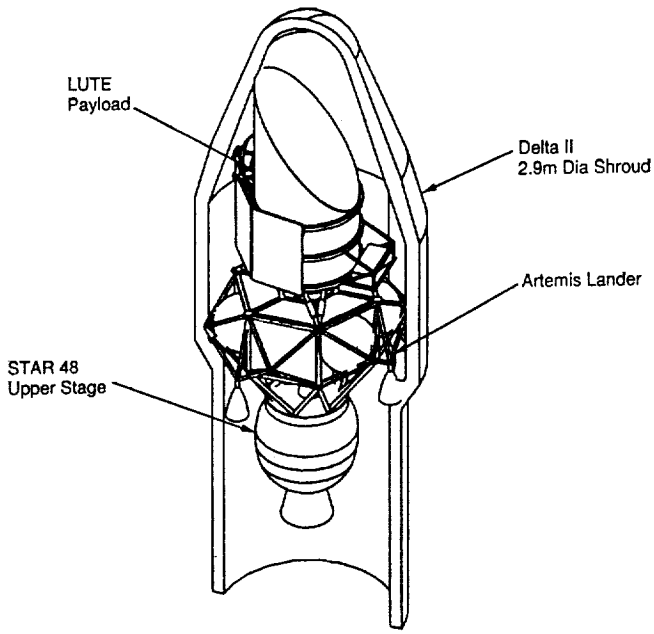

1-3925-2-381

Lunar Ultraviolet Telescope Exoeriment

System Schematic

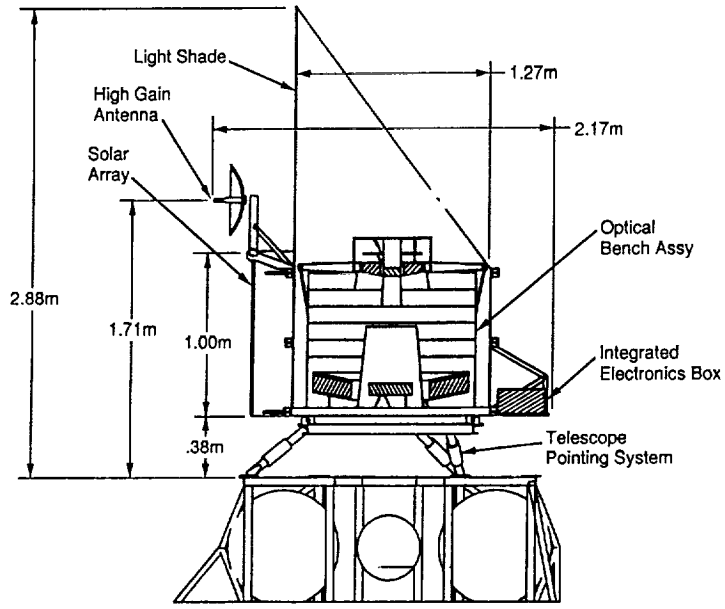

1-3927-2-383

Lunar Ultraviolet Telescope Experiment

Operational Configuration

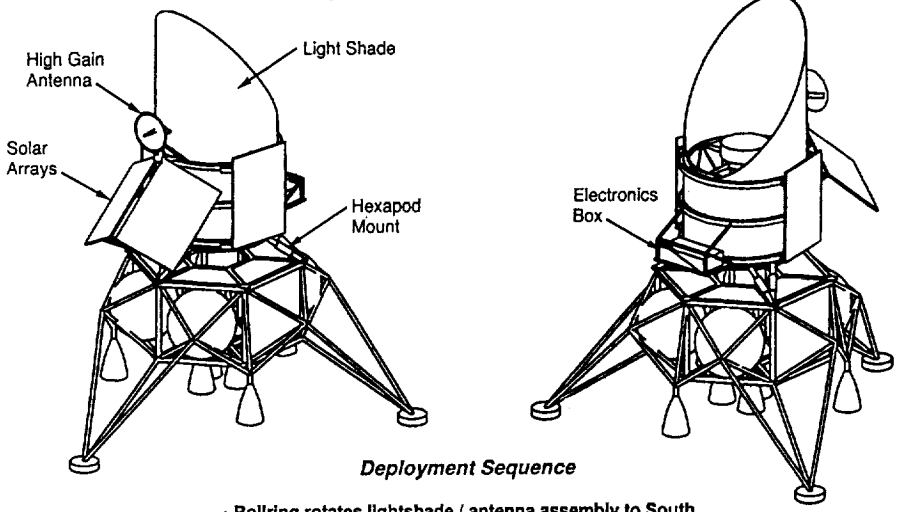

Deployment Sequence

- **Rollring rotates lightshade / antenna assembly to South**
- **Hexapod mount tilts entire assembly to zenith**
- **Deploy solar arrays**
- **Rotate Hi-gain antenna to acquire Earth**
- **Deploy aperture cover**
- **Begin electronics box louver deployment**
- **Begin fine alignment adjustments**

1-3929-2-385

APPENDIX F

LUTE HARDWARE TREE

Lunar Ultraviolet Telescope Experiment

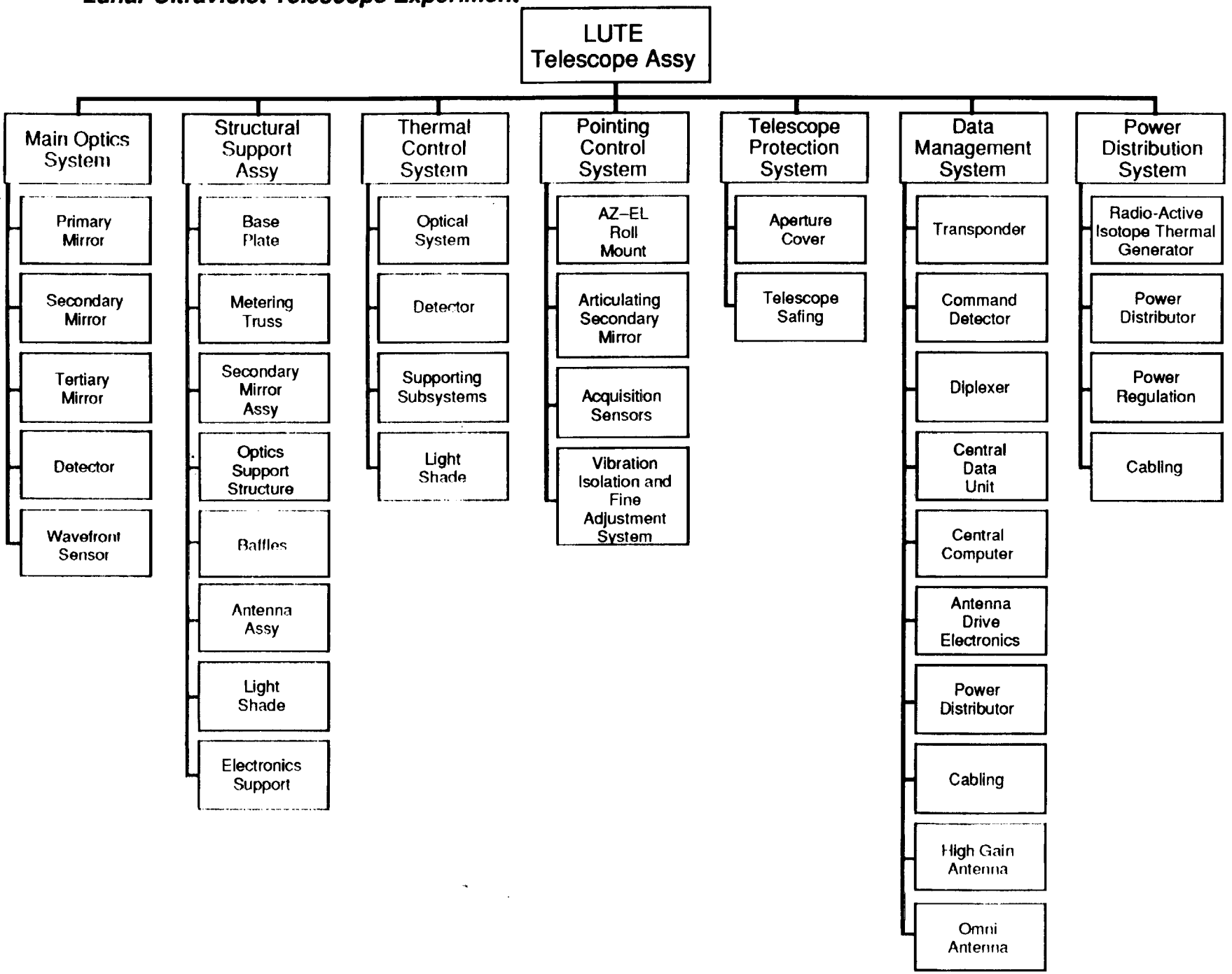

Lunar Ultraviolet Telescope Experiment

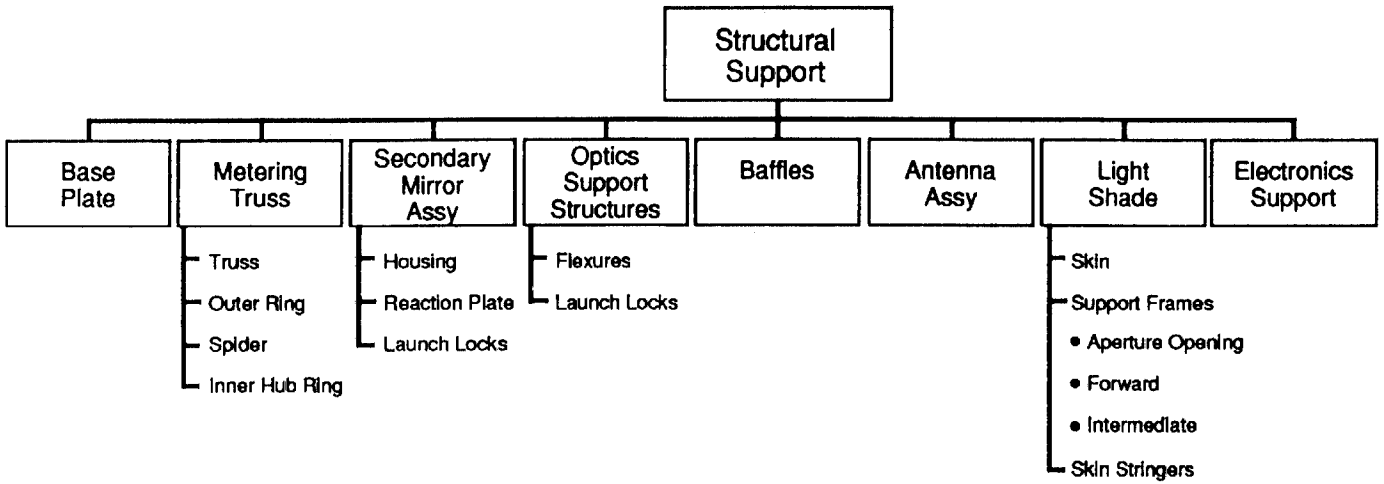

1-3738-2

Lunar Ultraviolet Telescope Experiment

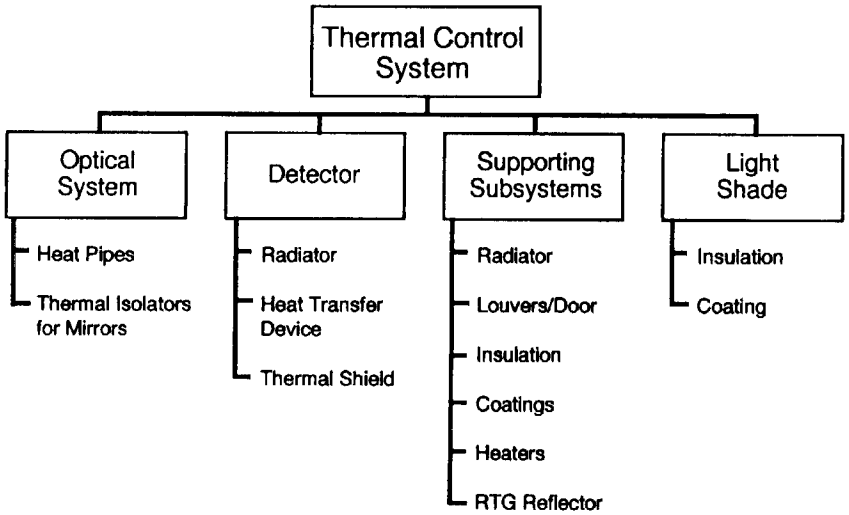

1-3739-2

Lunar Ultraviolet Telescope Experiment

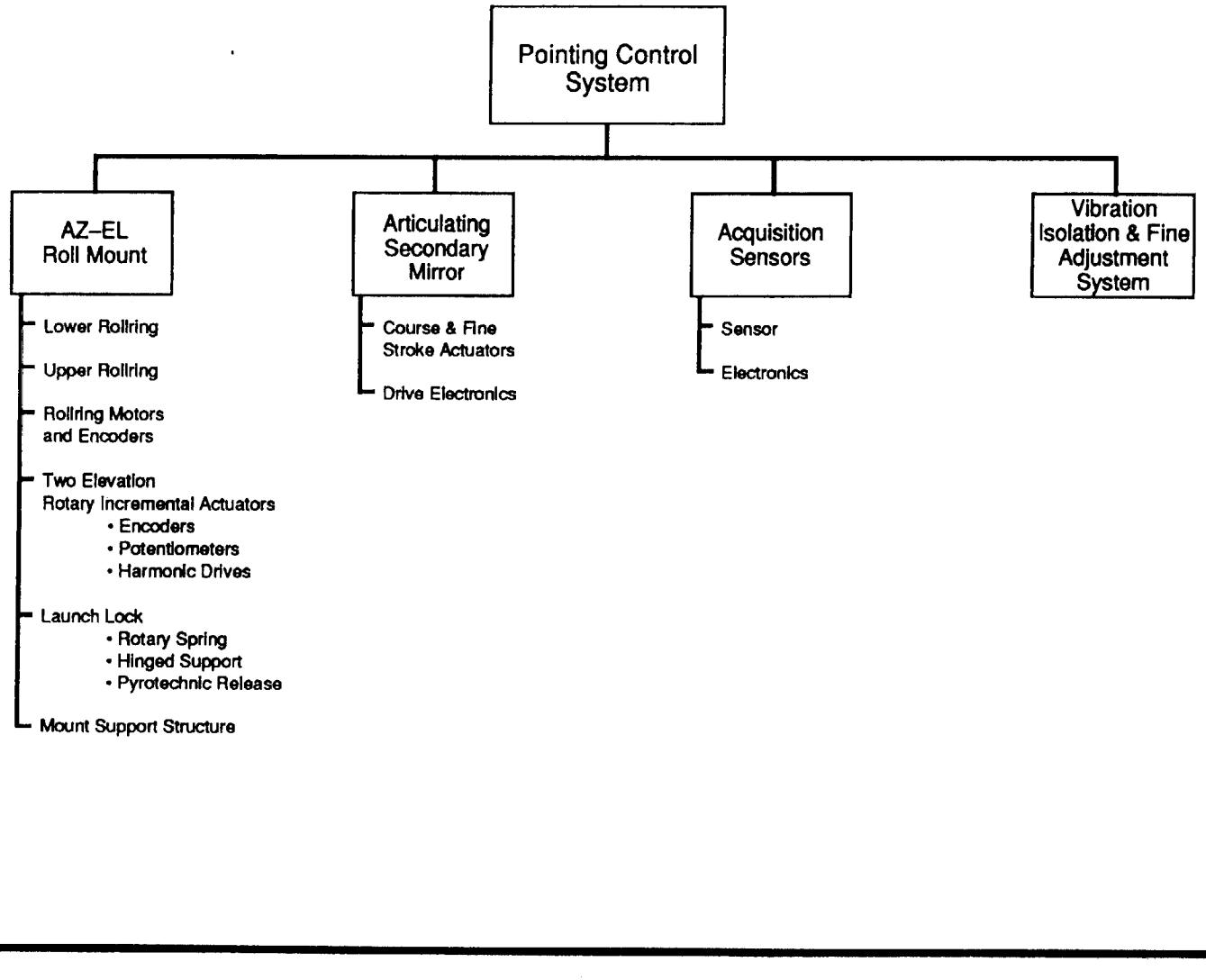

1-3740-2

Lunar Ultraviolet Telescope Experiment

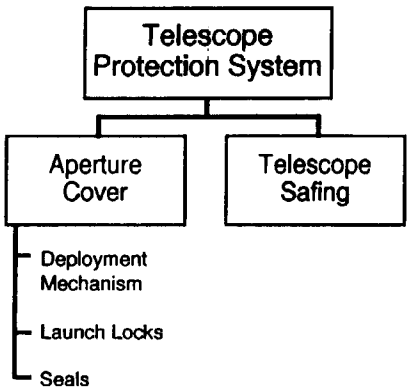

1-3741-2

APPENDIX G

APERTURE COVER CONCEPTS

APPENDIX G

LUTE APERTURE COVER CONCEPTS

List of Figures:

Figure 1 Aperture Cover Concept No. 1
2 Aperture Cover Concept No. 2
3 Aperture Cover Concept No. 3
4 Aperture Cover Concept No. 4
5 Aperture Cover Concept No. 5
6 Aperture Cover Concept No. 6
7 Aperture Cover Concept No. 7
8 Aperture Cover Concept No. 8

LUTE
Aperture Cover Concept #1

- Passive Deployment Method (Torsion Spring)
- Gravity Assisted Opening
- Opened Door is in Gravity Biased Position
- No Hard Stop Required, Simplifies Rate Control

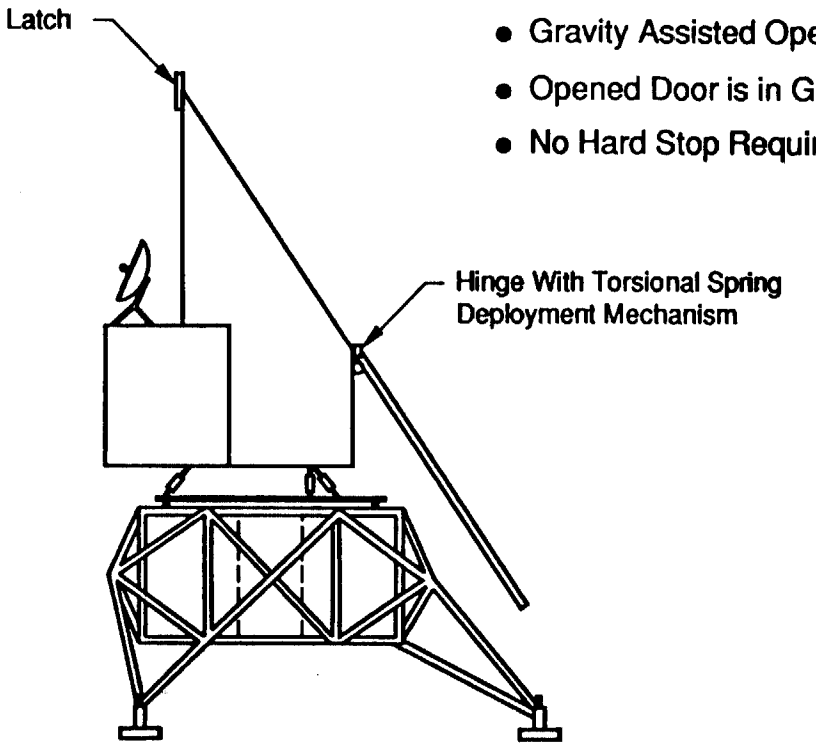

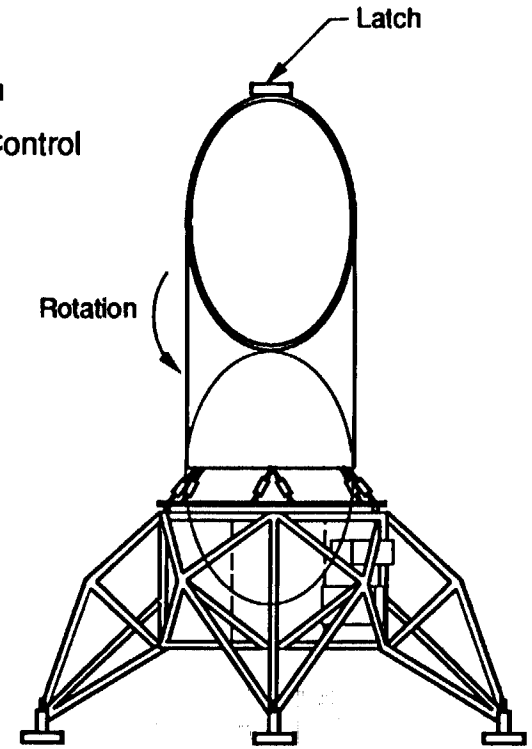

5-20478

LUTE
Aperture Cover Concept #2

- Requires Two Hinges
- Requires at Least Two Latches

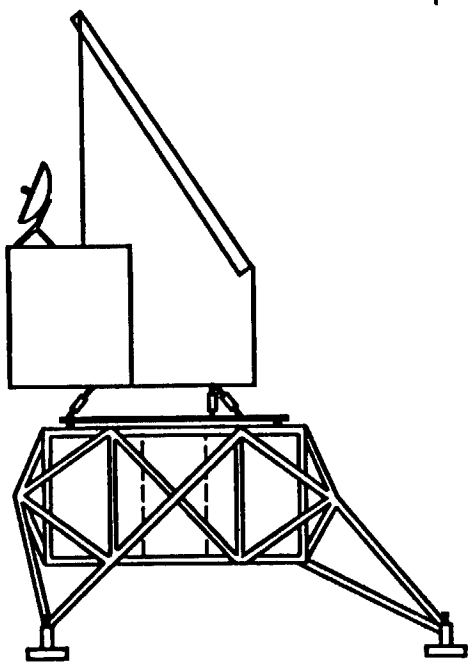

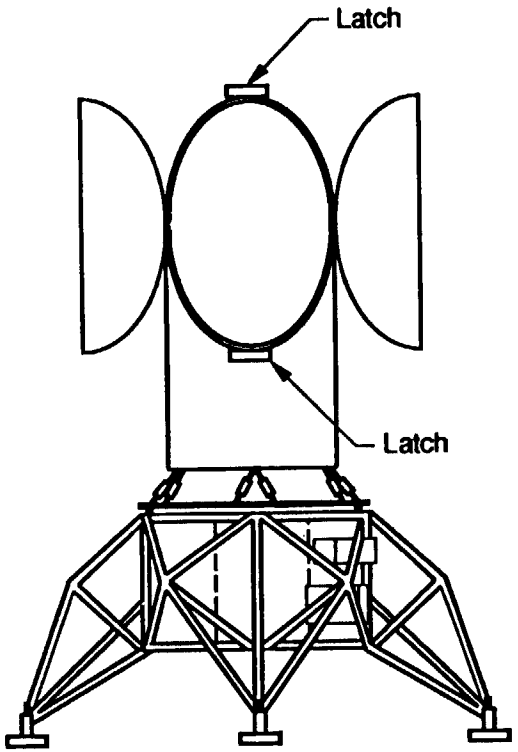

5-20477

LUTE
Aperture Cover Concept #3

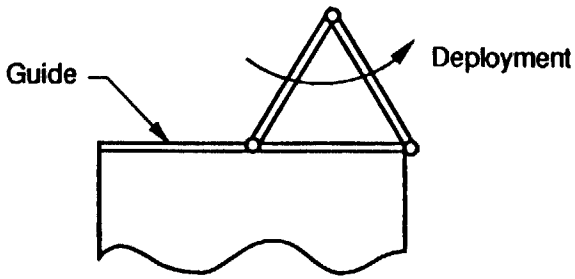

View A

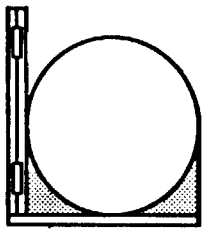

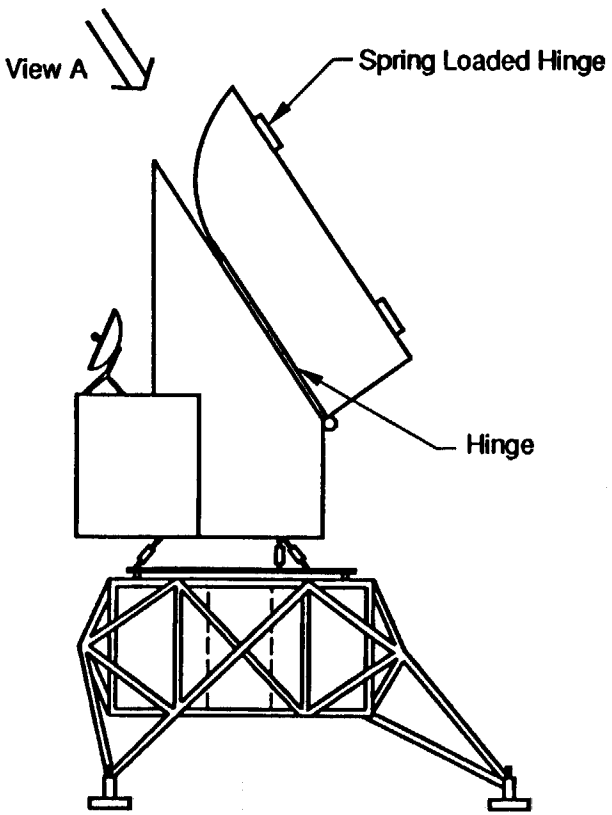

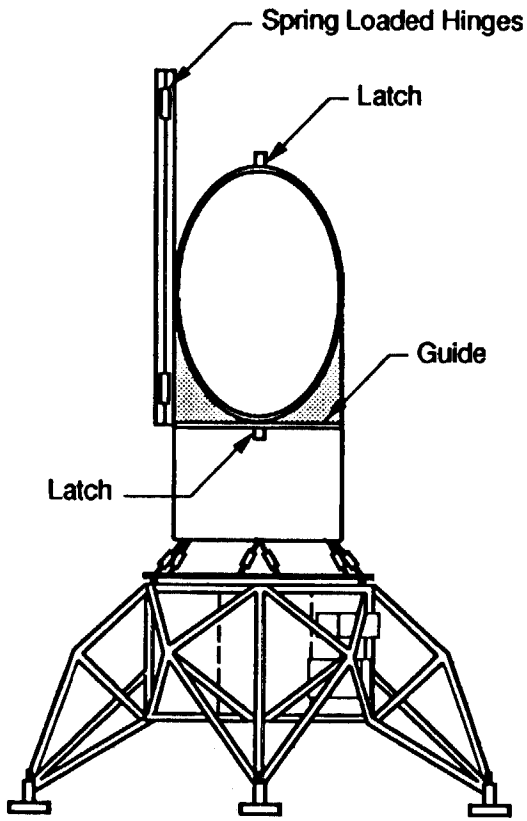

5-20480

LUTE
Aperture Cover Concept #4

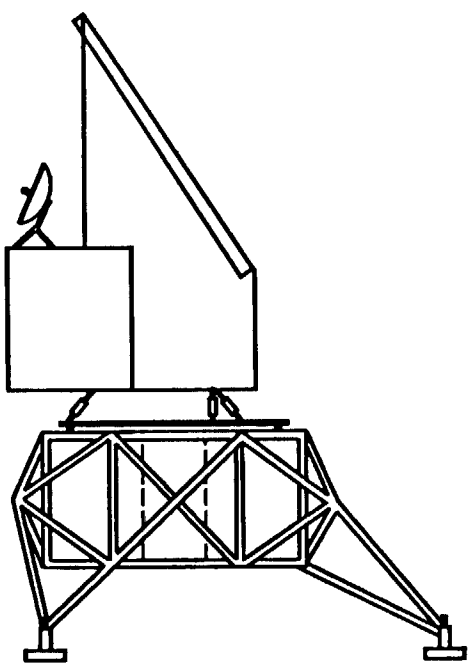

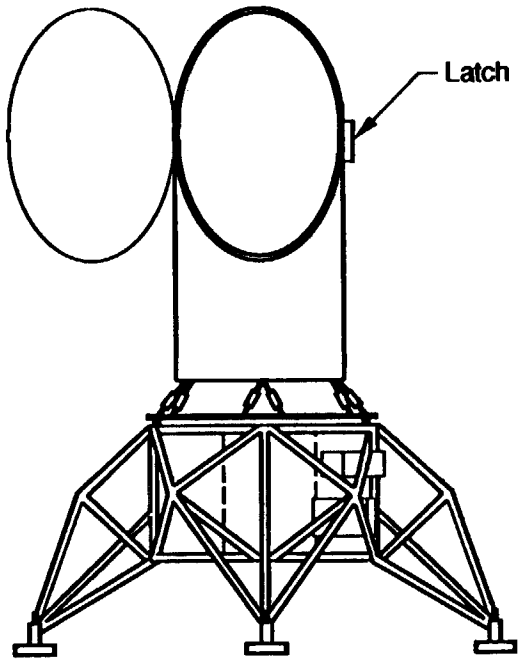

5-20474

LUTE
Aperture Cover Concept #5

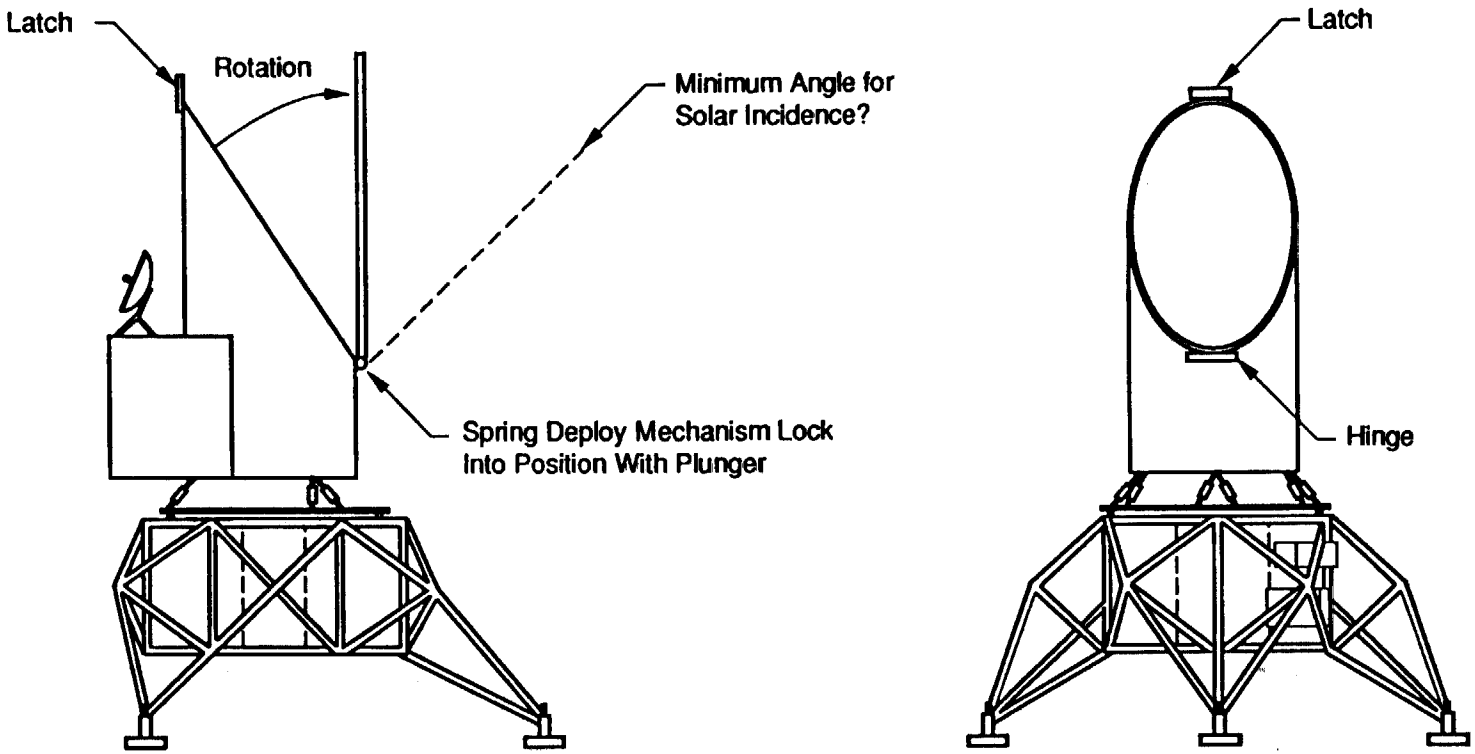

LUTE
Aperture Cover Concept #6

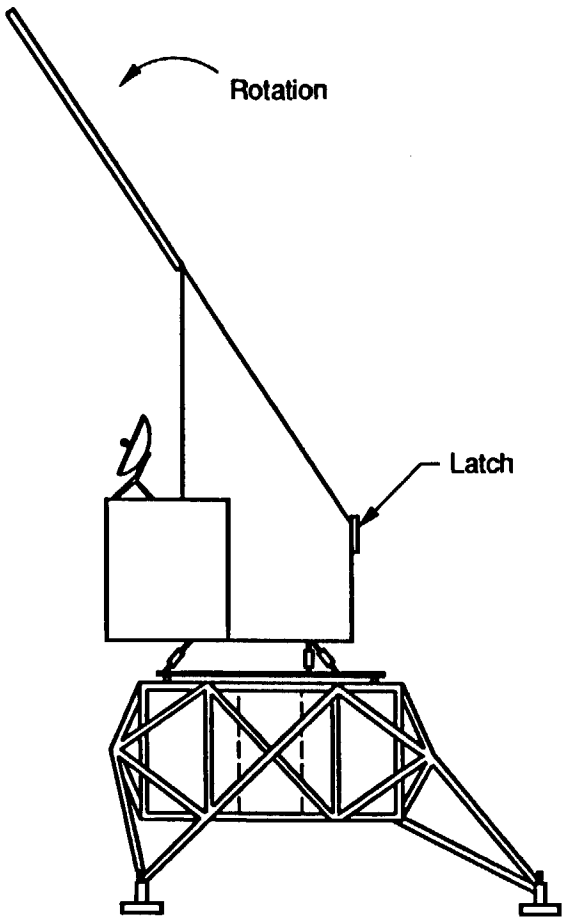

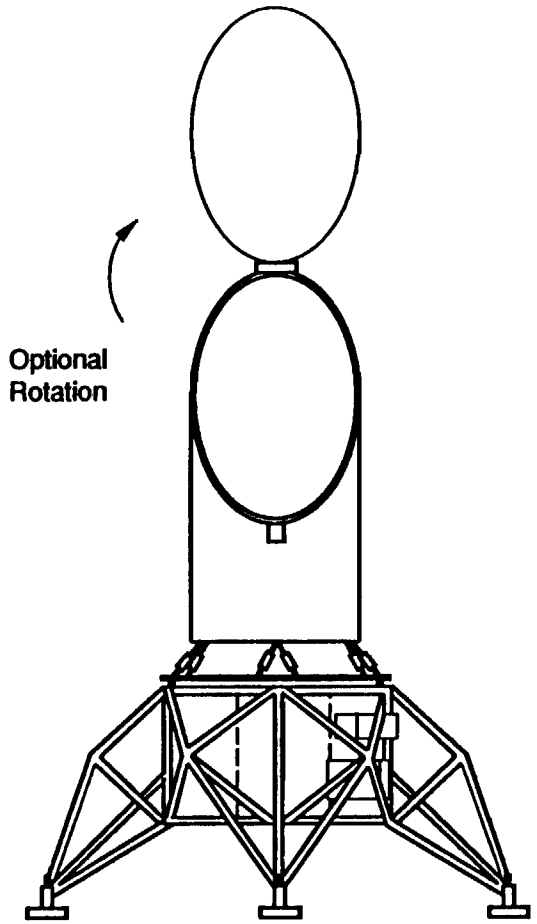

5-20476

LUTE
Aperture Cover Concept #7

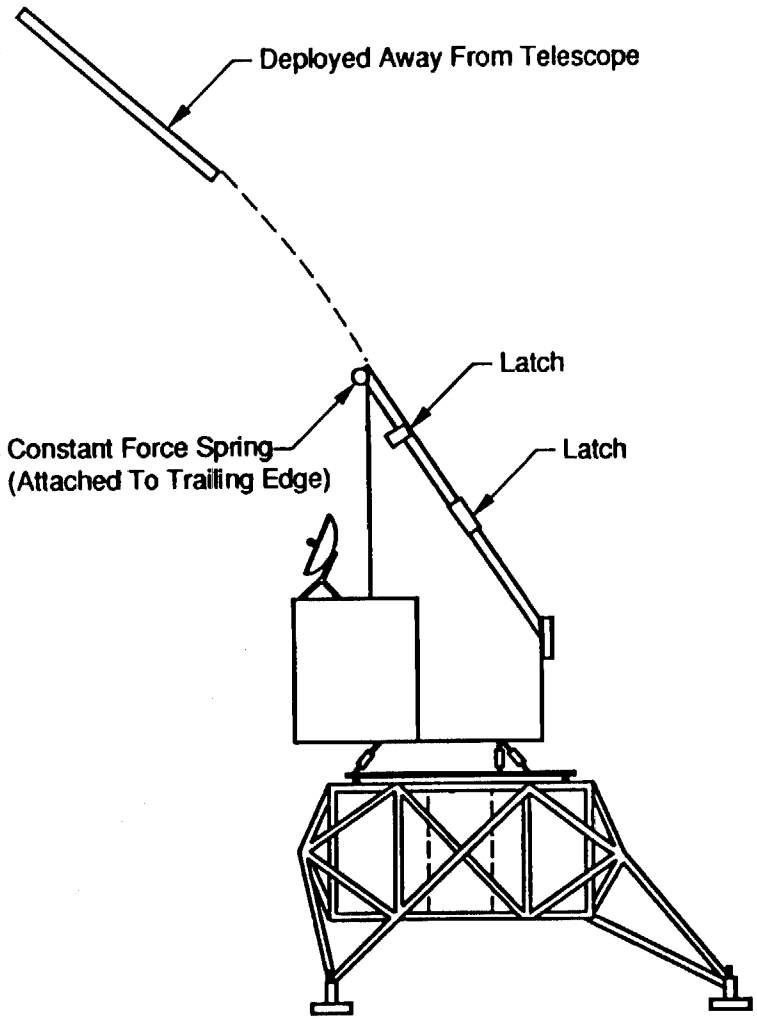

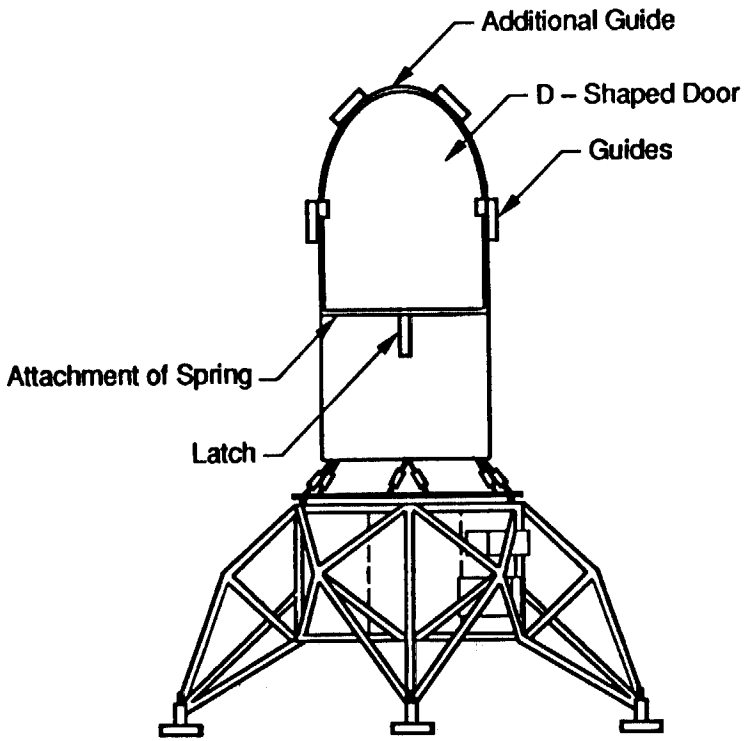

5-20479

LUTE
Aperture Cover Concept #8

- Fabric or mylar cover design options:
  (a) Fold down like accordion-style closet door.
  (b) Cover rolls up.

- Lightweight.

- Motor at bottom of elliptic opening.
  1. Gravity assisted opening.
  2. Reduces dust contamination of optics during cover retraction.

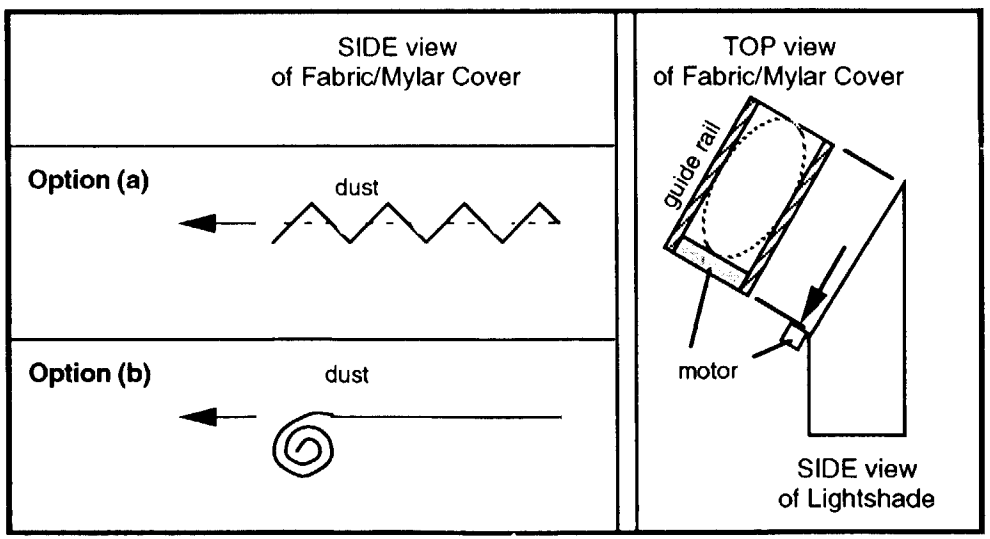

APPENDIX H

MECHANISMS

List of Figures:

Figure 1 Redundant Power Hinge
2 AD or HGA Active Hinge Assembly
3 Eddy Current Damper
4 Damper Qualification Status
5 Honeywell Damper
6 Honeywell Damper
7 Honeywell Damper
8 Hubble Latch
9 Holex Series 5800 Guillotines
10 ASE Pin Pull
11 Sn9400 Series Nut Separates
12 G&H Technology Nonexplosive Separation Nut
13 G&H Technology Nonexplosive Separation Nut
14 G&H Technology Nonexplosive Separation Nut
15 G&H Technology Nonexplosive Separation Nut
16 Starsys Research RL-50-C Launch Latch
17 Starsys Research RL-50-C Launch Latch
18 Fokker Space & Systems Thermal Knife
19 Fokker Space & Systems Thermal Knife

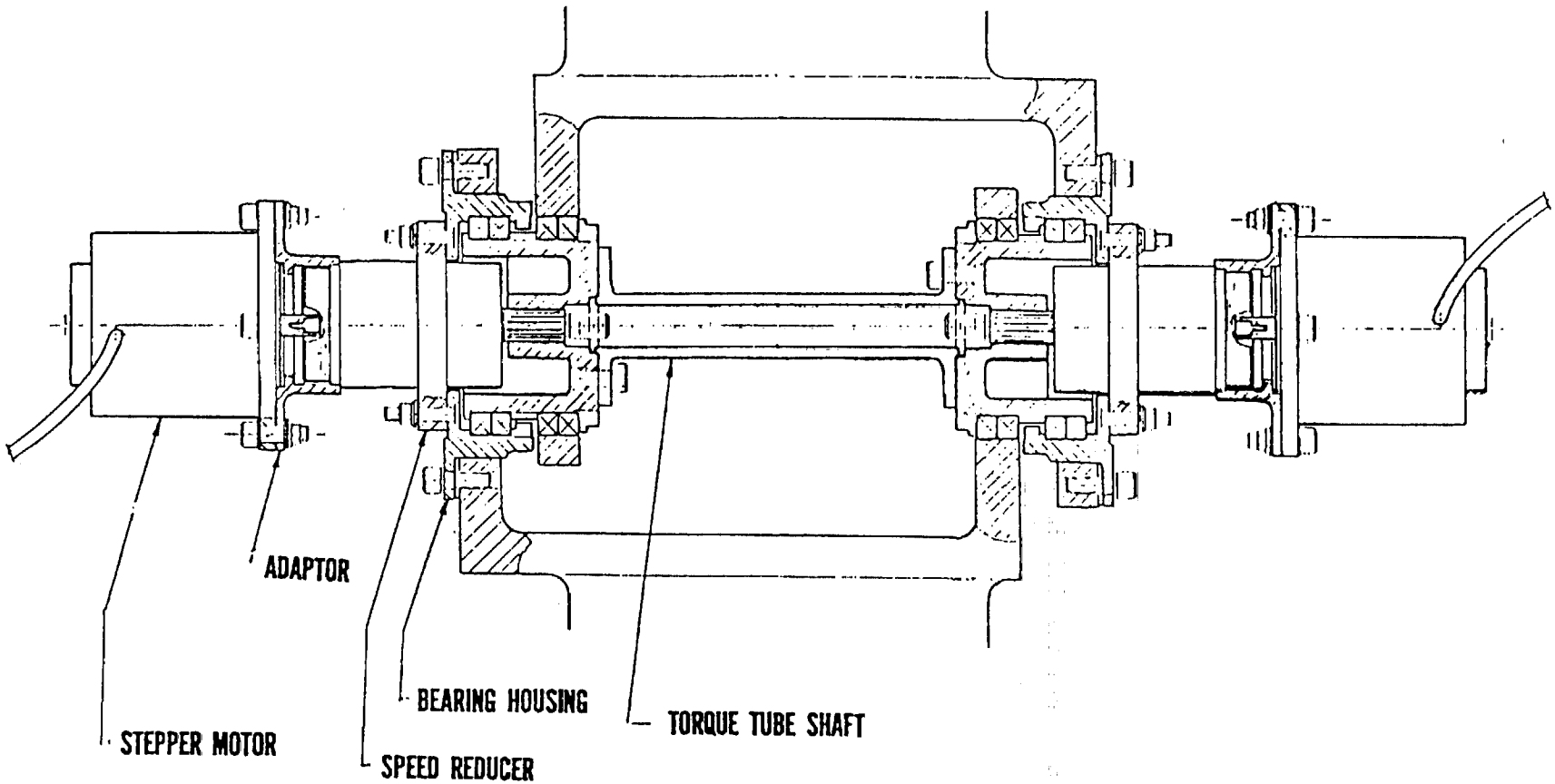

Redundant Power Hinge

AD OR HGA ACTIVE HINGE ASSEMBLY

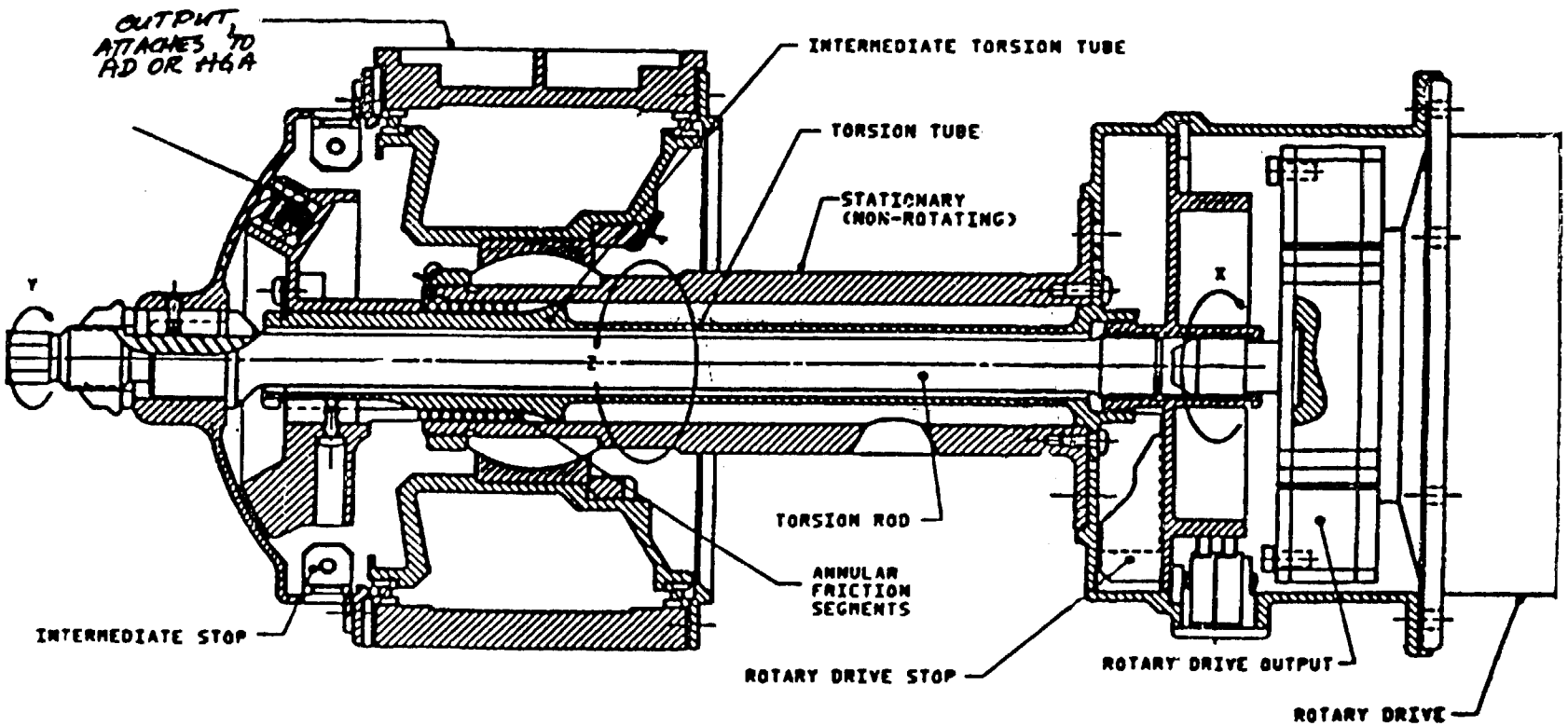

EDDY CURRENT DAMPER

R. C. Ellis*, R. A. Fink*, R. W. Rich*

ABSTRACT

A high torque capacity eddy current damper has been successfully developed as a rate limiting device for a large solar array deployment mechanism. The eddy current damper eliminates the problems associated with the outgassing or leaking of damping fluids. It also provides other performance advantages such as damping torque rates which are truly linear with respect to input speed, continuous 360 degree operation in both directions of rotation, wide operating temperature range, and the capability of convenient adjustment of unit damping rates by the user without disassembly or special tooling.

INTRODUCTION

The eddy current damper shown in Figure 1 consists of a copper alloy disk which rotates between opposed samarium cobalt magnets. Rotation of the disk in the magnetic field generates circulating eddy currents within the disk which create a damping torque proportional to rotation speed. The damping output can be dramatically increased by coupling the eddy current disk to a gearhead speed increaser (Figure 2). The overall damping rate is magnified by the square of the gear ratio since the gearhead acts to simultaneously increase disk speed while reducing the transmitted torque from the mechanical input of the unit. The damper design presented in this paper uses a four-stage planetary gearhead to boost the unit damping rate to 2260 N-m-sec/rad (20,000 in-lb/rad/sec.). Damping rates can be easily adjusted in the field by rotating the unit end bell, thereby misaligning magnets on either side of the eddy current disk.

The damper design also incorporates other special design features intended to minimize the size and weight of the unit and improve reliability.

* Honeywell Space and Aviation Systems, Durham, NC

DAMPER QUALIFICATION STATUS

Program	Customer	Status	Qual. temp (°C)	Qual. Vibr. Equiv. GRMS
Milstar	LMSC	Qualified	-51 to +104	18.6
MSAT	LMSC	Qualified	-51 to +104	18.6
Shuttle RMS	SPAR	Flown	-36 to +96	15.1
Radarsat	SPAR	Qualified	-70 to +60	12.2
TOPEX	Fairchild	Flown	-51 to +104	18.6
Milstar	Hughes	Qualified	-73 to +121 Non-op. -51 to +71 Oper.	26.3
DMSP	Astro	In fab.	-56 to +61	22.4

MAGNETIC DAMPER	P/N 2961068-1
DAMPING RATE (MAX.) IN-LB-SEC/RAD	10
DAMPING RATE (MIN.) IN-LB-SEC/RAD	5
INPUT TORQUE (MAX.) IN-LB	55
WEIGHT, (MAX.) OZ.	TBD

REVISIONS				
LTR	ZONE	DESCRIPTION	DATE	APPROVED
A		...	09-14-92	B.T.H. C.P.S.

NOTES:

1. DIRECTION OF ROTATION IS DEFINED WITH RESPECT TO VIEWING THE INPUT SHAFT END OF THE DAMPER.
2. BLACK LINE INDICATES NOMINAL DAMPING RATE SETTING.

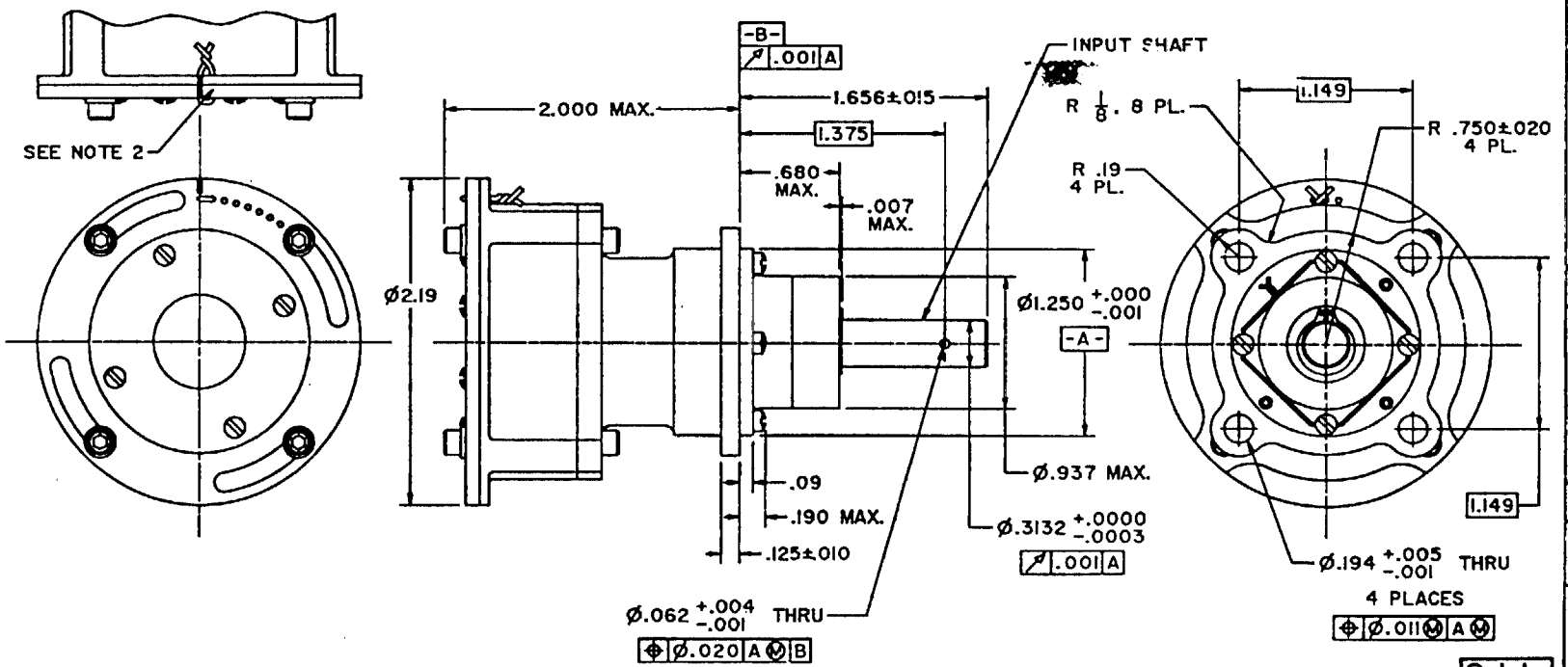

C.I.L.

DRAWN BY	DATE
D.R.GOSS	04-23-91
DESIGNED BY	DATE
W.B.S.	04-23-91
CHECKED BY	DATE
D.R.GOSS	04-27-91
APPROVED BY	DATE
C.P.S.	04-29-91

Honeywell

HONEYWELL INC. SPACE AND AVIATION SYSTEMS ELECTRO COMPONENTS DURHAM, NORTH CAROLINA

TITLE

PERFORMANCE AND OUTLINE
MAGNETIC DAMPER

SIZE	CODE IDENT NO.	DRAWING NO.	REV
C	90012	2941068	A

SCALE 2/1 SHEET 1 OF 1

DAMPER	2960946-1
DAMPING RATE (MAX.)	20,000 IN.-LBS.-SEC. MAX
DAMPING RATE (MIN.)	10,000 IN.-LBS.-SEC. MIN
INPUT TORQUE (IN.-LBS.) (MAX.)	700
ROTATION (CW OR CCW)	360°
WEIGHT (LBS.) (MAX)	1.54

REVISIONS				
LTR	ZONE	DESCRIPTION	DATE	APPR.
A	B4	UPTO END VIEW (ADDED) W/A DIM NOTED SPEC 12-7-86		
B		ADD: NOTES 3 & 4. SEE NOTE 3. RHVD (TABLE) HOLES OFFSET I.D. THR 5-3-86		
C		CALLOUT: #10(.190)-32UNC-3B --- MINIMUM WAS #8(.164)-32UNC-3B --- MINIMUM. CAB 4-16-86	16 APR 1986	
D		DAMPER & HOLES OFFSET DATA EXTENSIVELY REVISED. JCW 12-22-86		
E	B2 A2	CHG .500±.010 DIA WAS .500±.030 .402-.002 WAS .405-.005 (2 PL.) COMPANY NAME WAS "SPERRY" DRG 9-17-91	9-17-91	

NOTES:

1. THE PERCENTAGE OF FULL DAMPING RATE IS DETERMINED BY THE NUMBER OF ADJUSTMENT HOLES THAT THE SCRIBED LINES ARE OFFSET. VIEW B DEPICTS CONFIGURATIONS OF MAXIMUM AND MINIMUM DAMPING RATES.
2. THE FOLLOWING TABLE RELATES THE NUMBER OF HOLES THAT THE SCRIBE MARKS ARE OFFSET TO THE PERCENTAGE OF FULL DAMPING RATE.
3. THE FOUR END BELL ATTACHMENT SCREWS SHOULD BE TORQUED TO 4½ ± ½ IN.-LBS. MORE THAN REQUIRED TO OVERCOME THE RESISTANCE TORQUE OF THE LOCKING ELEMENT.
4. DIRECTION OF ROTATION IS DEFINED WITH RESPECT TO VIEWING THE INPUT SHAFT END OF THE DAMPER.

HOLES OFFSET	% FULL DAMPING RATE (NOMINAL)
0	100
1	97
2	92
3	84
4	74
5	62
6	57
7	41

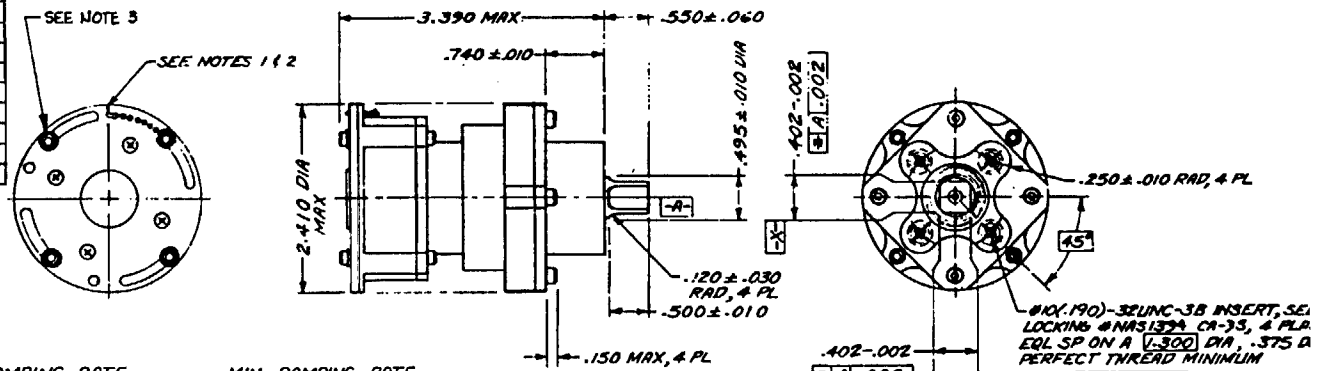

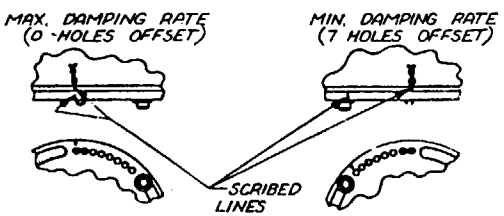

VIEW B

HONEYWELL

DRAWN BY	DATE
CHR & BTH	10-9-85
CHECKED BY	DATE
WBS	11.7.85
APPROVED BY	DATE

TITLE: PERFORMANCE & OUTLINE DAMPER

SIZE	CODE IDENT NO.	DRAWING NO.
C	90012	2940946

SCALE 1:1 | UNIT WT | SHEET 1 OF 1

DAMPER	2960946-2
DAMPING RATE (MAX.) IN-LB-SEC/RAD	6000
DAMPING RATE (MIN.) IN-LB-SEC/RAD	3000
DAMPING RATE (NOM.) IN-LB-SEC/RAD	4500
INPUT TORQUE (IN-LBS) (MAX.)	700
ROTATION (CW OR CCW)	360°
WEIGHT (LBS.) MAX	1.60

DWG NO. 2940946-2 SHEET 1 OF 1

REVISIONS				
LTR	ZONE	DESCRIPTION	DATE	APPROVED

NOTES:

1) DIRECTION OF ROTATION IS DEFINED WITH RESPECT TO VIEWING THE INPUT SHAFT END OF THE DAMPER.
2) BLACK LINE INDICATES NOMINAL DAMPING RATE SETTING.
3) SURFACE FINISH - PASSIVATED CRES PER QQ-P-35 CHEMICAL CONVERSION COATING FOR ALUMINUM PER MIL-C-5541

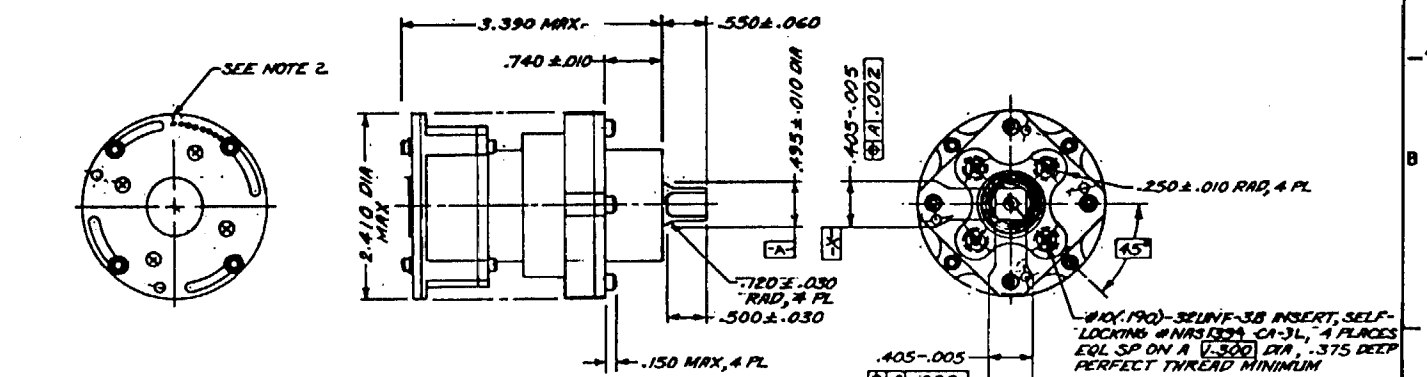

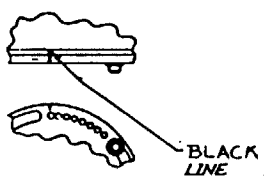

VIEW B

Honeywell

DRAWN BY M. L. T.	DATE 9 SEPT. 89	TITLE PERFORMANCE & OUTLINE DAMPER
CHECKED BY WBS	DATE 16 NOV. 1989	
APPROVED BY S.P.S.	DATE 11-16-89	
UNLESS OTHERWISE SPECIFIED DIMENSIONS ARE IN INCHES TOLERANCES ON FRACTIONS DECIMALS ANGLES		SIZE C · CODE IDENT NO. 90012 · DRAWING NO. 2940946-2 · REV LTR -

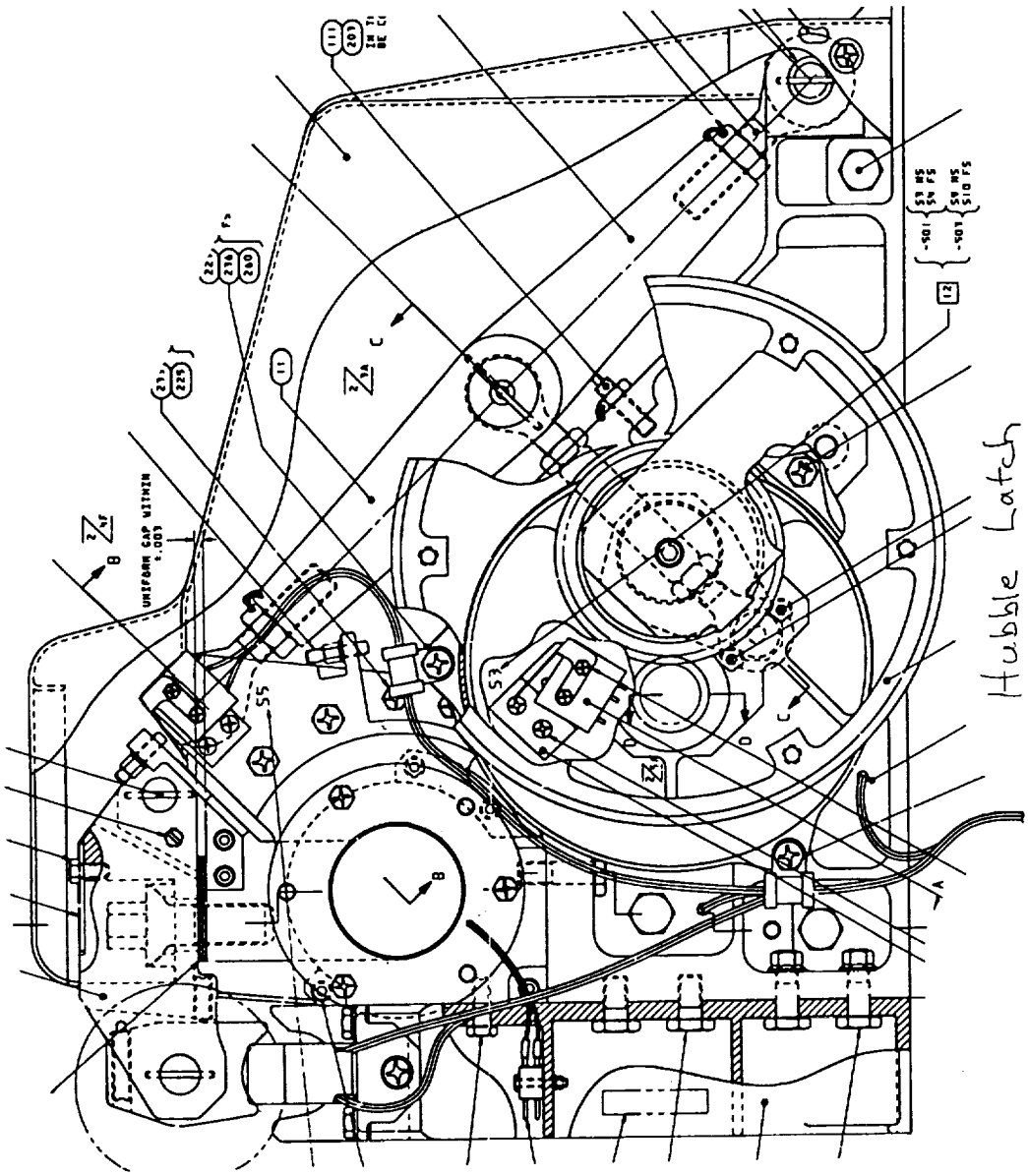
Hubble Latch

TECHNICAL DATA SHEET
HOLEX SERIES 5800 GUILLOTINES

DESCRIPTION

The HOLEX 5800 Series Guillotines were designed to incorporate the one amp-one watt No Fire characteristic in the versatile 2800 Series Guillotines. Additional handling safety is provided while retaining all the reliable operating characteristics of the 2800 Series.
The 5800 Series Guillotines are classified as "Class C" Explosives and may be shipped by air or surface transport.

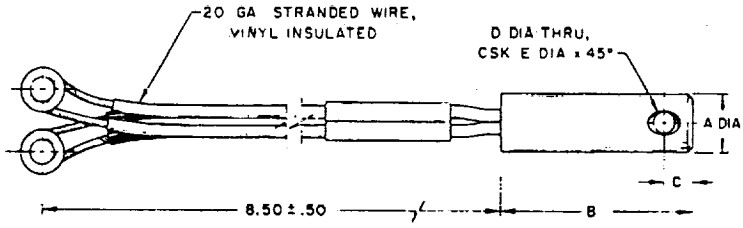

APPLICATION DATA

The 5800 series guillotines have been extensively tested for operation over a temperature range of −65°F to +160°F and are designed to meet most current military environmental specifications.

These guillotines will cut the following specific cables:
MODEL 5800—3/32 Dia 7 x 7 Cres Cable per MIL-C-5424
MODEL 5801—3/16 Dia 7 x 19 Cres Cable per MIL-C-5424
MODEL 5802—3/8 Dia 7 x 19 Cres Cable per MIL-C-5424
MODEL 5803—7/16 Dia 7 x 19 Cres Cable per MIL-C-5424
1/2 Dia 6 x 19 Galv Stl Commercial Cable

For applications involving other sizes and materials please contact HOLEX incorporated

HOLEX PART NO.	DIA A ± .005	DIM. B ± .035	DIM. C ± .025	DRILL D DIA	CSK E DIA	UNIT WT (OZ)
5800	.375	1.490	.200	#30 (.1285)	.188	7/8
5801	.500	2.01	.250	1/4 (.2500)	11/32	1
5802	.875	3.120	.870	7/16 (.4375)	5/8	3-1/2
5803	1.125	3.500	.800	9/16 (.5625)	7/8	6

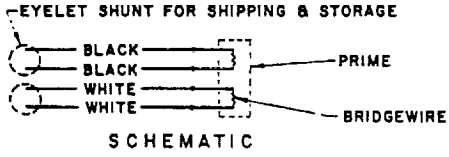

SCHEMATIC

FIRING CHARACTERISTICS

NO-FIRE CURRENT — 1.0 AMP FOR 1 MINUTE
ALL-FIRE CURRENT — 4.5 AMPERES
RECOMMENDED ALL-FIRE CURRENT — 5.0 AMPERES
BRIDGEWIRE RESISTANCE — 1.0 ± 0.1 OHM
PIN-TO-CASE RESISTANCE — 2 MEGOHMS AT 500 VDC
PIN-TO-CASE NO-FIRE — 100 VAC RMS

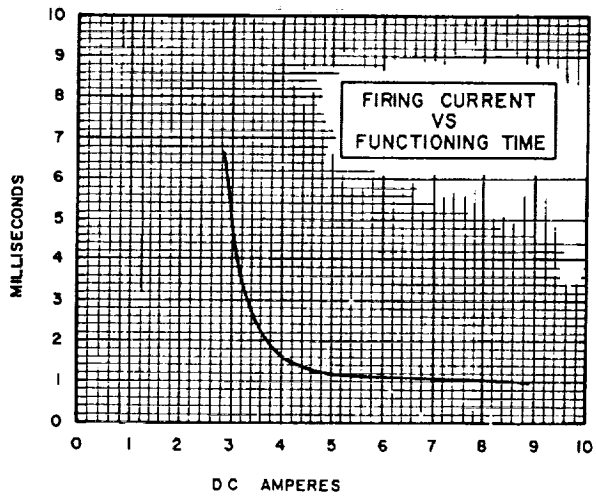

7/82

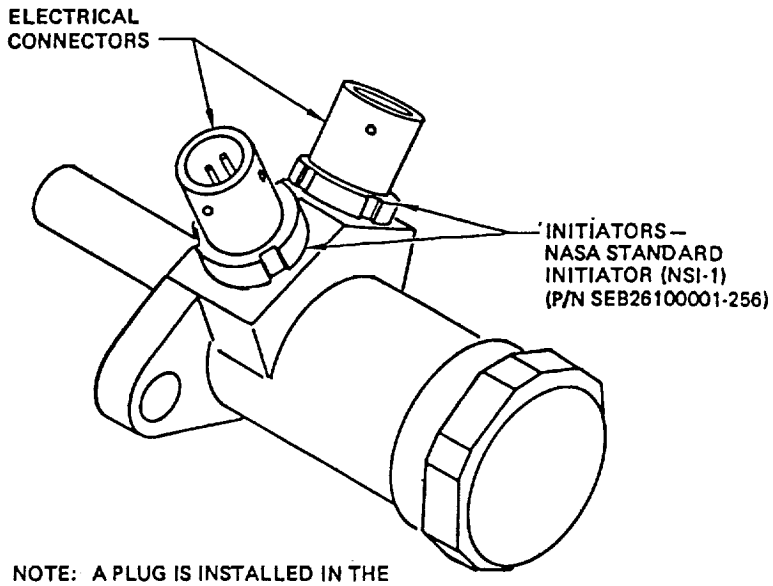

NOTE: A PLUG IS INSTALLED IN THE UNUSED INITIATOR PORT OF EACH PIN PULLER INSTALLED ON THE UMBILICAL BOOM.

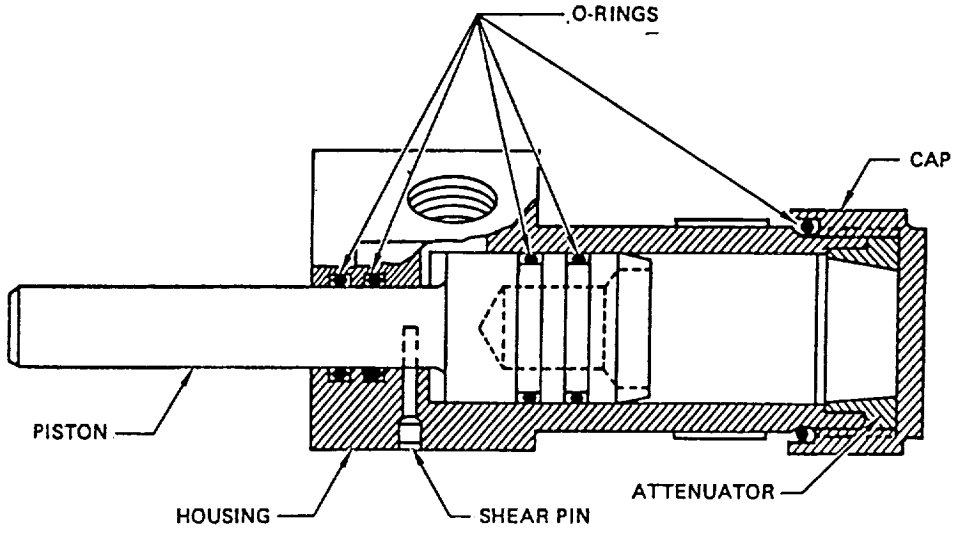

ASE Pin Puller

HOW THE SN9400 SERIES NUT SEPARATES

SEQUENCE OF OPERATION

1. High pressure gas produced by Power Cartridges is introduced into the pressure chamber.
2. Locking piston moves away from the bolt, unlocking the threaded segments engaging the bolt. Movement of the locking piston is stopped by the separator. This collision is isolated from the nut housing and surrounding structure, transmitting a very low shock level.
3. Threaded segments displace radially away from bolt.
4. Separator locks segments in open position.
5. If optional ejector is incorporated, ejector thrusts bolt out of structure joint.
6. Structure joint is cleanly separated.

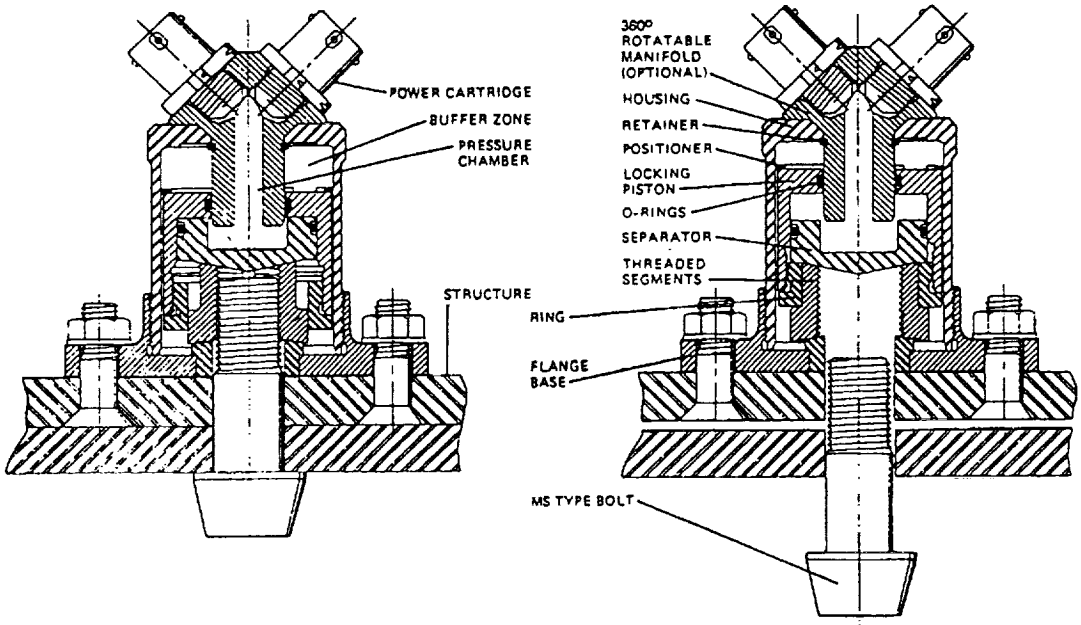

BEFORE ACTUATION

1. Bolt is threaded fully into nut segments.
2. Nut segments are fully supported by locking piston.
3. Structure joint is clamped up to tension rating of bolt.

AFTER ACTUATION

1. Gas pressure acts on locking piston, moving it away from bolt to unlock threaded segments.
2. Segments displace radially away from bolt.
3. Bolt ejects and structure joint separates.

MODEL 9421-2 NON-EXPLOSIVE SEPARATION NUT

Space-Grade Command Separable 1/4 Inch Fastener

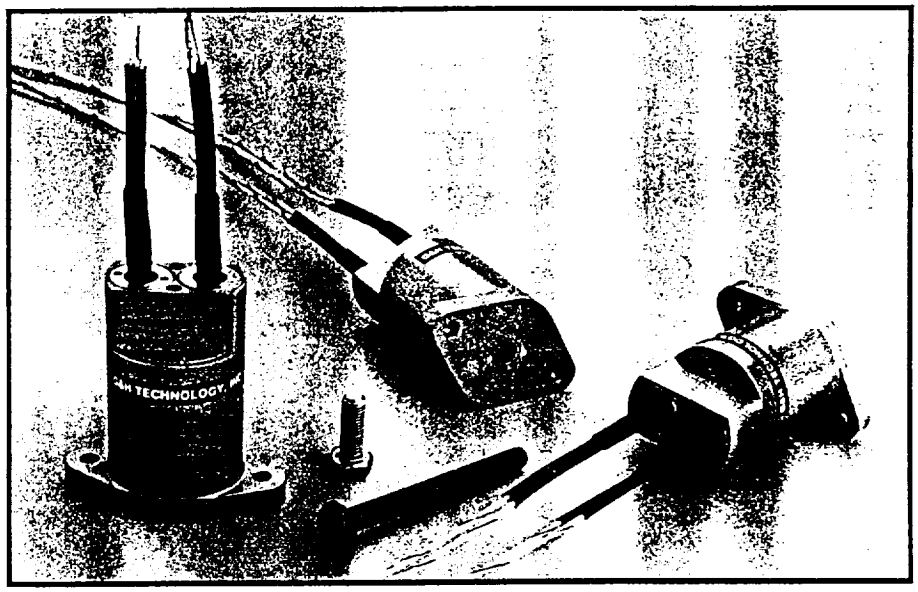

MAJOR DESIGN FEATURES:

- Efficient Redundant Separation
- Field Resettable for System Level Testing
- Temperature Ranges from -238ºF (-150ºC) to +250ºF (121ºC)
- Virtually Shockless Operation
- No Fragments or Debris
- High Strength Nut Carries Full Bolt Load. Tensile Loads to 5000 Pounds (22,050 Newtons)
- Safe Easy-to-Use Devices Contain No Explosives. Separation Nuts Can be Used Without Special Handling or Transportation Restrictions

PERFORMANCE:

Link Wire Resistance:	1.0 ±0.1 Ohms
Separation Voltage:	3.5 VDC Minimum
Separation Time:	20 Milliseconds Maximum at 4.5 Amperes
Bolt Load (1/4-28)	
Functional -	5,000 Pounds (22,050 Newtons)
Proof -	6,400 Pounds (28,224 Newtons)

G&H Technology, Inc.

THE G&H ELECTRO-MECHANICAL SEPARATION NUT

Reliable Minimum Shock Separation

The heart of the Model 9421-2 Separation Nut is a pair of G&H non-explosive spools, small electro-mechanical devices that have demonstrated unmatched performance in numerous space and military applications. Actuation of either one of these spools will initiate nut separation. The spools are insensitive to spurious or unintended signals and separation of the nut can not occur until the required electrical command is received.

Upon command, however, nut separation is reliable and ultra-rapid. The non-explosive spools unwind in milliseconds, freeing internal plungers. This movement releases enough spring force to push the nut locking sleeve out of position. The internal nut threads pull away, cleanly releasing their grip on the bolt.

Release of the bolt is extremely fast and no debris or contaminants are created. Complete and reliable separation occurs without the need for pyrotechnic devices. The result is safe, non-polluting and virtually shock-free separation.

Model 9421-2 Separation Nut
Ready to Actuate - Bolt Not Shown

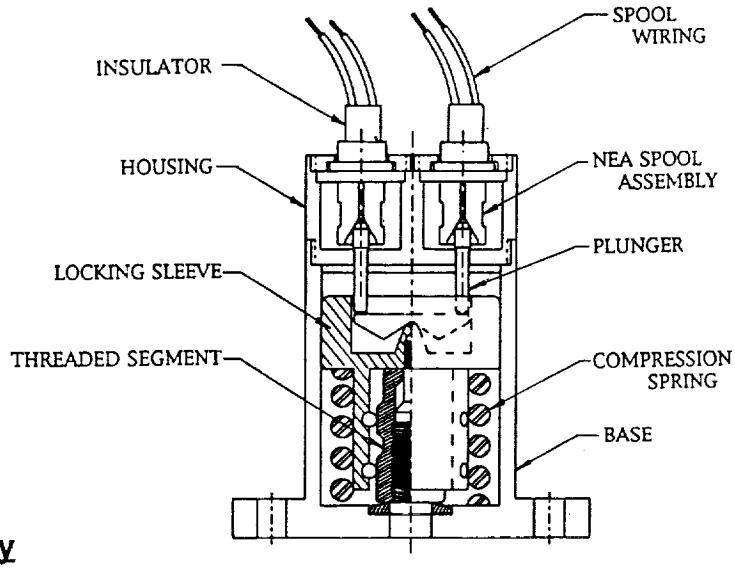

Redundancy

Each separation nut contains a pair of G&H non-explosive actuators. Complete separation will occur if either one, or both, of these actuators is fired. This provides complete electrical and mechanical redundancy, ensuring that these separation nuts perform when required.

G&H Technology, Inc., Special Products Division
1649 17th Street, Santa Monica, CA 90404 (310) 450-0561 FAX (310) 452-5478

FullyTested

The G&H 9421-2 non-explosive nut has been subjected to an intensive developmental and qualification testing program to establish its performance characteristics. Test fire separations were successful after environmental testing at both temperature and load extremes, demonstrating the reliability and effectiveness of these devices. The results are summarized below:

TEST NO.	TEST	TEST METHOD MIL-STD -1576	RESULTS
1	Insulation Resistance	2117	Passed. 5 Megohm minimum at 500 VDC
2	High Temperature Exposure 284±5°F (140±3°C) for 1 hour	3404	Passed. There was no evidence of bolt loosening or nut damage. Temperature exposure did not initiate nut separation
3	Temperature Cycling 8 cycles from -238°F (-150°C) to +250°F (121°C)	3407	Passed. There was no evidence of bolt loosening or nut damage due to temperature cycling
4	Shock 3,000 g at 10,000 Hz Three shocks in each direction of the three major orthogonal axes	3114	Passed. There was no evidence of bolt loosening or nut damage due to shock
5	Random Vibration 10 to 2000 Hz 22 grms 3 minutes in each direction	3113	Passed. There was no evidence of bolt loosening or nut damage due to vibration
6	Static Discharge 25 kv discharge from 500 pF capacitor	2205	Passed. Discharge did not initiate nut separation
7	No-Fire Verification 0.6 amps for 5 minutes	2404	Passed. Current did not initiate nut separation ,
8	Firing Tests -100°F (-73°C) and +250°F (121°C) 4.5 amps 2900 lb preload 4.5 amps 5000 lb preload		Passed. Nuts separated cleanly in less than 18.7 milliseconds at each temperature
9	Bridgewire Resistance	2201	Passed. 1.00 ±.05 ohm

A complete report on the G&H 9421-2 Separation Nut performance and environmental test program is available upon request. Contact your G&H marketing representative for information on metric and other size non-explosive separation nuts, additional nut applications, and your copy of the full test report.

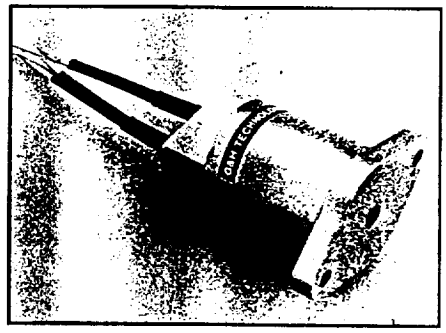

G&H Technology, Inc.

Shock Output Data

The shock generated by the non-explosive separation of these G&H nuts is significantly less than that typically caused by pyrotechnic separation devices . The low shock output during "firing" and separation of the G&H 9421-2 nut has been verified in a series of laboratory tests. The results of a typical test are shown at the right.

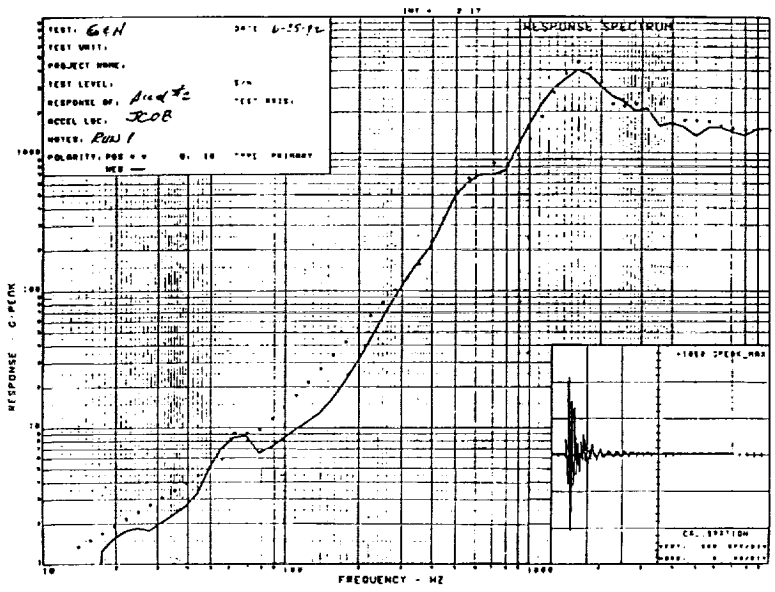

Resettable

G&H non-explosive nuts can be fired during system and subsystem level testing programs with no damage to attached equipment or the nuts themselves. This enables designers to establish full confidence in their system performance through a complete ground verification program. Customers can quickly and easily field refurbish these separation nuts with no special safety or handling restrictions. This makes them an attractive and economical alternative to other separation fasteners.

High Strength

Lightweight compact G&H 9421-2 Separation Nuts provide excellent fastening strength. They will carry the full torque and tension loads of the mating 1/4-28UNF bolts and are available in high strength materials for special ultra-high load applications. The mounting pattern uses standard NAS 618 hole limits and these units will replace most commonly used separation nuts. Their small size and light weight, 6.125 oz. (175 gm), make them ideal candidates for space applications.

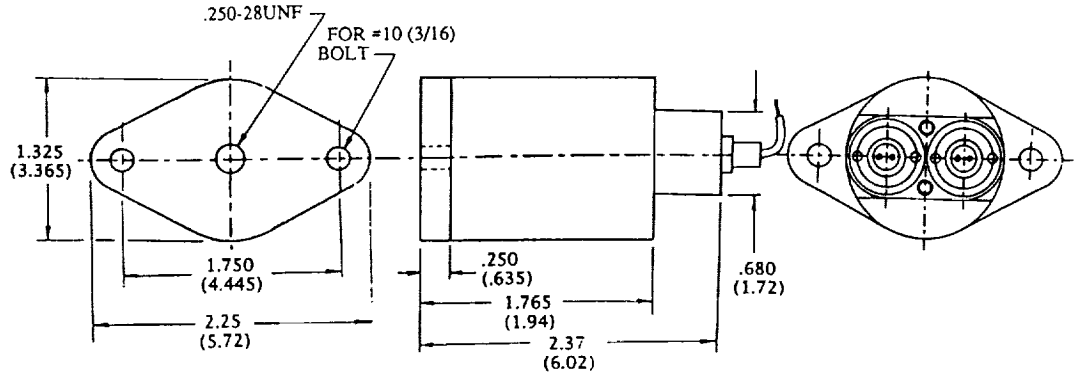

G&H Technology, Inc., **Special Products Division**
1649 17th Street, Santa Monica, CA 90404 (310) 450-0561 FAX (310) 452-5478

Description:

Starsys

The Starsys Research RL-50-C Launch Latch is a manually resettable release mechanism for use with moderate release loads (0-150 lbf). It provides an effective solution to small satellite solar panel release requirements. Powered by one SRC HOP linear motor, the RL-50-C is a "T-bar" type release latch which provides launch restraint and release equivalent to that of a pin puller. The latch is fully resettable, and can be operated hundreds of times during testing to fully verify performance.

The modular design minimizes component size and reduces interface requirements. The latch contains an integral limit switch for sensing latch release. All electrical connections are made through a standard 9 pin connector mounted to the latch.

Characteristics:

- Highly reliable operation:
  - HOP linear motor driven.
  - Resettability allows extensive testing of flight hardware prior to flight.
- All surfaces self lubricating.
- Designed for moderate launch and release loads.
- Self aligning geometry during re-latch.
- Optional kicker springs and active ejection ensure positive release.
- Multiple degrees of freedom are provided between the latch and the mating T-bar to accommodate misalignment and thermal strains.

Principle of Operation:

When the actuator is energized, it acts upon an internal "latch pin" causing it to slide relative to the mating, T-shaped release bar. The geometry of the latch pin and T-bar are such that this extension releases the T-bar. At the moment of release, loads are carried by high hardness coatings in line contact allowing high load release without galling or wear. Further extension of the actuator actively ejects the clevis from the latch body.

Re-latching is accomplished by extending the actuator, and locating the clevis within the latch body. As the actuator cools and retracts, the clevis is re-latched.

Specifications:

Physical envelope:	4.5" X 1.5" X 1"
Mass:	140 grams w/ actuator
Launch load capability:	200 lbf
Release load capability:	150 lbf
Power requirement:	10 watts at 28 volts
Time-for-release:	150 seconds from 0° C
Lifetime:	Minimum 500 releases
Degrees-of-freedom, latch/T-bar:	±2.5° conical misalignment allowable between the latch and T-bar

REVISIONS				
REV	DESCRIPTION	ECO #	DATE	APP
	INITIAL RELEASE			

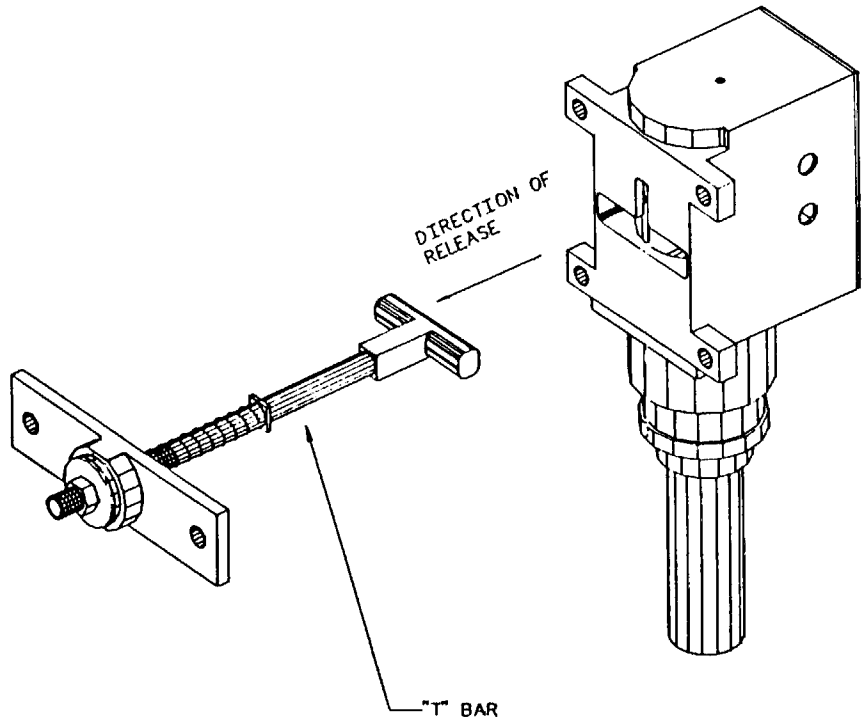

SHOWN JUST AFTER RELEASE

16 APR 92

APPROVED	DATE
PREP BY C POWERS	1/30/92
ENGINEERING	
MANUFACTURING	
QUAL ASSURANCE	
INTERPRET DRAWING PER ANSI Y14.5M 1982	

UNLESS OTHERWISE SPECIFIED
ALL DIMENSIONS ARE IN INCHES
.XX ±.01 .XXX ±.005
.XXXX ±.002 #3 √ X ±1°
FILLETS .035 MAX. .003 MIN.
BREAK SHARP EDGES .005 MAX.

STARSYS RESEARCH 5757 CENTRAL AVE., SUITE E, BOULDER, COLORADO 80301 (303) 444-6715

RL-50-C
LAUNCH RESTRAINT

MATERIAL	DWG NO.	
NA	AP-7003	
SCALE NA	DO NOT SCALE THIS DRAWING	SHEET 2 OF 2

THERMAL KNIFE*

General purpose Release system

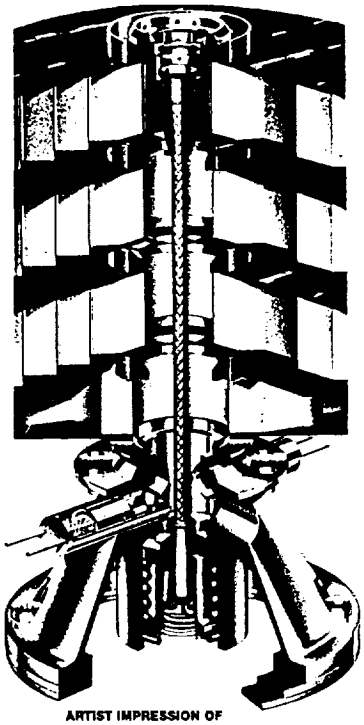

ARTIST IMPRESSION OF THERMAL KNIFE RELEASE SYSTEM

Fokker Space & Systems has developed an alternative release system for space applications. The thermal knife system which is based on Kevlar cables being degraded by two heating elements, has numerous advantages over using pyrotechnic devices. The thermal knife wa. used for the first time in 1988 on a CNES antenna release experiment at the Soviet space station MIR. This successful release system is part of Fokker's Avanced Rigid Array (ARA) solar arrays, but is also applicable to antennae, payloads and jettison systems.

Advantages:
- no risk of spontaneous release
- minimum release shock
- ground testing of flight units possible
- requires low current to release
- low weight
- high flexibility in release requirements

DESCRIPTION OF THE THERMAL KNIFE

This highly reliable release system can be applied to almost every system to be released in space. It is based on the use of Kevlar cables for example, to keep solar arrays together during launch.

Kevlar is used because of its strength and its capacity to degrade when heated above 600 Centigrade. Within the thermal knife two ceramic plates are pressed against the Kevlar cable. These plates are electrically heated for a period of about one minute. This period depends on the diameter of the cable, environmental conditions and required tension in the cable. The tension in the cable decreases gradually, preventing any sudden shocks. Because this release system is not sensitive to electromagnetic disturbances, the possibility of a spontaneous release has been eliminated.

The thermal knives can be used many times, so that perfor-

* THERMAL KNIFE IS PATENTED IN THE USA UNDER NO. 4 540.873 (10098)

THERMAL KNIFE

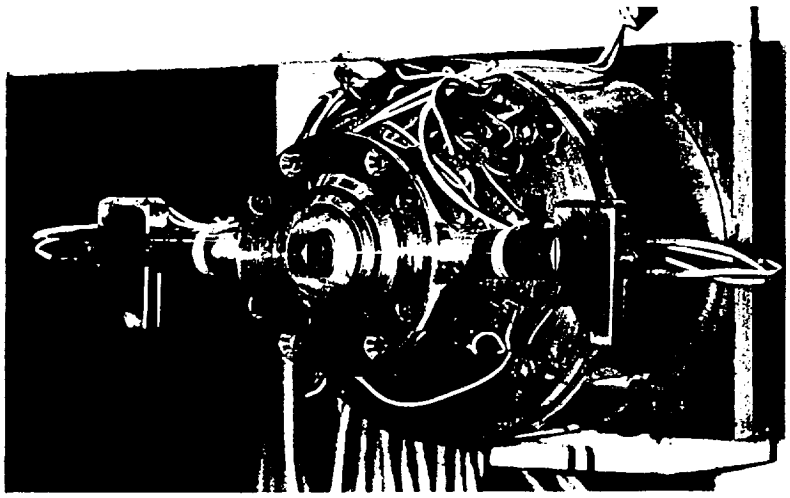

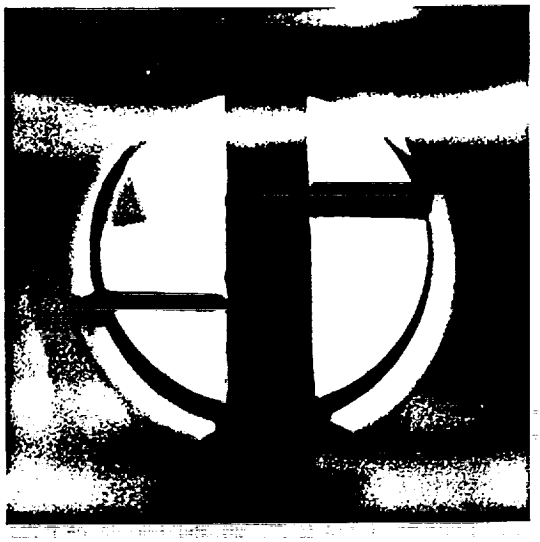

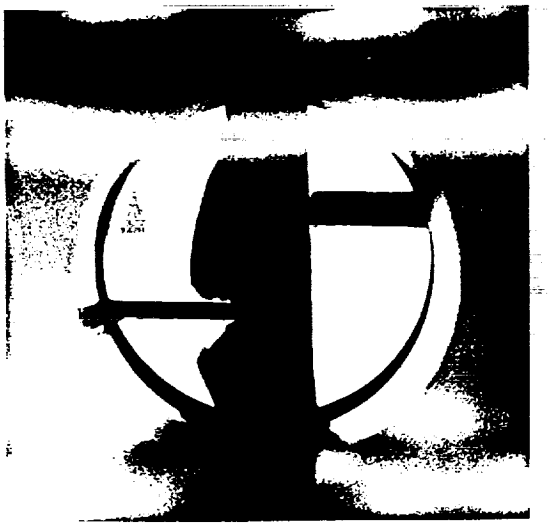

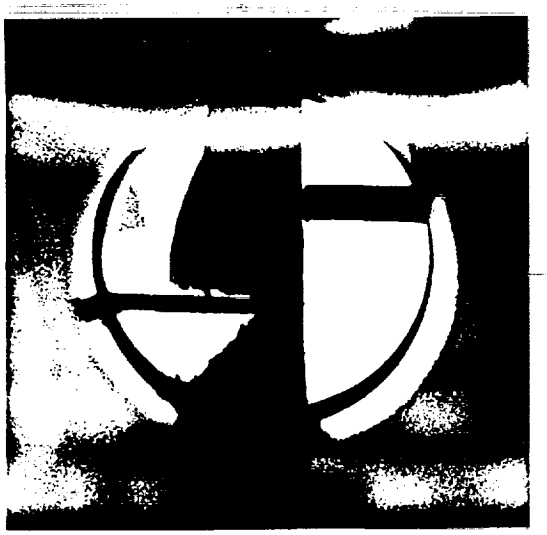

During the Advanced Rigid Array qualification program, the thermal knife successfully passed a series of tests, such as:

- cutting under atmospheric and vacuum conditions at room temperature
- vibration tests in flight configuration
- thermal cycling under dry air and vacuum conditions
- humidity test
- contamination test
- life test

The thermal knife has proven to survive at least 15 cuttings under several conditions during the qualification program

APPLICATIONS

INMARSAT 2	TELECOM 2	POLAR PLATFORM
SAX	SOHO	ARTEMIS
CNES/MIR	HISPASAT	DRS

TOP TO BOTTOM:
DEGRADATION OF THE KEVLAR CABLE INSIDE THE THERMAL KNIFE

Fokker Space & Systems B.V.

Hoogoorddreef 15
1101 BA Amsterdam-Z. doost
The Netherlands
Telephone (0201 6059
Telex 11526 FMHS NL
Datafax (0201 6056036
Cables Fokplanes Amsterdam

5003 1/DW/2028/3000/3 91

APPENDIX I

LUTE MISSION OPERATIONS PLAN

LUTE Mission Operations Plan

Purpose

This document presents the methodology to be used in the development of LUTE mission operations capabilities appropriate for accomplishing the LUTE mission objectives.

Scope

The scope of this document emcompasses the activities necessary to prepare for and successfully execute LUTE operations.

Operations Philosophy

The purpose of the LUTE program is to enhance our knowledge of the universe by exploring the ultraviolet spectrum from an instrument on the moon. NASA will provide the instrument and a means of controlling and monitoring the functions of the instrument for use primarily by the scientific and educational community. The function of monitoring and controlling the LUTE will be performed by the LUTE Operations Team (LOT) within the LUTE Operations Control Center (LOCC). The LOCC will provide communications to and from the instrument to control the instrument configuration and to evaluate the returned information from the instrument. Routine operations and maintainence of the LOCC will be the responsibility of the LOT.

Operations of the LUTE will be determined by a planned sequence of instrument operations and configurations known as the mission timeline which will be developed under the direction of the LUTE Management Team (LMT). This timeline will be developed to ensure that mission success criteria will be met during the LUTE operational period. NASA will work with the scientific and educational community to establish mission success criteria based on their desires and operational capabilities of the LUTE.

It is intended for the LOT to be comprised primarily of personnel from the scientific and educational community. It will be the responsibility of NASA to cerify both the personnel of the LOT and the guidelines and procedures to be used during the mission in order to ensure mission success.

It is desired to draw upon existing resources within NASA and the scientific and educational community to develop the LOCC. It will be the responsibility of NASA to verify and certify the LOCC facility for operational readiness to support the mission as the primary control center. Routine operations of the facility will be the responsibility of the LOT. Although the LUTE and LOCC will be provided as a service to the scientific and educational community, NASA will maintain a vested interest in the instrument performance and the science return for the mission. NASA will provide technical support as needed throughout the mission to ensure nominal operations of the LUTE and LOCC.

It is desired to make LUTE operations and science data easily accessible to necessary and interested individuals and institutions. The LOCC will have a substantial capability for access and dissemination of this information. Remote electronic access capabilities will be established commensurate with security requirements of the LOCC data systems.

Operations Development

Two critical areas which will be very important to the overall success of the LUTE mission are the development of the LUTE Operations Control Center and development of the LUTE Operations Team. The following paragraphs detail the philosophy which will be used in these areas of operations development.

LUTE Operations Control Center

The LOCC will be located at a selected location which has the necessary facilities required to accomplish LUTE mission operations objectives. It is desired that this location be an institution which has a vested interest in the success of the LUTE, such as an educational institution or a related research institution. Itis also desired that the LOCC be developed from much of the existing infrastructure within that institution and within NASA. It is the responsibility of NASA to direct thedevelopment and certify the operational readiness of the LOCC. However, it is the responsibility of the LUTE Operations Team to maintain the facility for day-to-day operations of the LUTE.

LUTE Operations Team

The LUTE Operations Team will consist of all individuals involved in the operations of the LOCC and the LUTE. This team will consist of individuals who have the responsibility of maintaining the LOCC for day-to-day operations, such as hardware, software, and communications support. The LOT will also consist of ground controllers responsible for valid science return from the LUTE along with the health and status of the instrument. It will be the responsibility of NASA to certify these individuals for LUTE operations in order to achieve mission goals.

Operations Phases

Prelaunch

Prior to launch, LUTE will be prepared for mission operations by subjecting the LOCC and spacecraft to end-to-end testing. Telemetry from the LUTE will be transmitted to the LOCC where it will be displayed and verified. Commands will also be transmitted to the instrument in the launch facility from the LOCC and verified for valid execution.

Landing

LUTE landing and instrument verification will occur prior to normal operations. Communications will be established between LUTE and the LOCC utilizing NASA Communications (NASCOM) after landing and prior to normal operations.

Normal Operations

Upon successful landing and instrument verification, normal operations will begin. NASCOM will provide necessary communication to the LOCC for instrument control and for health and status monitoring. The LOCC will be designed and prepared to support continuous support during the normal operations period. The LUTE configuration will be controlled as directed by the LUTE operations schedule. The LOCC will provide the capability to transmit commands to control the instrument configuration. Likewise,information from the instrument will be transmitted to the LOCC for monitoring by ground controllers responsible for instrument configuration and engineering support.

Ground Systems

Operations of the LUTE will require ground systems to perform specific functions to accomplish LUTE mission goals. The primary ground system will be the LUTE Operations Control Center (LOCC). Within the LOCC will be the Scientific Data Center (SDC), the Engineering Support Center (ESC), and the Education and Media Support Center (EMSC).

LUTE Operations Control Center

The function of the LOCC will be the execution of mission operations while processing and displaying engineering and scientific data for the LUTE OperationsTeam (LOT). In addition, the LOCC will provide for the dissemination of LUTE operations and science information to interested educational institutions and media services. These functions will be accomplished by the following facilitieswithin the LOCC. These facilities can be within the LOCC or remotely dispersed and connected electronically.

Scientific Data Center

This portion of the LOCC will distribute and archive the scientific data from the LUTE telemetry downlink. The data will be provided to the interested parties of the scientific community for analysis to determine its value for mission success.

Engineering Support Center

This portion of the LOCC will process and display the engineering data from the LUTE telemetry downlink. This data will be monitored and analyzed to determine the health and configuration status of the instrument in order to maintain proper operations of the instrument.

Education and Media Services Center

This portion of the LOCC will compile and maintain information about LUTE operations for distrubution to interested educational and media services. Information provided by the EMSC will include completed operations, scheduled operations, and information regarding the viewing targets. The EMSC will interface with the SAC and the ESC to obtain the desired information for the interested educational institutions and media services.

LUTE RESPONSIBILITIES

LUTE Management Team

-Establish operations policy
-Select and certify the LUTE Operations Team
-Develop and certify the LUTE Operations Control Center
-Certify instrument operations guidelines and ground operations procedures
-Establish mission success criteria with the scientific community

LUTE Operations Team

-Perform LUTE mission operations
-Operate and maintain hardware, software, and communications needed for prelaunch testing and mission support
-Monitor instrument performance and provide necessary enginnering support from the ESC, SDC, and the EMSC
-Coordinate the dissemination of LUTE operations information to interested institutions

LUTE OPERATIONS CONTROL CENTER

-Located at institution selected by the LUTE Management Team
-Serves as the focal point for reception of LUTE real time information
-Provide distribution of information to each center within the LOCC

Centers can be within the LOCC or remotely dispersed

ENGINEERING SUPPORT CENTER

-Provide information to engineering support personnel to monitor health and status information of the LUTE

SCIENTIFIC DATA CENTER

-Distribute and archive science information for the scientific community

EDUCATION AND MEDIA SERVICES CENTER

-Coordinate the dissemination of LUTE operations to the scientific community.

APPENDIX J

LUTE MIRROR MATERIALS REPORT

LUNAR ULTRAVIOLET TELESCOPE EXPERIMENT (LUTE)

DESIGN PHASE A: MIRROR MATERIALS REPORT

By Terrie M. Rice

George C. Marshall Space Flight Center
Materials and Processes Laboratory
EH43 - Project Engineering Branch
Marshall Space Flight Center, AL 35812

AUGUST 23 , 1993

LUNAR ULTRAVIOLET TELESCOPE EXPERIMENT (LUTE)

DESIGN PHASE A: MIRROR MATERIALS REPORT

Prepared by:

Terrie M. Rice

Terrie M. Rice
Materials Engineer
EH43/Project Engineering Branch
Materials and Processes Laboratory
George C. Marshall Space Flight Center

Approved by:

Dennis E. Griffin
Chief, EH43/Project Engineering Branch
Materials and Processes Laboratory
George C. Marshall Space Flight Center

TABLE OF CONTENTS

SECTION	PAGE
1.0 Introduction	1
1.1 Scope	1
1.2 LUTE System Description	1
2.0 Mirror Materials	2
2.1 Introduction	2
2.2 Mirror Material Comparison Factors	2
2.3 Mirror Material Discussion for Beryllium (Be)	4
2.4 Mirror Material Discussion for Silicon Carbide	7
2.5 Be/SiC Comparison	11
3.0 Conclusion	13
References	14-15

LIST OF FIGURES (1 only)

Figure: LUTE concept as depicted on lunar surface.

LIST OF TABLES

TITLE	PAGE
1. Table 1: I-250, I-70, and 0-50 Material Characteristics	5
2. Table 2: Instrument Grades of Beryllium	5
3. Table 3: Structural Grade Material Characteristics	6
4. Table 4: Typical SiC Mirror Material Properties	8
5. Table 5: Reaction Bonded SiC Characteristic Properties	9
6. Table 6: CVD SiC Characteristic Properties	10
7. Table 7: Mirror Material Properties (properties are at 300 and 159 K)	11

ACRONYMS and SYMBOLS

1. LUTE = Lunar Ultraviolet Telescope Experiment

2. Be = Beryllium

3. SiC = Silicon Carbide

4. RB SiC = Reaction Bonded Silicon Carbide

5. CVD SiC = Chemically Vapor Deposited Silicon Carbide

6. E = Young's Modulus

7. YS = Yield Strength

8. W = Watts

Note: On page of the report W represents weight.

9. I = Moment of Inertia

10. υ = Poisson's Ratio

11. MYS = MicroYield Strength

12. BRDF = Bidirectional Reflectance Distribution Function

13. UV = Ultraviolet

14. CTE = Coefficient of Thermal Expansion

15. UTS = Ultimate Tensile Strength

16. NNS = Near -Net-Shape

17. HIP = Hot Isostatic Pressing

18. IBS = Ion Beam Sputtering

ACRONYMS and SYMBOLS (CONTINUED)

19. rms = Root Mean Square

20. k = Thermal Conductivity

21. Cp = Specific Heat

22. cc = Centimeters Cubed

23. MPa = MegaPascal

24. GPa = GigaPascal

25. J = Joule

26. Kg = Kilogram

27. K = Kelvin

28. ppm = Parts Per Million

29. KSI = KiloPounds per Square Inch

30. sec = second

31. μ = micro

32. sq = square

33. cm = centimeter

1.0 INTRODUCTION

1.1 Scope

The LUTE phase A report on mirror materials is an overview of information accumulated from a 4 month long investigation of Beryllium and Silicon Carbide . The main objectives of this study were to 1) build a Be and SiC material property database and 2) recommend an optical material for the primary mirror based on mirror material comparison factors /figures of merit (see SEC. 2) .Some of the topics addressed for these two state of the art lightweight optical materials are material properties, material stability, material toxicity, processing and fabrication. References are listed at the end of the mirror material report. As a design aid , an indexed mirror material data book is also provided.

1.2 LUTE System Description

The Lunar Ultraviolet Telescope Experiment (LUTE) , modeled in Figure 1, is a 1 meter class transit(fixed declination), UV imaging telescope. The LUTE will be placed on the Lunar surface by an unmanned lander and remotely operated . The wavelength region of interest for LUTE is between 100 and 350 nm.

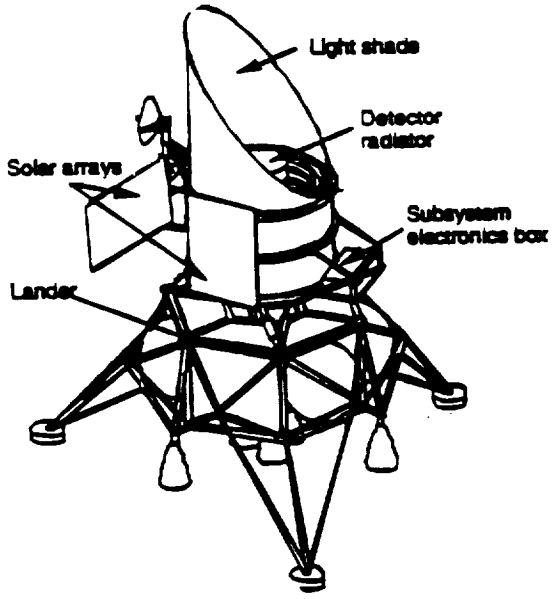

Figure : LUTE concept as depicted on Lunar surface

2.0 MIRROR MATERIALS

2.1 Introduction

The selection of substrate materials for an optical system is a very complex task; many areas have to be analysed such as structural, thermal, and material properties. Other areas that also have to studied are ease of fabrication, polishability, surface scatter, and the cost of the mirror blank.The LUTE program has keyed in on two mirror materials (Beryllium and Silicon Carbide) that designers throughout the world consider for high performance optical systems. Properties for these two materials are presented in tabular form throughout this report for comparison and reference.

2.2 Mirror Material Comparison Factors

Standard comparison factors and/or figures of merit for selection of optical systems are listed below :

1. Structural
   a. Specific stiffness - E(Young's Modulus)/ρ(Density)
   b. Specific Stength - YS(Yield Strength)/ρ(Density)
   c. Fracture Toughness - the behavior of a material with a crack present.
   d. Mirror Weight - W
   e. Area Weight Density - W/A is the weight per unit area, A=mirror area
   f.. Flexural Rigidity (D) - measure of structural stiffness given by

$$D=IE/(1-\nu^2)$$

Where I = Moment of inertia
E = Young's Modulus
ν = Poisson's ratio

k. Characteristic Length (L)- this property is useful for the characterization of active, deformable mirrors. L is the measure of the spatial extent of influence of a figure control actuator. A decrease in the the ratio of actuator spacing to characteristic length increases the accuracy to which the shape of a mirror can be controlled. L is given by:

$$L = (R^2D/t_eE)^{1/4}$$

Where R = mirror radius of curvature

t_e = thickness of solid mirrror having the same area weight density.

2. Temporal Stability

a. Temporal Instability - A permanent change that takes place in a component as a function of time in a fixed environment.

b. Microyield Strength (MYS)- this property is a sensitive measurement of the resistance of a material to becoming permanently deformed under cyclic loads. Prior history of the material affects this property significantly. High MYS is a desirable property.

c. Dimensional Instability - the time dependent dimensional change in response to internal or external influences .

3. Thermal Stability

a. Steady State Thermal Distortion Coefficient - CTE/k

b. Homogeneity of Thermal Expansion

c. Thermal Instability - a reversible dimensional change measured in a fixed environment after a change from another fixed environment that is independent from the environmental path.

f. Transient Thermal Distortion Coefficent - (CTE-ρ-Cp)/k

g. Hysteresis due to Thermal Cycling - A distortion that can be either permanent or reversible and is defined as the change measured in a fixed environment that is dependent on the environmental path to the fixed environment.

4. Optic Measurements

a. Surface Figure

b. Surface Microroughness (rms)

c. Optical Scatter

d. Bidirectional Reflectance Distribution Function (BRDF) - BRDF characterizes the directionality of the radiation reflected from a surface. The definition of BRDF is the ratio of the measured radiance (L) emitted from the sample surface to the irradiance (E) incident on the sample.

e. UV reflectance (normal incidence)

5. Manufacturability

a. Material availability

b. Material Polishability

c. Material Toxicity

d. Component Size
e. Overall Maturity of Technology
f. Cost

Other areas that need to be analyzed when evaluating materials for optical systems for space applications are environmental conditions the materials will be exposed to such as the space vacuum , radiation environment, atomic oxygen, and micrometeroid and orbital debris.

2.3 Mirror Material Discussion for Beryllium (Be)

In general, Be has the following favorable characteristics: 1) low density, 2) high specific heat, 3) high elastic modulus, 4) high infrared reflectance, 5) high thermal conductivity, 6) low X-ray absorption, 7) athermalized systems can be produced from Be materials, 8) Be components can be readily fastened with inserts, 9) Be components can be produced to near - net - shape by Hot Isostatic Pressing (HIPing) with little or no machining or material waste and 10) Be mirror substrates are polishable bare or coated.

Some of Be's unfavorable characteristics are 1) moderate thermal expansion, 2) low microyield, 3) anisotropy (directional properties), 4) toxicity, and 5) thermal induced porosity .

Several different Be materials and fabrication methods are utilized in the production of Be optics. Due to the high anisotropic nature of single crystal Be (hexagonal close - packed), it is not used for Be optics. Since Be is prone to anisotropic behavior, random orientation of the grains is required. Thus, Be optics and practically all Be parts are produced by powder metallurgical processes as opposed to the crystal growth process.

Be powders can be produced by the following methods: 1) attrition, 2) impact attrition, 3) rotary atomization, and 4) inert gas atomization . Even when consolidated under high temperatures and pressures ,the attritioned Be (fine powder of small flakes) component will have definite anisotropy due to the alignment of the flat surfaces of the Be flakes. The gas atomization of Be produces spherical shaped multicrystalline granules of Be. By utilization of the gas atomized Be powder, a more uniform Be mirror blank can be produced by HIPing . Material Properties for several different Be powders are detailed in the Tables 1, 2, and 3.

TABLE 1: I-250, I-70, and 0-50 Material Characteristics

Property	Grade		
	I-250	I-70	0-50
0.2% YS (KSI)	79	30	33
UTS (KSI)	95	38	48
%ELONGATION	3	3	3
MYS (KSI)	14	1.7 - 1.8	1.8
% BeO	2.0	0.7	0.5
Grain Size (microns)	2.5	10	9

Where I-250 = Instrument/Structural grade of Be
I-70 = Optical grade of Be
0-50 = Optical grade of Be

TABLE 2: Instrument Grades of Beryllium

Property	Grade		
	I-250	I-220	I-400
0.2% YS (KSI)	79	50	--
UTS (KSI)	95	65	80
% ELONGATION	3	2	--
MYS (KSI)	14	7.2	13
% BeO	2.0	2.1	6.7
Grain Size (microns)	2.5	6-8	1-3

TABLE 3: Structural Grade Material Characteristics

Property	Grade	
	I-250	S-200
0.2% YS (KSI)	79	38
UTS (KSI)	95	58
%ELONGATION	3	3
%BeO	2.0	1.7
Grain Size (microns)	2.5	8-10

Note: Tables 1-3 are excerpts from Reference # 1.0.1 .

The I-250 grade of Be is relatively new and is designed to function as both a structural and instrument material. It has a minimum MYS of 14 KSI, low oxide content, high yield and ultimate strength, and ductility eqivalent to structural grade Be materials. I-250 is also isotropic . Although I-250 may not be suitable for bare mirror applications due to its high oxide content, a coated I-250 optic would be highly dimensionally stable based on the material properties. I-250 would also be a good material for an optical bench due to its high strength, high ductility, and isotropy.

Be optics can be fabricated by several methods such as machining, epoxy bonding, brazing , or near-net-shape (NNS) processing (see Reference # 1.0.3). The newest method for Be fabrication is near-net-shape processing. For this process , Be powder is HIPed around non-Beryllium (copper) tooling. The tooling is then leached out chemically using a nitric acid solution. Most waste, and machining operations that are associated with detailed components are eliminated with this process. Structures as large as 1.2 m can be produced with this process.The NNS process is a tailorable cost-effective process for the manufacture of optics, optical support structures, and other Be components.

In order to produce a dimensionally stable Be optic, Be material properties must be satisfied by certain requirements. For example, a highly isotropic Be material is produced by utilization of atomized spherical Be powder that is HIPed. Other material properties and their requirements for the production of

dimensionally stable Be optics are as follows: 1) high microyield which is the result of a fine grain size, high oxide, texture strengthening material, 2) low optical scatter as a result of a low oxide, low impurity, high density, basal plane oriented Be material, 3) optics survivability which is due to a fine grain size, high purity, low oxide, low x-ray absorbtion, high microyield strength material, 4) thermal cycle stability due to isotropy and high thermal conductivity, 5) temporal stability from lack of stress gradients and residual stress, and 6) high thermal conductivity which is due to large grain size and low oxide content of the Be material. In short, Be optical materials are very well understood, characterized, documented (see Reference #1.0.2) and can be tailored to produce temporally and thermally stable optics.

Be is toxic in fine particle form (less than 10 microns). Be particles are produced when Be is machined , ground , sanded, or chemically processed. Be is not toxic in solid form . Touching , feeling ,and eating solid Be metal or accidentally cutting oneself with solid Be metal would not have toxic effects. Hybrid type structures where Al or Ti are bonded to Be assemblies to replace mount pad locations allow flexibility for modifying, lapping, polishing, threading, and /or line drilling of the mounting surfaces . This procedure effectively removes potential toxicity hazards associated with other manufacturing alternatives that would release airborne Be particles.

Overall Be is a highly designable, lightweight, rigid, and thermally stable material that should be considered where stiffness, weight, and stability are highly critical. Although initial material costs are high, Be becomes a cost effective material in the "finished product" form (see Reference # 1.0.3).

2.4 Mirror Material Discussion for Silicon Carbide (SiC)

Traditionally, SiC has been used for high temperature applications such as reaction tubes and furnace components used in semiconductor processing chambers, heating elements, refractory ware, abrasives, and coatings for wear and corrosion resistance. However, SiC exhibits favorable properties for use as a substrate for solar collectors and concentrators, laser mirrors, and astronomical telescopes. Some of the properties of SiC that are favorable to the production of optical substrates are: 1) low density, 2) low coefficient of thermal expansion, 3) high thermal conductivity, 4) high thermal shock resistance, 5) high specific stiffness for lightweight designs, 6) high fracture toughness relative to glass and glass ceramics, 7) high hardness for enhanced polishability, and 8) low static and dynamic thermal distortion characteristics required for dimensional

stability. SiC is also the material of choice for mirrors for use in the vacuum ultraviolet (LUTE environment) and X-ray regions (see Reference #1.0.7).

On the other hand , SiC does has some unfavorable characteristics such as :1) anomalous scatter in some cases, 2) the material is difficult to fasten and machine , 3) optical coatings like Si cladding or Ion Beam Sputtered (IBS) amorphous SiC are required for improved polishability and surface finish, and 4) the technology is less mature than Be optic technnology. Table 4 list the typical (average) properties of SiC.

TABLE 4: Typical SiC Mirror Material Properties

Property	
Density, g/cc	2.92
Elastic Modulus, GPa	311
Specific Modulus, relative	10.7
Thermal Conductivity, W/m-K	156
Specific heat, J/Kg-K	1255.2
Coefficient of Thermal Expansion, ppm/K	2.6
Diffusivity, relative	0.43
Microyield Strength, MPa	none

Note: Table 4 is an exert from Reference # 1.0.6.

There are two crystal forms of SiC , alpha and beta. Alpha SiC has a hexagonal crystal structure with some anisotropy exhibited in its thermal expansion properties. Beta SiC has a cubic crystal structure that has some anisotropy present in the

elastic modulus. Although there are a number of fabrication processes that exist for the production of SiC, the processes associated with the fabrication of optical components are Reaction Bonding (RB) [a powder processing technology (sintering or hot pressing of powders)] and Chemical Vapor Deposition (CVD) (a high temperature , low pressure process that deposits high purity beta SiC) .

RB SiC is a material with a two phase microstructure consisting of SiC grains in a silicon (Si) matrix . The SiC slurry is cast, dried, and fired. A porous body is formed which is refired to fill the porous body with pure Si yielding a 100% dense material. It is highly formable and repairable in the manufacturing process due to the tailorability of the slurry and other process parameters. RB SiC can be fabricated into near net shape lightweight mirrors and RB SiC also has a mature, low cost manufacturing process. RB SiC mirrors have been fabricated in sizes ranging from a few centimeters to two meters, with uncoated polished surfaces that have surface roughnesses < 30 Angstrom rms . Low scatter surfaces with a surface roughness of 10 Angstroms rms can be obtained on the bare two phase material utilizing polishing techniques developed by Hughes Danbury Optical Systems. Ultra-low scatter surfaces (≤ 5 Angstrom rms) can be obtained for a RB SiC optic with a coating such as Ion Beam Sputtered (IBS) amorphous SiC. When exposed to cryogenic temperatures, bare and amorphous SiC coated mirrors are thermally stable. In short, RB SiC is a competitive material for large optics. Characteristic properties of RB SiC are listed in Table 5.

TABLE 5: Reaction Bonded SiC Characteristic Properties

Properties

Flexural Strength (MPa)	280-385
Young's Modulus (GPa)	280-350
Thermal Conductivity (W/m-K)	155
Specific Heat (J/Kg-K)	670
CTE (ppm/K)	2.57
Grain Size(microns)	varies
Density (g/cc)	varies (approximately) 2.9

Note: Table 5 is excerpted from Reference # 2.0.6 .

CVD SiC has high UV reflectance and exhibits a low scatter surface. A scalable CVD process for SiC has been developed to produce a dense , high purity beta SiC that possesses material properties that are excellent for optical applications . Material characterization measurements for physical, thermal, mechanical, and optical properties have been conducted and the results show that CVD SiC is a dense, highly pure, single phase (cubic) material capable of being polished to ≤ 3 angstrom rms. The material is homogeneous in terms of CTE and also has a very high elastic modulus , high strength, hardness, relatively high heat capacity, and thermal conductivity. CVD SiC has good retention of mechanical properties up to 1500 degrees Celsius and the material also exhibits superior thermal and cryogenic stability (-190 to 1350 degrees C). It is highly resistant to atomic oxygen and electron beam degradation (see reference # 2.0.3). The CVD process is also scalable; for example, monolithic 0.5 meter diameter mirrors have been produced. Disks up to 60 cm in diameter and plates 76 cm by 46 cm wide with thicknesses up to 13 mm have also been produced. Currently, there is work being done on scaling the process to produce a mirror 1.5 meter in diameter. All of the positive material attributes of CVD SiC such as durability, strength, high stiffness -to -weight ratio, good thermal distortion resistance, and thermal stability establish the material as a good candidate material for current and future optical applications especially where high optical tolerances (ultra-low scatter surfaces) are required. Characteristic Properties of CVD SiC are listed in Table 6 .

TABLE 6: CVD SiC Characteristic Properties

Properties

Flexural Strength (MPa)	550
Young's Modulus (GPa)	470
Thermal Conductivity (W/m-K)	250
Specific Heat (J/Kg-K)	700
CTE (ppm/K)	2.4
Grain Size (microns)	2-10
Density (g/cc)	3.2

Note: Table 6 is exerted from Reference # 2.0.6.

Most forms of SiC are non-toxic. Reaction Bonded SiC is a hot pressed powder that is relativily non-toxic. Solid pieces of polycrystalline SiC are also relatively non-toxic. The only form that is toxic is SiC whiskers.

In conclusion , RB SiC offers a low cost mature technology with relatively good properties; whereas, CVD SiC offers the best properties with the least mature manufacturing technology. CVD SiC is the best SiC material suited for the LUTE wavelength region (CVD SiC has high ultraviolet reflection and can be manufactured with the lowest scatter surface). Overall, both SiC materials are excellent lightweight mirror substrates.

2.5 Be /SiC comparison

The performance of an optical system is related to the physical and mechanical properties of a material, material compatability with other system components, and dimensional stability. From the previous descriptions of both Be and SiC , it is evident that both materials are good candidates for the LUTE program optics . The material property table shown below lists both Be and SiC properties for comparison purposes.

TABLE 7: Mirror Material Properties

Properties	Be 300K-150K	SiC 300K-150K
Young's Modulus (GPa)	290	310-462
Density (g/cc)	1.85	2.82-3.21
Specific Stiffness(10E5)	159	112-147
Fracture Strength (MPa)	241	>275
Microyield Strength (MPa)	>7	none
Fracture Toughness (MPa m)	9	3
Coefficient of Thermal Expansion (ppm/K)	11.3-3.4	2.4-0.6
Thermal Conductivity (W/m-K)	194-316	160-150
Specific Heat (J/Kg-K)	1840-840	710-330
Thermal Diffusivity (sq cm/sec)	0.57-2.05	0.83-1.40
Steady State Distortion Coefficient (μm/W)	0.06-0.01	0.02-<0.01
Transient Distortion Coefficient (μsec/sq cmK)	19.8-1.7	2.9-0.4

Note: Table 7 is exerted from reference # 1.0.7.

SiC is a lightweight material that has structural characteristics that are between glass and Be . On the other hand, Be has the best mechanical properties and can be used to produce the lightest mirror designs. The data from Table 7 shows that Be has the lowest density of the two mirror materials.However, SiC has a Young's Modulus that is higher than Be; therefore, SiC is the stiffer of the two materials. The specific stiffness (stiffness to weight ratio) of Be is higher than SiC which is an extremely important property in the sense that deformations of the mirror substrate under load could feasibly result in optical figure distortion . Thus, Be on a weight for weight basis will not be as susceptible to deform under load as SiC.

The thermal properties of Be and SiC contribute to the dimensional stability of mirror substrates fabricated from these materials. Since Be and SiC have relatively high thermal conductivities, Be and SiC mirror substrates attain thermal equilibrium quite rapidly resulting in small thermal gradients . The high specific heat of Be indicates that Be can absorb large amounts of heat. Therefore, deformation would not occur unless a significant amount of heat was imparted into the mirror substrate. The high diffusivity of both Be and SiC enables these materials to rapidly equalize the temperature of a mirror substrate resulting in little or no thermal gradient which could lead to distortion. The CTE of Be is moderate (11.3-3.4 ppm/K) in comparison to SiC which has a CTE range of 2.4 -0.6 ppm/K; therefore, SiC is not as likely to experience dimensional movements due to temperature variations. In short, both Be and SiC thermal properties indicate high thermal stability for optics.

Based on all material presented, a Be optic fabricated from spherical powders would be a good choice for the LUTE mirror substrate except in the area of ultraviolet reflectance. An appropriate optical coating may be the solution to this problem. (NOTE: problems associated with bi-metallic bending should be a part of a coating trade study if Be is the final optical material choice for LUTE). Be has the most mature manufacturing base in comparison to SiC mirror materials. Reaction Bonded SiC is a competitive material to Be in the sense that the manufacturing process is low cost , tailorable, and with the aid of ultra-low scatter coatings surface roughnesses of ≤ 5 Angstroms rms can be achieved. Although the overall properties of CVD SiC are exceptional, CVD SiC can only be produced in limited geometrical forms. The cost effectiveness of this material is also questionable since the production process is not as mature as RB SiC or Be.

3.0 Conclusion

The comparison study of Be vs. SiC for the LUTE program has resulted in the in the following ranking for the optical material choices based on mature manufacturing

technology : 1) HIPed spherical Be, 2) RB SiC , and 3) CVD SiC . The optical materials rank as follows for use in the LUTE wavelength region: 1) CVD SiC, 2) RB SiC, and 3) HIPed spherical Be. CVD SiC technologies should be tracked for final selection of the LUTE primary mirror optic.

REFERENCES

1.0 Beryllium

1. James M. Marder, "A comparison of microdeformation in I-70, 0-50, and a new instrument grade of beryllium (I-250)", SPIE Vol. 1335 Dimensional Stability, pp. 108-116.

2. Dr. Don H. Killpatrick, "Beryllium- An Overview", From Proceedings of Aluminum, Beryllium, and Silicon Carbide Optics Seminar, February 23-24, 1993, Oak Ridge National Laboratory.

3.Larry A. Grant, Robert E. Hardesty, " Fabrication of Stable Lightweight Beryllium Optical Support Structures", SPIE Vol. 1335 Dimensional Stability, 1990, pp.140-155.

4. S.J.Kishner, G.J. Gardopee, M.B. Magida, R.A. Paquin, " Large stable mirrors: a comparison of glass, beryllium, and silicon carbide", SPIE Vol. 1335 Dimensional Stability, 1990, pp. 127-139.

5. J.A. Wells, C.M. Lombard, " Lessons Learned in Recent Mirror Fabrication", SPIE Vol. 1485 Reflective and Refractive Optical Materials for Earth and Space Applications , 1991, pp.2-12.

6. Thomas B. Parsonage, " Selecting mirror materials for high -performance optical systems", SPIE Vol. 1335 Dimensional Stability, 1990, pp. 119-126.

7. R.A. Paquin , "Silicon Carbide Optical Systems", From Proceedings of Aluminum, Beryllium, and Silicon Carbide Optics Seminar, February 23-24, 1993, Oak Ridge National Laboratory ----(Material Comparison Chart).

2.0 Silicon Carbide

1. Matthew B. Magida, Roger A. Paquin, James J. Richmond, "Dimensional stability of bare and coated reaction bonded silicon carbide", SPIE Vol. 1335 Dimensional Stability, 1990.

2. Michael A. Pickering, Raymond L. Taylor, and Joseph T. Keeley, " Chemically Vapor Deposited Silicon Carbide (SiC) for Optical Applications", SPIE Vol. 1118 Space Optical Materials and Space Qualification of Optics , 1989, pp. 2-13.

REFERENCES (Continued)

2.0 (continued)

3. J.S. Goela, M. A. Pickering, R.L. Taylor, " Chemically Vapor Deposited Silicon and Silicon Carbide Optical Substrates for Severe Environments", SPIE Vol. 1330 Optical Surfaces Resistant to Severe Environments (1990), pp. 25-38.

4. Roger A. Paquin, Matthew B. Magida and Cynthia L. Vernold, " Larger Optics from silicon carbide", SPIE Vol. 1618 Large Optics II , 1991, pp. 53-59.

5. R.A. Paquin , "Silicon Carbide Optical Systems", From Proceedings of Aluminum, Beryllium, and Silicon Carbide Optics Seminar, February 23-24, 1993, Oak Ridge National Laboratory ----(Material Comparison Chart).

6. Bud Graves," Silicon Carbide Structural Ceramics ", From Proceedings of Aluminum, Beryllium, and Silicon Carbide Optics Seminar, February 23-24, 1993, Oak Ridge National Laboratory-----(Characteristic Property Chart).

7. Ronald P. Williams, " Silicon Cladding of Silicon Carbide Substrates", From Proceedings of Aluminum, Beryllium, and Silicon Carbide Optics Seminar, February 23-24, 1993, Oak Ridge National Laboratory.

3.0 Stability (General)

1. Roger A. Paquin , " Dimensional Stability: An Overview ", SPIE Vol. 1335 Dimensional Stability , 1990, pp. 2-19.

2. Stephen F. Jacobs, "Unstable Optics", SPIE Vol. Dimensional Stability, 1990, pp. 20-44.

NOTE 1: The Proceedings from the Aluminum, Beryllium, and Silicon Carbide Optics Seminar, February 23-24, 1993, Oak Ridge National Laboratory are excellent references for Al, Be, and SiC . Topics addressed in the proceedings are toxicity of the optical materials, material properties (structural, thermal, and optical) of Al, Be, and SiC , and manufacturing considerations.

NOTE 2: The indexed literature search data book which accompanies this report contains the references listed in this report as well as other supporting information.

APPENDIX K

MIRROR MATERIAL PROPERTIES

LUNAR ULTRAVIOLET TELESCOPE EXPERIMENT (LUTE) PD22 / Paul L. Luz
Mirror Material Temperature-Dependent Properties Nov 9, 92

Material: Beryllium O-50

Temp. T (K)	Density rho (kg/m^3)	CTE (per K)	Conductivity k (W/m-K)	Specific heat Cp (J/kg-K)	FIGURES OF MERIT: Thermal Diffusivity [k/rho-Cp] (cm^2/sec)	FIGURES OF MERIT: Steady-state Distortion [CTE/k] (cm/MW)	FIGURES OF MERIT: Transient Distortion [CTE-rho-Cp/k] E-6(sec/cm^2-K)	Young's Modulus E (GPa)	Poisson's Ratio mu (—)	YTS (MPa)
0°	1856									
5		3.16E-10								
10		9.60E-10	26			3.69E-03		321.25	0.0334	
15		2.31E-09	34			6.79E-03				
20	*1856*	4.83E-09	55	1.6		8.78E-03	2.61E-05	321.25	0.0334	
25	1856	9.14E-09	68.5		221.00	1.33E-02	4.14E-05			
30		1.61E-08	85.6			1.88E-02		321.25	0.0334	
35		2.67E-08	104			2.57E-02				
40	*1856*	4.24E-08	120	10.0		3.53E-02	6.59E-04	321.25	0.0334	
45		6.48E-08								
50	1856	9.61E-08			33.40		2.88E-03	321.25	0.0334	
55		1.38E-07								
60	*1856*	1.94E-07	150	34.1		1.29E-01	8.18E-03	321.25	0.0334	
65		2.66E-07								
70		3.56E-07	175			2.03E-01		321.25	0.0334	
75	1856	4.67E-07			11.60		4.03E-02			
80	*1856*	5.99E-07	195	90.4		3.07E-01	5.15E-02	321.25	0.0334	
85		7.52E-07								
90		9.26E-07	220			4.21E-01		321.25	0.0334	
95		1.12E-06								
100	1856	1.32E-06	245	202.9	6.30	5.39E-01	2.10E-01	321.16	0.0335	
105		1.54E-06	250			6.16E-01				
110		1.77E-06						321.06	0.0336	
120	*1856*	2.27E-06	260	354.0		8.73E-01	5.74E-01	321.03	0.0338	
130		2.82E-06	250			1.13E+00		320.94	0.0339	
140		3.41E-06						320.74	0.0341	
150		4.01E-06		636.0				320.52	0.0345	
160		4.62E-06						320.33	0.0347	
170		5.24E-06						320.11	0.0351	
180		5.84E-06						319.86	0.0355	
190		6.43E-06						319.55	0.0360	
200	1854	7.00E-06		1112.9	1.30		5.38E+00	319.23	0.0363	
210		7.54E-06						318.89	0.0368	
220		8.07E-06						318.54	0.0373	
230		8.57E-06						318.20	0.0378	
240		9.04E-06						317.76	0.0384	
250	*1852*	9.50E-06	236	1535.5		4.03E+00	1.14E+01	317.38	0.0389	
260		9.94E-06						316.94	0.0395	
270		1.04E-05						316.50	0.0399	
273.16		1.05E-05	218			4.82E+00				
280		1.08E-05						316.04	0.0407	
290		1.11E-05						315.59	0.0413	
294.26	1850	1.13E-05	220	1875.0		5.14E+00	1.78E+01	*315.36*	0.0416	172
300	1849	1.15E-05	200	1832.6	0.59	5.75E+00	1.95E+01	315.13	0.0419	
						^	^			
						near zero is good	*near zero is good*			

REFERENCE:
- D.H. Killpatrick, REPORT ON THE PROPERTIES OF BERYLLIUM, Oak Ridge National Laboratory, May 1990.
- Swenson, "HIP beryllium: Thermal expansivity from 4 to 300K and heat capacity from 1 to 108K", JOURNAL OF APPLIED PHYSICS, 70(6), Sept. 1991.

LUNAR ULTRAVIOLET TELESCOPE EXPERIMENT (LUTE)
Mirror Materials Selection

PD22 / Paul L. Luz
Mar 19, 93

Material: CVD Silicon Carbide

					FIGURES OF MERIT					
Temp. T (°K)	Density rho (kg/m^3)	CTE (per °K)	Conductivity k (W/m-K)	Specific heat Cp (J/kg-K)	Thermal Diffusivity [k/rho-Cp] (cm^2/sec)	**Steady-state Distortion** [CTE/k] (cm/MW)	**Transient Distortion** [CTE-rho-Cp/k] E-6(sec/cm^2-K)	Young's Modulus E (GPa)	Poisson's Ratio mu (—)	Flexural Strength (MPa)
0°										
100										
123	= 3210		179	250	2.23					
128	= 3210	= 4.00e-7	= 179	= 250	= 2.23	= 2.23E-01	= 1.79E-01			
133		4.00E-7								
150										
173	= 3210	8.00E-7	223	400	1.74	= 3.59E-01	= 4.61E-01			
200										
223	= 3210	= 1.35e-6	235	= 550	1.33	= 5.74E-01	= 1.01E+00			
250										
273	= 3210	1.90E-6	202	700	0.90	= 9.41E-01	= 2.11E+00			
294.26	3210							461-466		595
298			193		0.80					
						^	^			
						near zero is good	*near zero is good*			

REFERENCE: "CVD Silicon Carbide™", CVD Materials, Technical Bulletin #107, Morton Advanced Materials, date unknown.

LUNAR ULTRAVIOLET TELESCOPE EXPERIMENT (LUTE) PD22 / Paul L. Luz
Mirror Materials Selection Nov 30, 92

Material: UTOS CERAFORM® Silicon Carbide (siliconized SiC)

					FIGURES OF MERIT					
Temp. T (°K)	Density rho (kg/m^3)	CTE (per °K)	Conductivity k (W/m-°K)	Specific heat Cp (J/kg-°K)	Thermal Diffusivity [k/rho-Cp] (cm^2/sec)	**Steady-state Distortion** [CTE/k] (cm/MW)	**Transient Distortion** [CTE-rho-Cp/k] E-6(sec/cm^2-°K)	Young's Modulus E (GPa)	Poisson's Ratio mu (—)	YTS (MPa)
0°										
25										
50										
75		1.02e-6 ?								
100		1.13e-6 ?	125 ?			= 9.04E-01				
125										
150		1.40e-6 ?	175 ?			= 8.00E-01				
175										
200		1.75e-6 ?	200 ?			= 8.75E-01				
225										
250		2.20e-6 ?	190 ?			= 1.16E+00				
273.16		1.60e-6 ?								
294.26										
300	2920	2.57E-6	156	670		1.65E+00		311		
						^ *near zero is good*	^ *near zero is good*			

REFERENCE: "UTOS CERAFORM® Silicon Carbide (siliconized SiC)", United Technologies Optical Systems, date unknown.

APPENDIX L

LUTE TELESCOPE STRUCTURAL DESIGN STUDY REPORT (STUDY REPORTS BY OPTICAL COMPANIES)

FINAL REPORT

LUTE Primary Mirror Study

May 14, 1993

Litton
Itek Optical Systems

for **Marshall Space Flight Center**
under Purchase Order No. H-19669D

Introduction

This brief study of primary mirror options for the Lunar Ultraviolet Telescope was conducted to evaluate the potential of either a passive or active mirror configuration to achieve "diffraction-limited" performance in the lunar surface environment, described in the LUTE telescope analyses done by the MSFC task team. Itek therefore started from the premise that any acceptable design must achieve the desired weight given in the overall LUTE weight statement, and must achieve a WFE of .03μm rms in the environment of the LUTE analyses. This report provides summary data describing active and passive mirror configurations which have an acceptable weight and would provide high quality wavefront performance. This information is in the form of presentation material used for a final briefing held at Itek on May 10, 1993. As appendix material, we include copies of memos and other information provided in the course of our study activity, as well as some information describing Itek-manufactured hardware, made to meet similar requirements for other programs.

Summary

To summarize the mirror structural analysis results in the light of the error budget, it appears that the goal of operation at near-diffraction-limited performance in the vacuum ultraviolet (0.1-0.35μm) is extremely restrictive. In a formal sense, there appears to be no simple combination of materials and common processes from which a passive lightweight mirror can be constructed to achieve the desired mirror performance (0.01 μm rms WFE) over the range of temperatures (and temperature distribution) seen by the LUTE primary in a full lunation. The solution to the dilemma is then to:

1. Reduce the optical performance goal to less than diffraction-limited (0.1 μm rms total WFE), thus reducing the scientific mission,
2. Thermally control mirrors and metering structure to a smaller temperature range, or
3. Adopt an active primary mirror configuration

Our evaluation of mirror performance over the lunar temperature range shows that achievable fused silica or SiC passive lightweight mirror designs will yield ~0.05μm rms wavefront error, and have mass/area ratios of 39.1 kg/m^2 and 33.3 kg/m^2 respectively. (Use of either of these materials for such a lightweight mirror is a low risk based on currently operational hardware.) A SiC mirror "cold figured" at the average operating temperature of 190K will yield a WFE of .03 μm rms. These thermally-induced errors exceed diffraction-limited performance requirements by factors of 3 to 5. Reducing system performance to accommodate this level of mirror capability might be acceptable, if overall scientific output is not strongly degraded. However, should sufficient power be available, using active thermal control with one of these materials may allow achieving diffraction-limited performance. For example, a total system error budget of 0.05 μm rms WFE is feasible for swings limited to about 50K. However, any final system goals for mirror weight and performance must be set on the basis of more detailed analysis than we have been able to provide here: these comments are for exemplary purposes only. It is safe to say that we have met the limit of the state of the art in this area, and we recommend that it would be cost-effective to do something other than try to develop even more advanced passive mirror approaches.

If an active mirror solution is required, because both the performance and weight goals are deemed to be firm, then we can certainly indicate that this technology also has a reasonable degree of maturity, based on almost twenty years of hardware development, under Itek and Government sponsorship. We can provide hardware specifics, if required in the future for review committee purposes, but at this time, a good summary of the Pepi/Nagle evaluation is that they were able to use their standard methodology, and interpolated into previously defined design curves to develop the parametric description and sketches of the active mirror baseline concept shown in the briefing.

From this evaluation, it appears that the reference mirror can be launched, land on the moon and (analytically) operate over the entire thermal cycle to the specified level. However, as also noted, to achieve the operating performance, a simple open-loop controller based on the analytic predictions is probably not sufficient, and some version of a "standard" active optic control system would be required for performance maintenance. The additional elements of the standard figure maintenance system are a wavefront sensor (either direct measurement or wavefront data inferred from deconvolution of the scientific imagery), a processor to derive the primary mirror surface shape (as well as alignment errors) from the wavefront, and a control system to drive the active mirror into the desired shape.

For the LUTE application, a simplifying assumption is that the constancy of the environment, and the truly repetitive nature of the thermal cycle, will allow a detailed analytical prediction of mirror distortion as a function of time, which would be phased with the varying temperature distribution within the telescope. Thus, once wavefront and temperature measurements are made over the first lunation, for validation and "calibration" of the predictive model, it should be possible to use the time and temperature distribution (only) to control the mirror, using the calibrated model. It is likely that the operating bandwidth of this "active" mirror control system will be in the .001 hz regime, so that the number of independent degrees of freedom will be modest, and the number and precision of thermal sensors should not be extreme. Finally, because there is likely to be small, but measurable, hysteresis of the mirror actuators, an occasional recheck of wavefront performance with the wavefront sensor will be a useful part of the system operating timeline. A second use for the WFS would be to check system optical alignment.

As a practical matter, we enumerate the hardware required for the active mirror system:

- Active mirror, with (nominally) 90 actuators (number depends on material and environment)
- Actuator drive electronics (1 card including amplifier, 12-15 IC chips, D/A, power supply and data bus interconnects)
- Wavefront sensor (CCD camera with ancillary pupil imaging optics and shear grating)
- Processing and control electronics (a 486-class, RISC computer, similar to existing Litton ATD unit. Memory of 16 megabytes would be more than ample for all active mirror functions.)
- Thermal sensors, of the order of 50-100 maximum, located strategically within the telescope.

Based on twenty years of development and hardware demonstration under various environmental conditions, at Itek and elsewhere, we feel that use of an active mirror for LUTE is a low to moderate risk, even though such a mirror has not yet flown in space. While we certainly agree that the additional parts count, failure modes and assembly complexity make an active mirror less attractive than a passive one, it should not be ruled out if the performance and mission cannot be supported by existing passive mirror technology.

LUTE

Mirror and Mirror Mount Design Methodology

J. Pepi

This material describes Itek's general methodology of designing passive and active primary mirrors for aerospace environments, and is based on a short course given by J. Pepi under the auspices of the SPIE.

MIRROR DESIGN ENVIRONMENTS AND REQUIREMENTS

- Launch or aircraft random, acoustic, and acceleration loadings
- Orbital gravity release (zero-g)
- Gravity orientation shifts
- Assembly-induced mount loadings
- Onboard vibration sources
- Manufacturing polishing pressures
- Temperature soak
- Operational temperature swings and gradients

Minimum weight to meet payload requirements

Adequate strength

Stringent optical performance to a fraction of a wavelength of light

DESIGN FLOW CHART

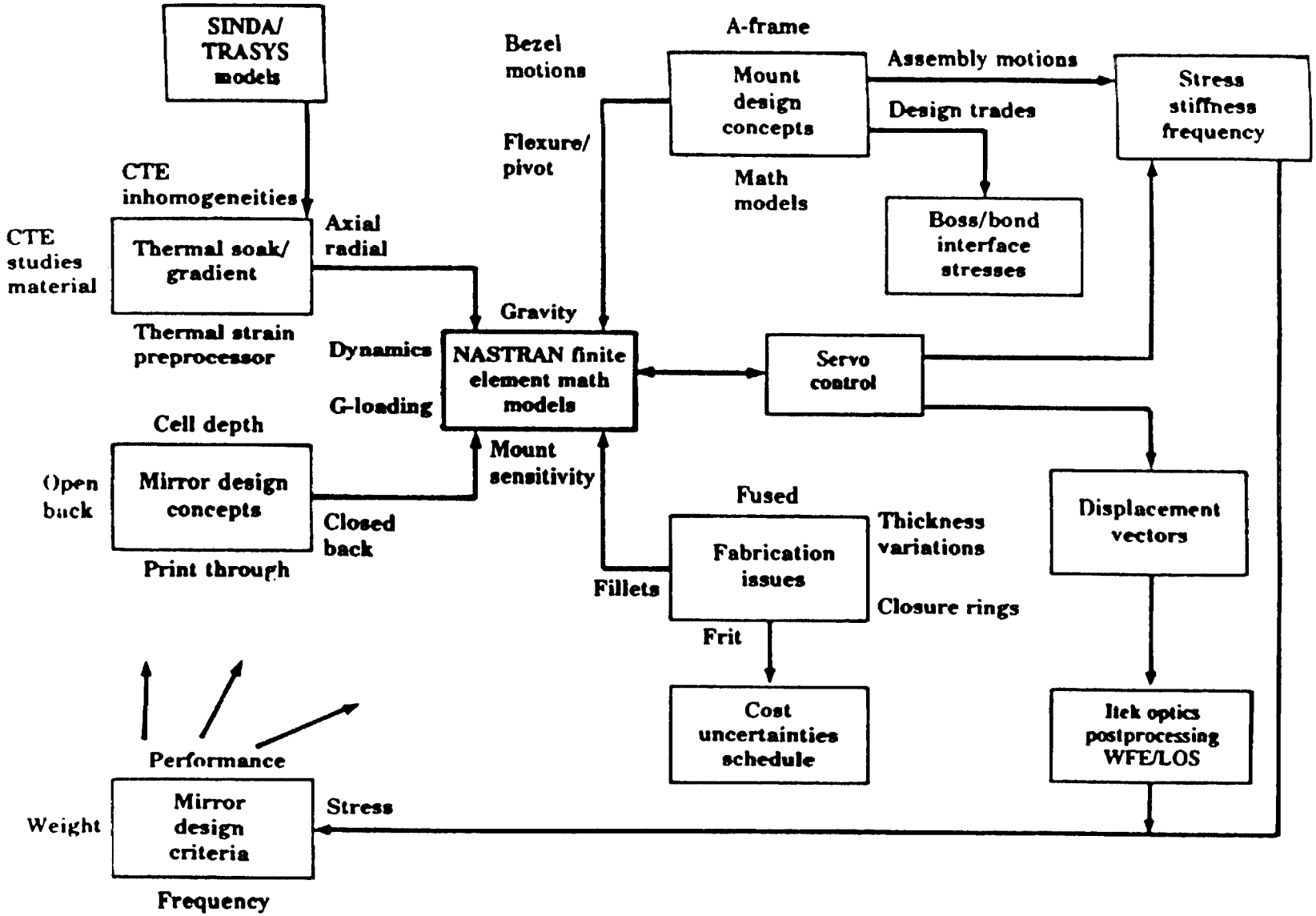

LIGHTWEIGHT MIRROR DESIGN OPTIONS

- Thin Meniscus Solid
- Closed Back Sandwich
  - Hexagonal Core
  - Square Core
  - Triangular Core
  - Fusion, Frit, Weld, Braze Processes
- Open Back Construction
  - Triangular Core

All Designs must Evaluate Material Selection;
Mount Location, Number and Type; and
Mirror Shape - in conjunction with the
Design Environments, Criteria, and
Requirements

LIGHTWEIGHT ACTIVE OPTIC

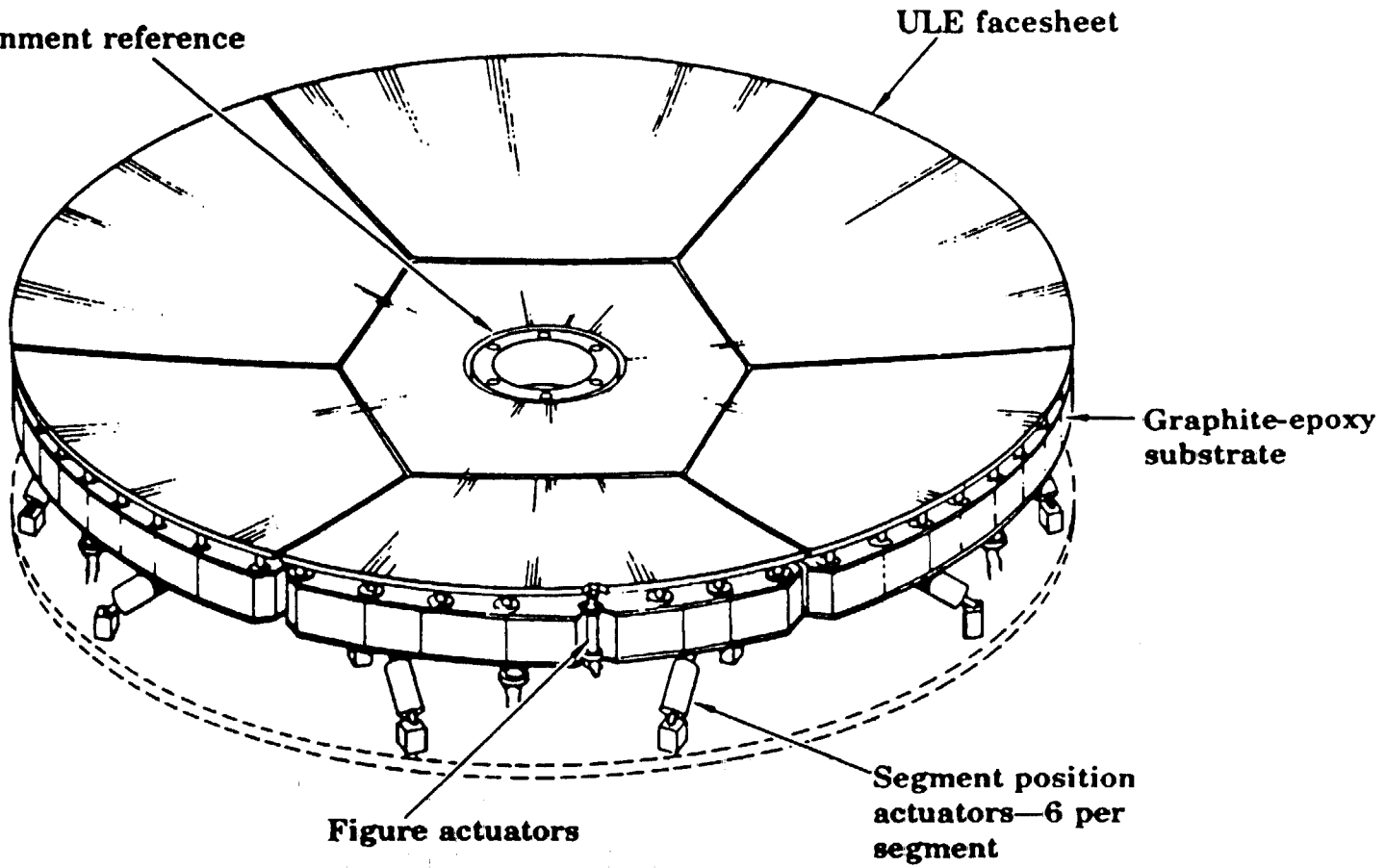

86-037

GRAVITY DISTORTIONS

Optical Axis Vertical

Horizontal Loading

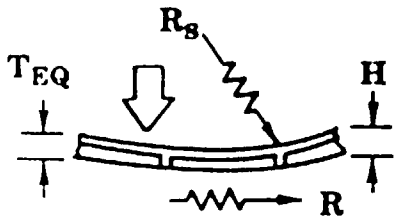

$$\text{sag} = \frac{K_1 \,(\text{weight density})\, R^4\, H}{T_{EQ}^{\,3}}$$

Optical Axis Horizontal

Vertical Loading

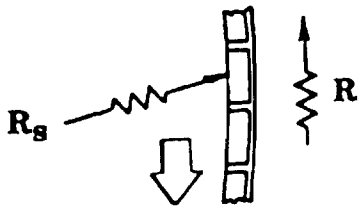

$$\text{sag} = \frac{K_2 \,(\text{weight density})\, R^5\, H}{R_S\, T_{EQ}^{\,3}}$$

Gravity

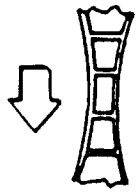

sag = minimal

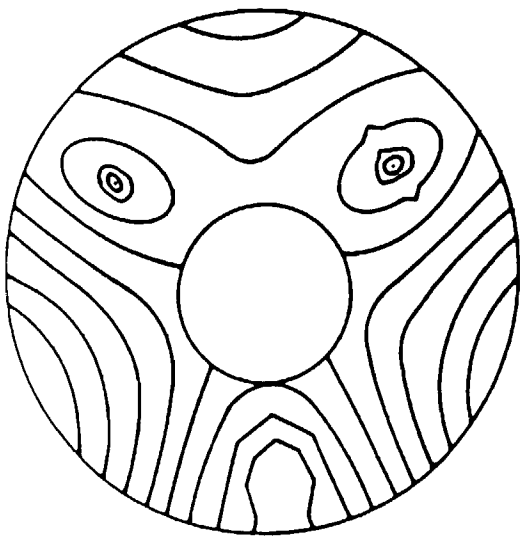

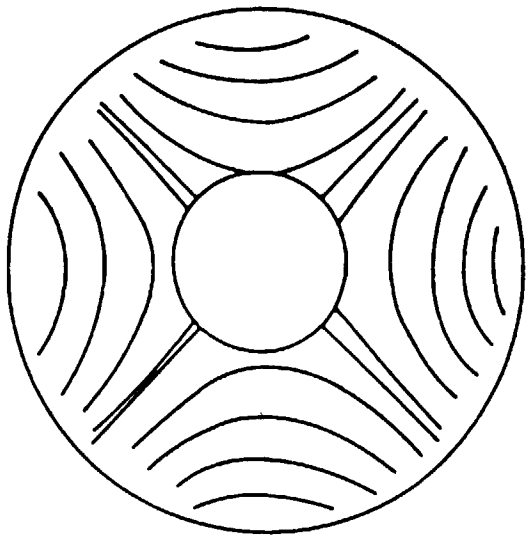

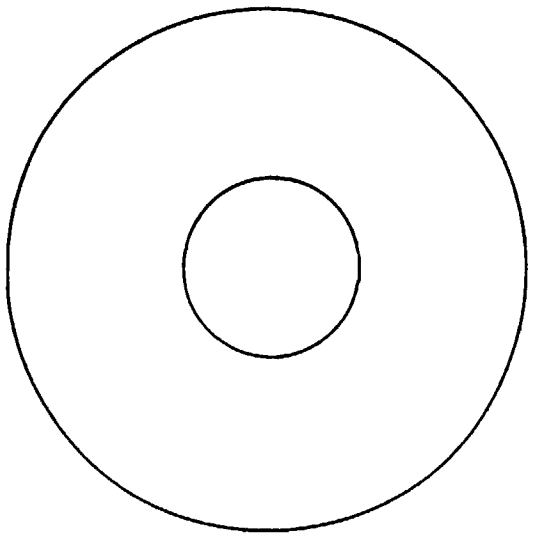

86-037

DESIGN REQUIREMENTS FOR THE PRIMARY MIRROR MOUNT

- Stiffness in all directions to maximize mirror rigid body frequencies
- Strength in all directions to resist launch load stresses
- Rigidity to preclude buckling
- Flexibility to minimize mount-induced assembly loading mirror distortion
- Flexibility to minimize mount-induced distortion from mirror/interface thermal mismatch
- Flexibility to minimize assembly/thermally induced stresses
- Pseudo-kinematic in nature to achieve isolation

SIX-DEGREE-OF-FREEDOM TANGENT BAR MOUNT SCHEME

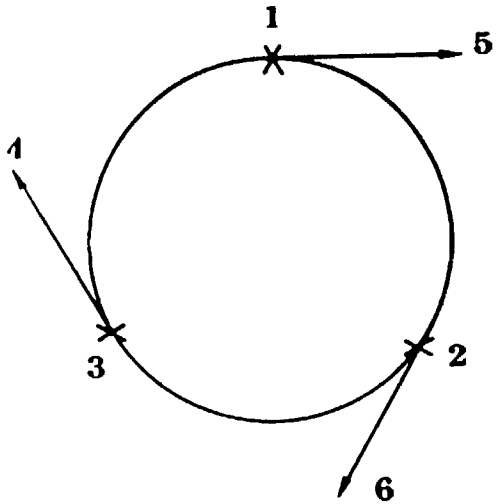

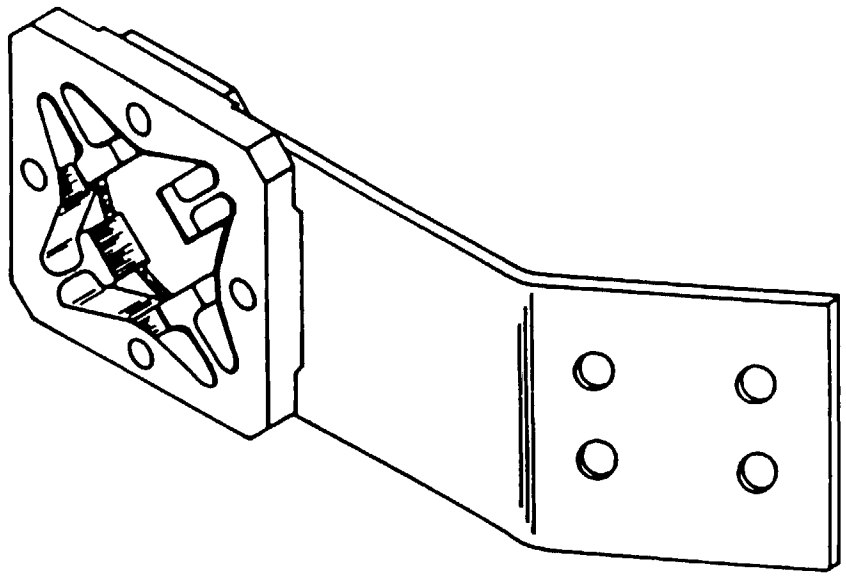

86-037

PSUEDO-KINEMATIC MOUNT

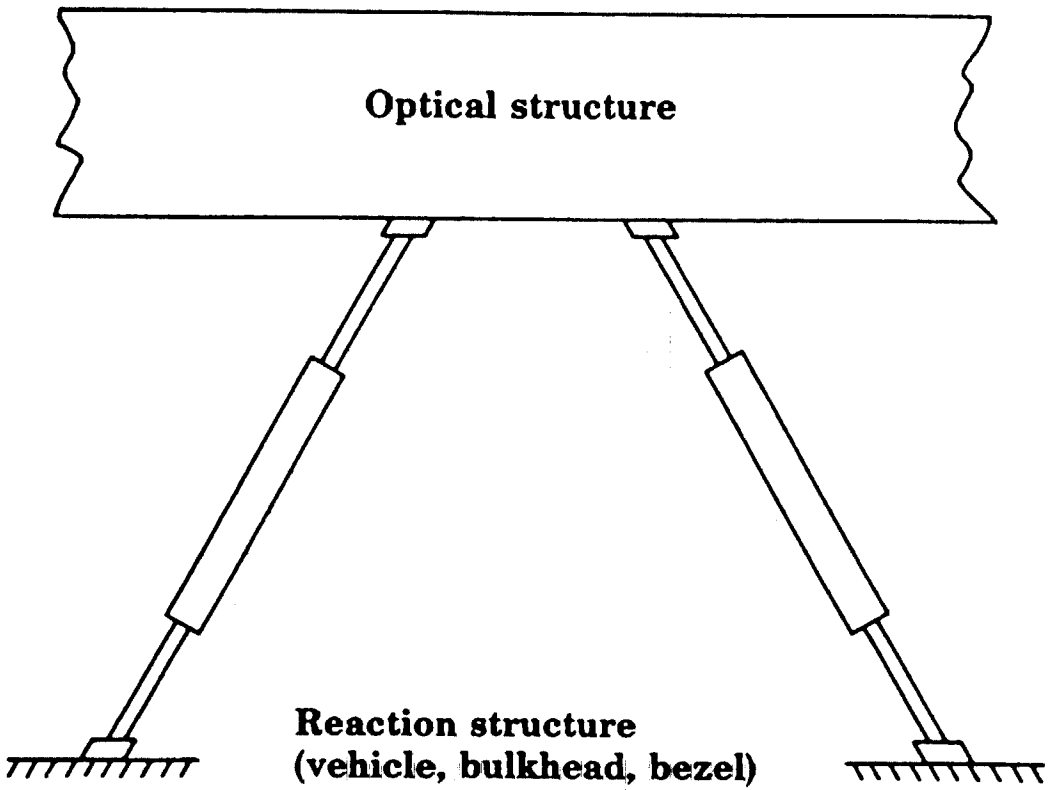

86-037

MATERIAL CONSIDERATIONS

$$F.M. \sim \frac{EKS}{\rho \alpha \Delta \alpha}$$

F. M.	=	Figure of merit
E	=	Modulus of Elasticity
K	=	Thermal conductivity
S	=	Strength
ρ	=	Density
α	=	Coefficient of Thermal Expansion (CTE)
$\Delta\alpha$	=	CTE Inhomogeneity

COMPARISON OF MIRROR CANDIDATE MATERIAL

Properties at Room Temperature

	Fused Silica	ULE	Zerodur	Borosilicate	Beryllium	Aluminum	Silicon Carbide	
							CVD	Reaction Bonded
Young's modulus of elasticity, E psi	10.6×10^6	9.8×10^6	13.1×10^6	9.1×10^6	44.0×10^6	10.6×10^6	66.8×10^6	52.8×10^6
Poisson's Ratio	0.25	0.18	0.25	0.20	0.07	0.33	0.21	0.14
Coefficient of thermal expansion, α/°C	0.56×10^{-6}	$0 \pm 0.03 \times 10^{-6}$	$0 \pm 0.05 \times 10^{-6}$	3.1×10^{-6}	11.2×10^{-6}	23.2×10^{-6}	1.9×10^{-6}	2.1×10^{-6}
CTE variation, ppb/°C	5	10	15	30	100	100	50	50
Thermal conductivity, K BTU/hr ft°F	0.79	0.76	0.95	0.79	87	109	115	99
Density, ρ (lb/in.^{3})	0.0796	0.0795	0.091	0.080	0.067	0.100	0.116	0.106
Mechanical figure of Merit (E/ ρ)	133	123	144	114	656	106	576	498
Thermal figure of merit K/α	1.4	25.3	19.0	0.3	7.7	4.7	60.0	47.0

THERMAL FIGURE OF MERIT

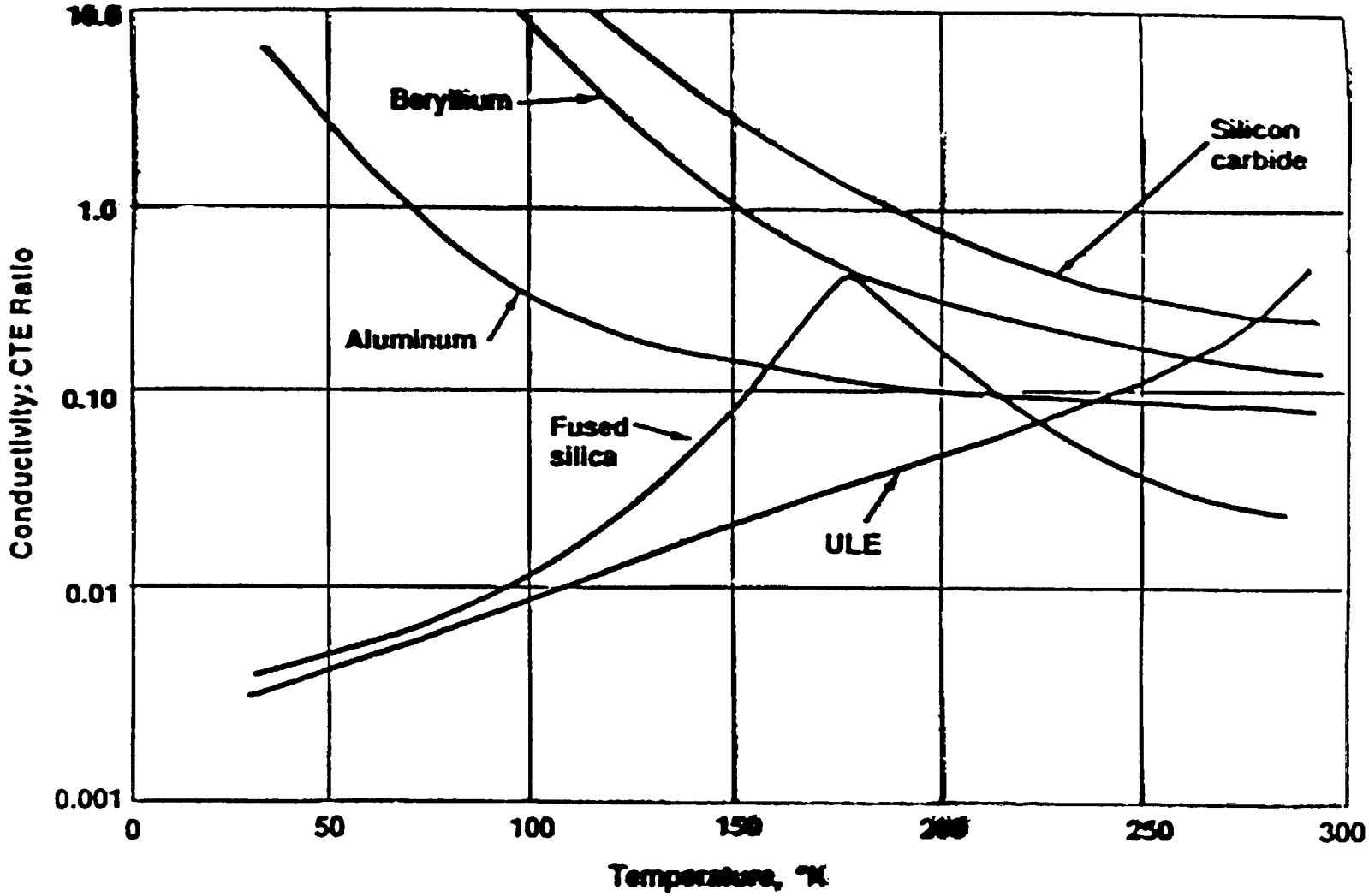

Litton

Itek Optical Systems

NASTRAN MODELING

Superposition of Facesheet on Boule CTE Inhomogeneity Study

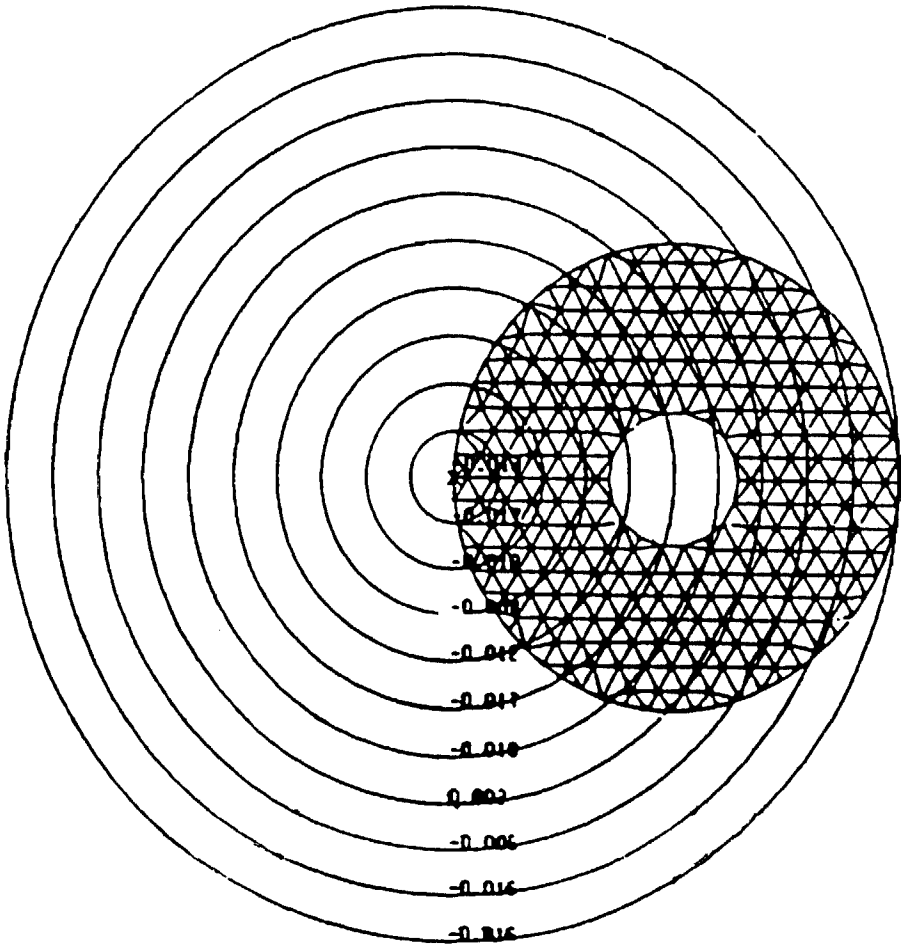

ACTIVE MIRROR DESIGN

- A mirror must be made active when the optical performance requirements cannot be met without excessive weight or high-risk manufacture
- The use of ultralight technology for active mirror designs results in "super" ultralightweight mirrors
- The choice of active versus passive performance depends on weight and performance requirements. In general, concepts exceeding a 2-m diameter dictate some form of active mirror compensation

SURFACE CONTROL ACTUATOR SCHEMATIC

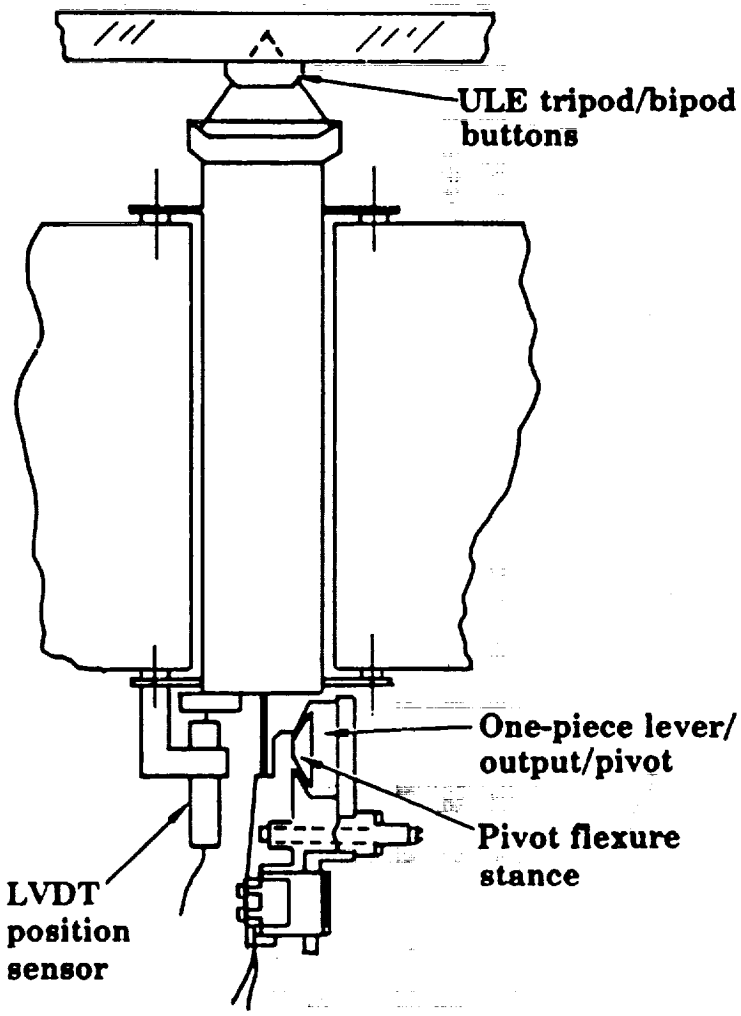

ONE EXAMPLE OF A 4-M-DIAMETER WEIGHT COMPARISON FOR VARIOUS APPROACHES

Passive **Active**

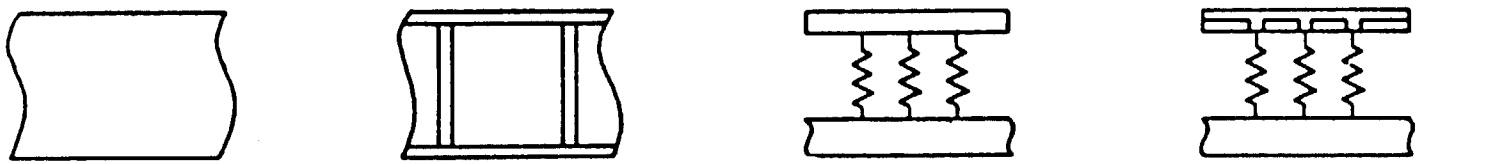

Solid
26,400 lb

Ultralight Design
3,000 lb
(88% lightweight)

Solid Facesheet
1,800 lb
(93% lightweight)

Ultralight Facesheet
760 lb
(97% lightweight)

- All designs sized to meet performance, stiffness, and strength goals

COMPOSITE DESIGN APPLICATIONS

- As a lightweight material for spacecraft and aircraft payload limitations
- As a stiff back structure to a flexible glass mirror
  - Low CTE at operational temperatures in cryogenic region
  - Match of total thermal strain to glass over cryogenic soak
  - Minimum CTE variation through depth to minimize distortion—cryogenic and orbital thermal variations (hot and cold)
  - Thermal conductivity to preclude excessive gradients
  - Dimensional stability—outgassing—microcrack phenomena
- As an optical metering structure—dimensional stability
- As a supportive structure—high strength and stiffness

Teal Ruby
InfraRed Telescope Unit

This telescope was made to serve as the wide-field optical collector for a test of IR focal plane components. In general, it was to have a relatively wide field, a moderately warm front end, and a cold rear section, all in a very light flight package to yield near diffraction limited imagery in the MWIR. The combination of lightweighted fused silica mirrors and graphite-epoxy structure shown here achieved these goals at a total flight weight of under 60 lb.

NOMINAL ITU DESIGN

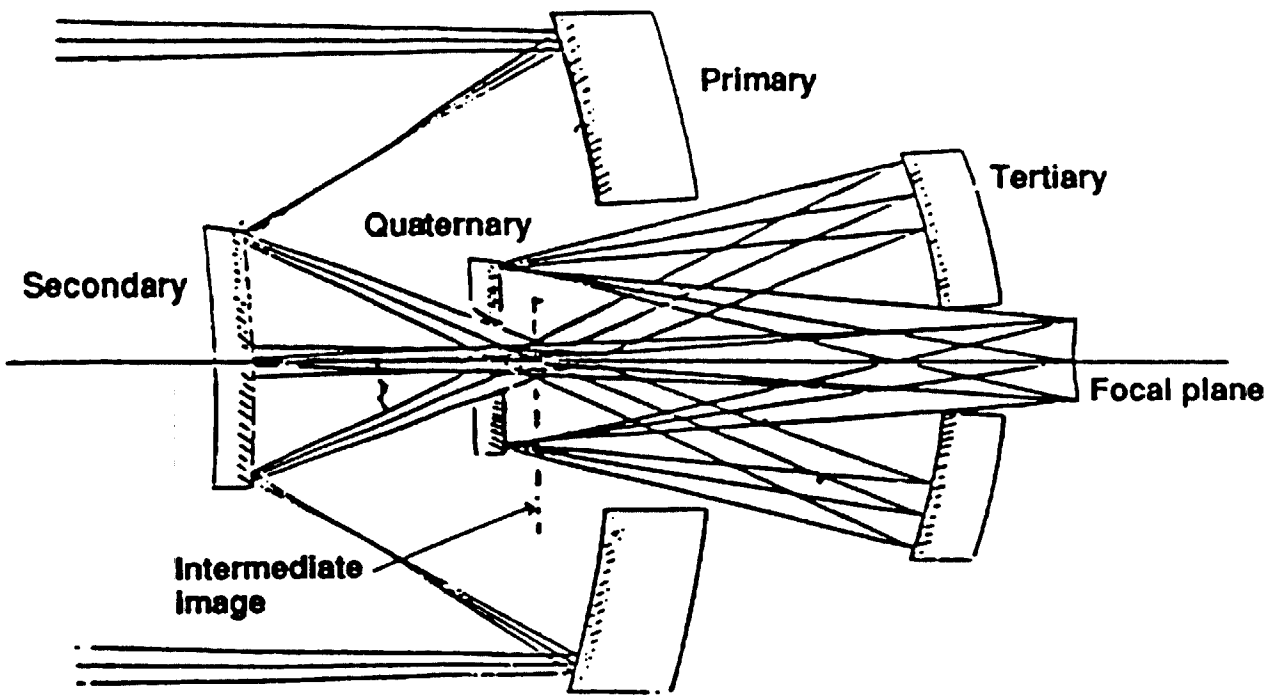

TELESCOPE SCHEMATIC

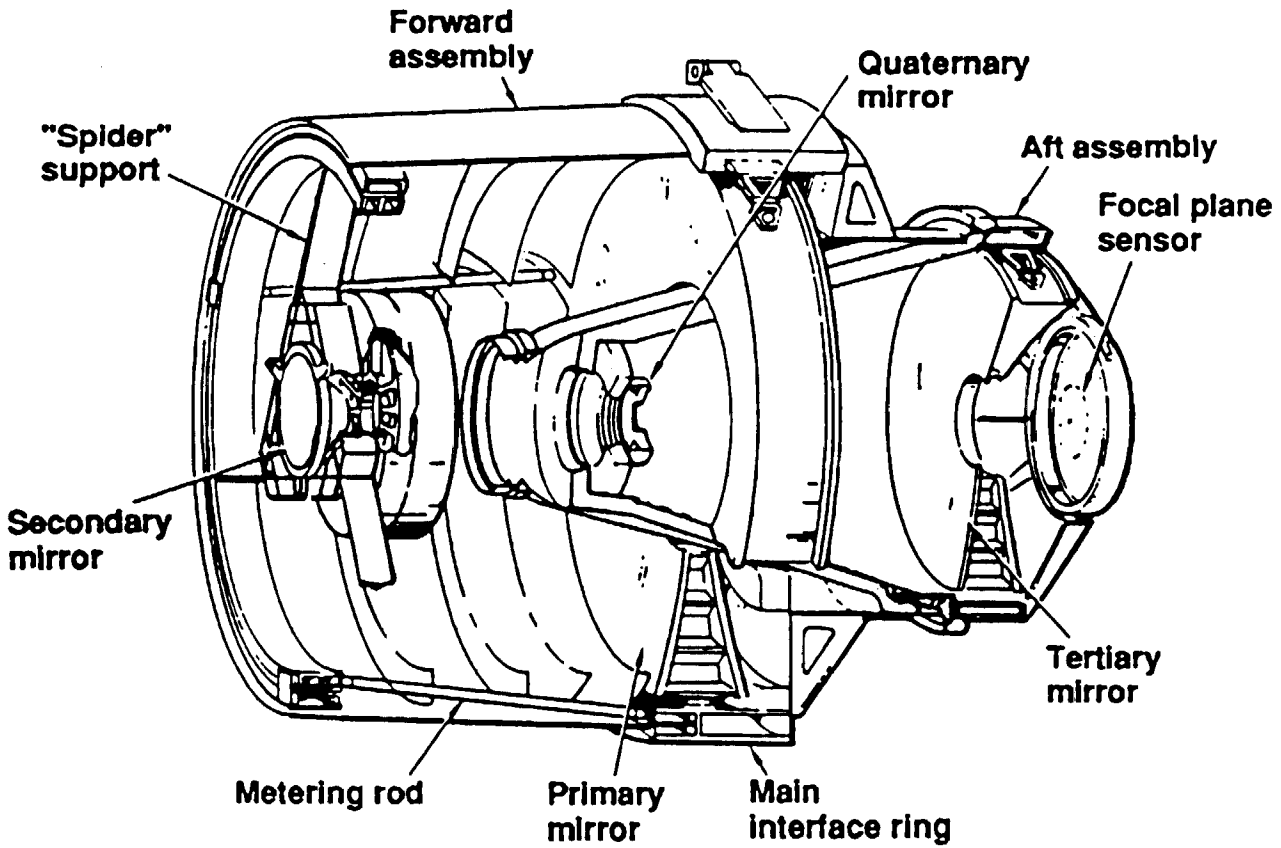

LUTE Mirrors

R. Nagle

The following material applies this design methodology to the LUTE requirements and environment, and describes the mirror configurations coming closest to achieving these goals.

LUTE PASSIVE PRIMARY MIRROR DESIGN SUMMARY

Requirements:

Aperture:	40 Inch with 20 Inch Central Hole
Spherical Radius:	80 Inch, Concave
Minimize Weight, Weight/Area:	25 KG/M^2
RMS WFE:	<0.04 Microns

Loads:

Temperature Soak:	From NASA Structural Analysis
Temperature Grad:	From NASA Structural Analysis
Gravity Release:	1G → 1/6G
Launch (Acceleration Vibration + Acoustic):	20G

Candidate Materials:

Fused Silica, ULE, Beryllium, Silicon Carbide

LUTE PASSIVE PRIMARY MIRROR DESIGN SUMMARY

Requirements, loads, and candidate materials for the Lute Primary Mirror were obtained from NASA's structural and thermal analysis reports.

An evaluation of equal stiffness/weight and equal weight passive mirror designs show that all materials yield a WFE greater than 0.04 microns rms, and weight/area greater than 25Kg/m^2. For diffraction limited performance, a WFE of <0.01 microns rms is desired. Even "cold figuring" a SiC mirror (best performance over temperature range) at the average operating temperature of 190K, only yields a WFE equal to 0.03 microns rms.

LUTE PASSIVE PRIMARY MIRROR DESIGN SUMMARY (Continued)

RESULTS:

Equal Stiffness/Weight Designs:

All Designs Yield RMS WFE > 0.04 Microns
Weight/Area Range from 25 KG/M^2, Be → 41.8 KG/M^2, ULE

Equal Weight Designs:

All Designs Yield RMS WFE > 0.04 Microns

Equal Stiffness/Weight (Cold Figured at 190°K)

SiC Only Material to Yield RMS WFE < 0.04 Microns
Weight/Area = 33.3 KG/M^2

FIGURE 1 PASSIVE PRIMARY MIRROR CONCEPTS (Minimum Weight Designs Based On Equal Stiffness To Weight)

The lightweight configurations selected for each material was based on optimum performance for minimum weight while considering the ease of manufacturing.

FIGURE 1

PASSIVE PRIMARY MIRROR CONCEPTS

MINIMUM WEIGHT DESIGNS BASED ON EQUAL STIFFNESS/WEIGHT

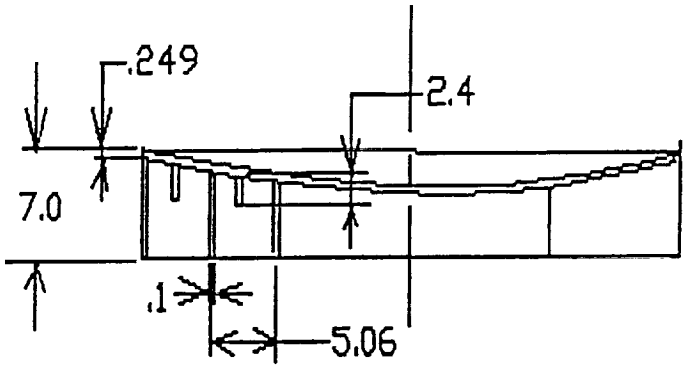

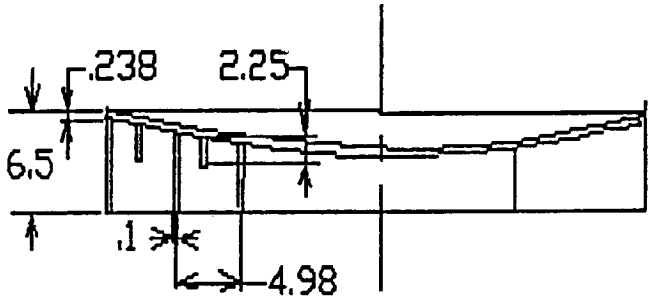

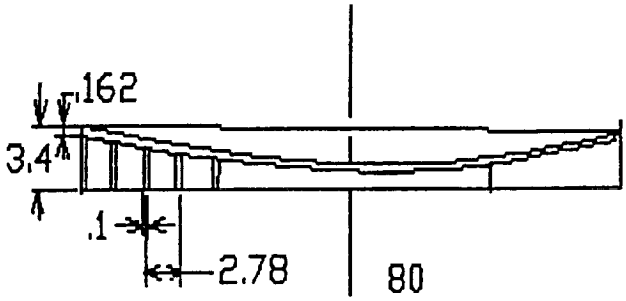

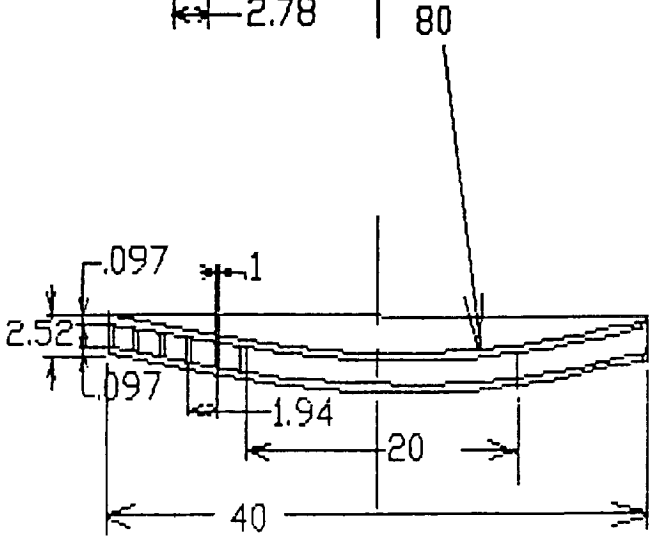

MAT'L	WT/AREA (KG/M^2)	RMS WFE @ 190 K
ULE	41.8	.075
FS	39.1	.060
SIC	33.3	.060
Be	25.4	.275

FIGURE 2 PASSIVE PRIMARY MIRROR CONCEPTS (MINIMUM WEIGHT DESIGNS BASED ON EQUAL WEIGHT)

Increasing the section, and consequently the weight, improves the WFE performance over the equal stiffness/weight designs, but still not diffraction limited performance.

FIGURE 2 -

PASSIVE PRIMARY MIRROR CONCEPTS

MINIMUM WEIGHT DESIGNS BASED ON EQUAL WEIGHT

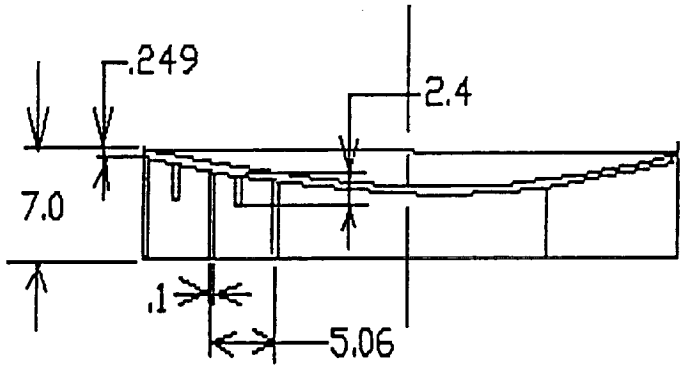

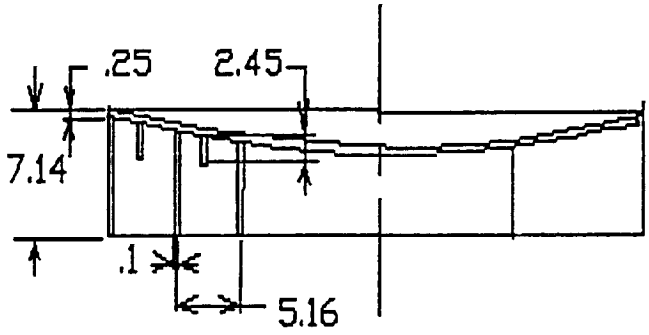

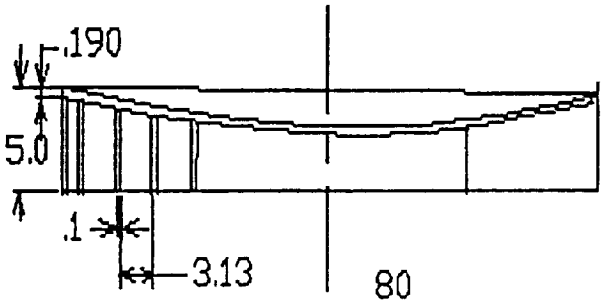

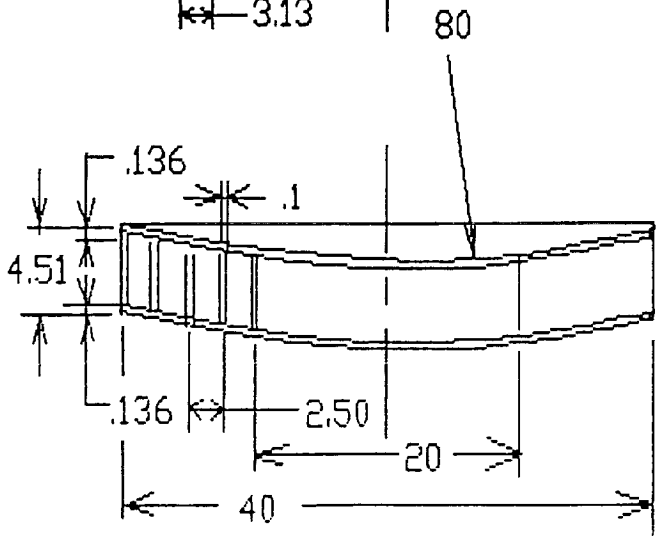

MAT'L	WT/AREA (KG/M^2)	RMS WFE @ 190 K
ULE	41.8	.075
FS	41.8	.040
SiC	41.8	.050
Be	41.8	.225

FIGURE 5 SOAK AND GRADIENT COMBINED (EQUAL STIFFNESS/WEIGHT MIRROR DESIGNS)

These equal stiffness/weight mirror thermal performance curves show that fused silica and SiC are the best performers, but exceed the WFE limit of 0.01 microns rms.

Figure 5

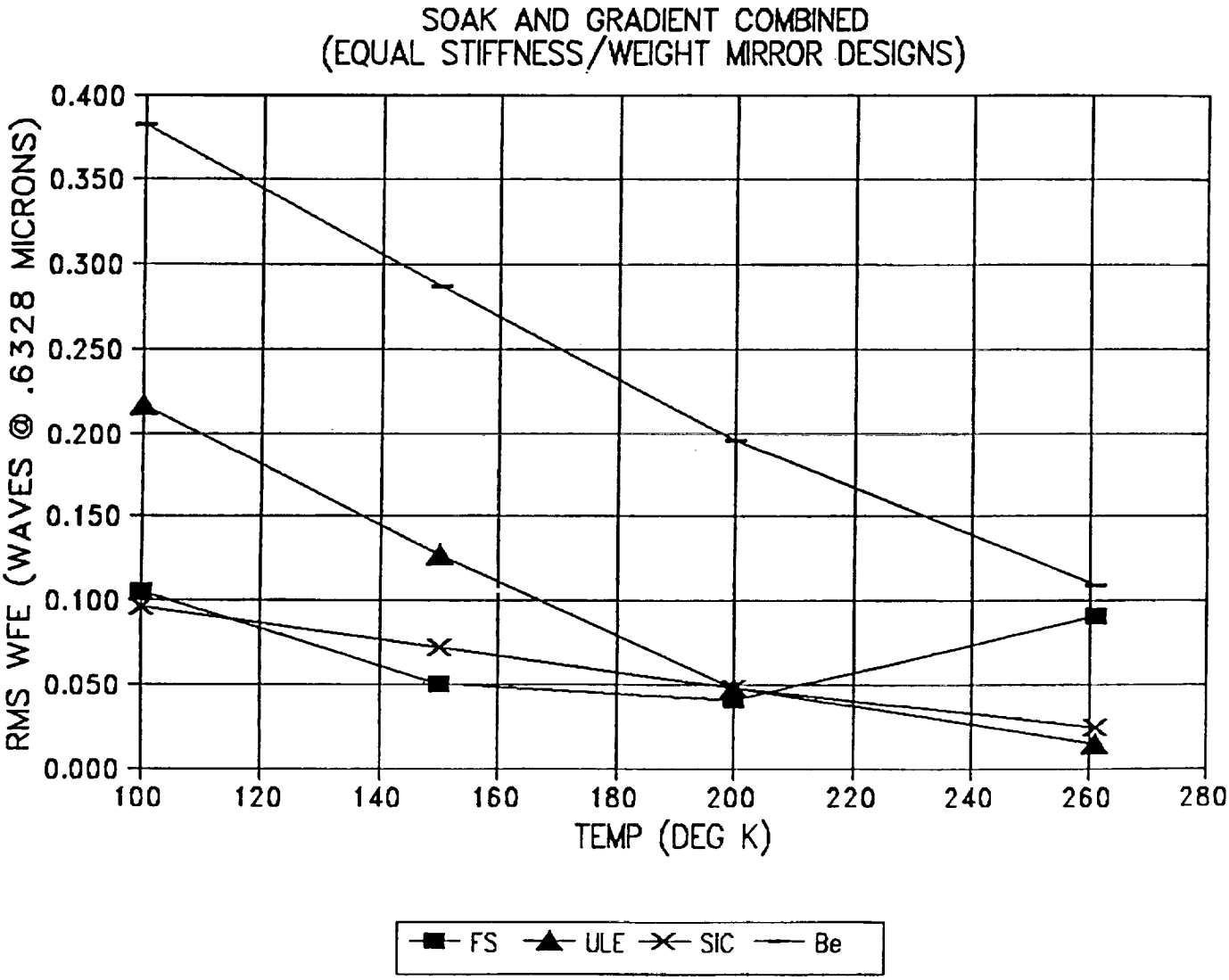
SOAK AND GRADIENT COMBINED
(EQUAL STIFFNESS/WEIGHT MIRROR DESIGNS)
RMS WFE (WAVES @ .6328 MICRONS)
0.400
0.350
0.300
0.250
0.200
0.150
0.100
0.050
0.000
100
120
140
160
180
200
220
240
260
280
TEMP (DEG K)
FS
ULE
SIC
Be

FIGURE 8 SOAK AND GRADIENT COMBINED (EQUAL WEIGHT MIRROR DESIGNS)

These equal weight mirror thermal performance curves show improvement over the equal stiffness/weight mirror performance curves, but still exceed the WFE limit of 0.01 microns rms.

Figure 8

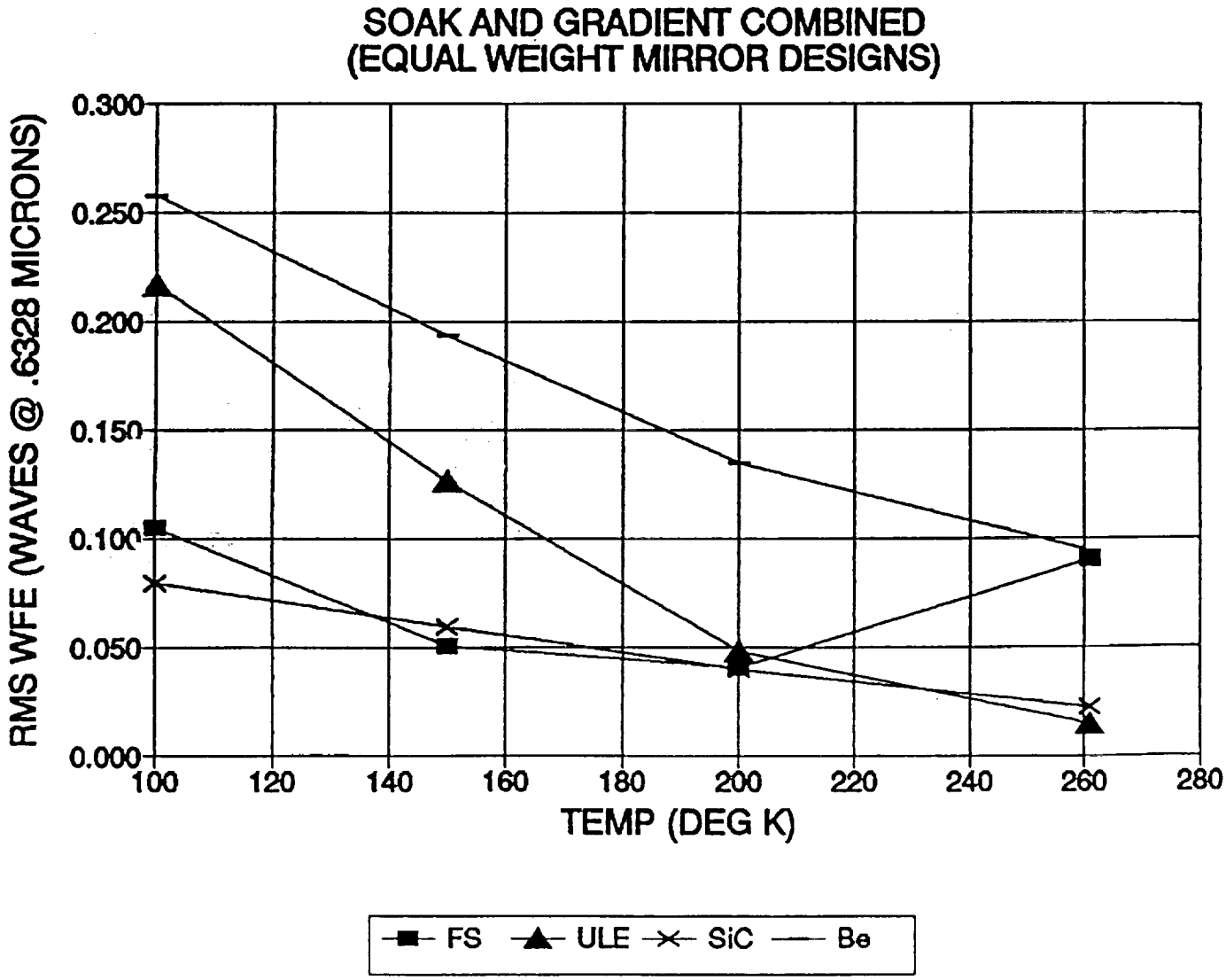
SOAK AND GRADIENT COMBINED
(EQUAL WEIGHT MIRROR DESIGNS)
RMS WFE (WAVES @ .6328 MICRONS)
0.300
0.250
0.200
0.150
0.100
0.050
0.000
100
120
140
160
180
200
220
240
260
280
TEMP (DEG K)
FS
ULE
SiC
Be

SOAK AND GRADIENT COMBINED (EQUAL STIFFNESS/WEIGHT MIRROR DESIGNS)

"Cold figuring" the mirror at the average operating temperature of 190K improves thermal performance, but still exceeds the WFE limit of 0.01 microns rms.

Figure 8a

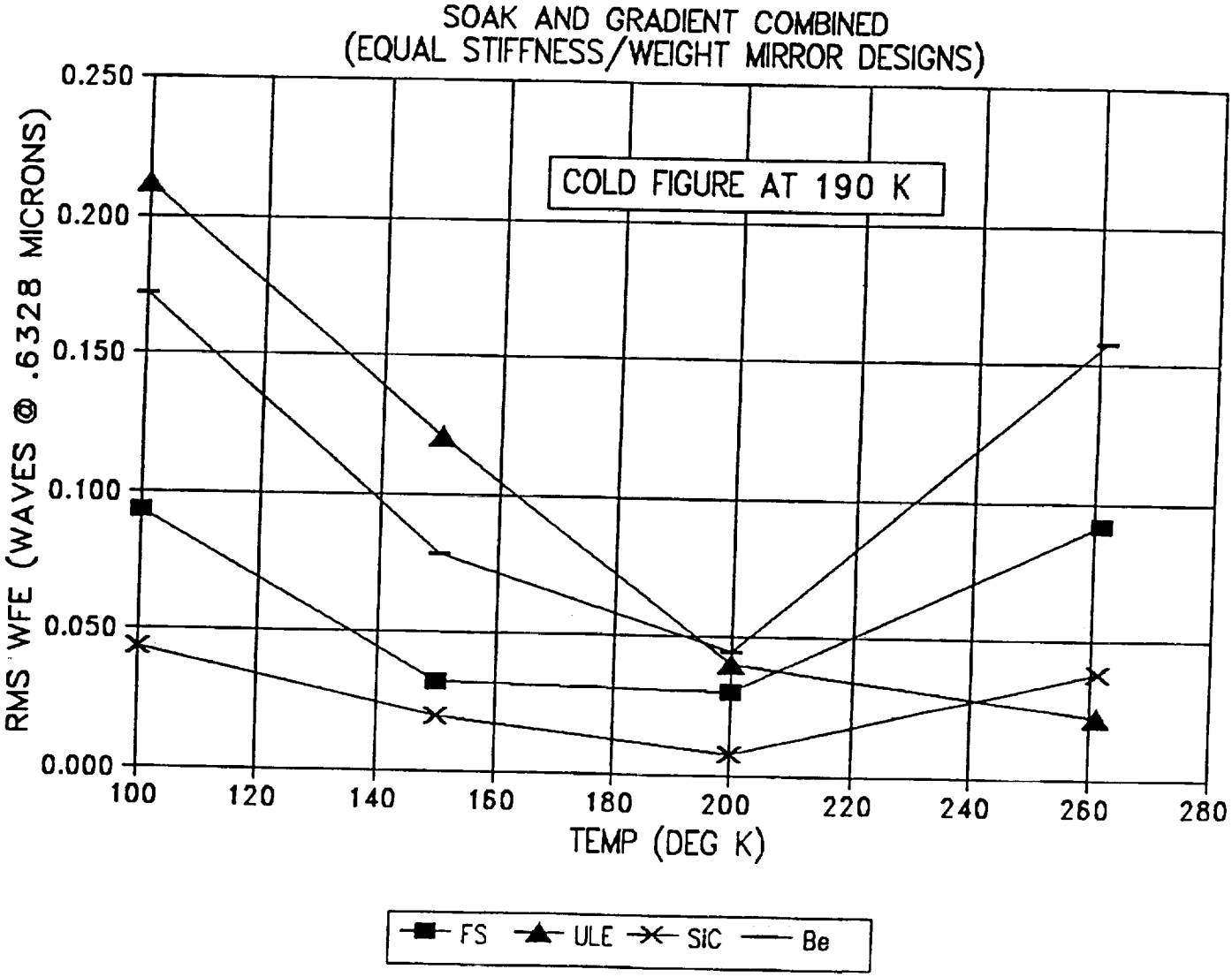
SOAK AND GRADIENT COMBINED
(EQUAL STIFFNESS/WEIGHT MIRROR DESIGNS)
COLD FIGURE AT 190 K
RMS WFE (WAVES @ .6328 MICRONS)
0.250
0.200
0.150
0.100
0.050
0.000
100
120
140
160
180
200
220
240
260
280
TEMP (DEG K)
FS
ULE
SiC
Be

LUTE ACTIVE PRIMARY MIRROR DESIGN SUMMARY

Requirements, loads, and candidate materials for the Lute Primary Mirror were obtained from NASA's structural and thermal analysis reports.

Evaluation of the active mirror design concepts show that all materials yield a facesheet + actuator weight/area less than 25Kg/m^2. Weight of the mirror support is not included as part of this weight/area since this structure is common to both an active or passive mirror approach.

LUTE ACTIVE PRIMARY MIRROR DESIGN SUMMARY

Requirements:

Same As Passive Design

Loads:

Same as Passive Design

Candidate Materials:

Same as Passive Design

Results:

Facesheet Material	Facesheet + Actuator Weight/Area	Facesheet Thickness	Approximate Number of Actuators
SiC	12.6 KG/M^2	0.15 Inch	90
Fused Silica	15.4 KG/M^2	0.25 Inch	90
Beryllium	18.2 KG/M^2	0.35 Inch	120
ULE	20.6 KG/M^2	0.325 Inch	144

ACTIVE MIRROR DESIGN CONCEPT

A thin solid facesheet is supported by an array of piezoelectric actuators. The actuators have a pin flexure at the facesheet end to minimize moment loads to the mirror. The other end of the actuator is bonded to a hexagonal shaped fitting that fits into the support structure cells. Also note that the actuators are aligned to the spherical radius to further reduce thermal interaction loads between the support structure and the PM facesheet.

FIGURE 1

ACTIVE MIRROR DESIGN CONCEPT

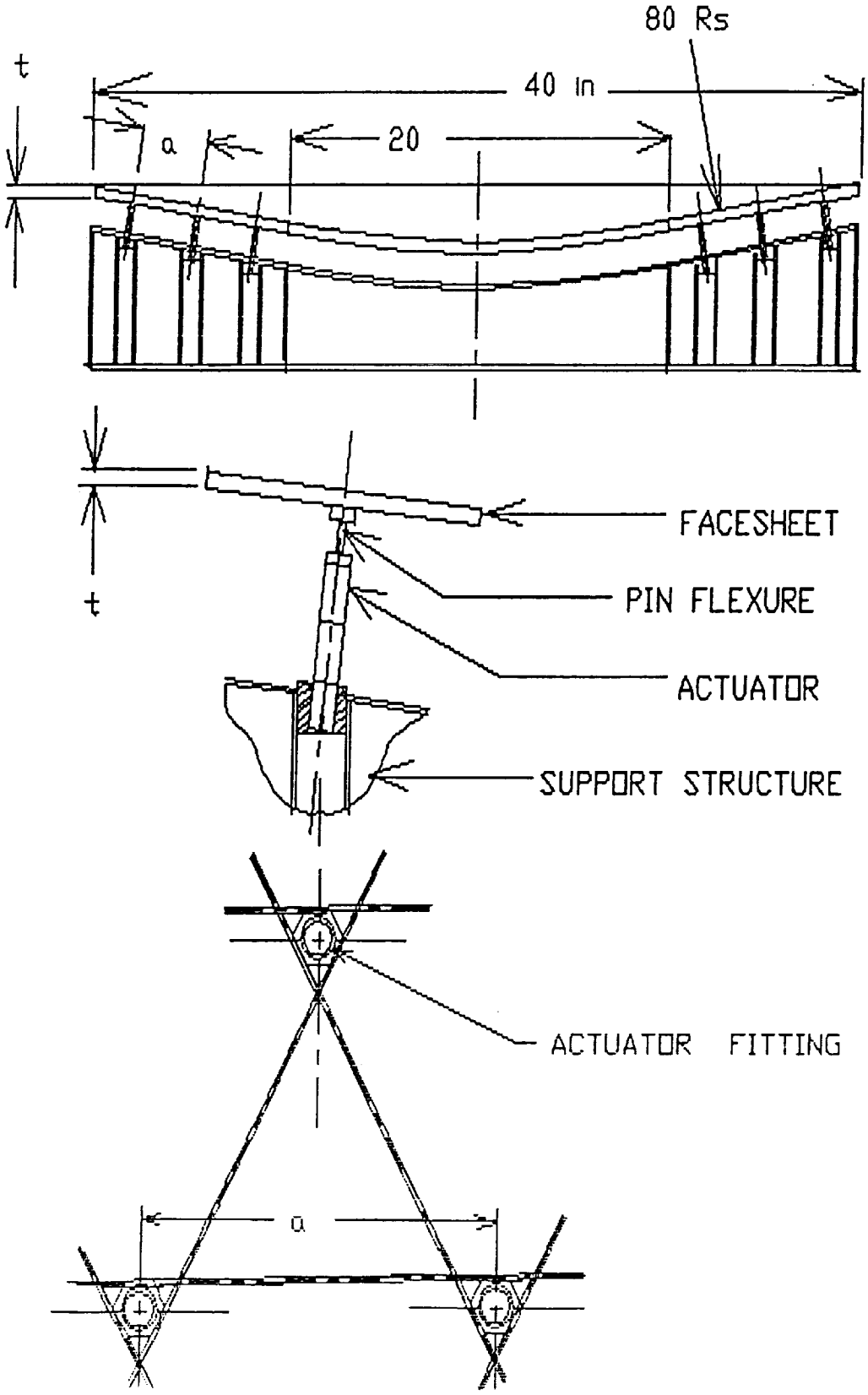

ACTIVE MIRROR DESIGN TRADE CURVES (SiC FACESHEET)

Facesheet thickness is traded against actuator spacing for constant mirror performance (stress, WFE, weight/area).

The direction of the arrows on each curve establishes a design space of acceptable facesheet thicknesses and actuator spacing. The point in this design space that yields minimum weight (minimum facesheet thickness and maximum actuator spacing) is chosen as the design point. For this material (SiC), the design point is 0.15 inch facesheet thickness with a 3.5 inch actuator spacing.

Figure 2

SiC Facesheet

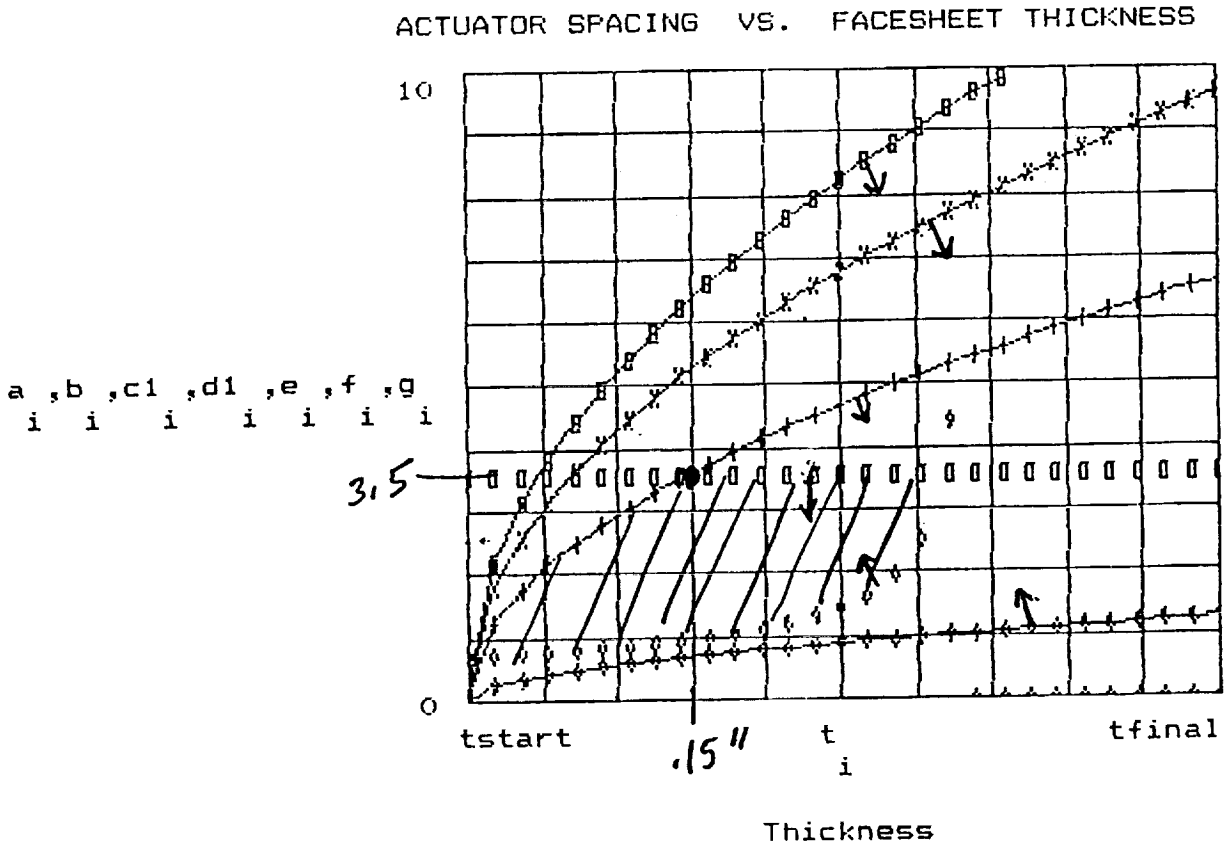

KEY

Curve 1 - Launch Survivability	=	line
Curve 2 - Gravity Sag	=	line with X
Curve 3 - HEL Load (Gradient)	=	line with O
Curve 4 - HEL Load (Soak)	=	line with plus sign
Curve 5 - Surface Correction	=	line with diamond
Curve 6 - correctibility (power)	=	no line with O
Curve 7 - Weight per Area	=	no line with diamond

LUTE PRIMARY MIRROR ASSEMBLY

A layout of the 3.5 inch actuator spacing over the primary mirror area yields 90 total actuators.

The hexagon shaped support structure is compatible for attachment of the hexapod, metering structure, and tertiary mirror assembly.

LUTE PRIMARY MIRROR ASSY

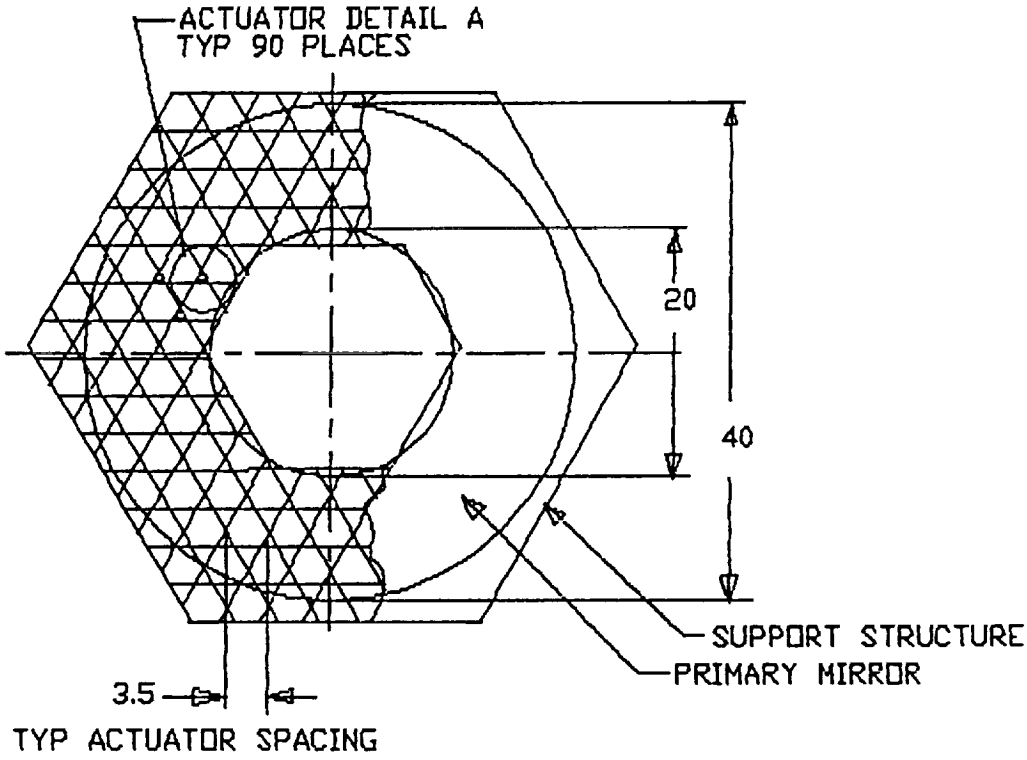

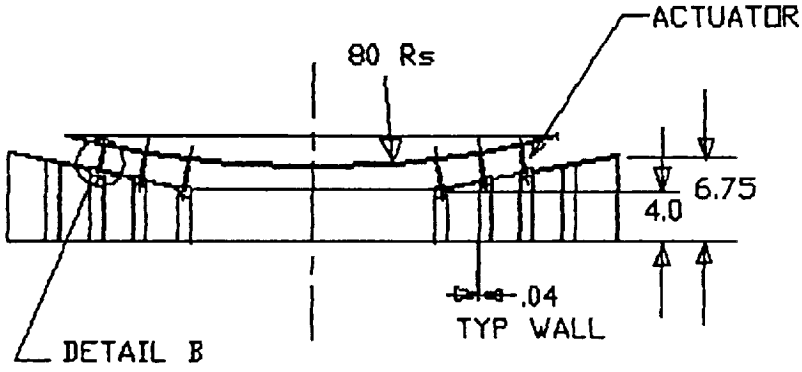

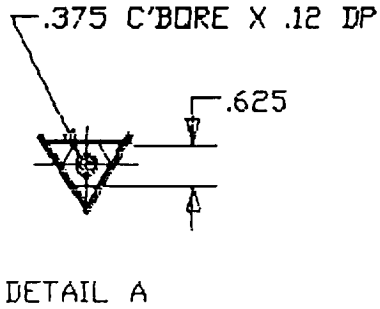

DETAIL A

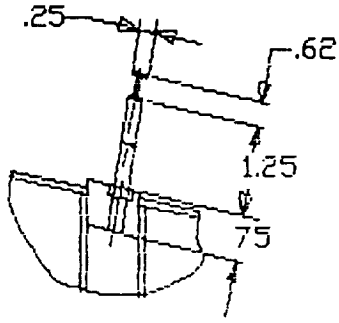

DETAIL B

LUTE WAVEFRONT CONTROL CONSIDERATIONS

System Block Diagram

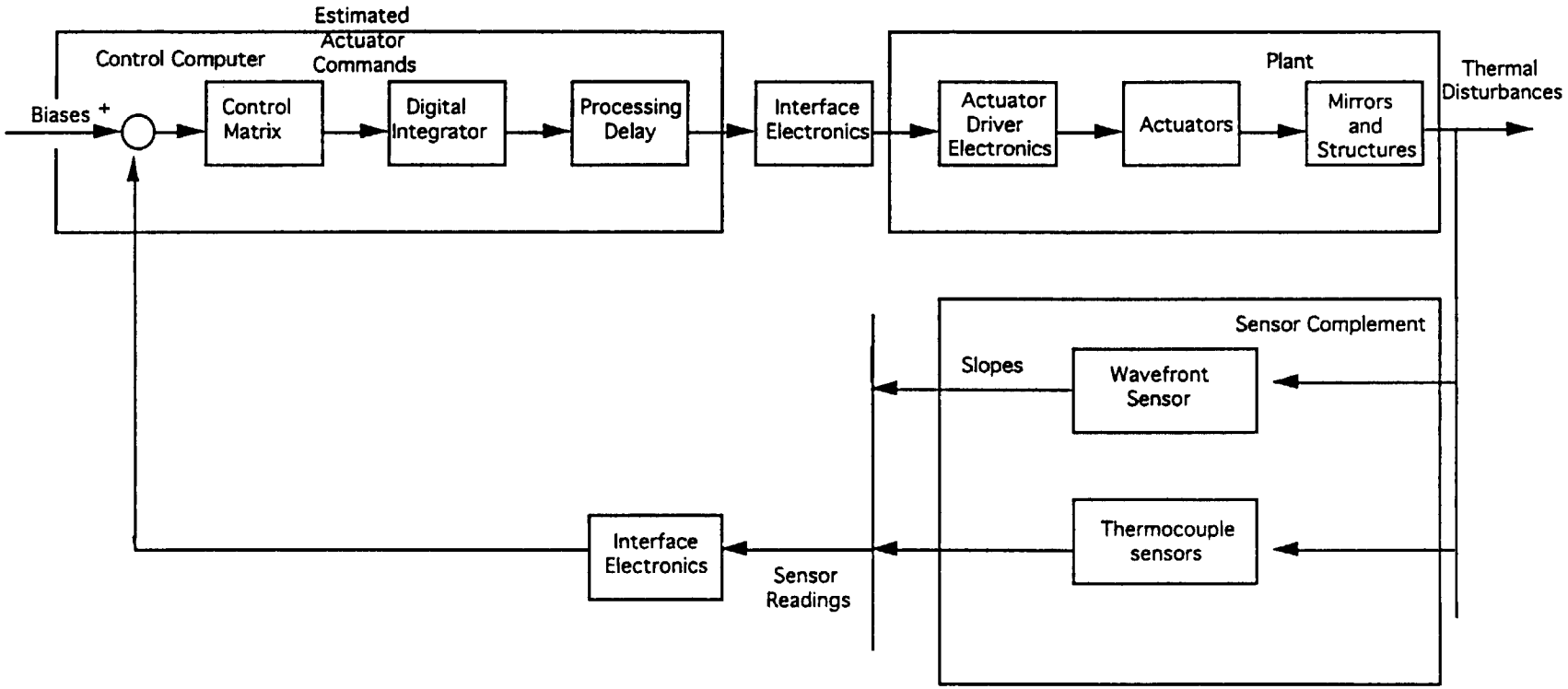

System Electronics (Example)

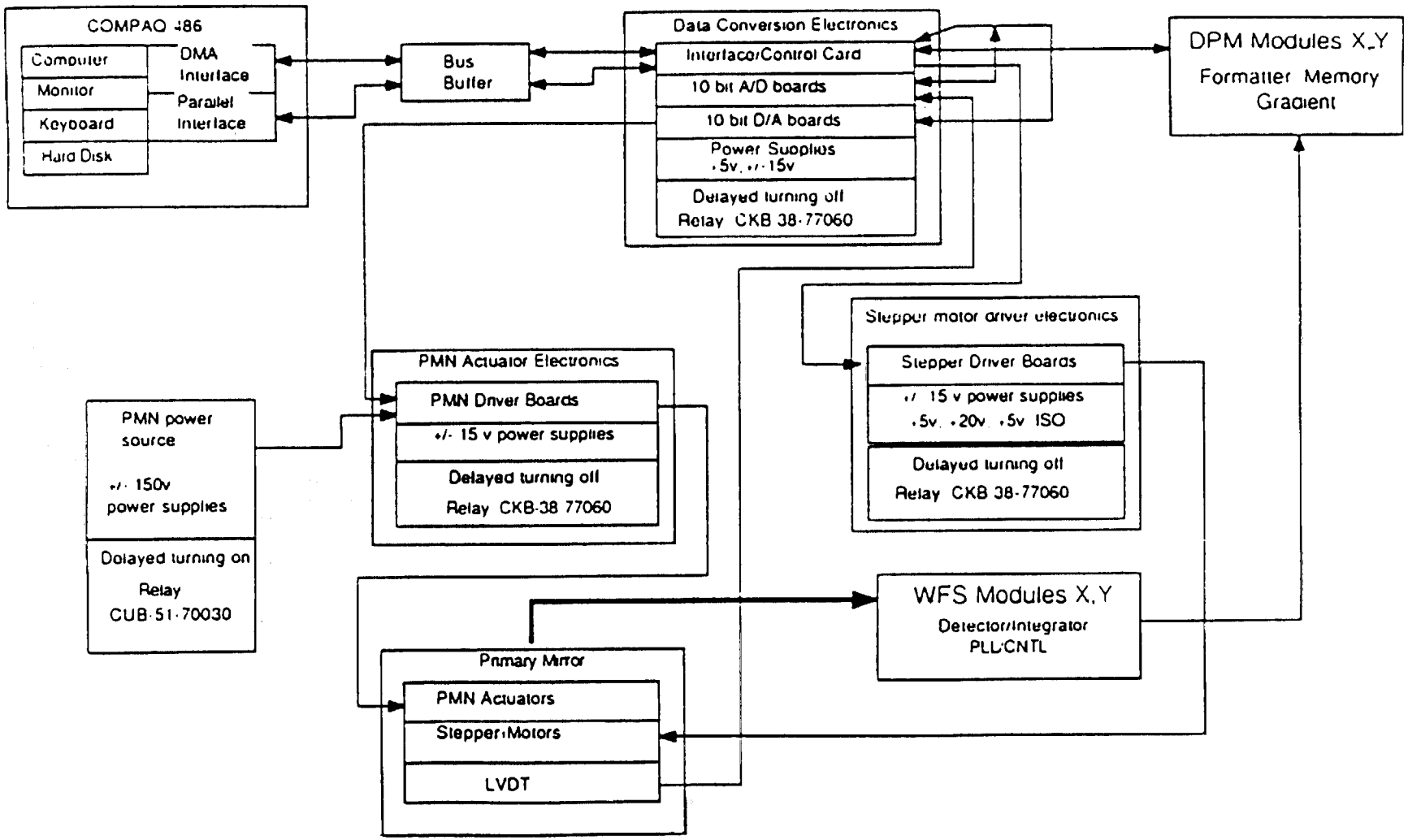

What Is The Plant

- All systems that make up the Hardware
  - Electronics
  - Optics
  - Mechanisms
  - Structures
- Some examples
  - Actuator drive electronics
  - Deformable mirrors
  - Actuated primary mirror assemblies
  - Adjustable secondaries

Example of A Primary Mirror Assembly (Plant)

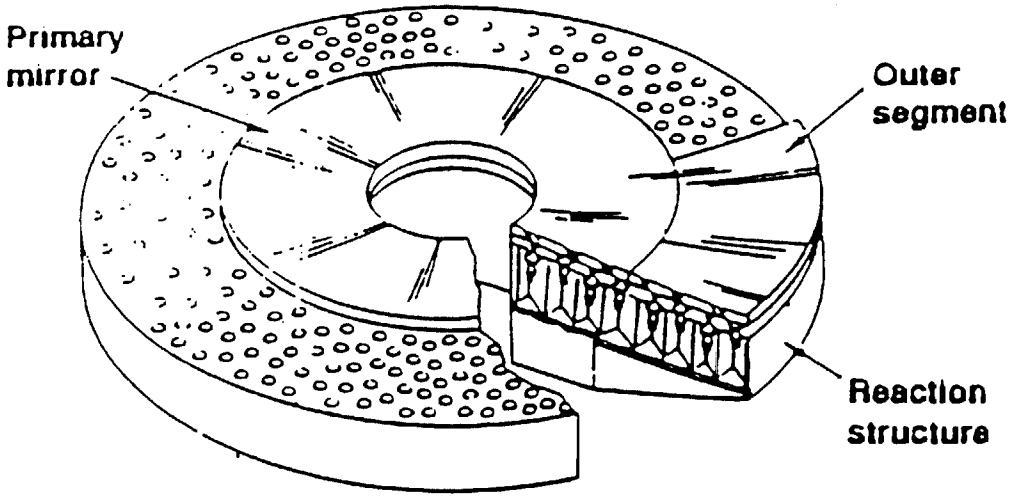

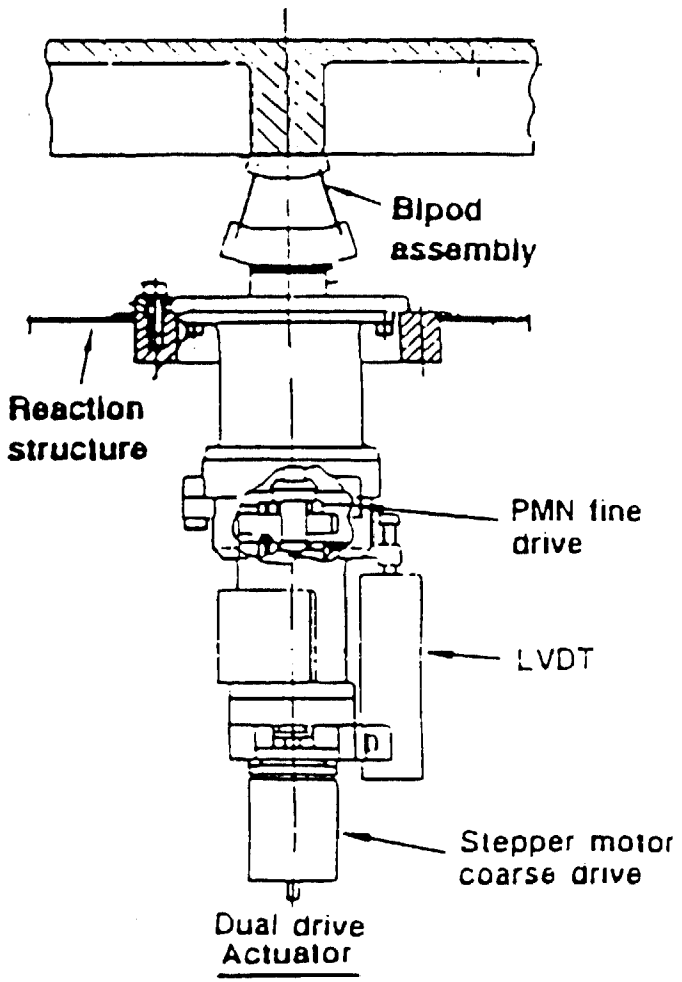

- Lightweighted (70%) ULE segmented facesheet provides high stiffness-to-weight
- Graphite-epoxy reaction structure provides lightweight, stiff foundation for primary mirror
- Actuator provides mechanism for correction of primary mirror
- Bipod assembly connects mirror to actuator and provides radial compliance and lateral stiffness for primary mirror
- 70 kg/m^2 areal density (823 kg) for fully populated PMA

Sensor System

- Traditional systems utilize a real-time wavefront sensor
  - Shearing interferometers
  - Hartmann sensors
- Main requirement is to determine the form of the wavefront error in order to determine the appropriate corrections
- Several options available
  - Direct measurements (traditional way)
  - Inferential measurements
    - » estimate error from images
    - » Electro-mechanical sensors such as thermo-couples and strain gauges
  - Educated guess

LUTE Considerations

- Space Based System
  - Low power and weight
  - Remote operation
- Guide Star availability unknown
  - Artificial source difficult to implement
- Extremely Low Bandwidth
  - Fraction of a Lunar day

LUTE Sensor Options

- Very Low Duty Cycle Wavefront Sensor
  - May be most power hungry option
  - Data storage may be large
  - May not be most efficient use of all available data
- Estimate From Imagery
  - Large Communication impact
    - » transmitting large number (≈50 to 100) of high resolution actuator commands will require a substantial bandwidth
- Strain Gages
  - This technique has been shown to be too insensitive

LUTE Sensor Options Continued

- Thermo-couples
  - Can be low power
  - Thermal environment is source of system wavefront error
  - Requires understanding of wavefront changes from thermal changes

Suggested LUTE Configuration

- Use thermo-couples to infer the system quality
  - Need to investigate requirements
    - » resolution
    - » range
    - » how many sensors and locations
- Real-time Wavefront sensor
  - Use for system initialization on the Lunar surface
  - Use for determination of system response to thermal changes
    - » Update model periodically
  - Back up sensor

Estimator

- Control Matrix Determined From Measured Influence Functions
- What Is An Influence Function?
  - Response of all wavefront sensor samples to a unit displacement of an actuator
  - Influence functions are measured in place
  - Determines the sensor plant interactions

LUTE Estimator

- Measure The Thermal Influence Function
  - Applying heat to the system in a controlled fashion on the moon will be difficult
  - Determine the thermal influence functions by measuring the thermal state of the system at the same time as measuring the wavefront sensor outputs
    - » Requires the measurement of the wavefront influence functions
- Determine the System quality and necessary corrections as a function of time
  - Store data in a look-up table
  - Use look-up table for subsequent corrections

APPENDIX M

MATERIAL PROPERTIES FOR THERMAL ANALYSES

The following material is a compilation of memos and working notes generated during this brief study effort.

Litton

Itek Optical Systems

FACSIMILE TRANSMISSION

DATE:	3/2293
TOTAL PAGES (Including This)	4

TO: Max Nein, MSFC 544-0619	RECEIVING STATION 205 544-5861
FROM: Len Solomon	SENDING STATION NO. (617)276-3306
PROJECT: LUTE	SENDERS TELEPHONE NO. 617 276-2038
SUBJECT: LUTE Memo #1	

REMARKS/SPECIAL INSTRUCTIONS:

In the spirit of getting you the information as I receive it, here is the first of the material we spoke about. While it is primarily qualitative, I think Chris makes the desired points:

- **The overall laboratory system-level budget of 1/30 wave or tighter is likely to be a major cost driver, if not a nearly impossible task.**
- **Alignment effects on the overall budget should be traded against size and weight, in terms of cost impact.**
- **Be sure to minimize the number and difficulty of the stated requirements; each one costs something to verify, and small ones cost more.**

Note: Passive mirror data to come shortly.

Len Solomon

Litton

Itek Optical Systems

Memorandum

To: Len Solomon Date: Fri, Mar 19, 1993

From: Chris Ullathorne

Subject: LUTE Error Budget and System Design Comments

Since John Pepi is providing commentary on the design of the primary mirror and the effect the lunar thermal environment has on the mirror performance I will restrict my comments to general note on the form of the error budget and the system design. Additionally, I have a few specific suggestions that I believe may improve the MSFC design and provide higher confidence in the error budget.

First, the strawman error budget is not in a form that is particularly "friendly" to an instrument manufacturer. Terms that we would normally group together are scattered about which makes it difficult for a manufacturer to know an adequate system has been produced. The attached figure is a typical layout for an error budget that we would produce, it includes many of the issues that are of concern here. The most noticeable difference with our format is that a laboratory based, or "as built" condition, of the system is separately tracked, allowing the manufacturer to have a so called "buy off condition" for the assembly. Additionally, this form provides for a convenient means to assess the benefits of spending resources to improve the system assembly, versus spending them to control the environmental impacts. If we were to evenly divide the top level wavefront error of 0.05 waves RMS between the laboratory and environmental terms, the resulting requirement for the laboratory assembled system would be in the $1/30^{th}$ wave wavefront class. This class of system would not be produced easily, especially considering that the distribution between the Laboratory system and the Environmental errors would more likely be on the order of 40/60 rather than 50/50.

Next, worrying about angstrom level errors is a bit premature at this stage of the design and may probably be unnecessary to ever consider. My intuition tells me that changes in errors at this level will have insignificant impact on the error budget. Additionally, such levels of error will be meaningless with respect to the system point spread function or encircled energy requirements, which, more likely than not, are the more important system level requirements. I would urge anyone doing an error budget to remember that the functions of an error budget are to help perform first-and second-order design/manufacturing trades and to help with the processes of manufacturing and integration. Regardless of what happens in the design or assembly stages, the final measure of the value of a design or assembly is going to be against the more critical system requirements, which in this case may be the point spread function and or encircled energy. Therefore, the error sources that one should track are those that impact these requirements the most.

One final comment about the degree of precision of the error budget. Unfortunately, error budgets get a great deal of overexposure and unnecessary attention, therefore, the precision reflected in any published error budget implies that the individual terms will be verified to that level or better. This can place very difficult requirements on manufacturing metrology systems which in turn will strongly drive the overall cost.

Finally, I would suggest that the effect of the active wavefront correction be more visible in the error budget. This can be most easily done by showing the before and after correction terms. This allows for a quick assessment of the worth of the active correction and some insight into the degree of correction assumed.

Regarding the system optical design, the first issue that jumps at me is the speed of the optical design and the apparent speed of the primary mirror. It isn't shown, but the F# of the primary mirror appears to be fairly fast, which is good from the standpoint of keeping the overall system short but is detrimental where the line-of-sight and wavefront error sensitivities are concerned. Additionally a fast overall system F# has the same results on the line-of-sight and wavefront sensitivities. These terms may have a significant impact on the system by complicating the system alignment and by making the on station alignment stability requirements drive the thermal control designs. I would suggest that an alignment sensitivity study be performed in order to assess the feasibility of aligning and maintaining that alignment. This study should not be very difficult to perform. All that is necessary is to perturb, one at a time, each mirror in decenters and tilts, and record the resulting wavefront and line-of-sight changes in the lens design.

Suggested LUTE Error Budget Form

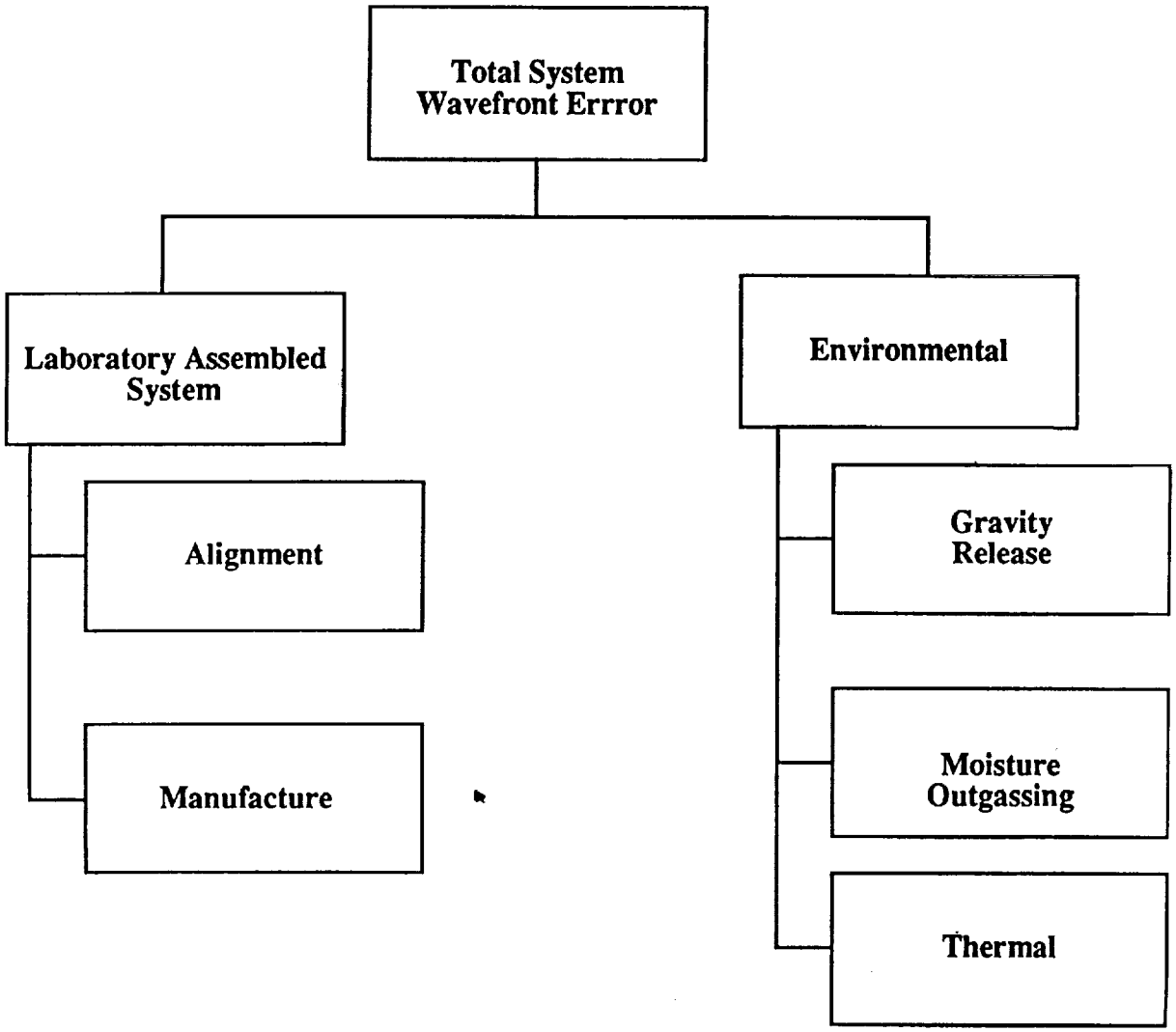

Litton

Itek Optical Systems

Memorandum

To: J. Pepi

Date: Thu, Mar 25, 1993

From: R. Nagle (RJN)

Log No: 270-93-013

Subject: LUTE – Passive Primary Mirror Design Concepts

cc: L. Solomon, C. Roberts, C. Ullathorne

Several Lunar Ultraviolet Telescope (LUTE) passive primary mirror concepts were evaluated for thermal performance in a lunar environment, where the temperature varies between 120K and 261K.

Mirror design concepts were based on equal stiffness to weight and equal weight. The equal stiffness to weight mirror concepts are shown in Figure 1; equal weight mirror concepts are shown in Figure 2. As shown, the LUTE primary mirror geometry has a 40 inch diameter aperture with a 20 inch diameter central hole; and a radius of curvature of 80 inches.

The lightweight configuration selected for each material was based on optimum performance for minimum weight, while considering the ease of manufacturing. For example, the ULE, Fused Silica, and SiC concepts have an open, flat back shape with a triangular core configuration for minimum weight and ease of manufacturing; compared to a closed back, meniscus shape configuration. In addition, the ULE and Fused Silica concepts have intermediate depth ribs to further reduce the weight. The Beryllium concept must be a closed back, meniscus shape to allow for uniform thickness nickel coatings to be applied on the front and back surfaces to reduce the "bimetal" thermal distortion.

Of the candidate material choices (ULE, Fused Silica, SiC, and Beryllium) for this mirror application; the SiC concept yielded the best performance for minimum weight, followed by Fused Silica, ULE, and Beryllium. Figures 3, 4, and 5 show the thermal performance for the equal stiffness to weight material configurations; and Figures 6,7, and 8 show the thermal performance for the equal weight material configurations, over the operating temperature range. As shown, the SiC equal stiffness to weight and equal weight configurations yield the best performance over most of the temperature range, followed by the Fused Silica, ULE, and Beryllium mirror configurations. These figures also show that the thermal performance is driven primarily by the soak conditions.

All mirror concepts show increased performance for the deeper, equal weight configurations. However, increasing the depth beyond those shown in Figure 2 will result in decreasing performance due to the bulk thermal expansion (Δ CTE x depth x T soak) thru the depth of the section.

Attachments (8)
/map

FIGURE 1

PASSIVE PRIMARY MIRROR CONCEPTS

MINIMUM WEIGHT DESIGNS BASED ON EQUAL STIFFNESS/WEIGHT

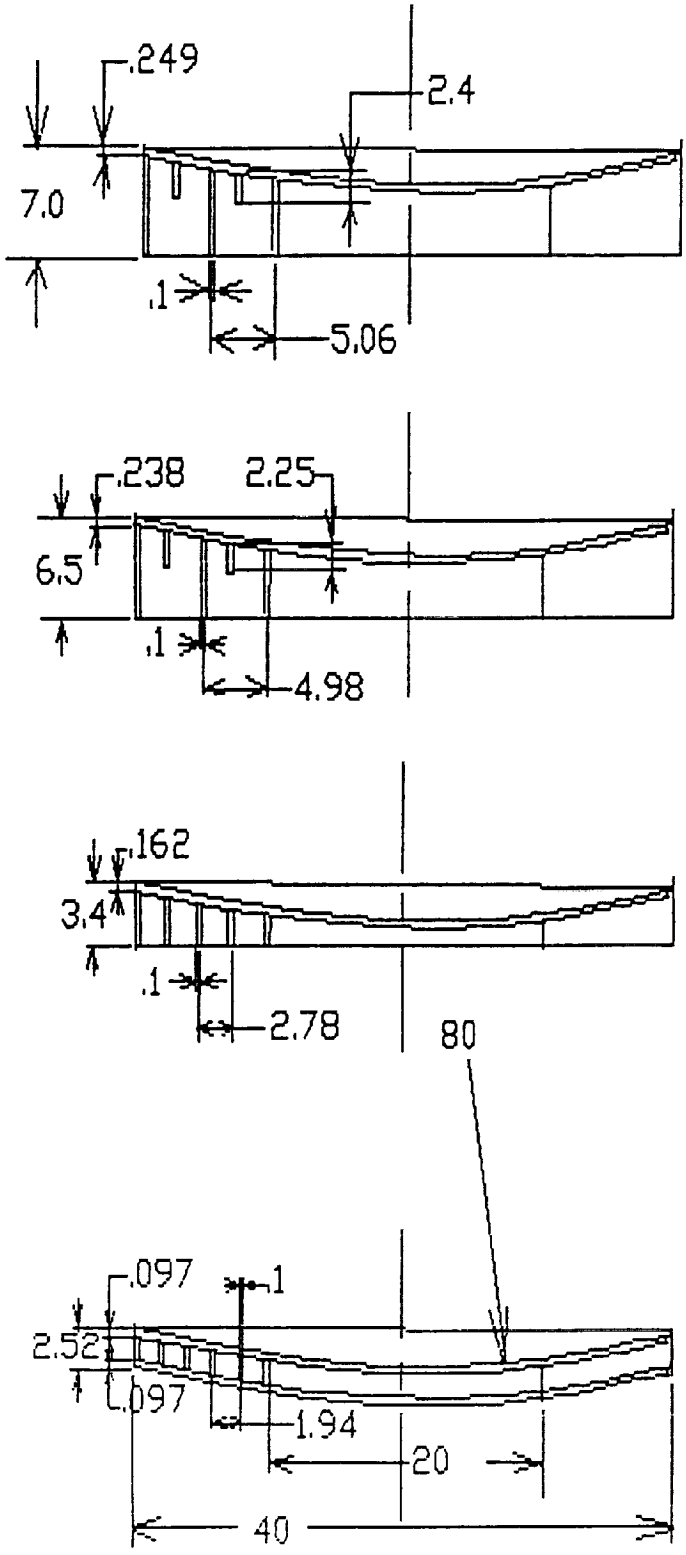

MAT'L	WT/AREA (KG/M^2)	RMS WFE @ 190 K
ULE	41.8	.075
FS	39.1	.060
SIC	33.3	.060
Be	25.4	.275

FIGURE 2

PASSIVE PRIMARY MIRROR CONCEPTS

MINIMUM WEIGHT DESIGNS BASED ON EQUAL WEIGHT

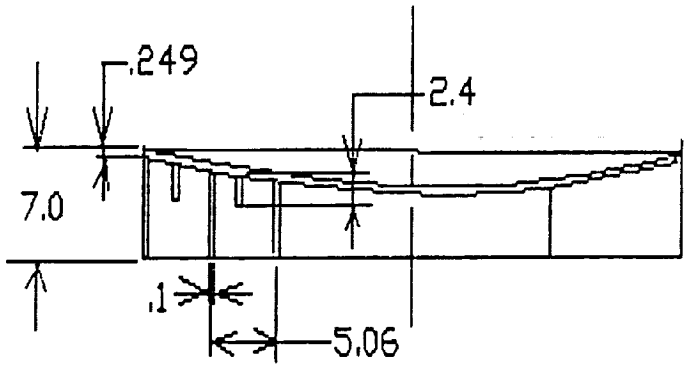

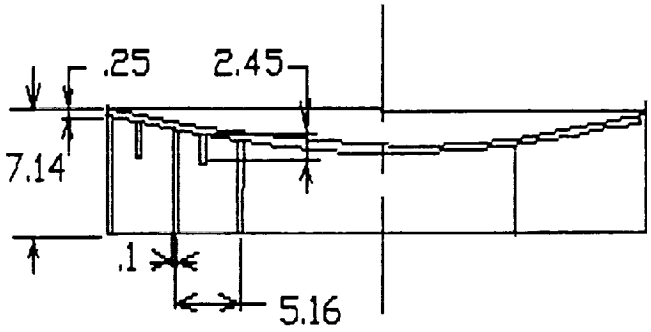

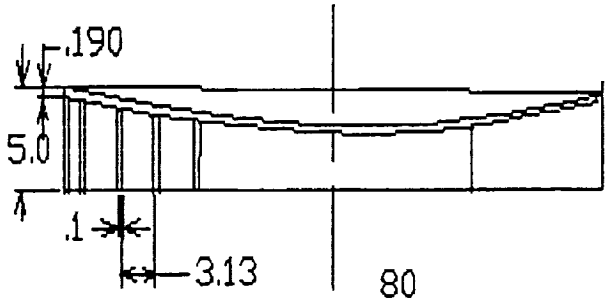

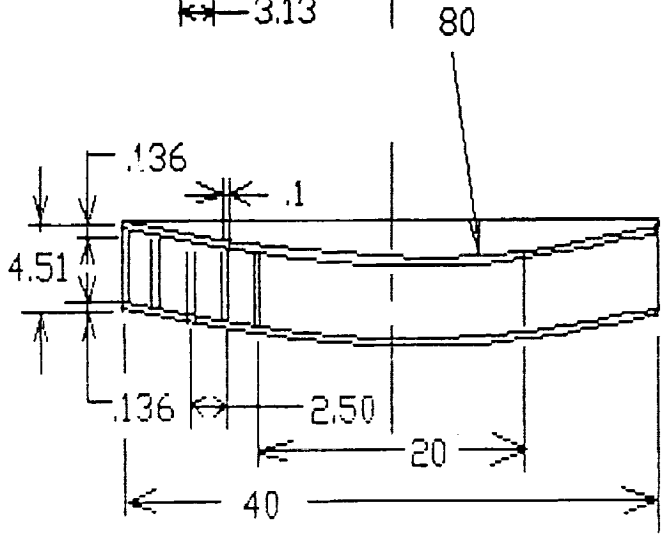

MAT'L	WT/AREA (KG/M^2)	RMS WFE @ 190 K
ULE	41.8	.075
FS	41.8	.040
SiC	41.8	.050
Be	41.8	.225

Figure 3

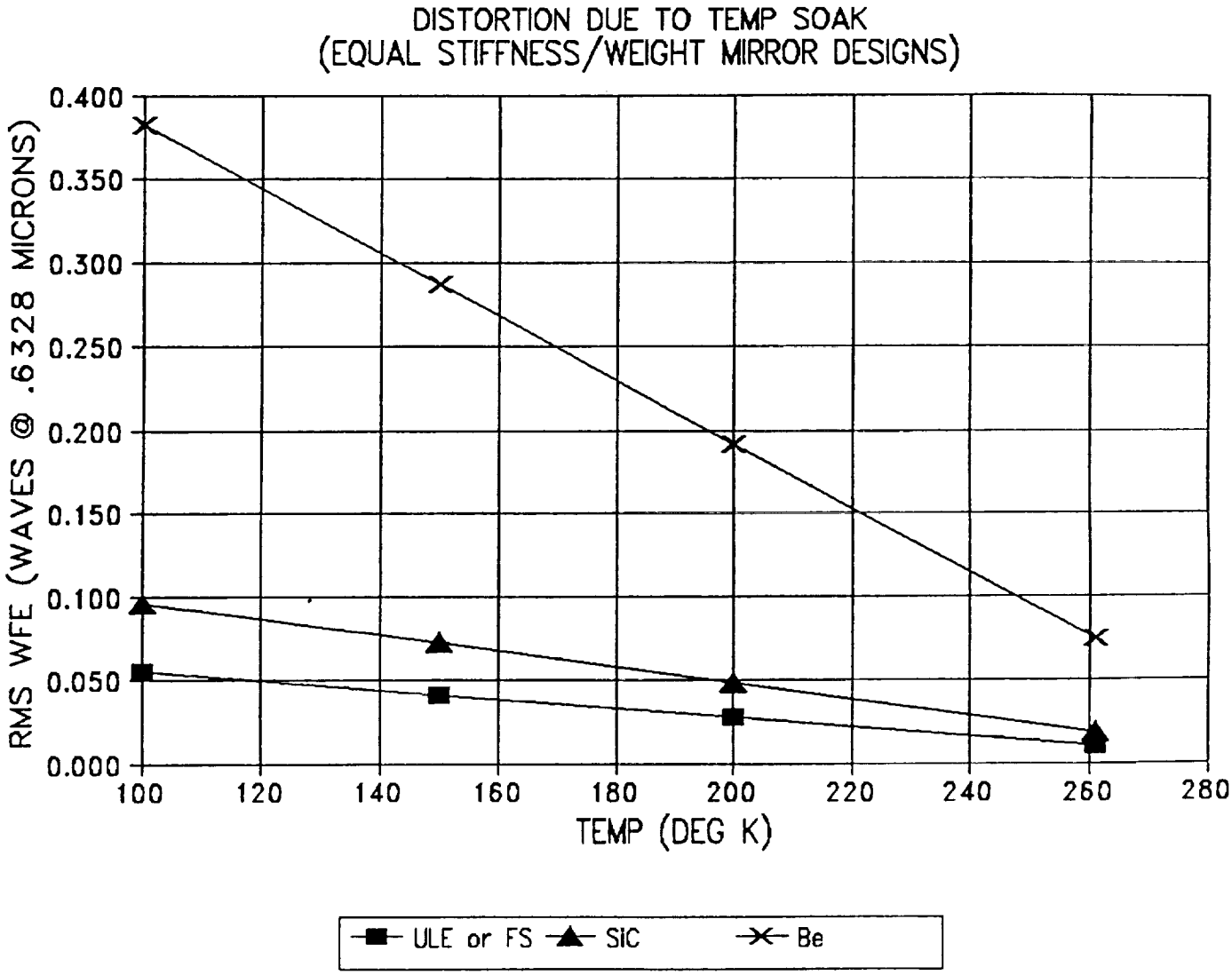
DISTORTION DUE TO TEMP SOAK
(EQUAL STIFFNESS/WEIGHT MIRROR DESIGNS)
RMS WFE (WAVES @ .6328 MICRONS)
0.400
0.350
0.300
0.250
0.200
0.150
0.100
0.050
0.000
100
120
140
160
180
200
220
240
260
280
TEMP (DEG K)
ULE or FS
SiC
Be

Figure 4

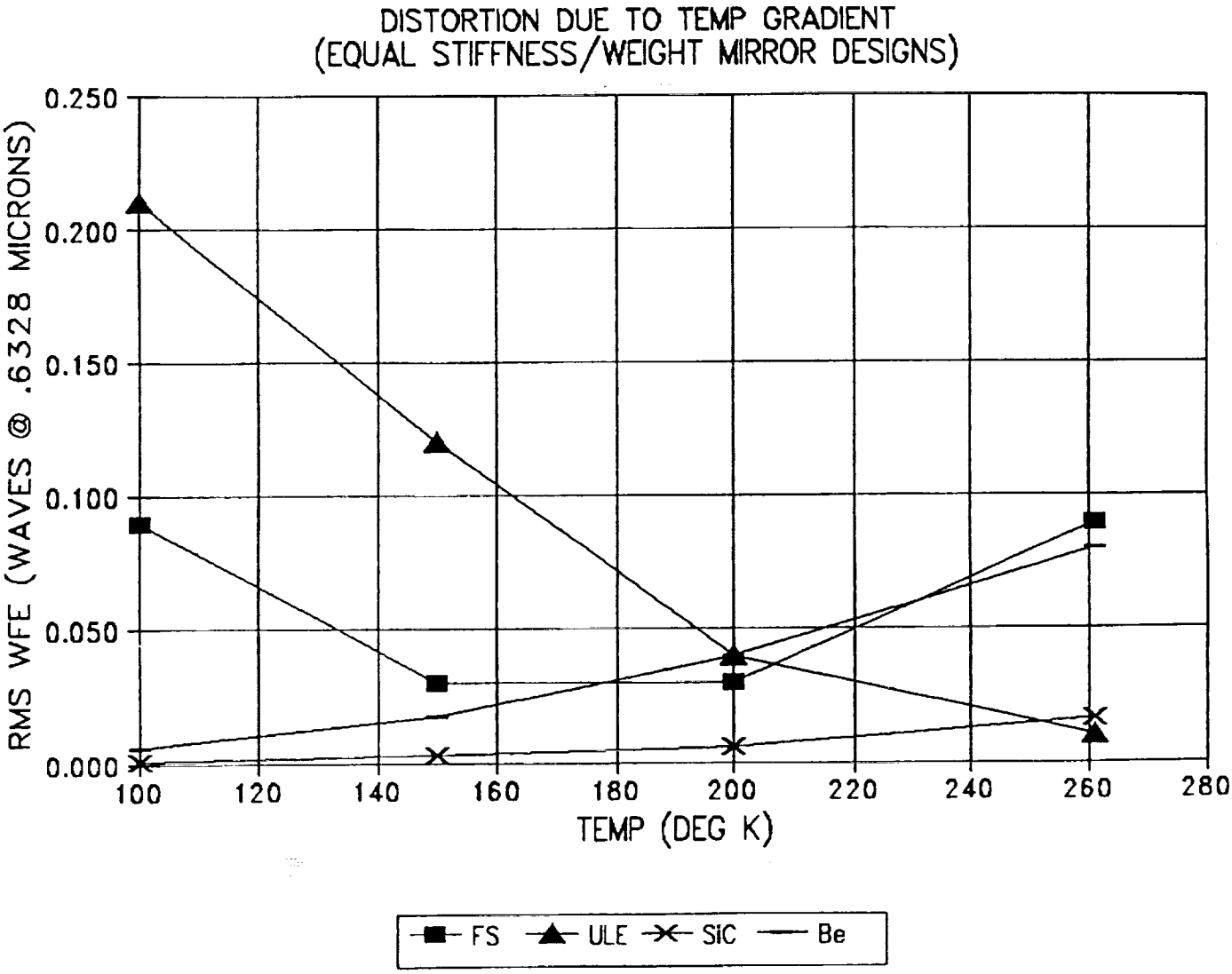
DISTORTION DUE TO TEMP GRADIENT
(EQUAL STIFFNESS/WEIGHT MIRROR DESIGNS)
RMS WFE (WAVES @ .6328 MICRONS)
0.250
0.200
0.150
0.100
0.050
0.000
100
120
140
160
180
200
220
240
260
280
TEMP (DEG K)
FS
ULE
SiC
Be

Figure 5

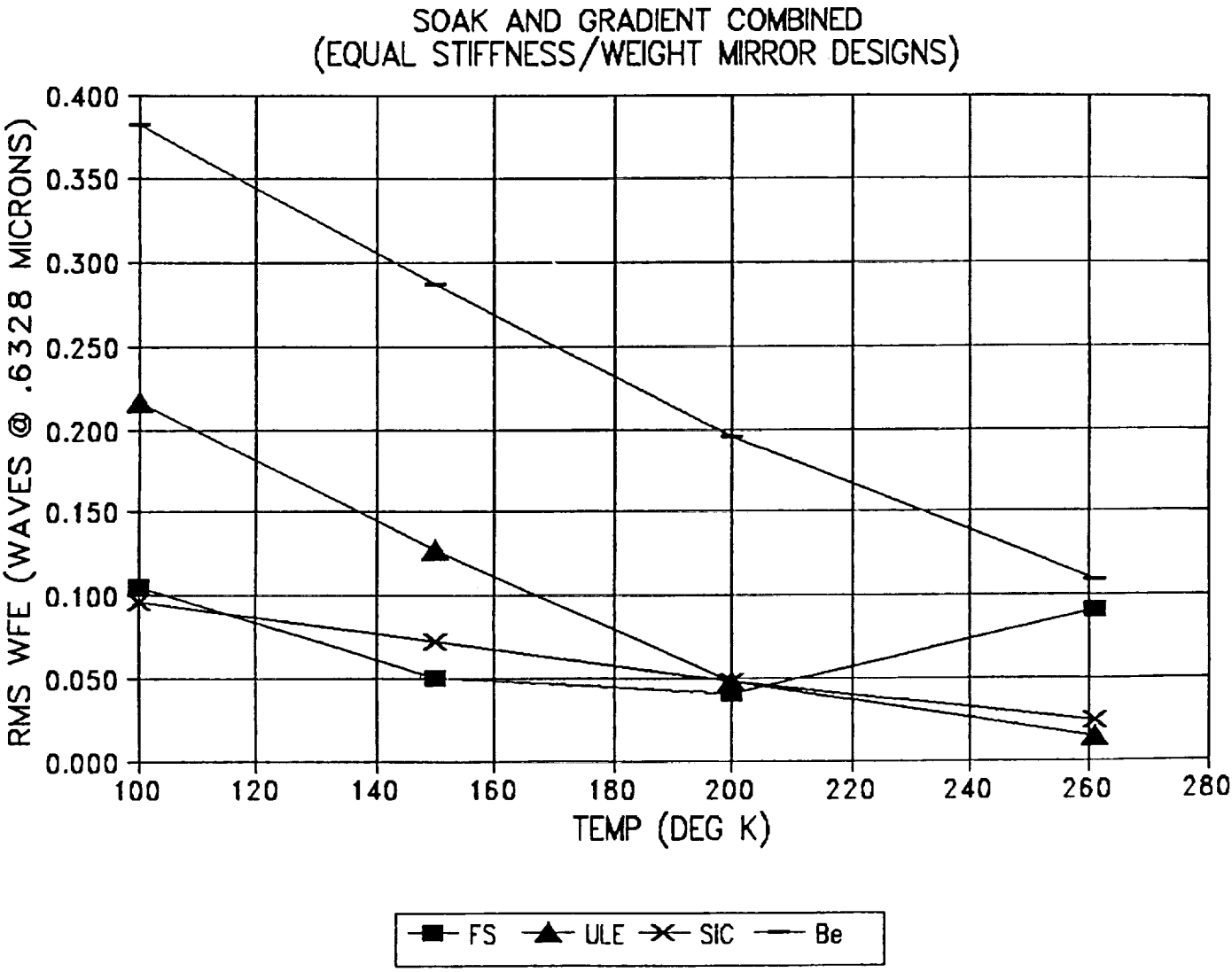
SOAK AND GRADIENT COMBINED
(EQUAL STIFFNESS/WEIGHT MIRROR DESIGNS)
RMS WFE (WAVES @ .6328 MICRONS)
0.400
0.350
0.300
0.250
0.200
0.150
0.100
0.050
0.000
100
120
140
160
180
200
220
240
260
280
TEMP (DEG K)
FS
ULE
SIC
Be

Figure 6

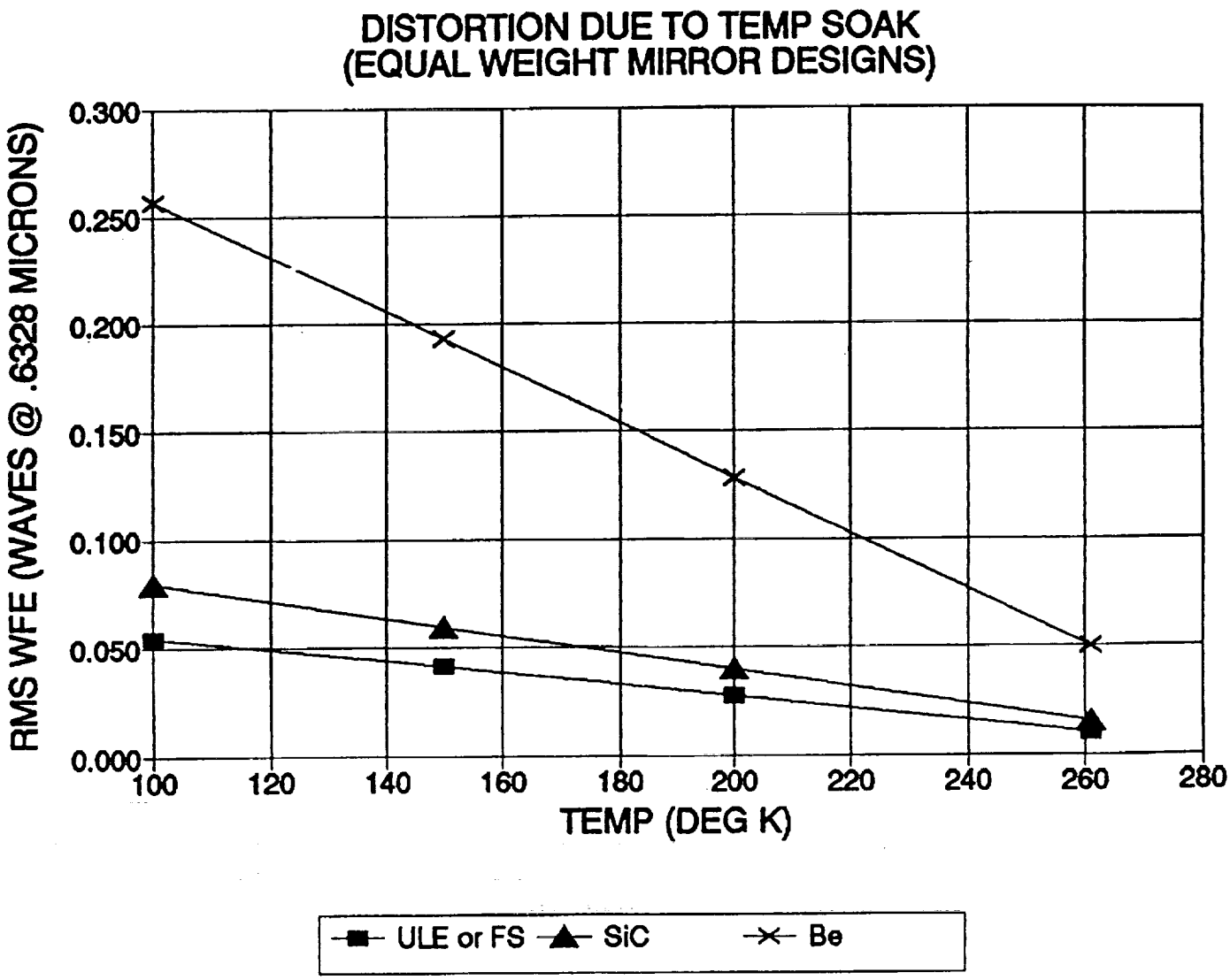
DISTORTION DUE TO TEMP SOAK
(EQUAL WEIGHT MIRROR DESIGNS)
RMS WFE (WAVES @ .6328 MICRONS)
0.300
0.250
0.200
0.150
0.100
0.050
0.000
100
120
140
160
180
200
220
240
260
280
TEMP (DEG K)
ULE or FS
SiC
Be

Figure 7

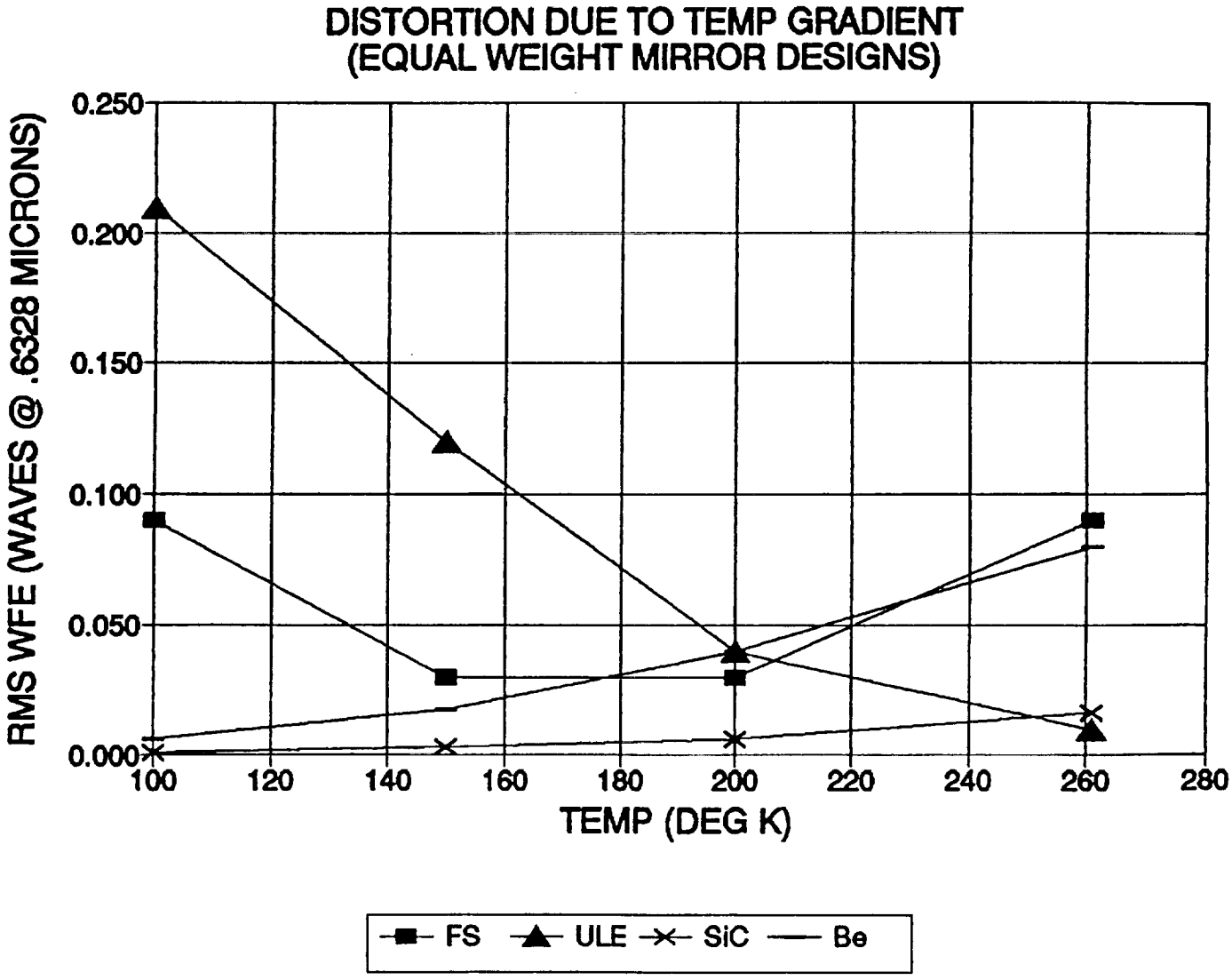
DISTORTION DUE TO TEMP GRADIENT
(EQUAL WEIGHT MIRROR DESIGNS)
RMS WFE (WAVES @ .6328 MICRONS)
0.250
0.200
0.150
0.100
0.050
0.000
100
120
140
160
180
200
220
240
260
280
TEMP (DEG K)
FS
ULE
SiC
Be

Figure 8

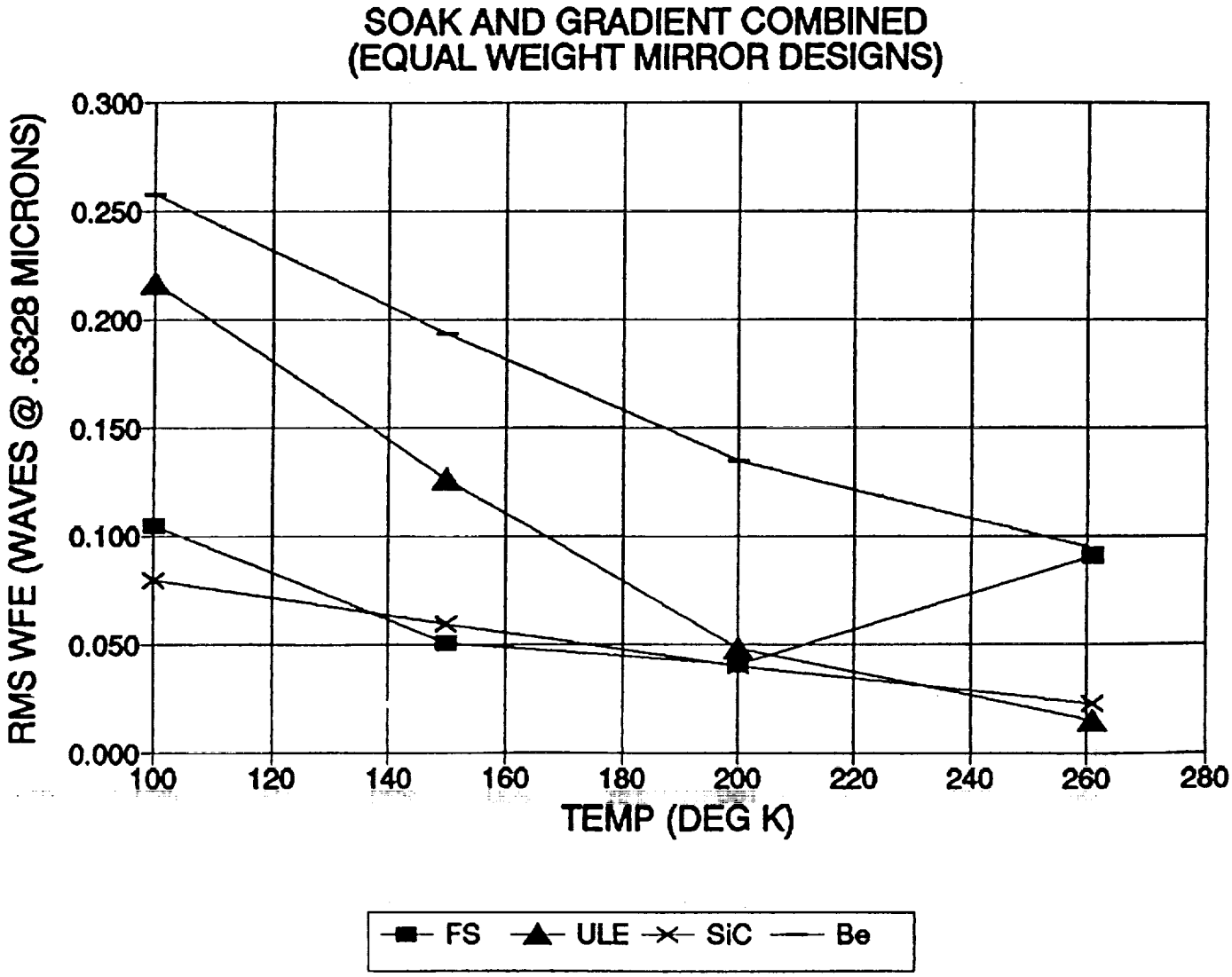
SOAK AND GRADIENT COMBINED
(EQUAL WEIGHT MIRROR DESIGNS)
RMS WFE (WAVES @ .6328 MICRONS)
0.300
0.250
0.200
0.150
0.100
0.050
0.000
100
120
140
160
180
200
220
240
260
280
TEMP (DEG K)
FS
ULE
SiC
Be

#3

Litton

Itek Optical Systems

Memorandum

To: L. Solomon

Date: Thu, Mar 25, 1993

From: J. Pepi

Log No: 270-93-014

Subject: LUTE Passive Mirror Performance

Reference: (a) LUTE Passive Primary Mirror Design Concepts, 25 March, 1993, 270-013-93, R. Nagle (Itek)
(b) LUTE Thermal Control System Analysis and Design (Draft), MSFC, December 1992, S. Walker Et. Al.
(c) LUTE Structural Analysis, Feasible Study, MSFC, Dated 1 February 1993, P.L. Luz

The memorandum of reference (a) describes the performance of the various material candidate and design options. Thermal soaks are based on the extremes at the lunar day environment noted in reference (b). Errors induced by soak are due to expansion inhomogeneities and are after focus removal; radius changes are assumed compensated by either the metering structure or articulating secondary mirror. Values utilized for inhomogeneity are known values of 10 ppb/°C for ULE and fused silica, a presumed value of 15 ppb/°C for Silicon Carbide, and an estimated value of 50 ppb/°C for Beryllium. Thermal gradients are based on figures (1) and (2) from the analyses of reference (b) at the specified temperatures, while performance is based on the analysis of reference (c) and instantaneous coefficient of expansion values obtained from the literature.

/map

Distribution:
R. Nagle
C. Ullathorne

FIGS 1, 2

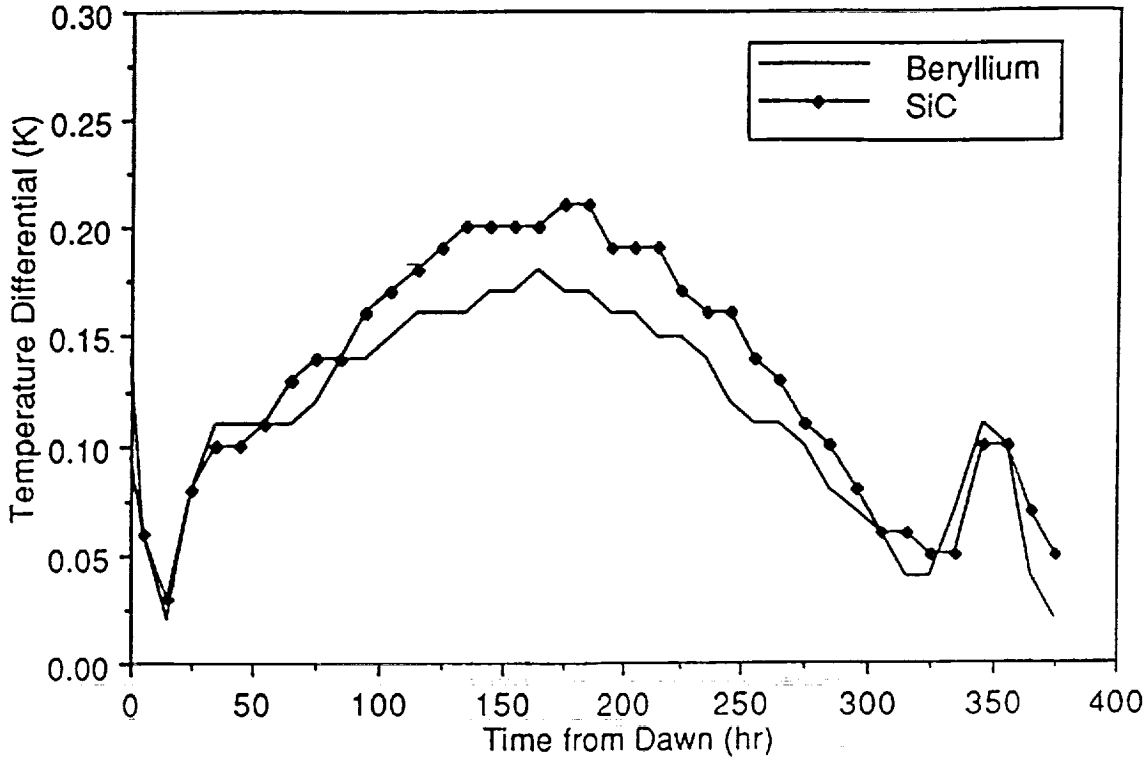

Figure 37. Temperature differential for beryllium and silicon carbide primary

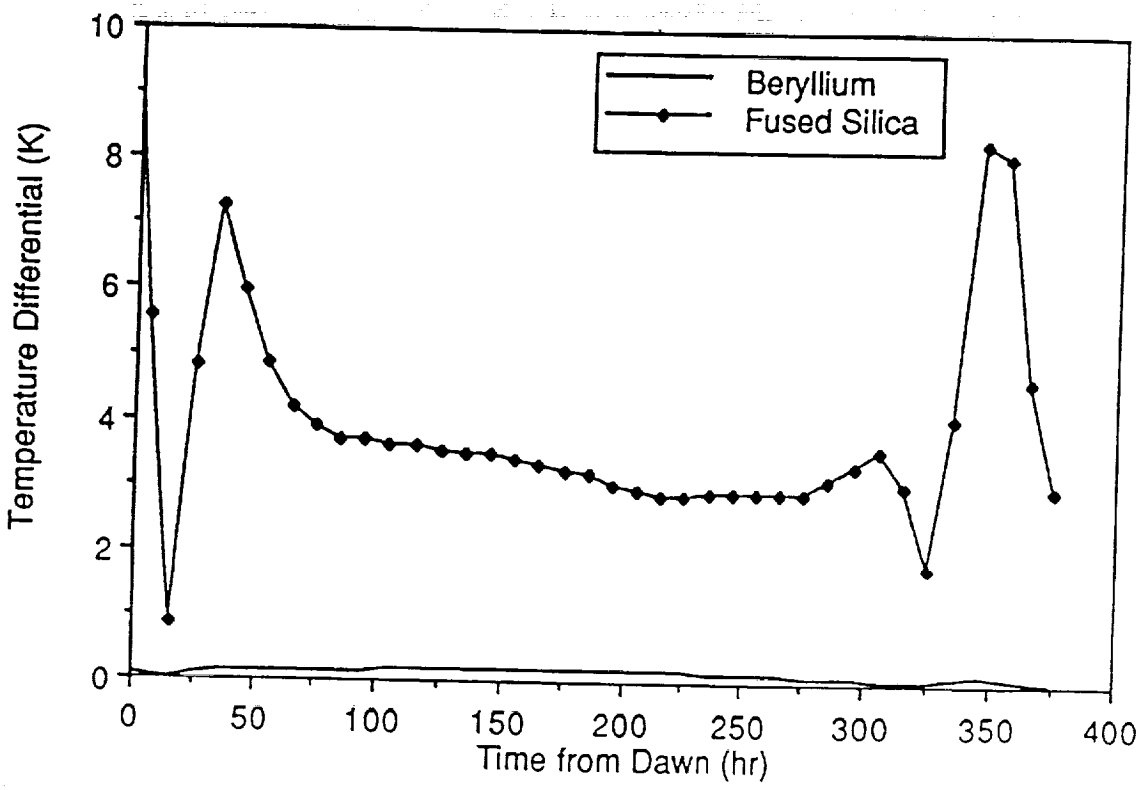

 Figure 38. Temperature differential for beryllium and fused silica primary

Litton #4

Itek Optical Systems

Memorandum

To: J. Pepi Date: Mon, Apr 5, 1993

From: R. Nagle Log No: 270-93-016

Subject: LUTE – Active Primary Mirror Design Trades

Reference: (1) Itek Memo 270-93-013, "LUTE – Passive Primary Mirror Design Concepts", by R. Nagle, 3/25/93

(2) Itek Memo 270-93-014, "LUTE Passive Mirror Performance", by J. Pepi 3/25/93

Active primary mirror design trades were conducted to evaluate the increase in thermal performance over the LUTE passive mirror design concepts shown in Reference (1). The active mirror designs traded actuator spacing against facesheet thickness for constant optical wavefront error contributors of 0.0144 waves rms at 0.6328 microns. The active mirror design trades also considered facesheet stress due to launch loads and surface correction, facesheet correctability due to reaction structure distortion, and weight per area of the facesheet plus actuators. Several candidate facesheet materials (ULE, Fused Silica, SiC, and Beryllium) were considered in the trades.

Figure 1 shows a typical active primary mirror design concept for any of the facesheet materials. The actuator configuration is a cylindrical, stacked PMN device which is pin connected to the facesheet and fixed to the support structure. The support structure is graphite/epoxy with an "eggcrate core" and front and back sheets.

Figure 2 thru 5 show the design trade curves for the various facesheet materials. The various curves bound a design zone which is shown cross-hatched. The location in this design zone which yields the lowest weight per area is selected for the point design; and the corresponding facesheet thickness and actuator spacing is indicated. These curves were based on the material, geometry, and load inputs shown in the Appendix; and the thermal data shown in Reference (2). The design equations are also shown in the Appendix.

Results of this trade study have shown that the SiC facesheet design yields the lowest facesheet plus actuator weight/area (12.6Kg/m^2) followed by the fused silica, beryllium, and ULE designs (15.4, 18.2, 20.6) respectively.

Figures 6 thru 8 shown the thermal performance for equal stiffness to weight passive mirror designs which are "cold figured" at the average operating temperature of 190K. These curves shown there is a significant increase in

performance over the designs shown in Reference (1), which were not "cold figured". Here again, the silicon carbide design yields the best performance over the operating temperature range.

Attachments (8) plus Appendix

/map

Distribution:
L. Solomon
C. Robbert
C. Ullathorne

C-6.

FIGURE 1

ACTIVE MIRROR DESIGN CONCEPT

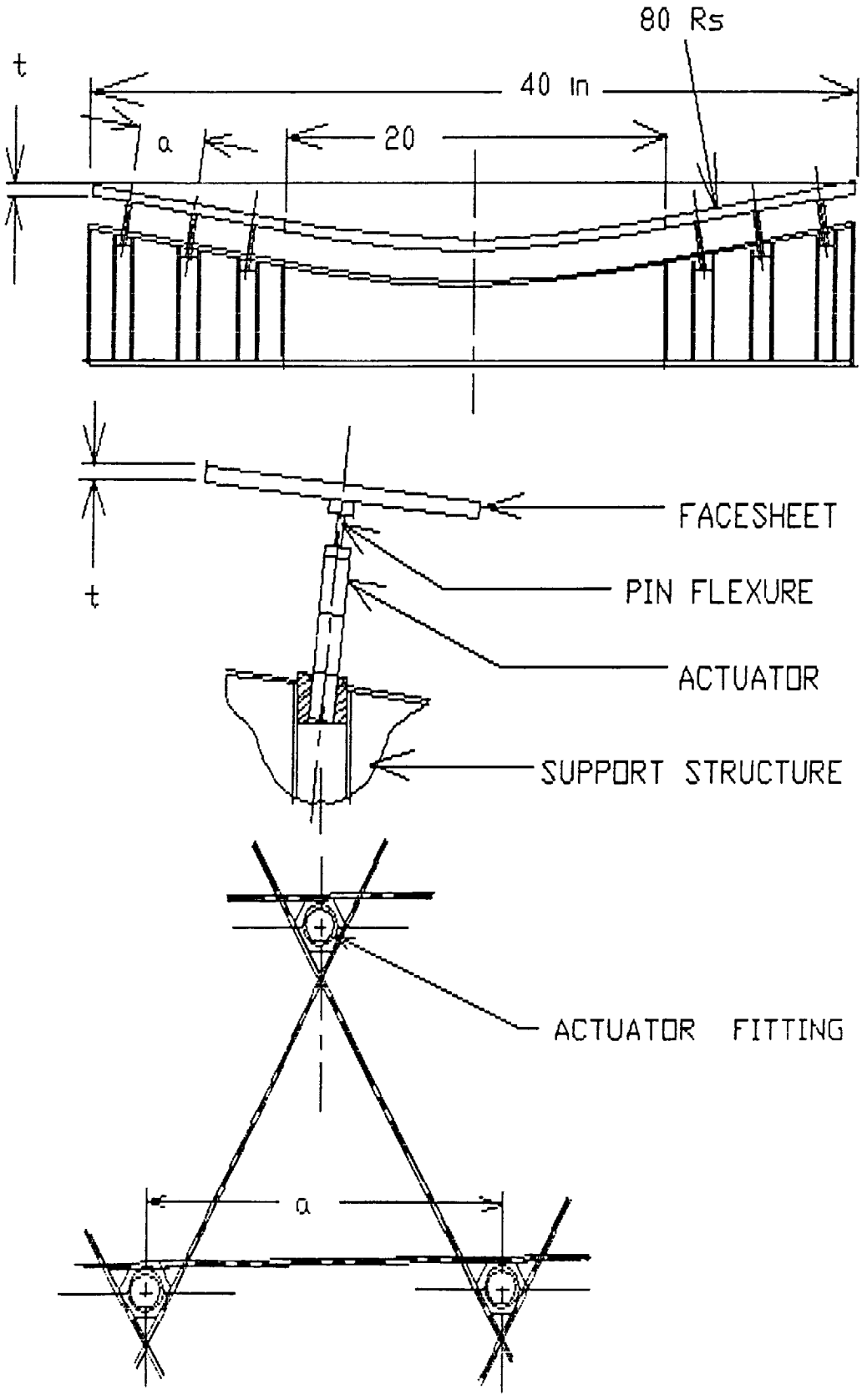

Figure 2

SiC Facesheet

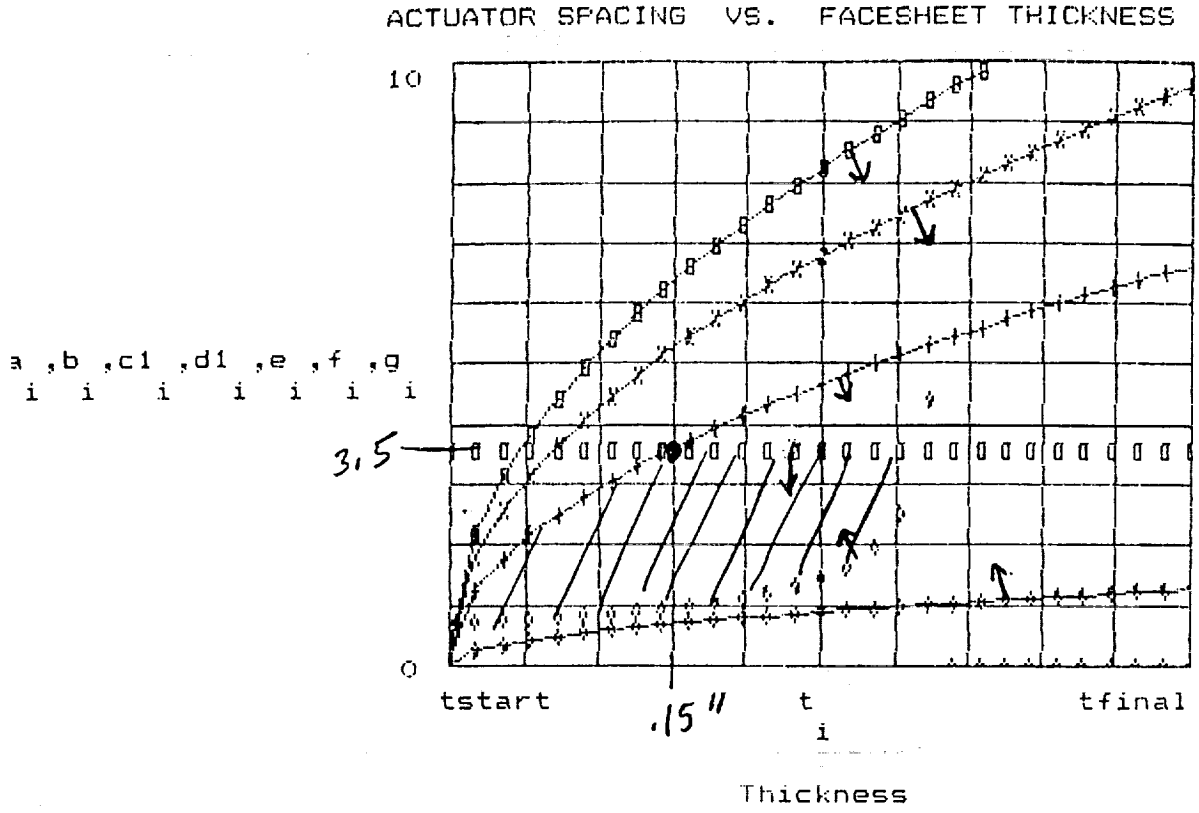

KEY

Curve 1 - Launch Survivability	=	line
Curve 2 - Gravity Sag	=	line with X
Curve 3 - HEL Load (Gradient)	=	line with O
Curve 4 - HEL Load (Soak)	=	line with plus sign
Curve 5 - Surface Correction	=	line with diamond
Curve 6 - correctibility (power)	=	no line with O
Curve 7 - Weight per Area	=	no line with diamond

Figure 3

Fused Silica Facesheet

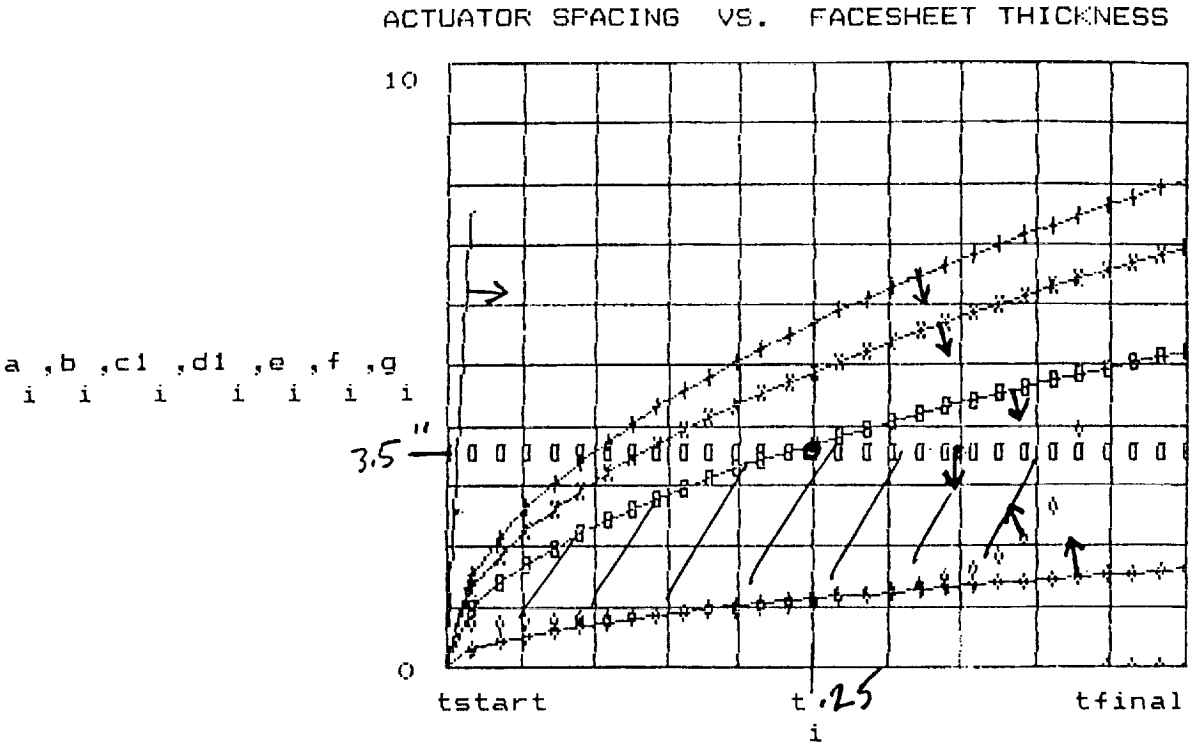

tstart = 0 tfinal = 0.5

KEY

Curve 1 - Launch Survivability = line
Curve 2 - Gravity Sag = line with X
Curve 3 - HEL Load (Gradient) = line with O
Curve 4 - HEL Load (Soak) = line with plus sign
Curve 5 - Surface Correction = line with diamond
Curve 6 - correctibility (power) = no line with O
Curve 7 - Weight per Area = no line with diamond

Figure 4

Beryllium Facesheet

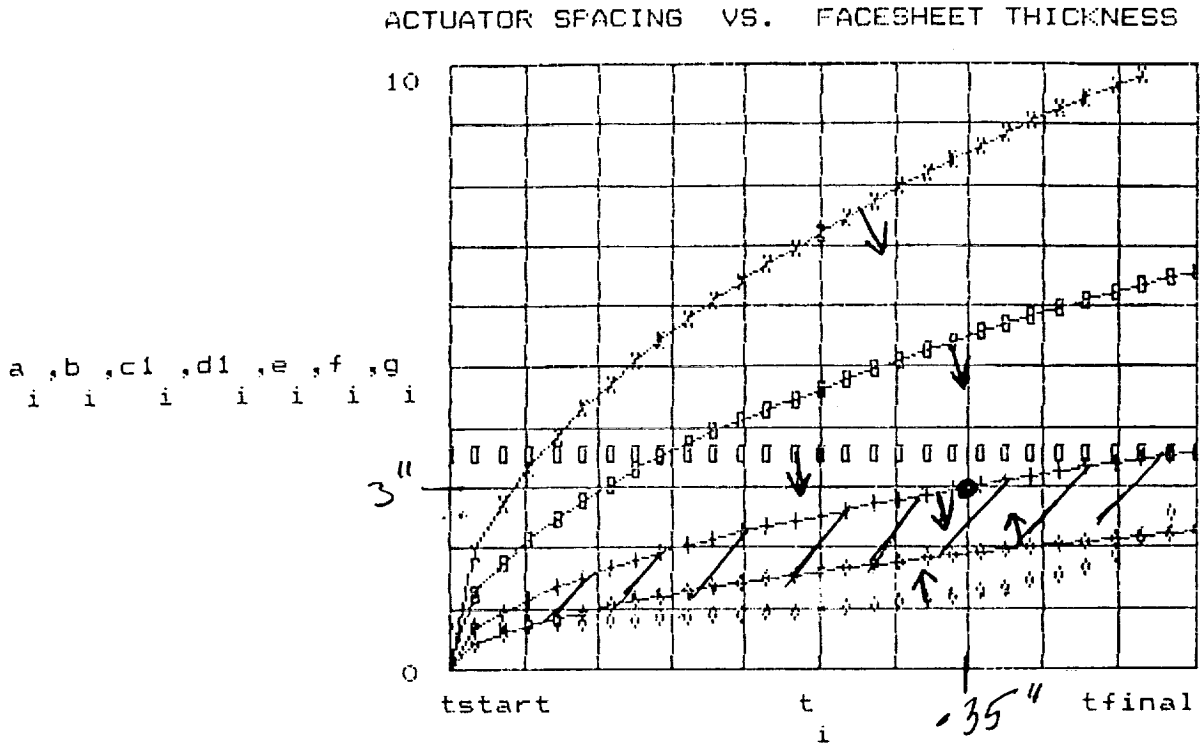

KEY

Curve 1 - Launch Survivability = line
Curve 2 - Gravity Sag = line with X
Curve 3 - HEL Load (Gradient) = line with O
Curve 4 - HEL Load (Soak) = line with plus sign
Curve 5 - Surface Correction = line with diamond
Curve 6 - correctibility (power) = no line with O
Curve 7 - Weight per Area = no line with diamond

Figure 5

ULE Facesheet

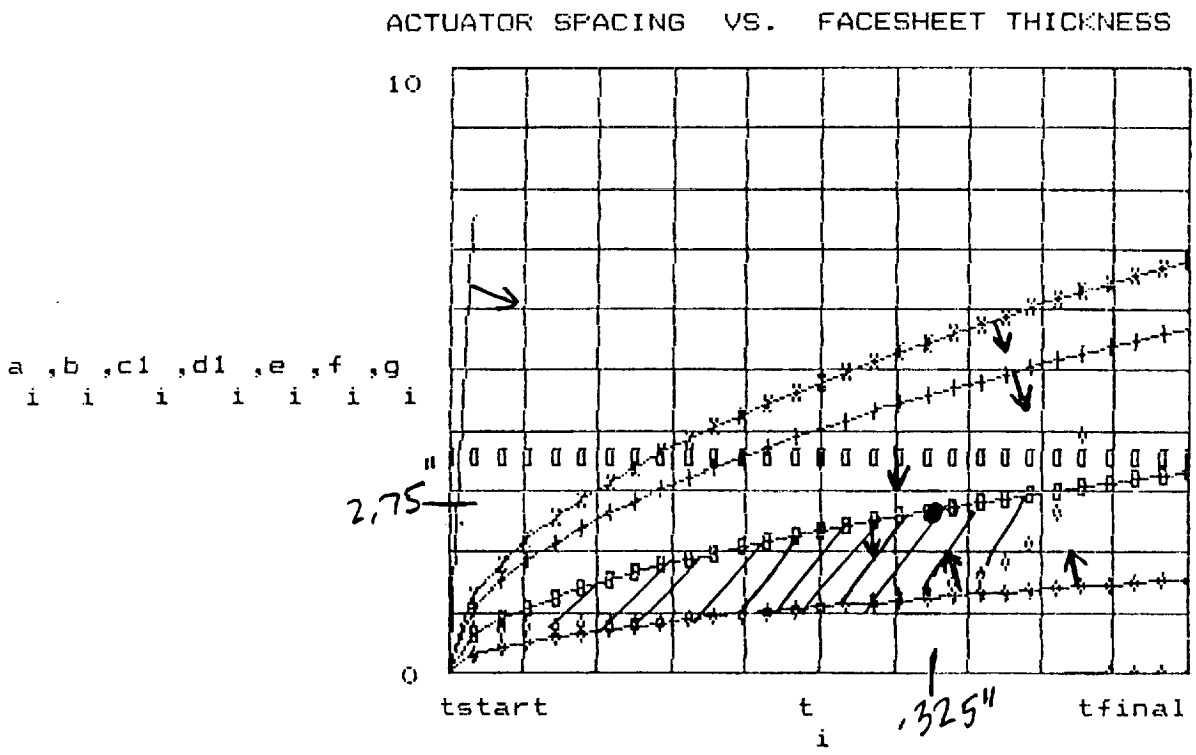

tstart = 0 tfinal = 0.5

KEY

Curve 1 - Launch Survivability = line
Curve 2 - Gravity Sag = line with X
Curve 3 - HEL Load (Gradient) = line with O
Curve 4 - HEL Load (Soak) = line with plus sign
Curve 5 - Surface Correction = line with diamond
Curve 6 - correctibility (power) = no line with O
Curve 7 - Weight per Area = no line with diamond

Figure 6

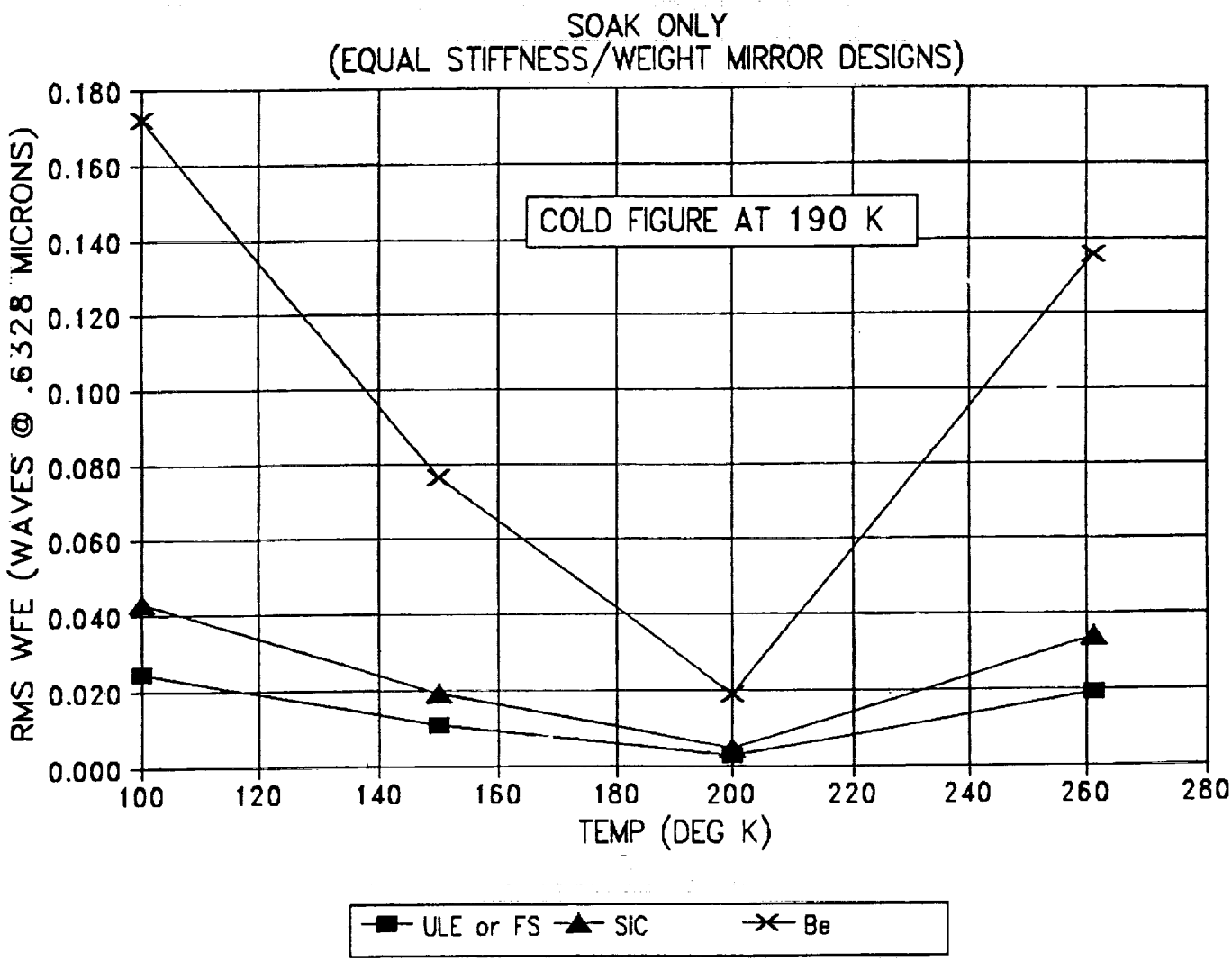
SOAK ONLY
(EQUAL STIFFNESS/WEIGHT MIRROR DESIGNS)
COLD FIGURE AT 190 K
RMS WFE (WAVES @ .6328 MICRONS)
0.180
0.160
0.140
0.120
0.100
0.080
0.060
0.040
0.020
0.000
100
120
140
160
180
200
220
240
260
280
TEMP (DEG K)
ULE or FS
SiC
Be

Figure 7

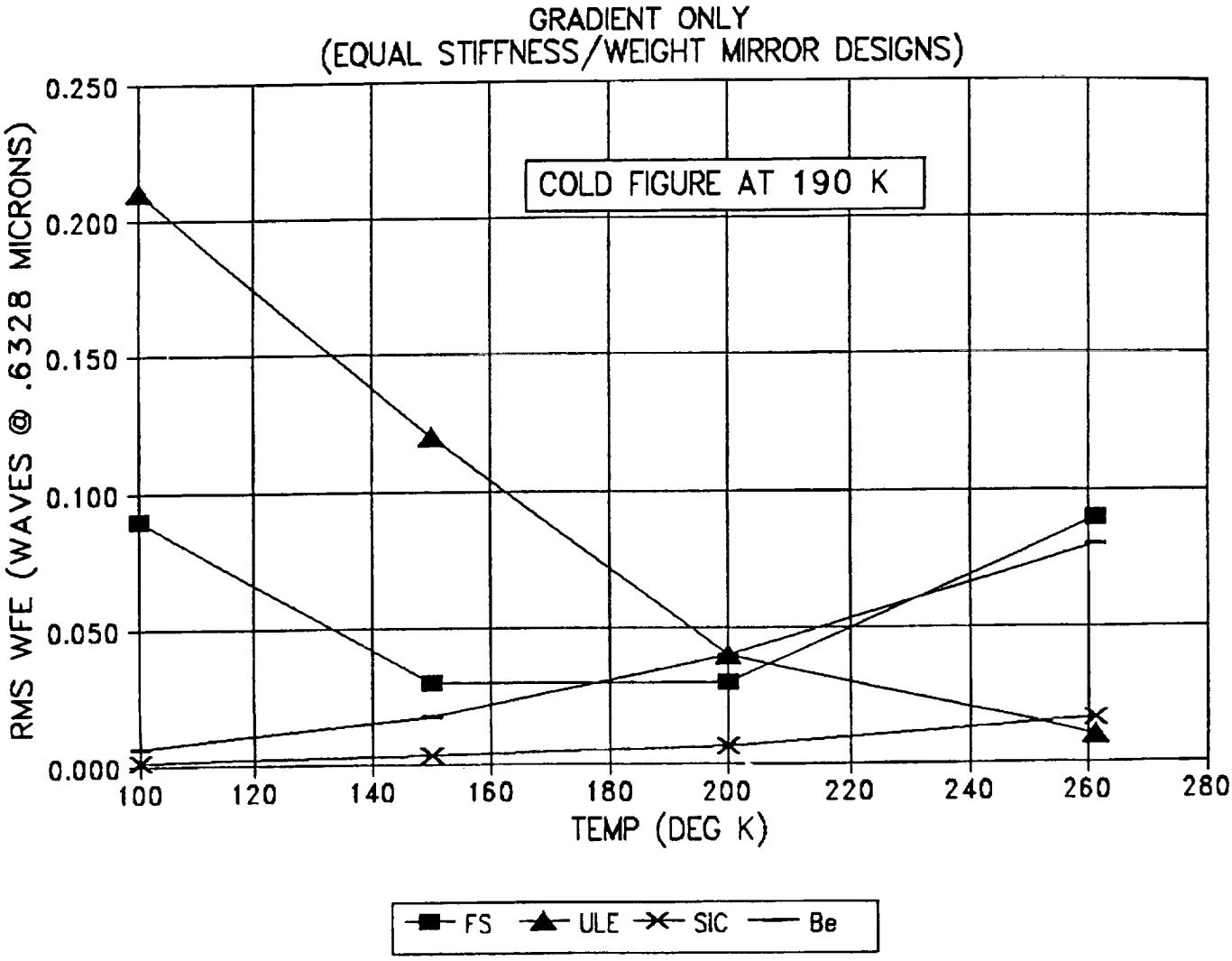
GRADIENT ONLY
(EQUAL STIFFNESS/WEIGHT MIRROR DESIGNS)
COLD FIGURE AT 190 K
RMS WFE (WAVES @ .6328 MICRONS)
0.250
0.200
0.150
0.100
0.050
0.000
100
120
140
160
180
200
220
240
260
280
TEMP (DEG K)
FS
ULE
SIC
Be

Figure 8

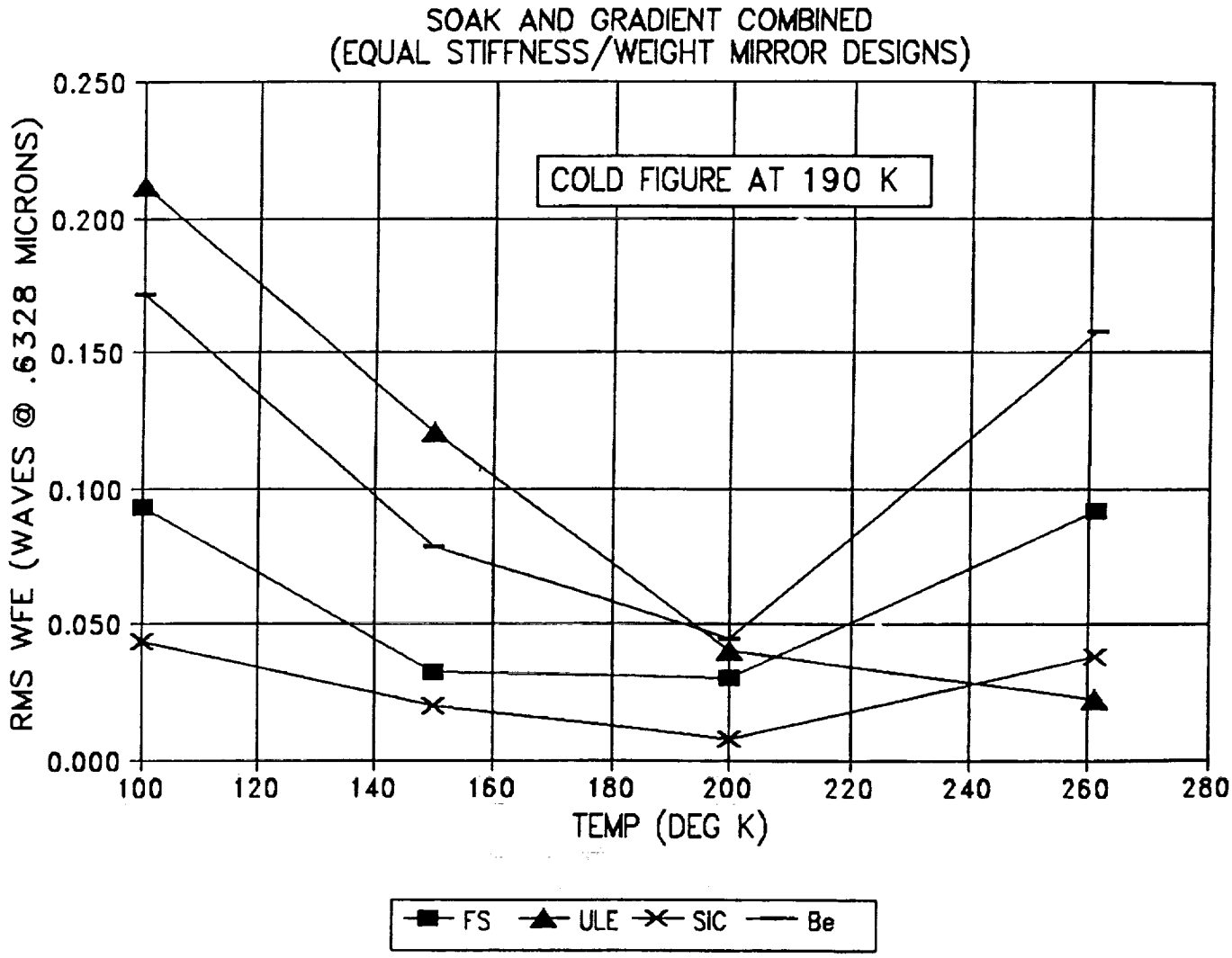
SOAK AND GRADIENT COMBINED
(EQUAL STIFFNESS/WEIGHT MIRROR DESIGNS)
COLD FIGURE AT 190 K
RMS WFE (WAVES @ .6328 MICRONS)
0.250
0.200
0.150
0.100
0.050
0.000
100
120
140
160
180
200
220
240
260
280
TEMP (DEG K)
FS
ULE
SIC
Be

APPENDIX

LARGE ACTIVE MIRROR DESIGN

This file is designed to study the various design parameters (facesheet thickness, actuator spacing, structural and thermal properties, actuator stiffness, etc.) for large active mirror designs.

The values for the following parameters may be changed to plot new design curves for various design conditions.

Note: All units must be consistant.

FS

Facesheet thickness/fine figure actuator spacing relations:

$\sigma := 1000$ psi ..... Facesheet allowable stress

$\rho := .079$ lb/in^3 ..... Weight Density

nu := .167 ..... Poisson's Ratio

$E := 10.6 \cdot 10^{6}$ psi ..... Modulus of Elasticity

$\alpha := .17 \cdot 10^{-6}$ in/in/F ..... Coeff. Thermal Expansion

$dCTE := .003 \cdot 10^{-6}$ in/in/F.....Delta Coeff. Therm. Expan.

$Cp := .543$ $Btu/lb/^{o}F$ .... Specific Heat

$K := .039$ $BTU/hr\ in\ ^{o}F$ ..... Thermal Conductivity

tstart := 0 inches ..... Minimum facesheet thickness to be incremented.

tfinal := .5 inches .... Maximum facesheet thickness

FS

(A2)

Ts := 311 deg F..... soak temperature

Tg := 13 deg F ..... gradient

G := 20 ..... Gravity load factor

$SEgs := .9 \cdot 10^{-6}$ inches .. RMS SE due to gravity sag

$SEhg := .9 \cdot 10^{-6}$ inches .. RMS SE due to HEL load (gradient)

$SEhs := .9 \cdot 10^{-6}$ inches .. RMS SE due to HEL load (soak)

$Qabs := 6.6041$ $BTU/hr\ in^2$ ... Absorbed HEL Flux Loading

$\tau := .13889$ hours ..... HEL exposure time

$W := 1.6 \cdot 10^{-4}$ inches ..... Actuator stroke

Dp := 40 inches .... Panel Diameter

Rs := 80 inches ..... Mirror spherical radius

$rrms := .9 \cdot 10^{-6}$ inches .. Residual RMS SE

$irms := 140 \cdot 10^{-6}$ inches ....Input RMS SE

Wact := .018 Lb ..... Actuator Weight

$wpa := .035$ Lb/in^2 ..... Desired weight per unit area

******** END OF PARAMETER INPUT DATA *********

$$tincr := \frac{tfinal - tstart}{ndp} \qquad tincr = 0.018$$

(A3)

LARGE ACTIVE MIRROR DESIGN

This file is designed to study the various design parameters (facesheet thickness, actuator spacing, structural and thermal properties, actuator stiffness, etc.) for large active mirror designs.

The values for the following parameters may be changed to plot new design curves for various design conditions.

Note: All units must be consistant.

Facesheet thickness/fine figure actuator spacing relations:

ULE

$\sigma := 1000$ psi ..... Facesheet allowable stress

$\rho := .079$ lb/in^3 ..... Weight Density

nu := .176 ..... Poisson's Ratio

$E := 9.8 \cdot 10^{6}$ psi ..... Modulus of Elasticity

$\alpha := .42 \cdot 10^{-6}$ in/in/F ..... Coeff. Thermal Expansion

$dCTE := .006 \cdot 10^{-6}$ in/in/F.....Delta Coeff. Therm. Expan.

$Cp := .452$ $Btu/lb/^{o}F$ .... Specific Heat

$K := .024$ $BTU/hr\ in\ ^{o}F$ ..... Thermal Conductivity

tstart := 0 inches ..... Minimum facesheet thickness to be incremented.

tfinal := .5 inches .... Maximum facesheet thickness

ULE

(A4)

Ts := 311 deg F..... soak temperature

Tg := 13 deg F ..... gradient

G := 20 ..... Gravity load factor

$SEgs := .9 \cdot 10^{-6}$ inches .. RMS SE due to gravity sag

$SEhg := .9 \cdot 10^{-6}$ inches .. RMS SE due to HEL load (gradient)

$SEhs := .9 \cdot 10^{-6}$ inches .. RMS SE due to HEL load (soak)

$Qabs := 6.6041$ BTU/hr in^2 ... Absorbed HEL Flux Loading

$\tau := .13889$ hours ..... HEL exposure time

$W := 1.6 \cdot 10^{-4}$ inches ..... Actuator stroke

Dp := 40 inches .... Panel Diameter

Rs := 80 inches ..... Mirror spherical radius

$rrms := .9 \cdot 10^{-6}$ inches .. Residual RMS SE

$irms := 140 \cdot 10^{-6}$ inches ....Input RMS SE

Wact := .018 Lb ..... Actuator Weight

$wpa := .035$ Lb/in^2 ..... Desired weight per unit area

******** END OF PARAMETER INPUT DATA *********

$$tincr := \frac{tfinal - tstart}{ndp} \qquad tincr = 0.018$$

A5

LARGE ACTIVE MIRROR DESIGN

This file is designed to study the various design parameters (facesheet thickness, actuator spacing, structural and thermal properties, actuator stiffness, etc.) for large active mirror designs.

The values for the following parameters may be changed to plot new design curves for various design conditions.

Note: All units must be consistant.

Facesheet thickness/fine figure actuator spacing relations:

Be

$\sigma := 2000$ psi ..... Facesheet allowable stress

$\rho := .067$ lb/in^3 ..... Weight Density

nu := .025 ..... Poisson's Ratio

$E := 43.5 \cdot 10^{6}$ psi ..... Modulus of Elasticity

$\alpha := 3.9 \cdot 10^{-6}$ in/in/F ..... Coeff. Thermal Expansion

$dCTE := .028 \cdot 10^{-6}$ in/in/F.....Delta Coeff. Therm. Expan.

$Cp := .452$ $Btu/lb/^{o}F$ .... Specific Heat

$K := 10.6$ $BTU/hr\ in\ ^{o}F$ ..... Thermal Conductivity

tstart := 0 inches ..... Minimum facesheet thickness to be incremented.

tfinal := .5 inches .... Maximum facesheet thickness

ORIGINAL PAGE IS OF POOR QUALITY

Be

(A6)

Ts := 167 deg F..... soak temperature

Tg := .36 deg F ..... gradient

G := 20 ..... Gravity load factor

SEgs := $.9 \cdot 10^{-6}$ inches .. RMS SE due to gravity sag

SEhg := $.9 \cdot 10^{-6}$ inches .. RMS SE due to HEL load (gradient)

SEhs := $.9 \cdot 10^{-6}$ inches .. RMS SE due to HEL load (soak)

Qabs := 6.6041 BTU/hr in^2 ... Absorbed HEL Flux Loading

τ := .13889 hours ..... HEL exposure time

W := $1.6 \cdot 10^{-4}$ inches ..... Actuator stroke

Dp := 40 inches .... Panel Diameter

Rs := 80 inches ..... Mirror spherical radius

rrms := $.9 \cdot 10^{-6}$ inches .. Residual RMS SE

irms := $140 \cdot 10^{-6}$ inches ....Input RMS SE

Wact := .018 Lb ..... Actuator Weight

wpa := .035 Lb/in^2 ..... Desired weight per unit area

******** END OF PARAMETER INPUT DATA *********

$$tincr := \frac{tfinal - tstart}{nop} \qquad tincr = 0.018$$

(A7)

LARGE ACTIVE MIRROR DESIGN

This file is designed to study the various design parameters (facesheet thickness, actuator spacing, structural and thermal properties, actuator stiffness, etc.) for large active mirror designs.

The values for the following parameters may be changed to plot new design curves for various design conditions.

Note: All units must be consistant.

Facesheet thickness/fine figure actuator spacing relations:

SiC

$\sigma := 8000$ psi ..... Facesheet allowable stress

$\rho := .106$ lb/in^3 ..... Weight Density

nu := .14 ..... Poisson's Ratio

$E := 52.8 \cdot 10^{6}$ psi ..... Modulus of Elasticity

$\alpha := .83 \cdot 10^{-6}$ in/in/F ..... Coeff. Thermal Expansion

$dCTE := .0083 \cdot 10^{-6}$ in/in/F.....Delta Coeff. Therm. Expan.

$Cp := .161$ $Btu/lb/^{o}F$ .... Specific Heat

$K := 9.6$ $BTU/hr\ in\ ^{o}F$ ..... Thermal Conductivity

tstart := 0 inches ..... Minimum facesheet thickness to be incremented.

tfinal := .5 inches .... Maximum facesheet thickness

SiC

(A8)

Ts := 167 deg F..... soak temperature

Tg := .54 deg F ..... gradient

G := 20 ..... Gravity load factor

$SEgs := .9 \cdot 10^{-6}$ inches .. RMS SE due to gravity sag

$SEhg := .9 \cdot 10^{-6}$ inches .. RMS SE due to HEL load (gradient)

$SEhs := .9 \cdot 10^{-6}$ inches .. RMS SE due to HEL load (soak)

$Qabs := 6.6041$ BTU/hr in^2 ... Absorbed HEL Flux Loading

$\tau := .13889$ hours ..... HEL exposure time

$W := 1.6 \cdot 10^{-4}$ inches ..... Actuator stroke

Dp := 40 inches .... Panel Diameter

Rs := 80 inches ..... Mirror spherical radius

$rrms := .9 \cdot 10^{-6}$ inches .. Residual RMS SE

$irms := 140 \cdot 10^{-6}$ inches ....Input RMS SE

Wact := .018 Lb ..... Actuator Weight

$wpa := .035$ Lb/in^2 ..... Desired weight per unit area

******** END OF PARAMETER INPUT DATA **********

$$tincr := \frac{tfinal - tstart}{ndp} \qquad tincr = 0.018$$

(A9)

CURVE 1 LAUNCH SURVIVABILITY

$$a_i := \left[\frac{\sigma}{.199 \cdot \rho \cdot G}\right]^{.5} t_i^{.5}$$

a - actuator spacing

t - facesheet thickness

$$a = \begin{bmatrix} 0 \\ 18.402 \\ 26.024 \\ 31.873 \\ 36.803 \\ 41.147 \\ 45.075 \\ 48.686 \\ 52.048 \\ 55.205 \\ 58.191 \\ 61.031 \\ 63.745 \\ 66.348 \\ 68.853 \\ 71.269 \\ 73.607 \\ 75.872 \\ 78.072 \\ 80.211 \\ 82.295 \\ 84.327 \\ 86.311 \\ 88.251 \\ 90.149 \\ 92.008 \\ 93.83 \\ 95.618 \\ 97.372 \end{bmatrix}$$

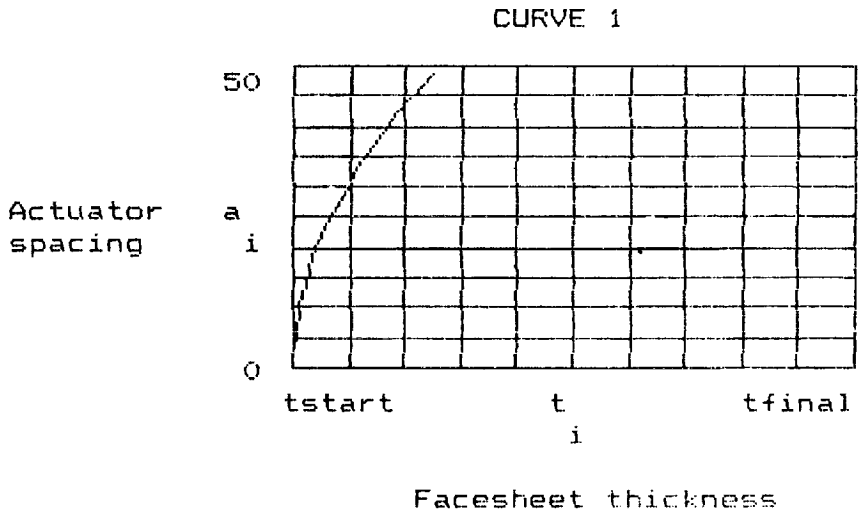

tstart = 0 tfinal = 0.5

CURVE 2 GRAVITY SAG

$$b_i := \left[\frac{SEgs \cdot E}{.0134 \cdot \rho \cdot \left[1 - nu^2\right]}\right]^{.25} \cdot t_i^{.5}$$

b_i - actuator spacing

a_i - facesheet thickness

$b =$

0
1.816
2.569
3.146
3.632
4.061
4.449
4.805
5.137
5.449
5.743
6.024
6.292
6.549
6.796
7.034
7.265
7.489
7.706
7.917
8.122
8.323
8.519
8.71
8.898
9.081
9.261
9.437

Actuator spacing

CURVE 2

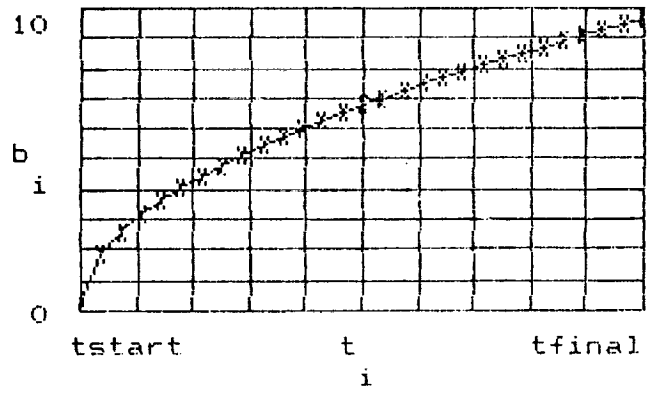

Facesheet thickness

tstart = 0 tfinal = 0.5

CURVE 3 HEL LOAD (GRADIENT)

$$c1_i := \left[\frac{SEhg \cdot t_i}{.0074 \cdot \alpha \cdot Tg}\right]^{.5}$$

$$c_i := \left[\frac{SEhg \cdot K}{.0074 \cdot \alpha \cdot Qabs}\right]^{.5}$$

c_i - actuator spacing

$$c1 = \begin{bmatrix} 0 \\ 2.201 \\ 3.113 \\ 3.813 \\ 4.403 \\ 4.922 \\ 5.392 \\ 5.824 \\ 6.226 \\ 6.604 \\ 6.961 \\ 7.301 \\ 7.625 \\ 7.937 \\ 8.236 \\ 8.526 \\ 8.805 \\ 9.076 \\ 9.339 \\ 9.595 \\ 9.844 \\ 10.088 \\ 10.325 \\ 10.557 \\ 10.784 \\ 11.006 \\ 11.224 \\ 11.438 \\ 11.648 \end{bmatrix}$$

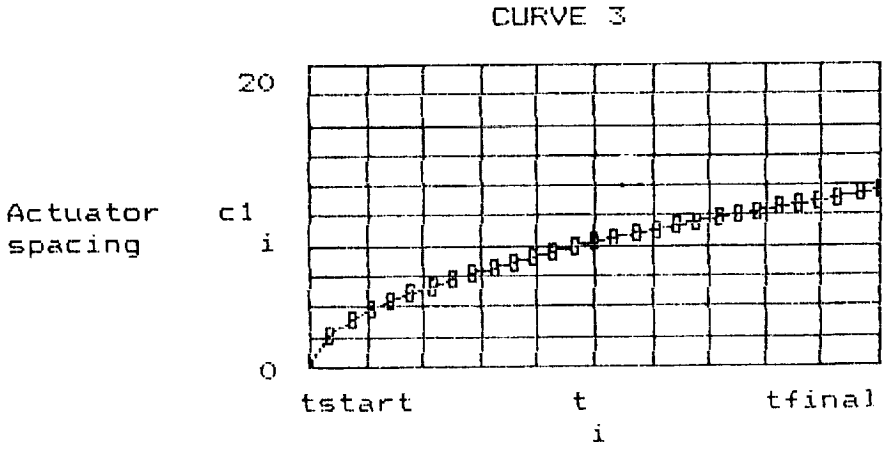

A12

CURVE 4 HEL LOAD (SOAK)

$$d_i := \left[\frac{SEhs \cdot \rho \cdot Cp}{Qabs \cdot \tau \cdot dCTE \cdot .0074}\right]^{.5} \cdot t_i$$

d_i – actuator spacing

t_i – facesheet thickness

$$d1_i := \left[\frac{SEhs \cdot t_i}{.0074 \cdot dCTE \cdot Ts}\right]^{.5}$$

$d1 =$

0
1.252
1.77
2.168
2.503
2.799
3.066
3.312
3.54
3.755
3.958
4.152
4.336
4.513
4.684
4.848
5.007
5.161
5.311
5.456
5.598
5.736
5.871
6.003
6.132
6.259
6.383
6.504
6.624

Actuator spacing

CURVE 4

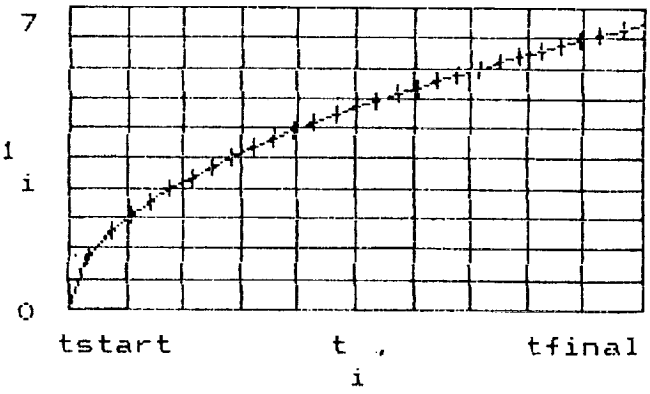

Facesheet thickness

tstart = 0 tfinal = 0.5

CURVE 5 FACESHEET STRESS DUE TO SURFACE CORRECTION

$$e_i := \left[\frac{3 \cdot E \cdot W}{\sigma \cdot \left[1 - nu^2\right]}\right]^{.5} \cdot t_i^{.5}$$

e_i – actuator spacing

t_i – facesheet thickness

$$e = \begin{bmatrix} 0 \\ 0.24 \\ 0.34 \\ 0.416 \\ 0.48 \\ 0.537 \\ 0.588 \\ 0.636 \\ 0.679 \\ 0.721 \\ 0.76 \\ 0.797 \\ 0.832 \\ 0.866 \\ 0.899 \\ 0.93 \\ 0.961 \\ 0.99 \\ 1.019 \\ 1.047 \\ 1.074 \\ 1.101 \\ 1.127 \\ 1.152 \\ 1.177 \\ 1.201 \\ 1.225 \\ 1.248 \\ 1.271 \end{bmatrix}$$

Actuator spacing

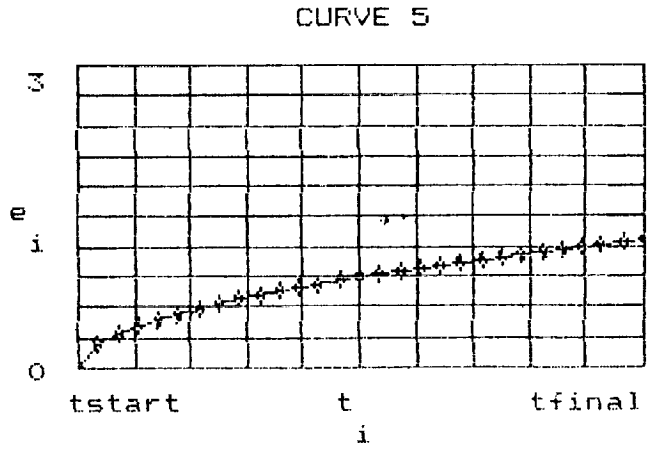

tstart = 0 tfinal = 0.5

A14

CURVE 6 POWER CORRECTION

$K1 := 2.5$

$$CF := \frac{rrms}{irms} \qquad CF = 0.006$$

$$f_i := \left[\frac{\pi \cdot Dp^2}{4 \cdot \left[\frac{K1}{CF}\right]^{.77}} \right]^{.5}$$

f - actuator spacing

$$f = \begin{bmatrix} 3.569 \\ 3.569 \end{bmatrix}$$

CURVE 6

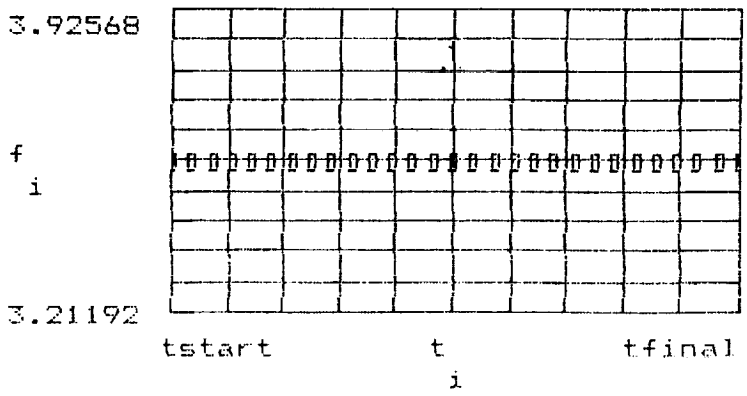

tstart = 0 tfinal = 0.5

A15

CURVE 7 WEIGHT PER UNIT AREA

$$g_i := \left[\frac{Wact}{wpa - \left[\rho \cdot t_i\right]}\right]^{.5}$$

g_i - actutor spacing

t_i - facesheet thickness

$$g = \begin{bmatrix} 0.717 \\ 0.737 \\ 0.759 \\ 0.784 \\ 0.81 \\ 0.84 \\ 0.873 \\ 0.91 \\ 0.952 \\ 1.001 \\ 1.058 \\ 1.127 \\ 1.21 \\ 1.316 \\ 1.455 \\ 1.651 \\ 1.954 \\ 2.526 \\ 4.403 \\ 4.32i \\ 2.51i \\ 1.947i \\ 1.646i \\ 1.452i \\ 1.314i \\ 1.209i \\ 1.125i \\ 1.057i \\ i \end{bmatrix}$$

Actuator spacing g_i

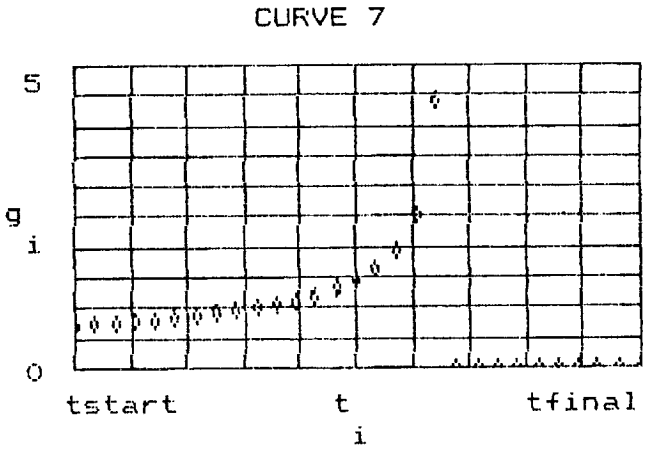

tstart = 0 tfinal = 0.5

HUGHES

HUGHES DANBURY OPTICAL SYSTEMS, INC.
a subsidiary

PR D15-0013A

LUTE PRIMARY MIRROR
MATERIALS AND DESIGN STUDY REPORT

February 1993

Prepared for:
National Aeronautics and Space Administration
George C. Marshall Space Flight Center
Marshall Space Flight Center
Alabama 35812
Order No. H-11994D

HUGHES DANBURY OPTICAL SYSTEMS, INC.
100 WOOSTER HEIGHTS ROAD
DANBURY, CT 06810-7589

All or a portion of the Work Discussed herein was Supported by NASA/MSFC

HUGHES

Hughes Danbury Optical Systems, Inc.
a subsidiary

PUBLICATION REVIEW:

Prepared by: _____ 2/26/93
Greg Ruthven, Project Engineer — Date

Approved by: _____ 26 Feb 93
Mark Stier, Program Manager — Date

_____ 2/26/93
George Bossers, Director Advanced Development Lab — Date

REVISION RECORD:

Revision	Date	Affected Pages
A	2-26-93	i through vi, 1-1, 2-1, 2-2, 3-1 through 3-12, 4-1 through 4-22, 5-1, 5-2, 6-1, 7-1, 8-1, A-1 through A-23, B-1 through B-29

TABLE OF CONTENTS

Section	Title	Page
1	INTRODUCTION	1-1
2	SUMMARY OF RESULTS	2-1
3	PRIMARY MIRROR DESIGN AND PERFORMANCE REQUIREMENTS	3-1
3.1	Optical Design	3-2
3.2	Wavefront Error Allocation	3-3
3.3	Weight Allocation	3-4
3.4	Quasi-Static Loads	3-6
3.5	Microroughness	3-7
3.6	Coating Reflectance	3-8
3.7	Metering Structure	3-9
3.8	Design Specification	3-12
4	PRIMARY MIRROR CANDIDATE MATERIALS AND CONFIGURATIONS	4-1
4.1	Substrate Materials and Designs	4-1
4.2	Usage History	4-2
4.3	Thermal Performance	4-2
4.4	Structural Performance and Mass Properties Estimates	4-9
4.5	Active Primary Mirror Design Option	4-18
5	SELECTION CRITERIA AND EVALUATION	5-1
5.1	Recommended Candidates	5-1
5.2	Basis of Selection	5-1
5.3	Candidate Design Producibilty Status	5-2
6	CONCLUSIONS	6-1
7	CANDIDATE TOPICS FOR FURTHER STUDY	7-1
8	ACKNOWLEDGEMENTS	8-1
APPENDIX A	ALLOWABLE THERMAL AND CTE GRADIENTS	A-1
APPENDIX B	MIRROR MATERIAL CRYOGENIC PROPERTIES AND FIGURES OF MERIT	B-1

LIST OF ILLUSTRATIONS

Figure	Title	Page
3-1	We Have Assumed the MSFC Optical Design Concept "LTT100" as the Baseline for Our Study	3-1
3-2.	Critical Requirements Were Addressed to Ensure the Recommended Design(s) Meet Ground Testing and In-Operation Scenarios	3-2
3-3	The LUTE Wavefront Error Allocation (Based on the HST WFE Budget).	3-3
3-4	UV-to-IR Normal Incidence Reflectances of Candidate Coatings	3-8
3-5	Various Candidate Metering Truss Designs Are Available for LUTE	3-9
3-6	Results from Other Programs Can Be Applied to LUTE Specific Investigations	3-10
3-7	The Support Structure with Metering Rod Design Allows A High CTE Material to Be Used in the Presence of Large Side-To-Side Temperature Gradients	3-11
4-1	The Lute Study Investigation Yielded Various Mirror Geometries.	4-3
4-2	LUTE PM Materials and Design Study Thermal Considerations	4-5
4-3	LUTE PM Materials and Design Study Performance Results (Closed Back and Single Arch-Diametral DT.)	4-6
4-4	LUTE PM Materials and Design Study Performance Results (Meniscus and Single Etch-Radially Symmetric $\Delta L/L$)	4-8
4-5	Major Structural Considerations Quantified to Determine Leading Candidate Designs.	4-9
4-6	Existing Mirror Finite Element Models Used as Cross-Check for Scaling Laws	4-14
4-7	Mirror Deformation Patterns Decomposed to Determine Wavefront Error after Tilt and Focus is Removed	4-15
4-8	A Beryllium, Single Arch Primary Mirror Design is Clearly Superior for 1g-to-1/6g Effects.	4-17
4-9	Primary Mirror Residual Distortion After Active Correction Via Figure Control Actuators	4-21
4-10	Several Design Concepts Exist for Primary Mirror Figure Control Actuators.	4-21

LIST OF TABLES

Table	Title	Page
3-1	LUTE Telescope Weight Budget Defined to Conduct Feasibility Study	3-5
3-2	Weight Contingency Schedule	3-6
3-3	Specifications for LUTE Primary Mirror	3-12
4-1	LUTE Substrate Materials	4-1
4-2	Cryogenic Mirror Performance Data	4-4
4-3	Meniscus Mirror - Three Point Supported - Performance Results	4-10
4-4	Open Back Mirror - Three Point Supported - Performance Results	4-11
4-5	Closed Back Mirror - Three Point Supported - Performance Results	4-12
4-6	Single Arch Mirror - Three Point Supported - Performance Results	4-13
4-7	LUTE Telescope Mass Properties	4-19

SECTION 1
INTRODUCTION

The major objective of the Lunar Ultraviolet Telescope Experiment (LUTE) Primary Mirror Materials and Design Study is to investigate the feasibility of the LUTE telescope primary mirror. We took a systematic approach to accomplish this key goal by first understanding the optical, thermal and structural requirements and then deriving the critical primary mirror-level requirements for ground testing, launch, and lunar operations.

After summarizing our results in Section 2, Section 3 discusses those requirements which drove the selection of material and the design for the primary mirror. Most important of these are the optical design which we assumed to be the MSFC baseline (i.e. 3 mirror optical system), telescope wavefront error (WFE) allocations, the telescope weight budget, and the LUTE operational temperature ranges. Section 3 also discusses mechanical load levels, reflectance and microroughness issues, options for the LUTE metering structure and initiates an outline for the LUTE telescope sub-system design specification.

Section 4 presents our primary mirror analysis and results. We discuss the six material substrate candidates and show four distinct mirror geometries which we considered for our study. With these materials and configurations together with varying the location of the mirror support points, a total of 42 possible primary mirror designs resulted. We also investigated the polishability of each substrate candidate and present a usage history of 0.5 meter and larger precision cryogenic mirrors (the operational low end LUTE temperature of 60 K is the reason we feel a survey of cryogenic mirrors is appropriate) that have been flown or tested. Sections 4.3 and 4.4 present performance data in summary form via bar charts; more detailed analysis is provided in the data tables. Additional material is provided in Appendix A. Material cryogenic properties are provided in Appendix B. Section 4 concludes with a mass properties summary to aid both telescope feasibility and telescope material selection along with information required for launch vehicle applicability and performance. The active primary mirror design approach is also discussed and its impact on weight and performance is assessed.

We describe the leading mirror materials and configurations in Section 5 with rational on these selections and our assessment of producing such a primary mirror.

We conclude our study with a set of recommendations not only with respect to the LUTE primary mirror but also on other topics related to the overall feasibility of the LUTE telescope sub-system.

SECTION 2
SUMMARY OF RESULTS

The ability to design, build, test and successfully launch and operate a 1-meter class diffraction-limited telescope operating over a 200 K temperature range appears to be feasible, albeit very technically challenging. From our understanding of the requirements, a primary mirror areal density (mass per unit area) of 28 kg/m^2 is necessary and must have a wavefront error of less than ~1/30th wave rms at 0.6328 μm of which no more than ~1/46th wave rms can be caused by thermally induced distortions. The primary mirror can not have a 1-g to 1/6-g residual (after telescope re-alignment) distortion of more than ~ 1/200th wave rms. The ability to fabricate such a 1-m cryo mirror that weighs less than 22 kg and is diffraction limited is unproven at this time.

After evaluating all of the candidates in our trade space, a single arch mirror design, fabricated from beryllium is the leading candidate for the LUTE primary mirror. This design is marginally acceptable in terms of residual 1-g deformation. All other candidate designs have poorer performance. This leading candidate design is very strongly based on our engineering judgment that use of a cryogenic metrology mount (to simulate 1/6-g deformation in a 1-g environment) would be an excessively high risk approach. We believe a logical approach to 1-g testing and verification is one which does not utilize a cryo "met" mount.

We have briefly assessed an active primary mirror design option which uses figure control actuators to compensate for mirror distortions. In addition to a significant weight penalty we doubt that the level of figure error correction required (better than 90%) is attainable. A further disadvantage of an active primary mirror is the need to periodically determine what figure corrections are needed and the need to actuate them reliably over several years. We have, therefore, rejected the active primary mirror design option.

We have also briefly assessed the concept of fabricating the tertiary mirror directly on the same substrate as the primary mirror. This approach would avoid the need for a separate mount for the tertiary mirror and make the optical system less sensitive to thermally-induced misalignments. Although we have done no analysis, in the judgment of our optical fabrication experts it is feasible to fabricate the tertiary mirror and the primary mirror on the same substrate.

Thermally induced mirror deformations must be closely monitored. The ±100 K range of operating temperatures is an exceptionally severe environment for a precision optical system. Our analyses show that the allowable temperature gradient across the mirror diameter or through its thickness is highly dependent on the particular temperature at which the measurement is taking place. This is due to the fact that each candidate primary mirror material has a different temperature dependence of its coefficient of thermal expansion (CTE.) For a single arch design a lower operating temperature (e.g. 60 K) is preferred if the CTE at the lower temperatures is lower than its room temperature value.

At 60 K, a side-to-side (i.e. diametral) gradient of approximately 1 K is allowable. From our discussions with MSFC this value seems realistic based on preliminary thermal analyses. However an area which needs further investigation is the allowable variation in CTE (and $\Delta L/L$) of the substrate itself. Our calculations show that the beryllium $\Delta L/L$ inhomogeneity must be maintained to within less than 1%. This represents a technical challenge and further discussions with beryllium vendors is certainly warranted. This issue is also important in the overall architecture of the LUTE mission and may determine whether operating temperatures should be more closely controlled via a telescope thermal control system.

SECTION 3
PRIMARY MIRROR DESIGN AND PERFORMANCE REQUIREMENTS

Our derivation of the LUTE primary mirror top level requirements is based on the three-mirror telescope configuration as baselined by MSFC and shown in Figure 3-1. The driving requirements include both wavefront error and weight allocations. Mirror performance predictions were calculated using these allocations as guidelines in our design effort and these calculations ultimately resulted in a recommended substrate and mirror geometry design which we feel is warranted for further investigation.

Study logic flow is summarized in Figure 3-2. Efforts centered around the Primary Mirror Assembly design and, in particular, three aspects of this assembly: 1) the candidate mirror substrates, 2) candidate mirror designs, and 3) whether active mirror correction capability is required. To a lesser degree we evaluated whether LUTE should have active thermal control to minimize the large operational temperature range as currently baselined. We show further study logic and discuss analytical results in Sections 4.3 and 4.4.

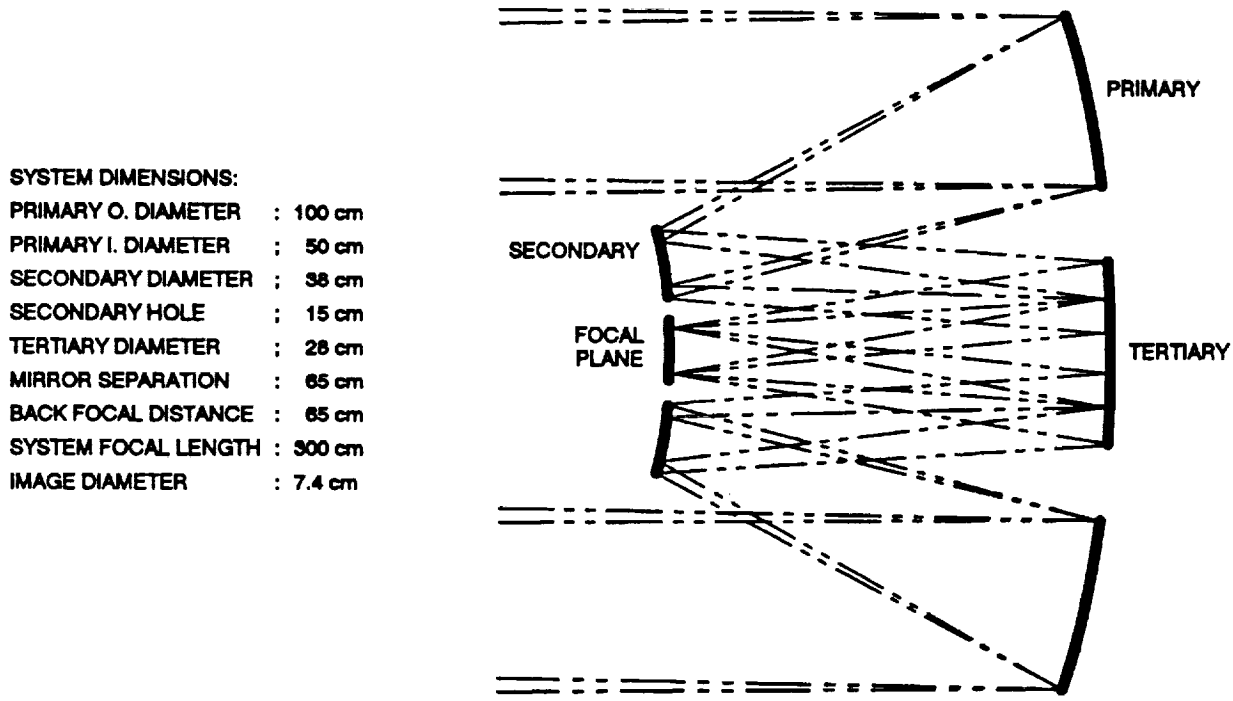

Figure 3-1. We Have Assumed the MSFC Optical Design Concept "LTT100" as the Baseline for Our Study.

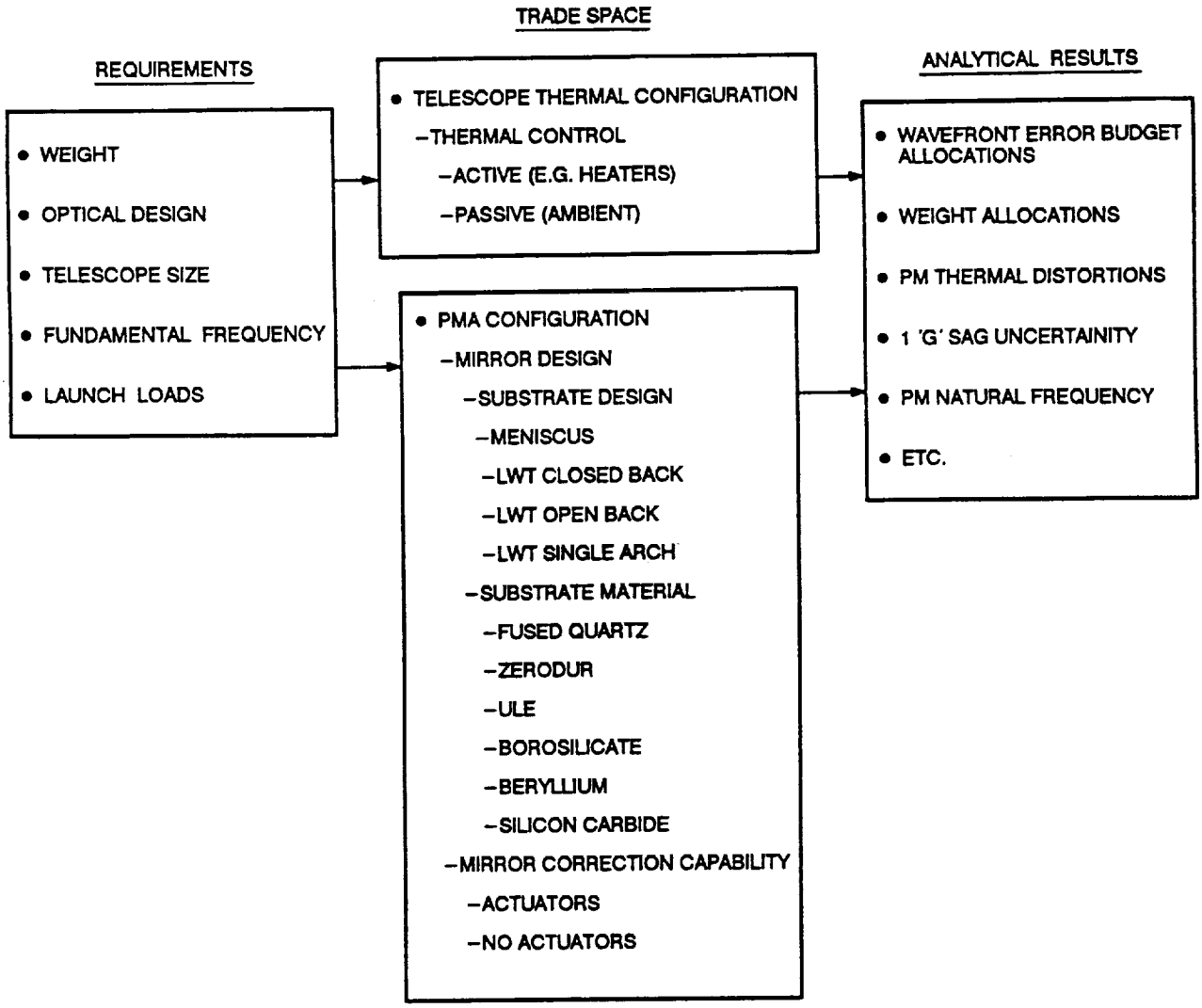

Figure 3-2. Critical Requirements Were Addressed to Ensure the Recommended Design(s) Meet Ground Testing and In-Operation Scenarios.

3.1 OPTICAL DESIGN

The optical design for LUTE was provided by MSFC. The need for a third optical element is derived from the need for a wide field of view. The LUTE concept is presently defined as a "transit" telescope that surveys the sky using only lunar rotation (and lunar precession.) It increases its effective sensitivity for faint objects by having a wide field of view to a focal plane fully populated with CCD's. This allows the integration time per object to be increased. The wide field system also increases the swath width of the sky that can be surveyed. No optical design analyses were performed as part of this study.

3.2 WAVEFRONT ERROR ALLOCATION

We developed a wavefront error allocation (Figure 3-3) for LUTE using that of the Hubble Space Telescope as a starting point. There are, however, significant differences in the two systems, and the LUTE allocation reflects its unique environment. The allocation forms a first-cut judgment of an equitable distribution of difficulty, but much more analytical work is required and considerable revisions to the allocation are likely to be needed in the future. Note that we have assumed that the secondary mirror has a re-alignment capability such that low-order wavefront errors are fully correctable.

The top-level value of 1/20 wave is a "round number" that, lacking analytical support, we believe will provide a reasonably good image quality at ultraviolet wavelengths. The majority of the budget has been allocated to the primary mirror. Only a small portion of the budget is available for primary mirror fabrication-related errors since we believe that the changes in the shape of the primary mirror from earth to moon may be particularly difficult to meet.

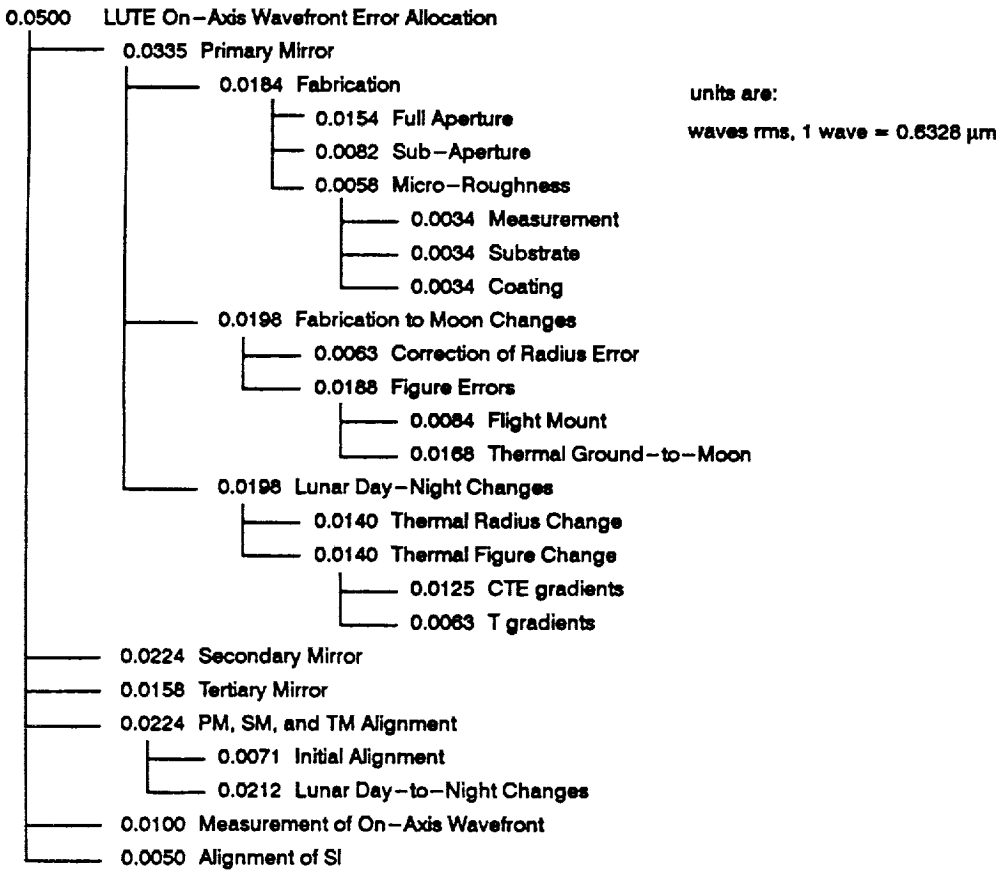

Figure 3-3. The LUTE Wavefront Error Allocation (Based on the HST WFE Budget).

There are three key contributors to post-launch changes in the shape of the primary mirror. First there is the change in deformation due to gravity. The HST mirror was precisely supported during fabrication/metrology such that it was measured in its 0-g configuration. As noted above, we believe that the use of a similar metrology mount for ground testing at LUTE's cryogenic operating temperatures would likely add more uncertainty to the interferometric data than an alternate approach that avoids the use of a cryo met mount. This decision has a very major impact on the mirror geometry selection as described below.

The second key contributor to wavefront errors is the "bulk" (mean) temperature change from the room temperature fabrication to the lunar environment. The primary effect of such a change is a radius of curvature change in the primary mirror that can be essentially eliminated by a focus mechanism at the secondary mirror. The budget allows for higher order errors, such as trefoil, spherical aberration, etc. that might be caused by CTE non-uniformities in the mirror substrate or residual effects of the mirror mount.

The third key contributor to wavefront error will be thermal gradients in the telescope. LUTE mass limitations preclude the use of a power system that can provide a stable thermal environment. Thus, as the 28 day long lunar "day" progresses there will be a changing thermal distribution in the telescope. If the mirror has a gradient in its CTE then a temperature change will produce a non-correctable figure error. Unfortunately, even if the mirror substrate has a perfectly uniform CTE, a thermal gradient in the mirror will produce a figure error. We have separated these two effects as an analytical tool for the study of primary mirror material and geometry.

3.3 WEIGHT ALLOCATION

Our weight budget allocations are based on our understanding of the LUTE telescope subsystem. We have assumed that an allocation of 84 kg total mass has been given to the telescope subsystem based on LUTE system engineering analyses done at MSFC. We have sub-allocated this 84 kg total into five major categories. They are:

- Mirrors
- Structure
- Electronics
- Thermal Control
- Alignment Sensor

These major categories and the weight allocations are shown in Table 3-1.

TABLE 3-1
LUTE TELESCOPE WEIGHT BUDGET DEFINED TO CONDUCT FEASIBILITY STUDY

Major Element	Sub-Assembly/Component	Weight (lbs)	Weight (kg)
1) Mirrors	Primary Mirror	48	21.9
	Secondary Mirror	6	2.7
	Tertiary Mirror	3	1.4
	Sub-Total	57	25.9
2) Structure	Baffle Subassembly		
	• Main	9	4.1
	• Central	2	0.9
	• SM	1	0.5
	Sub-Total	12	5.5
	Mirror Mounts		
	• PM	5	2.3
	• SM	3	1.4
	• TM	2	0.9
	Sub-Total	10	4.5
	Main Bulkhead Subassembly		
	• Main bulkhead	12	5.5
	• S/C interface fittings (3)	3	1.4
	Sub-Total	15	6.8
	Metering Bar Subassembly		
	• Metering bars (3)	3	1.4
	• Interface fittings (6)	3	1.4
	Sub-Total	6	2.7
	SM Subassembly		
	• Spider	4	1.8
	• Hub	3	1.4
	• Spider ring	3	1.4
	• Spider flexures (3)	3	1.4
	• Actuators (6)	6	2.7
	• Cabling	4	1.8
	Sub-Total	23	10.5
3) Electronics	ACE	3	1.4
	TCE	3	1.4
	DMS	3	1.4
	ASE	3	1.4
	Sub-Total	12	5.5
4) Thermal Control	Heaters	2	0.9
	Thermocouple	2	0.9
	MLI	3	1.4
	Sub-Total	7	3.2
5) Alignment Sensor	Sensor	10	4.5
	Sensor mount	2	0.9
	Sub-Total	12	5.5
	Total (w/o reserve):	154.0	70
	Reserve	31.6	14
	TOTAL	185.6	84

Based on our experience with other flight programs, we believe that a nominal value of 18% of the total 84 kg should be held in reserve for contingency factors. It is our experience that at this early stage in the development of a program, it is absolutely necessary to carry (at least) such a factor. As shown in Table 3-2, this schedule changes as a function of program maturity.

TABLE 3-2
WEIGHT CONTINGENCY SCHEDULE

Design Maturity	Contingency Factor (%)			
	Structures	Mechanisms	Wire/Cable	Therm. Control
Conceptual Estimate (Based on sketches, descriptions, experience, or finite element model)	18	18	33	18
Layout calculation (Equivalent to major mod's of existing hardware or soft mockup)	13	13	18	13
Prereleased drawings	3	3	8	8
Released drawings	1	1	2	2
Actual/measured weight	0	0	0	0

3.4 QUASI-STATIC LOADS

Once our weight allocations were established, we conducted a "zeroth order" stress analysis on several telescope components to ensure that some level of credibility existed for those allocations. We used a quasi-static load of 15-g's rms, applied singly in each of three orthogonal directions. The 15-g level is considered a limit load factor. Factors of safety of 1.25 and 1.5 for yield and ultimate criteria were used to assess the resulting design load factors. These design load factors are fully consistent with other flight programs that have used for expendable launch vehicles (ELV) including Titan IV, Delta II, and Atlas/Centaur.

A coupled loads analysis will eventually be required in order to attain more specific loads at each location of the telescope subsystem. This analysis will take into consideration the contribution of both "rigid" and "elastic" body effects due to transient, random vibration, steady state, and acoustic environments during ascent. However, this analysis may be deferred until a more definitive architecture for both the telescope subsystem and the spacecraft is in place.

The fundamental frequency of the telescope subsystem and each component is also a variable in the determination of flight load levels. There are generally two overriding concerns when trying to determine requirements for natural frequencies. The first is what is termed "avoidance frequencies." We desire the telescope to be sufficiently stiff relative to the ELV to avoid possible amplification of loads which might result if the elastic body (e.g. the telescope) dynamically couples into the launch vehicle modes. As an example, the Titan IV vehicle has two distinct avoidance frequencies; from 6-10 Hz in the lateral direction and 17-24 Hz in the axial (e.g. thrust) direction. If a high mass system's natural frequency is sitting between these bands, dynamically amplified loads will probably occur.

The second fundamental frequency requirement is derived from control system servo/structural interaction concerns. If the telescope has a closed loop servo system such as a fast steering mirror it is highly desirable that the structural modes be considerably higher than the bandwidth of the servo. Since we do not envision any closed loop active systems being implemented for LUTE, this requirement is not of concern here.

To address fundamental frequency requirements we have set as a guideline that we desire that the telescope be sufficiently stiff so that no amplification of loads will exist during ascent. To this end we have derived a requirement that the telescope, assuming a fixed base at the spacecraft interface (i.e. approximately 0.25 meters aft of the primary mirror virtual vertex), should have a fundamental frequency of at least 50 Hz. With this top level telescope requirement we have determined that a primary mirror natural frequency, assuming a three point rigid mount, should be greater than 150 Hz. This requirement has been used in our assessment of primary mirror substrates and designs.

3.5 MICROROUGHNESS

We have allocated a small portion of the LUTE wavefront error budget for the effects of mirror roughness at high spatial frequencies. The effects of microroughness become increasingly important as the operating wavelength decreases. Microroughness increases the amount of wide angle scatter that would increase the stray light seen by the focal plane detector. We have done no analysis in support of the allocation.

The applicability of beryllium mirror for the LUTE ultraviolet wavelengths also remains somewhat in question. We have considerable experience in polishing beryllium mirrors "bare" (uncoated) but they may exhibit too much scatter to be suitable for wavelengths as short as 0.1 μm. It is possible to overcoat beryllium mirrors with either beryllium or aluminum to reduce the amount of scatter, but one must then be careful about the magnitude of any thermal-induced "bi-metallic" effects. Analytical models of the effects of thin films have an additional uncertainty associated with the uncertainty in the

mechanical properties of very thin films. It is our judgment that beryllium mirrors can be polished to meet LUTE's scatter requirements but we currently lack physical proof.

The lunar environment is well-known to be dusty. Furthermore, dust particles are likely to travel very long distances in the airless environment. Thus, although it may be possible to fabricate a very smooth optical surface, lunar dust contamination could severely degrade system performance, both in terms of stray light rejection and throughput. Protection from dust, perhaps including sensors, a protective cover, and a means for *in situ* cleaning may be required by LUTE, but we have not included such subsystems in the weight budget.

3.6 COATING REFLECTANCE

We have computed the normal incidence reflectance of several candidate coatings for the LUTE telescope. The reflectances (plotted for a single reflection; note that LUTE requires three reflections) are shown in Figure 3-4. For the majority of materials that are well-known to be good reflectors at visible wavelengths, the UV reflectance shows a dramatic decrease. Silicon carbide and beryllium are somewhat exceptions to this trend, but neither exhibit excellent UV reflectance.

Aluminum appears to be an excellent reflector at wavelengths as short as 0.1 μm. However, it must be emphasized that the plotted values are for bare aluminum, without an oxide layer as would result if an aluminized mirror were exposed even to very small amounts of oxygen. A typical approach to this problem is to immediately follow the aluminum deposition with, for example, magnesium fluoride, while the mirror remains under high vacuum. The overcoating prevents oxidation of the aluminum without significantly absorbing UV photons. We have not computed reflectances for overcoated materials as part of this study.

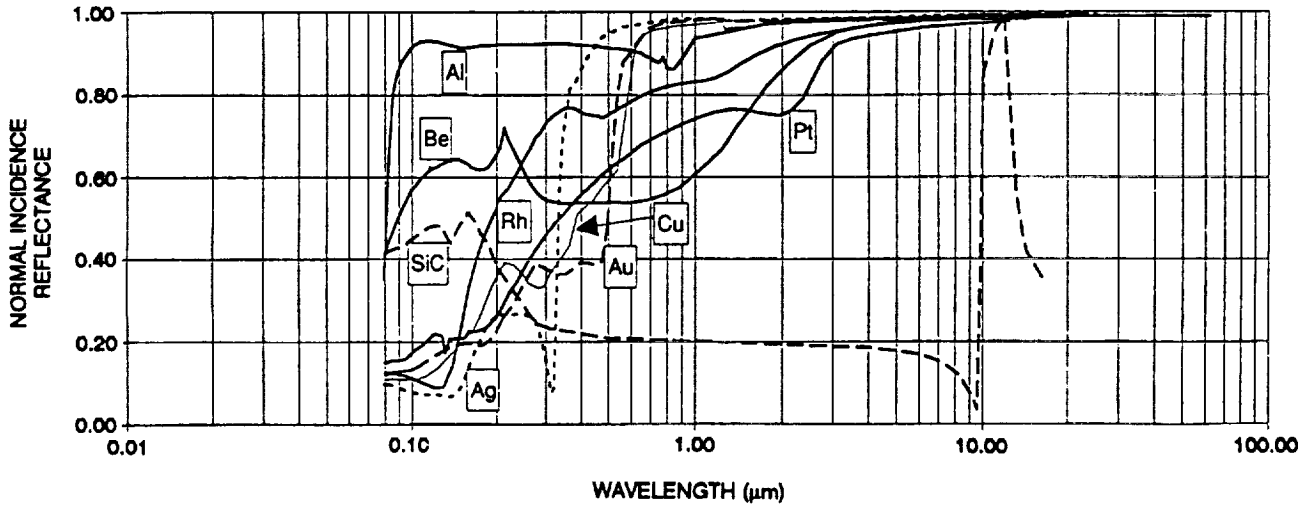

Figure 3-4. UV-to-IR Normal Incidence Reflectances of Candidate Coatings.

Optical coating of the LUTE mirrors remains a key issue for wavefront error performance. That is, since the operating temperature is far below the coating deposition temperature, and since the coating material will probably have a very different CTE than the substrate, coating stresses may deform the mirrors. The addition of an overcoat compounds this problem since it adds a third material. Analytical study of the wavefront effects of coatings is difficult since it is unclear that thin films have the same mechanical properties as the bulk material.

An alternative to overcoating remains a possibility for LUTE, but it is as-yet, an untried approach. Future LUTE studies should consider re-coating the mirror(s) in situ. Presumably there is insufficient oxygen in the lunar environment to oxidize the freshly-coated aluminum, and there would be no need for an overcoat layer.

3.7 METERING STRUCTURE

Several candidate metering structures are available to use for the LUTE telescope subsystem. These candidates are summarized in Figure 3-5.

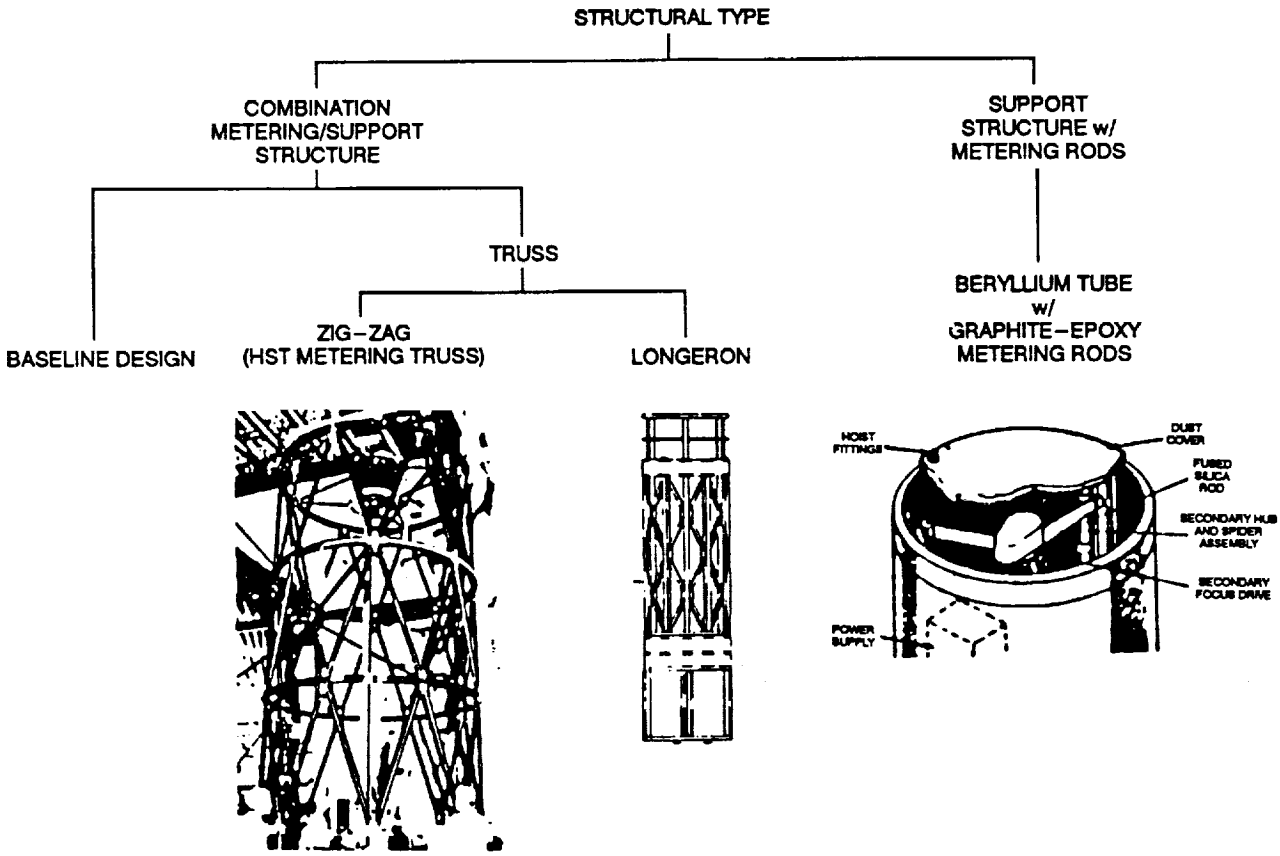

Figure 3-5. Various Candidate Metering Truss Designs Are Available for LUTE. Active thermal control could dictate preference. "Baseline Design" is a ring stiffened tube.

Although we did not conduct analyses on the LUTE metering structure, results conducted on other programs showing the optimum truss design for a given weight (see Figure 3-6) are directly applicable when considering a design which yields a high fundamental frequency for low weight. It is of interest that the "baseline design" (i.e. a ring-stiffened tube) for this particular trade space far surpasses both truss designs.

A variation of the metering structure is a support structure with metering rods. This design concept was successfully implemented on the OAO-C, an 80-cm UV orbiting telescope. Schematically shown

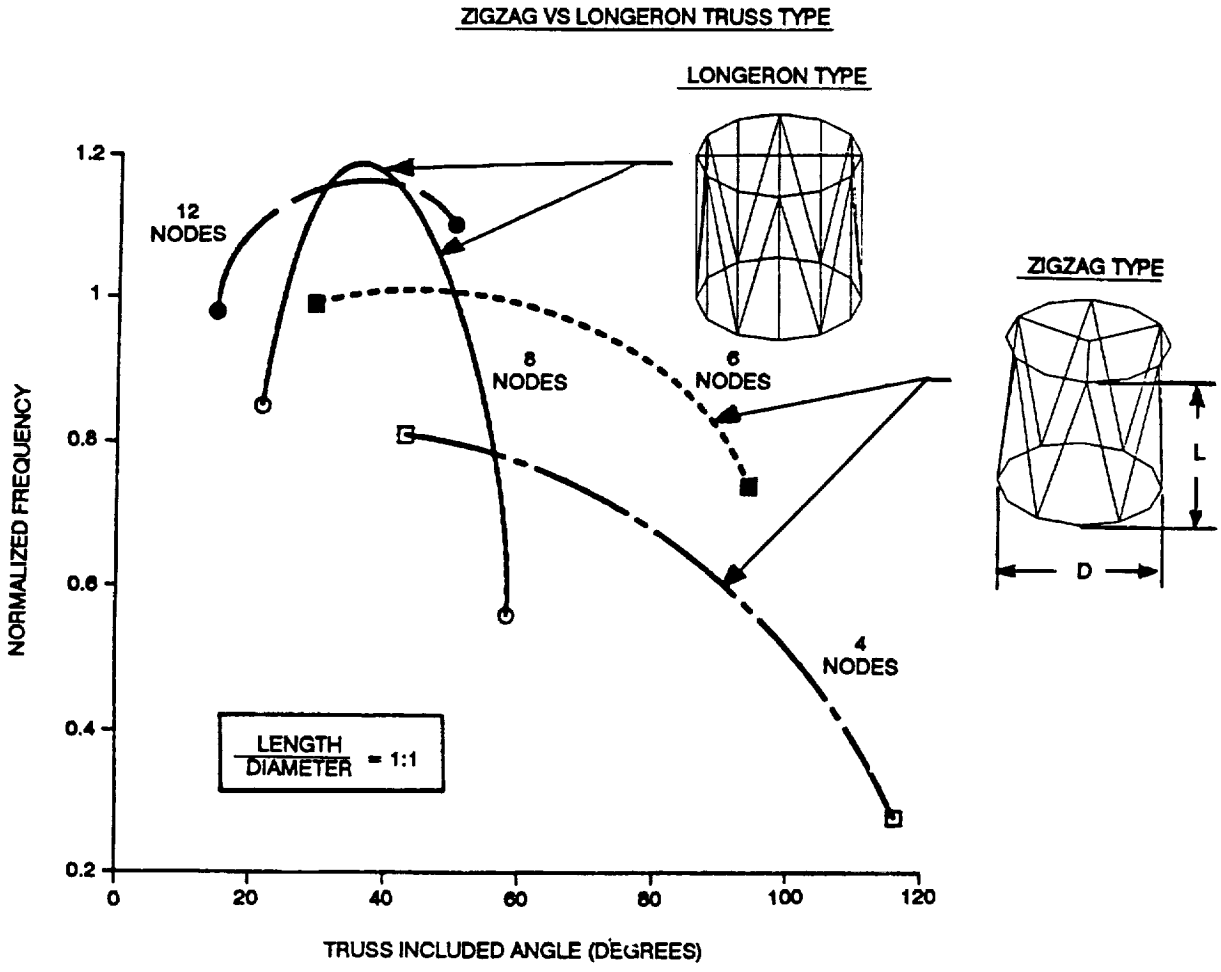

Figure 3-6. Results from Other Programs Can Be Applied to LUTE Specific Investigations. Metering structure type trades obtain high frequency and low weight.

in Figure 3-7 (for a Gregorian Telescope), this design is especially attractive if fabricated from beryllium, due to its outstanding stiffness to weight ratio. However, since beryllium's CTE properties would require the telescope to maintain very tight lateral temperature control, low CTE metering rods are employed to maintain primary mirror to secondary mirror despace and decenter within acceptable limits. These metering rods are attached to the main baffle by axial flexures at their centers and tangential flexures at their ends. With this design, should the structure "hot-dog" due to a side-to-side temperature gradient, both primary and secondary mirrors would decenter equal amounts with no relative tilts.

- ALLOWS THE USE OF BERYLLIUM FOR MAIN SUPPORT STRUCTURE
  - –OUTSTANDING STIFFNESS TO WEIGHT PERFORMANCE
  - –HIGH CTE
- APPROACH EMPLOYS LOW CTE METERING RODS TO MAINTAIN MIRROR SPACING

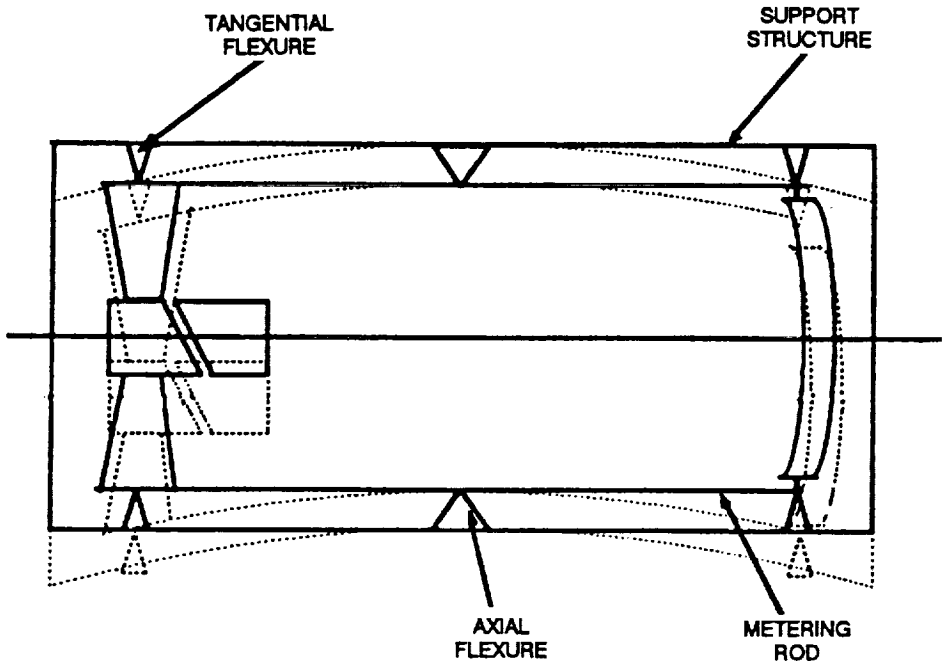

Figure 3-7. The Support Structure with Metering Rod Design Allows A High CTE Material to Be Used in the Presence of Large Side-To-Side Temperature Gradients.

3.8 DESIGN SPECIFICATION

Our design specification for the LUTE primary mirror is the combination of information described in the preceding paragraphs. The driving requirements which form the basis of this specification are shown in Table 3-3.

TABLE 3-3
SPECIFICATIONS FOR LUTE PRIMARY MIRROR

Item	Requirements/Goals
Optical Design	3 mirror telescope Diffraction limited @ 0.6328 μm 1 meter class Operating wavelength = 0.1 to 0.35 μm Throughput: > TBD BRDF: < TBD PM WFE: < 1/30 waves rms @ 0.6328 μm
Mechanical Configuration	Passive primary mirror Passive telescope thermal control Mass < 84 kg (including contingency)
Environment	Operating temperature range: - 260 K to 60 K - lunar day/night period Launch loads: - 15 g's (limit) x FOS Yield FOS = 1.25 Ultimate FOS = 1.5
Fundamental Frequency	Telescope: > 50 Hz Primary mirror: > 150 Hz

SECTION 4
PRIMARY MIRROR CANDIDATE MATERIALS AND CONFIGURATIONS

We conducted an extensive investigation of candidate primary mirror substrate materials and geometries which was then evaluated against the requirements, as stated in Section 3.8, to assess their suitability for the LUTE telescope.

4.1 SUBSTRATE MATERIALS AND DESIGNS

A broad range of substrate materials were investigated and evaluated against the applicable LUTE telescope requirements. The substrate materials we investigated are shown in Table 4-1.

TABLE 4-1
LUTE SUBSTRATE MATERIALS

Materials/Supplier	Evaluation Criteria
1) Glasses	
• Fused Quartz/Silica	• Repeatability
- Corning 7940	• Homogeneity
- Heraeus Suprasil	• Isotropy
- Heraeus Herasil	• Size Availability
• Ultra-Low Expansion (ULE)	• Inspectability
- Corning 7971	• Specific Stiffness
• Borosilicate	• Lightweighting Compatibility
- Corning Pyrex	• Cryogenic Heritage
- Ohara E6	• Polishability
2) Ceramics	• Conductivity and Specific Heat
• Zerodur	• Coating Compatibility
- Schott Glaswerks	• Strength
• Silicon Carbide (Reaction Bonded)	• Cost
- Carborundum	• Schedule
3) Metallics	
• HIP Beryllium	
- Battelle	

Fused quartz and fused silica are both amorphous silicon dioxide (SiO2) but differ in that fused quartz is manufactured from mined, high purity quartz crystals while fused silica is synthetic. From prior programs we have obtained an extensive library on the CTE, $\Delta L/L$, Young's Modulus, and Poisson's Ratio characteristics as a function of temperature, ranging from room temperature (293 K) to ~ 1 K. Although our library on these parameters for the remaining materials is not as extensive as for fused quartz, the data on hand is from several sources and, we feel, is a good representation of actual values.

We continue to develop our experience base in both silicon carbide and beryllium substrates (see Paragraph 4.2). Although there are a number a candidate silicon carbide vendors, we have worked closely with Carborundum Specialty Products (CSP) Corporation using their reaction-bonded SiC. Reaction bonded SiC is an open network of alpha SiC crystals which has its pores completely filled with silicon, thereby producing a material which is 100% dense.

Our beryllium substrate candidate design is centered around the fabrication technique termed hot isostatic pressing (HIP) which uses beryllium powder in a high temperature, high pressure environment to produce near-net-shape optics.

Along with the substrate candidates mentioned above we also evaluated a number a primary mirror geometries. Figure 4-1 shows that a large range of structural designs are available for use as the LUTE primary mirror.

4.2 USAGE HISTORY

Performance data from demonstrated telescopes and mirrors with apertures greater than or equal to 0.5 meter in diameter that are exposed to cryogenic environments is summarized in Table 4-2. This information was employed in areal density (mass per unit area) surveys along with understanding the cryogenic cooling-induced deformation of the mirror. Our survey of demonstrated mirrors at cryogenic temperatures revealed a wide range of substrate material, mirror design and performance.

4.3 THERMAL PERFORMANCE

Figure 4-2 shows the flow of our approach to evaluating mirror materials and geometries for thermal distortion effects. There are two outputs, the allowable thermal gradient and the allowable $\Delta L/L$ gradient that would meet the wavefront error budget. We emphasize here that the structural analysis sensitivities were scaled from analyses done for another cryogenic telescope program.

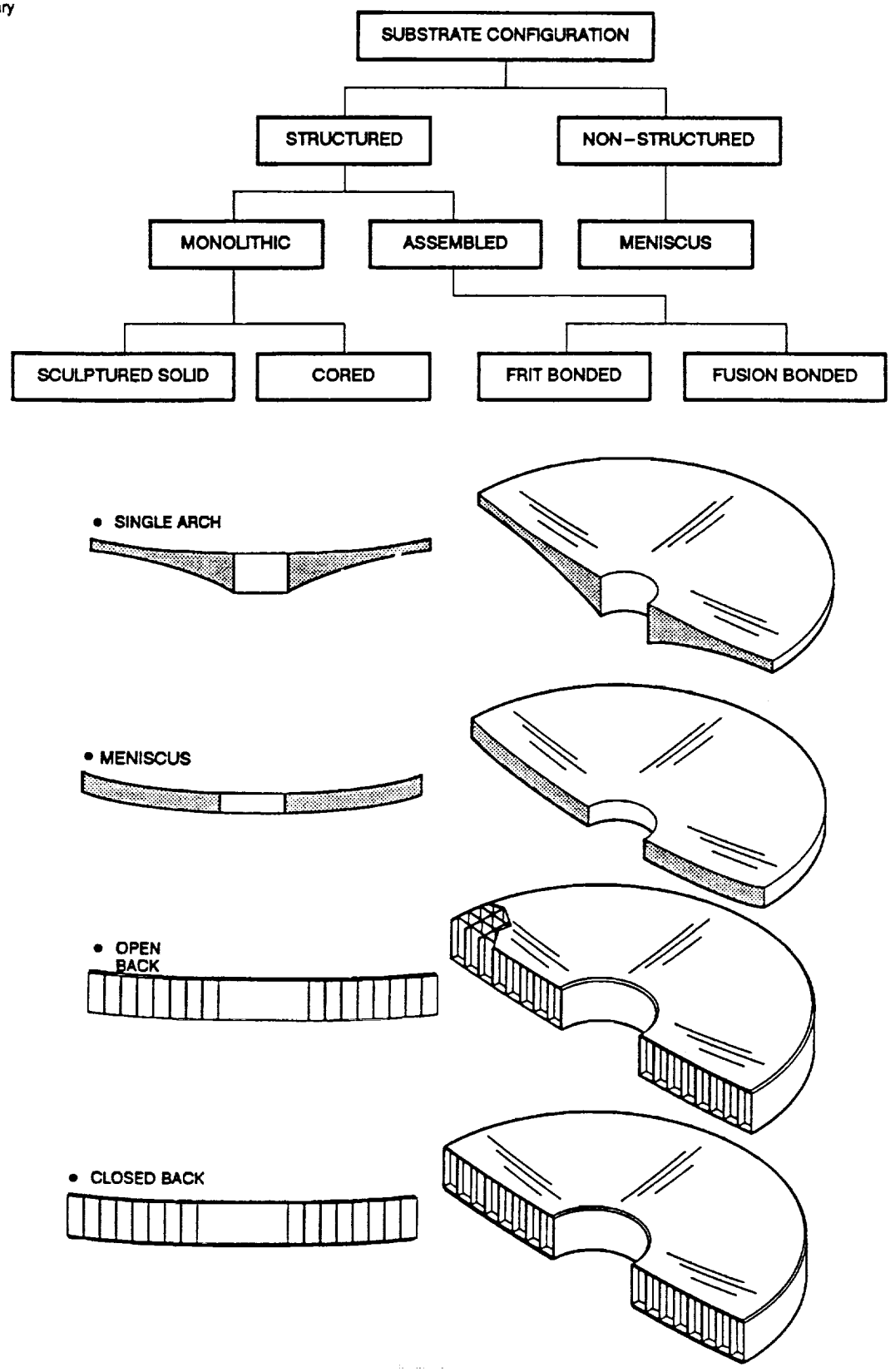

Figure 4-1. The Lute Study Investigation Yielded Various Mirror Geometries.

TABLE 4-2
CRYOGENIC MIRROR PERFORMANCE DATA

Name	Dia. (m)	Density (kg/m^2)	Temp. (K)	Cryo WF Distor'n (rms @ 0.63 μm)	Config/Mat'l
RADC/HDOS	0.4	23	110	n/a	Closed Back HIP Beryllium
ARC/Steward	0.4	55	80	0.18	Closed Back Pyrex
ARC/U of A	0.5	96	6	0.30	Double Arch Fused Silica
ARC/U of A	0.5	78	10	0.26	Single Arch Heraeus TO8E
GIRL	0.5	127	8	n/a	Open Back Zerodur
DARPA/EK	0.5	23	8	0.19	Closed Back Fused Silica
ARC/HDOS	0.5	28	8	0.46	Single Arch Beryllium
Aerosp./ISO	0.6	70	10	0.16	Open Back Fused Quartz
IRAS/HDOS	0.6	45	25	0.68	Open Back HIP Beryllium
Heraeus/Itek	0.7	57	15	0.52	Closed Back Fused Quartz
HAC/AOA	0.7 × 0.6	52	80	0.50	Open Back Fused Quartz
HAC/AOA	0.9 × 0.4	70	80	0.50	Open Back Fused Quartz
RADC/HDOS	1.0	23	110	0.37	Open Back HIP Beryllium

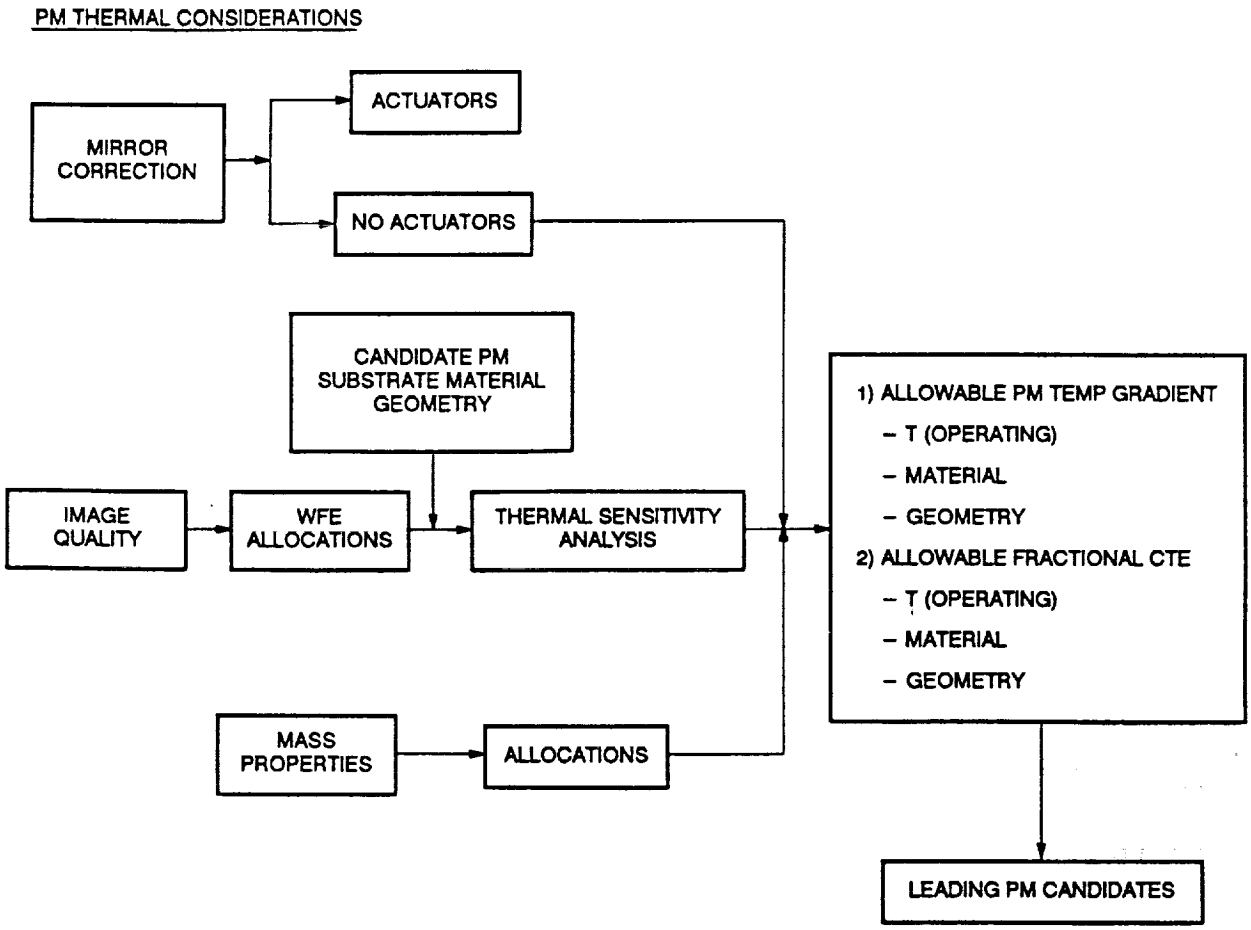

Figure 4-2. LUTE PM Materials and Design Study Thermal Considerations.

We did not generate new finite element models specifically for the LUTE study and the results are only approximate. Unfortunately, the effects of a thermal gradient that may exist in the primary mirror is also a function of the thermal conductivity of the mirror material. Both beryllium and silicon carbide have extremely high thermal conductivities compared to the glassy materials. Thus, beryllium and silicon carbide mirrors would not tend to develop significant thermal gradients. As part of this study we did not compute the thermal gradients that would actually be developed in the primary mirror in the lunar environment. This portion of the study is therefore based upon choosing materials and geometries based upon relative sensitivities and not on predicted deformations.

Figure 4-3 shows several examples of the results of our investigation into thermal gradient effects on the primary mirror wavefront error. The intent of the investigation was to determine if one material and one mirror geometry exhibited a particular insensitivity to thermal gradients. The wavefront error

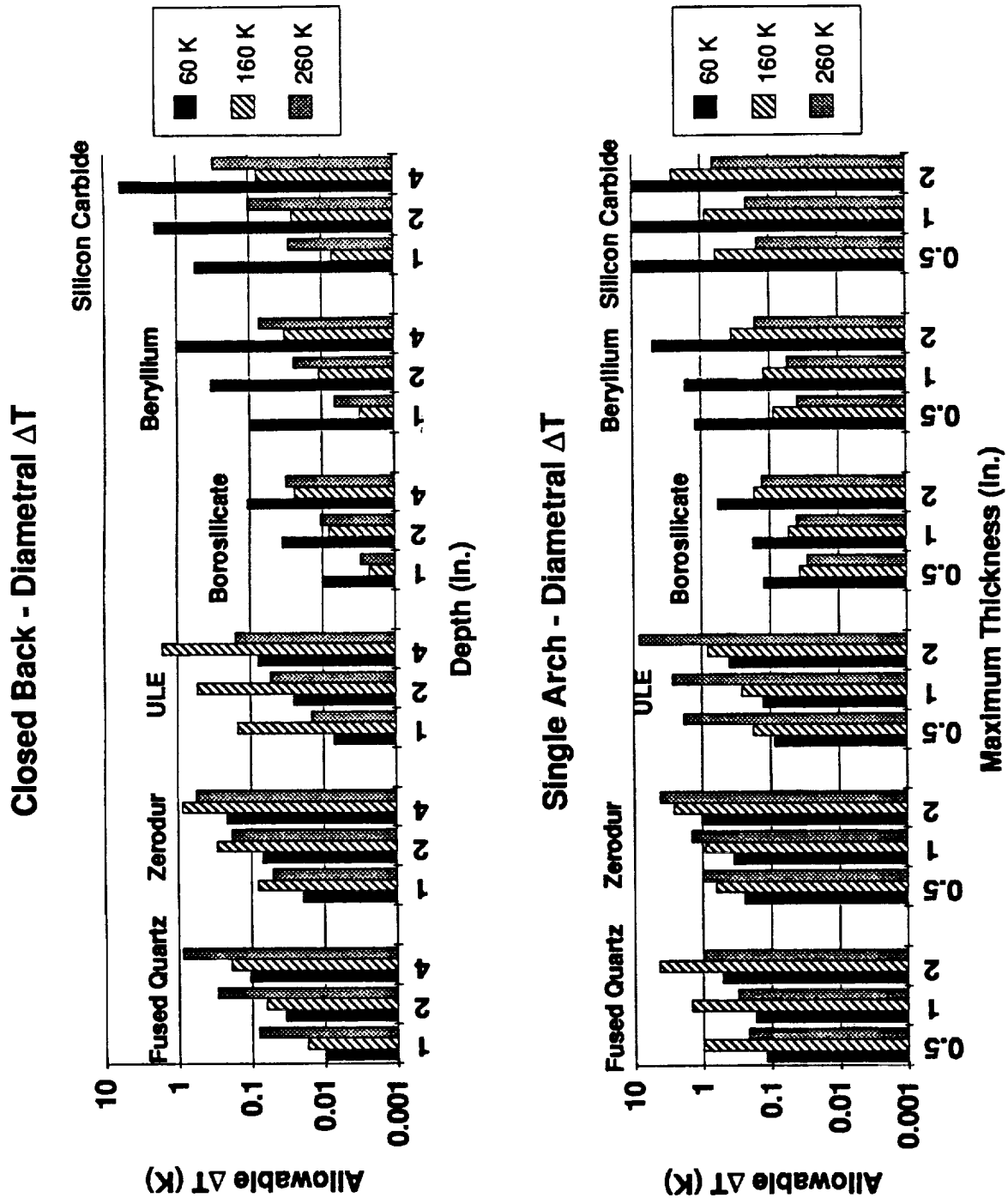

Figure 4-3. LUTE PM Materials and Design Study Performance Results (Closed Back and Single Arch-Diametral ΔT.)

budget used for this effect was 0.0063 waves rms (1 wave=0.6328 μm.) We computed the wavefront deformation assuming that the lowest order deformations could be removed by realignment of the secondary mirror.

The analysis uses the CTE of each material at the designated temperatures. We chose 60 K (the coldest temperature), 160 K (the "mean" temperature) and 260 K (the highest temperature) for the comparisons.

Inspection of Figure 4-3 shows that the single arch mirror has a consistently lower sensitivity to diametral thermal gradients than does the closed back mirror geometry. That is, the single arch mirror can tolerate larger thermal gradients than the closed back mirror before exceeding the wavefront error budget for this effect. Note that one limitation of this comparison is that mass is not constant between the various cases.

It is clear from Figure 4-3 that materials with a lower CTE can tolerate larger thermal gradients than materials with higher CTE's. For example, borosilicate (e.g. Pyrex) has a higher CTE at all three temperatures than beryllium and has a lower modulus. Therefore borosilicate mirrors are particularly sensitive to optical deformation from thermal gradients. Silicon carbide has an even lower CTE than beryllium, and combined with its high modulus it has superior low temperature performance. However, note that at 260 K, fused quartz is superior due to its very low CTE at that temperature. Thus, it is clear that the preferred material and geometry are a function of operating temperature and operating temperature range.

Figure 4-4 compares the sensitivities of a meniscus geometry with that of a single arch in terms of the effects of gradients in CTE (actually $\Delta L/L$.) We have used the actual CTE's of the various materials, integrated over three different temperature ranges. The wavefront error budget for the bulk ΔT (293 K to 160 K) was 0.0168 waves rms. The budget for 60 K to 160 K and for 160 K to 260 K was 0.0125 waves. In all cases the lowest order aberrations were neglected as they were assumed to be correctable using a secondary mirror mechanism.

The single arch geometry is more tolerant of a radially symmetric CTE variation than the meniscus geometry. In the 60 K to 160 K range the material most tolerant of CTE gradients is silicon carbide. In that temperature range it has an exceptionally low $\Delta L/L$, even lower than the glass and its high stiffness is an additional advantage.

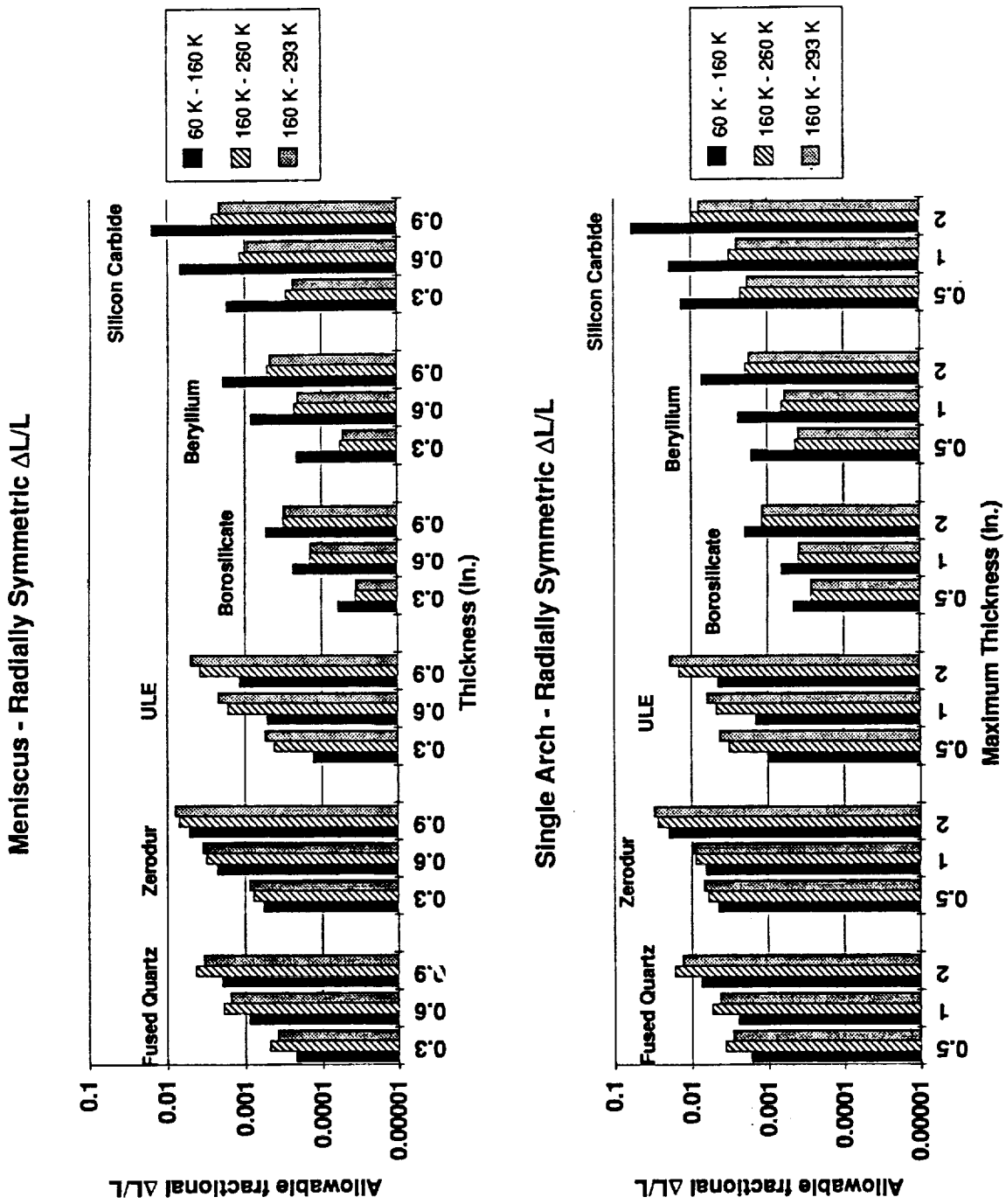

Figure 4-4. LUTE PM Materials and Design Study Performance Results (Meniscus and Single Arch-Radially Symmetric ΔL/L).

However, at the higher temperatures the glasses have the largest tolerance for CTE gradients. Beryllium, the preferred material from a structural (mass) viewpoint, does not fare very well in this comparison. It requires that the center to edge $\Delta L/L$ variation not exceed about 0.1%. Such a tolerance on a beryllium mirror's CTE gradient may be achievable but we have confirmed this as part of our study.

4.4 STRUCTURAL PERFORMANCE AND MASS PROPERTIES ESTIMATES

The logic used to assess the structural applicability of a particular substrate and mirror design for use as the LUTE primary mirror is shown in Figure 4-5. The critical requirements when making this assessment is the weight allocation of 21.8 kg (see paragraph 3.3), fundamental frequency greater than 150 Hz, and a 5/6-g release uncertainty of less than 0.0063 waves rms at 0.6328 μm.

The structural analyses conducted to assess each candidate design against the above requirements is summarized in Tables 4-3 through 4-6. These results present 1 g sag, fundamental frequency, and weight estimate results for each mirror geometry and substrate material investigated. For the meniscus, closed back and open back mirror designs, the effects of varying the mirror mount locations (e.g. at the 2/3 radius points versus edge supported) is also presented. These results are very good indicators for the relative performance of one design versus another. However, as previously stated, we

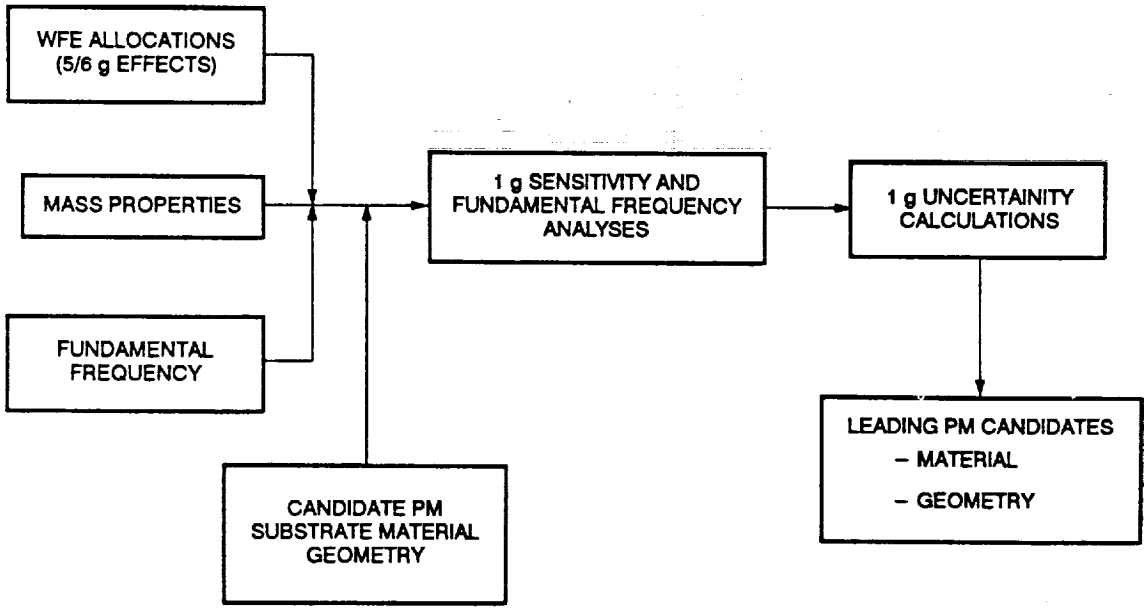

Figure 4-5. Major Structural Considerations Were Quantified to Determine Leading Candidate Designs.

TABLE 4-3
MENISCUS MIRROR - THREE POINT SUPPORTED - PERFORMANCE RESULTS

				Spread Sheet for Calculating 1-g Sag & Fund. Frequency										G. Puthven 12/10/92	
							Mirror Supported at Outer Diameter				Mirror Supported at 2/3 Radius				
Mirror Type	Radius (inch)	Equiv. Thickness (inch)	Density (lbs/in^3)	Weight (lbs)	Young's (psi)	Nu	Defl'n (in)	Defl'n (um)	Est. WFE (um) Z(8-23)-um	Freq (Hz)	Defl'n (in)	Defl'n (um)	Est. WFE (um) Z(8-23)-um	Freq (Hz)
1) Meniscus	20.69	0.3	0.079	24.53	10200000	0.17	0.01608	408.6	51.1	24.7	0.00366	92.8	23.2	51.8
• Fused Quartz	20.69	0.6	0.079	49.06	10200000	0.17	0.00402	102.1	12.8	49.4	0.00091	23.2	5.8	103.6
	20.69	0.9	0.079	73.59	10200000	0.17	0.00179	45.4	5.7	74.0	0.00041	10.3	2.6	155.3
• Zerodur	20.69	0.3	0.091	28.26	13200000	0.24	0.01389	352.9	44.1	26.6	0.00316	80.2	20.1	55.7
	20.69	0.6	0.091	56.51	13200000	0.24	0.00347	88.2	11.0	53.1	0.00079	20.1	5.0	111.4
	20.69	0.9	0.091	84.77	13200000	0.24	0.00154	39.2	4.9	79.7	0.00035	8.9	2.2	167.1
• ULE	20.69	0.3	0.079	24.53	9600000	0.22	0.01640	416.7	52.1	24.4	0.00373	94.7	23.7	51.3
	20.69	0.6	0.079	49.06	9600000	0.22	0.00410	104.2	13.0	48.9	0.00093	23.7	5.9	102.5
	20.69	0.9	0.079	73.59	9600000	0.22	0.00182	46.3	5.8	73.3	0.00041	10.5	2.6	153.8
• Borosilicate	20.69	0.3	0.088	26.39	9500000	0.22	0.01821	462.5	57.8	23.2	0.00414	105.1	26.3	48.7
	20.69	0.6	0.088	52.79	9500000	0.22	0.00455	115.6	14.5	46.4	0.00103	26.3	6.6	97.3
	20.69	0.9	0.088	79.18	9500000	0.22	0.00202	51.4	6.4	69.6	0.00046	11.7	2.9	146.0
• Beryllium	20.69	0.3	0.067	20.80	42000000	0.07	0.00339	86.2	10.8	53.7	0.00077	19.6	4.9	112.7
	20.69	0.6	0.067	41.61	42000000	0.07	0.00086	21.8	2.7	107.4	0.00019	4.9	1.2	225.4
	20.69	0.9	0.067	62.41	42000000	0.07	0.00038	9.6	1.2	161.2	0.00009	2.2	0.6	338.1
• Silicon Carbide	20.69	0.3	0.106	32.91	47000000	0.2	0.00463	117.6	14.7	46.0	0.00105	26.7	6.7	96.5
	20.69	0.6	0.106	66.83	47000000	0.2	0.00116	29.4	3.7	92.0	0.00026	6.7	1.7	193.0
	20.69	0.9	0.106	98.74	47000000	0.2	0.00051	13.1	1.6	138.0	0.00012	3.0	0.7	289.5

TABLE 4-4
OPEN BACK MIRROR - THREE POINT SUPPORTED - PERFORMANCE RESULTS

				Spread Sheet for Calculating 1-g Sag & Fund. Frequency									G. Puthven 12/10/92	
							Mirror Supported at Outer Diameter				Mirror Supported at 2/3 Radius			
Mirror Type	Radius (inch)	Depth (inch)	Density (lbs/in^3)	Weight (lbs)	Young's (psi)	Nu	Def'n (in)	Def'n (um)	Est. WFE (um) Z(6-23)-um	Freq (Hz)	Def'n (in)	Def'n (um)	Est. WFE (um) Z(6-23)-um	Freq (Hz)
2) Open Back	20.69	1	0.079	32.71	10200000	0.17	0.00228	58.0	19.3	66.6	0.00052	13.19	4.62	137.4
- Fused Quartz	20.69	2	0.079	49.06	10200000	0.17	0.00074	18.7	6.2	116.4	0.00017	4.26	1.49	242.0
	20.69	4	0.079	81.77	10200000	0.17	0.00018	4.6	1.5	236.3	0.00004	1.01	0.36	495.8
- Zerodur	20.69	1	0.091	37.67	13200000	0.24	0.00197	50.1	16.7	70.8	0.00045	11.39	3.99	147.8
	20.69	2	0.091	56.51	13200000	0.24	0.00064	16.2	5.4	124.1	0.00014	3.67	1.28	260.4
	20.69	4	0.091	94.19	13200000	0.24	0.00015	3.8	1.3	264.3	0.00003	0.87	0.31	553.4
- ULE	20.69	1	0.079	32.71	9600000	0.22	0.00233	59.2	19.7	64.8	0.00053	13.45	4.71	136.0
	20.69	2	0.079	49.06	9600000	0.22	0.00075	19.1	6.4	114.2	0.00017	4.33	1.52	239.6
	20.69	4	0.079	81.77	9600000	0.22	0.00018	4.6	1.5	234.0	0.00004	1.03	0.36	490.9
- Borosilicate	20.69	1	0.086	36.19	9600000	0.22	0.00259	65.7	21.9	61.8	0.00059	14.93	5.22	129.1
	20.69	2	0.086	52.79	9600000	0.22	0.00083	21.2	7.1	108.4	0.00019	4.81	1.68	227.5
	20.69	4	0.086	87.98	9600000	0.22	0.00020	5.0	1.7	222.1	0.00005	1.15	0.40	466.9
- Beryllium	20.69	1	0.067	27.74	42000000	0.07	0.00048	12.2	4.1	142.6	0.00011	2.78	0.97	299.0
	20.69	2	0.067	41.61	42000000	0.07	0.00015	3.9	1.3	251.1	0.00004	0.90	0.31	526.8
	20.69	4	0.067	69.35	42000000	0.07	0.00004	0.9	0.3	514.4	0.00001	0.21	0.07	1079.1
- Silicon Carbide	20.69	1	0.106	43.88	47000000	0.3	0.00066	16.7	5.6	122.1	0.00015	3.80	1.33	256.0
	20.69	2	0.106	65.83	47000000	0.3	0.00021	5.4	1.8	215.0	0.00005	1.22	0.43	451.0
	20.69	4	0.106	109.71	47000000	0.3	0.00005	1.3	0.4	440.9	0.00001	0.29	0.10	924.9

TABLE 4-5
CLOSED BACK MIRROR - THREE POINT SUPPORTED - PERFORMANCE RESULTS

				Spread Sheet for Calculating 1-g Sag & Fund. Frequency										G. Ruthven 12/10/92	
							Mirror Supported at Outer Diameter				Mirror Supported at 2/3 Radius				
Mirror Type	Radius (inch)	Depth (inch)	Density (lbs/in^3)	Weight (lbs)	Young's (psi)	Nu	Defl'n (in)	Defl'n (um)	Est. WFE (um) Z(6-23)-um	Freq (Hz)	Defl'n (in)	Defl'n (um)	Est. WFE (um) Z(6-23)-um	Freq (Hz)
3) Closed Back	20.69	1	0.079	36.98	10200000	0.17	0.00139	35.19	11.73	84.1	0.00031	8.00	2.80	176.4
• Fused Quartz	20.69	2	0.079	52.33	10200000	0.17	0.00039	9.84	3.28	159.0	0.00009	2.24	0.78	333.6
	20.69	4	0.079	85.04	10200000	0.17	0.00012	3.12	1.04	282.6	0.00003	0.71	0.26	592.6
• Zerodur	20.69	1	0.091	41.44	13200000	0.24	0.00128	30.39	10.13	90.5	0.00027	6.91	2.42	189.8
	20.69	2	0.091	60.28	13200000	0.24	0.00033	8.50	2.83	171.1	0.00008	1.93	0.68	358.9
	20.69	4	0.091	97.96	13200000	0.24	0.00011	2.69	0.90	303.9	0.00002	0.61	0.21	637.6
• ULE	20.69	1	0.079	36.98	9800000	0.22	0.00141	35.89	11.96	83.3	0.00032	8.16	2.86	174.7
	20.69	2	0.079	52.33	9800000	0.22	0.00040	10.04	3.35	157.5	0.00009	2.28	0.80	330.3
	20.69	4	0.079	85.04	9800000	0.22	0.00013	3.18	1.06	279.7	0.00003	0.72	0.25	586.7
• Borosilicate	20.69	1	0.085	39.71	9600000	0.22	0.00157	39.83	13.28	79.0	0.00036	9.06	3.17	165.9
	20.69	2	0.085	56.30	9600000	0.22	0.00044	11.14	3.71	149.5	0.00010	2.53	0.89	313.6
	20.69	4	0.085	91.49	9600000	0.22	0.00014	3.53	1.18	265.5	0.00003	0.80	0.28	556.9
• Beryllium	20.69	1	0.067	30.51	42000000	0.07	0.00029	7.43	2.48	183.1	0.00007	1.69	0.59	384.0
	20.69	2	0.067	44.38	42000000	0.07	0.00008	2.08	0.69	348.2	0.00002	0.47	0.17	726.1
	20.69	4	0.067	72.12	42000000	0.07	0.00003	0.66	0.22	614.9	0.00001	0.15	0.06	1289.7
• Silicon Carbide	20.69	1	0.106	48.27	47000000	0.2	0.00040	10.13	3.38	166.7	0.00009	2.30	0.81	328.8
	20.69	2	0.106	79.21	47000000	0.2	0.00011	2.83	0.94	296.4	0.00003	0.64	0.23	621.6
	20.69	4	0.106	114.10	47000000	0.2	0.00004	0.90	0.30	526.8	0.00001	0.20	0.07	1104.4

TABLE 4-6
SINGLE ARCH MIRROR - THREE POINT SUPPORTED - PERFORMANCE RESULTS

				Spread Sheet for Calculating 1-g Sag & Fund. Frequency						G. Ruthven 12/10/92
							Mirror Supported at Inner Diameter			
Mirror Type	Radius (inch)	Max Thickness (inc	Density (lbs/in^3)	Weight (lbs)	Young's (psi)	Nu	Defl'n (in)	Defl'n (um)	Est. WFE (um) Z(6-23)-um	Freq (Hz)
4) Single Arch	20.69	0.5	0.079	24.8	10200000	0.17	0.00090	22.9	0.62	104.3
• Fused Quartz	20.69	1	0.079	49.5	10200000	0.17	0.00062	15.7	0.43	119.4
	20.69	2	0.079	99.1	10200000	0.17	0.00021	5.3	0.14	187.9
• Zerodur	20.69	0.5	0.091	28.1	13200000	0.24	0.00079	20.0	0.54	111.5
	20.69	1	0.091	56.2	13200000	0.24	0.00054	13.8	0.37	127.5
	20.69	2	0.091	112.3	13200000	0.24	0.00018	4.7	0.13	200.8
• ULE	20.69	0.5	0.079	24.8	9800000	0.22	0.00103	26.1	0.71	97.6
	20.69	1	0.079	49.5	9800000	0.22	0.00071	18.0	0.49	111.6
	20.69	2	0.079	99.1	9800000	0.22	0.00024	6.1	0.16	175.6
• Borosilicate	20.69	0.5	0.085	26.4	9500000	0.22	0.00103	26.1	0.71	97.6
	20.69	1	0.085	52.8	9500000	0.22	0.00071	18.0	0.49	111.6
	20.69	2	0.085	105.7	9500000	0.22	0.00024	6.1	0.16	175.6
• Beryllium	20.69	0.5	0.067	21.5	42000000	0.07	0.00019	4.8	0.13	227.4
	20.69	1	0.067	42.9	42000000	0.07	0.00013	3.3	0.09	260.3
	20.69	2	0.067	85.8	42000000	0.07	0.00004	1.1	0.03	409.8
• Silicon Carbide	20.69	0.5	0.106	32.2	47000000	0.2	0.00025	6.4	0.17	196.6
	20.69	1	0.106	64.4	47000000	0.2	0.00018	4.4	0.12	224.7
	20.69	2	0.106	128.8	47000000	0.2	0.00006	1.5	0.04	353.8

did not generate detailed finite element models (FEM) for every candidate. We developed scaling laws and applied them where applicable. The results generated by these scaling laws were occasionally checked with a FEM to ensure that we obtained reasonable results. An example of one such model is shown in Figure 4-6 and the resulting 1-g sag results shown graphically in Figure 4-7.

The uncertainty in the primary mirror deformation caused by the 5/6-g change in acceleration is a critical requirement in our overall approach to the LUTE telescope design. The 5/6-g uncertainty budget item is that amount of wavefront error which the mirror can exhibit when going from a 1-g earth environment to the lunar surface environment of 1/6-g.

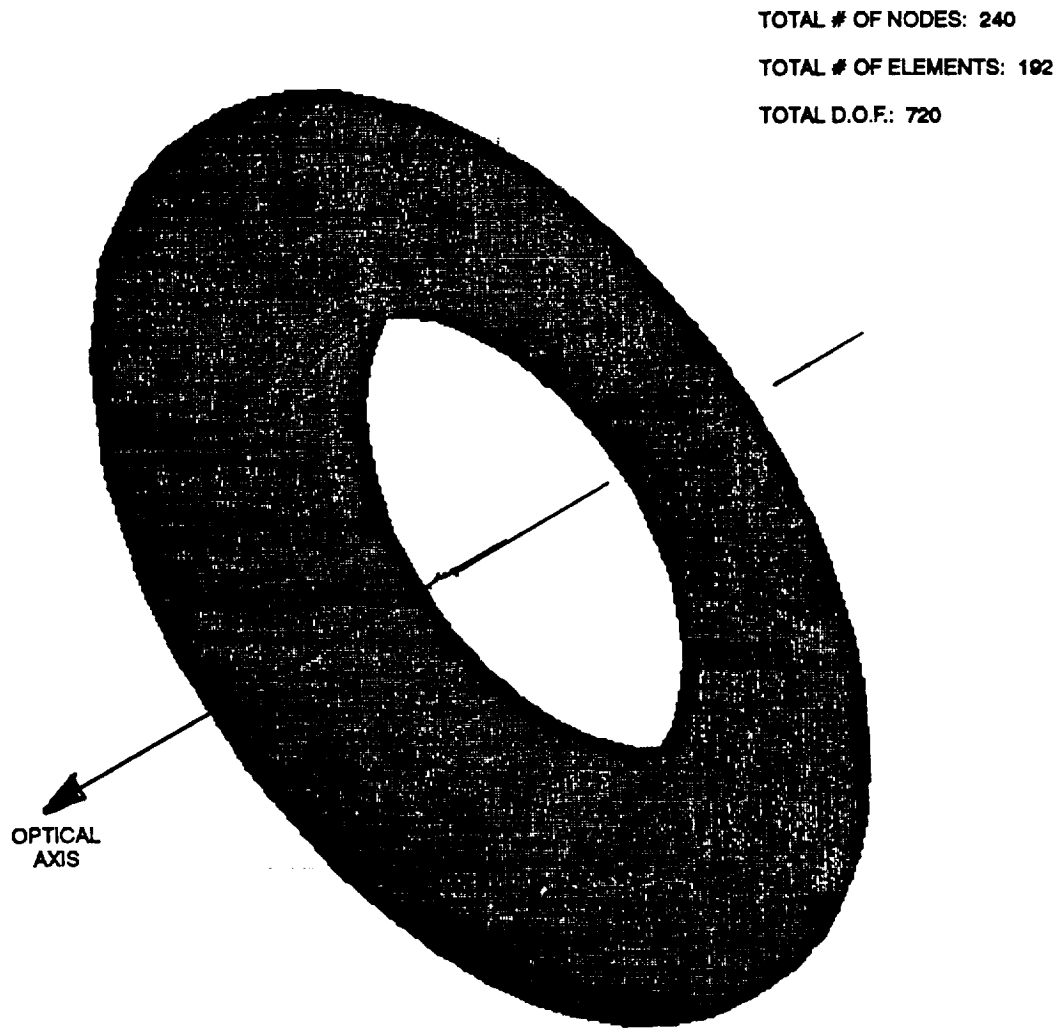

Figure 4-6. Existing Mirror Finite Element Models Used as Cross-Check for Scaling Laws.

EXAMPLE:

- 1g NORMAL TO OPTICAL AXIS
- SINGLE ARCH MIRROR DESIGN
- LINES OF CONSTANT DISTORTION SHOWN

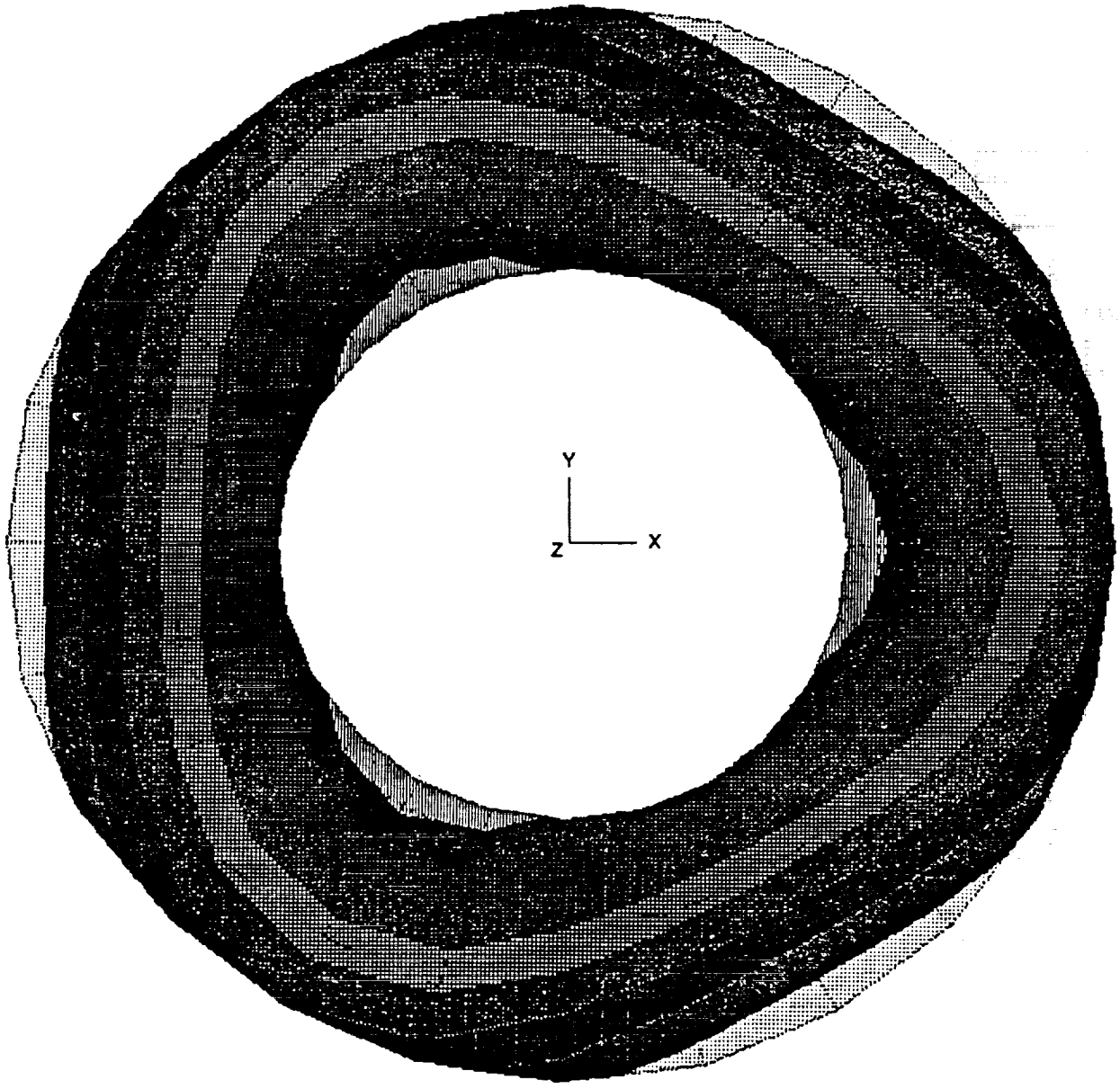

Figure 4-7. Mirror Deformation Patterns Decomposed to Determine Wavefront Error after Tilt and Focus is Removed.

The Hubble Space Telescope (HST) program used a "0-g metrology mount" to simulate the on-orbit 0-g environment. Because the metrology mount is always somewhat imperfect some residual error will exist. HDOS conducted a number of tests to correlate the HST metrology mount/mirror with a FEM of that system. We were able to correlate very well with test data. For instance, when the mirror was deformed in an astigmatic shape (sometimes referred to as "saddle") the mirror was interferometrically measured and compared to the predicted deformation. The mirror and FEM correlated to within 4%. For the LUTE primary mirror our wavefront error allocation for this effect is 0.0063 waves rms at 0.6328 μm.

For the LUTE telescope the scenario of using a metrology mount is in question since LUTE operates over a very wide temperature range compared with HST is ± 4° F. It is our judgment that the ability to design, fabricate and test a cryogenic metrology mount for LUTE would be a high risk approach. That is, the uncertainty of the metrology mount's performance operating over such a large temperature range could easily overshadow the 1-g effects we would be trying to measure. A similar concern affected the approach we used on the Infrared Astronomical Satellite (IRAS) program. We believe that a conservative approach to the LUTE primary mirror would be to have a mirror sufficiently stiff (at least in so far as non-realignable wavefront errors are concerned) that one can do without a cryogenic metrology mount.

If a cryogenic metrology mount is not used the question remains as to what is the uncertainty value for the 5/6-g effects. We believe, based on HST and other programs that we will be able to correlate the physical mirror characteristics to a FEM model to within 10%. Thus we can analytically predict how the mirror will deform in a 1/6-g cryogenic environment by correlating our model to 1-g cryogenic tests that do not utilize a metrology mount. We note here that it will be necessary to know the Young's modulus and Poisson's ratio of the mirror material throughout its operating temperature range.

Figure 4-8 shows the 1g uncertainty factors for the mirror candidates. Several items are noteworthy. The results shown are for 1-g; they should be multiplied by 5/6 to reflect the moon's 1/6-g environment. The second item to note is our assumption that LUTE will employ despace, decenter, and tilt capabilities via the secondary mirror subassembly. With this assumption, all the results shown in Table 4-3 through 4-6 and Figure 4-8 have piston, tilt and focus contributions removed from the estimated wavefront error.

From Figure 4-8 it is clearly seen that a beryllium single arch mirror is superior to all other candidates in terms of 1-g wavefront error uncertainty. The reason for this is that for the single arch the 1-g

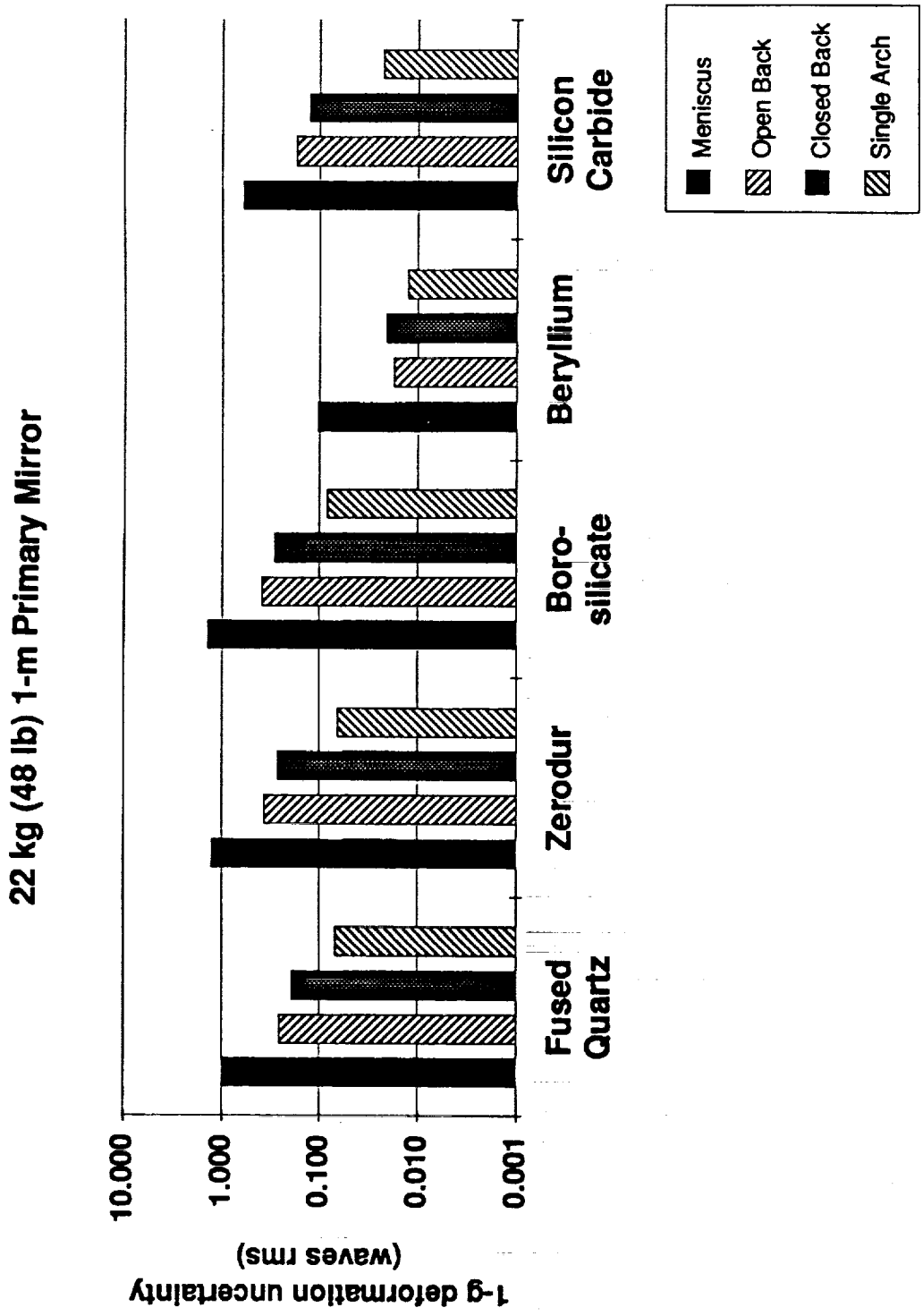

Figure 4-8. A Beryllium, Single Arch Primary Mirror Design is Clearly Superior for 1g-to-1/6g Effects.

results are dominated by focus error (i.e. Zernike polynomial terms Z4.) Our assumption of a focus mechanism makes focus error inconsequential. However, even though the single arch design has superior performance it is still just marginally acceptable in terms of the 0.0063 waves-rms requirement. In a future study a more refined investigation of this configuration and a revisiting of the overall error budget is warranted.

The mass properties estimates are presented in Table 4-7. The coordinate system used for the mass properties determination is such that the "X" direction is along the telescope optical axis (i.e. along the thrust axis of the launch vehicle) and the "Y" and "Z" axes are perpendicular to the "X" axis. The spacecraft interface in assumed to be 0.25 m aft of the (virtual) location of the primary mirror's vertex.

4.5 ACTIVE PRIMARY MIRROR DESIGN OPTION

The passive telescope design results presented show that due to the extreme operating temperature ranges, the ability to meet the top level primary mirror wavefront error budget of 0.0335 waves rms (at 0.6328 μm) is very challenging. An alternative design approach would be to employ figure control actuators which provide the ability to correct the mirror's surface figure in a closed loop fashion via an alignment/wavefront sensor.

We have conducted a first order analysis on the effects of figure control actuators on overall performance. Shown in Figure 4-9, the residual error which exists after correction has taken place as a function of mirror spatial frequency error suggests that for the anticipated low frequency errors associated with both temperature and substrate $\Delta L/L$ variations, a large portion (~ 80%) of these errors can be negated with the use of figure control actuators. This correction capability prediction is for a meniscus mirror design where a moderate number of actuators (approximately 16) are located on the rear surface of the primary mirror. The number of actuators could be optimized by targeting a specific set of aberrations caused by the thermal distortion sources (i.e material CTE gradients and variations in the mirror's thermal environment.)

A schematic of the figure control actuators is provided in Figure 4-10. This design employs a dual mode approach which provides large dynamic range while simultaneously providing fine adjustment capability. HDOS actuator technology has been demonstrated on several DoD programs, on the NASA HST Program and in HDOS laboratories.

TABLE 4-7
LUTE TELESCOPE MASS PROPERTIES

		LUTE Telescope							
		Hardware Family Tree & Mass Properties Estimates							
				Determine CG Location			Inertia Properties (in-lbs-sec^2)		
Major Element	Sub-Ass'y/Component	Weight (lbs)	Weight (kg)	Datum Dist.(x) (in)	- Wt * x (in-lbs)	r(x) (in)	Mr(x)^2	Ixo	Iyo=Izo
1) Mirrors									
	- Primary Mirror	48	21.8	9	432.0	-7.3	6.7	26.6	13.5
	- Secondary Mirror	6	2.7	33	198.0	16.7	4.3	0.6	0.3
	- Tertiary Mirror	3	1.4	6	18.0	-10.3	0.8	0.1	0.1
	Sub-Total:	57	25.9		648.0		11.8	27.3	13.9
2) Structure	Baffle Sub-Ass'y								
	- Main	9	4.1	18	162.0	1.7	0.1	10.0	5.1
	- Central	2	0.9	5	10.0	-11.3	0.7	0.5	0.3
	- SM	1	0.5	30	30.0	13.7	0.5	0.3	0.2
	Sub-Total:	12	5.5		202.0		1.2	10.7	5.5
	Mirror Mounts								
	- PM	5	2.3	6	30.0	-10.3	1.4	0	0
	- SM	3	1.4	33	99.0	16.7	2.2	0	0
	- TM	2	0.9	5	10.0	-11.3	0.7	0	0
	Sub-Total:	10	4.5		139.0		4.2	0	0
	Main Bulkhead Sub-Ass'y								
	- Main bulkhead	12	5.5	2	24.0	-14.3	6.4	9.6	4.8
	- S/C interface fittings (3)	3	1.4	2	6.0	-14.3	1.6	0	0
	Sub-Total:	15	6.8		30.0		8.0	9.6	4.8
	Metering Bar Sub-Ass'y								
	- Metering bars (3)	3	1.4	18	54.0	1.7	0.0	0	1.1
	- Interface fittings (6)	3	1.4	18	54.0	1.7	0.0	0	0
	Sub-Total:	6	2.7		108.0		0.0	0	1.1
	SM Sub-Ass'y								
	- Spider	4	1.8	36	144.0	19.7	4.0	0	0
	- Hub	3	1.4	36	108.0	19.7	3.0	1	0.5
	- Spider ring	3	1.4	36	108.0	19.7	3.0	3.3	1.5
	- Spider flexures (3)	3	1.4	36	108.0	19.7	3.0	0	0
	- Actuators (6)	6	2.7	34	204.0	17.7	4.8	0	0
	- Cabling	4	1.8	18	72.0	1.7	0.0	0	0
	Sub-Total:	23	10.5		744.0		17.8	4.3	2

TABLE 4-7 (Continued)
LUTE TELESCOPE MASS PROPERTIES

3) Electronics	• ACE	3	1.4	1	3.0	-15.3	1.8	0	0
	• TCE	3	1.4	1	3.0	-15.3	1.8	0	0
	• DMS	3	1.4	1	3.0	-15.3	1.8	0	0
	• ASE	3	1.4	1	3.0	-15.3	1.8	0	0
	Sub-Total:	12	5.6		12.0		7.3	0.3	0.1
4) Thermal Control	• Heaters	2	0.9	18	36.0	1.7	0.0	0	0
	• Thermocouples	2	0.9	18	36.0	1.7	0.0	0	0
	• MLI	3	1.4	18	54.0	1.7	0.0	0	0
	Sub-Total:	7	3.2		126.0		0.0	0	0
5) Alignment Sensor	• Sensor	10	4.5	38	380.0	21.7	12.1	2	1
	• Sensor mount	2	0.9	38	76.0	21.7	2.4	0	0
	Sub-Total:	12	5.5		456.0		14.6	2	1
	Total (w/o Reserve):	154.0	70		2465.0		65.1	54.2	31.4
	Reserve:	31.6	14	18	569.16	1.7	0.2		
	Total:	185.6	84				65.3		
				CG Location:	16.3	Total Inertia:			
				(in)		Ix=Ixo		54.2	
				(WRT S/C I/F)		Iy=Iz=Mr^2+Iy(o)			96.5

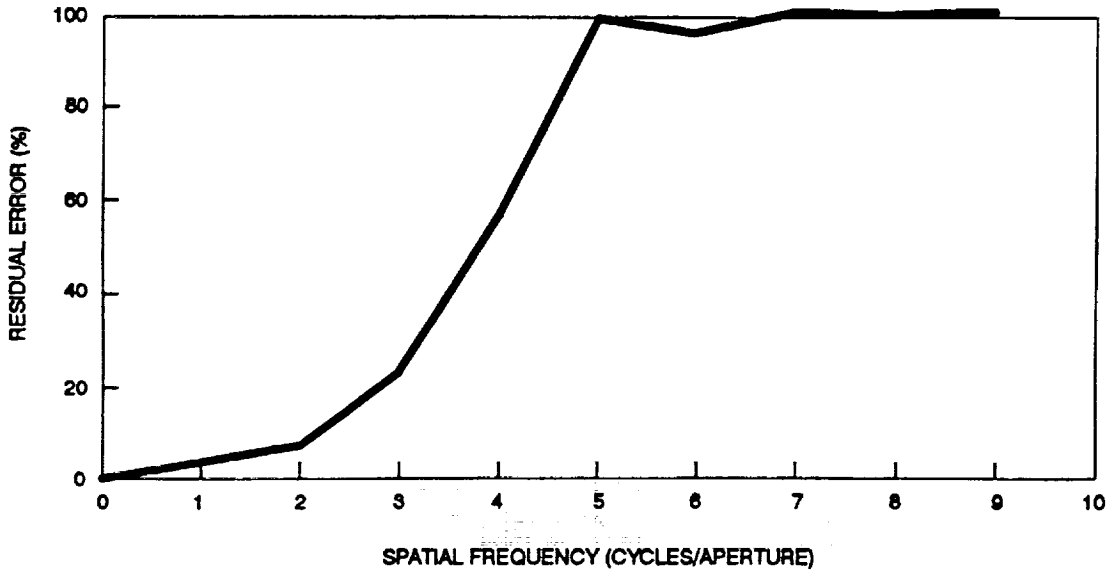

Figure 4-9. Primary Mirror Residual Distortion After Active Correction Via Figure Control Actuators. Additional analyses are required to determine LUTE specific performance.

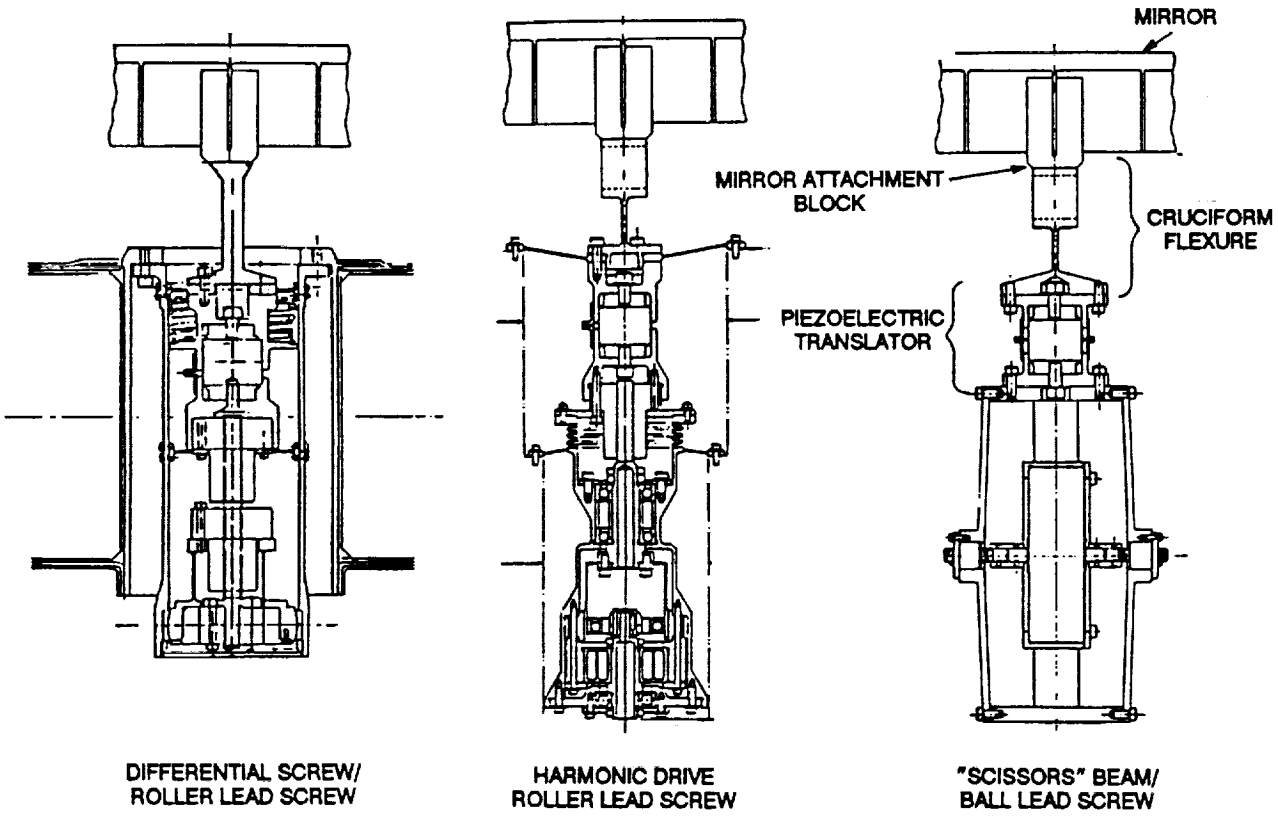

Figure 4-10. Several Design Concepts Exist for Primary Mirror Figure Control Actuators.

Our mass estimate for each actuator is about 1 kg. With approximately 16 actuators needed for 80% wavefront error correction capability a total mass of about 18 kg would be required. The weight allocations as presented in Figure 3-3 would need to be modified if an active mirror approach is adopted.

Our preliminary assessment of active figure compensation for the primary mirror shows that, along with a weight penalty, the ability to adequately compensate for the mirror distortion would be seriously in question. The residual 5/6-g effects of a beryllium meniscus design (a meniscus mirror is probably required if figure control actuators are to be used) with a weight consistent with the mass allocation is still three times larger than the error budget allocation of 0.0063 waves-rms at 0.6328 μm. All other substrate material candidates would yield even poorer results because of their lower specific stiffness (E/ρ) values. For instance, a fused quartz meniscus design would require a correction factor of better than 99%, a value which is certainly not attainable. We have tentatively concluded that the option of active control the primary mirror distortions is not viable.

SECTION 5
SELECTION CRITERIA AND EVALUATION

5.1 RECOMMENDED CANDIDATES

A beryllium single arch design is the leading candidate for the LUTE primary mirror. The next tier of leading candidates would include an open or closed back beryllium design. All glass and ceramic candidates of suitable low mass exhibit excessive 1-g deformations and thus cannot be considered viable materials. Mass is the key driver for the choice of beryllium.

5.2 BASIS OF SELECTION

The premise that leads us to recommend a beryllium single arch design is that a cryogenic metrology mount is a high risk approach which, in our engineering judgment, is not required to verify primary mirror 1-g to 1/6-g performance. The performance uncertainty of a cryogenic metrology mount may dwarf the mirror deformation effects which we would be trying to measure.

Verification of 1-g to 1/6-g effects can be predicted using 1-g interferometric test measurements of the mirror. These results, using both a room temperature metrology mount (for mirror fabrication) and other support fixturing, can be correlated to a finite element model of the mirror. The degree to which the model and interferometric measurement results do not correlate is the level of uncertainty which will exist when transitioning from earth to lunar gravity environments. We have recommended a slightly conservative correlation uncertainty factor of 10% for LUTE. This being the case, a single arch beryllium mirror design is the only candidate which approaches the allowable 1-g to 1/6-g uncertainty level of 0.0084 waves-rms (0.084 waves times 0.10) for the allowable primary mirror mass of 22 kg.

The thermal performance of the single arch beryllium mirror is good. In general, the mirror candidate geometries are more sensitive to a diametral variation of $\Delta L/L$ than a radial or axial variation. At the lower operating temperatures an allowable diametral temperature gradient of ~1 K is acceptable for the single arch beryllium candidate. However at higher operating temperatures an allowable gradient of only ~0.1 K is tolerable. LUTE system level trades must address this issue and whether an active telescope thermal control system should be considered. With the active thermal control system, an increase in the allowable temperature gradient as well as an increase in the allowable variation in material CTE would be realized.

5.3 CANDIDATE DESIGN PRODUCIBILTY STATUS

The ability to fabricate a 1-m class diffraction limited cryogenic primary mirror with an areal density of 28 kg/m^2 has not been proven to date. HDOS has designed and fabricated a 0.5 m, 28 kg/m^2 optic and cryogenically tested it to 8 K. The cryogenic distortion (i.e the amount of distortion transitioning from room temperature to cryogenic temperatures) was approximately 0.5 waves rms. This suggests that cryo null figuring will be required to meet the LUTE wavefront requirements. Note that the repeatability of the thermally-induced distortion must be exceptionally high for cryo null figuring to be successful. Such high repeatability has not been shown to date but may nonetheless be achievable in beryllium.

Cryo null figuring is an extension of traditional metrology and mirror fabrication techniques. In this process, metrology data is gathered at a discreet cryogenic temperature (this temperature is chosen based on worst case predicted mirror deformations.) The inverse wavefront error is figured into the mirror at room temperature so that subsequent further cooling the mirror wavefront is optimized at this discreet temperature. The advantages of using a cryo-null figuring approach are further enhanced if the operating temperature range of the telescope is reduced by the use of an active thermal control system.

Our current beryllium facilities can easily handle a 1-m class optic. Most recently we fabricated and tested a 1-m, closed back HIP beryllium optic. A low scatter surface roughness of approximately 20Å rms was achieved.

SECTION 6
CONCLUSIONS

No areas were identified in this study that would indicate that the LUTE mission is not feasible. Nonetheless, development of an ultra-lightweight, 1-m telescope with visible wavelength diffraction-limited performance for operation at cryogenic temperatures with a ±100 K temperature range would undoubtedly prove to be exceptionally difficult. We are unaware of any existing hardware that has met such requirements. No 1-m beryllium mirror has even been polished to such stringent wavefront error requirements.

The choice of beryllium was driven by the mass budget. For the currently allowable mass, beryllium is the only material that has a sufficiently small 1-g to 1/6-g deformation uncertainty.

The ability of beryllium to meet the LUTE primary mirror requirement is perhaps most uncertain due to the possibility that any cryogenic deformation will not be sufficiently repeatable to be able to be removed adequately with cryo null figuring. Furthermore a beryllium mirror cannot tolerate more than about 0.1% $\Delta L/L$ variation throughout the mirror substrate.

There are at least two LUTE system parameters that should be considered for revision following the results of this study; the first, being the LUTE mass budget. Should a substantial increase in lunar lander payload mass become available the selection of beryllium must be revisited. Other materials, particularly fused quartz, have shown a much higher degree of thermal cycling-induced deformation repeatability. They are likewise known to be suitable for exceptionally high performance optical systems.

The second LUTE system parameter that has had a major impact on this study is the temperature range over which the telescope must operate. Mirror substrate material properties such as coefficient of thermal expansion, thermal conductivity, etc. are strong functions of temperature. Any change to the LUTE operating temperature will require that the choice of optical materials be re-evaluated. This is clearly an iterative process since the evaluation of primary mirror thermal gradients requires knowledge of the material, while knowledge of the thermal gradients is required for the evaluation of the mirror wavefront deformation.

SECTION 7
CANDIDATE TOPICS FOR FURTHER STUDY

The following tasks remain as high priority candidates for further study to support the LUTE program.

- Re-evaluation of mirror material and geometry trades based upon revisions to the lunar lander payload mass budget and revisions to the operating temperature range.
- Analysis of three candidate beryllium mirror concepts (single arch, structured open back, and structured closed back) to identify the optimum geometry.
- Optical analysis to determine mirror alignment sensitivities in support of the concept to fabricate the tertiary mirror on same substrate as primary mirror.
- Ultraviolet scatter measurements on small (3-5 cm diameter) polished and coated beryllium mirrors.
- Analysis of the candidate materials to identify the optimum temperature range for each material to achieve its optimum performance.
- Structural analysis of the entire telescope assembly (in addition to the primary mirror) to show that the weight allocations are feasible.
- Further investigation into the utility of active correction of primary mirror surface deformations.
- Investigation into the CTE and $\Delta L/L$ uniformity of hot isostatic pressed beryllium.
- Optical analysis to support a re-evaluation of the existing wavefront error allocation to check its suitability for an ultraviolet wavelength telescope.
- Optical design trades to support optimization of the location of the focal plane.

SECTION 8
ACKNOWLEDGEMENTS

Mike Krim's help in many areas has been immeasurable. We would also like to thank Aaron Turner for the normal incidence ultraviolet reflectance computations, Alan Green and Bill Meyer for insightful discussions regarding optical fabrication, and Charlie Schaub for comments on the suitability of beryllium mirrors for UV applications.

APPENDIX A
ALLOWABLE THERMAL AND CTE GRADIENTS

Appendix A contains a set of tables and charts that support the trades between the candidate mirror materials and geometries. The materials evaluated include fused quartz, Zerodur, ULE, borosilicate, beryllium, and silicon carbide. For each mirror material we evaluated four mirror geometries: meniscus, open back, closed back, and single arch.

The charts are simply a graphical representation of the tabulated values and do not contain any additional information. However, the charts enable one to quickly detect trends.

The last set of tables document the mirror deformation sensitivities used in the previous tables and charts. Note that the sensitivity values do not include the lowest order primary mirror wavefront errors associated with rigid body motions or focus error because we assume that a secondary mirror alignment mechanism will be available. Also note that we computed more deformation sensitivities than were plotted in the previous charts; these data are provided for completeness.

TABLE A-1
MENISCUS RADIAL GRADIENT SENSITIVITY

			budget (waves rms, 1 wave = 0.6328 μm)					
			0.0168	0.0125	0.0125	0.0063	0.0063	0.0063
	Meniscus							
	Radial Gradient Sensitivity		T range			operating T		
	for 1E-6 ΔL/L		293 K-160 K	160 K-60 K	160 K-260 K	160 K	60 K	260 K
		Z5-Z23						
Material	Thickness (in.	μm rms	allowable fractional ΔL/L			allowable center-to-edge radial ΔT (K)		
Fused Quartz	0.3	0.748	0.00039	0.00023	0.00049	0.059	0.007	0.013
	0.6	0.188	0.00155	0.00090	0.00196	0.235	0.028	0.050
	0.9	0.084	0.00348	0.00202	0.00439	0.526	0.063	0.113
Zerodur	0.3	0.578	0.00090	0.00059	0.00080	0.037	0.014	0.058
	0.6	0.146	0.00358	0.00234	0.00317	0.147	0.057	0.231
	0.9	0.065	0.00805	0.00525	0.00713	0.331	0.128	0.520
ULE	0.3	0.779	0.00057	0.00013	0.00043	0.011	0.005	0.109
	0.6	0.196	0.00226	0.00053	0.00171	0.042	0.021	0.431
	0.9	0.087	0.00509	0.00120	0.00385	0.095	0.047	0.972
Borosilicate	0.3	0.803	0.00004	0.00006	0.00004	0.002	0.007	0.002
	0.6	0.202	0.00014	0.00024	0.00015	0.009	0.029	0.007
	0.9	0.090	0.00032	0.00054	0.00033	0.019	0.064	0.015
Beryllium	0.3	0.182	0.00005	0.00022	0.00006	0.005	0.068	0.002
	0.6	0.046	0.00021	0.00086	0.00023	0.019	0.269	0.009
	0.9	0.020	0.00049	0.00198	0.00053	0.044	0.619	0.020
Silicon Carbic	0.3	0.162	0.00024	0.00177	0.00030	0.035	0.676	0.009
	0.6	0.041	0.00095	0.00700	0.00118	0.138	2.670	0.035
	0.9	0.018	0.00216	0.01594	0.00269	0.314	6.082	0.079

TABLE A-2
MENISCUS DIAMETRAL GRADIENT SENSITIVITY

			budget (waves rms, 1 wave = 0.6328 μm)					
			0.0168	0.0125	0.0125	0.0063	0.0063	0.0063
	Meniscus							
	Diametral Gradient Sensiti		T range			operating T		
	for 1E-6 ΔL/L		293 K-160 K	160 K-60 K	160 K-260 K	160 K	60 K	260 K
		Z5-Z23						
Material	Thickness (in.	μm rms	allowable fractional ΔL/L			allowable diametral ΔT (K)		
Fused Quartz	0.3	0.066	0.00443	0.00257	0.00558	0.670	0.080	0.144
	0.6	0.017	0.01718	0.00996	0.02167	2.601	0.309	0.557
	0.9	0.007	0.04173	0.02420	0.05262	6.318	0.751	1.354
Zerodur	0.3	0.051	0.01026	0.00668	0.00909	0.422	0.163	0.663
	0.6	0.013	0.04023	0.02623	0.03565	1.655	0.638	2.600
	0.9	0.006	0.08717	0.05682	0.07724	3.586	1.382	5.633
ULE	0.3	0.069	0.00642	0.00151	0.00486	0.120	0.059	1.225
	0.6	0.017	0.02606	0.00614	0.01972	0.488	0.238	4.974
	0.9	0.008	0.05537	0.01305	0.04190	1.037	0.506	10.569
Borosilicate	0.3	0.071	0.00041	0.00069	0.00041	0.024	0.082	0.019
	0.6	0.018	0.00161	0.00272	0.00163	0.096	0.322	0.074
	0.9	0.008	0.00362	0.00613	0.00367	0.216	0.725	0.166
Beryllium	0.3	0.016	0.00061	0.00247	0.00067	0.055	0.774	0.025
	0.6	0.004	0.00243	0.00989	0.00266	0.222	3.095	0.100
	0.9	0.002	0.00486	0.01978	0.00533	0.444	6.190	0.200
Silicon Carbid	0.3	0.014	0.00278	0.02050	0.00346	0.404	7.819	0.101
	0.6	0.004	0.00974	0.07174	0.01211	1.413	27.367	0.354
	0.9	0.002	0.01948	0.14349	0.02423	2.826	54.734	0.708

TABLE A-3
OPEN BACK DIAMETRAL GRADIENT SENSITIVITY

			budget (waves rms, 1 wave = 0.6328 μm)					
			0.0168	0.0125	0.0125	0.0063	0.0063	0.0063
	Open Back							
	Diametral Gradient Sensiti		T range			operating T		
	for 1E-6 ΔL/L		293 K-160 K	160 K-60 K	160 K-260 K	160 K	60 K	260 K
		Z5-Z23						
Material	Depth (in.)	μm rms	allowable fractional ΔL/L			allowable diametral ΔT (K)		
Fused Quartz	1	0.849	0.00034	0.00020	0.00043	0.052	0.006	0.011
	2	0.272	0.00107	0.00062	0.00135	0.163	0.019	0.035
	4	0.066	0.00443	0.00257	0.00558	0.670	0.080	0.144
Zerodur	1	0.656	0.00080	0.00052	0.00071	0.033	0.013	0.052
	2	0.210	0.00249	0.00162	0.00221	0.102	0.039	0.161
	4	0.051	0.01026	0.00668	0.00909	0.422	0.163	0.663
ULE	1	0.884	0.00050	0.00012	0.00038	0.009	0.005	0.096
	2	0.283	0.00157	0.00037	0.00118	0.029	0.014	0.299
	4	0.069	0.00642	0.00151	0.00486	0.120	0.059	1.225
Borosilicate	1	0.912	0.00003	0.00005	0.00003	0.002	0.006	0.001
	2	0.292	0.00010	0.00017	0.00010	0.006	0.020	0.005
	4	0.071	0.00041	0.00069	0.00041	0.024	0.082	0.019
Beryllium	1	0.206	0.00005	0.00019	0.00005	0.004	0.060	0.002
	2	0.066	0.00015	0.00060	0.00016	0.013	0.188	0.006
	4	0.016	0.00061	0.00247	0.00067	0.055	0.774	0.025
Silicon Carbid	1	0.184	0.00021	0.00156	0.00026	0.031	0.595	0.008
	2	0.059	0.00066	0.00486	0.00082	0.096	1.855	0.024
	4	0.014	0.00278	0.02050	0.00346	0.404	7.819	0.101

TABLE A-4
CLOSED BACK DIAMETRAL GRADIENT SENSITIVITY

			budget (waves rms, 1 wave = 0.6328 μm)					
			0.0168	0.0125	0.0125	0.0063	0.0063	0.0063
	Closed Back							
	Diametral Gradient Sensiti		T range			operating T		
	for 1E-6 ΔL/L		293 K-160 K	160 K-60 K	160 K-260 K	160 K	60 K	260 K
		Z5-Z23						
Material	Depth (in.)	μm rms	allowable fractional ΔL/L			allowable diametral ΔT (K)		
Fused Quartz	1	0.534	0.00055	0.00032	0.00069	0.083	0.010	0.018
	2	.0.148	0.00197	0.00114	0.00249	0.299	0.036	0.064
	4	0.049	0.00596	0.00346	0.00752	0.903	0.107	0.193
Zerodur	1	0.413	0.00127	0.00083	0.00112	0.052	0.020	0.082
	2	0.115	0.00455	0.00296	0.00403	0.187	0.072	0.294
	4	0.038	0.01376	0.00897	0.01220	0.566	0.218	0.889
ULE	1	0.556	0.00080	0.00019	0.00060	0.015	0.007	0.152
	2	0.154	0.00288	0.00068	0.00218	0.054	0.026	0.549
	4	0.051	0.00869	0.00205	0.00657	0.163	0.079	1.658
Borosilicate	1	0.573	0.00005	0.00009	0.00005	0.003	0.010	0.002
	2	0.159	0.00018	0.00031	0.00018	0.011	0.036	0.008
	4	0.053	0.00055	0.00092	0.00055	0.033	0.109	0.025
Beryllium	1	0.130	0.00007	0.00030	0.00008	0.007	0.095	0.003
	2	0.036	0.00027	0.00110	0.00030	0.025	0.344	0.011
	4	0.012	0.00081	0.00330	0.00089	0.074	1.032	0.033
Silicon Carbid	1	0.193	0.00020	0.00149	0.00025	0.029	0.567	0.007
	2	0.054	0.00072	0.00531	0.00090	0.105	2.027	0.026
	4	0.018	0.00216	0.01594	0.00269	0.314	6.082	0.079

TABLE A-5
SINGLE ARCH RADIAL GRADIENT SENSITIVITY

			budget (waves rms, 1 wave = 0.6328 μm)					
			0.0168	0.0125	0.0125	0.0063	0.0063	0.0063
	Single Arch							
	Radial Gradient Sensitivity		T range			operating T		
	for 1E-6 ΔL/L		293 K-160 K	160 K-60 K	160 K-260 K	160 K	60 K	260 K
		Z5-Z23						
Material	Max. Thick. (in	μm rms	allowable fractional ΔL/L			allowable center-to-edge ΔT (K)		
Fused Quartz	0.5	0.098	0.00298	0.00173	0.00376	0.451	0.054	0.097
	1	0.067	0.00436	0.00253	0.00550	0.660	0.078	0.141
	2	0.022	0.01328	0.00770	0.01674	2.010	0.239	0.431
Zerodur	0.5	0.075	0.00697	0.00455	0.00618	0.287	0.111	0.451
	1	0.052	0.01006	0.00656	0.00891	0.414	0.159	0.650
	2	0.017	0.03077	0.02005	0.02726	1.266	0.488	1.988
ULE	0.5	0.102	0.00434	0.00102	0.00329	0.081	0.040	0.829
	1	0.070	0.00633	0.00149	0.00479	0.118	0.058	1.208
	2	0.023	0.01926	0.00454	0.01457	0.361	0.176	3.676
Borosilicate	0.5	0.105	0.00028	0.00047	0.00028	0.016	0.055	0.013
	1	0.072	0.00040	0.00068	0.00041	0.024	0.081	0.018
	2	0.024	0.00121	0.00204	0.00122	0.072	0.242	0.055
Beryllium	0.5	0.024	0.00041	0.00165	0.00044	0.037	0.516	0.017
	1	0.016	0.00061	0.00247	0.00067	0.055	0.774	0.025
	2	0.005	0.00180	0.00733	0.00197	0.164	2.292	0.074
Silicon Carbid	0.5	0.021	0.00186	0.01367	0.00231	0.269	5.213	0.067
	1	0.015	0.00260	0.01913	0.00323	0.377	7.298	0.094
	2	0.005	0.00812	0.05979	0.01009	1.177	22.806	0.295

TABLE A-6
SINGLE ARCH DIAMETRAL GRADIENT SENSITIVITY

			budget (waves rms, 1 wave = 0.6328 μm)					
			0.0168	0.0125	0.0125	0.0063	0.0063	0.0063
	Single Arch							
	Diametral Gradient Sensiti		T range			operating T		
	for 1E-6 ΔL/L		293 K-160 K	160 K-60 K	160 K-260 K	160 K	60 K	260 K
		Z5-Z23						
Material	Max. Thick. (ir	μm rms	allowable fractional ΔL/L			allowable diametral ΔT (K)		
Fused Quartz	0.5	0.043	0.00679	0.00394	0.00857	1.028	0.122	0.220
	1	0.030	0.00974	0.00565	0.01228	1.474	0.175	0.316
	2	0.010	0.02921	0.01694	0.03683	4.422	0.526	0.948
Zerodur	0.5	0.033	0.01585	0.01033	0.01404	0.652	0.251	1.024
	1	0.023	0.02274	0.01482	0.02015	0.936	0.360	1.469
	2	0.008	0.06538	0.04262	0.05793	2.690	1.036	4.225
ULE	0.5	0.045	0.00984	0.00232	0.00745	0.184	0.090	1.879
	1	0.031	0.01429	0.00337	0.01081	0.267	0.131	2.728
	2	0.010	0.04430	0.01044	0.03352	0.829	0.405	8.455
Borosilicate	0.5	0.046	0.00063	0.00107	0.00064	0.038	0.126	0.029
	1	0.032	0.00091	0.00153	0.00092	0.054	0.181	0.041
	2	0.010	0.00290	0.00490	0.00293	0.173	0.580	0.132
Beryllium	0.5	0.010	0.00097	0.00396	0.00107	0.089	1.238	0.040
	1	0.007	0.00135	0.00550	0.00148	0.123	1.719	0.056
	2	0.002	0.00405	0.01649	0.00444	0.370	5.158	0.167
Silicon Carbic	0.5	0.009	0.00419	0.03086	0.00521	0.608	11.771	0.152
	1	0.006	0.00609	0.04484	0.00757	0.883	17.104	0.221
	2	0.002	0.01855	0.13665	0.02307	2.691	52.127	0.674

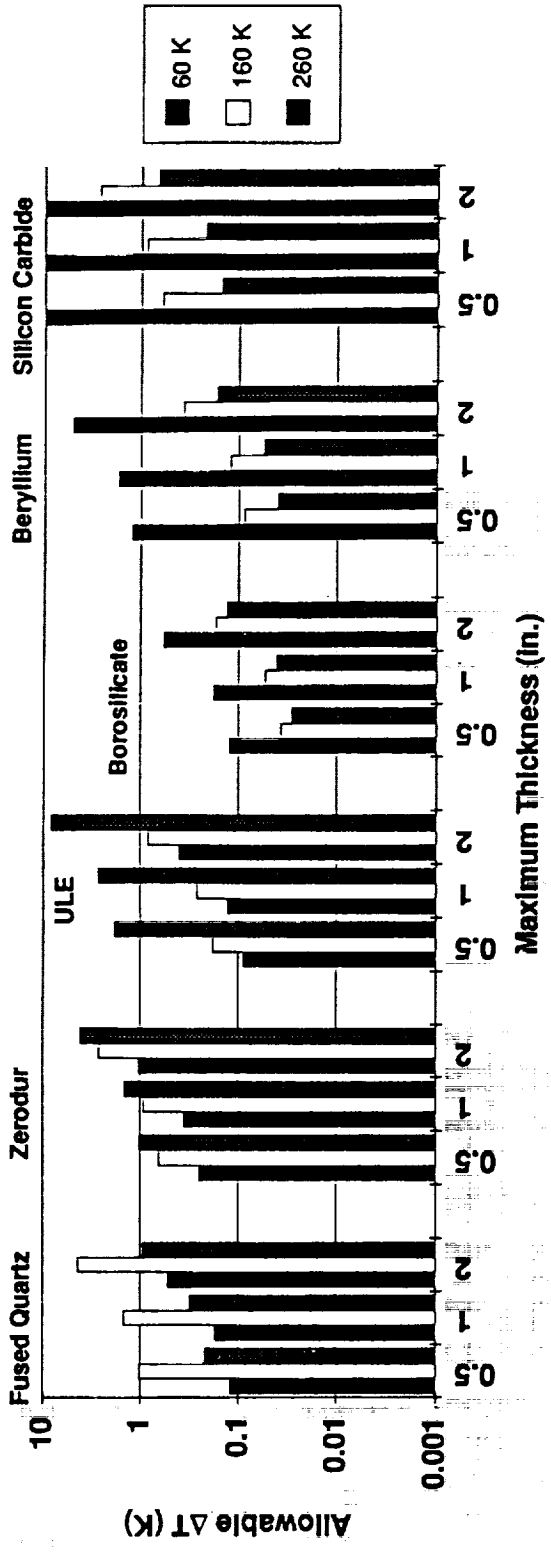

Figure A-1. Single Arch-Diametral ΔT.

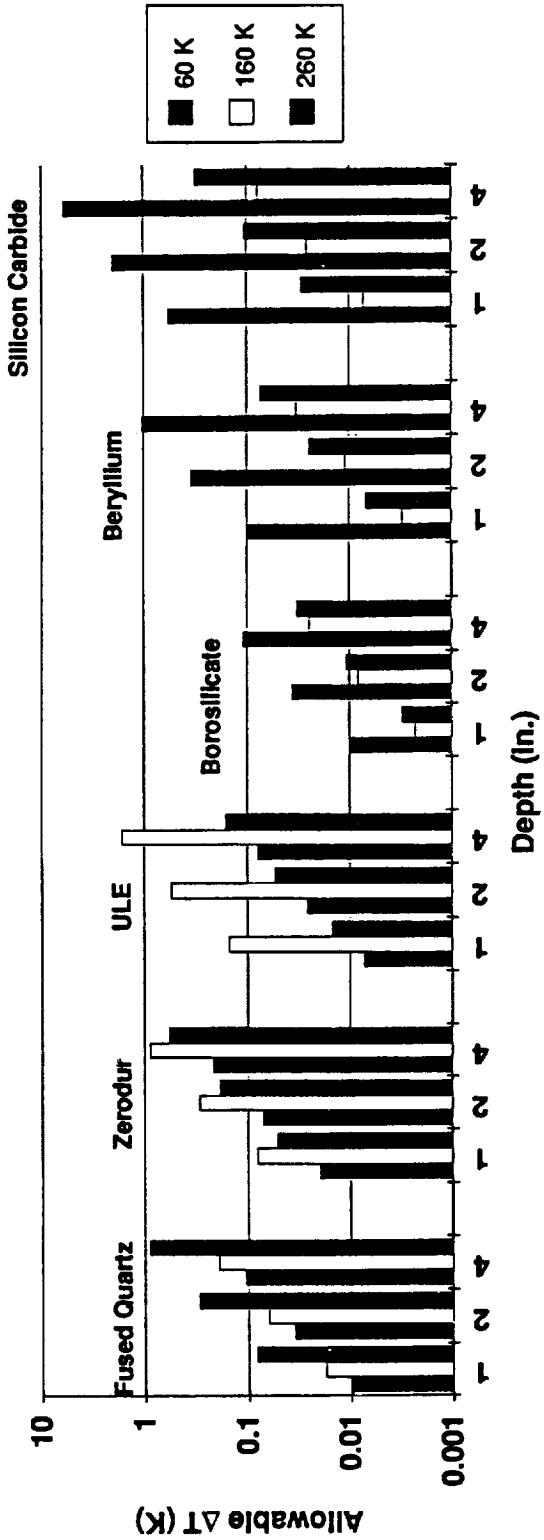

Figure A-2. Closed Back-Diametral ΔT.

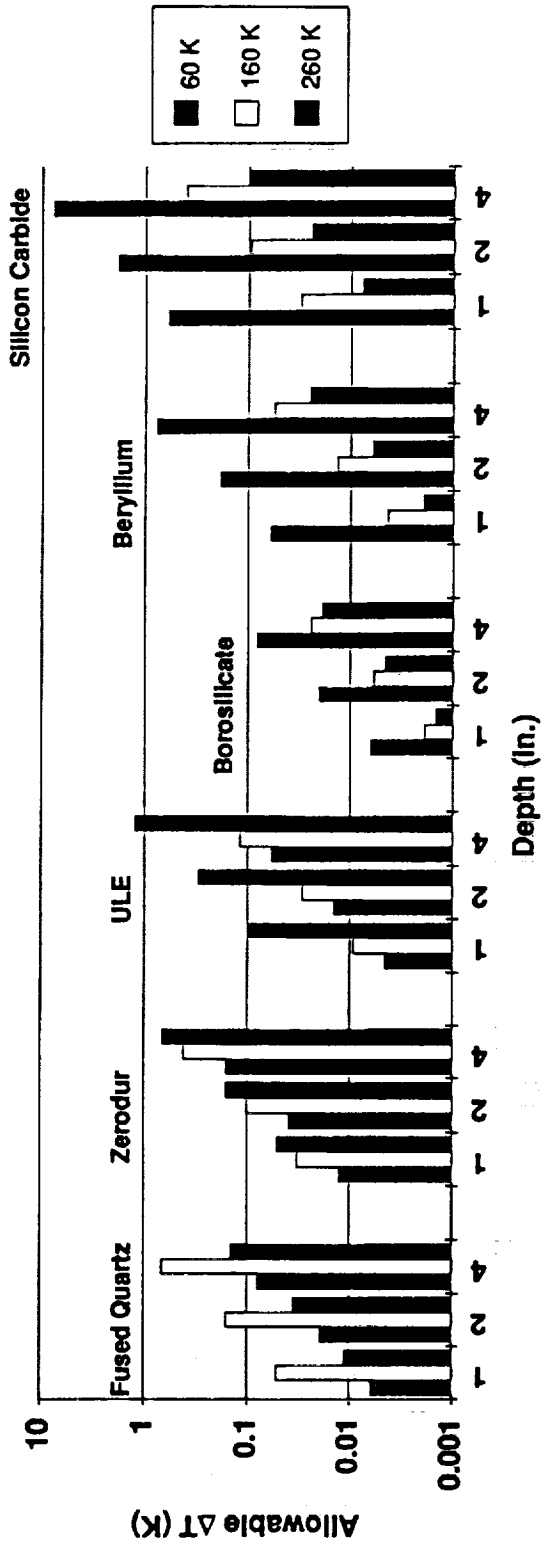

Figure A-3. Open Back-Diametral ΔT.

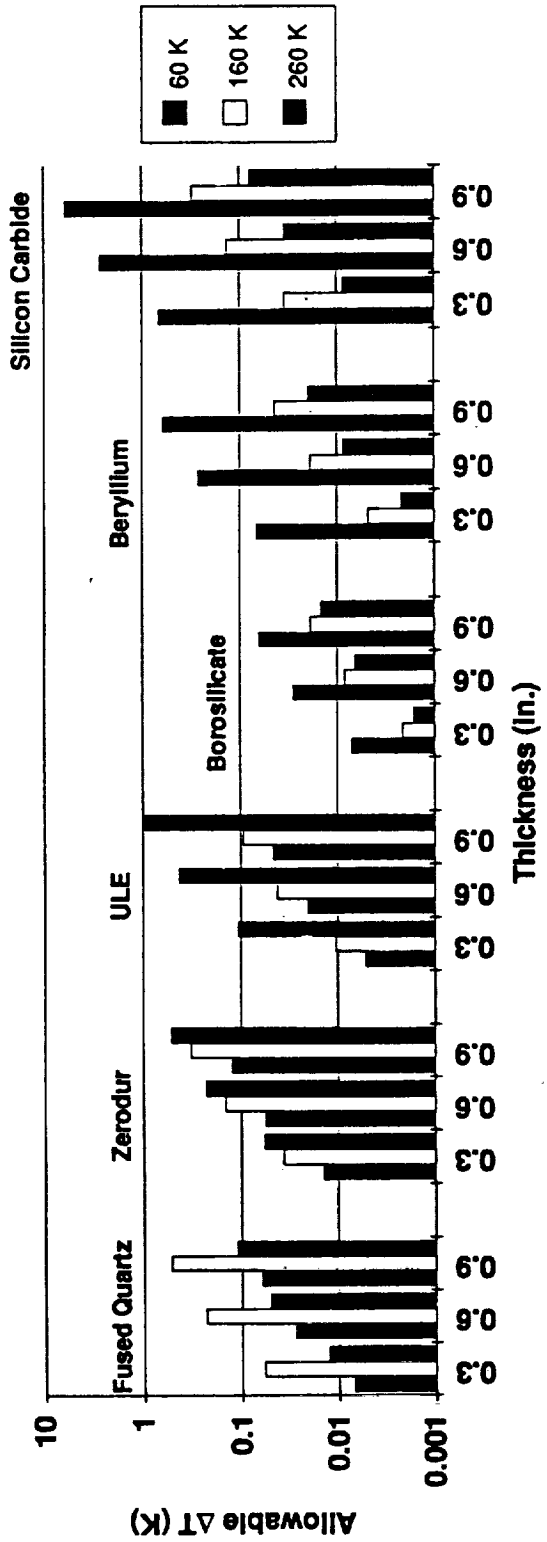

Figure A-4. Meniscus-Radially Symmetric ΔT.

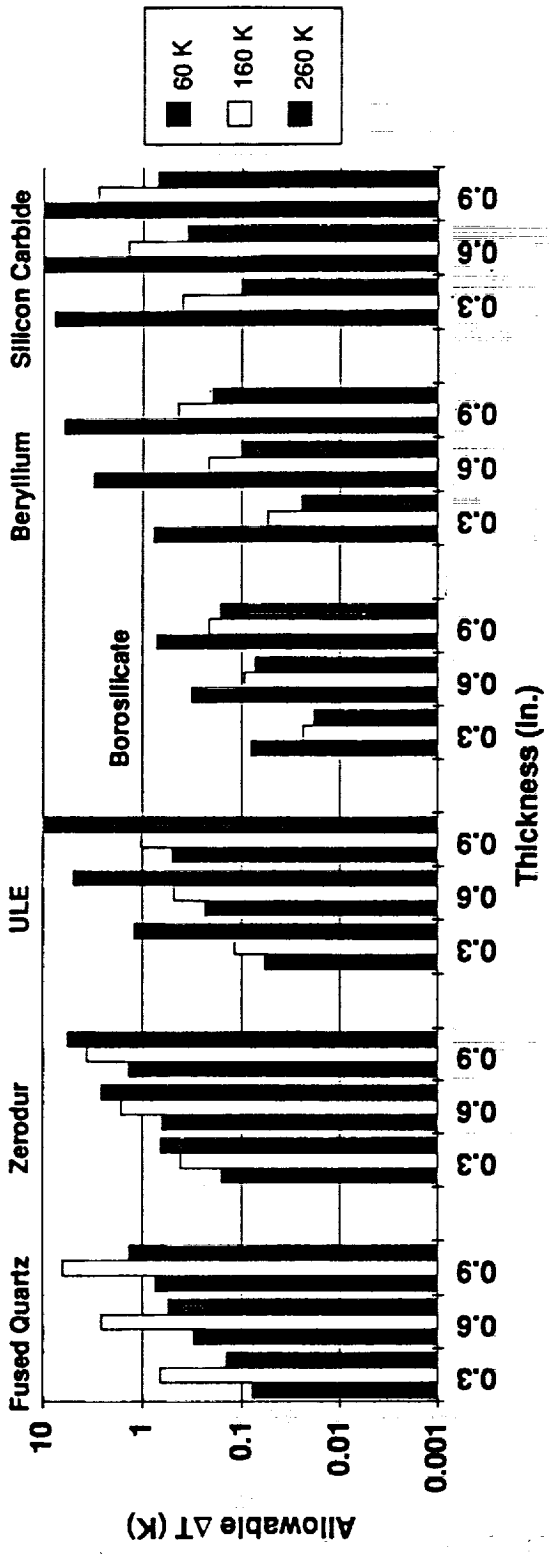

Figure A-5. Meniscus-Diametral ΔT.

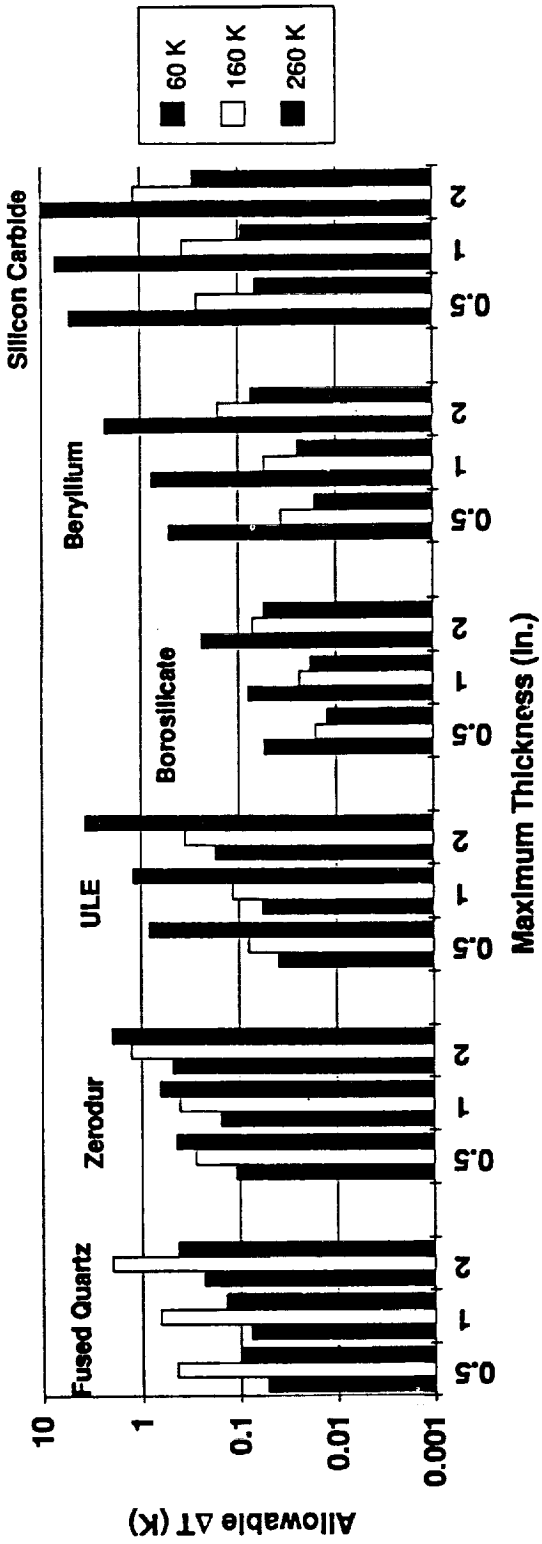

Figure A-6. Single Arch-Radially Symmetric ΔT.

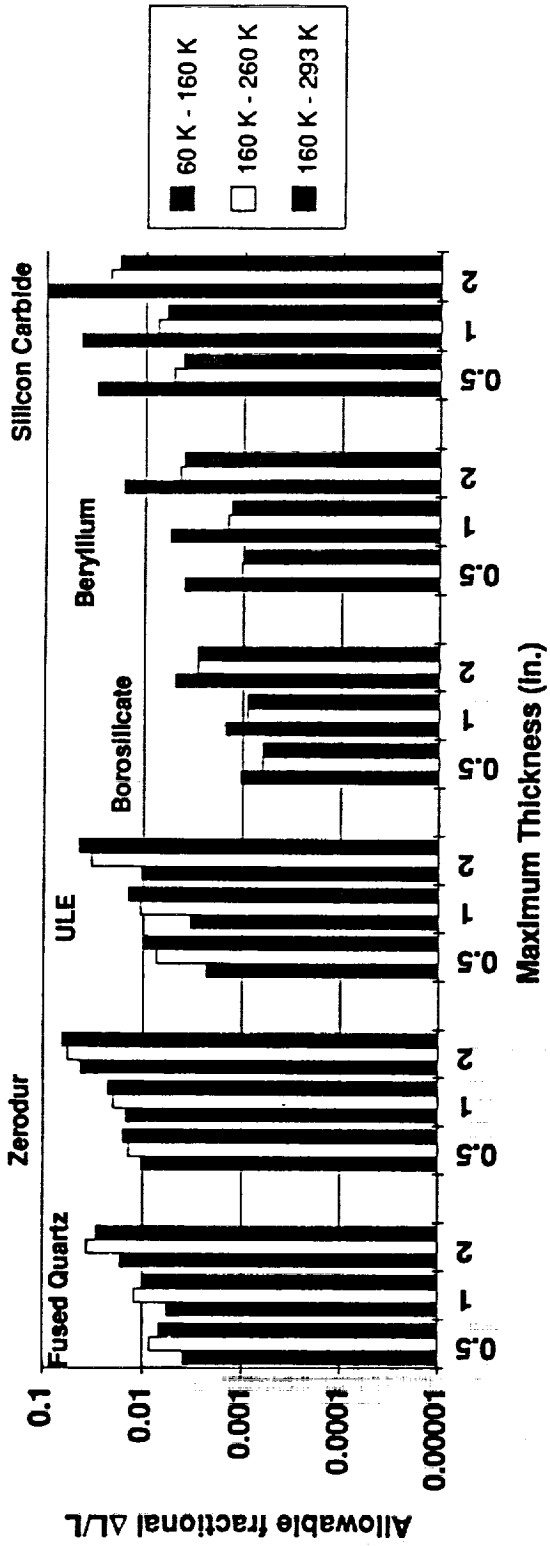

Figure A-7. Single Arch-Diametral ΔL/L.

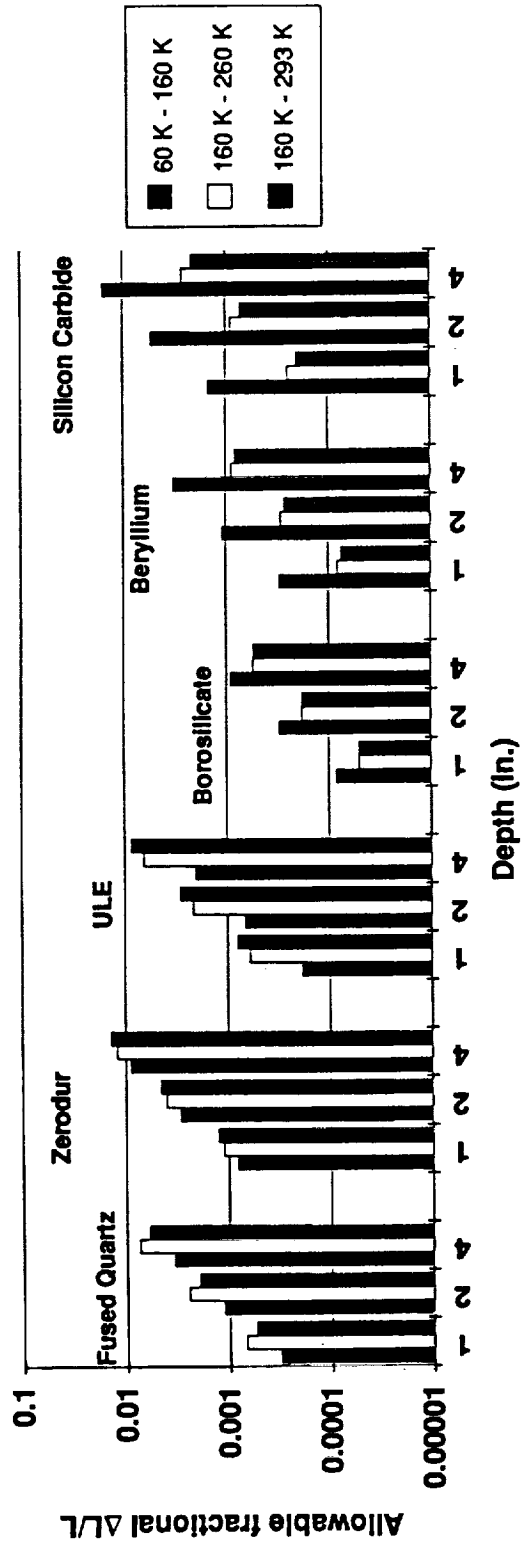

Figure A-8. Closed Back-Diametral ΔL/L.

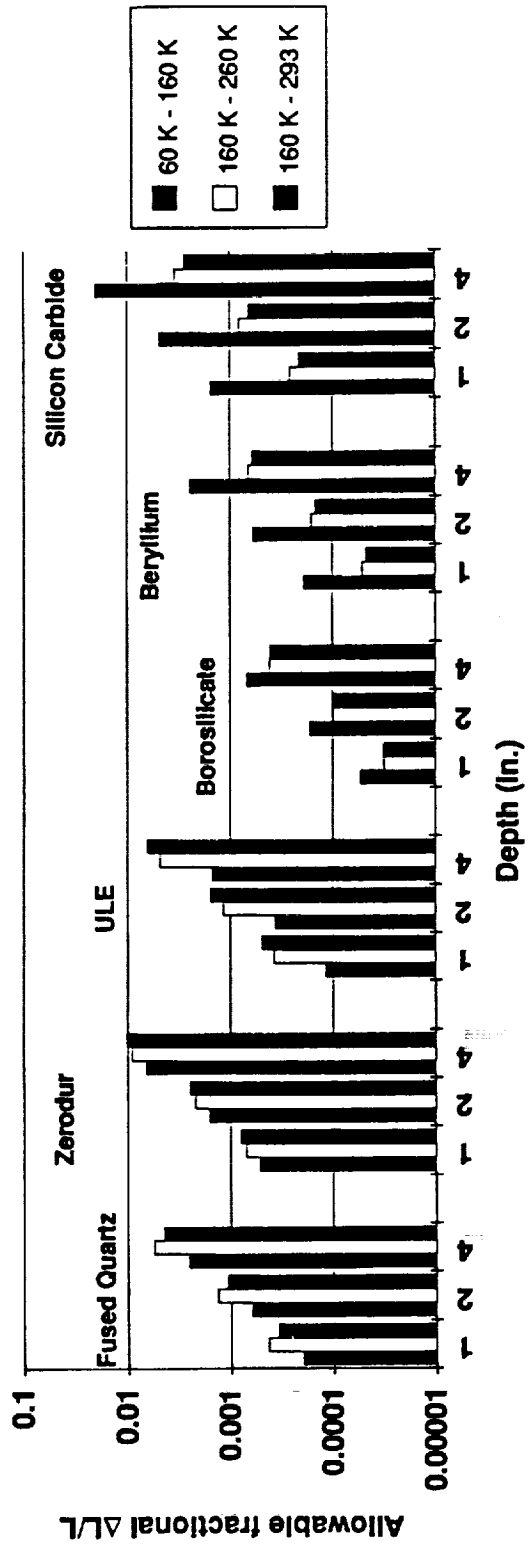

Figure A-9. Open Back-Diametral ΔL/L.

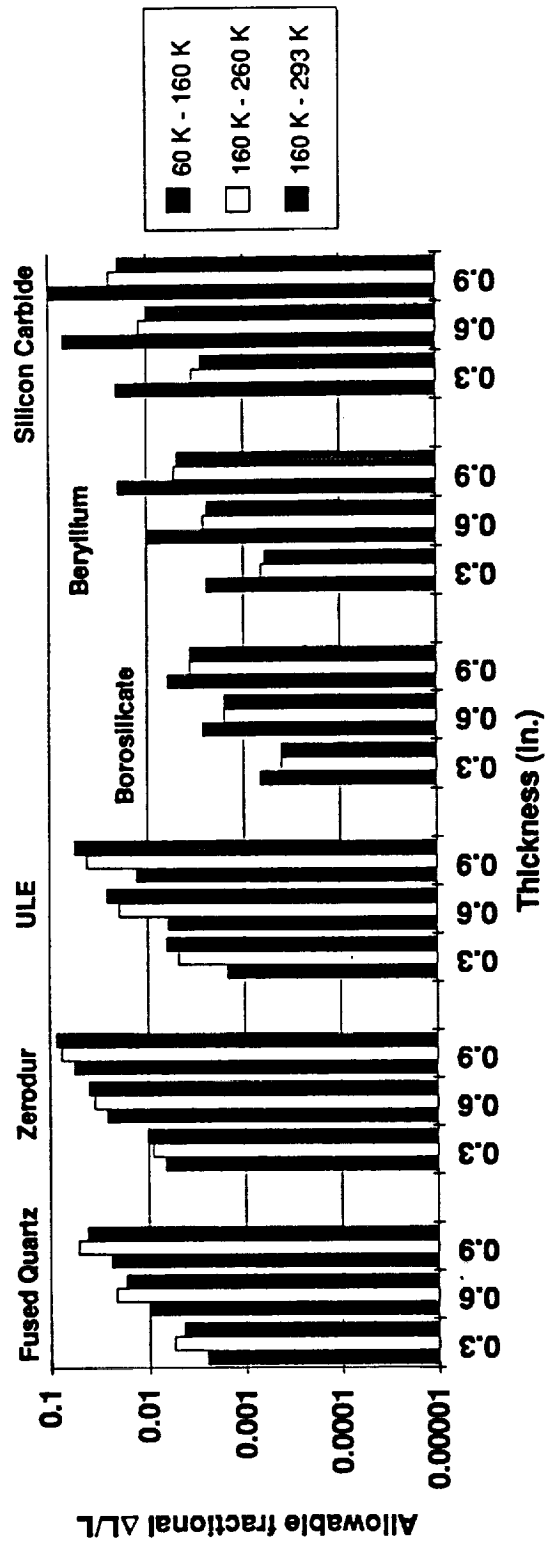

Figure A-10. Meniscus-Diametral ΔL/L.

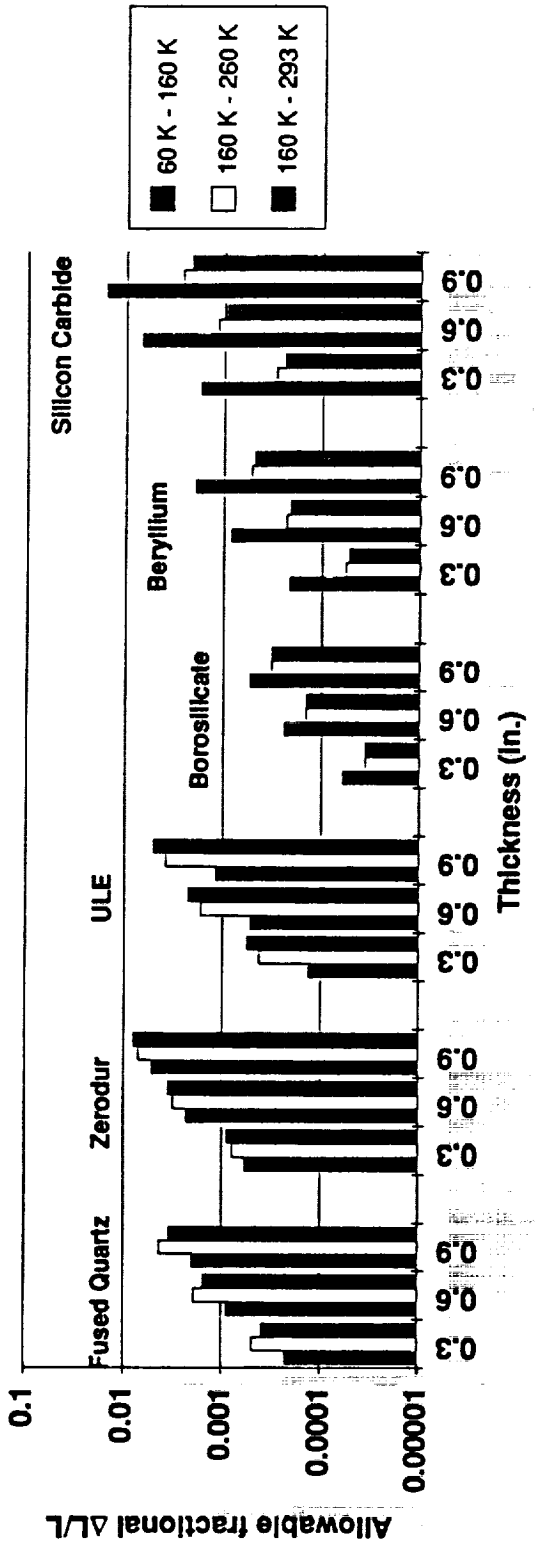

Figure A-11. Meniscus-Radially Symmetric ΔL/L.

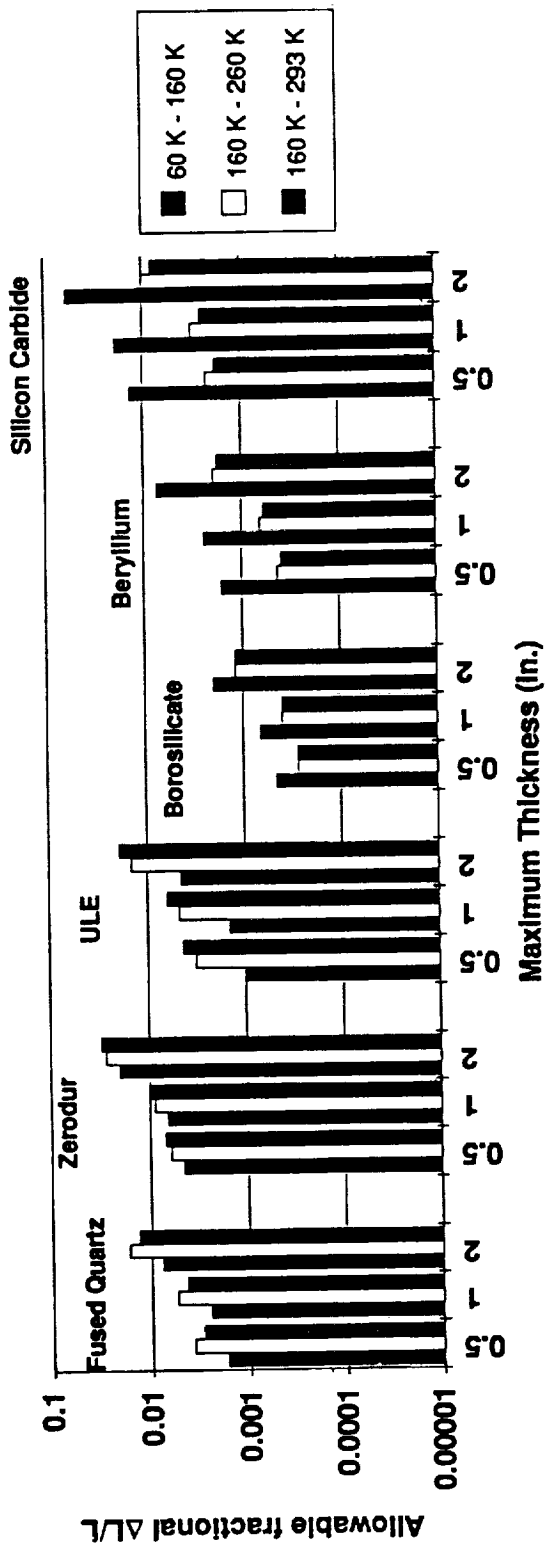

Figure A-12. Single Arch-Radially Symmetric ΔL/L.

TABLE A-7
PRIMARY MIRROR MENISCUS - ΔL/L

		Primary Mirror ΔL/L = (CTE * ΔT) Sensitivities		
		Diametral Gradient	Radial Gradient	Axial Gradient
		ΔL/L = 1.0e-6	ΔL/L = 1.0e-6	ΔL/L = 1.0e-6
		Est. WFE (um-rms)	Est. WFE (um-rms)	Est. WFE (um-rms)
Mirror Type	Thickness (inch)	Z(5-23)	Z(5-23)	Z(5-23)
1) Meniscus	0.3	0.066	0.748	0.0555
• Fused Quartz	0.6	0.017	0.188	0.0140
	0.9	0.007	0.084	0.0062
• Zerodur	0.3	0.051	0.578	0.0429
	0.6	0.013	0.146	0.0108
	0.9	0.006	0.065	0.0048
• ULE	0.3	0.069	0.779	0.0578
	0.6	0.017	0.196	0.0146
	0.9	0.008	0.087	0.0065
• Borosilicate	0.3	0.071	0.803	0.0596
	0.6	0.018	0.202	0.0150
	0.9	0.008	0.090	0.0067
• Beryllium	0.3	0.018	0.162	0.0135
	0.6	0.004	0.046	0.0034
	0.9	0.002	0.020	0.0015
• Silicon Carbide	0.3	0.014	0.162	0.0121
	0.6	0.004	0.041	0.0030
	0.9	0.002	0.018	0.0013

TABLE A-8
PRIMARY MIRROR OPEN BACK - ΔL/L

		Primary Mirror ΔL/L = (CTE * ΔT) Sensitivities					
		Diametral Gradient		Radial Gradient		Axial Gradient	
		ΔL/L = 1.0e-6		ΔL/L = 1.0e-6		ΔL/L = 1.0e-6	
		Est. WFE (um-rms)		Est. WFE (um-rms)		Est. WFE (um-rms)	
Mirror Type	Depth (inch)	Z(5-23)		Z(5-23)		Z(5-23)	
2) Open Back	1	0.849		0.145		0.0093	
• Fused Quartz	2	0.272		0.046		0.0030	
	4	0.066		0.011		0.0007	
• Zerodur	1	0.656		0.112		0.0072	
	2	0.210		0.036		0.0023	
	4	0.051		0.009		0.0006	
• ULE	1	0.884		0.151		0.0097	
	2	0.283		0.048		0.0031	
	4	0.069		0.012		0.0008	
• Borosilicate	1	0.912		0.155		0.0100	
	2	0.292		0.050		0.0032	
	4	0.071		0.012		0.0008	
• Beryllium	1	0.206		0.035		0.0023	
	2	0.066		0.011		0.0007	
	4	0.016		0.003		0.0002	
• Silicon Carbide	1	0.184		0.031		0.0020	
	2	0.059		0.010		0.0006	
	4	0.014		0.002		0.0002	

TABLE A-9
PRIMARY MIRROR CLOSED BACK - ΔL/L

		Primary Mirror ΔL/L = (CTE * ΔT) Sensitivities		
		Diametral Gradient	Radial Gradient	Axial Gradient
		ΔL/L = 1.0e-6	ΔL/L = 1.0e-6	ΔL/L = 1.0e-6
		Est. WFE (um-rms)	Est. WFE (um-rms)	Est. WFE (um-rms)
Mirror Type	Depth (inch)	Z(5-23)	Z(5-23)	Z(5-23)
3) Closed Back	1	0.534	0.087	0.0063
• Fused Quartz	2	0.148	0.024	0.0018
	4	0.049	0.008	0.0006
• Zerodur	1	0.413	0.068	0.0049
	2	0.115	0.019	0.0014
	4	0.038	0.006	0.0005
• ULE	1	0.556	0.091	0.0066
	2	0.154	0.025	0.0018
	4	0.051	0.008	0.0006
• Borosilicate	1	0.573	0.094	0.0068
	2	0.159	0.026	0.0019
	4	0.053	0.009	0.0006
• Beryllium	1	0.130	0.021	0.0015
	2	0.036	0.006	0.0004
	4	0.012	0.002	0.0001
• Silicon Carbide	1	0.193	0.019	0.0014
	2	0.054	0.005	0.0004
	4	0.018	0.002	0.0001

TABLE A-10
PRIMARY MIRROR SINGLE ARCH - ΔL/L

		Primary Mirror ΔL/L = (CTE * ΔT) Sensitivities					
			Diametral Gradient		Radial Gradient		Axial Gradient
			ΔL/L = 1.0e-6		ΔL/L = 1.0e-6		ΔL/L = 1.0e-6
			Est. WFE (um-rms)		Est. WFE (um-rms)		Est. WFE (um-rms)
Mirror Type	Max. Thick. (inch)		Z(5-23)		Z(5-23)		Z(5-23)
4) Single Arch	0.5		0.043		0.098		0.0151
• Fused Quartz	1		0.030		0.067		0.0104
	2		0.010		0.022		0.0034
• Zerodur	0.5		0.033		0.075		0.0117
	1		0.023		0.052		0.0081
	2		0.008		0.017		0.0026
• ULE	0.5		0.045		0.102		0.0157
	1		0.031		0.070		0.0109
	2		0.010		0.023		0.0036
• Borosilicate	0.5		0.046		0.105		0.0162
	1		0.032		0.072		0.0112
	2		0.010		0.024		0.0037
• Beryllium	0.5		0.010		0.024		0.0037
	1		0.0072		0.016		0.0025
	2		0.0024		0.0054		0.00083
• Silicon Carbide	0.5		0.0093		0.021		0.0033
	1		0.0064		0.015		0.0023
	2		0.0021		0.0048		0.00074

APPENDIX B
MIRROR MATERIAL CRYOGENIC PROPERTIES AND FIGURES OF MERIT

Appendix B contains a series of figures that describe the variation in mirror material properties with temperature. Since LUTE will operate over a very wide temperature range, and since mirror material properties at cryogenic temperatures can differ dramatically from the room temperature values, we used the following data in the analyses presented in this report.

How do they vary with temperature?

	Density	*Young's Modulus*	*Specific Stiffness*	*Poisson's Ratio*	*Coefficient of Thermal Expansion*	*Fractional Dimensional Change*	*Thermal Conductivity*
Preferred Magnitude	small	large	large	large	small	small	large
metric units	kg/(m^3)	Pa	(m^2)/(s^2)	---	1/K	[ref. 293 K]	W/(m K)
symbol	rho	E	E/rho	nu	alpha	ΔL/L	k

St. State Thermal Distortion	*Specific Heat*	*Thermal Diffusivity*	*Transient Thermal Distortion*
small	large	large	small
m/W	J/(kg K)	(m^2)/s	s/[(m^2) K]
alpha/k	C	D = k/(rho C)	alpha/D

Figure B-1. Material Property Figures of Merit.

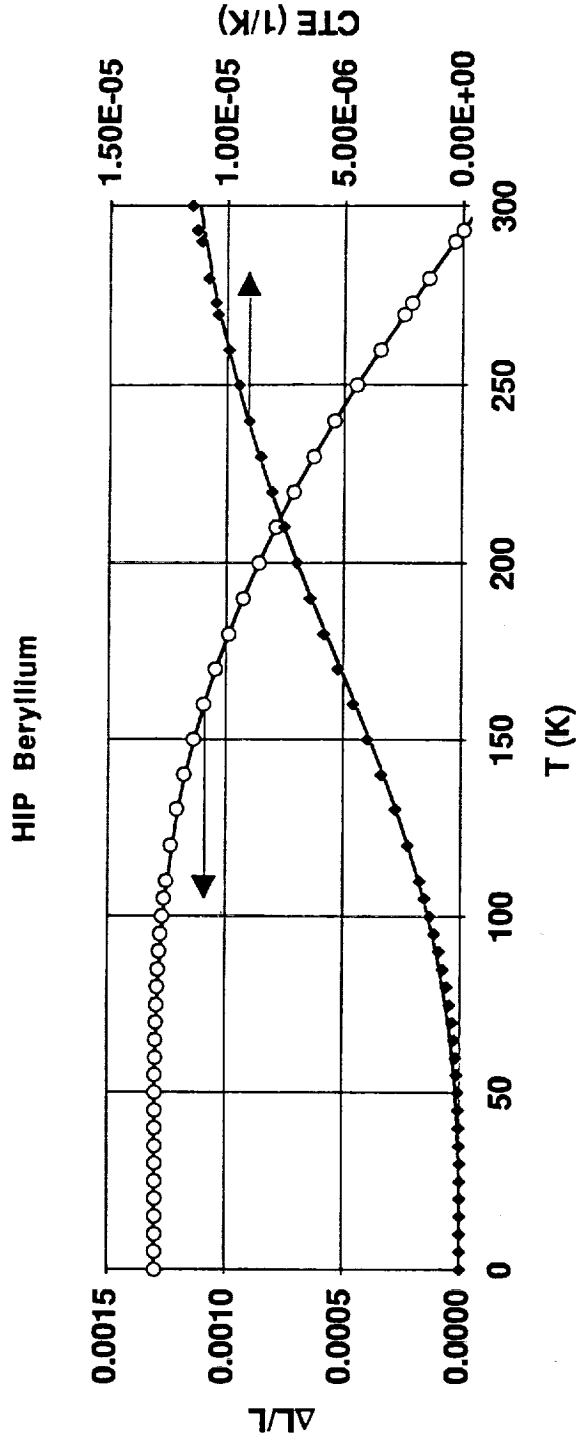

Figure B-2. Hot Isostatic Pressed Beryllium Coefficient of Thermal Expansion and Integrated Thermal Contraction.

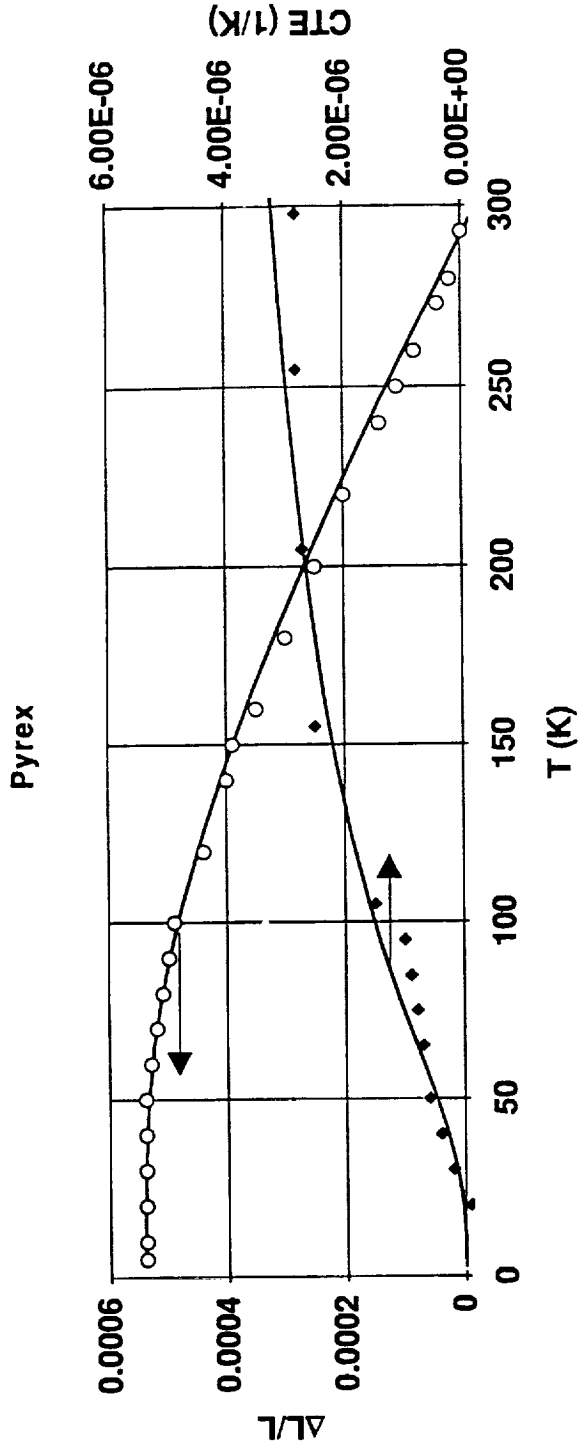

Figure B-3. Pyrex Coefficient of Thermal Expansion and Integrated Thermal Contraction.

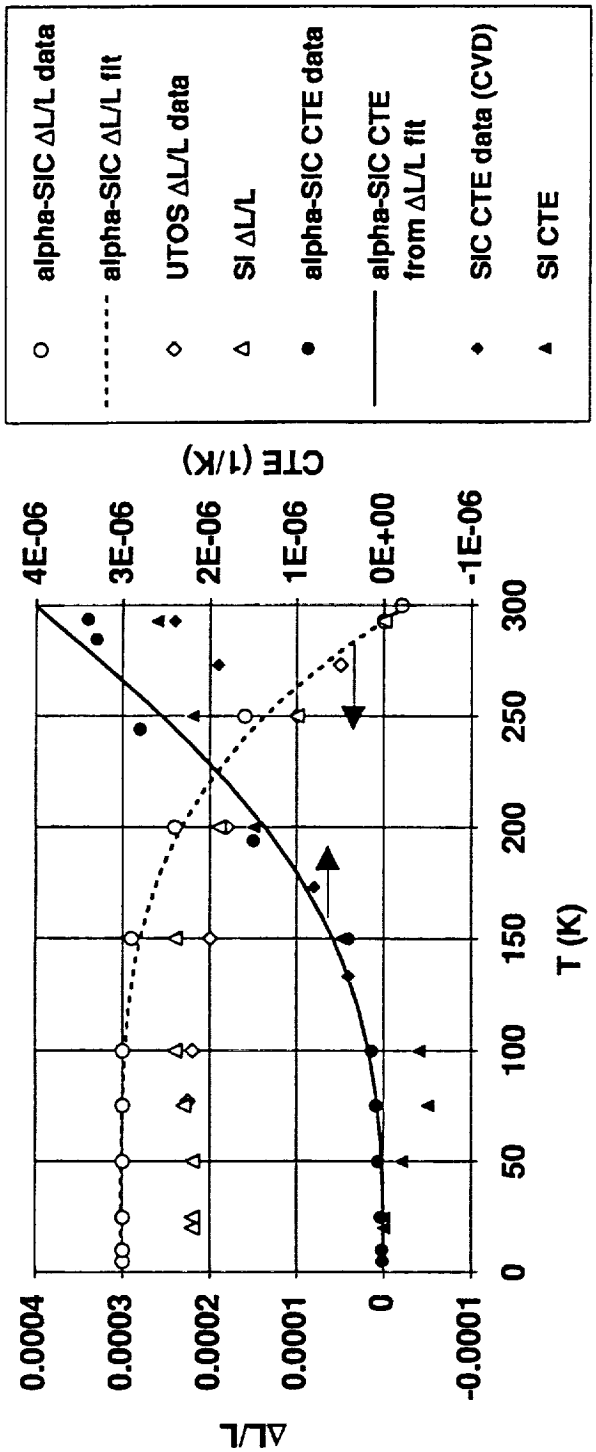

Figure B-4. Silicon Carbide and Silicon Coefficients of Thermal Expansion and Integrated Thermal Contraction. (Data is for the alpha form of silicon carbide and is only approximately correct for reaction-bonded silicon carbide.)

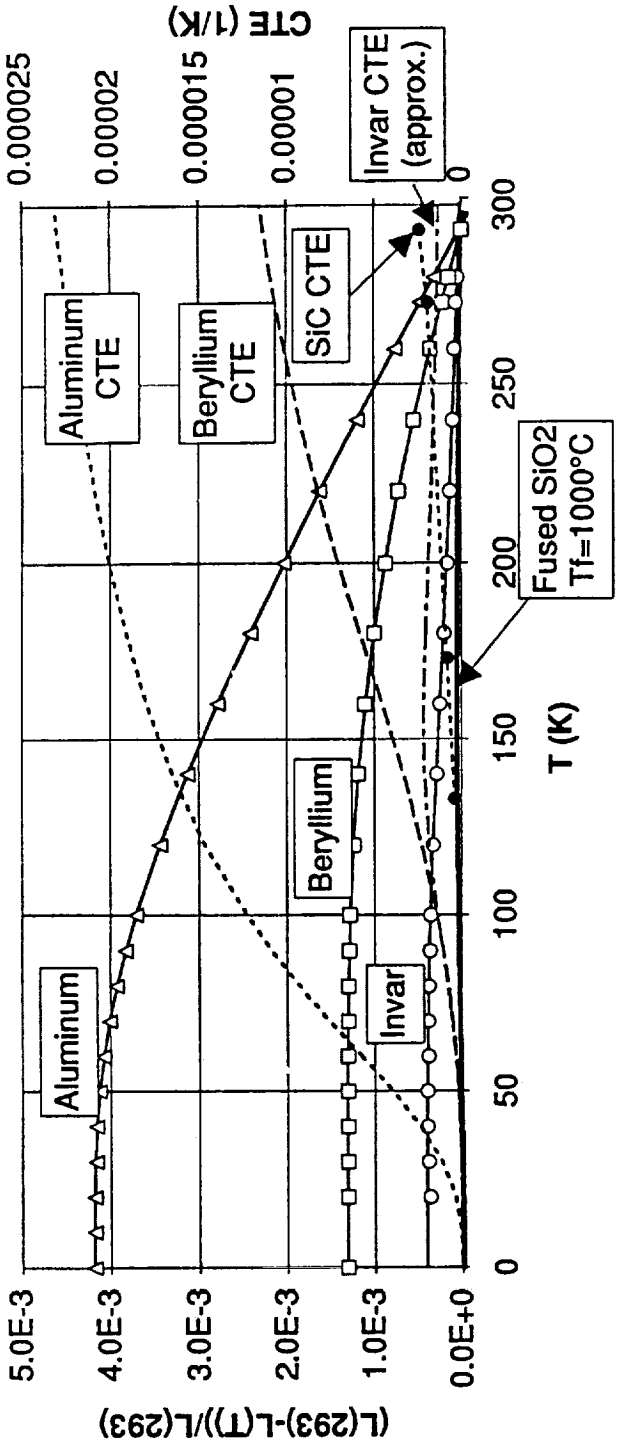

Figure B-5. Comparison of Coefficients of Thermal Expansion and Integrated Thermal Contraction for Metals, Silicon Carbide, and Fused Quartz.

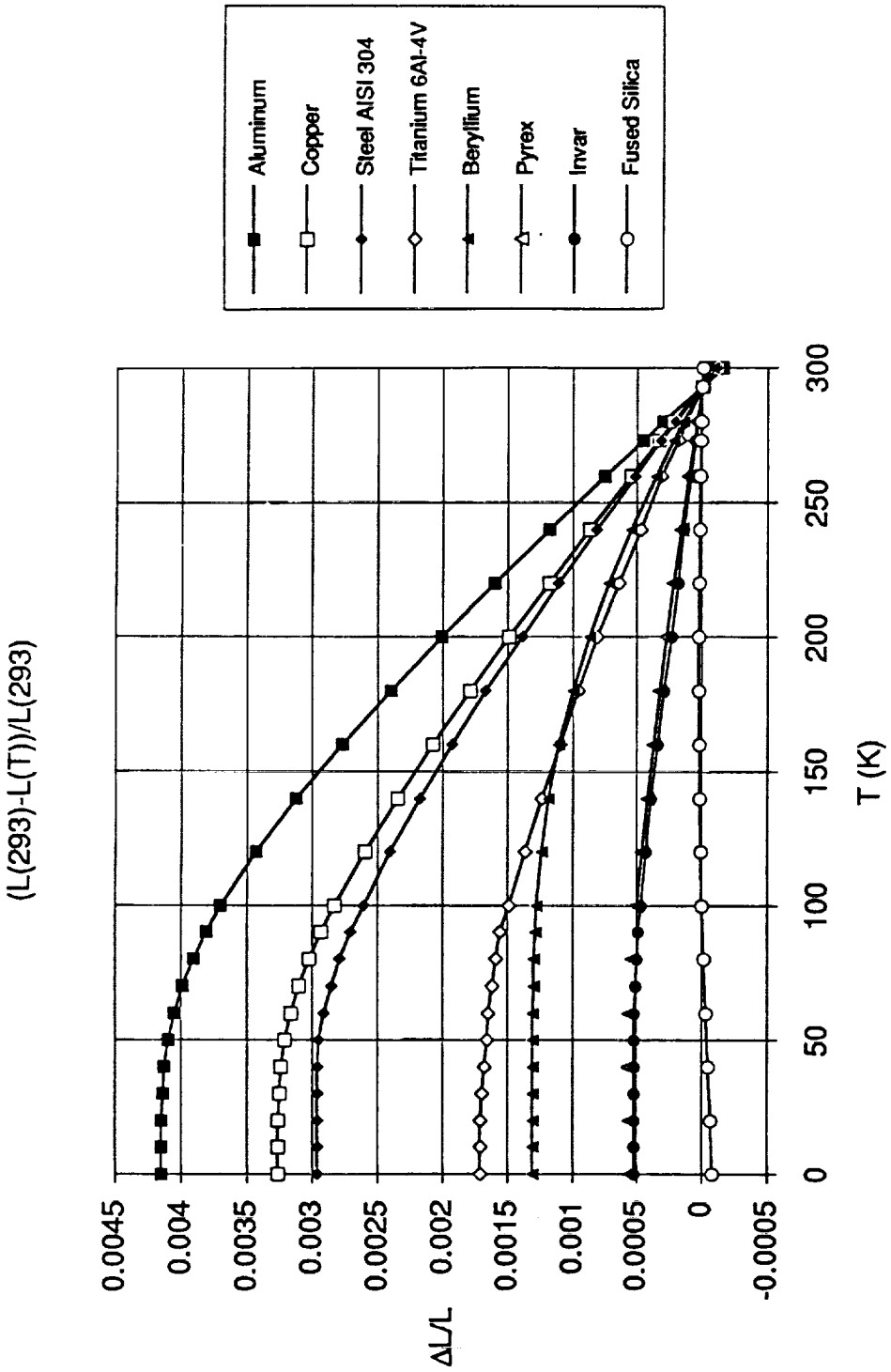

Figure B-6. Comparison of Integrated Thermal Contraction for Metals and Fused Quartz.

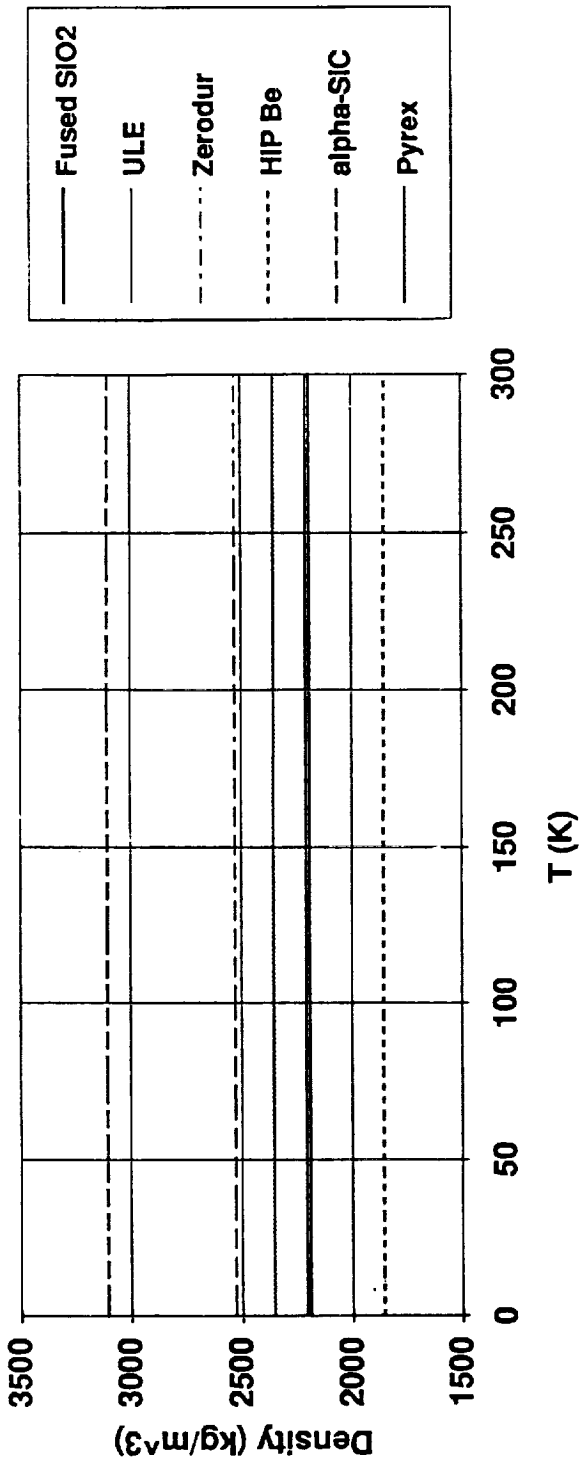

Figure B-7. Density of Candidate Mirror Materials.

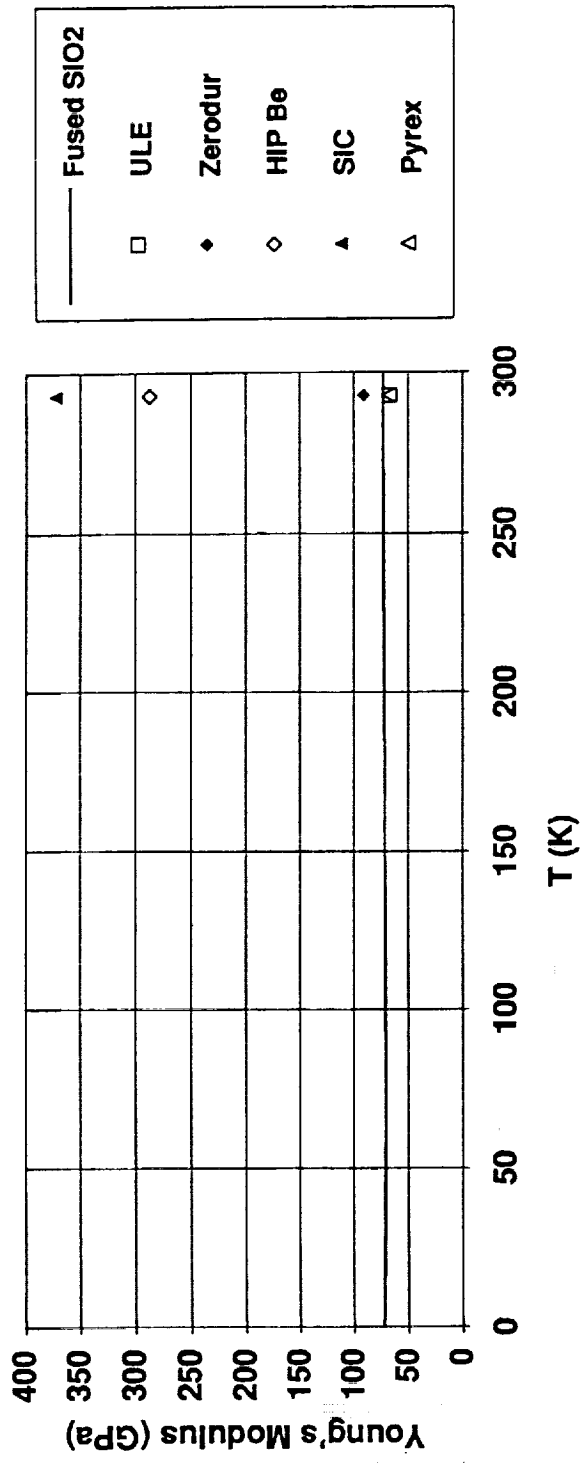

Figure B-8. Young's Modulus of Candidate Mirror Materials.

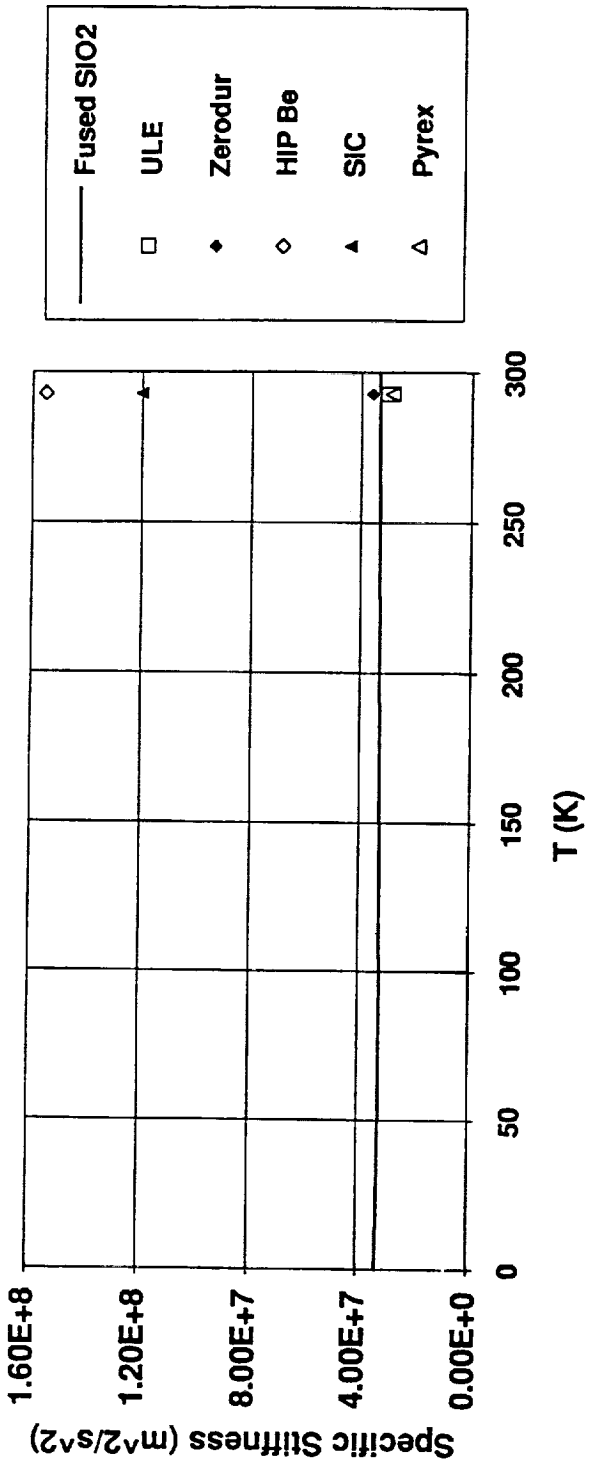

Figure B-9. Specific Stiffness of Candidate Mirror Materials.

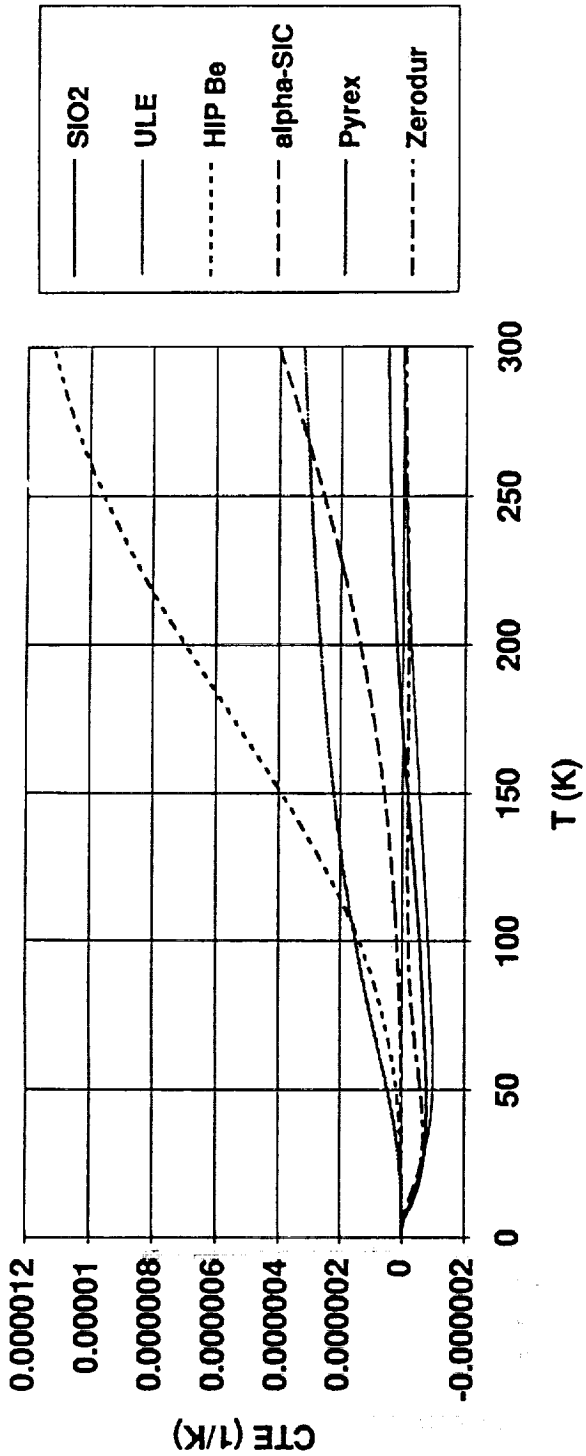

Figure B-10. Coefficient of Thermal Expansion of Candidate Mirror Materials.

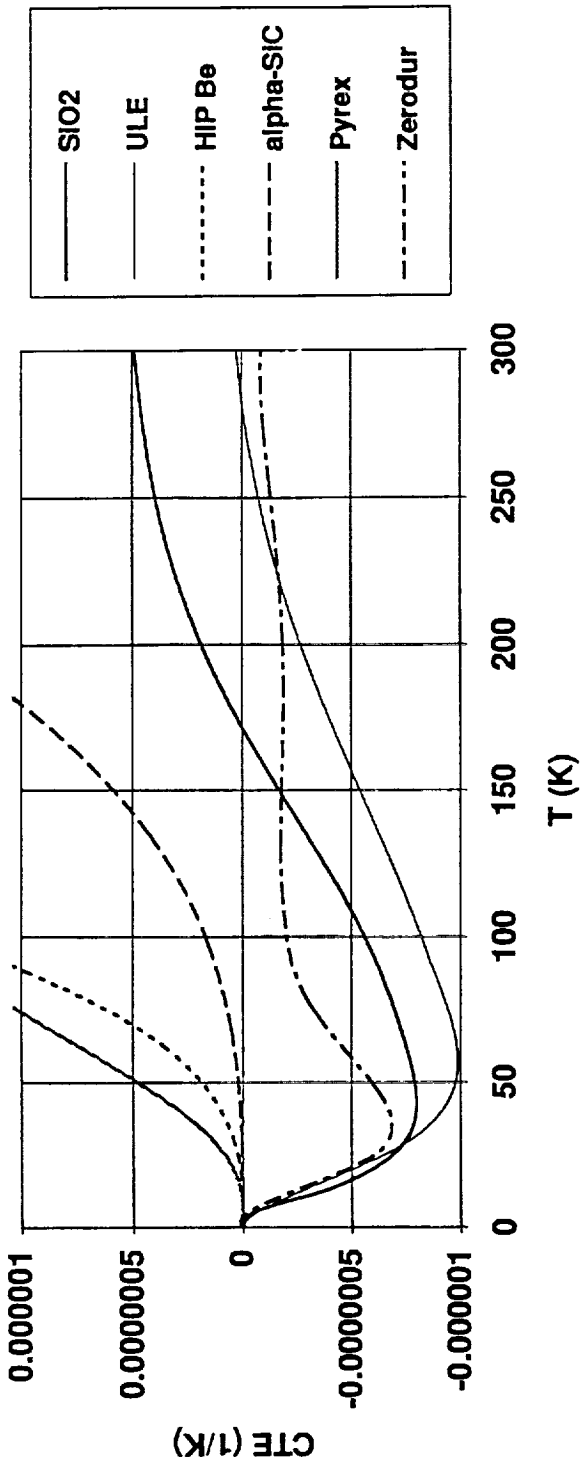

Figure B-11. Coefficient of Thermal Expansion of Candidate Mirror Materials. (Expanded vertical scale of Figure B-10.)

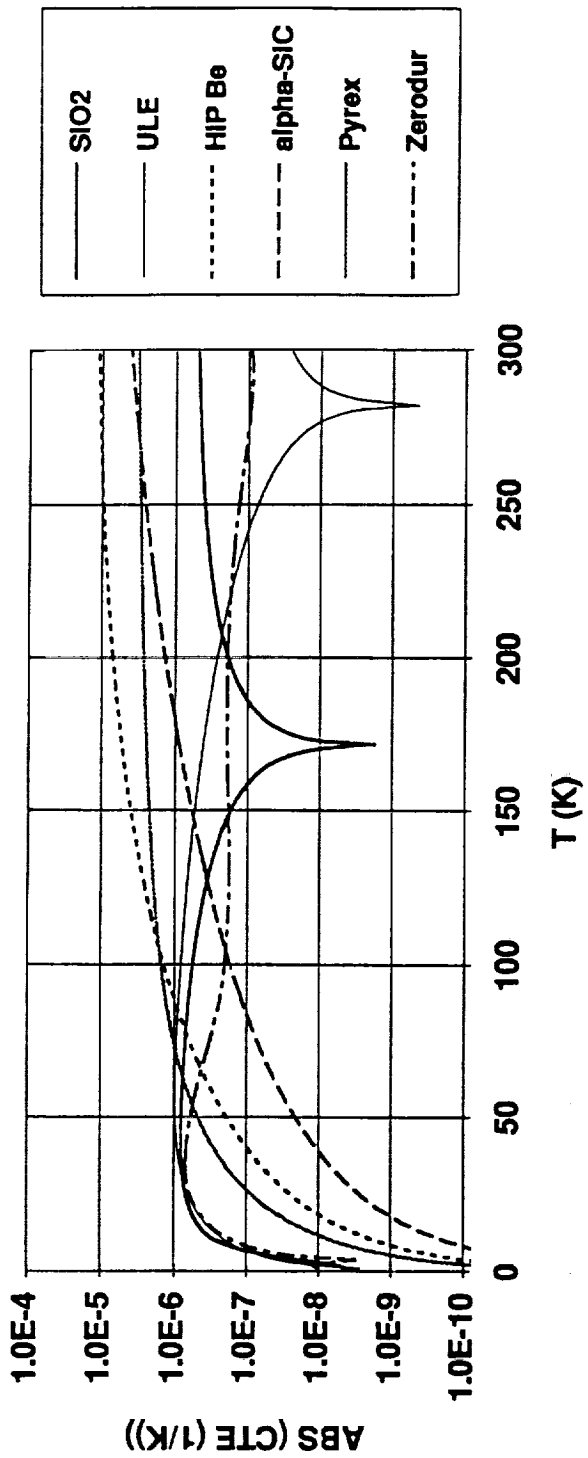

Figure B-12. Coefficient of Thermal Expansion of Candidate Mirror Materials. (Semi-log plot of absolute values of the CTE's shown in Figure B-10.)

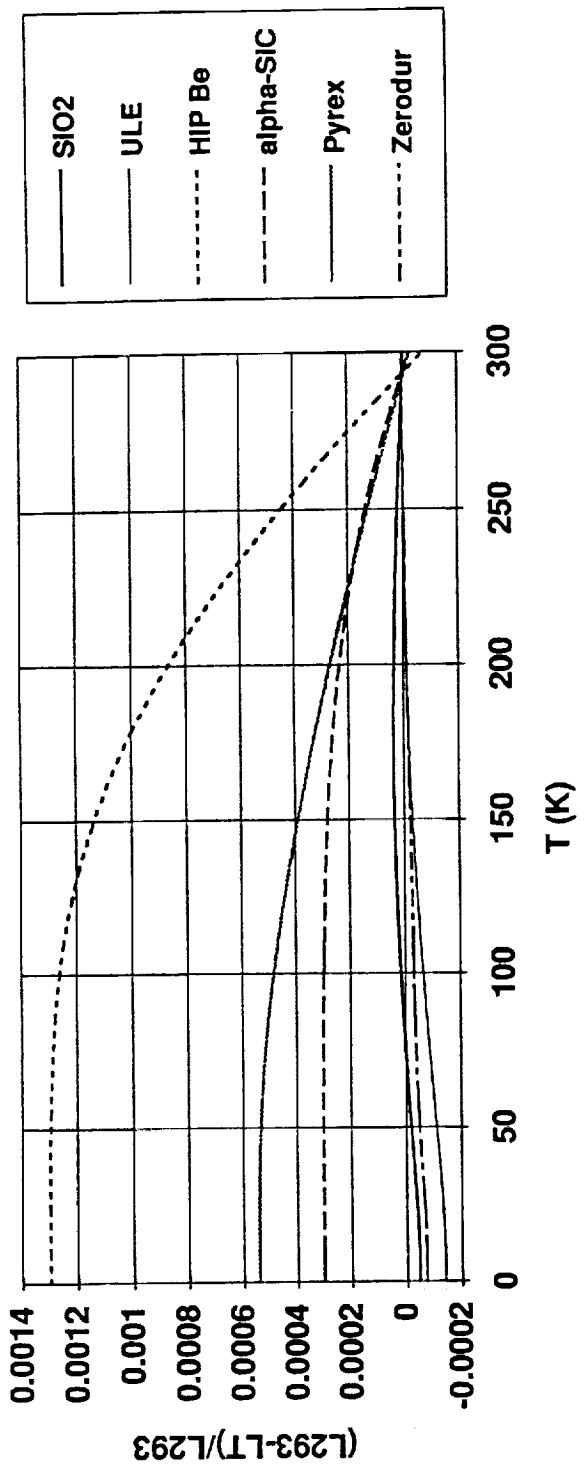

Figure B-13. Integrated Thermal Contraction of Candidate Mirror Materials. Reference temperature is 293 kelvins. Note that fused quartz, Zerodur, and ULE have a net expansion upon cooling to very low temperatures.

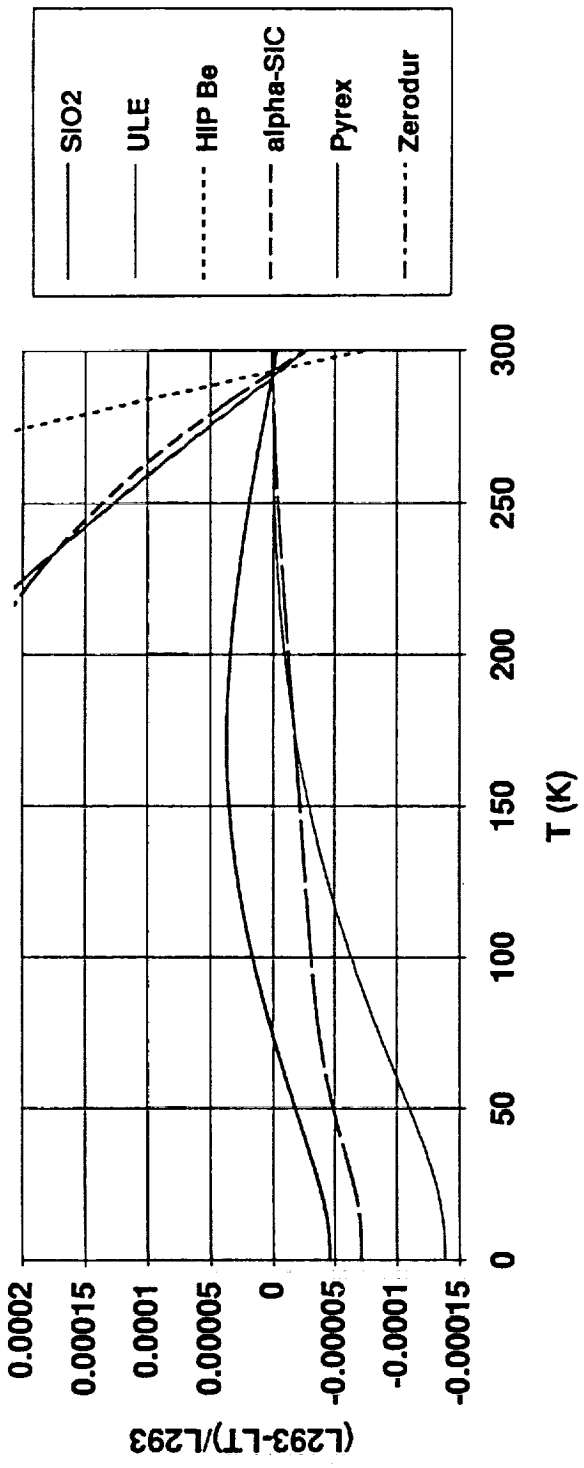

Figure B-14. Integrated Thermal Contraction of Candidate Mirror Materials. (Expanded vertical scale of Figure B-13.)

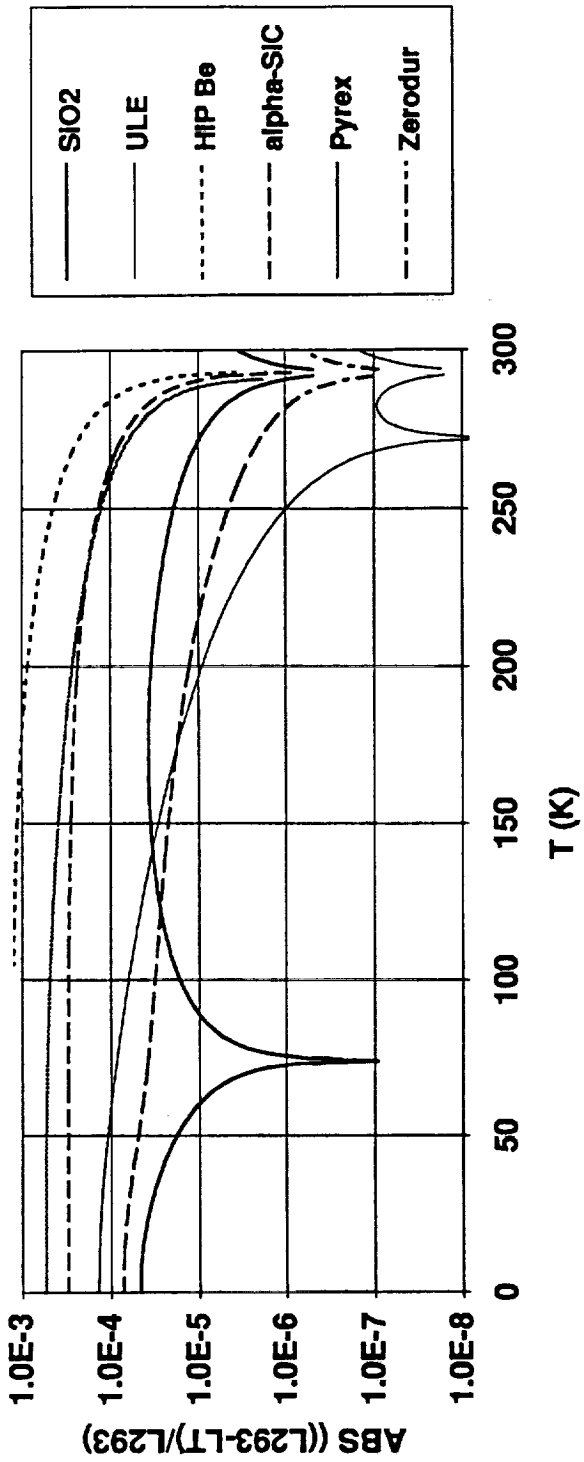

Figure B-15. Integrated Thermal Contraction of Candidate Mirror Materials. (Semi-log plot of the absolute values of the ΔL/L's of Figure B-13.)

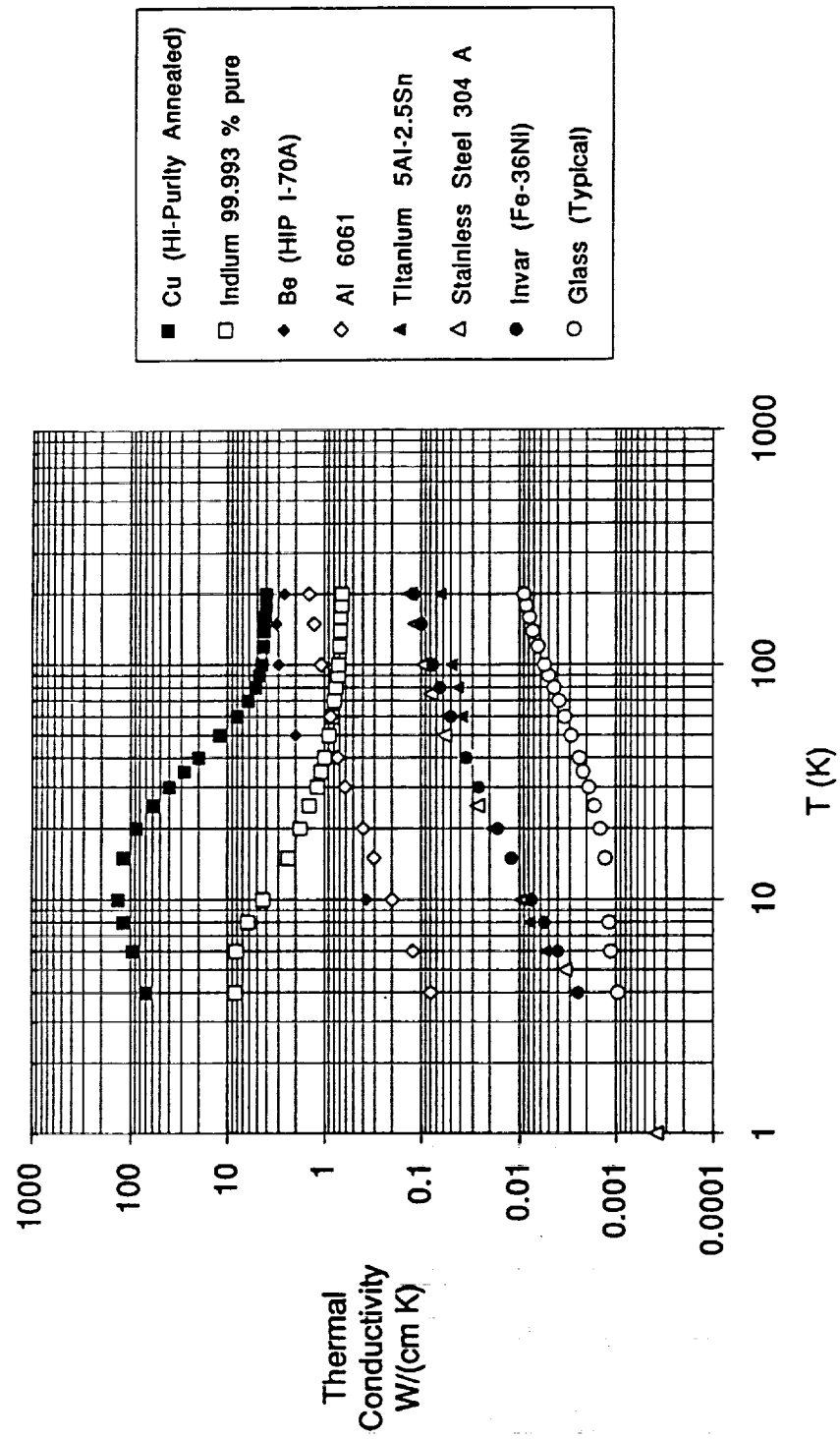

Figure B-16. Thermal Conductivity of Metals and Glass.

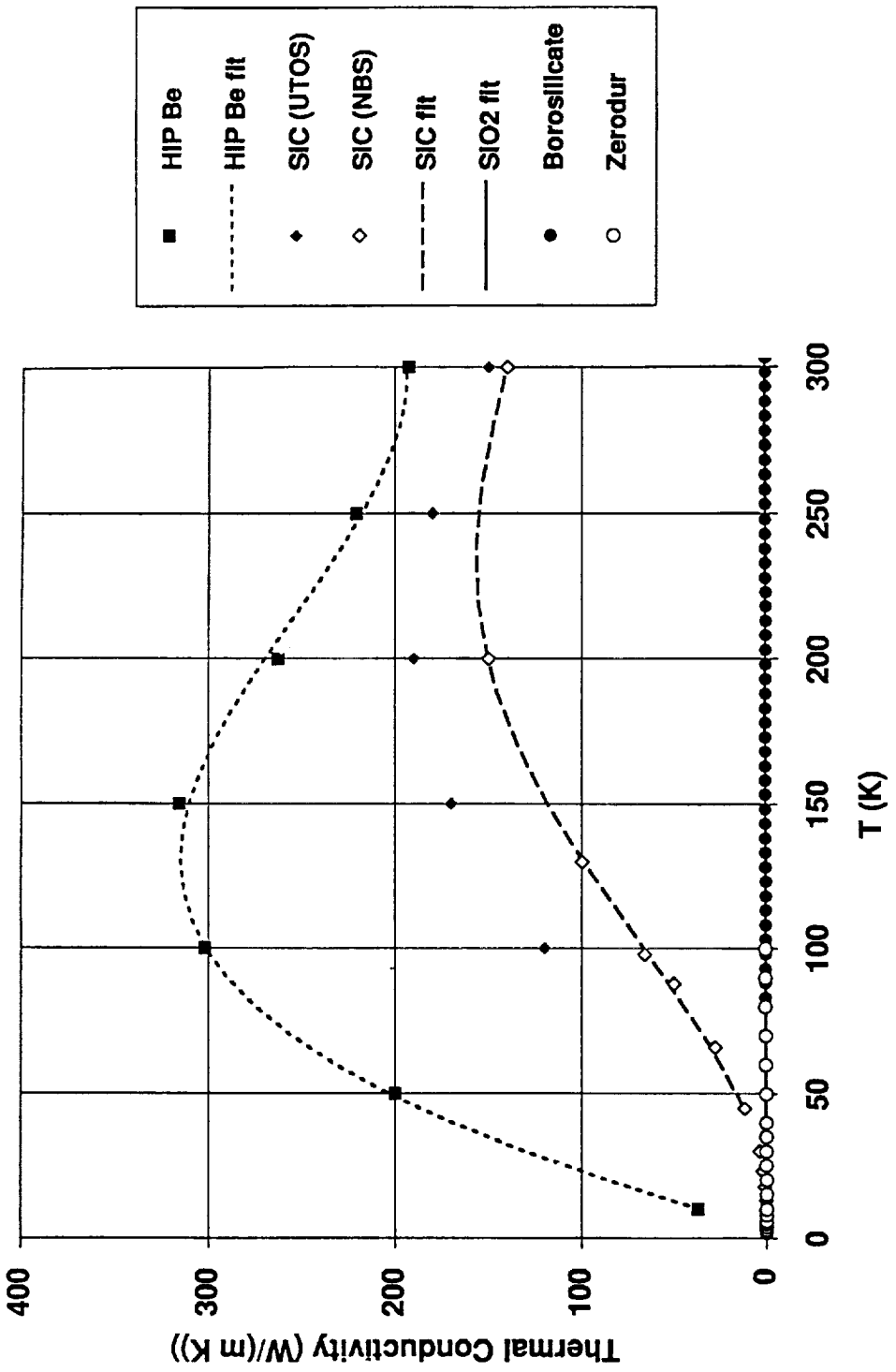

Figure B-17. Thermal Conductivity of Candidate Mirror Materials.

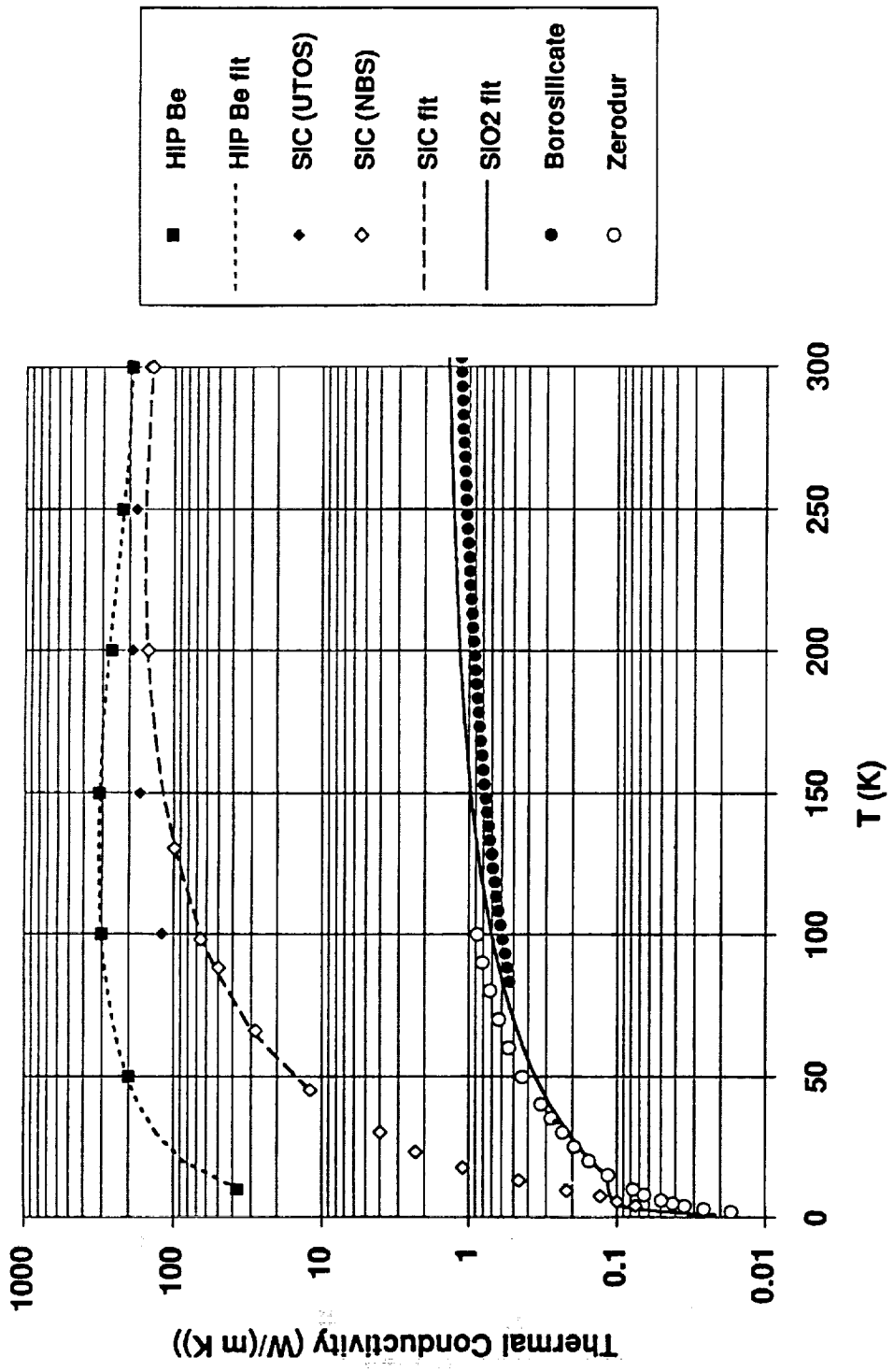

Figure B-18. Thermal Conductivity of Candidate Mirror Materials. (Semi-log plot of Figure B-17.)

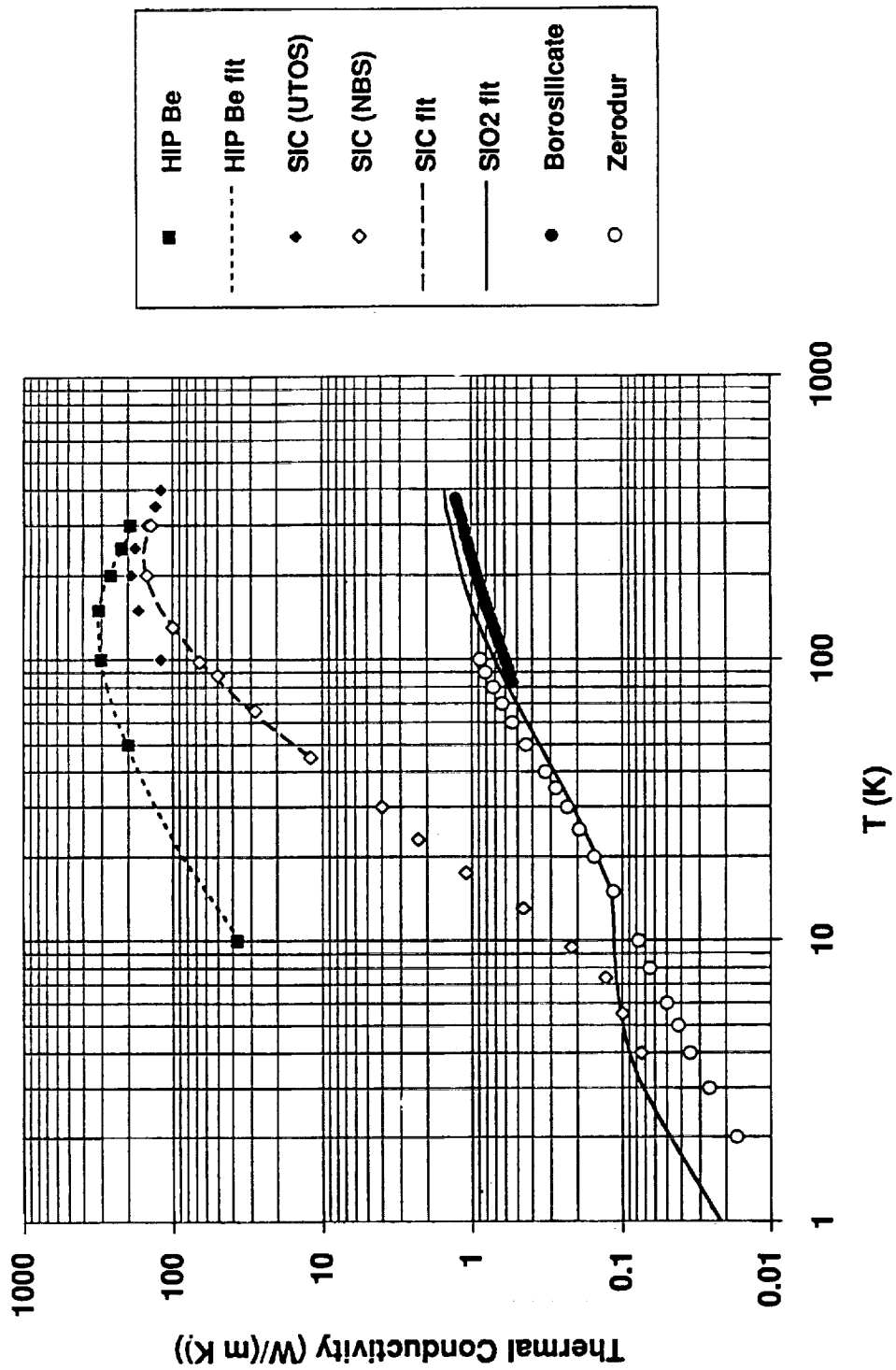

Figure B-19. Thermal Conductivity of Candidate Mirror Materials. (Log-log plot of Figure B-17.)

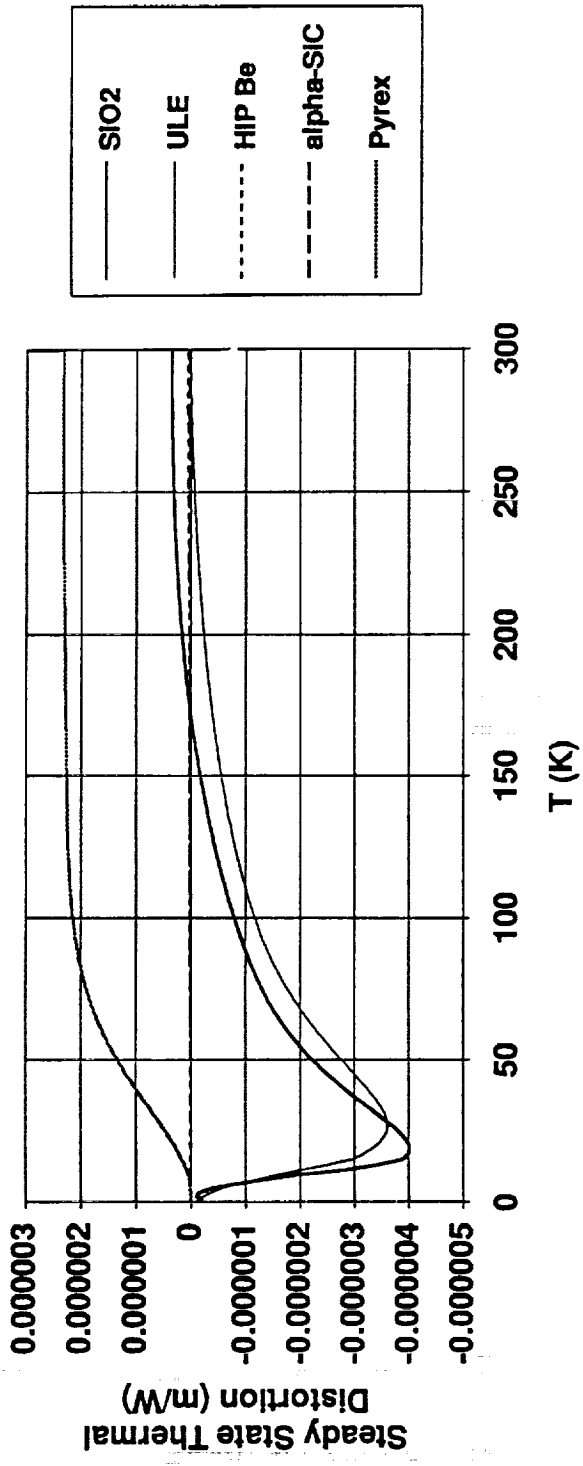

Figure B-20. Steady State Thermal Distortion Coefficient of Candidate Mirror Materials.

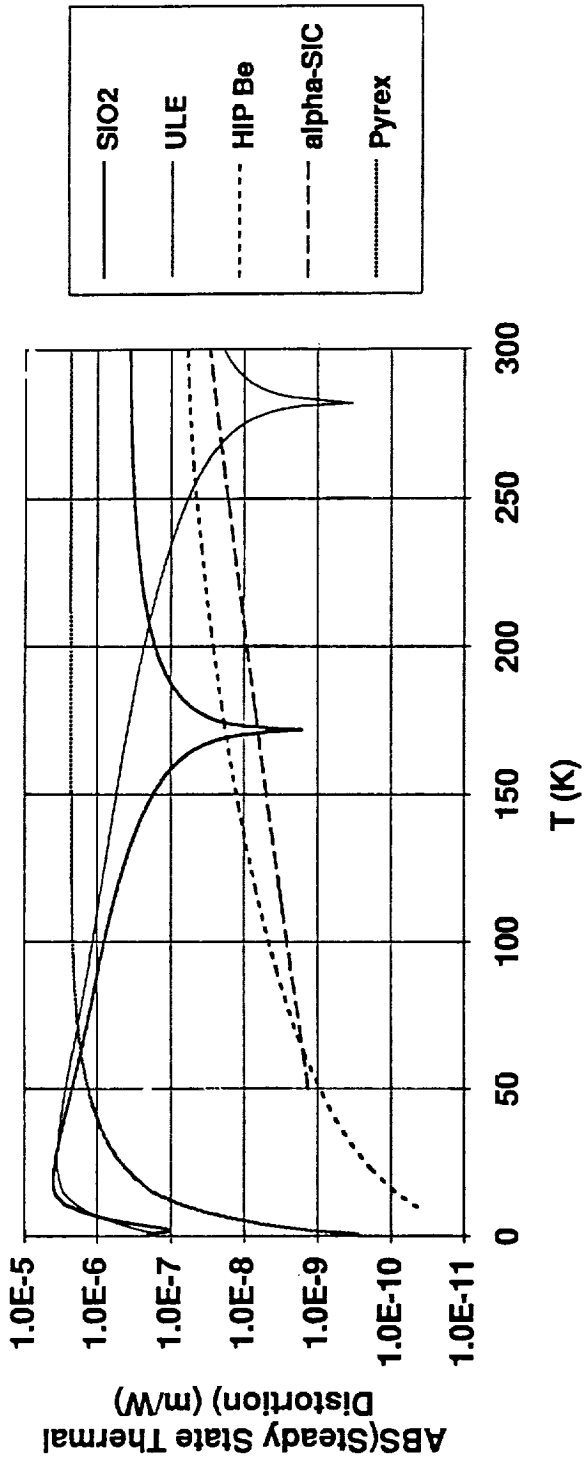

Figure B-21. Steady State Thermal Distortion Coefficient of Candidate Mirror Materials. (Semi-log plot of the absolute values of the SSTD's of Figure B-20.)

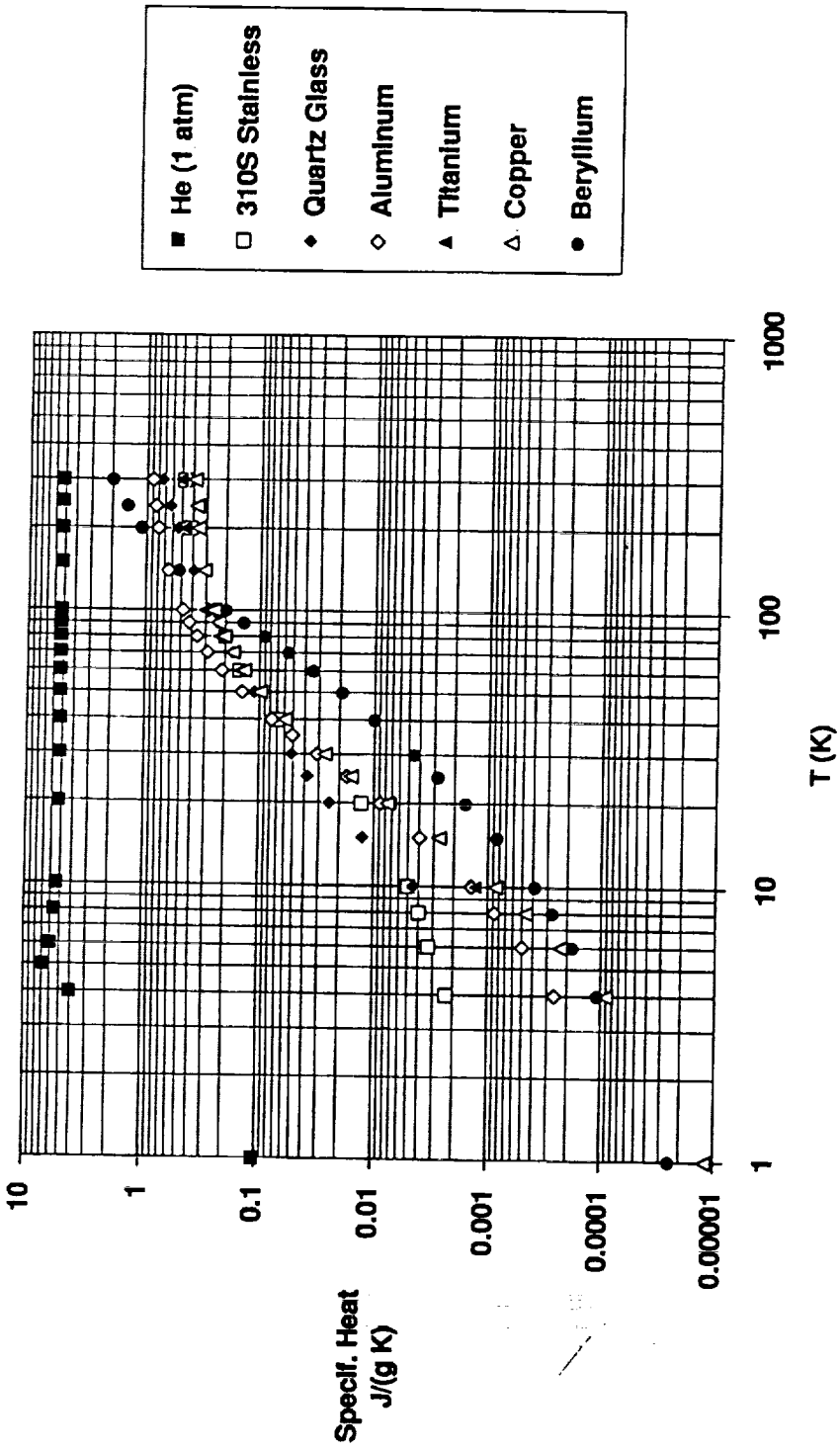

Figure B-22. Specific Heat of Helium, Metals, and Fused Quartz.

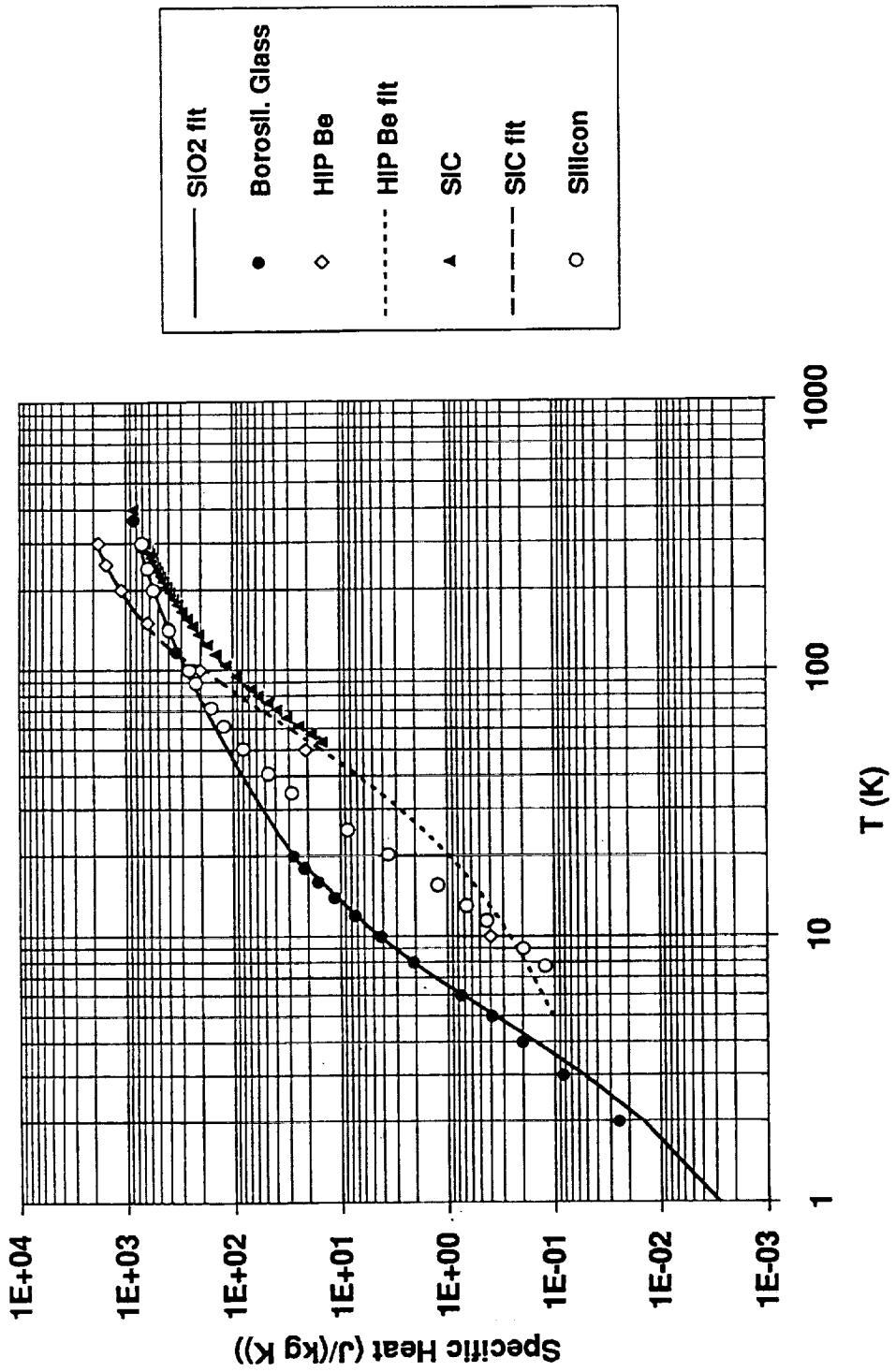

Figure B-23. Specific Heat of Candidate Mirror Materials.

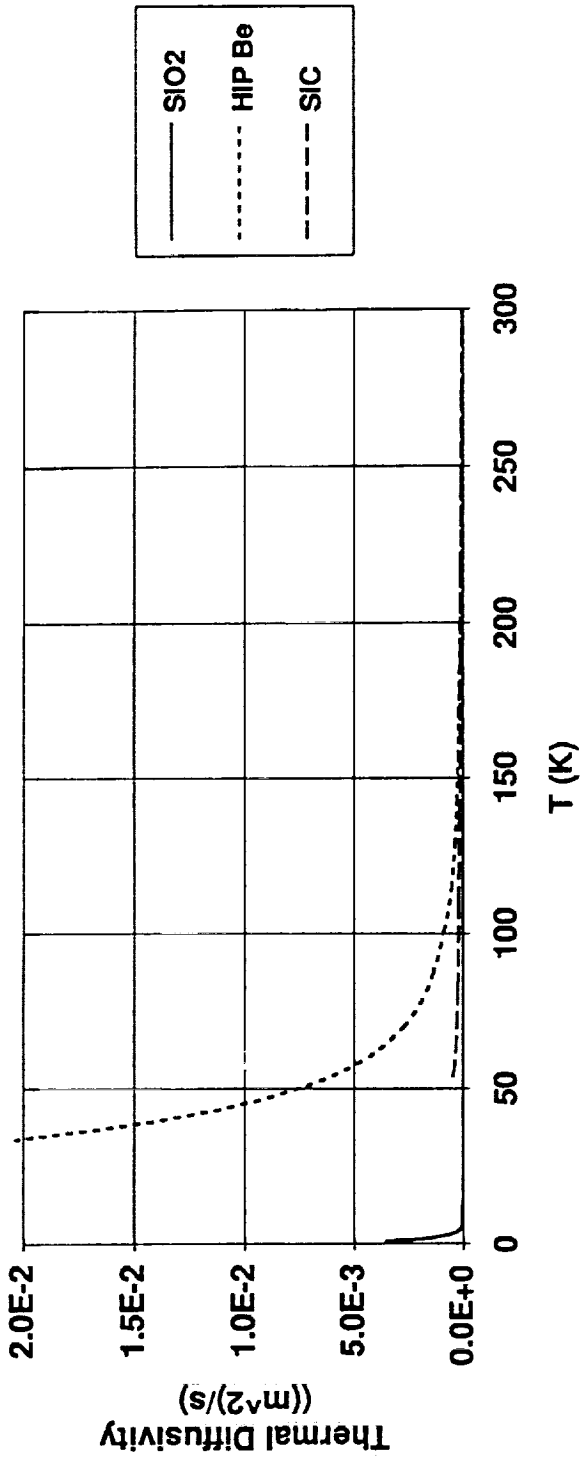

Figure B-24. Thermal Diffusivity Coefficient for Candidate Mirror Materials.

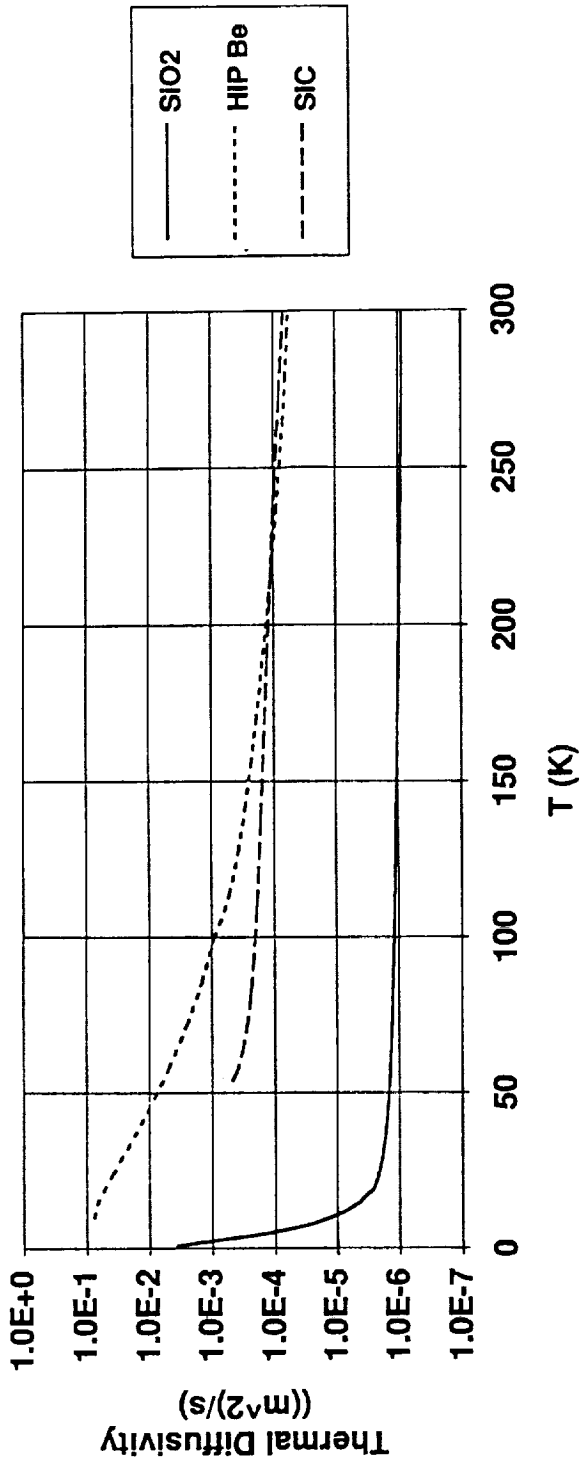

Figure B-25. Thermal Diffusivity Coefficient for Candidate Mirror Materials. (Semi-log plot of Figure B-24.)

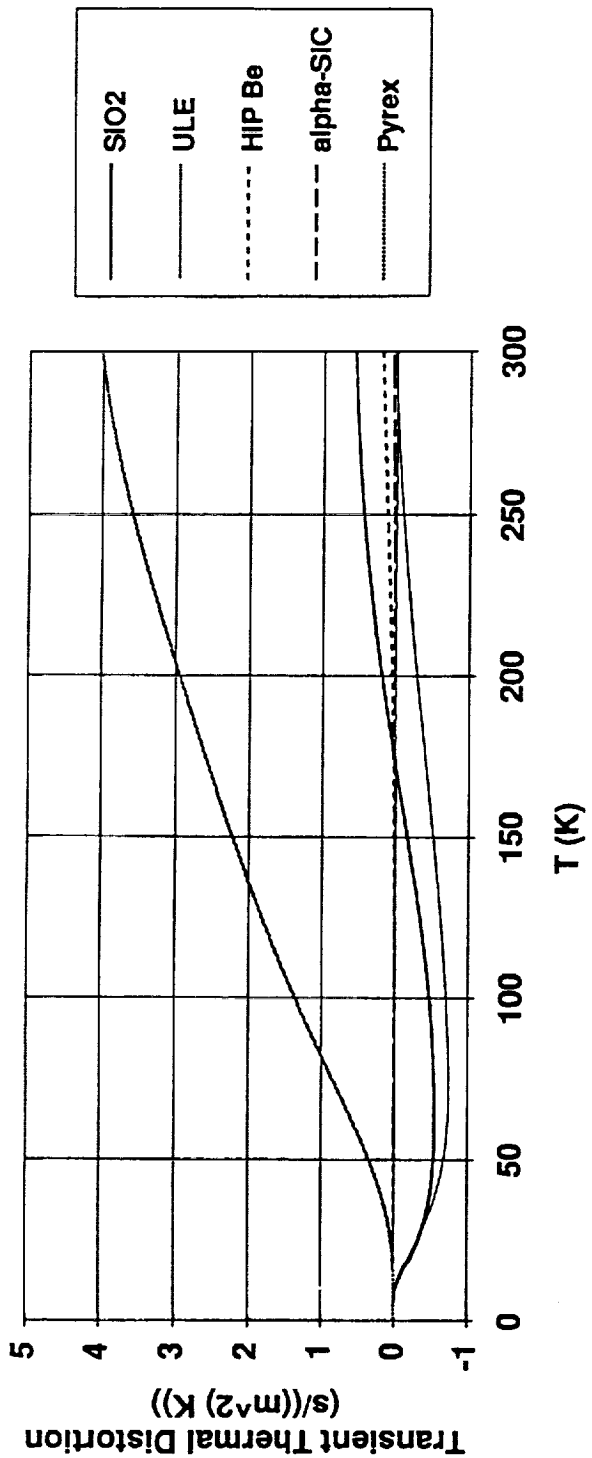

Figure B-26. Transient Thermal Distortion Coefficient for Candidate Mirror Materials.

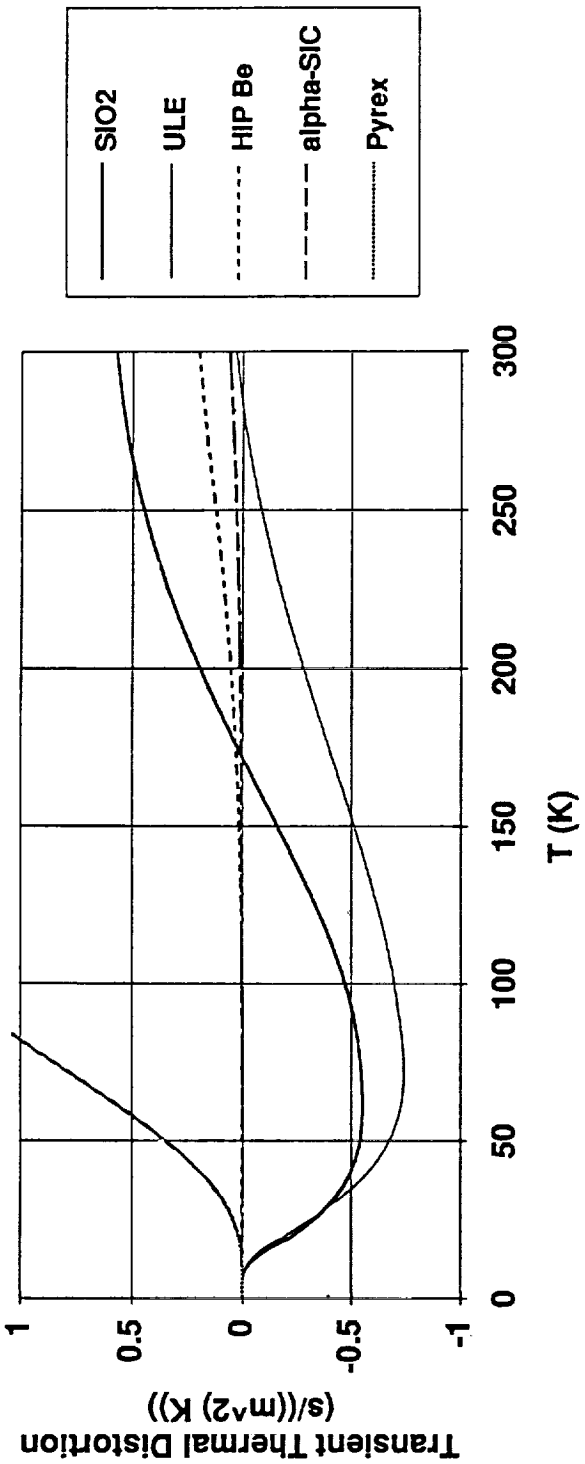

Figure B-27. Transient Thermal Distortion Coefficient for Candidate Mirror Materials. (Expanded vertical scale of Figure B-26.)

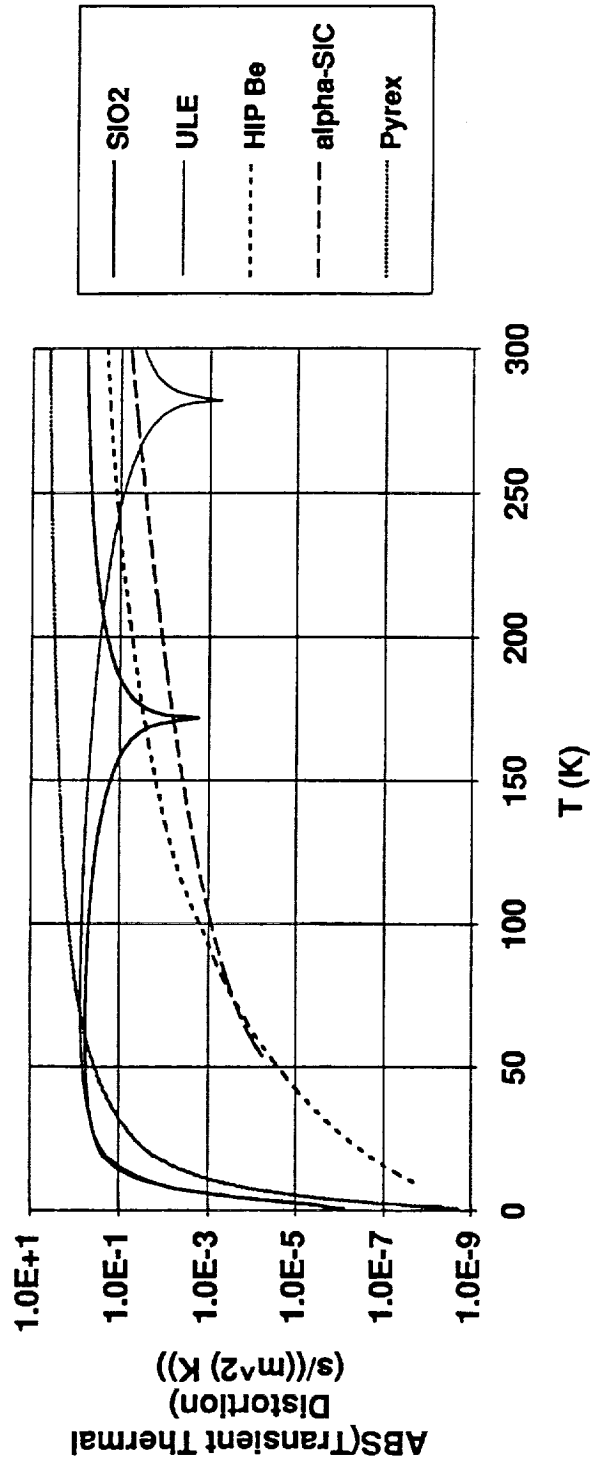

Figure B-28. Transient Thermal Distortion Coefficient for Candidate Mirror Materials. (Semi-log plot of the absolute values of the TTD's of Figure B-26.)

HUGHES DANBURY OPTICAL SYSTEMS, INC.
a subsidiary

PR D15-0015

LUTE TELESCOPE STRUCTURAL DESIGN STUDY REPORT

MAY 1993

Prepared for:

National Aeronautics and Space Administration
George C. Marshall Space Flight Center
Marshall Space Flight Center
Alabama 35812

Order No. H-19671D

HUGHES DANBURY OPTICAL SYSTEMS, INC.
100 WOOSTER HEIGHTS ROAD
DANBURY, CT 06810-7589

HUGHES

Hughes Danbury Optical Systems, Inc.
a subsidiary

Project Report No.: PR D15-0015

Title: LUTE Telescope Design Study Report

Prepared by: _____ 1/9/93
Greg Ruthven, Project Engineer — Date

Approved by: _____ 9 July 93
Mark Stier, Program Manager — Date

Approved by: _____ 7/16/93
George Bossers, Director
Advanced Development Lab — Date

REVISION RECORD:

Revision	Date	Affected Pages
Release	July 12, 1993	i through v, 1-1, 2-1, 3-1 through 3-14 4-1 through 4-4, 5-1 through 5-4, 6-1, A-i

TABLE OF CONTENTS

Section	Title	Page
1	INTRODUCTION	1-1
2	SUMMARY OF RESULTS	2-1
3	UVTA DESIGN DESCRIPTION AND STRUCTURAL ANALYSES	3-1
3.1	Study Logic	3-1
3.2	Primary/Tertiary Mirrors	3-3
3.3	Secondary Mirror Assembly (SMA)	3-5
3.4	Baffles	3-8
3.5	Metering Structure Assembly	3-10
3.6	Main Bulkhead	3-12
3.7	Weight Estimates	3-13
4	PRIMARY-TO-SECONDARY MIRROR DESPACE PREDICTIONS	4-1
4.1	Thermally Induced	4-1
4.2	Secondary Mirror Focus Mechanism Range	4-3
5	MECHANICAL LAYOUTS	5-1
5.1	Overall UTVA	5-1
6	RECOMMENDATIONS	6-1
APPENDIX A	LUTE VIEWGRAPHS FROM 4 MAY 1993 TECHNICAL TELECON	A-I

LIST OF ILLUSTRATIONS

Figure	Title	Page
3-1	Telescope Structural Configuration Trades Conducted in Order to Meet Strawman Set of Requirements	3-2
3-2	Our LUTE Telescope is Based on a 3 Mirror Optical Design and a Very Aggressive Weight Budget	3-4
3-3	1.03 Meter f/1.0 LUTE Primary Mirror	3-6
3-4	0.3 Meter f/0.6 LUTE Tertiary Mirror	3-7
3-5	Beryllium Construction Techniques Successfully Employed on the VUE Telescope are Directly Applicable to LUTE	3-9
3-6	Results from Main Baffle NASTRAN Model Confirms Design Meets Fundamental Frequency Requirements	3-11
5-1	The "Exploded" View of the LUTE Telescope Provides Insight into Assembly Sequences Along with Material and Fabrication Techniques	5-2
5-2	"Side" View of the LUTE Telescope	5-3
5-3	"Top" Views of the LUTE Telescope Sections "A-A" and "B-B" Highlights the Main Bulkhead and Primary/Tertiary Mirrors, Respectively	5-4

LIST OF TABLES

Table	Title	Page
3-1	A Consistent Set of Requirements Have Been Maintained Throughout the LUTE Studies	3-3
3-2	Fundamental Frequency Requirements Based on Ground Testing Diagnostics and Spring-Mass Coupling	3-8
3-3	LUTE Calculated Weight Estimates Compared to Allocations and Assessed to Determine Telescope Feasibility	3-14
4-1	A Material with a Low CTE Over the Entire Operating Temperature Range is Preferred So That Wavefront Distortions Caused by Telescope Axial Temperature Gradients are Minimized	4-3
4-2	Scaled Results from a Similar Optical Design Were Used to Calculate Allowable Telescope Axial Temperature Gradients	4-3
4-3	Identification of Despace Error Sources Have Been Made. Additional Analyses and Test Data Required to Fully Quantify These Effects on Optical Performance	4-4

SECTION 1

INTRODUCTION

The major objective of the Lunar Ultraviolet Transit Experiment (LUTE) Telescope Structural Design Study was to investigate the feasibility of designing an ultra-lightweight 1-m aperture system within optical performance requirements and mass budget constraints. This study uses the results from our previous studies on LUTE as a basis for further developing the LUTE structural architecture.

After summarizing our results in Section 2, Section 3 begins with the overall logic we used to determine which telescope "structural form" should be adopted for further analysis and weight estimates. Specific telescope component analysis showing calculated fundamental frequencies and how they compare with our derived requirements are included. "First-order" component stress analyses to ensure telescope optical and structural component (i.e. mirrors & main bulkhead) weights are realistic are presented. Layouts of both the primary and tertiary mirrors showing dimensions that are consistent with both our weight and frequency calculations also form part of Section 3.

Section 4 presents our calculated values for the predicted thermally induced primary-to-secondary mirror despace motion due to the large temperature range over which LUTE must operate. Two different telescope design approaches (one which utilizes fused quartz metering rods and one which assumes the entire telescope is fabricated from beryllium) are considered in this analysis. We bound the secondary mirror focus mechanism range (in despace) based on these two telescope configurations.

In Section 5 we show our overall design of the UVTA (Ultraviolet Telescope Assembly) via an "exploded view" of the sub-system. The "exploded view" is annotated to help aid in the understanding of each sub-assembly. We also include a two view layout of the UVTA from which telescope and telescope component dimensions can be measured.

We conclude our study with a set of recommendations not only with respect to the LUTE structural architecture but also on other topics related to the overall feasibility of the LUTE telescope sub-system.

SECTION 2

SUMMARY OF RESULTS

Based on this and the previous LUTE study, we remain convinced that the ability to design, build, test and successfully launch and operate a 1-meter class diffraction limited telescope operating over a large temperature range appears to be feasible. The major thrust of this study was to show that the telescope structural form or "architecture" could meet its weight and frequency allocation while still meeting its optical performance requirements. We have shown the weight and frequency requirements to be achievable by fabricating the telescope from beryllium. We have also taken advantage of a telescope architecture which allows efficient use of the available weight by designing deterministic load paths which results in non-complex telescope interfaces. The secondary mirror focus mechanism range is dependent on a number of error sources which have been identified. We have estimated that the anticipated range is well within that currently available (e.g. Hubble Space Telescope) and therefore does not represent a technology risk to the LUTE program.

After evaluating a number of telescope structural architectures we believe that a telescope which uses an "inverted tripod" metering structure in concert with a "single taper" primary mirror design can meet the stringent telescope sub-system weight requirement of 84 kg even assuming a 18% weight contingency factor. Our calculated telescope sub-system weight is 83 kg including this factor. By adopting this design approach significant weight savings are realized in the areas of the telescope light baffle and main bulkhead. This design concept not only meets the weight requirement but meets the derived telescope fundamental frequency requirement of $\geq$ 50Hz. This design also affords us the ability to assemble and align the telescope subassemblies "off-line" so that parallel integration activities can take place.

As mentioned in our previous LUTE study, the extreme temperature range ($\pm$ 100 K) over which the telescope must operate represents a significant challenge in terms of meeting wavefront requirements. Assuming this temperature range the secondary mirror focus mechanism should have a minimum despace range (i.e. travel along the optical axis) of approximately $\pm$1 mm. As a point a reference, the HST focus mechanism has a range of approximately $\pm$ 3 mm.

SECTION 3

UVTA DESIGN DESCRIPTION AND STRUCTURAL ANALYSES

3.1 STUDY LOGIC

The logic used to assess the structural design of the Ultraviolet Telescope Assembly (UVTA) is shown in Figure 3-1. We relied heavily on the results from the MSFC LUTE Interim Technical Assessment Report and the HDOS LUTE PM Material & Design Study to formulate this logic. This included the assessment of the MSFC telescope structural architecture in terms of both weight and fundamental frequency performance. The results of the Hubble Space Telescope-like metering truss design approach used in the MSFC baseline design were used as a benchmark and point of departure for our study.

Based on prior programs such as the Orbiting Solar Laboratory (OSL) where we studied several structural forms for a 1-m telescope, we qualitatively knew the performance of a "ring-stiffened" metering structure as compared to the HST type structure. We therefore focused our attention on two other metering structure designs. The first was a metering bar approach where low coefficient-of-thermal expansion (CTE) material is used to maintain PM-to-SM spacing while decenter errors are minimized via a set of axial and tangential flexures. This structural configuration allows the use of high CTE material (e.g. beryllium) to be used for the load carrying structure.

The other configuration we investigated we termed an "inverted tripod" design where the secondary mirror assembly (SMA) is supported via a metering structure which utilizes the "real estate" between the PM and tertiary mirror (TM). This design approach has a disadvantage in that the metering structure locally obscures a small portion of the converging optical beam at three locations. This is in contrast to a more conventional telescope design which utilizes a SM spider. However we have qualitatively discussed these effects and have determined this design approach to be acceptable.

Our assessments of these two configurations were done in a serial logic form. We made calculations to assess the metering bar and went through the logic "gate" on whether this design option was warranted for further study. We concluded that with the baseline beryllium optics which we recommended in the PM Design Study, a metering design approach to the LUTE telescope did not display any advantages

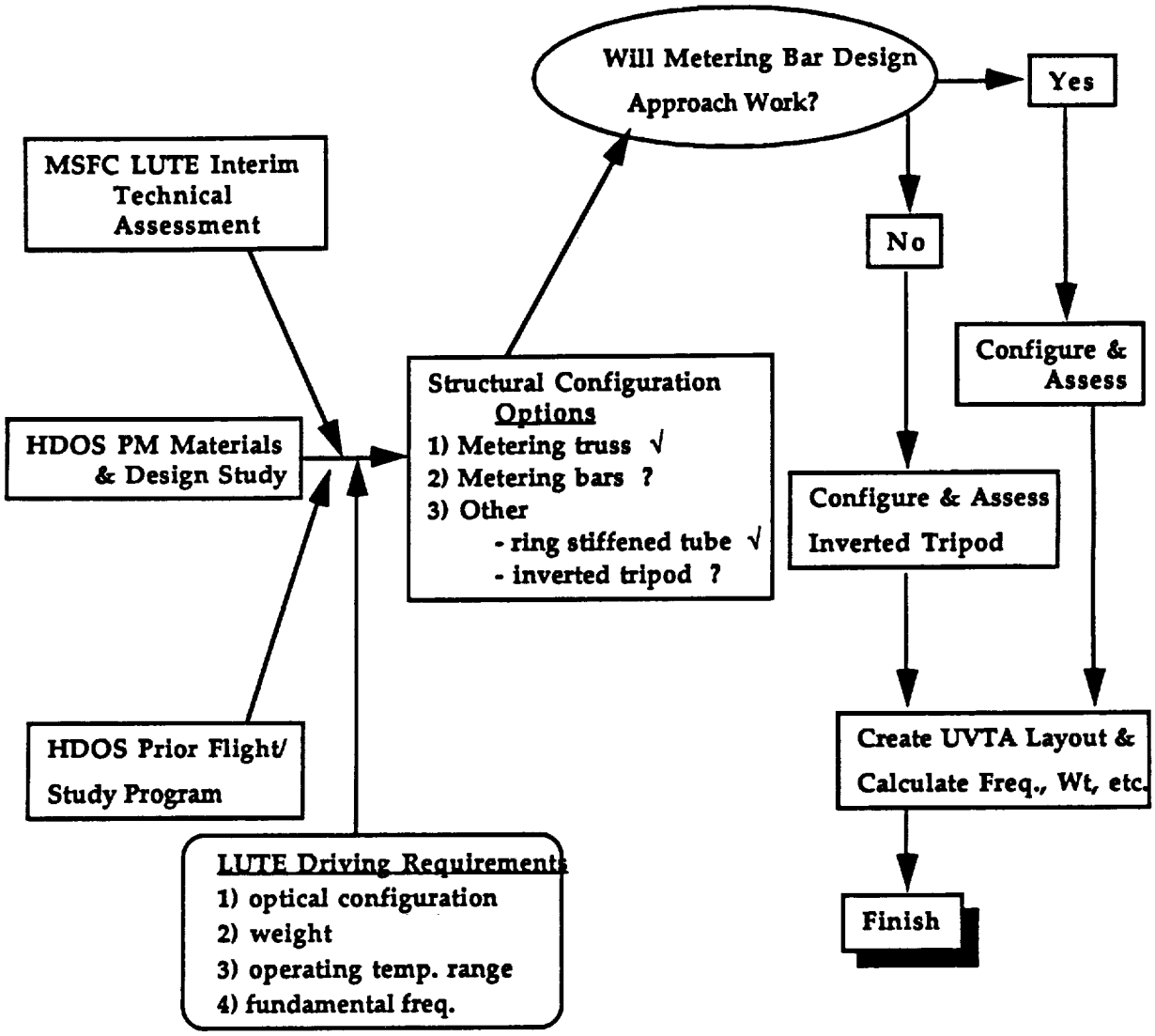

Figure 3-1. Telescope Structural Configuration Trades Conducted in Order to Meet Strawman Set of Requirements.

(this is discussed further in Section 4). We therefore assessed the inverted tripod design and concluded that, to first order, this design will meet the optical performance, weight and fundamental frequency requirements shown in Table 3-1.

TABLE 3-1
A CONSISTENT SET OF REQUIREMENTS HAVE BEEN MAINTAINED THROUGHOUT THE LUTE STUDIES

• Optical Design	• 3 mirror telescope • Diffraction limited @ 0.63 μm • 1 meter diameter C.A. • Operating W.L. = 0.1-0.35 μm
• Telescope Weight	• ≤ 84 kg
• Operating Temperature Range	• 260K - 60 K
• Fundamental Frequency	• Telescope: > 50 Hz • Primary Mirror: > 150 Hz

The inverted tripod design "cut-away" isometric layout is shown in Figure 3-2. There are several design features worth noting. The first is the ability of this design to meet its weight allocation of ≤84 kg. This is possible because of the significant lightweighting possible of the telescope main bulkhead which acts as both the telescope "backbone" along with the interface structure for the telescope hexapod actuators. This lightweighting is made possible only by the implementation of the single taper PM design. This PM design locates the PM mirror mounts at the inner hole ID and therefore the main bulkhead top faceplate can be relatively small in diameter. The second weight benefit of the inverted tripod design is that the telescope light shade is no longer a load carrying structure. It does not need to support the 10.5 kg SMA but only its self weight.

Sections 3.2 through 3.6 will describe each of the major sub-assemblies and/or components and give results of weight calculations, fundamental frequency and "first order" stress calculations due to launch vehicle ascent loads. We summarize the UVTA telescope weight estimate with particular attention to the weight associated with the "structural" components.

3.2 PRIMARY/TERTIARY MIRRORS

During our LUTE PM Study we tentatively concluded that an integral PM/TM design was preferable. Consultations with our optical fabrication personnel indicated that in fact the fabrication of this mirror is feasible.

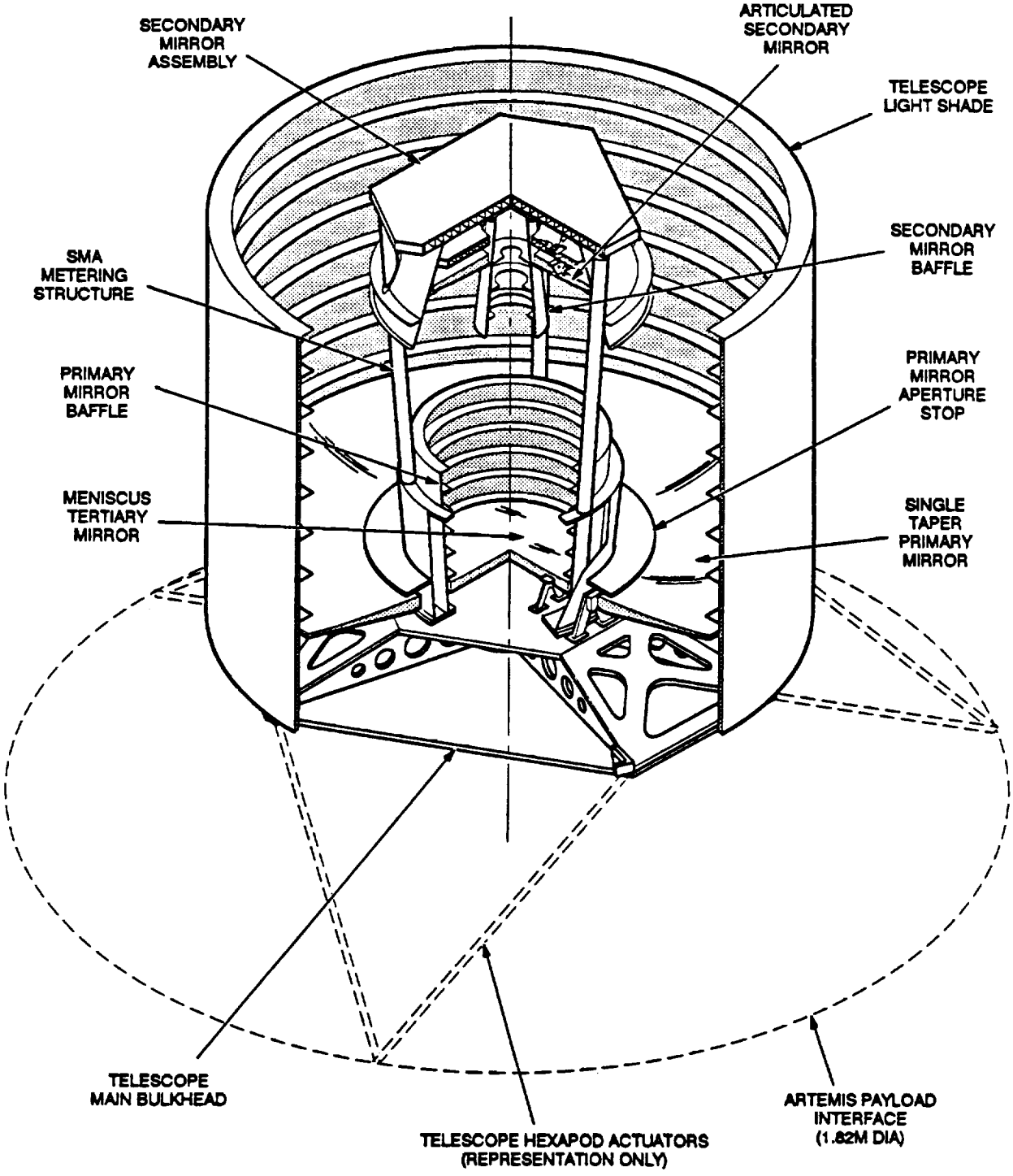

Figure 3-2. Our Lute Telescope is Based on a 3 Mirror Optical Design and a Very Aggressive Weight Budget.

Based on the decision to baseline the inverted tripod metering structure design we have reassessed our original conclusion. Aside from the configuration decision there is a weight penalty associated with an integral PM/TM design. For our single taper mirror design with an inner "hub" thickness of 25 mm, the weight of the portion of the mirror which is a "non-optical" (i.e. an annulus with an OD = 474 mm and an ID of 306 mm) is approximately 5 kg. Assuming the weight allocation of 2.3 kg for the PM mounts would be adequate to accommodate both this increased weight and the weight of the TM, a savings of 0.9 kg would be realized because the TM mounts would no longer be required. The net weight increase to the telescope system would be 4.1 kg, or an increase of 6%.

Figures 3-3 and 3-4 are the LUTE primary and tertiary mirror layouts. The PM is supported by three sets of bipod flexures fabricated from titanium with a thickness of 2.5 mm and a width of 12 mm. The TM is supported by a similar set of flexures. Both mirrors are fabricated from beryllium and each slightly oversized to accommodate edge rolloff effects and beveling during fabrication. We have assumed 10 mm margin for rolloff and 3 mm for beveling (both on the radius). The weights are 22 kg and 3 kg for the PM and TM, respectively.

NASTRAN analyses of these mirrors indicate their frequency requirements are met with margin. These requirements are specified in Table 3-2. Assuming a fixed base, three point attachment to the mirror, the fundamental frequency of the PM and TM are 260 and 1950 Hz, respectively. The hand-calculated maximum stress levels in the mirror assuming a 15 g rms ascent load with factors of safety (FOS) of 1.25 and 1.5 for yield and ultimate are 2700 and 800 psi, respectively.

Our PM design is of a similar form of that which HDOS fabricated and which was subsequently cryo tested at Ames Research Center (ARC) in the 1987-1988. That mirror, fabricated from optical grade I-70A hot isostatic pressed (HIP) beryllium was a 0.5 m diameter optic with an areal density of 28 kg/m^2 and was tested at 80 K and 8 K. The room temperature (293 K) figure was ~0.06 waves rms @ 0.6328 μm and the cryo distortion transitioning from 293 K to 80 K was 0.21 waves rms.

3.3 SECONDARY MIRROR ASSEMBLY (SMA)

The SMA is composed of the secondary mirror (SM), a set of actuators to provide 5 degrees-of-freedom for the SM, a SM hub which reacts the loads imparted to the SM, and the SMA hub which is the main load carrying member of the SMA The SMA hub also provides the interface to the metering structure. The SM baffle will be discussed in Section 3.4.

The SM design is essentially the same as we are using for the TM. That is, a HIP'd beryllium meniscus mirror with a thickness of 12 mm with the same "overage" to account for rolloff and beveling. "Pockets" at three locations on the rear or "R2" surface of the mirror allow the mirror to be supported as close to its center-of-gravity

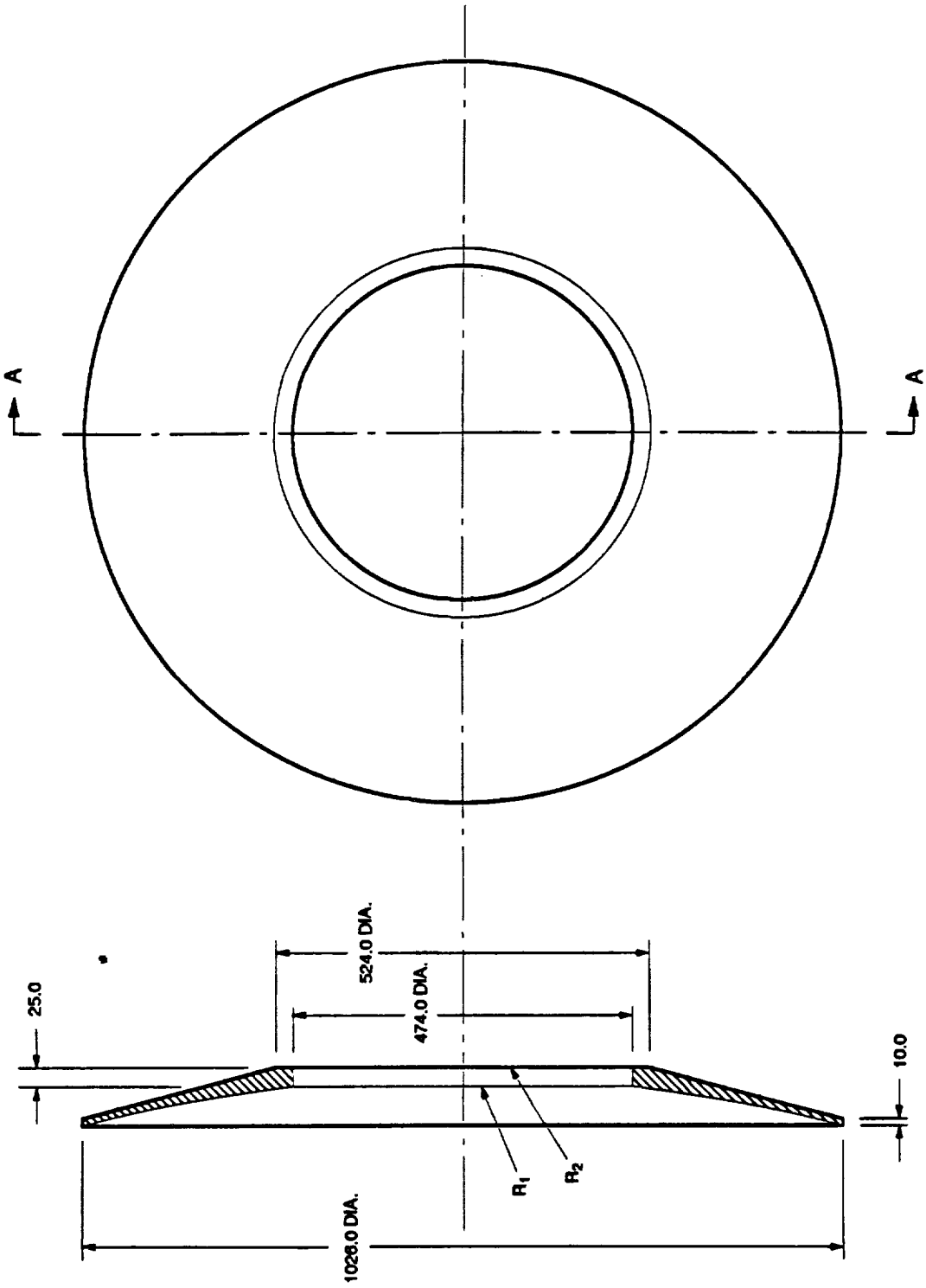

Figure 3-3. 1.03 Meter f/1.0 Lute Primary Mirror.

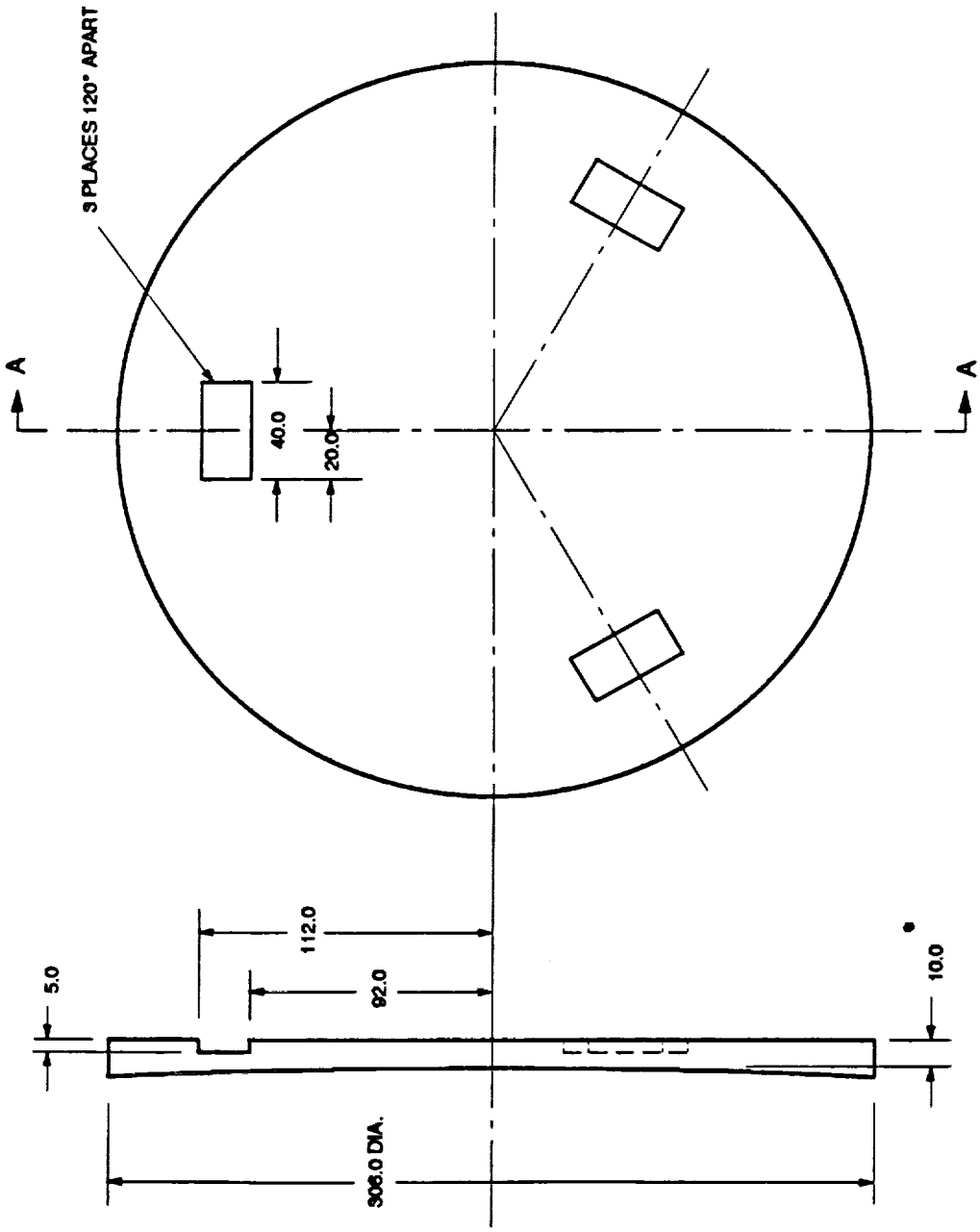

Figure 3-4. 0.3 Meter f/0.6 Lute Tertiary Mirror.

TABLE 3-2
FUNDAMENTAL FREQUENCY REQUIREMENTS BASED ON GROUND TESTING DIAGNOSTICS AND SPRING-MASS COUPLING

- Lute Telescope 50 Hz
  - Primary Mirror Assembly 100 Hz
    - * Primary Mirror 150 Hz
    - * Main Bulkhead 500 Hz
  - Secondary Mirror Assembly 300 Hz
    - * Secondary Mirror 800 Hz
    - * SM Hub 500 Hz
    - * SM Delta Frame 500 Hz
  - Metering Structure 60 Hz
  - Tertiary Mirror Assembly 500 Hz
    - * Tertiary Mirror 1000 Hz

(CG) as possible via 3 sets of bipod flexures. Additional bending moments during ascent would cause the flexures to be heavier if we didn't employ these "pockets." A calculated first mode of 1045 Hz and a stress level of 6100 psi meets the requirements.

The SM hub and delta frame are both lightweighted designs which utilize a square core structure sandwiched between two faceplates that are 1.5 mm thick with an overall thickness dimension of 19 mm. This same type of construction was used on a number of components on the Visible/Ultraviolet Experiment telescope which flew in the late 1980's. The construction technique used to fabricate these sections was to EDM (electro-discharge machine) a number of small diameter holes in the faceplates and core structure and to lock wire them together during the brazing operation. The wires were removed after the brazing operation. Figure 3-5 is a photograph of the forward end of the VUE telescope showing two lightweighted bulkheads which are nominally 50 mm in depth. Brazed connection between the bulkheads and other telescope structure can also be seen along with local inserts in the core structure to accept threaded connections. Hand calculations to determine the fundamental frequency of the two LUTE 19 mm deep lightweighted structures show that the 500 Hz first mode requirements are met (800 and 725 Hz for the hub and frame, respectively).

3.4 BAFFLES

All of the UVTA baffles are fabricated from aluminum. We considered issues such as material size availability, the baffle not being a load carrying member (except its own self weight) and ease of fabrication when determining these designs. For instance, the main baffle could not be fabricated from a single sheet of beryllium.

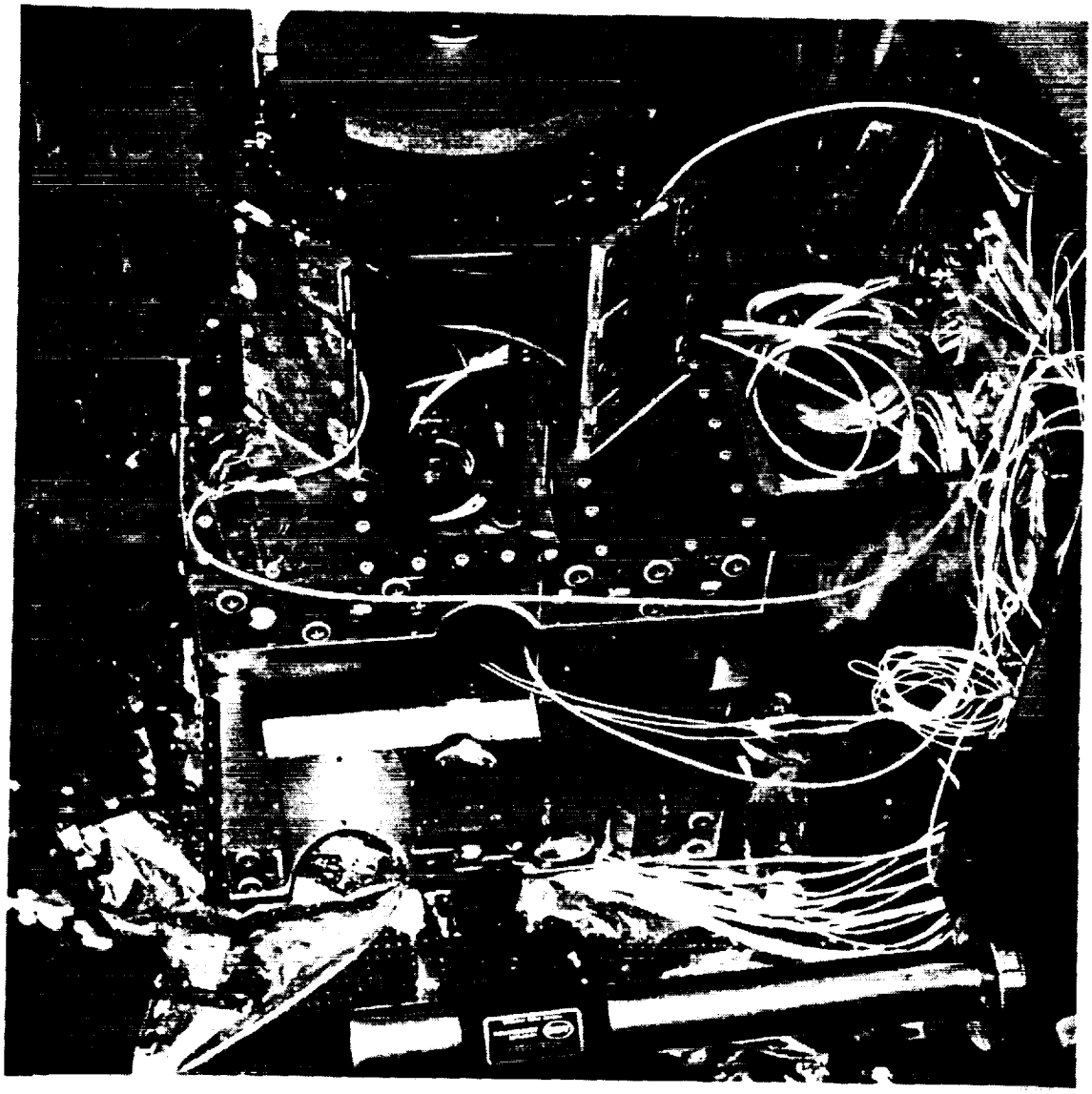

Figure 3-5. Beryllium Construction Techniques Successfully Employed on the VUE Telescope are Directly Applicable to Lute.

The main baffle is nominally 1120 mm in diameter and 960 mm in length. Its construction is a ring-stiffened structure with a wall thickness of 0.4 mm. Internal vanes which are 25 mm deep are attached to this shell and act as both structural stiffeners and stray light control vanes. Figure 3-6 is the NASTRAN modal analysis of this structure which shows a first bending mode frequency of 230 Hz and weight of 5.9 kg. This weight is slightly higher than the original estimate of 4.1 kg and is due to the further definition of the packaging requirements of the SMA.

Both the SM baffles are of similar construction to that of the PM baffle. Aluminum is again used for both SM baffles which are truncated cones with vanes located on the OD and ID. These baffles are attached the SM delta frame through a series of pinned and bolted joints. The combined weights of both of these structures is 2.1 kg.

The central baffle (primary baffle) has two functions. It's first function is to act as a stray light control component. We again have kept it's shell thickness the same as all other UVTA baffles. However this baffle also aids in the stiffening of the metering structure. In order to decrease the effective cantilevered length of the metering structure and thereby increase its natural frequency, we've connected the central baffle to not only the main bulkhead top faceplate but also the beryllium tubes which form part of the metering structure. As will be discussed in the next section, this "closes" the metering structure on its ID while a second stiffening shell, considered part of the metering structure assembly, "closes" the structure on its OD.

3.5 METERING STRUCTURE ASSEMBLY

Our inverted tripod structure takes advantage of the annular region between the PM ID and TM OD to package the metering structure. This structure is connected to the main bulkhead via an interface flange which is pinned and bolted to the top faceplate. Our current concept for this design is to utilize 6 beryllium tubes that are 34 mm in diameter with a wall thickness of 2.5 mm. These six tubes extend from the main bulkhead interface flange in a slightly canted orientation (i.e. the origin of the term "inverted") to a point approximately 240 mm from the main bulkhead interface. Three of the six structural tube members are terminated at this location to minimize distortion at the image plane due to this obscuration. The three members that are terminated are "capped" with three sections of an annular ring. These sections are brazed to the top of the members and to the periphery of the three structural members which continue up to the SMA. This adds significant rigidity to the structure. To further add stiffness of this structure an outer shell is attached to all six tube members. By designing this structure in this fashion the effective cantilevered length of the metering structure is significantly reduced.

NASTRAN analysis of this structure has been completed. Assuming that the cantilevered length is approximately 560 mm (the distance from the termination of three metering structure tube members to the SMA support location), and using the SMA calculated weight estimate of 7.2 kg, our analysis shows the first bending

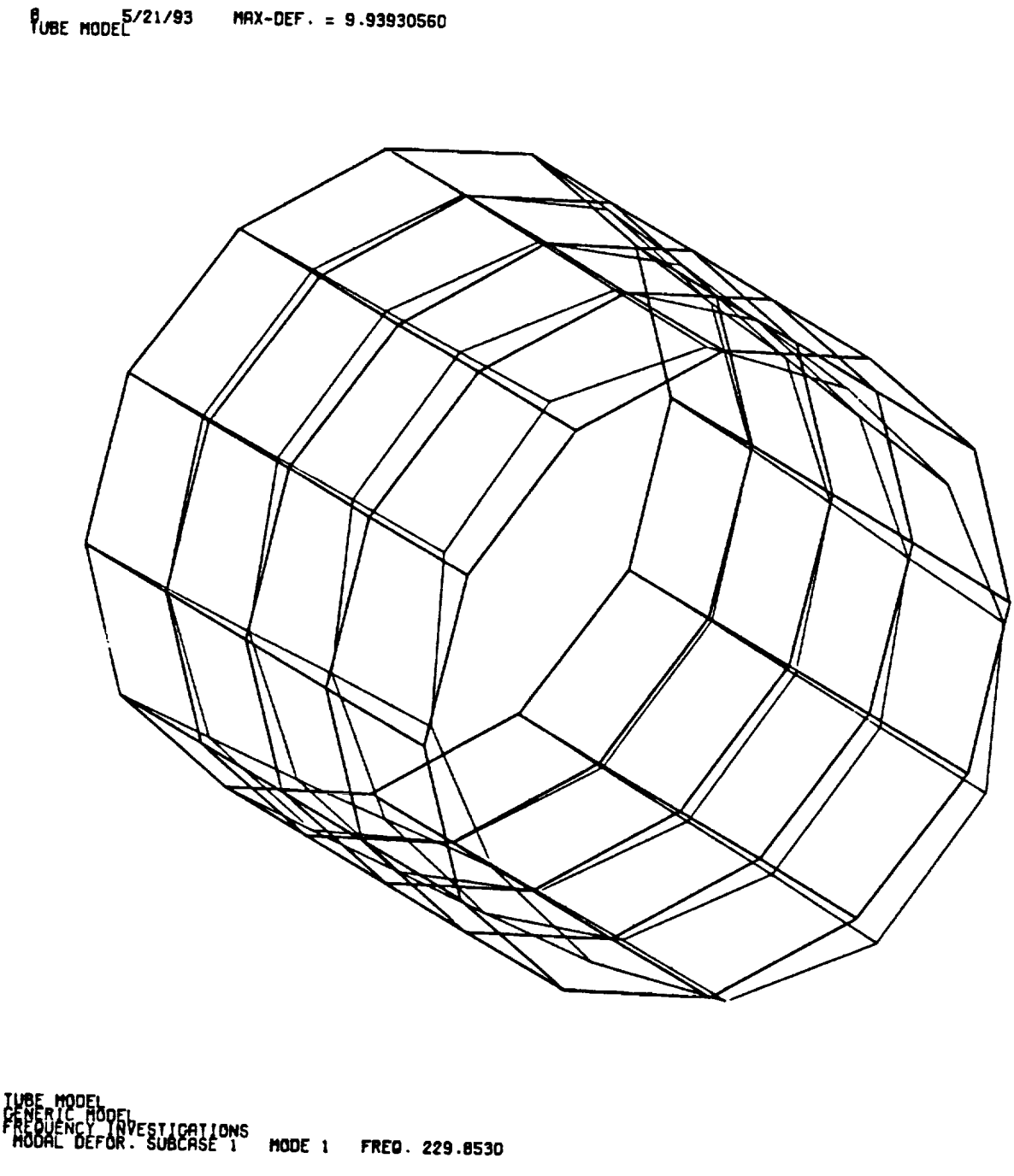

Figure 3-6. Results from Main Baffle NASTRAN Model Confirms design meets fundamental frequency requirements.

mode of the metering structure is 65 Hz. The first torsional mode of this structure is 104 Hz. The 60 Hz derived requirement is satisfied with this design approach and therefore we feel comfortable that ascent and lunar performance can be achieved.

The total weight of this structure is 2.2 kg which includes the weight of the 3 short and long beryllium tubes, the 3 annular ring "caps", the main bulkhead interface flange, and the 240 mm long metering structure closure cylinder. The "caps" and the interface flange are both 2.5 mm thick while the truncated cylinder is 1.3 mm thick. Hand stress analysis show that tube stress levels are low. A calculated stress of 9200 psi in a tube is well within the nominal values for yield and ultimate failure criteria for extruded beryllium structural shapes.

3.6 MAIN BULKHEAD

Our main bulkhead design is one of the major reasons why we feel that the 84 kg telescope weight requirement is feasible. To develop this concept we combined the fact that the PM single taper design requires its mounts to be located near its central hub and that the telescope main baffle must only be self supporting.

Lightweighting of this structure is evident. Minimization of weight is accomplished through the use of lightening holes and cutouts. Shear panels, which "beam" the loads from the top to bottom faceplates and then transfer these loads to the telescope hexapod actuators utilize these techniques. Three plates connecting the six shear panels have been designed to maintain structural stability while adding structural stiffness to the main bulkhead. These plates also have been lightweighted via "cutouts". The telescope main baffle only requires connection to the lower faceplate/shear panel locations at six locations due to its low weight. Local "L" brackets are used to make this connection through the OD of the main baffle. Where the main baffle is not connected to these six locations, non-load carrying secondary structure is used to control contamination and reflections off the lunar lander and/or surface. To facilitate PM and TM alignment, six local raised pads are located on the top faceplate of the main bulkhead. This allows tight tolerances to be maintained over a relatively small area.

The bulkhead is fabricated from beryllium. There are 3 "field splices" of the larger faceplate because of manufacturer limitations on maximum available size. These splices occur directly over three of the shear panels. All main bulkhead plate thickness are nominally 2.5 mm. Faceplate, shear panels and plates are brazed together to make a continuous, rigid, and deterministic structure. We used hand calculations to show that a first mode of 870 Hz and a maximum stress level of 5200 psi suggests this design is robust. We believe that more detailed analysis would continue to show this design meets its requirements.

3.7 WEIGHT ESTIMATES

The UVTA telescope weight estimates for the HDOS strawman design is shown in Table 3-3. This weight estimate reflects the updates to the original design concept use in the PM Materials & Design Study in terms of the metering structure, main bulkhead, baffles, and SMA. No attempt was made to assess the original allocations made to the electronics, alignment sensor and thermal control.

We have concluded that the original "structural" weight allocations are reasonable and except for some redistribution of weight, our original estimates were reasonable. There appears to be no outstanding issues with respect to launch survivability or dynamic characteristics which would indicate that these estimates will significantly increase.

TABLE 3-3
LUTE CALCULATED WEIGHT ESTIMATES COMPARED TO ALLOCATIONS AND ASSESSED TO DETERMINE TELESCOPE FEASIBILITY

Major Element	Sub-Ass'y/ Component	Weight Allocation(kg)		Calculated Estimate (kg)	
1) Mirrors	Primary		21.8		21.8
	Secondary		2.7		2.7
	Tertiary		1.4		1.4
	Sub-Total:		25.9		25.9
2) Structure					
	Baffles:				
	Main	4.1		5.9	
	Primary		0.9		0.9
	Secondary		0.5		2.1
	Sub-Total:		5.5		8.9
	Mirror Mounts:				
	PM		2.2		0.9
	SM		1.4		0.7
	TM		0.9		0.7
	Sub-Total:		4.5		2.3
	Main Bulkhead S. Ass'y:				
	Main bulkhead		5.4		6.8
	S/C I/F fittings (3)	1.4		1.4	
	Sub-Total:		6.8		8.2
	Metering Struc. S. Ass'y:				
	Metering structure	1.3		1.5	
	I/F fittings (6)		1.3		0.7
	Sub-Total:	2.6		2.2	
	SM Sub-Assembly				
	Spider		1.8		0
	Spider flexures		1.4		0
	Delta Frame	1.4		1.3	
	Hub		1.4		1.4
	Actuators		2.7		2.7
	Cabling		1.8		1.8
	Sub-Total:		10.5		7.2
3) Electronics					
	ACE		1.2		1.2
	TCE		1.2		1.2
	DMS		1.2		1.2
	ASE		1.2		1.2
	Sub-Total:		4.8		4.8
4) Thermal Control					
	Heaters		0.9		0.9
	Thermocouples		0.9		0.9
	MLI		1.5		1.5
	Cabling		2.0		2.0
	Sub-Total:		5.3		5.3
5) Alignment Sensor					
	Sensor	3.5		3.5	
	Sensor mount	0.5		0.5	
	Sub-Total:		4.0		4.0
	Total (w/o reserve):	69.9		68.8	
	Reserve:		14.1		13.9
	TOTAL:		84.0		82.7

SECTION 4

PRIMARY-TO-SECONDARY MIRROR DESPACE PREDICTIONS

4.1 THERMALLY INDUCED

Early in the study we traded metering structure design options. Using the work completed and documented in the MSFC "LUTE Interim Report" with respect to the Hubble Space Telescope (HST) type metering truss design, we investigated two additional types of structures. The first is a metering bar design approach where low coefficient-of-thermal expansion (CTE) material (i.e. fused quartz) is used to maintain the spacing between the primary and secondary mirrors in the presence of bulk temperature changes. This design approach is beneficial when considering a telescope design whose bulk temperature change, about some mean, is relatively small. This design approach possibly allows the elimination of the secondary mirror adjust mechanism thereby saving weight and reducing telescope complexity. Our "LUTE Primary Mirror Materials and Design Study Report", PR D15-0013A, discusses additional aspects of this design and includes a schematic of how this design approach could be implemented.

Based on the weight allocation of 84 kg for the telescope assembly, we concluded that the material of choice for LUTE is beryllium. This being the case, we calculated the amount of PM-to-SM despace if we assumed an all beryllium telescope and a telescope assembly temperature of 293 K (i.e. room temperature). These calculations also assumed that the mean temperature of the operational LUTE is 160 K with a range of temperature about this mean of ± 100 K. We used the data included in PR D15-0013A to account for CTE as a function of temperature. The calculations are as follows using the primary mirror as the reference.

- Beryllium structure:

  (ΔL) mean-to-cold = {(ΔL) for 160K - 60 K} = 130 μm

  (ΔL) mean-to-hot = {(ΔL) for 160K - 260 K} = 487 μm

Therefore for beryllium, the worst case is for the mean-to-hot case when the PM-to-SM spacing "grows" by 487 μm. However for a telescope which uses the same material throughout its optical "train", the telescope is athermalized. What is implies is that even though the spacing has changes by 487 μm, the radius of curvature of the primary and secondary mirror has changes by the same ratio. Therefore by definition, the wavefront error is identically zero (of course due to material inhomogeneities it is not identically zero.)

When we considered the metering bar approach several issues were immediately evident. First was that the temperature "swings" of the telescope is measured in "100's" of degrees not "a few degrees" which we typically would anticipate when considering a metering bar design and secondly, the optics are beryllium, not the more conventional "glass" optics where radius of curvature matching with "glass" metering rods could be accomplished. As a example of why a metering rod approach is not appropriate for LUTE, we continue similar calculations as shown above.

- Fused quartz metering rods:

$$(\Delta L) \text{ mean-to-cold} = \{(\Delta L) \text{ for } 160K - 60\ K\} = 36\ \mu m$$

$$(\Delta L) \text{ mean-to-hot} = \{(\Delta L) \text{ for } 160K - 260\ K\} = 13\ \mu m$$

These calculations show that even though the relative motion between the mirrors is much less, this motion obviously does not match the corresponding radius of curvature changes that the beryllium mirrors undergo. If the mirrors were fabricated from fused quartz (it is our opinion that this could only happen if the telescope weight allocation of 84 kg was significantly relaxed), then an assessment of the wavefront errors caused by the uncertainty of these values (remember material inhomogeneities, etc.) would need to be undertaken.

We made similar calculations to assess the impact of axial (i.e. along the telescope's length) temperature gradients on telescope performance. In this case, a telescope which uses the same material for both the structure and the optics does not necessarily enjoy any benefit when considering thermally induced deformations. This is shown in the Table 4-1 were we calculated allowable telescope axial temperature gradients to meet the PM-to-SM alignment requirement of 0.0212 waves rms (@ 0.6328 μm) due to lunar day-to-night changes as shown in PR D15-0013A. These results show that for axial temperature gradients, the all beryllium telescope will require a focus mechanism based on our understanding of the thermal analysis results presented in the MSFC report which suggests that the telescope axial gradients will be in excess of the 0.3K allowed. Conversely, a large benefit would be realized if the fused quartz metering bar design was chosen based on the allowable axial gradient. However as discussed, the PM-to-SM separation due to bulk temperature results clearly shows that LUTE is not suitable for the metering bar approach.

We did not conduct a LUTE-specific optical sensitivity analysis. In lieu of this we scaled sensitivity results from a similar three mirror telescope design. These sensitivities are shown in Table 4-2. We recommend that further work be undertaken to determine the specific optical sensitivities and that further analysis on PM-to-SM decenter (i.e. motion perpendicular to the optical axis) and relative tilts between the two elements be considered when bounding the allowable temperature gradients. From the results presented above we believe our inverted tripod design approach for the LUTE metering structure is appropriate.

TABLE 4-1
A MATERIAL WITH A LOW CTE OVER THE ENTIRE OPERATING TEMPERATURE RANGE IS PREFERRED SO THAT WAVEFRONT DISTORTIONS CAUSED BY TELESCOPE AXIAL TEMPERATURE GRADIENTS ARE MINIMIZED

Operating Temp (K)	Allowable Axial Temp Gradient (K)	
	Beryllium	Fused Quartz
260	0.3	30
160	—	—
60	1.5	4

TABLE 4-2
SCALED RESULTS FROM A SIMILAR OPTICAL DESIGN WERE USED TO CALCULATE ALLOWABLE TELESCOPE AXIAL TEMPERATURE GRADIENTS

Secondary Mirror Motion	Wavefront Distortion Sensitivity (waves rms @ 0.6328 μm)
• 1 μm despace	0.02
• 1 μm decenter	0.004
• 1 arcsec tilt	0.017

4.2 SECONDARY MIRROR FOCUS MECHANISM RANGE

To assess the precise amount of despace motion which the telescope must accommodate, a number of analyses and/or tests must first be conducted. These include:

a) LUTE-specific wavefront error sensitivity analyses
b) Metering structure material $\Delta L/L$ characteristics:
   1) uncertainty
   2) repeatability
   3) homogeneity
c) Assembly misalignments
d) Launch induced misalignment
e) Exact operational bulk and temperature gradients
f) 5/6's g release

We have attempted to begin this assessment assuming an all beryllium telescope which is aligned and tested in 1g at 293 K. These results are shown in Table 4-3. These values should be considered as a preliminary assessment which will need to be updated as the LUTE specific "architecture" in terms of structural form and material choice is baselined.

One must apply considerable margin to account for the error sources shown in Table 4-3 which are "tbd." We believe the LUTE secondary mirror mechanism should have a minimum despace range of ±1 mm. For reference, the HST SM mechanism has a despace range of approximately ±3 mm.

TABLE 4-3
IDENTIFICATION OF DESPACE ERROR SOURCES HAVE BEEN MADE. ADDITIONAL ANALYSES AND TEST DATA REQUIRED TO FULLY QUANTIFY THESE EFFECTS ON OPTICAL PERFORMANCE

Despace Error Source	Estimated Despace Motion (μm)	Equiv. Defocus Error (waves-rms)
• Initial misalignment	0.4	0.008
• 5/6 g release uncertainty	0.3	0.006
• Launch residual	tbd	tbd
• Bulk temp. effects		
- 260 K to 160 K	490	0
- 160 K to 60 K	130	0
• Temp. gradients		
- PM, SM, TM	tbd	tbd
- Metering structure	tbd	tbd
• ΔL/L effects		
- PM, SM, TM	tbd	tbd
- Metering structure	tbd	tbd

SECTION 5

MECHANICAL LAYOUTS

5.1 OVERALL UTVA

Our recommended LUTE telescope design described in detail in Section 3 is based on a set of requirements which dictates that the telescope have diffraction limited performance while at the same time be light weight and structurally stiff. Shown earlier in Figure 3-2, the isometric view of our telescope highlights the major telescope components which we believe will meet this set of requirements.

Figure 5-1 is an "exploded" view of the telescope providing further definition of its components, the material which the component is fabricated from, insight into the fabrication technique which we recommend for its construction, and other pertinent information to help in the overall understanding of form and function. Figures 5-2 and 5-3 provide the more classical "side" and "top" views of the telescope. These figures are "to scale" to show that all components are consistent with volume constraints and that no interferences occur which could jeopardize the overall telescope architecture.

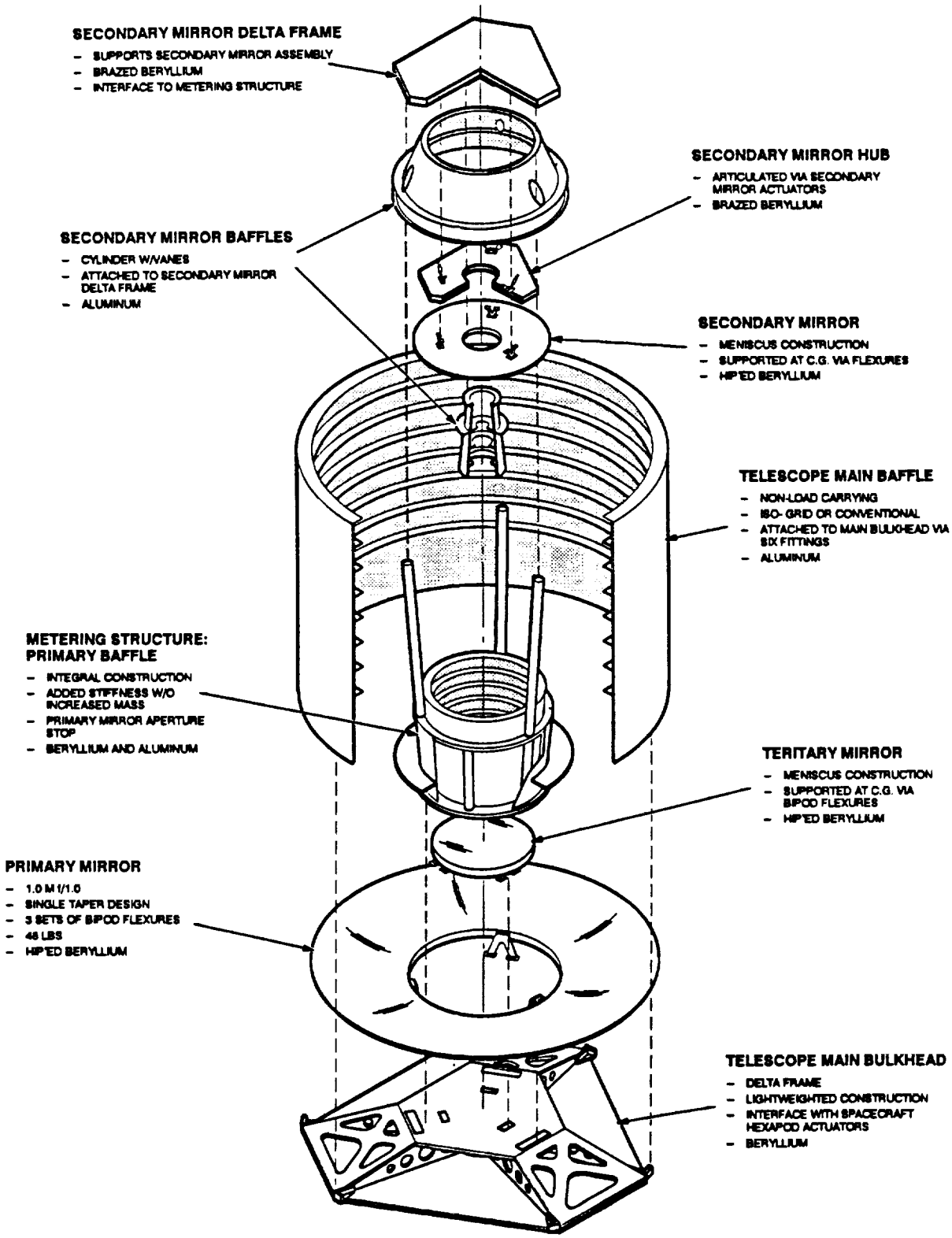

Figure 5-1. The "Exploded" View of the Lute Telescope Provide Insight into Assembly Sequences along with Material and Fabrication Techniques.

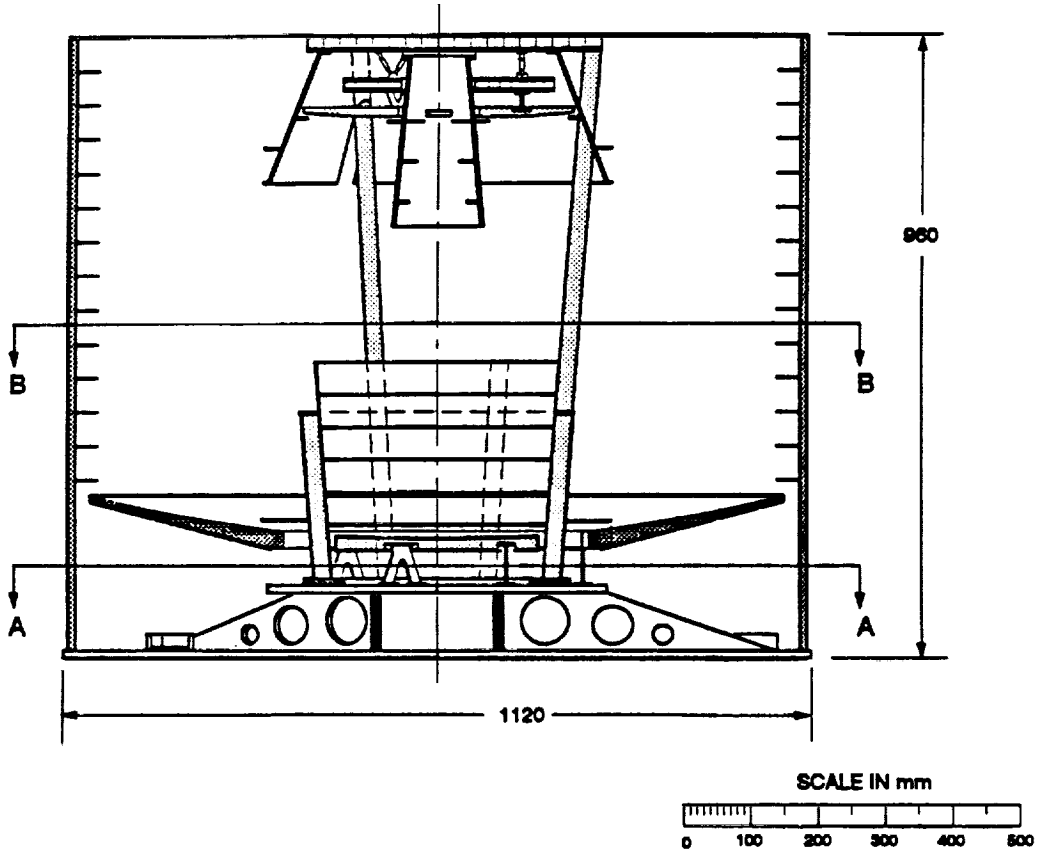

Figure 5-2. "Side" View of the Lute Telescope.

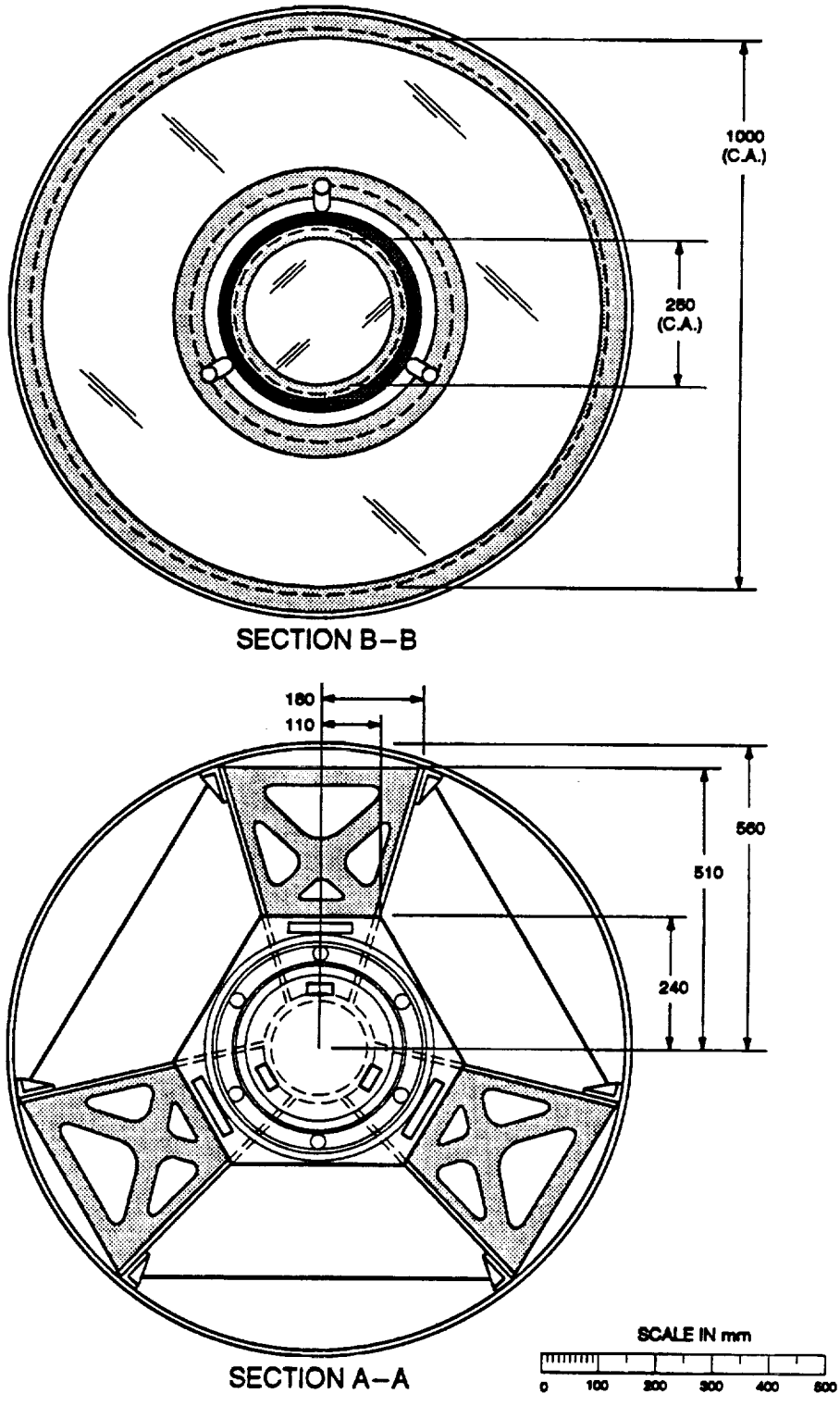

Figure 5-3. "Top Views of the Lute Telescope Sections "A-A" and "B-B" Highlights the Main Bulkhead and Primary/Tertiary Mirrors, Respectively.

SECTION 6

RECOMMENDATIONS

Our current investigation of the feasibility of the LUTE telescope substantiates the conclusions from our pervious LUTE study. That is, no areas have been identified that would indicate that the LUTE mission is not feasible. However, development of an ultra-lightweight, 1-m class telescope with visible wavelength diffraction-limited performance for operation across a temperature range of 60 - 260 K would undoubtedly prove to be very difficult. Following are some additional tasks and/or tests which warrant attention in the overall development of the telescope sub-system.

1) Use of other launch/lander vehicles could impact the conclusions made in our LUTE studies. A revisit of these studies is warranted if allowable telescope mass is significantly increased from 84 kg.

2) Sub-scale material testing of beryllium to quantify homogeneity as a function of location. Fabricate a full scale primary mirror blank, remove small sections and conduct CTE measurements as a function of temperature. Repeat these tests several times to extract repeatability data. Literature searches along with obtaining vendor information would complement this task.

3) Design and fabricate a brassboard (i.e. non-flight unit) of the LUTE telescope to investigate:

   a) thermally induced deformations of the telescope sub-system over the anticipated operating temperature range.
   b) simulate lunar "dust" applied to the telescope optical surfaces and correlate encircled energy degradation as a function of dust "buildup" with optical performance modeling.

4) Topics included in our previous study report:

   a) UV scatter measurements on small (3-5 cm diameter) polished and coated beryllium mirrors.
   b) Analysis of the candidate PM materials to identify the optimum temperature range for each material to achieve its optimum wavefront performance.
   c) Conduct optical analyses to:
      - support a re-evaluation of the existing wavefront error allocation to check its suitability for a UV telescope.
      - determine mirror alignment sensitivities in support of the concept to fabricate the TM on the same substrate as the PM.

APPENDIX A

LUTE VIEWGRAPHS FROM 4 MAY 1993 TECHNICAL TELECON

Lunar Ultraviolet Transit Experiment Study

Technical Telecon

Greg Ruthven
Mark Stier

4 May 1993

Agenda

- **Objective**
- **Study Logic**
- **Telescope Configuration Description**
- **Performance Results**
- **Summary**

Objective

- **Conceptualize LUTE UVTA mechanical/structural architecture and assess its feasibility**

Present results showing:

1) Overall configuration
2) Weight estimates
3) Fundamental frequency
4) Maximum stress levels
5) Secondary mirror focus range

LUTE
Telescope Structural Design Study

Study Logic

Hughes
Danbury Optical Systems

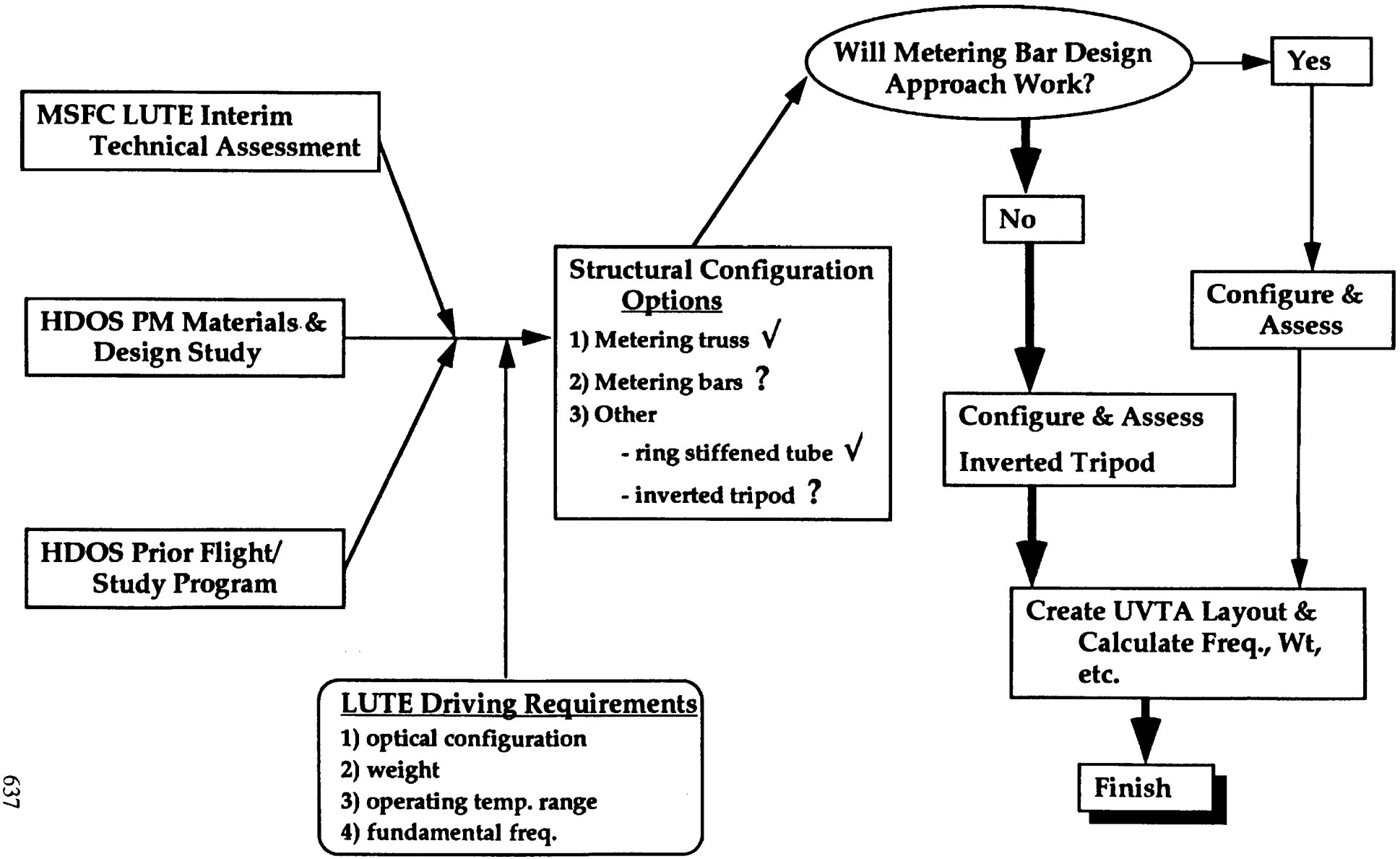

Requirements

Item	Requirement	Comments
• Optical Design	• 3 mirror telesope • Diffraction limited @ 0.63 μm • 1 meter diameter • Operating wavelength: 0.1 to 0.35 μm	• Baseline MSFC design
• Weight	• Max. telescope weight: 84 kg	• Includes 18 % contingency
• Operating Temp Range	• 260 K to 60 K	• Nominal temperature range
• Fundamental Freq.	• >50 Hz (Telescope) • > 150 (Primary Mirror)	• Based on other programs

Fundamental Frequency Allocations

- **Allocations based on two criteria:**
  - **Springs in series:** • $K_{(eff)} = 1/\{1/K_{(1)} + 1/K_{(2)} + 1/K_{(n)}\}$
  - **Ground testing:** • **Major resonances sufficiently separated for diagonosing test anomolies**

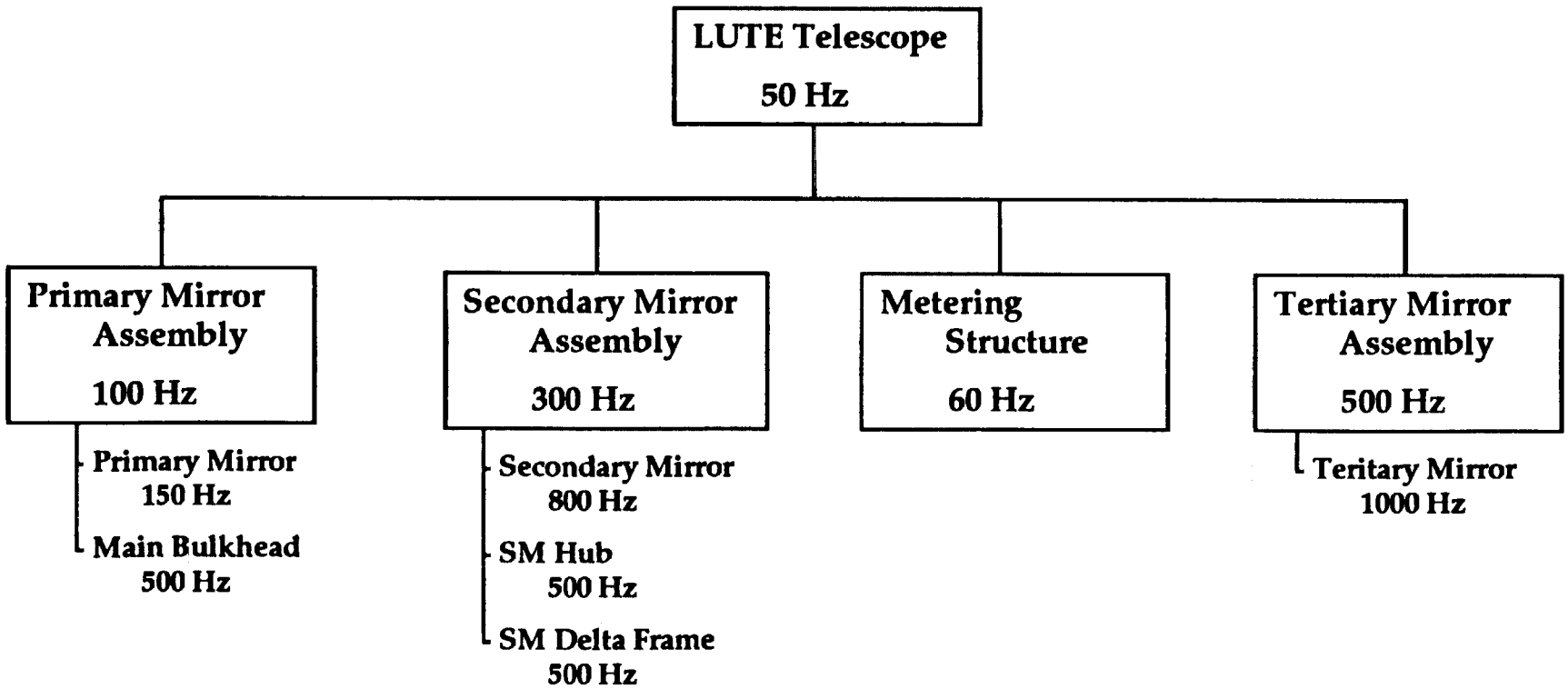

639

Optical Sensitivities & Wavefront Error Budget

- **WFE estimates scaled from similiar optical designs**

Sensitivity	WFE (@ 0.6328 μm)
• 1 μm of SM despace	0.02 waves rms
• 1 μm of SM decenter	0.004 waves rms
• 0.01 deg of SM tilt	0.6 waves rms

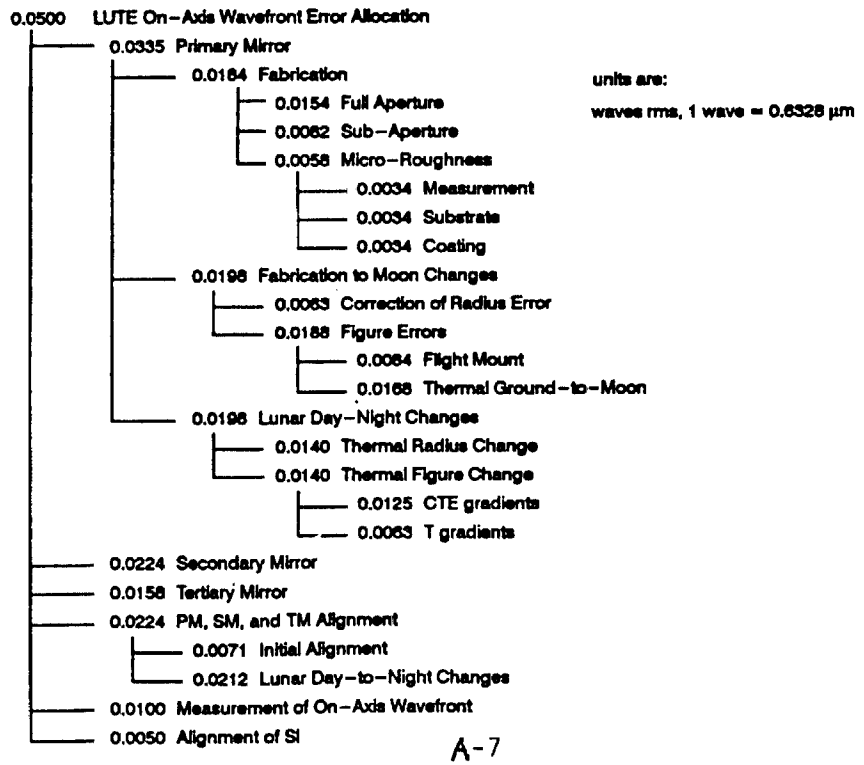

Metering Bar Design Approach

- **Metering bar design option assessed for thermal effects:**

Advantages:

1) Elimination of focus mechanism possible
2) Allows use of beryllium main support structure
3) Low CTE material for metering bars maintain despace.
4) Decenter control via axial & tangential flexures

Disadvantges:

1) May only be suitable for Δ(CTE) & temperature gradients

Example: Assume fused quartz metering rods; investigate despace:

- **Bulk temperature effects:**

(ΔL) mean-to-cold = {(ΔL) for 160 K - 60 K} = 36 μm, but requires 130 μm for Be mirrors
(ΔL) mean-to-hot = {(ΔL) for 160 K - 260 K} = 13 μm, but requires 487 μm for Be mirrors

Therefore, required focus mechanism range (worst) = 487 μm - 13 μm ~ 0.5 mm

- **Axial temperature gradients effects:**

Allowed temp gradient @ 260 K = 30 K (F.Q.) vs. 0.3 K (Be)
@ 60 K = 4 K (F.Q.) vs 1.5 k (Be)

{Sensitivity(first order): 1μm (despace) = 0.02 waves rms WFE (bugeted value)}

Even an all beryllium telescope requires focus mechanism if axial temperature gradient exceeds 0.3 K

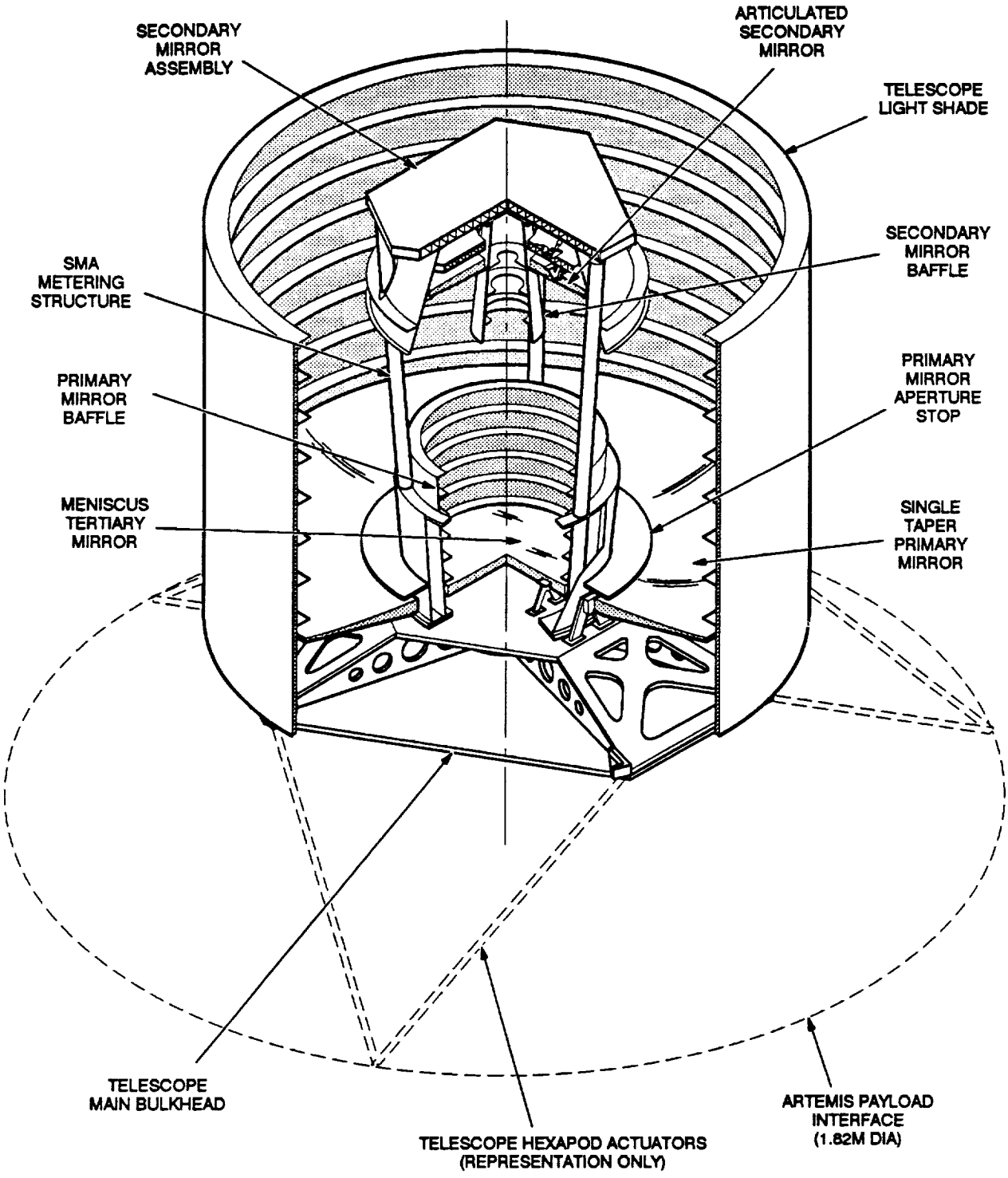
SECONDARY MIRROR ASSEMBLY
ARTICULATED SECONDARY MIRROR
TELESCOPE LIGHT SHADE
SECONDARY MIRROR BAFFLE
SMA METERING STRUCTURE
PRIMARY MIRROR BAFFLE
PRIMARY MIRROR APERTURE STOP
MENISCUS TERTIARY MIRROR
SINGLE TAPER PRIMARY MIRROR
TELESCOPE MAIN BULKHEAD
TELESCOPE HEXAPOD ACTUATORS (REPRESENTATION ONLY)
ARTEMIS PAYLOAD INTERFACE (1.82M DIA)

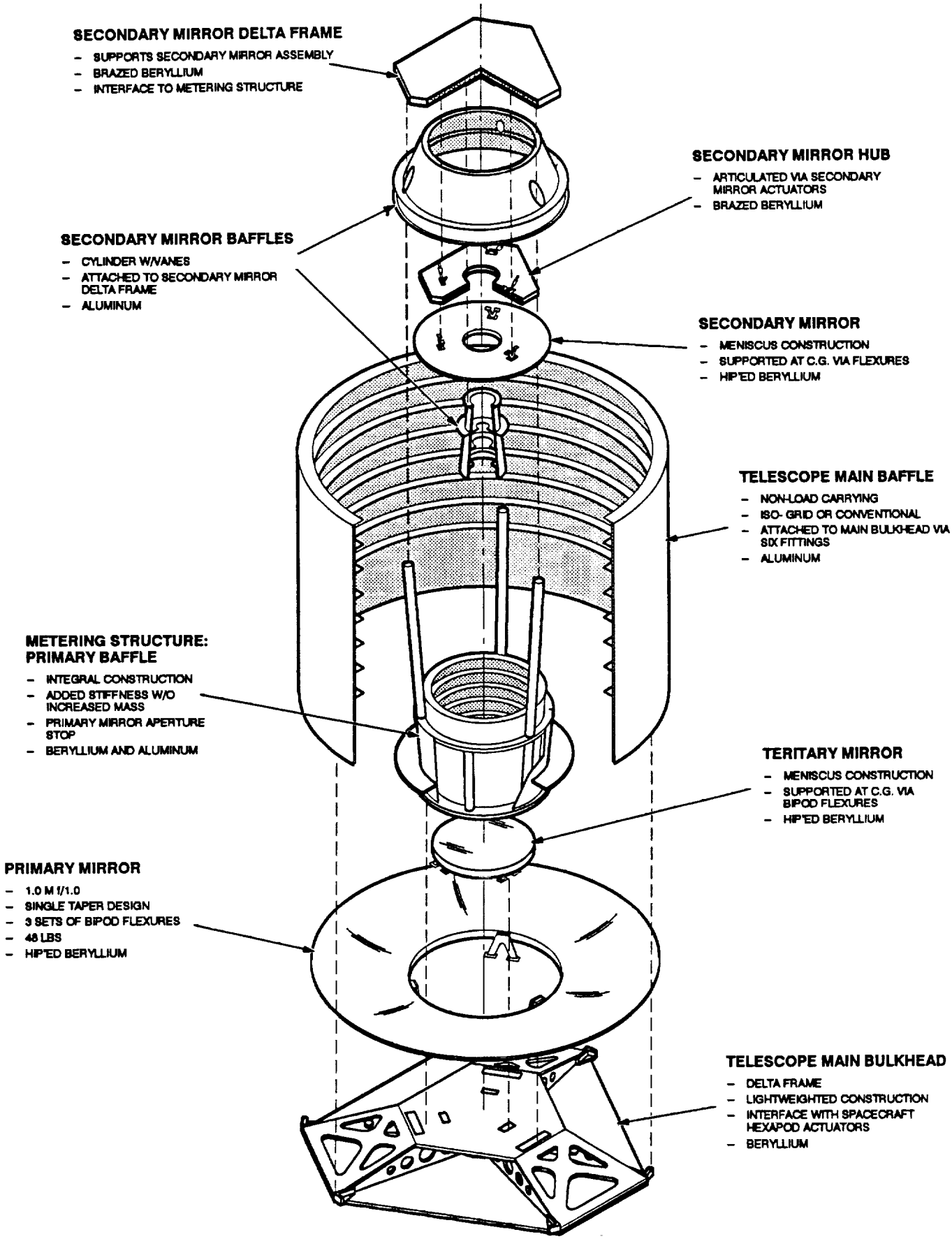
SECONDARY MIRROR DELTA FRAME
- SUPPORTS SECONDARY MIRROR ASSEMBLY
- BRAZED BERYLLIUM
- INTERFACE TO METERING STRUCTURE
SECONDARY MIRROR HUB
- ARTICULATED VIA SECONDARY MIRROR ACTUATORS
- BRAZED BERYLLIUM
SECONDARY MIRROR BAFFLES
- CYLINDER W/VANES
- ATTACHED TO SECONDARY MIRROR DELTA FRAME
- ALUMINUM
SECONDARY MIRROR
- MENISCUS CONSTRUCTION
- SUPPORTED AT C.G. VIA FLEXURES
- HIP'ED BERYLLIUM
TELESCOPE MAIN BAFFLE
- NON-LOAD CARRYING
- ISO- GRID OR CONVENTIONAL
- ATTACHED TO MAIN BULKHEAD VIA SIX FITTINGS
- ALUMINUM
METERING STRUCTURE: PRIMARY BAFFLE
- INTEGRAL CONSTRUCTION
- ADDED STIFFNESS W/O INCREASED MASS
- PRIMARY MIRROR APERTURE STOP
- BERYLLIUM AND ALUMINUM
TERITARY MIRROR
- MENISCUS CONSTRUCTION
- SUPPORTED AT C.G. VIA BIPOD FLEXURES
- HIP'ED BERYLLIUM
PRIMARY MIRROR
- 1.0 M f/1.0
- SINGLE TAPER DESIGN
- 3 SETS OF BIPOD FLEXURES
- 48 LBS
- HIP'ED BERYLLIUM
TELESCOPE MAIN BULKHEAD
- DELTA FRAME
- LIGHTWEIGHTED CONSTRUCTION
- INTERFACE WITH SPACECRAFT HEXAPOD ACTUATORS
- BERYLLIUM

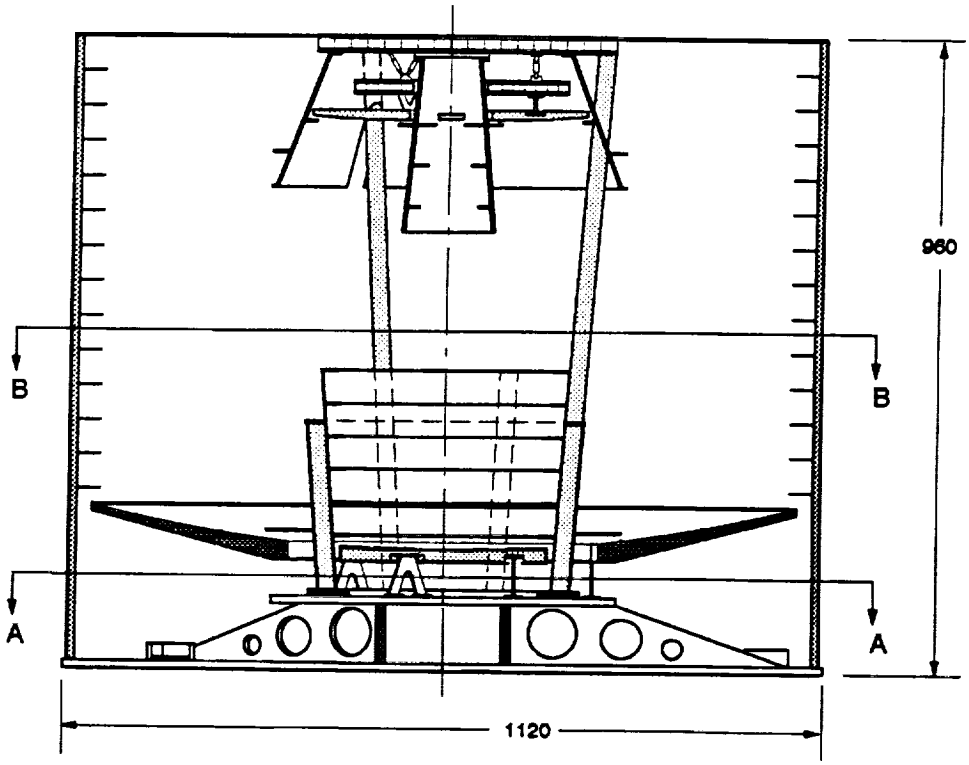
960
B
B
A
A
1120

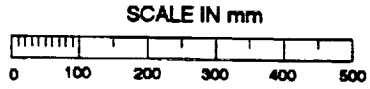
SCALE IN mm
0
100
200
300
400
500

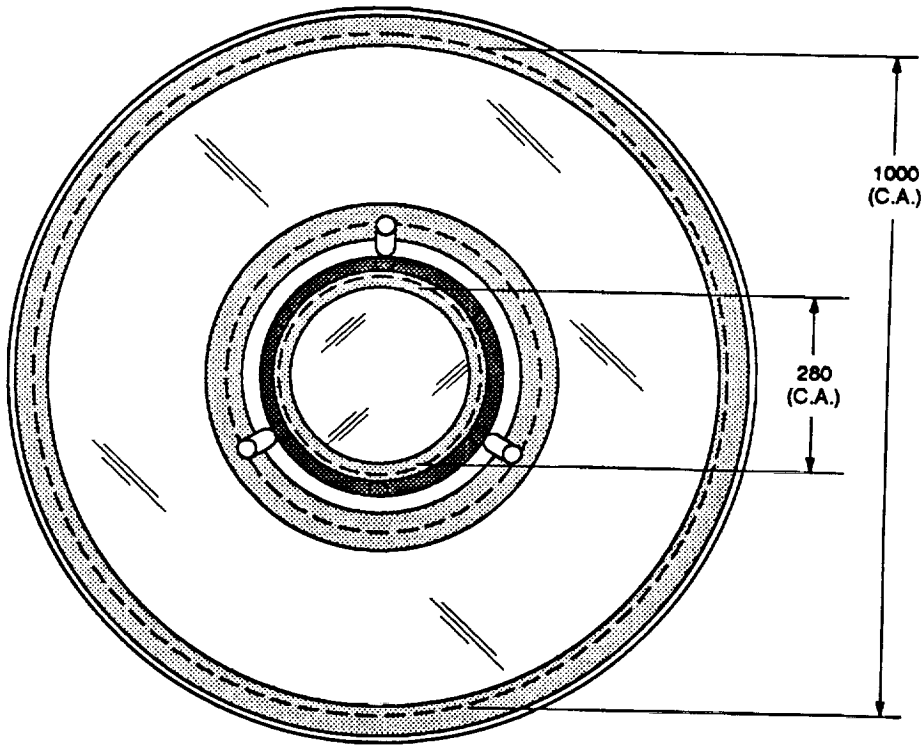

SECTION B–B

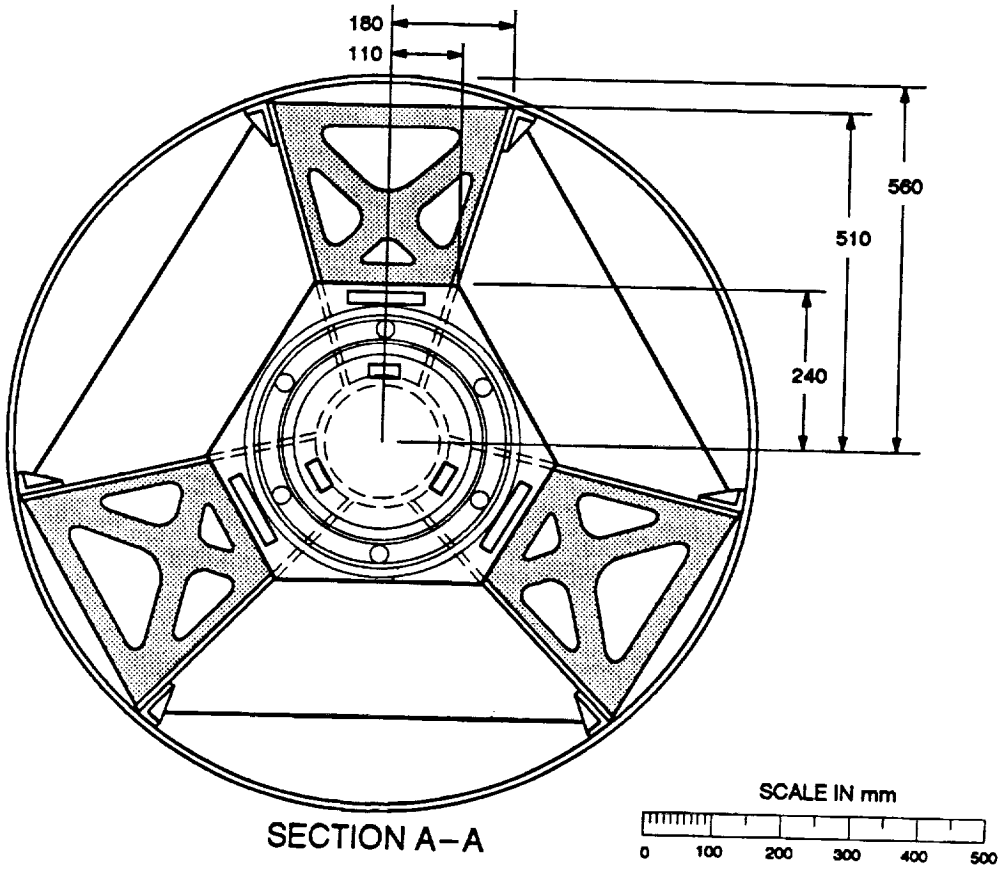

SECTION A–A

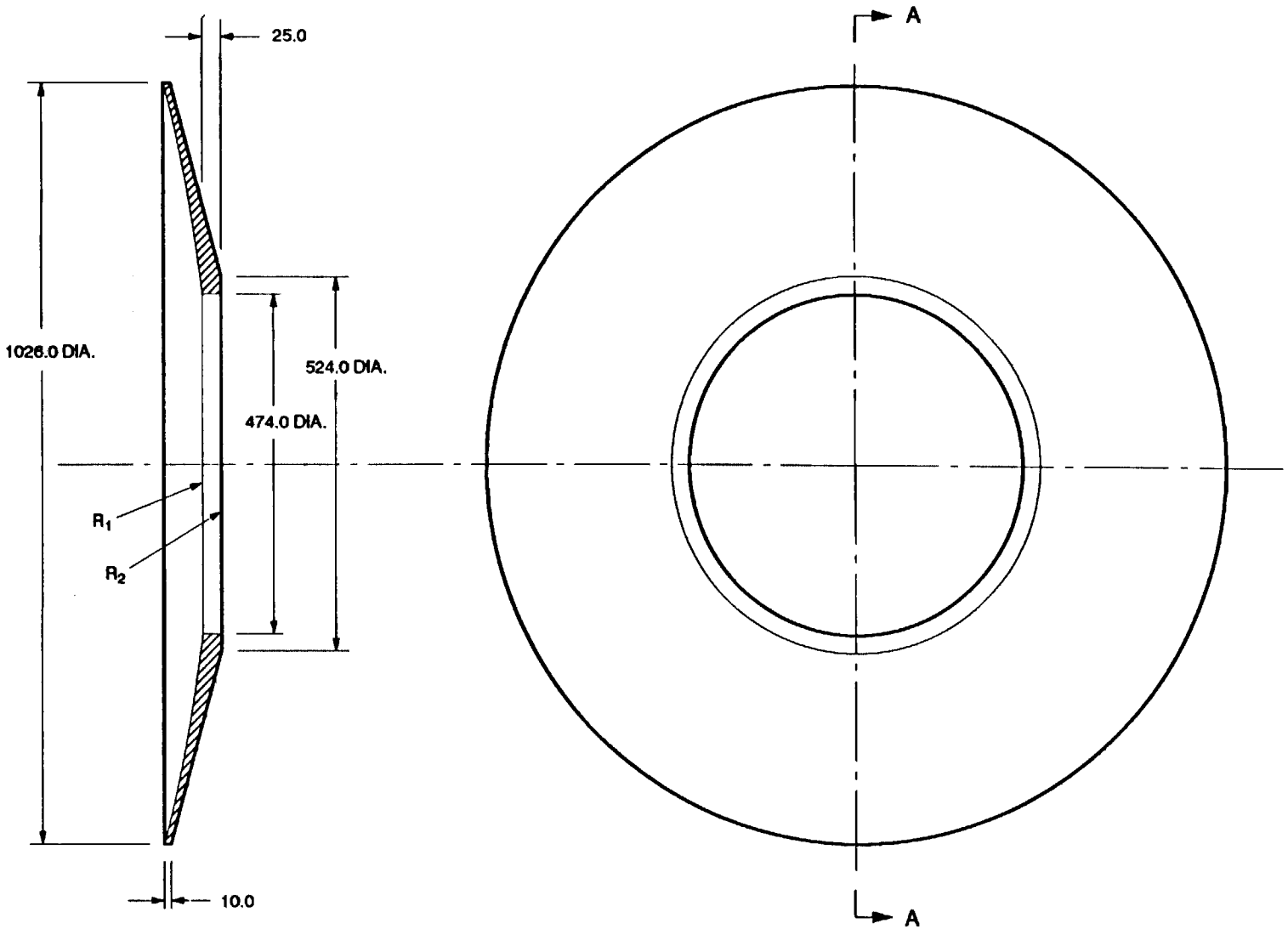

SECTION A–A

1.03 METER f/1.0 LUTE PRIMARY MIRROR

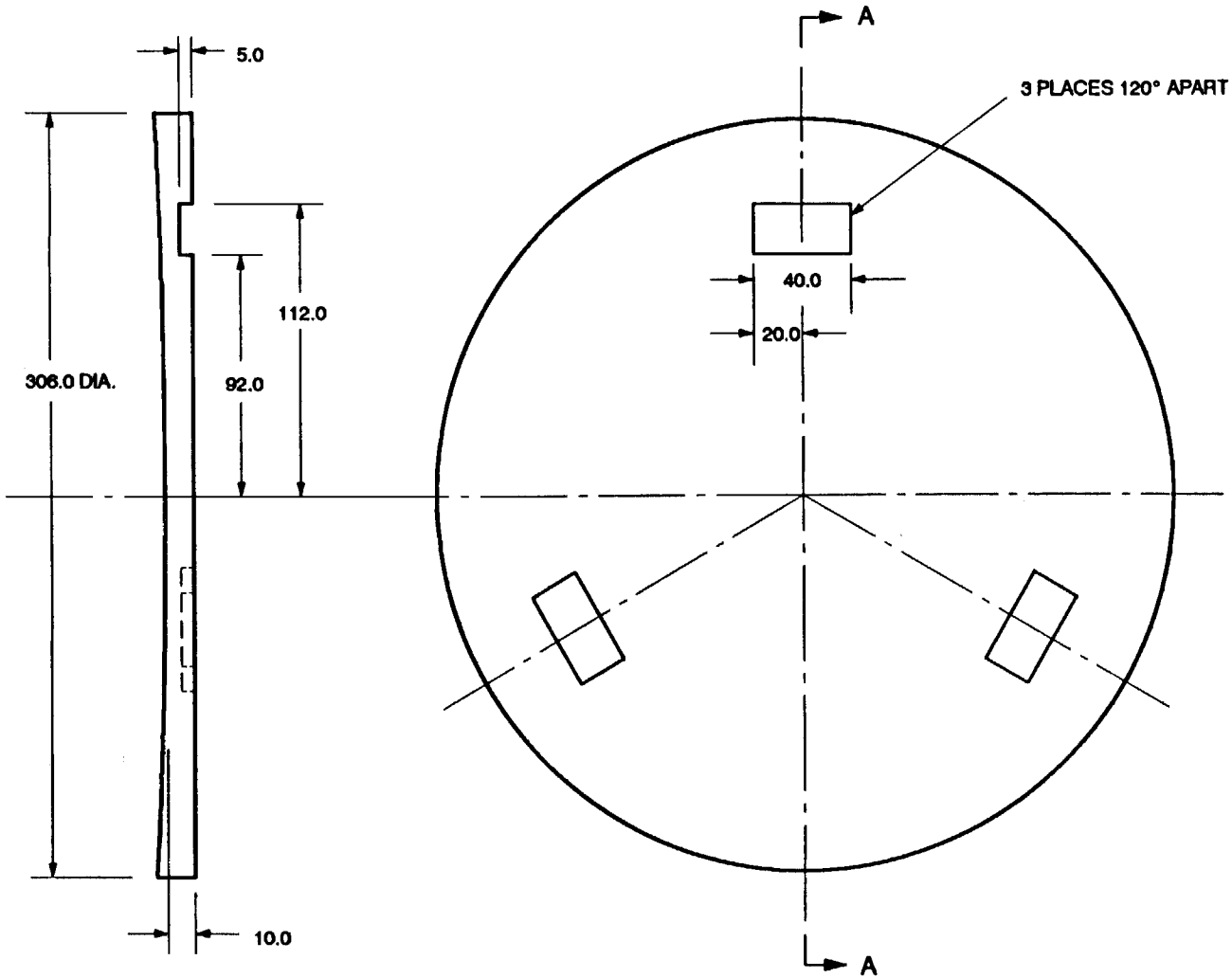

SECTION A–A

0.3 METER f/0.6 LUTE TERTIARY MIRROR

Inverted Tripod Design Approach

- **Question:** Can we use the conclusions from the "PM Materials & Design Study" to help configure the UTVA structural architecture?
- **Answer:** Yes.....but it wasn't obvious at first !!!!

The Driver: PM leading candidate geometry is a "single arch" mounted @ its inner rim.

- Can HDOS fabricate an integral PM/TM?

Yes.....but, from the current study results.....

Separate mirrors are preferred.....

Why?
- Weight penalty for integral PM/TM = 10 lbs; but more importantly.....
- Take advantage of the geometry to configure the telescope

Why? Significant weight savings for separate PM/TM design apparoach in areas of:

1) Main Bulkhead

2) Main Baffle

Weight Estimate (1)

- **Current study concentrated on "structural" weight (i.e. main baffle, metering structure, etc)**
  - **one-for-one comparison desired (allocation vs estimate)**
  - **thermal control, electronics, SM actuators still considered allocations**

		LUTE OBSERVATORY			
		Weight Estimate			
Major Element	Sub-Ass'y/Component	Weight Allocations		Weight Estimate	
		(lbs)	(kg)	(lbs)	(kg)
1) Mirrors					
	- Primary Mirror	48	21.8	48	21.8
	- Secondary Mirror	6	2.7	6	2.7
	- Tertiary Mirror	3	1.4	3	1.4
	Sub-Total:	57	25.9	57	25.9
2) Structure	Baffle Sub-Ass'y				
	- Main	9	4.1	13.0	5.9
	- Central	2	0.9	2.0	0.9
	- SM	1	0.5	4.6	2.1
	Sub-Total:	12	5.5	19.6	8.9
	Mirror Mounts				
	- PM	5	2.3	2.0	0.9
	- SM	3	1.4	1.5	0.7
	- TM	2	0.9	1.5	0.7
	Sub-Total:	10	4.5	5	2.3
	Main Bulkhead Sub-Ass'y				
	- Main bulkhead	12	5.5	14.9	6.8
	- S/C interface fittings (3)	3	1.4	3	1.4
	Sub-Total:	15	6.8	18	8.1
	Metering Struc. Sub-Ass'y				
	- Metering struc bars (3)	3	1.4	3.4	1.5
	- Interface fittings (6)	3	1.4	1.5	0.7
	Sub-Total:	6	2.7	4.9	2.2
	SM Sub-Ass'y				
	- Spider	4	1.8	0	0.0
	- Spider ring (Delta frame)	3	1.4	2.8	1.3
	- SM hub	3	1.4	3.1	1.4
	- Spider flexures (3)	3	1.4	0	0.0
	- Actuators (6)	6	2.7	6	2.7
	- Cabling	4	1.8	4	1.8
	Sub-Total:	23	10.5	15.9	7.2

LUTE
Telescope Structural Design Study

Weight Estimate (2)

Hughes
Danbury Optical Systems

3) Electronics	• ACE		3	1.4	3	1.4
	• TCE		3	1.4	3	1.4
	• DMS		3	1.4	3	1.4
	• ASE		3	1.4	3	1.4
	Sub-Total:		12	5.6	12	5.6
4) Thermal Control	• Heaters		2	0.9	2	0.9
	• Thermocouples		2	0.9	2	0.9
	• MLI		3	1.4	3	1.4
	Sub-Total:		7	3.2	7	3.2
5) Alignment Sensor	• WF Sensor		10	4.5	10	4.5
	• Sensor mount		2	0.9	2	0.9
	Sub-Total:		12	5.6	12	5.6
	Total (w/o Reserve):		154.0	70	151.3	69
	Reserve:		31.6	14	31.1	14
	Total:		185.6	84	182.4	83

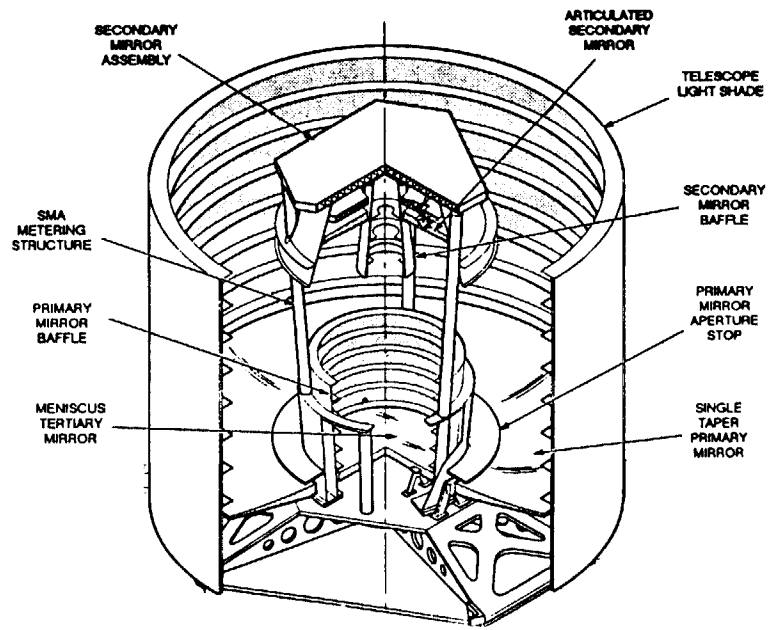

Fundamental Frequency Estimate

- Major components assessed via hand calculations & NASTRAN

Component:	Requirement	Calculated Value
• Primary Mirror Assembly		
- Primary Mirror	150 Hz	260 Hz
- Main Bulkhead	500	870
• Secondary Mirror Assembly		
- Secondary Mirror	800 Hz	1045
- SM Hub	500	800
- SM Delta Frame	500	725
• Metering Structure (w/ rigid SMA)	60Hz	65 Hz
• Teritary Mirror Assembly		
- Teritary Mirror	1000 Hz	1950 Hz
• Telescope Light Shade	200 Hz	242 Hz

Launch Induced Stresses

- **Telescope design is frequency driven.....stress levels are low**
  - **Hand calculations made of major components**
  - **Quasi-static limit load factor of 15 g's rms was assumed**
  - **F.O.S. of 1.25 & 1.5 for yield & ultimate used**

Component:	Est. Max Stress Level (psi)	Margin of Safety	Nature
- Primary Mirror	2700	>1	Bending
- Main Bulkhead	5200	>1	Bending
- Secondary Mirror	6100	>1	Bending
- SM Hub	4000	>1	Bending
- Metering Structure	9200	>1	Tension
- Teritary Mirror	800	>1	Bending
- Main Baffle	250	>1	Bending

SM Focus Mechanism Range

- **Basic Assumptions:** 1) LUTE telescope aligned and tested in 1g @ 293 K
  2) Telescope structure & optics are beryllium

Despace Error Source Source	Estimated Despace Motion (μm)	Equiv. Defocus Error (waves-rms)
• Initial misalignment	0.4	0.008
• 5/6 g release uncertainity	0.3	0.006
• Launch residual	tbd	tbd
• 260 K to 160 K	490	0
• 160 K to 60 K	130	0
• Δ(CTE) and T grad. effects	tbd	tbd
- PM		
- SM		
- TM		

We are uncertain at this time the SM focus mechanism requirements, but "worst case" estimate (F.Q. metering bars) → ± 1mm range

Conclusions

- Updated weight calculations consistent with previous allocations
- Fundamental frequency req'mts met
  - component designs are frequency driven, not stress driven
- SM focus mechanism required
- Image quality degradation effects due to metering structure needs further study
- Telescope design driven by mass budget & ΔT
  - use of other launch/lander vehicle would have major impact

Appendix A. Material Properties

Table A1. Regolith Thermal Conductivity[10]

Temperature (Kelvin)	Thermal conductivity (W/m-K)
0	0.00116
100	0.00116
150	0.00120
200	0.00128
250	0.00140
300	0.00158
350	0.00183
400	0.00217
450	0.00241

Table A2. Regolith Density times Specific Heat[41]

Temperature (Kelvin)	Density x Specific Heat (W-hr/m^3-K)
0	84.75
100	148.92
200	306.99
300	405.5
400	483.4

Table A3. Beryllium Thermal Conductivity[54]

Temperature (Kelvin)	Thermal conductivity (W/m-K)
36.7	104
60	150
70	175
79	195
85	210
250	236
273.2	218
300	200
350	178
400	161
500	139

[10] Cremers, C. J., Birkebak, R. C., and White, J. E. (1972), "Thermal Characteristics of the Lunar Surface Layer," International Journal of Heat and Mass Transfer, Vol. 15.
[41] Jones, W. P., Watkins, J. R., and Calvert, T. A. (1975), "Temperatures and Thermophysical Properties of the Lunar Outermost Layer." The Moon 13, D. Reidel Publishing Company, Dordrecht, Holland.
[54] "Beryllium Optical Properties," Brush Wellman, Inc., Beryllium Mining Division

February 8, 1994
9:20 AM

Table A4. Beryllium Density times Specific Heat[13]

Temperature (Kelvin)	Density x Specific Heat (W-hr/m^3-K)
60	17.49
80	46.40
100	104.18
120	181.73
150	326.51
200	571.39
250	788.34
300	940.86
600	1342.55

Table A5. Silicon Carbide (Ceraform™) Thermal Conductivity[13]

Temperature (Kelvin)	Thermal conductivity (W/m-K)
40	120
100	120
150	175
200	200
250	190
300	156
350	135

Table A6. Silicon Carbide (Ceraform™) Density times Specific Heat[14]

Temperature (Kelvin)	Density x Specific Heat (W-hr/m^3-K)
73	136.28*
298	543.44

* Projected based on fused silica behavior

Table A7. Fused Silica Thermal Conductivity[14]

Temperature (Kelvin)	Thermal conductivity (W/m-K)
40	0.4
73	0.7
173	1.0
273	1.3
298	1.38
373	1.44

---

[12] "Beryllium Optical Properties," Brush Wellman, inc., Beryllium Mining Division

[13]United Technologies Optical Systems, West Palm Beach, Florida, CERAFORM data sheet.

[14]Data received from Corning, November, 1992.

Table A8. Fused Silica Density times Specific Heat[15]

Temperature (Kelvin)	Density x Specific Heat (W-hr/m^3-K)
73	102.5
273	422.7
298	453.4
373	461.1

Table A9. Additional Material Properties

Material	Property	Value	Units
MLI	Eff. conductivity	0.0002077	W/m-K
Aluminum	Conductivity	237	W/m-K
Aluminum	Specific heat	0.2508	W-hr./kg-K
Aluminum	Density	2702	kg/m^3
Beryllium	Density	1850	kg/m^3
Silicon carbide	Density	2920	kg/m^3
Fused silica	Density	2204	kg/m^3

[14] Data received from Corning, November, 1992.

APPENDIX N

LUTE SYSTEM SAFETY PLAN

National Aeronautics and
Space Administration

CT 1724.3

George C. Marshall Space Flight Center
Marshall Space Flight Center, Alabama 35812

Lunar Ultraviolet Telescope Experiment (LUTE)

System Safety Plan

DRAFT

Marshall Space Flight Center (MSFC)
Lunar Ultraviolet Telescope Experiment (LUTE)
System Safety Plan

1.0 INTRODUCTION

1.1 SCOPE

This document presents the MSFC System Safety Plan for the LUTE. Existing MSFC documentation, techniques, and procedures are used to the maximum extent reasonable to prevent costly and unnecessary generation of new documentation and procedures in developing the plans to comply with the requirements of new projects.

The policies and procedures in this document will provide the most effective and economical means of implementing the system safety program. This plan presents the minimum requirements for the safety policies and procedures which will govern the conduct of those activities. These requirements will be followed during fabrication, inspection, testing, transport, pre-launch, and operation of the LUTE and associated support equipment.
The contents of this document are based on the assumption that the LUTE will be launched at the Eastern Test Range and that the ground processing of LUTE will be performed at Kennedy Space Center (KSC).

1.2 PURPOSE

The purpose of this plan is to establish system safety objectives and to maintain an effective and timely system safety program for the LUTE flight instruments, personnel and equipment, spacecraft and instrument interfaces.

1.3 REFERENCE DOCUMENTATION

The following documents shall be used as guidelines in the design, fabrication, testing and integration of the LUTE and, to the extent applicable, form a part of this document.
Unless otherwise specified, the latest issue of each document shall be used.

a. ESMCR 127.1, "Eastern Space and Missile Center Regulation, Range Safety"

b. MIL-STD-882, "Military Standard System Safety Program Requirements"

c. NHB 1700.1(V1-A), "Basic Safety Manual"

d. NHB 1700.1(V3-A), "System Safety"

e. MMI 1700.6, "MSFC Operational Readiness Program"

f. KSC 1710.2B, "KSC Safety Practices Handbook"

g. GP 1098F, "KSC Ground Operations Safety Plan"

h. Office of Science and Technology Policy letter, "Nuclear Safety Review and Approval Procedures for Minor Radioactive Sources in Space Operations," dated June 16, 1970.

i. MMI 1711.2C, "Reporting, Investigation, and Action on Mishaps Involving MSFC Employees, Property, Program Hardware, and Program Critical Problems"

2.0 SAFETY ORGANIZATION

2.1 SYSTEM SAFETY RESPONSIBILITY

All safety aspects of the instrument are the responsibility of the LUTE Project Manager (PM). The LUTE PM may, at his discretion, appoint a MSFC Project System Safety representative to implement and oversee the System Safety Program. The role of PM or the System Safety representative is to ensure that potential hazards to equipment and personnel are identified and controlled, and to assure the observance of safety criteria for launch site ground operations. As a minimum, Category I and Category II hazards will be identified and corrective actions will be taken to eliminate or accept these hazards. The responsibilities of the PM or System Safety representative will include, but not be limited to, the following:

a. Assure the identification of all hazards associated with the LUTE and its associated equipment, and eliminate the hazards or institute controls for the residual hazards.

b. Assure that hazard listing sheets, if required, are filled out and that hazard analyses are performed, where appropriate, to define the hazards.

c. Conduct drawing, specification, assembly, and test procedure reviews to assure minimizing of hazards and control of hazards.

d. Supervise the preparation of system safety documentation, including any necessary to fulfill expendable launch vehicle requirements for safety certification.

e. Supervise the preparation of nuclear safety documentation for minor and major nuclear sources which will be required for reviews by the Interagency Nuclear Safety Review Panel (INSRP) or by the NASA Nuclear Safety Coordinator.

f. Assure all system safety requirements are met and all safety procedures are observed.

g. Participate in design reviews, including the INSRP reviews, to assure that safety standards are observed and carried out in the design of all equipment and procedures.

h. Provide the LUTE Project Office with all required safety documentation for review and approval.

3.0 SYSTEM SAFETY ANALYSIS

3.1 PRELIMINARY SYSTEM SAFETY ASSESSMENT

A preliminary system safety assessment will be conducted by the PM/System Safety representative and the following will be documented:

a. A description of identifiable hazards associated with the LUTE or the support equipment.

b. Identification of components, interfaces and events that can present or can develop into Category I, II, or III hazards.

c. A description of plausible hazardous effects on the equipment and on personnel.

d. A description of proposed techniques for eliminating or controlling hazards.

3.2 HAZARD LEVELS

Hazards are classified, according to severity, as follows (per MIL-STD-882B, as referenced by ESMCR 127-1):

Category I - Personnel loss
System loss

Category II - Severe injury
Severe occupational illness
Major system damage

Category III - Minor injury
Minor occupational illness
Minor system damage

Category IV - Less than minor injury
Less than minor occupational illness
Less than minor system damage

3.3 SYSTEM SAFETY ANALYSES

3.3.1 HAZARD ANALYSIS

A hazard analysis will be performed in a systematic manner on the LUTE, its Ground Support Equipment (GSE), and ground launch site and flight operations to identify hazardous subsystems and functions. The hazard analysis shall be initiated early in the design phases and will be kept current throughout the developmental phase. The analysis will consist of a comprehensive, qualitative assessment of the design of the LUTE and GSE from a safety viewpoint.

3.3.2 HAZARD ANALYSIS LISTING

A separate hazard listing will be generated for each specific hazard identified. The hazard listing will document the causes, controls, and verification methods for each hazard.

3.3.3 MISSILE SYSTEM PRELAUNCH SAFETY PACKAGE (MSPSP)

As required by ESMCR 127.1, a MSPSP addressing all Category I, II, III, and IV hazards will be generated. The MSPSP shall be based on the system safety analysis tasks that have been performed and shall provide a comprehensive evaluation of the overall system safety assessment and identify operating limits and constraints.

4.0 LAUNCH SITE AND GROUND PROCESSING PROCEDURE APPROVAL

Launch site and ground processing procedures will comply with ESMCR 127.1 and will be developed and submitted per the contract schedule. Any hazardous operation or procedure will be identified and submitted to the launch site 75 days prior to the delivery of the LUTE hardware at the launch or ground processing site.

5.0 SAFETY NONCOMPLIANCE WAIVER REQUESTS

When a specific safety requirement cannot be met, a waiver request will be submitted that states the reason for the noncompliance, the proposed method of controlling any additional risk, and the residual risk after the application of the additional controls. Each waiver request will address only one hazard and will be submitted when it is determined that one is required.

6.0 INCIDENT REPORTING

6.1 GENERAL

All incidents/accidents involving the safety of flight hardware and associated GSE or personnel shall be reported to the MSFC Safety and Mission Assurance Office and the MSFC LUTE Project Office in accordance to MMI 1711.2C.

The System Safety representative will participate in mishap investigations which involve hardware and personnel through all phases of LUTE fabrication, testing, and checkout.

7.0 SAFETY TRAINING AND CERTIFICATION

Test and operational personnel will be required to complete training courses for certain critical or hazardous operations as prerequisites for personnel certification. All training courses require system and industrial safety inputs to emphasize critical and hazardous procedures.

8.0 SYSTEM SAFETY DATA SUBMITTALS AND SCHEDULES

Data submittals:

Preliminary System Safety Assessment and MSPSP..... PDR

Missile System Prelaunch Safety Package..... CDR

Updated Missile Prelaunch Safety Package....75 days prior to delivery to launch site

APPENDIX O

LUTE PRELIMINARY HAZARD ANALYIS REPORT

National Aeronautics and
Space Administration

CT 1724.9

July 1993

George C. Marshall Space Flight Center
Marshall Space Flight Center, Alabama 35812

LUNAR ULTRAVIOLET TELESCOPE EXPERIMENT (LUTE)

PRELIMINARY HAZARD ANALYSIS REPORT

Lunar Ultraviolet Telescope Experiment
Preliminary Hazard Analysis Report

Prepared by:

Michael J. Galuska / 7/6/93

CT21/Michael J. Galuska Date
Systems Safety Engineer
Safety Assessment Team

Approved by:

James E. Hatfield / 7/6/93

CT21/James E. Hatfield Date
Supervisory Lead, Systems
Safety Engineering Office

John M Livingston / 7/20/

CT21/John M. Livingston Date
Chief, Systems Safety
Engineering Office

Concurrence:

Robert O. McBrayer / 7/21/93

PF21/Robert O. McBrayer Date
LUTE Project Manager

John L. Frazier / 7-21-93

EJ 23/John L. Frazier Date
LUTE Chief Engineer

Table of Contents

Table of Contents.....i

List of Figures.....ii

List of Abbreviations and Acronyms.....iii

1.0 Introduction.....1
- 1.1 Purpose.....1
- 1.2 Approach.....1
- 1.3 Hazard Classification.....1

2.0 Documents.....2

3.0 Analysis.....3
- 3.1 LUTE Overview.....3
- 3.2 Subsystem Description.....3
  - 3.2.1 Thermal Control.....3
  - 3.2.2 Structures and Mechanical Ground Support Equipment.....3
  - 3.2.3 Main Optics and Telescope.....3
  - 3.2.4 Pointing Control.....4
  - 3.2.5 Command and Data Management System.....4
  - 3.2.6 Power Distribution.....4
- 3.3 Preliminary Hazard Analysis.....5

4.0 Preliminary Safety Risk Assessment Summary.....6
- 4.1 System Safety Risk Assessment.....6
  - 4.1.1 Human Factors.....6
  - 4.1.2 Materials.....6
  - 4.1.3 Structures and Handling.....6
  - 4.1.4 Thermal Control System.....6
  - 4.1.5 Electrical Power System.....6
  - 4.1.6 Command and Data Management System.....7
  - 4.1.7 Pressurized Systems.....7
  - 4.1.8 Pointing and Alignment.....7
- 4.2 Conclusion.....7

PHA Worksheets.....Appendix

List of Figures

Figure 1, Space Shuttle Preliminary Hazard Analysis Instructions.....8

Figure 2, List of Generic Hazards.....9

Figure 3, Risk Matrix Test for Agreement Between Closure Classification and Risk.....11

Figure 4, Conceptual LUTE Launch Configuration.....12

Figure 5, Radioisotope Heater Unit.....13

Figure 6, Conceptual Pointing System Components.....14

Figure 7, Command and Data Management System Conceptual Block Diagram.....15

Figure 8, General Purpose Heat Source Radioisotope Thermoelectric Generator.....16

List of Abbreviations and Acronyms

ALARA	As Low As Reasonably Achievable
ANSI	American National Standards Institute
CA	Catastrophic
CCD	Change Coupled Device
CDMS	Command and Data Management System
CR	Critical
dBA	Decibel, A-scale
DOF	Degrees of Freedom
EGSE	Electrical Ground Support Equipment
ELV	Expendable Launch Vehicle
ESMCR	Eastern Space and Missile Center Regulation
ETR	Eastern Test Range
GSE	Ground Support Equipment
IECEC	Intersociety Energy Conversion Engineering Conference
L of O	Likelihood of Occurrence
LSSO	Launch Site Safety Office
MGSE	Mechanical Ground Support Equipment
MOP	Maximum Operating Pressure
mw/cm2	Milliwatts Per Square Centimeter
NDI	Non-destructive Inspection
PHA	Preliminary Hazard Analysis
PuO2	Plutonium Dioxide
QA	Quality Assurance
RF	Radio Frequency
RHU	Radioisotope Heater Unit
RTG	Radioisotope Thermoelectric Generator
TBD	To Be Determined

1.0 Introduction

1.1 Purpose

The purpose of this PHA for the LUTE is to identify safety critical areas, to identify and evaluate hazards and to identify the safety design and operations requirements needed in the program concept phase. This PHA will also provide a knowledge of potential risks for alternative concepts.

1.2 Approach

Since the LUTE is a payload which will be launched at the ETR from an unmanned ELV, the safety requirements specified by ESMCR 127-1 will be imposed. The techniques and format described in NSTS 22254A, "Space Shuttle Methodology for Conduct of Space Shuttle Program Hazard Analyses," was used to perform this PHA. This analysis was performed on a subsystems basis using the instructions specified by figures 1 through 3 and covers the LUTE payload. The lander, ELV, and potential interface hazards were not analyzed in this PHA. Also, an analysis will be performed to evaluate the potential for orbital debris generation in both nominal and malfunction conditions, which is required by NMI 1700.8. The methods for conducting this orbital debris analysis are TBD.

1.3 Hazard Classification

Hazards are classified, according to severity, as follows:

Catastrophic (Category I) - Personnel loss, system loss.

Critical (Category II) - Severe injury, severe occupational illness, major system damage.

Marginal (Category III) - Minor injury, minor system damage.

2.0 Documents

ANSI B30 Series, "American National Standard, Standards for Cranes, Derricks, Hoists, Hooks, Jacks, and Slings"

A. Schock, "Light-Weight Radioisotope Heater Unit," 1981 IECEC Paper 819175

CT 1724.3, "Lunar Ultraviolet Telescope Experiment (LUTE) System Safety Plan," Draft, dated January 25, 1993

ESMCR 127-1, "Eastern Space and Missile Center Requirements Range Safety"

JSC 20793, "Manned Space Vehicle Battery Safety Handbook"

"Lunar Ultraviolet Telescope Experiment Draft Interim Technical Assessment," dated January 1993

MIL-B-5087B, "Bonding, Electrical, and Lightning Protection for Aerospace Systems"

MIL-STD-1522A, "Military Standard/Standard General Requirements for Safe Design and Operation of Pressurized Missiles and Space Systems"

MSFC-HDBK-505B, "Structural Strength Program Requirements"

MSFC-HDBK-527B, "Materials Selection List for Space Hardware Systems"

MSFC-SPEC-522B, "Design Criteria for Controlling Stress Corrosion Cracking"

NFPA 70, "National Electric Code"

NHB 1700.1 (V1-A), "Basic Safety Manual"

NMI 1700.8, "Policy for limiting Orbital Debris Generation"

NSTS 22254A, "Space Shuttle Methodology for Conduct of Space Shuttle Program Hazard Analysis"

3.0 Analysis

3.1 LUTE Overview

LUTE is a 1-M class, fixed declination, ultraviolet imaging telescope. The LUTE will be placed on the lunar surface by an unmanned lander and launch/transfer vehicle. The payload and vehicle will be launched from the Eastern Test Range and the payload will be processed at KSC. The launch configuration for LUTE is shown on figure 4. The LUTE will produce a multiple bandpass (1000 Angstrom to 3000 Angstrom) ultraviolet survey of more than 300 square degrees of the sky, with repeat observations at monthly and annual intervals to allow studies of variability and proper motion.

3.2 Subsystem Description

3.2.1 Thermal Control

The purpose of the thermal control subsystem is to maintain the LUTE optical subsystem, LUTE detector, LUTE light shade, and LUTE electronics within their thermal qualification limits for the duration of the mission.

It is anticipated that the LUTE will be cooled and heated passively and by using heaters. The optics detector will be cooled using a passive radiator and heated on the lunar surface using electrically powered heaters. If the electrical power solar array concept is used, the electronics for LUTE will be heated using radioisotope heating units. As depicted in figure 5, each RHU contains a small PuO2 fuel pellet in a capsule which has a heat output of 1 watt at the beginning of its life. The electronics will be cooled by a passive radiator. If the electrical RTG power concept is used, electrical heaters will provide heating for the electronics.

3.2.2 Structures and Mechanical Ground Support Equipment

For this analysis, it was assumed that MGSE will be required to move and lift the LUTE during ground operations at KSC and the ETR. It was also assumed that the flight hardware would be designed to accommodate handling. It is anticipated that some nitrogen inerting gas will be required.

3.2.3 Main Optics and Telescope

The LUTE will use a three mirror configuration. The focal plane is located in front of the telescope. The mirror material candidates are beryllium, fused silica, and silicon carbide.

3.2.4 Pointing Control

The pointing system provides the means of orienting the LUTE and its subsystems. The pointing systems component arrangement is shown in figure 6. Telescope mount actuators, secondary mirror alignment actuators and a sunshade/solar array/antenna roll mechanism are used to perform this function.

3.2.5 Command and Data Management System

The CDMS contains two antennas, which includes one steerable high-gain antenna and an omnidirectional antenna. The deployment of the high-gain antenna will occur automatically on landing on the lunar surface or will be commanded from the ground. The power required will be less than TBD watts and the power density is TBD mW/cm2. It is assumed that functional testing will be performed at KSC. A block diagram of the CDMS is shown in figure 7.

3.2.6 Power Distribution

The power distribution subsystem is required to provide a minimum TBDWe average electrical power. There are two concepts for providing power to the LUTE. One concept is a TBDWe solar array power system, which will restrict LUTE operations to sunlit periods. The other concept is a TBDWe RTG which allows the LUTE to operate continuously.

The solar array system power concept contains a TBD square meter solar array, a lithium bromine battery, and a power distribution regulator. The lithium bromine battery is used to deploy the solar arrays after the LUTE and lunar lander land on the moon.

The RTG system power concept would contain one RTG with TBD Plutonium bricks. Figure 8 shows a cross-sectional view of an RTG that was used on the Galileo mission. A prelaunch cooling system must be provided.

C-8.

3.3 Preliminary Hazard Analysis

Contents:

(1) Human Factors

(2) Materials

(3) Structure/Handling

(4) Thermal Control

(5) Power (Concepts 1 and 2)

(6) Command and Data Management

(7) Pressurized Systems

(8) Pointing and Alignment

The worksheets are enclosed in the Appendix.

4.0 Preliminary Safety Risk Assessment Summary

4.1 System Safety Risk Assessment

4.1.1 Human Factors

All the potential human factors hazard sources were found to be critical in severity, which could result in personnel injury. The controls required to eliminate these hazards are typical for ground processing. The elimination of access to hot surfaces, sharp edges, access to moving parts, and exposure to high noise sources will control human factors hazards.

4.1.2 Materials

In order to control the potential flammability and toxicity hazards associated with materials used during ground processing, materials will be selected using MSFC-HDBK-527 and will be approved by the KSC LSSO.

4.1.3 Structures and Handling

Structural failure of the MGSE or the payload attach points have the potential of causing a catastrophic hazard. All slings will be designed in accordance with ANSI B30 and ESMCR 127-1, paragraph 3.6, and proofload tested as required by KSC and ETR. Non-destructive inspection will be performed on shackles and eyebolts following each proofloading. Flight hardware will be designed in accordance with MSFC structural design requirements.

4.1.4 Thermal Control System

If the solar array concept is used, the thermal control system will use RHU's which contain a small amount of PuO2. These units are classified as small radiological sources which, as a minimum, will require NASA Headquarters approval for use. During ground processing, personnel exposure will be kept to a minimum. Also, the thermal control system may contain heat pipes which may require hazard controls that are typically applied to pressurized systems.

4.1.5 Electrical Power System

The electrical power system has two options for power sources, which may be an RTG or a set of solar arrays with a lithium bromine battery. An RTG is classified as a major ionizing radiation source, which requires the user to follow the nuclear safety review process. The NASA procedures, interagency review, and approval for the use of this type of device are outlined in Chapter 8 of NHB 1700.1 (V1-A). All nominal and off-nominal conditions will be assessed for acceptable risk to ensure that

the general public and range personnel are not overexposed to RTG-emitted ionizing radiation. The solar array power concept has several hazards which will be controlled. The potential for explosion of the lithium bromine and inadvertent deployment of the solar arrays during ground processing and launch will be completely assessed when the design becomes more mature. The hazards associated with both of these options are controllable and have been previously addressed in the design of spacecraft that have previously flown.

4.1.6 Command and Data Management System

Hazard controls will be implemented to prevent personnel overexposure to RF non-ionizing radiation during ground processing. Safety inhibits and shielding will be provided in accordance with ESMCR 127-1 and KSC non-ionizing radiation requirements.

4.1.7 Pressurized Systems

All flight and GSE pressurized systems will comply with the design, fabrication and testing requirements specified by MIL-STD-1522 and ESMCR 127-1. Compliance with these requirements will prevent personnel injury and payload and facility damage that can be caused by a ruptured pressurized line.

4.1.8 Pointing and Alignment

The pointing and alignment system has the capability to tilt or rotate the LUTE experiment. Controls will be implemented that will prevent inadvertent rotation or tilting of the LUTE during transportation, ground processing operations, and launch.

4.2 Conclusion

The LUTE concept design has been reviewed and found to meet current NASA safety requirements. The hazard controls and methods of verification are listed in the hazard reports which are enclosed in the Appendix. Overall, all of the safety design concerns for the LUTE have been previously addressed in the design of spacecraft that have previously flown.

SPACE SHUTTLE PRELIMINARY HAZARD (PHA) ANALYSIS INSTRUCTIONS

PHA NO. _____

MISSION PHASE: Flight Operations, Mission Operations, Turnaround, Etc.. ENGINEER: _____

SUBSYSTEM OR OPERATION: Identify EPS, ECLSS, GN&C, Etc. DATE: 06/30/86

EFFECTIVITY: Ascent, On-Orbit, Entry, Approach and Landing Turnaround SHEET 1 of 1

HAZARDOUS CONDITION	HAZARD CAUSES	HAZARD EFFECT	SEVERITY LEVEL	SAFETY REQUIRE-MENTS	HAZARD ELIMINATION/ CONTROL PROVISIONS	VERIFICATIONS	LIKELIHOOD OF OCCURRENCE
Use the checklist below to identify potentially hazardous conditions. 1. Can the system/ subsystem fail to operate as intended? 2. Can the system/subsystem operate inadvertently (untimely)? 3. Are there generic hazards? (See figure 2) Record the identified hazards	Enter brief description of how each hazardous condition is created, i.e., rupture of the 02 tank; wiring insulation overheating and igniting; etc.	Record the potential effect of each hazardous condition on critical equipment, personnel or the general public, i.e., loss of vehicle; emergency landing in inhabited area; etc.	Identify the severity level as one of the following for each hazardous condition: CA- Catastrophic CR- critical MR - Marginal	Identify the existing or proposed safety requirement that will eliminate or control the hazardous condition by document and paragraph number.	Identify proposed hazard reduction methods for open hazards and implemented reduction methods for controlled hazards.	Identify the methods used to verify the hazard controls. Include sufficient detail/explanation of testing, inspection, and analysis which mitigate the hazard and support hazard closure or risk rationale. Verification methods include analyses, tests, inspections, & operations & maintenance requirements. Identify the verification reference by document number and title	Assess the controls that are in place and classify them as one of the following: Probable; Infrequent; Remote; or Improbable.

Figure 1 Space Shuttle Preliminary Hazard Analysis (PHA) Instructions

GENERIC HAZARD	GENERIC HAZARD TYPE
I. CONTAMINATION/CORROSION	A. CHEMICAL DISASSOCIATION B. CHEMICAL REPLACEMENT/COMBINATION C. MOISTURE D. OXIDATION E. ORGANIC (FUNGUS/BACTERIAL, ETC.) F PARTICULATE
II. ELECTRICAL DISCHARGE/SHOCK	A. EXTERNAL SHOCK B. INTERNAL SHOCK C. STATIC DISCHARGE D. CORONA E. SHORT
III. ENVIRONMENTAL/WEATHER	A. FOG B. FUNGUS/BACTERIAL C. LIGHTNING D. PRECIPITATION (RAIN/SNOW/SLEET/HAIL) E. SOLAR/COSMIC RADIATION F. SAND/DUST G. VACUUM H. WIND I. TEMPERATURE EXTREMES
IV. FIRE/EXPLOSION	A. CHEMICAL CHANGE (EXOTHERMIC/ENDOTHERMIC) B. FUEL AND OXIDIZER IN PRESENCE OF PRESSURE AND IGNITION SOURCE C. PRESSURE RELEASE/IMPLOSION D. HIGH HEAT SOURCE
V. IMPACT/COLLISION	A. ACCELERATION (INCLUDING GRAVITY) B. DETACHED EQUIPMENT C. MECHANICAL SHOCK/VIBRATION/ACOUSTICAL D. METEROIDS/METEORITES E. MOVING/ROTATING EQUIPMENT
VI. LOSS OF HABITABLE ENVIRONMENT	A. CONTAMINATION B. HIGH PRESSURE C. OXYGEN CONTENT D. LOW PRESSURE E. TOXICITY F. LOW TEMPERATURE G. HIGH TEMPERATURE

Figure 2 List of Generic Hazards (Page 1 of 2)

GENERIC HAZARD	GENERIC HAZARD TYPE
VII. PATHOLOGICAL/PHYSIOLOGICAL/ PSYCHOLOGICAL	A. ACCELERATION/SHOCK/IMPACT/VIBRATION B. ATMOSPHERIC PRESSURE (HIGH, LOW, RAPID CHANGE) C. HUMIDITY D. ILLNESS E. NOISE F. SHARP EDGES G. SLEEP, LACK OF H. VISIBILITY (GLARE, WINDOW/HELMET FOGGING) I. TEMPERATURE J. WORKLOAD, EXCESSIVE
VIII. RADIATION	A. ELECTROMAGNETIC B. RADIOACTIVE ELEMENT
IX. TEMPERATURE EXTREMES	A. HIGH B. LOW C. VARIATIONS

Figure 2 List of Generic Hazards (Page 2 of 2)

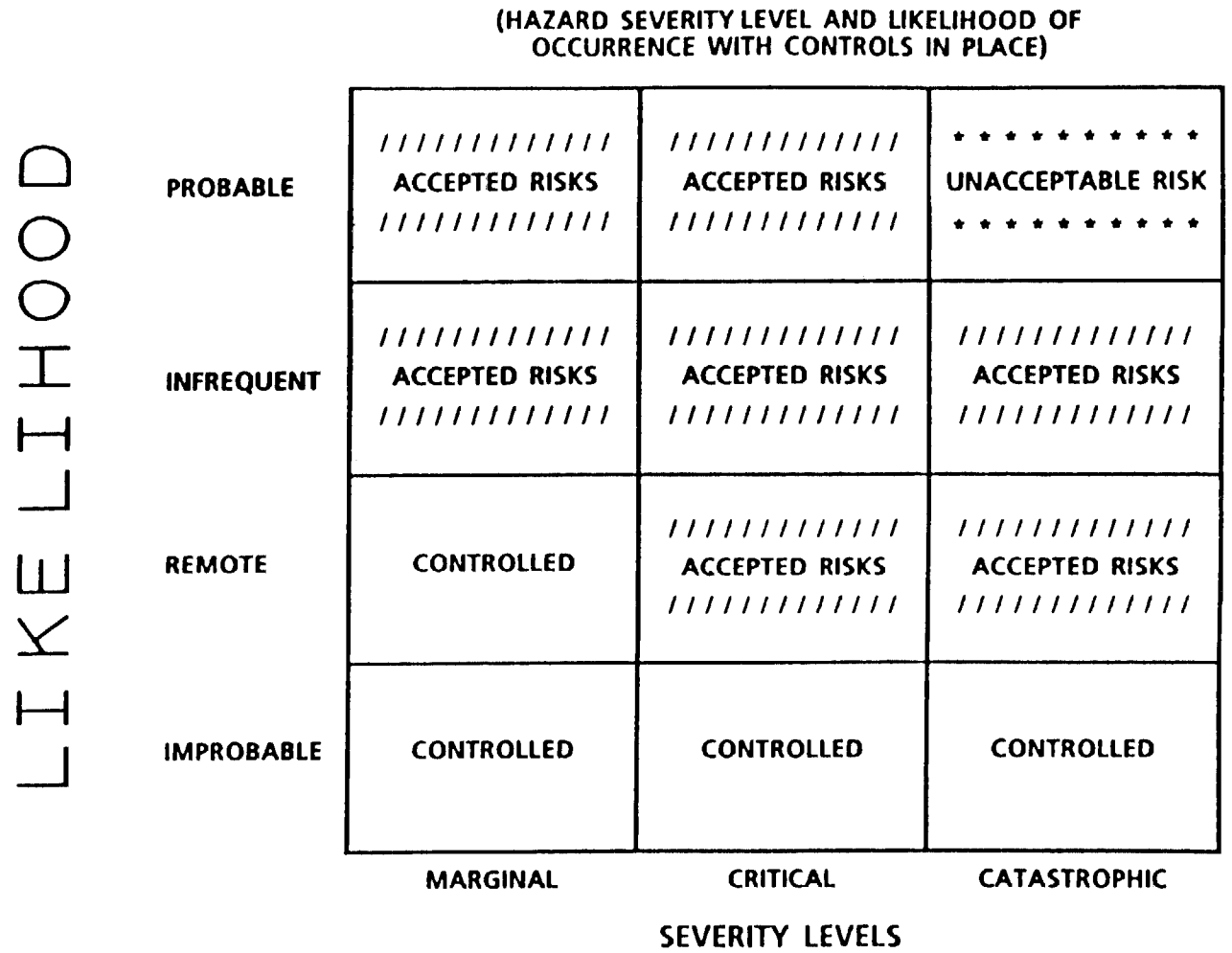

Figure 3 Risk Matrix Test for Agreement Between Closure Classification and Risk

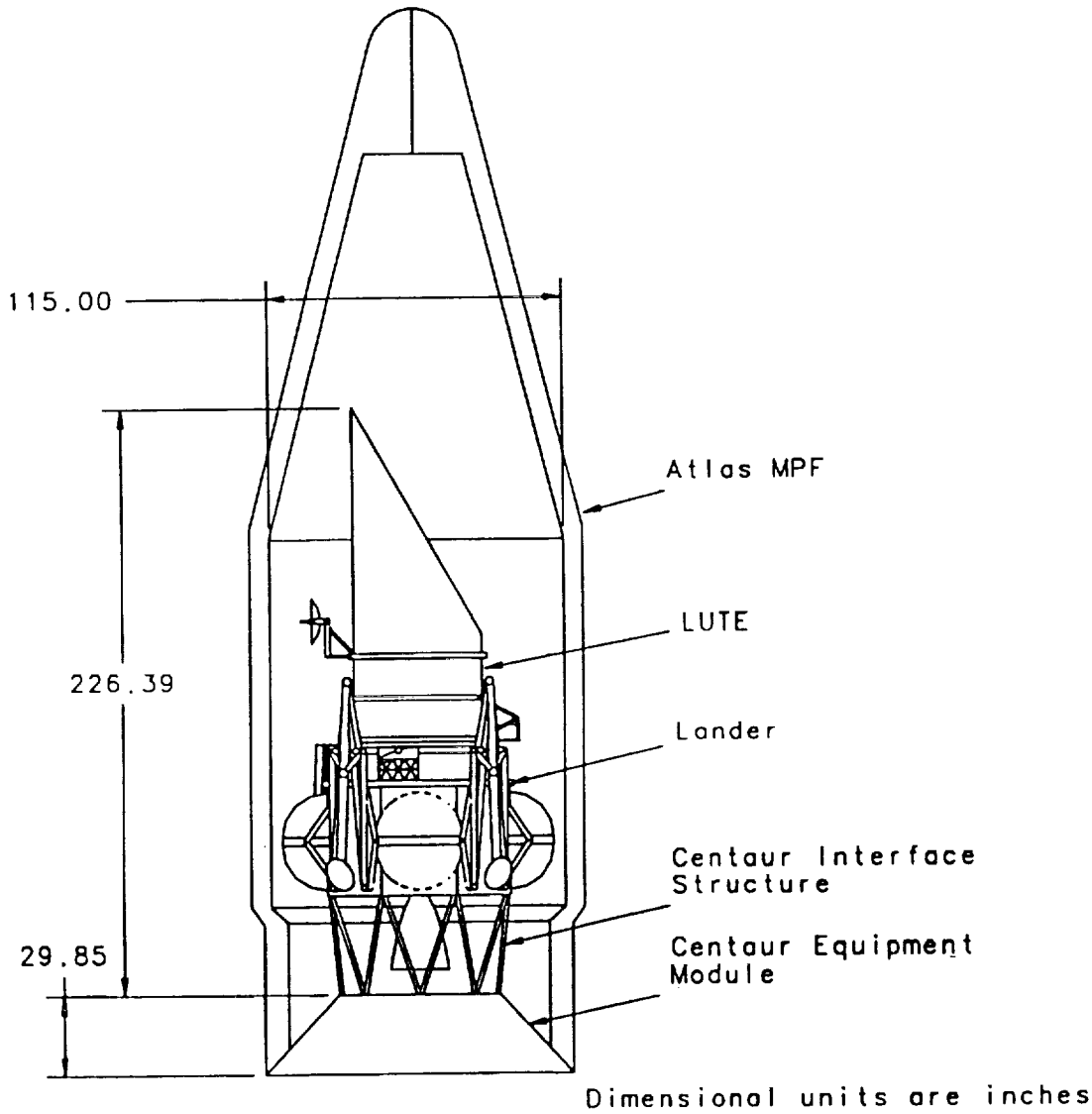

Figure 4 Conceptual LUTE Launch Configuration

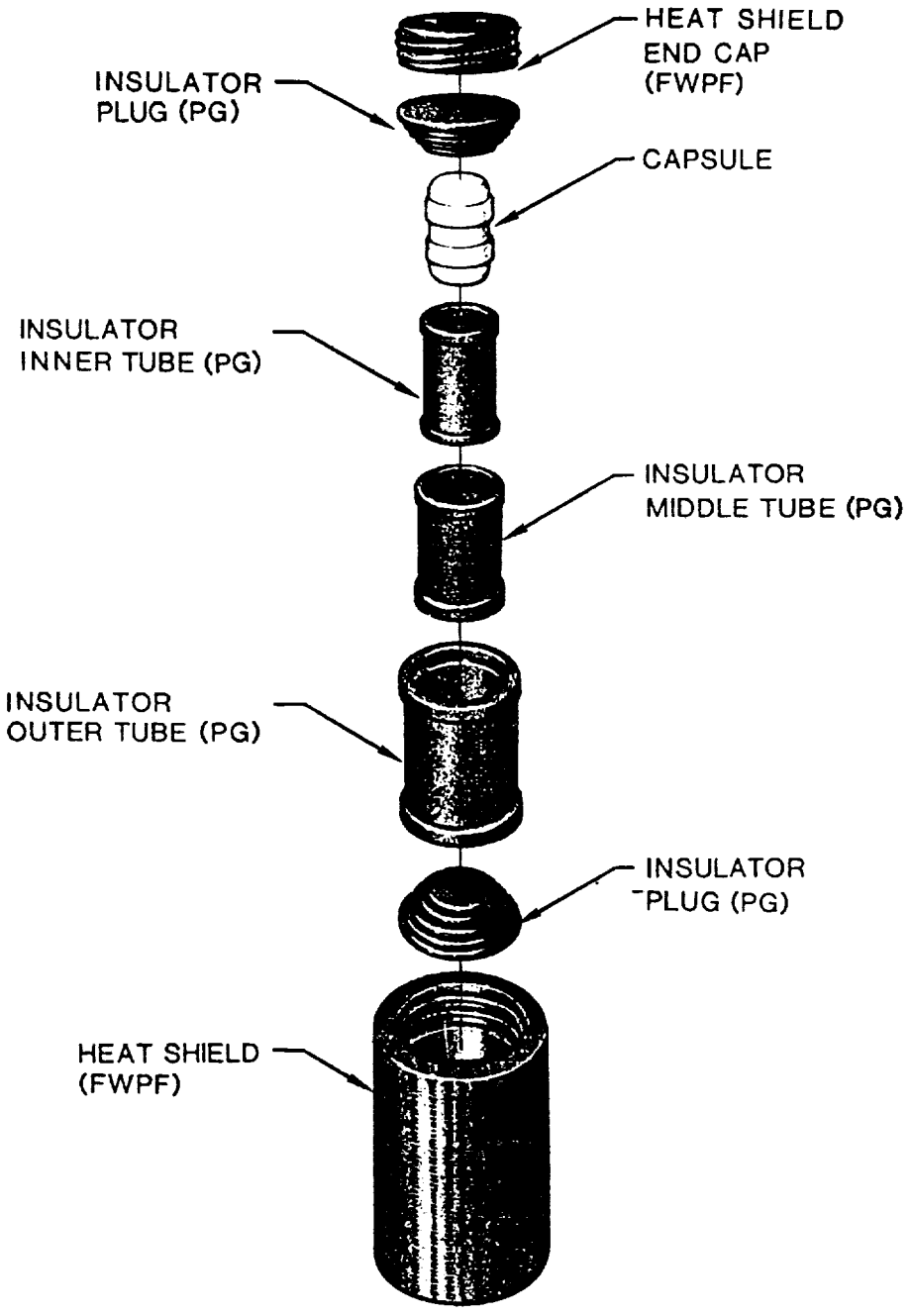

Figure 5 : RADIOISOTOPE HEATER UNIT

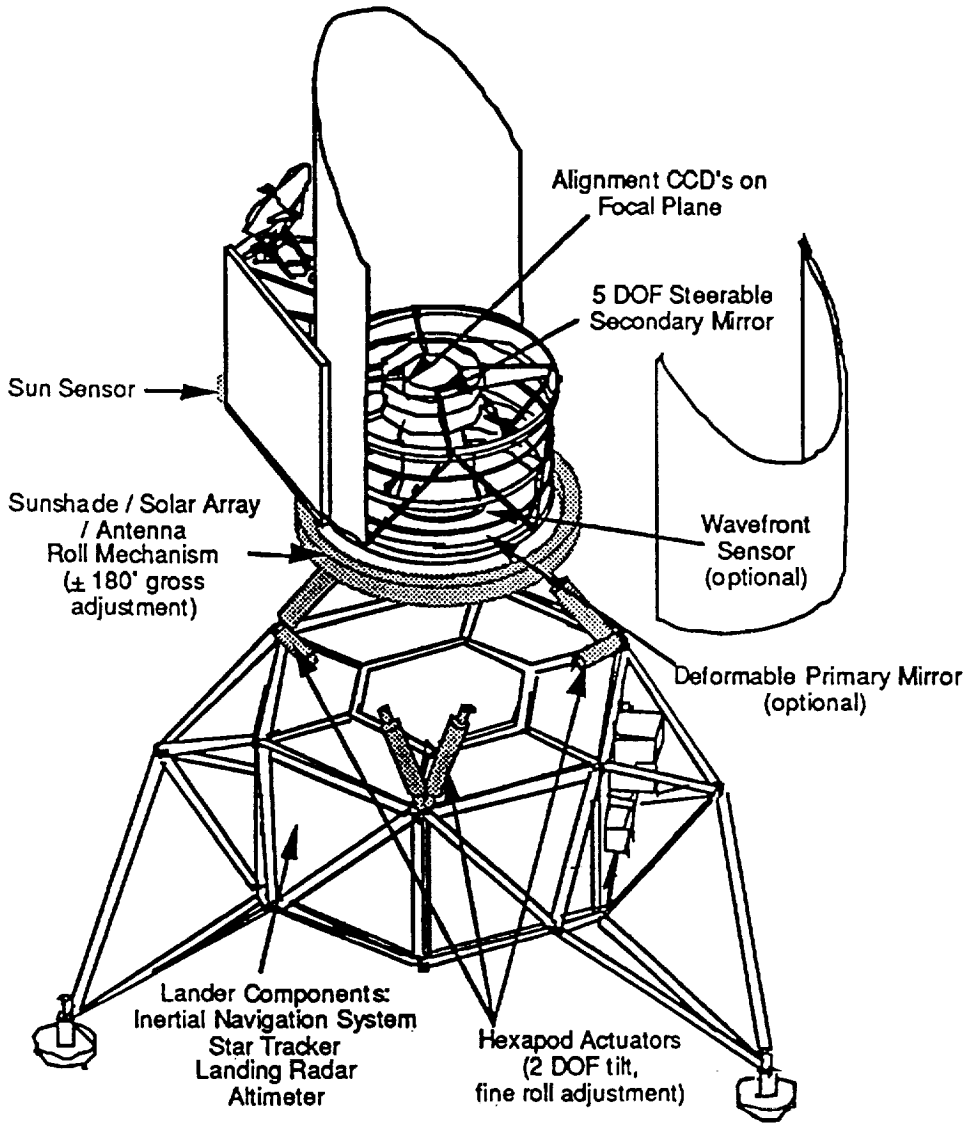

Figure 6 Conceptual Pointing System Components

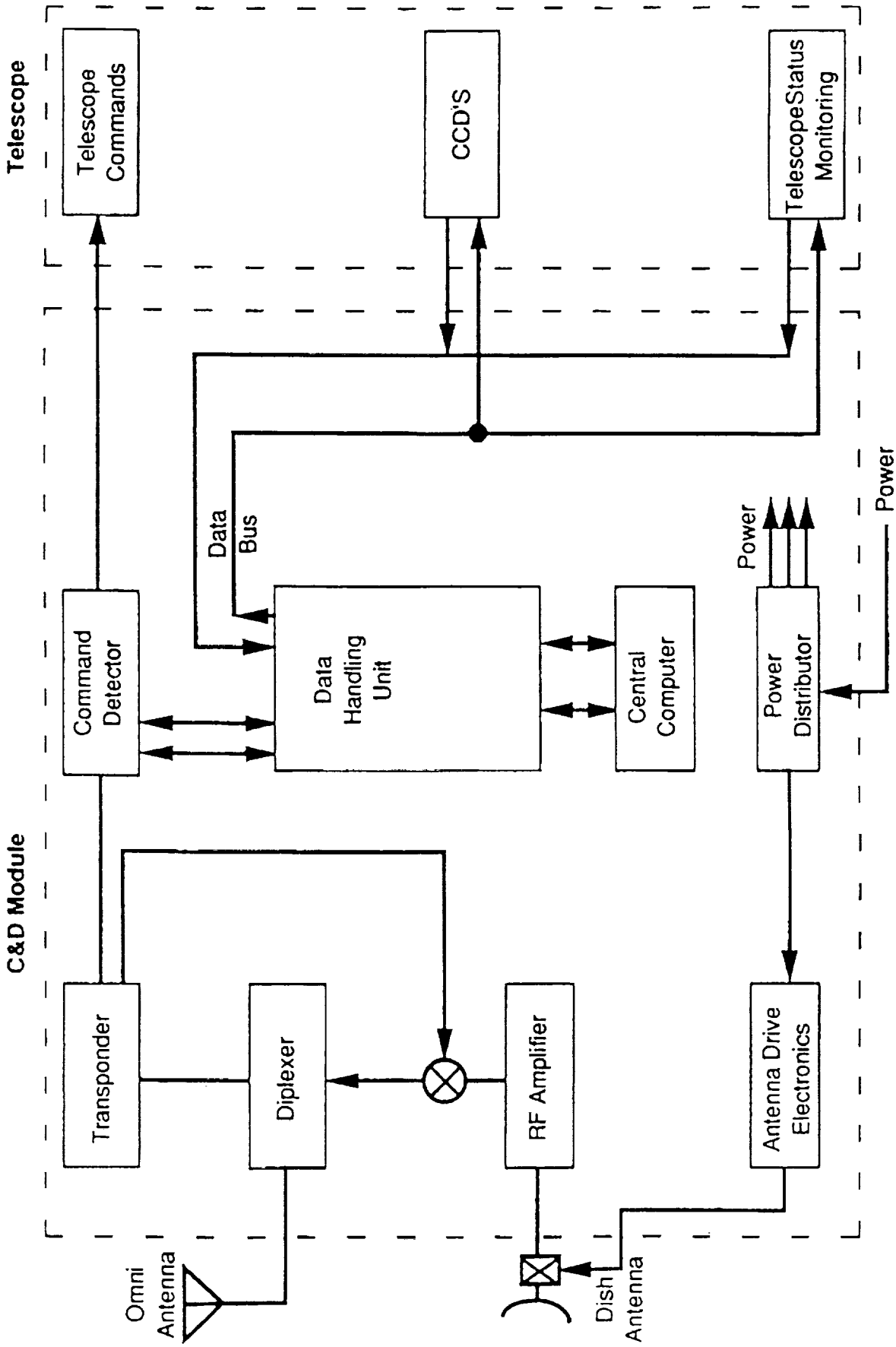

Figure 7 Command and Data Management System Conceptual Block Diagram

GENERAL PURPOSE HEAT SOURCE - RADIOISOTOPE THERMOELECTRIC GENERATOR

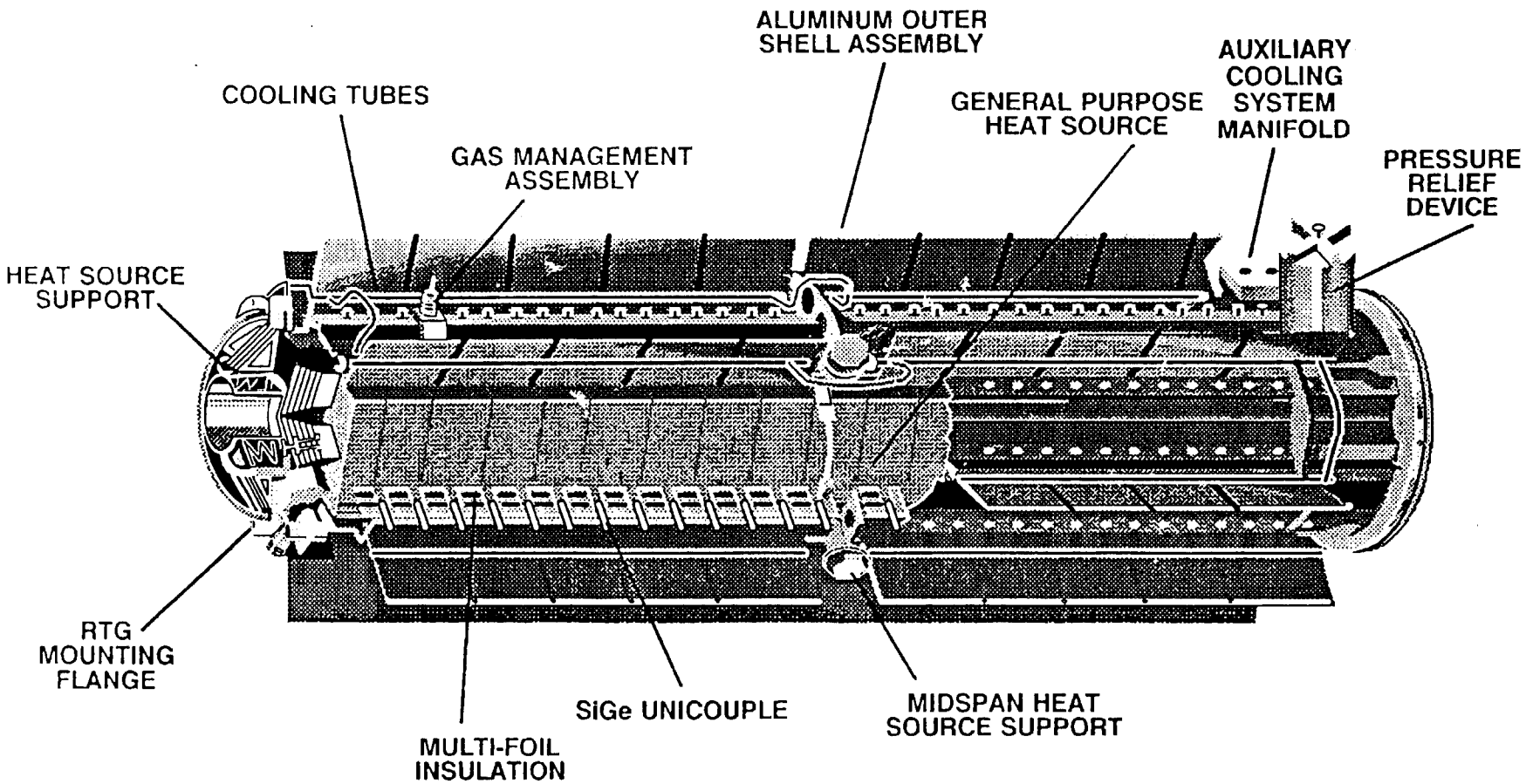

- **POWER OUTPUT** - 285 WATTS
- **FUEL LOADING** - 4400 WT; 132,50
- **WEIGHT** - 124 LBS
- **SIZE** - 16.6 IN × 44.5 IN

Figure 8

APPENDIX

PROJECT: LUTE SUBSYSTEM: Human Factors Hazard Report HF-1 1

HAZARD	HAZARD CAUSE	HAZARD EFFECT	SEVERITY LEVEL	SAFETY REQUIREMENT	HAZARD ELIMINATION/CONTROL	VERIFICATION	L OF O
High noise level	Exposure of personnel to noise levels >85dBA without protection	Personnel Injury	CR	ESMCR 127-1, 3.7	Limit the use of GSE with high noise levels.	Analysis & testing	Remote
					Provide personnel with hearing protection if noise levels exceed 85dBA.	Inspection	Remote
Touch temperature of payload or GSE exceeds 113 degrees F	Exposure of personnel to high touch temperatures	Personnel Injury	CR		Insulate high temperature surfaces to maintain touch temperature below 113 degrees F.	Analysis & inspection	Improbable
Sharp edges	Exposure of personnel to accessible sharp surfaces or protrusions	Personnel Injury	CR		Eliminate accessible sharp surfaces or protrusions.	Analysis & inspection	Improbable
Exposure to moving parts	Exposure of personnel to high energy moving parts (fans, belts, drives, etc.)	Personnel Injury	CR		Eliminate accessible moving parts on GSE by providing guards or other protective devices.	Analysis & inspection	Improbable

PROJECT: LUTE SUBSYSTEM: Materials Hazard Report M-1 2

HAZARD	HAZARD CAUSE	HAZARD EFFECT	SEVERITY LEVEL	SAFETY REQUIREMENT	HAZARD ELIMINATION/CONTROL	VERIFICATION	L OF O
Hazardous materials are used during ground processing that create a fire.	(1) Flammable material is used.	Fatality, personnel injury, loss of vehicle or facility hardware	CA	ESMCR 127-1, paragraph 3.10	(1) Use non-flammable materials.	Use materials approved by KSC LSSO and MSFC HDBK 527	Improbable
	(2) Hazardous materials are used during ground processing which can create a toxic environment.	Fatality, personnel injury, loss of vehicle or facility hardware	CA	ESMCR 127-1, paragraph 3.10	(2) Use only materials that are ETR/KSC approved for low toxicity.	Analysis	Improbable
	(3) Plastic films are used which retain an electrostatic charge that presents an ignition source.	Fatality, personnel injury, loss of vehicle or facility hardware	CA	ESMCR 127-1, paragraph 3.10	(3) Use only approved plastic materials during ground processing.	Analysis	Improbable

HAZARD	HAZARD CAUSE	HAZARD EFFECT	SEVERITY LEVEL	SAFETY REQUIREMENT	HAZARD ELIMINATION/CONTROL	VERIFICATION	L OF O
Structural failure of GSE or flight hardware attach points	(1) Loads exceeded	Fatality, personnel injury, loss of vehicle or facility hardware	CA	ESMCR 127-1, paragraph 3.6	(1) MGSE slings are designed and used in accordance with ANSI B30 and ESMCR 127-1, paragraph 3.6 and will be prooftested as required by KSC and ETR. Flight Hardware will be designed using the factors of safety specified by MSFC-HDBK-505B.	(1) Proofload testing of slings Stress analysis of flight hardware	Remote
	(2) Corrosion of MGSE	Fatality, personnel injury, loss of vehicle or facility hardware	CA		(2) Stress corrosion resistant materials will be selected from MSFC-SPEC-522B. MGSE parts will be protected from corrosion by coatings and finishes.	(2) Design analysis	Remote
	(3) Improper use of equipment or operations error	Fatality, personnel injury, loss of vehicle or facility hardware	CA		(3) All procedures that will be used at ETR or KSC will be validated prior to use.	(3) QA inspection	Remote
	(4) Propagation of crack-like defects in MGSE	Fatality, personnel injury, loss of vehicle or facility hardware	CA		(4) NDI testing will be performed on single failure points, welds, and on shackles and eyebolts.	(4) NDI testing performed after proofloading	Remote

HAZARD	HAZARD CAUSE	HAZARD EFFECT	SEVERITY LEVEL	SAFETY REQUIREMENT	HAZARD ELIMINATION/CONTROL	VERIFICATION	L OF O
Overexposure to radiation from RHU's during ground processing of LUTE	(1) Improper handling and long duration exposure during ground processing	Personnel injury	CR	ESMCR 127-1, paragraph 3.9.3	(1) Operating procedures will be conducted in a manner which will limit exposure of personnel to the RHU's.	Analysis & inspection	Improbable
					Radiation surveys will be performed on RHU's prior to bringing RHU's to KSC or ETR	Testing	Improbable
Radiation overexposure to RHU's following an aborted launch resulting in vehicle breakup	(2) Structural failure of nuclear source containment	Personnel injury	CR		(2) Maximum exposure levels established by KSC and ETR health physicians will be complied with.	Inspection	Improbable
					The RHU container is capable of withstanding worst case launch abort loads and environments.	Analysis & testing	Improbable

HAZARD	HAZARD CAUSE	HAZARD EFFECT	SEVERITY LEVEL	SAFETY REQUIREMENT	HAZARD ELIMINATION/CONTROL	VERIFICATION	L OF O
Rupture of heat pipes during ground operations	(1) Ground operations pressures/loads may exceed the stress level heat pipes can withstand.	Release of flammable liquid and shrapnel results in personnel injury or death	CA	ESMCR 127-1, paragraph 3.9.3	(1) An ultimate safety factor of equal or greater than 4 will be used in the design.	(1) Analysis & testing	Remote
	(2) Heat pipes contain cracks or flaws which may propagate to failure	Release of flammable liquid and shrapnel results in personnel injury or death	CA	ESMCR 127-1, paragraph 3.9.3	(2) Heat pipes will be subject to fracture control.	(2) Analysis	Remote
	(3) Failed on heaters may result in the overpressurization of heat pipes.	Release of flammable liquid and shrapnel results in personnel injury or death	CA	ESMCR 127-1, paragraph 3.9.3	(3) Heater controls will be designed to the required fault tolerance.	(3) Analysis	Remote
	(4) Excessive ground handling loads	Release of flammable liquid and shrapnel results in personnel injury or death	CA	ESMCR 127-1, paragraph 3.9.3	(4) All ground handling operations will be per validated procedures.	(4) Inspection of procedures	Remote

HAZARD	HAZARD CAUSE	HAZARD EFFECT	SEVERITY LEVEL	SAFETY REQUIREMENT	HAZARD ELIMINATION/CONTROL	VERIFICATION	L OF O
Electrical shock to personnel	(1) Exposed terminals/circuitry	Personnel injury or fatality	CA	ESMCR 127-1, paragraph 3.14	(1) EGSE and flight hardware terminals with >30 VAC or VDC will be covered or otherwise made inaccessible.	(1) Design analysis and inspection	Remote
	(2) Inadequate fusing and ground fault protection of EGSE.	Personnel injury or fatality	CA	ESMCR 127-1, paragraph 3.14	(2) Bonding and grounding will be compliant to MIL-B-5087B.	(2) Bonding resistance test	Remote
					Electrical connections will be designed to prevent inadvertent contact of pins during mating (scoop proof).	Design analysis	Remote
					EGSE and flight hardware will be designed with overcurrent protection. EGSE will be designed to meet NFPA70.	Design analysis	Remote
	(3) Improper use of EGSE	Personnel injury br fatality	CA	ESMCR 127-1, paragraph 3.14	(3) Procedures will be developed and validated prior to equipment delivery to KSC/ETR.	(3) Inspection	Remote

HAZARD	HAZARD CAUSE	HAZARD EFFECT	SEVERITY LEVEL	SAFETY REQUIREMENT	HAZARD ELIMINATION/CONTROL	VERIFICATION	L OF O
Explosion of Lithium Bromine battery	(1) Physical abuse of battery	Personnel Injury, fatality, or loss of hardware	CA	ESMCR 127-1, paragraph 3.14.7	(1) Procedures will be developed to handle the battery properly.	Inspection	Improbable
	(2) Overheating of battery	Personnel Injury, fatality, or loss of hardware	CA	ESMCR 127-1, paragraph 3.14.7	(2) Cell temperatures will be controlled below the manufacturer's stated upper limit.	Thermal analysis	Improbable
	(3) External short circuit from EGSE or from LUTE circuitry	Personnel Injury, fatality, or loss of hardware	CA	ESMCR 127-1, paragraph 3.14.7	(3) Fuses or circuit protection devices will be provided in EGSE and in the LUTE	Design analysis	Improbable
	(4) Forced discharge of a cell below zero voltage could cause the cell to explode.	Personnel Injury, fatality, or loss of hardware	CA	ESMCR 127-1, paragraph 3.14.7	(4) All cells will have shunt diodes attached to them.	Design analysis	Improbable

HAZARD	HAZARD CAUSE	HAZARD EFFECT	SEVERITY LEVEL	SAFETY REQUIREMENT	HAZARD ELIMINATION/CONTROL	VERIFICATION	L OF O
Inadvertent deployment of solar arrays during ground processing and launch	(1) Structural failure causes deployment during launch	Personnel injury or flight hardware damage during ground processing	CR	ESMCR 127-1, 3.3.4.7	(1) Solar array mechanism will be designed to withstand worst case launch loads.	Structural analysis and/or test	Improbable
	(2) Electrical relay failure during checkout or launch	Personnel injury or flight hardware damage during ground processing	CR	ESMCR 127-1, 3.14.11	(2) Fault tolerance will be designed into the flight system and EGSE.	Design analysis & test	Improbable
	(3) Commanding or software error during ground processing or launch	Personnel injury or flight hardware damage during ground processing	CR	ESMCR 127-1, 3.14.11	(3) Fault tolerance will be designed into the flight system and EGSE.	Design analysis & test	Improbable

HAZARD	HAZARD CAUSE	HAZARD EFFECT	SEVERITY LEVEL	SAFETY REQUIREMENT	HAZARD ELIMINATION/CONTROL	VERIFICATION	L OF O
Personnel exposure to large doses of radiation from RTG	(1) Loss of containment due to handling mishap	Personnel fatality	CA	ESMCR 127-1, paragraph 3.9	(1) RTG container will be designed to withstand to maintain its structural integrity for the worst case handling accident.	Analysis & testing	Improbable
					All RTG MGSE handling equipment will be designed and used in accordance with ANSI B30 and ESMCR 127-1, paragraph 3.6.	Proofload testing	Improbable
					All procedures that will be used at ETR or KSC will be validated prior to use.	QA inspection	Improbable
	(2) Loss of containment due to launch abort which results in vehicle breakup	Personnel fatality	CA	ESMCR 127-1, paragraph 3.9	(2) A risk assessment will be performed which will evaluate the probability and consequences of a worst case launch abort scenario.	Analysis & testing	Remote

HAZARD	HAZARD CAUSE	HAZARD EFFECT	SEVERITY LEVEL	SAFETY REQUIREMENT	HAZARD ELIMINATION/CONTROL	VERIFICATION	L OF O
Personnel exposure to large doses of radiation from RTG	Explosion of stage during fueling (Atlas) or explosion of Delta stage (TBD) on the pad	Personnel fatality	CA	ESMCR 127-1, paragraph 3.9	A risk assessment will be performed which will evaluate the probability and consequences of an explosion of the ELV during ground processing.	Analysis & testing	Remote

HAZARD	HAZARD CAUSE	HAZARD EFFECT	SEVERITY LEVEL	SAFETY REQUIREMENT	HAZARD ELIMINATION/CONTROL	VERIFICATION	L OF
Personnel exposure to radiation from RTG during normal ground processing activities	Provisions to control exposure are not instituted	Personnel injury	CR	ESMCR 127-1, paragraphs 3.9.1 & 3.9.2	RTG will be installed into LUTE late in the ground processing.	Inspection of procedures	Remote
					Procedures will be developed incorporating ALARA philosophy and exposure limit will be approved by Radiation Protection Officer.	Inspection of procedures	Remote
					Radiation surveys shall be performed on RTG prior to delivery to ETR	Test	Remote

HAZARD	HAZARD CAUSE	HAZARD EFFECT	SEVERITY LEVEL	SAFETY REQUIREMENT	HAZARD ELIMINATION/CONTROL	VERIFICATION	L OF O
RTG produces enough heat flux to exceed the thermal qualification of flight launch vehicle or lander vehicle propulsion systems	Loss of cooling to RTG during or after vehicle stacking	Explosion results in personnel injury of fatality and/or loss of flight and ground hardware	CA	ESMCR 127-1, paragraph 3.9.1.2	Determine cooling requirements for RTG. An onboard cooling system as required (TBD). Provide a reliable redundant GSE cooling system for RTG for prelaunch.	Analysis & testing Analysis &testing Analysis & testing	Improbable Improbable Improbable

PROJECT: LUTE SUBSYSTEM: CDMS Hazard Report C-1

HAZARD	HAZARD CAUSE	HAZARD EFFECT	SEVERITY LEVEL	SAFETY REQUIREMENT	HAZARD ELIMINATION/CONTROL	VERIFICATION	L OF O
Personnel exposure to hazardous RF levels	(1) Inadvertent operation of RF transmitter during ground processing	Personnel injury (TBD, power density of the RF transmitter is presently undetermined)	CR (TBD)	ESMCR 127-1, paragraph 3.8	(1) Safety inhibits will be provided where necessary to protect personnel during ground processing.	Design analysis	Improbable
	(2) Personnel located too close to emitter	Personnel injury (TBD, power density of the RF transmitter is presently undetermined)	CR (TBD)	ESMCR 127-1, paragraph 3.8	(2) RF equipment will be designed and located to allow test and checkout without presenting a hazard.	Analysis & inspection of operating procedures	Improbable

HAZARD	HAZARD CAUSE	HAZARD EFFECT	SEVERITY LEVEL	SAFETY REQUIREMENT	HAZARD ELIMINATION/CONTROL	VERIFICATION	L OF O
Rupture of GSE pressurized systems (experiment purge or RTG cooling system)	(1) Rupture due to inadequate design margins	Personnel injury or fatality and loss of flight and facility hardware	CA	ESMCR 127-1, paragraph 3.12	(1) All tanks, piping, fittings, and components will use design, fabrication, and testing requirements specified by MIL-STD-1522 and ESMCR 127-1, paragraph 3.12.	Analysis, testing & inspection	Improbable
	(2) Rupture due to failure of pressure regulations	Personnel injury or fatality and loss of flight and facility hardware	CA	ESMCR 127-1, paragraph 3.12	(2) Pressure relief devices will be provided to maintain the system below MOP.	Analysis, testing & inspection	Improbable

HAZARD	HAZARD CAUSE	HAZARD EFFECT	SEVERITY LEVEL	SAFETY REQUIREMENT	HAZARD ELIMINATION/CONTROL	VERIFICATION	L OF O
Collision with ELV fairing and LUTE due to inadvertent tilting or rotation of LUTE deck	(1) Inadvertent command during launch and ground processing	Personnel injury or flight hardware damage	CR	ESMCR 127-1, paragraph 3.14.11	(1) Fault tolerance will be designed into the flight system and EGSE.	Design analysis & testing	Improbable
	(2) Educated short or bent pin in electrical connector	Personnel injury or flight hardware damage	CR		(2) A bent pin in an electrical connector or an educated short will not bypass the fault tolerance used to control this hazard. A post-mate test of electrical connectors will be performed.	Design analysis & testing	Improbable
	(3) Structural failure causes system to tilt at launch	Personnel injury or flight hardware damage	CR	ESMCR 127-1, paragraph 3.3.4.7	(3) Rolling mechanism and actuators will be designed to withstand worst case launch loads.	Analysis and/or testing	Improbable

HAZARD	HAZARD CAUSE	HAZARD EFFECT	SEVERITY LEVEL	SAFETY REQUIREMENT	HAZARD ELIMINATION/CONTROL	VERIFICATION	L OF O
Inadvertent rotation or tilt of LUTE during transportation or lifting operations	(1) Inadvertent command during lifting or transportation	Personnel injury or hardware damage	CR	ESMCR 127-1, paragraph 3.3.4.7	(1) LUTE will be unpowered during lifting or transportation, or fault tolerance will be designed into the system.	Design analysis	Improbable
	(2) Structural failure causes LUTE to tilt or rotate	Personnel injury or hardware damage	CR		(2) LUTE pointing and alignment system will be designed to worst case lifting and transportation loads.	Design analysis	Improbable

APPENDIX P

LUTE RELIABILITY PLAN

NASA
National Aeronautics and
Space Administration

George C. Marshall Space Flight Center
Marshall Space Flight Center, Alabama 35812

June 14,1993

RELIABILITY PLAN

FOR THE

LUNAR ULTRAVIOLET

TELESCOPE EXPERIMENT (LUTE)

Systems Safety and Reliability Office

MSFC - Form 454 (Rev. October 1976)

PAGE 708 INTENTIONALLY BLANK

PRECEDING PAGE BLANK NOT FILMED

RELIABILITY PLAN
FOR THE
LUNAR ULTRAVIOLET
TELESCOPE EXPERIMENT (LUTE)

Prepared By:

Alvin J. Eidson
PRC, Safety and Mission Assurance Mission Services
Reliability and Maintainability

Approved By:

Danny Garcia
Reliability Engineer
Reliability and Maintainability Engineering Office, CT11

Bill Cole
Reliability Engineer
Reliability and Maintainability Engineering Office, CT11

Frank Pizzano
Technical Assistant to the Director
Systems Safety and Reliability Office, CT01

Charles R. Mauldin
Director
Systems Safety and Reliability Office, CT01

TABLE OF CONTENTS

1.0 INTRODUCTION 1
1.1 Purpose 1
1.2 Scope 1

2.0 RELIABILITY PROGRAM MANAGEMENT 1
2.1 Organization and Responsibilities 1
2.2 Reliability Planning and Control 4
2.2.1 Reliability Planning and Status Reporting 4
2.2.2 Reliability Task Control 4
2.2.3 Reliability Training 5
2.2.4 Supplier Control 5
2.2.5 Use of Previously Designed, Fabricated, or Flown Hardware . 5

3.0 RELIABILITY ENGINEERING 6
3.1 General 6
3.2 Design Specifications 6
3.3 Failure Mode and Effects Analyses (FMEA) and Critical Items List (CIL) 9
3.4 Electrical, Electronic, and Electromechanical (EEE) Parts 10
3.5 Problem/Failure Reporting and Correction 10
3.6 Limited Life Items 11
3.7 ALERT System Participation 11
3.8 Review Support 11
3.9 Configuration Control Board Support 12

4.0 TESTING 12
4.1 Reliability Evaluation 12

LIST OF ILLUSTRATIONS

FIGURE 1: NHB 5300.4 (1A-1) CROSS REFERENCE MATRIX 2

FIGURE 2: LUTE S&MA ORGANIZATIONAL INTERFACES 3

FIGURE 3: RELIABILITY ENGINEERING TASK MATRIX 7

FIGURE 4: LUTE RELIABILITY TASK SCHEDULE 8

ABBREVIATIONS AND ACRONYM LIST

ALERT	Acute Launch Emergency Reliability Tip
CCB	Configuration Control Board
CDCR	Critical Design and Cost Review
CDR	Critical Design Review
CIL	Critical Items List
EEE	Electrical, Electronic, and Electromechanical
FMEA	Failure Mode and Effects Analysis
FRR	Flight Readiness Review
GIDEP	Government-Industry Data Exchange Program
LLI	Limited Life Item
LUTE	Lunar Ultraviolet Telescope Experiment
MPRACA	MSFC Problem Reporting and Corrective Action
MSFC	Marshall Space Flight Center
PAR	Performance Assurance Requirements
PAS	Problem Assessment System
PDR	Preliminary Design Review
R&M	Reliability and Maintainability
S&E	Science and Engineering
S&MA	Safety and Mission Assurance
SS&R	Systems Safety and Reliability

DOCUMENT REFERENCE LIST

NHB 5300.4(1A-1)	Reliability Program Requirements for Aeronautical and Space System Contractors
CR 5320.9	Payload and Experiment Failure Mode and Effects Analysis and Critical Items List Groundrules
MMI 5310.2	ALERTs and SAFE-ALERTs - Reporting of NASA parts, Materials, and Safety Problems

RELIABILITY REQUIREMENTS

1.0 INTRODUCTION

1.1 Purpose

This plan shall serve as the implementing directive for management of reliability program activities for the Lunar Ultraviolet Telescope Experiment (LUTE). The activities described herein are structured to reflect the unique nature of the LUTE project in that the hardware will be designed and built in-house by NASA/MSFC.

1.2 Scope

This document is applicable to all LUTE activities conducted in-house by Marshall Space Flight Center (MSFC). This plan was developed in accordance with the requirements given in NHB 5300.4(1A-1), Reliability Program Requirements For Aeronautical And Space System Contractors as tailored for the LUTE program. A cross reference matrix which shows the applicability of NHB 5300.4 (1A-1) paragraphs and the implementing paragraphs of this document is given in figure 1. This document will be updated to reflect reliability concerns of other organizations, as well as program perturbations as they occur and are identified.

2.0 RELIABILITY PROGRAM MANAGEMENT

2.1 Organization and Responsibilities

The efforts required for implementation of the LUTE Reliability Program, as outlined herein, will be accomplished by three organizational units of the Marshall Space Flight Center (MSFC). These units are the Safety and Mission Assurance (S&MA) Office (CR01), the Science and Engineering (S&E) Directorate (EA01), and the Program Development Office (PA01). The heads of these organizations report to the MSFC Center Director (Figure 2).

The LUTE Project Manager reports to the Director of the Program Development Office. The Project Manager is responsible for all LUTE activities including design, development, and test and verification of all LUTE hardware and software, including control of all resources.

FIGURE 1

NHB 5300.4 (1A-1) CROSS REFERENCE MATRIX

NHB 5300.4 (1A-1) PARAGRAPH	APPLICABLE (Y/N)	LUTE RELIABILITY PLAN PARAGRAPH
1A100	N	
1A101	N	
1A102	N	
1A103	N	
1A104	N	
1A105	N	
1A106	N	
1A200 Organization	Y	2.1
1A201 R Program Plan	Y	2.2
1A202 R Program Control	Y	2.2
1A203 R Progress Reporting	Y	2.2.1
1A204 R Training	Y	2.2.3
1A205 Supplier Control	Y	2.2.4
1A206 Previous Hardware Use	Y	2.2.5
1A207 Reliability of GFP	N	
1A300 R Eng. General	Y	3.1
1A301 Design Specs.	Y	3.2
1A302 Standardization	N	
1A303 R Prediction	N	
1A304 FMEA	Y	3.3
1A305 Parts Stress Analysis	Y	3.4
1A306 Worst-Case Analysis	N	
1A307 Trend Analysis	N	
1A308 Special Analysis	N	
1A309 Software Assurance	N	
1A310 Maintainability/Ser.	N	
1A311 EEE Parts	Y	3.4
1A312 Materials & Processes	N	
1A313 EEE Packaging	Y	3.4
1A314 Design Review Prog.	Y	3.8
1A315 Problem Reporting	Y	3.5
1A400 Testing General	N	
1A401 R Evaluation Plan	N	
1A402 Testing	Y	4.0
1A403	N	
1A404	N	
1A405	N	
Limited Life Item Control	Y	3.6
Alert System Part.	Y	3.7

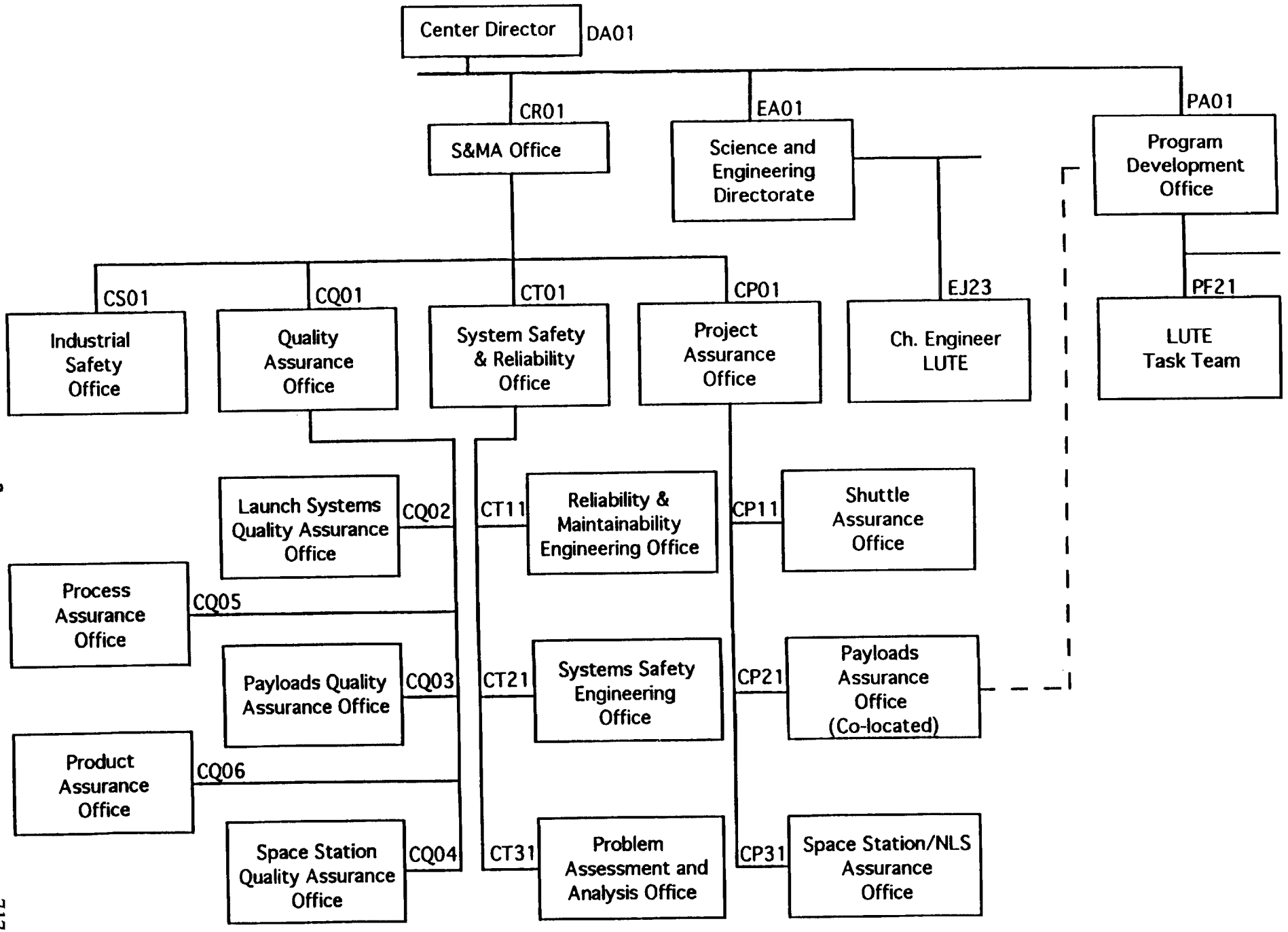

FIGURE 2:
LUTE S&MA ORGANIZATIONAL INTERFACES

The Chief Engineer reports to the Deputy Director for Space Systems, and is responsible for the engineering design, fabrication, assembly, and testing of the hardware. The Chief Engineer is also responsible for developing in-house activities within authorized guidelines, and assuring adequate and appropriate engineering activities across all S&E Laboratories. In addition, he is responsible for establishing and documenting materials, components, workmanship, testing, and reporting criteria for all instruments and hardware developed, consistent with project requirements, MSFC engineering practices, and general experiment resources constraints.

Responsibility for the management of the LUTE Reliability Program shall reside within the S&MA Office. As shown in Figure 2, reliability activities are within the purview of the director of the Systems Safety and Reliability (SS&R) Office (CT01). Within the SS&R Office, the Chief of the Reliability and Maintainability (R&M) Engineering Office (CT11) is responsible for direct oversight of the LUTE Reliability Program tasks. Although the management of the reliability program is organizationally independent from the LUTE Project Office, all reliability program activities shall be closely coordinated with project management through the S&MA representative co-located in the LUTE Project Office. Reliability interfaces with design engineering shall be coordinated with the Chief Engineer and the appropriate element of the S&E Directorate (see Figure 2 for organizational relationship).

2.2 Reliability Planning and Control

2.2.1 Reliability Planning and Status Reporting

The Reliability and Maintainability Engineering Office (CT11) shall be responsible for the development of reliability program requirements, planning and control of reliability tasks, support to project offices, and other programmatic tasks. CT11 is responsible for the development and maintenance of the Reliability Program Plan and supports the co-located S&MA representative with manpower estimates, task schedules, and by performing other programmatic tasks as required, including the preparation of reliability program status reports for presentation at program milestone reviews. CT11 solicits the other SS&R organizations for input as necessary.

2.2.2 Reliability Task Control

Overall responsibility for LUTE Reliability Program tasks rests with the Director of the Systems Safety and Reliability (SS&R) Office. Accountability for the individual reliability tasks described in this plan belongs to the Chief of the SS&R Office (CT11 or CT31) identified as responsible for the task. Office chiefs shall delegate authority for task performance to task lead engineers who shall assure that the task is performed in

accordance with this plan and other applicable requirements. Task lead engineers shall receive support from other MSFC office personnel and contractor personnel assigned to support the R&M Engineering Office as required. Task lead engineers shall report status to office and higher S&MA management periodically; coordinate activities with the LUTE project co-located S&MA representative; and interface with S&E personnel as required.

2.2.3 Reliability Training

The chief of the Reliability and Maintainability Engineering Office (CT11) shall be responsible for assuring that personnel, which are assigned to LUTE reliability tasks, have received proper training.

2.2.4 Supplier Control

The Reliability and Maintainability Engineering Office (CT11) is responsible for coordinating with MSFC offices involved in obtaining LUTE components from suppliers to ensure that these components meet the reliability requirements of the overall LUTE program. This applies to all items obtained from any supplier. CT11 shall provide guidance and controls to assure the adequacy of reliability program controls used by suppliers and that reliability has been integrated into the design. Items obtained from suppliers not required to have a formal reliability program shall be controlled by selected appropriate reliability task requirements.

2.2.5 Use of Previously Designed, Fabricated, or Flown Hardware

Where it is proposed to use previously designed, fabricated, or flown hardware in the LUTE, it shall be verified that the proposed hardware will comply with the reliability requirements of the LUTE program as well as the performance requirements. Where it is considered that such hardware has demonstrated compliance with the reliability requirements of LUTE, substantiating documentation shall be required to be submitted by suppliers or NASA offices , as appropriate. The documents shall:

a. Compare the performance, design, interface, qualification, and test requirement for LUTE (as delineated in other documents related to this procurement) with the corresponding previous requirements. For noncompliance hardware, a problem report shall be written into the Problem Assessment System (PAS) and rationale information including additional testing etc. or a description of what modification will be made to achieve compliance shall be given for closure.

b. Compare reliability requirements for the LUTE with the corresponding previous requirement. For non-compliance, describe what will be done to achieve compliance or provide a rationale and supporting information stating why the non-compliance is considered acceptable. In addition, state

how any modifications proposed will be shown to comply with the reliability requirements of this document.

c. Compare the manufacturing information for the LUTE hardware proposed with that of the previous hardware. As a minimum, this comparison shall include the name and location of the manufacturer, the date of manufacture, and any design, parts or material changes, as well as any modification to packaging techniques, fabrication or assembly processes.

d. Describe all test and flight experience with the proposed LUTE hardware and include a description of all failures or anomalies, their cause, and corrective action taken.

Documentation shall be submitted and updated as applicable.

3.0 RELIABILITY ENGINEERING

3.1 General

Reliability engineering consists of a number of interrelated technical assurance tasks that shall be conducted as an integral part of the LUTE program. These tasks include design definition and review, reliability analysis, interfaces with other assurance activities, control of general design practices, and problem identification, evaluation, correction and prevention. Figure 3 shows the reliability engineering tasks that are to be performed for the LUTE project and the organizational responsibilities for implementation of the tasks.

The reliability engineering tasks outlined herein will be conducted in a manner to assure that the LUTE design complies with the reliability requirements contained in MSFC-RQMT-TBD, "Lunar Ultraviolet Telescope Experiment (LUTE) Project Requirements Document (PRD)." This section elaborates on the reliability task responsibilities and provides details on the implementation approach to be followed. Figure 4 shows the schedule for delivery of reliability engineering task products.

3.2 Design Specifications

MSFC's reliability group, in conjunction with other MSFC groups, shall review for concurrence all design specifications or shall ensure that they are independently reviewed for compliance with reliability requirements prior to their release. This review shall ensure that the set of specifications covers all items of hardware and software at the appropriate levels, that each is complete in its contents, and is functionally and physically consistent with interfacing design specifications and reliability requirements. These reviews shall also

	CT11	CT31	S&E	CQ03	CQ06
Reporting	P	S	-	-	-
FMEA	P	-	S	-	-
CIL	P	-	S	-	S
Reliability Design Specifications	P/S	P/S	S	-	-
Problem/Failure Reporting and Correction	S	P	S	-	S
Limited Life Items List/Status	P	-	S	S	-
Alerts	S	P	S	-	-
Review Support	P	S	-	-	-
CCB Support	P	S	S	-	-
Reliability Testing	P	S	S	-	S
EEE Parts	S	-	P	-	-

P = Primary Responsibility
S = Support Responsibility

Figure 3

Reliability Engineering Task Matrix

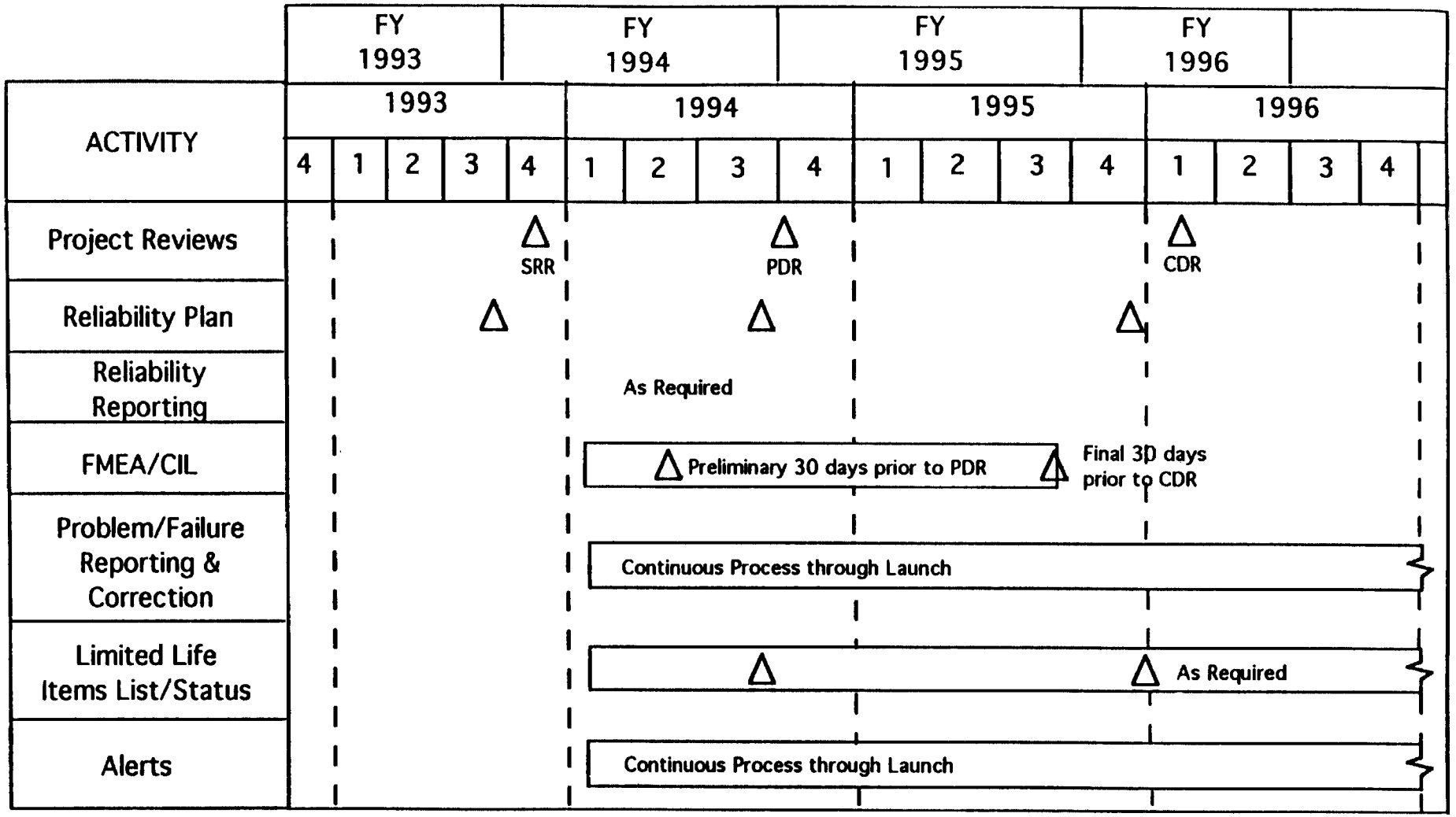

Note: This schedule is preliminary and will be updated when approved program schedules are released.

Legend
△ Submittal

FIGURE 4:
LUTE RELIABILITY TASK SCHEDULE

be conducted whenever individual specifications change. The documentation of design specification reviews shall be included in reliability status reporting.

3.3 Failure Mode and Effects Analyses (FMEA) and Critical Items List (CIL)

As an integral part of the LUTE design phase, an FMEA analysis shall be developed to determine possible modes of failure and their effects on mission objectives and system safety. The primary objective of these analyses shall be to identify critical and catastrophic failure modes to enable removal from the system or control the susceptibility to such failure or their effects. The analyses shall be performed for all LUTE flight hardware, systems interfaces, and critical Ground Support Equipment (GSE) in accordance with MSFC CR 5320.9 "Payload and Experiment Failure Mode and Effects Analysis/Critical Items List Groundrules."

Based on the results of the FMEA, a Critical Items List (CIL) shall be developed in accordance with CR 5320.9. The CIL will identify and bring to management's attention all single failure points and areas which do not meet the programs failure tolerance requirements. The CIL items that remain in the design as risks shall contain risk retention rational as to why the risk is acceptable.

The FMEA/CIL shall be performed in a timely manner to facilitate prompt action by design organizations and project management. The findings shall be a major consideration in design and management reviews and will provide criteria and data for other types of analysis including design improvements, testing, operations, and analyses of mission risks.

Important applications include:

a. Determining need for redundancy, fail-safe design features, and/or further derating.

b. Supporting LUTE systems safety analyses and hazard analyses.

c. Supporting establishment of safety requirements in testing and operations.

d. Assuring that the test program is responsive to known and suspected potential failure modes.

e. Supporting studies to establish tradeoffs of reliability versus performance, weight and cost.

f. Establishing frequency of monitoring in testing, checkouts, and mission use.

g. Supporting mission operations activities such as designing fault isolation sequences and alternate-mode-of-operation planning.

h. Supporting establishment of quality assurance requirements for determining mandatory inspection points for critical items during manufacturing and hardware acceptance.

The Reliability and Maintainability Engineering Office (CT11) shall be responsible for conducting the FMEA/CIL analysis with support from the Product Assurance Office (CQ06) and the appropriate elements of the S&E Directorate as required.

3.4 Electrical, Electronic, and Electromechanical (EEE) Parts

The Electrical, Electronic, and Electromechanical Parts Branch (EB13) shall be responsible for all EEE parts control activities on the LUTE program. These activities shall include review of parts selection, Screening and qualification criteria, parts stress analysis, EEE packaging, and other efforts as required to assure conformance with LUTE program requirements.

3.5 Problem/Failure Reporting and Correction

A closed loop problem reporting and corrective action system will be implemented by the Problem Assessment and Analysis Office (CT31) as part of the reliability program. The purpose of this system will be to ensure adequate remedial and recurrence prevention action for actual and suspected functional nonconformances/failures having safety or mission success implications. Formal problem reporting will begin with Acceptance Test Procedures; however, problems at qualification or requalification of previously flown or used hardware shall also be reported. The LUTE problem/failure reporting and correction process shall utilize the MSFC Problem Reporting and Corrective Action (MPRACA) system.

The MPRACA report provides input to the closed-loop problem reporting and corrective action system. Reports will be completed for all problem/failure incidents encountered in the LUTE program. The project office and the Product Assurance Office (CQ06) are responsible for initiating and submitting the report to S&MA for input into the MPRACA system. The report form documents the date, time, and other pertinent information of the problem/failure incidents, provides ample room to discuss any pertinent information, analyzes the nature and cause of the incident, assesses failure criticality, and identifies any corrective action. The closed-loop reporting system is designed to enhance problem status tracking, ensure timely problem closure action, ensure adequate problem recurrence control, and ensure that reports are provided to management for program monitoring and audit.

The LUTE Failure Analysis Review Board (FARB) will review all MPRACA reports

for adequate close-out. The purpose of the FARB is to evaluate the adequacy and timeliness of analyses, proposed corrective actions for all reports assigned for analysis, and review for concurrence of disposition those events not requiring in-depth analysis.

3.6 Limited Life Items (LLI)

The Reliability and Maintainability Engineering Office (CT11) with support from the Payloads Quality Assurance Office (CQ03) shall be responsible for coordinating the development and maintenance of a limited life items list. This list will be developed in cooperation with the appropriate elements of the Science and Engineering Directorate. The list will identify all hardware that is subject to degradation because of age, operating time, or cycles, and will identify the service limiting parameters. CT11 with support from CQ03 and S&E will provide status reports, to be submitted at milestone reviews, which will include life limits, usage to date, and time remaining for each item.

3.7 ALERT System Participation

Problems with parts, materials, equipment, or diminishing sources of supply will be reported through the GIDEP ALERT System. MSFC participation in GIDEP is as required by MMI 5310.2D.

As required by MMI 5310.2D, upon receipt of an ALERT from GIDEP, CT31 sends a copy to the LUTE project ALERT actionee, appointed by the Project Manager. The Project ALERT actionee is responsible for determining whether or not the ALERT impacts LUTE hardware. The LUTE project co-located S&MA representative is responsible for monitoring the status of the ALERT and assuring that the ALERT impact is determined and closure is expedited. If it is determined that there is an impact to LUTE hardware, the extent of the impact will be determined and project management will be informed. A statement of ALERT status is provided to CT31, regardless of impact, in order to close the ALERT.

ALERTs are due as generated. Responses to ALERTs are due 10 working days after receipt of the ALERT. Status summaries covering each applicable ALERT or notice will be included at milestone reviews.

3.8 Review Support

The Payloads Assurance Office (CP21) shall have the primary responsibility for representing reliability at all project status, program, requirements, design, and flight readiness reviews. The Reliability and Maintainability Engineering Office (CT11) and the Problem Assessment and Analysis Office (CT31) will provide the status of the various reliability tasks, as detailed in this plan, to the CP21 representative for presentation at these reviews. Assistance will be provided to these reviews by the Payloads Quality

Assurance Office (CQ03) who will assist in providing limited life item data and the Product Assurance Office (CQ06) who will assist in providing CIL retention rationale.

3.9 Configuration Control Board Support

The Payloads Assurance Office (CP21) shall provide a representative to the project manager's Configuration Control Board (CCB). CT11 will review all documents submitted to the CCB for reliability impact, will coordinate the reviews within S&MA as required, and will provide inputs to CP21 to support CCB meetings.

4.0 TESTING

4.1 Reliability Evaluation

Reliability will participate in the test programs to ensure achievement of reliability objectives and requirements. Specifically, Reliability will provide inputs to test planning; and monitor/review/assess test results to assure that:

1. Specification reliability requirements are verified by test, where applicable.

2. Environmental test levels for critical items reflect the design specifications, and results support the rationale for retention documented in the CIL.

3. Functional tests sufficiently verify operability of critical circuits, mechanisms, etc. based on the critical failure modes/causes shown in the FMEA/CIL.

4. Any exceedance of specification limits are evaluated for impact on operational usage of the component/system.

5. Failures are assessed for possible trends, recurrence prevention actions initiated where appropriate, and any impacts on the FMEA/CIL identified. Reliability assessments of failures will be reflected in the CIL, as applicable.

APPENDIX Q

LUTE INTEGRATED PROGRAM PLAN FINAL REPORT

System Studies & Simulation
4717 University Drive, Suite 100
Huntsville, Alabama 35816
Telephone: (205) 837-3999
Telefax: (205) 837-3939

LUTE Integrated Project Management Network

Addendum To: Lunar Ultraviolet Telescope Experiment (LUTE) Integrated Program Plan Final Report

8/3/93

prepared by

Ms. Janice F. Smith,
System Studies and Simulation, Inc.

and

Mr. Larry Forrest,
John M. Cockerham & Associates, Inc.

prepared for

LUTE Project Office
Marshall Space Flight Center,
National Aeronautics and Space Administration

S3 Report Number: 5307-00-9307-S

Preface

This document is an addendum to the final report delivered under delivery order H-20750D, "Lunar Ultraviolet Telescope Experiment (LUTE) Integrated Program Plan" for the NASA Marshall Space Flight Center (MSFC). The work was performed by Systems Studies and Simulation, Inc. in conjunction with John M. Cockerham & Associates, Inc. (JMCA). All opinions expressed in this report are solely those of the authors and should not necessarily be interpreted as the positions or views of NASA.

Table of Contents

	Preface	2
Section 1.	Introduction	3
Section 2.	Risk Management and Network Simulations	4
	Benefits of Risk Management	4
	Benefits of Network Simulations	5
Section 3.	Risk Management for the LUTE Project Office	6
	Significance of the LUTE Integrated Network Chart	6
	RISNET Probabilistic Operation and Capabilities	8
	RISNET Graph and Display	8
	Network Data Collection	8
	Understanding the LUTE Network Chart	9
	Additional RISPLOT Capabilities	10
Section 4.	Conclusion	11

Section 1. Introduction

This addendum describes the integrated project management network developed for the Lunar Ultraviolet Telescope Experiment (LUTE) Project Office and supplements the final report for the task under which the network was developed[1]. The LUTE integrated project management network charts were designed to provide LUTE project managers with a frame work for strategic planning and risk management throughout the life of the project. The charts were created to assist managers in developing an integrated plan of project activities, and to graphically display the plan as an integrated network that shows the project activities, all critical interfaces, and schedules. The documents presents

- The benefits of Risk Management and network simulations (Section 2),
- The Risk Management process performed for LUTE and describes the LUTE integrated project management network charts (Section 3), and
- Conclusions regarding extensions of the network analysis (Section 4).

---

[1] See the following report:
"Lunar Ultraviolet Telescope Experiment (LUTE) Integrated Project Plan - Final Report", System Studies and Simulation, 5307-00-9307-F, 13 July 1993

Benefits of Risk Management

Traditional project management is reactive. After award of the prime contract, planning virtually stops. Tracking and control the project becomes paramount. As problems occur, management reacts. Change is resisted at all levels and change only occurs after there has been program breakage. The decision process is reactive. Planning is inflexible and program uncertainties are intuitively addressed, if at all.

Risk Management is a new and revolutionary management concept. It is a proactive process of decision analysis and planning. It is continuous. As a project plan is being executed, the plan is continually challenged and improved through the process of Risk Management. The process incorporates the knowledge of project uncertainties and risks into strategic planning. Risk Management is predictive and deals with management strategies to avoid or reduce the impact of problems yet to occur.

Risk Management uses the program knowledge as it is generated to challenge the plans and change what needs to be changed. Risk management embraces change as a means to continually revitalize a program through cost and risk reduction. Risk management methods allow the project manager to:

A. Identify and track performance and programmatic uncertainties;
B. Identify problems and potential problems;
C. Quantify uncertainties and problems in terms of the likelihood of program impact and the magnitude of the impact;
D. Quantify, classify, track and update performance and programmatic risks;
E. Develop and maintain strategic level networks of integrated activities, schedules, costs and risks;
F. Develop Risk Mitigation options;
G. Conduct performance, cost, schedule and risk trade studies for research, development and production alternatives;
H. Perform "What-if" analyses; and
I. Restructure projects due to budgetary changes

Probabilistic network simulation is one of the most valuable tools available for the support of Risk Management. The Risk Information System and Network Evaluation Technique (RISNET) simulation is such a tool. It was the first widely used and accepted model on the market. RISNET has 18 years of application experience and has been used on many hundreds of projects. Over the years RISNET has been continually improved and updated to meet the requirements of Risk Management. RISNET is engineered for management to understand and the for analyst to use. The key benefits of RISNET are listed below.

Key RISNET Benefits

A. The network display allows management to easily see and understand their project.
B. The network and other displays provide a means for management to communicate with the risk analysts.
C. The model allows for traditional (deterministic) planning to begin the planning process and probabilistic information to be later added.
D. It is a cost estimating model and a cost risk model.
E. It is an integrated cost, schedule and risk model. (i.e. changes to the cost, schedule or risk in one part model will predict the effects in areas of the model).
D. Once developed the network simulation model can inexpensively operated for what-if analyses, problem solving, and program perturbations.
E. The model allows rapid replanning of budgetary resources.
F. The model automatically plans contingency funds for risk.
G. RISNET helps avoids the sub-optimization of resources, i.e. where one manager may be expediting his program activity through the expenditure of additional resources when there is no probable benefit to the overall project.

Section 3. Risk Management for the LUTE Project Office

The following discussion concerns the initial risk management planning effort for the LUTE project office. This effort was directed toward the development of the initial deterministic network model and the network chart display.

Significance of the LUTE Integrated Network Chart

In order to appreciate the meaning, utility, and limitations of the network chart, one must understand the place the RISNET tool occupies in project management. Project management takes place at two levels: the control level where daily progress is monitored and people react to problems as they occur, and the strategic level where the manager attempts to foresee problems before they occur and to determine the effects current problems will have on activities not yet initiated. RISNET assists the project manager in planning at the strategic level, and in risk management.

The LUTE network chart represents the initial step in developing an optimized, time-phased structure of LUTE project activities. It is a snapshot of the current level of planning within the project, which at this point (LUTE Phase A) is comparatively low. The LUTE network currently consists of a group of high level activities representing a level-of-effort expenditure of resources. The planning effort has not evolved to the point of a baseline plan. The baseline plan is the initial goal of the next LUTE phase and will include the flow of program decisions, significant accomplishments, the interrelationship between program activities and the time phased program costs.

Because the network is a visual display, one can easily see how the project flows from start to finish. The activities are color coded using the major Work Breakdown Structure (WBS) level codes. The purpose is to enable the manager to quickly see the location of activities with the same WBS code within the network. A legend is displayed on the chart which matches the WBS codes with each color. Management can easily see all decision points within the project elements and interactions between the elements. The more important milestones are annotated. Because the total float and free float[2] are displayed, the manager can see which activities can be delayed or accelerated, if need be.

---

2 Total float is the amount of time the start of an activity may be delayed without impacting the project end date. Free float is the amount of time the start of an activity may be delayed without impacting the successor activity.

RISNET Probabilistic Operation and Capabilities

RISNET is a probabilistic network analyzer which addresses both the cost and schedule uncertainties of a project. RISNET can generate baseline budget estimates for budget preparation, perform "what-if" exercises, sensitivity studies, and cost estimates. It can conduct cost and schedule assessments, produce trade-off studies and predict the impact of program risks and help evaluate risk mitigation alternatives.

RISNET functions by performing a Monte Carlo simulation to evaluate the characteristics of a network. The network can be simulated deterministically (fixed conditions) or probabilistically (with uncertainties). A deterministic simulation performs one iteration to determine the most probable critical path, baseline budget estimate, and/or program cost to identify milestones. It is used to calibrate the network. Calibrate means to ensure that no logic errors exist and that milestones occur in the network as scheduled. This calibrated network is often referred to as the baseline network against which all future networks are evolved. A probabilistic simulation performs multiple iterations using Monte Carlo techniques to determine time and cost probability distributions for selected program milestones, critical path families, and arc criticality summaries.

RISNET Graph and Display

RISNET uses the results of a network simulation to generate a variety of reports and graphs for display either on a terminal or output to a printer or graphics plotter. The time-phased network chart of the integrated program activities is produced by the graphics package RISPLOT.

The time-phased network is produced in three phases. The first phase yields a deterministic network that serves as a baseline for the project. In the second phase, node logic and schedule uncertainties are added. Finally, fixed and variable costs and cost uncertainties are added to each activity.

Network Data Collection

The key to accurate risk assessment using RISNET is the construction of a logically related interactive activity network. The network is used to create a database that the model can analyze deterministically and statistically.

The first step is to examine all available program information to determine what are the individual activities that make up a program and what are their interrelationships. Toward that end, the key personnel in all of the major LUTE technical areas were interviewed. The interviews focused on obtaining information on activities to be performed in a given technical area for all phases of the LUTE project up to launch, the scheduling of the activities, and their estimated durations. In addition, the analysts studied program plans, schedules, and work breakdown structures.

The following is a list of the LUTE Project key technical personnel who were interviewed to provide the network data:

NASA Personnel	*Topic*	*Telephone Number*
Robert McBrayer	Overall Program	(205) 544-1926
Max Nein	Overall Program	(205) 544-0619
John Frazier	Overall Program	(205) 544-1953
Jason Porter	Science Requirements	(205) 544-7607
Tim Baldridge	CCD and Electronics	(205) 544-5314
William Jones	Optics and FPA	(205) 544-3479
Sherry Walker	Thermal Analysis and Control	(205) 544-0501
Reggie Alexander	Thermal Analysis and Control	(205) 544-9289
Paul Luz	Structures	(205) 544-0512
Terrie Rice	Materials and Processes	(205) 544-4549
Connie Carrington	Pointing and Control	(205) 544-4869
Don Williams	Electrical Power - RTG	(205) 544-0491
Harold Blevins	Communications and Data Handling	(205) 544-0492
James Hilliard	Software	(205) 544-3739
Tom Dickson	Lander	(205) 544-0530
Tim Kauffman	Systems Engineering	(205) 544-4079
Keith Robinson	Operations	(205) 544-2054
James McCarter	Mission Planning and Lunar Environment	(205) 544-0536
Mark Gerry	Layouts - Configuration Status	(205) 544-0510
Andrew Prince	Cost Estimation	(205) 544-8360
Edward Trentham	Mission Assurance	(205) 544-0667
Michael Galuska	Safety	(205) 544-3743

The time-phased network chart network uses activity-on-arrow nomenclature. That is, activities are described on arrows (lines) connected between nodes or milestones. Each node is represented as a small box. The user has the option to display the node identifier within each box. The red diamonds drawn over some of the node boxes indicate milestones that are scheduled to occur at that time. The length of each solid portion of the activity line corresponds to its duration. If the activity is on the critical path, a double line is drawn; otherwise, a single line is used. A critical path describes the activities for which there is no slack time available. If the activity is non-critical, free float is represented as a dashed line appended to the solid line. The activity description consists of three parts: a unique activity identifier, a verbal description, and an optional WBS code. The WBS code may be up to ten characters long. The activity duration and total float is shown below the activity line with the mnemonic codes of T and F respectively. Activity duration (T) and total float (F) are recorded in days. When an activity is continuous, T is set equal to C on the chart. If there is not enough room to write the entire activity description on the line, then at least the activity number is written, and the entire description is added to the overflow table located at the bottom of the network. Figure 1 illustrates the network layout.

Figure 1. Network Chart Layout

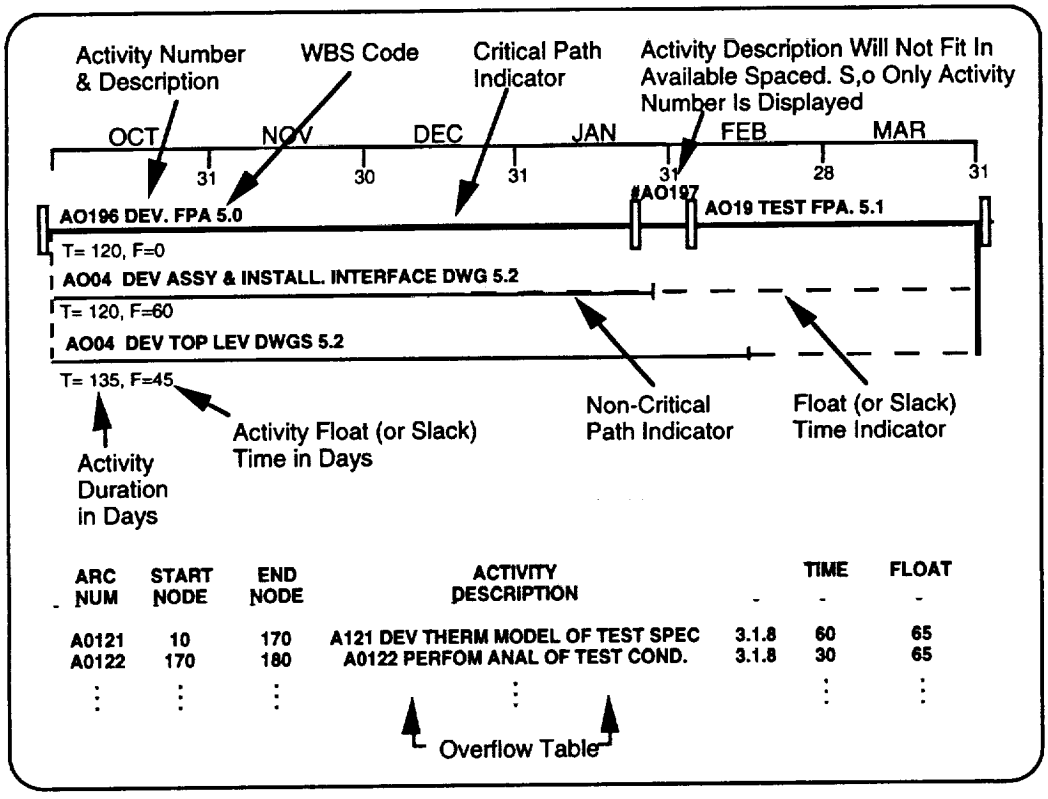

For this network the color coding scheme is as follows:

Color Code	*Activity*
Red	Systems Engineering
Blue	Project Management
Green	Software
Cyan	Mission Operations
Magenta	Ground Support
Orange	Telescope
Violet	Test

Additional RISPLOT Capabilities

RISNET can display the network in four different formats: deterministic plot, network logic plot, family of critical paths plot, and Gantt charts. A deterministic plot displays the most probable shape of the network based on the node logic. Furthermore, the deterministic plot may be displayed as a window (time slice) plot or as a zoned plot. A zoned plot is a sorted plot that has each element plotted in its own horizontal area of the plot page without any logic interfaces to other related activities. A network logic plot is a time-phased logic plot in which the node logic, except the and/all rule, is plotted above each node. A family of critical paths plot shows all of the activities determined to be critical during at least one iteration of the probabilistic simulation. Currently there is insufficient planning information to support these graphics for the LUTE Project.

Section 4. Conclusion

The LUTE network chart communicates the current program plan of future activities to the people responsible for making decisions. The activities describing the LUTE Project need to be defined in more detail and in terms of decisions and significant accomplishments.

Risk Management is an iterative and intellectual planning process that is enhanced by the use of the RISNET tool. The network chart is not an end unto itself. The network chart is simply a manifestation of the planning effort and status. The effort to accumulate the network activity information is beneficial in forcing the project members to plan more thoroughly. Many problems are resolved in advance of their occurrence and there is consideration given to new ideas and alternatives that may otherwise have been overlooked.

If implemented for the LUTE Project, Risk Management will be used to continually assess critical program areas for the purpose of reducing or eliminating cost, schedule and performance risks.

LUNAR U/V TELESCOPE EXPERIMENT ROBERT McBRAYER

ARC NO.	DESCRIPTION	CODE	EARLY START	EARLY FINISH	DAYS DUR.
A0004	DEV ASSY & INSTALL INTERFACE DMGS (P)	1.2	10CT93	29MAR94	180.0
A0005	DEV PRELIM GENERATION BREAKDOWN (P)	1.2	10CT93	29MAR94	180.0
A0006	DEV PRELIM CABLE INTERCONNEC DIA. (P)	1.2	10CT93	29MAR94	180.0
A0007	DEV PRELIM LMDR/LMCH VEH I/F AGRMNT (P)	1.2	10CT93	31JAN94	123.0
A0019	DEV PRELIM SYSTEM SCHEMATICS (P)	1.2	10CT93	29MAR94	180.0
A0022	DEV PRELIM CONFIG CONTROL PLAN (P)	1.2	10CT93	29MAR94	180.0
A0151	DEV TOP LEVEL DRAWINGS	1.2	10CT93	30SEP94	365.0
A0183	DEV PRELIM PCA	1.3	10CT93	31JAN94	123.0
A0193	PROVIDE ADMIN SUPPORT	1.6	10CT93	24SEP98	1820.0
A0194	PROVIDE PROCUREMENT MANAGEMENT	1.4	10CT93	24SEP98	1820.0
A0247	PROJECT MANAGEMENT	1.0	10CT93	24SEP98	1820.0
A0253	DEV MISSION NEED STATEMENT	1.0	10CT93	30NOV93	61.0
A0025	UPDATE ASSY & INSTALL INTERFACE DMGS (U)	1.2	10CT94	29MAR95	180.0
A0026	UPDATE GENERATION BREAKDOWN (U)	1.2	10CT94	29MAR95	180.0
A0027	UPDATE CABLE INTERCONNECTION DIA. (U)	1.2	10CT94	29MAR95	180.0
A0028	UPDATE LANDER INTERFACE AGREEMENT (U)	1.2	10CT94	29MAR95	180.0
A0041	UPDATE SYSTEM SCHEMATICS (U)	1.2	10CT94	29MAR95	180.0
A0152	DEV DETAILED DESIGN DRAWINGS	1.2	10CT94	30SEP95	365.0
A0186	PREP FOR NON-ADVOCACY REVIEW	1.0	10CT94	29MAR95	180.0
A0189	DEV PRELIM GSE RQMTS	1.5	10CT94	30SEP95	365.0
A0242	BASELINE CONFIGURATION CONTROL PLAN (B)	1.2	10CT94	29MAR95	180.0
A0248	PRR	1.0	10CT94	10CT94	.0
A0187	DEV PROJECT PLAN	1.0	30MAR95	28MAY95	60.0
A0188	DEV FINAL PCA	1.3	29MAY95	30SEP95	125.0
A0153	DEV DETAILED MANUFACTURING DRAWINGS	1.2	10CT95	29SEP96	365.0
A0195	PROVIDE CONFIGURATION MANAGEMENT	1.2	10CT95	24SEP98	1090.0
A0217	BASELINE ASSY & INSTALLATION DMGS (B)	1.2	10CT95	29SEP96	365.0
A0218	BASELINE GENERATION BREAKDOWN (B)	1.2	10CT95	29SEP96	365.0
A0219	BASELINE CABLE INTERCON. DIA. (B)	1.2	10CT95	28MAR96	180.0
A0220	BASELINE LANDER I/F AGREEMENT (B)	1.2	10CT95	28MAR96	180.0
A0229	BASELINE SYSTEM SCHEMATICS (B)	1.2	10CT95	28MAR96	180.0
A0249	PDR	1.0	10CT95	10CT95	.0
A0073	ACQUIRE OPS CNTR FACILITY	1.4	30SEP96	28MAR98	545.0
A0250	CDR	1.0	30SEP96	30SEP96	.0
A0251	FLT & GND OPS RR	1.0	30SEP97	30SEP97	.0
A0252	IRR	1.0	27JUN98	27JUN98	.0
A0012	DEV PRELIM MASS STATUS REPORT (P)	2.1.5	10CT93	29MAR94	180.0
A0137	DEV PRELIM QUALITY ASSURANCE PLAN (P)	2.4	10CT93	30SEP94	365.0
A0140	DEV PRELIM SAFETY PLAN (P)	2.4.1	10CT93	30SEP94	365.0
A0141	DEVELOP MSL SYS PRELAUNCH SAFETY PKG	2.4.1	10CT93	30SEP95	730.0
A0144	DEV PRELIM HAZARD ANALYSIS FOR P/L (P)	2.4.1	10CT93	30SEP95	730.0
A0147	PROVIDE RTG PSAR SUPPORT	2.4.1	10CT93	30SEP95	730.0
A0171	DEV PRELIM RELIABILITY PLAN	2.4.1	10CT93	30SEP94	365.0
A0174	DEV PRELIM FMEA/CIL	2.4.1	10CT93	30SEP94	365.0

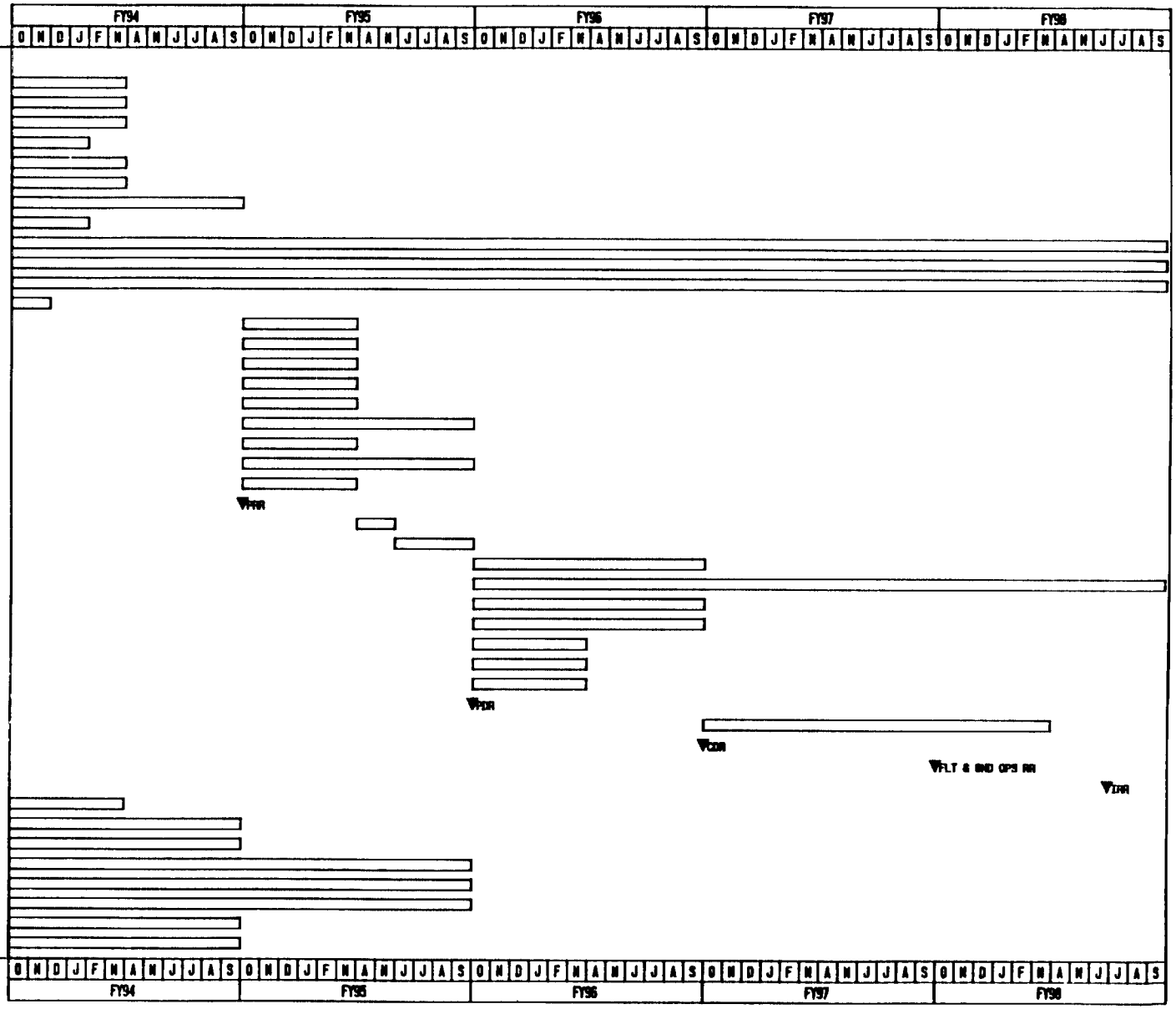

Plot Date: 09/20/93 Run Date: 09/08/93 Page 1: 5

LUNAR U/V TELESCOPE EXPERIMENT ROBERT McBRAYER

ARC NO.	DESCRIPTION	CODE	EARLY START	EARLY FINISH	DAYS DUR.
A0176	DEV LIMITED LIFE ITEMS LIST	2.4.1	10CT93	30SEP94	365.0
A0244	DEV PRELIM ENV MEASURE SYS ANALYSES (P)	2.1.6	10CT93	29MAR94	180.0
A0033	UPDATE MASS STATUS REPORT (U)	2.1.5	10CT94	29MAR95	180.0
A0036	DEV PRELIM MATERIALS USAGE LIST (P)	2.4	10CT94	29MAR95	180.0
A0038	UPDATE HAZARD ANALYSES FOR PAYLOAD (U)	2.4.1	10CT94	29MAR95	180.0
A0046	DEV HARDWARE TEST PLANS	2.3	10CT94	29MAR95	180.0
A0130	UPDATE QUALITY ASSURANCE PLAN (U)	2.4	10CT94	30SEP95	365.0
A0172	UPDATE RELIABILITY PLAN	2.4.1	10CT94	30SEP95	365.0
A0175	UPDATE FMEA/CIL	2.4.1	10CT94	30SEP95	365.0
A0177	UPDATE LIMITED LIFE ITEMS LIST	2.4.1	10CT94	30SEP95	365.0
A0185	DEV TEST VERIF/VALIDATION PLANS	2.3	10CT94	30SEP95	365.0
A0226	UPDATE SAFETY PLAN (U)	2.4.1	10CT94	30SEP95	365.0
A0243	DELAY	2.3	10CT94	29JUN95	272.0
A0245	BASELINE ENV MEASURE SYS ANALYSES (B)	2.1.6	10CT94	29MAR95	180.0
A0049	DEV PRELIM PAYLOAD VERIFICATION PLAN (P)	2.3	30JUN95	31JAN96	216.0
A0055	UPDATE HARDWARE TEST PLANS	2.3	10CT95	28MAR96	180.0
A0138	BASELINE QUALITY ASSURANCE PLAN (B)	2.4	10CT95	29SEP96	365.0
A0142	UPDATE NSPSP	2.4.1	10CT95	29SEP96	365.0
A0145	BASELINE HAZARD ANALYSIS FOR PAYLOAD (B)	2.4.1	10CT95	28MAR96	180.0
A0148	PROVIDE RTG USAR SUPPORT	2.4.1	10CT95	29SEP96	365.0
A0173	UPDATE RELIABILITY PLAN	2.4.1	10CT95	29SEP96	365.0
A0222	BASELINE MASS STATUS REPORT (U)	2.1.5	10CT95	28MAR96	180.0
A0225	BASELINE MATERIALS USAGE LIST (B)	2.4	10CT95	28MAR96	180.0
A0227	BASELINE SAFETY PLAN	2.4.1	10CT95	29SEP96	365.0
A0228	BASELINE PAYLOAD VERIFICATION PLAN (B)	2.3	10CT95	28MAR96	180.0
A0143	UPDATE NSPSP	2.4.1	30SEP96	26JUN98	635.0
A0146	UPDATE HAZARD ANALYSIS	2.4.1	30SEP96	26JUN98	635.0
A0149	PROVIDE RTG FSAR SUPPORT	2.4.1	30SEP96	29SEP97	365.0
A0072	DEV COMM INTERFACE TEST PLANS	2.3	30SEP97	26JUN98	270.0
A0150	PROVIDE RTG NSRP SUPPORT	2.4.1	30SEP97	26JUN98	270.0
A0067	LUTE SYSTEM INTEGRATION	2.2	27JUN98	24SEP98	90.0
A0008	DEV THERMAL TEST PLAN FOR SPECIMEN	3.1.8	10CT93	30OCT93	30.0
A0009	DEV PRELIM POWER SYSTEMS ANALYSES (P)	3.1.6	10CT93	29MAR94	180.0
A0013	DEV PRELIM STRUCTURES ANALYSES (P)	3.1.4	10CT93	29MAR94	180.0
A0015	DEV PRELIM OPTICAL/FPA SYS ANALYSES (P)	3.1.1	10CT93	29MAR94	180.0
A0020	DEV PRELIM DETECTOR ANALYSES (P)	3.1.3	10CT93	29MAR94	180.0
A0111	DEV RTG FUNC RQMTS	3.1.6	10CT93	29MAR94	180.0
A0120	DESIGN LIGHT BAFFLES	3.1.4.6	10CT93	29MAR94	180.0
A0121	DEV THERMAL MODEL OF TEST SPECIMEN	3.1.8	10CT93	29NOV93	60.0
A0127	PERF DETECTOR THERMAL CTL TRADE STUDIES	3.1.8	10CT93	29MAR94	180.0
A0129	PERF ELEC BOX THERMAL CTL TRADE STUDIES	3.1.8	10CT93	29DEC93	90.0
A0134	VERIFY DETECTOR THERMAL RQMTS	3.1.8	10CT93	29MAR94	180.0
A0135	VERIFY ELEC THERMAL RQMTS	3.1.8	10CT93	27FEB94	150.0
A0154	CHARACTERIZE VIBRATION DISTURBANCES	3.1.9	10CT93	30SEP94	365.0

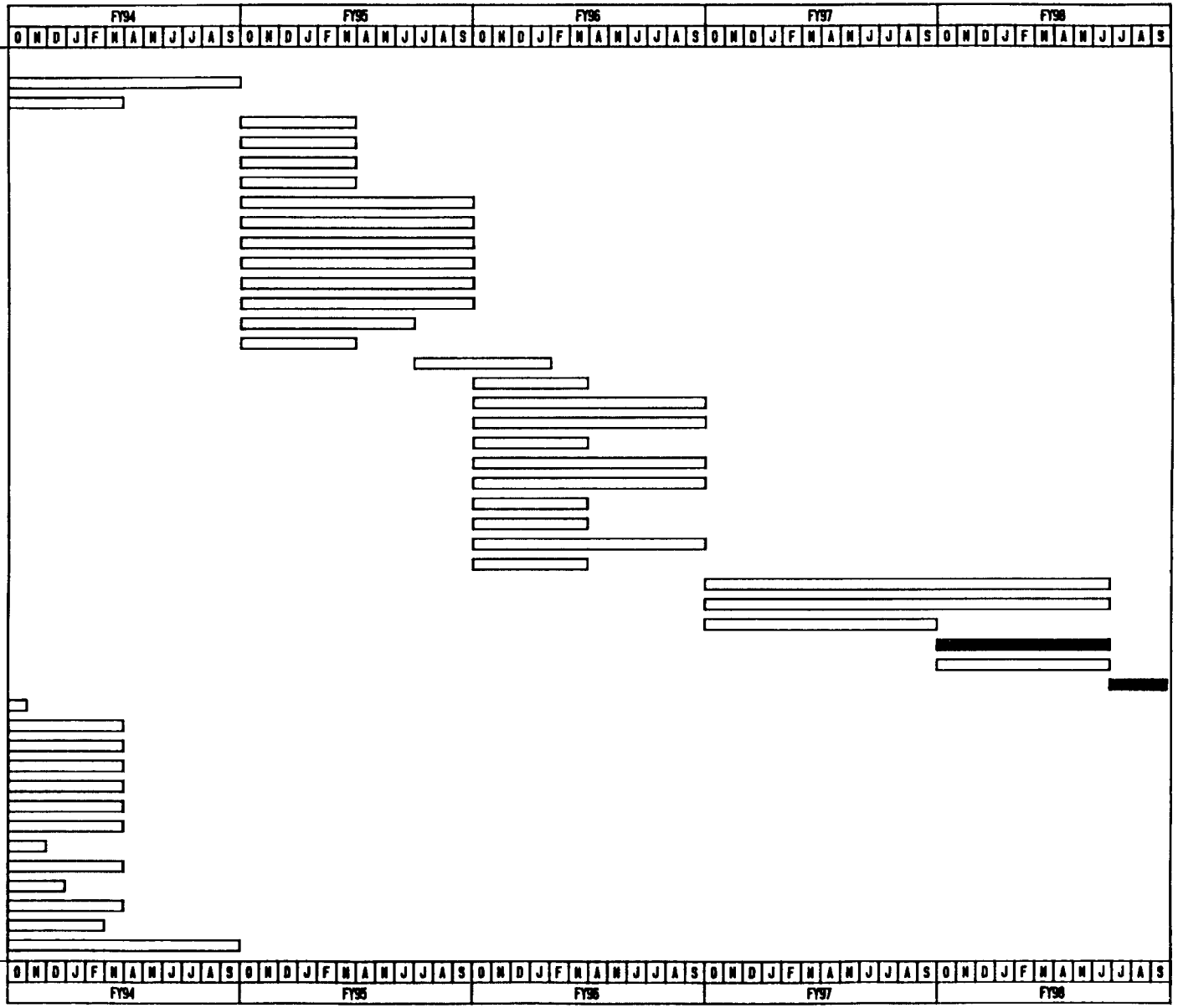

Plot Date: 09/28/93 Run Date: 09/08/93 Page 2: 5

LUNAR U/V TELESCOPE EXPERIMENT ROBERT McBRAYER

ARC NO.	DESCRIPTION	CODE	EARLY START	EARLY FINISH	DAYS DUR.
A0158	ID VIBRATION ISOLATION SYS & RQMTS	3.1.9	10CT93	30SEP94	365.0
A0160	ID RQMTS FOR 2ND MIRROR ACTUATION SYS	3.1.9	10CT93	30SEP94	365.0
A0162	DETERMINE C&DH REDUNDANCY RQMTS	3.1.7	10CT93	30SEP94	365.0
A0163	DETERMINE TRANSMISSION LINKS RQMTS	3.1.7	10CT93	30SEP94	365.0
A0164	DETERMINE DATA FORMAT RQMTS	3.1.7	10CT93	30SEP94	365.0
A0165	DETERMINE C&DH POWER RQMTS	3.1.7	10CT93	30SEP94	365.0
A0166	REFINE TRANSMIT/DATA HANDLING EQUIP LIST	3.1.7	10CT93	30SEP94	365.0
A0167	ID ELECTRONICS THERMAL STABILITY ISSUES	3.1.7	10CT93	30SEP94	365.0
A0168	DET COMM & COMPUT COMPAT W/GSC MECHANISM	3.1.7	10CT93	30SEP94	365.0
A0169	DET LOCATION & ANT OF COMM & COMP EQUIP	3.1.7	10CT93	30SEP94	365.0
A0178	ANALYZE ANTENNAE SUPPORT STRUCTURE	3.1.4.9	10CT93	30SEP94	365.0
A0179	REFINE DESIGN OF ELEC SPT STRUCTURE	3.1.4.10	10CT93	30SEP94	365.0
A0180	UPDATE LNCHER & LANDER INTER LOADS/DSGNS	3.1.4	10CT93	30SEP94	365.0
A0181	REFINE OPTICAL STRUCTURE MODELS	3.1.4	10CT93	30SEP94	365.0
A0182	DEV CONTAMINATION PLAN	3.1.4	10CT93	29MAR94	180.0
A0245	DELAY	3.1.4.11	10CT93	31DEC93	92.0
A0122	PERFORM ANALYSIS OF TEST CONDITIONS	3.1.8	30NOV93	29DEC93	30.0
A0123	SUPPORT THERMAL TESTS	3.1.8	30DEC93	29MAR94	90.0
A0125	PERF THERMAL CTL/OPTICAL SYS TRADES	3.1.8	30DEC93	27JUN94	180.0
A0138	PERF THERMAL CTL ELEC BOX ANALYSES	3.1.8	30DEC93	28JAN94	30.0
A0119	DETERMINE SUN SHADE CHARACTERISTICS	3.1.4.11	1JAN94	29MAR94	88.0
A0131	PERF THERMAL CTL DETECTOR ANALYSES	3.1.8	29JAN94	27FEB94	30.0
A0132	PERF THERMAL CTL OPTICAL SYS ANALYSES	3.1.8	28FEB94	28APR94	60.0
A0136	ID CRIT LUNAR THERMAL ENVIRON PARAMETERS	3.1.8	28FEB94	27JUN94	120.0
A0124	CORRELATE ANALYSES TO TEST RESULTS	3.1.8	30MAR94	27JUN94	90.0
A0128	PERF THERMAL CTL SYSTEM LEVEL ANALYSES	3.1.8	30MAR94	13MAY94	45.0
A0133	DEV THERMAL CTL SYS DESC DOCS	3.1.8	29APR94	12JUN94	45.0
A0126	PROVIDE INPUT TO PRD DOCS	3.1.8	28JUN94	27JUL94	30.0
A0029	UPDATE THERMAL ANALYSES	3.1.8	10CT94	29MAR95	180.0
A0030	UPDATE POWER SYSTEMS ANALYSES (U)	3.1.6	10CT94	29MAR95	180.0
A0034	UPDATE STRUCTURES ANALYSES (U)	3.1.4	10CT94	29MAR95	180.0
A0064	DESIGN & DEV CCD/SP BD & PROTO S/W	3.1.2	10CT94	30SEP95	365.0
A0078	UPDATE OPTICAL SYSTEM & FPA ANALYSES (U)	3.1.1	10CT94	29MAR95	180.0
A0112	DEV RTG TEST & ENVIRON FUNC SPECS	3.1.6	10CT94	29MAR95	180.0
A0113	PRODUCE RTG INTERFACE DWGS	3.1.6	10CT94	29MAR95	180.0
A0114	DEV RTG SYS INTEG SPECS	3.1.6	10CT94	29MAR95	180.0
A0155	REV POINT & ALIGNMENT PROTOTYPE DESIGNS	3.1.9	10CT94	30SEP95	365.0
A0159	DEV PROTOTYPE TEST PLANS	3.1.9	10CT94	30SEP95	365.0
A0161	DESIGN ACTUATION SYS FOR 2ND MIRROR	3.1.9	10CT94	30SEP95	365.0
A0170	TEST ANTENNAE DEPLOYMENT	3.1.7	10CT94	30SEP95	365.0
A0184	DEV DETAILED SYS STRESS ANALYSIS	3.1.4	10CT94	30SEP95	365.0
A0238	BASELINE DETECTOR ANALYSES (U)	3.1.3	10CT94	29MAR95	180.0
A0065	DEV CCD/SP ENGINEERING MODEL	3.1.2	10CT95	29SEP96	365.0
A0116	DEV RTG TEST PLAN	3.1.6	10CT95	29MAR96	180.0

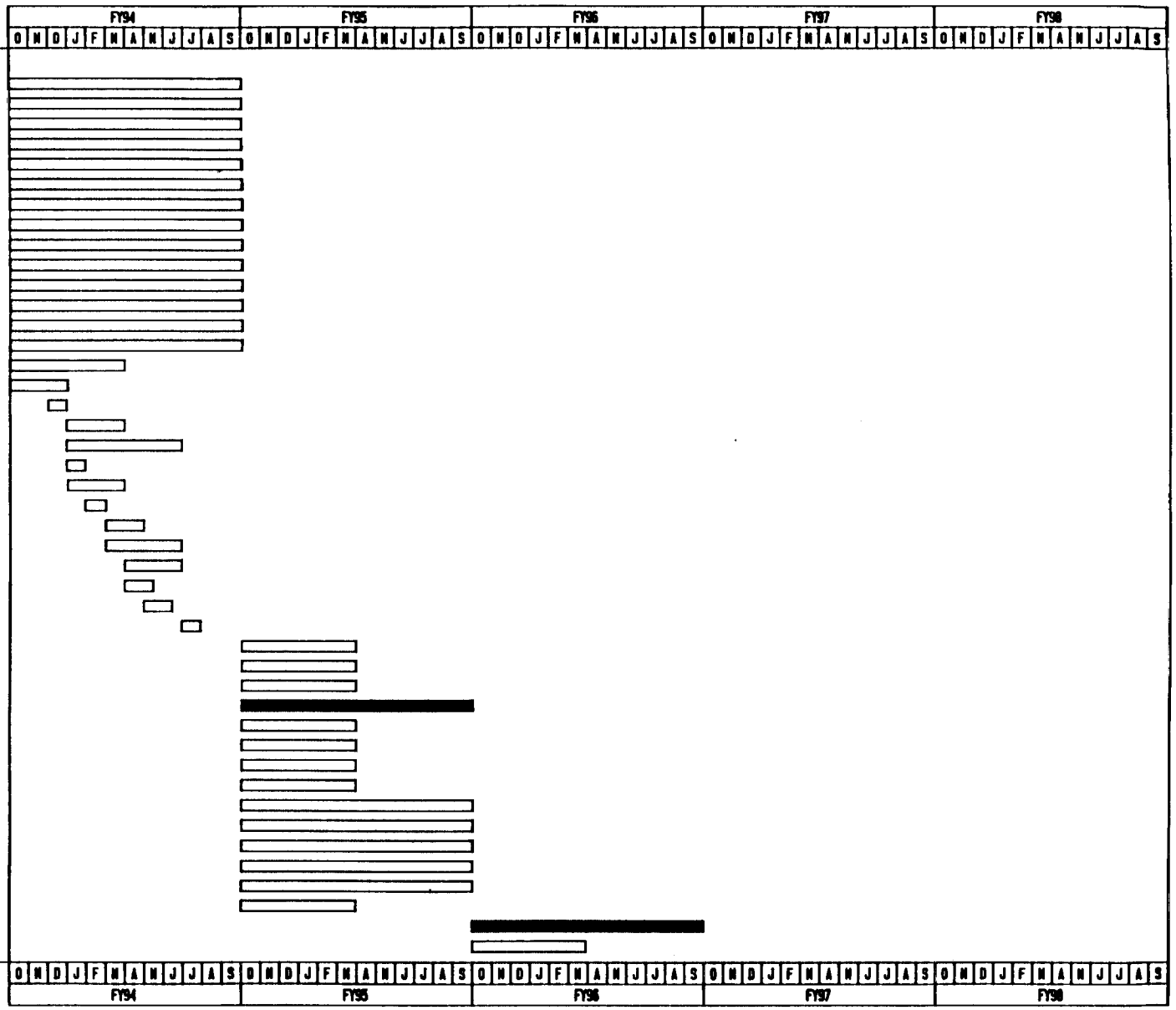

LUNAR U/V TELESCOPE EXPERIMENT ROBERT McBRAYER

ARC NO.	DESCRIPTION	CODE	EARLY START	EARLY FINISH	DAYS DUR.
A0156	BUILD POINT & ALIGNMENT PROTOTYPE	3.1.9	10CT95	28MAR96	180.0
A0191	BUILD/TEST OPTICAL SYS STRUCT PROTO	3.1.4	10CT95	29SEP96	365.0
A0221	BASELINE POWER SYSTEM ANALYSES (B)	3.1.6	10CT95	28MAR96	180.0
A0223	BASELINE STRUCTURES ANALYSES (B)	3.1.4	10CT95	28MAR96	180.0
A0224	BASELINE OPTICAL/FPA SYS ANALYSES (B)	3.1.1	10CT95	28MAR96	180.0
A0157	PERF TESTS ON POINT & ALIGNMENT PROTO	3.1.9	29MAR96	26JUN96	90.0
A0066	FAB, ASSY & TEST CCD/SP	3.2.2	30SEP96	21JUN98	630.0
A0075	FAB, ASSY & TEST TELESCOPE	3.2	30SEP96	21JUN98	630.0
A0079	DEV S/W TOP LEVEL FUNCTIONAL RQMTS	4.0	10CT93	30SEP94	365.0
A0080	DEV FLIGHT S/W DETAILED FUNC RQMTS	4.1.1	10CT94	29MAR95	180.0
A0081	DEV SCIENCE DATA DETAILED FUNC RQMTS	4.2.1	10CT94	29MAR95	180.0
A0082	DEV LAUNCH VEH DETAILED FUNC RQMTS	4.4.1	10CT94	29MAR95	180.0
A0083	DEV EGSE DETAILED FUNC RQMTS	4.5.1	10CT94	29MAR95	180.0
A0084	DEV LANDER DETAILED FUNC RQMTS	4.3.1	10CT94	27JUN95	270.0
A0094	DEV S/W SIMULATOR FUNCTIONAL RQMTS	4.0	10CT94	29MAR95	180.0
A0085	DEV S/W TEST PLANS & PROCEDURES	4.0	30MAR95	25SEP95	180.0
A0086	BEG FLIGHT S/W DESIGN	4.1.2	30MAR95	24DEC95	270.0
A0087	BEG SCIENCE DATA S/W DESIGN	4.2.2	30MAR95	24DEC95	270.0
A0088	LAUNCH VEH S/W DESIGN	4.4.2	30MAR95	24DEC95	270.0
A0089	BEG EGSE S/W DESIGN	4.5.2	30MAR95	24DEC95	270.0
A0095	CONT S/W SIMULATOR FUNC RQMTS	4.0	30MAR95	25SEP95	180.0
A0096	DESIGN SIMULATOR S/W	4.0	30MAR95	28MAR96	365.0
A0090	LANDER S/W DESIGN	4.3.2	25DEC95	19SEP96	270.0
A0091	CONT FLIGHT S/W DESIGN	4.1.2	25DEC95	19SEP96	270.0
A0092	CONT SCIENCE DATA S/W DESIGN	4.2.2	25DEC95	19SEP96	270.0
A0093	CONT EGSE S/W DESIGN	4.5.2	25DEC95	19SEP96	270.0
A0106	CODE SIMULATOR S/W	4.0	25DEC95	19SEP96	270.0
A0097	CODE FLIGHT S/W	4.1.3	29MAR96	28MAR97	365.0
A0098	CODE SCIENCE DATA S/W	4.3.3	29MAR96	28MAR97	365.0
A0099	CODE EGSE S/W	4.5.3	29MAR96	28MAR97	365.0
A0100	CODE LANDER S/W	4.3.3	29MAR96	24SEP96	180.0
A0110	CODE LAUNCHER S/W	4.4.3	29MAR96	26JUN96	90.0
A0107	TRAIN SIMULATOR USERS	4.0	30SEP96	28MAR97	180.0
A0101	V & V FLIGHT S/W	4.1.4	29MAR97	23DEC97	270.0
A0102	V & V SCIENCE DATA S/W	4.2.4	29MAR97	23DEC97	270.0
A0103	V & V LANDER S/W	4.3.4	29MAR97	23DEC97	270.0
A0104	V & V LAUNCH VEH S/W	4.4.4	29MAR97	23DEC97	270.0
A0105	V & V EGSE S/W	4.5.4	29MAR97	23DEC97	270.0
A0108	USE SIMULATOR IN S/W V & V EFFORT	4.0	29MAR97	23DEC97	270.0
A0063	DEV THERMAL TEST PLANS	5.1.7	10CT94	29MAR95	180.0
A0077	PERF OPTICAL/THERMAL/MATERIAL SUBSYS TST	5.1	10CT94	29SEP96	730.0
A0109	INTEGRATE S/W WITH H/W	5.3	27JUN98	24SEP98	90.0
A0192	PERFORM SHAKE TEST OF TELESCOPE/LANDER	5.3.1	27JUN98	24SEP98	90.0
A0042	DEV FIELDN GND INTEG REQ DOC (P)	8.0	10CT94	29MAR95	180.0

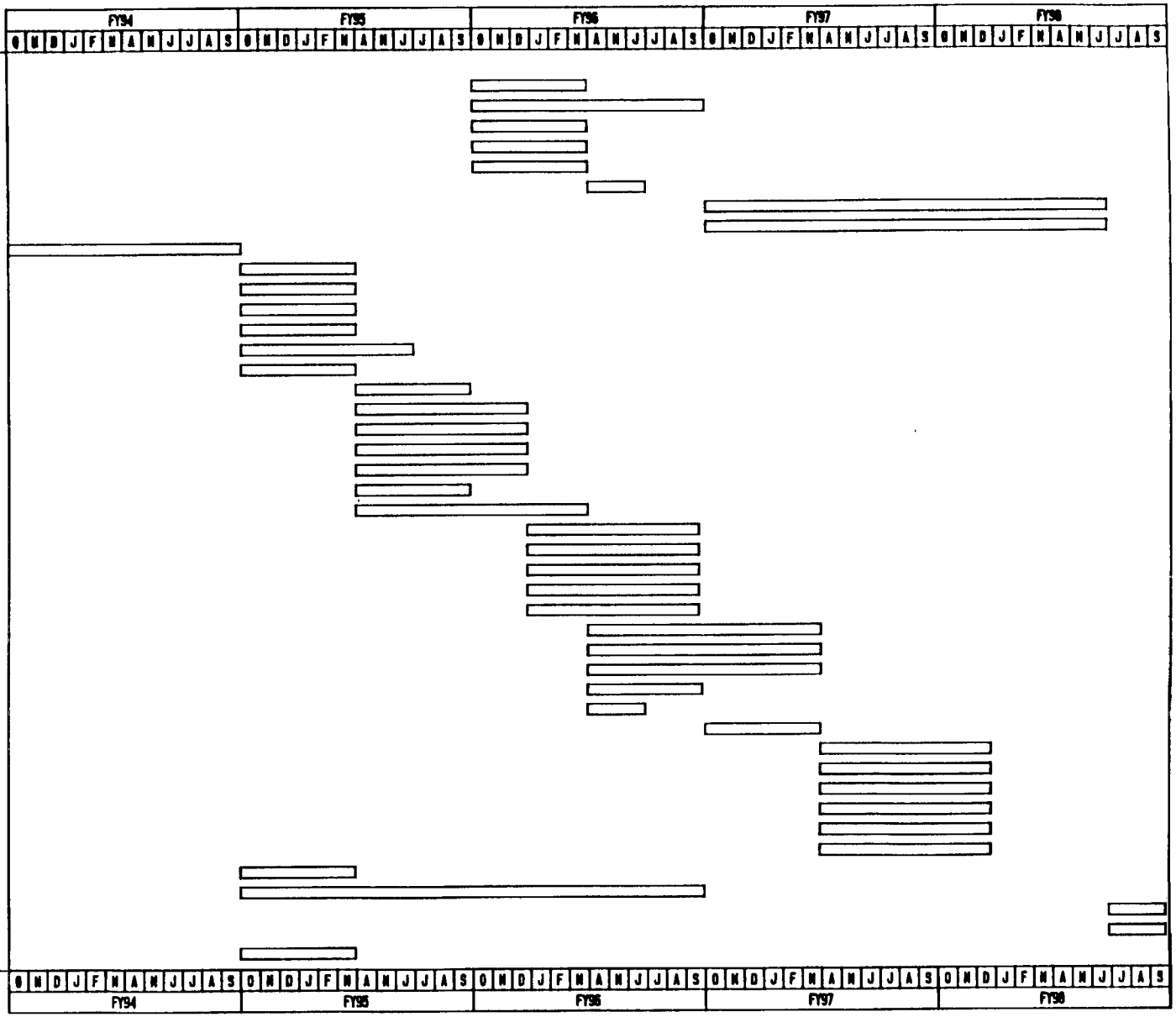

Plot Date: 09/26/93 Run Date: 09/08/93 Page 4.5

LUNAR U/V TELESCOPE EXPERIMENT ROBERT McBRAYER

ARC NO.	DESCRIPTION	CODE	EARLY START	EARLY FINISH	DAYS DUR.
A0051	UPDATE GROUND INTEG REQMTS (U)	8.0	10CT95	28MAR96	180.0
A0058	DEV PRELIM IP & CL (P)	8.0	30SEP96	28MAR97	180.0
A0231	BASELINE GND INTEG REQ DOC (B)	8.0	30SEP96	28MAR97	180.0
A0236	BASELINE IP & CL (B)	8.0	30SEP97	28MAR98	180.0
A0001	DEV MISSION OBJECTIVE REQMT DOCS (P)	9.1	10CT93	30SEP94	365.0
A0002	DEVELOP PART 1 CEI SPECS	9.1	10CT93	30SEP94	365.0
A0021	DEV OPS PLAN	9.4	10CT93	29MAR94	180.0
A0118	DETERMINE LANDING SITE	9.1	10CT93	29MAR94	180.0
A0238	DEV PRELIM FLT OPS PLAN (P)	9.3	10CT93	29MAR94	180.0
A0023	UPDATE CEI PART 1 SPECS (B/U)	9.1	10CT94	30SEP95	365.0
A0043	DEV PRELIM FLIGHT DEF DOC (P)	9.3	10CT94	29MAR95	180.0
A0044	DEV PRELIM DATA FLOW/DATA SYSTEMS (P)	9.4.2	10CT94	29MAR95	180.0
A0045	DEV PRELIM OPS GUIDELINES (P)	9.4	10CT94	29MAR95	180.0
A0047	DEV PRELIM OPS CENTER DATA BASE (P)	9.4.2	10CT94	29MAR95	180.0
A0048	DEV PRELIM OPS CENTER VERIF PLAN (P)	9.4.2	10CT94	29MAR95	180.0
A0049	UPDATE OPS PLAN	9.4	10CT94	29MAR95	180.0
A0068	DEV OPS PROCEDURES	9.0	10CT94	30SEP95	365.0
A0198	DEV PRELIM LAUNCH SITE RQMTS	9.1	10CT94	30SEP95	365.0
A0215	DEV SCIENCE REQMTS DOCS (B)	9.1	10CT94	30SEP95	365.0
A0240	UPDATE FLT OPS PLAN (U)	9.3	10CT94	29MAR95	180.0
A0052	UPDATE FLIGHT DEF DOC (U)	9.3	10CT95	28MAR96	180.0
A0054	UPDATE OPS GUIDELINES (U)	9.4	10CT95	28MAR96	180.0
A0056	UPDATE OPS CENTER DATA BASE (U)	9.4.2	10CT95	28MAR96	180.0
A0057	UPDATE OPS CENTER VERIFICATION PLAN (U)	9.4.2	10CT95	28MAR96	180.0
A0069	DEV OPS CONCEPTS	9.0	10CT95	29SEP96	365.0
A0070	ANALYSE CTL CNTR EQUIP & S/W REQMTS	9.4	10CT95	29SEP96	365.0
A0216	BASELINE CEI SPECS (B)	9.1	10CT95	29SEP96	365.0
A0233	UPDATE DATA FLOW/DATA SYSTEMS (U)	9.4.2	10CT95	28MAR96	180.0
A0241	BASELINE FLT OPS PLAN (B)	9.3	10CT95	28MAR96	180.0
A0071	DEV OPS CNTR PROCEDURES & MANUALS	9.0	30SEP96	29SEP97	365.0
A0232	BASELINE FLT DEF DOCS (B)	9.3	30SEP96	28MAR97	180.0
A0234	BASELINE DATA FLOW/DATA SYSTEMS (B)	9.4.2	30SEP96	28MAR97	180.0
A0235	BASELINE OPS GUIDELINES (B)	9.4	30SEP96	28MAR97	180.0
A0237	BASELINE OPS CTR DATA BASE (B)	9.4.2	30SEP96	28MAR97	180.0
A0239	BASELINE OPS CTR VERIFICATION PLAN (B)	9.4.2	30SEP96	28MAR97	180.0
A0074	OPS CNTR EQUIP INSTALL & CHECKOUT	9.4	29MAR98	24SEP98	180.0

FY94 FY95 FY96 FY97 FY98

O N D J F M A M J J A S O N D J F M A M J J A S O N D J F M A M J J A S O N D J F M A M J J A S O N D J F M A M J J A S

Plot Date: 09/26/93 Run Date: 09/08/93 Page 5: 5

REPORT DOCUMENTATION PAGE

Form Approved
OMB No. 0704-0188

1. AGENCY USE ONLY *(Leave blank)*	2. REPORT DATE	3. REPORT TYPE AND DATES COVERED
	April 1994	Technical Memorandum

4. TITLE AND SUBTITLE

Lunar Ultraviolet Telescope Experiment (LUTE)
Phase A Final Report

5. FUNDING NUMBERS

6. AUTHOR(S)

Robert O. McBrayer, et al.

7. PERFORMING ORGANIZATION NAME(S) AND ADDRESS(ES)

George C. Marshall Space Flight Center
Marshall Space Flight Center, Alabama 35812

8. PERFORMING ORGANIZATION REPORT NUMBER

M-746

9. SPONSORING/MONITORING AGENCY NAME(S) AND ADDRESS(ES)

National Aeronautics and Space Administration
Headquarters Astrophysics Division
Washington, DC 20546

10. SPONSORING/MONITORING AGENCY REPORT NUMBER

NASA TM-4594

11. SUPPLEMENTARY NOTES

This report is compiled from various Preliminary Design, Science and Engineering, and Safety and Mission Assurance Office members of the LUTE Task Team.

12a. DISTRIBUTION/AVAILABILITY STATEMENT

Unclassified—Unlimited
Subject Category: 89

12b. DISTRIBUTION CODE

13. ABSTRACT *(Maximum 200 words)*

The Lunar Ultraviolet Telescope Experiment (LUTE) is a 1-meter telescope for imaging from the lunar surface the ultraviolet spectrum between 1,000 and 3,500 angstroms. There have been several endorsements of the scientific value of a LUTE. In addition to the scientific value of LUTE, its educational value and the information it can provide on the design of operating hardware for long-term exposure in the lunar environment are important considerations.

This report provides the results of the LUTE phase A activity begun at the George C. Marshall Space Flight Center in early 1992. It describes the objective of LUTE (science, engineering, and education), a feasible reference design concept that has evolved, and the subsystem trades that were accomplished during the phase A.

14. SUBJECT TERMS	15. NUMBER OF PAGES
astronomy, lunar, LUTE, telescope, ultraviolet (UV)	772
	16. PRICE CODE A99

17. SECURITY CLASSIFICATION OF REPORT	18. SECURITY CLASSIFICATION OF THIS PAGE	19. SECURITY CLASSIFICATION OF ABSTRACT	20. LIMITATION OF ABSTRACT
Unclassified	Unclassified	Unclassified	Unlimited